Quarterly Publication

ISSN 2383 - 3572

Global Journal of Environmental Science and Management

Volume 11, Number 3, Summer 2025

Global Journal of Environmental Science and Management (GJESM)

(QUARTERLY PUBLICATION)

OPEN ACCESS

Publisher and Editor-in-Chief
Professor J. Nouri
GJESM Publisher INC, USA
Email: *nourijafar@gmail.com*
gjesm.publication@gmail.com

Managing Editor
Professor D. Sivakumar
Kalasalingam Academy of Research and Education, Tamil Nadu, India
Email: *sivakumar.gjesm@gmail.com*

Technical Editor
Professor M. Samimi
Kermanshah University of Technology: Kermanshah, Iran
Email: *m.samimi@kut.ac.ir*

Assistant Editor
Dr. S.M. Tehrani
International Journal of Human Capital in Urban Management
Email: *tehranishohre@gmail.com*

Page Designer
A. Rezaye Soltanabadi
Imajgaran Danesh

Editorial Contact Information
621 W. Chapman Ave, Orange, CA 92868
USA
Phone: +1(949)405 0540
Email: *gjesm.publication@gmail.com*
editor@gjesm.net

Website: https://www.gjesm.net/
https://www.gjesm.com/

Publication Center
GJESM Publisher INC
publisher@gjesm.net
gjesm.publication@gmail.com

Editorial Board

Professor V.K. Gupta; *University of Johannesburg,* ***South Africa***

Professor M. Sillanpää; *Lappeenranta University of Technology,* ***Finland***

Professor A. Fauzi Ismail; *Universiti Technologi Malaysia,* ***Malaysia***

Professor A.T. Peterson; *University of Kansas,* ***USA***

Professor A. Cerda; *University of Valencia,* ***Spain***

Professor J.-D. Gu; *University of Hong Kong,* ***P.R. China***

Professor S.I. Allakhverdiev; *Russian Academy of Sciences,* ***Russia***

Professor D. Wen; *University of Leeds,* ***UK***

Professor T. Yigitcanlar; *Queensland University of Technology,* ***Australia***

Professor A. Z. Aris, *Universiti Putra Malaysia,* ***Malaysia***

Professor K. Yetilmezsoy, *Yildiz Technical University,* ***Turkey***

Professor K.E. Noll; *Illinois Institute of Technology,* ***USA***

Professor J. Nouri; *Tehran University of Medical Sciences,* ***Iran***

Professor D. Sivakumar; *Kalasalingam Academy of Research and Education,* ***India***

Professor J. Aravind; *Saveetha Institute of Medical and Technical Sciences,* ***India***

GJESM is licensed under a "Creative Commons Attribution 4.0 International (CC-BY 4.0)"

Publication authorization is certified by the Ministry of Culture and Islamic Guidance; No. 93/3629; 14 May 2014
Scientific-Research grade is accredited by the Ministry of Science, Research and Technology; No. 3/18/59975; 20 June 2015

Let s work together to publish the knowledge
and science to serve better the environment

Circulation: 500

***p*ISSN 2383 - 3572** ***e*ISSN 2383 - 3866**

Aims and Scope

Global Journal of Environmental Science and Management (GJESM) is an international scholarly refereed research journal which aims to promote the theory and practice of environmental science and management. A broad outline of the journal's scope includes; peer reviewed original research articles, case and technical reports, reviews and analyses papers, short communications and notes to the editor, in interdisciplinary information on the practice and status of research in environmental science and management, both natural and man-made. The main aspects of research areas include, but are not exclusive to; environmental chemistry and biology, environments pollution control and monitoring, transport and fate of pollutants in the environment, concentrations and dispersion and trace of wastes in air, water, and soil, point and non-point sources pollution, heavy metals and organic compounds in the environment, atmospheric pollutants and trace gases, solid and hazardous waste management; soil biodegradation and bioremediation of contaminated sites; environmental impact assessment, industrial ecology, ecological and human risk assessment; improved energy management and auditing efficiency and environmental standards and criteria.

Vision and Mission

Global Journal of Environmental Science and Management (GJESM) publishes original. Peer-reviewed and technical environmental articles serve those environmental science and management through the on time quarterly publication with reliable information. GJESM is an integral partner with the scientific and technical communities, delivering superior information products and services that foster communication, build insights and enables individual and collective advancement in environmental research. Providing environmental science and management information to the general public with descriptions of contemporary advances in environmental issues to be used in improving environmental protection and management.

Abstracting and Indexing

Web of Science (ESCI); Scopus; Scimago Journal Rank (SJR); ProQuest (Agricultural and Environmental Science + Natural Science Collection + Ulrichsweb); Chemical Abstract (CAS); CABI Abstract; Global Health Abstract; Agricola; Committee on Publication Ethics (COPE); PubMed-NCBI; DOAJ; Open J-Gate; Google Scholar; Academia.edu; Geomar; WorldCat; Academic Resource Index; Environmental XPRT; Information Matrix for the Analysis of Journals (MIAR); Bibliothek Humburg; ScienceMedia; JournalTOCs; MSRT; ISC; RICeST; SID; Civilica; Magiran.

Global Journal of Environmental Science and Management
GJESM

Publisher and Editor-in-Chief
Professor J. Nouri

eISSN 2383 3866
pISSN 2383 3572

Quarterly Full Open Access Peer Reviewed Publication

Journal Abbreviation: Global J. Environ. Sci. Manage.



CALL FOR PAPERS

Publication benefits in GJESM Journal

- *Online Publication Journal*
- *Online Submission and Reviewing*
- *Online Status Inquiry*
- *Double Blind Review*
- *Fast-Track Review and Publication*
- *Immediate Publication on the Net*
- *Article Podcasts Implementation*
- *Indexed in Scopus Database with CiteScore = **7.9***
- *Scopus Percentile (WORLD TOP-TEN: 95th in Social Science)*
- *Scopus **Q1** Category*
- *Indexed in Web of Science Database with **IF = 3.1***
- *Web of Science JCR with **Q2** Category*

Indexed by Scopus

Clarivate Web of Science™ Core Collection, ESCI Journals

Journal Citation Reports 2023 — Clarivate Analytics — 3.1 — Journal Impact Factor

Journal Website:
https://www.gjesm.net
https://www.gjesm.com

Email:
gjesm.publication@gmail.com

Phone:
+1(949)405 4538
+1(949)405 0540

Address: 623 W. Chapman Ave, Orange, CA 92868 USA

Global
Journal of Environmental Science and Management

CONTENTS

Volume 11, Issue 3, Summer 2025

Neuro-fuzzy inference system and white shark optimization of coagulation-flocculation of aquaculture wastewater treatment **(857-874)**

A.F. Mohamed; H. Rezk (SAUDI ARABIA)

A spatial slip plane-based vegetation model for slope reinforcement and shallow landslide mitigation **(875-896)**

I.G. Tejakusuma; E.H. Sittadewi; A. Mulyono; T. Handayani; A. Tohari; H.E.H. Fatahillah; Z. Zakaria; E.B. Budiman; N. Utami (INDONESIA)

The potential of carbon emission reduction through the transition to battery electric vehicles **(897-914)**

W. Kongwee; W. Achariyaviriya; D. Rinchumphu; P. Suttakul; A. Achariyaviriya; N. Chanpichaigosol; V. Vichiensan; M. Kii; P. Iamtrakul; Y. Hayashi (THAILAND/ JAPAN)

Microplastic contamination in river and its impact on fish health **(915-940)**

U. Yanuhar; E.N. Wiratno; H. Suryanto; D.R. Machfuda; N.R. Caesar (INDONESIA)

Carbon footprint associated with a small-scale emissions reduction initiative for sustainable event management **(941-962)**

V. de cadenet; P. Parinyakulset; W. Komkum; P. Boondaeng; P. Raksa (THAILAND)

The role of marine protected areas in enhancing coral cover and reef fish communities **(963-982)**

Z.A. Harahap; D.G. Bengen; I.W. Nurjaya; S.B. Agus; Y. Naulita; R.M. Siringoringo (INDONESIA)

Eco-friendly pest management in integrated rice-fish farming systems using plant-derived biopesticides to promote sustainable agriculture **(983-1000)**

Wiratno; I.M. Trisawa; I. Taufik; I. Ardi; L. Thesiana; E. Kusrini; D. Susanti; E.W. Minarni; A. Nurawan; A. Jufri; Sukamto; Y. Apriyana; N. Sutrisna; Y. Surdianto; B. Susanto; U. Susanto (INDONESIA)

The significance of clean energy, education, and environmental managament in fostering a sustainable future **(1001-1018)**

J. Fábregas; A. Palencia (COLOMBIA)

Monsoonal influence on particulate organic carbon variability through satellite data analysis **(1019-1034)**

C.K. Tito; D.G. Bengen; T. Prartono; A. Damar; A.J. Wahyudi (INDONESIA)

Removal of cadmium and lead using a sub-bituminous coal resin modified with xanthate groups **(1035-1056)**

F. Fuentes Gandara; W. Cabrera-Lafaurie; I. Piñeres-Ariza; E. Espinosa-Fuentes; J. Marrugo-Negrete; J. Pinedeo-Hernández (COLOMBIA)

Conserving biodiversity, carbon, and community values in a fragmented landscape **(1057-1078)**

A. Susilowati; Y. Lisnawati; H.H. Rachmat; H. Kurniawan; W.C. Adinugroho; R. Imanuddin; D.J. Sudrajat; I.W.S. Dharmawan; M. Iqbal; S. Fahmi; L.M. Nugraha; E. Novriyanti; E. Sutrisno; A.B. Siswanto (INDONESIA)

Passenger car emissions in urban areas based on local vehicle fleet and environmental conditions **(1079-1096)**

A. Valdés-Montenegro; F.G. Gonzalez-Olivardia; C. Pinzón-Acosta (PANAMÁ)

Infrared precipitation on climate hazards using rainfall dataset over inter-tropical convergence zone **(1097-1124)**

A. Purwandani; Supari; W. Ambarwulan; U. Haryoko; I.P. Dewi; Y. Anantasena; Y.S. Djajadihardja; H. Sadmono; S.I. Sachoemar; D. Nugroho (INDONESIA)

Ambient air nitrogen dioxide concentration and the growing incidence of asthma in school-aged children **(1125-1142)**

P.N. Sari; D. Driejana; A.P. Yudison; D. Agustian; A.B. Kurnia (INDONESIA)

Spatiotemporal analysis of rainfall variability using satellite precipitation in watersheds **(1143-1162)**

M.D. Syaifullah; A. Purwandani; M. Kudsy; Tukiyat; S. Tikno; A.E. Sakya; F.H. Widodo; S. Bahri; Muktiyono (INDONESIA)

Tracking Coronavirus 2019 pandemic-related waste generation in urban waterways **(1163-1184)**

R.G. Banal; I.L.M. Abad (PHILIPPINES)

Sustainability of natural tourism attraction and satisfaction **(1185-1198)**

Y. Yuliana; A.M. Ningsih; V. Kristiana; A.P. Maharani; C. Syahni (INDONESIA)

Allometric equations model for estimating an above and below ground biomass of dipterocarp forest in the tropics **(1199-1220)**

I. Heriansyah; Luthfy Abdullah; J.S. Rahajoe; R. Susanti; Y. Lisnawati; Subarudi; R. Dewi; Darwo ,; Mawazin; Abdurachman; Karmilasanti; N. Wakhid; D. Wicaksono; R. Effendi; A.S. Yunianto; M.A. Qirom; N. Mindawati (INDONESIA)

Carcinogenic and non-carcinogenic hazards associated with trace elements and organochlorines from fish consumption in tropical river watershed **(1221-1240)**

D. Dwiyitno; G.R. Barokah; D. Yogaswara; R. Grandiosa; E. Frimawaty; F. Ariyani; H.E. Irianto; Y. Sani (INDONESIA)

The impact of renewable energy technology innovation on the low-carbon economic transition **(1241-1258)**

X.Y. Liu; X. Shao; X. Li; C. Dong (CHINA)

Integrating building information modeling and bayesian network for enhanced go/no-go decisions in building demolition projects **(1259-1280)**

T.J.W. Adi; Y.P. Devia; N. Andriyani (INDONESIA)

Sustainable approach for biocontrol of biostimulants derived from endophytic bacteria and seaweed extracts **(1281-1298)**

Y. Suryadi; D.N. Susilowati; W. Wartono; H. Hanudin; E. Korlina; N. Gunaeni; E. Diningsih; M. Asaad; S. Widawati; S. Suliasih (INDONESIA)

Bibliometrics analysis and the role of nanocatalysts in wastewater remediation **(1299-1318)**

J. Aravind; M. Kamaraj; P. Suresh Babu (INDIA)

A bibliometric study on Sordariales fungi covering genetic diversity, ecological interactions and biotechnological applications **(1319-1342)**

N.F. Wulandari; A.R. Syam; L. Alhamd; B. Gunadi; Yosmaniar; E. Widjaja; B.N. Utomo; S. Wahyuwardani; R. Widiastuti; T. Kadarini; D. Safar (INDONESIA)

Application of marine bacterial alginate lyases in wastewater treatment, biofilm removal and green technology **(1343-1360)**

M.U.K. Anjung; H. Nursyam; A.A. Prihanto; E. Chasanah (INDONESIA)

Global J. Environ. Sci. Manage. 11(3): 857-874, Summer 2025, Serial #43

Global Journal of Environmental Science and Management
(GJESM)

Homepage: https://www.gjesm.net/

Podcasts

ORIGINAL RESEARCH ARTICLE

Neuro-fuzzy inference system and white shark optimization of coagulation-flocculation of aquaculture wastewater treatment

A.F. Mohamed[1], H. Rezk[2,*]

[1] *Industrial Engineering Department, College of Engineering and Architecture, Umm Al-Qura University, Mecca, Saudi Arabia*

[2] *Department of Electrical Engineering, College of Engineering in Wadi Alddawasir, Prince Sattam bin Abdulaziz University, Wadi Alddawasir, Saudi Arabia*

ARTICLE INFO

Article History:
Received 22 January 2025
Revised 25 Feburary 2025
Accepted 01 April 2025

Keywords:
Artificial intelligence
Biopolymers
Coagulation-flocculation
Treatment of wastewater

ABSTRACT

BACKGROUND AND OBJECTIVES: Polymeric flocculants derived from the coagulation-flocculation procedure, such as chitosan, effectively remove algal-bacterial biomass from wastewater treatment, demonstrating efficiencies comparable to ferric salts at reduced dosages. For effective coagulation-flocculation in the treatment of aquaculture wastewater, it is crucial to determine accurate measurements for three primary input factors: potential of hydrogen, chitosan dose, and settling time. This study seeks to establish the most effective operating conditions for coagulation-flocculation by fine-tuning the three input parameters.

METHODS: Artificial intelligence and recent optimzation algorithms are integrated to achieve the purpose of this study work. Initially, an adaptive neuro-fuzzy inference system model of the wastewater treatment process was built based on experimental data. The white shark optimizer is utilized to assess the most effective chitosan dosage, potential of hydrogen value, and settling time necessary for minimizing turbidity and salinity levels. Throughout the optimization procedure, the controlling parameters act as design variables, and the goal is to maximize the objective function, which is the combined total of turbidity and salinity removal.

FINDINGS: The adaptive neuro-fuzzy inference system turbidity removal model has root mean square error values of 3.52e-05 and 1.51 for training and testing data, respectively. The R-squared values for testing and training are 0.76 and 1.0, respectively. The adaptive neuro-fuzzy inference system demonstrated a significant improvement over the analysis of variance, decreasing the root mean square error from 2.8 to 0.836, which represents a 70 percent decline. The estimated R-squared value rose by 11.76 percent, from 0.68 with analysis of variance to 0.76 with adaptive neuro-fuzzy inference system. In the context of salinity removal, the adaptive neuro-fuzzy inference system demonstrated root mean square error values of 7.13e-06 for the training phase and 2.045 for the testing phase. The R-squared values for training and testing are 1.0 and 0.82, respectively, and adaptive neuro-fuzzy inference system reduced the root mean square error from 6.8 with analysis of variance to 1.135 with adaptive neuro-fuzzy inference system achieving an 83.5 percent reduction. Through the analysis of variance, the R-squared value for prediction was 0.765, which improved by 7.2 percent to reach 0.82 when utilizing the adaptive neuro-fuzzy inference system.

CONCLUSION: Adaptive neuro-fuzzy inference system succseded to present an accurate model of wastewater treatment process and white shark optimizer defined accutrelly the values of chitosan dose, pontential of hydrogen, and settling time to reduce turbidity and salinity. Thus, improving chitosan-based coagulation-flocculation presents substantial ecological benefits by lowering the use of toxic chemicals and decreasing sludge formation, ultimately contributing to reduced pollution.

DOI: 10.22034/gjesm.2025.03.01

This is an open access article under the CC BY license (http://creativecommons.org/licenses/by/4.0/).

NUMBER OF REFERENCES
33

NUMBER OF FIGURES
9

NUMBER OF TABLES
7

*Corresponding Author:
Email: *hr.hussien@psau.edu.sa*
Phone: +554 741 6732
ORCID: 0000-0001-9254-2744

Note: Discussion period for this manuscript open until Sep 1, 2025 on GJESM website at the "Show Article".

INTRODUCTION

One industry that contributes to the pollution of surface waters is aquaculture (Alsaleh, 2024). The effluent from aquaculture exhibits a specific hue, high concentrations of suspended solids, notable turbidity, and a considerable amount of organic material. Additionally, it has a lot of nutrients, especially phosphate and nitrogen. When these substances are released into surface water without being properly treated, eutrophication results. At present, coagulation and flocculation are recognized as the most effective techniques for managing wastewater in aquaculture. It has been demonstrated that this method works well for treating the majority of pollutant parameters in aquaculture effluents (Kurniawan *et al.,* 2023). Wastewater treatment is crucial for a variety of reasons. First and foremost, it facilitates the removal of pollutants from wastewater, thereby increasing the supply of fresh water and decreasing the demand for natural resources (Silva, 2023). Secondly, by removing different pollutants before releasing the effluent back into the environment, wastewater treatment is vital for protection the environment and public health. Furthermore, managing wastewater effectively plays a crucial role in the sustainable utilization of resources. Additionally, safe, and healthy environments require effective wastewater treatment systems, mainly in urban areas where water pollution has caused by fast urbanization (Altowayti *et al*., 2022). In wastewater treatment, flocculation, or coagulation, is frequently utilized to eliminate solid particles and impurities from water. Numerous coagulants and flocculants are utilized to enhance the flocculation process's efficacy. Flocculants in water treatment has gained significant attention thanks to their various merits, containing their widespread availability, environmental friendliness, biodegradability, and prominent structural features. Several elements impact the procedure, including the potential of hydrogen (pH), temperature, mixing rate, and the dosages of coagulants and flocculants (Zaki *et al*., 2023). It has been exposed that bentonite treated with chitosan and polyglutamic acid may proficiently eliminate turbidity, total nitrogen, phosphorus, and chemical oxygen demand from starch wastewater at high removal rates (Zhang *et al*., 2023a). This technique of coagulation-flocculation is widely used in the treatment of natural and industrial wastewater to effectively eliminate radionuclides, phosphates, dyes, and suspended particles. In urban wastewater treatment facilities, coagulation/flocculation has also been employed as a pretreatment for ammonium recovery, with good removal efficiencies for turbidity, chemical oxygen demand, and total suspended solids (Barros *et al*., 2022). Furthermore, to eliminate organic and phenolic compounds from wastewater from olive mills, a combined coagulation-flocculation/adsorption technique was devised, leading to notable removal efficiencies for total suspended solids, and total phenolic content (Abu-Dalo *et al*., 2022). In wastewater treatment, artificial intelligence (AI) has been utilized for a range of purposes. AI-based models enhance sustainable wastewater management by optimizing treatment processes, improving efficiency, and reducing resource consumption. In the field of aquaculture, AI assists in the surveillance of water quality and the prediction of treatment demands, ultimately fostering healthier ecosystems. As an example, it is used for monitoring and managing membrane fouling, optimize models, and process parameters (Zhang *et al*., 2023b). The main application of artificial intelligence and machine learning lies in biological wastewater treatment processes (Singh *et al*., 2023). Modelling using AI provided good wastewater treatment procedure simulation precision. In the realm of wastewater treatment plants, regression trees, gene expression programming, and artificial neural networks are instances of AI-based tools used for the prediction of influent parameters (Aghdam *et al*., 2023). AI also efficiently used with water treatment processes including desalination, membrane filtration, disinfection and coagulation/flocculation (Safeer *et al*., 2022). In wastewater treatment, metaheuristic algorithms are applied to decrease energy expenditure and improve the overall performance of treatment facilities. These techniques, which use artificial neural networks to forecast oxygen pumping requirements, are used to reduce aeration energy usage (Salles *et al*., 2022). Examples of these algorithms are Particle Swarm Optimization, and Simulated Annealing. Compared to the default proportional-integral (PI) controller, the suggested method could dynamically modify the oxygen pumping requirement and lower consumed

electrical energy. The PI controller offers the advantage of dynamically adjusting its reference value with metaheuristic algorithms, leading to lower electricity usage compared to conventional controllers. Evaluating, optimizing, and comparing control laws has also been done using multiobjective genetic algorithms and wastewater treatment plant models, producing effective frameworks for wastewater treatment optimization. Furthermore, classification algorithms utilizing metaheuristic techniques have been established to assess the characteristics of wastewater treatment effluent in relation to influent factors, facilitating the efficient management and operation of treatment facilities (Elsayed *et al*., 2022). Using a dataset generated by a wastewater treatment reactor, the study assessed the efficacy of 23 machine-learning classification algorithms, considering two sets of variables related to effluent quality and removal efficiency. Analysis of all the techniques examined revealed that the ensemble bagged trees approach delivered the best overall classification accuracy. Improved performance in several applications, including optimal location of photovoltaic and wind based system in electrical networks (Nassar *et al*., 2025), pramter identification of fuel cells (Fathy and Alanazi, 2023), classification systems (Oyediran *et al*., 2025) and energy management in microgrids (Alhumade *et al*., 2023) are among the benefits of white shark optimizer (WSO). In comparison with other energy management schemes, WSO reduced the quantity of consumed hydrogen fuel by 34.17 percent (%) and boosted efficacy to 9.5%. WSO presented faster setting time features and improved fluctuation damping performance in power system. In comparison to other algorithms, WSO achieved the most significant outcomes in terms of loss minimization, enhancement of voltage profiles, and reduction of greenhouse gas emission reduction in photovoltaic-based distribution generation. Furthermore, WSO has been effectively used in unmanned aerial vehicle (UAV) path planning, exhibiting improved avoidance of local optimization and a faster convergence rate (Nadana Ravishankar *et al*., 2023). Neuro-fuzzy computation integates the advanteges of neural and fuzzy techniques (Sada and Ikpeseni, 2021; Kridakorn Na Ayutthaya *et al*., 2024). By merging the learning abilities of neural networks with fuzzy logic, the Adaptive neuro-fuzzy inference system (ANFIS) boosts prediction accuracy and is capable of modeling nonlinear relationships. Contrasting analysis of variance (ANOVA), ANFIS can handle uncertainty and provide more accurate predictions. In contrast to machine learning models, ANFIS is proficient in dealing with uncertainty and imprecision. However, it may struggle with training in highly dynamic environments, where simpler models like decision trees can operate more swiftly. It is successfully implemented in several enginnering application including prediction of biodiesel dynamic (Kassem *et al*., 2017), Vehicle-to-vehicle wireless charging Nadana (Rahman and Ali, 2025), electrical conductivity prediction (Ahmadianfar *et al*. ,2022). Consequently, the present study establishes a dependable ANFIS model aimed at simulating the process of eliminating salinity and turbidity from wastewater. Three process parameters are taken into consideration to boost turbidity and salinity removal: settling time, pH, and chitosan dosage. An ANFIS model of the wastewater treatment process was initially constructed based on experimental data. Utilizing the latest optimization techniques, the ideal chitosan dosage, pH, and settling duration have been determined to effectively increase turbidity and lower salinity. In accordance with No Free Lunch theory in optimization, no single optimizer can solve all problems effectively. Consequently, white shark optimizer is applied and to validate its suppository, a comparison with slime mould algorithm, particle swarm optimization, Jelly fish, Harris hawks optimization and elite evolutionary strategy Harris hawks optimization was carried out. This study has been contacted in Saudi Arabia in 2024.

MATERIALS AND METHODS

Utilizing AI for optimizing coagulation-flocculation in aquaculture presents challenges, particularly the high costs of computation required for processing data in real time. Table 1 illustrates the dataset used in the study, which was obtained from an open access journal (Iber *et al*., 2023). It depicts the link between two outputs (turbidity and salinity removal) and three input factors (chitosan dose, pH, and settling time).

This study combines ANFIS with white shark optimization to effectively model and enhance the wastewater treatment process. ANFIS is a

Table 1: Input and output data set

No.	Chitosan dosage (mg/L)	pH	Settling time (Min)	Turbidity removal (%)	Salinity removal (%)
1	5	5	17.5	79.88	14.29
2	20	5	17.5	81.27	14.29
3	5	7.5	17.5	85.66	21.43
4	20	7.5	17.5	82.22	14.29
5	5	6.25	5	85.5	21.43
6	20	6.25	5	83.9	21.43
7	5	6.25	30	84.94	21.43
8	20	6.25	30	87.67	7.14
9	12.5	5	5	79.74	14.29
10	12.5	7.5	5	81.82	7.14
11	12.5	5	30	85.2	7.14
12	12.5	7.5	30	85.78	14.29
13	12.5	6.25	17.5	85.5	21.43

combination technique that combines neural networks and fuzzy logic. ANFIS, as seen in Fig. 1, comprises many levels, which are discussed below (Buriboev and Muminov, 2022).

In the fuzzification layer, the Gaussian membership function (GMF) is utilized to identify the MF associated with each input, using Eq. 1 (Zanganeh, 2020):

$$\mu_{X_i}(\alpha) = e^{-\left(\frac{\alpha - c_i}{a_i}\right)^2} \quad (1)$$

Where, a_i and c_i are adjustable parameters associated with the GMF.

α is the input variable

X_i is fuzzy set associated with premise input variables

Product layer: The degrees of membership are used to determine the ith rule's firing strength (ω_i), using Eq. 2 (Zanganeh, 2020):

$$\omega_i = \mu_{X_i}(\alpha) \times \mu_{Y_i}(\beta) \quad (2)$$

β is the input variable

Y_i is fuzzy set associated with premise input variables

$\mu_{X_i}(\alpha)$ is the degrees of membership for α

$\mu_{Y_i}(\beta)$ is the degrees of membership for β

Normalization layer: The weight-total-weight relationship can be described, using Eq. 3 (Zanganeh, 2020):

$$\overline{\omega_i} = \frac{\omega_i}{\sum \omega_i} \quad (3)$$

Defuzzification layer: The adaptive nodes will be determined, using Eq. 4 (Zanganeh, 2020):

$$\overline{\omega_i} f_i = \overline{\omega_i}\gamma = \overline{\omega_i}\left(p_i\alpha + q_i\beta + r_i\right) \quad (4)$$

Where, p_i, q_i, and r_i are the modifiable subsequent parameters.

Output layer: Output is computed using combined amount of inputs from the layers that came before it.

WSO operates as an optimization system that draws on the impressive behaviors of great white sharks, notably their superior hearing and olfactory abilities while navigating and foraging. The primary phases of WSO can be categorized and presented in (Braik *et al.,* 2022). Once a white shark recognizes the whereabouts of prey through the wave action constructed by prey movements, it attempts to undulant fashion, using Eq. 5 (Braik *et al.,* 2022):

$$s_i(t+1) = u\left[s_i(t) + \rho_1 \cdot c_1\left(P_{Gbest}(t) - P_i(t)\right) + \rho_2 \cdot c_2\left(P_{ibest}(t) - P_i(t)\right)\right] \quad (5)$$

Where, the index i=1, 2,..., n communicates the white shark sequence, s is the acceleration, P_{gbest} is the global best location, P denotes current location, P_{best} denotes the current best-accomplished location. c_1 and c_2 represent two arbitery values. u denotes the constriction factor. p_1, p_2, and u are estimated as Eqs. 6, 7 and 8 (Nadana Ravishankar *et al*., 2023):

$$\rho_1 = \rho_{\max} + \left(\rho_{\max} - \rho_{\min}\right)e^{-(4t/t_{\max})^2} \quad (6)$$

$$\rho_2 = \rho_{\max} + \left(\rho_{\max} - \rho_{\min}\right)e^{-(4t/t_{\max})^2} \quad (7)$$

$$u = \frac{2}{\left|2 - \tau - \sqrt{\tau^2 - 4\tau}\right|} \quad (8)$$

Where,
t is current iteration
t^{max} is maxumum number of iterations
ρ_{min} is the intial velocity
ρ_{max} is the subordinate velocity
τ is the acceleration coefficient

Movement in the direction of the best prey: When white sharks smell the perfume of their prey or observe the waves produced by the target's movement, they invariably swim toward it. The prey may either run away or move to a different location to find food. Despite this, its scent remains in the original spot. As a result, the white shark adjusts its location, as indicated by Eq. 9 (Lepe-Silva *et al.*, 2024):

$$P_i(t+1) = \begin{cases} P_i(t) \neg \oplus P_0 + high \cdot a + low \cdot b; \ rand < m \\ P_i(t) + s_i(t) / f; \ rand \geq m \end{cases} \quad (9)$$

Where,
$P_i(t+1)$ is the new position
a and b are a single-dimensional binary vectors
P_0 is the is the logical vector
f signifies frequency, the *high* and *low* values are maximum and minimum limits, and m is the movement force and may be defined as Eq. 10 (Braik *et al.*, 2022):

$$m = \frac{1}{\left|a_0 + e^{\frac{t_{max}/2 - t}{a_1}}\right|} \quad (10)$$

Where, a_0 and a_1 are positive constants.

The step of progress toward the greatest white shark is characterized using Eq. 11 (Braik *et al.*, 2022):

$$P_i(t+1) = \begin{cases} P_{Gbest}(t) + r_1 \cdot D \cdot \text{sgn}(r_2 - 0.5); \ r_3 < s_s \\ P_i(t); \ otherwise \end{cases} \quad (11)$$

Where, r_1, r_2 and r_3 are arbitery values, D is the distance.

The following relation defined the fish school behavior using Eq. 12 (Braik *et al.*, 2022):

$$P_i(t+1) = \frac{P_i(t) + P_i(t+1)}{2 \cdot rand} \quad (12)$$

The global illustrative scheme is provided in Fig. 2.

ESULTS AND DISCUSSION

Thirteen points were utilised in the measurement process to construct the ANFIS models for salinity and turbidity removal. The data is organized into two segments. The initial segment, which includes nine points, serves to train the model, whereas the second segment is used to evaluate the model with the remaining information. By implementing a hybrid training method, the model is trained through backpropagation during the backward process and applies least square error (LSE) in the

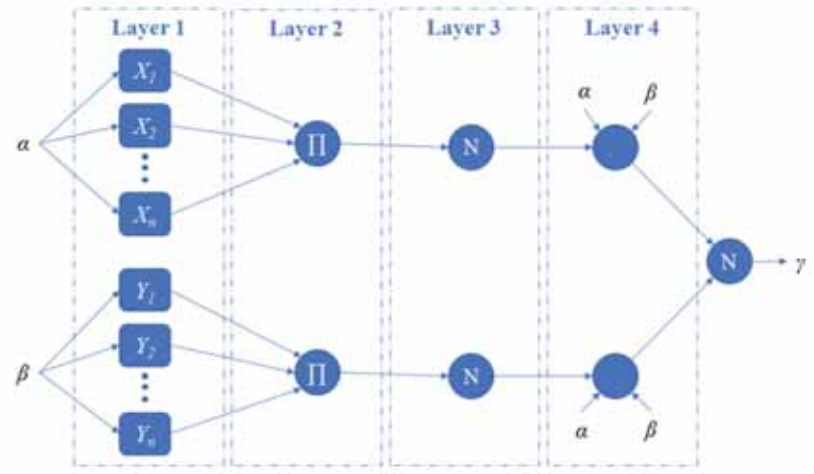

Fig. 1: ANFUS architecture

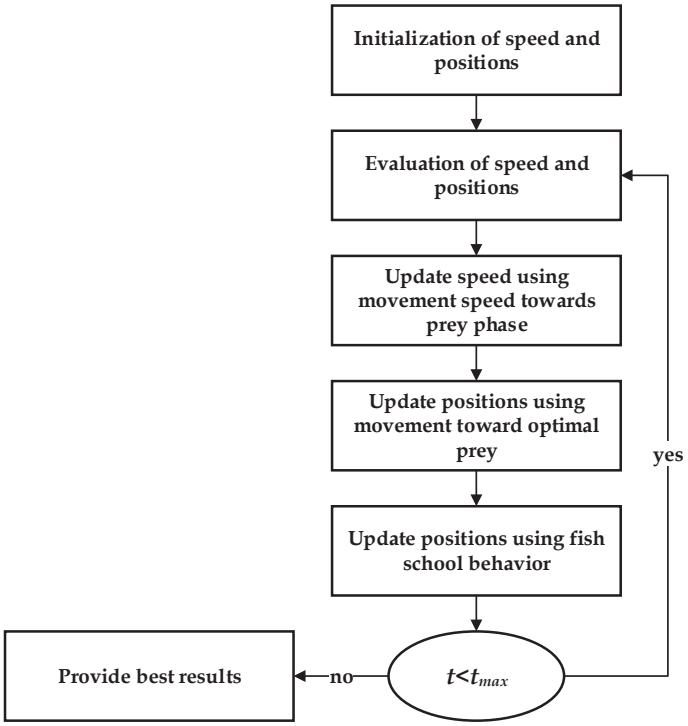

Fig. 2: WSO flow digram

Table 2: Numerical assessment of ANFIS models of turbidity removal and salinity removal

RMSE			R-squared		
Training	Testing	All	Training	Testing	All
Model of turbidity removal					
3.52e-05	1.507	0.836	1.0	0.76	0.91
Model of salinity removal					
7.13e-06	2.045	1.135	1.0	0.82	0.96

forward direction. The subtractive clustering (SC) developed the system's rules, which numbered nine in this work. The two models were then trained until the RMSE was reduced. The metrics deemed statistically significant for the ANFIS models created are show in Table 2.

According to Table 2, the RMSE values for the ANFIS model concerning turbidity reduction are 3.52e-05 and 1.507, respectively. For the training set, the R-squared coefficient is 1.0, while for the testing set, it is 0.76. With the use of ANFIS, the RMSE experienced a significant decline of 70%, falling from 2.8 in ANOVA to 0.836 in ANFIS (Iber *et al.*, 2023). With ANFIS, the R-squared value for prediction increased by 11.76%, from 0.68 using ANOVA to 0.76 by ANFIS. A higher R-squared value produced by ANFIS relative to ANOVA demonstrates improved predictive accuracy and a better fit for the model. For the salinity reduction model developed using ANFIS, the RMSE coefficients are 7.1309e-06 for the training data and 2.0453 for the testing data. For training and testing, the R-squared values are, respectively, 1.0 and 0.82. The RMSE dropped by 83.5% when utilizing ANFIS as opposed to ANOVA, going from 6.8 when using ANOVA to 1.1345 when using ANFIS. With ANFIS, the R-squared value for prediction increased by 7.2% from 0.765 using ANOVA to 0.82 by ANFIS. ANFIS improves prediction accuracy compared to ANOVA by modeling nonlinear relationships more effectively. Lowering

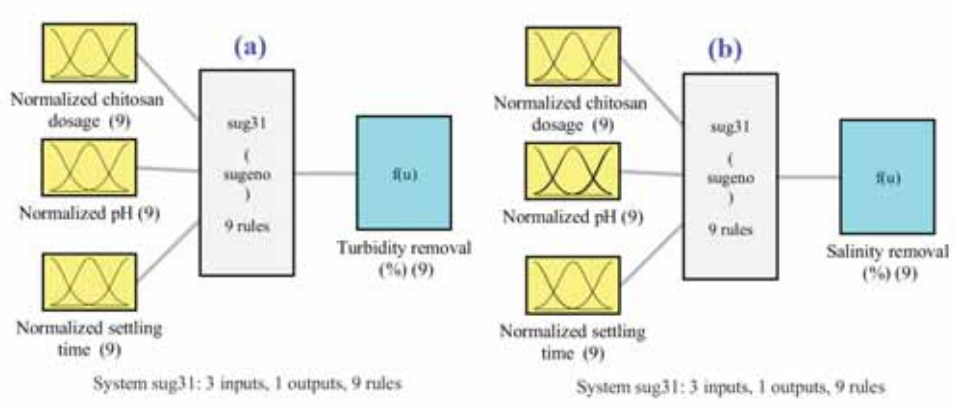

Fig. 3: ANFIS turbidity and salinity model architecture

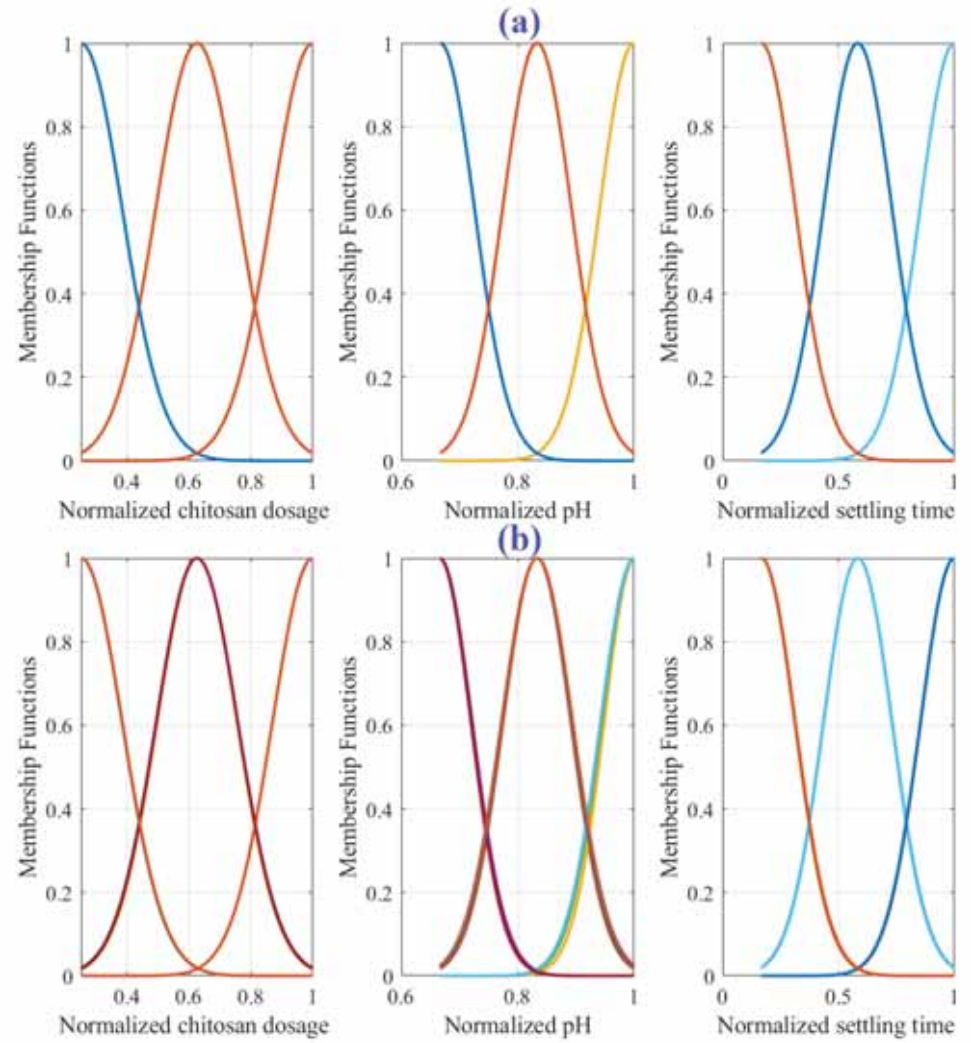

Fig. 4: Fuzzy Model of Turbidity and Salinity Inputs' MFs

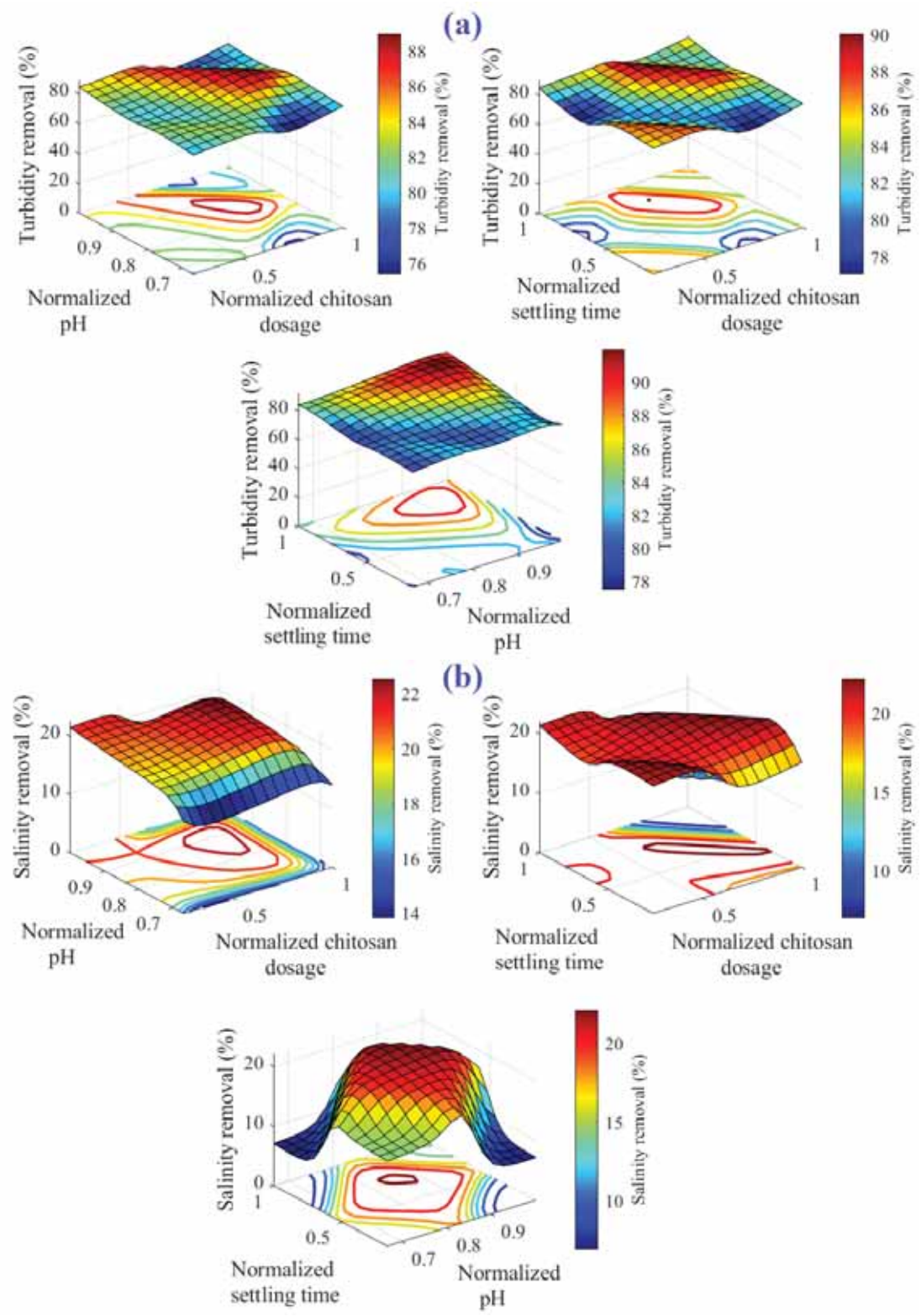

Fig. 5: Three-dimensional surface of ANFIS models, [a] turbidity removal and [b] salinity removal

the RMSE increases the dependability of the model, resulting in predictions that are both more accurate and consistent. Fig. 3 shows the three-input, single-output ANFIS models for salinity and turbidity removal. Fig. 4 depicts the outlines of membership functions (MFs) with a Gaussian form.

The contours of the input-output function for the system are depicted in Fig. 5, which also includes a three-dimensional spatial description for each combination of two inputs. The output reaches its maximum value at dark red, but its lowest value is at dark blue. The results indicated that a higher dosage of chitosan is advantageous for the removal of both turbidity and salinity. Furthermore, an increase in pH levels contributes positively to the removal of turbidity and salinity.

When the inputs and outputs of the model are properly recorded, the ANFIS models developed can predict performance with remarkable precision. This is made evident by plotting the anticipated outputs of the ANFIS model versus the experimental data, as shown in Fig. 6a and

Fig. 6:

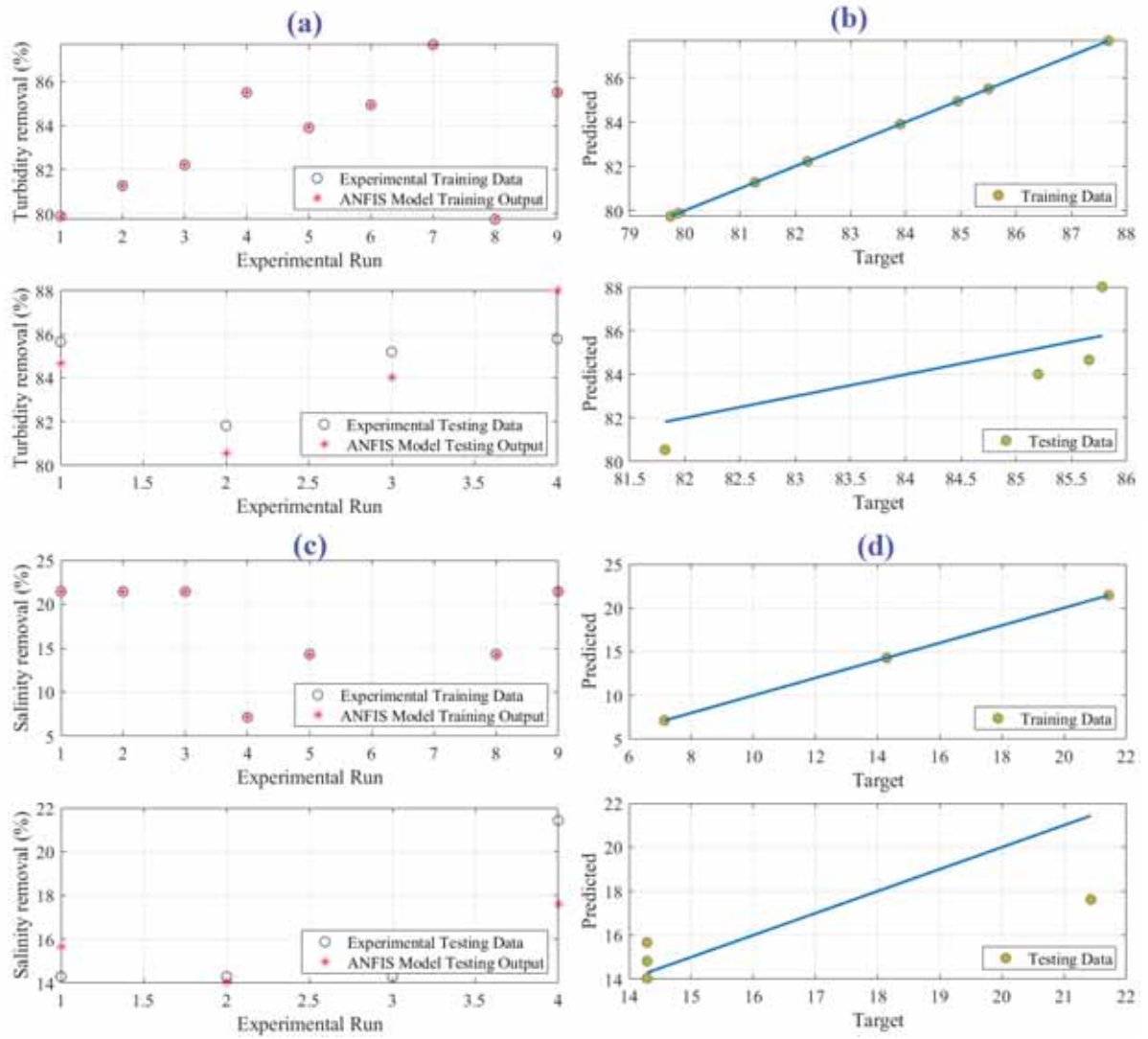

Fig. 6: Prediction accuracy of ANFIS models [a] ANFIS model of turbidity removal: projected and experimental data, [b] one hundred precision line of ANFIS model of turbidity removal, [c] assumed and experimental data of the ANFIS salinity removal model and [b] one hundred precision line of ANFIS model of salinity removal

Table 3: Validation of the ANFIS model

Method	Chitosan dosage (mg/L)	pH	Settling time (Min)	Turbidity removal (%)	Salinity removal (%)	Total Difference
Exp. (Iber *et al.*, 2023)	5	7.5	30	90.80	22.40	0.0
RSM (Iber *et al.*, 2023)	5	7.5	30	87.67	21.43	4.1
ANFIS	5	7.5	30	89.22	20.1	3.88

Table 4: Optimized results

Method	Chitosan dosage (mg/L)	pH	Settling time (Min)	Turbidity removal (%)	Salinity removal (%)	TPI (%)
Exp. (Iber *et al.*, 2023)	5	7.5	17.5	85.66	21.43	107.09
RSM Iber *et al.*, 2023)	5	7.5	30	87.67	21.43	109.1
ANFIS and WSO	0.25 (norm.) 5	1.0 (norm.) 7.5	0.4255 (norm.) 12.765	93.48	20.56	114.1

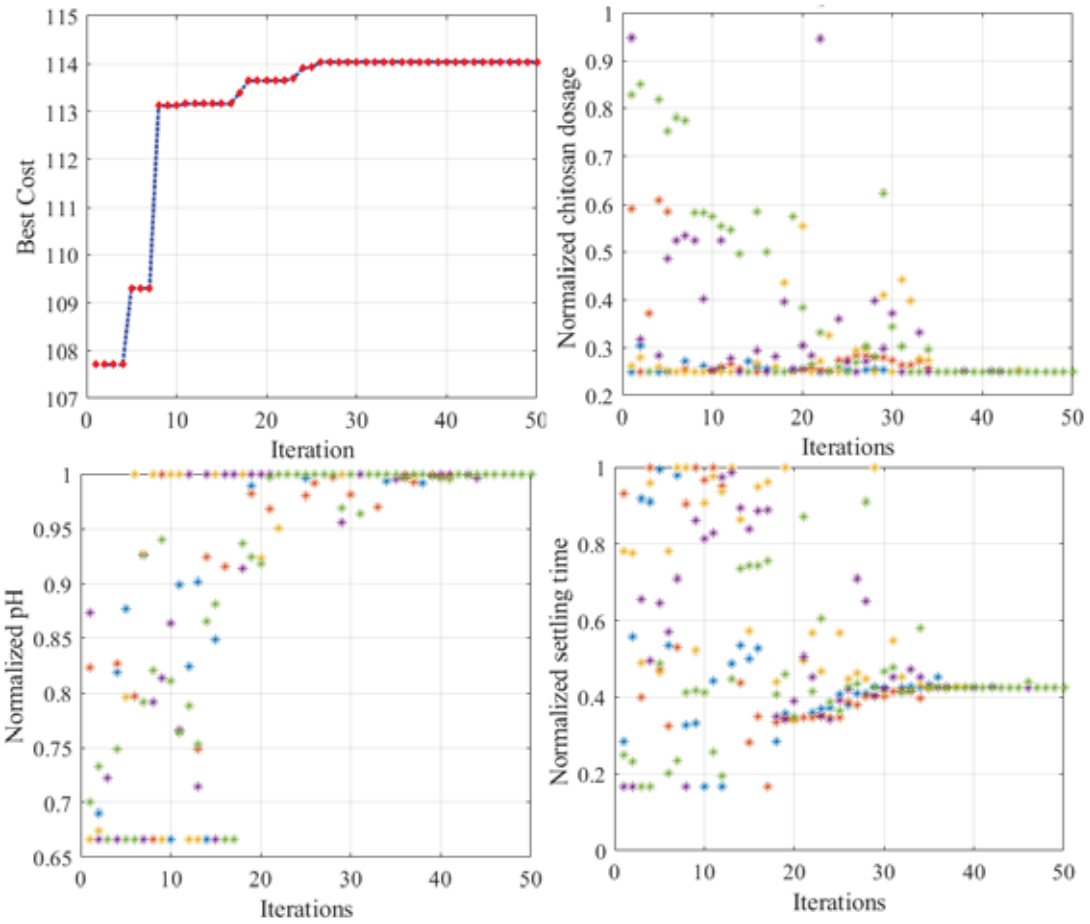

Fig. 6: Particles convergence during optimization [a] best objective function, [b] normalized sulfur concentration, [c] normalized run time and [d] normalized biomass concentration

Table 5: Details description of 30 runs with different algorithms

No.	WSO	SMA	PSO	JS	HHO	EESHHO	No.	WSO	SMA	PSO	JS	HHO	EESHHO
1	114.05	114.05	113.06	113.78	110.1	112.93	16	114.05	114.05	113.06	112.71	113.63	113.05
2	114.05	114.05	113.06	112.47	107.11	114.01	17	114.05	114.05	114.04	111.96	113.9	113.06
3	114.05	113.06	113.06	113.06	114.03	113.06	18	114.05	113.04	113.06	113.99	109.66	113.05
4	114.05	114.05	114.05	112.95	113.17	113.06	19	114.05	113.06	113.07	113.91	114.05	113
5	114.05	114.05	114.05	112.96	114.04	113.01	20	114.05	114.05	113.07	112.03	112.32	112.89
6	114.05	113.04	113.07	113.01	111.42	113.05	21	114.05	113.06	114.05	112.84	112.36	111.42
7	114.05	114.05	113.06	113.07	113.93	114.05	22	114.05	114.05	113.07	113.05	114.04	112.73
8	114.05	114.05	113.07	113.06	113.96	114.04	23	114.05	114.05	113.07	112.87	114.05	112.74
9	114.05	113.06	113.07	113.83	113.93	113.06	24	114.05	114.05	113.07	112.79	112.37	112.89
10	114.05	114.05	113.06	112.67	111.54	112.82	25	114.05	114.05	113.07	113.56	114.04	114.05
11	114.05	113.04	114.05	113.05	113.84	113.05	26	114.05	114.05	112.03	113.07	112.39	113.03
12	114.05	114.05	113.06	114.03	113.94	111.96	27	114.05	114.05	113.06	113.06	114.04	113.06
13	114.05	114.05	113.06	113.06	114.04	113.03	28	114.05	114.05	113.06	113.06	113.98	113.03
14	114.05	113.06	113.07	113.06	114.02	112.53	29	114.05	114.05	113.06	111.99	113.27	113.06
15	114.02	114.05	113.07	112.2	112.06	114.05	30	114.05	114.05	113.06	112.71	113.63	113.05

6c. The calculated and measured results closely matched. The plots in Fig. 6b and 6d represent the predictions in relation to the 100 percent precision line across the training and testing durations.

Table 3 shows the validation results of the constructed ANFIS models. As shown in Table 3, the ANFIS model lowered the total difference from 4.1 (based on ANOVA results) to 3.88, achieving a reduction of 5.37 %.

After validating the constructed model, the next step is to ascertain the ideal values for chitosan dosage, pH, and settling time to improve the effectiveness of turbidity and salinity removal. Consequently, after obtaining consistent ANFIS models of turbidity removal and salinity removal, WSO is employed to define optimal values of the inputs. During the optimization process, the parameters that control the system, including pH, chitosan dosage, and settling time, are utilized as design variables. The aim is to maximize the objective function, defined as the sum of turbidity removal and salinity removal. The optimzation argument is formulated using Eq. 13.

$$x = \underset{x \in R}{\arg\max} \left(y1 + y2 \right) \tag{13}$$

Where, x denotes set of normalized inputs. $y1$ and $y2$ are the percentage of the turbidity removal and salinity removal respectively.

The optimal values and the percentages for turbidity and salinity removal are illustrated in Table 4, utilizing data from the experimental method, RSM approach, and WSO. Integrating ANFIS and WSO increased the total performance index (TPI) by 6.55% and 4.6% compared measured data and ANOVA. In this scenario, the turbidity removal efficiency rose from 85.66% (based on experimental data) to 93.48% by utilizing the proposed methodology, achieving an increase of roughly 7.82%. Fig. 6 displays the particles motion throughout optimization. As presented in Fig. 6a, the highest TPI of 114.1 % is obtained at iteration no. 40. The respective optimal values of 0.25, 1.0, and 0.4255 correspond to the normalized dosage of chitosan, the normalized pH level, and the normalized settling time.

To validate the suppository of WSO, an evaluation with slime mould algorithm (SMA) (Li *et al.,* 2020), particle swarm optimization (PSO), Jelly fish (JS) (Chou and Truong, 2021), Harris hawks optimization (HHO) (Heidari *et al*., 2019), and elite evolutionary strategy Harris hawks optimization (EESHHO) (Li *et al*., 2021) was carried out. In order to eliminate arbitrary results, the algorithms are processed 30 times, followed by a thorough numerical analysis. Table 5 and Fig. 7 show the results of 30 runs. The estimates and presentation of various statistical indicators, including the maximum and minimum values, average, median, variance, and standard deviation, can be found in Table 6. The standard deviation of cost function values (TPI) varies from 114.045 to 112.976. The greatest average score of 114.045 is reached by SWO, followed by PSO (113.781), and the lowest average value of 112.976 by HHO. STD scores vary from 0.004 to 1.619. SWO has the highest score for STD at 0.004, then comes the SMA at 0.423, while HHO has the most severe STD at 1.619. This validates the effectiveness of WSO in pinpointing the ideal values associated with maximum TPI.

Additional tests including ANOVA and Tukey also performed. Table 7 displays the ANOVA results, whereas Fig. 8 depicts the ranking, supporting WSO's remarkable performance. It illustrates remarkable average fitness and considerable differences, reinforcing its status as the leading performer.

The findings from the Tukey test, illustrated in Fig. 9, confirm the outcomes derived from ANOVA. Specifically, the average outcomes generated by PSO, JS, HHO, and ESSHHO were significantly lower

Table 6: Statistical assessment of optimizers under examination

Metric	WSO	SMA	PSO	JS	HHO	EESHHO
Best	114.046	114.046	114.046	114.032	114.046	114.046
Worst	114.022	113.043	112.031	111.96	107.11	111.422
Mean	114.045	113.781	113.194	113.004	112.976	113.058
Median	0	0.192	0.179	0.292	2.622	0.31
Variance	114.046	114.046	113.065	113.053	113.915	113.038
SD	0.004	0.439	0.423	0.541	1.619	0.557

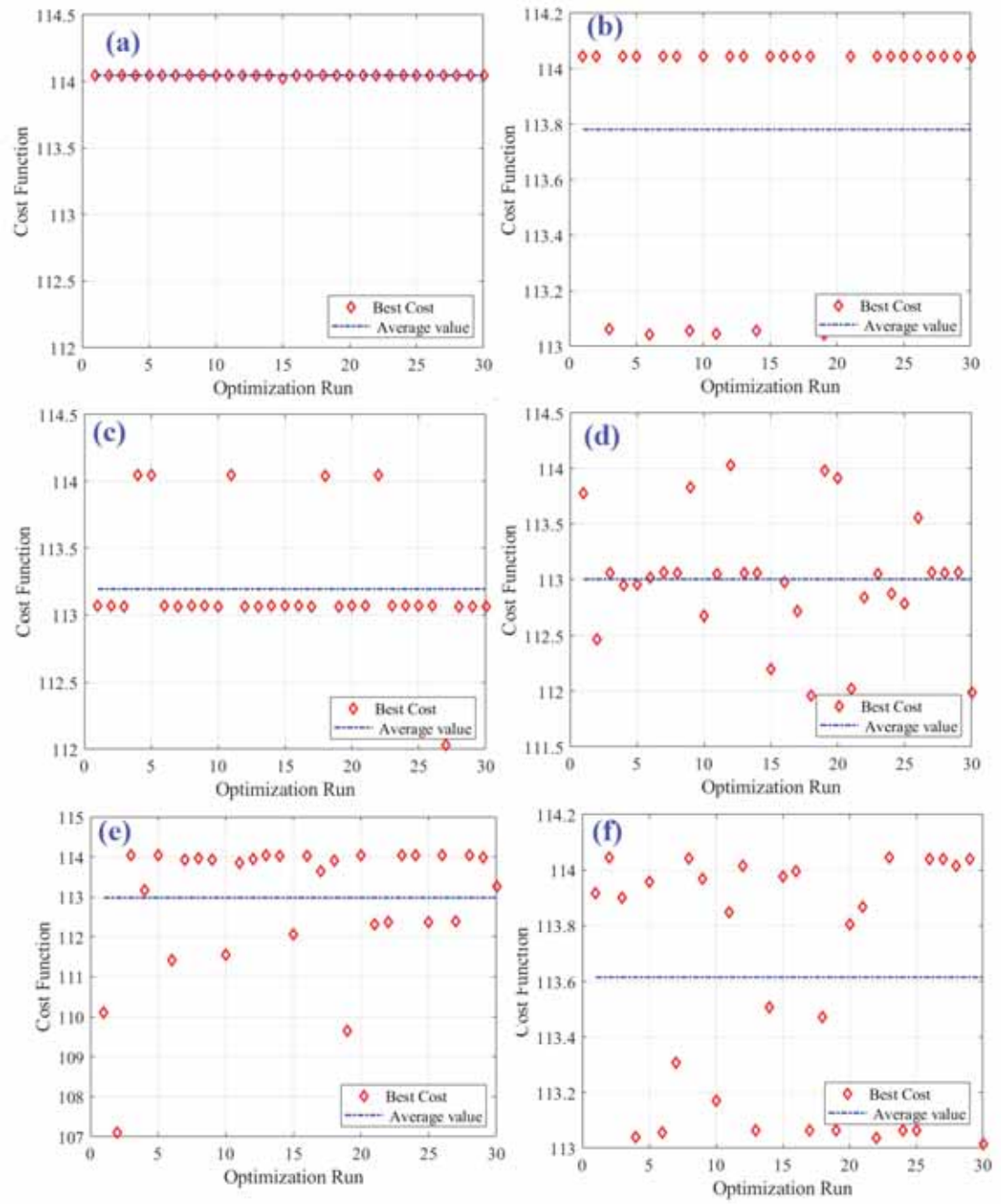

Fig. 7: Characteristics for 30 runs include, [a] WSO, [b] SMA, [c] PSO, [d] JS, [e] HHO and [f] FBI

Table 7: ANOVA statistical metrics

Source	df	SS	MS	F	Prob
Columns	5	31.125	6.225	10.04	1.856e-08
Error	174	107.892	0.620		
Total	179	139.017			

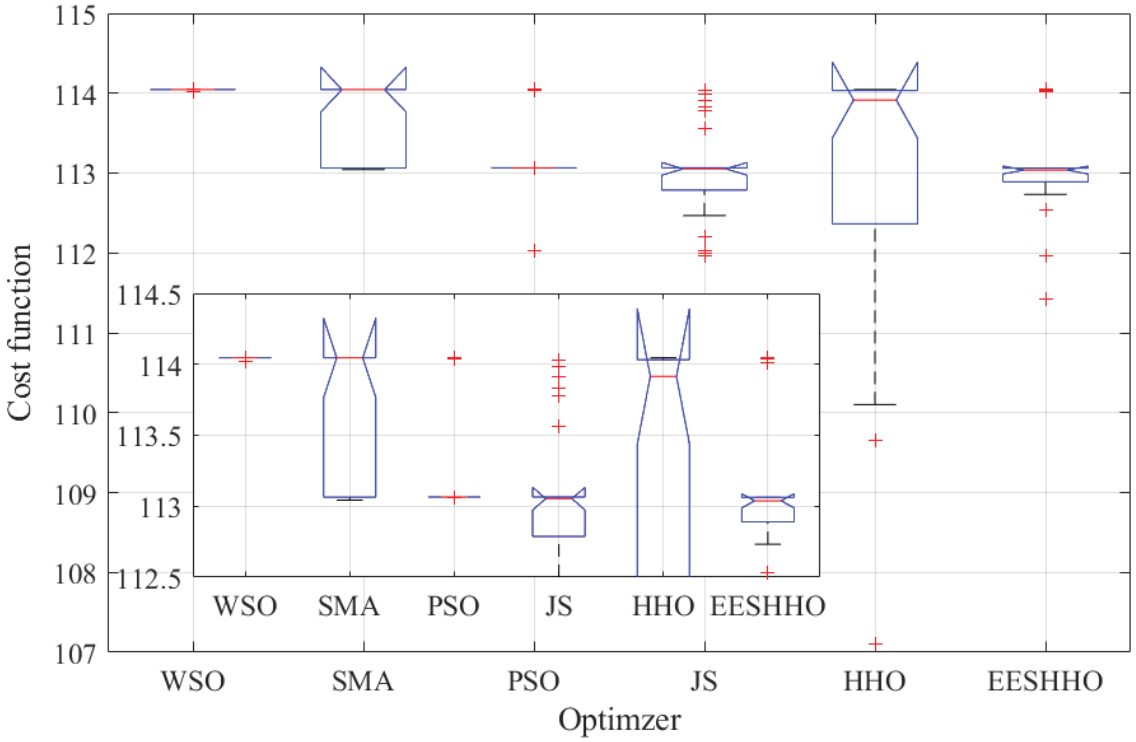

Fig. 8: ANOVA ranking

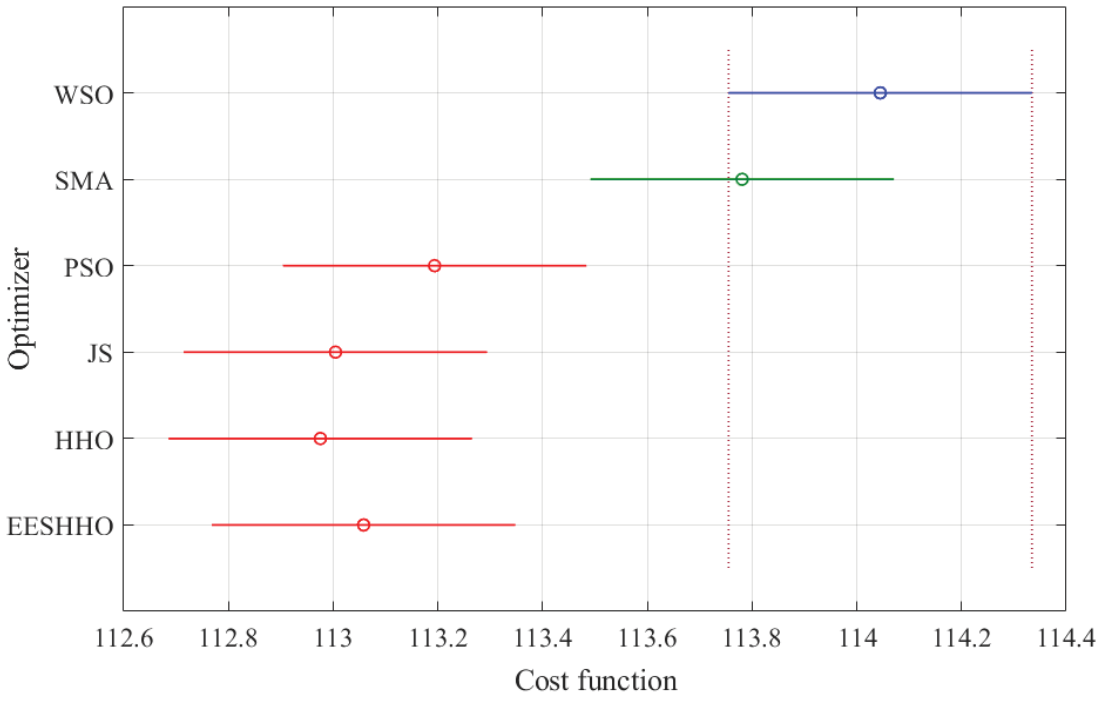

Fig. 9: Tukey test

than those achieved by WSO, with SMA delivering the second-best performance after the WSO.

CONCLUSION

This study aims to achieve its objectives by combining artificial intelligence with contemporary optimization algorithms. Initially, an ANFIS model of the wastewater treatment process was built based on experimental data. The White Shark Optimizer (WSO) is then used to calculate the optimal chitosan dose, pH, and settling time for reducing turbidity and salinity. The main aim of this study is to design a credible ANFIS model that can accurately represent the removal of turbidity and salinity from effluent generated by shrimp farming. Three process parameters are used to increase turbidity and salinity removal: chitosan dose, pH, and settling time. The initial step involved constructing an ANFIS model of the wastewater treatment process, relying on experimental data. To enhance turbidity and salinity, the White Shark Optimizer (WSO) is employed to ascertain the best chitosan dosage, pH, and settling duration. The ANFIS framework for turbidity removal has RMSE metrics of 3.5211e-05 and 1.5069 for training and testing data, respectively. Training and testing had R-squared levels of 1.0 and 0.76, respectively. ANFIS reduced the RMSE from 2.8 via ANOVA to 0.836 with ANFIS (a 70% reduction). There was an 11.76% increase in the R-squared value for predictions, moving from 0.68 with ANOVA to 0.76 with ANFIS. The ANFIS model for salinity reduction achieved RMSE scores of 7.1309e-06 for the training set and 2.0453 for the testing set. The R-squared values for training and testing are 1.0 and 0.82, respectively. When in comparison with ANOVA, ANFIS lowered the RMSE from 6.8 to 1.1345 (an 83.5% reduction). The R-squared value for prediction rose 7.2% from 0.765 using ANOVA to 0.82 using ANFIS. In conclusion, the ANFIS machine learning model's lower RMSE and high coefficient-of-determination values indicate that the modeling phase has been successful. The analysis of measured data alongside ANOVA indicated that the integration of ANFIS and WSO enhanced the total performance index (TPI) by 6.55% and 4.6%, respectively. To confirm the effectiveness of the WSO method, it was compared with SMA, PSO, JS, HHO, and EESHHO. The average cost function value ranges from 114.045% to 112.976 percent. SWO possesses the highest average value (114.045), which is followed by PSO (113.781%), and HHO has the lowest average value (112.976%). The STD results vary from 0.004 to 1.619, with SWO getting the highest value at 0.004, SMA at 0.423, and HHO with the worst at 1.619, proving SWO's supremacy in determining the ideal parameters for greatest performance. To summarize, modern optimization algorithms combined with artificial intelligence can substantially enhance wastewater treatment processes by decreasing energy requirements, forecasting the most effective treatment strategies, and improving system performance. WOS can be refined for wastewater treatment by integrating it with other optimizers to enhance convergence speed and solution precision. By integrating the exploration strengths of WSO with algorithms that prioritize exploitation, hybrid methods can more effectively address the intricate and multi-faceted issues associated with wastewater treatment. Future research can improve ANFIS and white shark optimization in wastewater treatment by enhancing scalability, enabling real-time implementation, and integrating them with other treatment technologies. This leads to optimizing treatment efficiency and decreasing costs

AUTHOR CONTRIBUTIONS

H. Rezk, as the corresponding author, has contributed the research proposal making, built the simulation model, and writing the manuscript, A.F. Mohamed participated in the preparation of manuscript, performed results analysis, and optimization process using MHs.

ACKNOWLEDGEMENT AND FUNDING

The authors extended their appreciation to Umm Al-Qura University for funding this research work through the project number [25UQU 4290444GSSR04NI].

CONFLICT OF INTEREST

The authors declare that there are no conflict of interest regarding the publication of this manuscript. In addition, the ethical issues, including plagiarism, informed consent, misconduct, data fabrication and/or falsification, double publication and/or submission, and redundancy, were observed by the authors.

OPEN ACCESS

©2025 The author(s). This article is licensed under a Creative Commons Attribution 4.0 International License, which permits use, sharing, adaptation, distribution and reproduction in any medium or format, as long as you give appropriate credit to the original author(s) and the source, provide a link to the Creative Commons license, and indicate if changes were made. The images or other third-party material in this article are included in the article's Creative Commons license, unless indicated otherwise in a credit line to the material. If material is not included in the article's Creative Commons license and your intended use is not permitted by statutory regulation or exceeds the permitted use, you will need to obtain permission directly from the copyright holder. To view a copy of this license, visit: http://creativecommons.org/licenses/by/4.0/

PUBLISHER'S NOTE

GJESM Publisher remains neutral with regard to jurisdictional claims with regard to published maps and institutional affiliations.

Positive AI Statement

During the preparation of this work the author(s) have used [NAME TOOL / SERVICE] in order to [REASON]. After using this tool/service, the authors reviewed and edited the content as needed and take full responsibility for the content of the publication. Furthermore, the GPTZero detector will evaluate the manuscript utilizing Generative AI, ensuring a high detection rate. If the manuscript relies heavily on Generative AI and AI-assisted technologies, it will be archived without further options for appeal.

Negative AI Statement

The author(s) declare that no AI tools or services were not used or not highly applied during the preparation of this work.

ABBREVIATIONS

%	Percent
a	A single-dimensional binary vectors
a_0	Constant
ANOVA	Analysis of variance
AI	Artificial intelligence
ANFIS	Adaptive neuro-fuzzy inference system
b	*A* single-dimensional binary vectors
c_i	Constant
EESHHO	Elite evolutionary strategy Harris hawks optimization
D	Distance
HHO	Harris hawks optimization
GMF	Gaussian membership function
JS	Jelly fish
LSE	Least square error
MFs	Membership functions
P	Current location
P_{best}	Current best-accomplished location
P_{gbest}	Global best location
P_0	Logical vector
ρ_{max}	Subordinate velocity
ρ_{min}	Intial velocity
$P_i(t+1)$	New position
PI	Proportional-integral
pH	Potential of hydrogen
PSO	Particle swarm optimization
RMSE	Root mean square error
SC	Subtractive clustering
SMA	Slime mould algorithm
t	Current iteration
TPI	Total performance index
t^{max}	Maxumum number of iterations
UAV	Unmanned Aerial Vehicle
X_i	fuzzy set associated with premise input variables
ωi	Firing strength
WSO	White shark optimizer
y_1	Percentage of the turbidity removal
y_2	Percentage of salinity removal
Y_i	Fuzzy set associated with premise input variables
α	Input variable

β	Input variable
$\mu_{X_i}(\alpha)$	Degrees of membership for α
$\mu_{Y_i}(\beta)$	Degrees of membership for β
τ	Acceleration coefficient

REFERENCES

Abu-Dalo, M.; Abdelnabi, J.; Al-Rawashdeh, N.A.; Albiss, B.; Al Bawab, A., (2022). Coupling coagulation-flocculation to volcanic tuff-magnetite nanoparticles adsorption for olive mill wastewater treatment. Environ. Nanotechnol. Monit. Manage., 17: 100626 **(26 pages).**

Aghdam, E.; Mohandes, S.R.; Manu, P., Cheung, C.; Yunusa-Kaltungo, A.; Zayed, T., (2023). Predicting quality parameters of wastewater treatment plants using artificial intelligence techniques. J. Cleaner Prod., 405: 137019 **(12 pages).**

Ahmadianfar, I.; Shirvani-Hosseini, S.; He, J.; Samadi-Koucheksaraee, A.; Yaseen, Z.M., (2022). An improved adaptive neuro fuzzy inference system model using conjoined metaheuristic algorithms for electrical conductivity prediction. Sci. Rep., 12(1); 4934 **(34 pages).**

Alhumade, H.; Rezk, H.; Louzazni, M.; Moujdin, I. A.; Al-Shahrani, S., (2023). Advanced energy management strategy of photovoltaic/PEMFC/lithium-ion batteries/supercapacitors hybrid renewable power system using white shark optimizer. Sensors. 23(3): 1534 **(17 pages).**

Alsaleh, M., (2024). The impact of aquaculture economics expansion on marine water quality in the EU region. Reg. Stud. Mar. Sci., 77: 103625 **(13 pages).**

Altowayti, W.A.H., Shahir, S.; Othman, N.; Eisa, T.A.E.; Yafooz, W.M.; Al-Dhaqm, A., Soon, C.Y.; Ali, A., (2022). The role of conventional methods and artificial intelligence in the wastewater treatment: a comprehensive review. Processes. 10(9): 1832 **(31 pages).**

Barros, A.; Vecino, X.; Reig, M.; Cortina, J.L., (2022). Coagulation and flocculation optimization process applied to the sidestream of an urban wastewater treatment plant. Water. 14(24): 4024 **(26 pages).**

Braik, M.; Hammouri, A.; Atwan, J.; Al-Betar, M.A.; Awadallah, M.A., (2022). White Shark Optimizer: A novel bio-inspired meta-heuristic algorithm for global optimization problems. Knowledge-Based Syst. 243: 108457 **(29 pages).**

Buriboev, A.; Muminov, A., (2022). Computer State Evaluation Using Adaptive Neuro-Fuzzy Inference Systems. Sensors. 22(23): 9502 **(20 pages).**

Chou, J.S.; Truong, D.N., (2021). A novel metaheuristic optimizer inspired by behavior of jellyfish in ocean. Commun. Appl Math. Comput. 389: 125535 **(47 pages)**

Elsayed, A.; Siam, A.; El-Dakhakhni, W., (2022). Machine learning classification algorithms for inadequate wastewater treatment risk mitigation. Process Safety Environ. Protect. 159: 1224-1235 **(11 pages).**

Fathy, A.; Alanazi, A., (2023). An efficient white shark optimizer for enhancing the performance of proton exchange membrane fuel cells. Sustainability. 15(15): 11741 **(21 pages).**

Heidari, A.A.; Mirjalili, S.; Faris, H.; Aljarah, I.; Mafarja, M.; Chen, H., (2019). Harris hawks optimization: Algorithm and applications. Future Gener. Comput. Syst., 97: 849-872 **(24 pages).**

Kassem, Y.; Çamur, H.; Esenel, E., (2017). Adaptive neuro-fuzzy inference system (ANFIS) and response surface methodology (RSM) prediction of biodiesel dynamic viscosity at 313 K. Procedia Comput. Sci., 120: 521-528 **(8 pages).**

Kridakorn Na Ayutthaya, T.; Jakrawatana, N.; Rinchumphu, D.; Owatsakul, V., (2024). Application of artificial neural networks for predictive model of municipal solid waste collection in tourist cities. Global J. Environ. Sci. Manage., 10(4): 1859-1876 **(18 pages).**

Kurniawan, S.B.; Imron, M.F.; Abdullah, S.R.S.; Othman, A.R; Hasan, H.A., (2023). Coagulation–flocculation of aquaculture effluent using biobased flocculant: From artificial to real wastewater optimization by response surface methodology. J. Water Process Eng. 53: 103869 **(20 pages).**

Iber, B.T.; Torsabo, D.; Chik, C.E.N.C.E.; Wahab, F.; Sheikh Abdullah, S.R.; Abu Hassan, H.; Kasan, N.A., (2023). Response surface methodology (RSM) approach to optimization of coagulation-flocculation of aquaculture wastewater treatment using chitosan from carapace of giant freshwater prawn Macrobrachium rosenbergii. Polymers. 15(4): 1058 **(23 pages).**

Lepe-Silva, F.; Crawford, B.; Cisternas-Caneo, F.; Barrera-Garcia, J.; Soto, R., (2024). A Binary Chaotic White Shark Optimizer. Math., 12(20): 3171 **(35 pages).**

Li, C., Li, J.; Chen, H.; Heidari, A.A., (2021). Memetic Harris Hawks Optimization: Developments and perspectives on project scheduling and QoS-aware web service composition. Expert Syst. Appl., 171: 114529 **(18 pages).**

Li, S.; Chen, H.; Wang, M.; Heidari, A. A.; Mirjalili, S., (2020). Slime mould algorithm: A new method for stochastic optimization. Future Gener. Comput. Syst., 111: 300-323 **(23 pages).**

Nadana Ravishankar, T.; Ramprasath, M.; Daniel, A.; Selvarajan, S.; Subbiah, P.; Balusamy, B., (2023). White shark optimizer with optimal deep learning based effective unmanned aerial vehicles communication and scene classification. Sci. Rep., 13(1): 23041 **(18 pages).**

Nassar, S. M.; Saleh, A.A.; Eisa, A.A.; Abdallah, E.M.; Nassar, I.A., (2025). Optimal Allocation of Renewable Energy Resources in Distribution Systems using Meta-Heuristic Algorithms. Results Eng. 104276 **(16 pages).**

Oyediran, M.O.; Ajagbe, S.A.; Ojo, O.S.; Alshahrani, R.; Awodoye, O.O., Adigun, M.O., (2025). White shark optimizer via support vector machine for video-based gender classification system. Multimedia Tools Appl., 1-17 **(17 pages)**.

Rahman, M.S.; Ali, M.H., (2025). Adaptive Neuro Fuzzy Inference System (ANFIS)-Based Control for Solving the Misalignment Problem in Vehicle-to-Vehicle Dynamic Wireless Charging Systems. Electron., 14(3): 507 **(22 pages).**

Sada, S.O.; Ikpeseni, S.C., (2021). Evaluation of ANN and ANFIS modeling ability in the prediction of AISI 1050 steel machining performance. Heliyon. 7(2) **(9 pages).**

Safeer, S.; Pandey, R.P.,;Rehman, B., Safdar, T.; Ahmad, I.; Hasan,

S.W.; Ullah, A., (2022). A review of artificial intelligence in water purification and wastewater treatment: Recent advancements. J. Water Process Eng. 49: 102974 **(18 pages).**

Salles, R.; Mendes, J.; Antunes, C.H.; Moura, P.; Dias, J., (2022). Dynamic Setpoint optimization using metaheuristic algorithms for wastewater treatment plants. In IECON 2022–48th Annual Conference of the IEEE Industrial Electronics Society. 1-6 **(6 pages).**

Silva, J.A., (2023). Wastewater treatment and reuse for sustainable water resources management: a systematic literature review. Sustainability. 15(14): 10940 **(31 pages).**

Singh, N.K.; Yadav, M.; Singh, V.; Padhiyar, H.; Kumar, V., Bhatia; S.K.; Show, P.L., (2023). Artificial intelligence and machine learning-based monitoring and design of biological wastewater treatment systems. Bioresour. Technol. 369: 128486 **(8 pages).**

Zaki, N.; Hadoudi, N.; Charki, A.; Bensitel, N.; Ouarghi, H. E.; Amhamdi, H.; Ahari, M.H., (2023). Advancements in the chemical treatment of potable water and industrial wastewater using the coagulation–flocculation process. Sep. Sci. Technol. 58(15-16): 2619-2630 **(11 pages).**

Zanganeh, M., (2020). Improvement of the ANFIS-based wave predictor models by the particle swarm optimization. J. Ocean. Eng. Sci., 5(1): 84-99 **(15 pages).**

Zhang, Y.; Li, M.; Zhang, G.; Liu, W.; Xu, J.; Tian, Y.; Xie, X., (2023a). Efficient treatment of the starch wastewater by enhanced flocculation–coagulation of environmentally benign materials. Sep. Purif. Technol. 307: 122788 **(12 pages).**

Zhang, S.; Jin, Y.; Chen, W.; Wang, J.; Wang, Y.; Ren, H., (2023b). Artificial intelligence in wastewater treatment: A data-driven analysis of status and trends. Chemosphere. 336: 139163 **(8 pages).**

AUTHOR (S) BIOSKETCHES

Mohamed , A.F., Ph.D., Associate Professor, Industrial Engineering Department, College of Engineering and Architecture, Umm Al-Qura University , Saudi Arabia.
- Email: *afmohamed@uqu.edu.sa*
- ORCID: 0000-0003-3559-9650
- Web of Science ResearcherID: KPB-0491-2024
- Scopus Author ID: 56785001200
- Homepage: https://scholar.google.co.uk/citations?user=Bg6Et_0AAAAJ&hl=el

Rezk, H., Ph.D., Associate Professor, Department of Electrical Engineering, College of Engineering in Wadi Alddawasir, Prince Sattam bin Abdulaziz University, Wadi Alddawasir, Saudi Arabia.
- Email: *hr.hussien@psau.edu.sa*
- ORCID: 0000-0001-9254-2744
- Web of Science ResearchrID: M-2100-2019
- Scopus Author ID: 55425573200
- Homepage: https://scholar.google.com.eg/citations?user=R0pThmwAAAAJ&hl=en

HOW TO CITE THIS ARTICLE

Mohamed, A.F.; Rezk, H., (2025). Neuro-fuzzy inference system and white shark optimization of coagulation-flocculation of quaculture wastewater treatment. Global J. Environ. Sci. Manage., 11(3): 857-874.

DOI: 10.22034/gjesm.2025.03.01

URL: https://www.gjesm.net/article_722377.html

Global J. Environ. Sci. Manage. 11(3): 875-896, Summer 2025, Serial #43

Global Journal of Environmental Science and Management
(GJESM)

Homepage: https://www.gjesm.net/

Podcasts

ORIGINAL RESEARCH PAPER

A spatial slip plane-based vegetation model for slope reinforcement and shallow landslide mitigation

I.G. Tejakusuma[1,*], E.H .Sittadewi[1], A. Mulyono[2], T. Handayani[3], A. Tohari[1], H.E.H. Fatahillah[4], Z. Zakaria[5], E.B. Budiman[4], N. Utami[3]

[1] *Research Center for Geological Disaster, National Research and Innovation Agency, Indonesia*

[2] *Research Centre for Environmental and Clean Technology, National Research and Innovation Agency, Indonesia*

[3] *Research Centre for Sustainable Production System and Life Cycle Assessment, National Research and Innovation Agency, Indonesia*

[4] *Research Center for Mining Technology, National Research and Innovation Agency, Indonesia*

[5] *Faculty of Geological Engineering, Universitas Padjadjaran, Indonesia*

ARTICLE INFO

Article History:
Received 24 December 2024
Revised 28 February 2025
Accepted 03 April 2025

Keywords:
Hydromechanical stabilization
Landslide-prone areas
Permeability contrast
Slip plane distribution
Subsurface characterization

ABSTRACT

BACKGROUND AND OBJECTIVES: Vegetation is essential for reducing shallow landslides by providing hydromechanical stability. However, effective slope stabilization requires understanding the spatial distribution of slip planes, a crucial aspect that remains underexplored in landslide mitigation studies. This study sought to establish a new vegetation intervention model that merges the hydromechanical properties of plants with the arrangement of slip planes, with the goal of strengthening slopes and decreasing the likelihood of landslides.

METHODS: Geological field investigations, electrical resistivity tomography, light detection and ranging drone surveys, geomorphological analysis, three-dimensional terrain modelling, and isopach map development combine vegetation's hydromechanical effects. Field observations and interviews were utilized to perform a vegetation inventory, aimed at assessing the conditions prior to and following the landslide. The landslide risks map was created by combining slope and lithology thickness above the slip plane using reclassification and weighting analyses. Based on this map and the hydromechanical characteristics of chosen plant species, vegetation interventions were subsequently developed.

FINDINGS: The landslide area comprises brown breccia with moderate permeability and grey marl with low permeability, exceeding 40 meters in thickness. The slip plane aligns with the breccia-marl interface and follows the slope's dip, resulting in a heightened risk of landslides. Slip plane depth varies with breccia thickness (0.5–4.5 meters). Prior to the landslide, the area was characterized by vegetation mainly composed of garden plants, bamboo, and selectively harvested woody species, which had a limited impact on slope stabilization. The depletion and transition areas are divided into high, medium, and low landslide risk zones based on slopes and breccia thickness. Plants were selected based on root depth, evapotranspiration capacity, and canopy density properties.

CONCLUSION: In high-risk zones (breccia 3–4.5 meters, slopes >30 degrees), deep-rooted trees of >4.5 meters, fast-growing tree species with high evapotranspiration, and dense canopies such as *Paraserianthes falcataria*, Eucalyptus sp., and Acacia mangium, are recommended, with wider spacing to prevent additional loading. *Bambussa* sp. is also suitable due to its fibrous roots and high water absorption. Medium-risk zones (breccia 1–3 meters, slopes 10–30 degrees) benefit from species with >3 meters' root depths, including *Leucaena leucocephala*, *Artocarpus heterophyllus*, *Gmelina arborea*, *Mangifera indica*, *Swietenia sp.*, *Bambussa sp.*, and *Chrysopogon zizanoides*. Low-risk zones (breccia <1 meter, slopes <10 degrees) can support shallow-rooted, economically valuable crops such as *Cocos nucifera*, *Musa paradisiaca*, *Zea mays*, *Vigna unguiculata*, *Manihot esculenta*, *Capsicum annuum* and *Solanum lycopersicum*. Cover crops can be integrated across all zones for stability and erosion control. This vegetation-focused strategy serves as a model for reinforcing slopes and mitigating shallow landslides effectively.

DOI: 10.22034/gjesm.2025.03.02

This is an open access article under the CC BY license (http://creativecommons.org/licenses/by/4.0/).

NUMBER OF REFERENCES
107

NUMBER OF FIGURES
6

NUMBER OF TABLES
6

*Corresponding Author:
Email: ***
Phone: ***
ORCID: ***

Note: Discussion period for this manuscript open until Sep 1, 2025 on GJESM website at the "Show Article".

INTRODUCTION

The presence of vegetation is vital for mitigating landslide risks, as it helps to stabilize soil, decrease surface runoff, and improve slope stability through its hydromechanical influence. The ability of vegetation to reinforce slopes has been studied previously by Fernandes and Guiomar (2016); Kim *et al.* (2017); Perez (2017); Dinorah (2017); Patil *et al.* (2021); Li (2021), and Stokes and Yildiz (2023). Research has been conducted on the hydromechanical functions of vegetation, as demonstrated by the works of Mulyono *et al.* (2018); Fata *et al.* (2021); and Netto *et al.* (2024). The presence of vegetation is critical in minimizing landslide threats by reinforcing soil stability (Phewnil *et al.,* 2024). It effectively stabilizes slopes through its ability to absorb, release, and evaporate water (Monteleone and Sabatino, 2014). Additionally, plant roots contribute to soil reinforcement (Zayadi *et al.*, 2022; Song *et al.*, 2024; Tejakusuma *et al.,* 2024). Emadi-Tafti (2021) explained that effective slope reinforcement occurs when tree roots penetrate and anchor into the landslide slip plane. The advancement of vegetation-based slope stabilization has transitioned from straightforward bioengineering methods to more complex models that utilize hydromechanical enhancements, merging plant growth with soil behaviour and hydrological processes (Gong *et al.*, 2024). Sittadewi *et al.* (2024) stated that implementing an agroforestry system with deep penetrating root trees and multi-season crops on slide-prone slopes can strengthen soil structure, facilitate water retention, and reduce erosion, thereby enhancing slope stability and minimizing landslide risks. By incorporating recent studies on root-soil interactions, choosing suitable plant species, and applying hydrological modeling, the slope reinforcement model can be adapted to meet diverse geological, climatic, and socio-economic conditions (DiBiagio *et al.*, 2024). This advanced knowledge not only improves the effectiveness of vegetation-based stabilization but also aids in creating more sustainable, cost-efficient, and eco-friendly landslide mitigation strategies globally (Niyomukiza *et al.*, 2023). Optimal slope reinforcement occurs when the vegetation on the slope possesses tree and root traits that correspond with the depth conditions of the slip plane. A canopy formed by above-ground vegetation diminishes the kinetic energy of raindrops, leading to improved infiltration into the ground. Root systems bind soil layers and increase soil cohesion. Both above-ground and below-ground plant indicators were crucial for improving slope stability (Lann *et al.*, 2024). Slope reinforcement using vegetation is particularly effective in preventing shallow landslides. The presence of appropriate vegetation on the ground can yield effective hydromechanical effects, which contribute to minimizing the risk of slope failure and ensuring long-term stability of slopes. Besides the vegetation, another very important factor is the spatial distribution of landslide slip plane depth, which is, in other words, soil depth. Soil and rock conditions, as do the soil depths, vary across different locations. Bruijnzeel (2004) indicates that roots are crucial in managing shallow landslides of <3 meters (m) depth, whereas geological and climatic conditions have a greater impact on deeper landslides. These differences affect slope stability about vegetation. Stabilization effects are most pronounced when soil depths are up to 3 m and decrease for depths exceeding 3 m. As depth increases, the slip plane shifts beyond the zone accessible to root growth, which diminishes the effectiveness of soil reinforcement. Deep-rooted plants are necessary to stabilise soil layers thicker than 3 m. Consequently, successful landslide hazard mitigation hinges on a thorough understanding of the spatial depth conditions of the slip plane. This knowledge is vital for identifying the most suitable vegetation to be cultivated in such environments. However, there is a notable absence in the existing literature regarding this topic, as it has not been sufficiently examined or considered in the slope reinforcement efforts. Previously, the relationship between the depth of the spatial slip plane and the hydromechanical characteristics of vegetation has not been examined. This study reviews gaps in knowledge on slip plane distribution and vegetation's role in landslide mitigation, highlighting limited research on slip plane distribution and its integration with hydrological and vegetation factors. It lays the foundation for new insights into how vegetation dynamics affect slope stability and offers a novel contribution to landslide research. The uniqueness of the current study is found in its integration of the hydromechanical properties of vegetation with the distribution of slip planes, a critical area that has been largely overlooked in prior studies. Its methodological innovation combines field data, geological

modelling, risk-zone development, and species-specific considerations, offering a comprehensive understanding of vegetation's influence on slip plane migration and reactivation. Although integrating vegetation dynamics with slip plane data in slope stability models is still developing, models like Slope Stability Models (Murgia *et al*., 2022) and geographic information system (GIS)-based slip surface models (Schmaltz and Mergili, 2018) incorporate root system composition and density to assess slope stability. Nevertheless, the comprehensive integration of these elements is still restricted, underscoring the necessity for additional studies. This study seeks to establish a new model for vegetation intervention that merges the hydromechanical properties of plants with the arrangement of slip planes, with the goal of strengthening slopes and decreasing the likelihood of landslides. This study has been carried out in Banar area, Sukajaya District, Bogor Regency, West Java, Indonesia in 2025.

MATERIALS AND METHODS

Study area

The study area was one of many sites affected by the massive landslides triggered by a hefty rainfall that struck the Sukajaya region on January 1, 2020. The landslide in Banar has destroyed village residences and caused four fatalities. The geographical coordinates of the landslide site are south (S) 06 degrees (°) 36.329 minutes (') and east (E) 106°30.767'. It is accessible from Bogor City, located approximately 42 kilometers (km) to the west (Fig. 1).

Landslide Geology and Geomorphology

Landslide geology in the Banar was investigated through field surveys from the source to the toe of the landslide area. Observations featured rock exposures, the stratigraphic arrangement of lithology, and the depth of sediment layers. Grain size was analyzed using sieve analysis American society for testing and materials (ASTM) D6913/D6913M

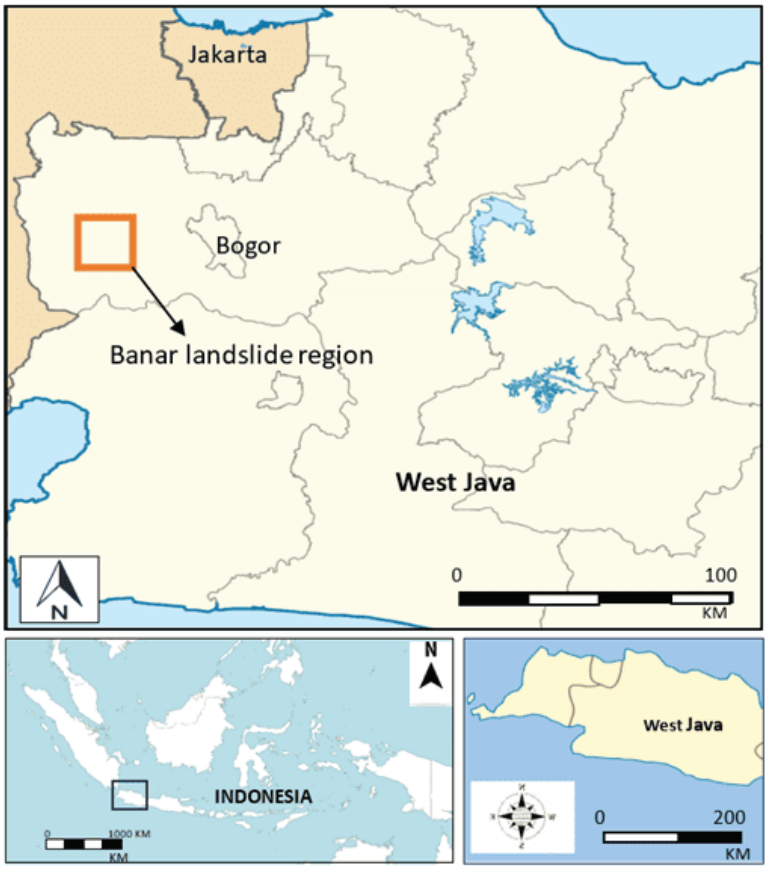

Fig. 1: Geographical location of the study area in Banar region, Sukajaya, West Java, Indonesia

and ASTM D7928, and permeability was estimated using Saxton and Rawls (2006). The depletion and transition zones, identified as areas at risk for future landslides, were analyzed comprehensively. In contrast, the accumulation zone, while relatively stable, could still accumulate debris from future incidents. Geological conditions were reconstructed to assess slope instability risks. A light detection and ranging (LiDAR) drone was used to penetrate dense vegetation, providing high-resolution topographic data for geomorphological analysis and three-dimensional (3D) terrain modelling.

Subsurface landslide characterization and 3D modelling

The electrical resistivity tomography (ERT) method mapped the slip plane in unstable depletion and transition zones. By employing cutting-edge inversion methods and 3D modeling, ERT effectively defined the rock formations and stratigraphic structures. Data were collected with an automatic resistivity system (ARES) and 48 electrodes across five survey lines: two north-south (5 m spacing), two east-west (3 m spacing), and one additional north-south (3 m spacing). Utilizing a dipole-dipole setup allowed for high-resolution imaging and the detection of lateral resistivity, which proved effective in identifying rock layers and slip planes (Falae *et al.*, 2019). Resistivity data were processed in Res2Dinv using smoothness-constrained least-squares inversion (Loke *et al.*, 2015). The processing encompassed LiDAR-derived topographic adjustments at a resolution of 0.1 m/pixel, applied smoothness constraints to decrease noise levels, and employed half-unit electrode spacing to improve subsurface detail (Loke, 2025). Two-dimensional (2D) resistivity models were interpolated into 3D for spatial continuity (Mostafaei and Ramazi, 2018; Salarian *et al.*, 2020). The upper boundary aligned with LiDAR digital elevation model (DEM) data, while lithological interpretations from 2D models and field observations constrained lithology thickness above the slip plane, the final 3D model and isopach map aid hydromechanical analysis and landslide mitigation.

Vegetation identification and intervention model

Field observations and detailed descriptions of plant life were utilized to perform a vegetation inventory at the landslide site. Interviews were conducted with local residents affected by the landslide to assess vegetation conditions prior to the landslide. The proper planting of vegetation, tailored to its distinct hydromechanical properties, enhances slope stability by leveraging the hydromechanical effects of the plants. The slope intervention model using vegetation was developed by selecting plant species based on the thickness of the layer above the slip surface and-the slope gradient. To assist in formulating the plant intervention plan, the spatial thickness distribution of the lithology located above the slip plane was created. The plant selection prioritized fast-growing species, native to the local area, with appropriate root depth, evapotranspiration (ET) capacity and canopy. Field observations and relevant literature provided data regarding plant evapotranspiration, root structures, and canopy information.

RESULTS AND DISCUSSION

Landslide geomorphology and geology

The geomorphology of the landslide area in Banar illustrates the landslide pathway from the depletion zone to the transition zone and then to the landslide toe in the accumulation zone, as seen in Fig. 2. Data collected from the LiDAR drone survey significantly enhanced the analysis of landslide geomorphology (Fig. 2). In the depletion zone, a typical horseshoe-shaped of the landslide head scarp, near-vertical slope (Fig. 2, 3A and Fig. 4-Line 3) can be observed with the rock outcropped on the wall side of the scarp (Fig. 3A). The landslide's geomorphology is defined by distinct variations in slope. In the depletion zone, the slopes are steep, exceeding 30°, which places it in the high-risk classification. The transition zone consists of moderate slopes ranging from 10° to 30°, categorized as moderate risk. In contrast, the accumulation zone has gentle slopes between 0° and 10°. The prominent horseshoe-shaped structure seen in the landslide (Fig. 3) serves as evidence of previous landslide activity. The landslide follows a N 95° E trajectory in the depletion and transition zones, curving to N 135° E in the accumulation zone. The orientation of the slopes runs from west to east-southeast, which aligns with the trajectory of the landslide. This suggests a hydrogeological context in which groundwater flow is likely moving towards the east-southeast. The landslide movement demonstrates a sliding process initiated by debris slide within the depletion zone. It transforms into slide-flow or hyper concentrated flow

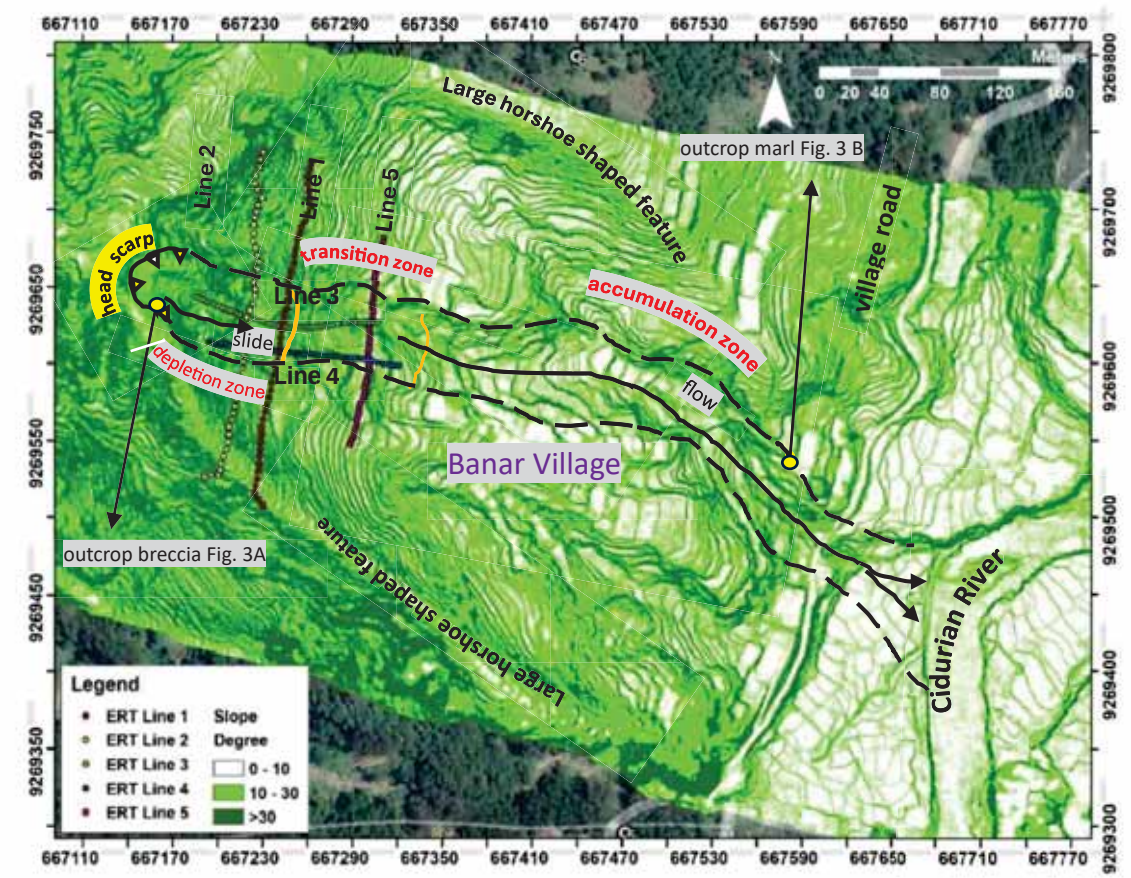

Fig. 2: Geomorphology and slope characteristics of the Banar landslide area derived from the LiDAR drone, highlighting a steep slope in the depletion zone, a moderate slope in the transition zone, and a gentle slope in the accumulation zone. A sizeable horseshoe-shaped feature is visible

within the transition zone, and finally transforms into lower sediment concentration flow within the accumulation zone. The total distance of the landslide's movement measures approximately 563 m, with widths ranging from 51 meters to 22 m along its path (Fig. 2). Based on field observations, the geology of the Banar landslide consists of breccia from the surface to the exposed depth of approximately 2.5 m in the landslide depletion zone (Figs. 2 and 3) and thinning downslope to about 0.5 m in the accumulation zone (Figs. 2 and 3). This breccia rock is characterized by its brown hue and loose, poorly sorted texture. It has an open fabric that includes subrounded to subangular pieces of andesite, tuff, and pumice, with sizes varying from 5 centimeters (cm) to 1 m, as well as a matrix containing silt, sand, and a small amount of clay.

A sandy tuff matrix with high permeability dominates the breccia in some places. The vertical profile of the outcrop exhibits a completely weathered dark brown to brownish black humus soil layer (soil horizon O) at the surface of approximately 45 cm thick, transitioning with gradationally contact to highly - moderately weathered brown breccia rock to a depth of around 2.5 m (Fig. 3). In various areas, a thin colluvial layer, roughly 0.3 m thick, can be found beneath the breccia, followed by a thick deposit of grey marl that has an exposed thickness of more than 1 m. The contact between breccia and marl exhibits an irregular unconformity (Fig. 3), indicating a distinct discontinuity between these rock layers. This irregular interface implies distinctions in the history of deposition, lithological composition, and structural processes that may influence slope stability and landslide susceptibility. The breccia exhibits greater thickness near the landslide depletion zone,

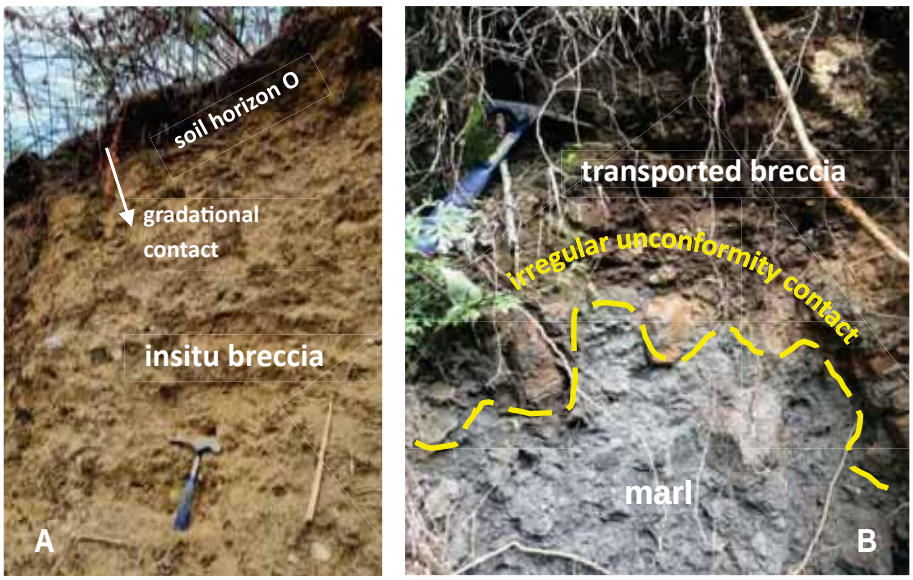

Fig. 3: Outcrop of breccia exposed in the depletion zone at the head scarp of the landslide (left, A), also showing the O soil horizon. Marl overlain by transported breccia on an irregular unconformity contact, exposed in the accumulation zone (right, B)

becoming progressively thinner as it extends toward the transition and accumulation zones along the landslide path. The grain size composition of breccia ranges from 20.53 percent (%) to 21.89% clay, 45.63% to 46.99% silt, and 31.12% to 33.04% sand, while that of marl ranges from 33.67% to 34.42% clay, 57.72% to 58% silt, and 7.86% to 8.63% sand. The estimated permeability of breccia ranges from 9.13 to 10.99 cm/day, while that of marl ranges from 0.269 to 0.368 cm/day. As noted by Weil and Brady (2017), breccia is characterized by moderate permeability, whereas marl displays low permeability. This observation implies that the upper layer of sediment has a higher permeability compared to the lower layer, which has lower permeability and could serve as a potential sliding plane. Local geology significantly influences landslides in the Banar area. The upper layer consists of moderately permeable breccia (up to 4.5 m thick), underlain by low-permeability marl (>40 m thick). The breccia-marl contact serves as the slip plane. The bedding's orientation follows the slope, which raises the likelihood of landslides. Investigations underscore the importance of geological structure and bedding alignment in the context of landslide events

LaHusen and Grant (2023) show that even slight increases in bedding dip raise the likelihood of cataclinal (parallel to bedding) landslides, which are often more severe than non-cataclinal ones. Vick *et al.* (2020) note that unstable rock masses tend to follow pre-existing structural discontinuities, such as foliation, joint planes, or faults. The limited thickness of the breccia layer highlights the essential function of vegetation in promoting slope stabilization. Consequently, choosing the right types of vegetation is vital for enhancing slope stability. Mapping breccia thickness, isopachs, and slip plane depth will guide vegetation-based slope interventions for enhanced stability. Slope gradient is a key factor in landslide mitigation through vegetation. Risk levels in the Banar landslide zone are determined by evaluating the steepness of the slopes and the thickness of the breccia. High-risk slopes (>30°) require deep-rooted trees for hydromechanical benefits and shrubs for surface protection. Strategic vegetation planning is crucial in areas like the head scarp, where slopes exceed 30°. Moderate-risk slopes (10°–30°) suit medium- to deep-rooted vegetation, while low-risk slopes (0°–10°) benefit from shallow-rooted plants or grasses for erosion control. Employing lighter plant biomass species on steep slopes prone to instability is recommended to mitigate risks. Wider tree spacing is recommended on steep slopes to reduce soil instability, while moderate-risk slopes can accommodate denser planting for better stabilization.

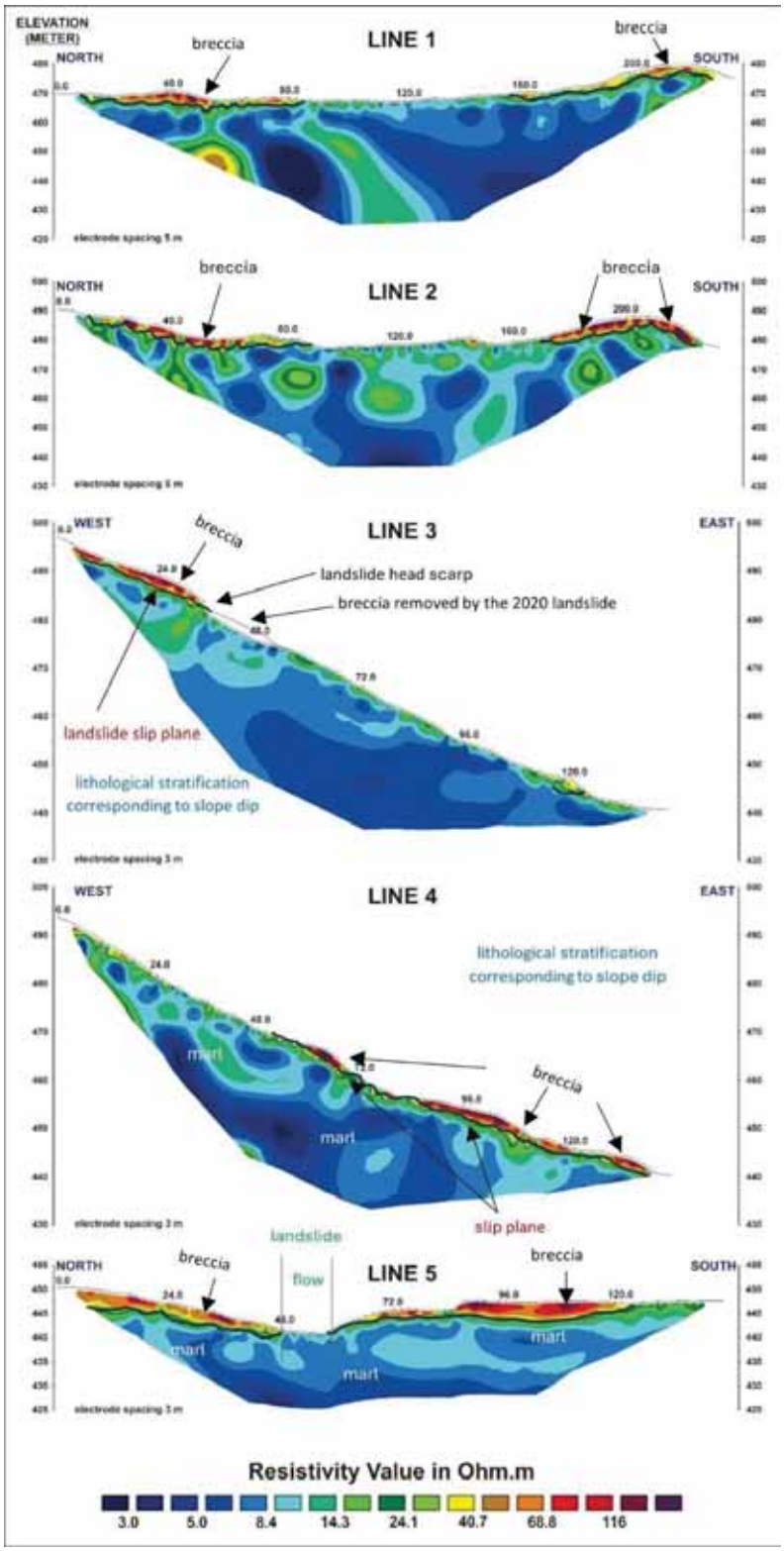

Fig. 4: Subsurface lithological conditions of the Banar landslide show a shallow breccia layer overlying a thick marl layer that acts as the sliding plane

Landslide subsurface geology and 3D model

The geoelectrical survey provided valuable insights into subsurface stratigraphy in landslide-prone areas. By combining field surveys with ERT data from five lines located in the depletion and transition zones (Fig. 4), two separate rock layers were distinguished: marl (<40 Ohm meter (Ohm-m) and breccia (>40 ohm-m). The stratigraphic profile shows breccia as the uppermost layer, overlying up to 40 m of marl. This permeability contrast significantly impacts slope stability. Bedding planes align with the slope dip, influencing groundwater flow and potential failure surfaces (Fig. 4). Marl, a low-permeability layer, serves as a sliding plane. The orientation of the slip plane in relation to the breccia-marl boundary and the slope's inclination elevates the likelihood of landslide reactivation, attributed to the contrasting materials and their structural alignment. Breccia's high permeability allows water infiltration, while marl traps water, raising pore pressure and reducing shear strength. Parallel alignment with the slope dip increases shear stress, especially during heavy rainfall or seismic events, making reactivation more likely. This geological feature is vital for assessing slope stability and landslide risk. The breccia thickness in the depletion and transition zones is shallow, ranging from 0.5 to 4.5 m. The orientation of the slip plane in relation to the breccia-marl boundary and the slope's inclination, coupled with the limited thickness of the breccia, emphasizes the vital importance of vegetation in slope reinforcement. Breccia thickness along the slip plane was mapped using 2D cross-sections and 3D modelling, providing a detailed spatial representation of the landslide slip plane (Figs. 4 and 5). This mapping elucidates the thickness, depth, and extent of the unstable breccia mass. Measurements showed that the width varied across the different survey lines. The landslide narrows southward along ERT line 5, suggesting a shift from sliding to flow. The 3D block diagram (Fig. 5) shows breccia overlying marl with varying thicknesses. The interface between the breccia and marl acts as the slip plane and is aligned with the slope's inclination, making the area particularly vulnerable to landslides.

Vegetation in the landslide area

The post-landslide vegetation inventory results are presented in Table 1, identifying forest plants, fruit-bearing plants, crop plant and pioneer species. Based on feedback from local residents, the types of vegetation present before and after the landslide has not significantly altered.

Evapotranspiration, root and canopy

In Banar, an inventory of local species, including forest, fruit-bearing, and pioneer species, was

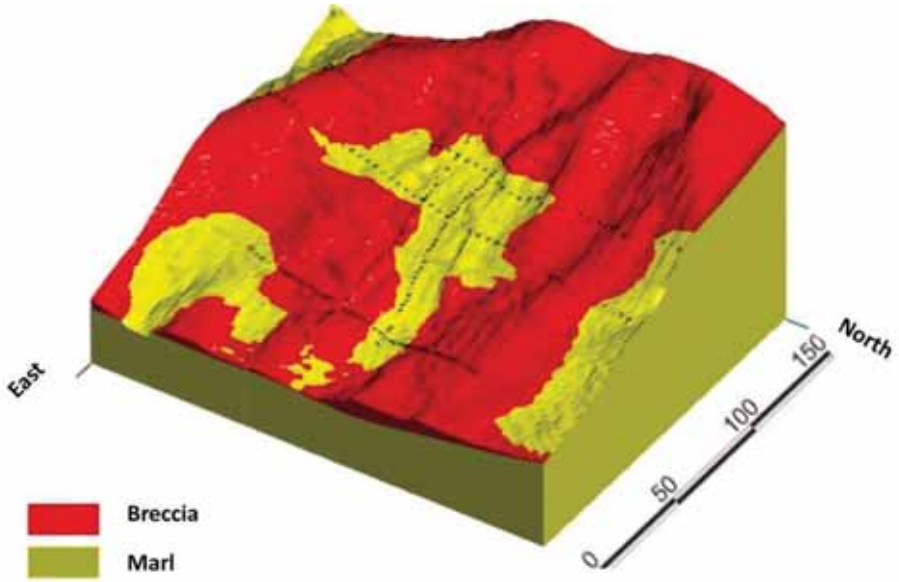

Fig. 5: Block diagram of the Banar landslide depletion and transition zones, illustrating the spatial distribution of breccia (red) and marl (yellow) and the depositional relationship between these layers

Table 1: Results of vegetation inventory in the Banar landslide area

Plant group	Species name	Canopy	Abundance
Forest plant			
	Maesopsis eminii Engl	Moderately dense	vvvvv
	Bambussa sp.	Fairly dense	vvv
	Paraserianthes falcataria	Fairly dense	vvv
	Arenga pinnata Merr	Moderately dense	vv
	Swietenia mahagoni	Moderately dense	vvv
	Sandoricum koetjape	Dense	v
	Hibiscus macrophyllu, Roxb.	Moderately dense	v
	Calliandra calothyrsus	Moderately to dense	vv
Fruit-bearing plant			
	Durio zibethinus	Dense	vvvv
	Garcinia mangostana	Very dense	vvv
	Bouea macrophylla	Moderately to very dense	vv
	Syzygium aromaticum	Moderately dense	v
	Mangifera caesia	Dense and spreadly	vv
	Muntingia calabura	Moderately dense	v
	Artocarpus integer sp	Dense	v
	Ananas comosus Merr	Dense foliage	v
	Musa paradisiaca	Moderately dense	v
	Cocos nucifera	Moderately open	v
Crop plant			
	Manihot esculenta	Light to moderately dense	vv
	Vigna unguicilata	Open to moderately dense	vv
	Solanum lycopersicum	Moderately open	vv
	Capsicum annum	Moderately dense	vvv
	Zea mays	Moderately dense	vv
Pioneer species			
	Borreria alata, L	Light to moderately dense	vv
	Melastoma affine D.Don	Moderately dense	vvvv
	Clidemia hirta (L.) D.Don	Moderately to highly dense	vv
	Agetarum conyzoides L	Light to moderately dense	vvv
	Mikania micrantha, Kunth	Highly dense	vv

conducted alongside a literature review of their root characteristics and evapotranspiration rates. At the research site and surrounding areas, the vegetation canopy is readily observable. The selection of suitable plants can significantly bolster slope stability, rendering this method vital for successful landslide management and recovery efforts. Vegetation significantly influences slope stability by regulating interception, evapotranspiration, soil aggregation, and root reinforcement (Graf *et al.*, 2019). Interception occurs when the canopy captures rainfall and evaporates before reaching the soil. The extent of leaf area and the width of the canopy are crucial elements, as a greater leaf area index is associated with increased interception (Yang *et al.*, 2019). Evapotranspiration, the combined process of evaporation and transpiration, reduces soil saturation and prevents water build up above the slip surface, lowering pore water pressure in permeable rocks. For optimal results in plant-based slope stabilization, it is best to select species known for their high evapotranspiration rates. Generally, plants that have deep roots and wide-spreading canopies show increased levels of evapotranspiration. Total and specific root length correlate positively with evapotranspiration (Szota, 2024). Key influencing factors include plant density, rainfall, soil type (Mulyono *et al.*, 2018), solar radiation, humidity, temperature, wind, vegetation cover, species composition, and growth rates (Graf *et al.*, 2019). The study conducted by González-Ollauri and Mickovski (2017) revealed that the presence of vegetation significantly contributes to slope stability by absorbing water, which leads to a 12.84% reduction in moisture levels and a threefold increase in matric suction compared to fallow slopes. Plants play a vital role in slope stabilization through root reinforcement, increasing soil shear strength and

stability (Bao *et al.*, 2024; Taib *et al.*, 2020). Lobmann *et al.* (2020) highlight the strong link between slope stability, vegetation type and root structure. *Leucaena leucocephala* had taproots, and their lateral roots grew horizontally and profusely; their tap and lateral roots (both VH-type) had high reinforcement capacities (Saifuddin and Normaniza, 2016). Strong and intricate root systems establish a connection that secures soil particles, curtails erosion, and diminishes the landslide risk. While tree roots provide strength, shrubs also effectively mitigate shallow landslides, increasing the factor of safety (FoS) from 1.50 to 3.53 (Lann *et al.*, 2024). The parameters of root cohesion and root depth play a vital role, with elevated values resulting in improved slope stability. For instance, root cohesion values ranging from 5 to 25 kilo Pascal (kPa) and root depths up to 2.0 m significantly enhanced slope safety factors (Ahmed and Hussain, 2023). As roots decompose, their tensile strength and cohesion decrease, weakening the soil's resistance to shear forces and impacting long-term slope stability. Simulations reveal that fresh roots of *Chrysopogon nemoralis* and *Chrysopogon zizanioides* contribute to slope stability improvements of up to 45°, but this advantage lessens over time due to decomposition. Root decay alters the soil's mechanical and hydraulic properties (Phan *et al.*, 2025), potentially redistributing stress and triggering or reactivating slip planes, particularly on steep slopes or in weak geological conditions. Apart from the depth of their roots, some plant species, including bamboo, significantly contribute to landslide prevention. *Bambusa vulgaris* has a dense, fibrous root system stabilizes slopes by binding soil and reducing erosion (Balasuriya *et al.*, 2018). Its effectiveness is especially notable in high-rainfall, landslide-prone areas (Maddalwar *et al.*, 2024). Farmers report its primary benefits as landslide prevention (33%) and soil erosion reduction (30.5%) (Ananfack *et al.*, 2023). To assess vegetation's role in slope stability, detailed data on species' growth patterns, hydromechanical traits, root development, water retention, and soil interactions are essential. Understanding how plants support slopes, reduce erosion, and stabilize soil relies heavily on these factors. However, there is still a lack of data concerning particular plant types. Plants with high evapotranspiration rates increase soil suction more effectively than those with low rates, while deep-rooted plants draw water from deeper layers, affecting vertical moisture distribution. This increased suction enhances soil shear strength and reduces the risk of shallow landslides. Plants possess a range of root structures that affect the stability of slopes; however, there is insufficient research regarding the root traits and depth associated with specific tree species. Table 2 presents tropical species with varying root depths and evapotranspiration rates that can be applied for slope reinforcement and shallow landslide mitigation based on the limited available literature. Canopy descriptions are based on field observation. All selected species are fast-growing, making them suitable for rapid slope stabilization.

Roots are commonly used in bioengineering to improve slope stability, especially in infrastructure earthworks (Boldrin *et al.*, 2020). They improve the tensile strength of the soil, especially at shallow levels, where erosion and slope failures commonly occur (Masi *et al.*, 2021; Ni *et al.*, 2018). Root effectiveness depends on architecture and mass; shallow mat root systems prevent erosion but are less effective against slope failures (Masi *et al.*, 2021), Hydrological reinforcement, through evapotranspiration-induced matric suction, also boosts soil shear strength (Boldrin *et al.*, 2020). The interaction between root systems and different soil types boosts cohesion, aids in water infiltration, and delivers mechanical support, with roots proving to be more effective in stabilizing clay soils than sandy ones (Cheng *et al.*, 2024). In vegetated slopes, roots help prevent erosion, alter water flow, and reduce pore pressure, enhancing stability, while bare slopes are more prone to erosion, lower water retention, and higher pore pressure, increasing failure risk.

Vegetation intervention

Vegetation intervention in landslide-prone or post-landslide areas should align with slip plane depth and overlying rock or soil thickness. Strategic plant placement based on hydromechanical properties enhances slope stability and reduces shallow landslide risks. Important considerations for selecting plants involve choosing species that grow quickly, develop deep root systems that extend to the slip plane, and possess canopy traits that enhance evapotranspiration. Climate variability must be considered in vegetation models for landslide mitigation. During intense rainfall, plants with extensive root systems promote improved water

Table 2: Root depth, ET and canopy of some tropical species

Species	Root Depth (m)	ET (mm/day)	Canopy
	Source	Source	Source
Bambussa sp.	1,5 - 2	2-4	Fairly dense
	Tardio *et al.* (2018)	-	Observation
Acasia mangium	6,4	6-7	Fairly dense
	Kadir *et al.* (1998) Germon *et al.* (2018)	Germon *et al.* (2018)	Observation
Eucalyptus sp.	8-11,5	2.7-4	Not too dense
	Pinherio *et al*. (2016)	Pinherio *et al*. (2016);, Liu *et al.* (2017)	Observation
Leucaena leucocephala	1-4	4-6	Moderately dense
	Verma (2016), Pachas *et al.* (2016)	Verma (2016)	Observation
Casuarina equisetifolia	2.5	-	Moderately to sparse
	Purwono (2022)		Observation
Gmelina arborea	2-4	3-5	Moderately to fairly dense
	Kumar and Nair (2011)	Kumar and Nair (2011)	Observation
Artocarpus heterophyllus	2-5	3-5	Dense
	Orwa *et al.* (2009)	Orwa *et al.* (2009)	Observation
Paraserianthes falcataria	3-5	2	Moderately to fairly dense
	Pinheiro *et al.* (2021)	Pinheiro *et al.* (2021)	Observation
Swietenia sp.	-	4.32	Moderately dense
		Joseph *et al*. (2022)	Observation
Pinus merkusii	1,5 -2	-	Relatively sparse
	Utomo *et al.* (2019)	-	Observation
Mangifera indica	6	4-6	Dense and spread
	Oktaviano *et al.* (2015)	Da Silva (2024)	Observation
Crysophogon zizanoides	>3 m	8.56 – 35.6	Sparse
	Truong and Vanoh (2021)	Milani (2019), Boodia (2025)	Observation

infiltration. Although this can be advantageous, it may also lead to a reduction in soil shear strength, thereby heightening the risk of landslides. Musdalipa *et al*. (2018) note that plant roots create macropores, enhancing water movement into the soil. This model highlights deep-rooted species for managing heavy rainfall and their higher resistance to wind and erosion during extreme weather events. Local species are preferred for their adaptability, ease of application, and cost-effectiveness. Plant roots strengthen soil structure, increasing shear strength (Feng *et al.*, 2020). They facilitate water infiltration (Wang *et al.*, 2020) and regulate soil moisture by absorbing and directing water flow (Li *et al.*, 2021). The choice of vegetation must reflect the slope conditions, emphasizing the use of trees that are not overly heavy to prevent the possibility of landslides. Woody plants with strong, deep roots enhance soil stability by resisting movement. Trees with roots reaching 5 m improve the FoS (Lann *et al.*, 2024). Feng *et al.* (2020) found that slopes reinforced by exponential root branching systems exhibit more substantial hydrological and mechanical stability than those with uniform root branching. An isopach map depicting the distribution of breccia thickness in the Banar landslide source region was produced to assist in implementing vegetation-focused measures that enhance slope stability and help prevent landslides. The slope map from the LiDAR drone, as described and presented in Fig. 2, overlays this figure. To analyze the distribution of landslide risk, slope and breccia thickness were integrated through the processes of reclassification and weighting analyses. Reclassification categorized data based on suitability, as detailed in Table 3 while weighting assigned priority to each parameter during raster summation (Table 4). Higher weights were given to factors with greater landslide influence. The final risk distribution was reclassified (Table 5) and visualized in Fig. 6.

Landslide risk mapping using GIS involves subjective and objective uncertainties. Human judgment in choosing parameters, setting reclassification

Table 3: Reclassification of value and criteria from each parameter

No.	Parameter	Value	Criteria	Description
1	Slope	5	>30°	High risk landslide
		3	10° – 30°	Moderate risk landslide
		1	<10°	Low risk landslide
2	Thickness of volcanic breccia	5	3 – 4.5 m of thickness	High risk landslide
		3	1 – 3 m of thickness	Moderate risk landslide
		1	< 1 m of thickness	Low risk landslide

Table 4: Study parameters and weighting value

No.	Parameter	Explanation	Weight
1	Slope	Slope gradient or steepness is a key factor in landslide susceptibility, as steeper slopes increase downslope gravitational force, reducing stability. High-gradient areas are more prone to failure, especially when combined with rainfall, geological conditions, or human activities.	5
2	Thickness of breccia	Breccia, a volcanic rock with subrounded to subangular fragments, overlies marl and influences slope stability by adding weight and affecting shear stress. Its impact depends on slope gradient and rainfall, with thicker breccia remaining stable on gentle slopes but potentially failing on steeper ones.	2

Table 5: Reclassification of value and criteria from landslide risk level

No.	Parameter	Value	Criteria	Description
1	Landslide risk level	5	>35	High risk zone
		3	7 – 35	Moderate risk zone
		1	<7	Low risk zone

thresholds, and making weighting decisions leads to subjective uncertainties. Conversely, objective uncertainties are caused by factors such as data accuracy, resolution, geological imperfections, and the limitations inherent in models. To ensure accurate risk assessment, direct observations and established references were used. Slope angle follow key studies (Castellazzi and Previtali, 2024), with slope classes simplified from five to three. Lithological thickness reclassification is based on Bruijnzeel (2004); Cohen and Schwartz (2017), emphasizing tree roots' role in reducing shallow landslides of < 3 m and < 1 m. Slope is weighted higher due to its stronger link to landslides (Michael and Samanta, 2016; Çellek, 2022), while geological factors have lower spatial resolution and predictive strength (Reichenbach *et al*., 2018). Objective uncertainties are reduced by using high-resolution data, including a 0.1 m/pixel DEM from Real-Time Kinematic LiDAR, closely spaced resistivity measurements (3 m and 5 m) across five ERT lines, and field observations for geological verification. Based on the abundance of local species in the Banar landslide area, several tropical species are suitable for slope stabilization and shallow landslide prevention. Additionally, these species can provide economic benefits to local communities (Table 6 and Fig. 6). The plants are selected based on their fast-growing, canopy, depth of root systems, slip plane depth, breccia thickness, and slope gradients. The insufficient body of literature concerning the hydro-mechanical traits of plants, particularly in relation to root depth and evapotranspiration, hinders the selection process for plants.

Future studies are essential to establish universal patterns or equations that connect tree height with root depth across different species and ecosystems, as well as evapotranspiration and canopy dynamics. For HR, *Paraserianthes falcataria*, *Eucalyptus* sp., *Acacia mangium*, and *Bambussa* sp. are suitable species. *Paraserianthes* and *Albizia* species are the same scientific name for Sengon trees (local name in Indonesia). The roots of Albizia trees provide additional cohesion to the soil and can significantly improve the lack, particularly in steep slopes

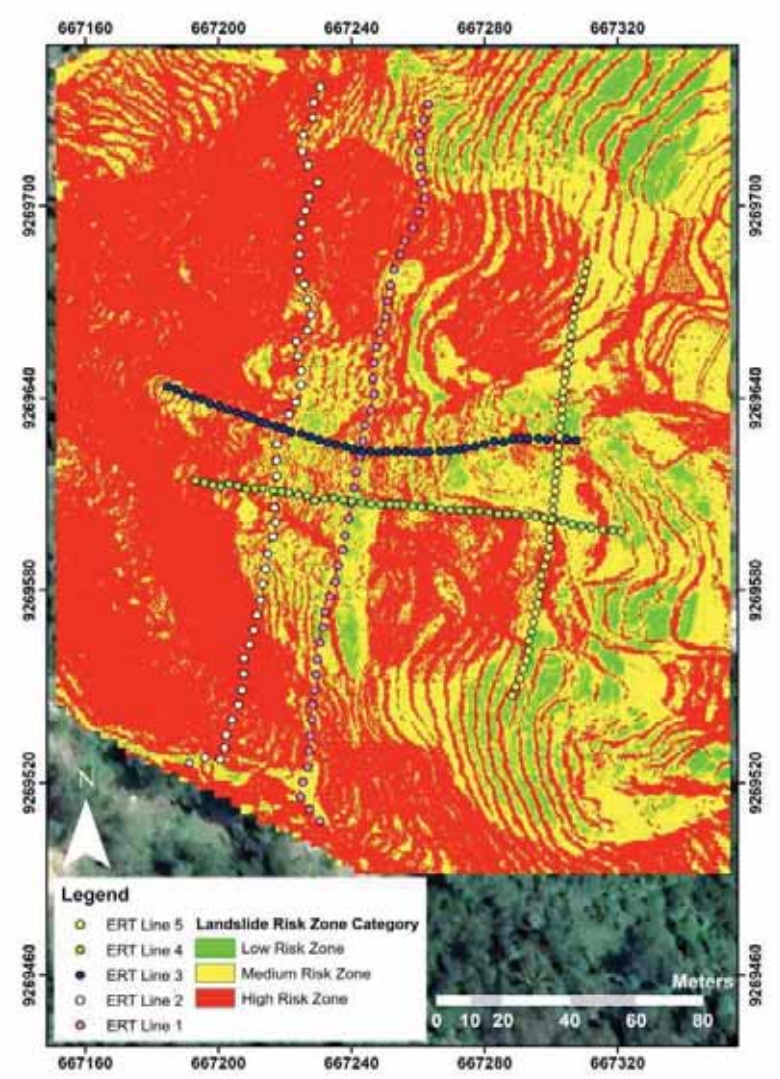

Fig. 6: Landslide risk zones in the depletion and transition areas of Banar, classified for vegetation intervention into high-risk (HR), medium-risk (MR), and low-risk (LR) zones.

(Ahmed and Hussain, 2023; Wang *et al.*, (2019) and maintaining lower moisture levels in the soil (Kim *et al.*, 2017). *Acacia mangium* has shown high shear strength values (up to 50.2 kPa) and is effective in binding soil layers (Abdullah *et al.*, 2011). Even during its early-stage establishment (28 weeks), its roots exhibited a tensile strength of 10.18 ± 0.62 mega pascal (MPa), a Young's modulus of 325.18 ± 21.72 MPa, and a mechanical reinforcement of 3.15 kPa (Phan *et al.*, 2024). Eucalyptus trees play a vital role in stabilizing slopes during the ecosystem's adjustment and vegetation recovery phases (Facadio *et al.*, 2023). Their robust root systems have demonstrated the ability to enhance the FoS of slopes by 22-34% when utilized for reinforcement (Tsige *et al.*, 2019). For MR, *Leucaena leucocephala, Artocarpus heterophyllus, Gmelina arborea, Mangifera indica*, *Swietenia* sp., *Bambussa* sp., and *Crysophogon zizanoides* are recommended. *Swietenia* sp. have deep root systems that provide substantial mechanical reinforcement to slopes by anchoring the soil and preventing landslides (Ng *et al.*, 2018). The root system of *Gmelina arborea* is shallow and is well-known for its swift growth and application in agroforestry. It plays a significant role in slope stabilization by rapidly building biomass and reinforcing the soil with its roots (Obiazi and Ojeifo,

Table 6: Vegetation for interventions in Banar for slope reinforcement and shallow landslide mitigation

Species name	Note
Plants for HR	
Paraserianthes falcataria	Local species
Eucalyptus, sp	Tropical species
Acasia mangium	Local species
Bambussa, sp	Local species
Plants for (MR)	
Artocarpus heterophyllus	Local species
Gmelina arborea	Tropical species
Mangifera indica	Local species
Bambusa, sp	Local species
Chrysopogon zizanoides	Tropical grass species
Leucaena leucocephala	Tropical species
Swietenia sp.	Local species
Plants for low risk zone (LR)	
Cocos nucifera	Local species
Musa paradisiaca	Local species
Zea mays	Local species
Manihot esculenta,	Local species
Vigna unguicilata,	Local species
Solanum lycopersicum,	Local species
Capsicum annum	Local species
Cover Crops for reinforcement in all zones	
Agetarum conyzoides L	Local species
Melastoma affine D.Don	Local species
Borreria alata L	Local species
Mucuna bracteata,	LCC (Legume cover crops)
Calopogonium muconoides,	LCC
Centrosoma pubescens	LCC
Calopogonium caeruleum	LCC
Pueraria javanica	LCC

2020). For LR, cultivating shallow-rooted plants with low to medium evapotranspiration rates and economic benefits is recommended. Suitable species for these conditions include *Musa paradisiaca* (banana), *Cocos nucifera* (coconut), *Zea mays* (corn), *Solanum lycopersicum* (tomato), *Vigna unguiculata* (peanut), *Manihot esculenta* (cassava), and *Capsicum annum* (chili). The plants that have been selected feature both indigenous species and tropical types that can easily adapt. While concerns about invasive species exist, some invasive woody plants can improve soil quality, increase carbon sequestration, and enhance nitrogen and phosphorus availability (González Giro *et al*., 2023). Voigtlaender *et al*. (2019) indicate propose that the practice of intercropping invasive species that fix nitrogen with native species that do not can improve the long-term nitrogen content of soil in tropical plantation settings. Plant biomass, both above- and below-ground, plays a crucial role in slope stability by increasing shear strength and matric suction, with plant-induced suction expected to rise as root biomass increases due to plant maturity or greater biodiversity. (Yildiz *et al*., 2019). To ensure soil protection in regions at risk of landslides, it is necessary to adopt extra precautions prior to the trees achieving maturity. Without adequate ground cover, raindrop impact can lead to surface erosion, further infiltration and increasing slope instability. The primary tree species selected for slope stabilization in Banar area require a long growth period, leaving open spaces between trees that remain vulnerable to erosion. In the early stages of slope recovery, fast-growing plants and grasses that cover the ground extensively serve as vital pioneer species. The root tensile strength of three tested grass species increased with root diameter (Yin *et al.*, 2024). Several pioneer species observed in Banar are listed in Table 1.

To enhance stability and reduce erosion, cover crops can be utilized in every risk zone within the Banar

landslide area (Table 6). In addition to pioneer species that serve as ground cover, open spaces between trees can be filled with cover crops, including LCC. By mitigating the kinetic energy of raindrop impacts, these crops contribute to maintaining soil moisture for future plant growth, reducing evaporation, and enhancing the retention of water from rainfall and irrigation (Sharma *et al*., 2018). Furthermore, they are crucial in minimizing soil erosion caused by wind and water while reducing airborne dust emissions and mechanical disturbances (Blanco-Canqui *et al.,* 2015). By vying for water, light, and nutrients, cover crops effectively suppress weed growth, and they can also release allelopathic compounds that hinder the development of weeds (Rouge *et al*., 2022; Masilionyte *et al*., 2017). Additional benefits include increased organic matter, nutrients and microbial activity; improved soil fertility; fixing atmospheric nitrogen; benefit to the agroecosystem; and more effective pest control (Quintarelli, *et al*., 2022). Furthermore, the use of cover crops contributes to the enrichment of soil organic matter, particularly when they are paired with materials rich in Carbon : Nitrogen ratio, facilitating nutrient availability for plant growth (Hubbard et al., 2013). Several species classified as LCC that can be used are presented in Table 6. Cover crop local species include *Ageratum conyzoides L.*, *Melastoma affine D. Don*, *Borreria alata L*. Meanwhile, LCC species consist of *Mucuna bracteata*, *Calopogonium mucunoides*, *Centrocema pubescens*, *Calopogonium caeruleum*, and *Pueraria javanica* (Ma'ruf *et al*., 2017) as well as *Pennisetum clandestinum*, *Portulaca grandiflora*, *Oxalis triangularis*, *Tradescantia* spp., *Soleirolia soleirolii*, *Dymondia margaretae*, *Lavandula* spp., and *Ajuga reptans*. Furthermore, leguminous plants are especially advantageous because they improve soil health and contribute to erosion control (Sharma *et al.,* 2018). Long-term monitoring data on plants and their interactions with soil are another point to investigate in the future. Slip plane stability is influenced by soil moisture and groundwater fluctuations, with vegetation playing a key role. Groundwater levels and soil type affect moisture content, and depletion can lead to vegetation degradation (Ridwan *et al.,* 2024). In arid regions, groundwater and soil moisture are vital for growth in groundwater-dependent vegetation (GDV) (Maihemuti *et al*., 2021). Understanding the fluctuations in moisture and groundwater levels is essential for grasping plant development and the overall water budgets within ecosystems. Seasonal soil moisture variations impact slope stability, as excess moisture weakens slip planes, while dry conditions cause soil cracking. Vegetation stabilizes slopes by reducing moisture in wet periods and preventing erosion through root systems and transpiration. Loss of vegetation or excessive moisture increases the risk of slope failure. Models assessing slope stability that exclude the hydromechanical impacts of vegetation encounter major limitations. They often underestimate the reinforcement provided by roots, overlook the interactions between water and vegetation, and fail to recognize the dynamic nature of vegetation (Ning *et al*., 2020). Roots enhance slope stability by strengthening soil shear resistance, and models that overlook this may lead to inaccurate predictions (Yin *et al*., 2024). The interaction between vegetation and water, including the ways in which root systems facilitate drainage and impact moisture retention, is essential for ensuring stability. Preferential flow influences slope stability by affecting water infiltration and redistribution. Excluding these factors prevents accurate representation of pore water pressure, which is key to slope failure, especially during heavy rainfall (Qiu *et al*., 2022). Furthermore, models that do not take into account seasonal fluctuations in root development and water absorption might be inadequate in predicting stability during various seasons or after disturbances like droughts or intense rainfall (Ai *et al*., 2022). The impact of vegetation on slope stability can change over time. Vegetation influences slip plane migration or reactivation through root reinforcement, hydrological changes, and ecological succession (Noviandi *et al*., 2022; Fraccica *et al*., 2023; Wang *et al*., 2020; Chen *et al*., 2021). Ignoring these evolving effects in models can lead to inaccurate forecasts of long-term stability, particularly in locations where vegetation is essential for slope support (Huang *et al*., 2023). Neglecting plant growth and decay may overlook critical feedback mechanisms, such as how plant cover mitigates erosion and enhances stability, leading to a distorted understanding of slope behaviour in natural conditions (Lann *et al*., 2024). This study introduces a vegetation intervention model that improves slope stability by integrating spatial slip plane data with specific vegetation traits, such as root depth,

canopy density, and evapotranspiration in risk zones. In contrast to earlier models that view vegetation as uniform, this approach merges hydromechanical functions of vegetation with slip plane mapping, resulting in improved stability predictions. The model provides practical solutions, like optimizing tree spacing in high-risk areas, offering a framework for managing landslide-prone slopes. It is adaptable to different geological, climatic, and socio-economic contexts by considering local factors, making it applicable in a range of settings. To achieve effective management, a well-organized approach is essential for navigating the trade-offs between different conservation values. This requires an understanding of stakeholder preferences and objectives, as well as a careful balance between the benefits of fast-growing species and the necessity of maintaining biodiversity (Regan *et al.*, 2023). Additionally, conservation planning should take into account the long-term ecological effects that may arise from the selection of fast-growing species, including possible shifts in species composition and changes in ecosystem dynamics van Lanen *et al.*, 2025). Adapting the model for different geological, climatic, and socio-economic contexts requires flexibility and customization. The model can be adapted for wider use by taking into account local soil types, climate conditions, and socio-economic factors. Although vegetation-based approaches are recognized for their cost-effectiveness and environmental benefits, several challenges must be addressed to ensure successful implementation. The obstacles encompass economic viability, community support, and technical constraints tied to the specific conditions of the site. Future research and collaboration with local stakeholders will be key to refining the model for diverse regions, ensuring its scalability and long-term success in landslide mitigation and slope reinforcement (Yazdani *et al.*, 2024).

CONCLUSION

A spatial slip plane-based vegetation model for slope reinforcement and shallow landslide mitigation holds great potential but faces challenges related to climate variability, plant succession, and long-term monitoring. Future research addressing these issues is essential for enhancing model sustainability and reliability. The integration of climate predictions, a thorough understanding of plant succession, and the creation of effective monitoring systems will strengthen the management and mitigation of shallow landslide risks, ensuring that vegetation-based solutions adapt successfully to changing environmental conditions. This study presents a novel intervention model integrating vegetation's hydromechanical functions for slope reinforcement aligned with the spatial distribution of the landslide slip plane. Achieving effective stabilization is contingent upon the depth of the slip plane and the intentional design of vegetation. The Banar landslide spans approximately 563 m, starting as a debris slide in the depletion zone and transitioning to slide flow along an N 95° E trajectory. It curves to N 135° E in the accumulation zone, where it becomes a lower sediment concentration flow. The trajectory of the movement corresponds to the west-to-east-southeast incline, implying that groundwater is also moving in that direction. LiDAR data reveals a typical horseshoe-shaped head scarp and steep slopes exceeding 30°. The landslide is controlled by a moderately permeable breccia layer (0.5–4.5 m thick) overlying low-permeability grey marl (>40 m thick), with the breccia-marl contact serving as the slip plane. Higher permeability in the breccia (9.13–10.99 cm/day) compared to the marl (0.269–0.368 cm/day) facilitates water infiltration, while the parallel bedding orientation with the slope further increases instability. Given these conditions, the presence of vegetation significantly contributes to the stability of slopes. The Banar landslide area is classified by breccia thickness and slope steepness. HR zones (breccia 3–4.5 m, slopes >30°) require deep-rooted trees, surface-protecting shrubs, and lighter biomass with wider spacing to maintain stability. MR zones (breccia 1–3 m, slopes 10°–30°) are suitable for medium- to deep-rooted vegetation with denser planting to enhance stabilization. In comparison, LR zones (breccia <1 m, slopes <10°) are best suited for shallow-rooted plants or grasses to control erosion. The slope intervention model focuses on selecting local species that grow quickly, as well as other tropical species that are adaptive and have medium to high evapotranspiration rates. It incorporates a combination of deep to moderately rooted plants, and cover crops as ground cover. Additionally, vegetation with moderate to high canopy density is integrated to enhance overall slope stability. This holistic strategy aims to enhance the beneficial impacts of vegetation

in strengthening slopes. In HR the spacing and density of tree planting need to be carefully regulated, with wider spacing to prevent excessive loading. The appropriate vegetation for HR zone includes *Paraserianthes falcataria, Eucalyptus* sp., *Acacia mangium*, and *Bambussa* sp. For MR, *Leucaena leucocephala, Artocarpus heterophyllus, Gmelina arborea, Mangifera indica, Swietenia* sp., *Bambussa* sp. *and Chrysopogon zizanoides* are recommended. In LR, seasonal and productive crops such as *Cocos nucifera, Musa paradisiaca*, *Zea mays*, *Solanum lycopersicum, Capsicum annuum*, *Manihot esculenta*, and *Vigna unguiculata* can be planted to provide daily benefits for local communities. Additionally, cover crops such as *Ageratum conyzoides* L., *Melastoma affine* D. Don, *Borreria alata* L., *Mucuna bracteata*, *Calopogonium mucunoides*, *Pueraria javanica*, and others can be integrated in all zones to enhance slope stabilization and prevent erosion. This vegetation-focused strategy serves as a model for strengthening slopes and mitigating shallow landslides, fostering sustainable land management practices and better safeguarding communities and infrastructure in regions at risk of landslides.

AUTHOR CONTRIBUTIONS

I.G. Tejakusuma, the first and corresponding author, contributed to the conceptualization, methodology, observations, acquisition of data, data analysis, statistical analysis, preparation of photos and figures, original draft preparation, obtaining funding, and critical revision. E.H. Sittadewi conducted conceptualization, observations, acquisition data, data analysis, statistical analysis, obtaining funding, administration support, original draft preparation, and critical revision. A. Mulyono supported observations, literature review, original draft preparation, data acquisition, editing, and critical revision. T. Handayani performed the methodology, observation, original draft preparation, data acquisition, data analysis, reviewing and editing, and critical revision. A Tohari, obtaining funding, methodology, acquisition data, original draft preparation, supervision, and material support. H.E.H. Fatahillah performed analysis and interpretation of data, original draft preparation, statistical analysis, and preparation of photos and figures. Z. Zakaria performed the original draft preparation, supervision, validation, and review. E.B. Budiman conducted the original draft preparation, preparation of pictures and figures, literature review, validation, and technical support. N. Utami conducted the original draft preparation, a literature review, and administrative support.

ACKNOWLEDGEMENT

The authors gratefully acknowledge the Research Organization for Earth Sciences and Maritime (ORKM) – National Research and Innovation Agency (BRIN) for funding this research through the 2025 Rumah Program Kebencanaan dan Sumber Daya Kebumian [B-34263/III.4/TK.02.00/12/2024].

CONFLICT OF INTEREST

The authors declare that there is no conflict of interest regarding the publication of this manuscript. The ethical issues, including plagiarism, informed consent, misconduct, data fabrication and/or falsification, double publication and/or submission, and redundancy have been completely observed by the authors.

OPEN ACCESS

©2025 The author(s). This article is licensed under a Creative Commons Attribution 4.0 International License, which permits use, sharing, adaptation, distribution and reproduction in any medium or format, as long as you give appropriate credit to the original author(s) and the source, provide a link to the Creative Commons license, and indicate if changes were made. The images or other third-party material in this article are included in the article's Creative Commons license, unless indicated otherwise in a credit line to the material. If material is not included in the article's Creative Commons license and your intended use is not permitted by statutory regulation or exceeds the permitted use, you will need to obtain permission directly from the copyright holder. To view a copy of this license, visit: http://creativecommons.org/licenses/by/4.0/

PUBLISHER'S NOTE

GJESM Publisher remains neutral with regard to jurisdictional claims in published maps and institutional afflictions.

Positive AI Statement

During the preparation of this work the author(s) have used [NAME TOOL / SERVICE] in order to

[REASON]. After using this tool/service, the authors reviewed and edited the content as needed and took full responsibility for the content of the publication. Furthermore, the GPTZero detector will evaluate the manuscript utilizing Generative AI, ensuring a high detection rate. If the manuscript relies heavily on Generative AI and AI-assisted technologies, it will be archived without further options for appeal.

Negative AI Statement

The author(s) declare that no AI tools or services were not used or not highly applied during the preparation of this work.

ABBREVIATIONS

°	Degrees
“	Minutes
%	Percent
2D	Two-dimensional
3D	Three-dimensional
ASTM	American society for testing and materials
ARES	Automatic resistivity system
C	Carbon
cm	Centimeter
E	East
ERT	Electrical resistivity tomography
HR	High risk
kPA	Kilo Pascal
GDV	Groundwater-dependent vegetation
GIS	Geographic information system
km	Kilometer
LCC	Legume cover crops
LiDAR	Light detection and ranging
LR	Low risk
m	Meter
Ohm-m	Ohm-meter
MPA	Mega pascal
MR	Medium risk
N	North
sp	Species

REFERENCES

Abdullah, M.N.; Osman, N.; Ali, F.H., (2011). Soil-root shear strength properties of some slope plants. Sains. Malays., 40(10): 1065-1073 **(9 pages)**.

Ahmed, S.A.; Hussain, M.S., (2023). Evaluation of slope stabilization by vegetation reinforcement: modelling aspects. Polytech. J., 13(1): 99-108 **(10 pages)**.

Ai, Z.; Zhang, H.; Wu, S.; Jiang, C.; Yan, Q.; Ren, Z., (2022), Study on the slope dynamic stability considering the progressive failure of the slip surface under earthquake. Front. Earth Sci. 10: 1-13 **(13 pages)**.

Ananfack, G.R.K.; Temgoua, E.; Avana Tientcheu, M.L., (2023). Farmers' local knowledge of soil fertility in bamboo plantations in the Western Highlands, Cameroon. Adv. Bamboo Sci., 4: 1-10 **(10 pages)**.

Balasuriya, A.D.H.; Jayasingha, P.; Christoper, W. A. P. P., (2018). Application of bioengineering to slope stabilization in Sri Lanka with special reference to Badulla District. Prof. Geol., 47-51 **(5 pages)**.

Bao, H.; Xin-lin, A.; Yue-sheng, G.; Heng-xing, L.; Guan-miao, G.; Han, Z., (2024). Evolution analysis of root reinforcement mechanical effect of typical plant. China J. Highw. Transp., 37(6): 98-110 **(12 pages)**.

Blanco-Canqui, H.; Shaver, T.M.; Lindquist, J.L.; Shapiro, C.A.; Elmore, R.W.; Francis, C.A.; Hergert, G.W., (2015). Cover crops and ecosystem services: Insights from studies in temperate soils. Agron. J., 107(6): 2449-2474 **(26 pages)**.

Boldrin, D.; Leung, A.K.; Bengough, A.G., (2020). Hydro-mechanical reinforcement of contrasting woody species: A full-scale investigation of a field slope. Géotechnique. 71(11): 970–984 **(15 pages)**.

Boodia, N., (2025). Mathematical models to predict evapotranspiration of selected plant species for phytoremediation. Proceedings of the 11th International Conference on Agriculture. 9(1): 1–15 **(15 pages)**.

Bruijnzeel, L.A., (2004). Hydrological functions of tropical forests: Not seeing the soil for the trees? Agri. Ecosyst. Environ., 104(1): 185-228 **(44 pages)**.

Castellazzi, G.; Previtali, M. (2024). A Multi-Criteria GIS-based approach for risk assessment of slope instability driven by glacier melting in the Alpine area. Appl. Sci., 14(24): 1-23 **(23 pages)**.

Çellek, S., (2022). Effect of the slope angle and its classification on landslides. Him. Geol., 43(1): 85–95 **(11 pages)**.

Chen, M.; Tang, C.; Li, M.; Xiong, J.; Luo, Y.; Shi, Q.; Zhang, X.; Tie, Y.; Feng, Q., (2022). Changes of surface recovery at coseismic landslides and their driving factors in the Wenchuan earthquake-affected area. Catena. 210(105871): 1-14 **(14 pages)**.

Cheng, P.; Wu, L.; Zhang, H.; Zhou, J., (2024). Inclusion of root water absorption and reinforcement in upper bound limit stability analysis of vegetated slopes. Computers and Geotechnics, 169: 1-12 **(12 pages)**.

Cohen, D,; Schwartz, M., (2017). Tree-root control of shallow landslides. Earth Surf. Dynam., 5: 451–477 **(27 pages)**.

Da Silva, M.J.; De Moura, M.S.B.; Carvalho, H.F.D.S.; Dos Santos, C.V.B.; Leitão, M.D.M. V. B. R., Campeche, L. F. D. S. M.; da Silva, T.G.F., (2024). Evapotranspiration and crop coefficient of 'Kent'mango in an important fruit-growing hub in Brazil. Irrig. Drain., 73(4): 1391-1407 **(17 pages)**.

DiBiagio, A.; Capobianco, V.; Oen, A.; Tallaksen, L.M., (2024). State-of-the-art: parametrization of hydrological and mechanical

reinforcement effects of vegetation in slope stability models for shallow landslides. Landslides. 21: 2417-2446 **(30 pages)**.

Dinorah, P.C., (2017). Assessment of the Role of Vegetation as Part of Ecosystem-Based Risk Reduction Measures Used for Shallow Landslides in Rasuwa District, Nepal. M.Sc. Thesis, University of Twente. The Netherlands.

Emadi-Tafti, M.; Ataie-Ashtiani, B.; Hosseini, S.M., (2021). Integrated impacts of vegetation and soil type on slope stability: A case study of Kheyrud Forest, Iran. Ecol. Model., 446: 1-15 **(15 pages)**.

Facadio, A.C.; Sato, A. M.; Netto, A.L.C., (2023). Eucalyptus planting in pasture matrix and erosive reactivation of gullies in the Sesmaria River Basin (SP/RJ): A cycle of instability in headwater valleys. Rev. Bras. Geomorfol., 24(00): 1-30 **(30 pages)**.

Falae, P. O.; Kanungo, D. P.; Chauhan, P.K.S.; Dash, R.K., (2019). Recent Trends in Application of Electrical Resistivity Tomography for Landslide Study, in: Chattopadhyay, J., Singh, R., Prakash, O. (Eds), Renewable Energy and its Innovative Technologies. Springer, Singapore.

Fata, Y.A.; Hendrayanto; Murtilaksono, K.; Erizal, (2021). The role of hydro-mechanical vegetation in slope stability: A review. IOP Conference Series: Earth Environ. Sci., 794: 1-9 **(9 pages)**.

Feng, S., Liu, H. W.; Ng, C.W.W., (2020). Analytical analysis of the mechanical and hydrological effects of vegetation on shallow slope stability. Comput. Geotech., 118: 1-9 **(9 pages)**.

Fernandes, J.P.; Guiomar, N., (2016). Simulating the stabilization effect of soil bioengineering interventions in Mediterranean environments using limit equilibrium stability models and combinations of plant species. Ecol. Eng., 88: 122-142 **(21 pages)**.

Fraccica, A.; Romero, E.; Fallas, J. E., (2023). The impact of soil-vegetation-atmosphere interaction on a landslide initiation under torrential storms: a case study. E3S Web Conference. 382 **(6 pages)**.

Germon, A.; Guerrini, I.A.; Bordron, B.; Bouillet, J.; Nouvellon, Y.; Gonçalves, J.L.M.; Jourdan, C.; Paula, R.R.; Laclau, J., (2018). Consequences of mixing Acacia mangium and Eucalyptus grandis trees on soil exploration by fine roots down to a depth of 17 m. Plant Soil. 424(1): 203–220 **(18 pages)**.

Gong, C.; Ni, D. R.; Liu, Y.; Li, Y.; Huang, Q.; Tian, Y.; Zhang, H., (2024). Herbaceous vegetation in slope stabilization: a comparative review of mechanisms, advantages, and practical applications. Sustainability. 16(17):7620 **(18 pages)**.

González Giro, Z.; Olivera, R.P.; Mandado, R.L.; Hu, J.; Font Vila, L.; Sleutel, S.; Fievez, S.; De Neve., (2023). Invasive woody plants in the tropics: a delicate balance between control and harnessing potential benefits. A review. Agron. Sustainable Dev., 43(41): 1-25 **(25 pages)**.

Gonzalez-Ollauri, A.; Mickovski, S.B., (2017). Hydrological effect of vegetation against rainfall-induced landslides. J. Hydrol., 549: 374-387 **(14 pages)**.

Graf, F.; Bast, A.; Gartner, H.; Yildiz, A., (2019). Effects of mycorrhizal fungi on slope stabilisation functions of plants, in: W. Wu. (Eds), Recent Advances in Geotechnical Research. Springer Series in Geomechanics and Geoengineering. Springer International Publishing. AG. 57-77 **(21 pages)**.

Huang, F.; Xiong, H.; Chen, S.; Lv, Z.; Huang, J.; Chang, Z.; Catani, F., (2023). Slope stability prediction based on a long short-term memory neural network: comparisons with convolutional neural networks, support vector machines and random forest models. Int. J. Coal Sci. Technol., 10(18): 1-14 **(14 pages)**.

Hubbard, R.K.; Strickland, T.C.; Phatak, S., (2013). Effects of cover crop systems on soil physical properties and carbon/nitrogen relationships in the coastal plain of southeastern USA. Soil Tillage Res., 126: 276-283 **(8 pages)**.

Joseph, P.; Baillard, K.; Claude, J.P.; Abati, Y.; Ely-Marius, S.; Sophie, S.; Jean-Francois, Y.; Simphor, J.E.; Major, P., (2022). Natural Regeneration of indigenous species under plantation forests of Mahoganis (Swietenia macrophylla and Swietenia xaubrevilleana): The Case of Martinique. Open Access Library J., 9(1): 1-23 **(23 pages)**.

Kim, J.H.; Fourcaud, T.; Jourdan, C.; Maeght, J-L.; Mao, Z.; Metayer, J.; Meylan, L.; Pierret, A.; Rapidel, B.; Roupsard, O.; de Rouw,A,; Sanchez, M. V.; Wang, Y.; Stokes, A., (2017). Vegetation drives slope stability and its variability through hydrological impacts. Geophys. Res. Lett., 44(10): 4897-4907 **(11 pages)**.

Kumar, B.M.; Nair, P.K.R., (2011). Tropical Homegardens: A Time-Tested Example of Sustainable Agroforestry. Springer.

Kadir, W.R.; Kadir, A.A.; Van Cleemput, O.; Rahman, Z.A., (1998). Field grown Acacia mangium: How intensive is root growth? J. Trop. For. Sci., 10(3): 283 – 291 **(9 pages)**.

LaHusen, S.R.; Grant, A.R.R., (2024). Complex landslide patterns explained by local intra-unit variability of stratigraphy and structure: Case study in the Tyee Formation, Oregon, USA. Eng. Geol., 329: 1-14 **(14 pages)**.

Lann, T.; Bao, H.; Lan, H.; Zheng, H.; Yan, C.; Peng, J., (2024). Hydro-mechanical effects of vegetation on slope stability: A review. Sci. Total Environ., 926: 1-26 **(26 pages)**.

Li, J.; Wang, X.; Jia, H.; Liu, Y.; Zhao, Y.; Shi, C.; Zhang, F.; Wang, K., (2021). Assessing the soil moisture effects of planted vegetation on slope stability in shallow landslide-prone areas. J. Soils Sediments. 21: 2551-2565 **(14 pages)**.

Liu, W.; Wu, J.; Fan, H.; Duan, H.; Li, Q.; Yuan, Y.; Zhang, H., (2017). Estimations of evapotranspiration in an age sequence of Eucalyptus plantations in subtropical China. Plos One. 12(4): 1-15 **(15 pages)**.

Lobmann, M.T.; Geitner, C.; Wellstein, C.; Zerbe, S., (2020). The influence of herbaceous vegetation on slope stability – A review. Earth Sci. Rev., 209: 1-17 **(17 pages)**.

Loke, M.H., (2025). Tutorial: 2-D and 3-D electrical imaging surveys. Tutorial Notes - 6th February 2025 Update.

Loke, M.H.; Wilkinson, P. B.; Chambers, J. E.; Uhlemann, S. S.; Sorensen, J. P. R., (2015). Optimized arrays for 2-D resistivity survey lines with a large number of electrodes. J. Appl. Geophys., 112: 136-146 **(11 pages)**.

Maddalwar, S.; Kumar, T.; Tijare, G.; Agashe, A; Kotangale, P.; Sawarkar, A.; Singh, L., (2024). A global perspective on a bioengineering approach to landslide mitigation using bamboo diversity. Adv. Bamboo Sci., 8: 1-11 **(11 pages)**.

Maihemuti, B.; Simayi, Z.; Alifujiang, Y.; Aishan, T.; Abliz, A.; Aierken, G., (2021). Development and evaluation of the soil water balance model in an inland arid delta oasis: Implications for sustainable groundwater resource management. Global Ecol. Conserv., 25: 1-15 **(15 pages)**.

Ma'ruf, A.; Zulia, C.; Safrudin, (2017). Legume Cover Crop di Perkebunan Kelapa Sawit. Forthisa Karya.

Masi, E.B.; Segoni, S.; Tofani, V., (2021). Root Reinforcement in Slope Stability Models: A Review. Geosciences. 11(5): 1-24 **(24 pages)**.

Masilionyte, L.; Maiksteniene, S.; Kriauciuniene, Z.; Jablonskyte-Rasce, D.; Zou, L.; Sarauskis, E., (2017). Effect of cover crops in smothering weeds and volunteer plants in alternative farming systems. Crop Prot., 91: 74-81 **(8 pages)**.

Michael, E.A.; Samanta, S., (2016). Landslide vulnerability mapping (LVM) using weighted linear combination (WLC) model through remote sensing and GIS techniques. Model. Earth Syst. Environ., 2(2) 88: 1-15 **(15 pages)**.

Milani, M.; Marzo, A.; Toscano, A.; Consoli, S.; Cirelli, G. L.; Ventura, D.; Barbagallo, S., (2019). Evapotranspiration from Horizontal Subsurface Flow Constructed Wetlands Planted with Different

Perennial Plant Species. Water. 11(10): 2159: 1-21 **(21 pages)**.
Monteleone, S.; Sabatino, M., (2014). Hydrogeological hazards and weather events: Triggering and evolution of shallow landslides. Int. Soil Water Conserv. Res., 2(2): 23-29 **(7 pages)**.
Mostafaei, K.; Ramazi, H., (2018). Compiling and verifying 3D models of 2D induced polarization and resistivity data by geostatistical methods. Acta Geophy, 66: 959–971 **(13 pages)**.
Mulyono, A.; Subardja, A.; Ekasari, I.; Lailati, M.; Sudirja, R.; Ningrum, W., (2018). The hydromechanics of vegetation for slope stabilization. Global Colloquium on Geosciences and Engineering 2017, IOP Conference Series: Earth Environ. Sci., 118: 1-6 **(6 pages)**.
Murgia, I.; Giadrossich, F.; Mao, Z.; Cohen, D.; Capra, G.F.; Schwarz, M., (2022). Modeling shallow landslides and root reinforcement: A review. Ecol. Eng., 181 (106671): 1-17 **(17 pages)**.
Musdalipa, A.; Suhardi, S.; Faridah, S.T., (2018). Pengaruh Sifat Fisik Tanah dan Sistem Perakaran Vegetasi Terhadap Imbuhan Air Tanah. Agritechno. 11(1): 35-39 **(5 pages)**.
Netto, A.L.; Bolsas, L.; Facadio, A.C.; Silva, I.B.; Thomaz, E.L., (2024). Vegetation changes C. fire affect soil water behavior and enhance landslides in the mountainous region of Rio de Janeiro state, southeast Brazil. Catena. 241: 1-14 **(14 pages)**.
Ng, C. W.W.; Leung, A.K.; Ni, J.J., (2018). Bioengineering for slope stabilisation using plants: Hydrological and mechanical effects. In Proceedings of China-Europe Conference on Geotechnical Engineering: Volume 2, Cham: Springer International Publishing. 1287-1303 **(17 pages)**.
Ni, J.J.; Leung, A.K.; Ng, C.W.W.; Shao, W., (2018). Modeling hydro-mechanical reinforcements of plants to slope stability. Comput. Geotech., 95: 99–109 **(10 pages)**.
Ning, T.; Li, Z.;Feng, Q.; Chen, W.; Li, Z., (2020). Effects of forest cover change on catchment evapotranspiration variation in China. Hydrol. Process. 34: 2219–2228 **(9 pages)**.
Niyomukiza, J.B.; Eisazadeh, A.; Tangtermsirikul, S., (2023). Recent advances in slope stabilization using porous vegetation concrete in landslide-prone regions: A review. J. Build. Eng. 76: 1-22 **(22 pages)**.
Noviandi, R.; Gomi, T.; Sidle, R. C.; Ritonga, R. P.; Hasunuma, Y., (2022). Do Vegetation Root Systems Affect Landslide Mobility? A Flume Experiment. EGU General Assembly Conference Abstracts. EGU22-9004.
Obiazi, C.C.; Ojeifo, I.M., (2020). The relevance of Gmelina arborea (Roxb.) in agroforestry systems and medicine. J. Biodivers. Environ. Sci., 17(3): 1-6 **(6 pages)**.
Orwa, C.; Mutua, A.; Kindt, R.; Jamnadass, R.; Anthony, S., (2009). Agroforestry Database: A Tree Reference and Selection Guide Version 4.0. World Agroforestry Centre.
Oktaviano, Y., Sunaryo, Suryanto, A., (2015). Characterization of plant mango (Mangifera indica L.) cantek, ireng, empok, jempol in Tiron suburb, Banyakan district, Kediri. J. Prod. Tanam., 3(2): 91 – 97 **(7 pages)**.
Pachas, A.N.A.; Shelton, H.M.; Lambrides, C.J.; Dalzell, S.A.; Macfarlane, D.; Murtagh, G.J., (2016). Water use, root activity and deep drainage within a perennial legume-grass pasture: A case study in southern inland Queensland, Australia. Tropical Grasslands - Forrajes Tropicales. 4(3): 129–138 **(10 pages)**.
Patil, U.D.; Shelton III, A.J.; Aquino, E., (2021). Bioengineering solution to prevent rainfall-induced slope failures in tropical soil. Land, 10(299): 1-21 **(21 pages)**.
Perez, J.; Salazar, R.C.; Stokes, A., (2017). An open-access database of plant species useful for controlling soil erosion and substrate mass movement. Ecol. Eng., 99: 530-534 **(5 pages)**.
Phan, T.N.; Kraithong, P.; Likitlersuang, C.; Likitlersuang, S., (2024). A Comprehensive Study on Young Roots of Acacia mangium Willd. Species for Soil Bioengineering. Land Degrad. Dev., 35(17): 5124-5136 **(13 pages)**.
Phan, T.N.; Leung, A.K.; Nguyen, T.S.; Kamchoom, V.; Likitlersuang, S., (2025). Modelling root decomposition effects on root reinforcement and slope stability. Comput. Geotech., 179: 1-15 **(15 pages)**.
Phewnil, O.; Pattamapitoon, T.; Semvimol, N.; Wararam, W.; Duangmal, K.; Intaraksa, A.; Chunkao, K.; Maskulrath, P.; Hanthayung, S.; Wichittrakarn, P., (2024). Effects of landslide hazards on quality of stream water and sediments. Global J. Environ. Sci. Manage., 10(3): 1099-1116 **(18 pages).**
Pinheiro, R.C.; Bouillet, J.-P.; Pivello, V.R.; Aló, L.L.; Costa, V.E.; Meersche, K.V.D.; Guerrini, I.A.; Laclau, J.-P., (2021). Roots take up labeled nitrogen from a depth of 9 m in a wooded savanna in Brazil. Soil Biol. Biochem., 160: 1-8 **(8 pages)**.
Pinheiro, R.C; Deus Jr, J.C; Nouvellon, N.; Campoe, O.C.; Stape, J.L.; Aló, L.L.; Guerrini, I.A.; Jourdan, C.; Laclau, J.P., (2016). A fast exploration of very deep soil layers by Eucalyptus seedlings and clones in Brazil. For. Ecol. Manage., 366: 143 - 152 **(10 pages)**.
Purwono, N.A.S., (2022). Growth rate analysis Casuarina equisetifolia of the case study Pacitan and Samas coast area. IOP Conference Series: Earth Environ. Sci., 1095: 1-13 **(13 pages)**.
Qiu, D.; Xu, R.; Wu, C.; Mu, X.; Zhao, G.; Gao, P., (2022). Vegetation restoration improves soil hydrological properties by regulating soil physicochemical properties in the Loess Plateau, China. J. Hydrol., 609(3-4): 1-13 **(13 pages)**.
Quintarelli, V.; Radicetti, E.; Allevato, E.; Stazi, S.R.; Haider, G.; Abideen, Z.; Bibi, S.; Jamal, A.; Mancinelli, R., (2022). Cover Crops for Sustainable Cropping Systems: A review. Agriculture. 12: 2076: 1-21 **(21 pages)**.
Regan, T. J.; MacHunter, J.; Sinclair, S. J.; Bruce, M. J.; Neil, J.; Parker, E.;Nam, B., (2023). Structured decision making to navigate trade-offs between multiple conservation values in threatened grasslands. Conserv. Sci. Pract., 5(7): 1-15 **(15 pages)**.
Reichenbach, P.; Rossi, M.; Malamud, B.D.; Mihir, M.; Guzzetti, F., (2018). A review of statistically-based landslide susceptibility models. Earth-Sci. Rev., 180: 60–91 **(31 pages)**.
Ridwan, I.; Kadir, S.; Nurlina, N., (2024). Wetland degradation monitoring using multi-temporal remote sensing data and watershed land degradation index. Global J. Environ. Sci. Manage., 10(1): 83-96 **(14 pages).**
Rouge, A.; Adeux, G.; Busset, H.; Hugard, R.; Martin, J.; Matejicek, A.; Moreau, D.; Guillemin, J.; Cordeau, S., (2022). Weed suppression in cover crop mixtures under contrasted levels of resource availability. Eur. J. Agron., 136: 1-10 **(10 pages)**.
Salarian, S.; Asghari, O.; Abedi, M.; Alilou, S.K., (2020). Geostatistical-based geophysical model of electrical resistivity and chargeability data applied to image copper mineralization in the Ghalandar deposit, Iran. Int. J. Min. Geo-Eng., 54(2): 153-160 **(8 pages)**.
Saxton, K.E. and Rawls, W.J., (2006). Soil water characteristic estimates by texture and organic matter for hydrologic solutions. Soil Sci. Soc. Am. J., 70(5): 1569-1578 **(10 pages)**.
Sharma, P.; Singh, A.; Kahlon, C.S.; Brar, A.S.; Grover, K. K.; Dia, M.; Steiner, R. L., (2018). The role of cover crops towards sustainable soil health and agriculture—A review. Am. J. Plant Sci., 9: 1935-1951 **(16 pages)**.
Sittadewi, E.H.; Tejakusuma, M.; Mulyono, A.; Handayani, T.; Tohari, A.; Zakaria, Z., (2024). Post-landslide restoration through multistrata agroforestry-based land management in the West Bogor area of Indonesia. Trees For. People. 16: 1-12 **(12 pages)**.
Schmaltz, E.M.; Mergili, M., (2018). Integration of root systems into a GIS-based slip surface model: computational experiments in a generic hillslope environment. Landslides. 15: 1561–1575 **(15 pages).**
Song, X.; Tan, Y.; Lu, Y., (2024). Microscopic analyses of the

reinforcement mechanism of plant roots in different morphologies on the stability of soil slopes under heavy rainfall. Catena. 241: 1-15 **(15 pages)**.
Stokes, A.; Yildiz, A., (2023). The reinforcement of soil by plant roots. Encyclopedia of Soils in the Environment (Second Edition). 5: 115-122 **(12 pages)**.
Szota, C.; Sanjappa, S.; Fletcher, T.D.; Farrell, C., (2024). Larger shrubs can maintain high infiltration and evapotranspiration rates in experimental biofiltration systems impacted by high sediment loads. Urban For. Urban Green., 101: 1-10 **(10 pages)**.
Saifuddin, M and Normaniza, O., (215). Rooting characteristics of some tropical plants for slope protection. J. Trop. For. Sci., 28(4): 469–478 **(10 pages)**.
Taib, A.M.; Taha, M.R.; Rahman, N.A.; Yazid, M.R. M.; Khoiry, M.A., (2020). The effect of soil-root interaction by vetiver grass on slope stability. J. Eng. Sci. Technol., 15: 46–57 **(12 pages)**.
Tejakusuma, I.G.; Sittadewi, E.H.; Handayani, T.; Hernaningsih, T.; Wisyanto, W.; Rifai, A., (2024). Root growth and arbuscular mycorrhizal fungi on woody plants for vegetative stabilization of tropical slopes. Global J. Environ. Sci. Manage., 10(1): 267-286 **(10 pages).**
Tsige, D.; Senadheera, S.; Talema, A., (2019). Stability analysis of plant-root-reinforced shallow slopes along mountainous road corridors based on numerical modelling. Geosciences. 10(1): 1-19 **(19 pages)**.
Truong, P. and Vanoh, R., (2021). The role of Vetiver grass in protecting unstable slopes. Agrikultura CRI J., 2(1): 16-23 **(19 pages)**.
Tardio, G.; Mickovski, S.B.; Rauch, H.P.; Fernandez, J.P.; Acharya, M.S., (2018). The Use of Bamboo for Erosion Control and Slope Stabilization: Soil Bioengineering Works. Bamboo - Current and Future Prospects. Chapter 7. 105-132 **(27 pages)**.
Utomo, B.; Manalu, H.; Dalimunthe, A., (2019). Root Morphological Analysis of 10 Forest Tree Species in an Effort to Design a Rooter System in the Bukit Barisan Forest. Proc. 1st Int. MIPAnet Conf. Sci. Math., 1: 117-124 **(8 pages)**.
Van Lanen, N.J.; Duchardt, C.J.; Pejchar, L.; Shyvers, J.E.; Aldridge, C.L., (2025). Considering multiecosystem trade-offs is critical when leveraging systematic conservation planning for restoration. Global Change Biol., 31(1): 1-8 **(8 pages)**.
Verma, S., (2016). A review study on Leucaena leucocephala: A multipurpose tree. International J. Sci. Res. Sci. Eng. Technol., 2(2): 103-105 **(3 pages)**.
Vick, L.M.; Böhme, M.; Rouyet, L.; Bergh S.G.; Corner, G.D.; Lauknes T.R., (2020). Structurally controlled rock slope deformation in northern Norway. Landslides. 17: 1745–1776 **(32 pages)**.
Voigtlaender, M.; Brandani, C.B.; Caldeira, D.R.M.; Tardy, F., (2019). Nitrogen cycling in monospecifc and mixed-species plantations of *Acacia mangium* and *Eucalyptus* at 4 sites in Brazil. For. Ecol. Manage., 436: 56–67 **(2 pages)**.
Wang, X.; Hong, M.M.; Huang, Z.; Zhao, Y.F.; Ou, Y.S.; Jia, H.X.; Li, J., (2019). Biomechanical properties of plant root systems and their ability to stabilize slopes in geohazard-prone regions. Soil Tillage Res., 189: 148–157 **(10 pages)**.
Wang, X.; Ma, C.; Wang, Y.; Wang, Y.; Li, T.; Dai, Z.; Li, M., (2020). Effect of root architecture on rainfall threshold for slope stability: variabilities in saturated hydraulic conductivity and strength of root-soil composite. Landslides. 17: 1965–1977 **(13 pages)**.
Wang, H.; Zhang, G.; Li, N.; Zhu, P., (2020). Variation in soil erosion resistance of slips deposition zone with progressive vegetation succession on the Loess Plateau. China J. Soils Sediments. 20: 234-248 **(15 pages)**.
Weil, R.R.; Brady N. C., (2017). The Nature and Properties of Soils, 15th. Ed. Pearson Education.
Yang, B.; Lee, D.K.; Heo, H.K.; Biging, G., (2019). The effects of tree characteristics on rainfall interception in urban areas. Landsc. Ecol. Eng., 15: 289–296 **(8 pages)**.
Yazdani, F.; AliPanahi, P.; Sadeghi, H., (2024). A comparative study of environmental and economic assessment of vegetation-based slope stabilization with conventional methods. J. Environ. Manage., 359:121002.
Yildiz, A.; Graf, F.; Springman, S.M., (2019). An investigation of plant-induced suction and its implications for slope stability. Themed issue on the 5th Italian Workshop on Landslides. 172(6): 520-529 **(10 pages)**.
Yin, W.; Pan, Y.; Yang, M.; Li, Z., (2024). The root reinforcement on the slope under the condition of colonization of various herbaceous plants. Heliyon, 10: 1-12 **(12 pages)**.
Zayadi, R.; Putri, C.A.; Irfan, M.N.; Kusuma, Z.; Leksono, A.S.; Yanuwiadi, B., (2022). Soil reinforcement modelling on a hilly slope with vegetation of five species in the area prone to landslide in Malang, Indonesia. Environ. Res. Eng. Manage., 78(3): 56-72 **(17 pages)**.

AUTHOR (S) BIOSKETCHES

ejakusuma, I.G., Dr., Professor, Research Center for Geological Disaster, National Research and Innovation Agency, Indonesia.
- Email: *iwan004@brin.go.id*
- ORCID: 0000-0002-2660-4828
- Web of Science ResearcherID: 2655-2023
- Scopus Author ID: 6504148333
- Homepage: https://brin.go.id/

Sittadewi, E.H., M.Sc., Senior Researcher, Research Center for Geological Disaster, National Research and Innovation Agency, Indonesia.
- Email: *euth001@brin.go.id*
- ORCID: 0000-0002-3061-9758
- Web of Science ResearcherID: 2865-2023
- Scopus Author ID: 57200330811
- Homepage: https://brin.go.id/

Mulyono, A., Dr., Senior Researcher, Research Center for Environmental and Clean Technology, National Research and Innovation Agency, Indonesia.
- Email: *asep033@brin.go.id*
- ORCID: 0000-0002-4403-5948
- Web of Science ResearcherID: NA
- Scopus Author ID: 57201061998
- Homepage: https://brin.go.id/

AUTHOR (S) BIOSKETCHES

Handayani, T., Dr., Professor, Research Center for Sustainable Production System and Life Cycle Assessment, National Research and Innovation Agency, Indonesia.
- Email: *asep033@brin.go.id*
- ORCID: 0000-0002-4403-5948
- Web of Science ResearcherID: NA
- Scopus Author ID: 58170210000
- Homepage: https://brin.go.id/

Tohari, A., Dr., Senior Researcher, Research Center for Geological Disaster, National Research and Innovation Agency, Indonesia.
- Email: *adri001@brin.go.id*
- ORCID: 0000-0002-6662-0697
- Web of Science ResearcherID: NA
- Scopus Author ID: 16235175900
- Homepage: https://brin.go.id/

Fatahillah, H.E.H., M.GeoSc., Junior Researcher, Research Center for Mining Technology, National Research and Innovation Agency, Indonesia.
- Email: *hilm006@brin.go.id*
- ORCID: 0009-0007-6403-9835
- Web of Science ResearcherID: NA
- Scopus Author ID: 58934858500
- Homepage: https://brin.go.id/

Zakaria, Z., Dr., Associate Professor, Faculty of Geological Engineering, Universitas Padjadjaran, Indonesia.
- Email: *zufialdi.zakaria@unpad.ac.id*
- ORCID: 0000-0001-5670-0813
- Web of Science ResearcherID: NA
- Scopus Author ID: 56909598300
- Homepage: https://ftgeologi.unpad.ac.id/

Budiman, E.B., Dipl.Ing., Senior Engineer, Research Center for Mining Technology, National Research and Innovation Agency, Indonesia.
- Email: *even001@brin.go.id*
- ORCID: 0009-0000-3756-5150
- Web of Science ResearcherID: NA
- Scopus Author ID: 57225940187
- Homepage: https://brin.go.id/

Utami, N., M.Sc., Senior Researcher, Research Center for Sustainable Production System and Life Cycle Assessment, National Research and Innovation Agency, Indonesia.
- Email: *rrno001@brin.go.id*
- ORCID: 0009-0006-2813-0685
- Web of Science ResearcherID: NA
- Scopus Author ID: 57225386223
- Homepage: https://brin.go.id/

HOW TO CITE THIS ARTICLE

Tejakusuma, I.G.; Sittadewi, E.H.; Mulyono, A.; Handayani, T.; Tohari, A.; Fatahillah, H.E.H.; Zakaria, Z.; Budiman, E.B.; Utami, N., (2025). A spatial slip plane-based vegetation model for slope reinforcement and shallow landslide mitigation. Global J. Environ. Sci. Manage., 11(3): 875-896.

DOI: 10.22034/gjesm.2025.03.02

URL: https://www.gjesm.net/article_722401.html

Global J. Environ. Sci. Manage. 11(3): 897-914, Summer 2025, Serial #43

Global Journal of Environmental Science and Management
(GJESM)

Homepage: https://www.gjesm.net/

Podcasts

ORIGINAL RESEARCH PAPER

The potential of carbon emission reduction through the transition to battery electric vehicles

W. Kongwee[1], W. Achariyaviriya[2,3,*], D. Rinchumphu[4], P. Suttakul[5], A. Achariyaviriya[5], N. Chanpichaigosol[5], V. Vichiensan[6], M. Kii[7], P. Iamtrakul[8], Y. Hayashi[9]

[1] *Integrated Science Program Multidisciplinary and Interdisciplinary School, Chiang Mai University, Chiang Mai, Thailand*

[2] *Department of Electrical Engineering, Faculty of Engineering, Chiang Mai University, Chiang Mai, Thailand*

[3] *Research Unit for City Environment and Disaster Management, Chiang Mai University, Chiang Mai, Thailand*

[4] *Department of Civil Engineering, Faculty of Engineering, Chiang Mai University, Chiang Mai, Thailand*

[5] *Department of Mechanical Engineering, Faculty of Engineering, Chiang Mai University, Chiang Mai, Thailand*

[6] *Department of Civil Engineering, Faculty of Engineering, Kasetsart University, Bangkok, Thailand*

[7] *Division of Sustainable Energy and Environmental Engineering, Graduate School of Engineering, Osaka University, Osaka, Japan*

[8] *Center of Excellence in Urban Mobility Research and Innovation, Faculty of Architecture and Planning Thammasat University, Khlong Luang, Pathumthani, Thailand*

[9] *Tokai Gakuen University, 2-901 Nakahira, Tenpaku-ku, Nagoya 468-8514, Japan*

ARTICLE INFO

Article History:
Received 08 March 2025
Revised 16 May 2025
Accepted 20 June 2025

Keywords:
Agent-based transport simulation
Battery electric vehicle
Carbon emissions assessment
Internal combustion engine vehicle

ABSTRACT

BACKGROUND AND OBJECTIVES: Thailand is a significant emitter of greenhouse gases especially emissions from the energy sector, originated from the transportation sector. The government is prioritizing carbon reduction efforts in Thailand; concurrently, the battery electric vehicle industry is experiencing global growth. It stresses the need to decrease carbon emissions in transportation by moving towards battery electric vehicles. Conversely, Thailand lacks a comprehensive understanding of how battery electric vehicles influence carbon emissions. The study objectives were to explore the carbon reduction potential of the transition to electric vehicles and develops methods for estimating carbon emissions using micro-simulations.

METHODS: The Multi-Agent Transport Simulation was used for simulation of the traffic in Phuket, Thailand. There were two attributes for simulation: a road network and an agent's plan. The road network contained details of road segments in Phuket. The agent's plan comprised trips for Phuket residents, formulated from population assumptions based on survey data. The simulation model was validated against actual traffic reports from main roads in Phuket and used to estimate carbon emissions at the individual level. Subsequently, scenarios were created by analyzing the proportions of internal combustion engine vehicles in relation to battery electric vehicles on the network to evaluate carbon emissions.

FINDINGS: The model captures general travel behavior trends. Despite moderate alignment between simulated and observed traffic speeds and trip durations, the model demonstrates reasonable validity for representing typical travel behavior in Phuket. Nonetheless, the modest coefficient of determination value, along with the exaggerated trip durations, points to possible constraints in the network intricacies and population estimates. For carbon emission estimation, the emission trend exhibited an approximately linear relationship. Increasing the proportion of battery electric vehicles to 10 per cent resulted in an approximate 7 per cent reduction in total carbon emissions. Notably, emissions from internal combustion engine vehicles decreased by roughly 10 percent, in contrast to the 3 percent increase in emissions from battery electric vehicles.

CONCLUSION: Model accuracy could be enhanced by incorporating more detailed input data, including a greater variety of vehicle types, and a more complete transport network (such as minor roads). Furthermore, thorough survey data encompassing population activity times, home addresses, and workplace coordinates would significantly boost the model's performance. Even though the model can provide any probability of battery electric vehicle proportion. In the practical way, an optimal proportion depends on subsidization from government departments. The anticipated outcomes are intended to serve as guidelines for detailed planning policies focused on enhancing the quantity of battery electric vehicles and minimizing carbon output in Thailand's transportation system.

DOI: 10.22034/gjesm.2025.03.03

This is an open access article under the CC BY license (http://creativecommons.org/licenses/by/4.0/).

NUMBER OF REFERENCES
35

NUMBER OF FIGURES
9

NUMBER OF TABLES
4

*Corresponding Author:
Email: *witsarut.a@cmu.ac.th*
Phone: +66 5394 4140
ORCID: 0000-0002-1832-0761

Note: Discussion period for this manuscript open until Sep 1, 2025 on GJESM website at the "Show Article".

INTRODUCTION

According to the Global Climate Change Risk Index 2021, Thailand was ranked as the ninth most vulnerable country to the impact of climate change (Eckstein *et al.,* 2021). This vulnerability underscores the critical requirement for Thailand to transition toward a low-carbon society (Tangkitvanich, 2023). The electric power and transportation sectors rank as the top two sources of greenhouse gas (GHG) emissions, which are crucial targets for initiatives focused on emissions reduction (Energy Policy and Planning Office, 2024; Santoso *et al.,* 2024; Nassef *et al.,* 2025). In response to the need for reducing emissions in the transportation sector, the government introduced the "30@30" policy framework. This policy aims to increase battery electric vehicle (BEV) production to 30 percent of total manufacturing by 2030. This initiative fosters the growth of zero-emission vehicles (ZEVs) and backs initiatives aimed at decreasing carbon emissions in the transportation sector (Energy Policy and Planning Office, 2021). Regarding to Phuket province, it encompasses a total area of approximately 570.034 square kilometers, incorporating its surrounding islands. Administratively, it is divided into three districts: Mueang Phuket, Kathu, and Thalang. These districts encompass seventeen sub-districts and 96 villages. The province's total population stands at 417,891, consisting of 197,101 males and 220,790 females, resulting in an average population density of 769.55 people per square kilometer. The main economic sector is tourism. Phuket's gross provincial product (GPP) reaches 99,545 million Baht, with a per capita GPP of 165,343 Baht. The province hosts approximately 1,236,480 tourists annually, facilitated by an infrastructure of 1,405 hotels and accommodations. Healthcare services are robust, with nine hospitals and 21 Sub-district Health Promoting Hospitals (HPHs) available to residents and visitors. Education features 118 schools and two universities (Phuket Provincial Statistical Office, 2023). Given the information above, Phuket has been selected to develop as the pilot smart city to promote the economy and quality of life (Poolsawud, 2017). It is noteworthy that Phuket serves as an appropriate pilot study for the potential for reducing GHG emissions. In order to effectively decrease GHG emissions, precise measurement is an essential initial step, acting as a benchmark for analyzing and creating reduction strategies. Traditionally, GHG emissions from the transportation sector are estimated using either a top-down or bottom-up approach. The top-down approach calculates emissions based on the total fuel consumed, providing relatively accurate results. However, it faces challenges in assessing GHG emissions within a hypothetical context that entails modifications in traffic or travel behavior, due to its insufficient resolution to capture dynamic traffic situations. On the other hand, the bottom-up approach estimates emissions using activity data, such as vehicle kilometers traveled (VKT), offering greater flexibility for modeling behavior- or policy-driven scenarios. Moreover, this technique works well with microscopic simulation models, yielding outputs in the form of comprehensive activity data. In this study, a microsimulation-based approach is proposed to establish a baseline of transportation activity data. Real-world fuel efficiency functions are then applied to estimate fuel consumption and greenhouse gas (GHG) emissions. Scenarios involving different proportions of internal combustion engine vehicles (ICEVs) and BEVs are analyzed to assess their impact on emission outcomes. Furthermore, the relationship between the increasing share of BEVs and the corresponding rate of GHG emission reduction is investigated. The findings deliver insights that can bolster data-driven approaches to sustainable transportation planning. This study aims to assess the potential for carbon reduction from the transition to electric vehicles and to develop microsimulation-based methods for estimating carbon emissions. The research was conducted in Phuket Province, Thailand, in 2022.

Influenced factor on vehicle energy consumption

Vehicle energy consumption is influenced by several factors, which can be broadly categorized into four groups: ambient temperature, route characteristics, driving behavior, traffic speed. The heating, ventilation, and air conditioning (HVAC) system is impacted by ambient temperature since vehicles must expend energy to keep the interior comfortable (Li *et al.*, 2016). Furthermore, route characteristics significantly impact energy consumption. The overall distance of the route, with longer distances requiring more energy and elevation changes, where uphill segments increase energy use. The condition of the road surface, especially if it is subpar, can elevate

Table 1: Summary of related studies on factors influencing vehicle energy consumption

Countries	Route-related factors				Behavior-related factors							Sources
	Urban route	Rural route	Road slope	Traffic speed	HVAC	Velocity	Acceleration	Payload	ICEV	HEV	BEV	
Australia	✓	✓	✓	✓	✓	✓	✓				✓	Li *et al.* (2016)
China	✓	✓		✓	✓						✓	Ma *et al.* (2021)
China	✓			✓	✓	✓	✓				✓	Zhang *et al.* (2019)
Thailand	✓	✓	✓		✓	✓	✓	✓	✓	✓	✓	Janpoom *et al.* (2023)
USA, Italy, Belgium	✓	✓		✓		✓	✓	✓	✓		✓	Fiori *et al.* (2019)

energy usage due to additional resistance and the requirement for slower speeds. The layout and complexity of the route, including whether it is straight or involves many turns, affect energy efficiency. Speed limits, along with the average speed sustained on the road, are important factors, with steady speeds proving to be more energy efficient (Ma *et al.*, 2021). Drivers' behavior is response, particularly in how they apply acceleration and braking. According to Zhang *et al*. (2019), the combination of low acceleration and low deceleration is linked to the least energy consumption, while high acceleration and high deceleration patterns are associated with the greatest energy expenditure. These findings indicate that smoother driving behavior, characterized by more moderate use of the accelerator and brake pedals, can effectively reduce energy use. Traffic speed significantly affects energy consumption rates, with different effects observed between BEVs and ICEVs powertrains. Compared to ICE vehicles, BEVs are more energy-efficient at low-speed traffic due to regenerative braking and high part-load powertrain efficiency. The variation in energy consumption at low versus high traffic speeds is considerably more pronounced in ICEVs than in BEVs (Fiori *et al.*, 2019). Additionally, vehicle payload has been found to have a minor effect on energy consumption (Janpoom *et al.*, 2023). As shown in Table 1, a variety of studies provide valuable information regarding the dynamics of energy use in vehicles across different nations. The route characteristics commonly considered include route types (urban and rural), slope, and traffic speed. Furthermore, a number of behavior-related elements are commonly studied, including HVAC, velocity, acceleration, and payload. Various powertrain types are also considered. In this paper, an analysis is conducted focusing on the following factors: urban routes, traffic speed, and two types of powertrains—ICEVs and BEVs.

Macroscopic evaluation of GHG emissions

The Intergovernmental Panel on Climate Change (IPCC) provides a guideline for estimating GHG emissions through a tiered framework of increasing accuracy and data requirements (IPCC, 2019). In Tier 1, default emission factors and straightforward national data are utilized. Conversely, Tier 2 incorporates country-specific emission factors and more intricate data for greater accuracy. Tier 3 involves the most advanced methods, using detailed models or measurements with high-resolution, location-specific data for the highest accuracy. Furthermore, the Global Protocol for Community-Scale Greenhouse Gas Emission Inventories (GPC) provides a standardized framework for cities to measure and report their GHG emissions. The GPC categorizes emissions into three scopes based on their source and relationship to the city boundary. Scope 1 covers all direct GHG emissions from sources found within the boundaries of the city. Scope 2 relates to indirect emissions that occur due to the consumption of electricity provided by the grid. Scope 3 encompasses all other indirect emissions that occur beyond the city boundary but are driven by activities taking place within the city. Angin *et al.* (2022) examine GHG emissions from everyday motorized vehicles in Jember, East Java,

Indonesia. The analysis was based on secondary data collected between 2018 and 2020, focusing on vehicle counts, classifications, and projections for the year 2030. The analysis revealed that by 2030, carbon emissions from daily vehicles in Jember are expected to reach 3.85 megatons of carbon dioxide equivalent ($MtCO_2eq$). Motorcycles are predicted to be the primary contributors, with an estimated emission of 2.06 $MtCO_2eq$ by 2030. Emissions from vehicles on eight main streets in Jember ("Golden Triangle") GPC with global gridded were predicted to total 62,190.52 tons of carbon dioxide equivalent ($tonCO_2eq$) in 2030. The GHG transportation emissions in the city boundary are in scope 1. Ahn *et al.* (2023) assessed fossil fuel carbon dioxide ($FFCO_2$) emissions from 78 global cities in the C40 network. They compared city-reported inventories with global emission datasets, namely the Emissions Database for Global Atmospheric Research (EDGAR) and the Open-source Data Inventory for Anthropogenic CO_2 (ODIAC). The study examines Scope 1 emissions across five key major sectors: residential, commercial, industrial, energy, and transportation. Results indicate that the total annual $FFCO_2$ emissions from these cities amount to approximately 890 $MtCO_2eq$. On average, transportation is the largest contributor, accounting for 51 percent (%) of citywide $FFCO_2$ emissions. Furthermore, transportation can be considered Scope 3 when outside transportation is necessitated by city activities. Wiedmann *et al.* (2021) presented a comprehensive assessment of Scope 1, 2, and 3 greenhouse gas emissions for 79 global C40 cities using a city-specific multiregional input–output model. The study reveals that total emissions amount to 4.4 Gigatons of carbon dioxide equivalent ($GtCO_2eq$), with Scope 3 emissions alone contributing 1.8 $GtCO_2eq$. This constitutes roughly 41% of the city's total emissions, underscoring the important influence of consumption-based emissions that happen outside the city's limits. Emissions were categorized into seven sectors, with transport accounting for 15% of Scope 3 emissions, making it one of the top contributors alongside electricity and food. The results underscores that an exclusive focus on territorial emissions (Scopes 1 and 2) fails to capture the full extent of urban climate consequences. Integrating Scope 3 is essential for effective low-carbon infrastructure and consumption strategies. Jia *et al.* (2018) studied GHG emissions in Nanning, using the GPC framework to calculate emissions across various sectors. For instance, they include industrial energy, transportation, household and commercial energy, industrial processes, and waste management. The analysis underscored the necessity of taking into account both direct emissions and emissions from electricity consumption. The study found that Nanning's total GHG emissions grew from 6.56 $MtCO_2eq$ in 1994 to 55.44 $MtCO_2eq$ in 2015, with an average annual increase rate of 10.69%. The major contributors to emissions were industrial energy consumption (29.72-61.09%), transportation (10.75-41.87%), and industrial processes (7.40-14.99%). Over 90.94% of Nanning's emissions were related to coal usage throughout the study period (1994-2015). Table 2 provides a summary of relevant studies on the application of the GPC Framework for assessing macroscopic GHG emissions.

GHG emissions evaluation using microsimulation

Macroscopic approaches for estimating GHG emissions in the transportation sector typically rely on aggregated activity data, such as fuel sales or VKT, combined with average emission factors. The methods specified in the IPCC and GPC frameworks are advantageous for national or city-wide inventories; however, they have limitations in accurately reflecting the dynamic characteristics of real-world traffic and driver behavior. Therefore, macroscopic methods are not capable of providing detailed emission estimates at the trip or activity level within a city, making them unsuitable for analyzing trip-level policies or regulatory measures. Improving accuracy can be achieved by directing the study towards a microscopic scale, thus positioning microsimulation, which centers on agent-based transport simulation, as an alternative method for estimating carbon emission. A rising collection of studies has attempted to assess carbon emissions in urban transport by employing various modeling strategies. Rostami-Shahrbabaki *et al.* (2021) investigated the impact of increasing BEV adoption on urban carbon emissions through a microsimulation-based model applied to the city of Munich. By integrating both microscopic and macroscopic emission modeling techniques, the study evaluated six scenarios with BEV shares ranging from 0.5% to 100%. Results demonstrated a linear decline in Tank-to-Wheel (TTW) emissions as BEV adoption increased, culminating in zero local

Table 2: Overview of studies applying the GPC framework for macroscopic GHG emission assessment

Cities	Scopes			Sectors							Sources
	1	2	3	Residential	Commercial	Industrial	Construction	Energy	Transportation	Waste	
Jember, Indonesia	✓								✓		Angin *et al.* (2022)
C40 Cities	✓			✓	✓	✓		✓	✓		Ahn *et al.* (2023)
C40 Cities	✓	✓	✓	✓		✓	✓	✓	✓		Wiedmann *et al.* (2021)
Nanning, China	✓	✓		✓	✓	✓		✓	✓	✓	Jia *et al.* (2018)

emissions under a fully electrified fleet. Using the microsimulation technique, it was estimated that internal combustion engine vehicles have around 15% higher fuel consumption and carbon emissions in comparison to macroscopic models. This highlights the influence of detailed driving behavior modeling. Moreover, energy consumption for BEVs was shown to be 40% lower in the microscopic model, primarily due to regenerative breaking, which accounted for about 25% in energy savings. However, well-to-tank (WTT) emissions initially increased with greater EV penetration due to the carbon intensity of electricity generation. A key drawback of this study is the insufficient model validation. Conversely, Ma *et al.* (2015) examined the future of transport-related carbon emissions in Beijing by developing a spatial population microsimulation framework. This study merged extensive demographic statistics with travel survey data to assess individual travel patterns and emissions in the city from 2000 to 2010, and to project future trends up to 2030. Several policy scenarios were tested, including investments in public transport, compact urban development, and the adoption of low-emission vehicle technologies. The findings revealed that the combination of several policy interventions has the potential to decrease transport-related carbon emissions by up to 43% relative to the typical business-as-usual scenario. Validation of the model was conducted using independent traffic count data and modal share statistics, affirming its reliability in illustrating both spatial and temporal emission patterns. The methodology developed by Hasan *et al.* (2022) utilizes microsimulation to evaluate the long-term environmental consequences of various urban traffic management strategies. The research was carried out on a 3.5-kilometer stretch of the E10 highway in Abu Dhabi, United Arab Emirates. This area is characterized by high traffic density and a strong reliance on private vehicles, which make up approximately 80% of the modal share. The study simulated four scenarios: a business-as-usual case, a conventional bus service, a bus rapid transit (BRT) system, and an autonomous vehicle-based bus rapid transit (AV-BRT) system. The outcomes revealed that the AV-BRT scenario attained the greatest reductions in environmental impact by the year 2045. These reductions included decreases in energy consumption, CO_2 emissions, nitrogen oxides (NO_x) emissions, and particulate matter (PM) emissions compared to the baseline scenario. The models were validated using real 2015 traffic data. Lastly, Makridis *et al.* (2020) used a microsimulation model to evaluate emissions resulting from different vehicle technologies. These included human-driven vehicles, automated vehicles (AVs), and connected and automated vehicles (CAVs). While CAVs demonstrated improved traffic flow and reduced emissions relative to AVs, they still exhibited higher emissions per kilometer compared to human-driven vehicles. The study underscored the necessity of realistic vehicle dynamics modeling, pointing out that standard car-following models frequently exaggerate acceleration, which results in flawed emissions calculations. Validation was performed using the European EMEP/EEA emissions inventory model and the CO_2MPAS model both of which are standard in EU vehicle certification. Furthermore, the study incorporated the Microsimulation Free-flow Acceleration Model (MFC), validated against real-world acceleration data from thousands of vehicles across Europe. This analysis utilizes microsimulation to investigate a range of assumptions in multiple cities worldwide (Table 3). It is interesting to note that

Table 3: Research related to microsimulation

Validation	Cities	Analysis	Assumption	Sources
-	Munich, Germany	Impact of increasing the number of EVs	Increase of EVs can significantly decrease carbon.	Rostami-Shahrbabaki *et al.* (2021)
Independent traffic count data, modal share statistics	Beijing, China	Estimate and project transport-related carbon emissions	Future demographic, travel behavior, and policy impacts influence emission trends	Ma *et al.* (2015)
Real 2015 traffic data	Abu Dhabi, UAE	Evaluate impacts of different urban traffic management	AV-BRT scenario reduces environmental impact	Hasan *et al.* (2022)
Real-world acceleration data	Antwerp, Belgium	Analyze the impact of AVs and CAVs on traffic and carbon	CAVs improve traffic flow better than AVs. CAVs reduce carbon more than AVs	Makridis *et al.* (2020)

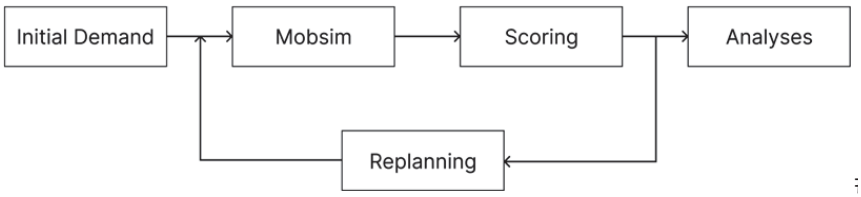

Fig. 1: MATSim framework

the important data needed to do microsimulation are road networks and the travel behavior of the population. The models will undergo validation using actual traffic reports and demographic density data. Subsequently, statistical values will be utilized for evaluation in the validation process. This study uses a microsimulation model by using road networks and the travel behavior of Phuket in an agent-based mobility simulation.

Multi-agent transport simulation (MATSim)

MATSim (Horni *et al.*, 2024) is an agent-based mobility simulation on a virtual transport network based on travel demand scenarios as indicated in Fig. 1. This tool can simulate and examine the traffic features in the virtual transport network throughout spatial and temporal dimensions. Each agent in MATSim consistently optimizes its daily activity plan while vying for space-time slots against all other agents on the transportation network. This approach is akin to the iterative cycle of route assignment, yet it advances by including various choice (Ziemke *et al.*, 2021), mode choice (Hörl, 2021), or destination choice (Briem *et al.*, 2019) into the iterative loop.

The primary demand stems from the daily activity sequences of the population in the study area, which are obtained from empirical data via sampling or discrete choice modeling. Every agent possesses a memory containing a fixed number of day plans, each plan composed of a daily activity chain and an associated score, which is interpreted as an econometric utility. Thus, each agent optimizes this initial demand individually. MATSim mobility simulation (mobsim) generates route planning (Ziemke *et al.*, 2015). All agents chooses a plan from its memory, based on the plan scores. QSim serves as the default method for conducting mobsim. It operates on a queue-based and time-step approach. Upon an agent entering a link from an intersection, it gets appended to the end of the current waiting queue. The agent remains in this position until the required time for traversing the link at free-flow conditions has elapsed, until it reaches the forefront of the waiting queue, and until it can proceed onto the subsequent link. Entry of an agent is prohibited if the link's storage capacity is exceeded. Scores are assessed following every simulation run, reflecting the effectiveness of the executed plans. Typically, a fraction of the agents, often around 10 percent, are granted the opportunity to duplicate their selected plan and undergo replanning. Replanning, four dimensions are usually considered for MATSim: departure time (Ziemke *et al.*, 2021), route (Zhuge et al. 2021), mode (Hörl, 2021), and destination (Tchervenkov et al., 2020). Replanning of MATSim provides various methods for adjusting plans. These

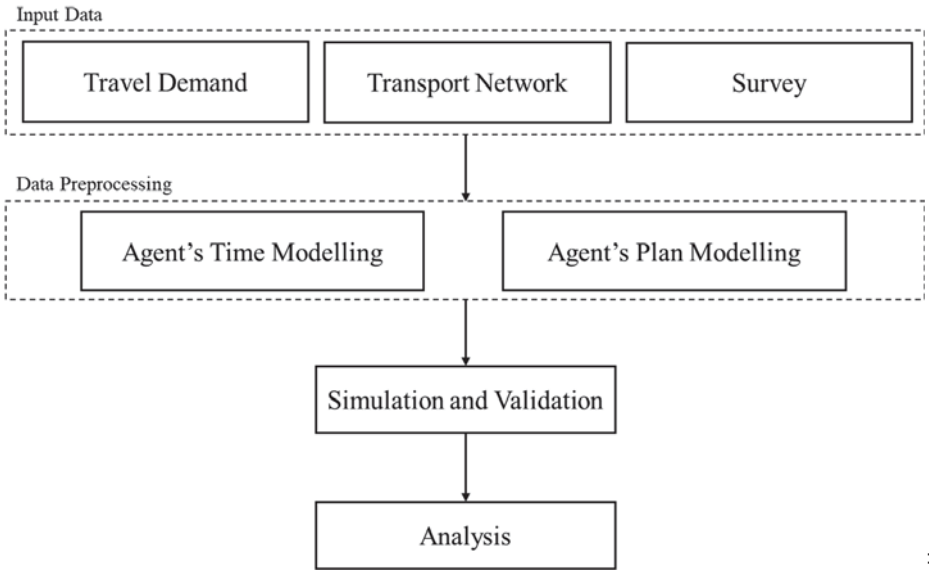

Fig. 2: Research framework.

methods include random changes, approximate recommendations, and solutions to find the best current option in each iteration.

MATERIALS AND METHODS

The methodology consists of four main components: input data collection, data preprocessing, simulation and validation, and analysis. The overall research workflow is illustrated in Fig. 2. The input data includes five essentials datasets which comprises of the travel demand, the road network, traffic analysis zone (TAZ), point of interests (POIs), and questionnaire survey. Input data passes preprocessing in the next step, which consists of two processes: agent time modeling and agent plan modeling. Agent time modeling establishes the starting times for agents' commutes to their workplaces and their return home. Agent plan modeling generates the geographic coordinates of residential locations and workplaces. Subsequently, the agents' plans are synthesized by integrating spatial coordinates with time profiles. Once the agent plans are finalized, they are utilized as inputs within the simulation model, together with the road network. The outcomes of the simulation are then validated against reported traffic data.

Input data

The travel demand, TAZ, and road network data were obtained from the Feasibility Study on Engineering, Economic, and Financial Viability, and Environmental Impact Assessment for the Muang Mai, Koh Kaew, Kathu Expressway Project (Expressway Authority of Thailand, 2023). The Origin-Destination (O-D) matrix indicates the number of trips made per day between each pair of zones, as illustrated in Fig. 3(a). The TAZ data of Phuket consists of 341 zones, each associated with corresponding population data, as shown in Fig. 3(b). Covering about 700 kilometers, the Phuket Road network is situated in an area of 543 square kilometers. It provides information on each road segment, including lengths, road capacities, and free-flow speeds. The road network is shown in Fig. 3(c). The POI data, obtained from OpenStreetMap (OSM), included both the geographic locations and place types used to indicate activity location, as shown in Fig. 3(d). Questionnaire survey data were obtained from the Phuket Air-Front Smart City as a Business-Life Regenerative Innovation Gateway Hub for Transformation (AIR SC-BRIGHTER 2050) project (Hayashi et al., 2022), which include information on individuals' departure times to workplaces. Furthermore, the spatial and demographic features of Phuket were included to enhance the spatial analysis of environmental effects in travel behavior modeling (Raungratanaamporn *et al.*, 2024).

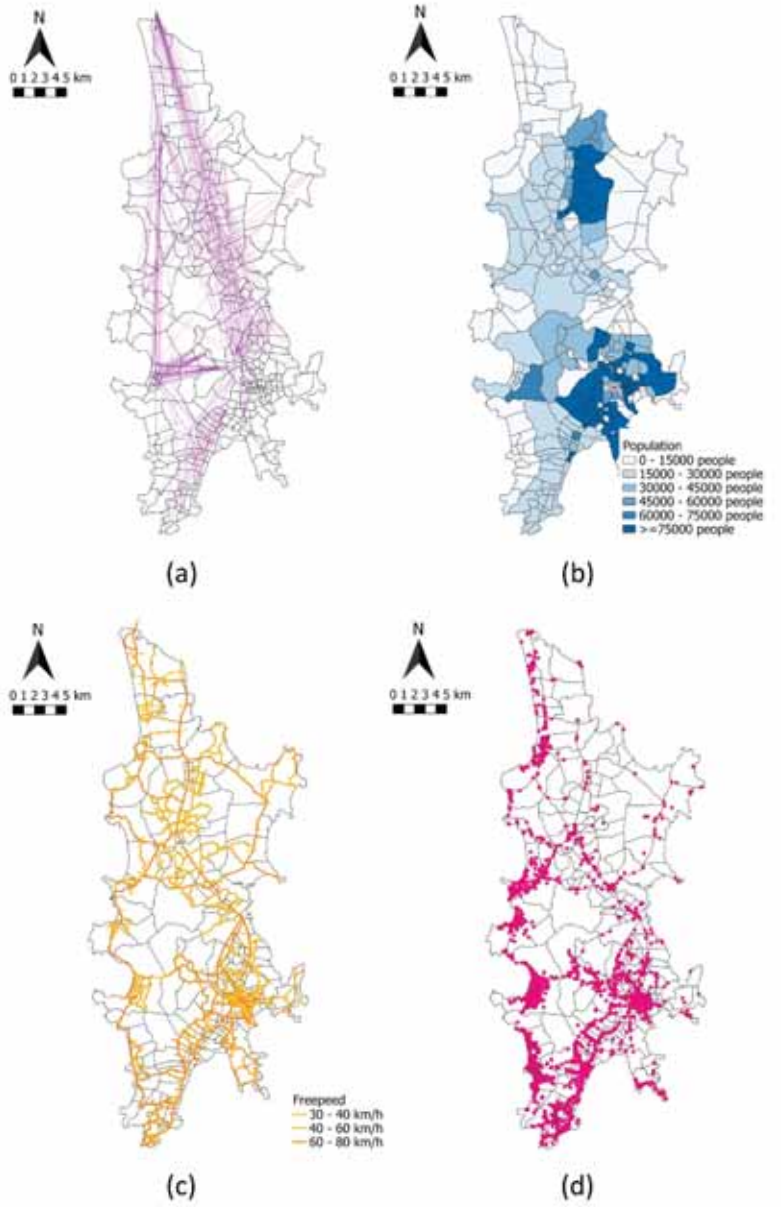

Fig. 3: Input data for preprocessing (a) interzone demands travel between zones more than 120 trips per day, (b) spatial distribution of population density, (c) road networks, (d) spatial distribution of activity

Agent time modelling

The departure time for individuals commuting to work is shown as a histogram in Fig. 4(a), based on data from the questionnaire survey. The departure time distribution that was observed is estimated by fitting a log-normal distribution. Nevertheless, due to the absence of return time data from the survey, the return time distribution is assumed based on peak traffic demand as reported by Expressway Authority of Thailand (2023). Fig. 4(b) displays the fitted curves for both departure and return.

Agent's plan modelling

In this study, agents represent the population of Phuket. Each agent's home location is assigned through a two-step process. First, a zone is selected

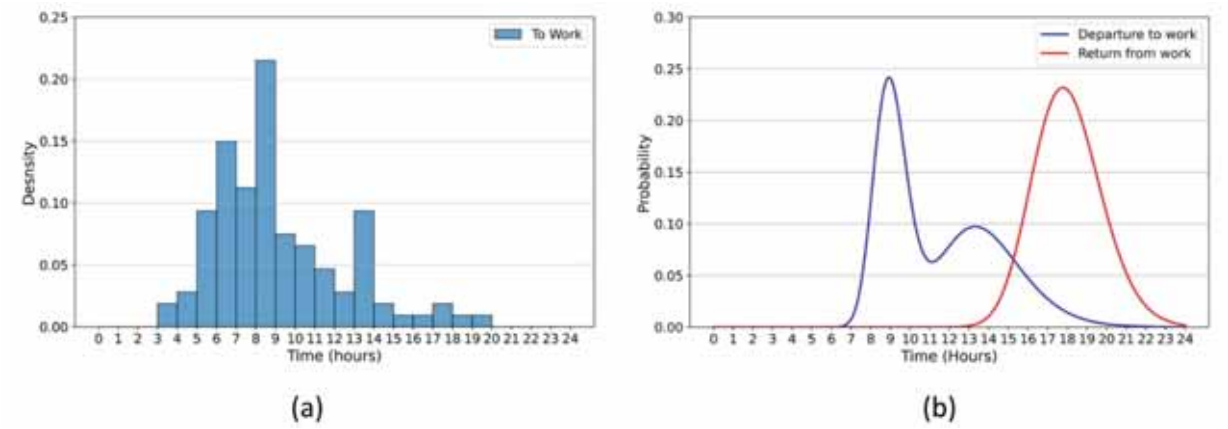

Fig. 4: Agent time modelling (a) observed departure time distribution from the questionnaire survey, and (b) fitted time model

based on the population density provided by the TAZ dataset. Subsequently, a specific home location within the selected zone is randomly assigned according to the spatial distribution of POIs in that zone. The agent's workplace zone is subsequently assigned based on the interzonal travel probabilities derived from the O-D matrix. Within the selected destination zone, the exact workplace location is also randomly assigned using the local POI distribution. Once the origin and destination of each agent have been established, the departure and return times are allocated according to the agent time model outlined in the preceding section. It should be noted that several assumptions are applied to simplify agent behavior and trip generation. First, each agent is assumed to perform only one round-trip activity per day, consisting of a commute from home to work and a return from work to home. Second, all agents are assigned vehicles with the same characteristics, following the default vehicle configuration in the MATSim framework.

Scenario and assumptions

This study considers four vehicle adoption scenarios based on the proportion of BEVs and ICEVs in Phuket. The baseline scenario is derived from current accumulated registered vehicle data, with 136,600 ICEVs and 2,302 BEVs, resulting in an ICEV share of 98.34 percent and a BEV share of 1.66 percent (Department of Land Transport, 2025). To explore potential electrification impacts, three additional scenarios are defined as follows: a 10% BEV scenario with 90% ICEVs and 10% BEVs, a 20% BEV scenario with 80% ICEVs and 20% BEVs, and a 30% BEV scenario with 70% ICEVs and 30% BEVs.

Traffic congestion index

The congestion index (CI) quantifies the relative difference between the free-flow speed and the average speed of vehicles, serving as a metric in this study to determine the congestion level of each road segment. A higher CI indicates greater congestion, while a lower CI suggests smoother traffic flow. This index underscores differences from free-flow conditions, making it ideal for analyzing traffic performance across each road section. The CI is calculated using Eq. 1 (Wang *et al.*, 2018):

$$CI = \frac{T_f - T_c}{T_f} \quad (1)$$

Where, T_f denotes the free-flow speed of the road segment, and T_c is the average speed of vehicle (agents) who drive on road segments.

Simulation and validation

The road network and agent travel plans are used as inputs to the MATSim simulation framework. The simulation covers a full-day period, running from 00:00 to 23:59, to capture daily travel activities of all agents who were assumed as residents within a typical workday. The vehicle type was assumed to be passenger cars. The model yields two distinct types of outputs. The first type is disaggregated data, which includes the travel behaviors of individual agents, such as the routes they select and the durations of

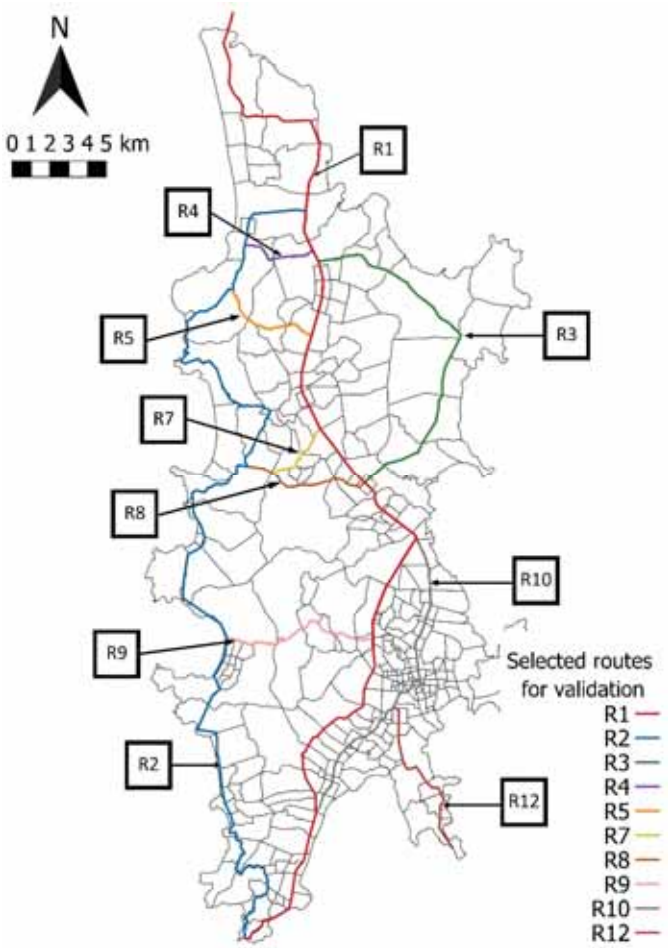

Fig. 5: The selected routes for validation

their trips. The second type consists of aggregated traffic statistics, which provide average speeds across road segments and overall travel time. To validate the simulation results, 10 candidate routes were selected based on their connectivity to major functional areas of the city. These areas include the airport, central business districts, residential zones, and popular tourist destinations, as illustrated in Fig. 5. Because of their substantial travel demand and relevance to the network, these routes are considered representative of overall traffic conditions in Phuket. For each designated route, the average traffic velocity was analyzed over two time intervals: morning and evening, incorporating both simulated data and observed traffic statistics from official reports. The comparison was conducted using standard statistical metrics, including the coefficient of determination (R^2), mean absolute error (MAE), and root mean square error (RMSE).

Carbon emission estimation

Carbon emissions are estimated based on each agent's travel speed across each road segment and are aggregated over the entire travel route. Since vehicle energy consumption varies with speed, this study accounts for dynamic driving behavior throughout the network. The link between the speed of vehicles and their energy usage is established from empirical data obtained in Thailand (Achariyaviriya et al., 2024), and the fitted consumption curves are illustrated in Fig. 6. These curves are used to estimate segment-level energy use and, subsequently, carbon emissions. The conversion of energy consumption into carbon emissions is achieved through the use of

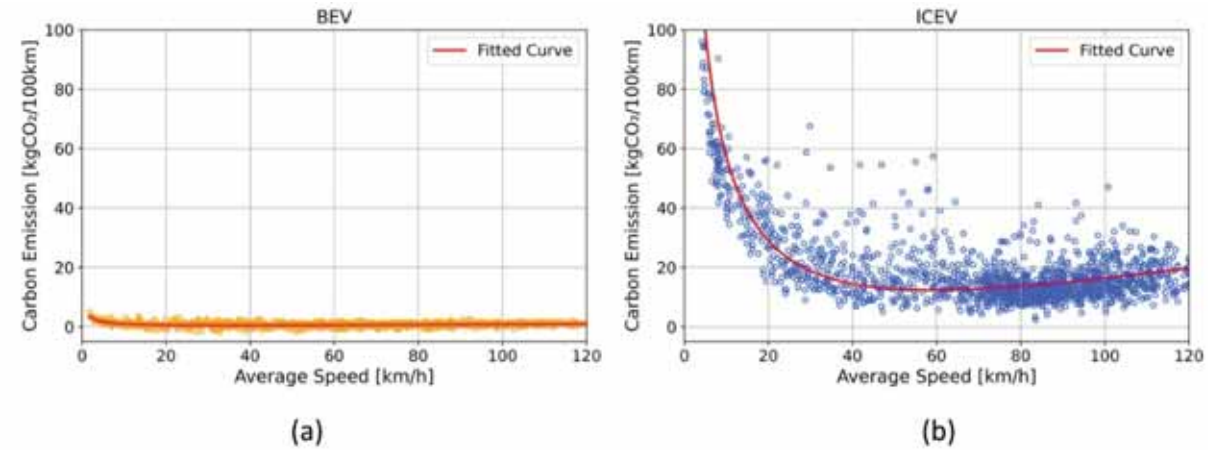

Fig. 6: Carbon emission rates of (a) BEV, (b) ICEV.

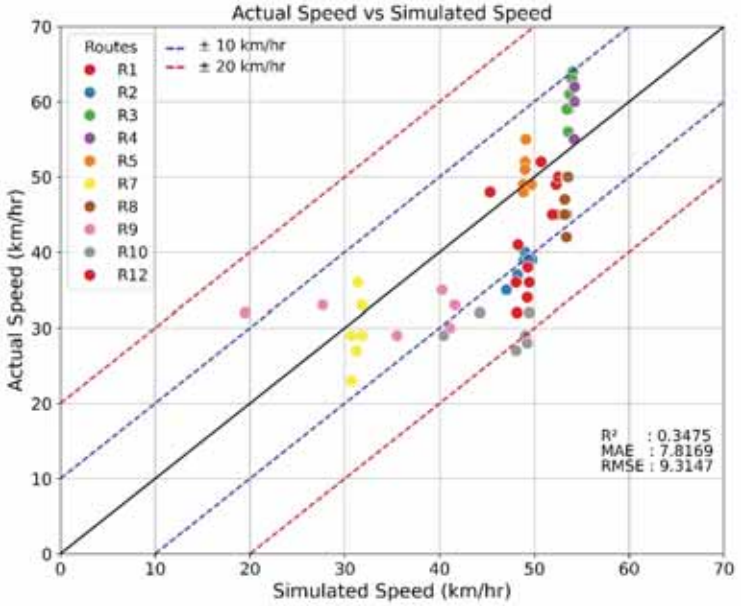

Fig. 7: The scatter plot between actual and simulation speed.

emission factors. For electricity from Thailand's grid mix, the factor is 0.4857 kilograms of carbon dioxide equivalent per kilowatt-hour ($kgCO_2eq/kWh$), while for motor gasoline, it is 2.2376 kilograms of carbon dioxide equivalent per liter ($kgCO_2eq/L$).

RESULTS AND DISCUSSION

Model validation

Fig. 7 presents a scatter plot comparing actual traffic speeds with simulated speeds to validate the model. The result shows that the r-square is 0.3475, the mean absolute error is 7.8169 kilometers per hour (km/h), and the root mean square error is 9.3147 km/h. Furthermore, the simulation results show that the average leg duration of agents is approximately 29 minutes and 22 seconds. Conversely, the survey indicates that the average travel time is 24 minutes and 4 seconds. This suggests that while the model captures general travel behavior trends, certain discrepancies remain, particularly in trip duration estimation. In spite of a moderate alignment observed between the simulated traffic speeds and

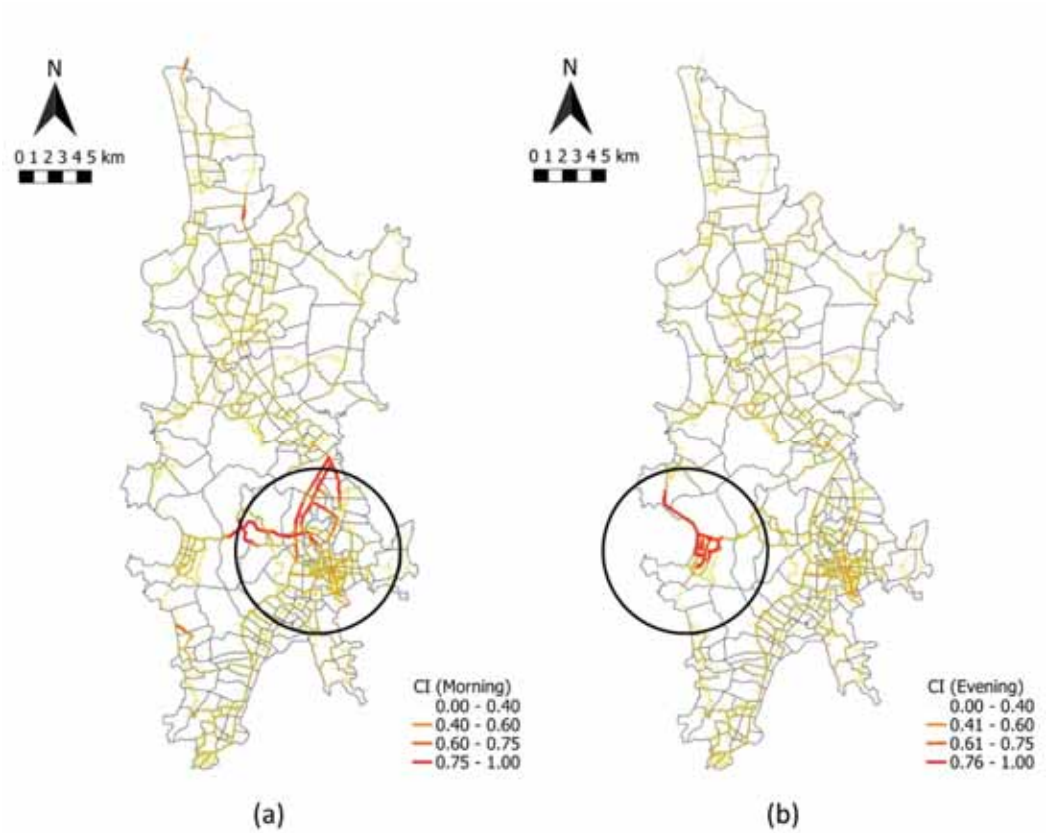

Fig. 8: Congestion index across Phuket during two time periods: (a) morning and (b) evening. Roads are color-coded based on congestion severity, where red indicates higher congestion levels

actual trip durations, the model effectively represents typical travel behavior in Phuket with reasonable validity. However, the relatively low R^2 value and overestimated trip durations suggest limitations in network detail and population assumptions.

The observed discrepancies between the simulation results and actual traffic data can be attributed to several modeling assumptions and data limitations. The road network contained only major roads. Conversely, the real traffic, with passengers taking into account both main and minor roads, influences their route selection. There was only one vehicle type. It was not represented the real transport that varied vehicle types because they were different mobilities and speeds. The survey questionnaire ought to be enhanced by incorporating diverse population types, as well as the timestamps that reflect when individuals performed their activities. Moreover, coordinates of houses and workplaces should be surveyed. To include more information, the model would be nearly the actual traffic.

Peak-time traffic

Fig. 8 illustrates the spatial distribution of traffic congestion during the morning and evening peak hours. In the morning, heavy congestion is observed around the Old Phuket Town (the circle in Fig. 8(a)), particularly along Route R1, and along Route R9. Route R9 shows consistently high congestion levels because the Old Phuket Town has long served as Phuket's Central Business District (CBD), hosting key commercial, governmental, and cultural institutions. Conversely, during the evening rush hour, traffic congestion on these roads diminishes. However, traffic intensity increases noticeably in Patong (the circle in Fig. 8(b)) and along several roads near the west coast. This points to a transformation in travel habits, probably attributed to the variety of entertainment options and tourist attractions that operate after sunset.

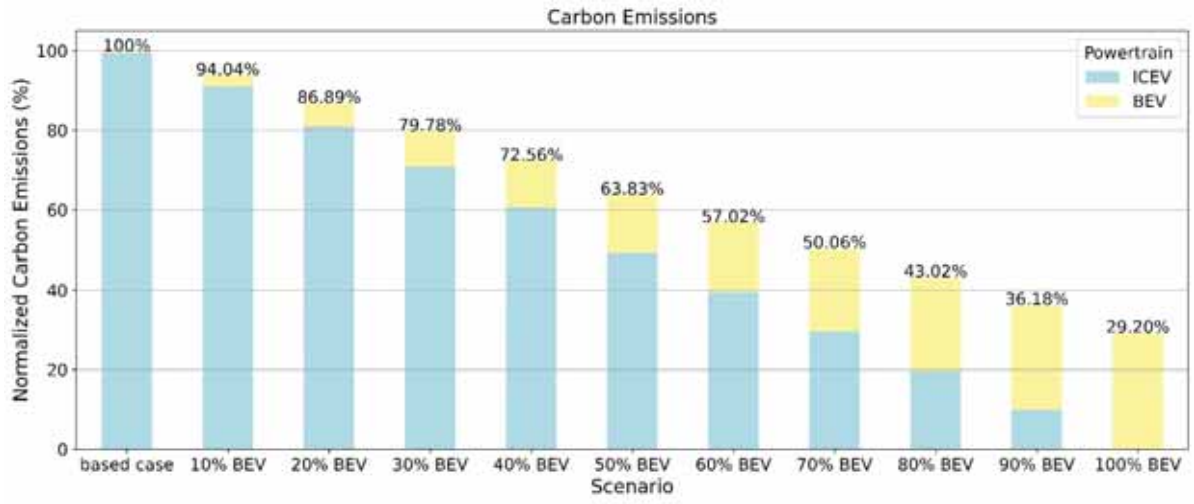

Fig. 9: Simulated carbon emissions under different BEV adoption scenarios. The chart presents the normalized total carbon emissions as a function of BEV penetration rate

Table 4: Normalized carbon emission contributions by powertrain under various BEV adoption scenarios

Powertrain	Scenario										
	Base Case	10% BEV	20% BEV	30% BEV	40% BEV	50% BEV	60% BEV	70% BEV	80% BEV	90% BEV	100% BEV
ICEV (%)	99.5	91.05	80.91	70.82	60.57	49.19	39.52	29.64	19.64	9.91	0
BEV (%)	0.5	2.99	5.98	8.96	11.99	14.64	17.50	20.42	23.38	26.27	29.20

Note: Percentages refer to the share of total carbon emissions, not the number of vehicles.

Carbon emission evaluation

In Fig. 9, the results of carbon emissions are shown for different BEV adoption scenarios, with emissions normalized against the baseline case. In the base case, BEVs contribute only 0.50% of total emissions, while ICEVs account for 99.50%. As the proportion of BEVs increases from 10% to 100%. The data exhibited an approximately linear relationship. The proportions of normalized carbon emission contributions are summarized in Table 4. Notably, the total carbon emissions decreased approximately 7% whereas the proportion of BEVs increased 10%. This reduction is primarily driven by a 10% decrease in emissions from ICEVs, while emissions from BEVs increase by only 3% due to their lower emission intensity. Overall, this trend illustrates that a transition towards the adoption of BEVs can bring about significant environmental improvements, given that BEVs generate much lower total emissions. These findings highlight the environmental value of promoting BEV use in urban transportation systems. To convert these environmental advantages into practical policy, it is crucial to combine the potential for carbon emission reduction with a thorough total cost of ownership (TCO) assessment. While the simulation highlights the environmental advantages of increasing BEV adoption, the economic feasibility for both users and policymakers remain a critical consideration. TCO, which includes vehicle purchase cost, maintenance, energy consumption, and residual value, provides an overall view of long-term affordability. By combining TCO analysis with carbon reduction outcomes, policymakers can identify scenarios where BEV adoption offers the best cost-benefit balance. This strategy enables the creation of focused subsidy programs that not only improve the economic

viability of BEVs but also maximize the environmental returns on public investment.

CONCLUSION

This study applied an agent-based simulation model using MATSim, which was validated against actual traffic data from Phuket. The verified model was then employed to evaluate carbon emissions across different BEV adoption scenarios. The key findings are summarized as follows; 1) Model accuracy can be enhanced by incorporating more detailed input data, including a greater variety of vehicle types, a more complete transport network (such as minor roads), and comprehensive survey data covering population activity times, home and workplace coordinates. 2) Increasing BEV adoption yields substantial emission reductions. As an illustration, boosting the percentage of BEVs to 10% yields roughly a 7% reduction in total carbon emissions. The simulation model demonstrates that increasing the proportion of BEVs can effectively reduce carbon emissions in the context of Thailand, particularly in tourism-intensive regions such as Phuket. Furthermore, while the model provides insights into different BEV adoption scenarios, the successful implementation of BEV expansion is heavily dependent on the presence of necessary infrastructure. In particular, the deployment of charging stations. Government subsidies and coordinated public-sector support are essential to achieve an optimal BEV adoption rate that aligns with Thailand's unique socio-economic and geographic conditions. This study highlights the utility of integrating agent-based simulation for carbon emissions estimation, offering valuable insights for policymakers aiming to foster low-carbon urban transportation systems. Future studies ought to take into account spatial and behavioral aspects that impact BEV adoption, including the layout of urban areas, travel behaviors, and access to charging facilities. Furthermore, integrating the carbon intensity of the electricity grid and analyzing Well-to-Wheel (WTW) emissions under various energy transition scenarios would provide a more comprehensive understanding of BEV impacts. While the simulation provides valuable insights into the potential carbon reductions from BEV adoption, it is important to acknowledge that certain behavioral responses are not yet fully captured in the current MATSim-based model. For instance, the availability and spatial distribution of charging infrastructure may lead individuals to alter their destination choices or trip patterns, affecting OD demand between zones. Moreover, the lower cost per kilometer associated with BEVs, when contrasted with conventional vehicles, might lead to a rise in travel demand, potentially mitigating the anticipated decrease in emissions. These complex behavioral adjustments are difficult to model accurately without further enhancements to the simulation framework. Consequently, the future advancement of the model should incorporate more detailed representations of charging behavior, cost sensitivity, and dynamic travel decision-making to enhance its reflection of real-world mobility. To conclude, this study underscores the significance of agent-based modeling as a valuable resource for analysis and decision-making in the transition to low-carbon urban transport. The model captures individual travel behavior and links it to emissions outcomes. This study also contributes to advancing research methods in transport and environmental planning. It helps translate broad policy goals into practical, location-specific strategies. As apprehension about climate change intensifies on both national and local fronts, the necessity for effective planning tools is becoming more critical. The simulation results from this study can help support decision-making on subsidy policies aimed at promoting electric vehicle adoption, providing a clear overview of potential impacts.

AUTHOR CONTRIBUTIONS

W. Achariyaviriya conceived the research idea and contributed to the development of the methodology. W. Kongwee conducted the data collection, performed the formal analysis and validation, and prepared the original draft of the manuscript. D. Rinchumphu supervised the first author and reviewed the paper draft. P. Suttakul provided vehicle energy consumption data and supervised the first author on emission calculation. A. Achariyaviriya reviewed the paper draft. V. Vichiensan provided road network data and supported the implementation of the simulation method. M. Kii supervised the first author on the simulation method and reviewed the paper draft. N. Chanpichaigosol reviewed and edited the manuscript draft. P. Iamtrakul acquired the funding and reviewed the paper draft. Y. Hayashi also acquired funding.

ACKNOWLEDGMENTS

This study was partially supported by Chiang Mai University, Thailand. The authors gratefully acknowledge the support provided by the Faculty of Engineering, Chiang Mai University. In particular, we wish to express our appreciation to the Master's Degree Program in Master of Arts and Science (Integrated Science), Chiang Mai University, under the CMU Presidential Scholarship. This research was also funded by the National Research Council of Thailand (NRCT) under the project entitled "Air-front Smart City: A Business-Life Regenerative Innovation Gateway Hub as Transformer of Economic-system for the Region towards 2050" which is a part of e-ASIA Joint Research Program (e-ASIA JRP), [Contract No. N11A670702].

CONFLICT OF INTEREST

The authors declare that there is no conflict of interests regarding the publication of this manuscript. In addition, the ethical issues, including plagiarism, informed consent, misconduct, data fabrication and/or falsification, double publication and/or submission, and redundancy have been completely observed by the authors.

OPEN ACCESS

©2025 The author(s). This article is licensed under a Creative Commons Attribution 4.0 International License, which permits use, sharing, adaptation, distribution and reproduction in any medium or format, as long as you give appropriate credit to the original author(s) and the source, provide a link to the Creative Commons license, and indicate if changes were made. The images or other third-party material in this article are included in the article's Creative Commons license, unless indicated otherwise in a credit line to the material. If material is not included in the article's Creative Commons license and your intended use is not permitted by statutory regulation or exceeds the permitted use, you will need to obtain permission directly from the copyright holder. To view a copy of this license, visit: http://creativecommons.org/licenses/by/4.0/

PUBLISHER'S NOTE

GJESM Publisher remains neutral with regard to jurisdictional claims in published maps and institutional afflictions

Positive AI Statement

During the preparation of this work the author(s) have used Artificial Intelligence (AI) [ChatGPT] in order to check for typographical errors and improve sentence structure for manuscript writing. After using this tool/service, the authors reviewed and edited the content as needed and take full responsibility for the content of the publication.

(For this reason, the GPTZero detector will evaluate the manuscript utilizing Generative AI, ensuring a high detection rate. If the manuscript relies heavily on Generative AI and AI-assisted technologies, it will be archived without further options for appeal).

Negative AI Statement

The author(s) declare that no AI tools or services were not used or not highly applied during the preparation of this work.

ABBREVIATIONS

%	Percent
AVs	Automated vehicles
AV-BRT	Autonomous vehicle-based bus rapid transit
BEV	Battery electric vehicles
BRT	Bus rapid transit
CAVs	Connected and automated vehicles
CBD	Central Business District
CI	Congestion index
CO_2	Carbon dioxide
EDGAR	Emissions Database for Global Atmospheric Research
EMEP/EEA	Air pollution emission inventory guidebook
$FFCO_2$	Fossil fuel carbon dioxide
GHG	Greenhouse gas
Gigaton	1000 kilogram
GPC	Global Protocol for community-scale greenhouse gas emission inventories
GPP	Gross provincial product
$GtCO_2eq$	Gigatonnes of carbon dioxide equivalent

HPHs	Health Promoting Hospitals
HVAC	Heating, ventilation, and air conditioning
ICEVs	Internal combustion engine vehicles
IPCC	Intergovernmental Panel on Climate Change
kgCO_2eq	Kilotons of carbon dioxide equivalent
kgCO_2eq/kWh	Kilograms of carbon dioxide equivalent per kilowatt-hour
kgCO_2eq/L	Kilograms of carbon dioxide equivalent per liter
km/h	Kilometers per hour
kWh	kilowatt-hour
MAE	Mean absolute error
MATSim	Multi-agent transport simulation
MFC	Microsimulation free-flow acceleration model
Mobsim	Mobility simulation
MtCO_2eq	Megatons of carbon dioxide equivalent
NO_x	Nitrogen oxides
O-D	Origin-destination
ODIAC	Open-source Data Inventory for Anthropogenic CO_2
OSM	OpenStreetMap
PM	Particulate matter
POIs	Point of interests
R^2	Coefficient of determination
RMSE	Root mean square error
T_f	Free-flow speed
T_c	Average speed of vehicle
TAZ	Traffic analysis zone
TCO	Total cost of ownership
tonCO_2eq	Tons of carbon dioxide equivalent
TTW	Tank-to-wheel
VKT	Vehicle kilometers traveled
WTT	Well-to-tank
WTW	Well-to-wheel
ZEVs	Zero-emission vehicles

REFERENCES

Achariyaviriya, W.; Wongsapai, W.; Rinchumphu, D.; Tippayawong, N.; Tippayawong, K.Y.; Suttakul, P., (2024). A comparative study of vehicle powertrain efficiency: Data-driven analyzing energy consumption and environmental impact. Transport. Eng., 18 **(16 pages).**

Ahn, D.Y.; Goldberg, D.L.; Coombes, T.; Kleiman, G.; Anenberg, S.C., (2023). CO_2 emissions from C40 cities: Citywide emission inventories and comparisons with global gridded emission datasets. Environ. Res. Lett., 18(3) **(16 pages).**

Angin, R.; Irawati; Setyaningtyas, R.; Adawiyah, P.R., (2022). Using the IPCC Formula to Calculate CO_2 emissions from everyday motorized vehicles as the baseline for climate change mitigation policies. IOP Conference Series: Earth Environ. Sci., 1105(1) **(7 pages).**

Briem, L.; Mallig, N.; Vortisch, P., (2019). Creating an integrated agent-based travel demand model by combining mobiTopp and MATSim. Procedia Comput. Sci., 151: 776-781 **(6 pages).**

Department of Land Transport, (2025). Number of vehicle registered.

Eckstein, D.; Künzel, V.; Schäfer, L., (2021). Global Climate Risk Index 2021 **(50 pages).**

Energy Policy and Planning Office, (2021). Promoting electric vehicles approach.

Energy Policy and Planning Office, (2024). Carbon Dioxide (CO2) Emissions from energy use in 2023.

Expressway Authority of Thailand, (2023). Feasibility Study on Engineering, Economic, and Financial Viability, and Environmental Impact Assessment for the Muang Mai, Koh Kaew, Kathu Expressway Project in Phuket Province **(77 pages).**

Fiori, C.; Arcidiacono, V.; Fontaras, G.; Makridis, M.; Mattas, K.; Marzano, V.; Thiel, C.; Ciuffo, B., (2019). The effect of electrified mobility on the relationship between traffic conditions and energy consumption. Transp. Res. Part D Transp. Environ., 67: 275-290 **(16 pages).**

Hörl, S., (2021). Integrating discrete choice models with MATSim scoring. Procedia Comput. Sci., 184: 704-711 **(8 pages).**

Hasan, U.; Whyte, A.; AlJassmi, H., (2022). A microsimulation modelling approach to quantify environmental footprint of autonomous buses. Sustainability. 14(23) **(31 pages).**

Hayashi, Y.; Iamtrakul, P.; Redillas, M., (2022). Air-front Smart City: A Business-Life Regenerative Innovation Gateway Hub as Transformer of Economic-system for the Region towards 2050.

Horni, A.; Nagel, K.; Axhausen, K., (2024). The multi-agent transport simulation MATSim **(208 pages).**

IPCC, (2019). 2019 Refinement to the 2006 IPCC Guidelines for National Greenhouse Gas Inventories. Intergovernmental Panel on Climate Change. **(23 pages).**

Janpoom, K.; Suttakul, P.; Achariyaviriya, W.; Fongsamootr, T.; Katongtung, T.; Tippayawong, N., (2023). Investigating the influential factors in real-world energy consumption of battery electric vehicles. Energy Rep., 9: 316-320 **(5 pages).**

Jia, J.; Gong, Z.; Xie, D.; Jian, H.; Chen, C., (2018). Study of urban carbon dioxide equivalent (CO2e) accounting based on the comparable GPC framework: a case of the underdeveloped city, Nanning, China. J. Integr. Environ. Sci., 15(1): 59-81 **(23 pages).**

Li, W.; Stanula, P.; Egede, P.; Kara, S.; Herrmann, C., (2016). Determining the Main Factors Influencing the Energy

Consumption of Electric Vehicles in the Usage Phase. Procedia CIRP. 48: 352-357 **(6 pages).**

Ma, J.; Mitchell, G.; Heppenstall, A., (2015). Exploring transport carbon futures using population microsimulation and travel diaries: Beijing to 2030. Transp. Res. Part D. Transp. Environ., 37: 108-122 **(15 pages).**

Ma, X.; Miao, R.; Wu, X.; Liu, X., (2021). Examining influential factors on the energy consumption of electric and diesel buses: A data-driven analysis of large-scale public transit network in Beijing. Energy. 216 **(12 pages).**

Makridis, M.; Mattas, K.; Mogno, C.; Ciuffo, B.; Fontaras, G., (2020). The impact of automation and connectivity on traffic flow and CO_2 emissions. A detailed microsimulation study. Atmos. Environ., 226 **(9 pages).**

Nassef, A.M.; Ghadbane, H.E.; Sayed, E.T.; Rezk, H., (2025). Reducing hydrogen consumption in hybrid electric vehicles using aquila optimization algorithm. Global J. Environ. Sci. Manage., 11(2): 695-710 **(16 pages).**

Raungratanaamporn, I.; Iamtrakul, P.; Chayphong, S.; Hayashi, Y.; Le Phuc, T., (2024). Spatial Estimation of Carbon Emissions in a Tourist City: A Geostatistical Approach for Phuket, Thailand. Proceeding of the IEEE Intetrnational Smart Cities Conference. (ISC2), 1–6 **(6 pages).**

Phuket Provincial Statistical Office, (2023). Phuket Provincial Statistical Report **(228 pages).**

Poolsawud, J., (2017). Phuket Smart City: The first pilot smart city of an intelligent urban Development in Thailand.

Rostami-Shahrbabaki, M.; Fehn, F.; Ricci, G. L.; Bogenberger, K., (2021). Effects of Different Shares of Electric Vehicles in Cities on Global CO2 Emissions: A Microsimulation-Based Analysis. 2021 IEEE International Intelligent Transportation Systems Conference (ITSC). 3190-3197 **(8 pages).**

Santoso, A.D.; Daulay, H.; Priyanti, A.; Silalahi, M.; Yaumidin, U.K.; Irawati, N.; Sumartono, H.; Astuti, P.; Farandy, A.R.; Parikesit, A.; Manti, M.F.; Indriasari, E.; Joelijani, W.; Wahyuni, S., (2024). Conversion of motorcycles to electric vehicles towards sustainable mobility. Global J. Environ. Sci. Manage., 10(SI): 181-200 **(20 pages).**

Tangkitvanich, S., (2023). Adapt Thailand to low-carbon economy and society.

Tchervenkov, C.; Hörl, S.; Balac, M.; Dubernet, T.; Axhausen, K.W., (2020). An improved replanning strategy for congested traffic conditions in MATSim. Procedia Comput. Sci., 170: 779-784 **(6 pages).**

Wang, W.X.; Guo, R.J.; Yu, J., (2018). Research on road traffic congestion index based on comprehensive parameters: Taking Dalian city as an example. Adv. Mech. Eng., 10(6), **(8 pages).**

Wiedmann, T.; Chen, G.; Owen, A.; Lenzen, M.; Doust, M.; Barrett, J.; Steele, K., (2021). Three-scope carbon emission inventories of global cities. J. Ind. Ecol., 25(3): 735-750 **(16 pages).**

Zhang, J.; Wang, Z.; Liu, P.; Cui, D.; Li, X., (2019). Analysis on influence factors of energy consumption of electric vehicles based on real-world driving data. Int. Conf. on Appl. Energy 2019 **(7 pages).**

Zhuge, C.; Bithell, M.; Shao, C.; Li, X.; Gao, J., (2021). An improvement in MATSim computing time for large-scale travel behaviour microsimulation. Transportation. 48(1): 193-214 **(22 pages).**

Ziemke, D.; Nagel, K.; Bhat, C., (2015). Integrating CEMDAP and MATSIM to increase the transferability of transport demand models. Transp. Res. Rec. J. Transp. Res. Board., 2493: 117-125 **(9 pages).**

Ziemke, D.; Knapen, L.; Nagel, K., (2021). Expanding the analysis scope of a MATSim transport simulation by integrating the FEATHERS activity-based demand model. Procedia Comput. Sci., 184: 753-760 **(8 pages).**

AUTHOR (S) BIOSKETCHES

Kongwee, W., M.Sc. Student, Integrated Science Program Multidisciplinary and Interdisciplinary School, Chiang Mai University, Chiang Mai, Thailand.
- Email: *worawut_kongwee@cmu.ac.th*
- ORCID: 0009-0006-7255-6229
- Web of Science ResearcherID: NA
- Scopus Author ID: 59907914900
- Homepage: https://urbanintelligence.eng.cmu.ac.th/graduate-students/worawut-kongwee/

Achariyaviriya, W., Ph.D., Assistant Professor, [1]Department of Electrical Engineering, Faculty of Engineering, Chiang Mai University, Chiang Mai, Thailand. [2]Research Unit for City Environment and Disaster Management (CEDM), Chiang Mai University, Chiang Mai, Thailand.
- Email: *witsarut.a@cmu.ac.th*
- ORCID: 0000-0002-1832-0761
- Web of Science ResearcherID: NA
- Scopus Author ID: 57212228172
- Homepage: https://urbanintelligence.eng.cmu.ac.th/experts/witsarut-achariyaviriya/

Rinchumphu, D., Ph.D., Associate Professor, Department of Civil Engineering, Faculty of Engineering, Chiang Mai University, Chiang Mai, Thailand.
- Email: *damrongsak.r@cmu.ac.th*
- ORCID: 0000-0002-6037-4974
- Web of Science ResearcherID: IUN-3065-2023
- Scopus Author ID: 57219602276
- Homepage: https://urbanintelligence.eng.cmu.ac.th/experts/urban-management-experts/damrongsak-rinchumphu/

AUTHOR (S) BIOSKETCHES

Suttakul, P., Ph.D., Assistant Professor, Department of Mechanical Engineering, Faculty of Engineering, Chiang Mai University, Chiang Mai, Thailand.
- Email: *pana.s@cmu.ac.th*
- ORCID: 0000-0002-2946-8921
- Web of Science ResearcherID: NA
- Scopus Author ID: 56724686000
- Homepage: https://me.eng.cmu.ac.th/staff/85

Achariyaviriya, A., Ph.D., Associate Professor, Department of Mechanical Engineering, Faculty of Engineering, Chiang Mai University, Chiang Mai, Thailand.
- Email: *aree.a@cmu.ac.th*
- ORCID: 0009-0000-6579-3046
- Web of Science ResearcherID: NA
- Scopus Author ID: 6507900489
- Homepage: https://me.eng.cmu.ac.th/staff/37

Chanpichaigosol, N., Ph.D., Researcher, Department of Mechanical Engineering, Faculty of Engineering, Chiang Mai University, Chiang Mai, Thailand.
- Email: *ch.nuttaponn@gmail.com*
- ORCID: 0000-0001-7532-0381
- Web of Science ResearcherID: NA
- Scopus Author ID: 57933951100
- Homepage: https://urbanintelligence.eng.cmu.ac.th/graduate-students/nuttapon-chanpichaigosol/

Vichiensan, V., Ph.D., Associate Professor, Department of Civil Engineering, Faculty of Engineering, Kasetsart University, Bangkok, Thailand.
- Email: *fengvmv@ku.ac.th*
- ORCID: 0000-0003-2444-352X
- Web of Science ResearcherID: AAF-7557-2020
- Scopus Author ID: 8440258100
- Homepage: https://en.eng.ku.ac.th/?professor=varameth-vichiensan

Kii, M., Ph.D., Professor, Division of Sustainable Energy and Environmental Engineering, Graduate School of Engineering, Osaka University, Osaka, Japan.
- Email: *kii@see.eng.osaka-u.ac.jp*
- ORCID: 0000-0003-1774-4308
- Web of Science ResearcherID: AAE-6786-2021
- Scopus Author ID: 8576152700
- Homepage: https://see.eng.osaka-u.ac.jp/topics/topics_en/13151

Iamtrakul, P., Ph.D., Associate Professor, Center of Excellence in Urban Mobility Research and Innovation (UMRI), Faculty of Architecture and Planning Thammasat University (Rangsit Campus), Khlong Luang, Pathumthani, Thailand.
- Email: *pawinee@ap.tu.ac.th*
- ORCID: 0000-0003-1362-2995
- Web of Science ResearcherID: ADM10592022
- Scopus Author ID: 16506714300
- Homepage: https://www.expertise-grad.tds.tu.ac.th/professors/14

Hayashi, Y., Ph.D., Distinguished Professor, Tokai Gakuen University, 2-901 Nakahira, Tenpaku-ku, Nagoya 468-8514, Japan.
- Email: *y-hayashi@tokaigakuen-u.ac.jp*
- ORCID: 0000-0001-5491-1967
- Web of Science ResearcherID: NA
- Scopus Author ID: 56742185800
- Homepage: https://www.isc.chubu.ac.jp/hayashi/Eprofile.html

HOW TO CITE THIS ARTICLE

Kongwee, W.; Achariyaviriya, W.; Rinchumphu, D.; Suttakul, P.; Achariyaviriya, A.; Chanpichaigosol, N.; Vichiensan, V.; Kii, M.; Iamtrakul, P.; Hayashi, Y., (2025). The potential for carbon emission reduction from the transition to battery electric vehicles. Global J. Environ. Sci. Manage., 11(3): 897-914.

DOI: 10.22034/gjesm.2025.03.03

URL: https://www.gjesm.net/article_725364.html

Global J. Environ. Sci. Manage. 11(3): 915-940, Summer 2025, Serial #43

Global Journal of Environmental Science and Management
(GJESM)

Homepage: https://www.gjesm.net/

Podcasts

ORIGINAL RESEARCH PAPER

Microplastic contamination in the river and its impact on fish health

U. Yanuhar[1,*], E.N. Wiratno[1], H. Suryanto[2], D.R. Machfuda[1], N.R. Caesar[1]

[1] Study Program of Aquatic Resources Management, Faculty of Fisheries and Marine Sciences, Brawijaya University, Jl. Veteran Malang, East Java, Indonesia

[2] Department of Mechanical and Industrial Engineering, Faculty of Engineering, Universitas Negeri Malang, Jl. Semarang 5, Malang 65145, Indonesia

ARTICLE INFO

Article History:
Received 04 December 2024
Revised 08 February 2025
Accepted 10 April 2025

Keywords:
Fish blood
Fish histology
Microplastics
Porong river
Water quality

DOI: 10.22034/gjesm.2025.03.04

ABSTRACT

BACKGROUND AND OBJECTIVES: In recent years, microplastic waste has become a global environmental problem, especially in rivers and its impact on fish health. The Porong River is one of the main rivers in East Java, Indonesia, flowing through residential areas and industrial zones in the regencies of Mojokerto and Sidoarjo, before emptying into the Java Sea. The infiltration of microplastics from both domestic and industrial sources into aquatic ecosystems is a major issue. These microplastics have the potential to carry harmful additives and water-soluble toxins, which can adversely affect marine organisms and increase environmental contamination. This study aims to evaluate the impact of microplastic contamination in the Porong River on fish health.

METHODS: The study was carried out at Porong River, where five sampling stations were established and three replications were performed each location. Observed parameters included microplastic abundance, water quality, histological changes in fish organs, fish blood hematological parameters, and Canonical Correspondence Analysis.

FINDINGS: The study indicated that the Porong River is contaminated with microplastics, detected in both water and sediment, with polyethylene terephthalate being the most prevalent. The highest recorded levels were 94.3 particles per liter in the water and 166.1 particles per kilogram in the sediment. Microplastics were also detected in fish gills and intestines. Microplastic affects the blood composition and tissue structure of fish. Hematological analysis indicates deviations in blood cell parameters as an indication of physiological stress in fish. With an average neutrophil percentage of 11.82, surpassing the values seen in healthy fish. Furthermore, lymphocyte levels were found to be below normal at the majority of the sampling stations. Fish gills showed mild damage across all observation stations, with the highest tissue damage score at Station 2 (24.4 percent) and the lowest at Station 5 (9.74 percent). An observed positive correlation exists between microplastics in both the gills and sediment, alongside the parameters of edema and hyperplasia. Microplastic in the intestines has a lesser impact on structural tissue changes compared to the gills.

CONCLUSION: Exposure to microplastics has affected fish health and disturbed the balance of the aquatic ecosystem in the Porong River. The outcomes of the current study can serve as a basis for developing regulations that effectively address and reduce plastic waste in rivers, ultimately minimizing microplastic contamination in water ecosystems.

This is an open access article under the CC BY license (http://creativecommons.org/licenses/by/4.0/).

NUMBER OF REFERENCES
106

NUMBER OF FIGURES
11

NUMBER OF TABLES
6

*Corresponding Author:
Email: *oktoruun@ub.ac.id*
Phone: + 812 5269 5056
ORCID: 0000-0003-3360-8752

Note: Discussion period for this manuscript open until Sep 1, 2025 on GJESM website at the "Show Article".

INTRODUCTION

The Porong River is located in the province of East Java, Indonesia, with a length of about 42 kilometers. The river flows through the regencies of Mojokerto and Sidoarjo, before reaching the Java Sea. It significantly contributes to the economic well-being of the local community, particularly for fishermen, aquaculture, and related industries. However, the river has faced significant pollution challenges such as from the Lapindo mudflow, which has been started since 2006, leading to a decline in water quality (Caesar *et al.,* 2022; Maulana *et al.,* 2023). Besides industrial operations, the rising population living adjacent to the river has exacerbated pollution by improperly disposing of household waste, which has negatively impacted water quality. Due to its proximity to industrial areas and densely populated communities, the Porong River accumulates plastic pollution (Piranti and Wibowo, 2020). Among the various pollutants, plastic waste is particularly concerning which poses a serious risk to the sustainability of aquatic ecosystems (Takarina *et al.,* 2024). In the long term, plastic will degrade to micro and nanoplastic accumulated in water, sediment, and aquatic organisms (Basri *et al.,* 2024). The presence of plastic waste may interfere with the ecological stability of rivers and jeopardize the survival of aquatic orgaisms (Nurhasanah *et al.,* 2024). This issue requires stronger waste management policies and greater community effort to reduce its environmental impact. The widespread use of plastic can be attributed to its cost-effectiveness and versatility. Globally, manufacturing of plastic reached 359 million tons in the last two years, with plastic waste projected to reach 26 billion tons by the year 2050 (Jiao *et al.,* 2024; Nakano *et al.,* 2025). The rampant use of plastic has caused a notable impact on the environment. After being disposed of, plastic packaging retains its chemical integrity but gradually disintegrates into smaller particles through the action of microbes and heat, eventually breaking down into carbon dioxide and water (Shi *et al.*, 2023). In Sidoarjo Regency, only about 20 percent (%) of plastic waste is managed by the Environmental and Parks Department, leaving a significant amount unprocessed. The National Waste Management Information System, in 2020, Sidoarjo Regency recorded 1,860.24 microplastic particles in aquatic environments, particularly in rivers like the Porong River (Samudra *et al.*, 2024). Microplastics pose a serious issue because they are durable and can easily spread throughout the environment (Gigault *et al.*, 2021). Microplastics spread by currents and accumulate in rivers both in water and sediment. Microplastics penetrate aquatic ecosystems and subsequently enter various organisms, leading to accumulation that significantly affects the health of the ecosystem (Iskandar *et al.*, 2024). At the top of the food chain, fish are a key indicator of aquatic ecosystem health (Brien *et al.*, 2016; Utari *et al.,* 2024), because fish are highly sensitive to environmental changes, including pollution. In aquatic habitats, the immune system is essential for safeguarding against pathogens and various environmental challenges (Alava *et al*., 2017). While previous studies have reported microplastic contamination in the Porong River (Samudra *et al.*, 2024; Salamah *et al*., 2024; Buwono *et al.,* 2021a), limited studies have explored its biological effects on microplastics on aquatic organisms, particularly fish health. The presence of microplastics in water bodies disrupts the food chain, impacting various aquatic organisms. Microplastics can be ingested by a wide range of aquatic species, from the smallest to the largest, eventually affecting the health and safety of the human food chain (Scherer *et al*., 2023; Sabilillah *et al.,* 2023). Implementing a unified plastic waste management initiative that covers river basins and coastal areas is of utmost importance. While the case study centers on Recife, Brazil, the proposed approach is adaptable to other contexts, including Indonesia's Porong River. The initiative emphasizes the essential importance of engaging the community, fostering collaboration among various agencies, and implementing a thorough, integrated approach to plastic waste management (Moura *et al.,* 2020). Most existing studies in East Java river rivepager focus on microplastic abundance and type, and also accumulation in water and sediment (Samudra *et al*., 2024; Firdaus *et al.,* 2020; Lestari *et al*., 2020), so needs further understanding of their physiological impacts on fish species. Consequently, it is crucial to assess how fish physiologically respond to exposure to microplastics. This study represents the first in-depth investigation of microplastic accumulation in the Porong River and its effects on the physiological parameters of local fish, including changes in hematological profiles, gill tissue histopathology, and water quality—areas that have not been thoroughly



Fig. 1: Geographic location of the study area along with the sample collection sites in the Porong River in Sidoarjo, in Indonesia

explored in this region before. The objective of this study is to investigate the effects of microplastic pollution on the health of fish in the Porong River, focusing on changes in blood cell composition, gill tissue structure, and overall water quality. The study was conducted at the five-station points along the Porong River in Sidoarjo, Indonesia from 2024 to 2025.

MATERIALS AND METHODS

Research design

This study utilized a descriptive research design to systematically and accurately present data samples in a factual manner (Kim *et al.*, 2017). The study site was in the Porong River, which is a continuation of the Brantas River located in Sidoarjo City, East Java Province, Indonesia. This river originates in Mojokerto City (Lengkong Baru Dam). The study's design featured observations at five designated sampling locations, referred to as Station 1 to Station 5, with each site being observed three times. Samples were collected from these five points along the Porong River in Sidoarjo (Fig. 1). The analysis of microplastic content was conducted at the Central Research and Clinical Diagnostic Laboratory for Healthy Animal Wildlife in Malang. At the freshwater laboratory unit of Brawijaya University in East Java, Indonesia, an evaluation of fish gill damage, hematological parameters of fish blood, and water quality were carried out. This river flows eastward and empties into the Madura Strait. Geographically, the Porong River is located between 112.5° east (E) - 112.9°E and 7.3° south (S) - 7.5°S. In 2013, the area around the Porong River consisted of various types of land cover, including settlements, industry, rice fields, ponds, and areas affected by Lapindo mud.

Water sample collection

The water sample was collected at five stations along the Porong River, Sidoarjo, using a bottle as a container. To ensure the integrity of the water samples during transport to the laboratory, they were stored in a cooler filled with ice. Fish sampling was performed three times at five stations, with each sampling occurring two weeks apart, fishing gear. To ensure the fish remained alive during their journey to the laboratory, they were secured in plastic bags with water and oxygen added.

Measuring microplastic abundance

The method established by Buwono *et al*. (2021b) was utilized to determine the abundance of microplastics. Water samples collected from the observation station were filtered using a stainless steel sieve with a 0.5 mm mesh size to separate larger particles. The residue that remained on the sieve was carefully poured into a test tube using a funnel, and then washed with distilled water to ensure that all microplastic particles were completely gathered. The sample was subsequently dried in an oven at 80 degrees Celsius (°C) for 24 hours (h). Once the samples were dried, 2 milliliters (mL) of 30% hydrogen peroxide (H_2O_2) was added to each sample, which was then covered with aluminum foil to prevent contamination. Incubation was performed in a water bath at 80°C for 24 h. to ensure complete decomposition of organic matter. The processed sample was then filtered using Whatman filter paper No. 41 and left to dry. An Optilab device and scanning electron microscope (SEM) were employed to observe and identify microplastics, ensuring the accuracy of the results obtained. The abundance of microplastics in the water sample was calculated using Eq. 1 (Buwono *et al*., 2021b):

$$\text{Microplastic abundance} = \frac{\text{Number of Microplastic particles (i)(particles)}}{\text{Filtered water volume (m3)}} \quad (1)$$

Blood sampling and hematology

Fish was anesthetized by immersion in water containing clove oil. 0.3 milliliters per liter (mL/L) (5-6 drops) of clove oil. Blood was sucked through the caudal vein using a 5 mL syringe. The hematological analysis included the measurement of blood parameters such as red and white blood cell counts via a hemocytometer, hemoglobin (Hb) levels assessed with a Sahli haemometer, and hematocrit levels obtained using a microhematocrit tube, which was then centrifuged at 6000 rotation per minutes (rpm). Leukocyte differentiation (monocytes, lymphocytes, basophils, eosinophils, and neutrophils) was determined by preparing blood smears and staining them with Giemsa solution. Platelet counts, macronuclei, micronuclei, and erythrocyte indices—such as mean corpuscular hemoglobin (MCH), mean corpuscular hemoglobin concentration (MCHC), and mean corpuscular volume (MCV), were also analyzed (Khan *et al*., 2022; Rasheed *et al*., 2023). All blood parameters underwent three separate counts to enhance precision.

Determining percentage of tissue damage

The gill organs of Tawes fish (*Barbonymus gonionotus*) from observation stations of the Porong River were taken. Histology analysis followed previously published methods (Rashid *et al*., 2025). The Organ tissues were fixed in 10% formalin solution, followed by the preparation of histological slides, which were subsequently using hematoxylin-eosin. Microscopic observation with an Optilab Camera was conducted at 100x to 400x magnification. Using the semi-quantitative method, observations were made in five different fields to view for tissue damage (hyperplasia, fusi, and necrosis/cell damage). Using Eq. 2, the percentage of damage for each field of view was computed based on the count of damaged cells and is categorized using a scoring system ranging from 1 to 4 (Yanuhar *et al*., 2020):

$$\text{Percentage of damage} = \frac{\text{Number of damaged cells}}{\text{Number of analyzed cells}} \times 100\% \quad (2)$$

The obtained percentage damage has scores ranging from 0 to 3 (Aminin et al., 2024), with criteria as follows:

-Score 0: No damage at all.

-Score 1: Mild damage with a percentage of <30%.

-Score 2: Moderate damage with a percentage of 30%-70%.

-Score 3: Severe damage with a percentage of >70%.

Measuring water quality

The water quality parameters were observed in physical parameters (temperature, total suspended solid (TSS), and total dissolved solids (TDS) and

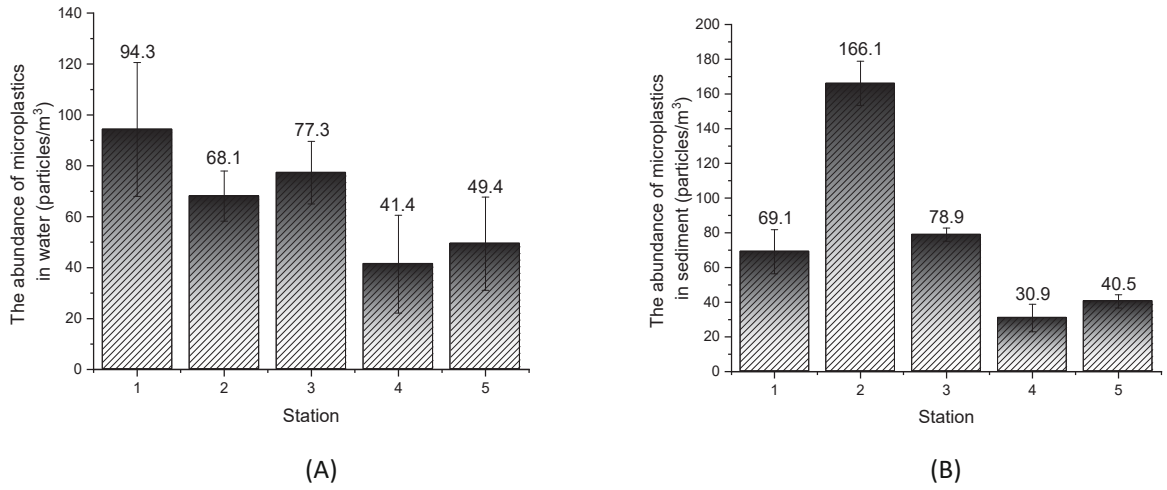

Fig. 2: Total average microplastic abundance at each station : (A) In water; (B) In sediment

chemical parameters; such as dissolved oxygen (DO), potential of hydrogen (pH), ammonia, phosphate, carbon dioxide (CO_2), total organic matter (TOM), and biochemical oxygen demand (BOD). At each station, water samples were taken following a predetermined schedule of repetitions. Water quality testing was conducted using both in-situ (on-site) and ex-situ (laboratory) methods. In-situ testing was performed using instruments such as a DO meter and pH meter. Concurrently, ex-situ measurements such as TOM demanded titration for analytical purposes.

Data analysis

The research data were analyzed using Microsoft Office Excel, origin 19b, and PAST (PAleontological Statistics), with statistical testing conducted using analysis of variation (ANOVA) and canonical correspondence analysis (CCA). The average values of water quality parameters and fish blood cell profiles were computed using Microsoft Excel. The resulting data were displayed in graphical format to enhance clarity and conciseness in numerical representation, including ANOVA results. PAST software was utilized for CCA, a statistical method that visually represents the correlation and proximity between fish blood cell profile variables and water quality parameters.

RESULTS AND DISCUSSION

Microplastic abundance in the Porong River

At all monitoring locations in the Porong River, microplastics were identified in both the water and sediment, as depicted in Fig. 2. The abundance of microplastics in river water varied across monitoring stations (Fig. 2A). Station 1 exhibited the highest concentration, reaching 94.3 particles per cubic meter (particles/m³), while Station 4 recorded the lowest abundance at 41.4 particles/m³. These variations are believed to be shaped by a range of influences, including the distance from pollution sources, the dynamics of water currents, and the diverse environmental conditions present along the river. Stations located closer to primary pollution sources are more likely to contain higher microplastic concentrations (Salamah *et al*. 2024).

The levels of microplastics found in sediment samples showed variation among the different sampling sites (Fig. 2B). The highest concentration reached 166.1 particles/m³ at Station 2, while the lowest concentration with 30.9 particles/m³ was found at Station 4. Compare to another study on the Brantas River, East Java, Indonesia indicates that microplastic in the Porong River is lower than Brantas River with a maximum value of 5192.59 particles/m^3 (Buwono *et al.*, 2021) at Brantas River outfall. Brantas River is the biggest river in Java so it may accumulate microplastic contaminants. The levels of microplastics found in sediment samples showed variation among the different sampling sites (Alimi *et al*., 2018). Acting as the final destination for pollutants, sediments entrap microplastics that are carried along by flowing

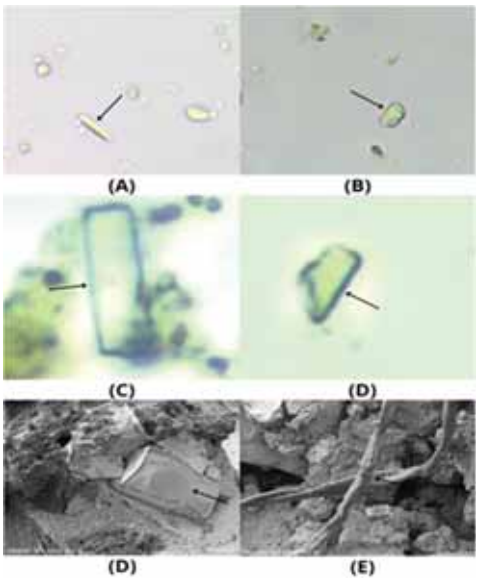

Fig. 3: Microplastics type found in Porong River; In water : (A) PP, (B) PET; In sediment : (C) PET, (D) PP (microscope optics, M.100x); (E) PET; (D) PE fiber (SEM, M500x)

water within their strata. Water samples contained diverse microplastic types, with polypropylene (PP) (Fig. 3A) and polyethylene terephthalate (PET) (Fig. 3B) being the most prevalent. PET was found at all monitoring stations, whereas PP was only found at Station 3. The two dominant microplastic types in sediment samples were PET (Fig. 3C) and PP (Fig. 3D), with PET present at all sampling stations, while PP was absent at Station 5. Different degradation processes and pollution sources lead to variations in the types and distribution of microplastics. Larger particles are from plastics in the early stages of fragmentation, whereas smaller particles suggest further degradation due to ultraviolet exposure, microbial activity, and mechanical abrasion by river currents (Dimassi *et al*., 2022). The identification of PET in sediment and water samples highlights its status as a prevalent plastic pollutant in the Porong River, primarily resulting from its extensive use in dairy-related products including as bottles, food packaging, and polyester textiles. In contrast, PP was detected only at certain locations, such as Station 3 in water samples, indicating PP as localized pollution sources from industrial discharge, or domestic waste containing polypropylene-based products (Binelli *et al*., 2022). At Station 5, PP was not detected in the sediment, possibly because of environmental conditions that affect its deposition, such as water flow, sedimentation rates, and the approaches used for plastic waste disposal. The concentration of microplastics in both sediments and water is largely influenced by their physical properties, such as size, shape, and density, which contribute to their tendency to settle and accumulate at the bottom of aquatic environments. At Stations 2 and 3, it is apparent that microplastic concentrations in the sediment are greater than those present in the water layer above. Furthermore, the spread of microplastics in water systems is notably impacted by a range of elements, including human-induced activities, the type of land use nearby, and the unique properties of the sediment (Gonzalez-Saldias *et al*., 2024; Go *et al.,* 2024). Microplastic contamination can significantly disrupt aquatic food web structures by entering the bodies of lower trophic level organisms, such as zooplankton and phytoplankton. These indigestible particles interfere with feeding behavior, hinder growth, and reduce nutritional intake. Therefore, the consequences also affect predators at higher trophic levels via processes including bioaccumulation and biomagnification. Furthermore, microplastics can impair organismal behavior and physiology, thereby altering interspecific interactions and disrupting energy flow across the ecosystem. Prolonged exposure to such disturbances may ultimately lead

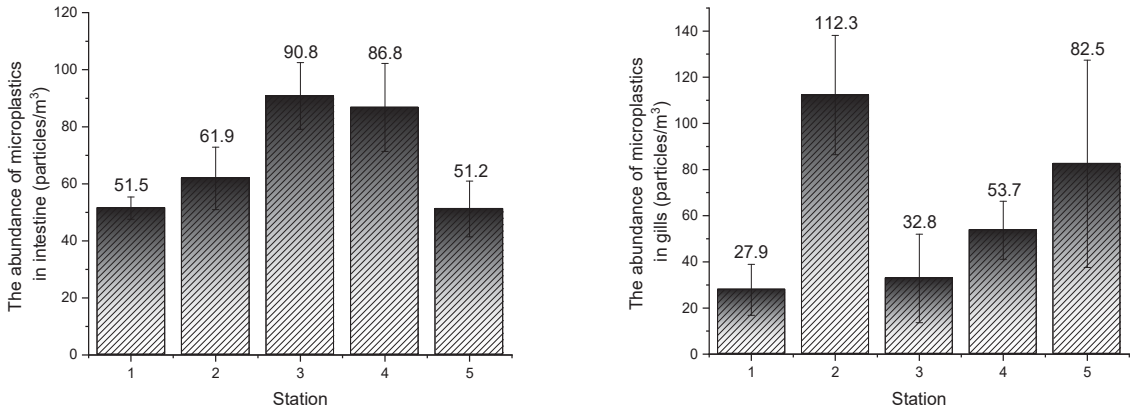

Fig. 4: Average abundance of microplastics : (A) in intestine; (B) in gills

to imbalances and the deterioration of aquatic ecosystem functionality (Chae *et al*., 2017). Extended bioaccumulation of microplastics in fish may cause numerous chronic effects, including physiological, behavioral, and reproductive disturbances, along with ecological repercussions. This situation endangers not just the health of individual fish but also the viability of fish populations and the overall stability of aquatic ecosystems.

Microplastics in fish organs

Microplastics were also found in the gills and intestines of Tawes fish from the Porong River, with abundance as shown in Fig. 4. The levels of microplastics present in the gills and intestines of fish differ from one station to another (Fig. 4A and 4B). In gill, the highest microplastic was recorded at fish from Station 3 with a content of 90.8 particles/m³, while Station 5 had the lowest microplastic content with a value of 51.2 particles/m³. In intestine, the highest microplastics were found at Station 2 with a concentration of 3 particles/m³, while the lowest was at Station 1, with a concentration of 27.9 particles/m³. Other studies indicate that Brantas River outfall (East Java, Indonesia) has fish gill containing microplastic of 2861.11 particles/gram (Buwono et al., 2021). The disparity in microplastic levels is influenced by various elements, including the levels of plastic pollution, the nature of the habitat, and the feeding behaviors of fish, which determine their chances of ingesting microplastics. Huang *et al*. (2022) reported that the stations closer to pollution sources with human activity tend to indicate higher microplastic concentrations in fish intestines. Serving as respiratory organs, the gills of fish are particularly permeable to tiny particles, rendering them more prone to the buildup of accumulation (Hajji *et al*., 2024). Fish and other aquatic organisms can ingest microplastics, which may subsequently be transferred to humans through the consumption of contaminated seafood. This process happens when individuals ingest fish or seafood products that contain microplastics. Once ingested, these particles can reach the human digestive system, where they may be absorbed, leading to oxidative stress, cytotoxic effects, and potential migration to other body tissues (Pal *et al*., 2025). Effective strategies are vital to alleviate these issues, which should encompass reducing single-use plastic consumption, upgrading waste management systems to curb plastic pollution in aquatic ecosystems, and fostering research to deepen the understanding of the long-term health consequences of microplastics and to devise effective interventions (Alberghini *et al*., 2023).

Microplastic particles were identified in the intestines of Tawes fish from the Porong River, with the largest particles found at Station 3 and the smallest at Station 5. Correspondingly, the microplastics found in the gills displayed size differences, with the largest observed at Station 5 and the smallest at Station 1. The study of microplastics revealed two key types present in the intestines: PET (Fig. 5A) and PP (Fig. 5B). PP was only detected in samples from Stations 1 and 4, while PET was in all stations. In the gills of

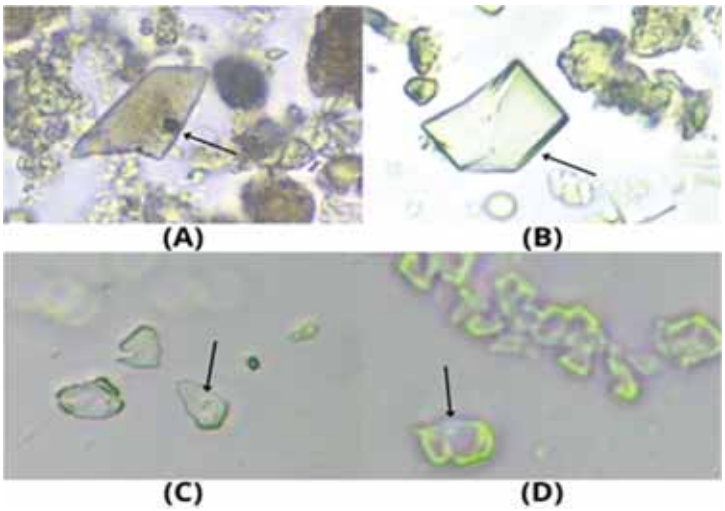

Fig. 5: Type microplastics in gills : (A) PET; (B) PP; (C) PET; (D) PP

Tawes fish, PET (Fig. 5C) and PP (Fig. 5D) were also found. PET was present at all stations, whereas PP was only found at Stations 3 and 5. Microplastic size and distribution differences are shaped by the degree of plastic breakdown, the digestive systems of fish, the movement of water, microbial activity, and the impact of UV radiation (Yee *et al*., 2021). The Porong River is predominantly polluted by PET microplastics, which underscores its significant utilization in various industrial and household applications, coupled with a slow rate of degradation. In contrast, PP was detected at fewer stations, specifically in the gills of fish from Stations 3 and 5, indicating that PP includes a local pollution source, such as domestic and industrial discharges. Moreover, the flow velocity of the river, sedimentation processes, and turbulence can impact the movement and buildup of microplastics in distinct parts of the river (Li *et al*., 2019; Zakiah *et al.,* 2025). ANOVA indicates that each station's result abundance of microplastic is significantly different (α=95%, p=0.0256; n=5).

Fish hematology analysis

Results of hematological analysis of fish are presented in Fig. 6. The average erythrocyte count of Tawes fish ranged from 1,266,667 to 2,280,000 cells/mm^3, with an overall average of 1,616,000 cells/mm^3 (Fig. 6A). Station 1 recorded the highest average erythrocyte count at 2,280,000 cells/mm^3, while Station 2 had the lowest at 1,266,667 cells/mm^3. Despite these variations, the erythrocyte counts at all stations remained within the normal range for Tawes fish, which is between 1,000,000 and 3,000,000 cells/mm^3. Fluctuations in erythrocyte counts may alter hematological parameters, yet the levels found in the sampled fish are still within the normal range, which implies that they are not under significant physiological stress. The average hematocrit level of Tawes fish ranged from 19% to 34% (Fig. 6B), with an overall average of 27%. The highest hematocrit level of 34% was observed at Station 1, in contrast to Station 2, which had the lowest at 19%. The hematocrit levels at Stations 2 and 3 were below the normal range, whereas those at Stations 1, 4, and 5 were in the normal range for Tawes fish 27.3% - 37.8% (Hertika *et al*., 2024).

The hematocrit measurement reveals the relationship between erythrocytes and plasma, indicating the percentage of red blood cells present in fish blood. This parameter is linked to the erythrocyte count and can be recognized as a measure of fish health that is influenced by their age. The younger fish usually exhibit higher hematocrit values (Ahmed *et al*., 2020; Yanuhar *et al*., 2021). Environmental changes or pollution can drop hematocrit levels as a physiological response to stress. Furthermore, conditions such as illnesses, reduced appetite, or nutritional inadequacies—like insufficient dietary protein or vitamin shortages—may contribute to a reduction in hematocrit levels (Imanpoor *et al*., 2021).

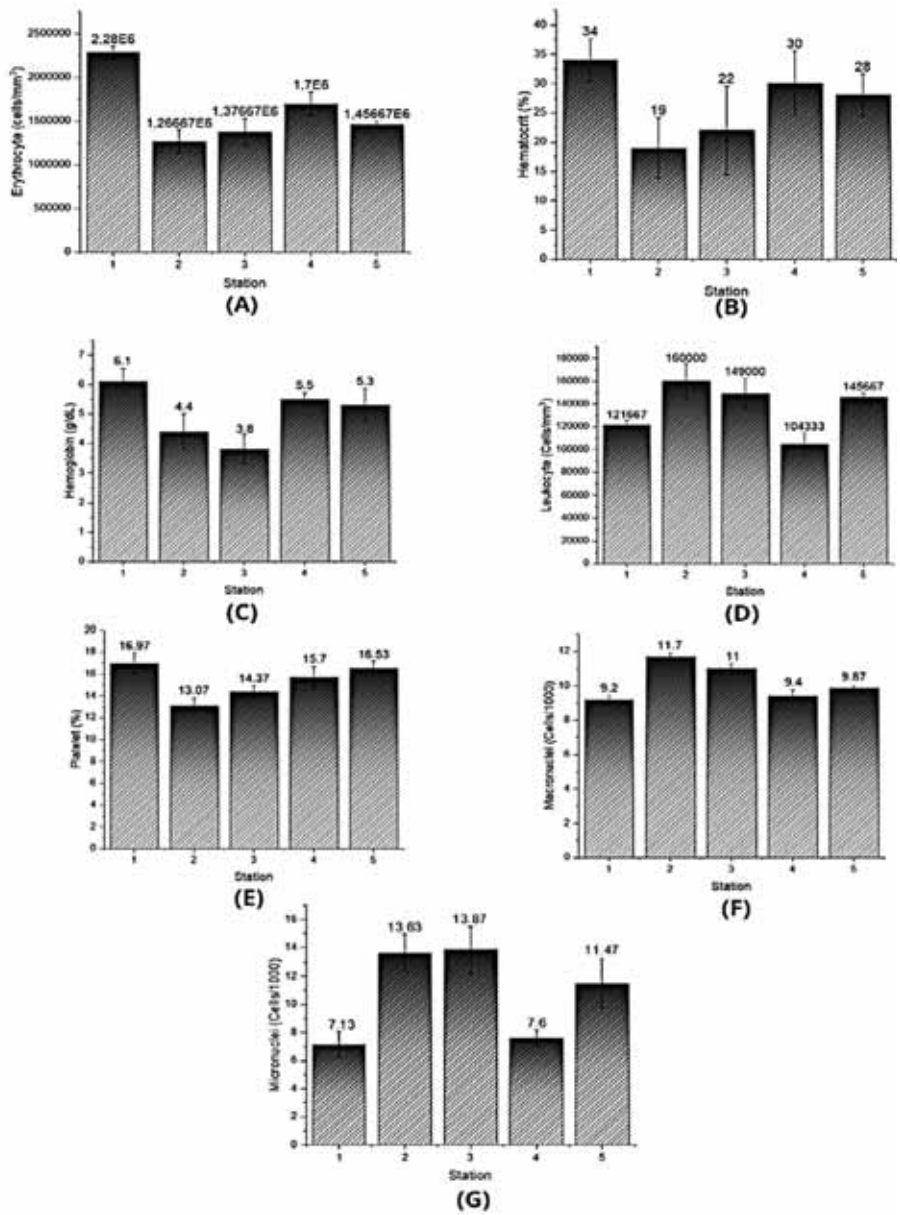

Fig. 6: Fish Hematology : (A) Erythrocyte ; (B) Hematocrit, (C) Hemoglobin, (D) Leukocyte, (E) Platelet, (F) Macronuclei, (G) Micronuclei

The average hemoglobin level of Tawes fish ranged from 3.8 to 6.1 grams/deciliter (g/dL), with an average of 5.03 g/dL (Fig. 6C). The highest hemoglobin level was recorded at Station 1 with a value of 6.1 g/dL, while the lowest one was recorded at Station 3 with a value of 3.8 g/dL. The hemoglobin levels at Stations 2 and 3 were identified below the normal status (5.05-8.33 g/dL, Jo *et al.*, 2025), whereas those at Stations 1, 4, and 5 remained within the normal status for the Tawes fish. The primary function of hemoglobin is to facilitate the movement of oxygen from the gills to various body tissues while also transporting carbon dioxide back to the gills for excretion (Nikinmaa *et al.*, 2019). The presence of low hemoglobin levels points to disruptions in hematopoiesis linked to microplastic exposure, potentially leading to lower metabolic rates and diminished energy production (Abdel-Tawwab *et al.*, 2019). ANOVA indicates that each station's result hemoglobin is significantly different (α=95%, p=0.0476; n=5). The average leukocyte count

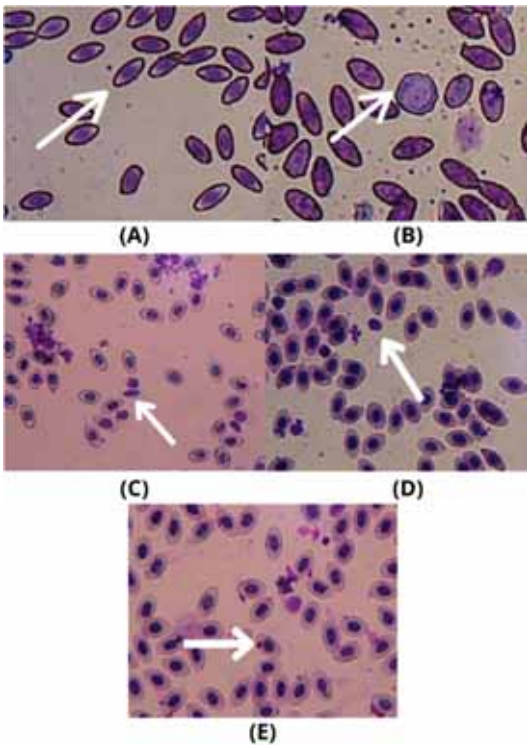

Fig. 7: Observation of Fish Blood Morphology : (A) Erythrocyte; (B) Leukocyte, (C) Platelet, (D)) Macronuclei, (E) Micronuclei

of Tawes fish ranged from 121,667 to 160,000 cells/mm³, with an overall average of 136,133 cells/mm³ (Fig. 6D). Station 2 recorded the highest leukocyte count at 160,000 cells/mm³, while Station 1 had the lowest at 121,667 cells/mm³. While the leukocyte count at Station 2 surpassed the normal range, the counts at Stations 1, 3, 4, and 5 were consistent with the normal leukocyte levels for Tawes fish, which range between 20,000 and 150,000 cells/mm³ (Ismarica *et al*., 2025). The average platelet count of Tawes fish ranged from 13.07% to 16.97%, with an overall average of 15.33% (Fig. 6E). Station 1 recorded the highest average platelet count at 16.97%, while Station 2 had the lowest at 13.07%. The average platelet count is below the normal range for fish, which is between 20% and 30% (Chen and Luo., 2023). The average macronucleus count in Tawes fish ranged from 9.2 to 11.7 cells per 1,000, with an overall average of 10.2 cells per 1,000 (Fig. 6F). Station 2 recorded the highest average macronucleus count at 11.7 cells per 1,000, while Station 1 had the lowest at 9.2 cells per 1,000. Interestingly, areas with elevated levels of microplastics were found to have a greater quantity of macronuclei cells in fish blood samples. The average micronucleus count in Tawes fish ranged from 7.13 to 13.87 cells per 1,000, with an average of 10.74 cells per 1,000 (Fig. 6G). The highest average micronucleus count was recorded at Station 3 with a value of 13.87 cells per 1,000, while the lowest one was at Station 1 with a value of 7.13 cells per 1,000. The average micronucleus is within the normal range (8 - 23 cells per 1,000, Farkha *et al*., 2021). The blood morphology of fish, as observed under a microscope, is depicted in Fig. 7, revealing that the erythrocytes maintain a normal structure (Fig. 7A). The number and shape of erythrocytes serve as important indicators of fish health. A reduction in the number of erythrocytes might suggest infection, stress, or anemia, whereas a higher count could signify an adaptive response to low oxygen levels or alterations in environmental conditions. Several factors influence erythrocyte levels in fish, including environmental conditions, age, sex, nutrition, and dissolved oxygen availability. The primary function of erythrocytes is to transport hemoglobin, facilitating oxygen delivery from the gills or lungs to body tissues. Furthermore,

erythrocytes contain a high concentration of carbonic anhydrase, an enzyme that accelerates the reaction between carbon dioxide and water, enabling the transport of carbon dioxide from tissues to the gills for excretion. A decrease in erythrocyte count in infected fish may suggest the presence of pathogens, prompting an immune response that results in a reduction of erythrocytes as the organism strives to combat the infection (Chen and Luo, 2019). The morphology of fish leukocytes remained normal (Fig. 7B). Leukocytes, or white blood cells, function as the primary cellular defense mechanism in fish. Several factors influence leukocyte levels, including sex, age, nutrition, infections, and environmental pollution. Leukocytes play a crucial role in immune responses, as fish increase immune cell production when exposed to infections or foreign substances (Firdaus and Zamri, 2016). Higher leukocyte counts in sick fish suggest an activated immune response. An uptick in the total number of leukocytes suggests a boost in immune function, particularly among phagocytic cells responsible for engulfing and neutralizing foreign entities. This immune response is a natural defense mechanism to combat pathogens and environmental stressors (Biller *et al*., 2018).

The morphology of fish platelets remained normal (Fig. 7C). Platelets are cytoplasmic fragments of megakaryocytes with diameters ranging from 3 to 5 micrometers (µm). The essential function of platelets lies in hemostasis, where they prevent severe bleeding. Furthermore, they are important for immune protection, as they help to localize attacks from pathogens and support both wound healing and the clotting process. Platelets release thromboplastin, an enzyme that polymerizes fibrinogen, a key component in the blood coagulation process. As red blood cell production (polycythemia) increases, platelet regeneration also escalates, which contributes to a more rapid formation of clots. However, during infections, platelet levels generally decrease (Chandrashekar *et al*., 2018). Conversely, platelet counts may rise in response to hemorrhages or ulcers, as platelets are produced to promote blood clotting and prevent further bleeding (Manon and Karsdal, 2016). The fish macronuclei exhibited a typical morphology (Fig. 7D). The nucleus consists of both a micronucleus and a heteromeric-type macronucleus. The macronucleus plays a crucial role in ensuring survival, while the micronucleus is responsible for reproduction. Structurally, the macronucleus contains dense DNA granules situated along the periphery, linked by central areas where DNA diffusion is minimal. This organelle is rich in DNA, with RNA also playing a significant role in its composition. The DNA within the macronucleus is associated with chromosomes or chromosome-like structures (Wang *et al*., 2024). Macronuclei are essentially enlarged cell nuclei containing larger DNA granules compared to normal-sized nuclei. An elevated count of macronuclei frequently serves as a sign of cellular stress due to adverse environmental conditions. Exposure to environmental pollutants, such as microplastics, can induce stress responses in fish, leading to macronuclear abnormalities (Sarasamma *et al*., 2020). The morphology of micronuclei in fish is still in normal status (Fig. 7E). Micronuclei are chromatin bodies in the cytoplasm containing chromosome fragments that fail to integrate into the nucleus during cell division. Micronuclei can serve as indicators of fish health, with higher counts possibly reflecting exposure to harmful substances or pathogens in their environment. Several factors influence the cytological analysis of fish blood, including sex, body size, spawning stage, species resilience, environmental adaptation, genetic variation, and blood sampling procedures (Nabi *et al*. 2022).

Differential Leukocyte

The average monocyte count in Tawes fish ranged from 9.14% to 19.32%, with an overall average of 13.96% (Table 1). Station 2 recorded the highest monocyte count (19.32%), while Station 1 had the lowest (9.14%). These measurements are higher than the standard monocyte range for Tawes fish (3.9%–5.9%, Steckert *et al*. 2019), implying that environmental stressors, infections, or pollutants may have triggered an immune response. The average lymphocyte count ranged from 39.27% to 74.44%, with an overall average of 59.75%. Station 1 exhibited the highest lymphocyte count (74.44%), while Station 2 had the lowest (39.27%). Compared to the normal range (68%–86%, Reda *et al*. 2016), lymphocyte levels at Stations 2, 3, 4, and 5 fell below normal, indicating potential immunosuppression due to stress, infection, or environmental pollutants, which may increase disease susceptibility).

The average basophil count ranged from 4.43%

Table 1: Average differential leukocyte results at each station

Station	Monocyte (%)	Lymphocyte (%)	Basophil (%)	Neutrophils (%)	Eosinophil(%)
1	9.1 ± 0.3	74.44 ± 1.5	4.43 ± 0.6	7.27 ± 1.5	4.72 ± 0.8
2	19.32 ± 0.4	39.27 ± 30.3	5.2 ± 0.5	15.68 ± 4.3	5.64 ± 1.5
3	16.83 ± 0.4	54.19 ± 5.3	8.67 ± 1.2	13.91 ± 2.1	3.28 ± 0.8
4	10.88 ± 0.9	67.7 ± 2.1	6.42 ± 1.6	10.54 ± 0.8	4.47 ± 0.4
5	13.65 ± 1.8	63.15 ± 3.1	8.06 ± 0.7	11.71 ± 1.9	3.43 ± 1.5

to 8.67%, with an overall average of 6.56% (Table 1). Station 3 recorded the highest basophil count (8.67%), while Station 1 had the lowest (4.43%). These values surpass the normal range (0.10%–3.88%, Abdelhamid *et al*., 2019), suggesting a heightened immune response. The average eosinophil levels fluctuated from 3.28% to 5.64%, resulting in a mean of 4.31%. The highest count was observed at Station 2, reaching 5.64%, while Station 3 had the lowest count at 3.28%. Since the values fall within the normal range (2.40%–8%, Sulieman *et al*., 2024), eosinophil levels indicate a stable immune response, particularly against parasites and allergens. ANOVA indicates that each station results in eosinophil cells significantly different (α=95%, p=0.0347; n=5). The average neutrophil count ranged from 7.27% to 15.68%, with an overall average of 11.82%. The neutrophil count at Station 2 was the highest, reaching 15.68%, while Station 1 reported the lowest count of 7.27%. Although the neutrophil count at Station 1 fell within the normal range of 6% to 8%, the counts at Stations 2, 3, 4, and 5 were above the normal thresholds (Havixbeck *et al*., 2016). This indicates a potential physiological stress linked to water contamination. The heightened levels of monocytes, basophils, and neutrophils found at several stations imply that environmental stressors might be influencing the health of Tawes fish, prompting an immune response to external threats. Microscopic observations of fish blood morphology are presented in Fig. 8. Blood morphology of monocyte, lymphocyte, basophil, and Eosinophil indicate abnormal (swelling cells, arrow sign) (Fig. 8A-D). Examination under a microscope confirmed that the structure of fish neutrophils was consistent with normal characteristics (Fig. 8E). The increase in neutrophil levels may be attributed to sudden environmental changes, requiring fish to adjust and maintain homeostasis. Furthermore, being exposed to contaminated water may trigger a rise in neutrophil levels, given that these immune cells are vital for inflammation response and protection against pathogens. Neutrophils, a type of white blood cell, act as the first line of defense, responding to cytokine signals at infection or inflammation sites, leading to elevated counts in peripheral blood (Chmielewski and Strzelec, 2018).

Advanced blood cell count calculation

Advanced blood cell count calculations were conducted to determine the parameters of MCV, MCH, and MCHC, with the quantified values presented in Fig. 9. The average MCV of Tawes fish ranged from 20 to 35 µm³, with an overall average of 28 µm³ (Fig. 9A). Station 2 recorded the highest MCV at 35 µm³, while Station 1 had the lowest at 20 µm³. The average MCV remained within the normal range for Tawes fish blood, which is between 12.36 and 528.57 µm³ (Elarabany *et al*., 2017). MCV indicates the average size of red blood cells and is determined by the erythrocyte count as well as hematocrit measurements. A high MCV occurs when hematocrit levels are increased while the erythrocyte count is reduced (Fazio, 2019). An increase in MCV may result from the release of immature erythrocytes into the bloodstream. MCV values can serve as an important indicator for assessing erythrocyte production efficiency during the erythropoiesis process (Buttarello, 2016). The average MCH of Tawes fish ranged from 14 to 19 pico gram (pg), with an average of 16 pg (Fig. 9B). The peak MCH value of 19 picograms was observed at Station 5, in contrast, Station 1 exhibited the lowest mean corpuscular MHC at 14 pg. These findings indicate that the average MCH remained within the normal range for Tawes fish blood, which is between 5.07 and 120.86 pg (Bbole *et al*., 2016). MCH represents the average hemoglobin content in a single red blood cell, expressed in picograms (pg). It demonstrates hemoglobin's role in transporting oxygen across the body. Lower levels of hemoglobin may point to anemia or gill damage due to toxic feed exposure. A low MCH value indicates structural damage to the erythrocyte membrane.

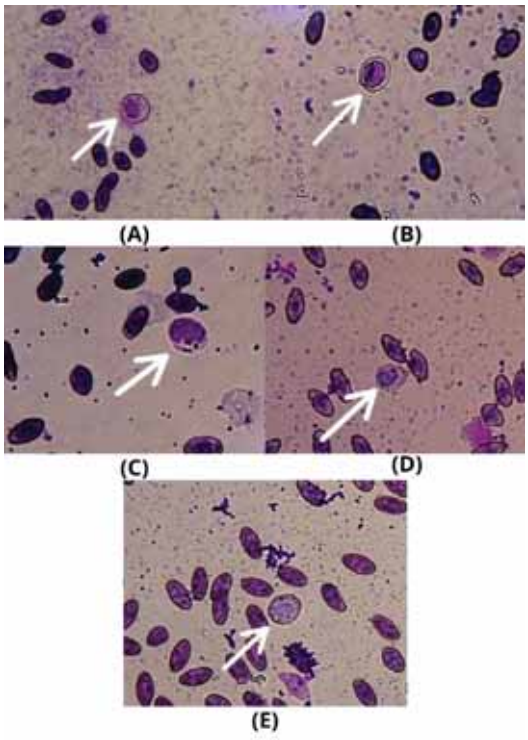

Fig. 8: Observation of fish blood morphology : (A) Monocyte ; (B) Lymphocyte, (C) Basophil, (D) Eosinophil, (E) Neutrophils

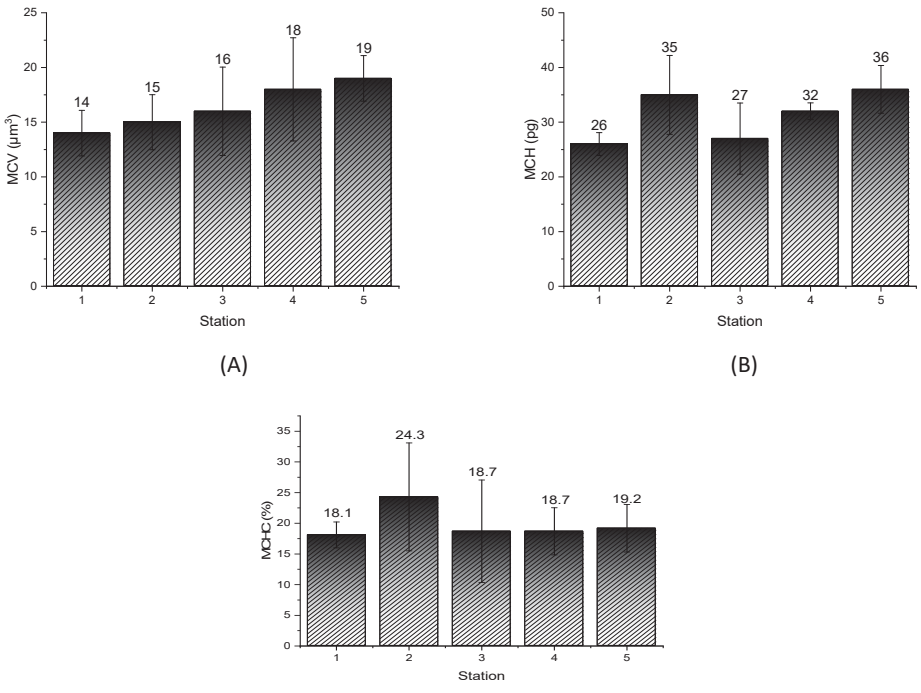

Fig. 9: Advanced blood cell count calculations: (A) MCV, (B) MCH, and (C) MCHC

Table 2. Scoring of edema damage to the gills

Station	Sampling			Average (%)	Score	Damage level
	1	2	3			
1	143	150	148	35.51	2	Moderate damage
2	128	135	133	31.88	2	Moderate damage
3	115	110	118	27.62	1	Mild damage
4	123	121	130	30.11	2	Moderate damage
5	48	55	53	12.56	1	Mild damage

Note: the scoring criteria: Score 0: No damage at all; Score 1: Mild damage with about <30%; Score 2: Moderate damage with range 30%-70%; Score 3: Severe damage with a percentage of >70% (Aminin *et al*., 2024).

Abnormal erythrocyte release from the spleen, or hypoxia, can disrupt hemoglobin formation, so it can reduce hemoglobin circulation and further affect oxygen transport. An increase in both MCH and MCV is indicative of a regenerative anemia response, commonly associated with the breakdown of red blood cells (Doig and Zhang, 2017). MCHC is the average concentration of hemoglobin in a single red blood cell and is directly proportional to hemoglobin levels. The average MCHC of Tawes fish ranged from 14.6% to 24.3%, with an overall average of 18.0% (Fig. 9C). Station 2 recorded the highest MCHC of 24.3%, while Station 4 had the lowest by 14.6%. The MCHC at Station 2 remained within the normal range 19.84% - 87.73% (Patra *et al*., 2024) but the other Stations were below the normal range for Tawes fish blood. A low MCHC value indicates abnormal hemoglobin synthesis, which may impair blood osmoregulation and lead to anemia.

Gill damage analysis

Gill damage in Tawes fish was observed under an optical microscope with a magnification of 10 times. An assessment of the gill tissue was conducted, and the identified damage was quantified using a scoring system as outlined in equation (2). The analysis revealed three types of gill damage: edema, hyperplasia, and lamellar fusion. As the main respiratory organ, gills possess a thin structure and extensive surface area to optimize gas exchange. Nevertheless, this anatomical characteristic makes them particularly vulnerable to foreign substances like microplastics. Structural damage to the gills can impair the exchange of oxygen and carbon dioxide, ultimately causing respiratory dysfunction in fish (Zink and Wood, 2024). The condition known as edema is marked by the swelling of cells, which may occur due to pollutants entering the gill organs or from an overaccumulation of fluid within body tissues. Edema is identified by the stretching or detachment of the basal membrane and the narrowing of cells, leading to impaired gill function, so the respiratory process and body metabolism begin to be disrupted (Shah *et al*., 2020; Hakim *et al.,* 2024). The presence of edema was detected in the gills of the fish sample, as depicted in Fig. 10A. Damage assessment for edema was carried out using Eq.2, with the outcomes summarized in Table 2. Based on the scoring results (Table 2), moderate damage was observed at stations 1, 2, and 4, indicating a medium level of water pollution. Meanwhile, stations 3 and 5 showed mild damage, which suggests a low level of water pollution. The highest average score was recorded at station 1, with a score of 35.51%, while the lowest average score was at station 5, with a score of 12.56%. Hyperplasia can occur in both the secondary and primary lamellae. Hyperplasia in the secondary lamellae occurs due to excessive division of epithelial cells. In the primary lamellae, hyperplasia is caused by excessive division of chloride cells (Macirella and Brunelli, 2017; Purnama *et al.,* 2025). The process of hyperplasia causes the epithelial tissue at the tips of the filaments to thicken, taking on a shape similar to a baseball bat, or it can lead to thickening of the epithelium near the lamellae's base (Mohamad *et al*., 2021). The hyperplasia damage is shown in Fig. 10B.

The scoring results (Table 3) indicate that moderate damage occurred at stations 1 and 2, indicating a moderate level of water pollution. Observations at stations 3, 4, and 5 revealed minor damage, which points to a moderate level of water pollution. The highest average score was recorded at station 1 with a score of 30.27%, while the lowest average score was found at station 5 with a score of 10.63%.

Lamellar fusion is a tissue alteration caused by continuous hyperplasia, leading to adhesion on both

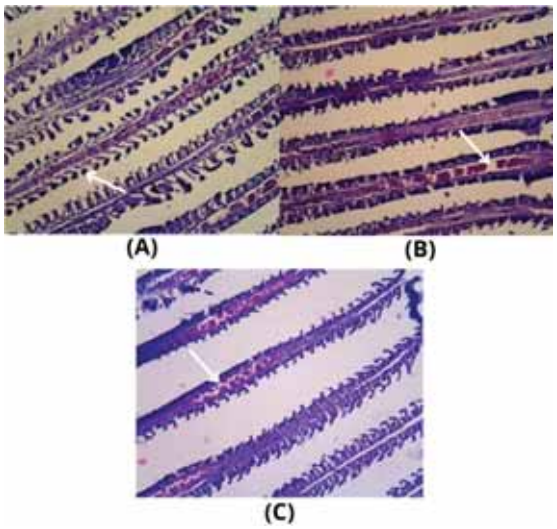

Fig. 10: Gill damage: (A) Edema, (B) Hyperplasia, and (C) Lamellar fusion

Table 3: Scoring of hyperplasia damage to the gills

Station	Sampling			Average (%)	Score	Damage level
	1	2	3			
1	121	129	126	30.27	2	Moderate damage
2	118	127	130	30.19	2	Moderate damage
3	53	63	60	14.17	1	Mild damage
4	95	98	95	23.19	1	Mild damage
5	42	50	40	10.63	1	Mild damage

Note: the scoring criteria: Score 0: No damage at all; Score 1: Mild damage with about <30%; Score 2: Moderate damage with range 30%-70%; Score 3: Severe damage with a percentage of >70% (Aminin *et al.*, 2024).

sides of the lamellae. The term fusion describes a condition where gas diffusion efficiency diminishes due to hyperplasia-induced damage to the gill epithelium and secondary lamellae (Abdel-Gaber *et al.,* 2023). The form of lamellar fusion damage is shown in Fig. 10C. Given the results of the identified lamellar fusion damage in fish gills, damage scoring can be executed using the existing formula. The scoring results for lamellar fusion damage in fish gills are shown in Table 4, which shows that mild damage occurred at stations 1 to 5, indicating a low level of water pollution. The average score at station 2 was the highest, standing at 24.4%, in contrast to station 5, which recorded the lowest average score of 9.74%. Gill organ damage was relatively high at station 1 and lowest at station 5. This was influenced by several factors and activities occurring near the sampling points. The high damage at station 1 was due to its location in the middle of a residential area and industrial activities. Correspondingly, stations 2 to 4 displayed similar percentage figures, attributed to their location near human activities. Station 5 had the lowest damage level because it was located near the sea, far from human activity. Gill tissue damage is thought to be affected by the exposure to harmful substances found in the water (Kostic *et al.*, 2017; Noor *et al.,* 2025). The poor condition of the Porong River, along with its proximity to residential and industrial activities, may contribute to the presence of toxic substances entering the water. This statement supports the analysis results, which show histological damage in fish from the Porong River, with percentages ranging from 9.74% to 35.51%. This damage disrupts the efficient transfer of oxygen and carbon dioxide, which in turn results in respiratory problems for fish. The consequences of gill damage

Table 4: Scoring of lamellar fusion damage to the gills

Station	Sampling			Average (%)	Score	Damage level
	1	2	3			
1	100	98	105	24.40	1	Mild damage
2	80	82	85	19.89	1	Mild damage
3	50	47	48	11.67	1	Mild damage
4	71	78	75	18.04	1	Mild damage
5	38	43	40	9.74	1	Mild damage

Note: the scoring criteria: Score 0: No damage at all; Score 1: Mild damage with about <30%; Score 2: Moderate damage with range 30%-70%; Score 3: Severe damage with a percentage of >70% (Aminin *et al*., 2024).

Table 5: Average results of temperature, TSS, and TDS measurements

Parameters	Station				
	1	2	3	4	5
Temperature (°C)	29.27	29.97	28.8	28.83	27.17
TSS (mg/L)	23.33	24.13	22.33	58	47.67
TDS (mg/L)	416.33	420.3	419.3	598.3	599

are critical to fish survival, as disrupted respiration can lead to physiological stress, decreased activity, metabolic imbalances, and, in severe cases, mortality. Consequently, the damage to gill tissues resulting from microplastics is a major concern for the health and survival of fish within aquatic environments (Ghost, 2024).

Water quality

Physics parameters

The average measurement of temperature, TSS, and TDS for each station are shown in Table 5. The lowest average temperature was recorded at Station 5, at 27.17°C, while the highest average temperature was observed at Station 2, at 29.97°C. The elevated temperature observed at Station 2 was probably affected by topographical elements that enhanced heat retention. An increasing temperature within a certain range can enhance the proliferation of aquatic organisms (Hutchins and Fu, 2017). Water temperature is influenced by land surface variations and pollutants from agricultural, livestock, and residential activities (Cheng *et al*., 2022), and also by ambient factors, such as water currents, turbulence, sunlight exposure, and turbidity. Indonesian Government Regulation No. 22 of 2021 on Environmental Protection and Management stated that the temperature of water should not deviate by more than 3°C. In line with these guidelines, the temperature levels in the Porong River are maintained within the acceptable ranges for Class II water quality, which continues to support healthy aquatic ecosystems. The lowest average TSS was recorded at Stations 1 and 3, with a value of 23.33 milligrams per liter (mg/L), while the highest average TSS was observed at Station 4, reaching 58 mg/L (Table 5). The increasing TSS at Station 4 was likely due to the accumulation of upstream waste, which increased TSS concentrations at Stations 4 and 5. The minimal tidal activity recorded at Stations 1 to 3 was responsible for the lowest TSS levels at Station 3. Furthermore, TSS levels are significantly impacted by river discharge rates, as stronger currents contribute to higher sediment production in aquatic environments (Beermann *et al*., 2018). TSS concentrations are influenced by organic matter input, land runoff, and seasonal variations. The presence of suspended solids in water is attributed to both biological elements, such as phytoplankton, zooplankton, and bacteria, and non-biological elements, which consist of inorganic particles (Buana *et al*., 2018). Indonesian Government Regulation No. 22 of 2021 stated that the Class II water quality standard for TSS is 50 mg/L. Results indicate that TSS in the Porong River complies with Class II standards at four stations, except at Station 4 that higher than the 50 mg/L threshold. It means that TSS at station 4 does not meet Class II standards but remains within Class III standards, which permit its use for freshwater aquaculture, livestock, and agriculture.

TDS measurements indicated that the lowest

Table 6: Average measurement results of DO, pH, ammonia, phosphate, nitrate, CO_2, TOM, and BOD

Parameters	Station				
	1	2	3	4	5
DO (mg/L)	5.5	5.2	4.93	5.17	5.73
pH	7.89	8.07	8.03	7.85	7.9
Ammonia (mg/L)	0.16	0.13	0.14	0.16	0.11
Orthophosphate (mg/L)	0.3	0.16	0.13	0.12	0.14
Nitrate (mg/L)	1.01	1.03	1.01	1.02	1.26
CO_2 (mg/L)	13.94	13.29	13.30	12.63	13.29
TOM (mg/L)	14.43	14.02	14.86	19.49	20.68
BOD (mg/L)	4.57	5.60	5.5	4	4.27

average TDS was recorded at Station 1, with a value of 416.3 mg/L, while the highest average TDS was observed at Station 5, at 599 mg/L (Table 5). The high TDS levels observed at Station 5 were linked to the dynamics of water flow, which led to an accumulation of TDS concentrations at both Stations 4 and 5. In contrast, Station 1 exhibited lower TDS levels due to minimal waste accumulation. TDS concentrations tend to rise in downstream areas due to sedimentation at river estuaries, where poorly soluble metals undergo prolonged dilution before settling in bottom sediments (Gantayat *et al.*, 2023). Agricultural practices, residential waste, and industrial discharges significantly impact TDS levels in aquatic ecosystems. Changes in TDS concentrations can impact water salinity and ion composition, potentially affecting the toxicity of specific ions (Mount *et al.*, 2016; Syamsu *et al.*, 2024). Indonesian Government Regulation No. 22 of 2021 has established that TDS quality standard for Class II water is 1000 mg/L. Following this standard, the TDS levels in the Porong River are maintained within acceptable thresholds for Class II water quality, ensuring favorable conditions for aquatic species.

Chemical parameters

DO level of the water river has the lowest average value at Station 3 (4.93 mg/L), while the highest was at Station 5 (5.73 mg/L) (Table 6). The increasing DO levels at Station 5 are due to the presence of phytoplankton and aquatic plants, which contribute to oxygen production through photosynthesis. Conversely, the lower DO levels at Station 3 were likely due to the limited vegetation around the river, which reduced oxygen availability. In water bodies, DO concentrations vary continuously due to the consumption and generation of oxygen by aquatic organisms, diffusion, and seasonal fluctuations (Bulbul and Mishra, 2022). DO of water environments originates from aeration and photosynthesis by aquatic plants. Aeration, as the primary source of DO in rivers, occurs when the water surface interacts with the atmosphere to restore equilibrium. When the concentration of oxygen in water decreases below saturation levels, this process facilitates its dissolution into the water (Marce *et al.*, 2024). The Class II water quality standard for DO is 4 mg/L based on Indonesian Government Regulation No. 22 of 2021. So, the DO concentrations in the Porong River remain within acceptable limits for Class II water quality, supporting aquatic life. The analysis of pH levels showed that Station 4 exhibited the lowest average pH of 7.85, in contrast to Station 2, which had the highest average pH of 8.07 (Table 6). The highest pH values were observed at Stations 2 and 3, whereas the lowest was recorded at Station 4. These results indicate that the Porong River has a predominantly alkaline water condition. The pH levels in aquatic ecosystems can fluctuate due to several influences, including photosynthesis, respiration, air temperature, the discharge of industrial waste, and the geological features of the riverbed substrate (Caesar *et al.*, 2023). Ammonia concentrations showed that the lowest average value was recorded at Station 5 (0.11 mg/L), while the highest was observed at Stations 1 and 4 (0.16 mg/L) (Table 6). Elevated ammonia levels at Stations 1 and 4 were attributed to household waste from residential areas and fish metabolism from aquaculture activities. Conversely, the lowest level of ammonia detected at Station 5 was due to a limited buildup of pollutants. Ammonia sources in aquatic environments include metabolic waste, such as feces and decomposing organic matter (Yang *et al.*, 2025). The main nitrogenous waste produced by aquatic animals is ammonia, which is expelled through the gills during metabolism. In fish farming areas, the levels

of ammonia are typically increased because of the accumulation of fish excrement. Additionally, ammonia pollution in rivers is influenced by rising temperatures, dissolved oxygen levels, and pH (Srivastava *et al*. 2022). Indonesian Government Regulation No. 22 of 2021 has set the Class II water quality standard for ammonia is 0.2 mg/L. This standard stated that ammonia concentrations in the Porong River remain within acceptable limits, supporting aquatic life.

Orthophosphate concentrations showed that the lowest average value was recorded at Station 4 (0.12 mg/L), while the highest was at Station 1 (0.30 mg/L) (Table 6). The increased phosphate levels at Station 1 were associated with household waste and runoff from agriculture, while the minimum levels were detected at Stations 1 and 2. Orthophosphate can originate from agricultural activities, industrial waste, and domestic sewage. High orthophosphate levels in water bodies can promote excessive algae growth, eutrophication, and ecosystem degradation (Badamasi *et al*., 2019). Detergents in household waste significantly contribute to high levels of orthophosphate, as they contain phosphate ions as fundamental compounds. Phosphates tend to dissolve in water as dominant phosphorus compounds, particularly under anaerobic conditions (Li *et al*., 2019). Indonesian Government Regulation No. 22 of 2021 has established that the Class II water quality standard for orthophosphate is 0.2 mg/L. According to this standard, the levels of orthophosphate in the Porong River are in accordance with Class II water quality standards at four different locations. However, Station 1 exceeds this threshold but remains within the Class III standard (1 mg/L), allowing its use for freshwater aquaculture, livestock, and agriculture. Nitrate concentrations revealed that the lowest average value was recorded at Stations 1 and 3 (1.01 mg/L), while the highest was at Station 5 (1.26 mg/L) (Table 6). The increased nitrate levels at Station 5 were caused by the accumulation of organic fertilizer residues from downstream agricultural, plantation, and aquaculture activities, whereas Stations 1 and 3 showed the lowest nitrate concentrations. Nitrate concentrations in water bodies can fluctuate due to both natural processes and human activities, such as agriculture, industry, and domestic waste disposal (Craswell, 2021). Elevated nitrate levels can lead to eutrophication, which promotes unchecked growth of algae and aquatic vegetation. This process disrupts the balance of aquatic ecosystems, compromises water quality, and may cause widespread fish die-offs due to decreased dissolved oxygen availability. Conversely, low nitrate concentrations indicate better water quality (McGoff *et al*., 2017). Indonesian Government Regulation No. 22 of 2021 has established that the Class II water quality standard for nitrate is ≤10 mg/L. Thus, nitrate concentrations in the Porong River remain within the standard to support aquatic life. Carbon dioxide (CO_2) concentrations showed that the lowest average value was recorded at Station 4 (12.63 mg/L), while the highest was at Station 1 (13.94 mg/L) (Table 6). Elevated measurements at Station 1 were linked to the discharge of household waste, while the minimal levels observed at Station 4 were a result of lower pollutants and organic matter, promoting ideal conditions for photosynthesis among aquatic plants. High CO_2 concentrations in water bodies can be caused by household waste, urban runoff, and organic matter decomposition (Akhtar *et al*., 2021). CO_2 concentrations in water are influenced by nutrient availability. Sedimentation and reduced turbidity can promote photosynthesis increasing oxygen production and decreasing CO_2 levels (Reitsema *et al*., 2018). It is found that CO_2 levels in the Porong River (12.63–13.94 mg/L) are lower than tolerable CO_2 concentration for aquatic organisms (5 - 10 mg/L) so this condition is less optimal for aquatic life. TOM concentrations are shown in Table 6. The lowest average TOM was recorded at Station 2 (14.02 mg/L), while the highest was at Station 5 (20.68 mg/L). The significant TOM concentrations recorded at Station 5 were due to an increased presence of organic pollutants in the estuary, while the minimal levels at Station 2 reflected lower pollution impacts. High TOM levels in water bodies can reduce dissolved oxygen and pH negatively affecting water quality (Ariadi *et al*., 2019). When there is too much organic matter, it can cause eutrophication, which leads to rampant growth of aquatic life and disrupts the balance of ecosystems. High TOM levels are typically caused by dissolved or suspended organic and inorganic particles that degrade over time (Singh *et al*., 2021). The standard for TOM is 80 mg/L (Indonesian Government Regulation No. 22 of 2021) for Class III water quality. Thus, TOM concentrations in the Porong River comply with Class III standards, making it suitable for freshwater aquaculture, livestock, and agriculture. The results of BOD measurements indicated that the lowest average BOD was recorded at Station 4, with a value of 4 mg/L, while the highest was found at Station 2, measuring 5.6 mg/L (Table 6). Stations 2 and 3 showed the highest average BOD values, in contrast

to Station 4, which had the lowest readings. BOD represents the amount of dissolved oxygen required by microorganisms to decompose organic matter under aerobic conditions. BOD measures the oxygen demand for the decomposition of organic matter rather than providing an accurate representation of its actual quantity (Wei *et al*., 2023). Elevated BOD levels in water often result from organic waste entering the aquatic environment. High BOD concentrations can significantly reduce dissolved oxygen levels, impairing the ability of aerobic bacteria to degrade organic matter. With the further reduction of oxygen levels, anaerobic bacteria become the primary agents of decomposition, possibly causing unpleasant odors in the water (Dissanayaka *et al*., 2022). Indonesian Government Regulation No. 22 of 2021 has set the BOD standard for Class II water quality at 3 mg/L. This standard indicates that BOD concentration in the Porong River is higher than the Class II water quality limit so river water is less optimal for supporting aquatic life. ANOVA indicates that each station result in BOD is significantly different (α=95%, p=0.0387; n=5). The statistical analysis indicates that the abundance of microplastics varies significantly between observation stations and also shows discrepancies in water quality. From a chemical perspective, microplastics can act as vectors for hazardous substances such as heavy metals, pesticides, and organic pollutants that adhere to their surfaces. These contaminants can contribute to a reduction in DO levels and elevate BOD and COD, as they promote increased microbial activity during the decomposition process. Furthermore, microplastics can indirectly influence water pH by gathering materials that disturb the acid-base equilibrium. Biologically, microplastics induce stress and toxicity in aquatic organisms, leading to tissue damage, impaired growth, and in severe cases, mortality—ultimately reducing biodiversity. Additionally, microplastics create environments conducive to the colonization of pathogenic microorganisms through biofilm formation, which can lead to the destabilization of the natural microbial ecosystem. Thus, the presence of microplastics not only signifies environmental contamination but also actively degrades water quality and threatens the ecological integrity of aquatic ecosystems (Banaee *et al.,* 2023).

Analysis of relationships between parameters using CCA

The CCA was conducted to identify and explain the relationships between the influence of biotic and abiotic habitat factors caused by microplastics. The outcomes deliver vital information that can inform focused mitigation strategies and improve the effectiveness of environmental management policies. The CCA results reveal a positive correlation between microplastics in the gills and the neutrophil and eosinophil parameters.

This correlation indicated that microplastic exposure in the gills triggers an immune response, identified by the increased number of neutrophils and eosinophils. This reaction is linked to oxidative stress or irritation of gill tissue resulting from microplastic particles, which trigger an immune response. Additionally, the correlation between microplastics in the gills and MCH/MCHC suggests potential alterations in the blood's oxygen transport capacity. Damage to erythrocytes or disruptions in ion homeostasis caused by particles affect hemoglobin-related parameters. The study reveals a negative correlation between sediment microplastics and the platelet and hematocrit values. It suggests a possible blood coagulation disorder or hemodilution due to microplastic exposure because compounds within particles interfere with red blood cell and platelet production or stability. Furthermore, the correlation between microplastics in water and the lymphocyte and hematocrit parameters is positive. This findings indicate that microplastics found in water may stimulate the adaptive immune system, as demonstrated by the elevated lymphocyte count. The rise in hematocrit levels may also indicate a physiological response to environmental stress, such as mild hypoxia, potentially caused by interactions between microplastics and the fish's respiratory or metabolic systems. The CCA results identified a positive correlation observed between microplastic in the gills and sediment with edema and hyperplasia parameters. When gills are exposed to microplastics, it causes edema and an increase in epithelial thickness, primarily due to enhanced cell proliferation (hyperplasia). Edema indicates heightened environmental stress, while hyperplasia is often associated with an increased toxic load affecting the gill tissues. Conversely, the link between microplastics found in the intestines and histopathological parameters is not strongly established.. Microplastic exposure in the intestines has a lesser impact on structural tissue changes compared to the gills. However, no significant correlation is found between microplastic in sediment and gills with the lamellar fusion parameter. This result

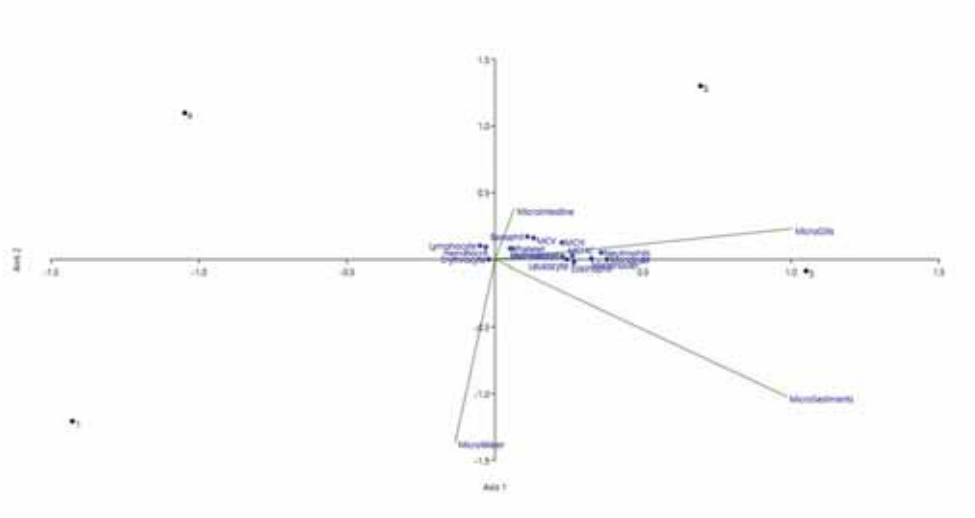

(A)

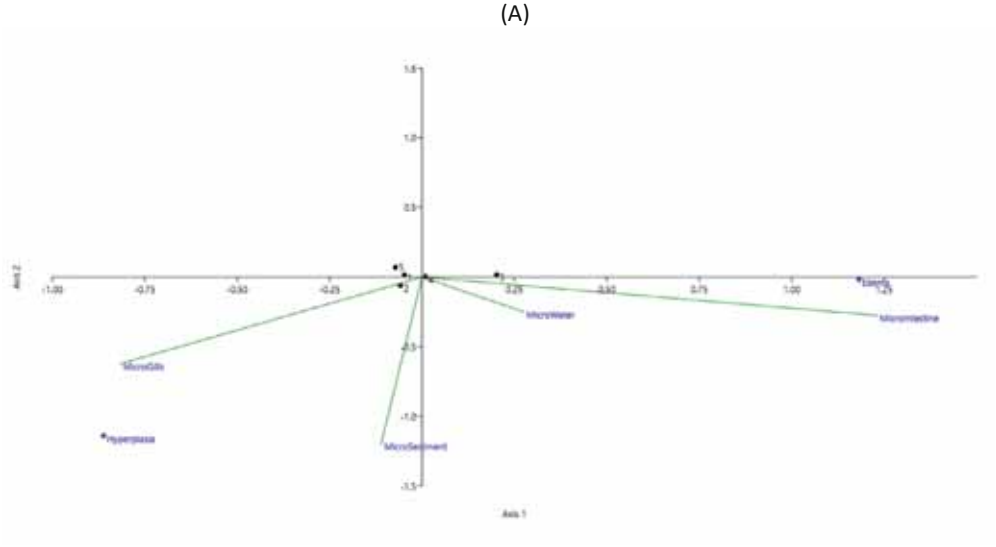

(B)

Fig. 11: CCA test results microplastic Test : (A) with hematology test, (B) with hepatology test

points to the possibility that lamellar fusion is subject to other factors that were excluded from this analysis. Based on the findings, microplastic contamination in the Porong River has negatively impacted fish health status.

CONCLUSION

Evaluation of microplastic contamination in the Porong River and its effects on fish health has been conducted. The data showed that microplastics were prevalent throughout all sampling sites, occurring in both the water and sediment. The highest concentration of microplastics was found at Station 1, with a value of 94.3 particles/m^3, while the lowest concentration was recorded at Station 4, with a value of 41.4 particles/m^3. In sediment, microplastic concentrations of 30.9 particles/m^3 were found at Station 4, and 166.1 particles/m^3 were found at Station 2. These findings reveal that sediments serve as more significant deposition sites for microplastics in comparison to water. The hematological analysis of fish indicated significant deviations in blood cell parameters. The neutrophil count had an average value of 11.82%. This value is higher than the normal range (6%–8%), obtained at Stations 2, 3, 4, and 5. Furthermore,

lymphocyte counts at these four stations were also lower than the normal level (68%–86%), indicating a possible state of immunosuppression caused by environmental stress or microplastic contamination. When lymphocyte counts decrease, fish become less capable of defending themselves against infections and various pathogens in the environment. Histopathological analysis of fish gills indicates a mild damage level at all observation stations, with the highest damage level scored at Station 2 (24.4%) and the lowest at Station 5 (9.74%). The observed damage to the gills featured edema, hyperplasia, and lamellar fusion, indicating responses to microplastic exposure. Edema indicates high environmental stress, while hyperplasia is usually associated with increased toxic load affecting the gill tissues. The process of lamellar fusion can hinder the efficiency of gas diffusion, leading to disruptions in both respiration and the fish's overall metabolism. Water quality analysis showed that temperature ranged from 27.17°C to 29.97°C, with the highest value found at Station 2. The highest TSS concentration was found at Station 4 (58 mg/L), likely due to the accumulation of waste from upstream. The correlation between microplastics and water quality indicators suggests that the physical and chemical characteristics of water play a significant role in the distribution and accumulation of microplastics in the river. Based on the CCA analysis, microplastics in gills and sediment showed a positive correlation with edema and hyperplasia parameters, indicating that microplastic exposure can trigger immune responses in fish marked by increased numbers of neutrophils and eosinophils. Overall, the findings of this study emphasize that microplastic pollution in the Porong River adversely affects the fish health. The accumulation of microplastics in fish organs causes disturbances in hematological parameters, structural changes in gill tissues, and shows correlations with various water quality parameters. Consequently, enhanced efforts are necessary to enforce regulations regarding plastic waste management, particularly in the industrial and residential sectors near the Porong River. While the presence and composition of microplastics have been analyzed, further studies are needed to accurately identify and trace the specific sources of pollution, including both industrial and domestic waste. To mitigate the negative impacts of microplastic contamination, policymakers should strengthen regulations on plastic production and consumption—especially targeting single-use plastics—and implement effective waste management systems at both local and national levels. Raising awareness through public education campaigns is essential for informing individuals about proper plastic disposal techniques and the long-term hazards of microplastic pollution. Additionally, it is essential to enhance environmental monitoring programs to routinely assess microplastic concentrations and their effects on aquatic life. Supporting research and innovation in biodegradable materials and promoting eco-friendly alternatives to conventional plastics are also crucial steps toward reducing plastic dependency and ensuring the health of freshwater ecosystems. Furthermore, this study presents only a limited view of contamination levels, and the long-term effects of bioaccumulation, along with the broader ecological implications, remain insufficiently investigated. Future research is recommended to investigate the long-term biological effects on fish populations and to develop sustainable solutions for pollution control. By highlighting organ-specific accumulation and hematological alterations, the results pave the way for investigations into toxicity mechanisms, long-term bioaccumulation, and trophic transfer within aquatic food webs. These insights play a key role in evaluating potential risks to human consumers, informing public health guidelines, and crafting effective environmental policies aimed at reducing plastic pollution.

AUTHOR CONTRIBUTIONS

U. Yanuhar, as the first author and the corresponding author, as a granted receiver, conducted the research design and data analysis and wrote the main manuscript. E.N. Wiratno, performed the preparing data and laboratory analysis, H. Suryanto supervised all data analysis and revised manuscripts, D.R. Machfuda, prepared the materials, data collection and analysis, N.R. Caesar, has done the data collection, and analysis. All authors read and put comments to improve the manuscript.

ACKNOWLEDGMENTS

The authors acknowledge the Faculty of Fisheries and Marine Sciences of Brawijaya University for funding the Research Professors 2024 with Contract Number: [3703/UN10.F06/KS/].

CONFLICT OF INTEREST

The authors declare that there are no conflicts of interest regarding the publication of this manuscript. In addition, the ethical issues, including plagiarism, informed consent, misconduct, data fabrication and/or falsification, double publication and/or submission, and redundancy, were observed by the authors.

OPEN ACCESS

©2025 The author(s). This article is licensed under a Creative Commons Attribution 4.0 International License, which permits use, sharing, adaptation, distribution, and reproduction in any medium or format, as long as you give appropriate credit to the original author(s) and the source, provide a link to the Creative Commons license, and indicate if changes were made. The images or other third-party material in this article are included in the article's Creative Commons license unless indicated otherwise in a credit line to the material. If material is not included in the article's Creative Commons license and your intended use is not permitted by statutory regulation or exceeds the permitted use, you will need to obtain permission directly from the copyright holder. To view a copy of this license, visit:

http://creativecommons.org/licenses/by/4.0/

PUBLISHER'S NOTE

GJESM Publisher remains neutral with regard to jurisdictional claims in published maps and institutional afflictions.

☐ Positive AI Statement

During the preparation of this work the author(s) have used [NAME TOOL / SERVICE] in order to [REASON]. After using this tool/service, the authors reviewed and edited the content as needed and took full responsibility for the content of the publication. Furthermore, the GPTZero detector will evaluate the manuscript utilizing Generative AI, ensuring a high detection rate. If the manuscript relies heavily on Generative AI and AI-assisted technologies, it will be archived without further options for appeal.

☑ Negative AI Statement

The author(s) declare that no AI tools or services were not used or not highly applied during the preparation of this work.

ABBREVIATIONS

%	Percent
°C	Degree Celsius
µm	Micrometer
µm³	Cubic micrometer
ANOVA	Analysis of variance
BOD	Biochemical oxygen demand
CCA	Canonical correspondence analysis
cells/mm³	Cells per cubic millimeter
CO_2	Carbon dioxide
DO	Dissolved oxygen
DNA	deoxyribonucleic acid
g/dl	Gram/deciliter
H_2O_2	Hydrogen peroxide
Hb	Hemoglobin
kg	Kilogram
L	Liter
m	Meter
MCH	Mean corpuscular hemoglobin
MCHC	Mean corpuscular hemoglobin concentration
MCV	Mean corpuscular volume
mg/L	Miligram/Liter
Ml	Milliliter
ml/L	Milliliter/Liter
mm	Millimeter
PAST	Paleontological STatistics
particles/m³	Particles per cubic meter
pg	Picogram
pH	Potential of hydrogen
PE fiber	Polyethylene Fiber
PET	Polyethylene terephthalate
PP	Polypropylene
Rpm	Revolutions per minute
SEM	Scanning electron microscope
TDS	Total dissolved solids

TOM	Total organic matter
TSS	Total suspended solids
UV	Ultraviolet

REFERENCES

Abdel-Gaber, R.; Al Quraishy, S.; Alghamdi, M.; Aljawdah, H.M.; Maodaa, S.N.; Al-Shaebi, E.M., (2023). DNA barcoding of Argyrops filamentous (Perciformes: Sparidae) based on mitochondrial COI gene and histopathological evaluation of gills infected by monogeneans. Indian J. Anim. Res., 1626: 1-6 (6 pages).

Abdelhamid, A.M.; Refaey, M.A.; Salem, M.F.; El-Kattan, M.A.M., (2019). Factors affecting fish blood profile: A-effect of nutritional treatments. Egypt. J. Aquat. Biol. Fish., 23(2): 517-526 (**10 pages**).

Abdel-Tawwab, M.; Monier, M.N.; Hoseinifar, S.H.; Faggio, C., (2019). Fish response to hypoxia stress: growth, physiological, and immunological biomarkers. Fish Physiol. Biochem., 45: 997-1013 (**17 pages**).

Ahmed, I.; Reshi, Q.M.; Fazio, F., (2020). The influence of the endogenous and exogenous factors on hematological parameters in different fish species: a review. Aquac. Int., 28: 869-899 (**31 pages**).

Akhtar, N.; Syakir Ishak, M.I.; Bhawani, S.A.; Umar, K., (2021). Various natural and anthropogenic factors responsible for water quality degradation: A review. Water 13(9): 2660. (**35 pages**).

Alava, J.J.; Cheung, W.W.; Ross, P.S.; Sumaila, U.R., (2017). Climate change–contaminant interactions in marine food webs: Toward a conceptual framework. Global. Change Biol., 23(10): 3984-4001 (**18 pages**).

Alberghini, L; Truant, A; Santonicola, S; Colavita, G; Giaccone, V. (2023). Microplastics in Fish and Fishery Products and Risks for Human Health: A Review. Int. J. Environ. Res. Public Health, 20(1), 789 (**17 Pages**).

Ali, B.; Anushka; Mishra, A., (2022). Effects of dissolved oxygen concentration on freshwater fish: A review. Int. J. Fish. Aquat. Stud., 10(4): 113-127 (**15 pages**).

Alimi, O.S.; Budarz, J.F.; Hernandez, L.M.; Tufenkji, N., (2018). Microplastics and nanoplastics in aquatic environments: aggregation, deposition, and enhanced contaminant transport. Environ. Sci. Technol., 52(4): 1704-1724 (**21 pages**).

Aminin, A.; Arfiaty, D.; Andayani, S., (2024). Histopathological changes and Metallothionein levels in Filopaludina javanica during depuration. Adv. Sustain. Sci. Eng. Technol., 6(3): 02403019-01 - 02403019-08 (**8 pages**).

Anggraini, R.R.; Risjani, Y.; Yanuhar, U., (2020). Plastic litter as pollutant in the aquatic environment: A mini-review. Sci. J. Fish. Mar., 12: 167-180 (**14 pages**).

Ariadi, H.; Fadjar, M.; Mahmudi, M., (2019). The relationships between water quality parameters and the growth rate of white shrimp (Litopenaeus vannamei) in intensive ponds. Aquac. Aquar. Conserv. Legis., 12(6): 2103-2116 (**14 pages**).

Badamasi, H.; Yaro, M.N.; Ibrahim, A.; Bashir, I.A., (2019). Impacts of phosphates on water quality and aquatic life. Chem. Res. J., 4(3): 124-133 (**10 pages**).

Banaee, M; Multisanti, C.R; Impellitteri, F; Piccione, G; Faggio, C., (2024). Environmental toxicology of microplastic particles on fish: A review. Comp. Biochem. Physiol. C, 110042 (**19 Pages**).

Bbole, I.; Mumba, C.; Mupenda, N.; Kefi, A.S., (2016). Analysis of growth performance and haematological parameters of Oreochromis niloticus fed on a varying diet of Moringa oleifera Lam. leaf meal as an additive protein source. Int. J. Fish. Aquacult., 8(11): 105-111 (**7 pages**).

S. Basri K.; Daud, A.; Birawida, A.B.; Maming, M.; Mukono, H.J.; Arsyad, D.S., (2024). Microplastic polymers in shellfish and fish in the coastal area. Global J. Environ. Sci. Manag., 10(4): 1477-1500 (**24 pages**).

Beermann, A.J.; Elbrecht, V.; Karnatz, S.; Ma, L.I.; Matthaei, C.D.; Piggott, J.J.; Leese, F., (2018). Multiple-stressor effects on stream macroinvertebrate communities: A mesocosm experiment manipulating salinity, fine sediment and flow velocity. Sci. Total Environ., 610: 961-971 (**11 pages**).

Biller, J.D.; Takahashi, L.S., (2018). Oxidative stress and fish immune system: phagocytosis and leukocyte respiratory burst activity. An. Acad. Bras. Ciênc., 90(4): 3403-3414 (**12 pages**).

Binelli, A.; Torre, C.D.; Nigro, L.; Riccardi, N.; Magni, S., (2022). A realistic approach for the assessment of plastic contamination and its ecotoxicological consequences: A case study in the metropolitan city of Milan (N. Italy). Sci. Total Environ., 806: 150574 (**19 pages**).

Buana, S.; Tambaru, R.; Selamat, M.B.; Lanuru, M.; Massinai, A., (2021). The role of salinity and Total Suspended Solids (TSS) to abundance and structure of phytoplankton communities in estuary Saddang Pinrang. IOP Conference Series: Earth Environ. Sci., 860: 012081 (**9 pages**).

Buttarello, M., (2016). Laboratory diagnosis of anemia: are the old and new red cell parameters useful in classification and treatment, how?. Int. J. Lab. Hematol., 38(1): 123-132 (**10 pages**).

Buwono, N.R.; Risjani, Y.; Soegianto, A., (2021). Contamination of microplastics in Brantas River, East Java, Indonesia and its distribution in gills and digestive tracts of fish Gambusia affinis. Emerg. Contam., 7: 172-178 (**7 pages**).

Buwono, N.R.; Risjani, Y.; Soegianto, A., (2021). Distribution of microplastic in relation to water quality parameters in the Brantas River, East Java, Indonesia. Environ. Technol. Innov., 24: 101915 (**10 pages**).

Caesar, N.R.; Yanuhar, U.; Faqih, A.R.; Anitasari, S.; Ciptadi, G.; Musa, M.; Bisri, M.; Wardani, N.P., (2024). Correlation between water quality and surfactant pollution in the Porong River. BIO-Web Conference. 117(2024): 01010) (**8 pages**).

Caesar, N.R.; Yanuhar, U.; Musa, M.; Ciptadi, G.; Suryanto, H.; Wahyudi, Y.A.; Soelistyoadi, R.N., (2023). Heavy metals contamination and their impacts on fish responses in Porong River, East Java, Indonesia. Evergreen. 10(3): 1218-1230 (**13 pages**).

Chae, Y.; An, Y.J., (2017). Effects of micro-and nanoplastics on aquatic ecosystems: Current research trends and perspectives. Mar. Pollut. Bull., 124(2), 624-632 (**8 pages**).

Chandrashekar, A.; Singh, G.; Garry, J.; Sikalas, N.; Labropoulos, N., (2018). Mechanical and biochemical role of fibrin within a venous thrombus. Eur. J. Vasc. Endovasc. Surg., 55(3): 417-424 (**8 pages**).

Chen, H.; Luo, D., (2023). Application of haematology parameters for health management in fish farms. Rev. Aquac., 15(2): 704-737 (**34 pages**).

Cheng, C.; Zhang, F.; Shi, J.; Kung, H.T., (2022). What is the relationship between land use and surface water quality? A review and prospects from remote sensing perspective. Environ. Sci. Pollut. Res., 29(38): 56887-56907 (**21 pages**).

Chmielewski, P.P.; Strzelec, B.J.F.M., (2018). Elevated leukocyte count as a harbinger of systemic inflammation, disease progression, and poor prognosis: a review. Folia Morphol., 77(2): 171-178 (**8 pages**).

Craswell, E., (2021). Fertilizers and nitrate pollution of surface and ground water: an increasingly pervasive global problem. SN Appl. Sci., 3(4): 518 (**24 pages**).

Dimassi, S.N.; Hahladakis, J.N.; Yahia, M.N.D.; Ahmad, M.I.; Sayadi, S.; Al-Ghouti, M.A., (2022). Degradation-fragmentation of marine plastic waste and their environmental implications: A critical review. Arab. J. Chem., 15(11): 104262 (**31 pages**).

Dissanayaka, D.M.O.N.; Pinsarani, W.G.J.R.; Himanujahn, S.; Athapattu, B.C.L., (2022). Assessing the impact of eutrophication and hourly discharge on dissolved oxygen fluctuation of urban water system linked to an estuary. J. Eng. Technol., 10(2): 40-51 (**12 pages**).

Doig, K.; Zhang, B., (2017). A methodical approach to interpreting the red blood cell parameters of the complete blood count. Am. Soc.

Clin. Lab. Sci., 30: 173-185 (**13 pages**).
Elarabany, N.; Bahnasawy, M.; Edrees, G.; Alkazagli, R., (2017). Effects of salinity on some haematological and biochemical parameters in Nile tilapia, Oreochromus niloticus. A Agric. For. Fish., 6(6): 200-205 (**6 pages**).
Farkha, D.K.; Diana, A.; Feni, I., (2021). Hematology and micronuclei analysis of tilapia (Oreochromis niloticus) from Selorejo Reservoir, Ngantang, Malang, Indonesia. Russ. J. Agric. Socio-Econ. Sci., 112(4): 142-148 **(7 pages**).
Fazio, F., (2019). Fish hematology analysis as an important tool of aquaculture: a review. Aquaculture 500: 237-242 (**6 pages**).
Firdaus, M.; Trihadiningrum; Y.; Lestari, P., (2020). Microplastic pollution in the sediment of Jagir Estuary, Surabaya City, Indonesia. Mar. Pollut. Bull., 150: 110790 (**8 pages**)
Firdaus-Nawi, M.; Zamri-Saad, M., (2016). Major components of fish immunity: a review. Pertanika J. Trop. Agric. Sci., 39(4): 393-420 (**28 pages**).
Gantayat, R.R.; Viswanathan, P.M.; Ramasamy, N.; Sabarathinam, C., (2023). Spatial and temporal variations of geochemical processes and toxicity of water, sediments, and suspended solids in Sibuti River Estuary, NW Borneo. Environ. Sci. Pollut. Res., 30: 92692–92719 (**28 pages**).
Ghosh, T., (2024). Microplastics bioaccumulation in fish: its potential toxic effects on hematology, immune response, neurotoxicity, oxidative stress, growth and reproductive dysfunction. Toxicol. Rep., 101854 (**22 page**).
Gigault, J.; El Hadri, H.; Nguyen, B.; Grassl, B.; Rowenczyk, L.; Tufenkji, N.; Feng, S.; Wiesner, M., (2021). Nanoplastics are neither microplastics nor engineered nanoparticles. Nat. Nanotechnol., 16(5): 501-507 (**7 pages**).
Go, M. ; Ybanez, A.; Ilano, A.; Cababat, F.; De La Calzada, L., (2024). Microplastics in beach sediments, seawater, and common fish in tourist destinations. Global J. Environ. Sci. Manage., 10(4): 1993-2008 **(16 pages).**
Gonzalez-Saldias, F.; Sabater, F.; Gomà, J., (2024). Microplastic distribution and their abundance along rivers are determined by land uses and sediment granulometry. Sci. Total Environ., 933, 173165 (**8 Pages**).
Hajji, A.L.; Lucas, K.N., (2024). Anthropogenic stressors and the marine environment: From sources and impacts to solutions and mitigation. Mar. Pollut. Bull., 205: 116557 (**19 pages**).
Hakim, L.; Riani, E.; Iswari, M.Y.; Cordova, M.R., (2024). Microplastic contamination in the gut and gills of commercial marine fish. Global J. Environ. Sci. Manage., 10(4): 1897-1916 (**20 pages**).
Havixbeck, J.J.; Rieger, A.M.; Wong, M.E.; Hodgkinson, J.W.; Barreda, D.R., (2016). Neutrophil contributions to the induction and regulation of the acute inflammatory response in teleost fish. J. Leukoc. Biol., 99(22): 241-252 (**12 pages**).
Hertika, A.M.S.; Risjani, Y.; Buwono, N.R.; Kei, S.A.A.; Heratiana, Y.Y.; Nur, Z.K.; Ashari, F.I.A.; Alfarisi, M.A.; Halimah, M.F., (2024). Blood and micronuclei analysis of Tawes fish (Barbonymus gonionotus) correlation with water quality in the Boon Pring Ecotourism Area, Turen, Malang Regency. IOP Conference Series: Earth Environ. Sci., 1328(1): 012016 (**13 pages**).
Huang, D.; Chen, H.; Shen, M.; Tao, J.; Chen, S.; Yin, L.; Zhou, W.; Wang, X.; Xiao, R.; Li, R., (2022). Recent advances on the transport of microplastics/nanoplastics in abiotic and biotic compartments. J. Hazard. Mater., 438: 129515 (**18 pages**).
Hutchins, D.A.; Fu, F., (2017). Microorganisms and ocean global change. Nat. Microbiol., 2: 1-11 (**11 pages**).
Imanpoor, M.; Imanpoor, M.R.; Roohi, Z., (2017). Effects of dietary vitamin C on skeleton abnormalities, blood biochemical factors, haematocrit, growth, survival and stress response of Cyprinus carpio fry. Aquac. Int., 25: 793-803 (**11 pages**).
Iskandar, M.R.; Park, Y.G.; Surinati, D.; Nugroho, D.; Cordova, M.R., (2024). Estimation of bottom microplastic flux in the Indonesian seas. Mar. Pollut. Bull., 209, 117047 (**6 pages**).
Ismarica, I.; Helda, M.; Dewi, C.D., (2025). Addition of garlic (Allium sativum) extract in fry as immunostimulant on survival and blood profile of pomfret fish (Colossoma macropomum). BIO Conference. 156: 03027 (**9 pages**).
Jiao, H.; Ali, S.S.; Alsharbaty, M.H.M.; Elsamahy, T.; Abdelkarim, E.; Schagerl, M.; Al-Tohamy, R.; Sun, J., (2024). A critical review on plastic waste life cycle assessment and management: Challenges, research gaps, and future perspectives. Ecotoxicol. Environ. Saf., 271: 115942 (**17 pages**).
Jo, A.H.; Yu, Y.B.; Choi, J.H.; Lee, J.H.; Choi, C.Y.; Kang, J.C.; Kim, J.H., (2025). Microplastics induce toxic effects in fish: Bioaccumulation, hematological parameters and antioxidant responses. Chemosphere. 375: 144253 (**12 pages**).
Khan, G.B.; Akhtar, N.; Khan, M.F.; Ullah, Z.; Tabassum, S.; Tedesse, Z., (2022). Toxicological impact of zinc nano particles on tilapia fish (Oreochromis mossambicus). Saudi J. Biol. Sci., 29(2): 1221–1226 (**6 pages**).
Kim, H.; Sefcik, J.S.; Bradway, C., (2017). Characteristics of qualitative descriptive studies: A systematic review. Res. Nurs. Health., 40(1): 23-42 (**20 pages**).
Kim, J.H.; Yu, Y.B.; Choi, J.H., (2021). Toxic effects on bioaccumulation, hematological parameters, oxidative stress, immune responses and neurotoxicity in fish exposed to microplastics: A review. J. Hazard. Mater., 413: 125423 (**18 pages**).
Kostić, J.; Kolarević, S.; Kračun-Kolarević, M.; Aborgiba, M.; Gačić, Z.; Paunović, M.; Višnjić-Jeftić, Ž.; Rašković, B.; Poleksić, V.; Lenhardt, M.; Vuković-Gačić, B., (2017). The impact of multiple stressors on the biomarkers response in gills and liver of freshwater breams during different seasons. Sci. Total Environ., 601: 1670-1681 (**12 pages**).
Lestari, P.; Trihadiningrum, Y.; Wijaya, B.A.; Yunus, K.A.; Firdaus, M., (2020). Distribution of microplastics in Surabaya River, Indonesia. Sci. Total Environ., 726: 138560 (**12 pages**)
Li, L.; Pang, H.; He, J.; Zhang, J., (2019). Characterization of phosphorus species distribution in waste activated sludge after anaerobic digestion and chemical precipitation with Fe3+ and Mg2+. Chem. Eng. J., 373: 1279-1285 (**7 pages**).
Li, Y.; Wang, X.; Fu, W.; Xia, X.; Liu, C.; Min, J.; Zhang, W.; Crittenden, J.C., (2019). Interactions between nano/micro plastics and suspended sediment in water: Implications on aggregation and settling. Water Res., 161: 486-495 (**10 pages**).
Macirella, R.; Brunelli, E., (2017). Morphofunctional alterations in zebrafish (Danio rerio) gills after exposure to mercury chloride. Int. J. Mol. Sci., 18(4): 824 (**19 pages**).
Manon-Jensen, T.; Kjeld, N.G.; Karsdal, M.A., (2016). Collagen-mediated hemostasis. J. Thromb. Haemost., 14(3): 438-448 (**11 pages**).
Marcé, R.; Gómez-Gener, L.; Carey, C.C., (2024). Oxygen. In Wetzel's Limnology. Academic Press. 237-274 (**38 pages**).
Maulana, M.R.; Saiful, S.; Muchlisin, Z.A., (2023). Microplastics contamination in two peripheral fish species harvested from a downstream river. Global J. Environ. Sci. Manage., 9(2): 299-308 **(10 pages).**
McGoff, E.; Dunn, F.; Cachazo, L.M.; Williams, P.; Biggs, J.; Nicolet, P.; Ewald, N.C., (2017). Finding clean water habitats in urban landscapes: professional researcher vs citizen science approaches. Sci. Total Environ., 581: 105-116 (**12 pages**).
Mohamad, S.; Liew, H.J.; Zainuddin, R.A.; Rahmah, S.; Waiho, K.; Ghaffar, M.A.; Nhan, H.T.; Loh, J.Y.; Lim, L.S.; Chang, Y.; Liang, L., (2021). High environmental temperature and low pH stress alter the gill phenotypic plasticity of Hoven's carp Leptobarbus hoevenii. J. Fish Biol., 99(1): 206-218 (**13 pages**).
Mount, D.R.; Erickson, R.J.; Highland, T.L.; Hockett, J.R.; Hoff, D.J.; Jenson, C.T.; Norberg-King, T.J.; Peterson, K.N.; Polaske, Z.M.; Wisniewski, S., (2016). The acute toxicity of major ion salts to Ceriodaphnia dubia:

I. Influence of background water chemistry. Environ. Toxicol. Chem., 35(12): 3039-3057 (**19 pages**).

Moura, M.R.; FalcÃ£o, S.M.; da Silva, A.C.; Neto, A.R.; Montenegro, S.M.; da Silva, S.R., (2020). Developing a Plastic Waste Management Program: From River Basins to Urban Beaches (Case Study). J. Eng. Technol. Sci., 52(1), 108-120 (**13 Pages**).

Nabi, N.; Ahmed, I.; Wani, G.B., (2022). Hematological and serum biochemical reference intervals of rainbow trout, Oncorhynchus mykiss cultured in Himalayan aquaculture: Morphology, morphometrics and quantification of peripheral blood cells. Saudi J. Biol. Sci., 29(4): 2942-2957 (**16 pages**).

Nakano, H.; Alfonso, M.B.; Phinchan, N.; Jandang, S.; Manap, M.A.; Chavanich, S.; Viyakarn, V.; Müller, M.; Wong, C.; Bacosa, H.P.; Celik, M., (2025). Aquatic microplastics research in the ASEAN region: Analysis of challenges and priorities. Mar. Pollut. Bull., 210: 117342 (**13 pages**).

Nikinmaa, M.; Berenbrink, M.; Brauner, C.J., (2019). Regulation of erythrocyte function: multiple evolutionary solutions for respiratory gas transport and its regulation in fish. Acta Physiol., 227(2): e13299 (**16 pages**).

Noor, S.Y.; Riani, E.; Hariyadi, S.; Butet, N.A.; Cordova, M.R., (2025). Microplastic accumulation in respiratory and digestive systems of selected fish from Banten Bay, Indonesia. Environ. Monit. Assess., 197(4): 1-21 (**21 pages**).

Nurhasanah; Hasrianti; Hakim, L.; Riani, E.; Iswari, M.Y.; Cordova, M.R., (2024). Microplastic contamination in the gut and gills of commercial marine fish. Global J. Environ. Sci. Manage., 10(4): 1897-1916 (**20 pages**).

O'Brien, A.; Townsend, K.; Hale, R.; Sharley, D.; Pettigrove, V., (2016). How is ecosystem health defined and measured? A critical review of freshwater and estuarine studies. Ecol. Indic., 69: 722-729 (**8 pages**).

Pal, D; Prabhakar, R; Barua, V.B;. (2025). Microplastics in aquatic systems: A comprehensive review of its distribution, environmental interactions, and health risks. Environ Sci Pollut Res 32, 56–88 (**32 pages**).

Patra, A.; Das, S.; Das, S.; Mandal, A.; Mondal, N.S.; Ghosh, A.R., (2024). Assessing haematological parameters and probable toxicity analysis in two coastal fish species at harbouring areas of Digha coastal belt, West Bengal, India. Environ. Res., 249: 118318 (**17 pages**).

Piranti, A.S.; Wibowo, D.N., (2020). The use of phytoplankton communities for assessment of water quality in the Wadaslintang Reservoir in Indonesia. J. Water Land Dev., 46: 170-178 (**9 pages**).

Purnama, D.; Zamani, N.P.; Bengen, D.G.; Cordova, M.R., (2025). Study on plastic ingestion in Carcasses Sea Turtles on Enggano Island, Indonesia. Egypt. J. Aquat. Biol. Fish., 29(1): 27 – 53 (**27 pages**).

Rasheed, A.; Iqbal, K.J.; Safdar, A.; Nasir, A.; Jabeen, R.; Tara, N.; Ali, S.; Zeeshan, M.; Abbas, S.; Muhammad, S.A., (2023). Toxicological effects of zinc oxide nanoparticles on hemato-biochemical profile of common carp (Cyprinus carpio). J. King Saud Univ. Sci., 35(7): 102835 (**7 pages**).

Rashid, E.; Hussain, S.M.; Ali, S.; Sarker, P.K.; Nasir, S.; Al-Anazi, K.M.; Nazish, N., (2025). New insights into the effects of polystyrene microplastics on freshwater fish, Labeo rohita: Assessment on histopathology, mineral composition, bioaccumulation and antioxidant activity. Water Air Soil Pollut., 236(1): 1-10 (**10 pages**).

Reda, R.M.; Mahmoud, R.; Selim, K.M.; El-Araby, I.E., (2016). Effects of dietary acidifiers on growth, hematology, immune response and disease resistance of Nile tilapia, Oreochromis niloticus. Fish Shellfish Immunol., 50: 255-262 (**8 pages**).

Reitsema, R.E.; Meire, P.; Schoelynck, J., (2018). The future of freshwater macrophytes in a changing world: dissolved organic carbon quantity and quality and its interactions with macrophytes. Front. Plant Sci., 9: 629 (**15 pages**).

Sabilillah, A.M.; Palupi, F.R.; Adji, B.K.; Nugroho, A.P., (2023). Health risk assessment and microplastic pollution in streams through accumulation and interaction by heavy metals. Global J. Environ. Sci. Manage., 9(4): 719-740 **(21 pages).**

Salamah, L.N.; Al-Zamzami, I.M.; Pramudia, Z.; Susanti, Y.A.D.; Dhea, L.A.; Kurniawan, A., (2024). Distribution of microplastics in Lusi Island, Sidoarjo, Indonesia. IOP Conference Series: Earth Environ. Sci., 1328: 012012 (**8 pages**).

Samudra, D.; Aunurohim, A.; Setiawan, E., (2024). Preliminary Report of Microplastic (MPs) Presence on East Java Freshwater Sponges at Brantas Porong River. BIO Web Conference. 94: 04019 (**10 pages**).

Sarasamma, S.; Audira, G.; Siregar, P.; Malhotra, N.; Lai, Y.H.; Liang, S.T.; Chen, J.R.; Chen, K.H.C.; Hsiao, C.D., (2020). Nanoplastics cause neurobehavioral impairments, reproductive and oxidative damages, and biomarker responses in zebrafish: Throwing up alarms of wide spread health risk of exposure. Int. J. Mol. Sci., 21(4): 1410 (**29 pages**).

Scherer, C.; Weber, A.; Stock, F.; Vurusic, S.; Egerci, H.; Kochleus, C.; Reifferscheid, G., (2020). Comparative assessment of microplastics in water and sediment of a large European river. Sci. Total Environ., 738, 139866 (**11 pages**).

Shah, N.; Khan, A.; Ali, R.; Marimuthu, K.; Uddin, M.N.; Rizwan, M.; Rahman, K.U.; Alam, M.; Adnan, M.; Muhammad; Jawad, S.M., (2020). Monitoring bioaccumulation (in gills and muscle tissues), hematology, and genotoxic alteration in Ctenopharyngodon idella exposed to selected heavy metals. Biomed. Res. Int., 1: 6185231 (**16 pages**).

Shi, H.; Frias, J.; Sayed, A.E.D.H.; De-la-Torre, G.E.; Jong, M.C.; Uddin, S.A.; Rajaram, R.; Chavanich, S.; Najii, A.; Fernández-Severini, M.D.; Ibrahim, Y.S., (2023). Small plastic fragments: A bridge between large plastic debris and micro-& nano-plastics. TrAC Trends Anal. Chem., 168: 117308 (**8 pages**).

Singh, G.; Singh, A.; Singh, P.; Shukla, R.; Tripathi, S.; Mishra, V.K., (2021). Chapter 9: The fate of organic pollutants and their microbial degradation in water bodies. In pollutants and water management: resources, strategies and scarcity. John Wiley & Sons Ltd. 210-240 (**31 pages**).

Srivastava, R.K.; Shetti, N.P.; Reddy, K.R.; Aminabhavi, T.M., (2020). Sustainable energy from waste organic matters via efficient microbial processes. Sci. Total Environ., 722: 137927 (**16 pages**).

Steckert, L.D.; Furtado, W.E.; Jerônimo, G.T.; Tancredo, K.R.; Hashimoto, G.S.D.O.; Pereira, S.A.; Martins, M.L., (2019). Hematological analysis and relative condition factor in naturally parasitized Nile tilapia. Lat. Am. J. Aquat. Res., 47(3): 502-512 (**11 pages**).

Sulieman, H.M.A.; Habeeb, T.H., (2024). Influence of different water environments on the differential leukocyte counts in Nile tilapia. Vet. J., 14(4): 617-625 (**9 pages**).

Syamsu, D.A.; Deswati, D.; Syafrizayanti, S.; Putra, A.; Suteja, Y., (2024). Presence of microplastics contamination in table salt and estimated exposure in humans. Global J. Environ. Sci. Manage., 10(1): 205-224 **(20 pages).**

Takarina, N.D.; Chuan, O.M.; Adiwibowo, A.; Jeffery, F.N.A.; Zamri, N.Z.A.B.N.M.; Adidharma, M.A., (2024). (2024). Microplastic contamination in different tissues of commercial fish in estuary area. Global J. Environ. Sci. Manage., 10(4): 1917-1932 (**16 pages**).

Utari, D.; Hawa, N.I.; Fizumli, G.; Agustina, H., (2024). Evaluation of community behavior regarding the risk of plastic micro-pollution on the environment health. Global J. Environ. Sci. Manage., 10(2): 605-620 **(16 pages).**

Wang, N.; Zheng, X.; Leptihn, S.; Li, Y.; Cai, H.; Zhang, P.; Wu, W.; Yu, Y.; Hua, X., (2024). Characteristics and phylogenetic distribution of megaplasmids and prediction of a putative chromid in Pseudomonas aeruginosa. Comput. Struct. Biotechnol. J., 23: 1418-1428 (**11 pages**).

Wei, G.; Wei, T.; Li, Z.; Wei, C.; Kong, Q.; Guan, X.; Qiu, G.; Hu, Y.; Wei, C.; Zhu, S.; Liu, Y., (2023). BOD/COD ratio as a probing index in the O/H/O process for coking wastewater treatment. Chem. Eng. J., 466:

143257 (**13 pages**).
Yang, J.; Zhang, J.; Du, X.; Gao, T.; Cheng, Z.; Fu, W.; Wang, S., (2025). Ammonia inhibition in anaerobic digestion of organic waste: a review. Int. J. Environ. Sci. Technol., 22: 1-16 (**16 pages**).
Yanuhar, U.; Musa, M.; Putri, R.D.; Caesar, N.R.; Junirahma, N.S., (2020). Histopathology of gill tissue koi carp (Cyprinus carpio) infected Myxobolus sp. with treatment of diflubenzuron. IOP Conference Series: Earth Environ. Sci., 456: 012080 (**7 pages**).
Yanuhar, U.; Raharjo, D.K.W.P.; Caesar, N.R.; Junirahma, N.S., (2021). Hematology response of catfish (Clarias sp.) as an indicator of fish health in tuban regency. IOP Conference Series: Earth Environ. Sci., 718(1): 012059 (**7 pages**).
Yee, M.S.L.; Hii, L.W.; Looi, C.K.; Lim, W.M.; Wong, S.F.; Kok, Y.Y.; Tan, B.K.; Wong, C.Y.; Leong, C.O., (2021). Impact of microplastics and nanoplastics on human health. Nanomaterials. 11(2): 496. nano11020496 (**22 pages**).
Zakiah; Riani, E.; Taryono; Cordova, M.R., (2024). Assessment of sediment grain size and its correlation with microplastic accumulation and characteristics in the Kahayan River, Indonesia. Environ. Forensics, 25(6): 474-487 (**14 pages**).
Zink, L.; Wood, C.M., (2024). The effects of microplastics on ionoregulatory processes in the gills of freshwater fish and invertebrates: A prospective review. Comp. Biochem. Physiol. A Mol. Integr. Physiol, 295, 111669 (**7 pages**).

AUTHOR (S) BIOSKETCHES

Name, N., Aff.

Yanuhar, U., Dr., Professor, Biotechnology of Waters Environment, FPIK, Brawijaya University, Jl. Veteran, Malang, East Java, Indonesia.
- Email: *doktoruun@ub.ac.id*
- ORCID: 0000-0003-3360-8752
- Web of Science ResearcherID: ACM-6270-2022
- Scopus Author ID: 55022874000
- Homepage: https://fpik.ub.ac.id/dosen/prof-dr-uun-yanuhar-s-pi-m-si/

Wiratno, E.N., M.Sc., Program of Aquatic Sciences Management, Faculty of Fisheries Marine Science, Brawijaya University, Malang, East Java, Indonesia.
- Email: *ekwan13@ub.ac.id*
- ORCID: 0009-0005-2587-805X
- Web of Science ResearcherID: 0000-0002-4296-2174
- Scopus Author ID: 56996209400
- Homepage: https://fpik.ub.ac.id/dosen/ekwan-nofa-wiratno-s-si-m-si/

Suryanto, H., Dr., Professor, Material Manufacture, Center Excellent for Cellulose Composite (CECCom), Department of Mechanical and Industrial Engineering, Faculty of Engineering, Universitas Negeri Malang, Jl. Semarang 5, Malang, 65145, Indonesia.
- Email: *heru.suryanto.ft@um.ac.id*
- ORCID: 0000-0001-7037-1868
- Web of Science ResearcherID: R-7921-2019
- Scopus Author ID: 55992540200
- Homepage: https://pakar.um.ac.id/Data/Peneliti/u=e617ceab-bc5f-43c7-b1bc-fb2f45cb705e

Machfuda, D.R., Bachelor student, Program of Aquatic Sciences Management, Faculty of Fisheries Marine Science, Brawijaya University, Malang, East Java, Indonesia.
- Email: *defarizqi03@student.ub.ac.id*
- ORCID: 0009-0009-8964-8252
- Web of Science ResearcherID: NA
- Scopus Author ID: NA
- Homepage: https://fpik.ub.ac.id/

Caesar, N.R., Ph.D. candidate, Program of Aquatic Sciences Management, Faculty of Fisheries Marine Science, Brawijaya University, Malang, East Java, Indonesia.
- Email: *nicorahmancaesar@gmail.com*
- ORCID: 0000-0002-9859-4681
- Web of Science ResearcherID: U-1064-2017
- Scopus Author ID: 57205470854
- Homepage: https://fpik.ub.ac.id/dosen/nico-rahman-caesar-s-pi-m-p/

HOW TO CITE THIS ARTICLE

Yanuhar, U.; Wiratno, E.N.; Suryanto, H.; Machfuda, D.R.; Caesar, N.R., (2025). Microplastic contamination in river and its impact on fish health. Global J. Environ. Sci. Manage., 11(3): 915-940.

DOI: 10.22034/gjesm.2025.03.04

URL: https://www.gjesm.net/article_722662.html

Global J. Environ. Sci. Manage. 11(3): 941-962, Summer 2025, Serial #43

Global Journal of Environmental Science and Management
(GJESM)

Homepage: https://www.gjesm.net/

Podcasts

CASE STUDY

Carbon footprint associated with a small-scale emissions reduction initiative for sustainable event management

V. de Cadenet*, W. Komkum, P. Raksa, P. Boondaeng, P. Parinyakulset

School of Environmental Engineering, Unit of Greenhouse Gas Management, Technopolis Suranaree University of Technology, Nakhon Ratchasima 30000, Thailand

ARTICLE INFO

Article History:
Received 29 January 2025
Revised 02 April 2025
Accepted 06 May 2025

Keywords:
Carbon footprint
Small-scale emissions reduction
Sustainable event management
Greenhouse gas emissions
University agricultural fairs

ABSTRACT

BACKGROUND AND OBJECTIVES: In the modern era, it has become crucial to discover methods for minimizing carbon emissions and conserving energy. Simple energy-saving measures can not only reduce utility costs but also contribute to a healthier and more sustainable planet. This study focuses on the Suranaree Agricultural Fair 2025, a nine-day public event hosted by Suranaree University of Technology, located in Nakhon Ratchasima Province, Thailand, was selected as a case study to assess the environmental effects of large-scale academic gatherings. The event, promoting sustainable agricultural innovation and the Bio-Circular-Green Economy, was held across an area of 226,068.19 square meters and attended by 258,917 participants. The aim of this study was to evaluate the carbon footprint of the fair, pinpoint key sources of greenhouse gas emissions, and suggest strategies for emission reduction.

METHODS: A comprehensive carbon footprint assessment was conducted by evaluating emissions from travel, accommodation, food consumption, waste generation, electricity, and water usage. Data was collected via participant surveys, utility measurements, and waste assessments. Emissions were calculated using standard emission factors and presented in carbon dioxide equivalent values per person, per square meter, and per event hour.

FINDINGS: The total carbon footprint of the event was estimated at 1,524,844.09 kilograms of carbon dioxide equivalent. This equates to 5.89 kilograms per person, 6.74 kilograms per square meters, and 14,115.19 kilograms per hour of the event. More than 67 percent of the total emissions were attributed to food consumption and the participant travel. An investigation into emission patterns across various participant groups uncovered a range of behaviors and engagement levels that influence the carbon emission outcomes.

CONCLUSION: This study highlights the considerable environmental impact of large-scale academic fairs and establishes a crucial dataset for ongoing emissions monitoring. It offers targeted recommendations to enhance data collection, encourage low-carbon initiatives, and assist institutional efforts toward achieving carbon neutrality. These insights contribute to integrating sustainability principles into event management within the higher education sector.

DOI: 10.22034/gjesm.2025.03.05

This is an open access article under the CC BY license (http://creativecommons.org/licenses/by/4.0/).

NUMBER OF REFERENCES
53

NUMBER OF FIGURES
9

NUMBER OF TABLES
3

*Corresponding Author:
Email: *vorasiri@g.sut.ac.th*
Phone: +668 6909 8554
ORCID: 0009-0006-7038-3707

Note: Discussion period for this manuscript open until Sep 1, 2025 on GJESM website at the "Show Article".

INTRODUCTION

In recent years, the environmental impact of large-scale events has emerged as a critical concern in the context of climate change mitigation. Conferences, exhibitions, fairs, and academic events often entail high energy consumption, long-distance travel, and considerable waste production (Collins *et al.,* 2009; Gössling and Peeters, 2015; Ramely *et al.*, 2022; Clabeaux *et al.,* 2020). These activities collectively contribute significantly to greenhouse gas (GHG) emissions, making events an important focus for climate intervention efforts. With the rising awareness of environmental impacts, both public and academic institutions face mounting pressure to adopt sustainable practices in event management. Carbon accounting frameworks, particularly those based on life cycle assessment (LCA) methodologies, have been widely applied to quantify environmental burdens and support data-driven decision-making (Xuan *et al.,* 2025; Owen *et al.,* 2013; Calzavara, 2023). Several case studies have illustrated the carbon emissions linked to mega-events, pointing to the pressing requirement for dedicated strategies to mitigate these emissions. For instance, the carbon footprint evaluation of Expo Milano 2015, a universal exposition, indicated significant emissions linked to visitor transport, catering operations, and temporary infrastructure (Scorrano *et al.,* 2020). Similarly, Dolf and Teehan (2015) demonstrated that over 70 percent (%) of emissions associated with university sporting events originated from private vehicle and air travel, while Shah *et al.* (2024) reported comparable findings for academic conferences. Gössling and Peeters (2015) and Martellini *et al.* (2015) underscored the critical role of methodological tools, including LCA and event carbon foot printing in supporting decisions aimed at environmental enhancement. These techniques are suitable for both large-scale events and are increasingly pertinent to academic and community-scale gatherings. International frameworks such as the United Nations sustainable development goals (SDGs)—particularly SDG 12 (the Responsible Consumption and Production) and SDG 13 (Climate Action) (United Nations, 2015a, 2015b) and the Paris Agreement, create a policy framework that encourages organizations to track and reduce emissions in all areas, including education. The outcomes of the 28th Conference of the Parties (COP28) reinforced the role of non-state actors, including universities, in achieving net-zero targets through operational decarbonization and behavioral change. Consequently, evaluating carbon footprints has emerged as a fundamental aspect of environmental transparency and institutional responsibility, especially for higher education institutions that exemplify sustainability for future generations (Disterheft *et al.,* 2015; Lozano *et al.,* 2013). In the Southeast Asian context, Thailand has committed to achieving carbon neutrality by 2050 and net-zero GHG emissions by 2065, as outlined in its Nationally Determined Contributions (NDCs) (Thailand, 2022a; Thailand, 2022b). As centers of innovation and public institutions, universities are strategically positioned to significantly contribute to the advancement of national objectives through the execution of policies and demonstration initiatives (Leal Filho *et al.,* 2021; McCowan, 2020). In response to this challenge, Suranaree University of Technology (SUT), located in Nakhon Ratchasima Province, Thailand, organized the Suranaree Agricultural Fair, 2025, held from 11 to 19 January 2025 under the theme "Sustainable Agri-Innovation for bio-circular-green (BCG) economy: Creative agriculture, progressive innovation towards sustainability." Over the course of nine days, the event presented exhibitions, seminars, academic challenges, and public engagement efforts that highlighted agriculture and sustainability. In addition to its educational goals, the event was thematically aligned with the university's commitment to sustainability, particularly through the promotion of agri-innovation and the bio-circular-green (BCG) economy. The event organizers failed to carry out any structured sustainability interventions. In contrast, the carbon footprint analysis was intended to assess emissions generated across significant activity sectors and to create a solid foundation for future advancements. This initiative aligns with Suranaree University of Technology's Environmental and Energy Management Policy and its institutional goal of achieving carbon neutrality by 2035 (SUT, 2024a; 2024b). As the first carbon footprint assessment conducted for the Suranaree Agricultural Fair, this study seeks to identify key emission sources and propose mitigation strategies to inform sustainable event planning within higher education institutions. The main goal of this research was to create a dependable emissions baseline, pinpoint contributing sectors, and suggest mitigation

strategies to guide sustainable event planning within higher education institutions. This study has been carried out in Thailand Suranaree Agricultural Fair, in 2025.

MATERIALS AND METHODS

Event overview and participant categorization

The Suranaree Agricultural Fair 2025 was held on the premises of SUT over a continuous nine-day period, from 11 to 19 January 2025. The event featured exhibitions, academic seminars, product showcases, and cultural activities related to sustainable agriculture and innovation. To enable a more detailed and behavior-oriented examination of GHG emissions, participants in the event were classified into four main categories according to their institutional roles and levels of engagement: 1) university students, 2) faculty members and administrative staff, 3) members of the general public, and 4) co-organizers, including exhibitors and commercial vendors. This classification allowed for tailored emission estimates for each participant group, reflecting their unique travel habits, lodging choices, and consumption patterns. Such classification is consistent with recent studies on event-based carbon accounting that emphasize the value of participant profiling in identifying high-emission clusters and tailoring mitigation strategies accordingly.

Data collection

System boundaries

In accordance with the methodological principles of ISO 14067: 2018 (ISO, 2018) and the 2021 Intergovernmental Panel for Climate Change (IPCC) Guidelines for national GHG inventories, (IPCC, 2021a; 2021b) this study adopted a gate-to-gate system boundary approach. This method, frequently utilized in evaluating the carbon footprint of time-sensitive activities, emphasizes emissions produced within a specific spatial and temporal context (Martellini *et al.,* 2015). The selected boundary focused on direct and indirect emissions associated with; 1) Participant travel to and from the event. 2) Accommodation during the event participation. 3) Food consumption within the event. 4) Electricity and water use (measured by event-specific meters). 5) Waste generated during the operational period. The analysis excluded emissions that were not under the operational control of the event organizers. Specifically, upstream and downstream emissions associated with the production and transportation of materials, food items, and promotional goods brought in by vendors and exhibitors were omitted due to the absence of verifiable life cycle inventory data. This restriction is acknowledged, since these emissions can be considerable and ought to be included in future analyses to improve both accuracy and completeness. The adopted boundary ensures methodological transparency while maintaining compliance with internationally recognized GHG accounting standards.

Data collection procedures

A mixed-methods approach was employed to gather data related to emission-generating activities throughout the nine-day event, consistent with the system boundaries established for this study. The techniques for data collection involved systematic questionnaires, resource tracking, and direct waste assessments, all adhering to established environmental evaluation protocols. Real-time participant tracking was also implemented to normalize emissions across participant groups more accurately.

Questionnaires

Structured surveys were conducted at three main entrances to collect data on participant travel modes and distances, accommodation types, and food consumption preferences. This approach reflects earlier evaluations of carbon footprints for university and public events (Dolf and Teehan, 2015; Shah *et al.,* 2024). Survey questions included examples such as: "How did you travel to the event today?", "Did you stay overnight? If yes, where?", and "What type of meals did you consume?". A total of 3,667 complete responses were obtained. The sample size was determined using Taro Yamane's formula for finite populations (Yamane, 1967), ensuring statistical reliability at a 95% confidence level. To mitigate sampling bias and consider daily variations in participant behavior, data collection was conducted over multiple days and time slots.

Resource metering

The consumption of electricity and water was observed using specific sub-meters installed in crucial zones of the event, which encompassed exhibition

halls, seminar venues, vendor areas, and sanitation facilities. Daily readings from the meters were documented and assembled to produce. Emissions associated with these utilities were calculated using locally validated emission factors from recent Thai and Southeast Asian energy inventories (Almeida *et al.,* 2021), thereby reflecting context-specific environmental conditions.

Waste audits

On-site waste was collected, sorted, and weighed each day by the university's Building and Grounds Division, in partnership with the Center of Excellence in Biomass. Waste was divided into classifications such as general refuse, recyclable items, and compostable waste. These procedures followed the IPCC's waste emission guidelines (IPCC, 2006) and the Thai national emission factor framework provided by the Thailand Environmental Institute (TEI, 2012).

Participant Counting

Attendance was tracked in real time using a mobile application installed at all seven official event gates. Each entry was registered digitally between 09:00 and 21:00 and automatically displayed on a central monitoring dashboard. This system enabled accurate monitoring of visitor numbers over time, in accordance with the best practices used in contemporary event-scale GHG evaluations (Scorrano *et al.,* 2020; Mannheim and Avató, 2023). Although the study incorporated comprehensive data collection systems, it acknowledges limitations in the exclusion of emissions from materials, food, and merchandise brought in independently by exhibitors and co-organizers, due to the lack of verifiable inventory records. This emission is noted in interpreting final carbon footprint estimates.

Emission factors and calculation

The carbon footprint of the Suranaree Agricultural Fair 2025 was calculated following the methodological framework outlined in ISO 14067: 2018. The general emission equation used is defined as Eq. 1 (ISO, 2018):.

$$\text{Emission} = \text{Activity data} \times \text{emission factor} \quad (1)$$

Emission factors indicate the volume of GHG emissions generated per unit of activity assessed. These factors are typically expressed in kilograms of carbon dioxide equivalent ($kgCO_2eq$), which enables different types of GHGs to be reported in a common unit based on their global warming potential. The total emissions can be determined in a standardized and comparable manner by multiplying the emission factor by the measured quantity of the activity, which may include fuel consumption, electricity usage, or waste production. To ensure scientific rigor and comparability with international practices, emission factors were sourced from well-established databases and regulatory guidelines, including the Intergovernmental Panel on Climate Change IPCC (2014), Thailand GHG Management Organization (Thai National LCI Database, 2022), Thailand Greenhouse Gas Management Organization (2022), the Department of alternative Energy Development and Efficiency (DEDE, 2023), Thailand Industrial Information System, National Metal and Materials Technology Center Thailand (TIIS-MTEC-NSTDA, 2022), Environmental Institute (TEI, 2012), the United Kingdom Department for Environment, and Food and Rural Affairs (UK DEFRA) conversion factors and the United Kingdom's Department for business, as well as Energy and Industrial Strategy (BEIS, 2022). Emission factors were employed across a spectrum of activity areas relevant to event management. For transportation, these factors were assigned per kilometer (km) traveled and organized by mode of transportation, which includes private automobiles, public buses, and motorcycles. For accommodation, emissions were calculated per person per night, accounting for variations in energy intensity across lodging types such as homestays, hotels, and university dormitories. Food-related emissions were assessed by analyzing the quantity and nature of meals consumed, with specific factors distinguishing between vegetarian, mixed, and meat-heavy diets. Solid waste emissions were calculated per kilogram (kg) based on the composition of general waste, recyclables, and food waste. Electricity usage was quantified per kilowatt-hour (kWh) consumed, while water-related emissions were computed per cubic meter (m^3) of usage. To ensure contextual relevance to Thailand's energy grid and waste management infrastructure, country-specific emission coefficients were prioritized whenever possible (Kongritti, 2015). In cases where domestic data was incomplete or unavailable, supplemental factors from the UK

DEFRA database were used to maintain analytical consistency. This method embodies the leading practices in carbon accounting, while maintaining the methodological rigor of the findings derived from the Suranaree Agricultural Fair 2025.

Data analysis

The assessment of the collected information was arranged to provide a detailed analysis of the carbon footprint related to the Suranaree Agricultural Fair 2025. First, the overall GHG emissions were quantified, with results expressed in metric tons of carbon dioxide equivalent (tCO_2eq). Carbon intensity indicators were also calculated, including emissions per person ($kgCO_2eq$ per person), per square meter of event area ($kgCO_2eq$ per square meter), and per hour of event operation ($kgCO_2eq$ per hour) (Kongritti, 2015). The use of standardized metrics allowed for comparisons between similar events. Emissions were then categorized into major activity areas including transportation, accommodation, food consumption, utility usage, and waste management. This categorization allowed identification of the dominant sources contributing to the event's total footprint. An analysis of daily emission patterns was conducted to evaluate the differences in total emissions during the nine-day event period. This temporal analysis reflected the influence of program schedules, participant attendance, and public holidays on daily GHG outputs. Finally, a detailed analysis of emissions was conducted by participant type, encompassing both the total emissions for each group and the average emissions per capita. This disaggregation supported a deeper understanding of behavioral and logistical factors influencing carbon intensity among university students, faculty and staff,

Table 1: Emission factors used in carbon footprint assessment

Activity category	Emission factor	Unit	Sources
Private car (Gasoline)	0.16	$kgCO_2eq$/km-trip	IPCC, 2006; DEDE, 2023; IPCC, 2014
Electric vehicle (EV)	0.07	$kgCO_2eq$/km-trip	IPCC, 2006; DEDE, 2023; IPCC, 2014
Pickup truck (Diesel)	0.24	$kgCO_2eq$/km-trip	IPCC, 2006; DEDE, 2023; IPCC, 2014
Private van	0.26	$kgCO_2eq$/km-trip	IPCC, 2006; DEDE, 2023; IPCC, 2014
Taxi	0.18	$kgCO_2eq$/km-trip	IPCC, 2006; DEDE, 2023; IPCC, 2014
Motorcycle	0.05	$kgCO_2eq$/km-trip	IPCC, 2006; DEDE, 2023; IPCC, 2014
Public bus	0.03	$kgCO_2eq$/km-trip	IPCC, 2006; DEDE, 2023; IPCC, 2014
Public van	0.02	$kgCO_2eq$/km-trip	IPCC, 2006; DEDE, 2023; IPCC, 2014
Domestic flight	0.17	$kgCO_2eq$/km-trip	BEIS, 2022
International flight	0.11	$kgCO_2eq$/km-trip	BEIS, 2022
Diesel train	0.05	$kgCO_2eq$/km-trip	TEI, 2012
Electric train	0.71	$kgCO_2eq$/km-trip	Ecoinvent Centre, 2007; IPCC, 2007
Public boat	0	$kgCO_2eq$/km-trip	TEI, 2012
Regular meal	3.93	$kgCO_2eq$/meal	BEIS, 2022
Vegetarian meal	1.12	$kgCO_2eq$/meal	BEIS, 2022
Regular snack and drink	0.21	$kgCO_2eq$/meal	BEIS, 2022
Vegetarian snack and drink	0.14	$kgCO_2eq$/meal	BEIS, 2022
1-2 Star hotel	6.08	$kgCO_2eq$/person-night	TEI, 2012
3-Star hotel	8.1	$kgCO_2eq$/person-night	TEI, 2012
4-Star hotel	9.14	$kgCO_2eq$/person-night	TEI, 2012
5-Star hotel	14.21	$kgCO_2eq$/person-night	TEI, 2012
Homestay (No air-conditioning (A/C)	0.28	$kgCO_2eq$/person-night	TEI, 2012
Homestay (With A/C)	3.13	$kgCO_2eq$/person-night	TEI, 2012
Food waste	2.53	$kgCO_2eq$/kg	IPCC, 2006
Paper waste	2.93	$kgCO_2eq$/kg	IPCC, 2006
Plastic waste	2.32	$kgCO_2eq$/kg	IPCC, 2006
Textile waste	2	$kgCO_2eq$/kg	IPCC, 2006
Wood waste	3.33	$kgCO_2eq$/kg	IPCC, 2006
Other waste	2.32	$kgCO_2eq$/kg	IPCC, 2006
Electricity consumption	0.4999	$kgCO_2eq$/kWh	TIIS-MTEC-NSTDA, 2022; IPCC, 2014
Water consumption	0.5410	$kgCO_2eq/m^3$	TIIS-MTEC-NSTDA, 2022;

the general public, and co-organizers or vendors. An in-depth evaluation of emissions was carried out according to participant types, covering both the total emissions for each category and the per capita average emissions

RESULTS AND DISCUSSION

The results provide evidence-based insights for event organizers, university policymakers, and sustainability practitioners working toward climate-responsive operations.

Overall carbon footprint

The total carbon footprint of the Suranaree Agricultural Fair 2025 was estimated at 1,524.84 tCO_2eq. This figure represents the cumulative GHG emissions generated throughout the nine-day event, covering six primary activity categories: food consumption, participant transportation, accommodation, waste generation, electricity usage, and water consumption. Food consumption was the largest contributor, accounting for 559.07 tCO_2eq, or approximately 36.7% of total emissions. Participant travel followed, contributing 467.24 tCO_2eq, representing 30.6%. These results are consistent with previous studies identifying food provisioning and participant mobility as dominant sources of event-related emissions (Collins *et al., 2009*; Cerutti *et al*., 2018; Dolf and Teehan, 2015). The calculation of food emissions relied on consumption patterns provided by participants and specific emission factors for each meal, while travel emissions were estimated based on self-reported transportation methods, travel distances, and national fuel-specific emission factors (DEDE, 2023). Accommodation-related emissions totaled 335.23 tCO_2eq, primarily from overnight stays by members of the general public and co-organizers. This is consistent with studies highlighting the substantial carbon footprint of accommodations during events (Gössling and Peeters, 2015). Waste generation contributed 148.09 tCO_2eq, or 9.7 percent of total emissions, highlighting the importance of integrating waste reduction strategies into event management. The impact of electricity and water consumption was minimal, contributing 14.57 tCO_2eq (1.0%) and 0.64 tCO_2eq (0.04%), respectively, reflecting the efficient infrastructure and growing renewable energy integration in Thailand's grid (DEDE, 2023). In order to support benchmarking and comparative analyses, three normalized indicators of carbon intensity were derived. The carbon footprint was 5.89 $kgCO_2eq$ per person, based on a total attendance of 258,917 individuals. Emission intensity per unit area was 6.74 $kgCO_2eq$ per square meter, calculated from a total event area of 226,068.19 square meters. Emission intensity per operational hour was 14.16 tCO_2eq per hour, based on 108 hours of event operation across nine days. These uniform metrics serve as a benchmark for assessing the environmental impact of similar events and facilitate the formulation of sustainable event planning strategies (Ballarano *et al*., 2022). The distribution of emissions across categories is illustrated in Fig. 1. The findings reaffirm that food consumption and participant travel were the dominant sources of emissions, followed by accommodation and waste generation, while electricity and water usage had a minimal impact. This analysis emphasizes essential areas for intervention that can advance sustainable dietary practices, promote the use of low-carbon transportation, and enhance waste and accommodation management could substantially reduce the environmental footprint of future events. However, it is important to highlight that the total carbon footprint presented here excludes upstream and downstream emissions, including those associated with the production of food, merchandise, or booth materials. Based on prior LCA studies of similar events, these excluded emissions may contribute an additional 10-25% to the overall footprint to the overall footprint (Calzavara, 2023; Martellini *et al*., 2015). Despite being excluded because of inventory constraints, these emissions hold environmental importance and must be included in future evaluations for a more comprehensive and policy-relevant counting.

Emissions by activity type

The analysis of emissions by activity type offers deeper insight into the environmental dynamics of the Suranaree Agricultural Fair 2025. The contributions to emissions were evaluated across six primary categories food consumption, travel, accommodation, waste generation, electricity usage, and water use.

Food consumption

GHG emissions from food consumption were

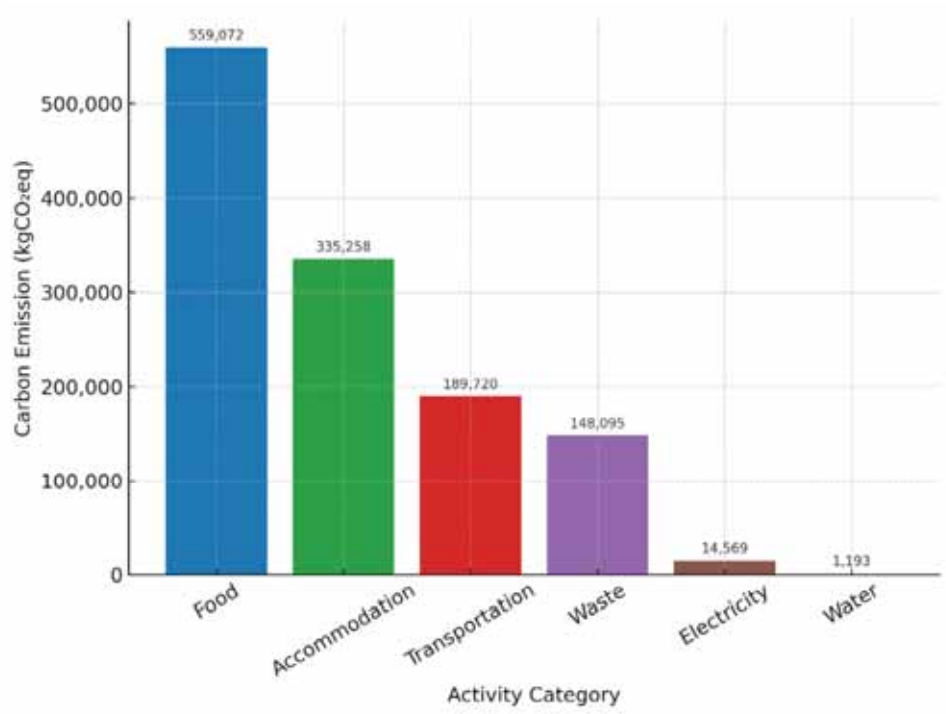

Fig. 1: Carbon footprint by activity category for the Suranaree Agricultural Fair 2025

assessed based on questionnaire data from participants detailing their usual meal choices. Conventional meals containing animal-based proteins, particularly red meat, were the most frequently reported and accounted for the highest food-related emissions. These meals are distinguished by their increased carbon intensity relative compared to plant-based alternatives (González-García *et al.*, 2018). Total food-related emissions amounted to 559.07 tCO_2eq, representing 36.7% of the event's carbon footprint (Fig. 1). As illustrated in Fig. 2, carbon emissions and carbon intensity from food consumption varied across participant groups, with students, faculty, the general public, and vendors exhibiting distinct patterns. These results emphasize the essential impact of food selections on event sustainability, showcasing the opportunity to lower emissions by encouraging plant-based meal alternatives and eco-friendly catering methods.

Transportation

Transportation-related emissions were primarily driven by private vehicles powered by fossil fuels. Gasoline-fueled vehicles contributed 146.65 tCO_2eq, while diesel vehicles accounted for 298.12 tCO_2eq, together representing over 90% of travel-related emissions. Emission estimates were derived from self-reported travel distances and modes of transportation, utilizing national emission factor (TIIS-MTEC-NSTDA, 2022). Average travel distances varied among participant groups, with students traveling 4.85 kilometers (km), faculty and staff 9.51 km, the general public 33.67 km, and co-organizers and vendors 98.69 km. These observations demonstrate the varied geographical backgrounds and functions of participants. The significant use of private vehicles is in line with earlier findings that pinpoint transportation as a primary contributor to emissions related to events (Dolf and Teehan, 2015; Scorrano *et al.*, 2020). As shown in Fig. 3, transportation-related emissions varied substantially among participant groups, with general public and co-organizers/vendors exhibiting particularly high emissions due to long-distance travel and the use of fossil-fuel vehicles. Although the domestic flight emissions data were based on a relatively small sample size of 16 participants, the total emissions amounted to 6,951 $kgCO_2eq$, corresponding to 434.44 $kgCO_2eq$

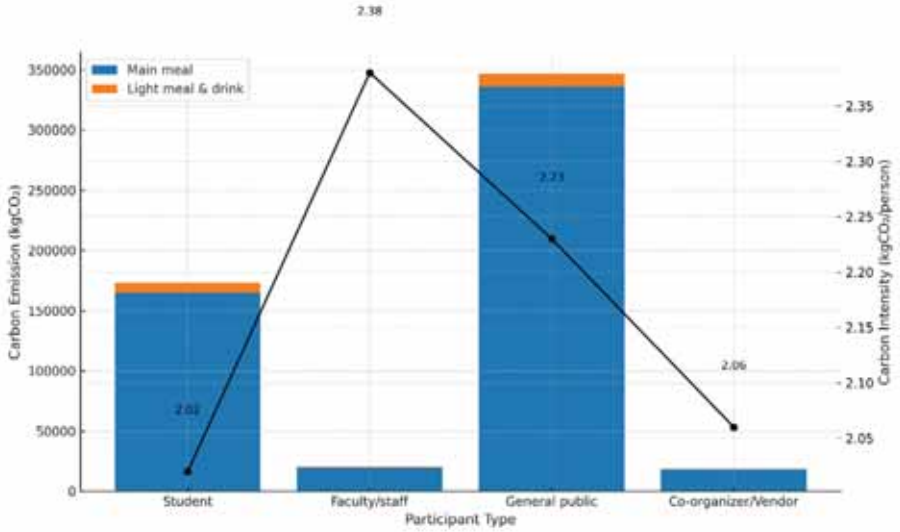

Fig. 2: Carbon emissions and intensity from food consumption by participant type at the Suranaree Agricultural Fair 2025

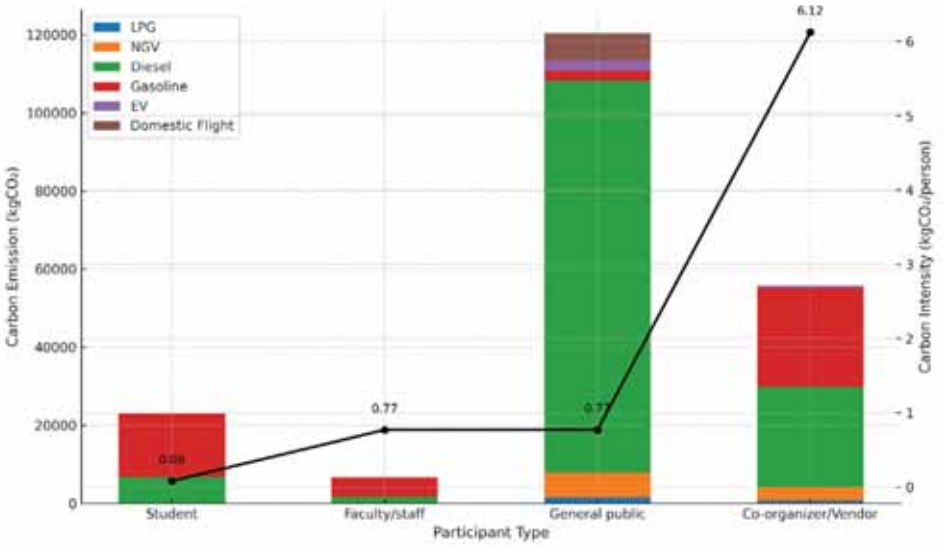

Fig. 3: Carbon emissions and carbon intensity from transportation activities among different participant groups at the Suranaree Agricultural Fair 2025

per person. This reveals that air travel, even within a confined group, has a substantial effect on the total carbon footprint, illustrating the disproportionate effect of aviation activities in comparison to other transportation options.

Accommodation

Accommodation emissions were influenced by lodging type and duration of stay. Guests reported staying at campsites, budget-friendly hotels, eco-lodges, and upscale hotels, with three-star hotels being the most common choice and contributing significantly to emissions. Although globally higher-tier hotels tend to generate greater emissions (Zhang and Xia, 2024), the context of a public university event likely influenced participant decisions toward mid-range options. Total emissions from accommodation reached 335,230.84 $kgCO_2eq$. The data from the survey shows that a significant number of student participants were from the local vicinity and did not necessitate overnight lodging. In contrast, vendors and co-organizers often stayed for extended

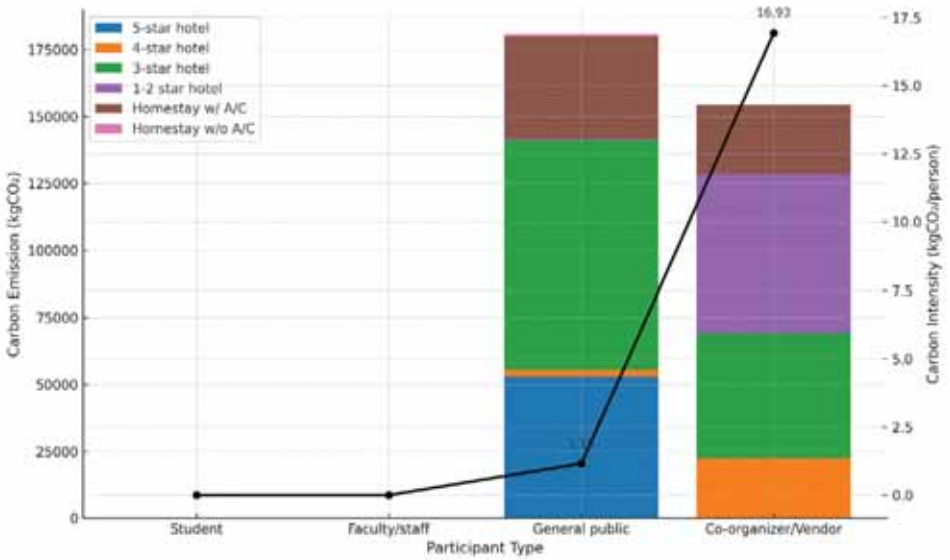

Fig. 4: Carbon emissions and carbon intensity from accommodation activities among different participant groups at the Suranaree Agricultural Fair 2025

durations, with some reporting up to 10 nights, thereby amplifying their proportional contributions. As illustrated in Fig. 4, accommodation-related emissions varied significantly among participant groups, with general public attendees and co-organizers/vendors contributing disproportionately due to prolonged stays in energy-intensive lodging facilities. These results imply that supporting eco-friendly certified lodging and promoting shared accommodation arrangements could be viable strategies for minimizing emissions in upcoming editions of the fair.

Waste generation

Waste-related emissions totaled 148.09 tCO_2eq, representing approximately 9.7% of the event's total carbon footprint. In conjunction with the Center of Excellence in Biomass, the university's Building and Grounds Division performed daily waste collection, sorting, and weighing. General waste accounted for the highest emissions due to its residual, non-recyclable nature. All remaining waste was processed into Refuse-Derived Fuel (RDF) and transported to a cement manufacturing facility for co-processing as an alternative fuel, thereby reducing landfill waste and enhancing resource circularity. Based on national and IPCC emission factors, this RDF strategy avoided approximately 248.80 tCO_2eq, comprising 106.63 tCO_2eq from coal substitution and 142.17 tCO_2eq from avoided landfill methane emissions (IPCC, 2006; TGO, 2022). However, previous studies emphasize that the environmental benefits of RDF depend heavily on accurate characterization of its biogenic and fossil carbon content (Velis *et al.*, 2010). Misjudgments, particularly in streams dominated by plastics, can cause fossil CO_2 emissions to be underreported, emphasizing the importance of implementing standardized RDF quality control for trustworthy carbon accounting. These findings underline the importance of complementing downstream waste-to-energy recovery with upstream waste minimization and segregation strategies. Future improvements may include composting organic fractions, promoting reusable or recyclable packaging, and selecting lower-emission materials. By implementing these strategies, the carbon footprint associated with event waste management could be substantially diminished, furthering the university's commitment to climate responsiveness. As shown in Fig. 5, domestic waste constituted the largest share of both carbon emissions and waste quantities generated during the Suranaree Agricultural Fair 2025. Although separate bins for food waste were provided, a substantial portion of plastic and food-contaminated materials were improperly disposed of as general waste, diminishing the effectiveness of waste separation initiatives.

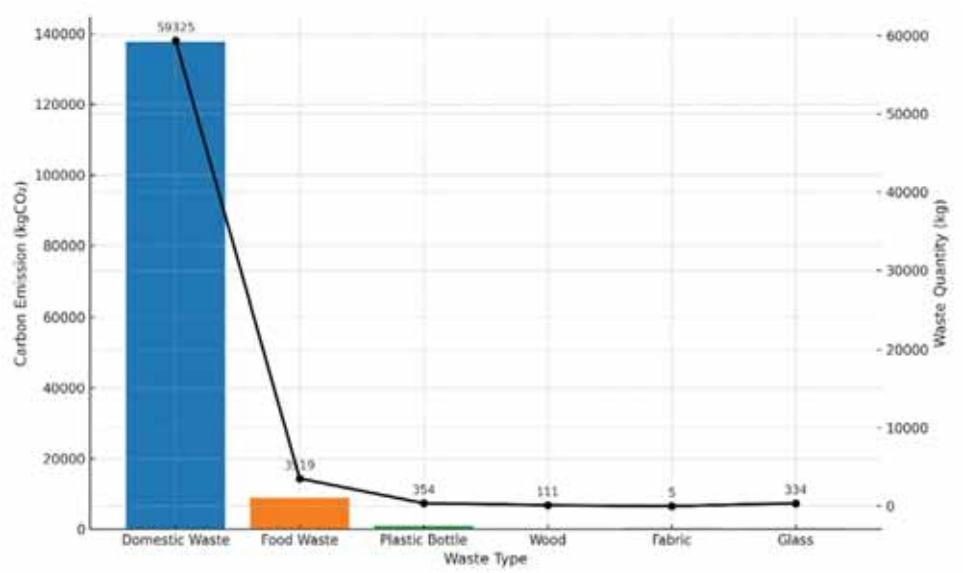

Fig. 5: Carbon emissions and waste quantities by waste type generated during the Suranaree Agricultural Fair 2025

Compared to the leading domestic waste stream, the contributions of food waste, plastics, wood, fabric, and glass were relatively minimal.

Electricity and water usage

Carbon emissions associated with electricity consumption during the Suranaree Agricultural Fair 2025 totaled 14,569.04 $kgCO_2eq$, based on actual metered usage over the nine-day event. Water usage contributed an additional 639.46 $kgCO_2eq$, with utility-related emissions accounting for 1.04% of the total carbon footprint. Emissions calculations were derived from daily meter readings in accordance with national emission factors (TEI, 2012; DEDE, 2023). While the national grid emission factor was utilized, the university's solar floating system enhanced the electricity supply, implying that the real carbon intensity might have been lower. Most activities were conducted outdoors, primarily food stands, which not only minimized the need for energy-intensive heating, ventilation, and air conditioning (HVAC) systems but also contributed to the event's significant food-related emissions, consistent with findings from previous studies of outdoor events (Collins *et al.*, 2009). As depicted in Fig. 6, daily utility emissions exhibited a stable trend, with a significant rise on the final day attributed to the closure ceremony and a large concert. This surge underscores how high-attendance events can temporarily elevate utility demands. Potential future developments may encompass enhanced tracking of renewable energy inputs along with specialized demand management strategies for major events.

Daily carbon footprint variation

The daily carbon emissions of the Suranaree Agricultural Fair 2025 varied significantly over the nine-day period, as illustrated in Fig. 7, which presents the distribution of emissions by activity category. These changes demonstrated alterations in attendee participation, event scheduling, and resource utilization behaviors. Daily emissions ranged from 112.82 $kgCO_2eq$ to 221.33 $kgCO_2eq$, with the highest emissions recorded on January 14. This peak corresponded with several high-profile activities, including nationally promoted exhibitions, an innovative showcase, and a public holiday that attracted a substantial number of off-campus visitors. Conversely, the least emissions were observed on January 15 and 16, midweek days that typically feature lower attendance and less demand on infrastructure. The observed temporal variation highlights the strong correlation between human activity levels and environmental impacts. The main factors influencing daily emission variations were food consumption and participant transportation, which increased in direct relation to the number of participants. Conversely, electricity and water usage

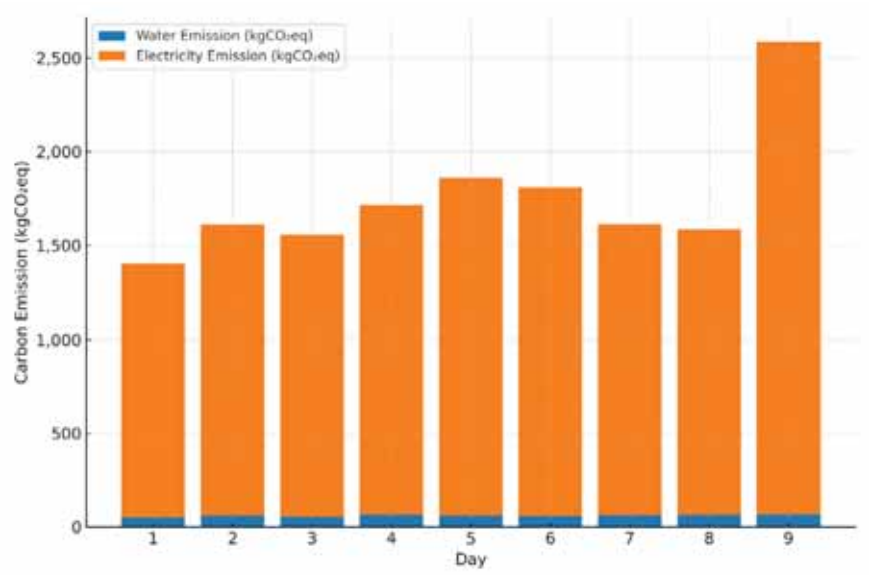

Fig. 6: Daily carbon emissions from electricity and water consumption during the Suranaree Agricultural Fair 2025

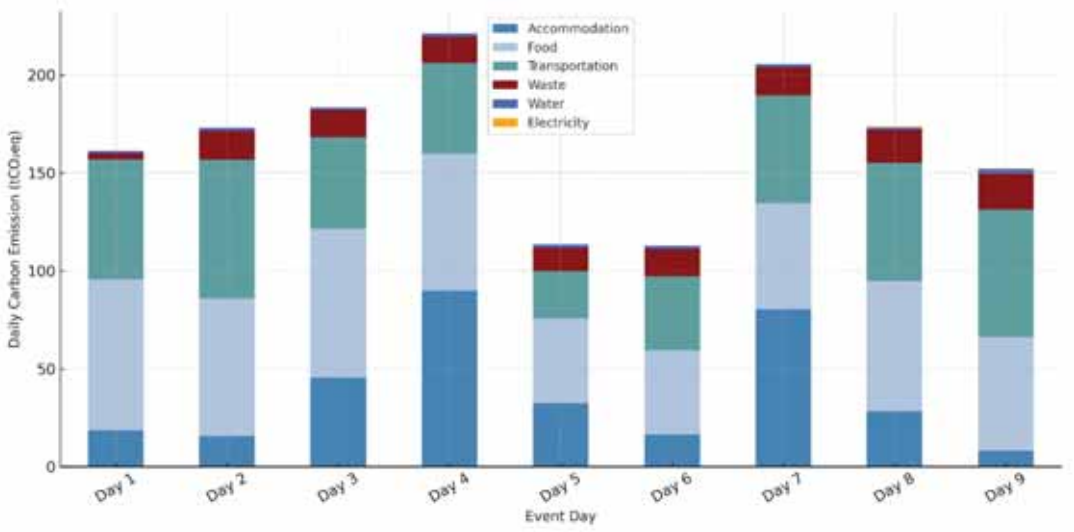

Fig. 7: Daily carbon emissions by activity type during the Suranaree Agricultural Fair 2025

remained consistent during the event, indicating steady baseline requirements for lighting, cooling, and sanitation services. Understanding these daily emission dynamics is critical for future event planning. Identifying peak emission days enables the design of targeted interventions, such as expanding public transport capacity, promoting plant-based meal options, optimizing waste management logistics, and distributing high-impact activities across multiple days to avoid concentrated environmental loads. This time-based analysis provides valuable insights for improving the sustainability of upcoming campus and national fairs.

Emissions by participant type

Examining carbon emissions by participant type in a disaggregated manner reveals crucial insights into the ways individual and group behaviors shaped the

total carbon footprint of the Suranaree Agricultural Fair 2025. As illustrated in Fig. 8 and detailed in Table 2, participants were categorized into four groups: SUT students, faculty and staff, the general public, and co-organizers or vendors. The evaluation of emissions focused on three key sectors: food consumption, travel, and accommodation, which collectively constituted the primary sources of GHG emissions linked to the event.

Emissions from accommodation were recorded as zero for SUT students, faculty, and staff, based on the assumption that most participants either resided on campus or lived within a short commuting distance. Consequently, overnight stays or lodging-related activities were not required for their participation. This belief aligns with conventional procedures in university-based carbon footprint analyses, where accommodation-related emissions for local populations are generally excluded unless they are specifically noted in participant surveys (Piccerillo *et al.*, 2023).

SUT students

Students from SUT contributed a total of 196,249.32 $kgCO_2eq$ to the overall carbon footprint of the Suranaree Agricultural Fair 2025. Of this amount, 173,168.48 $kgCO_2eq$ (approximately 88%) originated from food consumption, while 23,080.84 $kgCO_2eq$ resulted from travel activities. Emissions related to accommodation were minimal, given that the majority of students lived on campus or in adjacent living arrangements. A total of 85,705 student participants were recorded, yielding a relatively low per capita emission of 2.29 $kgCO_2eq$. These results illustrate the environmental benefits of situating events close to participant demographics as a means to decrease emissions, contributing to the larger goals of sustainable event management objectives.

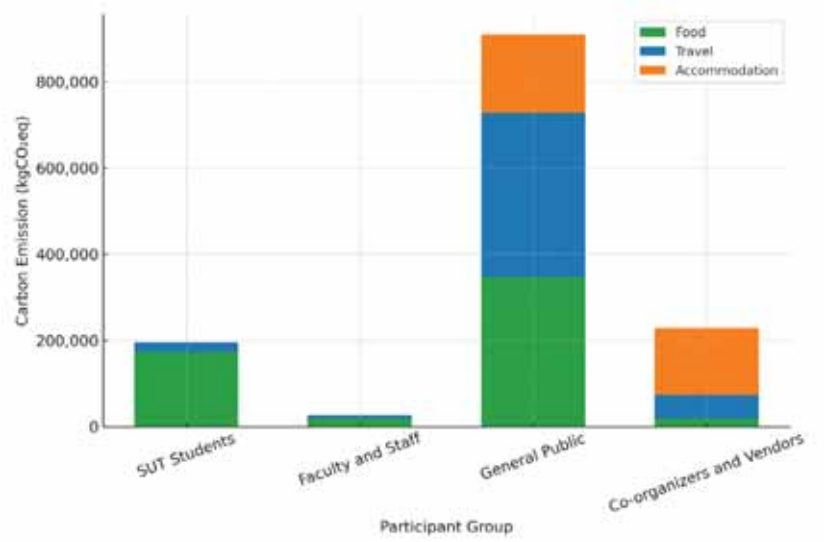

Fig. 8: Carbon emissions by participant type and activity category (food, travel, and accommodation)

Table 2: Emissions by participant group

Participant group	Emissions ($kgCO_2eq$)				Total emissions	Per capita emissions ($kgCO_2eq$/person)
	Participants	Food	Travel	Accommodation		
SUT Students	85,705	173,168.48	23,080.84	0	196,249.32	2.29
Faculty and Staff	8,609	20,488.20	6,660.87	0	402,150.34	46.71
General Public	155,482	346,667.11	381,662.14	180,831.01	527,498.12	3.39
Co-organizers and Vendors	9,122	18,748.67	55,833.83	154,399.83	228,982.33	25.10

Faculty and staff

Faculty and staff participants contributed a total of 27,149.07 $kgCO_2eq$ to the overall carbon footprint of the Suranaree Agricultural Fair 2025. Of this amount, 20,488.20 $kgCO_2eq$ (75%) originated from food consumption, while 6,660.87 $kgCO_2eq$ (approximately 25%) resulted from travel activities. Emissions related to accommodation were not documented, as it was assumed that the majority of participants were located within a commutable range of the campus. A total of 8,609 participants were recorded in this group, resulting in a per capita emission of 3.15 $kgCO_2eq$, notably higher than that of student participants. This variation largely signifies a heightened reliance on private transportation for routine commuting. These results highlight the necessity of encouraging low-carbon transportation alternatives, including carpooling, cycling, and the adoption of electric vehicles, as integral components of comprehensive strategies aimed at minimizing emissions from small-scale events and fostering sustainable event management.

General public

The general public constituted the largest participant group at the Suranaree Agricultural Fair 2025 and was responsible for the highest absolute emissions, totaling 909,160.26 $kgCO_2eq$. Of this amount, 346,667.11 $kgCO_2eq$ (38%) were attributed to food consumption, 381,662.14 $kgCO_2eq$ (42%) to travel activities, and 180,831.01 $kgCO_2eq$ (20%) to accommodation. A total of 155,482 participants were recorded in this group. The increased travel emissions are indicative of the high volume of visitors, many of whom come from outside the local area, often using private vehicles, van, or interprovincial transportation services. Accommodation emissions further indicate patterns of multi-day attendance and hotel stays. Despite the high absolute emissions, the per capita emission remained moderate at 5.85 $kgCO_2eq$ per person, due to the diluting effect of the large participant base. These results imply that future sustainable event management strategies should prioritize the promotion of low-carbon public transport, enhance local visitor involvement, and providing incentives for brief stays or the selection of eco-certified accommodations Co-organizers and vendors. Co-organizers and vendors contributed a total of 228,982.33 $kgCO_2eq$ to the overall carbon footprint of the Suranaree Agricultural Fair 2025. Of this amount, 18,748.67 $kgCO_2eq$ (8%) were associated with food consumption, 55,833.83 $kgCO_2eq$ (24%) with travel activities, and 154,399.83 $kgCO_2eq$ (68%) with accommodation. A total of 9,122 participants were recorded in this group, resulting in the highest per capita emissions at 25.10 $kgCO_2eq$ per person. The expanded footprint demonstrates a long-term presence at the site, full-day engagements, logistical operations, and overnight accommodations. Notably, higher travel emissions were driven by the fact that many vendors originated from other provinces and participated as part of a rotating national exhibition circuit. These results emphasize the importance of sustainability efforts aimed at vendors and co-organizers, including shared lodging solutions, eco-friendly accommodations, and low-emission transportation alternatives. Tailored mitigation strategies based on participant roles and behaviors are essential for advancing small-scale emissions reduction goals while maintaining successful and inclusive event management. The segmented analysis of emissions according to participant types highlighted specific environmental impact patterns driven by collective behaviors, mobility habits, and participation duration. Students and faculty, residing predominantly near the campus, contributed relatively low per capita emissions, whereas the general public and vendors exhibited higher absolute and per capita emissions due to long-distance travel, extended stays, and greater resource consumption. These conclusions emphasize the significance of developing targeted strategies for emissions reduction strategies that cater to the unique profiles of participants. The survey collected 3,667 complete responses out of a total participant base of 258,917, representing approximately 1.4% of all attendees. This sample size was determined using Yamane's formula, ensuring statistical validity at a 95% confidence level. Even though the methods used are suitable, there is still a chance of sampling bias, particularly if specific groups of participants are represented in excess. Therefore, emission estimates derived from this survey should be interpreted with an awareness of this limitation. It is important to recognize that non-respondents may have differed systematically from those who completed the survey. Participants who traveled far or needed to stay overnight might not have been fully represented due to constraints in

Table 3: Comparison of total and per capita carbon footprint across educational institutions and event-based case studies

Context	Per capita emission ($kgCO_2eq$/person/day)	Total emission (tCO_2eq)	Remarks	Sources
Institutional employees, Indonesia	20.33	523.83	Annual food and transport emissions	Haryanto *et al.* (2025)
Thai university students and staff	0.73 – 2.36	Not reported	Emissions from daily campus activity	Kongritti (2015)
U.S. University campus	21.64	Not reported	Includes air travel and facilities	Clabeaux *et al.* (2020)
Municipal bicycle lane, Thailand	N/A	200,000 avoided	Modal shift potential	Prasara-A and Bridhikitti (2022)
Walchand College, India	N/A	1,400	High impact from electricity and respiration	Kamble and Kavathekar (2021)
Czech forestry university	N/A	686	Forestland management with low Scope 3	Kubavá *et al.* (2018)
Hero Dolomites sports event, Italy	7.04	52.33	High share from upstream transport and accommodation	Calzavara (2023)
Suranaree Agricultural Fair 2025, Thailand	5.89	1,524.84	Large-scale 3-day public event	This study

availability, lack of visibility for the survey, or lower motivation to respond. These factors could introduce bias into participant-level emission estimates. Future assessments should consider broader outreach or digital tools to improve representativeness. Programs promoting low-carbon commuting, sustainable food initiatives, and organized accommodation planning can greatly enhance efforts towards reducing emissions on a small scale and managing events sustainably, especially in university settings and large public gatherings. As shown in Table 3, carbon emissions from event-based and educational settings vary significantly depending on system boundaries, duration, and participant characteristics. Institutional studies such as those by Haryanto *et al.* (2025); Clabeaux *et al.* (2020) and Kubová *et al.* (2018) indicate elevated daily per capita emissions, estimated between 20 and 21.6 $kgCO_2eq$ per individual each day, attributed to constant electricity consumption, commuting, and operational demands. In contrast, shorter-duration event studies such as Calzavara (2023) and the present research show moderate per capita values of 7.04 and 5.89 $kgCO_2eq$ per person per day, respectively, reflecting limited upstream inclusions and localized participation. Studies conducted in Thailand, such as Kongritti (2015) and the municipal bicycle lane analysis by Prasara-A and Bridhikitti (2022), reveal substantially lower footprints or mitigation potential, though they apply narrower scopes. Kamble and Kavathekar (2021) further highlight the scale of emissions from a single academic institution, reporting over 1,400 tCO_2eq annually, largely driven by electricity use. As a prominent short-term public event, the Suranaree Agricultural Fair produces emissions that are nearly equivalent to those of continuous operations, yet its per capita intensity remains comparatively lower due to the predominantly local attendance and absence of air travel. These findings indicate that despite the considerable differences in carbon intensity, using standardized per capita metrics facilitates meaningful comparisons. The fair's position near the center of this spectrum illustrates that even well-managed, short-term public events can carry notable environmental impacts—particularly on food, transport, and accommodation—if not strategically mitigated.

Carbon intensity

While absolute emissions provide an overview of the Suranaree Agricultural Fair 2025's total carbon impacts, per capita emissions reveal important disparities among participant groups. In this study, carbon intensity, defined as emissions per person ($kgCO_2eq$), as a consistent framework for comparing the environmental performance of multiple events (Ballarano *et al.*, 2022). As illustrated in Fig. 9, co-organizers and vendors recorded the highest emissions at 25.10 $kgCO_2eq$ per person, reflecting

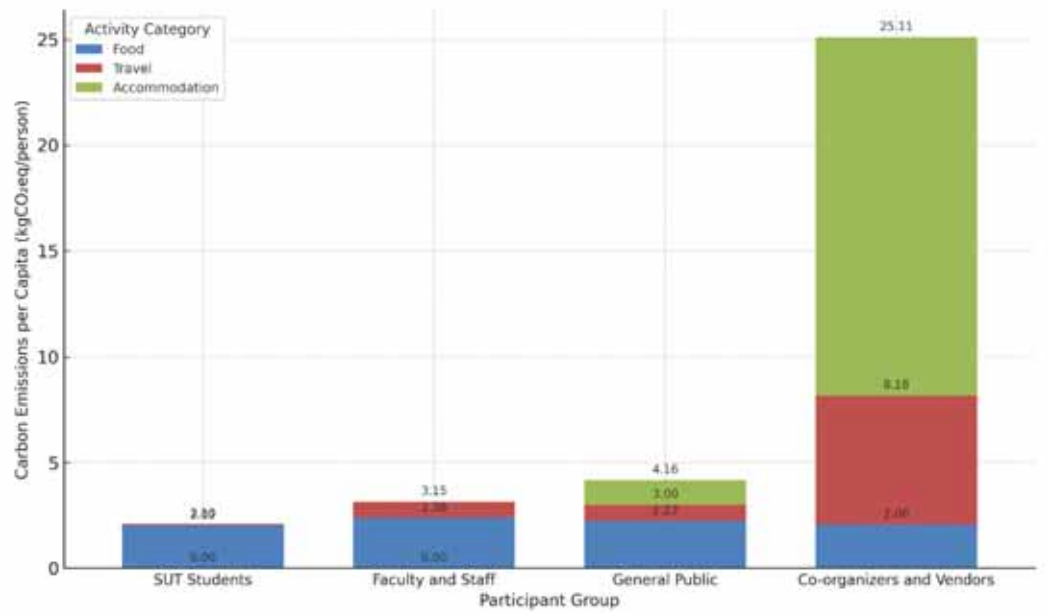

Fig. 9: Carbon intensity by participant type and activity category (food, travel, and accommodation) at the Suranaree Agricultural Fair 2025

their extended on-site presence, reliance on private transportation, and overnight stays. These insights emphasize the importance of eco-friendly lodging, vendor education programs, and emissions standards customized for exhibitors. In contrast, SUT students exhibited the lowest per emissions at 2.29 $kgCO_2eq$ per person, benefiting from residential proximity, minimal lodging needs, and likely use of low-emission commuting modes. Faculty and staff recorded slightly higher emissions at 3.15 $kgCO_2eq$ per person, primarily due to private vehicle commuting, highlighting opportunities for ride-sharing initiatives and electric vehicle incentives. The general public, representing the largest attendance group, recorded an emission of 5.85 $kgCO_2eq$ per person. While this figure is relatively moderate compared to other groups, it indicates a variety of transportation methods, shared lodging, and different lengths of stay. Considering the extent of public involvement, even minor decreases in per capita emissions could result in significant overall savings. These findings underscore the need for role-specific and behavior-specific strategies in sustainable event management. Concentrating exclusively on total emissions may overlook important chances for enhancing efficiency through small-scale adjustments in travel habits, dietary selections, and lodging practices.

The carbon footprint assessment of the Suranaree Agricultural Fair 2025 offers critical insights into the environmental impacts of large-scale academic events. The total footprint, estimated at 1,524.84 tCO_2eq, highlights the substantial emissions associated with multi-day gatherings. The observations corroborate prior studies that demonstrate how events with widespread public engagement, catering, and logistical arrangements can lead to elevated levels of GHG emissions (Dolf and Teehan, 2015; Clabeaux *et al.,* 2020; Scorrano *et al.,* 2020). Among the identified sources, food consumption and transportation were the dominant contributors, a pattern widely observed in the emissions profiles of public and institutional events (Collins *et al.,* 2009; Xuan *et al.,* 2025). The impact of food consumption and transportation-related emissions emphasizes the necessity for focused mitigation approaches, which include supporting plant-based food choices, improving public transportation, and fostering low-emission travel methods such as cycling and the use of electric vehicles. To facilitate benchmarking, the carbon intensity of the event was also assessed using normalized indicators, with a footprint of 6.74 $kgCO_2eq$ per square meter and 14,115.19 $kgCO_2eq$

per hour across the nine-day period. These metrics provide standardized performance indicators and allow comparison with other large-scale events. Scorrano *et al*. (2020) noted a similar event-hour footprint during the 2015 Expo Milan: Universal Expositions, emphasizing the relevance of normalized emission metrics for sustainable event planning. Analysis by participant type revealed distinct behavioral and logistical patterns. The highest per capita travel emissions were observed among faculty and staff, mainly due to their reliance on personal vehicles for commuting over moderate distances, a trend that corresponds with academic mobility studies (*Xuan et al.*, 2025). General public participants demonstrated moderate per capita emissions, but their large numbers and reliance on accommodation led to the highest total emissions. These patterns align with broader research highlighting the influence of participant behavior on event sustainability outcomes (Gössling and Peeters, 2015; Shah *et al.*, 2024). Electricity and water consumption accounted for only 1% of total emissions, reflecting effective energy practices such as the use of light-emitting diode (LED) lighting and demand management. This result reflects the conclusions drawn from university campus evaluations, where emissions related to utilities are frequently restricted (Clabeaux *et al.*, 2020). Nevertheless, the implementation of more disaggregated metering systems could enable zone-specific interventions to further optimize energy efficiency at future events. Despite its advantages, this study is subject to certain limitations. Although the survey sample of 3,667 respondents aligns with Yamane's formula for sample size determination (Yamane, 1967), generalizing behavioral patterns across all 258,917 participants may introduce bias. Moreover, emissions linked to materials provided by third-party vendors were not included because of the lack of reliable inventory data, implying that the overall emissions for the event could be slightly lower than reported. Nevertheless, this carbon footprint assessment establishes a critical baseline for institutional carbon management, directly supporting SUT's strategic objective of achieving carbon neutrality by 2035 (SUT, 2024b) and advancing small-scale emissions reduction initiatives within university-based events. The outcomes of this study align closely with the fair's theme, "Sustainable Agri-Innovation for BCG," by providing actionable data that integrate environmental accountability into event planning. Furthermore, the results contribute practical insights toward Thailand's National Bio-Circular-Green (BCG) Economy framework and global climate action goals under the UN Sustainable Development Goals (Leal Filho *et al.*, 2021; United Nations, 2022b). Implementing systematic carbon evaluations and initiatives for reducing emissions in event operations can act as a benchmark for advancing sustainable event management in the education and innovation sectors. The analysis centered on participants highlighted clear emission patterns tied to group interactions and logistical considerations. The general public contributed the highest total emissions, while co-organizers and vendors recorded the highest per capita emissions at 25.10 $kgCO_2eq$ per person, primarily due to extended stays, travel patterns, and accommodation needs. These patterns, consistent with previous studies (Gössling and Peeters, 2015), underscore the necessity of targeted mitigation strategies tailored to participant profiles. Conversely, SUT students demonstrated the lowest per capita emissions, underscoring the environmental advantages of promoting local engagement and supporting small-scale emissions reduction within sustainable event management frameworks.

Recommendations for sustainability event management

The findings of this study advocate for the development of tailored carbon mitigation strategies, such as vendor training programs, accommodation pooling initiatives, and public transportation incentives targeting high-impact participant categories. The execution of these strategies will encourage the adoption of low-carbon practices in university event planning and bolster the leadership of higher education institutions in advancing operations that are resilient to climate change.

Enhance data collection

Strengthening data collection frameworks is a critical first step. Incorporating carbon footprint-related questions into event registration would improve participant coverage and data accuracy. Ongoing input from stakeholders has been recognized as a crucial factor in promoting green campus initiatives (Suksod *et al.*, 2016). Subsequent to this evaluation, the findings were communicated

to the university administration, and initiatives were launched to gather vendor travel and material information beforehand, as well as to incorporate the emissions survey into the university's satisfaction survey process. These measures are designed to facilitate effective and sustainable tracking of emissions related to events

Expand the scope of assessment

Future evaluations should broaden their scope to include emissions associated with external inputs such as merchandise, booth infrastructure, and materials brought by vendors and exhibitors. A thorough evaluation would be consistent with the holistic carbon accounting methods suggested in recent sustainability reviews of higher education institutions (Sugiarto *et al.*, 2022).

Promote sustainable practices

SUT formally announced its Environmental and Energy Management Policy and Carbon Neutrality Roadmap on 11 November 2024, targeting net-zero emissions by 2035 (SUT, 2024a; 2024b). The Agricultural Fair takes place every year with different themes, but the 2025 edition was the inaugural effort to synchronize event activities with the newly established institutional objectives. While the overall planning process did not yet integrate structured sustainability interventions or decision-making protocols, the decision to conduct a carbon footprint assessment was a direct outcome of the university's sustainability commitments. This measure acted as a pivotal move to incorporate environmental accountability into future university activities and illustrates a larger institutional change towards climate-conscious planning. Targeted interventions are essential to address the event's primary emission sources: food, travel, and accommodation. Together, these categories accounted for approximately 90% of total emissions, underscoring their significance for emissions reduction initiatives. Encouraging food vendors to offer locally sourced, plant-based meals can help reduce food waste and promote the use of biodegradable or reusable packaging. Travel-related emissions can be reduced through public transportation promotion, carpooling initiatives, and incentives for low-emission commuting behaviors. For accommodation, partnerships with eco-certified lodging providers and promotion of shared stays among visitors and vendors could substantially lower emissions. Collaborating with students and key stakeholders in the development of these initiatives is crucial for fostering sustainable practices and facilitating small-scale emissions reduction within university events (Rahman *et al.*, 2023). Future editions could reduce electricity and water-related emissions by adopting LED and solar lighting, installing water-efficient fixtures, exploring greywater reuse systems for non-potable applications, and promoting the use of refillable cups to minimize single-use container waste. Advocating for compostable food packaging and offering incentives to attendees to minimize packaging waste. The use of the campus venue helped reduce emissions by utilizing existing infrastructure and enabling local access. Shaded pathways have been established to enhance walkability, and future designs may group activity areas to decrease the need for internal transport. While no formal partnerships were established, local vendors contributed indirectly by showcasing sustainability-focused products and services. Collaborations with businesses and local communities in the future could enhance efforts such as reusable packaging, carbon offset schemes, and sourcing low-carbon goods produced locally

Implement carbon offsetting measures

Adopting certified carbon offset programs would allow the university to address residual and unavoidable emissions. By adopting these mechanisms, the university would advance its climate neutrality aims and synchronize event operations with global carbon management strategies.

Institutionalizing continuous improvement

Routine carbon footprint assessments should be embedded into all major university events to track progress, identify opportunities for further emission reductions, and strengthen SUT's leadership in sustainable event management. This strategy is in accordance with international sustainability criteria and campus greening models that seek to encourage lasting transformation within academic settings (Sugiarto *et al.*, 2022). By adopting these recommendations, the university can further integrate sustainability into event planning and reinforce its commitment to achieving carbon neutrality by 2035. These efforts also support the broader BCG economy vision promoted through the Agricultural

Fair and position the university as a leader in climate-responsive education and action. The results of this preliminary evaluation are anticipated to inform targeted enhancements in vendor registration, travel arrangements, and data gathering for upcoming iterations of the fair.

CONCLUSION

This carbon footprint assessment of the Suranaree Agricultural Fair 2025 successfully quantified the GHG emissions associated with a multi-day academic event and identified the primary emission sources, specifically food consumption, participant travel, and accommodation activities, across diverse participant groups. Approximately 41% of total emissions were due to food consumption, with travel activities contributing roughly 31%. The total footprint of 1,524.84 tCO_2eq, corresponding to an average of 5.89 $kgCO_2eq$ per person, highlights the substantial environmental significance of such events, often underestimated in institutional sustainability initiatives. Calculated carbon intensities, 6.74 $kgCO_2eq$ per square meter and 14,115.19 $kgCO_2eq$ per event hour, provide valuable benchmarks for future monitoring and sustainable planning. Importantly, this study advances the integration of small-scale emissions reduction initiatives into sustainable event management frameworks. Utilizing a thorough participant-focused analysis, it separated emissions into various activity categories, which enriched the comprehension of the underlying behavioral and logistical influences. This approach offers a replicable model for academic institutions aiming to embed carbon management into operational practices. Practical recommendations, including promoting sustainable food provisioning, low-carbon commuting, eco-friendly accommodation, and improved data management, demonstrate that targeted interventions can meaningfully mitigate emissions. These initiatives are in strong alignment with SUT's sustainability goals and its dedication to reaching carbon neutrality by 2035. At the policy level, this research reinforces the role of universities as key drivers in advancing the BCG Economy framework and the UN SDGs, particularly Goal 13 on Climate Action and Goal 12 on Responsible Consumption and Production. By formalizing regular assessments of carbon footprints and embedding sustainability within event management, academic institutions can reinforce their leadership in supporting climate-resilient education and innovation ecosystems. Future research should focus on integrating life cycle assessment (LCA) methodologies to capture indirect emissions from material flows and supply chains, and on comparative studies across event types and institutional contexts. Investigating behavioral strategies to encourage participants to make low-carbon choices is a promising approach to improve sustainable event management practices

AUTHOR CONTRIBUTIONS

V. de Cadenet performed the conceptualized and managed the project, designed the methodology, performed data analysis, and led the manuscript writing. W. Komkum coordinated project operations, organized the data collection team, and served as the liaison with university departments to gather required information. P. Raksa conducted GHG emission calculations using provided emission factors and organized the data into activity-based categories. P. Boondaeng converted raw input data into participant-based emission metrics and revised calculations for accuracy and consistency. P. Parinyakulset facilitated waste management implementation during the event, managed electricity and water usage data, and provided information on waste sorting and collection. All authors reviewed and approved the final version of the manuscript.

ACKNOWLEDGMENT

The authors would like to thank SUT for supporting this study through the Sustainable Campus Initiative. This research was also financially supported by Technopolis, SUT, for field operations and data collection. Special appreciation is extended to the Office of Building and Grounds, the Center of Excellence in Biomass, and the Suranaree Agricultural Fair 2025 organizing committee for their collaboration, facility access, and logistical support. The authors also acknowledge the Division of Planning of SUT for providing detailed participant data from the registration application and event staff records. Lastly, sincere thanks go to all participants who contributed to the carbon footprint survey, making this research possible.

CONFLICT OF INTEREST

The authors declare that there is no conflict of interest regarding the publication of this manuscript. In addition, ethical issues, including plagiarism, informed consent, misconduct, data fabrication and/or falsification, double publication and/or submission, and redundancy, were observed by the authors.

OPEN ACCESS

©2025 The author(s). This article is licensed under a Creative Commons Attribution 4.0 International License, which permits use, sharing, adaptation, distribution and reproduction in any medium or format, as long as you give appropriate credit to the original author(s) and the source, provide a link to the Creative Commons license, and indicate if changes were made. The images or other third-party material in this article are included in the article's Creative Commons license, unless indicated otherwise in a credit line to the material. If material is not included in the article's Creative Commons license and your intended use is not permitted by statutory regulation or exceeds the permitted use, you will need to obtain permission directly from the copyright holder. To view a copy of this license, visit: http://creativecommons.org/licenses/by/4.0/

PUBLISHER'S NOTE

GJESM Publisher remains neutral with regard to jurisdictional claims with regard to published maps and institutional affiliations.

Positive AI Statement

During the preparation of this work the author(s) have used artificial intelligence (AI) ChatGPT (OpenAI) in order to assist with English language polishing, improving clarity of expression, and enhancing academic writing style. After using this tool/service, the authors reviewed and edited the content as needed and take full responsibility for the content of the publication.

(For this reason, the GPTZero detector will evaluate the manuscript utilizing Generative AI, ensuring a high detection rate. If the manuscript relies heavily on Generative AI and AI-assisted technologies, it will be archived without further options for appeal).

NEGATIVE AI STATEMENT

The author(s) declare that no AI tools or services were not used or not highly applied during the preparation of this work.

ABBREVIATIONS

%	Percent
BCG	Bio-circular-green
BEIS	Department for Business, Energy and Industrial Strategy
CO_2	Carbon dioxide
$kgCO_2eq$	kilogram carbon dioxide equivalent
COP	Conference of parties
DEDE	Department of Alternative Energy Development and Efficiency
DEFRA	Department for Environment, Food and Rural Affairs
EMS	Environmental management system
GHG	Greenhouse gas
IPCC	Intergovernmental Panel on Climate Change
ISO	International Organization for Standardization
kg	kilogram
$kgCO_2eq$	Kilogram of carbon dioxide equivalent
Km	kilometer
kWh	kilowatt-hour
LCA	Life cycle assessment
LCI	Life cycle inventory
LED	Light-emitting diode
LT-LEDS	Long-term low greenhouse gas emission development strategy
MBT	Mechanical biological treatment
tCO_2eq	Metric ton carbon dioxide equivalent
NDC	Nationally Determined Contribution
NSTDA	Nation al Science and Technology Development Agency

RDF	Refuse derived fuel
SBM	Slack based measure (from DEA modeling)
SDG	Sustainable development goal
SUT	Suranaree University of Technology
TEI	Thailand Environmental Institute
TGO	Thailand Greenhouse Gas Management Organization
TIIS-MTEC	Thailand Industrial Information System, National Metal and Materials Technology Center
UFRR	Federal University of Roraima
UK	United Kingdom
UK DEFRA	United Kingdom Department for Environment, Food and Rural Affairs
UNFCCC	United Nations Framework Convention on Climate Change

REFERENCES

Almeida, A.P.; Sousa, V.; Silva, C.M., (2021). Methodology for estimating energy and water consumption patterns in university buildings: Case study, Federal University of Roraima (UFRR). Heliyon. 7(1): e08642 (**13 pages**).

Ballarano, D.; Patella, S.M.; Asdrubali, F., (2022). Sustainable transportation for events: A systematic review. Sustainability. 14(23): 15815 (**22 pages**).

BEIS, (2022). Greenhouse gas reporting: conversion factors 2022. Department for Business, Energy and Industrial Strategy UK Government.

Calzavara, M., (2023). Application of ISO 14067 standard to assess events' carbon footprint: Hero Dolomites' case study, Master's thesis, Universita Ca'Foscari Venezia, curriculum of environmental monitoring and remediation, environmental science program (**10 pages**).

Cerutti, A.K.; Beccaro, G.L.; Bruun, S.; Bosco, S.; Donno, D.; Notarnicola, B.; Bounous, G., (2018). Carbon footprint in fruit production systems: A review of methodological approaches and results. J. Cleaner Prod., 175: 769–784 (**16 pages**).

Clabeaux, R.; Carbajales-Dale, M.; Ladner, D.; Walker, T., (2020). Assessing the carbon footprint of a university campus using a life cycle assessment approach. J. Cleaner Product., 273: 122600 (**7 pages**).

Collins, A.; Jones, C.; Munday, M., (2009). Assessing the environmental impacts of mega sporting events: Two options? Tourism Manage., 30(6): 828–837 (**10 pages**).

Defra, (2023). UK Government GHG conversion factors for company reporting. Department for Environment, Food and Rural Affairs (Defra), London, UK **(1 page).**

DEDE, (2023). Thailand emission factor database. Department of Alternative Energy Development and Efficiency Ministry of Energy, Bangkok, Thailand.

Disterheft, A., Caeiro, S., Ramos, M.R.; Azeiteiro, U.M., (2015). Environmental management systems (EMS) implementation processes and practices in European higher education institutions: Top-down versus participatory approaches. J. Cleaner Prod., 106: 134–144 (**11 pages**).

Dolf, M.; Teehan, P., (2015). Reducing the carbon footprint of spectator and team travel at the University of British Columbia's varsity sports events. Sport Manage. Rev., 18(2): 244–255 (**12 pages**).

Ecoinvent Centre, (2007). Ecoinvent data v2.2: Life cycle inventory database. Swiss Centre for Life Cycle Inventories.

González-García, S.; Esteve-Llorens, X.; Moreira, M.T.; Feijoo, G., (2018). Carbon footprint and nutritional quality of different human dietary choices. Sci. Total Environ., 644: 77–94 (**18 pages**).

Gössling, S.; Peeters, P., (2015). Assessing tourism's global environmental impact 1900–2050. J. Sustainable Tourism. 23(5): 639–659 (**21 pages**).

Haryanto, A.; Santoso, A.D.; Hanif, M.; Astuti, L.P.; Darmawan, M.; Wirawan, R.H.; Prasetyo, A.D., (2025). Strategies for sustainable behavior and emission reduction through individual carbon footprint analysis. Global J. Environ. Sci. Manage., 11(1): 243–260 (**18 pages**).

IPCC, (2006). 2006 IPCC guidelines for national greenhouse gas inventories: Volume 5 – Waste. Intergovernmental Panel on Climate Change (**215 pages**).

IPCC, (2007). Climate change 2007: Mitigation of climate change. Contribution of working group III to the fourth assessment report of the IPCC. Cambridge University Press (**851 pages**).

IPCC, (2014). Climate change 2014: Synthesis report. Contribution of working groups I, II and III to the fifth assessment report of the Intergovernmental Panel on Climate Change. Pachauri, R.K.; Meyer, L.A. (Eds.). Intergovernmental Panel on Climate Change (IPCC) (**151 pages**).

IPCC, (2021a). Climate change 2021: The physical science basis. Intergovernmental Panel on Climate Change (**3949 pages**).

IPCC, (2021b). 2021 refinement to the 2006 IPCC guidelines for national greenhouse gas Inventories. Intergovernmental Panel on Climate Change (**839 pages**).

ISO, (2018). ISO 14064-1:2018 - Greenhouse gases – Part 1: Specification with guidance at the organization level for quantification and reporting of greenhouse gas emissions and removals. Int. Organ. Standardization, Geneva, Switzerland (**38 pages**).

Kamble, N.N.; Kavathekar, B.R., (2021). Carbon footprint assessment of an educational institute: A case study. Proceedings of International Conference on Smart Systems

and Green Energy, India (**6 pages**).
Kongritti, N., (2015). Carbon footprint of students and personnel of Nakhon Ratchasima Rajabhat University. Res. Bus. Econ. J., 10: 86–94 (**9 pages**).
Kubová, P.; Hájek, M.; Třebický, V., (2018). Carbon footprint measurement and management: Case study of the school forest enterprise. BioResources, 13(2): 4521–4535 (**15 pages**).
Leal Filho, W.; Setti, A.F.; Boenecke, J.; Beynaghi, A.; Price, E.; Azeiteiro, U.M., (2021). Handling climate change education at universities: an overview. Environ. Sci. Europe. 33: 109 (**15 pages**).
Lozano, R.; Lukman, R.; Lozano, F.J.; Huisingh, D.; Lambrechts, W., (2013). Declarations for sustainability in higher education: Becoming better leaders, through addressing the university system. J. Clean. Prod., 48: 10–19 (**10 pages**).
Mannheim, V.; Avató, J., (2023). Examining the carbon footprint of conferences with an emphasis on energy consumption and catering. Energies. 18(2): 321 (**15 pages**).
Martellini, T.; Daddi, T.; Gagliardi, F.; Marrucci, L.; Marrucci, A.; Fabbri, E., (2015). Carbon footprint assessment in event management: Best practices and case studies. J. Clean. Prod., 93: 79–88 (**10 pages**).
McCowan, T., (2020). The impact of universities on climate change: A theoretical framework. Centre for Global Higher Education, Working Paper No. 55 (**44 pages**).
Owen, R., Fisher, E., McKenzie, K., (2013). Beyond reduction: Climate change adaptation planning for universities and colleges. Int. J. Sustainable High. Educ., 14(3): 246–263 (**18 pages**).
Piccerillo, L.; Misiti, F.; Digennaro, S., (2023). Assessing the environmental impact of a university sport event: The case of the 75th Italian National University Championships. Sustainability. 15(3): 2267 (**18 pages**).
Prasara-A, J.; Bridhikitti, A., (2022). Carbon footprint and cost analysis of a bicycle lane in a municipality. Global J. Environ. Sci. Manage., 8(2): 197–208 (**12 pages**).
Rahman, S.A.A.; Qureshi, M.I.; Saeed, M.N.; Khan, M.B., (2023). Green-smart university campuses: The mediating role of student engagement. SAGE Open. 13(4) (**15 pages**).
Ramely, A.; Ab. Talib, M.F.; Raziah, J.Z.R.; Mokhtar, M.F., (2022). Green event practices: Understanding the adaptation of event organisers through a systematic review. Malays. J. Sustainable Environ., 9(1): 119–140 (**22 pages**).
Scorrano, M.; Bimbo, F.; Castriota, S.; Vecchiato, D., (2020). Assessing the carbon footprint of large-scale events: The case of Milan Expo 2015. Sustainable Prod. Consum., 24: 258–266 (**9 pages**).
Shah, A.; Wan, Y.; Rubin, J.; Brennan, J.; Goldstein, B.P., (2024). Emissions analysis of academic events: The case for hybrid and local formats. Environ. Res. Lett., 19(1) **(13 pages)**.
Sugiarto, A., Lee, C.W. and Huruta, A.D., (2022). A systematic review of the sustainable campus concept. Behav. Sci., 12(5): 130 (**15 pages**).
Suksod, S.; Boonmee, K.; Wang, Y.; Keeratipranon, N., (2016). Green campus initiative and its impacts on quality of life of stakeholders in green and non-green campus universities. Sustainability. 8(10): 1005 (**16 pages**).
Suranaree University of Technology, (2024a). Green University Initiatives. (**1 page**).
Suranaree University of Technology, (2024b). Green University Initiatives. (**1 page**).
TEI, (2012). Emission factors for greenhouse gas inventories in Thailand. Thailand Environmental Institute (**55 pages**).
TIIS-MTEC-NSTDA, (2022). Thai National Life Cycle Inventory (LCI) Database: Electricity Emission Factors. Natl. Sci. Technol. Dev. Agency (NSTDA), Thailand.
Thai National LCI Database, (2022). Thai national life cycle inventory database. Thailand Greenhouse Gas Management Organization (TGO), Bangkok, Thailand (**1 page**).
Thailand Greenhouse Gas Management Organization, (2022). Thailand carbon footprint database and guidelines for GHG calculation. (**1 page**).
Thailand, (2022a). Thailand's second updated nationally determined contribution (NDC). United Nations Framework Convention on Climate Change (UNFCCC) (**36 pages**).
Thailand, (2022b). Long-term low GHG emission development strategy (LT-LEDS). United Nations Framework Convention on Climate Change (UNFCCC) (**63 pages**).
United Nations, (2015a). Goal 12: Ensure sustainable consumption and production patterns. Sustainable Development Goals (**1 page**).
United Nations, (2015b). Goal 13: Take urgent action to combat climate change and its impacts. Sustainable Development Goals (**1 page**).
United Nations, (2015c). Paris agreement. United Nations Framework Convention on Climate Change (UNFCCC) (**27 pages**).
Velis, C.A.; Longhurst, P.J.; Drew, G.H.; Smith, R.; Pollard, S.J.T., (2010). Production and quality assurance of solid recovered fuels using mechanical–biological treatment (MBT) of waste: A comprehensive assessment. Crit. Rev. Environ. Sci. Technol., 40(12): 978–1105 (**128 pages**).
Xuan, S.; Zhou, Z.K.; Zhou, J.X.; Xia, Q.F.; Qin, Y.N.; Wu, J.P., (2025). The impact of sporting events on carbon emissions and the emission reduction measures: A systematic review from 2019 to 2024. Pol. J. Environ. Stud., 34(1): 123–135 (**13 pages**).
Yamane, T., (1967). Statistics: An introductory analysis (2nd ed.). Harper and Row (**919 pages**).
Zhang, J.; Xia, B., (2024). Carbon emissions and its efficiency of tourist hotels in China from the supply chain based on the input–output method and Super-SBM model. Sustainability, 16(21): 9489 (**20 pages**).

AUTHOR (S) BIOSKETCHES

De Cadenet, V., Ph.D., Lecturer, School of Environmental Engineering, and Head, Unit of Greenhouse Gas Management, Technopolis, Suranaree University of Technology, 111 University Avenue, Nakhon Ratchasima 30000, Thailand.
- Email: *vorasiri@g.sut.ac.th*
- ORCID: 0009-0006-7038-3707
- Web of Science Researcher ID: MZQ-7319-2025
- Scopus Author ID: NA
- Homepage: https://beta.sut.ac.th/ie-envi/

Parinyakulset, P., M.Eng., Environmental Engineering, Head, Environmental Unit, Division of Buildings and Ground, Suranaree University of Technology, Nakhon Ratchasima, Thailand.
- Email: *chanid@sut.ac.th*
- ORCID: 0009-0001-6198-4088
- Web of Science Researcher ID: NA
- Scopus Author ID: NA
- Homepage: https://web.sut.ac.th/dbg/personnel_dbg.html

Komkum, W., B.Inf.Sc., Communication, Administration officer of Unit of Greenhouse Gas Management Technopolis, Suranaree University of Technology, Nakhon Ratchasima, Thailand.
- Email: *wasutha@g.sut.ac.th*
- ORCID: 0009-0004-3600-3622
- Web of Science ResearcherID: NA
- Scopus Author ID: NA
- Homepage: https://tn.sut.ac.th/?page=Info/infoMajor&ref=165&lang=en

Boondaeng, P., B.Eng., Environmental Engineering, Administration officer of Unit of Greenhouse Gas Management Technopolis, Suranaree University of Technology, Nakhon Ratchasima, Thailand.
- Email: *panuwit.bd@g.sut.ac.th*
- ORCID: 0009-0008-5696-8033
- Web of Science ResearcherID: NA
- Scopus Author ID: NA
- Homepage: https://tn.sut.ac.th/?page=Info/infoMajor&ref=165&lang=en

Raksa, P., B.Eng. Candidate, Undergraduate Student in Environmental Engineering, School of Environmental Engineering, Suranaree University of Technology, Nakhon Ratchasima, Thailand.
- Email: *phonchitafaiifight@gmail.com*
- ORCID: 0009-0006-4531-9359
- Web of Science ResearcherID: NA
- Scopus Author ID: NA
- Homepage: http://orcid.org/0009-0006-4531-9359

HOW TO CITE THIS ARTICLE

de Cadenet, V.; Komkum, Raksa, W.; Boondaeng, P.; Parinyakulset, P., (2025). Carbon footprint associated with a small-scale emissions reduction initiative for sustainable event management. Global J. Environ. Sci. Manage., 11(3): 941-962.

DOI: 10.22034/gjesm.2025.03.05

URL: https://www.gjesm.net/article_723652.html

Global J. Environ. Sci. Manage. 11(3): 963-982, Summer 2025, Serial #43

Global Journal of Environmental Science and Management
(GJESM)

Homepage: https://www.gjesm.net/

Podcasts

ORIGINAL RESEARCH ARTICLE

The role of marine protected areas in enhancing coral cover and reef fish communities

Z.A. Harahap[1,2], D.G. Bengen[2,*], I.W. Nurjaya[2], S.B. Agus[2], Y. Naulita[2], R.M. Siringoringo[3]

[1] *Department of Aquatic Resources Management, Faculty of Agriculture, Universitas Sumatera Utara, Medan, 20155, Indonesia*

[2] *Department of Marine Sciences and Technology, Faculty of Fisheries and Marine Science, IPB University, Bogor, 16680, Indonesia*

[3] *Research Center for Oceanography, National Research and Innovation Agency, Indonesia*

ARTICLE INFO

Article History:
Received 1 November 2024
Revised 03 February 2025
Accepted 10 April 2025

Keywords:
Biodiversity
Coral cover
Coral reef
Marine protected area

DOI: 10.22034/gjesm.2025.03.06

ABSTRACT

BACKGROUND AND OBJECTIVES: Coral reefs are vital ecosystems that support a diverse array of marine species and provide essential services such as coastal protection, fisheries, and tourism. Nevertheless, these ecosystems face growing threats from human-induced pressures, including overfishing, pollution, and the impacts of climate change. No-take zones within marine protected areas have proven to be valuable instruments for the protection of coral reefs and the enhancement of biodiversity. The study objectives were to evaluates the role of no-take zones in promoting coral cover, reducing coral degradation, and supporting the diversity and abundance of reef fish communities in the Tapanuli Tengah Marine Conservation area, North Sumatra, Indonesia.

METHODS: Field surveys were conducted in three no-take zones and adjacent non-protected areas. Coral cover was assessed using the underwater photo transect method, while reef fish communities were surveyed using the underwater visual census technique. The analysis focused on comparing coral health, fish populations, and species diversity in both protected and unprotected zones. Statistical analyses were used to evaluate correlations between coral cover and fish communities and the effectiveness of no-take zones in supporting biodiversity.

FINDINGS: Analysis demonstrated that no-take zones had a significantly higher percentage of hard coral cover and a lower level of macroalgal growth when compared to non-protected areas. Fish species richness and abundance were also substantially more significant in no-take zones. Prominent families of reef fish, such as Pomacentridae, Apogonidae, and Caesionidae, showed a strong connection to vibrant coral habitats. Conversely, disturbed regions were characterized by algae-dominated substrates and species that can withstand such conditions, including Acanthuridae and Lethrinidae.

CONCLUSION: This study highlights the effectiveness of no-take zones in improving coral reef health and enhancing reef fish biodiversity. The findings support expanding and strictly enforcing no-take zones to mitigate the impacts of overfishing and environmental degradation. It is essential to pursue further research to identify site-specific influences and long-term ecological results, thereby guaranteeing sustainable benefits for both marine ecosystems and coastal communities.

This is an open access article under the CC BY license (http://creativecommons.org/licenses/by/4.0/).

NUMBER OF REFERENCES
97

NUMBER OF FIGURES
6

NUMBER OF TABLES
1

*Corresponding Author:
Email: *dieter@indo.net.id*
Phone: +251 862 3644
ORCID: 0000-0002-3880-5117

Note: Discussion period for this manuscript open until Sep 1, 2025 on GJESM website at the "Show Article".

INTRODUCTION

Coral reefs represent some of the most expansive and ecologically varied ecosystems on Earth; coral reefs support a wide range of life, from tiny plankton to large fish. This astonishing range of biodiversity plays a vital role in sustaining the balance of ocean ecosystems and greatly influences human communities (Awak *et al.,* 2016; Azra *et al.,* 2023; Bellwood and Tebbett, 2024). Despite occupying less than 1 percent (%) of the ocean's surface, coral reefs sustain approximately 25% of all marine species, offering critical habitats for fish, mollusks, crustaceans, and numerous other organisms that depend on these ecosystems for protection, feeding, and reproduction (Kembrey *et al.,* 2024). Coral reefs, while ecologically significant, also deliver vital services to human communities, including protection against coastal erosion, support for fishing industries, and tourism opportunities, which together sustain millions of livelihoods globally. The extraordinary biodiversity and multifaceted benefits of coral reefs highlight the urgent need for protection amidst escalating environmental pressures (Burdett *et al.,* 2024; Hughes *et al.,* 2017). The "Coral Triangle", comprising Solomon Islands, Timor-Leste, Papua New Guinea, Malaysia, Philippines, and eastern Indonesia, is identified as the primary center of coral reef biodiversity worldwide (Green, 2008; Sobha *et al.,* 2023). Located in the Coral Triangle, Indonesia is known for its exceptional diversity of marine biodiversity. This area is home to approximately 569 species and 83 genera of stony corals, accounting for roughly 69% of the global species and 76% of the genera of stony corals worldwide (Hadi *et al.,* 2020). Recognized globally for their ecological diversity, the nation's coral reefs are home to over 70% of all species of reef-building corals, as well as a substantial variety of fish species that inhabit these ecosystems (De Clippele *et al.,* 2023). Recent studies underscore a significant decline in marine biodiversity, with coral reefs enduring substantial impacts from human activities (Camp *et al.,* 2024; Edgar *et al.,* 2023; L. Huang *et al.,* 2024; Obura *et al.,* 2022). These ecosystems are crucial not only for the survival of diverse marine species but also for the economic well-being of human communities through sectors such as fisheries, tourism, and coastal defense. Nevertheless, these essential habitats are facing growing challenges from a combination of overfishing, pollution, and the effects of climate change. Overfishing has led to the reduction of vital fish stocks, pollution has degraded water quality, and climate change has resulted in coral bleaching and increased ocean acidity, all of which threaten the structural and ecological integrity of coral reefs (Good and Bahr, 2021; O'Leary *et al.,* 2020). Globally, coral reefs face a range of complex challenges. Critical challenges involve the repercussions of overfishing, pollution, and especially the significant ramifications of climate change, such as higher sea temperatures, ocean acidification, and a rise in both the frequency and intensity of extreme weather phenomena. The intrinsic fragility and sensitivity of coral reef systems mean that even slight environmental fluctuations—like minor temperature or salinity changes—can have disastrous effects. These changes can trigger extensive coral mortality and lead to the degradation of the associated fish communities that rely on these habitats for survival and reproduction. The interaction between coral reefs and the fish populations that depend on them is one of the most thoroughly examined relationships within marine ecosystems. Coral reefs, particularly those dominated by Acropora and Millepora corals, provide critical habitat for a wide variety of fish species (Coker *et al.,* 2014), and their loss can have significant implications for fish biodiversity. Protecting coral habitats and the fish populations that rely on them is crucial, making conservation initiatives vital. Ecological disruption not only reduces biodiversity but also undermines the resilience of these ecosystems, complicating efforts towards their recovery and conservation (Hughes *et al.,* 2017; Selig and Bruno, 2010). The heightened exploitation of natural resources and the intensifying repercussions of global warming have brought to light the urgent need for comprehensive management strategies that bolster ecosystem resilience and enhance their ability to withstand and recover from various disturbances. In marine environments, no-take zone (NTZ) and marine protected areas (MPAs) have emerged as effective tools for conserving biodiversity and increasing the biomass of exploited species, as a key conservation strategy to protect and restore coral reef ecosystems and associated fish communities (Caughman *et al.,* 2024; Lusiana *et al.,* 2024). In-depth study indicates that properly enforced MPAs can markedly boost the diversity, abundance, size of individual organisms, and reproductive rates of fishes and invertebrates,

resulting in advantageous spillover effects to nearby unprotected zones (Benedetti-Cecchi *et al.,* 2024). However, it is important to note that the specific mechanisms and outcomes of MPAs in enhancing coral reef ecosystems can vary considerably across different regions, management contexts, and environmental conditions (Strain *et al.,* 2019). Among marine environments, coral reef ecosystems are some of the richest in biodiversity; however, they face growing threats from human impact and changes in the environment. NTZs can help fisheries recover and boost ecotourism by protecting coral reefs. However, they may cause short-term income loss for fishers and require investment in management. Involving local communities in decision-making can help balance these impacts and ensure long-term benefits. Since 2008, the waters of Tapanuli Tengah have been designated as a regional marine protected area. In 2020, this status was elevated with the issuance of Decree Number 87/KEPMEN-KP/2020 by the Minister of Marine and Fisheries of the Republic of Indonesia, officially recognizing it as a conservation area of coastal and small islands in Tapanuli Tengah and Adjacent Waters (MMAF, 2020). Nonetheless, the extent of community engagement in its management is markedly insufficient, which has limited the impact of conservation strategies. Depending on marine resources for their livelihoods, local communities have not been fully involved in managing the no-take zones. When communities are not involved, it often results in misunderstandings and pushback against conservation policies. Therefore, it is essential to actively involve these communities in the management process to secure long-term success. This study seeks to address two critical objectives. The first objective is to examine the relationship between coral cover and reef fish communities, focusing on their abundance and species diversity within the MPAs of Tapanuli Tengah. Understanding these dynamics is crucial to identifying the ecological linkages that sustain biodiversity in these systems. The second objective is to evaluate the effectiveness of MPAs in enhancing the health and resilience of coral reef and the fish species that are part of these environments. The study seeks to deliver practical insights into how MPAs contribute to the conservation of coral reef biodiversity and uphold the ecological balance necessary for their enduring sustainability by meeting these objectives. The study was conducted within the Tapanuli Tengah Marine Conservation area in North Sumatra, Indonesia. Data collection was executed in two distinct phases: initially, in 2021, observations were conducted outside NTZs, while in 2024, observations were undertaken at three specific locations of NTZs. This study has been carried out in the Tapanuli Tengah Marine Conservation Area in North Sumatra, Indonesia, in 2024.

MATERIALS AND METHODS

Study area

This study was conducted in the Tapanuli Tengah Marine Conservation Area in North Sumatra, Indonesia, focusing on coral reefs and reef fish. Three no-take zones were the focus of observations, including Mursala Island, where fishing and other disruptive activities are strictly prohibited. These areas were compared with locations outside the no-take zones to evaluate the conservation effectiveness of these protected areas. The specific sites for coral observations are shown in Fig. 1. This figure illustrates the geographic layout of the study sites, highlighting both the protected and non-protected areas, which enables a clear visual comparison of the ecological contexts within which the observations were made. Understanding the effects of conservation strategies on marine biodiversity relies heavily on this spatial separation.

Coral reef observation

The observational survey commenced from the mainland or coastal areas and extended into the adjacent waters. Designated stations were systematically monitored, employing self-contained underwater breathing apparatus (SCUBA) to facilitate underwater observations and capture photographic documentation (Hill and Wilkinson, 2004). The underwater photo transect (UPT) technique was employed to assess benthic reef cover, ensuring precision and reproducibility (Kohler and Gill, 2006). In this study, 50 photos were systematically analyzed, each annotated with 30 random points, using coral point count with excel extensions (CPCe) software for detailed analysis (Abrar *et al.,* 2024; Kohler and Gill, 2006). This strategy allowed for the assessment of multiple metrics, including the percentage of coral coverage, the diversity of benthic biota, and various substrate categories (Dumas *et al.,* 2009; Kornder *et al.,* 2021). The UPT method enables high-resolution

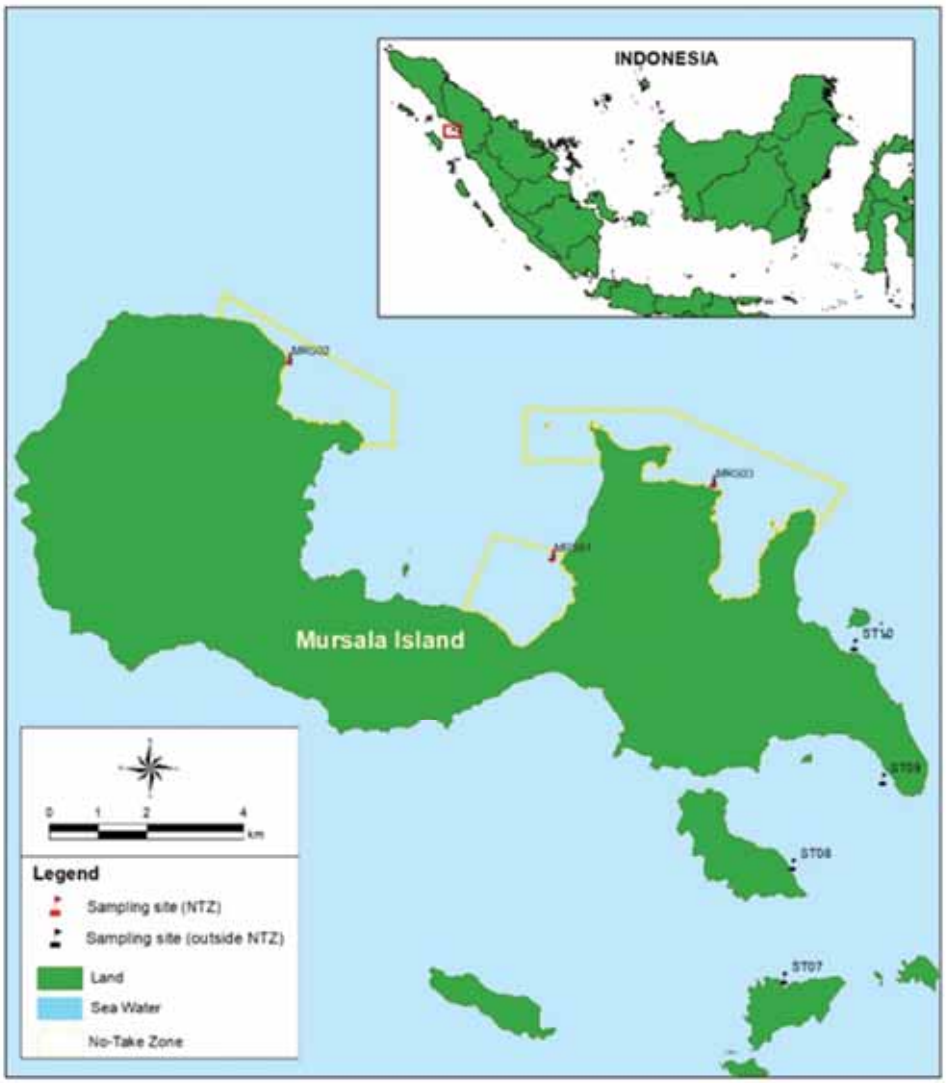

Fig. 1: Geographical location of the study area in Tapanuli Tengah Marine Conservation area, Indonesia

documentation of benthic ecosystems, facilitating detailed and consistent long-term monitoring of coral reef health while allowing for efficient quantification of coral cover and benthic composition across spatial and temporal scales (Prasetya and Santoso, 2022).

Coral cover

The evaluation of coral cover seeks to establish the status and categorization of coral reef areas, which is essential for assessing the ecological health and overall condition of the reef ecosystem. Percent cover of a lifeform category, using Eq. 1 (English *et al.,* 1997):

$$N_i = \frac{L_i}{N} x100\% \quad (1)$$

Where; Li : percent cover (%); Li : Total length of category; N : Length of transect

In many regions of Southeast Asia, coral reefs are assessed using a linear scale based on the percentage of live coral cover, as outlined by Bachtiar *et al.* (2019). According to this scale, reefs exhibiting more than 75% live coral cover are classified as being in "excellent" condition. Reefs with coral cover between 50% and 75% are categorized as being in "good"

condition, while those with coral cover ranging from 25% to 50% are deemed to be in "fair" condition. A reef is deemed to be in "poor" condition if it has less than 25% of its surface covered by live coral (Edinger and Risk, 2000).

Coral reef fish observation

Reef fish data were obtained through the underwater visual census (UVC) method along a 50-meter transect, with a field of view extending 2.5 meters on either side of the transect line (English *et al.,* 1997). At every specified data collection location, transects were set up, and fish data were documented through underwater video recordings taken during the day within the no-take zone reef. Divers utilized underwater video cameras to document the presence and behaviour of coral reef fish in shallow waters, capturing random yet comprehensive footage of fish communities (Kang *et al.,* 2022). The identification of species and the estimation of their abundance were conducted utilizing video image data. Observed fish were cross-referenced with identification guides, including (Frose and Pauly, 2024) and (Allen, 2003), to ensure accuracy. During dives, fish data were initially recorded on underwater slates and subsequently transferred to a Microsoft Excel datasheet for further processing and analysis. This strategy offered a comprehensive framework for the assessment of reef fish communities by combining visual census techniques with video documentation and rigorous data validation processes.

Community structure of coral reef fish

To characterize the community structure of reef fish, underwater visual surveys were conducted using SCUBA within designated survey plots. Throughout these surveys, the composition of species, their abundance, and the total length of all individuals measuring at least 15 centimeters (cm) were meticulously documented (Helder *et al.,* 2022). The identification of reef fish was guided by authoritative references, including Allen and Erdmann (2012), (Kuiter and Tonozuka, 2001), and FishBase online data (Froese and Pauly, 2024), which provide essential taxonomic, ecological, and distributional information. These resources, when combined, create a vital framework for studies related to biodiversity and ecology. The structure of coral reef fish communities was analyzed by calculating diversity indices, including Margalef richness index (D), Shannon-Wiener diversity index (H), Pielou's Evenness index (E), and Simpson dominance species index (C) (Fedor and Zvaríková, 2019; Gaertner *et al.,* 2008). The use of biodiversity metrics, including species richness, diversity, evenness, and dominance, is vital for analyzing the community structure and the general health of fish populations in coral reefs. These indices are instrumental in the monitoring, evaluation, and conservation of coral reef ecosystems, offering vital insights into biodiversity, ecosystem resilience, and functional processes. Furthermore, they are vital in monitoring alterations in fish community dynamics, identifying potential stressors, and shaping management and conservation strategies aimed at preserving the integrity and sustainability of reef ecosystems (Loiseau and Gaertner, 2015).

Statistical analysis

Correspondency analysis performed to investigate the correlation between reef fish family abundance and the percent cover of coral lifeforms (Chabanet *et al.,* 1997). This multivariate approach is often utilized to detect patterns and connections in categorical data, which makes it particularly adept at explaining the relationships between ecological variables. The analysis utilized a statistical computing environment that supports robust data visualization and interpretation. By employing this approach, the study intended to identify potential relationships or trends within the data that could shed light on the ecological dynamics between reef fish communities and the configuration of coral habitats.

RESULTS AND DISCUSSION

Coral cover

This study conducted an analysis of coral reef lifeforms both within and outside designated no-take zones in the Tapanuli Tengah Marine Conservation Area. The NTZs examined included MRS01, MRS02, and MRS03, while the non-protected areas comprised ST07, ST08, ST09, and ST10. The data presented in Fig. 2 reveal significant variations in coral composition between NTZs and adjacent unprotected areas, thereby substantiating the efficacy of conservation measures in preserving coral reef ecosystems (Wright, 2022). Within the NTZs, which are safeguarded from direct human disturbances such as fishing and boating, hard coral coverage is substantially higher

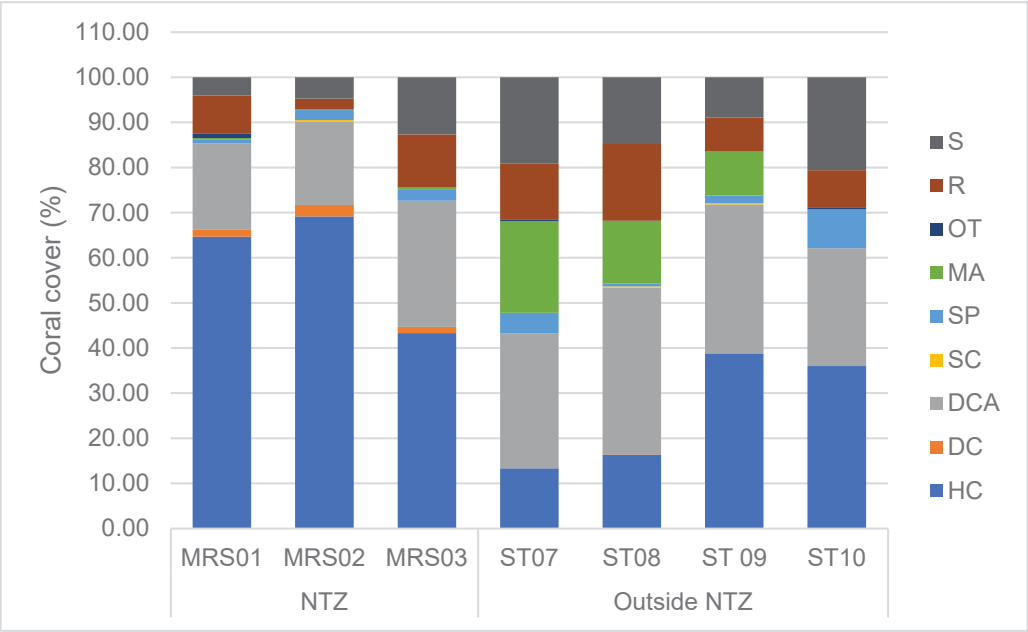

Fig. 2: Comparison of coral lifeforms in NTZ and outside NTZ

(MRS01: 64.64%, MRS02: 69.16%, MRS03: 43.30%) compared to sites outside these zones (ST07: 13.33%, ST08: 16.40%, ST09: 38.80%, ST10: 36.00%). Hard corals are fundamental to the formation of reef structures and are integral to marine biodiversity. They deliver important ecosystem services, including protection for coastlines and habitats for various fish species (Angkotasan *et al.,* 2023; Darling *et al.,* 2017). According to Edinger and Risk (2000), NTZs are categorized as having good conditions based on live coral cover, while non-protected areas are in fair condition. Live coral cover is considered a primary indicator of reef health (Gudka *et al.,* 2023). Conversely, the elevated levels of dead corals covered with algae outside the NTZs (ranging from 26.13% to 36.93%) indicate ecological degradation. When corals die and are overtaken by algae, coral reef ecosystems display symptoms of distress. This rampant algal proliferation hinders the development of new coral colonies, worsening the decline of the reef system (Shah, 2021). Algae-covered dead corals signify not only the mortality of reef-building organisms but also a shift in ecological balance, often precipitated by overfishing, which reduces herbivorous fish populations that control algal growth, and nutrient pollution from land-based sources (Zaneveld *et al.,* 2016). Such disruptions can weaken the resilience of coral reefs, increasing their susceptibility to further challenges such as climate change and ocean acidification (Stier and Osenberg, 2014). Moreover, the notable presence of macroalgae (20.33% at ST07 outside the NTZ) starkly contrasts with its minimal occurrence within protected zones (maximum 0.53%). The growth of macroalgae often occurs as a result of nutrient enrichment, which can impede coral health by blocking sunlight and suffocating young coral recruits, ultimately leading to a destabilization of the reef structure (D'Angelo and Wiedenmann, 2014). This study underscores the necessity for expanded and strictly enforced NTZs as a critical measure in maintaining coral health, which is vital for environmental conservation and the socio-economic stability of communities that rely on these ecosystems. Serving as rich biological resources, coral reefs play a critical role in providing essential services like food security, tourism prospects, and natural coastal protection. Therefore, maintaining their health is a key concern that impacts both ecological balance and human welfare, as well as economic resilience (Cinner *et al.,* 2016; Hughes *et al.,* 2017; Moberg and Folke, 1999). Additionally, integrating these protective zones with comprehensive strategies aimed at

mitigating anthropogenic impacts like nutrient runoff and overfishing in adjacent areas is crucial. A holistic approach to marine conservation can help preserve these vital ecosystems for future generations, while promoting sustainable economic practices that rely on healthy reefs (Halpern *et al.,* 2013; Kusumawati and Huang, 2015). The data highlights that while NTZs maintain healthier coral populations and lower incidences of environmental stress indicators like macroalgae and sedimentation, challenges such as coral mortality and algal overgrowth broadly affect coral reefs. This emphasizes the critical need for holistic environmental management approaches that go beyond NTZ limits to address the pervasive environmental stressors impacting coral reefs. Statistical analysis of 95% confidence intervals was employed as an indicator to estimate the range within which the population parameters are likely to fall. The live coral cover (hard coral) in NTZs was statistically greater than that in areas outside NTZs. The confidence interval values for the NTZ indicated that coral cover varied from (59.03±15.63%), whereas outside NTZs, it ranged from (26.13±12.85%). This evidence points to the conclusion that NTZs are superior in safeguarding or encouraging coral growth. The overlap in ranges implies that, although NTZs generally exhibit better coral cover, variability may still exist both within and outside NTZ areas.

Reef fish communities

The analysis of marine reserve sites within and adjacent to NTZs demonstrates significant differences in ecological metrics, as shown in the presented data (Fig. 3). In Fig. 3a, a thorough analysis of the fish families identified at various marine sites is illustrated, with a clear distinction made between those located inside and outside NTZs. The sites within the NTZs—MRS01, MRS02, and MRS03—exhibit a greater diversity of fish families, with counts ranging from 6 to 9. Conversely, at sites beyond the NTZs—namely ST07 to ST10—the number of fish families consistently falls between 6 and 7, which is notably lower. This observation suggests that NTZs play a significant role in enhancing or at least sustaining marine biodiversity. Fig. 3b explores the total species count per site, further supporting the positive impact of NTZs on marine life diversity. Notably, species richness within NTZs, particularly at sites MRS02 and MRS03, significantly exceeds that observed in areas outside the NTZs, with counts as high as 29 species compared to a maximum of 22 species outside the NTZs. Furthermore, the disparity in species richness emphasizes the ability of NTZs to function as biodiversity hotspots, which play a crucial role in boosting the productivity and ecological equilibrium of marine habitats. Studies have shown that areas with higher biodiversity often exhibit greater stability and productivity, as diverse species interactions can enhance resource utilization and energy transfer efficiency within the ecosystem (Erm *et al.,* 2024; Russ and Alcala, 2011). Additionally, other opinions have been expressed by (Stuart-Smith *et al.,* 2013) that higher species abundance and functional traits offer a clearer understanding of biodiversity and its role in ecosystem functions. In temperate climates, the even distribution of species allows each one to contribute significantly to ecological functions, resulting in increased stability and productivity. In contrast, tropical regions have higher species richness, but individual species contribute less to the overall ecosystem functions. Thus, functional diversity and evenness in species abundance provide better ecosystem stability and efficiency indicators. Finally, Fig. 3c quantifies the reef fish abundance in individuals per hectare, highlighting a stark contrast in population density. Sites within NTZs, especially MRS02, show a remarkably high abundance of 19,440 individuals per hectare, whereas the highest abundance outside the NTZs is considerably lower at 4,600 individuals at ST09. The data presented in Fig. 3 strongly supports the notion that no-take zones are effective in boosting both biodiversity and the numbers of reef fish. The observed patterns align with established ecological theories that protected areas, by restricting extractive activities like fishing, create refuges for marine life, thereby allowing for greater biodiversity and biomass accumulation (Hollitzer *et al.,* 2023). The considerable disparity in fish family diversity and species richness observed between NTZs and non-NTZ regions can be explained by the decrease in fishing pressure. This pressure typically removes certain key species, thereby modifying the natural composition of the community (Salema *et al.,* 2022). Moreover, the increased abundance of individuals within NTZs, as shown in Fig. 3c, may be indicative of successful reproductive and recruitment processes, suggesting that NTZs provide not only refuge but also suitable conditions for the growth

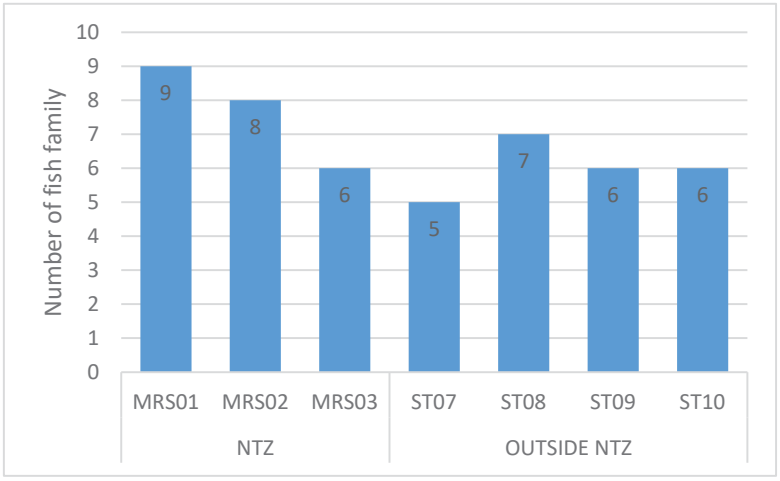

(a

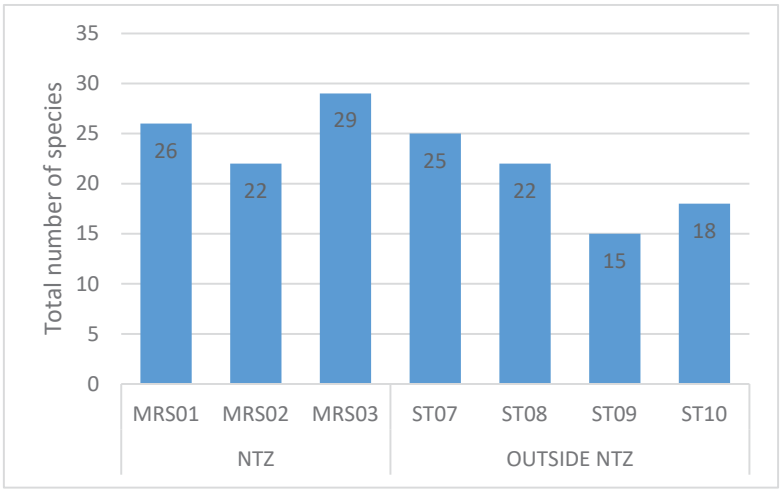

(b

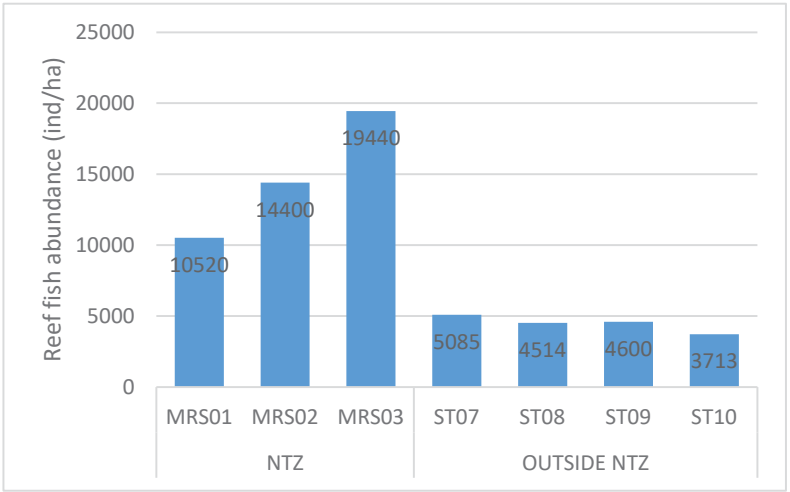

(c

Fig. 3: Comparative number of coral reef fish in NTZs and outside NTZs (a) family (b) Total number of species (c) fish abundance (individuals/ha)

and reproduction of various fish species (Bostedt *et al.,* 2020). Maintaining sustainable fish populations is particularly essential, as they significantly bolster the resilience of coral reef ecosystems against environmental shifts and disturbances. Additionally, the data underscores the need for continued support and potentially expanding NTZs as a conservation strategy. While NTZs are effective, the variability in results across differences in abundance at various sites implies that site-specific factors also play a crucial role in determining the success of these zones. The effectiveness of these protected areas may be influenced by various factors, including the quality of the habitat, closeness to pollution sources, and the enforcement of NTZ regulations (Ferreira *et al.,* 2022; Rodríguez-Rodríguez and Martínez-Vega, 2022). This study demonstrates that NTZs significantly enhance biodiversity and fish populations on coral reefs. The quantitative evidence supports expanding NTZs as an effective marine conservation strategy. The study underscores the necessity of implementing no-take zones in at-risk marine environments to facilitate the conservation and recovery of global biodiversity. Furthermore, confidence intervals serve to evaluate the reliability and validity of sample data employed in making estimates, clearly indicating that NTZs support significantly higher fish abundance and species richness compared to areas outside NTZs. Within NTZs, fish abundance is observed to range from 14,800 ± 5,059.19 ind/ha, with 95% confidence intervals offering a reliable estimate of the fish population within this range. In NTZs, the range of species richness is 25.67 ± 3.97 species, with confidence intervals supporting the precision of the diversity measurementsConversely, outside NTZs, fish abundance ranges from 4,478 ± 557.20 ind/ha, and species richness varies between 20 ± 4.31 species, with wider confidence intervals indicating greater variability (Fig. 3).

Reef fish diversity across marine reserves and surrounding areas

The entire dataset is presented in Fig. 4, which offers a comprehensive comparison of reef fish diversity and functional group abundance across both NTZs (MRS01, MRS02, MRS03) and areas outside these protected zones (ST07, ST08, ST09, ST10). This illustration distinctly highlights the significant variations in species richness, population densities, and the distribution of important fish families, offering essential insights into the ecological impacts of NTZs on marine biodiversity and the interactions within functional groups. Within NTZs, MRS03 exhibits the highest species richness with 29 species and the highest individual density at 19,440 individuals per hectare. These metrics contrast markedly with the sites outside NTZs, where species richness and individual density are significantly lower; for example, ST09 supports only 15 species and 4,600 individuals per hectare. Further investigation demonstrates that the improved biodiversity in NTZs can be largely credited to the existence and abundance of vital functional groups, particularly those consisting of herbivorous and coralivorous species. The Pomacentridae family, which includes many coralivorous species, is notably abundant in NTZs, with counts of 169, 261, and 410 individuals at MRS01, MRS02, and MRS03, respectively. In contrast, this family is entirely absent from unprotected sites. The absence of Pomacentridae outside NTZs highlights the susceptibility of coralivorous species to fishing pressures, which may significantly disrupt coral-algal dynamics and, by extension, the health of the coral reef itself. The role of coralivorous fish is vital in sustaining the balance within coral-dominated ecosystems. By selectively grazing on both coral and algae, they help avert algal overgrowth that could potentially overwhelm and damage coral structures (Knoester *et al.,* 2023). Herbivorous reef fish are the primary grazers of macroalgae on coral reefs (Cheal *et al.,* 2010; Cook *et al.,* 2025), such as those in the Scaridae family (e.g., parrotfish), are also significantly more abundant in NTZs. These species are essential for managing algal populations, preventing them from overtaking coral reefs. The distribution of Scaridae, however, shows variability between sites. For instance, while sites within NTZs exhibit higher numbers, the non-NTZ site ST07 supports a notable 99 individuals. This variation implies that specific environmental conditions, such as the accessibility of algal resources or targeted fishing activities, might play a role in determining the density of herbivorous species in unprotected areas (Altman-Kurosaki *et al.,* 2021). Carnivorous species, particularly those in the Serranidae family (e.g., groupers and basses), are also more abundant within NTZs. By regulating the numbers of smaller fish and invertebrates, these predators play a crucial role in maintaining the

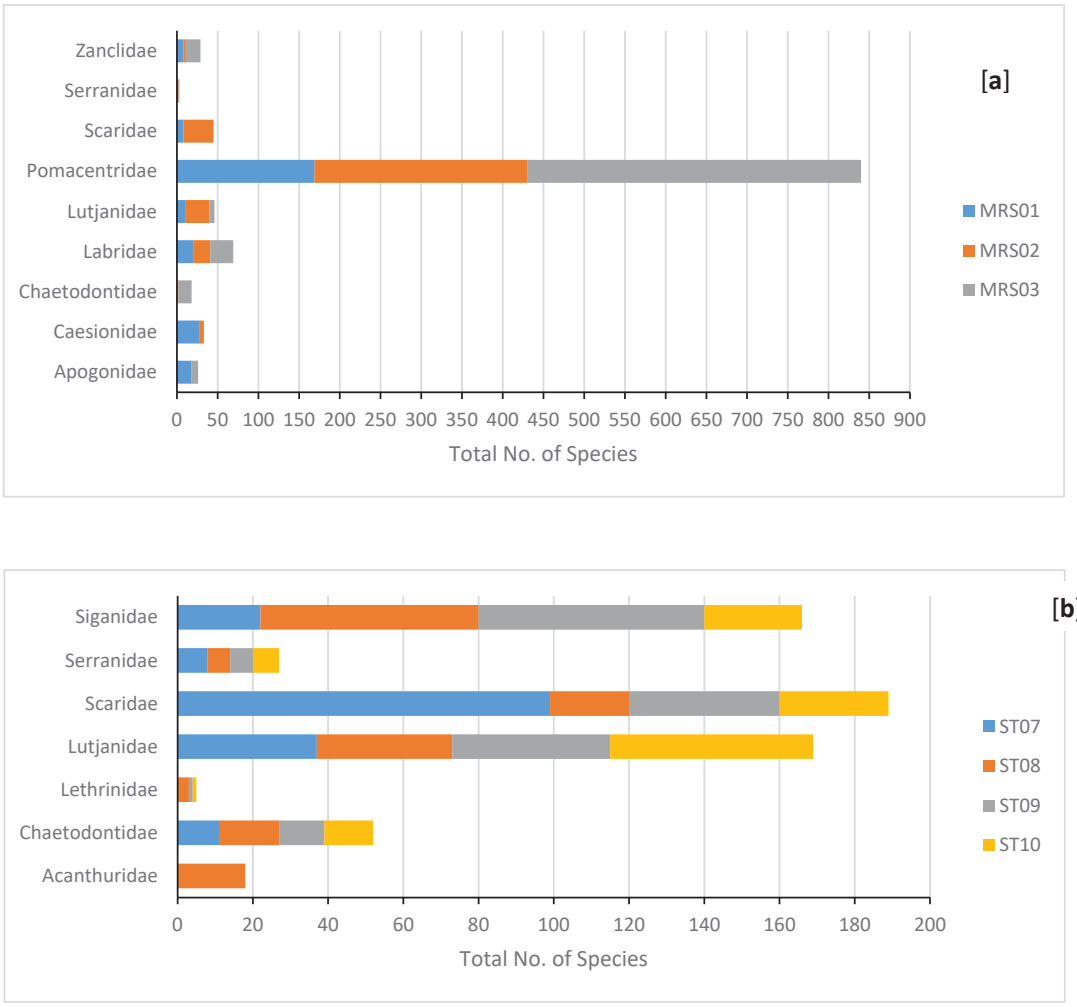

Fig. 4: Comparative abundance of fish families [a] no-take zone and [b] outside no-take zone

balance of the food web and fostering ecosystem stability (Boaden and Kingsford, 2015). In NTZs, the absence of fishing pressure allows these apex predators to thrive, which, in turn, helps control the abundance of herbivorous and coralivorous species and mitigates overgrazing and overgrazing-induced coral degradation. Apex predators play a vital role in preserving the structure and dynamics of marine ecosystems by ensuring the continuity of trophic cascades (Estes *et al.,* 2011). In contrast, the scarcity of both herbivorous and coralivorous fish in non-NTZ areas, alongside lower densities of carnivores, suggests that fishing pressures and habitat degradation may disrupt trophic interactions and reduce the ecological resilience of coral reef ecosystems. In the absence of adequate herbivorous and coral-eating species to manage algal proliferation and safeguard coral populations, these ecosystems could be at a higher risk of transitioning to algal-dominated conditions, which tend to be less diverse and more vulnerable to environmental fluctuations (Cook *et al.,* 2024). These findings underscore the crucial role of NTZs in sustaining marine biodiversity and maintaining the ecological functionality of coral reef ecosystems. The significantly higher abundance of herbivores, carnivores, and coralivores within NTZs highlights the protective benefits these areas provide in terms of maintaining healthy fish populations that fulfill essential ecological roles. Thus, the expansion and strict enforcement of NTZs ought to be seen as a

Table 1: Ecological diversity indices for reef fish in NTZs and outside NTZs of marine protected area

Indices	MRS01	MRS02	MRS03	ST07	ST08	ST09	ST10	P-value
Species Richness	26	29	22	25	22	15	18	0.13
Shannon-wiener (H')	2.61	1.89	1.85	1.37	1.80	1.49	1.55	0.06
Evenness (E)	0.80	0.56	0.60	0.43	0.58	0.55	0.54	0.14
Dominance (C)	0.11	0.25	0.26	0.37	0.22	0.27	0.27	0.23

crucial strategy for advancing biodiversity, improving the resilience of coral reefs to climate change, and fostering sustainable marine ecosystems that support both ecological integrity and the livelihoods of coastal populations.

Ecology indices

The ecological diversity indices for reef fish communities in NTZs (MRS01-MRS03) and areas outside NTZs (ST07-ST10) within the marine protected areas exhibit notable variations in species richness, diversity, evenness, and dominance. The total number of species, known as species richness, was typically greater in the NTZ, with MRS02 documenting the highest count at 29 species. In contrast, ST09 showed the lowest species richness, with only 15 species identified among the sites surveyed outside the protected area. These findings are consistent with earlier studies conducted by Kelaher (2014) who found that NTZs support higher species richness due to reduced fishing pressure and habitat protection. Although NTZs demonstrated slightly higher species richness, statistical analysis ($p = 0.127$) indicated that this difference was not statistically significant, suggesting that additional factors such as habitat complexity, recruitment dynamics (Moustaka *et al.,* 2024) and regional oceanographic conditions (Ceccarelli *et al.,* 2023) may also influence species composition. The Shannon-Wiener Diversity Index (H'), which measures species variety and abundance, was also higher inside NTZs, with MRS01 ($H' = 2.61$) recording the highest value, while ST07 had the lowest ($H' = 1.37$). This pattern indicates that NTZs have the potential to promote more resilient and diverse fish communities (Kembrey *et al.,* 2024). The difference was close to significance ($p = 0.0598$), indicating that marine protection plays a role in diversity but may not be the only factor (Sanchez *et al.,* 2024). Evenness (E), which shows how evenly species are distributed, was highest in MRS01 (0.80) and lowest in ST07 (0.43). When evenness is high, nearing a value of 1, it signifies that no particular species is overly dominant and that there is a more balanced distribution of species in NTZs. This condition typically reflects a more resilient ecosystem that can better withstand changes. Conversely, lower evenness in areas outside NTZs may point to an ecosystem that is more fragile, making it more prone to disturbances and slower in its recovery process. However, the difference was not statistically significant ($p = 0.140$), suggesting that competition and habitat differences influence evenness (Pereira *et al.,* 2024). Similarly, the Dominance Index (C), which measures whether a few species dominate, was lowest in MRS01 (0.11), indicating a balanced ecosystem, and highest in ST07 (0.37), showing dominance by a few species. This trend matches findings that overfishing in unprotected areas often leads to a few species dominating (Martin *et al.,* 2023). However, statistical tests ($p = 0.226$) did not confirm a significant difference between NTZs and outside NTZs. The lack of statistically significant differences in NTZs, as measured by diversity indices (species richness, H, E, and C) can be attributed to a combination of methodological limitations, NTZ characteristics, taxonomic variability, and broader environmental influences. To accurately evaluate the effectiveness of NTZs, it is crucial to adopt a multi-faceted strategy that integrates additional metrics, including phylogenetic and functional diversity (Matten *et al*., 2023), and takes into account external factors such as climate change and changes in land use (Häkkilä *et al.,* 2017). This comprehensive strategy will provide a more accurate understanding of the role of NTZs in biodiversity conservation.

The findings indicate that NTZs help maintain biodiversity by supporting more species, higher diversity, and a balanced ecosystem, but the differences observed were not consistently statistically significant. Moreovere, a range of factors like the structure of habitats, levels of fishing

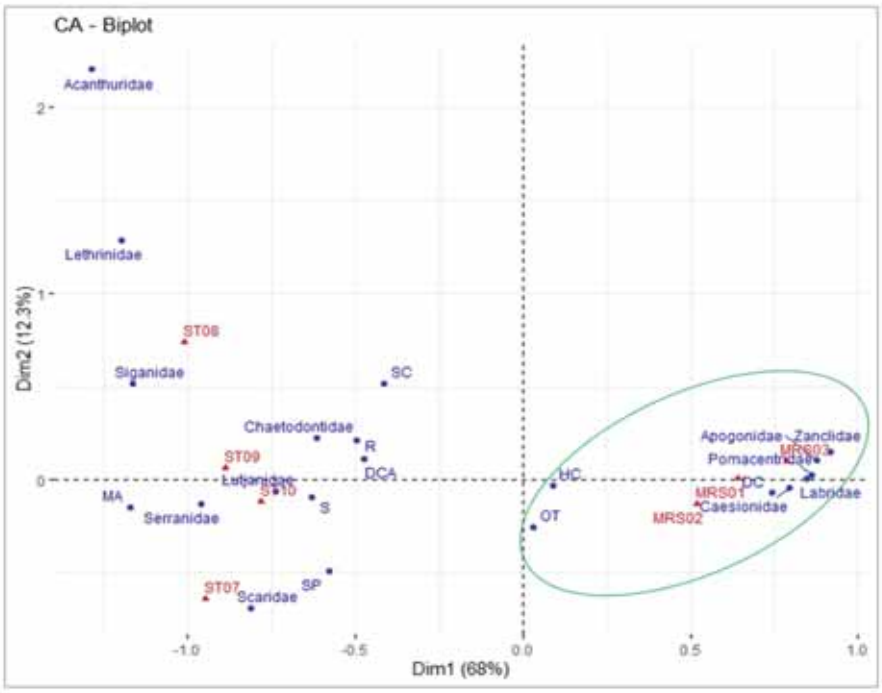

Fig. 5: Biplot graph of correspondence analysis across all sites with reef fish families and coral life forms

pressure, and changes in the environment may affect fish populations (Hernández-Andreu *et al.,* 2024; Hopf *et al.,* 2024; Varnes and Olsen, 2023). Future research should include long-term monitoring and habitat analysis to fully understand the benefits of no-take zones.

Relationship between coral cover and coral reef fish

The correspondence biplot visualizes the relationship between the abundance of reef fish families and coral lifeforms at NTZs and sites outside the NTZs (Fig. 5). Two principal dimensions are utilized in the biplot to represent the variability within the data: Dim1 (68%), which accounts for the greatest proportion of variation, and Dim2 (12.3%), capturing secondary gradients of association.

Fig. 5 demonstrates a clear distinction between the ecological conditions of NTZs and outside NTZs, highlighting how these areas differ in both fish family composition and the types of coral life forms present. The presence of fish families like Acanthuridae, Lethrinidae, and Sigannidae on the negative side of Dim1 indicates that they are more closely linked to degraded coral habitats located beyond the NTZs (ST07, ST08, ST09, ST10). These sites are dominated by dead coral (DC), dead coral with algae (DCA), and rubble (R). Acanthuridae feed on detritus and algae, which are abundant in degraded environments, as they are detritivorous (Russ *et al.,* 2018). Their abundance in such areas is strongly linked to the availability of dead substrate, which provides both food and shelter. Similarly, Lethrinidae and Sigannidae are known to exploit algae and detritus, making them well-suited to degraded coral environments (McCormick *et al.,* 2017). The fish families found here, such as Chaetodontidae and Scaridae, are often associated with more disturbed ecosystems where they may rely on macroalgae and detritus, their ability to adapt to disturbed ecosystems by altering their diet suggests a potential resilience to environmental changes (Russ and Leahy, 2017). These results support the concept that fish communities in impaired habitats tend to be less diverse and increasingly dependent on opportunistic resources (Rogers *et al.,* 2017). In contrast, Pomacentridae, Apogonidae, Zanclidae, and Caesionidae, found on the positive side of Dim1, are strongly associated with sites in the NTZs (MRS01, MRS02, MRS03), where hard coral (HC) is



Fig. 6: Analysis of the correlation between fish family abundance and hard coral cover in NTZs

more abundant. The proximity of these fish families to hard coral indicates their reliance on complex reef habitats for shelter, food, and breeding sites (Coker *et al.,* 2014; Hall and Kingsford, 2021). NTZs, through the prohibition of fishing, create healthier and more diverse coral environments, thereby supporting a larger array of fish species, especially those that are reliant on live coral (Kembrey *et al.,* 2024). The dominance of hard coral in NTZs further enhances the habitat's ability to support high biodiversity, as healthy reefs are essential for maintaining ecosystem function and structure (Harvey *et al.,* 2018). Additionally, sand (S) and sponge (SP) life forms are located closer to the fish families found outside the NTZs, further highlighting the degraded conditions of these sites. Outside of NTZs, macroalgae (MA) is more commonly found, often flourishing due to less competition from coral. This phenomenon is intensified by factors such as overfishing and habitat degradation (Seemann *et al.,* 2018). Fish families associated with macroalgae, such as Scaridae, may dominate in these disturbed areas, as they can graze on algae that thrive in coral-depleted environments (Wilson *et al.,* 2022). Overall, this correspondence analysis underscores the importance of NTZs in preserving reef biodiversity, where healthier, coral-dominated ecosystems support a more diverse range of fish families. The graph visually reinforces the concept that NTZs play a critical role in maintaining biodiversity by offering refuges for coral and associated fish species threatened by anthropogenic disturbances outside these protected areas. However, the efficacy of NTZs is often influenced by effective enforcement and community engagement, which are essential for optimizing conservation outcomes (Espinosa-Andrade *et al.,* 2020). Furthermore, long-term monitoring is vital for assessing coral reef ecosystems' ecological condition, evaluating conservation efforts' success, and adapting management strategies. Monitoring provides essential data on the health and trends of coral reefs, which are under significant pressure from both anthropogenic and natural factors (Obura *et al.,* 2019). By integrating these elements, NTZs can function as a potent mechanism for the preservation of coral reef ecosystems.

This correspondence analysis offers a visual tool to assess variations in fish family composition between protected and non-protected areas, highlighting the role of NTZs in supporting biodiversity and ecosystem health. In Fig. 6, the method is shown to analyze the habitat preferences of reef fish in relation to different hard coral species. Fish families such as Serranidae, Caesionidae, and Apogonidae exhibit a strong spatial association with coral species like Acropora Tabulate (ACT) and Coral Millepora (CME), as evidenced by their close proximity on the correspondence analysis biplot. The connections between coral structures and reef fish are not limited to basic habitat use; they include sophisticated functional relationships that are mutually beneficial. Corals provide critical

shelter from predation pressure for fish families, particularly for juvenile individuals. Research has documented by Leal *et al.* (2013) that juvenile fish comprise approximately 65% of individuals observed in association with Millepora coral colonies. The ecological interactions between reef fish families such as Serranidae, Caesionidae, and Apogonidae and coral species like Acropora Tabulate and Millepora represent intricate relationships crucial for coral reef ecosystems' biodiversity and ecological processes. These relationships include overall association trends and targeted habitat preferences, demonstrating the adaptations of fish species to the unique structural attributes of different coral varieties. The complex architecture of the Acropora Tabulate and Millepora colonies creates a variety of microhabitats that upport different life stages and ecological functions of the associated fish species. On the other hand, fish species like Lutjanidae, Pomacentridae, and Chaetodontidae appear further apart from certain coral types such as Coral Submassive (CS) and Coral Heliopora (CHL), possibly indicating that these fish families are associated with different coral structures, either for feeding or sheltering purposes (González-Rivero *et al.,* 2017; Harsindhi *et al.,* 2020). According to Hernández *et al*. (2023), various fish families display specific preferences for certain coral types; however, these preferences are not exclusively determined by the availability of coral. Instead, factors such as predator avoidance, metabolic changes, and ontogenetic vertical migration play significant roles in shaping the distribution patterns of these species. These behavioral elements can impact larval dispersal and connectivity, highlighting a sophisticated interaction between preferences for different coral types and the larger ecological framework. The biplot reveals some notable trends in how coral species and fish families are distributed across the plot. For instance, the Acropora Branching (ACB) coral species is located near fish families such as Labriidae, which may suggest a functional relationship between these coral structures and the fish's feeding or shelter needs (Floros and Schleyer, 2017). Likewise, the Coral Foliose (CF) and Coral Encrusting (CE) types show a closer relationship to species like Zanclidae and Scaridae, indicating potential ecological interactions. According to the biplot analysis, the no-take zone supports specific ecological connections between particular fish families and hard coral species. Some fish species appear to preferentially associate with particular coral structures, which likely offer critical resources such as feeding, spawning, and nursery grounds (Bonaldo *et al.,* 2017; Kembrey *et al.,* 2024). The insights gained from this research are vital for shaping future conservation strategies that aim to protect the critical interactions between coral and fish in designated conservation zones.

CONCLUSION

This study underscores the critical role of MPAs, particularly NTZs, in conserving and enhancing coral reef ecosystems. The results from the Tapanuli Tengah Marine Conservation Area provide robust evidence that well-enforced NTZs can significantly improve coral cover and biodiversity, particularly by increasing the abundance and diversity of reef fish communities. Sites within NTZs exhibited significantly higher hard coral coverage, lower incidence of macroalgal overgrowth, and greater fish abundance compared to adjacent non-protected areas, demonstrating the efficacy of these protected areas in fostering ecological resilience. Moreover, the results of the correspondence analysis indicated a specific relationship between the abundance of different fish families and coral lifeforms, underscoring the structural dependencies of reef fish on coral ecosystems. Fish families such as Pomacentridae, Apogonidae, and Caesionidae, which are closely associated with healthy coral environments, were more abundant in NTZs, where hard corals were prevalent. Conversely, non-protected regions, characterized by dead coral and macroalgae, exhibited a greater presence of fish families like Acanthuridae, Lethrinidae, and Sigannidae, which are generally linked to deteriorated coral environments. These findings substantiate the hypothesis that MPAs, and specifically NTZs, play a pivotal role in maintaining habitat quality and enhancing biodiversity by providing refuges for species reliant on live coral structures. The positive relationship observed between coral cover and reef fish populations underscores the essential connection between the vitality of coral reefs and the structure of the fish communities that rely on them. These results align with extensive global research indicating that NTZs provide effective refuges for marine species, contributing to the recovery and maintenance of ecosystem services such as biodiversity preservation, habitat provisioning,

and trophic stability. These findings emphasize the critical need to enhance and rigorously enforce NTZs in the study region and globally, serving as an essential strategy to combat the detrimental effects of overfishing, habitat destruction, and climate change on marine environments. Although this study offers significant insights into the ecological benefits of NTZs, further research is required to assess the influence of additional site-specific factors such as habitat complexity, local enforcement strength, and anthropogenic pressures on the success of these conservation areas. Furthermore, continuous monitoring programs play a key role in determining the resilience and adaptability of these ecosystems over time. It is essential to integrate multi-scale monitoring and management approaches to guarantee the lasting ecological benefits provided by NTZs. As the world faces escalating environmental challenges, the growth and proper management of MPAs, particularly (NTZs, are vital for the conservation of coral reefs and the protection of marine biodiversity. This approach has profound implications for ecosystem-based management and the resilience of coastal areas.

AUTHOR CONTRIBUTIONS

Z.A. Harahap contributed to crafting the research proposal, executing field sampling, performing data analysis and interpretation, and drafting the manuscript. D.G. Bengen performed the conception and design, critical revision of the manuscript, and supervision. I.W. Nurjaya performed a critical revision of the manuscript and supervision. S.A. Bahri performed the conception and design, critical revision of the manuscript, and supervision. Y. Naulita performed the conception and design, critical revision of the manuscript, and supervision. R.M. Siringoringo performed data collection and tabulation.

ACKNOWLEDGEMENT

Authors would like to sincerely thank The Indonesian Education Scholarship (BPI), The Center for Higher Education Funding Assessment, and the Ministry of Higher Education, Service, and Technology Indonesia [PUSLAPDIK-KEMDIKTISAINTEK] for their support in funding academic endeavors and enabling us to conduct this research. Authors are also deeply grateful to the Endowment Funds for Education Agency and the Ministry of Finance of the Republic of Indonesia for their support through a scholarship that enabled the completion of this research. Lastly, the group of authors appreciate all contributions from individuals and institutions that helped make this work possible.

CONFLICT OF INTEREST

The authors declare that there is no conflict of interest regarding the publication of this manuscript. In addition, the authors have completely observed the ethical issues, including plagiarism, informed consent, misconduct, data fabrication and/or falsification, double publication and/or submission, and redundancy.

OPEN ACCESS

©2025 The author(s). This article is licensed under a Creative Commons Attribution 4.0 International License, which permits use, sharing, adaptation, distribution and reproduction in any medium or format, as long as you give appropriate credit to the original author(s) and the source, provide a link to the Creative Commons license, and indicate if changes were made. The images or other third-party material in this article are included in the article's Creative Commons license, unless indicated otherwise in a credit line to the material. If material is not included in the article's Creative Commons license and your intended use is not permitted by statutory regulation or exceeds the permitted use, you will need to obtain permission directly from the copyright holder. To view a copy of this license, visit: http://creativecommons.org/licenses/by/4.0/

PUBLISHER'S NOTE

GJESM Publisher remains neutral with regard to jurisdictional claims in published maps and institutional afflictions.

Positive AI Statement

During the preparation of this work the author(s) have used [ChatGPT] in order to [assist with drafting and generating ideas for the manuscript]. After using this tool/service, the authors reviewed and edited the content as needed and took full responsibility for the content of the publication. Furthermore, the GPTZero detector will evaluate the manuscript utilizing Generative AI, ensuring a high detection rate.

If the manuscript relies heavily on Generative AI and AI-assisted technologies, it will be archived without further options for appeal.

Negative AI Statement

The author(s) declare that no AI tools or services were not used or not highly applied during the preparation of this work.

ABBREVIATIONS

%	Percent
ACB	Acropora branching
ACT	Acropora tabulate
C	Dominance species index
CB	Coral branching
CE	Coral encrusting
CF	Coral foliose
CHL	Coral heliopore
cm	Centimeter
CM	Coral massive
CME	Coral millepora
CMR	Coral mushroom
CS	Coral submassive
CPCe	Coral point count with excel extension
D	Richness index
DC	Dead coral
DCA	Dead coral with algae
E	Evennes index
H	Diversity index
HC	Hard coral
ind/ha	Individual per hectare
MA	Macroalgae
MPA	Marine protected area
NTZ	No-take zone
OT	Others
R	Rubble
R^2	Determinant
r	Correlation
S	Sand
SCUBA	Self-contained underwater breathing apparatus
SP	Sponge
UPT	Underwater photo transect
UVC	Underwater visual census

REFERENCES

Abrar, M.; Bengen, D.G.; Zamani, N.P.; Suharsono; Giyanto; Putra, R.D.; Ni, N.W.; Siringoringo, R.M.; Hadi, T.A.; Utama, R.S.; Hermanto, B.; Arbi, U.Y.; Hukom, F.D.; Alifatri, L.O.; Wouthuyzen, S.; Harrison, P., (2024). Spatial distribution of juvenile corals (Scleractinia) in the coastal and small islands of Sumatra, Indonesia. Reg. Stud. Mar. Sci., 80: 1-11 **(10 pages)**.

Allen, G.R., (2003). Reef Fish Identification: Tropical Pacific. New World Publications. **(457 pages).**

Allen, G.R.; Erdmann, M.V., (2012). Reef fishes of the East Indies. Vols. I–III. Tropical Reef Research, Perth, Australia. **(1292 pages).**

Altman-Kurosaki, N.T.; Smith, C.M.; Franklin, E.C., (2021). O'ahu's marine protected areas have limited success in protecting coral reef herbivores. Coral Reefs. 40(2): 305–322 **(17 pages).**

Awak, D.S.H.L.M.K.; Gaol, J.L.; Subhan, B.; Madduppa, H.H.; Arafat, D., (2016). Coral reef ecosystem monitoring using remote sensing data: case study in Owi Island, Biak, Papua. Procedia Environ. Sci., 33: 600–606 **(7 pages).**

Azra, M.N.; Aouissi, H.A.; Hamma, W.; Guerzou, M.; Noor, M.I.M.; Petrişor, A.I., (2023). A scientometric macroanalysis of coral reef research in the world. Ecosyst. Evol., 42(2): 108–116 **(9 pages).**

Bachtiar, I.; Suharsono, Damar, A.; Zamani, N.P., (2019). Practical resilience index for coral reef assessment. Ecosyst. Serv., 54(1): 117–127 **(11 pages).**

Bellwood, D.R.; Tebbett, S.B., (2024). Habitat trumps biogeography in structuring coral reef fishes. Coral Reefs, 43(6): 1599–1609 **(11 pages).**

Benedetti-Cecchi, L.; Bates, A.E.; Strona, G.; Bulleri, F.; Horta e Costa, B.; Edgar, G.J.; Hereu, B.; Reed, D.C.; Stuart-Smith, R.D.; Barrett, N.S.; Kushner, D.J.; Emslie, M.J.; García-Charton, J.A.; Gonçalves, E.J.; Aspillaga, E., (2024). Marine protected areas promote stability of reef fish communities under climate warming. Nat. Commun., 15(1): 1–14 **(14 pages)**.

Boaden, A.E.; Kingsford, M.J., (2015). Predators drive community structure in coral reef fish assemblages. Ecol. Soc. Am., 6(4): 1–33 **(33 pages)**.

Bonaldo, R.M.; Pires, M.M.; Guimarães Junior, P.R.; Hoey, A.S.; Hay, M.E., (2017). Small marine protected areas in Fiji provide refuge for reef fish assemblages, feeding groups, and corals. PLoS One. 12(1): 1-26 **(26 pages)**.

Bostedt, G.; Berkström, C.; Brännlund, R.; Carlén, O.; Florin, A.B.; Persson, L.; Bergström, U., (2020). Benefits and costs of two temporary no-take zones. Mar. Policy, 117(2020): 1-13 **(13 pages)**.

Burdett, H.L.; Albright, R.; Foster, G.L.; Mass, T.; Page, T.M.; Rinkevich, B.; Schoepf, V.; Silverman, J.; Kamenos, N.A., (2024). Including environmental and climatic considerations for sustainable coral reef restoration. PLoS Biol., 22(3): 1–17 **(17 pages)**.

Camp, E.F.; Braverman, I.; Wilkinson, G.; Voolstra, C.R., (2024). Coral reef protection is fundamental to human rights. Global

Change Biol., 30(9): 1–4 **(4 pages)**.
Caughman, A.M.; Gaines, S.D.; Bradley, D., (2024). Climate change reduces long-term population benefits from no-take marine protected areas through selective pressures on species movement. Glob. Chang. Biol., 30(3): 1–15 **(15 pages)**.
Ceccarelli, D.M.; Evans, R.D.; Logan, M.; Jones, G.P.; Puotinen, M.; Petus, C.; Russ, G.R.; Srinivasan, M.; Williamson, D.H., (2023). Physical, biological and anthropogenic drivers of spatial patterns of coral reef fish assemblages at regional and local scales. Sci. Total Environ., 904(2023): 2–23 **(24 pages)**.
Chabanet, P.; Ralambondrainy, H.; Amanieu, M.; Faure, G.; Galzin, R., (1997). Relationships between coral reef substrata and fish. Mar. Ecol. Prog. Ser., 16(2): 93–102 **(9 pages)**.
Cheal, A.J.; MacNeil, M.A.; Cripps, E.; Emslie, M.J.; Jonker, M.; Schaffelke, B.; Sweatman, H., (2010). Coral-macroalgal phase shifts or reef resilience: Links with diversity and functional roles of herbivorous fishes on the Great Barrier Reef. Coral Reefs, 29(4): 1005–1015 **(11 pages)**.
Cinner, J.E.; Pratchett, M.S.; Graham, N.A.J.; Messmer, V.; Fuentes, M.M.P.B.; Ainsworth, T.; Ban, N.; Bay, L.K.; Blythe, J.; Dissard, D.; Dunn, S.; Evans, L.; Fabinyi, M.; Fidelman, P.; Figueiredo, J.; Frisch, A.J.; Fulton, C.J.; Hicks, C.C.; Lukoschek, V.; Mallela, J.; Moya, A.; Penin, L.; Rummer, J.L.; Walker, S.; Williamson, D.H., (2016). A framework for understanding climate change impacts on coral reef social–ecological systems. Reg. Environ. Change, 16(4): 1133–1146 **(14 pages)**.
Coker, D.J.; Wilson, S.K.; Pratchett, M.S., (2014). Importance of live coral habitat for reef fishes. Rev. Fish Biol. Fish, 24(1): 89–126 **(37 pages)**.
Cook, D.T.; Schmitt, R.J.; Holbrook, S.J.; Moeller, H.V., (2024). Modeling the effects of selectively fishing key functional groups of herbivores on coral resilience. Ecol. Soc. Am., 15(1): 1–14 **(14 pages)**.
D'Angelo, C.; Wiedenmann, J., (2014). Impacts of nutrient enrichment on coral reefs: New perspectives and implications for coastal management and reef survival. Curr. Opin. Environ. Sustain., 7: 82–93 **(12 pages)**.
De Clippele, L.H.; Díaz, L.A.; Andradi-Brown, D.A.; Lazuardi, M.E.; Iqbal, M.; Zainudin, I.M.; Prabuning, D.; van Hooidonk, R.; Hakim, A.; Agung, F.; Dermawan, A.; Hennige, S.J., (2023). Evaluating annual severe coral bleaching risk for marine protected areas across Indonesia. Mar. Policy. 148: 1-11 **(11 Pages)**.
Dumas, P.; Bertaud, A.; Peignon, C.; Léopold, M.; Pelletier, D., (2009). A "quick and clean" photographic method for the description of coral reef habitats. J. Exp. Mar. Biol. Ecol., 368(2): 161–168 **(8 pages)**.
Edgar, G.J.; Stuart-Smith, R.D.; Heather, F.J.; Barrett, N.S.; Turak, E.; Sweatman, H.; Emslie, M.J.; Brock, D.J.; Hicks, J.; French, B.; Baker, S.C.; Howe, S.A.; Jordan, A.; Knott, N.A.; Mooney, P.; Cooper, A.T.; Oh, E.S.; Soler, G.A.; Mellin, C.; Ling, S.D.; Dunic, J.C.; Turnbull, J.W.; Day, P.B.; Larkin, M.F.; Seroussi, Y.; Stuart-Smith, J.; Clausius, E.; Davis, T.R.; Shields, J.; Shields, D.; Johnson, O.J.; Fuchs, Y.H.; Denis-Roy, L.; Jones, T.; Bates, A.E., (2023). Continent-wide declines in shallow reef life over a decade of ocean warming. Nature, 615(7954): 858–865 **(8 pages)**.
Edgar, G.J.; Stuart-Smith, R.D.; Heather, F.J.; Barrett, N.S.; Turak, E.; Sweatman, H.; Emslie, M.J.; Brock, D.J.; Hicks, J.; French, B.; Baker, S.C.; Howe, S.A.; Jordan, A.; Knott, N.A.; Mooney, P.; Cooper, A.T.; Oh, E.S.; Soler, G.A.; Mellin, C.; Ling, S.D.; Dunic, J.C.; Turnbull, J.W.; Day, P.B.; Larkin, M.F.; Seroussi, Y.; Stuart-Smith, J.; Clausius, E.; Davis, T.R.; Shields, J.; Shields, D.; Johnson, O.J.; Fuchs, Y.H.; Denis-Roy, L.; Jones, T.; Bates, A.E., (2023). Continent-wide declines in shallow reef life over a decade of ocean warming. Nature, 615(7954): 858–865 **(8 pages)**.
Edinger, E.N.; Risk, M.J., (2000). Reef classification by coral morphology predicts coral reef conservation value. Biol. Conserv., 92(1): 1-13 **(13 pages)**.
English, S.; Wilkinson, C.; Baker, V., (1997). Survey manual for tropical marine sources (2nd Edition) **(385 pages)**.
Erm, P.; Balmford, A.; Krueck, N.C.; Takashina, N.; Holden, M.H., (2024). Marine protected areas can benefit biodiversity even when bycatch species only partially overlap fisheries. J. Appl. Ecol., 61: 621–632 **(12 pages)**.
Espinosa-Andrade, N.; Suchley, A.; Reyes-Bonilla, H.; Alvarez-Filip, L., (2020).The no-take zone network of the Mexican Caribbean: assessing design and management for the protection of coral reef fish communities. Biodivers. Conserv., 29: 2069–2087 **(19 pages)**.
Estes, J. A.; Terborgh, J.; Brashares, J.S.; Power, M.E.; Berger, J.; Bond, W.J.; Carpenter, S.R.; Essington, T.E.; Holt, R.D.; Jackson, J.B.C.; Marquis, R.J.; Oksanen, L.; Oksanen, T.; Robert, T.P.; Pikitch, E.K.; Ripple, W.J.; Sandin, S.A.; Scheffer, M.; Schoner, T.W.; Shurin, J.B.; Sinclair, A.R.E.; Soulé, M.E.; Vistanen, R.; Wardle, D.A., (2011). Trophic downgrading of planet earth. Science. 333(6040): 301–307 **(7 pages)**.
Fedor, P.; Zvaríková, M., (2019). Biodiversity indices. Encyclopedia of Ecology: Volume 1-4, Second Edition 1: 337–346 **(10 pages)**.
Ferreira, H.M.; Magris, R.A.; Floeter, S.R.; Ferreira, C.E.L., (2022). Drivers of ecological effectiveness of marine protected areas: A meta-analytic approach from the Southwestern Atlantic Ocean (Brazil). J. Environ. Manage., 301: 113889 **(1 page)**.
Floros, C.; Schleyer, M.H., (2017). The functional importance of Acropora austera as nursery areas for juvenile reef fish on South African coral reefs. Coral Reefs, 36(1): 139–149 **(11 pages)**.
Froese, R.; Pauly, D. (Eds.), 2024. FishBase. World Wide Web electronic publication. www.fishbase.org., version (10/2024).
Gaertner, J.C.; Taquet, M.; Dagorn, L.; Mérigot, B.; Aumeeruddy, R.; Sancho, G.; Itano, D., (2008). Visual censuses around drifting fish aggregating devices (FADs): A new approach for assessing the diversity of fish in open-ocean waters. Mar. Ecol. Prog. Ser., 366: 175–186 **(12 pages)**.
González-Rivero, M.; Harborne, A.R.; Herrera-Reveles, A.; Bozec, Y.M.; Rogers, A.; Friedman, A.; Ganase, A.; Hoegh-Guldberg, O., (2017). Linking fishes to multiple metrics of coral reef structural complexity using three-dimensional technology. Sci. Rep., 7(1): 1-17 **(17 pages)**.
Good, A.M.; Bahr, K.D., (2021). The coral conservation crisis: Interacting local and global stressors reduce reef resiliency and create challenges for conservation solutions. SN Appl. Sci., 3(3):1-14 **(14 pages)**.
Green, A.; M.P.J., (2008). Delineating the coral triangle, its ecoregions and functional seascapes. Version 5.0. TNC coral triangle program report 1/08 **(44 pages)**.
Gudka, M.; Aboud, S.; Obura, D., (2023). Historical coral reef

benthic cover for the Western Indian Ocean (1970-2008). West. Indian Ocean J. Mar. Sci., 22(1): 103–115 **(13 pages)**.

Hadi, T.A.; Abrar, M.; Giyanto, G.; Prayudha, B.; Johan, O.; Budiyanto, A.; Dzumalek, A.R.; Alifatri, L.O.; Sulha, S.; Suharsono, S., (2020). The status of Indonesian coral reefs 2019. Research Center for Oceanography (RCO). Jakarta: 1–86 **(86 pages)**.

Häkkilä M.; Le Tortorec, E.; Brotons, L.; Rajasärkkä, A.; Tornberg, R.; Monkkonen, M., (2017) Degradation in landscape matrix has diverse impacts on diversity in protected areas. PLOS ONE. 12(9): 1–17 **(17 pages)**.

Hall, A.E.; Kingsford, M.J., (2021). Habitat type and complexity drive fish assemblages in a tropical seascape. J. Fish Biol., 99(4): 1364–1379 **(16 pages)**.

Halpern, B.S.; Klein, C.J.; Brown, C.J.; Beger, M.; Grantham, H.S.; Mangubhai, S.; Ruckelshaus, M.; Tulloch, V.J.; Watts, M.; White, C.; Possingham, H.P., (2013). Achieving the triple bottom line in the face of inherent trade-offs among social equity, economic return, and conservation. Proc. Natl. Acad. Sci. U.S.A., 110(15): 6229–6234 **(6 pages)**.

Harsindhi, C.J.; Bengen, D.G.; Zamani, N.P.; Kurniawan, F., (2020). Abundance and spatial distribution of reef fish based on coral lifeforms at Tidung Island, Seribu Islands, Jakarta Bay. AACL Bioflux, 13(2): 736–745 **(10 pages)**.

Harvey, B.J.; Nash, K.L.; Blanchard, J.L.; Edwards, D.P., (2018). Ecosystem-based management of coral reefs under climate change. Ecol. Evol., 8(12): 6354–6368 **(15 pages)**.

Helder, N.K.; Burns, J.H.R.; Green, S.J., (2022). Intra-habitat structural complexity drives the distribution of fish trait groups on coral reefs. Ecol. Indic., 142(2022): 1-11 **(11 pages)**.

Hernández, C.M.; Paris, C.B.; Vaz, A.C.; Jones, B.T.; Kellner, J.B.; Richardson, D.E.; Sponaugle, S.; Cowen, R.K.; Llopiz, J.K., (2023). Diverse patterns of larval coral reef fish vertical distribution and consequences for dispersal and connectivity. Coral Reefs, 42(2): 453–465 **(13 pages)**.

Hernández-Andreu, R.; Félix-Hackradt, F.C.; Schiavetti, A.; Jessyca, J.L.; Hackradt, C.W., (2024). Marine protected areas are a useful tool to protect coral reef fishes but not representative to conserve their functional role. J. Environ. Manage., 351(2024): 1-13 **(13 pages)**.

Hill, J.; Wilkinson, C.R., (2004). Methods for ecological monitoring of coral reefs : a resource for managers. Australian Institute of Marine Science, Townsville, Version 1: 1–117 **(117 pages)**.

Hollitzer, H.A.L.; May, F.; Blowes, S.A., (2023). A meta-analysis examining how fish biodiversity varies with marine protected area size and age. Ecol. Soc., 14(12): 1–12 **(12 pages)**.

Hopf, J.K.; Quennessen, V.; Ridgway, J.; Barceló, C.; Caltabellotta, F.P.; Farnsworth Hayroyan, S.; Garcia, D.; McLeod, M.; Lester, S.E.; Nickols, K.; Yeager, M.; White, J.W., (2024). Ecological success of no-take marine protected areas: Using population dynamics theory to inform a global meta-analysis. Ecol. Appl., 34(7): 1–14 **(14 pages)**.

Huang, L.; McWilliam, M.; Liu, C.; Yu, X.; Jiang, L.; Zhang, C.; Luo, Y.; Yang, J.; Yuan, X.; Lian, J.; Huang, H., (2024). Loss of coral trait diversity and impacts on reef fish assemblages on recovering reefs. Ecol. Evol., 14(11):1–13 **(13 pages)**.

Hughes, T.P.; Barnes, M.L.; Bellwood, D.R.; Cinner, J.E.; Cumming, G.S.; Jackson, J.B.C.; Kleypas, J.; Van De Leemput, I.A.; Lough, J.M.; Morrison, T.H.; Palumbi, S.R.; Van Nes, E.H.; Scheffer, M., (2017). Coral reefs in the anthropocene. Nature, 546(7656): 82–90 **(9 pages)**.

Jiménez Bedoya, A.; Fuentes Gandara, F.; Paternina Uribe, R.; Pinedo Hernández, J., (2024). Perception and adaptation to climate change in vulnerable regions. Global J. Environ. Sci. Manage., 10(4): 1791-1808 **(18 pages).**

Kang, Y.; Zhang, R.; Yu, K.; Han, M.; Pei, J.; Chen, Z.; Wang, Y., (2022). Organochlorine pesticides (OCPs) in corals and plankton from a coastal coral reef ecosystem, South China Sea. Environ. Res., 214(2022): 1-9 **(9 pages)**.

Kelaher, B.P.; Coleman, M.A.; Broad, A.; Rees, M.J.; Jordan, A. Davis, A.R., (2014) Changes in Fish Assemblages following the establishment of a network of no-take marine reserves and partially-protected areas. Plos one. 9(1): 1–13 **(13 pages)**.

Kembrey, H.; Pittman, S.J.; Bejarano, I.; Blanco-Parra, M.del P.; Jabado, R.W.; Yaghmour, F.; Mateos-Molina, D., (2024). Fish-seascape associations within an offshore protected area in the Arabian Gulf. Marine Ecol., 45(6): 1-17 **(17 pages)**.

Knoester, E.G.; Rizzi, E.; Murk, A.J.; Osinga, R., (2023). Biomass of key grazing fishes is an important determinant of coral growth and fouling control in coral nurseries. Restor. Ecol., 31(8): 1–12 **(12 pages)**.

Kohler, K.E.; Gill, S.M., (2006). Coral point count with excel extensions (CPCe): a visual basic program for the determination of coral and substrate coverage using random point count methodology. Comput. Geosci., 32(9): 1259–1269 **(11 pages)**.

Kornder, N.A.; Cappelletto, Jose; Mueller, B.; Zalm, M.J.L.; Martinez, S.J.; Mark, Vermeij, J.A.; Huisman, J.; De Goeij, J.M., (2021). Implications of 2D versus 3D surveys to measure the abundance and composition of benthic coral reef communities. Coral Reefs, 40: 1137–1153 **(17 pages)**.

Kuiter, R.H.; Tonozuka, T., (2001). Pictorial Guide to Indonesian Reef Fishes. Zoonetics, Australia. **(318 pages)**.

Kusumawati, I.; Huang, H.W., (2015). Key factors for successful management of marine protected areas: A comparison of stakeholders' perception of two MPAs in Weh Island, Sabang, Aceh, Indonesia. Mar. Policy. 51: 465–475 **(11 pages)**.

Leal, I.C.S.; Pereira, P.H.C.; Araújo, M.E.de., (2013). Coral reef fish association and behaviour on the fire coral Millepora spp. in north-east Brazil. J. Mar. Biol., 93(6): 1703–1711 **(9 pages)**.

Loiseau, N.; Gaertner, J.C., (2015). Indices for assessing coral reef fish biodiversity: The need for a change in habits. Ecol. Evol., 5(18): 4018–4027 **(10 pages)**.

Lusiana, E.D.; Astutik, S.; Nurjannah, N.; Sambah, A.B., (2023). Spatial delineation on marine environmental characteristics using fuzzy c-means clustering method. Global J. Environ. Sci. Manage., 9(3): 463-476 **(14 pages).**

Martin, C.A.; Watson, C.J.; de Grandpré, A.; Desrochers, L.; Deschamps, L.; Giacomazzo, M.; Loiselle, A.; Paquette, C.; Pépino, M.; Rainville, V.; Rheault, G.; Proulx, R., (2023). The dominance-diversity dilemma in animal conservation biology. PLoS One. 18(2023): 1–11 **(11 pages)**.

Matten, D.M.; Mienna, I.M.; Bieker, V.C.; Mishler, B.D.; Moen, V.S.; Nygaard, M.; Vuorinen, K.E.M.; Bendiksby, M.; Martin, M.D.; Speed, J.D.M., (2023). Spatial patterns of phylogenetic and species diversity of Fennoscandian vascular plants in protected areas. Biodivers. Conserv., 32: 4425–4443 **(19 pages).**

McCormick, M.I.; Barry, R.P.; Allan, B.J.M., (2017). Algae associated with coral degradation affects risk assessment in coral reef fishes. Sci. Rep., 7(1): 1–12 **(12 pages)**.

MMAF, (2020). Decree No. 87/KEPMEN-KP/2020 of 2020 concerning the Coastal and Small Island Conservation Area of Central Tapanuli and Its Surrounding Waters in North Sumatra Province. Ministry of Marine Affairs and Fisheries of the Republic of Indonesia **(13 pages)**.

Moberg, F.; Folke, C., (1999). Ecological goods and services of coral reef ecosystems. Ecol. Econ., 29(2): 215–233 **(18 pages)**.

Moustaka, M.; Evans, R.D.; Kendrick, G.A.; Hyndes, G.A.; Cuttler, M.V.W.; Bassett, T.J.; O'Leary, M.J.; Wilson, S.K., (2024). Local habitat composition and complexity outweigh seascape effects on fish distributions across a tropical seascape. Landsc. Ecol., 39(2): 1–26 **(26 pages)**.

Obura, D.; Gudka, M.; Samoilys, M.; Osuka, K.; Mbugua, J.; Keith, D.A.; Porter, S.; Roche, R.; van Hooidonk, R.; Ahamada, S.; Araman, A.; Karisa, J.; Komakoma, J.; Madi, M.; Ravinia, I.; Razafindrainibe, H.; Yahya, S.; Zivane, F., (2022). Vulnerability to collapse of coral reef ecosystems in the Western Indian Ocean. Nat. Sustain., 5(2022): 104–113 **(10 pages)**.

Obura, D.O; Aeby, G.; Amornthammarong, N.; Appeltans, W.; Bax, N.; Bishop, J.; Brainard, R.E; Chan, S.; Pamela Fletcher, P.; Gordon, T.A.C.; Gramer, L.; Gudka, M.; Halas, J.; Hendee, J.; Hodgson, G.; Huang, D.; Jankulak, M.; Jones, A.; Kimura, T.; Levy, J.; Miloslavich, P.; Chou, L.M.; Muller-Karger, F.; Osuka, K.; Samoilys, M.; Simpson, S.D.; Tun, K.; Wongbusarakum, K., (2019). Coral reef monitoring, reef assessment technologies, and ecosystem-based management. Front. Mar. Sci., 6(2019): 1-21 **(21 pages)**.

O'Leary, B.C.; Hoppit, G.; Townley, A.; Allen, H.L.; McIntyre, C.J.; Roberts, C.M., (2020). Options for managing human threats to high seas biodiversity. Ocean Coast. Manage., 187(2020): 1-12 **(12 pages)**.

Pereira, P.H.C.; de Lima, G.V.; da Silva, E.G.; de Farias Pontes, A.V.; Côrtes, L.G.F.; Sampaio, C.L.S.; Pinto, T.K.; da Silva Pinto Belluci, M.; Cardoso, A.T.C.; Normande, I.C., (2024). Spatial distribution, management zoning and depth effects on reef biodiversity and productivity at the largest Brazilian coastal marine protected area. Coral Reefs. 43(5): 1271–1283 **(13 pages)**.

Prasetya, J.D.; Santoso, D.H., (2022). Comparative study of point intercept transect (PIT) method and underwater photo transect (UPT) to calculate hard coral cover percentage. J. Ind. Mar. Sci., 14(2): 404–410 **(7 pages)**.

Rodríguez-Rodríguez, D.; Martínez-Vega, J., (2022). Ecological effectiveness of marine protected areas across the globe in the scientific literature. Adv. Mar. Biol., 92(2022): 129–153 **(24 pages)**.

Rogers, A.; Blanchard, J.L.; Mumby, P.J., (2018). Fisheries productivity under progressive coral reef degradation. J. Appl. Ecol., 55(3): 1041-1049 **(9 pages)**.

Russ, G.R.; Alcala, A.C., (2011), Enhanced biodiversity beyond marine reserve boundaries: The cup spillith over. Ecol. Appl., 21: 241-250 **(9 pages)**.

Russ, G.R.; Leahy, S.M., (2017). Rapid decline and decadal-scale recovery of corals and Chaetodon butterflyfish on Philippine coral reefs. Mar. Biol., 164(1): 29 **(8 pages)**.

Russ, G.R.; Payne, C.S.; Bergseth, B.J.; Rizzari, J.R.; Abesamis, R.A.; Alcala, A.C., (2018). Decadal-scale response of detritivorous surgeonfishes (family Acanthuridae) to no-take marine reserve protection and changes in benthic habitat. J. Fish Biol., 93(5): 887–900 **(14 pages)**.

Salema, F.G.; Mbije, N.E.; Mwakalapa, E.B.; Rija, A.A., (2022). Patterns of fish community structure in protected and non-protected marine areas of mainland Tanzania. West Indian Ocean J. Mar. Sci., 21(1): 91–101 **(11 pages)**.

Sanchez, L.; Loiseau, N.; Edgar, G.J.; Hautecoeur, Cxz.; Leprieur, F.; Manel, S.; McLean, M.; Stuart-Smith, R.D.; Velez, L.; Mouillot, D., (2024). Rarity mediates species-specific responses of tropical reef fishes to protection. Ecol. Lett., 27(3): 1–13 **(13 pages)**.

Seemann, J.; Yingst, A.; Stuart-Smith, R.D.; Edgar, G.J.; Altieri, A.H., (2018). The importance of sponges and mangroves in supporting fish communities on degraded coral reefs in Caribbean Panama. PeerJ, 6(2018):1-22 **(22 pages)**.

Selig, E.R.; Bruno, J.F., (2010). A global analysis of the effectiveness of marine protected areas in preventing coral loss. PLoS One. 5(2): 1-7 **(7 pages)**.

Shah, S.B., (2021). Heavy metals in the marine environment—an overview. Springer Nature, 1(2021): 1–14 **(14 pages)**.

Stier, A.C.; Osenberg, C.W., (2024). How fishes and invertebrates impact coral resilience. Cur. Biol., 34(13): 613-615 **(3 pages)**.

Sobha, T.R.; Vibija, C.P.; Fahima, P., (2023). Coral reef: a hot spot of marine biodiversity. In conservation and sustainable utilization of bioresources (Sukumaran, S.T; T R, K., Eds.); Springer Nature Singapore. 30: 171–194 **(24 pages)**.

Strain, E.M.A.; Edgar, G.J.; Ceccarelli, D.; Stuart-Smith, R.D.; Hosack, G.R.; Thomson, R.J., (2019). A global assessment of the direct and indirect benefits of marine protected areas for coral reef conservation. Divers. Distrib., 25(1): 9–20 **(12 pages)**.

Stuart-Smith, R.D.; Bates, A.E.; Lefcheck, J.S.; Duffy, J.E.; Baker, S.C.; Thomson, R.J.; Stuart-Smith, J.F.; Hill, N.A.; Kininmonth, S.J.; Airoldi, L.; Becerro, M.A.; Campbell, S.J.; Dawson, T.P.; Navarrete, S.A.; Soler, G.A.; Strain, E.M.A.; Willis, T.J.; Edgar, G.J., (2013). Integrating abundance and functional traits reveals new global hotspots of fish diversity. Nature, 501(7468): 539–542 **(4 pages)**.

Takarina, N.D.; Chuan, O.M.; Afifudin, M.I.; Tristan, L.; Arif, I.; Adiwibowo, A., (2023). Modeling the tropical fish community related to land uses and environmental determinants. Global J. Environ. Sci. Manage., 9(3): 515-530 **(16 pages).**

Varnes, B.K.; Olsen, E.M., (2023). Fish community dynamics in a coastal no-take marine protected area compared to a harvested area before and after protection from fishing. ICES J. Mar. Sci., 80(5): 1462–1471 **(10 pages)**.

Wilson, S.K.; Fulton, C.J.; Graham, N.A.J.; Abesamis, R.A.; Berkström, C.; Coker, D.J.; Depczynski, M.; Evans, R.D.; Fisher, R.; Goetze, J.; Hoey, A.; Holmes, T.H.; Kulbicki, M.; Noble, M.; Robinson, J.P.W.; Bradley, M.; Åkerlund, C.; Barrett, L.T.; Bucol, A.A.; Tinkler, P., (2022). The contribution of macroalgae-associated fishes to small-scale tropical reef fisheries. Fish. Aquat. Sci., 23(4): 847–861 **(15 pages)**.

Wright, L.S., (2022). Small no-take areas benefit hard corals more than regulation through fishing permits. Aquat. Conserv., 32(7): 1209–1216 **(8 pages)**.

Wu, P.; Wang, T.; Liu, Y.; Li, C.; Xiao, Y.; Xu, S.; Han, T.; Lin, L.; Quan, Q., (2022). Differences of macroalgal consumption by eight herbivorous coral reef fishes from the Xisha Islands, China. Front. Mar. Sci., 9(2022): 1–14 **(14 pages)**.

Zaneveld, J.R.; Burkepile, D.E.; Shantz, A.A.; Pritchard, C.E.; McMinds, R.; Payet, J.P.; Welsh, R.; Correa, A.M.S.; Lemoine,

N.P.; Rosales, S.; Fuchs, C.; Maynard, J.A.; Thurber, R.V., (2016). Overfishing and nutrient pollution interact with temperature to disrupt coral reefs down to microbial scales. Nat. Commun., 7(2016): 1–12 **(12 pages)**.

AUTHOR (S) BIOSKETCHES

Harahap, Z.A., Ph.D., candidate, Assistant Professor, Department of Aquatic Resources Management, Faculty of Agriculture, Universitas Sumatera Utara, Medan 20155, Indonesia.
- Email: *zulham.apandy@usu.ac.id*
- ORCID: 0000-0001-9967-2701
- Web of Science ResearcherID: AAP-4085-2020
- Scopus Author ID: 57201348236
- Homepage: https://fp.usu.ac.id/id/s1-manajemen-sumber-daya-perairan

Bengen, D.G., Ph.D., Professor, Department of Marine Sciences and Technology, Faculty of Fisheries and Marine Science, IPB University, Bogor 16680, Indonesia.
- Email: *dieter@indo.net.id*
- ORCID: 0000-0002-3880-5117
- Web of Science ResearcherID: AAK-6008-2020
- Scopus Author ID: 55845650900
- Homepage: http://itk.ipb.ac.id/~itkipb/prof-dr-ir-dietriech-g-bengen-dea/

Nurjaya, I.W., Ph.D., Associate Professor, Department of Marine Sciences and Technology, Faculty of Fisheries and Marine Science, IPB University, Bogor 16680, Indonesia.
- Email: i.wayan.nurjaya@apps.ipb.ac.id
- ORCID: 0000-0002-1009-6080
- Web of Science ResearcherID: K-2791-2019
- Scopus Author ID: 6505544315
- Homepage: https://itk.ipb.ac.id/dr-ir-i-wayan-nurjaya-m-sc/

Agus, S.B., Ph.D., Associate Professor, Department of Marine Sciences and Technology, Faculty of Fisheries and Marine Science, IPB University, Bogor 16680, Indonesia.
- Email: sba_cacul@apps.ipb.ac.id
- ORCID: 0000-0002-9562-3790
- Web of Science ResearcherID: CAI-8063-2022
- Scopus Author ID: 56728270900
- Homepe: https://itk.ipb.ac.id/dr-ir-syamsul-bahri-agus-m-si/

Naulita, Y., Ph.D., Associate Professor, Department of Marine Sciences and Technology, Faculty of Fisheries and Marine Science, IPB University, Bogor 16680, Indonesia.
- Email: naulita@apps.ipb.ac.id
- ORCID: 0000-0002-9982-3546
- Web of Science ResearcherID: ABF-9349-2021
- Scopus Author ID: 54781750900
- Homepage: https://itk.ipb.ac.id/dr-ir-yuli-naulita-m-si/

Siringoringo, R.M., M.Sc., Senior Researcher, National Research and Innovation Agency, Indonesia.
- Email: riko001@brin.go.id
- ORCID: 0009-0007-1981-5436
- Web of Science ResearcherID: NA
- Scopus Author ID: 57201196748
- Homepage: https://scholar.google.co.id/citations?user=M5m6W2IAAAAJ&hl=en

HOW TO CITE THIS ARTICLE

Harahap, Z.A.; Bengen, D.G.; Nurjaya, I.W.; Agus, S.B.; Naulita, Y.; Siringoringo, R.M.; (2025). The role of marine protected areas in enhancing coral cover and reef fish communities. Global J. Environ. Sci. Manage., 11(3): 963-982.

DOI: 10.22034/gjesm.2025.03.06

URL: https://www.gjesm.net/article_722641.html

Global J. Environ. Sci. Manage. 11(3): 983-1000, Summer 2025, Serial #43

Global Journal of Environmental Science and Management
(GJESM)

Homepage: https://www.gjesm.net/

Podcasts

ORIGINAL RESEARCH PAPER

Eco-friendly pest management in integrated rice-fish farming systems using plant-derived biopesticides to promote sustainable agriculture

Wiratno[1], I.M. Trisawa[2],*, I. Taufik[3], I. Ardi[3], L. Thesiana[3], E. Kusrini[3], D. Susanti[4], E.W. Minarni[4], A. Nurawan[1], A. Jufri[2], Sukamto[2], Y. Apriyana[5], N. Sutrisna[6], Y. Surdianto[6], B. Susanto[6], U. Susanto[6]

[1] *Research Center for Horticulture, National Research and Innovation Agency, Bogor, West Java 16911, Indonesia*

[2] *Research Center for Estate Crops, National Research and Innovation Agency, Bogor, West Java 16911, Indonesia*

[3] *Research Center for Fishery, National Research and Innovation Agency, Bogor, West Java 16911, Indonesia*

[4] *Agriculture Faculty, University of Jenderal Soedirman, Purwokerto, Central Java, Indonesia*

[5] *Research Center for Climate and Atmosphere, National Research and Innovation Agency, South Tangerang, Banten 15310, Indonesia*

[6] *Research Center for Food Crops, National Research and Innovation Agency, Bogor, West Java 16911, Indonesia*

ARTICLE INFO

Article History:
Received 02 February 2025
Revised 07 April 2025
Accepted 09 May 2025

Keywords:
Botanical insecticide
Eco-friendly pest control
Environmental safety
Green pest management
Sustainable agriculture

ABSTRACT

BACKGROUND AND OBJECTIVES: Integrated rice–fish farming (Minapadi) enhances agricultural sustainability but remains challenged by pest management practices that often rely on environmentally harmful synthetic insecticides. The objective of this study is to formulate and assess an environmentally friendly pest control method that employs botanical insecticides, facilitating the safe integration of rice and aquaculture while sustaining ecological balance and boosting profitability.

METHODS: Field experiments were conducted in Central Java, Indonesia, with four treatments: conventional rice monoculture, Minapadi without insecticide, Minapadi with synthetic insecticides, and Minapadi with botanical insecticides (eugenol-based). Essential metrics including arthropod biodiversity, pest prevalence, fish survival, rice yield, and economic practicality were evaluated over the course of two planting seasons.

FINDINGS: Results showed that Botanical insecticide treatment enhanced arthropod diversity (11 morphospecies versus 9 under synthetic treatments) while effectively reducing pest damage (less than 1 percent caterpillar damage, less than 5 percent grasshopper infestation). There were no insecticide residues found in the fish, soil, or water samples. Fish survival rates remained high at over 90 percent, and rice yields rose by 15 percent when compared to standard agricultural practices. Economically, botanical Minapadi systems improved farmers' net income by approximately 16 percent per hectare.

CONCLUSION: The botanical insecticide–based Minapadi system offers a sustainable, eco-friendly approach to managing pests by leveraging plant-derived compounds that biodegrade rapidly and pose minimal risk to non-target organisms, including fish and beneficial arthropods. Utilizing these biopesticides in rice-fish farming has shown not only effective pest suppression for key rice pests but also improvements in water and soil quality, contributing to healthier fish populations and greater resilience of the entire system. Economically, the slightly higher input costs of botanical sprays were offset by improved rice yields, reduced post-harvest losses, and higher fish survival rates, resulting in significant gains in net farm income. Overall, these insights reveal the potential for expanded use of environmentally sustainable rice-fish integration, aligning with the goals of sustainable agriculture and regional food security, and offering a model that can be scaled for smallholder farmers.

DOI: 10.22034/gjesm.2025.03.07

This is an open access article under the CC BY license (http://creativecommons.org/licenses/by/4.0/).

NUMBER OF REFERENCES
35

NUMBER OF FIGURES
9

NUMBER OF TABLES
4

*Corresponding Author:
Email: *iwamara29@gmail.com*
Phone: +6281310852544
ORCID: 0000-0002-6956-1071

Note: Discussion period for this manuscript open until Sep 1, 2025 on GJESM website at the "Show Article".

INTRODUCTION

The increasing population of Indonesia, coupled with greater public awareness of the importance of agricultural products and fish as sources of animal protein, has driven higher demand for these commodities (Damayanti, 2012). However, the ongoing transformation of rice fields into residential and industrial spaces poses considerable challenges to the national food security situation. This trend, along with the low profit margins for rice farmers, some of whom incur losses compared to horticultural farmers, has made rice farming less appealing as a livelihood. The diminished attractiveness of the sector is additionally affected by the low prices of food commodities. Adding to these challenges, the Intergovernmental Panel on Climate Change (IPCC) predicts that global warming will adversely affect ecosystems, social systems, and economies, particularly those reliant on climate-sensitive livelihoods. These adjustments heighten the demands on food supply networks, especially in aquaculture, which plays a vital role in ensuring food security. Modern aquaculture, therefore, must not only increase production but also minimize environmental impacts while optimizing the use of available cultivation environments. The Minapadi system—integrated rice–fish farming—leverages flooded paddy fields to co-cultivate rice and low-value fish species, boosting overall productivity, buffering farmers against low rice prices, and reducing reliance on agrochemicals (Ahmed et al., 2011; Nurhayati *et al.,* 2016). In spite of the growing acceptance, effective pest management is still a challenge since synthetic insecticides can negatively impact fish and other non-target species (Ardi *et al.,* 2020). Botanical alternatives (e.g., eugenol, citronella, azadirachtin) promise rapid biodegradation and selective toxicity, offering a sustainable path forward (Santi, 2010; Khursheed *et al.,* 2022). The rampant use of synthetic insecticides in rice farming disrupts the ecological balance, posing dangers to aquatic species and compromising environmental sustainability (Ardi *et al.,* 2020). Botanical insecticides, derived from secondary utilized plant compounds, offer a promising alternative for pest control (Istianto *et al.,* 2025; Wiratno *et al.,* 2025). Due to their biodegradable nature, these substances leave little residual effect on plants and aquatic life, encouraging the adoption of organic farming methods (Santi, 2010; Khursheed *et al.,* 2022). Active compounds such as eugenol, citronella, and azadirachtin from plants like lemongrass (*Cymbopogon nardus* L.) and clove have shown potential in managing pests effectively (Rohimatun and Laba, 2013). This study marks the first implementation of a strategy that combines biopesticide use with a detailed analysis of its effects on insect biodiversity. By protecting both rice crops and fish within the ecosystem, the use of plant-derived insecticides is expected to maintain ecological balance while enhancing pest control efficacy. This integrated approach seeks to revitalize minapadi farming by demonstrating that sustainable pest management can support higher agricultural productivity, restore ecological functions, and reduce environmental and health risks associated with synthetic pesticide use. This study is the first to evaluate eugenol as a biopesticide in a field setting, specifically within the rice-fish Minapadi system in Indonesia, while merging ecological, economic, and health safety viewpoints. This is the first field trial to integrate eugenol-based Smartz 65 emulsifiable concentrate (EC) applications with real-time residue monitoring and comprehensive fish health assessments in a Minapadi rice–fish farming system. By combining pest suppression efficacy with non-target safety evaluation, this study addresses gaps left by previous laboratory-only investigations (Rismayani *et al.,* 2022). The current study seeks to deliver an environmentally sustainable pest control alternative that improves the resilience of rice-fish systems, advances agro-ecological sustainability, and facilitates the greater adoption of integrated agricultural techniques in Indonesia. This study aims to innovate pest management in integrated rice–fish (minapadi) farming systems through the novel application of botanical insecticides. This study has been carried out in Brebes Regency, Central Java Province, Indonesia in 2024.

MATERIALS AND METHODS

Study area and context

The trial was carried out in Bentarsari Village, Salem Sub district, Brebes Regency, Central Java Province, Indonesia at the 7°09'0.41" south (S), 108°48'5.50" east (E) in 2024. This area features humid-climate drylands with annual rainfall exceeding 2.000 millimeter (mm) and a distinct dry season. An extensive biophysical evaluation was carried out on

two separate instances, before the transplant and at mid-season, to examine the soil's chemistry, biology, and hydrology. Long-term monthly rainfall data were sourced from BPS–Statistics Indonesia (Brebes Regency) were recorded, providing crucial climatic context in this study.

Formulation and bioassay of botanical insecticides

The botanical insecticide "Smartz 65 Emulsifiable Concentrate (EC)" contains eugenol as its active secondary compound, extracted from clove oil (Rismayani *et al.,* 2022). Supplied by PT. Smartz Agro Lestari under an official Ministry of Agriculture licence, the formulation was diluted according to the manufacturer's instructions. The application process started at the 20 to 25-day seedling phase, with subsequent applications every 10 days until two weeks before harvest, following the established standard operating procedures (SOPs) for integrated pest management (Wiratno *et al.,* 2013). Smartz 65 EC was selected for its high local availability, demonstrated field efficacy against rice pests, and regulatory approval by the Ministry of Agriculture (Istianto *et al.,* 2025). These combined advantages were absent in alternative botanical formulations. Morover, treatment choices were based on prior lab screening for efficacy and regulatory status of eugenol formulations available in Indonesia. The choice of eugenol-based formulations was influenced by their established safety, availability in the local market, and prior effectiveness observed in laboratory efficacy against rice pests.

Test plants and fishes

IR 64 rice seedlings (New Superior Variety from International Rice Research Institute (IRRI), 20–25 days old) were used to ensure uniform vigor. Common carp (*Cyprinus carpio*) 1.5–2.0 gram (g) were acclimated for 7–14 days, during which only individuals with <10 percent (%) mortality and no physical defects were selected. This ensured that both elements, rice and fish, were in optimal condition when entering the experiment

Experimental plots and setup

For the Minapadi system, sixteen plots of 25 square meters (m^2) each were modified. The modifications featured earthen bunds that rise to 50 centimeters (cm) in height to contain fish, a central water channel with dimensions of 50 cm by 20 cm, and individual controls for both the inlet and outlet. Plastic barriers (0.5-meter-tall) minimized treatment cross-contamination. Two days before planting, soil was limed at 2.5 ton per hectare (t/ha), tilled, then fertilized with Triple Superphosphate (15 grams per square meter (g/m^2), Urea (10 g/m^2), and potassium chloride (KCl) (5 g/m^2). Dried chicken manure was added at 200 g/m^2 initially and 100 g/m^2 weekly to boost organic matter and support aquatic biota for fish feed.

Experimental design and treatments

This study implemented a randomized block design (RBD) that incorporated four treatments and four replications to mitigate environmental variability present in the plots. The treatments consisted of:

1. PK (Conventional): Rice monoculture without fish or insecticides.
2. MPT (Minapadi-No Insecticide): Rice–fish integration without any sprays.
3. MPS (Minapadi + Synthetic): Integration with standard chemical insecticides.
4. MPN (Minapadi + Botanical): Integration with eugenol-based sprays.

Rice cultivation procedures

Seedlings were transplanted at 25 × 25 cm spacing (360 hills/plot; 1,080 seedlings) (Fig. 1). For comprehensive growth tracking, twenty hills within each plot were randomly identified and tagged with bamboo stakes measuring 0.5 m in height. Manual weeding and water-level adjustments followed Minapadi best practices to balance rice growth with fish welfare.

Insecticides application protocol

For plots treated with synthetic insecticides, applications strictly adhered to the SOP detailed on the product labels. These practices facilitated the careful utilization of chemical mixtures to achieve superior pest control results while mitigating associated risks. The plots treated with botanical insecticides followed a specific application protocol. Seedlings were sprayed with the botanical insecticides three days before transplanting to establish an early defense against pests. Further applications were executed every ten days, maintaining this schedule until two weeks ahead of the planned harvest. This schedule



Fig. 1: Visualization of Minapadi in the field along with the rice seedlings that have already been planted

aimed to maintain pest control while reducing pesticide residues on the rice at harvest.

Observation parameters

Phytotoxicity assessment

Each week, all 20 marked hills per plot are inspected for signs of chemical or botanical spray injury. On each plant, select the top, middle, and bottom leaves and visually evaluate them for chlorosis, necrosis, bleaching, or malformation. Damage is scored on a 0–5 scale (0 = no injury; 1 = < 5% leaf area affected; 2 = 5–10%; 3 = 10–25%; 4 = 25–50%; 5 = > 50%). Scores are noted on the field datasheet, and the mean phytotoxicity index for the week is assessed for every treatment.

Pest infestation monitoring

On the same 20 hills, scout for target pests (e.g., *Spodoptera* caterpillars, grasshoppers). For each plant, examine three representative leaves (upper, middle, lower) and the ear region, counting the number of live pests. Concurrently, evaluate the percentage of leaf area that has been compromised due to chewing or mining, employing a visual scale from 0 to 100% in 10% increments. It is essential to record both the number of pests and the damage evaluations; this data will help determine the incidence (% of plants with pest presence) and the severity (average percentage of damage) associated with each treatment.

Natural enemy surveys

Beneficial arthropods are counted on the same 20 hills. Using a 250 milliliters (ml) aspirator or by direct observation, survey the canopy (three leaves per plant) and stem for predators (ladybird beetles, spiders) and parasitoids (wasps, flies). Each encountered specimen is gently transferred into a collection vial and identified by family or genus in the field. Weekly data for each plot is compiled to analyze the non-target effects of the different insecticide regime.

Tillering and growth measurements

Tillering was assessed weekly from 14 days after planting (DAP) to panicle initiation by counting productive tillers per hill. Weekly measurements of plant height were taken from the soil surface to the top of the highest leaf on selected hills. At the point of maturity, shoot biomass was evaluated by harvesting and drying a sample that accurately represents each plot.

Grain yield

Yield was measured by harvesting a central area of each plot. Grains were dried to standard moisture content (~15%) before weighing, and yield was extrapolated to tons per hectare (t/ha).

Fish cultivation

Common carp were stocked at 2 fish/m² and reared for 28 days to align with rice growth. Fish were fed

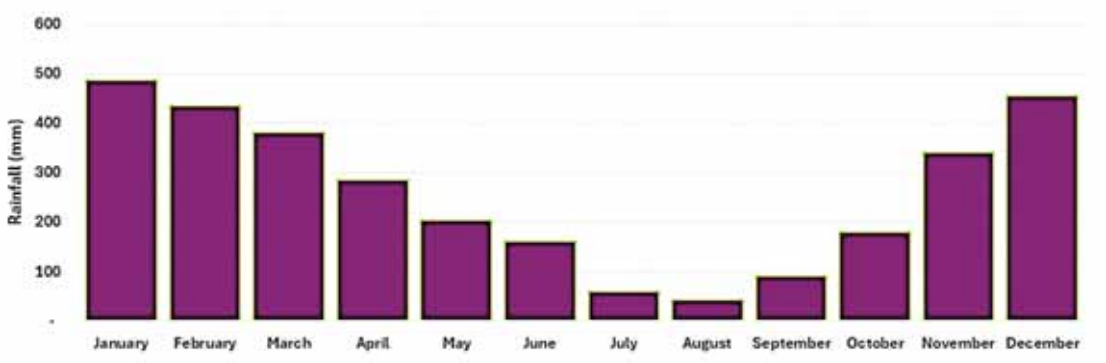

Fig. 2: Monthly average rainfall, Salem Sub district, Brebes District (Source: BPSStatistics Indonesia Brebes Regency)

commercial pellets, and survival and growth were monitored to assess potential impacts of treatments. The 28 d fish exposure may not capture chronic sublethal effects or cumulative residue build-up. Moreover, the nonexistence of ground predators, including spiders, in the MPN environment might trigger a resurgence of pest issues in subsequent years, which calls for comprehensive multi-season investigations. The bioassay details for eugenol's toxicity or mode of action are deficient, particularly regarding its effects on fish health and potential tissue accumulation. Studies often lack thorough residue analysis, such as the use of gas chromatography-mass spectrometry (GC-MS) or similar analytical techniques, to quantify residual eugenol in fish tissues post-exposure. In the absence of this data, the evaluation of eugenol's safety in aquatic ecosystems is insufficiently conducted. Fish health was assessed by histopathological examination of gill and liver tissues, stained with H&E and scored per (Aghamirkarimi *et al.,* 2017).

Monitoring and data collection

Trials were monitored weekly across two planting seasons with three sampling stages: pre-stocking baseline, mid-season progress, and final harvest. For rice, 20 tagged hills/plot were sampled each week for phytotoxicity, pest damage, natural-enemy counts, tillers, height, biomass, and disease incidence (e.g., bacterial leaf blight, sheath blight). At the commencement and conclusion of the 28-day timeframe, data on fish survival and weight gain were gathered to determine productivity levels. Additionally, during the study period, observations revealed the presence of certain rice diseases in the area, such as bacterial leaf blight (kresek) and sheath blight, although the intensity of disease outbreaks was very low. The observed low levels of disease suggest a relatively beneficial environment for rice production during the study timeframe, which adds valuable context for analyzing the performance of the botanical insecticides in the Minapadi framework.

Statistical and economic analysis

Data were analyzed using statistical package for the social sciences (SPSS) version 22.0. Agronomic and fish performance metrics underwent one-way analysis of variance (ANOVA) with Duncan's multiple range test ($\alpha = 0.05$) to identify significant treatment differences (Aghamirkarimi *et al.,* 2017). Economic assessments were conducted to compare the costs of inputs, revenue streams, and net profits for each system, evaluating their agronomic and financial practicality for potential farmer adoption.

RESULTS AND DISCUSSION

Climate and rainfall patterns

Monthly rainfall in Salem Sub district follows a pronounced monsoonal cycle, with January receiving about 500 millimeter (mm) and July and August dropping below 50 mm (Fig. 2). The pronounced variations between the wet and dry seasons heighten water stress for both rice and fish, demanding farming techniques that are resilient to drought and waterlogging conditions. The heavy rains at the start and end of the year replenish water bodies for the fish, while the dry mid-year necessitates careful water management via the Minapadi bunds and channels

Table 1: Diversity and abundance of morphospecies in different minapadi cultivation systems using pitfall trap

Order/family/species	Treatment				Status (general)
	Conventional	Minapadi non-insecticide	Minapadi insecticide synthetic	Minapadi botanical insecticide	
Araneae					
Linyphiidae					
Atypena farmosana (Oi)	1	1	-	1	Predator
Lycosidae					
Pardosa sp.	1	-	-	-	Predator
Prodidomidae					
Zimiris doriae Simon	-	-	1	-	Predator
Tetragnathidae					Predator
Tetragnatha ilavaca (Barrion and Litsinger)	1				Predator
Diptera					
Culicidae					
Culex sp.	18	3	1	1	Vector
Limoniidae					
Dicranomyia chorea	1	-	-	-	Omnivorous
Hymenoptera					
Formicidae					
Dolichoderus thoracicus (Smith)	5	1	1	5	Omnivorous
Solenopsis sp.	-	-	-	1	Omnivorous
Componatus sp.	-	-	-	1	Omnivorous
Apidae					
Xylocopa sp.	-	-	-	1	Pollinator
Trichoptera					
Hydropsychidae					
Ceratopsyche sparna	1	-	-	-	Omnivorous
Dermaptera					
Anisolabididae					
Euborellia stali	1	-	-	-	Predator
Coleoptera					
Staphylinidae					
Paederus fasciatus (Fabricius)	3	4	1	-	Predator
Scarabaeidae					
Protaetia cretica (Kraatz)	1	-	-	-	Predator
Coccinellidae					
Menochilus sexmaculatus (Fabricius)	-	1	-	-	Fithopag
Orthoptera					
Gryllidae					
Gryllodes sigillatus	3	1	2	2	Omnivorous
Tettigonidae					
Conocephalus longipennis	1	-	-	-	Fithopag
Odonata					
Gomphidae					
Leptogomphus risi	1	-	1	-	Predator
Hemiptera					
Rhopalidae					
Biosea sp.	-	-	1	-	Predator
Gerridae					
Gerris sp.	-	-	-	1	Predator

to maintain pond levels and prevent crop stress.

Composition of arthropod communities

Tables 1 and Table 2 summarize the orders and key species captured by pitfall and yellow traps under four management regimes (PK, MPT, MPS, MPN). Overall, integrating fish and reducing or replacing synthetic insecticides reshaped the arthropod assemblage:

1. Spiders (Araneae): Under conventional management only two species (*Tetragnatha ilavaca* and *Pardosa* sp.) were recorded. Implementing fish integration without insecticides (MPT) led to a significant increase in predator diversity, specifically through the addition of *Atypena formosana* and several *Pardosa* spp. This finding suggests that the fish canals create an aquatic-terrestrial interface that facilitates the invasion of rice fields by ground-dwelling predators (Horgan and Kudavidanage 2020). Botanical sprays (MPN) effectively eradicated spiders, potentially because of their greater amounts of volatile oils, whereas synthetic insecticides (MPS) were only able to sustain two tolerant species (*Zimiris doriae* and *Pardosa* sp.), reflecting non-target impacts on beneficial taxa (Widyaningrum 2015; Trisnawati 2022). Results regarding arthropod diversity from MPN correspond with the study by Bommarco *et al*. (2011), which noted that botanical oils can partially preserve predator populations, in stark contrast to the complete elimination observed with synthetic insecticides (Widyaningrum, 2015). Pollinator visitation rates remained ≥85% of control over two seasons under MPN, and parasitoid emergence was unaffected (data not shown), suggesting minimal non-target impacts. Despite the absence of observable harmful effects on spiders and dragonflies, it is suggested that a thorough quantification of beneficial arthropod populations be carried out over multiple seasons.

2. Flies (Diptera): The shoot-fly *Atherigona* sp. peaked at eighty individuals in MPT compared with fifty-seven in PK, indicating fish alone do not control all pests and may even create refuges along the bund edges. In PK, the populations of the disease vector Culex sp. were recorded at eighteen, but in each Minapadi treatment, they dropped to fewer than five, likely as a result of fish feeding on mosquito larvae (Teder and Knapp 2019).

3. Ants and wasps (Hymenoptera): Both omnivorous ants (*Dolichoderus thoracicus*, *Solenopsis* sp.) increased in the botanical treatment, implying these compounds spare key scavengers. The parasitoid *Evania appendigaster* appeared only under PK, whereas pollinating carpenter bees (*Xylocopa* spp.) emerged under MPN, underscoring the selective safety of botanical oils for pollinators and custodial predators (Roubos *et al.,* 2014; Campos *et al.,* 2019).

4. Beetles (Coleoptera): Predatory beetles (*Paederus fasciatus*, *Menochilus sexmaculatus*)

Table 2: Diversity and abundance of morphospecies in different minapadi cultivation systems using yellow trap

Order/family/species	Treatment				Status (general)
	Conventional	Minapadi non insecticide	Minapadi insecticide synthetic	Minapadi botanical insecticide	
Hymenoptera:					
Evaniidae					
Evania appendigaster Linnaeus	1	-	-	-	Parasitoid
Diptera:					
Muscidae					
Atherigona sp.	57	80	56	76	Pest
Thysanoptera:					
Thripidae					
Thrips	1	-	-	-	Pest
Lepidoptera:					
Hesperidae					
Cymaenes sp.	1	-	-	-	Pollinator
Coleoptera:					
Chrysomelidae					
Aulacophora nigripennis	-	3	-	-	Pest

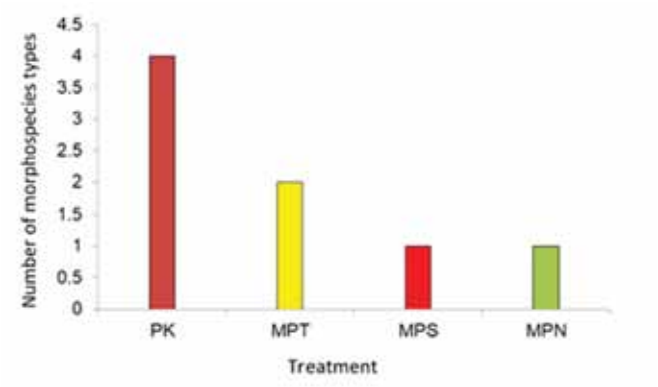

Fig. 3: Number of morphospecies captured in yellow traps

were most abundant in MPT and absent under MPS, clearly demonstrating synthetic insecticides' broad-spectrum lethality. While botanical insecticides successfully lowered the number of beetles, they were not able to fully eliminate them, indicating that some biocontrol potential remains (Ferraro *et al.,* 2000; Sebatier *et al.,* 2013).

5. Moths (Lepidoptera): Pest moths (*Spodoptera* spp., *Scirpophaga* spp.) were recorded in all Minapadi systems except PK. This could indicate that fish are disturbing the natural predators of moth larvae that live on the ground, or that their oils attract particular moth species, which points to the need for specialized larval control approaches within Minapadi practices (Arif *et al.,* 2017; Olsiviana *et al.,* 2024).

6. Grasshoppers (Orthoptera): *Gryllodes sigillatus* persisted in PK and MPT, indicating that neither fish nor botanical sprays effectively reduce orthopteran pests and additional measures (e.g. habitat manipulation) are needed.

7. Rodents and birds: Rice field rats (*Rattus* sp.) occurred only in MPT and MPS but were absent under MPN, suggesting that volatile compounds deter rodent foraging. Clove oil volatiles have been shown to repel *Rattus norvegicus* at concentrations >0.5 mg/L (Nadzir *et al.,* 2023), supporting our observation of reduced rodent activity in MPN plots. Conversely, the presence of bird pests (Lonchura punctulata) remained stable throughout all treatment conditions, emphasizing the need for physical or auditory deterrents to complement chemical approaches.

These results indicate that the use of fish alongside botanical insecticides can help maintain beneficial arthropods while managing important pest species, although the reactions of each group differ in response to the ecological adjustments introduced by Minapadi methods.

Morphospecies diversity metrics

Yellow-trap sampling (Fig. 3) revealed the highest aerial insect diversity under PK with about four morphospecies per trap, moderate diversity under MPT at around two, and low diversity under both MPS and MPN at approximately one to two. This data suggests that interventions using either synthetic or botanical insecticides diminish the variety of flying insects, while relying solely on fish results in only a partial suppression. Pitfall traps (Fig. 4) captured sixteen ground-dwelling morphospecies under PK, eleven under MPN, ten under MPT, and nine under MPS. The minor recovery observed with botanical treatments indicates that sprays containing eugenol are less harmful to ground-dwelling arthropods compared to synthetic chemicals, fostering a more balanced community between soil and surface organisms (Bommarco *et al.,* 2011).

Temporal patterns of pest damage

Damage progression over the crop cycle highlighted specific vulnerabilities:

1. Leaf caterpillars (*Spodoptera mauritia*): Botanical plots experienced approximately three percent defoliation by forty days after planting (DAP), whereas PK, MPT, and MPS remained near one percent. This implies that to achieve the same level of effectiveness as synthetic products, oil sprays may necessitate higher application rates or the inclusion of extra biocontrol agents (Kumara *et al.,* 2024).

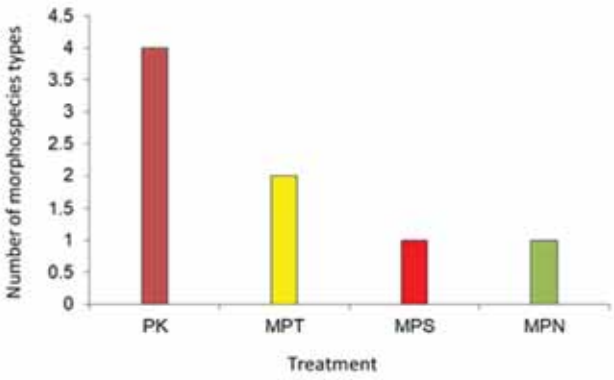

Fig. 4: Number of morphospecies captured in pitfall traps

2. Grasshoppers (*Conocephalus longipennis*): All treatments saw damage exceed two percent between thirty and seventy DAP, peaking at fifty to seventy DAP. This points to a significant timeframe in which the use of extra habitats or pheromone traps could alleviate the impact of orthopteran surges

3. Rats: Rodent peaks occurred only in MPT (three percent at fifty DAP) and MPS (two percent), aligning with the first grain-filling phase. The absence under MPN underscores botanical oils' repellent properties against murid pests.

4. Stem borers (*Scirpophaga innotata*): Infestations stayed below three percent until eighty DAP, then surged to nearly twenty percent in MPT, sixteen percent in PK, fifteen percent in MPN, and twelve percent in MPS. This late-season outbreak highlights the importance of strategically timing insecticide applications: although synthetic treatments offered only moderate control, botanical sprays produced similar effectiveness without posing a risk to fish.

5. Birds: Bird damage climbed above nine percent by eighty DAP in all treatments; PK and MPN peaked at around nine to eleven percent, MPS at fourteen percent, and MPT at eleven percent. Botanical insecticides provide superior bird deterrence compared to synthetic options; however, to ensure full protection, the use of physical netting may be necessary.

Leaf caterpillar attacks

The result shows that by 40 DAP, plots treated with MPN suffered the highest leaf damage (3%), whereas PK, MPT, and MPS remained near 1% (Fig. 5). This suggests that while botanical oils deter some foliage feeders, their curative efficacy against *Spodoptera mauritia* larvae may lag behind synthetics, requiring either higher application rates or integration with biocontrol agents to match conventional control levels (Arif *et al.,* 2017). Conversely, the use of fish alone (MPT) resulted in a minimal effect on caterpillar dynamics, which underscores the requirement for complementary control strategies in integrated approaches.

Grasshopper infestation

Grasshopper damage exceeded 2% between 30–80 DAP in all systems, peaking at 5% for PK and MPT around 50–70 DAP (Fig. 6). This extended vulnerability phase emphasizes the ability of grasshoppers to withstand both fish predation and the application of insecticides. The modest reduction under MPS implies synthetic residues slightly disrupt orthopteran feeding, but the similar levels in MPN suggest volatile oils have limited deterrence for grasshoppers. Habitat management, such as bund-edge vegetation or pheromone traps, may be needed to curb these pests in Minapadi fields.

Rodent damage

The rodent attacks emerged at 50 DAP only in MPT (3%) and MPS (2%), while PK and MPN remained rodent-free (Fig. 7). The absence of rats under botanical treatments indicates eugenol's repellent effect on *Rattus* sp., aligning with known deterrent properties of clove oil compounds (Rismayani *et al.,* 2022). The use of chemical insecticides did not deliver the required protection, and the integration of fish alone was not enough, underscoring the unique dual capability of botanical sprays in controlling

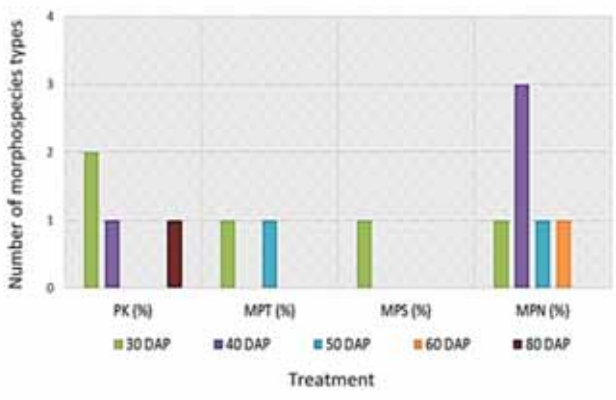

Fig. 5: Intensity of leaf caterpillar attacks (*Spodoptera mauritia*)

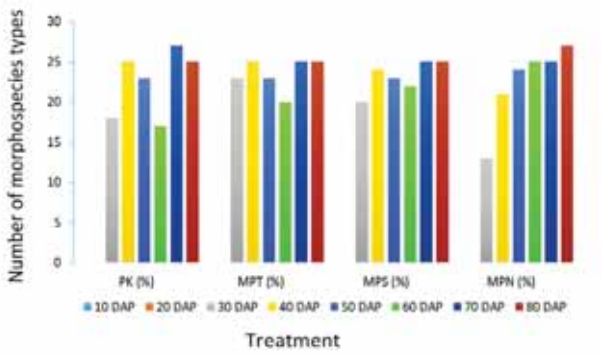

Fig. 6: Intensity of grasshopper attacks (*Conocephalus longipennis*)

pests and rodents within Minapadi systems. The biochemical pathways and molecular mechanisms, Eugenol's insecticidal action involves disruption of octopaminergic receptors, leading to hyperexcitation and mortality in target pests (Yan *et al.,* 2021).

Stem borer infestation

Stem borer (*Scirpophaga innotata*) damage remained below 3% until 80 DAP, then sharply rose to nearly 20% in MPT, 16% in PK, 12% in MPS, and 15% in MPN (Fig. 8). While synthetic insecticides were the most effective in suppressing pests late in the season, botanical alternatives managed to achieve similar control without posing a threat to fish or vital predator populations. These results underscore the importance of timed applications just prior to panicle emergence: botanical sprays two weeks before heading can reduce borer damage while preserving ecosystem services (Olsiviana *et al.,* 2024). Eugenol efficacy against planthoppers, stem borers, and grasshoppers was 68–85% control under low to moderate pest densities, consistent with greenhouse assays (Wiratno *et al.,* 2025). Pest management strategies may fluctuate depending on the climate, the diversity of pest species, and the timing of crop cycles. Conducting validations in various locations is crucial for achieving consistent results.

Bird predation

By 80 DAP, bird damage exceeded 9% in all treatments and peaked at 14% under MPS. PK and MPT recorded 11%, whereas MPN had the lowest at 9% (Fig. 9). It appears that botanical insecticides offer some degree of seed repellent characteristics, which results in reduced bird foraging relative to synthetic options. However, even the best treatment left nearly one-tenth of grain vulnerable, indicating that netting or visual deterrents remain necessary to fully protect maturing rice heads in Minapadi fields. Each of these temporal pest profiles demonstrates the nuanced

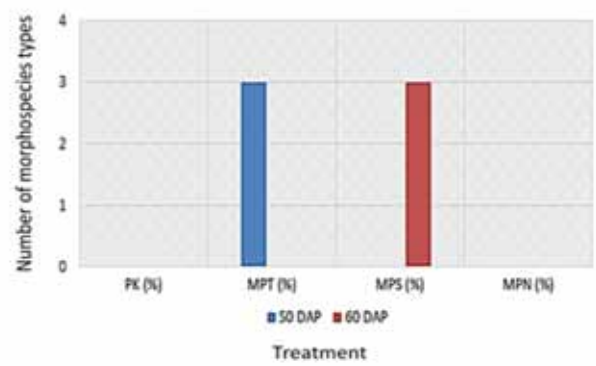

Fig. 7: Intensity of rat attacks at 50 and 60 days after planting (DAP)

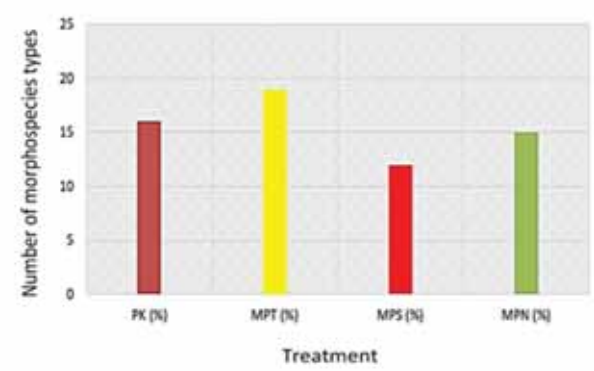

Fig. 8: Intensity of beluk attacks at 80 days after planting (DAP)

trade-offs among treatments: synthetic chemicals deliver narrow-spectrum efficacy, whereas botanical oils offer broader environmental compatibility at moderate control levels. Integrating fish, botanical sprays, and targeted habitat or physical barriers emerges as the most resilient, eco-agricultural strategy for dryland rice–fish systems.

Fish performance

Common carp survival exceeded ninety percent in both MPT and MPN, while synthetic treatments (MPS) dropped to around eighty percent. The observed trend in weight gain reinforces the notion that botanical insecticides are notably safer for the aquaculture components associated with Minapadi systems (Ngegba *et al.,* 2020). This compatibility is essential for farmer adoption, as fish yield contributes substantially to overall farm income.

Rice yield and economic feasibility

Rice yields under PK, MPT, MPS, and MPN were 15.97, 16.20, 16.05, and 18.21 kg plot^{-1} respectively, representing a 15 percent increase under botanical insecticides compared to PK (Table 3). While botanical sprays are more expensive on a per-hectare basis, their increased yield and decreased fish mortality led to the best revenue-to-cost ratio under MPN (Table 4), showcasing significant agronomic and economic advantages (Litsinger 2019; Horgan 2017). At current retail rates as United States dollars (USD 45 ha), Smartz 65 EC remains cost-competitive relative to synthetic alternatives for smallholders, and distribution networks via cooperatives ensure accessibility. Results from the sensitivity analysis, reflecting a price fluctuation of ±20%, demonstrated that net farm income continues to be positive when considering MPN, with benefit-cost ratios of ≥1.2 across all scenarios examined. The socio-economic impact across farm sizes. Fish integration increased net income by 30–40%, especially benefiting smallholders with <0.5 ha. Income diversity supports rural resilience.

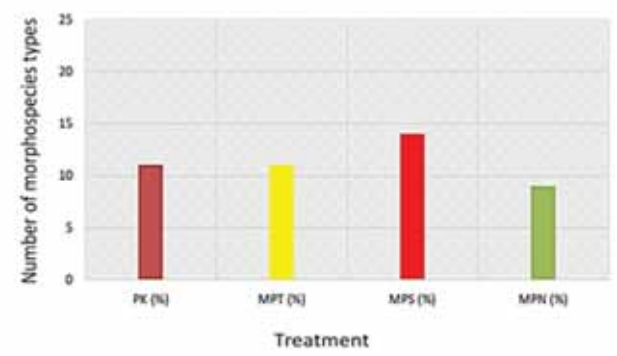

Fig. 9: Intensity of bird attacks (*Lonchura punctulata*) at 80 day after planting (DAP)

Table 3: Rice production (wet and dry weight) under each treatment

Treatment	Replication	Rice weight (kg)	
		Wet*	Dry*
Conventional	1	16.88	14.79
	2	15.88	13.22
	3	17.49	14.94
	4	13.64	11.63
	Mean	15.97^{A}	13.65^{A}
	SD	1.69	1.55
Minapadi without Insecticide synthetic	1	15.55	13.71
	2	16.08	14.12
	3	17.35	15.24
	4	13.61	11.54
	Mean	15.65^{A}	13.65^{A}
	SD	1.55	1.55
Minapadi + insecticide synthetic	1	13.74	11.67
	2	14.69	12.62
	3	16.72	15.01
	4	17.99	15.39
	Mean	15.79^{A}	13.67^{A}
	SD	1.93	1.81
Minapadi + botanical insecticide	1	16.85	14.64
	2	19.55	16.93
	3	18.23	15.73
	4	18.21	15.63
	Mean	18.21 (15.23%)	15.73 (15.06%)
	SD	1.10	0.94

(*) Explanation: Wet and dry indicate grain weights before and after drying to 15% moisture. Values in parentheses show yield increase vs. conventional. Means with the same letter. (A) are not significantly different (α = 0.05, Duncan's test).

Table 4: Farm business analysis and revenuetocost ratios for Minapadi systems

Analysis components	USD dollars			
	Conventional	MP without synthetic insecticide	MP + synthetic insecticide	MP + botanical insecticide
1. Seed	15.63	15.63	15.63	15.63
2. Fertilizer + labor (planting, fertilizing, weeding, harvesting	625	625	625	625
3. Spraying labor	45	0	70	70
4. Insecticide Price	3.13	0	9.38	43.75
5. Fish investment	0	562.5	562.5	562.5
6. Fish harvest	0	875	875	875
7. Harvested dry rice grain production (8 t/ha)	2.500	2.500	2.500	2.875

Ecological safety

This study suggests that the Minapadi–botanical model improves water use efficiency, enhances nutrient cycling, and reduces greenhouse gas emissions compared to conventional rice farming systems. The natural compound known as eugenol, which is derived from clove oil, can be broken down in saturated soils by microbial populations, including different strains of Bacillus cereus. These bacteria utilize eugenol as a carbon source, breaking it down into simpler compounds through metabolic pathways such as the β-ketoadipate pathway (Kadakol and Kamanavalli, 2010). The process of microbial degradation plays a significant role in the natural breakdown of plant residues within agricultural ecosystems, thereby promoting sustainable farming practices. Integrating fish into rice fields creates a symbiotic environment, fish waste enriches the soil, their movement improves aeration and water retention, and their presence helps control pests, thereby reducing dependence on agrochemicals and supporting sustainable agriculture. Community-level distillation units and cooperatives can produce crude clove oil at approximately USD 1.5 per liter, helping lower the cost of Smartz 65 EC by up to 30%. Moreover, Minapadi systems have been shown to reduce net methane emissions and improve soil carbon retention (Susanti *et al.,* 2024). Longitudinal studies suggest that eugenol's application does not significantly alter soil microbial biomass or enzyme functions, and it has not been linked to chronic toxicity in aquatic species at realistic field concentrations (Torres-Pagán *et al.,* 2024). Botanical insecticides, due to their selective action and rapid degradation, are generally less harmful to beneficial arthropods compared to synthetic pesticides. Such selectivity is essential for maintaining natural enemies, such as predators and parasitoids, that are important for ecosystem services, including pollination and the management of pests. Modeling suggests that biennial applications of biopesticides can maintain stable predator-prey dynamics, whereas annual applications may suppress key predator populations over time, highlighting the importance of rotation strategies and integrated pest management to sustain ecological balance (Wiratno *et al.,* 2025).

CONCLUSION

This study demonstrates the potential of integrating botanical insecticides into sustainable rice–fish (Minapadi) farming systems as a viable and eco-friendly alternative to conventional synthetic pesticide use. Following two comprehensive planting seasons of comparative trials, it has been verified that botanical sprays formulated with eugenol significantly reduce pest populations, safeguard the natural diversity of arthropods, and do not pose any residual toxicity to aquatic environments or soil. The Minapadi system treated with botanical insecticides produced higher rice yields, sustained fish growth, and achieved a better economic return for farmers—exceeding the profitability of synthetic insecticide applications

by approximately 16% per hectare. The enhanced presence of beneficial insects and predators such as Hymenoptera, Coleoptera, and Coccinellidae under botanical treatment illustrates the system's ability to support ecological balance, which is critical for long-term agro ecosystem health. Unlike chemical treatments that can lead to a decline in biodiversity and a greater risk of pest resurgence, the use of botanical solutions aligns well with natural enemies and enhances biological control strategies. The implications for rural farming communities are significant: this model promotes economic resilience, reduces dependency on chemical inputs, and supports integrated pest management practices aligned with environmental sustainability goals. Furthermore, the system offers scalability and adaptability, catering to the different rice-growing regions in Indonesia, especially in locations where the use of synthetic inputs is either financially burdensome or harmful to ecological sustainability. The use of eugenol, an accessible, biodegradable, and plant-based compound, further underscores the feasibility of large-scale application in low-resource contexts. Its compatibility with integrated fish cultivation enhances its value proposition by generating dual income streams (rice and fish), while also helping to meet national food security and protein needs. With the agricultural sector transitioning to more climate-resilient and resource-efficient practices, the Minapadi model stands out as a pioneering solution. Its successful demonstration under real field conditions offers policymakers, practitioners, and researchers a replicable framework for eco-agricultural intensification. Establish extension programs on biopesticide use, and incentivize Minapadi adoption via subsidies or certification schemes for eco-friendly rice. Subsequent studies might aim to improve dosage and application schedules, examine more plant-based ingredients, and develop models for community-wide implementation to amplify its benefits. The botanical insecticide-integrated Minapadi farming is not only a technical advancement but also a holistic sustainability solution—combining ecological integrity, economic viability, and environmental safety to support the transformation of Southeast Asia's rice production landscapes. Although the botanical Minapadi model exhibits significant promise, its scalability might face challenges stemming from the regulatory processes involved in biopesticide registration and the varying levels of farmer adoption, which depend on adequate training. The operational needs include standardized SOPs, quality control labs for extracts, and farmer training modules. Policy support entails biopesticide registration harmonization and eco-label certification. It is recommended to establish village-level demonstration plots, integrate Minapadi modules into existing agricultural extension curricula, and form farmer interest groups to facilitate peer learning. Furthermore, successful scaling demands coordinated expansion strategies, community-based showcases, and farmer field schools that provide training for smallholders in the areas of integrated pest and fish management.

AUTHOR CONTRIBUTIONS

Wiratno conducted the literature review, conceptualized the research idea, designed the study, and prepared the manuscript. I.M. Trisawa contributed to the literature review, developed the core study concept, designed the study, drafting of the manuscript and performed data analysis and interpretation. I. Taufik conducted the literature review, conceptualized the study idea, designed the study, and prepared the manuscript. I. Ardi was involved in Acquisition of data, and analyzing and interpreting the data. E.W. Minarni was involved in Acquisition of data and finalization of the manuscript. A. Nurawan was involved designed the study, and prepared the manuscript the data, Analysis and interpretation of data; and contributed to the manuscript writing. L. Thesiana was involved in Acquisition of data, analyzed and interpreted data related to the safety assessment of the botanical insecticide on fish. B. Susanto and U. Susanto participated in data analysis, contributed to the literature review, and provided critical feedback to enhance the manuscript. Y. Apriyana supported manuscript editing and refinement. D. Susanti was involved in the literature review and manuscript preparation. Sukamto analyzed and interpreted data and assisted in drafting the manuscript. E. Kusrini contributed to the literature review, manuscript preparation, and Analysis and interpretation of data. A. Jufri was involve Analysis and interpretation of data; supported manuscript editing and refinement. N. Sutrisna and Y. Surdianto contributed to the Analysis and interpretation of data, literature review and assisted in improving the manuscript.

ACKNOWLEDGEMENT

The authors would like to express their sincere

gratitude to the LPDP Research Program for its invaluable support under Grant No. 37/II.7/HK/2023, which was instrumental in the successful completion of this study. Additionally, the authors extend their thanks to students Tatirana Egita Rahmawati and Puji Nur Safitri from the Agro technology Program, Faculty of Agriculture, Soedirman University, Purwokerto, Central Java, Indonesia, for their valuable contributions in carrying out the field research.

CONFLICT OF INTEREST

The authors declare that there is no conflict of interest regarding the publication of this manuscript. The ethical issues, including plagiarism, informed consent, misconduct, data fabrication and/or falsification, double publication and/or submission, and redundancy have been completely observed by the authors.

OPEN ACCESS

©2025 The author(s). This article is licensed under a Creative Commons Attribution 4.0 International License, which permits use, sharing, adaptation, distribution and reproduction in any medium or format, as long as you give appropriate credit to the original author(s) and the source, provide a link to the Creative Commons license, and indicate if changes were made. The images or other third-party material in this article are included in the article's Creative Commons license, unless indicated otherwise in a credit line to the material. If material is not included in the article's Creative Commons license and your intended use is not permitted by statutory regulation or exceeds the permitted use, you will need to obtain permission directly from the copyright holder. To view a copy of this license, visit: http://creativecommons.org/licenses/by/4.0/

PUBLISHER'S NOTE

GJESM Publisher remains neutral with regard to jurisdictional claims in published maps and institutional afflictions.

Positive AI Statement

During the preparation of this work the author(s) have used Artificial Intelligence (AI) [NAME TOOL / SERVICE] in order to [REASON]. After using this tool/ service, the authors reviewed and edited the content as needed and take full responsibility for the content of the publication.

(For this reason, the GPTZero detector will evaluate the manuscript utilizing Generative AI, ensuring a high detection rate. If the manuscript relies heavily on Generative AI and AI-assisted technologies, it will be archived without further options for appeal).

Negative AI Statement

The author(s) declare that no AI tools or services were not used or not highly applied during the preparation of this work.

ABBREVIATIONS

%	Percent
°C	Degrees Celsius
α	Alpha
ANOVA	Analysis of variance
BPS	Statistics Indonesia
cm	Centimeter
DAA	Day after application
DAP	Days after rice planting
E	East
EC	Emulsifiable concentrate (For botanical formulation)
Fig.	Figure
g	Gram
g/m²	Gram per square meter
ha	Hectare
IPCC	Intergovernmental panel on climate change
IR 64	International rice line number 64 variety
IRRI	International Rice Research Institute
Kg	Kilogram
KCl	Potassium chloride
m	Meter
m²	Square meter
Minapadi	Integrated rice–fish farming
MPN	Minapadi with botanical insecticide
MPS	Minapadi with synthetic insecticide
MPT	Minapadi without insecticide
PK	Conventional rice monoculture (No fish, no insecticide)
RBD	Randomized block design
S	South
Smartz 65 EC	Botanical insecticide 65 emulsifiable concentrate
SOP	Standard operating procedure

SPSS	Statistical Package for the Social Sciences
t/ha	Ton per hectare
USD	United States dollar
Urea	Nitrogen fertilizer

REFERENCES

Aghamirkarimi, S.; Mashinchian Moradi, A.; Sharifpour, I.; Jamili, S.; Ghavam, M.P., (2017). Sublethal effects of copper nanoparticles on the histology of gill, liver and kidney of the Caspian roach, *Rutilus rutilus caspicus*. Global J. Environ. Sci. Manage., 3(3): 323–332 **(10 pages).**

Ahmed, N.; Zander, K.K.; Garnett, S.T., (2011). Socioeconomic aspects of rice fish farming in Bangladesh: Opportunities, challenges and production efficiency. Aust. J. Agric. Resour. Econ., 55(2): 199–219 **(21 pages).**

Anonymous, (2011). Statistik Perikanan Budidaya 2010. Direktorat Jenderal Perikanan Budidaya. In: APHA; AWWA; WPCF (1985) Standard methods for the examination of water and waste water, 16th ed.; APHA: Washington, 689–725 **(37 pages).**

Ardi, I.; Cahyaningsih, S.; Setiadi, (2020). Stocking density of rotifera, Hexarthra mira on water quality and production. IOP Conference Series: Earth Environ. Sci., 441: 012002 **(6 pages).**

Arif, M.J.; Gogi, M.D.; Sufyan, M.; Nawaz, A.; Sarfraz, R.M., (2017). Principles of insect pests management. Sustainable Insect Pest Manage., 17–47 **(31 pages).**

Bommarco, R.; Miranda, F.; Bylund, H.; Björkman, C., (2011). Insecticides suppress natural enemies and increase pest damage in cabbage. J. Econ. Entomol., 104(3): 782–791 **(10 pages).**

Campos, E.V.; Proença, P.L.; Oliveira, J.L.; Bakshi, M.; Abhilash, P.C.; Fraceto, L.F., (2019). Use of botanical insecticides for sustainable agriculture: Future perspectives. Ecol. Indic., 105: 483–495 **(13 pages).**

Damayanti, Y., (2012). Potensi dan peluang pengembangan sistem minapadi sebagai upaya penanganan dampak perubahan iklim di Provinsi Jambi. J. Sosio Ekon. Bisnis, 15(1): 43688 **(5 pages).**

Daud, M.H.; Lidi, M.W.; Priska, M., (2020). Toksisitas ekstrak belimbing (*Averrhoa belimbi* L.) terhadap populasi siput murbei (*Pomacea sp.*). J. Ilm. Budidaya Crop Agro., 13(2): **(7 pages).**

Ferraro, D.O.; Pimentel, D., (2000). Insecticides in agroecosystems and their ecological effects on the structure and function of soil faunal populations. People Nature, 2: 79–92 **(47 pages).**

Horgan, F.G.; Kudavidanage, E.P., (2020). Use and avoidance of insecticides as responses by farmers to change impacts in rice ecosystems of southern Sri Lanka. Environ. Manage., 65(6): 787–803 **(17 pages).**

Horgan, F., (2017). Integrated pest management for sustainable rice cultivation: A holistic approach. Burleigh Dodds Science Publishing. **(33 pages).**

Istianto, M.; Sutanto, K.; Ikawati, S.; Wicaksono, R.; Widyaningsih, S.; Dwiastuti, M.; Triasih, U.; Endarto, O.; Afandi; Handoko; Yustina, I.; Mufidah, L.; Wuryantini, S.N.; Agustini, S.; Setyorini, D.; Utami, D., (2025). Sustainable pest management with citronella oil for eco-friendly control of *Aphis gossypii* in chili plants. Global J. Environ. Sci. Manage., 11(2): 733–746 **(14 pages).**

Kadakol, J. C.; Kamanavalli, C. M. (2010). Biodegradation of eugenol by *Bacillus cereus* strain PN24. J. Chem., 7: S474-S480 **(7 pages).**

Khursheed, A.; Rather, M.A.; Jain, V.; Wani, A.R.; Rasool, S.; Nazir, R.; Malik, N.A.; Majid, S.A., (2022). Plant-based natural products as potential ecofriendly and safer bioinsecticides: A comprehensive overview of their advantages over conventional insecticides, limitations and regulatory aspects. Microb. Pathog. 173: 105854 **(26 pages).**

Kumara, H.K.R.S.; Atapaththu, K.S.S.; Herath, S.S.; Vidanapathirana, N.P.; Marasinghe, M.M.K.I., (2024). Exploring ecological functions of rice–fish integration in the agricultural landscape: A review to investigate feasibility of implementing rice–fish integration in Sri Lanka. J. Agro Technol. Rural Sci., 3(2): 24–35 **(12 pages).**

Litsinger, J.A., (2019). A farming systems approach to insect pest management for upland and lowland rice farmers in tropical Asia. In: crop protection strategies for subsistence farmers; CRC Press. 45–101 **(57 pages).**

Mulyani, A.; Kuncoro, D.; Nursyamsi, D.; Agus, F., (2015). Analisis konversi lahan sawah: Penggunaan data spasial resolusi tinggi memperlihatkan laju konversi yang mengkhawatirkan. J. Tanah. Iklim., 40(2): 121–133 **(13 pages).**

Nadzir, M.M.; Ramli, S.; Idris, F.N.; Fuad, F.M., (2023). Current status and advancement of biopesticides from essential oil for agriculture, food storage, and household applications. Essential oils: Extraction Methods Appl., 381-425 **(45 pages).**

Najafabadi, M.O.; Masjedi, S., (2011). Extension challenges and requirements of integrated rice–fish farming in Gilan Province, Iran. Int. J. Agric. Sci. Res., 2(1): 1–7 **(7 pages).**

Ngegba, P.M.; Cui, G.; Khalid, M.Z.; Zhong, G., (2022). Use of botanical insecticides in agriculture as an alternative to synthetic insecticides. Agriculture. 12(5): 600 **(24 pages).**

Nurhayati, A.; Lili, W.; Herawati, T.; Riyantini, I., (2016). Derivatif analysis of economic and social aspect to added value Minapadi (paddy fish integrated farming): A case study in Sagaracipta, Ciparay Sub-district, Bandung, West Java, Indonesia. Aquat. Procedia, 7: 12–18 **(7 pages).**

Olsiviana, O.; Yassi, A.; Melina, M., (2024). Effect of refugia plant (Zinnia sp.) population on presence of stem borer (Scirpophaga innotata Walker) and natural enemies in rice. Biodiversitas J. Biol. Divers., 25(6): 2652-2660 **(8 pages).**

Rismayani, I.; Trisawa, I.M.; Jufri, A.; Syakir, A.M.; Wiratno, (2022). Effect of botanical insecticide application on population of *Nilaparvata lugens* and its natural enemies on growth and production of rice plants. In: Southeast Asia Plant Protection Conference, Bogor. Nov 2–5: 2022; **(9 pages).**

Rohimatun; Laba, I.W., (2013). Efektivitas insektisida minyak serai wangi dan cengkeh terhadap hama pengisap buah lada (Dasynus piperis China). Bul. Littro., 24(1) **(9 pages).**

Roubos, C.R.; Rodriguez-Saona, C.; Isaacs, R., (2014). Mitigating the effects of insecticides on arthropod biological control at field and landscape scales. Biol. Control, 75: 28–38 **(11 pages).**

Santi, S.R., (2010). Senyawa aktif anti makan dari umbi gadung (*Dioscorea hispida* Dennst). J. Kimia, 4(1): 71–78 **(8 pages).**

Sukri, M.Z.; Suwardi, F., (2016). Kelompok Tani Program Intensifikasi Sistem Minapadi (INSISMINDI). J-Dinamika. 1(1): 53-59 **(7 pages).**

Susanti, W.I.; Cholidah, S.N.; Agus, F., (2024). Agroecological nutrient management strategy for attaining sustainable rice self-sufficiency in Indonesia. Sustainability. 16(2): 845 **(29 pages).**

Teder, T.; Knapp, M., (2019). Sublethal effects enhance detrimental impact of insecticides on non-target organisms: A quantitative synthesis in parasitoids. Chemosphere. 214: 371–378 **(8 pages).**

Torres-Pagán, N.; Muñoz, M.; Barbero, S.; Mamone, R.; Peiró, R.; Carrubba; Verdeguer, M., (2024). Herbicidal potential of the natural compounds carvacrol, thymol, eugenol, p-cymene, citral and pelargonic acid in field conditions: indications for better performance. Agronomy. 14(3): 537 **(14 pages).**

Trisnawati, D.W.; Fadilah, M.; Nurkomar, I., (2022). Diversity and composition of arthropod natural enemies in integrated rice–fish farming system (Minapadi) and its functions in agroecosystems. IOP

Conference Series: Earth Environ. Sci., 985(1): 012047 **(7 pages).**
Widyaningrum, I., (2015). Pest and weed suppressive mechanisms in complex rice systems at Malang, East Java, Indonesia. Ph.D. Diss.; Wageningen University: Wageningen, The Netherlands **(65 pages).**
Wiratno; Siswanto; Trisawa, I.M., (2013). Development of research, formulation, and utilization of plant-based pesticides. J. Agric. Res. Develop., 32(4): 150–155 **(6 pages).**
Wiratno; Sutanto, K.D.; Nurawan, A.; Taufik, I.; Surdianto, Y.; Sutrisna, N.; Rizal, M.; Karmawati, E.S.; Soetopo, D.; Trisawa, I.R.; Rahardjo, I.B., (2025). Eco-friendly botanical insecticides to control brown leafhoppers and their effects on predators and the aquatic environment. Global J. Environ. Sci. Manage., 11(1): 113–128 **(16 pages).**

AUTHOR (S) BIOSKETCHES

Wiratno., Ph.D., Senior researcher, Research Center for Horticulture, National Research and Innovation Agency, Jl. Raya Jakarta-Bogor KM 46, Cibinong, Indonesia.
- Email: *wiratno02@Yahoo.com*
- ORCID: 0000-0001-6286-3352
- Web of Science ResearcherID: NA
- Scopus Author ID: 53508154800
- Homepage: http://www.wur.nl/en/education-programmes/wageningen-university.htm

Trisawa, I.M., Ph.D., Senior researcher, Research Center for Estate Crops, National Research and Innovation Agency, Jl. Raya Jakarta-Bogor KM 46, Cibinong, Indonesia.
- Email: *iwamara29@gmail.com*
- ORCID: 0000-0002-6956-1071
- Web of Science ResearcherID: NA
- Scopus Author ID: 57196435731
- Homepage: https://www.ipb.ac.id/beranda/

Taufik, I., Ph.D., Senior researcher, Research Center for Fishery, National Research and Innovation Agency, Jl. Raya Jakarta-Bogor KM 46, Cibinong, Indonesia.
- Email: *imam026@brin.go.id*
- ORCID: 0000-0001-8118-5294
- Web of Science ResearcherID: NA
- Scopus Author ID: 57203918186
- Homepage: https://www.ipb.ac.id/beranda/

Thesiana, L., Ph.D., Senior researcher, Research Center for Fishery, National Research and Innovation Agency, Jl. Raya Jakarta-Bogor KM 46, Cibinong, Indonesia.
- Email: *loli002@brin.go.id*
- ORCID: 0000-0002-8827-9127
- Web of Science ResearcherID: NA
- Scopus Author ID: 57214665660
- Homepage: https://civil.ui.ac.id/

Surdianto, Y., Ph.D., Senior researcher, Research Center for Food Crops, National Research and Innovation Agency, Jl. Raya Jakarta-Bogor KM 46, Cibinong, Indonesia.
- Email: *y.surdianto@yahoo.com*
- ORCID: 0000-0002-4127-6092
- Web of Science ResearcherID: NA
- Scopus Author ID: 57222190320
- Homepage: https://www.ipb.ac.id/beranda/

Sutrisna, N., Ph.D., Senior researcher, Research Center for Food Crops, National Research and Innovation Agency, Jl. Raya Jakarta-Bogor KM 46, Cibinong, Indonesia.
- Email: *ntrisna.ns@gmail.com*
- ORCID: 0009-0006-5789-2611
- Web of Science ResearcherID: NA
- Scopus Author ID: 57217115108
- Homepage: https://www.ipb.ac.id/beranda/

Ardi, I., Ph.D., Senior researcher, Research Center for Fishery, National Research and Innovation Agency, Jl. Raya Jakarta-Bogor KM 46, Cibinong, Indonesia.
- Email: *idil001@brin.go.id*
- ORCID: 0000-0002-8843-0579
- Web of Science ResearcherID: NA
- Scopus Author ID: 57203909744
- Homepage: https://www.ipb.ac.id/beranda/

Susanti, D., Ph.D., Senior researcher, Agriculture Faculty, University of Jenderal Soedirman, Purwokerto, Central Java, Indonesia
- Email: *dyah.susanti@unsoed.ac.id*
- ORCID: 0000-0001-8176-4982
- Web of Science ResearcherID: AAE-8636-2021
- Scopus Author ID: 56526798000
- Homepage: https://www.unsoed.ac.id/

AUTHOR (S) BIOSKETCHES

Minarni, E.W., Ph.D., Senior researcher, Agriculture Faculty, University of Jenderal Soedirman, Purwokerto, Central Java, Indonesia
▪ Email: *endang.minarni@unsoed.ac.id*
▪ ORCID: 0000-0003-3971-5049
▪ Web of Science ResearcherID: NA
▪ Scopus Author ID: 57223021784
▪ Homepage: https://www.unsoed.ac.id/

Nurawan, A., Ph.D., Senior researcher, Research Center for Horticulture, National Research and Innovation Agency, Jl. Raya Jakarta-Bogor KM 46, Cibinong, Indonesia.
▪ Email: *agus197@brin.go.id*
▪ ORCID: 0000-0002-5737-1916
▪ Web of Science ResearcherID: NA
▪ Scopus Author ID: 57700788800
▪ Homepage: https://www.unpad.ac.id/

Jufri, A., Ph.D., Senior researcher, Research Center for Estate Crops, National Research and Innovation Agency, Jl. Raya Jakarta-Bogor KM 46, Cibinong, Indonesia.
▪ Email: *akhm002@brin.go.id*
▪ ORCID: 0009-0003-6388-3445
▪ Web of Science ResearcherID: NA
▪ Scopus Author ID: 58761133400
▪ Homepage: https://www.ipb.ac.id/beranda/

Sukamto, Ph.D., Senior researcher, Research Center for Estate Crops, National Research and Innovation Agency, Jl. Raya Jakarta-Bogor KM 46, Cibinong, Indonesia.
▪ Email: *Sukamto@brin.go.id*
▪ ORCID: 0000-0003-1861-8127
▪ Web of Science ResearcherID: NA
▪ Scopus Author ID: 5748306400
▪ Homepage: http://www.agri.tohoku.ac.jp/en/

Apriyana, Y., Ph.D., Senior researcher, Research Cente for Climate and Atmosphere , National Research and Innovation Agency, Jl. Raya Puspitek 60, Tangerang Selatan 15310, Indonesia.
▪ Email: *yaya028@brin.go.id*
▪ ORCID: 0000-0003-1809-6103
▪ Web of Science ResearcherID: NA
▪ Scopus Author ID: 57212866604
▪ Homepage: https://www.ipb.ac.id/beranda/

Susanto, B., Ph.D., Senior researcher, Research Center for Food Crops, National Research and Innovation Agency, Jl. Raya Jakarta-Bogor KM 46, Cibinong, Indonesia.
▪ Email: *bamb074@brin.go.id*
▪ ORCID: 0000-0003-1442-3699
▪ Web of Science ResearcherID: NA
▪ Scopus Author ID: 57427935900
▪ Homepage: https://www.ipb.ac.id/beranda/

Susanto, U., Ph.D., Senior researcher, Research Center for Food Crops, National Research and Innovation Agency, Jl. Raya Jakarta-Bogor KM 46, Cibinong, Indonesia.
▪ Email: *untu009@brin.go.id*
▪ ORCID: 0000-0002-0992-2349
▪ Web of Science ResearcherID: NA
▪ Scopus Author ID: 55971074300
▪ Homepage: https://www.ipb.ac.id/beranda/

Kusrini, E., Ph.D., Senior researcher, Research Center for Fishery, National Research and Innovation Agency, Jl. Raya Jakarta-Bogor KM 46, Cibinong, Indonesia.
▪ Email: *enik002@brin.go.id*
▪ ORCID: 0000-0003-3656-5014
▪ Web of Science ResearcherID: NA
▪ Scopus Author ID: 57217095187
▪ Homepage: https://www.ipb.ac.id/beranda/

HOW TO CITE THIS ARTICLE

Wiratno; Trisawa, I.M.; Taufik, I.; Ardi, I.; Thesiana, L.; Kusrini, E.; Susanti, D.; Minarni, E.W.; Nurawan, A.; Jufri, A.; Sukamto; Apriyana, Y.; Sutrisna, N.; Surdianto, Y.; Susanto, B.; Susanto, U., (2025). Eco-friendly pest management in integrated rice-fish farming systems using plant-derived biopesticides to promote sustainable agriculture. Global J. Environ. Sci. Manage., 11(3): 983-1000.

DOI: 10.22034/gjesm.2025.03.07

URL: https://www.gjesm.net/article_723768.html

Global J. Environ. Sci. Manage. 11(3): 1001-1018, Summer 2025, Serial #43

Global Journal of Environmental Science and Management
(GJESM)

Homepage: https://www.gjesm.net/

Podcasts

ORIGINAL RESEARCH PAPER

The significance of clean energy, education, and environmental management in fostering a sustainable future

J. Fábregas Villegas[1,2], A. Palencia Díaz[2,*]

[1] *Mechanical Engineering Program, Autonomous University of the Caribbean, Colombia*

[2] *Doctorate Program in Engineering, Technological University of Bolívar, Colombia*

ARTICLE INFO

Article History:
Received 17 March 2025
Revised 19 May 2025
Accepted 20 June 2025

Keywords:
Atmospheric transmittance
Environment
Solar energy
Sustainability
Wind energy

ABSTRACT

BACKGROUND AND OBJECTIVES: In Santa Cruz del Islote, an island located in the Colombian Caribbean, the lack of access to reliable electricity significantly affects the quality of life and educational opportunities of its inhabitants. The ongoing dependence on diesel generator-powered polygeneration systems is financially unsustainable, detrimental to the environment, and unstable in operation. The island experiences an average energy autonomy of only 11 hours. Consequently, this study intends to assess the viability of introducing renewable energy systems, particularly solar and wind energy, designed to suit the island's specific climatic and geographic characteristics, with the objective of boosting energy self-sufficiency and encouraging equitable educational access

METHODS: The study focused on the assessment of meteorological and energy data obtained from Santa Cruz del Islote to evaluate the viability of solar and wind energy. Solar irradiance levels were evaluated using historical data and the application of atmospheric transmittance models. Another approach to understanding wind behavior involved examining historical meteorological data, developing wind rose diagrams, performing frequency analysis, and utilizing probability density functions. The study also included an assessment of the island's available renewable energy resources.

FINDINGS: The results indicate that Santa Cruz del Islote receives high levels of solar irradiance throughout the year, with average daily values around 4,290 and peak values exceeding 5,780 watt-hours per square meter. The wind behavior analysis revealed predominant directions toward the north and north-northeast, with average wind speeds ranging from 2.6 to 4.7 meters per second, suggesting the feasibility of harnessing this available renewable resource. Wind energy potential, however, changes with the seasons, experiencing diminished availability between May to November. These findings support the design of hybrid renewable energy systems tailored to local conditions.

CONCLUSION: The findings demonstrate that Santa Cruz del Islote is equipped with enough renewable energy resources to enable a move away from fossil fuels. Implementing clean energy technologies would not only reduce environmental impact and operational costs but also enhance educational infrastructure and digital access. The merging of sustainable practices, technological progress, and social fairness is vital for the enduring resilience and advancement of insular communities including Santa Cruz del Islote.

DOI: 10.22034/gjesm.2025.03.08

This is an open access article under the CC BY license (http://creativecommons.org/licenses/by/4.0/).

NUMBER OF REFERENCES
43

NUMBER OF FIGURES
10

NUMBER OF TABLES
1

*Corresponding Author:
Email: *argpalencia@utb.edu.co*
Phone: +5730 1372 2376
ORCID: 0000-0003-4947-5659

Note: Discussion period for this manuscript open until Sep 1, 2025 on GJESM website at the "Show Article".

INTRODUCTION

Many rural communities in the Colombian Caribbean (CC) face serious development challenges as non-interconnected zones (NIZ), meaning they are not connected to the National Interconnected System (NIS) (Colmenares-Quintero *et al.,* 2022; Fábregas *et al.,* 2024). Historically, this has limited access to vital services, particularly in the fields of education, healthcare, and the economy. In response, the Institute for Planning and Promotion of Energy Solutions for non-interconnected zones (IPSE) has played a crucial role in expanding energy access in Colombia, especially in NIZ areas (Garces *et al.,* 2021; Castro *et al.,* 2023). IPSE advocates for projects centered around solar and wind energy, which substantially elevate living standards in these communities (Eras-Almeida *et al.,* 2023; Zamora-Muñoz *et al.,* 2025). Despite these efforts, many NIZ communities in the CC still lack 24 hours (h) electricity, affecting daily life and limiting progress in education, health, and economic development. Hevia (2021) conducted a study on open government initiatives in Latin America and the Caribbean, underscoring the critical role of connectivity, educational investment, and equity, while also pointing out the limitations of current educational governance models. Pedraza-jiménez *et al.* (2024) emphasize the value of community-based environmental education that fosters identity, respect for diversity, and ecological awareness, recognizing the interdependence between humans and nature. In alignment with this, Bernal *et al*. (2021) recommend an environmental education approach aimed at marginalized Caribbean communities, utilizing self-structuring pedagogical models and active learning techniques. Although the Coronovirus desease 2019 (COVID-19) pandemic disrupted implementation, it helped internalize environmental concepts and spark scientific curiosity (Gidarjati *et al.,* 2024). Manjarres and Salazar (2021) criticize the rigidity and lack of innovation in Colombia's educational model, advocating for public investment in education that strengthens human capital and integrates science and technology into national development. Plasencia-Díaz (2021) provides a critical viewpoint on the consequences of the pandemic, drawing attention to the heightened school dropout rates and the erosion of intellectual and human capital, especially in disadvantaged and poorly connected communities. This situation calls for a paradigm shift in education, enabling the design of resilient and sustainable long-term strategies. Herrera (2020) contributes to this perspective by stressing the necessity of revitalizing schools as hubs of solidarity, democracy, and territorial diversity, fostering public discourse and acknowledging educators and students as key players in driving change. From an institutional standpoint, Galindo (2021) stresses the urgency of reforming the Ministry of Education's management model, moving toward a more innovative, digital, and human rights-centered public administration to reduce inequalities. Acevedo-Tarazona and Lizcano-Herrera (2021) point out that education budgets have historically been insufficient, forcing local communities to assume responsibilities that should fall under the State. Consequently, Blanco *et al.* (2022) highlight the concept of education as an essential right and a continuous process that encourages individual development, honors human rights, and aids in the creation of a more equitable society. In this context, Santa Cruz del Islote (SCDI), a small island in the CC, faces major challenges in both education and energy autonomy. Despite the introduction of innovative strategies such as environmental education, insufficient infrastructure and scarce resources obstruct their sustainability. Another major hurdle is the island's lack of energy self-sufficiency, as it is heavily dependent on pricey external energy supplies, which limits the adoption of educational technologies and curtails school programs. Expanding solar and wind energy offers a sustainable way to improve quality of life (Alazzam *et al.,* 2024). It also strengthens education by ensuring stable and equitable learning conditions. The implementation of renewable energy in non-interconnected insular zones (NIIZ) is a key opportunity for sustainable development and educational improvement. Fábregas Villegas *et al.* (2024) highlight the importance of selecting renewable energy projects through comprehensive life cycle cost analysis to maximize economic, social, and environmental benefits. Jareemit and Srivanit (2024) build upon this idea with innovative solar control systems that improve energy capture by utilizing fuzzy entropy algorithms, which in turn boosts the efficiency of solar panels. Baranitharan *et al.* (2024) emphasize the potential of wind energy as a sustainable source, stressing the importance of accurate wind speed (WS) and direction forecasts to

optimize its use. This data is essential for designing reliable energy systems that can be efficiently integrated into local grids. Furthermore, Castro *et al.* (2021) bolster this argument through their analysis of international microgrid case studies, showing that the synergy of solar, wind, and battery storage technologies effectively secures energy supply in isolated communities. The energy transition is key to improving life in vulnerable NIZ. The use of statistical tools, climate modeling, and techno-economic analysis enables more precise and efficient planning of sustainable energy systems. (Trenggono *et al.,* 2025). The evaluation of wind resources via statistical distributions, notably the Weibull distribution, has been thoroughly validated as a reliable approach for estimating wind energy potential. Studies such as those by Ávila *et al.* (2022), Vega-Zuñiga *et al.* (2022), and Souza *et al.* (2024) agree that accurately estimating the shape and scale parameters of this distribution is essential for reliably modeling wind resource availability. Furthermore, the application of numerical models, including the weather research and forecasting model, demonstrated effectiveness in relation to the CC, delivering comprehensive representations of atmospheric dynamics in designated regions (Gil *et al.,* 2022). On the other hand, solar energy has also been the subject of detailed analysis. Mejía *et al.* (2021) highlight how meteorological conditions such as ambient temperature and irradiance affect the performance of photovoltaic systems in the CC. From an implementation viewpoint, Diaz *et al.* (2021) recommend a holistic strategy that integrates renewable resource evaluation with green logistics and economic assessment to develop an off-grid energy generation system for the CC. These types of studies underscore the importance of conducting periodic statistical analyses at meteorological stations to identify wind and solar potential in the region. In long-term energy planning, tools like the autocorrelation function and wind rose diagrams are essential (Fabregas *et al.,* 2020; Wang and Liu, 2021; Froese *et al.,* 2022; Jooss *et al.,* 2022; Qothrunada *et al.,* 2022). In contexts like SCDI, IPSE, with the support of the Government of Colombia (GC) through its action plans, promotes access to sustainable and dignified energy autonomy for communities that have historically been excluded from the NIS. This initiative is supported by Law 1715 of 2014 (Castaño-Gómez and García-Rendón, 2020), enacted by the Colombian Congress, which aims to promote the development and use of non-conventional energy sources. By leveraging renewable energy options including solar and wind, the objective is to secure a consistent energy supply for SCDI and simultaneously encourage local development, education, and environmental conservation. Although the initial implementation costs of these technologies may be higher than those of diesel generators, their long-term operation proves to be more efficient, cleaner, and economically viable. As a preliminary measure, studying essential geographical factors such as solar irradiation, wind speed, and climate trends is critical for accurately determining renewable energy potential. This technical analysis is crucial for designing future renewable energy solutions that are tailored, sustainable, and socially impactful. This study presents an energy assessment of the solar and wind renewable resources available in the SCDI locality, based on historical meteorological data from 2020 to 2024.

MATERIALS AND METHODS

Locality of Santa Cruz Del Islote

The locality of SCDI is situated in the Bolívar Department, located at latitude 09°47’15’’N, longitude 75°51’32’’W, and at an elevation of 1 meter above sea level. It has an estimated population of over 1,000 inhabitants, resulting in a population density of approximately 125,000 people per square kilometer. This makes it one of the most densely populated islets, according to census approximations provided by the National Administrative Department of Statistics (NADS). Based on the reported population figures, it is estimated that there are more than four individuals per household, as illustrated in Fig. 1.

SCDI is a Caribbean paradise that, despite its natural beauty, faces significant infrastructure challenges. One of the most pressing issues is its limited energy autonomy approximately 11 hours of electricity per day according to the National Monitoring Center (CNM). This limitation directly impacts the quality of life of its residents. The educational center in SCDI stands as a symbol of hope and resilience for a community surrounded by the Colombian Caribbean Sea. Nonetheless, the geographic isolation and socioeconomic circumstances present a distinct illustration of the obstacles that vulnerable areas

Fig. 1:

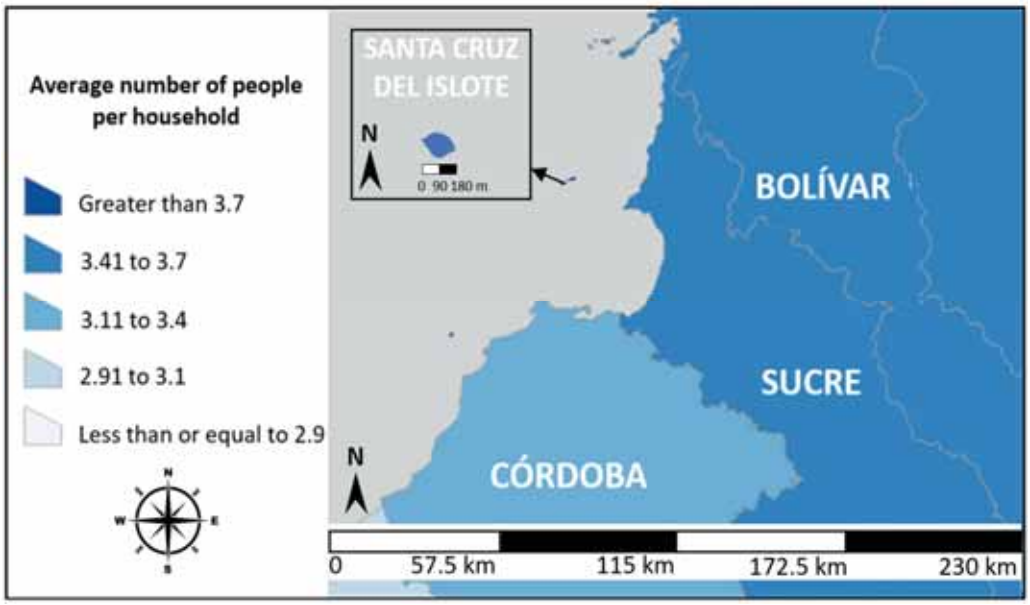

Fig. 1: Geographical location and the number of Inhabitants per Household in SCDI – Bolívar, Colombia

identified as NIIZ confront in achieving sustainable development and securing fundamental services including electricity. Education is a key tool for sustainable development, and in Santa Cruz del Islote, limited access to electricity directly affects educational quality. The unavailability of consistent power limits the application of educational technologies, curtails study hours, and endangers the refrigeration of food and essential pharmaceuticals. These issues conflict with several Sustainable Development Goals (SDGs), particularly Goal #7 (Affordable and Clean Energy), Goal #4 (Quality Education), and Goal #10 (Reduced Inequalities). Currently, the island's energy matrix relies heavily on fossil fuels, primarily through diesel generators. This source of energy is not just high-priced and polluting; it is also ineffective and inconsistent. There is an urgent need for an energy transition to improve residents' quality of life and ensure the right to a dignified education. In light of this reality, adopting renewable energy stands out as a sustainable and essential solution. Projects involving clean energy sources such as solar and wind power could not only enhance educational quality but also promote the comprehensive development of the community. SCDI currently operates a poly-generation energy system that integrates photovoltaic systems with a capacity of 67.5 kilowatt-peak (kWp) and a diesel combustion generator with a capacity of 100 kilowatt (kW), which includes 144 batteries, each with a capacity of 4,800 ampere-hours (Ah) at 2 volts (V).

Renewable energy in SCDI

Renewable energy sources like solar and wind offer sustainable solutions to reduce reliance on diesel generators. Solar energy utilizes plentiful sunlight, whereas wind power harnesses coastal winds to produce clean electricity. Together, these technologies can improve living conditions, support education, and promote environmental resilience.

Assessment of solar energy potential in SCDI

Atmospheric transmittance (AT) is a key parameter in assessing the solar potential of a region, as it determines the fraction of solar radiation that successfully passes through the Earth's atmosphere and reaches the surface. This occurrence is affected by various elements, such as the atmospheric chemical makeup, the elevation of the site, and the existence of aerosols, clouds, and contaminants. Each of these elements can attenuate, absorb, or scatter solar radiation, significantly affecting the amount of energy available for solar applications (Gutiérrez-Trashorras *et al.,* 2018). In the specific case of SCDI, a low-

altitude island located in the CC, AT takes on particular importance. Its geographic location near the equator provides high solar irradiance throughout the year. Nonetheless, higher levels of relative humidity and the potential for suspended marine particles may impact the quality of radiation reaching the surface. Understanding AT in this context is not only essential for accurately estimating the photovoltaic generation potential, but also for designing efficient solar systems tailored to local environmental conditions.

Bird and Hulstrom model

The bird and Hulstrom model (BHM) enables the calculation of total irradiance by combining the values of direct and diffuse irradiance on a horizontal surface. As one of the most comprehensive models available, it provides highly reliable results, using Eq. 1 (Benharrats and Mahi, 2023):

$$I_{TH} = I_{DH} + I_{dH} \quad (1)$$

Where;

I_{TH}: Total irradiance.

I_{DH}: Direct irradiance.

I_{dH}: Diffuse irradiance.

The direct irradiance on a horizontal surface can be determined using Eq., 2 (Budiyanto and Lubis, 2020):

$$I_{DH} = 0.9662 C_r \tau_r \tau_0 \tau_g \tau_w \tau_a sinsin A \quad (2)$$

Where;

C_r: Daily solar constant in W/m².

τ_r: Transmittance due to Rayleigh scattering by air molecules.

τ_o: Transmittance due to ozone absorption.

τ_g: Transmittance due to absorption by uniformly mixed gases.

τ_w: Transmittance due to water vapor absorption.

τ_a: Transmittance due to aerosol absorption and scattering.

A: Solar altitude angle in degrees.

The value of C_r varies according to Eq. 3 (Gutiérrez-Trashorras *et al.,* 2018):

$$C_r = C\left(1 + 0.033 cos \frac{360n}{365}\right) \quad (3)$$

Where;

C: Normalized solar constant = 1367 W/m².

n: Julian day.

To accurately model the attenuation of solar radiation as it passes through the atmosphere, it is essential to consider several distinct transmittance components. This encompasses the transmittance resulting from Rayleigh scattering by air molecules, the transmittance due to ozone absorption, the transmittance resulting from absorption by uniformly mixed gases, the transmittance due to water vapor absorption, and the transmittance caused by both absorption and scattering due to the presence of aerosols, using Eqs. 4, 5, 6, 7, and 8 (Vanegas *et al.,* 2020; Gutiérrez-Trashorras *et al.,* 2018):

$$\tau_r = e^{-0.0903 m_a^{0.84}\left(1 + m_a - m_a^{1.01}\right)} \quad (4)$$

$$\tau_0 = 1 - \left[0.1611\left[\left(L_o m_{rel}\right)\left(1 + 139.48 L_o m_{rel}\right)^{-0.3035}\right] + \frac{0.002715 L_o m_{rel}}{1 + 0.044 L_o m_{rel} + 0.003\left(L_o m_{rel}\right)^2}\right] \quad (5)$$

$$\tau_g = e^{-0.0127 m_a^{0.26}} \quad (6)$$

$$\tau_w = 1 - \frac{2.4959\left(WWm_{rel}\right)}{\left(1 + 79.034 WWm_{rel}\right)^{0.6828} + 6.385 WWm_{rel}} \quad (7)$$

$$\tau_a = 0.12445\alpha - 0.0162 + \left(1.003 - 0.125\alpha\right) e^{-\beta m_a\left(1.809\alpha + 0.5123\right)} \quad (8)$$

Where;

m_a: Optical air mass

L_o: Ozone layer thickness

m_{rel}: Relative air mass

WW: Precipitable water content in the vertical column

α: Mean particle size

β: Atmospheric turbidity coefficient

The product of all these coefficients, which account for the attenuation of direct radiation, is referred to as the global atmospheric transmittance of direct radiation.

Diffuse irradiance is calculated, using Eq. 9 (Vanegas *et al.,* 2020):

$$I_{dH} = I_{dr} + I_{da} + I_{dm} \quad (9)$$

Where;
I_{dr}: Scattering by air molecules.
I_{da}: Presence of dust and aerosols.
I_{dm}: Multiple reflections between the ground and the atmosphere.

The diffuse irradiance due to air molecules is calculated using Eq. 10 1ne 11 (Vanegas *et al.,* 2020):

$$I_{dr} = 0.79 C_r \tau_0 \tau_g \tau_w \tau_{aa} 0.5 \frac{1-\tau_r}{1-m_a+m_a^{1.02}} sinsin A \quad (10)$$

$$\tau_{aa} = 1-\left(1-\omega_o\right)\left(1-m_a+m_a^{1.06}\right)\left(1-\tau_a\right) \quad (11)$$

Where;
τ_{aa}: Transmittance due to aerosol absorption.
ω_o: Single scattering albedo.

Diffuse radiation due to aerosols is calculated using Eqs. 12, 13 and 14 (Silvera *et al.,* 2021):

$$I_{da} = 0.79 C_r \tau_0 \tau_g \tau_w \tau_{aa} F_c \frac{1-\tau_{as}}{1-m_a+m_a^{1.02}} sinsin A \quad (12)$$

$$F_c = 0.93 - 0.21 lnln\, m_a \quad (13)$$

$$\tau_{as} = \frac{\tau_a}{\tau_{aa}} \quad (14)$$

Where;
F_c: Fraction of energy at the Earth's surface due to aerosol scattering.
τ_{as}: Transmission coefficient due solely to aerosol scattering.

For the calculation of diffuse irradiance from multiple reflections, the reflection coefficients of all relevant surfaces must be considered, using Eq. 15 (Silvera *et al.,* 2021):

$$I_{dm} = \left(I_{DH} sinsin A + I_{dr} + I_{da}\right) \frac{\rho_g \rho'_a}{1-\rho_g \rho'_a} \quad (15)$$

To compute multiple reflections between the ground and the sky, using Eq. 16 (Silvera *et al.,* 2021):

$$\rho'_a = 0.0685 + \left(1+F_c\right)\left(1-\tau_{as}\right) \quad (16)$$

Using the aforementioned models, it is possible to perform an accurate assessment of the available solar potential for the locality of SCDI. The initial step in this process involves collecting historical meteorological data, which includes variables such as wind temperature (WT), relative humidity (RH), sunshine duration (SD), peak sun hours (PSHs), cloud cover factor (CCF), among others.

Peak sun hours

PSHs are a standardized measure that represents the amount of solar energy received by a surface in one day, expressed as the number of hours during which solar irradiance would be at 1000 W/m² the standard test condition for solar panels. This unit enables simple and consistent evaluation of solar resources across different regions and times of the year. PSHs are calculated from the total daily solar irradiation (TI_{TH}) in Wh/m^2, using Eq. 17 (Pérez *et al.,* 2017):

$$PSHs = \frac{TI_{TH}}{1000\, w/m^2} \quad (17)$$

Assessment of the wind energy potential in SCDI

The evaluation of wind energy potential in the locality of SCDI region requires an in-depth analysis of several meteorological and statistical parameters. Key components of this assessment include the study of wind rose diagrams to understand prevailing wind directions, the analysis of historical WS data, and the projection of wind behavior at different altitudes using vertical extrapolation models. Furthermore, the implementation of probability distribution laws, including the Weibull distributions, facilitates a more accurate illustration of WS variability over time. Furthermore, the analysis of wind frequency yields important information regarding the consistency and reliability of wind resources, which are vital for evaluating the feasibility and efficiency of wind energy systems within the region.

Probability density function of the distribution

The probability density function of the distribution (PDFD) provides the likelihood of different WSs occurring. This is vital for wind energy assessments, as the output power of a wind turbine is significantly affected by WS, generally proportional to the cube of the speed (Kassem *et a.,* 2018). By integrating the PDFD with the power curve of a wind turbine, one can estimate the expected energy output, capacity factor, and overall feasibility of wind power generation at a specific site such as SCDI.

Accurate representation of WS behavior is vital for determining the potential of wind energy. To achieve this, several probability distributions are commonly used in wind resource assessment. The following sections describe the Weibull, Gamma, and Logistic distributions, each offering unique characteristics that make them suitable for different types of WS data and analysis objectives. The Probability Density Function of the Weibull Distribution (PDFWD) is commonly used in wind energy studies due to its ability to model WS variability effectively. Its shape is determined by the scale and shape parameters. The Probability Density Function of the Gamma Distribution (PDFGD) is effective for representing data that is both asymmetric and strictly positive. Although it is less specific to WS analysis than the Weibull distribution, it can still provide valuable insights in certain contexts. The Probability Density Function of the Logistic Distribution (PDFLD) exhibits symmetry and possesses heavier tails, rendering it possibly beneficial in contexts where a more uniform distribution of WSs is expected. The mathematical expressions for each of the following probability distribution models *f(v);* Weibull, Gamma, and Logistic are presented as Weibull Distribution, using Eq. 18 (Kassem *et a.,* 2018):

$$f(v)=\left(\frac{k}{c}\right)\left(\frac{v}{c}\right)^{k-1} e^{-\left(\frac{v}{c}\right)^{k}} \quad (18)$$

Where;
v: Wind Speed
k: Shape parameter
c: Scale parameter

Gamma distribution was applied, using Eq., 19 (Nymphas and Teliat, 2024):

$$f(v)=\frac{v^{\xi-1}}{\beta^{\xi}\Gamma(\xi)}e\left(-\frac{v}{\beta}\right) \quad (19)$$

Where;
β: Shape parameter
ξ: Scale parameter in m/s.

Logistic Distribution was applied, using Eq., 20 (Kassem *et a.,* 2018):

$$f(v)=\frac{e^{\left(\frac{v-\mu}{\sigma}\right)}}{\sigma\left\{1+e^{\left(\frac{v-\mu}{\sigma}\right)}\right\}^{2}} \quad (20)$$

Where;
μ: location parameter.
σ: Scale parameter.

Hellman's law for WS extrapolation

WS is affected by obstacles, including surface irregularities and buildings, which interfere with the natural airflow. Wind measurements are typically taken in open areas at a standard height of 10 meters, and mathematical models are then applied to estimate how WS varies with height. This underscores the necessity of evaluating surface resistance factors, including the roughness of the terrain, any obstructions, and the height of the target for WS projection (Gunda *et al.,* 2021). The following sections present the Hellman power law and logarithmic wind profile equations, both of which are commonly used to estimate WS at different elevations, using Eq. 21 (Narasimalu *et al.,* 2018).

$$\frac{v}{v_0}=\left(\frac{H}{H_0}\right)^{\alpha} \quad (21)$$

Where;
v_0: Wind speed at 10 meters.
H_0: Reference height at 10 meters.
H: Desired height for wind speed estimation.
α: Wind shear coefficient for obstacles.

RESULTS AND DISCUSSION

This study presents the results derived from the analysis of the behavior and potential of renewable energy sources available in the locality of SCDI, as a strategy to enhance the community's energy autonomy. The purpose of the initiative is to cut down on reliance on external energy sources, especially diesel-powered generators, while also contributing to the enhancement of residents' quality of life, the advancement of sustainable development, and the fortification of educational processes within the community. The findings illustrated highlight the significant influence of these endeavors on the availability of clean energy through solar and wind renewable sources. The initial acquisition of historical meteorological data was carried out through nearby weather stations operated by the Institute of Hydrology, Meteorology and Environmental Studies (IDEAM) of Colombia, with additional support from the Prediction of Worldwide Energy Resources

(POWER) database, developed by the National Aeronautics and Space Administration (NASA).

Analysis of solar energy potential in SCDI

This section details the procedure for interpreting and examining meteorological data obtained from SCDI, intended to evaluate the behavior and potential of the solar energy resource in the area. The analysis initiates with crucial variables like air temperature, relative humidity, sunshine duration, and air density, all of which directly influence the efficiency and availability of solar energy. Understanding these data helps in pinpointing local climate patterns and allows for a more accurate appraisal of the practicality of adopting solar technologies within a sustainable energy transition framework for the community. Figs. 2 to 3 illustrate the monthly behavior of air temperature, relative humidity, and sunshine duration, based on measurements taken from 2020 to 2024.

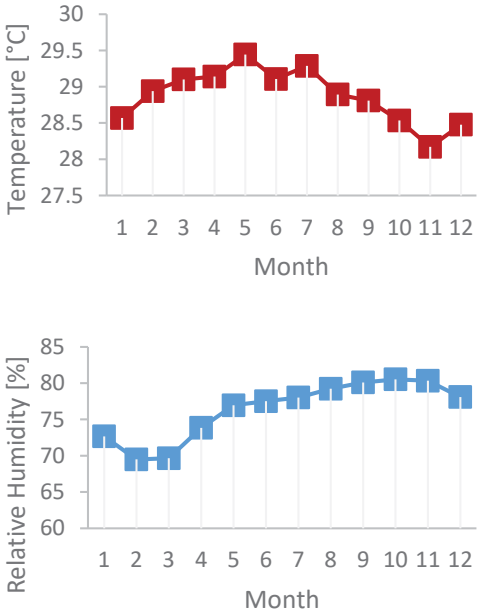

Fig. 2: Behavior of Ambient Temperature and Relative Humidity in the SCDI

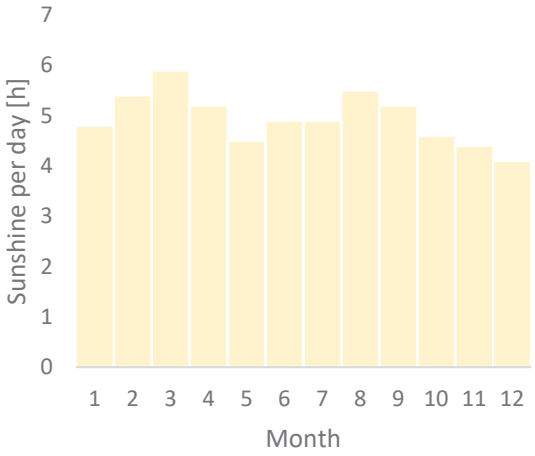

Fig. 3: Daily sunshine patterns throughout the 12 months of the year in SCDI

Table 1: Atmospheric transmittance behavior in SCDI

	Atmospheric transmittance factors				
	τ_r	τ_o	τ_g	τ_w	τ_a
JAN	0.9026	0.9842	0.9869	0.8609	0.6818
FEB	0.9079	0.9848	0.9871	0.8636	0.6989
MAR	0.9121	0.9850	0.9873	0.8649	0.7121
APR	0.9137	0.9849	0.9874	0.8639	0.7172
MAY	0.9128	0.9845	0.9873	0.8618	0.7143
JUN	0.9117	0.9843	0.9873	0.8617	0.7109
JUL	0.9122	0.9841	0.9873	0.8615	0.7126
AUG	0.9135	0.9843	0.9874	0.8622	0.7167
SEP	0.9130	0.9843	0.9873	0.8618	0.7150
OCT	0.9094	0.9842	0.9872	0.8606	0.7035
NOV	0.9039	0.9840	0.9869	0.8591	0.6860
DIC	0.9006	0.9838	0.9868	0.8582	0.6757

As shown in Fig. 2, the temperature behavior in SCDI reaches a minimum value of 28.17 degrees Celsius (°C) in November and a maximum of 29.44°C in May, with an average annual temperature of 28.9°C. Fig. 2 illustrates the relative humidity trends in the area, indicating minimum values of approximately 69.6 percent (%) RH during February and March, and maximum values around 80.5% RH in October and November. The annual average RH is 76.4%. Similarly, Fig. 3 presents the monthly sunshine duration in SCDI, highlighting March as the month with the highest solar exposure at 5.9 hours per day, and December as the lowest with 4.1 hours per day. On average, the annual sunshine lasts for roughly 5 hours daily.

Solar potential based on AT in SCDI

Using the BHM, equations 1 through 18 are applied to determine the available solar energy potential for the locality of SCDI, beginning with the calculation of atmospheric transmittance variables. Presented in Table 1 is the behavior of these atmospheric transmittance variables in SCDI for the period from 2020 to 2024, derived from the meteorological data previously examined.

Consequently, the appropriate values for direct, diffuse, and total solar irradiation are obtained based on the estimated AT and the influence of variables such as T, RH, SD, geographic latitude, elevation above sea level, moist air density, and other essential elements mentioned in the BHM.

Fig. 4 highlights that, for the month of December, the minimum daily solar irradiation potential for SCDI is observed, with a value of 3400 Wh/m². The maximum value of 5785.8 Wh/m² occurs in March, while the average is approximately 4290 Wh/m². According to Gutiérrez-Trashorras *et al.* (2018), and Benharrats and Mahi (2023), the solar radiation values provided through the BHM are representative for the effective utilization of the available solar resource. As a component of the preliminary study for expanding a photovoltaic generation system in SCDI, an assessment of the available solar radiation potential in the area was performed (Fig. 5). The aim was to identify the renewable energy resource and lay a strong technical groundwork for later phases of the project, including system sizing and cost assessment. This initial evaluation determined an average of 4.6 PSHs per day, indicating a moderately high and relatively stable solar availability throughout the year. This facilitates the detection of seasonal changes in solar capture, which will be vital for the upcoming design of energy storage systems. The results suggest that the solar potential is sufficient to meet the community's energy demand through a photovoltaic plant, ensuring 24 h energy autonomy. However, this analysis is limited to resource characterization. The

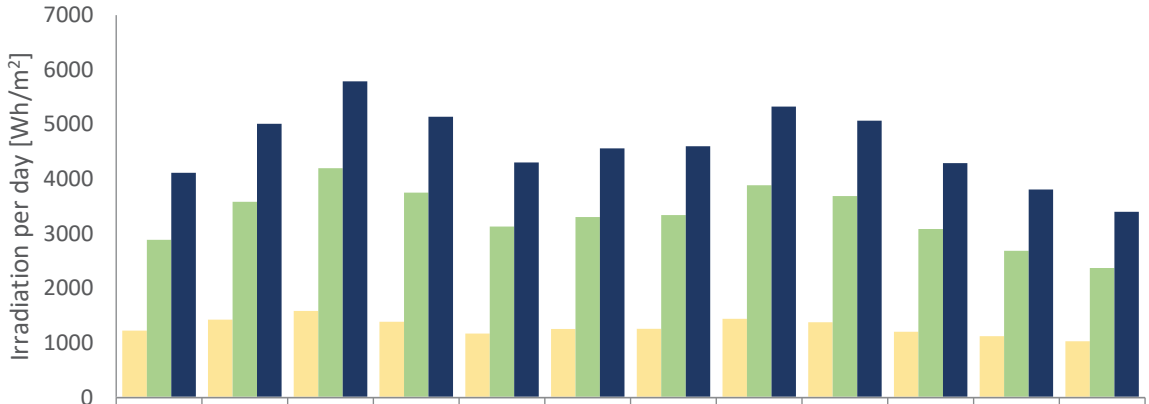

	1	2	3	4	5	6	7	8	9	10	11	12
IdH	1226.1	1425.8	1586.9	1388.9	1172.9	1255.2	1259.4	1441.5	1377.9	1205.5	1122.9	1030.1
IDH	2886.9	3582.9	4198.9	3749.6	3130.2	3305	3339	3884.5	3688.4	3084.8	2686	2370.7
ITH	4113	5008.7	5785.8	5138.4	4303.2	4560.2	4598.4	5326	5066.3	4290.3	3809	3400.7

Fig. 4: Daily Solar irradiation patterns throughout the 12 months of the year in SCDI

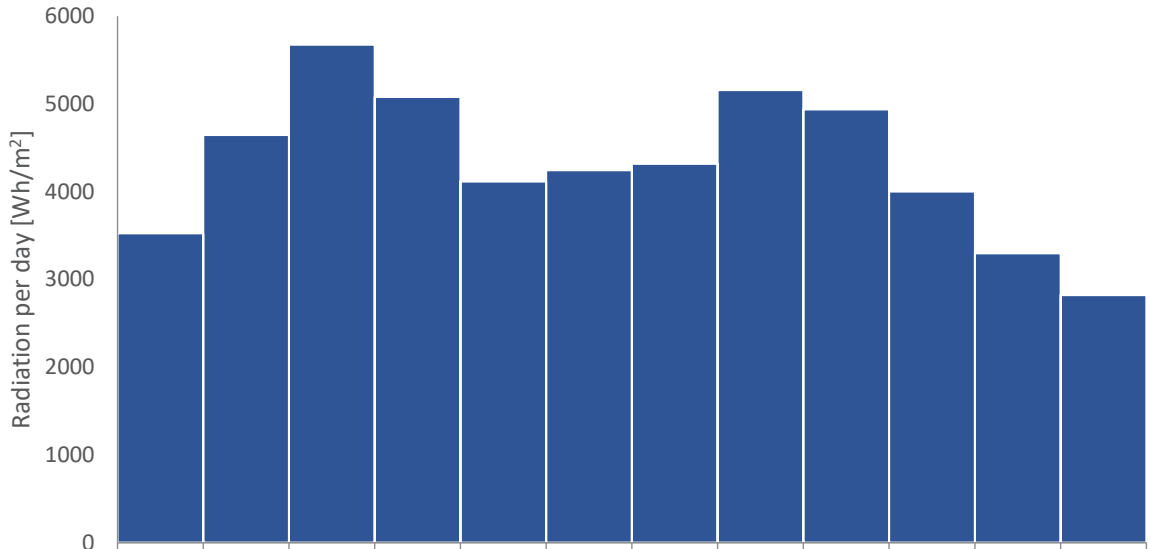

	1	2	3	4	5	6	7	8	9	10	11	12
RS	3524.3	4645.8	5673.8	5077.6	4114.9	4244	4315.4	5157.5	4936	4001.5	3297.3	2820.7

Fig. 5: Available solar radiation in the SCDI Location

precise sizing of the system and the assessment of its technical and economic viability will be covered in a later study that relies on the results presented in this document.

Wind energy potential analysis in SCDI

This section outlines the process of decoding and analyzing meteorological data collected in SCDI to evaluate the behavior and potential of wind energy resources in the region. The study emphasizes important variables, including WS and wind direction, that are crucial for evaluating the effectiveness and feasibility of wind energy systems. By interpreting these data, it is possible to identify local wind patterns

and assess the feasibility of implementing wind energy technologies as part of a sustainable energy transition strategy for the community. Figs. 6 and 7 illustrate the monthly variations in WS and direction, based on measurements recorded between 2020 and 2024.

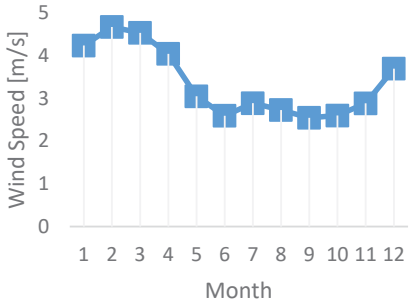

Fig. 6: Wind speed behavior throughout the 12 months of the year in SCDI

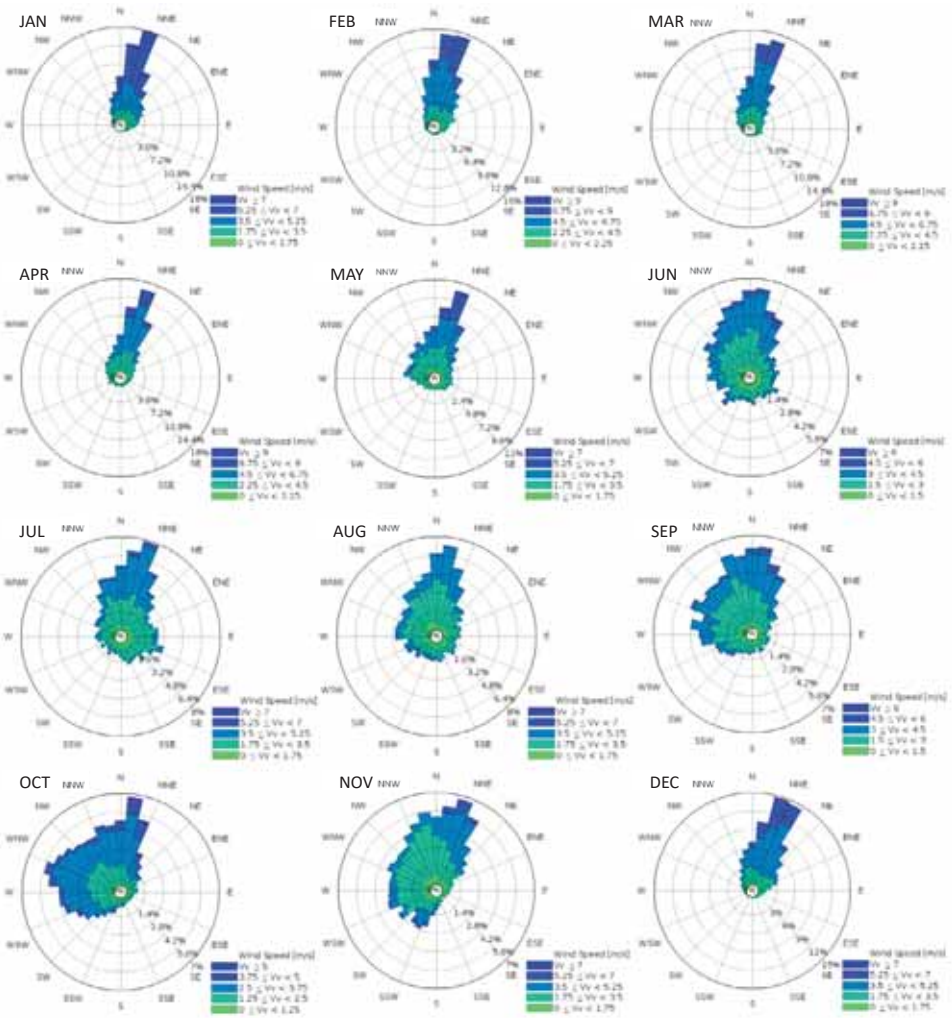

Fig. 7: Monthly wind rose diagrams in SCDI

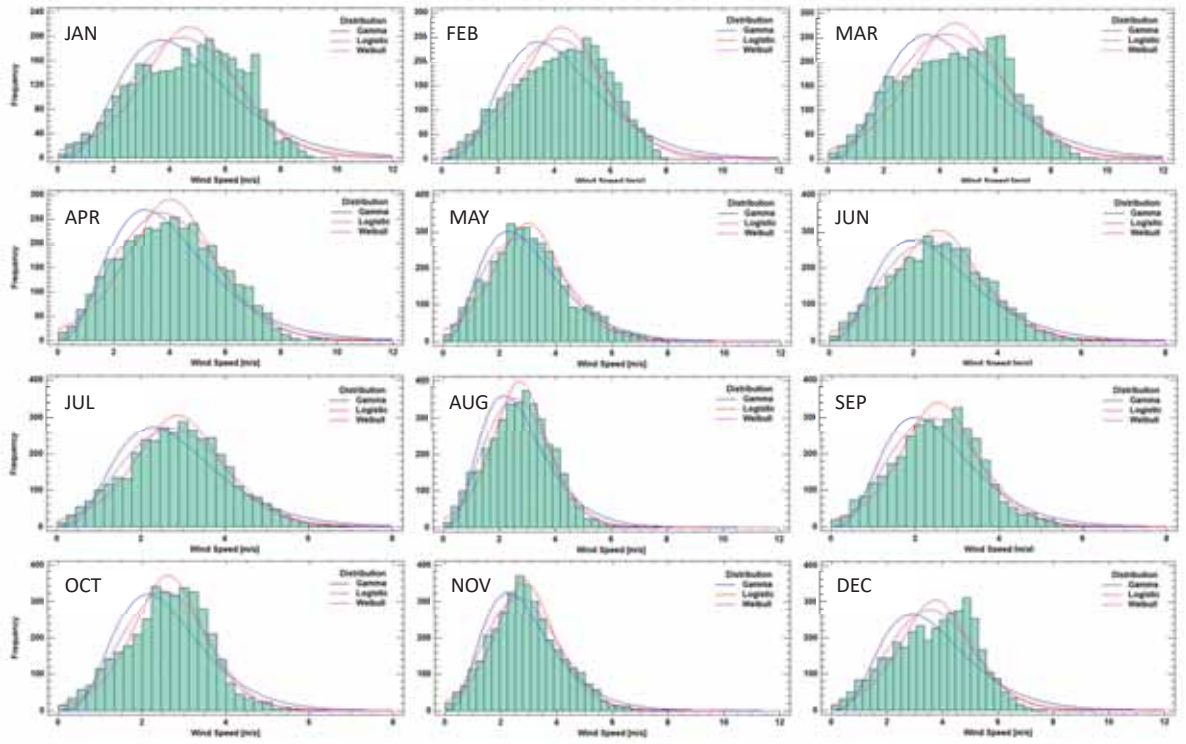

Fig. 8: Frequency histograms and PDFD of WS throughout the 12 months of the year in SCDI

Based on the obtained WS values, minimum and maximum speeds of 2.6 meters per second (m/s) and 4.7 m/s were observed, respectively, with an average value of 3.4 m/s (Fig. 6). It is essential to emphasize that these outcomes pertain to measurements taken at a reference height of 10 m above ground level. However, despite having minimum, maximum, and average WS values, these figures should not be directly used for sizing wind energy systems. Instead, statistical foundations such as WS frequency distribution studies and probability density functions should be applied for accurate energy potential assessments. Fig. 7 illustrates the wind direction behavior represented as wind roses, showing monthly patterns for the years 2020 through 2024. This illustration emphasizes the primary wind directions along with their occurrence frequency. The data reveals a greater frequency of winds from the north and north-northeast, with maximum wind speeds surpassing 9 m/s in particular months. The data show that the highest wind frequency is directed toward the north and north-northeast, with wind speeds most commonly falling within the range of 2.25 m/s to 4.5 m/s. The results imply that a horizontal axis wind turbine model (HAWT) can be installed with minimal necessity for directional adjustment mechanisms.

Once the WS behavior has been determined, PDFD laws such as Weibull, Gamma, and Logistic are applied. The aim is to pinpoint, each month, the areas exhibiting the greatest frequency density of WS occurs, based on statistical analyses of frequency, shape factors, and scale parameters.

Fig. 8 shows that WS behavior varies significantly throughout the year, highlighting the need for a detailed analysis to properly size a functional wind farm. In the last month and the early part of the year, there is a tendency for data density to gather around a WS of 4 m/s. In contrast, from May to November, the trend shifts to wind speeds between 2.5 m/s and 3 m/s. This pattern is reflected in the PDFWD, which provides a more accurate representation for wind energy studies, as noted by Kassem *et al.* (2018). Through the examining of WS's monthly behavior via PDFD, a yearly summary is created, as depicted in Fig.

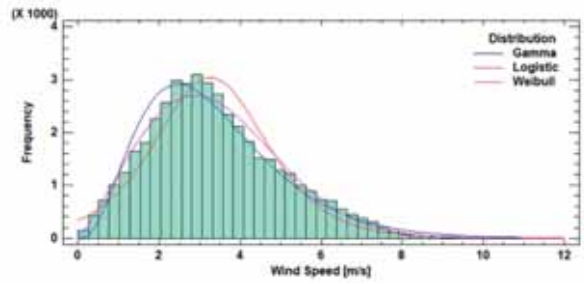

Fig. 9: Annual frequency histograms and PDFD of WS



	1	2	3	4	5	6	7	8	9	10	11	12
10m	1097.2	951.11	1059.4	757.23	336.57	242.55	202.94	157.19	215.63	167.9	172.32	727.73
25m	1612.2	1397.5	1556.6	1112.7	494.55	356.4	298.2	230.97	316.84	246.72	253.21	1069.3
50m	2157	1869.8	2082.6	1488.7	661.67	476.83	398.97	309.03	423.9	330.09	338.77	1430.7
100m	2885.9	2501.7	2786.4	1991.7	885.26	637.97	533.8	413.45	567.15	441.63	453.26	1914.1

Fig. 10: Wind energy potential at different heights throughout the 12 months of the year in SCDI

9. According to the PDFWD law and at the intersection point of the PDFGD and PDFLD a WS value of 3.1 m/s is identified. This value serves as the benchmark for energy design in wind turbine systems. The shape and scale factors used for replicating the PDFWD were k = 2.2 and c = 3.8 m/s, respectively.

The annual wind energy potential available for the SCDI locality is determined using wind behavior data and the PDFWD. In light of the results, Fig. 10 demonstrates how this potential behaves at various elevations, utilizing the equation from Hellman's law, which is presented in Equation 22. A significant increase in available wind power potential can be observed with height. However, from May to November, the daily wind resource potential remains low. The practicality of creating a wind energy generation site in proximity to the SCDI locality relies on the wind potential patterns depicted in Fig. 10. Nevertheless, as a naturally available resource, it can still be harnessed to benefit this vulnerable population. In a forthcoming study project, the authors aim to examine approaches for leveraging this existing wind potential. Additionally, it is important to highlight that providing energy access to a vulnerable population in an NIIZ, such as SCDI, aligns with the strategic objectives of the GC and the IPSE. Their

strategic plans focus on expanding sustainable energy solutions to marginalized communities, especially by implementing clean energy technologies. This initiative not only promotes social equity and energy inclusion but also contributes to national efforts toward energy decarbonization and environmental sustainability.

CONCLUSION

This study highlights the urgent need to transform the energy matrix of island communities such as SCDI, where limited electricity autonomy and continued dependence on fossil fuels pose not only economic and environmental challenges but also restrict access to fundamental rights such as education. Another thorough analysis of meteorological and energy data indicates that suitable conditions are present for the deployment of renewable energy technologies—specifically solar and wind energy customized to the island's specific geographic and atmospheric traits. The high annual solar irradiance and the presence of exploitable, albeit variable, wind patterns provide a solid foundation for the design of hybrid systems capable of delivering continuous, efficient, and sustainable energy supply. The potential for daily solar irradiance averaging 4,290 Wh/m² indicates a considerable resource that can be leveraged to assist this vulnerable population classified as NIIZ. The average daily wind energy potential of 745.4 Wh/m², projected at a height of 25 meters, while lower in magnitude compared to solar potential, indicates the presence of a viable natural resource for energy generation. This facilitates the creation of initiatives that encourage the utilization of clean energy sources. This shift towards sustainable energy will not just decrease pollutant emissions and operational expenses; it will also directly strengthen educational infrastructure, increase access to digital resources, and advance equity in learning opportunities. In this context, energy becomes a cross-cutting pillar for sustainable development, aligned with the Sustainable Development Goals (SDGs), particularly SDG 7 (Affordable and Clean Energy), SDG 4 (Quality Education), and SDG 10 (Reduced Inequalities). The implementation of clean energy solutions in the Southern Caribbean Islands is not only technically feasible but also socially imperative and ethically unavoidable. This investigation sets the stage for upcoming studies that seek to improve the application of solar and wind resources in order to create holistic strategies that enhance the resilience of island communities when confronted with energy, educational, and environmental obstacles.

ACKNOWLEDGEMENT

This study addresses the challenge of sustainable electrification in an island region with limited energy autonomy. It focuses on developing viable solutions to improve energy access and resilience in non-interconnected areas. The study is being carried out as part of the Ph.D. candidacy in the Doctoral Program in Engineering at the Technological University of Bolívar, Colombia.

CONFLICT OF INTEREST

The authors declares that there is no conflict of interests regarding the publication of this manuscript. In addition, the ethical issues, including plagiarism, informed consent, misconduct, data fabrication and/or falsification, double publication and/or submission, and redundancy have been completely observed by the authors.

OPEN ACCESS

©2025 The author(s). This article is licensed under a Creative Commons Attribution 4.0 International License, which permits use, sharing, adaptation, distribution and reproduction in any medium or format, as long as you give appropriate credit to the original author(s) and the source, provide a link to the Creative Commons license, and indicate if changes were made. The images or other third-party material in this article are included in the article's Creative Commons license, unless indicated otherwise in a credit line to the material. If material is not included in the article's Creative Commons license and your intended use is not permitted by statutory regulation or exceeds the permitted use, you will need to obtain permission directly from the copyright holder. To view a copy of this license, visit: http://creativecommons.org/licenses/by/4.0/

PUBLISHER'S NOTE

GJESM Publisher remains neutral with regard to jurisdictional claims in published maps and institutional afflictions.

Positive AI Statement

During the preparation of this work the author(s) have used Artificial Intelligence (AI) [NAME TOOL / SERVICE] in order to [REASON]. After using this tool/ service, the authors reviewed and edited the content as needed and take full responsibility for the content of the publication.

(For this reason, the GPTZero detector will evaluate the manuscript utilizing Generative AI, ensuring a high detection rate. If the manuscript relies heavily on Generative AI and AI-assisted technologies, it will be archived without further options for appeal).

Negative AI Statement

The author(s) declare that no AI tools or services were not used or not highly applied during the preparation of this work.

ABBREVIATIONS

%	Percent
°C	Degree Celsius
AT	Atmospheric transmittance
BHM	Bird and Hulstrom model
CC	Colombian Caribbean
CCF	Cloud cover factor
COVID-19	Coronovirus desease 2019
HAWT	Horizontal axis wind turbine model
IDEAM	Institute of hydrology, meteorology and environmental studies
NADS	National administrative department of statistics
NASA	National aeronautics and space administration
NIS	National interconnected system
NIIZ	Non-interconnected insular zones
NIZ	Non-interconnected zones
CNM	National Monitoring Center
PDFD	probability density function of the distribution
GC	Government of Colombia
PDFGD	Probability Density Function of the Gamma Distribution
PDFLD	Probability Density Function of the Logistic Distribution
PDFWD	Probability Density Function of the Weibull Distribution
POWER	Prediction of worldwide energy resources
IPSE	Institute for planning and promotion of energy solutions for non-interconnected zones
PSHs	peak sun hours
RH	Relative humidity
SCDI	Santa Cruz del Islote
SD	Sunshine duration
SDGs	Sustainable development goals
WS	Wind speed
WT	Wind temperature
I_{TH}	Total irradiance
I_{DH}	Direct irradiance
I_{dH}	Diffuse irradiance
I_{dr}	Scattering by air molecules
I_{da}	Presence of dust and aerosols
I_{dm}	Multiple reflections between the ground and the atmosphere
TI_{TH}	Total daily solar irradiation
τ_r	Transmittance due to Rayleigh scattering by air molecules
τ_o	Transmittance due to ozone absorption
τ_g	Transmittance due to absorption by uniformly mixed gases
τ_w	Transmittance due to water vapor absorption
τ_a	Transmittance due to aerosol absorption and scattering
τ_{aa}	Transmittance due to aerosol absorption
τ_{as}	Transmission coefficient due solely to aerosol scattering
A	Solar altitude angle in degrees
C	Normalized solar constant
C_r	Daily solar constant
h	Hours
n	Julian day
m_a	Optical air mass

L_o	Ozone layer thickness
m_{rel}	Relative air mass
m/s	Meters per second
Wh/m²	Watt-hours per square meter
m	Meter
km	kilometer
kW	kilowatt
kWp	kilowatt-peak
Ah	Ampere-hours
V	Volts
WW	Precipitable water content in the vertical column
α	Mean particle size
β	Atmospheric turbidity coefficient
ω_o	Single scattering albedo
F_c	Fraction of energy at the Earth's surface due to aerosol scattering
f(v)	probability distribution models
v	Wind Speed
k	Shape parameter
c	Scale parameter
β	Shape parameter
ξ	Scale parameter
μ	location parameter
σ	Scale parameter
v_0	Wind speed at 10 meters
H_0	Reference height at 10 meters
H	Desired height for wind speed estimation
α	Wind shear coefficient for obstacles

REFERENCES

Acevedo-Tarazona, Á.; Lizcano-Herrera, D., (2021). Misiones económicas en colombia y su incidencia en la educación técnica industrial (1930-1960). Rev. CS., (34): 241–264 **(24 pages).**

Alazzam, I.; Shatanawi, K.; Al-Weshah, R., (2024). Rainwater and fog harvesting from solar panels. Global J. Environ. Sci. Manage., 10(3): 955-968 **(14 pages).**

Ávila, A.; Pérez, D.; Jiménez, J., (2022). Análisis del potencial eólico a través de la función de distribución de weibull y rosa de los vientos. Ladee., 3(1): 40–46 **(7 pages).**

Baranitharan, B.; Sivakumar, D.; Selvan, M., (2024). Wind speed and direction on predicting wind energy availability for a sustainable ecosystem. Global J. Environ. Sci. Manage., 10(4): 1573–1592 **(20 pages).**

Benharrats, F.; Mahi, H., (2023). Clear sky global surface solar irradiance estimation from bird & hulstrom radiometric model/modis atmospheric data combination. J. Renew. Energ., 26(1): 31–39 **(9 pages).**

Bernal, G.; Congote, D.; Urrego, L.; Restrepo, S.; Quintero, J; Rivera, M.; Gutiérrez, M.; Builes, S.; Mateus, M.; Castilo, K.; Castro, C.; Muñoz, M., (2021). Experiencia de aprendizaje activo lúdico para generar conciencia ambiental en comunidades marginales / a playful active learning experience to generate environmental awareness in marginal communities. Braz. J. Anim. Environ. Res., 4(2): 1829–1856 **(28 pages).**

Blanco, Y.; Zuleta, M.; Vásquez, M., (2022). Models of public management in education: verticality versus horizontality. Rev. Venez. Gerenc., 27(100): 1405–1422 **(18 pages).**

Budiyanto, M.; Lubis, M., (2020). Physical reviews of solar radiation models for estimating global solar radiation in Indonesia. Energy Rep., 6: 1206–1211 **(6 pages).**

Castaño-Gómez, M.; García-Rendón, J., (2020). Análisis de los incentivos económicos en la capacidad instalada de energía solar fotovoltaica en Colombia. Lect. Econ., (93): 23–64 **(42 pages).**

Castro, A.; Troncoso-Mendoza, S.; Gallardo, R.; Zamora-Musa, R., (2021). A review: integration of renewable energies in the sustainability of the electric distribution grid. Int. J. Energy Econ. Policy., 11(4): 240–248 **(9 pages).**

Castro; J.; Buitrago, L.; Téllez, S.; Giraldo, S.; Zapata, J., (2023). Comunidades energéticas: modelos para el empoderamiento de los usuarios en colombia. Enerlac. Rev. Energ. Lat. Am. Caribe., 7(1): 110–133 **(24 pages).**

Chamorro, M.V.; Espinel-Blanco, E.; Rojas, J.P., (2020). Direct, diffuse and total solar radiation data set in La Guajira, Magdalena and Cesar Departments - Colombia. Data Brief., 33: 1–13 **(13 pages).**

Colmenares-Quintero, R.; Maestre-Gongora, G.; Baquero-Almazo, M.; Stansfield, K.; Colmenares-Quintero, J., (2022). Data analysis of electricity service in colombia's non-interconnected zones through different clustering techniques. Energies. 15(20): 1–16 **(16 pages).**

Diaz, L.; Ramirez, L.; Fabregas, J., (2021). Green logistics in off-grid renewable energy projects for the rural localities. Int. J. Tech. Phys. Probl. Eng., 13(3): 119–124 **(6 pages).**

Eras-Almeida, A.; Vásquez-Hernández, T.; Hurtado-Moncada, M.; Egido-Aguilera, M., (2023). A comprehensive evaluation of off-grid photovoltaic experiences in non-interconnected zones of colombia: integrating a sustainable perspective. Energies. 16(5): 1–23 **(23 pages).**

Fábregas Villegas, J.; Tovar Ospino, I.; Palencia Díaz, A., (2024). Electrification as a development and sustainability approach in rural areas using renewable energy sources. Global J. Environ. Sci. Manage., 10(4): 2115–2126 **(12**

pages).

Fabregas, J.; Valencia, G.; Vanegas, M., (2020). Statistical wind energy analysis and wind persistence assessment for cordoba and sucre departments' weather stations in the caribbean region of colombia. Int. J. Adv. Sci. Eng. Inf. Technol., 10(5): 1760–1766 **(7 pages).**

Froese, G.; Ku, S.; Kheirabadi, A.; Nagamune, R., (2022). Optimal layout design of floating offshore wind farms. Renew. Energy., 190: 94–102 **(9 pages).**

Galindo, V., (2021). Ministerio de educación nacional de colombia: un nuevo modelo de gestión y redes colaborativas para una educación con calidad. Opera., (29): 139–161 **(23 pages).**

Garces, E; Tomei, J.; Franco, C.; Dyner, I., (2021). Lessons from last mile electrification in colombia: examining the policy framework and outcomes for sustainability. Energy Res. Soc. Sci., 79: 102156 **(1 page).**

Gidarjati, M.; Matsumoto Gidarjati, M.; Matsumoto, T., (2024). Correlation between meteorological variables, air quality, and the Coronavirus-19 pandemic events. Global J. Environ. Sci. Manage., 10(4): 1961-1976 **(16 pages).**

Gil, S.; Cañón, J.; Martínez, J., (2022). Assessment and validation of wind power potential at convection-permitting resolution for the caribbean region of colombia. Energy. 244: 1–13 **(13 page).**

Gunda, I.; Chikuni, E.; Tazvinga, H.; Mudare, J., (2021). Estimating wind power generation capacity in zimbabwe using vertical wind profile extrapolation techniques: a case study. J. Energy South. Afr., 32(1): 14–26 **(13 pages).**

Gutiérrez-Trashorras, A.; Villicaña-Ortiz, E.; Álvarez-Álvarez, E.; González-Caballín, J.; Xiberta-Bernat, J.; Suarez-López, M., (2018). Attenuation processes of solar radiation. application to the quantification of direct and diffuse solar irradiances on horizontal surfaces in mexico by means of an overall atmospheric transmittance. Renew. Sustainable Energy Rev., 81: 93–106 **(14 pages).**

Herrera, D., (2020). El modelo de la alternancia y la desigualdad educativa territorial en la educación en colombia. Rev. Int. Pedagog. Innov. Educ., 1(2): 61–86 **(26 pages).**

Hevia, F., (2021). Gobierno abierto y educación en américa latina y el caribe. Estud. Sociol., 40(118): 85–122 **(38 pages).**

Jooss, Y.; Berg, E.; Jason, R.; Bracchi, T., (2022). Influence of position and wind direction on the performance of a roof mounted vertical axis wind turbine. J. Wind Eng. Ind. Aerodyn., 230: 1–11 **(11 page).**

Kassem, Y.; Gökçekus, H.; Çamur, H., (2018). Economic assessment of renewable power generation based on wind speed and solar radiation in urban regions. Global J. Environ. Sci. Manage., 4(4): 465–482 **(18 pages).**

Manjarres, J.; Salazar, R., (2021). El gasto público en los pilares de educación (cobertura, calidad, pertinencia y eficiencia): una revisión bibliográfica. Conocim. Global., 6: 76–96 **(21 pages).**

Mejía, S.; Vanegas, M.; Valencia, G.; Fábregas, J.; Acevedo, C., (2021). Effects of Environmental Conditions on Photovoltaic Generation System Performance with Polycrystalline Panels. Int. J. Adv. Sci. Eng. Inf. Technol., 11(5): 2031–2038 **(8 pages).**

Narasimalu, S.; Narasimhaumurthy, R.; Kannan, A., (2018). Geospatial model to estimate wind energy resource potential in remote locations. Asian Conf. Energy Power Transp. Electrific., 1(1): 1–7 **(7 pages).**

Nymphas, E.; Teliat, R., (2024). Evaluation of the performance of five distribution functions for estimating Weibull parameters for wind energy potential in Nigeria. Sci. Afr., 23: 1–20 **(20 pages).**

Pedraza-Jiménez, Y.; Hernández-Barbosa, R.; Alvear-Narváez, N., (2024). Editorial educación ambiental comunitaria. Tecné, Episteme y Didaxis: TED., 54: 7–10 **(4 pages).**

Pérez, M.; Morales, I.; Castro, E., (2017). The Hour Equivalent Solar Peak, Definition and Interpretation. J. Energ. Eng., 38(2): 124–131 **(8 pages).**

Plasencia-Díaz, A., (2021). ¿Hacia una nueva realidad educativa? complejidad, educación y poscovid. Educ. Pedagogía. 5(9): 10–13 **(4 pages).**

Qothrunada, D.; Satria, H.; Putra, Y., (2022). Analisis diagram windrose di konawe selatan. J. Sains Riset., 12(1): 22–26 **(5 pages).**

Silvera, O.; Vanegas, M.; Valencia-Ochoa, G., (2021). Wind and solar resource assessment and prediction using artificial neural network and semi-empirical model: Case study of the Colombian Caribbean region. Heliyon. 7(9): 1–13 **(13 pages).**

Souza, A.; Medeiros, E.; Bicalho, C.; Olinda, R., (2024). A comprehensive analysis of weibull distribution parameter estimation methods to improve wind potential assessment. Ciência e Natura. 46: 1–24 **(24 pages).**

Trenggono, S.W.; Meilano, I.; Latief, H.; Diantara, S.D.; Sakti, W.; Ketaren, D.G.K.; Winata, I.N.P.; Yuwono, T.; Syamdidi; Arthatiani, F.Y.; Kasim, K.; Radiarta, I.N., (2025). Innovation in the blue economy and environmental sustainability in marine and fisheries strategy

Global J. Environ. Sci. Manage., 11(2): 497-518 **(22 pages).**

Vega-Zuñiga, S.; Rueda-Bayona, J.; Ospino-Castro, A., (2022). Evaluation of eleven numerical methods for determining weibull parameters for wind energy generation in the caribbean region of colombia. Math. Model. Eng. Probl., 9(1): 194–199 **(6 pages).**

Wang, Z.; Liu, W., (2021). Wind energy potential assessment based on wind speed, its direction and power data. Sci. Rep., 11(1): 1–15 **(15 pages).**

Zamora-Muñoz, A.; Orozco-Gutierrez, M.; Lopez-Santiago, D.; Montenegro-Oviedo, J.; Ramos-Paja, C., (2025). Battery sizing method for microgrids—a colombian application case. Computation., 13(5): 1–20 **(20 pages).**

AUTHOR (S) BIOSKETCHES

Fábregas Villegas, J., Ph.D. candidate, Engineering, Technological University of Bolívar, Colombia. And Researcher, Mechanical Engineering Program, Autonomous University of the Caribbean, Colombia.
▪ Email: *jfabregas@utb.edu.co, jonathan.fabregas@uac.edu.co,*
▪ ORCID: 0000-0003-1924-8666
▪ Web of Science ResearcherID: GVS-8825-2022
▪ Scopus Author ID: 57353034200
▪ Homepage: https://investigaciones.uac.edu.co/grupos-de-investigacion-giima

Palencia Díaz, A., Ph.D., Professor, Doctorate Program in Engineering, Technological University of Bolívar, Colombia.
▪ Email: *argpalencia@utb.edu.co*
▪ ORCID: 0000-0003-4947-5659
▪ Web of Science ResearcherID: NA
▪ Scopus Author ID: 57353034200
▪ Homepage: https://www.utb.edu.co/profesores/argemiro-palencia-diaz

HOW TO CITE THIS ARTICLE

Fábregas Villegas, J.; Palencia Díaz, A., (2025). Building a Sustainable Future: The Role of Clean Energy, Education, and Environmental Engagement. Global J. Environ. Sci. Manag., 11(3): 1001-1018.

DOI: 10.22034/gjesm.2025.03.08

URL: https://www.gjesm.net/article_725363.html

Global J. Environ. Sci. Manage. 11(3): 1019-1034, Summer 2025, Serial #43

Global Journal of Environmental Science and Management
(GJESM)

Homepage: https://www.gjesm.net/

Podcasts

ORIGINAL RESEARCH PAPER

Monsoonal influence on particulate organic carbon variability through satellite data analysis

C.K. Tito[1,2], D.G. Bengen[1,*], T. Prartono[1], A. Damar[3,4], A.J. Wahyudi[2]

[1] *Department of Marine Science and Technology, Faculty of Fisheries and Marine Sciences, IPB University, IPB Dramaga Campus, Bogor, Indonesia*

[2] *Research Center for Oceanography, National Research and Innovation Agency, Jl. Pasir Putih I, Jakarta, Indonesia*

[3] *Department of Aquatic Resources Management, Faculty of Fisheries and Marine Sciences, IPB University, IPB Dramaga Campus, Bogor, Indonesia*

[4] *Center for Coastal and Marine Resources Studies, IPB University, IPB Dramaga Campus, Bogor, Indonesia*

ARTICLE INFO

Article History:
Received 04 February 2025
Revised 08 April 2025
Accepted 12 May 2025

Keywords:
Forecasting; Jakarta Bay
Monsoon
Particulate organic carbon (POC)
Riverine input

DOI: 10.22034/gjesm.2025.03.09

ABSTRACT

BACKGROUND AND OBJECTIVES: The concentration of particulate organic carbon serves as a key indicator of biological productivity within the euphotic zone. Estimating its variability delivers key perspectives on the overarching trends in. The objective of this study is to explore the distribution of particulate organic carbon over time and space, as well as to model its fluctuations in Jakarta Bay, thereby enriching the knowledge of organic carbon dynamics in coastal ecosystems.

METHODS: Monthly moderate-resolution imaging spectroradiometer satellite data for surface particulate organic carbon and chlorophyll-a during 2011 to 2023 periods were collected. In addition, seasonal in-situ data of salinity, sea surface temperature, dissolved oxygen, nitrate, and phosphate, were examined to assess the potential impact of natural processes on the fluctuations of particulate organic carbon variability in this bay. The seasonal autoregressive integrated moving average model was selected for particulate organic carbon forecast.

FINDINGS: The concentration of particulate organic carbon varied between approximately 230 and 340 within the observed range. Significant concentrations were noted in the nearshore areas owing to the river's outflow into the bay. The seasonal variation indicates that the highest concentrations occur during the north west monsoon. Meanwhile, the lowest concentrations were observed during the Inter-monsoon II. In spite of the considerable variability, the trend in particulate organic carbon is almost constant (Coefficient of determination 0.0002) from retrospective analysis to predictive modeling.

CONCLUSION: The results showed that in Jakarta Bay, particulate organic carbon variability is primarily influenced by a combination of biological production and physical transport processes modulated by monsoonal forcing. The predictions indicate that, under the current pressures, there will be negligible near-term shifts in the dynamics of particulate organic carbon along the northern coastline of Jakarta.

This is an open access article under the CC BY license (http://creativecommons.org/licenses/by/4.0/).

NUMBER OF REFERENCES	NUMBER OF FIGURES	NUMBER OF TABLES
51	4	3

*Corresponding Author:
Email: *dietriechbe@apps.ipb.ac.id*
Phone: +62 25 8629 083
ORCID: 0000-0002-3880-5117

Note: Discussion period for this manuscript open until Sep 1, 2025 on GJESM website at the "Show Article".

INTRODUCTION

The marine environment relies on organic substances to carry out important natural processes (Chester and Jickells, 2012). Studies have demonstrated that the concentrations of particulate organic carbon (POC) in seawater arise from natural processes connected to the actions of biota (Maciejewska and Pempkowiak, 2014). The coastal region has higher biological productivity because of the supply of nutrients from rivers, estuaries, wetlands, and terrestrial run-off (Bauer *et al*., 2013; Cai *et al*., 2011; Fan *et al*., 2018; Ridwan *et al.,* 2024). The addition of nutrients and carbon to coastal and marginal seas might influence marine productivity in both advantageous and adverse ways (Wahyudi *et al.*, 2023). In recent studies, various algorithms have been formulated to estimate POC concentrations based on ocean-color radiometry (Tran *et al.*, 2019). Current reviews of the available POC algorithms for oceanic environments reveal that empirical and semi-analytical techniques achieve the highest levels of accuracy (Stramski *et al*., 2008; Tran *et al*., 2019). However, these algorithms may not effectively capture the pronounced variability of POC in coastal waters, which exhibit more complex bio-optical properties (Liu *et al.*, 2015; Loisel *et al*., 2013; Rouf *et al*., 2021; Tran *et al*., 2019). POC concentration is an essential indicator of biological productivity in the euphotic zone and serves as a marker for pollution events in coastal regions influenced by human activities (Tran *et al*., 2019). Furthermore, predicting POC variability in the region provides valuable insights into the broader patterns of organic carbon variability. Considering the important role of POC on the coastal, monitoring a POC as one of the main variables in the area is necessary in areas such as Jakarta Bay. The tropical estuarine system of Jakarta Bay in Indonesia is heavily influenced by the considerable influx of domestic wastewater from the Jakarta metropolitan area which flows through 13 river estuaries, influencing its intricate biogeochemical dynamics. The continuous inflow of nutrients and organic matter from nearby rivers causes chronic eutrophication in Jakarta Bay (Damar *et al*., 2020; van der Wulp *et al*., 2016). The ecosystem in Jakarta Bay is mainly influenced by physical processes such as tides, wind, and river discharges, which contribute to spatial and temporal variations (Koropitan *et al*., 2009). The monsoon system plays a key role in controlling the wind, influencing both the dry and the rainy season (Aldrian and Susanto, 2003; Koropitan *et al*., 2009). This dry and rainy season intensity was associated with the El Niño–Southern Oscillation (ENSO) and Indian Ocean Dipole (IOD) (Aldrian and Susanto, 2003). The discharge of freshwater from 13 rivers into Jakarta Bay may impact the dynamics of the terrestrial carbon pool. This coastal ecosystem also serves as as a highly productive area where organic matter, that observed as POC, is dynamically produced and degraded, driven by complex biogeochemical and physical mechanism. Therefore, it is important to examine the variability of POC in Jakarta Bay and its corresponding rivers that contribute to the role of coastal waters in the carbon cycle. While previous works had investigated variability of MODIS-derived POC in the wider scale Indonesian waters (Triana *et al.*, 2021; Wahyudi *et al*., 2023), the current study provides novel findings by zeroing in on Jakarta Bay, an urbanized estuarine area facing unique human-induced challenges. This study is the first to link long-term POC estimates derived from satellites and to use a SARIMA-based prediction model adapted to the monsoon-controlled system of the Jakarta Bay. The combination of POC time-series forecasting and seasonal monsoon dynamics provides an innovative method for forecasting biogeochemical transitions, allowing for proactive environmental management in critically affected coastal regions. The aims of this study are 1) analyze spatial and temporal variations in sea surface POC, 2) determine potential drivers that may affect the spatial and temporal variations in POC, and 3) estimate and predict the variance of POC in coastal areas. The present study was thus conducted in Jakarta Bay, in Indonesia, in 2023.

MATERIALS AND METHODS

Study site

Characterized by an average depth of 12.5 meters (m), Jakarta Bay is found in the western region of Indonesia, close to the Sunda Strait. The bay covers an area of roughly 490 kilometers square (km^2), with a maximum width of 19.75 kilometers (km) and a length of 26.64 km (Damar *et al*., 2020). The spatial and temporal dynamics of the Jakarta Bay ecosystem are largely shaped by the monsoonal regime, which includes comprising the north west (NW) monsoon (December-March), the inter-monsoon I (April-May), the south east (SE) monsoon (June-September),



Fig. 1: Geographical location of Jakarta Bay at the edge of the Sunda Strait, Indonesia

and the inter-monsoon II(October-November) (Wahyudi *et al.*, 2023; Monerie *et al.*, 2021). In this study, sampling stations designated for in-situ data encompassed the northern areas of Jakarta Bay and segments of the adjacent Java Sea, with a coordinate range of 106.52° - 106.96° east (E), 5.52° - 6.05° south (S) (Fig. 1).

Data acquisition

Monthly POC and chlorophyll-a (Chl-a) concentrations were obtained from Ocean Colour remote sensing data collected by the moderate-resolution imaging spectroradiometer (MODIS) aboard the Aqua satellite spanning from May 2011 to August 2023. Data is resolved at a distance of 4 km, utilizing the mapped images (SMI) format. The MODIS Aqua satellite-derived POC product is based on a power-law algorithm applied to the blue-to-green band ratio. Unlike total suspended solids (TSS), which are generally assessed using algorithms based on red and near-infrared (NIR) bands, which are more reactive to sediment and inorganic particulates (Stramski *et al.*, 2008). The in-situ data of seawater parameters: sea surface temperature (SST), salinity (Sal), dissolved oxygen (DO), nitrate (NO_3-N), and phosphate (PO_4-P), from 2011 to 2022 (Table 1) were obtained from the Environmental Agency/Dinas Lingkungan Hidup Daerah Khusus Ibukota (DLH DKI) of Jakarta. Meanwhile, the in-situ data of seawater parameters in January and August 2023 were from this study.

Field measurements, sample collection, and laboratory analysis

Water samples were collected with a 3 liters (L) Van Dorn water sampler. SST and Sal were measured with a Horiba multi-parameter water quality meter U-52G onsite. DO measurements were conducted using the Winkler method. For determination of NO_3-N and PO_4-P, 150–300 mililitres (mL) water samples were pumped and filtered through a glass micro fiber filter (GF/F) (Whatman, 25 milimeters (mm) diameter, 0.7 micrometers (µm) pore-size) filter membrane at low pressure (<0.05 megapascal (MPa)). The filtrate was placed in a 100 mL plastic bottle and subsequently frozen to determine nutrient concentration. Once back in the laboratory, the concentrations of NO3-N and PO4-P were determined using a Spectrophotometer using Cadmium Reduction and Ascorbic Acid Reduction techniques (Baird *et al.*, 2017).

Data analysis

Owing to the restricted availability of in-situ data on POC concentration, the POC in Jakarta Bay was calibrated utilizing an equation model proposed by Triana *et al.* (2021). This study collected MODIS Aqua satellite data for surface POC during the period 2002–2021, together with in-situ data, that was analysed using elemental analyzer isotope ratio mass spectrometry (EA-IRMS; FLASH 2000/ DELTA V Advantage; Thermo Fisher Scientific). Furthermore, Triana *et al.* (2021) carried out a linear regression analysis on these pairs to create a calibration

Table 1: Summary of in-situ dataset on seawater parameters from 2011 to 2023

Year	Monsoon	Month	Parameters	Data sources
2011	Inter-monsoon I	May	Sal, SST, DO, NO_3-N, PO_4-P	DLH, DKI Jakarta
	SE monsoon	Jul.	Sal, SST, DO, NO_3-N, PO_4-P	DLH, DKI Jakarta
	Inter-monsoon II	Nov.	Sal, SST, DO, NO_3-N, PO_4-P	DLH, DKI Jakarta
2012	SE monsoon	Jul.	Sal, SST, DO, NO_3-N, PO_4-P	DLH, DKI Jakarta
	Inter-monsoon II	Oct.	Sal, SST, DO, NO_3-N, PO_4-P	DLH, DKI Jakarta
	NW monsoon	Dec.	Sal, SST, DO, NO_3-N, PO_4-P	DLH, DKI Jakarta
2013	SE monsoon	Jul.	Sal, SST, DO, NO_3-N, PO_4-P	DLH, DKI Jakarta
		Aug.	Sal, SST, DO, NO_3-N, PO_4-P	DLH, DKI Jakarta
		Sep.	Sal, SST, DO, NO_3-N, PO_4-P	DLH, DKI Jakarta
2014	Inter-monsoon II	Oct.	Sal, SST, DO, NO_3-N, PO_4-P	DLH, DKI Jakarta
	SE monsoon	Aug.	Sal, SST, DO, NO_3-N, PO_4-P	DLH, DKI Jakarta
		Sep.	Sal, SST, DO, NO_3-N, PO_4-P	DLH, DKI Jakarta
2015	Inter-monsoon II	Oct.	Sal, SST, DO, NO_3-N, PO_4-P	DLH, DKI Jakarta
2016	Inter-monsoon II	Nov.	Sal, SST, DO, NO_3-N, PO_4-P	DLH, DKI Jakarta
2017	SE monsoon	Aug.	Sal, SST, DO, NO_3-N, PO_4-P	DLH, DKI Jakarta
2018	SE monsoon	Sep.	Sal, SST, DO, NO_3-N, PO_4-P	DLH, DKI Jakarta
	Inter-monsoon I	Apr.	Sal, SST, DO, NO_3-N, PO_4-P	DLH, DKI Jakarta
	SE monsoon	Jul.	Sal, SST, DO, NO_3-N, PO_4-P	DLH, DKI Jakarta
2019	Inter-monsoon I	Apr.	Sal, SST, DO, NO_3-N, PO_4-P	DLH, DKI Jakarta
	SE monsoon	Jul.	Sal, SST, DO, NO_3-N, PO_4-P	DLH, DKI Jakarta
2020	SE monsoon	Sep.	Sal, SST, DO, NO_3-N, PO_4-P	DLH, DKI Jakarta
2021	NW monsoon	Mar.	Sal, SST, DO, NO_3-N, PO_4-P	DLH, DKI Jakarta
	SE monsoon	Aug.	Sal, SST, DO, NO_3-N, PO_4-P	DLH, DKI Jakarta
2022	NW monsoon	Mar.	Sal, SST, DO, NO_3-N, PO_4-P	DLH, DKI Jakarta
	SE monsoon	Aug.	Sal, SST, DO, NO_3-N, PO_4-P	DLH, DKI Jakarta
2023	NW monsoon	Jan.	Sal, SST, DO, NO_3-N, PO_4-P	This study
	SE monsoon	Aug.	Sal, SST, DO, NO_3-N, PO_4-P	This study

equation linking in-situ and satellite-derived POC data for use across all satellite datasets pertaining to Indonesian waters. According to Triana et al. (2021), the validation of in-situ POC data from the Sunda Strait in western Indonesia indicates that MODIS-derived POC data is adequately reliable, showing an R square (R^2) = 0.70, root mean square error (RMSE) = 40.12 and mean absolute percentage error (MAPE) = 32.56 percent (%), using Eq. 1 (Triana *et al*. 2021):

$$y = 0.557x + 8.838 \quad (1)$$

Where, y is MODIS-derived POC data and x is the calibrated MODIS-derived POC data for Jakarta Bay. Although there is no direct observational data for Jakarta Bay, its location in the western region of Indonesian waters, adjacent to the Sunda Strait, indicates possible hydrodynamic influences from the strait may be significant. Given its location at the periphery of the Sunda Strait, Jakarta Bay may experience significant water mass exchange driven by seasonal monsoonal circulation. Prior studies have demonstrated that monsoon dynamics promote the transfer of water between the Indian Ocean and the Java Sea through the Sunda Strait, leading to notable variations between seasons (Xu *et al*., 2018). Furthermore, the POC model validated by Triana *et al*. (2021) encompasses the northern waters of Jakarta, thereby providing a relevant framework for the study area. The Chl-a from the MODIS Aqua satellite was calibrated using an empirical model from Wouthuyzen *et al*. (2007) developed for Jakarta Bay. This model was created utilizing 48 data sets of in-situ Chl-a concentration measurements, along with MODIS satellite images that exhibited minimal cloud obstruction, acquired almost concurrently with the sampling timeframe. The dataset comprises 18 records from 2004, 15 from 2005, and 15 from 2006, with a total of 863 in-situ Chl-a concentration observations. The Chl-a estimation model, with R^2 = 0.72, using Eq. 2 (Wouthuyzen *et al*., 2007):

$$y = 432.79x^3 - 220.87\,x^2 + 34.46\,x - 1.28 \quad (2)$$

The analysis performed in this research encompasses spatial and temporal distributions,

seasonal patterns, and variations over the years. Quantum geographic information system (QGIS) (ver. 3.32.3-Lima, GNU General Public License, see https://qgis.org/en/site/) software was used to determine POC mean values and create maps. Pearson's correlation coefficient was employed to evaluate the relationship between POC concentration and other parameters of seawater. A one-way analysis of variance (ANOVA) was performed to test the statistical significance of variation as probability value (P) < 0.01) between the POC value. All statistical analyses were performed using StatPlus: mac LE.

POC forecast

The seasonal autoregressive integrated moving average (SARIMA) model was selected for estimating and predicting the variance of POC in coastal areas, as it is a time-series analysis technique that integrates autoregressive behavior with conventional seasonal trends (Wahyudi *et al*., 2023; Wahyudi and Febriani, 2024). The choice of the SARIMA model was based on the time series nature of MODIS derived POC. To attain higher-order seasonality, SARIMA was chosen and utilized, reflecting the conclusions of prior studies that highlighted monsoonal modulation as a primary contributor to POC variability in the coastal waters of Indonesia (Wahyudi *et al*., 2023; Triana *et al.,* 2021). Furthermore, SARIMA was selected over long short-term memory (LSTM) because of the small size of the data set and for interpretability of the local management forecast. To evaluate the stationarity of the series, the Augmented Dickey-Fuller (ADF) test was utilized, revealing a notable seasonal cycle with an annual frequency related to monsoonal conditions. The autocorrelation function (ACF) and partial autocorrelation function (PACF) plots showed significant seasonal lags at 12 months, adding weight to the idea of a SAR structure. The study employed monthly averages of the POC concentration as calculated from the observational data, and the time series was initially divided into training and validation datasets (70% and 30%, respectively) to facilitate the development of a reliable model and its performance evaluation. The optimal model according to the Bayesian Information Criterion (BIC) was selected for all the possible SARIMA parameters (p,d,q)×(P,D,Q,s) based on this grid search. The primary model was formulated and tested on raw POC data, exhibiting adequate performance that can be further optimized. Subsequently a Box-Cox transformation was used to adjust the forecast accuracy and to stabilize variation in the data. This modification produced a model that is more suitable because of the existing non-constant variance within the series.The best fitted refined model, SARIMA (2,1,1)×(2,1,0,12), was chosen by selecting the BIC minimum. Model fit then evaluated using Ljung-Box Q-statistic and Jarque-Bera test. Subsequently, the SARIMA model was implemented on the modified data, demonstrating a notable improvement in performance metrics, with a MAPE of 13.4%, RMSE of 50.4 micrograms per liter (µg/L) and reduced bias. After backward elimination, the final model was refitted to the complete dataset (Box-Cox transformed) and a 5-year prediction (60 months) was obtained. The forecasted values were then reverted to the original POC units for analysis. The Box-Cox transformation refers to a collection of power transformations designed to stabilize variance, facilitating a closer alignment of time-series or regression data with the assumptions of linear modeling, particularly normality and homoscedasticity. In time series forecasting, especially with models like ARIMA or SARIMA, the box-cox transformation is often used to stabilize fluctuating variance (heteroscedasticity), improve stationarity, and enhance model fit and forecast accuracy (Hyndman and Athanasopoulous, 2018). To monitor and visualize the trend, the entire hindcast and forecast time series were joined together, and a linear regression trendline was established to assess the long-term change direction. A 95 % confidence interval was added to show the range of possible predicted values.

RESULTS AND DISCUSSION

Spatial and temporal distribution of MODIS-derived POC concentrations

The spatial distribution analysis of MODIS-derived POC concentrations in northern waters of Jakarta Bay during 13 years (2011-2023) observations reveals that POC concentration decreased gradually due to the distance from coastal (Fig. 2). The highest concentrations of POC were detected in nearshore environments, with a yearly average of 286.70 miligrams per cubic meter (mg/m^3). The decline in POC concentrations from coastal to offshore regions is primarily governed by hydrodynamic transport. The highest concentrations of POC are found at river mouths, where terrestrial organic matter enters through runoff and human contributions. The

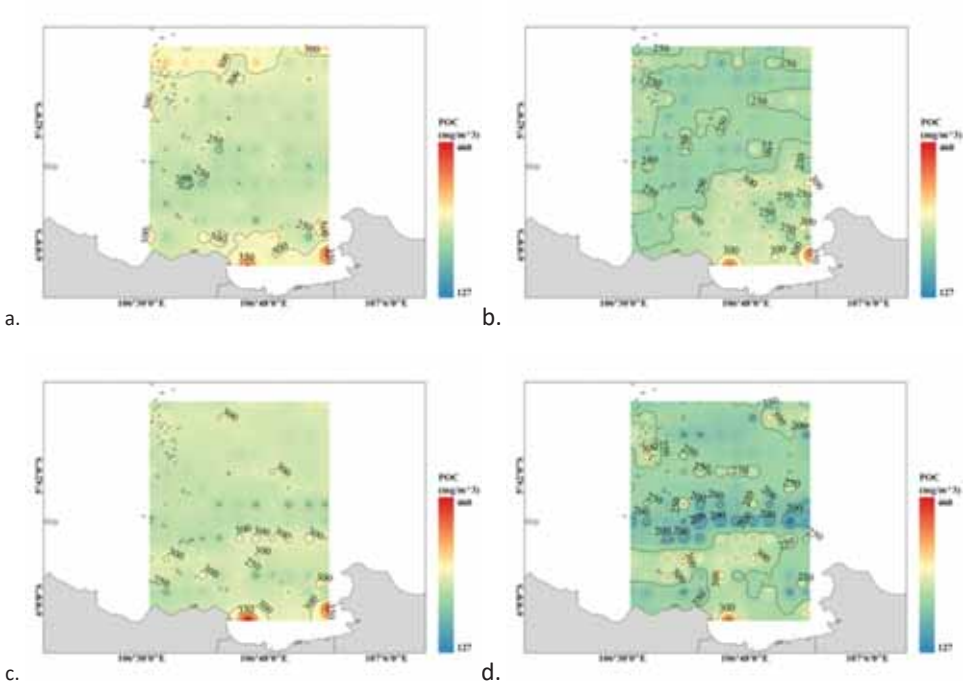

Fig. 2: Spatial and temporal patterns of the mean value of POC satellite data from May 2011 to August 2023 at northern part of Jakarta Bay in: a. the NW monsoon, b. the Inter-monsoon I, c. the SE monsoon, and d. the Inter-monsoon II

movement of surface currents and wind-driven circulation enhances the dispersal of POC, resulting in lower concentrations as one moves away from coastal area (Cai *et al*., 2015). During the NW monsoon, high river discharge increases POC flux into coastal waters and stratification slows offshore transport, retaining higher POC concentrations in nearshore zones. In the SE monsoon, stronger winds and enhanced mixing facilitate offshore advection, causing a slower decline in POC along the gradient. Meanwhile, in the inter-monsoon, weaker hydrodynamic forcing results in stabilized POC gradients.

The temporal analysis showed that POC concentration was highest during the NW monsoon and lowest during the Inter-monsoon II. The rainy season characterized by the NW monsoon leads to increased river flow, which enhances the delivery of nutrients and terrestrial organic matter. This influx stimulates biological activity, leading to elevated productivity and organic carbon production through natural processes. However, the rise in river discharge has contributed to a higher load of suspended sediments, which may cause an elevation in TSS rather than in POC. A substantial influx of inorganic particles from terrestrial runoff may impair water clarity, limiting light penetration and potentially affecting phytoplankton productivity. Reduced light availability, imposed limitations on the photosynthetic efficiency of periphytons and submerged macrophytes, which in turn influenced primary consumers (Shen *et al*., 2019). In the Inter-monsoon II, weakened hydrodynamic mixing results in moderate primary production, with lower nutrient replenishment from riverine sources. In addition, more stable water column conditions reduce phytoplankton turnover rates, leading to a gradual decline in POC accumulation (Wahyudi *et al*., 2023). Even with diminished rainfall and river discharge in the SE monsoon (dry season), POC concentrations stay at significant levels, though they are lower compared to the NW monsoon (rainy season). During this season, the decreasing intensity of rainfall and river discharge reduces the nutrient and organic materials input, while increased sunlight exposure maintains warm SST (Aldrian and Susanto, 2003). This warmer SST leading to increased rates of photosynthesis and of microbial activity. The processes involving microbes and zooplankton are essential for managing

POC dynamics, especially in coastal areas subject to seasonal fluctuations. Bacterial remineralization facilitates POC degradation, drives organic matter turnover, and regulate nutrient cycling. Zooplankton ingestion of phytoplankton alters autochthonous POC availability, influencing surface organic carbon concentrations. The processes involving microbes and zooplankton act as a natural means of removing POC, which contributes to the deposition of sediments and carbon sequestration (Steinberg *et al*, 2008). However, Wahyudi and Febriani (2024) found a negative correlation between POC and SST, which may indicate that POC remineralization is more enhanced with higher SST, and surface POC concentrations would decrease. Consequently, while greater sunlight and warmer SST are likely to boost primary production, the observed reduction in POC levels could suggest an increase in microbial degradation and carbon cycling, offsetting the carbon drawdown from local phytoplankton. The observed seasonal pattern suggests that POC variability in Jakarta Bay is primarily influenced by a combination of biological production and physical transport processes modulated by monsoonal forcing. In the nearshore area of the bay, the biogeochemistry process that stimulates POC concentration is not only influenced by the monsoon, but rather more affected by the water resident time. The average duration that a specific quantity of a substance remains in a designated reservoir is known as water residence time (Libes, 2009). Monsoonal variability plays a critical role in regulating POC residence time and transport pathways in Jakarta Bay (Mulsandi *et al*., 2024). During the NW monsoon (rainy season), Increased river discharge enhances terrestrial POC input, shortening POC residence time in surface waters due to elevated transport rates. The SE monsoon, characterized by dry conditions, sees stronger coastal currents that enhance the offshore movement of POC, thereby increasing lateral flow into deeper regions. In addition, Enhanced sediment resuspension and mixing prolongs POC residence time by redistributing organic matter through the water column. Meanwhile, during inter-monsoon, weakened hydrodynamic forcing stabilizes POC residence time, promoting gradual remineralization and transformation processes. Furthermore, transport routes reveal diminished variability, sustaining localized POC cycling in coastal zones (Zhang *et al*., 2021). Previous research showed that during the NW monsoon residence time of water in the Bay of Jakarta is 13.3 days (Suteja, 2016). In recent research, a hydrographic survey to develop a three-dimensional model based on particulate organic matter (POM), and it was found that the residence time of river water in May was about 15 days and that in September was about 50 days (Morimoto *et al*., 2019). A longer residence time leads to greater nutrient availability, thereby sustaining phytoplankton productivity and facilitating the formation of autochthonous POC (Grabowska, 2012) Meanwhile, shorter residence time, faster circulation and stronger currents expedite nutrient dispersal, reducing POC concentration. Due to the location of Jakarta Bay which is located at the edge of the Sunda Strait, this embayment may have significant influences from this strait. Studies have shown that monsoons drive water transport between the Indian Ocean and the Java Sea through the Sunda Strait, resulting in substantial inter-seasonal variability (Xu *et al*., 2018). During the SE monsoon, water moves from the Java Sea into the Indian Ocean, influenced by changes in sea surface heights and local wind patterns, whereas the NW monsoon reverses this flow, directing water back to the Java Sea (Hendiarti *et al*., 2002). Particularly during the SE monsoon season, water transported from the Java Sea brings high Chl-a concentrations, while water transported from the Indian Ocean during the NW monsoon season decreases Chl-a concentrations (Amri *et al*., 2014; Hendiarti *et al*., 2004). This higher Chl-a concentration in the SE monsoon will stimulate productivity to produce organic substances, and eventually enhance POC concentration. Amidst the NW monsoon, the diminished Chl-a concentration in water transported from the Indian Ocean might impede primary productivity by decreasing organic substances and lowering the POC concentration. ENSO and other interannual climate variability patterns exert significant influence on monsoonal POC dynamics by modulating hydrodynamic forcing, nutrient availability, and organic matter transport in coastal systems (Aldrian and Susanto, 2003). During El Nino, reduced precipitation and weakened river discharge limit terrestrial POC input. La Nina conditions lead to increased rainfall and elevated river input, which significantly enhance the flux of terrestrial POC, notably during peak monsoonal discharge periods. Biological production rates exhibit

Table 2: Mean values and ranges of in-situ seawater parameters from measurements in 2011 to 2023

Monsoon	Sal Practical salinity unit (psu)	SST Degree celcius (°C)	DO Miligrams per liter (mg/L)	NO_3-N Micromoles per liter (µmol/L)	PO_4-P Micromoles per liter (µmol/L)
NW monsoon	24.36 (22.10-27.76)	28.83 (26.33-30.21)	4.71 (3.14-6.17)	2.02 (1.31-3.06)	2.69 (1.16-3.47)
Inter monsoon I	25.22 (21.63-28.10)	29.27 (28.82-30.35)	5.04 (3.27-6.18)	1.00 (0.73-1.26)	2.04 (1.05-2.74)
SE monsoon	25.49 (20.00-29.78)	29.58 (28.21-30.57)	3.58 (1.59-5.55)	1.30 (0.36-2.09)	2.33 (1.28-3.47)
Inter monsoon II	26.76 (21.39-30.08)	29.25 (28.53-29.93)	4.25 (2.77-5.80)	1.77 (1.45-2.37)	1.64 (0.98-1.89)

distinct seasonal variability due to differences in hydrodynamic forcing, nutrient availability, and stratification (Lv *et al*., 2023).

Distribution of in-situ data in Jakarta Bay

The mean values and ranges of Sal, SST, DO, NO_3-N, and PO_4-P of Jakarta Bay are shown in Table 2. The mean value of Sal and SST was highest during the SE monsoon, meanwhile, the DO, NO_3-N, and PO_4-P were lower, compared to the NW monsoon. This time-based analysis illustrates the impact of monsoons on the physical and chemical properties of Jakarta Bay. Further analysis shows significant differences (ANOVA, $P < 0.01$) in the temporal patterns of Sal, as practical salinity unit (psu), meanwhile, no significant differences (ANOVA, $P > 0.01$) were found in the temporal patterns of SST, as degrees celcius (°C), DO, as miligrams per liter (mg/L), NO_3-N and PO_4-P, as micromoles per liter (µmol/L), concentrations for 4 monsoons.

The in-situ measurements indeed exhibit data gaps, particularly in terms of seasonal resolution. These constraints are largely attributed to logistical factors and the feasibility of conducting field campaigns. However, to minimize potential biases the Pearson correlation analysis was conducted using the seasonal average values of satellite data. This approach was justified by the relatively low standard deviation of 25 for POC dataset with a range of 230 to 340. This low standard deviation reflects reduced variability in the dataset, but it is still considerable enough to warrant careful analysis when utilizing seasonal averages, thereby bolstering the reliability of the seasonal depiction. Although the low standard deviation supports the use of seasonal averages, careful interpretation remains necessary to account for underlying environmental fluctuations. Furthermore, in-situ measurements of oceanographic parameters, including nutrient concentrations, SST, Sal, and DO, were utilized under the assumption that these variables effectively capture seasonal variability in the study area. In order to better address this concern, subsequent research should seek to integrate extra field measurements to improve seasonal resolution and validation accuracy.

Interannual variability

Over the 13 years (2011-2023), in general, POC concentration in Jakarta Bay has exhibited an almost flat slope (R^2 approximately 0.0002). Although the R^2 is negligible, a slight upward trend in concentrations was observed (Fig. 3). The slight upward trend of POC coincided with the elevated Chl-a, meanwhile, Sal and SST are negatively correlated with POC. Thus, the higher SST and Sal, the lower POC observed. The significant concentration of POC is attributed to the flow of land-derived POC from the river to the bay. Observations on land-derived POC discharge into Jakarta Bay remain limited, preventing direct identification of its role in elevated POC concentrations. Nevertheless, the increasing contributions of nutrient and organic matter from river systems are probably affecting this trend. Koropitan *et al*. (2009) reported a total river discharge of 224.70 m^3/s into Jakarta Bay, while van der Wulp *et al*. (2016) projected enhanced flows ranging from 90 to 377 m^3/s, with nitrogen and phosphorus loads reaching 174 t/d and 60 t/d, respectively. Nugrahadi *et al*. (2009) estimated organic carbon input from land at 107.6 t/d in February and 42 t/d in May. Additionally, Damar *et al*. (2020) observed a significant increase in concentrations of dissolved inorganic nitrogen and

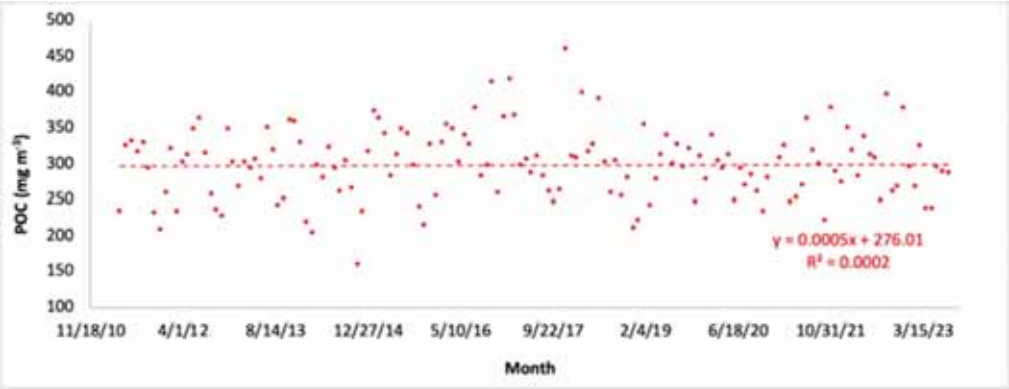

Fig. 3: The annual mean of POC concentration in Jakarta Bay from 2011 to 2023

phosphates, coupled with a rise in phytoplankton biomass, during the period from 2001 and 2019.

Further analysis (Table 3) showed that POC is significantly correlated to Chl-a ($P < 0.001$, Pearson's correlation coefficient (r) = 0.47), Chl-a is significantly correlated to Sal ($P < 0.001$, Pearson's r = -0.45), and SST is significantly correlated to PO_4-P ($P < 0.001$, Pearson's r = -0.46). There were no significant differences (ANOVA, $P > 0.01$) in the interannual variability of POC, Chl-a, Sal, SST, DO, NO_3-N, and PO_4-P concentrations over the 13 years. This relationship aligns with earlier research by Triana *et al*. (2021), which indicates that the levels of POC concentration are positively associated with Chl-a concentration and negatively associated with SST. The result analysis also indicates a negative correlation between higher POC concentrations and Sal in Jakarta Bay. The Sal distribution demonstrates an upward trend from nearshore to offshore area, resulting from the freshwater entering through the rivers. These findings support the increase in POC concentrations observed in nearshore areas compared to offshore regions in Indonesia (Triana *et al*., 2021).

The analysis showed that the annual mean POC in Jakarta Bay (297.99 mg/m^3) was higher than that in Sunda Strait (159.3 mg/m^3) (Triana *et al*., 2021). Jakarta Bay is a nearshore located in the western part of Indonesia waters, at the edge of the Sunda Strait. The higher concentrations of POC in Jakarta Bay align with earlier research conducted by Triana *et al*. (2021), which indicates that the distribution of POC in Indonesia shows a trend of rising concentrations from offshore to nearshore. Very high POC concentrations were located around the estuaries with large river run-off. These findings are consistent with a study showing that the transport of terrestrial organic carbon to estuaries is principally controlled by river discharge (Sato *et al*., 2006). The highest POC concentration in the east part of the bay may reflect the river discharge, whereas the Marunda River has a river discharge of 37.10 m^3/s, Angke River is 16.10 m^3/s, and Sunter River is 17.20 m^3/s (Cordova and Nurhati, 2019). Consequently, river discharge can be influenced by population density and human activities in the surrounding areas. Marunda River located in the eastern region of North Jakarta which borders directly with Bekasi Regency, has a high population of around 5 million inhabitants along the river and according to statistic data from Badan Pusat Statsistic (BPS), it is surrounded by high industry activities, more than 7,500 industries in 10 industrial areas (BPS-SBR, 2023). Flowing in the northwest part of Jakarta, the Angke River passes through both Tangerang in Banten and Jakarta. Approximately 6 million inhabitants settle in this area and there are 6 industrial areas with a land area reaching 4,450 hectares (BPS-STR, 2023). Meanwhile, the Sunter River that flows in the eastern part of Jakarta was adjacent to South and Central Jakarta.

Forecast and trend of POC

The forecast of POC concentration in the northern waters of Jakarta was conducted using a refined Seasonal ARIMA (SARIMA) model, optimized with Box-Cox transformation to stabilize variance. The final model, SARIMA (2,1,1)x(2,1,0)12, was used to project monthly POC values over a 5-year horizon (2023–2028). Presented in Fig. 4 are the forecast results, which

Table 3: The Pearson correlation matrix of parameters on an average scale

Variables	POC	Chl-a	Sal	SST	DO	NO_3-N	PO_4-P
POC	1.00						
Chl-a	0.47	1.00					
Sal	-0.37	-0.45	1.00				
SST	-0.24	-0.05	0.13	1.00			
DO	-0.02	-0.06	-0.01	0.32	1.00		
NO_3-N	0.03	-0.32	0.14	0.07	0.05	1.00	
PO_4-P	-0.15	0.03	-0.27	-0.46	-0.22	-0.26	1.00

Notes: Correlations in bold are significant at the 5% level.

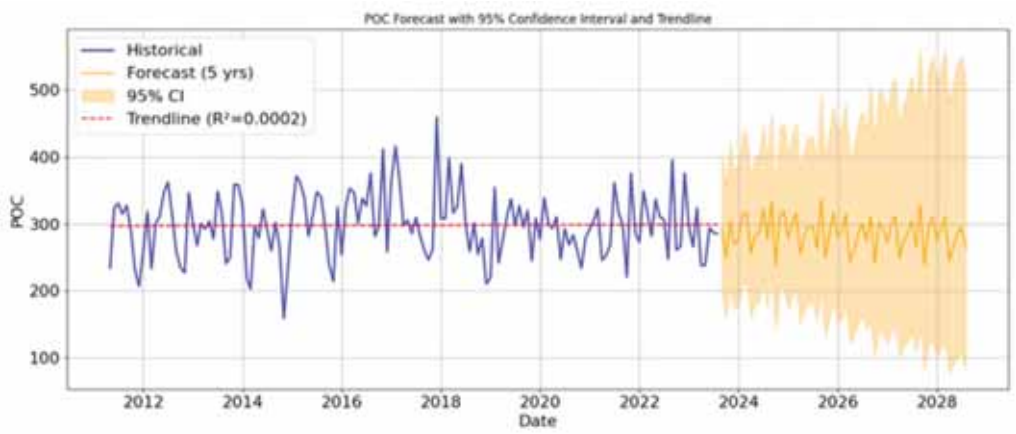

Fig. 4: Time series forecast of POC using SARIMA

encompass the historical POC record, the expected values, 95% confidence intervals, and a trendline that covers the full duration of the time series. Results from diagnostic checks supported the SARIMA model to account for seasonality in POC fluctuations. The ADF test (test = -7.66, p-value = 1.70e-11) also showed that, after first order differencing, the series was stationary, which supports the usage of SARIMA for seasonal prediction. The Ljung-Box Q-statistic (p = 0.992) indicated no notable residual autocorrelation, supporting the hypothesis of white noise and the suitability of the model specification. However, Jarque-Bera test (p = 0.0012) showed that the data significantly deviated from normality, and it is positively skewed (0.667) and leptokurtic (kurtosis = 4.18). The results highlight a potential residual structure that might influence the dependability of confidence intervals, indicating that further improvements may be needed in upcoming models. Forecasting uncertainty was tackled through the Box-Cox transformation of the dependent variable, successfully removing heteroscedasticity, as demonstrated by decreasing RMSE (from 97.5 mg/m³ to 50.35 mg/m³) and MAPE (from ~31% to ~13%). The POC concentrations in the study area appeared to have not changed greatly over the hindcast and forecast period (that is, from 230 to 340 mg/m³, mean = 286.7 ± 25 mg/m³, near flat trend R^2 = 0.0002) as there may be no obvious long-term changes. But the expanding 95% confidence intervals beyond 2026 show increasing uncertainty, indicating potential effects of unmodeled drivers, for example, riverine inputs, eutrophication, or climate anomalies. Nonetheless, the model demonstrates a commendable ability to reproduce the seasonal POC signal, which is promising for its application in forecasting seasonal to interannual anomalies for proactive planning and early warning. A stable POC trend in the water column could suggest an equilibrium in the carbon flux, with constant supply,

primary production and remineralization. Despite being labeled as stable systems, these may still conceal inefficiencies in organic carbon storage due to increasing environmental pressures, potentially jeopardizing carbon budgets in the long run. Furthermore, a lack of response to external stressors (e.g., rising SST, altered hydrodynamics) could indicate reduced system sensitivity, potentially affecting nutrient cycling, organic matter transformation, and coastal trophic interactions (Osterholz *et al*., 2021).

The forecasted POC values indicate a near-equilibrium state in organic carbon dynamics, with no substantial long-term changes likely resulting from consistent hydrodynamic flushing that inhibits excessive accumulation. By contrast, episodic increases of POC during the rainy season imply some deviation related to terrestrial influence. The forecast still exhibits a strong seasonal signal, which is related to monsoonal forcing and seasonal riverine discharge, confirming the significance of seasonal processes in determining POC variability in the Jakarta Bay. The predictions related to POC are significant early indicators of eutrophication, hypoxia, and the dynamics of sediment-carbon cycling dynamics in estuarine ecosystems. For Jakarta Bay, predicting seasonal peaks in POC, particularly during NW monsoon, is instrumental for targeted actions aiming at managing source of nutrient loads and managing wastewater discharge. Linking POC predictions with hydrodynamic models can aid in managing sediment and pinpointing eutrophication hotspots. These tools support a proactive strategy for adaptive environmental management and marine spatial planning.

Limitations and future research opportunities

The satellite-derived POC estimates in turbid coastal waters are biased due to the optical interferences, aerosol corrections, and algorithm constraints. High turbidity levels may mask POC signals and difficult differentiation from inorganic particles and colored dissolved organic matter (CDOM). In order to minimize the turbidity, locations closer to the coast were excluded in this study. Accuracy improvements in such waters can be achieved through in-situ validation and the development of localized bio-optical algorithms tailored to specific turbidity conditions (Loisel *et al*., 2013). The fate of POC in the form of sequestration, remineralization, or export was not evaluated in the present study, but this would be possible using targeted methodologies in future studies. Sediment trap collections can be used to assess POC flux and sequestration rates for different sedimentation peaks, especially during post-monsoon periods (Ma *et al*., 2021; Skylaki *et al*., 2024). Oxygen consumption data may provide information on remineralization rates with respect to POC inputs (Middelburg, 1989). POC transport can be simulated during monsoonal flows with the use of particle tracking models that recognize increased riverine input (NW monsoon) and decreased flow (SE monsoon) (Ma *et al*., 2021; Harrison *et al*., 2024). Integrating these estimates of fate would yield a fuller perspective on POC cycling within developed coastal areas. Separation of allochthonous and autochthonous sources of POC was not performed in the present study but could be estimated based on: stable isotope analysis that distinguishes terrestrial (allochthonous) from marine (autochthonous) carbon signatures (Wahyudi and Afdal, 2019); biomarker analysis that traces certain lipid and Chl-a derivatives; and CDOM fluorescence which can be used to assess terrestrial vs. marine organic matter contributions (Yuan *et al*., 2024). The lag effects between Chl-a and POC in the monsoonal season were not the focus of this study; nonetheless, existing literature suggests that POC generally lags behind Chl-a peaks during this season as a result of degradation, aggregation, and sedimentation, with the duration of these lags being associated with monsoonal intensity (Simanjutak and Lin, 2022). Effects of monsoon changes driven by the climate on POC dynamics were not considered, but could be a good topic for further study. POC fluxes might be influenced by higher precipitation, drought or both through riverine runoff, sediment resuspension, and stratification. One could consider projecting such dynamics using coupled model intercomparison project 6 (CMIP6) or regional climate projections under representative concentration pathways (RCPs) or shared socioeconomic pathways (SSPs) (Peng *et al*., 2023; Siabi *et al*., 2023). Evaluations using scenario models could investigate POC transport, remineralization, and sequestration during periods of intensified monsoon activity. Wind driven resuspension and atmospheric deposition also deserve more investigation as theseare factors in the surface POC variation. Wind-induced resuspension and atmospheric deposition, and their influence on surface POC were not considered in this study. An upcoming development could include the addition of models for wind-driven sediment

resuspension and aerosol transport, which may assist in addressing these conditions. Similarly, turbidity and shear stress metrics may characterize sediment dynamics and POC reworking by monsoonal turbulence. Stable isotope tracers would add another dimension to understanding sources and turnover times of POC. Moreover, the model does not consider the spatial variability within the sub-basins of Jakarta Bay, or the interaction of POC with oceanography (vertical mixing, benthic–pelagic coupling). In subsequent modeling endeavors, these processes might be evaluated to improve the explanation of POC dynamics in this coastal system and the broader context of carbon cycling in general.

CONCLUSION

Jakarta Bay, a tropical estuary in Indonesia, undergoes significant anthropogenic impacts due to wastewater effluent transported through 13 river estuaries linked to the Jakarta metropolitan area. Continuous inflows of nutrients and organic matter from nearby rivers contribute to ongoing eutrophication within the bay. The assessment of organic matter variability, measured as POC concentrations, can be conducted utilizing satellite observations based on ocean-color radiometry techniques. This study utilized MODIS satellite data during 2011 to 2023 and seasonal in-situ data of SST, Sal, DO, NO_3-N, and PO_4-P. This study seeks to examine the spatial and temporal distribution of POC, evaluate the environmental influences on its variability, and predict its distribution trends in Jakarta Bay. The 13-years hindcast satellite data product analysis indicates that in Jakarta Bay, POC variability is primarily influenced by a combination of biological production and physical transport processes modulated by monsoonal forcing. The spatial analysis of MODIS satellite data demonstrates that POC concentrations are highest in coastal waters and diminish gradually toward the bay's outer regions. The higher POC concentration in the nearshore waters primarily driven by terrestrial organic matter influx from river discharge. In the nearshore areas of the bay, the biogeochemistry process that drives POC concentration is influenced by the water resident time, rather than the monsoon regime. The seasonal pattern of POC in Jakarta Bay shows that the highest POC concentration is observed during the NW monsoon. During this time of year, the rise in river discharge results in an increased supply of nutrients and organic matter from terrestrial source. This influx stimulates biological activity, leading to elevated productivity and organic carbon production through natural processes. Conversely, the SE monsoon also exhibits high POC concentrations, despite reduced rainfall and river discharge limiting nutrient and organic matter influx. During this season, the heightened exposure to sunlight keeps SST warm, fostering ideal conditions for phytoplankton to produce organic carbon, which could later impact the increase in POC concentration. The observed seasonal pattern suggests that POC variability in Jakarta Bay is primarily influenced by a combination of biological production and physical transport processes modulated by monsoonal forcing. Observational data indicates a slight upward trend in POC concentrations which coincided with the elevated Chl-a. The enhanced river discharge, laden with high amounts of nutrients and organic matter, might elucidate the minor upward trend in POC concentration in Jakarta Bay. Forecasted POC values suggest no significant long-term trend, implying relative stability in organic carbon dynamics. This relative equilibrium is ikely maintained by regular hydrodynamic processes and periodic water mass flushing, which prevent significant accumulation or depletion of organic matter. Nonetheless, seasonal fluctuations, especially heightened land runoff during the rainy season, can still take place due to increased terrestrial runoff, resulting in temporary deviations from this equilibrium state. For future research analysis, it is highly recommended to use more in-situ data to account for natural processes and anthropogenic perturbations that drive the variability of POC concentration. Moreover, regular POC forecasts can assist in monitoring the risks associated with eutrophication, the dynamics of sediment and carbon, and the potential for oxygen depletion.

AUTHOR CONTRIBUTIONS

C.K. Tito performed the conceptualizing of the manuscript, drafting the original version, revising and editing the content, as well as contributing to visualization, data validation, acquisition of resources, development of methodology, conducting the investigation, managing the data, performing formal analysis, and securing funding. D.G. Bengen contributed to the conceptualization of the manuscript, participated in the review and editing process, and provided supervision. T. Prartono was involved in the manuscript's conceptualization, contributed to the review and editing, and provided supervisory support. A. Damar contributed to the conceptualization of

the manuscript, assisted in reviewing and editing the text, and provided supervision. A.J. Wahyudi played a role in manuscript conceptualization, reviewed and edited the manuscript, contributed to data validation, assisted in developing the methodology, conducted formal analysis, and provided supervision.

ACKNOWLEDGEMENT

Authors are grateful to Nofi Rahmawati Azzah a staff at the Environmental Agency of DKI Jakarta (DLH DKI Jakarta) for allowing us to access Jakarta Bay monitoring data for analysis in this research work. Great appreciation goes to Rustam Effendi Paembonan, Insaniah Rahimah, and Zulham Apandy Harahap from Marine Science, IPB University, and also M. Taufik Kaisupy and Suci Lastrini, technician staff at the Marine Biogeochemical Laboratory, Research Center for Oceanography, National Research and Innovation Agency, for their field survey and laboratory analysis support. The authors acknowledge Romanu Dwi Sasongko and Jejen Jenhar Hidayat for their assistance during data analysis. Authors also thank all the reviewers for their constructive comments on improving the manuscript. This study was funded by the Endowment Fund for Education Agency/Lembaga Pengelola Dana Pendidikan (LPDP), Ministry of Finance, Republic of Indonesia, for funding research through the Targeted Scholarships 2021, Grant No: [0001208/IPA/D/ASN-2021].

CONFLICT OF INTEREST

The authors declare that there is no conflict of interests regarding the publication of this manuscript. In addition, the ethical issues, including plagiarism, informed consent, misconduct, data fabrication and/or falsification, double publication and/or submission, and redundancy have been completely observed by the authors.

OPEN ACCESS

©2025 The author(s). This article is licensed under a Creative Commons Attribution 4.0 International License, which permits use, sharing, adaptation, distribution and reproduction in any medium or format, as long as you give appropriate credit to the original author(s) and the source, provide a link to the Creative Commons license, and indicate if changes were made. The images or other third-party material in this article are included in the article's Creative Commons license, unless indicated otherwise in a credit line to the material. If material is not included in the article's Creative Commons license and your intended use is not permitted by statutory regulation or exceeds the permitted use, you will need to obtain permission directly from the copyright holder. To view a copy of this license, visit: http://creativecommons.org/licenses/by/4.0/

PUBLISHER'S NOTE

GJESM Publisher remains neutral with regard to jurisdictional claims in published maps and institutional afflictions.

☑ Positive AI Statement

During the preparation of this work the author(s) have used Artificial Intelligence (AI) Co-pilot in order to refine sentence structures during the preparation of this work. After using this tool/service, the authors reviewed and edited the content as needed and take full responsibility for the content of the publication.

(For this reason, the GPTZero detector will evaluate the manuscript utilizing Generative AI, ensuring a high detection rate. If the manuscript relies heavily on Generative AI and AI-assisted technologies, it will be archived without further options for appeal).

☐ Negative AI Statement

The author(s) declare that no AI tools or services were not used or not highly applied during the preparation of this work.

ABBREVIATIONS

%	Percent
°C	Degree celcius
°E	East
°S	South
µg/L	Micrograms per liter
µm	Micrometers
µmol/L	Micromoles per liter
ANOVA	A one-way analysis of variance
ARIMA	Autoregressive integrated moving average
ACF	Autocorrelation function
ADF	Augmented dickey-fuller
BIC	Bayesian information criterion

BPS	Badan pusat statistik
CDOM	Colored dissolved organic matter
Chl-a	Chlorophyll-a
CMIP6	Coupled model intercomparison project 6
DLH DKI	Dinas lingkungan hidup daerah khusus ibukota
DO	Dissolved oxygen
EA-IRMS	Elemental analyzer - Isotope ratio mass spectrometry
ENSO	El niño–southern oscillation
et al.	And others
Fig.	Figure
GF/F	Glass micro fiber filter
i.e.	Id est (that is)
IOD	Indian ocean dipole
km	Kilometers
km^2	Kilometers per square
L	Liters
LSTM	Long short-term memory
m	Meters
mm	Milimeters
m^3/s	Cubic meters per second
mg/L	Miligrams per liter
mg/m^3	Miligrams per cubic meter
mL	Mililiters
MPa	Megapascal
MAPE	Mean absolute percentage error
MODIS	Moderate-resolution imaging spectroradiometer
NIR	Near-infrared
NO_3-*N*	Nitrate
NW	North west
P	P-value (Probability value)
PACF	Partial autocorrelation function
PO_4-*P*	Phosphate
POC	Particulate organic carbon
POM	Particulate organic matter
psu	Practical salinity unit
QGIS	Quantum geographic information system
RMSE	Root mean square error
R^2	R square (Coefficient of determination)
RCPs	representative concentration pathways
r	Correlation coefficient
SARIMA	Seasonal autoregressive integrated moving average (Seasonal ARIMA)
SE	South east
SSPs	or shared socioeconomic pathways
SMI	Standard mapped images
Sal	Salinity
SST	Sea surface temperature
t/d C	Tons per day carbon
TSS	Total suspended solids
UK	United Kingdom

REFERENCES

Aldrian, E; Susanto, D., (2003). Identification of three dominant rainfall regions within Indonesia and their relationship to sea surface temperature. Int. J. Climatol., 23(12): 1435-1452 **(18 pages).**

Amri, K.; Priatna, A.; Suprapto; (2014). Oceanographycal characteristic and phytoplankton abundance in Sunda Strait in east monsoon. Bawal. 6(6): 14–20 **(7 pages).**

Baird, R.B.; Eaton, R.B.; Rice, E.W., (2017). Standard methods for the examination of water and wastewater, 23rd ed. American Public Health Association, Vol. 23.

Bauer, J.E.; Cai, W.J.; Raymond, P.A.; Bianchi, T.S.; Hopkinson, C.S.; Regnier, P.A.G.. (2013). The changing carbon cycle of the coastal ocean. Nature. 504(7478): 61-70 **(10 pages).**

BPS-SBR, (2023). Bekasi regency in figures. BPS-Statistics of Bekasi Regency, Vol. 1.

BPS-STR, (2023). Tangerang Regency in figures. BPS-Statistics of Tangerang Regency, Vol. 1.

Cai, W.J.; Hu, X.; Huang, W.J.; Murrell, M.C.; Lehrter, J.C.; Lohrenz, S.E.; Chou, W.C.; Zhai, W.; Hollibaugh, J.T.; Wang, Y.; Zhao, P.; Guo, X.; Gundersen, K.; Dai, M.; Gong, G.C., (2011). Acidification of subsurface coastal waters, enhanced by eutrophication. Nat. Geosci., 4(11): 766-770 **(5 pages)**.

Cai, Y.; Guo, L.; Wang, X.; Aiken, G., (2015). Abundance, stable isotopic composition, and export fluxes of DOC, POC, and DIC from the Lower Mississippi River during 2006–2008, J. Geophys. Res. Biogeosci., 120: 2273–2288 (**17 pages**).

Chester, R.; Jickells, T., (2012). Marine geochemistry (3rd ed.). John Wiley & Sons.

Cordova, M.R.; Nurhati, I.S., (2019). Major sources and monthly variations in the release of land-derived marine debris from the Greater Jakarta area, Indonesia. Sci. Rep., 9(1): 1-9 **(9 pages)**.

Damar, A.; Colijn, F.; Hesse, K.J.; Adrianto, L.; Yonvitner; Fahrudin, A.; Kurniawan, F.; Prismayanti, A.D.; Rahayu, S.M.; Rudianto, B.Y.; Ramli, A., (2020). Phytoplankton biomass dynamics in tropical coastal waters of Jakarta Bay, Indonesia in the period between 2001 and 2019. J. Mar. Sci. Eng., 8(9): 1-17 **(17 pages).**

Fan, H.; Wang, X.; Zhang, H.; Yu, Z., (2018). Spatial and temporal variations of particulate organic carbon in the Yellow-Bohai Sea

over 2002-2016. Sci. Rep., 8(1): 1-9 **(9 pages)**.
Grabowska, M., (2012). The role of a eutrophic lowland reservoir in shaping the composition of river phytoplankton. Ecohydrol. Hydrobiol., 12(3): 231–242 (**12 pages**).
Harrison, L.C.; Graham, J.A.; Chowdhury, P.; Silva, T.A.M.; Hoehn, D.P.; Samanta, A.; Chakraborty, K.; Joseph, S.; Nair, T.M.B., Kumar, T.S., (2024). Monsoonal influence on floating marine litter pathways in the Bay of Bengal. Egusphere Preprint Repository, 1-22 (**22 pages**).
Hendiarti, N.; Siegel, H.; Ohde, T., (2002). Distinction of different water masses in and around the Sunda Strait: satellite observations and in-situ measurements. Proc. Porsec., 2: 674-679 (**6 pages**).
Hendiarti, N.; Siegel, H.; Ohde, T., (2004). Investigation of different coastal processes in Indonesian waters using SeaWiFS data. Deep Sea Research Part II: Topical Stud. Oceanogr., 51: 85-97 (**13 pages**).
Hyndman, R.J.; Athanasopoulos, G., (2018). Forecasting: Principles and practice. 2nd ed. OTexts.
Koropitan, A.F.; Ikeda, M.; Damar, A.; Yamanaka, Y., (2009). Influences of physical processes on the ecosystem of Jakarta Bay: a coupled physical-ecosystem model experiment. CES J. Mar. Sci., 66: 336-348 (**13 pages**).
Libes, S.M., (2009). Introduction to marine biogeochemistry. 2nd ed. Elsevier/Academic.
Liu, D.; Pan, D.; Bai, Y.; He, X.; Wang, D.; Wei, J.A.; Zhang, L., (2015). Remote sensing observation of particulate organic carbon in the Pearl River Estuary. Remote Sens., 7(7): 8683-8704 **(22 pages)**.
Loisel, H.; Vantrepotte, V.; Jamet, C.; NgocDat, D., (2013). Challenges and new advances in ocean color remote sensing of coastal waters. InTech. NTECH: London, UK.
Lv, H.; Wang, G.; Xu, W.; Zhang, Y.; Jiang, L., (2023). Seasonal variability of satellite- derived primary production in the South China Sea from an absorption-based model. Front. Mar. Sci. 10:1087604 (**14 pages**).
Ma, W.; Xiu, P.; Chai, F.; Ran, L.; Wiesner, M.G.; Xi, J.; Yan, Y.; Fredj, E., (2021). Impact of mesoscale eddies on the source funnel of sediment trap measurements in the South China Sea. Prog. Oceanogr., 194: 102566 **(14 pages)**.
Maciejewska, A.; Pempkowiak, J., (2014). DOC and POC in the water column of the southern Baltic. Part I. Evaluation of factors influencing sources, distribution and concentration dynamics of organic matter. Oceanologia. 56(3): 523-548 (**26 pages**).
Middelburg, J.J., (1989). A simple rate model for organic matter decomposition in marine sediments. Geochim. Cosmochim. Acta, 53(7): 1577-1581 **(5 pages)**.
Monerie, P.-A.; Robson, J.I.; Dunstone, N.J.; Turner, A.G., 2021. Skilful seasonal predictions of global monsoon summer precipitation with DePreSys3. Environ. Res. Lett., 16: 104035 (**13 pages**).
Morimoto, A.; Soeyanto, E.; Hayami, Y.; Sudaryanto, A.; Sachoemar, S., (2019). Residence time of river water in the Jakarta Bay. Japan Geoscience Union Meeting 2019.
Mulsandi, A.; Koesmaryono, Y.; Hidayat, R.; Faqih, A.; Sopaheluwakan, A., (2024). On the interannual variability of Indonesian Monsoon Rainfall (IMR): A literature review of the role of its external forcing. Jurnal Meteorologi Dan Geofisika, 24(2): 115–127 (**12 pages**).
Nugrahadi, M.S.; Yanagi, T.; Tejakusuma, I. G.; Adi, S.; Darmawan, R.A., (2009). Dissolved and particulate carbon in Jakarta Bay, Indonesia. Mar. Res. Indones., 34(1): 11-16 (**6 pages**).
Osterholz, H.; Burmeister, C.; Busch, S.; Dierken, M.; Frazão, H.C.; Hansen, R.; Jeschek, J.; Kremp, A.; Kreuzer, L.; Sadkowiak, B.; Waniek, J.J.; Schulz-Bull, D.E., (2021). Nearshore dissolved and particulate organic matter dynamics in the Southwestern Baltic Sea: Environmental drivers and time series analysis (2010–2020). Front. Mar. Sci., 8:795028 (**18 pages**).
Peng, S.; Wang, C.; Li, Z.; Mihara, K.; Kuramochi, K.; Toma, Y.; Hatano, R., (2023). Climate change multi-model projections in CMIP6 scenarios in Central Hokkaido, Japan. Sci. Rep., 13(1): 1-18 **(18 pages)**.
Rouf, M.A.; Golder, M.R.; Sumana, Z.A., (2021). Satellite-based observation of particulate organic carbon in the northern Bay of Bengal. Environ. Adv., 6: 100124 (**11 pages**).
Ridwan, I.; Kadir, S.; Nurlina, N., (2024). Wetland degradation monitoring using multi-temporal remote sensing data and watershed land degradation index. Global J. Environ. Sci. Manage., 10(1): 83-96 **(14 pages).**
Sato, T.; Miyajima, T.; Ogawa, H.; Umezawa, Y.; Koike, I., (2006). Temporal variability of stable carbon and nitrogen isotopic composition of size-fractionated particulate organic matter in the hypertrophic Sumida River Estuary of Tokyo Bay, Japan. Estuarine Coastal Shelf Sci., 68(1): 245-258 (**14 pages**).
Shen, X.; Sun, T.; Su, M.; Dang, Z.; Yang, Z., (2019). Short-term response of aquatic ecosystem metabolism to turbidity disturbance in experimental estuarine wetlands. Ecol. Eng., 136: 55-61 (**7 pages**).
Siabi, E.K.; Awafo, E.A.; Kabo-bah, A.T.; Derkyi, N.S.A.; Akpoti, K.; Mortey, E.M.; Yazdanie, M., (2023). Assessment of Shared Socioeconomic Pathway (SSP) climate scenarios and its impacts on the Greater Accra region. Urban Clim., 49: 101432 **(35 pages)**.
Simanjutak, F.; Lin, T-H., (2022). Monsoon effects on chlorophyll-a, sea surface temperature, and Ekman dynamics variability along the Southern Coast of Lesser Sunda Islands and its relation to ENSO and IOD based on satellite bbservations. RemoteSens., 14: 1682 (**28 pages**).
Steinbergh, D.K.; Mooy, B.A.S.V.; Buesseler, K.O.; Boyd, P.W.; Kobari, T., Karl, D.M., (2008). Bacterial vs. zooplankton control of sinking particle flux in the ocean's twilight zone. Limnol. Oceanogr., 53(4): 1327-1338 **(12 pages)**.
Stramski, D.; Reynolds, R.A.; Babin, M.; Kaczmarek, S.; Lewis, M.R.; Röttgers, R.; Sciandra, A.; Stramska, M.; Twardowski, M.S.; Franz, B.A.; Claustre, H., (2008). Relationships between the surface concentration of particulate organic carbon and optical properties in the eastern South Pacific and eastern Atlantic Oceans. Biogeosci., 5: 171-201 (**31 pages**).
Suteja, Y., (2016). Pollutant load and assimilation capacity of ammonium and Nitrate at northwest monsoon in Jakarta Bay. J. Mar. Aquat. Sci., 2(1): 16-22 (**7 pages**).
Skylaki, E.; Parinos, C.; Tsagkaraki, M.; Hatzianestis, I.; Christidi, A.; Skampa, E.; Nikolopoulou, I.; Kambouri, G.; Stavrakaki, I.; Velaoras, D.; Kouvarakis, G.; Triantaphyllou, M.V.; Kanakidou, M.; Mihalopoulos, N.; Gogou, A., (2024). A 1-Year Sediment Trap Study on the Downward Flux of Polycyclic Aromatic Hydrocarbons by Settling Particulate Matter in Deep Basins of the Aegean and Ionian Seas, Northeastern Mediterranean. J. Mar. Sci. Eng., Vol. 13(1): 1-24 (**24 pages**).
Tran, T.K.; Duforêt-Gaurier, L.; Vantrepotte, V.; FerreiraJorge, D.S.; Mériaux, X.; Cauvin, A.; d'Andon, F.; Loisel, H., (2019). Deriving particulate organic carbon in coastal waters from remote sensing: Inter-comparison exercise and development of a maximum band-ratio approach. Remote Sens., 11(23): 2849 **(29 pages)**.
Triana, K.; Wahyudi, A.J.; Murakami-Sugihara, N.; Ogawa, H., (2021). Spatial and temporal variations in particulate organic carbon in Indonesian waters over two decades. Mar. Freshwater Res., 72(12): 1782-1797 (**16 pages**).
van der Wulp, S.A.; Damar, A.; Ladwig, N.; Hesse, K.J., (2016). Numerical simulations of river discharges, nutrient flux and nutrient dispersal in Jakarta Bay, Indonesia. Mar. Pollut. Bull.,

110(2): 675-685 (**11 pages**).
Wahyudi, A.J.; Afdal, A., (2019). The origin of the suspended particulate matter in the seagrass meadow of tropical waters, an evidence of the stable isotope signatures. Acta Oceanol. Sin., 38: 136-143 (**8 pages**).
Wahyudi, A.J.; Febriani, F.; Triana, K., (2023). Multi-temporal variability forecast of particulate organic carbon in the Indonesian seas. Environ. Monit. Assess., 195(388): 1-20 (**20 pages**).
Wahyudi, J.; Febriani, F., (2024). Time-series forecasting of particulate organic carbon on the Sunda Shelf: Comparative performance of the SARIMA and SARIMAX models. Reg. Stud. Mar. Sci., 80: 103863 (**12 pages**).
Wouthuyzen, S.; Tan, C.K.; Ishizaka, J.; Son, T.P.H.; Ransi, V.; Tarigan, S.; Sediadi, A., (2007). Monitoring of algal blooms and massive fish kill in the Jakarta Bay, Indonesia using satellite imageries. Proceeding The First Joint PI Symposium of ALOS Data Nodes for ALOS Science Program, 1-4 (**4 pages**).
Xu, T.; Li, S.; Hamzah, F.; Setiawan, A.; Susanto, R.D.; Cao, G.; Wei, Z., (2018). Intraseasonal flow and its impact on the chlorophyll-a concentration in the Sunda Strait and its vicinity. Deep-Sea Research Part I: Oceanogr. Res. Papers. 136: 84-90 **(7 pages**).
Yuan, D.; Li S.;, Ye, C.; Liu, W.; Xu, J., (2024). Dissolved organic matter (DOM) rather than warming and eutrophication directly affects partial pressure of CO2 (pCO2) in mesocosm systems, Water Res., 267(11): 122448 (**15 pages**).
Zhang, Y.; Zhu, K.; Huang, C.; Kong, D.; He, Y., Wang, H.; Liu, W.; Xie, Z.; Wei, G.; Liu, Z., (2021). Asian winter monsoon imprint on the water column structure at the Northern South China Sea Coast. Front. Earth Sci., 9:680180 (**9 pages**).

AUTHOR (S) BIOSKETCHES

Tito, C.K., Ph.D. Candidate, [1] Department of Marine Science and Technology, Faculty of Fisheries and Marine Sciences, IPB University, IPB Dramaga Campus, Bogor, Indonesia. [2]Research Center for Oceanography, National Research and Innovation Agency, Jl. Pasir Putih I, Jakarta, Indonesia.
- Email: *camelliatito@apps.ipb.ac.id; came002@brin.go.id*
- ORCID: 0000-0003-2259-7023
- Web of Science ResearcherID: H-1860-2018
- Scopus Author ID: 57189297461
- Homepage: https://www.ipb.ac.id

Bengen, D.G, Ph.D., Professor, Department of Marine Science and Technology, Faculty of Fisheries and Marine Sciences, IPB University, IPB Dramaga Campus, Bogor, Indonesia.
- Email: *dietriechbe@apps.ipb.ac.id*
- ORCID: 0000-0002-3880-5117
- Web of Science ResearcherID: AAK-6008-2020
- Scopus Author ID: 55845650900
- Homepage: https://www.ipb.ac.id

Prartono, T., Ph.D., Professor, Department of Marine Science and Technology, Faculty of Fisheries and Marine Sciences, IPB University, IPB Dramaga Campus, Bogor, Indonesia.
- Email: *tripr@apps.ipb.ac.id*
- ORCID: 0000-0003-1304-2384
- Web of Science ResearcherID: GPP-1284-2022
- Scopus Author ID: 6507205997
- Homepage: https://www.ipb.ac.id

Damar, A., Ph.D., Professor, [1]Department of Aquatic Resources Management, Faculty of Fisheries and Marine Sciences, IPB University, IPB Dramaga Campus, Bogor, Indonesia. [2]Center for Coastal and Marine Resources Studies, IPB University, IPB Dramaga Campus, Bogor, Indonesia.
- Email: *adamar@apps.ipb.ac.id*
- ORCID: 0000-0002-5289-2747
- Web of Science ResearcherID: GPK-7500-2022
- Scopus Author ID: 26027787100
- Homepage: https://www.ipb.ac.id

Wahyudi, A.J., Ph.D., Professor, Research Center for Oceanography, National Research and Innovation Agency, Jl. Pasir Putih I, Jakarta, Indonesia.
- Email: *aanj001@brin.go.id*
- ORCID: 0000-0001-7435-4731
- Web of Science ResearcherID: H-6609-2014
- Scopus Author ID: 56712715300
- Homepage: https://www.brin.go.id/en

HOW TO CITE THIS ARTICLE

Tito, C.K.; Bengen, D.G.; Prartono, T.; Damar, A.; Wahyudi, A.J., (2025). Monsoonal influence on particulate organic carbon variability through satellite data analysis. Global J. Environ. Sci. Manage., 11(3): 1019-1034.

DOI: 10.22034/gjesm.2025.03.09

URL: https://www.gjesm.net/article_723950.html

Global J. Environ. Sci. Manage. 11(3): 1035-1056, Summer 2025, Serial #43

Global Journal of Environmental Science and Management
(GJESM)

Homepage: https://www.gjesm.net/

Podcasts

ORIGINAL RESEARCH PAPER

Removal of cadmium and lead using a sub-bituminous coal resin modified with xanthate groups

F. Fuentes-Gandara[1,*], W. Cabrera-Lafaurie[2], I. Piñeres-Ariza[3], E. Espinosa-Fuentes[4], J. Marrugo-Negrete[5], J. Pinedo-Hernández[5]

[1] *Department of Natural and Exact Sciences, Universidad de la Costa, Calle 58 Nº 55-66, Barranquilla, Colombia*

[2] *Corporación Universitaria de Ciencias Empresariales, Educación y Salud – Corsalud, Calle 64 N° 52-62, Barranquilla, Colombia*

[3] *Department of Physics, Faculty of Basic Sciences, Universidad del Atlántico, km 7 Antigua vía Puerto Colombia, Colombia*

[4] *Faculty of Engineering, Universidad Libre, Cra 51B #135 -100, Cra 46 N° 48-170, Barranquilla, Colombia*

[5] *Faculty of Basic Sciences, Department of Chemistry, Universidad de Córdoba, Cra 6 #77-305, Montería, Colombia*

ARTICLE INFO

Article History:
Received 16 February 2025
Revised 21 April 2025
Accepted 23 May 2025

Keywords:
Coal
Heavy metal
Isotherms
Removal
Wastewater

DOI: 10.22034/gjesm.2025.03.10

ABSTRACT

BACKGROUND AND OBJECTIVES: The increase in industrial effluent discharges from sectors such as smelting, electroplating, pharmaceuticals, and ceramics has led to a rise in heavy metal presence in ecosystems, posing a growing environmental risk. As the demand for more efficient materials rises, there has been a heightened interest in employing adsorbents obtained from biological origins and industrial waste, owing to their affordability, accessibility, and efficacy in eliminating heavy metals from aqueous environments. The objective of this study was to assess the potential of a modified adsorbent resin, synthesized from mineral coal waste originating in Cesar, Colombia, for the removal of cadmium and lead from aqueous solutions as a sustainable remediation strategy.

METHODS: The coal waste was chemically modified using sodium hydroxide and carbon disulfide to synthesize the adsorbent resin. Batch adsorption experiments were performed at hydrogen ion concentration levels from 3 to 8 to analyze the removal efficiency. The effect of hydrogen ion concentration on adsorption efficiency was examined, and the experimental results were analyzed using a comparative modeling technique. Adsorption equilibrium was assessed using the Freundlich, Langmuir, and Langmuir–Freundlich isotherms, while kinetic behavior was interpreted through pseudo-first- and second-order models.

FINDINGS: The results demonstrated that the removal efficiencies varied with potential of hydrogen, reaching maximum values when it was adjusted to 6, with 98 percent for lead and 97 percent for cadmium. The adsorption process conformed to the Freundlich isotherm, implying a multilayer adsorption mechanism, and the pseudo-second-order kinetics revealed that chemisorption was the prevailing mechanism.

CONCLUSION: The findings of this study underscored the effectiveness of modified mineral coal waste as a viable adsorbent for the extraction of cadmium and lead, suggesting a promising option for the treatment of industrial wastewater. Besides its exceptional performance, this strategy contributes to the valorization of solid waste from coal mining, encouraging a circular economy and minimizing the environmental impact associated with its disposal.

This is an open access article under the CC BY license (http://creativecommons.org/licenses/by/4.0/).

NUMBER OF REFERENCES **90**

NUMBER OF FIGURES **7**

NUMBER OF TABLES **3**

*Corresponding Author:
Email: *fabioar20@hotmail.com*
Phone: +300 5616 226
ORCID: 0000-0002-0681-0544

Note: Discussion period for this manuscript open until Sep 1, 2025 on GJESM website at the "Show Article".

INTRODUCTION

Industrial development and population growth in countries at various stages of development have exacerbated environmental concerns, including wastewater contamination with heavy metals, which poses global threats to biodiversity and human health (Ben-Ali *et al.,* 2017; Wattanakornsiri *et al.,* 2022). The introduction of heavy metals into aquatic ecosystems arises from a range of industrial activities, including mining, pesticide and battery manufacturing, electroplating, leather tanning, metal plating, steel metallurgy, pigment and dye synthesis, petroleum product production, as well as paper and textiles, and the discharge of leachate from landfills (Tambaru *et al.,* 2018; Tamizharasan *et al.,* 2023; Sulistyowati *et al.,* 2023). The presence of heavy metal elements in water resources is quite alarming, especially considering the harmful effects of these contaminants, their extensive distribution, environmental durability, and their ability to bioaccumulate in living organisms and biomagnification across trophic levels (Fuentes-Gandara *et al.,* 2021). Heavy metals are recognized as one of the major environmental issues and are considered among the most dangerous contaminants due to rigorous regulatory standards (Sabilillah *et al.,* 2023). Therefore, it is essential to eliminate them from wastewater and industrial discharges to safeguard both public health and the ecosystem (Jasim and Ajjam, 2024). In biological entities, exposure to heavy metals may result in numerous disorders and diseases, including complications in respiration, dysfunction of the endocrine system, obesity, developmental abnormalities in fetuses, neurological issues, infertility, miscarriages, multiple cancer types, and even fatal outcome (Mitra *et al.,* 2022; El Mouden *et al.,* 2023). In many regions of the world, lead (Pb) and cadmium (Cd) are identified as high-priority inorganic environmental pollutants (Akinterinwa *et al.,* 2022; Arul *et al.,* 2023). Annual global emissions of Cd and Pb from human activities are estimated at approximately 3000 and 120000 tons, respectively. Specifically, divalent cations Cd and Pb pose considerable threats when present in water bodies (Wang *et al.,* 2024a). Pb exposure can cause adverse effects on the human body, including mental retardation, impairment of the nervous and reproductive systems, anemia, damage to red blood cells and kidneys, hypertension, and cardiovascular problems. Severe lead exposure may result in infertility, miscarriages, and neonatal death (Arul *et al.,* 2023). Acute and chronic disorders associated with cadmium exposure include kidney damage, hypertension, emphysema, potential direct inhibition of deoxyribonucleic acid (DNA) mismatch repair, itai-itai disease, testicular atrophy, and certain types of cancer (Požgajová *et al.,* 2022). In light of the toxic risks posed by heavy metals, the advancement of research dedicated to the removal of these contaminants from wastewater is gaining significant importance (Karim *et al*., 2019; Li *et al*., 2021; Cheng *et al*., 2022) to ensure the protection of human health and the environment against the adverse effects of Cd and Pb contamination (Arul *et al.,* 2023). Various techniques are available for removing heavy metals from aqueous wastewater solutions, such as reverse osmosis, ultrafiltration, ion exchange, electrodeposition, chemical precipitation, and membrane filtration. Despite their advantages, these techniques present multiple drawbacks, including the creation of substantial waste, elevated operational costs, limited selectivity, and insufficient removal effectiveness (Khan *et al.,* 2020; Fakhar *et al.,* 2021). Among the diverse methods available for treating contaminated water, adsorption stands out as an effective and practical approach for removing heavy metals. Its advantages include operational simplicity, cost-efficiency, and high removal performance, positioning it as a favored option in physicochemical treatment strategies. Adsorption techniques are particularly appealing due to their adaptability for wastewater treatment (Gebretsadik *et al.,* 2020; Chakraborty *et al.,* 2022), often relying on adsorbents made from naturally abundant materials or byproducts from agricultural and industrial processes. Low-cost adsorbents are characterized by minimal processing requirements and accessibility, whether derived from natural sources or as industrial residues. Another major hurdle in this domain is the advancement of adsorbents that possess improved adsorption rates, selectivity, recyclability, and capacity, catering to the rising demand for efficient and eco-friendly solutions to heavy metal contamination (Jawad *et al.,* 2020). Studies have been carried out to explore methods for removing and recovering toxic metals using resins with unique functional characteristics (Gurnule and Katkamwar, 2012). Ion exchange materials, including zeolite and Purolite C105, have demonstrated exceptional

performance in extracting heavy metal ions from aqueous solutions. Zeolite achieved removal efficiencies of 98 percent (%) for copper (Cu), 93% for nickel (Ni), and 88% for Pb, while Purolite C105 showed removal rates of 94%, 97%, and 88% for the same metals, respectively (Mohammed *et al.,* 2013). The cationic resin Purolite® C100, applied in an acidic medium, was used for the remediation of Pb and Cu contamination. Ion exchange achieved removal efficiencies of 92.9% for Pb and 94.37% for Cu. These findings were derived from a dosage of Purolite® C100 resin that varied from 40 gram (g) to 80 g, within a potential of hydrogen (pH) range of 3 to 12 (Jasim and Ajjam, 2024). Selective ion exchange resins have been widely used for the removal of other heavy metals in aqueous solutions, such as chromium (Cr) (Gode and Pehlivan, 2003), Cd (Memon *et al.,* 2007; Wong *et al.,* 2014), aluminum (Al) and iron (Fe) using the aminomethylphosphonic acid functional chelating resin (Virolainen *et al.,* 2021). Coal fly ash, produced from coal-burning power plants, is acknowledged for its dusty waste nature, loose structure, and consistent pore distribution, rendering it a highly porous material with multiple uses (Patel, 2020). Its use as an adsorbent is particularly valued due to its accessibility, high efficiency in treatment processes, and cost-effectiveness (Sun *et al.,* 2022). When enhanced with sulfonated materials using alkaline fusion and hydrothermal processes, coal fly ash has shown to be effective in the simultaneous removal of Cd and methylene blue dye from wastewater. Under optimized conditions, adsorption capacities reached 93.53 milligrams per gram (mg/g) for Cd and 116.69 mg/g for methylene blue in single systems, and 85.49 mg/g for Cd and 100.23 mg/g for methylene blue in binary systems (Wang *et al.,* 2024b). The modification of fly ash through a low-temperature fusion method using potassium hydroxide (KOH) as an activator has significantly enhanced its adsorption capacity for the removal of heavy metals from aqueous solutions. This material proves to be highly effective in the removal of Pb, Cd, and Cu from wastewater. Under optimal conditions, the maximum adsorption capacities were reported as 337.41, 310.09, and 125 mg/g, respectively, in single-metal systems (Yang *et al.,* 2023). Fly ash modified with zeolites is classified as a high-efficiency adsorbent. In a batch process under optimal conditions, this material demonstrated great potential for metal removal, achieving removal efficiencies of 99.04% for Cu and 97.73% for Ni (Sireesha *et al.,* 2022). Lignite, recognized as the most immature form of coal, exists between peat and bituminous coal in the carbonization spectrum. Its defining features include a dark brown color and elevated reactivity. This material contains various functional groups such as phenolic hydroxyl, hydroxyl, aldehyde, carboxyl, and carbonyl. Additionally, lignite exhibits significant properties, including a notable capacity for cation exchange, a large surface area, and outstanding chemical and biological durability (Yuliani *et al.,* 2012). These features empower it to efficiently reduce the movement and environmental accessibility of heavy metals in soils and industrial discharges (Kamaraj *et al.,* 2025). Modifications with nanoferric iron have been recognized as a straightforward, efficient, and economical strategy, garnering substantial attention in scientific research. As an illustration, doping lignite with nanoferric iron has been proven to increase its ability to adsorb Cd by 36% (Pentari *et al.,* 2019). Furthermore, acidic treatments of lignite have been employed to further improve its capacity for removing metal ions from wastewater. After treatment with nitric acid (HNO_3), the adsorption of Pb ions by modified lignite was predominantly achieved through chemical adsorption involving mainly ion exchange, coordination, and chelation between the metal ions and the adsorbent (Wang *et al.,* 2021). A noteworthy material for environmental applications, particularly in addressing heavy metal contamination, is mercapto-modified coal gangue. Studies have demonstrated that incorporation of mercapto groups successfully generates functional sites that improve the adsorption of heavy metal ions, including mercury (Hg), Cd and Pb. This modification enables the material to achieve adsorption capacities of 110.4, 179.2 and 332.8 mg/g, for these metals, respectively (Shang *et al.,* 2021). Finally, considering that mineral coal waste is a low-cost material with limited economic reuse in many sectors, its disposal has caused significant degradation of natural resources and poses environmental risks. However, these residues exhibit resistance to high temperatures, dimensional stability, and high viscosity, allowing them to be used in the production of resins for metal ion exchange applications. In this context, the goal of this study is to analyze the capability of a chemically altered resin obtained from mineral coal waste for the extraction of Cd and Pb

from aqueous solutions, employing adsorption experiments backed by kinetic and isotherm modelling. The experimental development of this research was conducted in the laboratories of the Department of Natural and Exact Sciences at Universidad de la Costa and the Faculty of Basic Sciences at Universidad de Córdoba, in Colombia in 2023.

MATERIALS AND METHODS

The methodology involved the preparation of an adsorbent from sub-bituminous coal, which was chemically modified and characterized through compositional analyses (proximate and ultimate), alongside the application of fourier transform infrared spectroscopy (FTIR). Both unmodified (C) and modified (CM) coal samples were evaluated for the removal of Pb and Cd ions from aqueous solutions using batch adsorption experiments conducted under varying pH conditions. These tests encompassed equilibrium and kinetic studies that were aligned with mathematical models illustrating processes which seem to adhere to follow first or second order kinetics. In this study, analytical-grade chemical compounds were used, supplied by Merck. These compounds include sodium hydroxide (NaOH), lead nitrate ($Pb(NO_3)_2$, carbon disulfide (CS_2), hydrochloric acid (HCl) and tetrahydrated cadmium nitrate ($Cd(NO_3)_2 *4H_2O$).

Collection and characterization of coal

A sub-bituminous coal from a mine located in the Cesar Department-Colombia was selected, an area known for its high coal production, accounting for 53.1% of the national production in 2022 with 30.2 million tons (United Nations Development Programme-UNDP, 2024). This coal is sourced through open-pit mining, facilitating the simultaneous collection of different strata, thus ensuring consistency in its attributes. This coal exhibits favorable thermal characteristics, low sulfur and ash content, and low nitrogen oxide emissions. The surface area of the resin was determined using the Brunauer, Emmett, and Teller (BET) method with a Micromeritics Gemini III 2375 sorptometer. Nitrogen adsorption-desorption isotherms were analyzed to calculate the specific surface area (Benkő *et al.,* 2013). Standard tests to determine the volatile matter, moisture, and ash content of the coal were carried out in accordance with the American Society for Testing Materials (ASTM) standards, specifically ASTM D 5832, 2867, and 2866, respectively (Pereira *et al.,* 2018). The characterization process for the adsorbents was carried out by obtaining the infrared spectra of C and CM by mixing and macerating 1 milligram (mg) of the sample with 100 mg of potassium bromide (KBr). The mixture was compressed to form a pellet, which was analyzed with using FTIR with Shimadzu 8400 device in the range of 4000 to 400 per centimeter (/cm) to determine the functional groups involved in the adsorption of heavy metals. The identification of potential xanthate traces in the aqueous medium was conducted using ultraviolet visible (UV-Vis) spectroscopy with a spectrophotometer functioning within the 200–800 nanometer (nm) range. A calibration curve was prepared using standard solutions at concentrations of 0.2, 1.0, 2.5, 5.0, and 10.0 parts per million (ppm), measuring their absorbance within the characteristic xanthate ion range of 230–300 nm. For the leaching analysis, 10 milliliters (mL) of the supernatants were collected after suspending 0.5 g of functionalized carbon in 50 mL of distilled water were collected. These suspensions were stirred at room temperature for 24, 48, 72, 96, and 120 hour (h). The samples were then filtered using 0.45 micrometer (µm) membranes and analysed with the spectrophotometer (Fontenele *et al.,* 2007).

Resin preparation

Initially, the collected coal was immersed in an acetone solution for a duration of seven days to promote its expansion. It was then repeatedly rinsed with distilled water until the conductivity of the rinse water stabilized, followed by a drying period of 24 h. The obtained material was ground in a mill to reduce the particle size and then sieved to achieve a particle size of 0.225 millimeter (mm). To eliminate certain dyes and impurities, the material underwent rinsing with 0.1 molarity (M) HCl followed by rinsing with distilled water until a neutral pH was reached. Subsequently, 25 g of the obtained material were placed in a beaker, to which 0.42 liters (L) of a NaOH (4M) solution was added and mechanically stirred for 3 h. Then, 102 mL of pure CS_2 was added, and the mixture was stirred for 3.5 h. Subsequently, the mixture was allowed to rest for 16 h, filtered, continuously rinsed with deionized water, and dried

at 70 degrees Celsius (°C) (Liang *et al.,* 2010). The resulting product was referred to as CM.

Adsorption tests

The impact of pH on Pb and Cd adsorption was evaluated by combining 50 mg of CM and C with 10 mL of a 100 ppm solution of each metal separately at 25°C. The experiments were conducted over a pH range of 3 to 8, adjusted using 0.1 M HCl and 0.1 M NaOH. After 8 h of stirring, the solutions were filtered, and the concentrations were assessed via an inductively coupled plasma optical emission spectrometer (ICP-OES).

For the kinetic study of Pb and Cd, 50 mg of adsorbent (CM) were mixed with 10 mL of $Pb(NO_3)_2$ and $Cd(NO_3)_2{\cdot}4H_2O$ solution, at a concentration of 100 ppm of Pb^{2+} and Cd, at an optimal pH value of 6. Samples were filtered and concentration measurements were documented at 60-minutes (min) intervals over a total duration of 8 h (covering the range of 60-480 min). The quantity of adsorbed metal was computed, using eq. 1 (Kumar *et al.,* 2023):

$$[q_e] = \frac{(C_o - C_e) \times V}{W} \quad (1)$$

Where; C_0 (mg/L) indicates the initial concentration, C_e (mg/L) represents the equilibrium concentration, q_e (mg/g) the equilibrium adsorption capacity, V (L) Volume of solution and W (g) is the adsorbent mass.

For the isotherm study, solutions with different concentrations of $Pb(NO_3)_2$ and $Cd(NO_3)_2{\cdot}4H_2O$ (1 - 45 ppm) were prepared using CM and C for 8 h. The amount adsorbed of both metals was determined with an ICP-OES.

All adsorption equilibrium isotherm data were evaluated according to the Freundlich, Langmuir, and Langmuir-Freundlich isotherm models, using Eqs. 2, 3 and 4 (Cabrera-Lafaurie *et al.,* 2012):

$$q = K_F C_e^{1/nf} \quad (2)$$

$$\frac{q}{q_m} = \frac{K_L C_e}{1 + K_L C_e} \quad (3)$$

$$\frac{q}{q_m} = \frac{K_{LF} C_e^{1/n_{LF}}}{1 + K_L C_e^{1/n_{LF}}} \quad (4)$$

Where; q represents the quantity adsorbed, q_m denotes the hights adsorption capacity, K_F, K_L and K_{LF} signify the interaction coefficients of Freundlich, Langmuir, and Langmuir-Freundlich, respectively, and the parameter n_F y n_{LF} are dimension constants that reflects the degree of heterogeneity of the adsorbent.

The pseudo-first-order kinetic model has been used to describe sorption kinetics, according to Eq. 5 (Wang *et al.,* 2021).

$$\log(q_e - q_t) = \log q_e - K_1 / (2.303t) \quad (5)$$

Where; log (*qe-qt)* represents the logarithm of the equilibrium adsorption capacity. The parameter qt (mg/g) represents the amount adsorbed at a specific time t (min), while K_1 (per minute - /min) corresponds to the rate constant for the pseudo-first-order kinetic model.

The pseudo second (2nd) order kinetic model, which is based on equilibrium adsorption, using Eq. 6 (Wang *et al.,* 2021):

$$\frac{t}{q_t} = \frac{1}{K_2 q_e^2} + (1/q_e)t \quad (6)$$

Where; K_2 as gram per milligram per minute (g/mg/min) represents the rate constant of the pseudo-2nd -order equation. Tests were performed with wastewater for the small-scale application of the adsorbent employed. The samples were found to be contaminated with 100 ppm of Cd and Pb, and their concentration was determined. For this, 50 mg of adsorbent were blended with 10 mL of the sample. All adsorption experiments were carried out in triplicates.

RESULTS AND DISCUSSION

Material characterization

The obtained material, according to BET analysis, revealed a specific surface area of 2.1 square meter per gram (m^2/g), a mean pore diameter of 15.45 nm, and a pore volume of 7.9 cubic millimeters per gram (mm^3/g), indicating a mesoporous structure. As per the IUPAC classification, materials that have pore sizes ranging from 2 to 50 nm are categorized as mesoporous (Ren *et al.,* 2023). This characteristic is

especially advantageous for the adsorption of metal ions such as Pb and Cd, as it facilitates their diffusion into the internal structure and provides accessible active sites. In the charcoal samples, the moisture level was measured at 8.4%, the volatile material was found to be 71.23%, and the ash content stood at 4.89%. Furthermore, studies have shown that reduced moisture and ash content can boost the adsorption capacity of the adsorbent, thus enhancing the effectiveness of the activated carbon (Kim *et al.*, 2023). The values obtained for moisture, volatile matter, and ash are consistent with those reported by Fuentes *et al.* (2024) and Franco da Rocha *et al.* (2024), who described adsorbent materials with characteristics similar to those observed in this study. The FTIR spectra of samples C and CM are shown in Figs. 1 and 2, respectively. The infrared spectrum of C exhibits several characteristic bands. A broad and poorly defined band is observed between 3600 and 3000 /cm, corresponding to the stretching

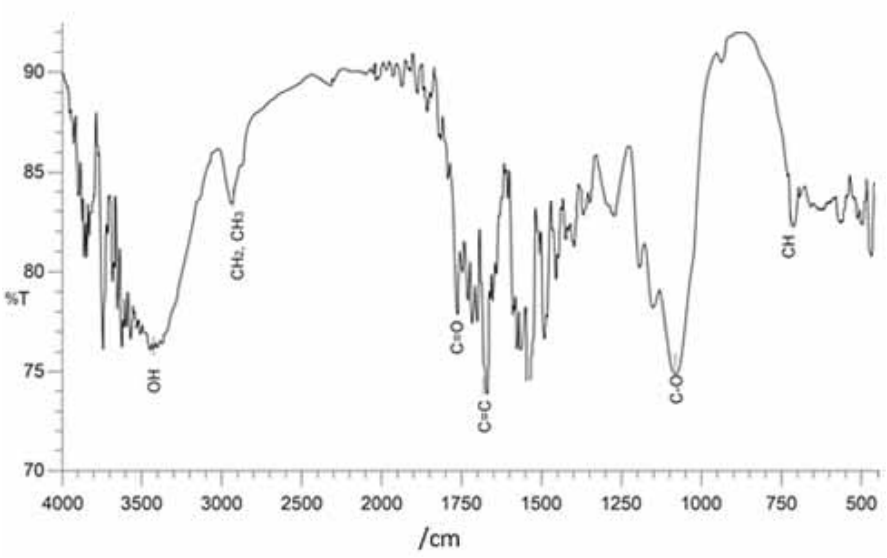

Fig. 1: FTIR spectra of C. %T is percentage transmittance

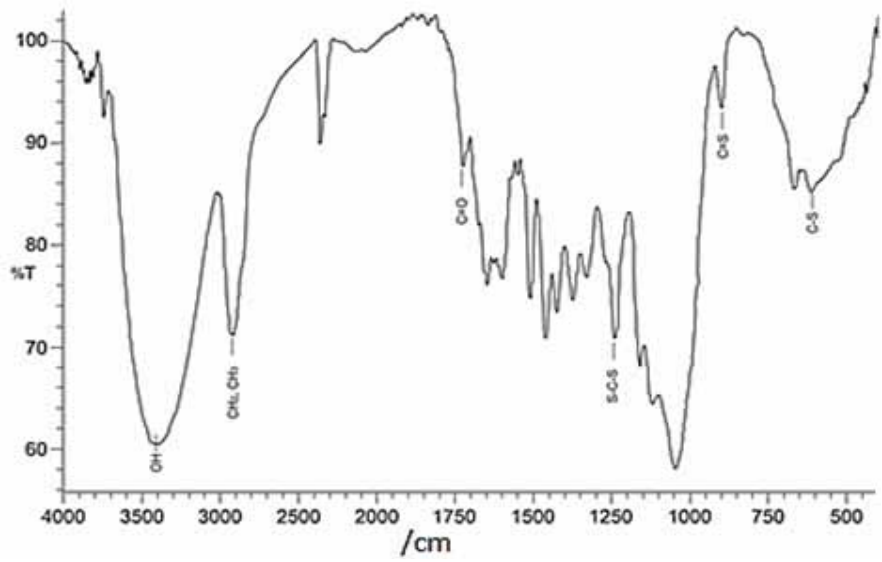

Fig. 2: FTIR spectra of CM

vibrations of oxygen (O) – hydrogen(H) groups. This implies that H bonds are present, probably related to remaining moisture or hydroxyl groups within the carbon structure. In the region between 3000 and 2800 /cm, signals are observed that are attributable to the stretching vibrations of methyl (CH_3) and methylene (CH_2) groups. The existence of these groups is often linked to carbonaceous compounds. Furthermore, bands appear at 1740 cm and 1620/cm, corresponding to the stretching vibrations of carbon C=O and C=C bonds, respectively. These results indicate the potential existence of carbonyl groups and double bonds in the carbon framework. The signals around 1400 and 1300/cm can be associated with the twisting and rocking vibrations of CH_3 and CH_2 groups. Finally, in the region near 1100 /cm, bands are observed that can be attributed to the stretching of C-O bonds, likely due to oxygenated compounds in the carbon. Meanwhile, the signals ranging from 800 and 600/cm are associated with the torsional vibrations of CH groups (He *et al*., 2017).

The infrared spectrum of the CM reveals supplementary traits that affirm the inclusion of xanthate groups. Signals in the region from 3000 to 2800 /cm, corresponding to the stretching vibrations of CH_2 and CH_3 groups, are still observable, albeit with lower intensity relative to the spectrum of unmodified C. New bands appear in the range of 1250–1000 /cm, which can be attributed to the stretching vibrations of C-O and sulfur (S) S-C-S bonds, characteristic of xanthate groups. The intense band at 1070 /cm is indicative of the presence of the C=S bond and C-S groups, confirming the functionalization of carbon with xanthate groups (Liang *et al.,* 2010). Furthermore, bands can be detected in the area ranging from 850 to 750 /cm, which further corroborates the existence of these groups. These findings affirm the successful enhancement of carbon through xanthates, leading to the introduction of new sulfur-containing functional groups and changes in the surface chemical composition of the material.

The UV-Vis spectroscopy results did not show the presence of xanthate group traces at any of the analyzed washing times. This indicates that the xanthate functionalization of the carbon is stable and that the material does not release detectable levels of these compounds into the aqueous solution under the experimental conditions employed. The lack of spectroscopic signals related to xanthates in the UV spectra implies that the employed synthesis and washing methods used are effective in eliminating any surplus reagent that is not attached to the surface of the material.

Effects of pH on Pb and Cd adsorption

Single-point adsorption experiments provide a straightforward and efficient method for gaining significant quantitative understanding of the influence of pH in heavy metal adsorption. pH is a key factor influencing the electrical state of the adsorbent surface, the level of ionic dissociation and the speciation of chemical species (Abou El-Reash, 2016; Zhu *et al.,* 2019). The influence of initial pH on the adsorption of Pb and Cd was examined across an initial pH spectrum ranging from 3.0 to 8.0. It is essential to emphasize that pH levels above 8 were excluded from this analysis, as they may cause the development of metal hydroxide precipitates, which would greatly obstruct the adsorption process and could lead to a misleading interpretation of adsorption (Nadarajah *et al.,* 2021). Fig. 3a-b presents the results obtained for adsorption on the adsorbents after 24 h of equilibrium at room temperature. A decrease in adsorption capacity at low pH levels is observed for both metals (Pb and Cd). This behavior was noted in both the C and CM. With the rise in pH of the solution, the adsorption capacity similarly increased, attaining a peak adsorption value at pH 6;this pattern was observed consistently for both adsorbents and metals. At this pH, the removal efficiencies reached 98% for Pb and 97% for Cd, indicating optimal adsorption conditions. The findings clearly demonstrate that pH levels have impacted the functional groups or surface charges of the adsorbent and the chemical speciation of the ions in the aqueous solutions. Furthermore, the effect of pH on adsorption capacity was evaluated through an analysis of variance (ANOVA), which showed significant differences for both metals, with an F-value of (5,12) surpassing 800 and a p-value < 0.001, confirming that pH has a crucial and statistically significant effect on removal efficiency.

The lower adsorption capacity at low pH is attributed to the increase in the concentration of hydronium ions (H_3O^+) as the pH of the solution decreases. This increase leads to competition between $H_3O^+$and metal cations for the active sites on the adsorbent, thereby affecting the adsorption capacity of Pb and Cd ions. This finding aligns with

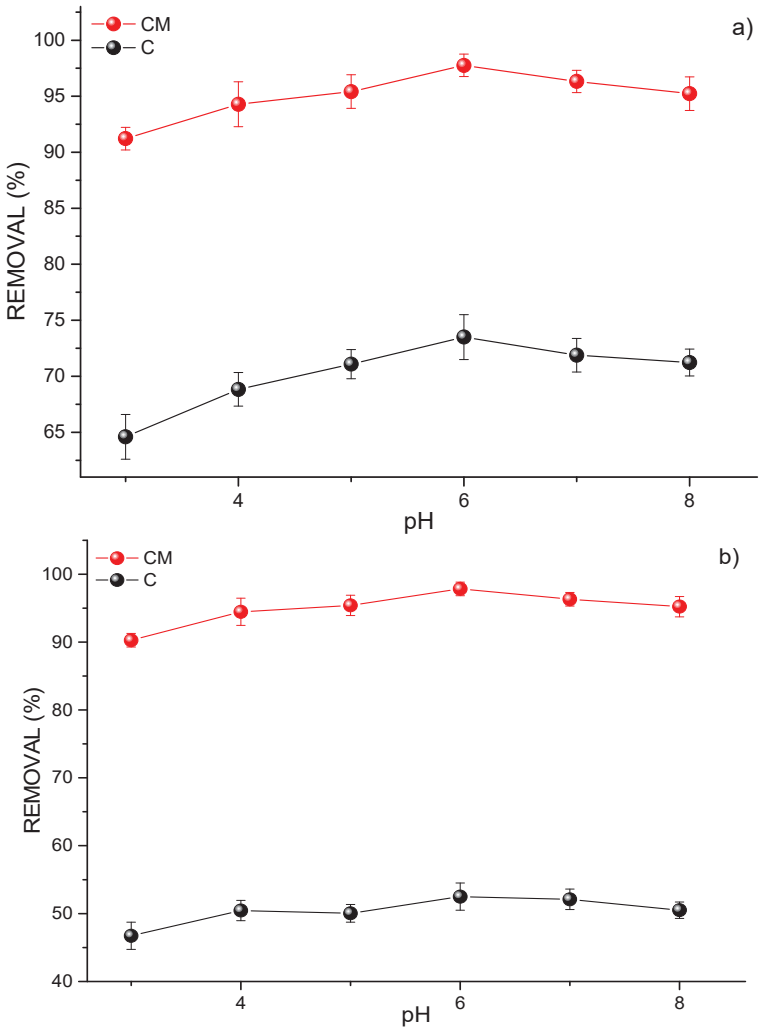

Fig. 3: Effect of solution pH on the adsorption of Pb (a) and Cd (b)

research that discusses the extraction of Pb^{2+} utilizing mesoporous activated carbons sourced from kenaf fiber through physical activation (Mandal *et al.,* 2021). Similar findings have been reported in other studies, where the adsorption of Pb^{2+} ions was highest at pH 6 in experiments conducted with activated carbons derived from apricot stone (Mouni *et al.,* 2021). Comparable findings were observed for different kinds of activated carbons at pH 6 (Purkait *et al.,* 2007). Likewise, comparable outcomes were obtained for the adsorption of Cd^{2+} on activated carbon derived from shrimp shell, with maximum removal % reported in the pH range of 6–7 (Guo *et al.,* 2021). This indicates that adsorption takes place more efficient at mildly acidic and neutral pH levels, contingent upon the characteristics of the adsorbent and the particular conditions involved. Speciation studies in aqueous solutions have shown that Pb and Cd ions remain predominantly in their Pb^{2+} and Cd^{2+} forms within the pH range of 5–6.5. At higher pH values, lead hydroxide ($Pb(OH)^{+}$) and cadmium hydroxide ($Cd(OH)^{+}$) emerge as new species (Pagnanelli *et al.,* 2003; Sheng *et al.,* 2004). These observations elucidate the reason behind the highest removal percentages for both chemical species occurring within this pH range. This behavior is also favored by the fact that, within the pH range of 5–6.5, the surface of the adsorbent becomes deprotonated

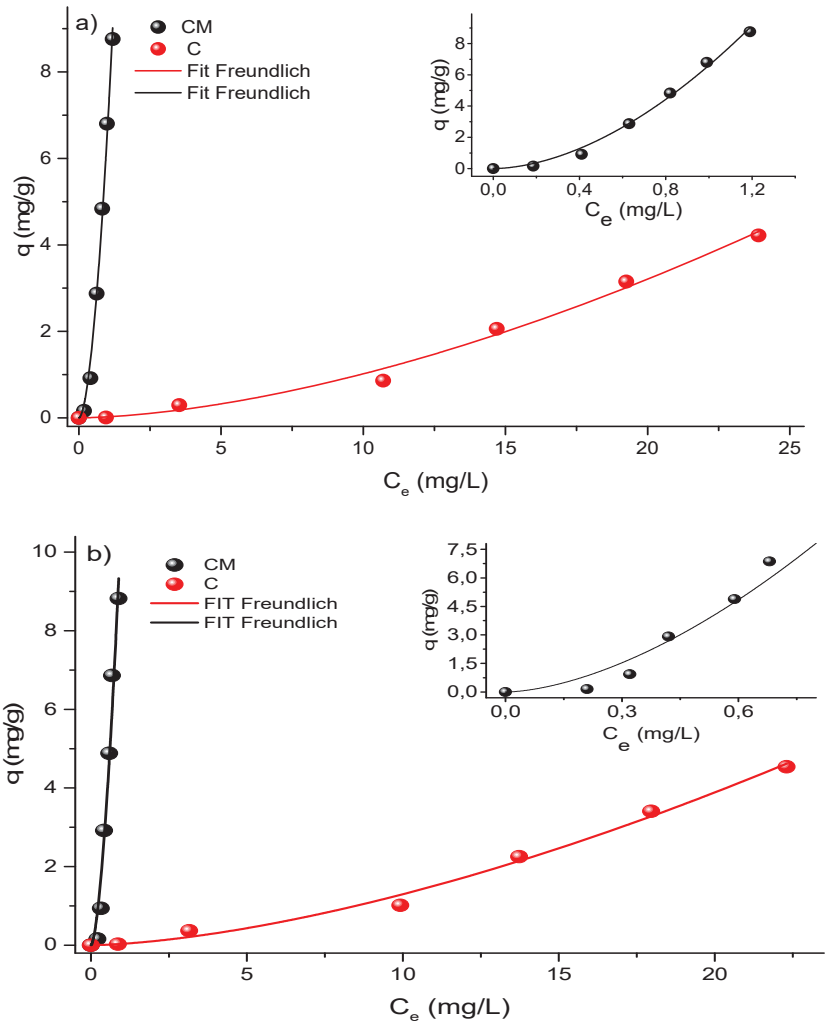

Fig. 4: Adsorption isotherms of Pb^{2+} (a) and Cd^{2+} (b) on C and CM.

and negatively charged. Consequently, a force of attraction is established between the negatively charged surface and the metal cations (Abbas *et al.,* 2016). When comparing the adsorption capacities of C and CM, as shown in Fig. 3, a significant improvement is observed in the removal properties of the modified adsorbent compared to the unmodified one. The adjusted resin exhibits a greater adsorption capacity throughout the complete range of pH levels assessed for both metals. This outcome is due to the chemical alteration of the surface by incorporating sulfur-containing groups, like xanthates, known for their strong attraction to heavy metals (Liang *et al.,* 2009).

Adsorption isotherms

Equilibrium isotherms are models that play a crucial role in explaining the interaction mechanism between the solute and the adsorbents. The adsorption process's efficiency is examined, offering insights into the affinity and attributes of the adsorbent. In general, the adsorption process depends on the pH of the solution, as evidenced by the results on the effect of pH on the adsorption capacities of metal ions. Thus, pH 6 was identified as the optimal condition for conducting equilibrium isotherm analyses. The equilibrium adsorption data for individual Pb and Cd ions are presented in Fig. 4a-b. It is important to note

Table 1: Adsorption isotherm parameters

Metal	Material	Lamgmuir-Freundlich					Freundlich			
		q_m (mg/g)	K_{FL}(L/mg)	n_{LF}	AIC	AICc	K_F(L/mg)	n_F	AIC	AICc
Pb^{+2}	C	6.820	0.0002	0.35	27.69	39.692	0.022	0.60	24.32	28.318
	CM	15.720	0.7799	0.36	46.19	54.192	6.606	0.56	21.50	24.496
Cd^{+2}	C	7.199	0.0002	0.34	30.14	38.141	0.034	0.63	29,50	32.501
	CM	11.535	4.81	0.30	20.91	28.913	11.32	0.60	9.70	12.698

that the adsorption capacities were considerably impacted by the changes implemented on the adsorbents (for instance, the addition of sulfur-containing groups), underscoring the efficiency of the process, which achieved an approximate 190% increase when to C. Studies have reported that sulfur-containing groups, particularly xanthates, exhibit high affinity for heavy metals and high stability constants for the metal complexes formed by these groups (Liang *et al.,* 2009; Panda *et al.,* 2008; Chakraborty *et al.,* 2006). Pb and Cd ions can be adsorbed onto the carbon resin via an ion exchange process, and/or complexation mechanisms. This is attributed to xanthate groups being classified as soft ligands based on the hard-soft acid-base (HSAB) concept, which exhibit a strong affinity for forming coordination complexes with divalent metals. According to HSAB principles, soft ligands have a strong affinity for soft acids such as Pb^{2+} and Cd^{2+}. These metals, categorized as borderline to soft Lewis acids, easily create stable coordination complexes with sulfur-containing groups (Wang *et al.,* 2016). This complexation is a chemisorption mechanism that entails the sharing of valence electrons from the lone pair on the sulfur atom and the empty orbitals of the metal ions.

Furthermore, the equilibrium adsorption capacity of the C and CM initially exhibited a significant increase with higher initial concentrations of metal ions. This occurrence can be linked to the increased driving forces generated by sharper concentration gradients when there are elevated initial metal ion concentrations. Three isotherm models (Freundlich, Langmuir, and Langmuir-Freundlich) were applied to evaluate the adsorption capacity, adsorption intensity, and to fit the experimental data of C and CM used for the removal of Pb^{2+} and Cd^{2+} ions from aqueous solutions. The results of the study are presented in Table 1. The Akaike Information Criterion (AIC) was employed to identify the adsorption isotherm model that best fits the experimental data. The AIC is a statistical tool that considers the number of parameters in the models being evaluated when ranking them, using Eq. 7 (Akpa and Unuabonah, 2011):

$$AIC = 2k - n_i\left[\ln\left(\frac{SSR}{n_i - k}\right)\right] \quad (2)$$

Where; the symbol k corresponds to the parameter count in the isotherm model, n_i refers to the amount of data points, and SSR is defined as the sum of "squared residuals. When the number of observations (*ni*) is small, the AIC should be corrected, using Eq. 8 (Akpa and Unuabonah, 2011):

$$AIC_c = AIC + \left[\frac{2k(k+1)}{n_i - k - 1}\right] \quad (8)$$

The adsorption isotherm model with the minimum *AICc* value was selected as the most appropriate to describe the experimental equilibrium data. Considering that the data corresponding to the Langmuir model yielded negative values, which lack physical significance, this model was excluded from the isotherm model analysis. In every case examined, the traditional Freundlich isotherm model was favored for representing the equilibrium data compared to other isotherm models that have three or comparable parameters. This aligns with findings from previous studies on the adsorption of heavy metals onto modified carbon-based materials (Mandal *et al.,* 2021; Liang *et al.,* 2009; Borji *et al.,* 2021). Furthermore, the heterogeneity factors presented in Table 1 showed a good correlation with non-homogeneous surfaces, as expected, given that the modified carbons contain both inorganic and organic fractions that may act as individual or simultaneous adsorption sites. This observed correlation validates that the altered carbon possesses a complex and uneven surface (heterogeneity), a trait that, based on the data, is linked

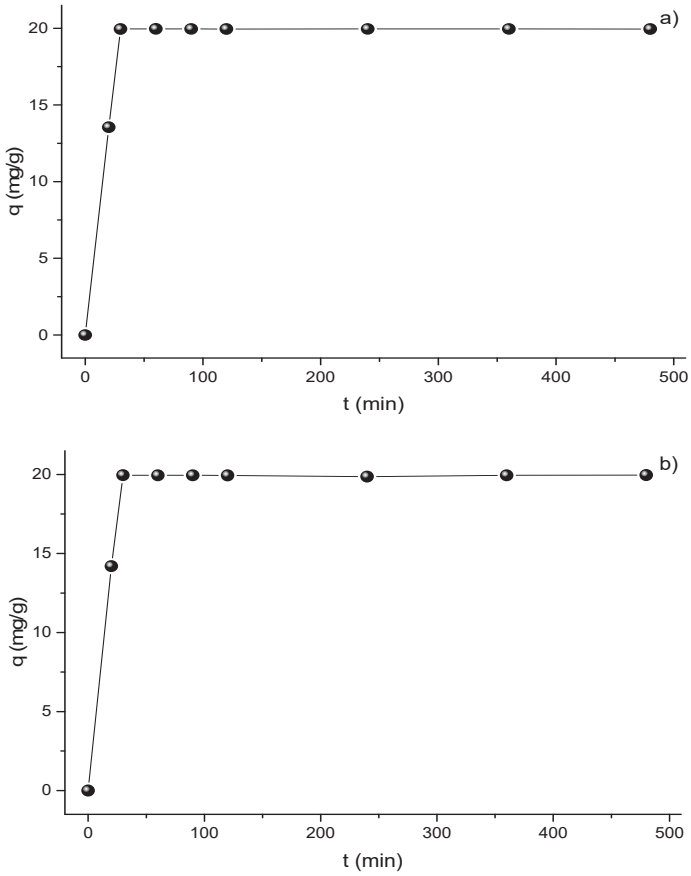

Fig. 5: Adsorption kinetics curve for Pb (a) and Cd (b)

to its structure and significantly impacts its capacity for heavy metal removal, influencing both the amount removed and the binding mechanisms. The results indicated that adsorption follows a Freundlich-type isotherm, characterizing the adsorption process as chemisorption. This is in agreement with the proposed adsorption mechanism, which entails a complexation process, leading to the formation of coordination complexes with Pb^{2+} and Cd^{2+}. Additionally, the Langmuir-Freundlich model is useful for defining the adsorption saturation point, as it includes the parameter q_m, which represents the maximum adsorption capacity of the material. This metric is vital for determining system constraints and potential effectiveness. According to the data presented in Table 1, the CM showed a q_m value of 15.720 mg/g for Pb and 11.535 mg/g for Cd, while the C exhibited significantly lower maximum capacities: 6.820 mg/g for Pb and 7.199 mg/g for Cd. The results demonstrate that the modified material exhibits a stronger attraction to metal ions, thus making it a superior alternative for the removal of metals from aqueous media.

Adsorption kinetics

Adsorption kinetics is significant as it helps to identify the rate at which metal ions are absorbed by the solid phase from aqueous solutions until equilibrium is attained. Furthermore, examining adsorption kinetics yields essential understanding of the adsorption mechanism, encompassing aspects invluding diffusion, surface reaction phenomena, and mass transfer. Adsorption kinetics were determined using solutions with a constant concentration of 100 ppm at pH 6, employing modified carbon while varying the contact time from 0.5 to 8 h. Two mathematical models were considered: the pseudo-first-order kinetic model and the pseudo-2nd-order kinetic model. From Fig. 5a-b,

Table 2: Adsorption kinetic parameters: Pseudo 2nd-order

Metal	qe (mg/g)	k_2 (/min)	$t_{1/2}=1/k_2qe$	R^2
Pb	20.00	0.020	0.1233	0.997
Cd	20.08	0.022	0.1118	0.996

it was noted that the adsorption process accelerates quickly within a brief time frame before reaching equilibrium. This behavior may be attributed to the progressive depletion of active sites on the CM as time progresses. Equilibrium was reached at 100 min, at which point the adsorbed concentration stabilized, with an adsorption capacity of 19.95 mg/g for Pb and 19.94 mg/g for Cd. Compared to other adsorbents used for the removal of heavy metals, the equilibrium time obtained in this study is competitive. Katariya *et al.* (2021) reported equilibrium times exceeding 120 min for the adsorption of Pb^{2+} and Cd^{2+} using a cationic ion-exchange resin modified with ethylenediaminetetraacetic acid (EDTA), while Wattanakornsiri *et al.* (2022) reported contact times close to 180 min using biosorbents derived from local fruit peels. The findings indicate that the xanthate-modified resin demonstrates effective adsorption kinetics, positioning it as a suitable option for the swift elimination of heavy metals in water-based environments. In addition to its rapid adsorption kinetics, the adsorption capacity of the xanthate-modified resin is comparable or superior to that of various materials reported in the literature. Mkilima *et al.* (2024) reported an adsorption capacity of 4.8 mg/g for Pb^{2+} using activated carbon derived from banana peel, while Mondal *et al.* (2024) documented 17.2 mg/g for Cd^{2+} in a biochar derived from macroalgae biomass. Additionally, Ofudje *et al.* (2015) reported an adsorption capacity of 22.1 mg/g for Pb^{2+} using alkali-modified coconut fruit as a biosorbent. These findings indicate the capability of the examined material for use in the remediation of contaminated water.

The pseudo-first-order kinetic model exhibited a correlation coefficient (R^2) close to zero, indicating a poor fit to the experimental data and suggesting that the adsorption process does not align with the assumptions of this kinetic model. Table 2 displays the rate constants for pseudo-2nd-order kinetic models concerning Pb and Cd, including the R^2 values. The agreement between the experimental data and the model predictions was assessed using R^2, which serve as a measure of how accurately the experimental data fit the kinetic models. A high R^2 value, close to 1, indicates that the model effectively describes the adsorption kinetics of metals.

The R^2 values derived from the linear regression analysis for both metal ions using the pseudo-first-order model were relatively low. Moreover, the equilibrium adsorption amounts, especially the discrepancy noted between the experimental adsorption capacity and the capacity estimated by the model, were significan. In contrast, the pseudo-2nd-order kinetic model yielded a much better fit, as indicated by higher correlation coefficients approaching unity (R^2 = 0.997). The graph illustrating t/qe in relation to t demonstrated a robust alignment between the experimentally derived values and the calculated values (Fig. 6a-b). Consequently, it can be inferred that the adsorption behavior of Pb and Cd ions onto CM adheres to the pseudo-2nd-order kinetic model. These findings are consistent with studies by Nadarajah *et al.* (2021), Liang *et al*. (2009), and Khalil *et al*. (2016), who examined the adsorption of Pb and Cd using modified carbon-based materials. These findings imply that the rate-controlling mechanism of the process is chemical adsorption or chemisorption, which depends on active sites instead of the concentration in the solution. This observation is consistent with the findings from adsorption isotherms and the proposed mechanism (complexation and ion exchange) (Yadav et al., 2013).

Laboratory-scale application

Studies focused on industrial wastewater aimed to analyze ion competition and the impact of natural organic matter (NOM) on the efficiency of metal ion removal in scenarios that more closely resemble real-world situations. Triplicate samples were taken, and the removal % of Pb and Cd were determined in water samples with an initial concentration (100 ppm) exceeding the permissible limit. This study was performed exclusively using the CM as this adsorbent demonstrated the highest efficiency for the removal of Pb and Cd compared to C. NOM

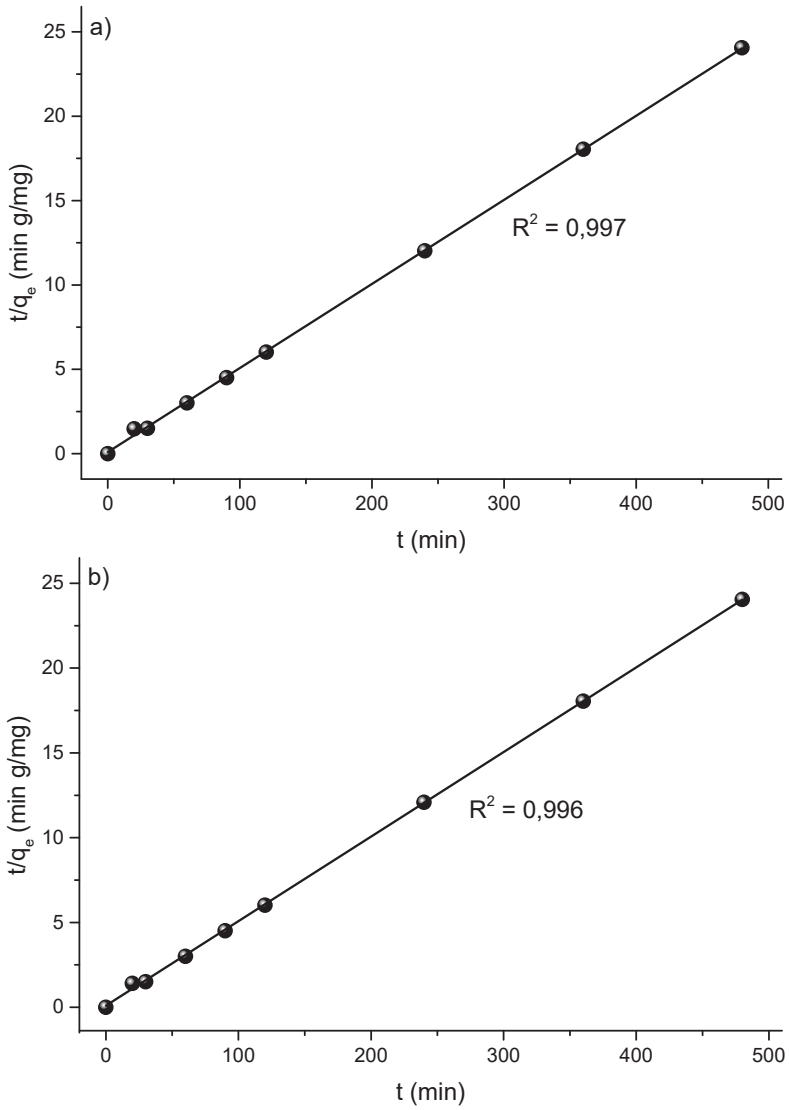

Fig. 6: Pseudo 2nd-order kinetics for the uptake of Pb (a) and Cd (b) on CM.

is well-known as a combination of polyfunctional organic acids, predominantly composed of humic and fulvic acids, which originate from the decomposition of organic materials from plants and animals. NOM is characterized as a complex mixture of organic acids and demonstrates significant reactivity with heavy metals (Jia *et al.*, 2021). The interactions occurring between NOM and heavy metals can substantially can greatly alter the chemical behavior of these metals in environmental systems, influencing their mobility, availability to organisms, and potential toxicity (Zhou *et al.*, 2023). The characterization of this matrix revealed the presence of Fe (0.6 ppm), vanadium (V) (0.2 ppm), Cu (1 ppm), total nitrogen (21 ppm), total hardness (251 ppm as calcium carbonate-$CaCO_3$), chlorides (30 ppm), sulfates (14 ppm), NOM, and a pH of 7.2. The removal efficiency of Cd and Pb across five reuse cycles is depicted in Fig. 7. In the initial cycle (cycle 0), the CM achieves excellent removal efficiencies of 99.11% for Cd and 92% for Pb, demonstrating high performance in complex wastewater matrices. With the advancement of reuse cycles, there is a gradual decrease in the efficiency of removal for both metals. By cycle 4, Cd falls to about 93%, whereas the removal

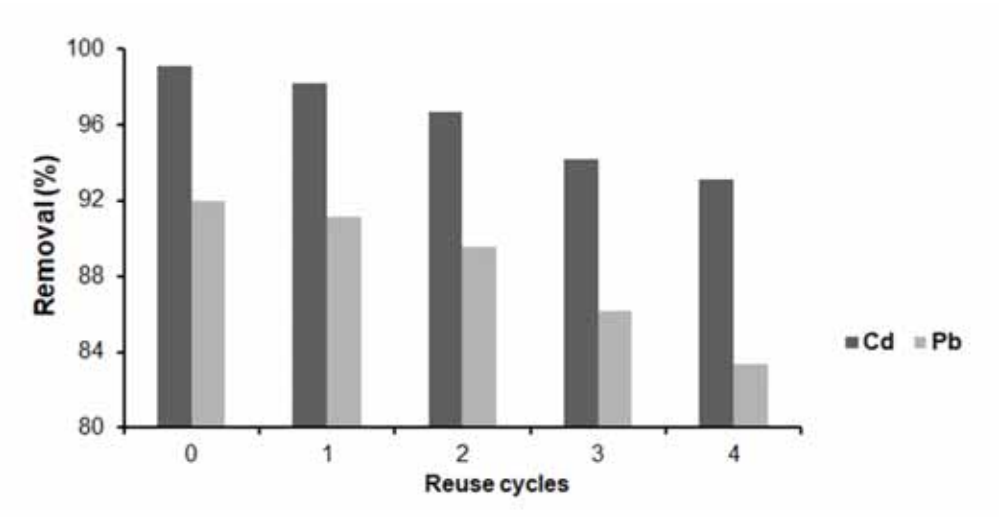

Fig. 7: % removal of heavy metals Pb and Cd in wastewater samples through reuse cycles.

of Pb declines sharply to roughly 83%, suggesting a more significant decrease in performance for Pb. This declining trend may be attributed to the saturation or partial deactivation of active sites on the CM surface, as well as potential structural changes in the material over repeated use. Furthermore, the competition for adsorption between metal ions and other substances present in the wastewater matrix could additionally obstruct removal efficiency during subsequent cycles. Despite this reduction, the material retains relatively high efficiency, particularly for Cd, suggesting strong and stable interactions between Cd^{2+} ions and the CM. As discussed in previous studies, NOM plays a crucial role in enhancing metal ion removal due to its diverse functional groups that facilitate ion exchange, chelation, and adsorption mechanisms (Tang *et al*., 2014). Humic and fulvic acids, vital constituents of NOM, possess the ability to form stable complexes with heavy metals, which may also aid in the prolonged immobilization of Cd^{2+} and Pb^{2+} over multiple cycles (Du *et al*., 2011; Wang *et al*., 2017). Overall, while reuse cycles affect the efficiency, the CM still performs effectively, particularly in the removal of Cd, underscoring its potential for application in sustainable wastewater treatment systems. Additionally, the pH of the wastewater sample analyzed falls within the optimal range for the adsorption of both Cd^{2+} and Pb^{2+}, minimizing proton competition and the formation of less adsorbable metal hydroxide species. Overall, these results validate that ionic competition in actual wastewater did not impede the effectiveness of the adsorbent. On the contrary, the presence of NOM may have played a synergistic role, enhancing heavy metal uptake. These results reinforce the applicability of CM as a selective and effective adsorbent for treating industrial effluents contaminated with heavy metals.

Another comparative assessment of CM's performance relative to other adsorbents found in the literature (Table 3) emphasizes its considerable capability for heavy metal extraction. For Cd removal, the modified resin synthesized in this study demonstrated exceptional efficiency, reaching a removal rate of 99.11%. This surpasses the performance of several widely studied adsorbents, such as phosphate-modified sludge biochar (Zhou *et al*., 2024), bioadsorbents derived from aged refuse (Manimekalai *et al*., 2024), ion exchange resin (Marszałek *et al*., 2023), a graphene oxide–silica composite (Mahmoudi *et al*., 2020), and bamboo stem-derived biochar (Sable *et al*., 2024). Significantly, it exceeded the performance of activated carbon made from banana peels (Mklima *et al*., 2024). Its performance is comparable to that of carbon dots, as reported by Bhattacharjee *et al*. (2023). With respect to Pb removal, the enhanced resin accomplished a remarkable removal rate of 92.00%. Even though some materials exhibited somewhat greater efficiencies, such as sulfur-ferromagnetic nanoparticles (Song *et al*., 2022), the resin still holds a competitive edge.

Table 3: Cd and Pb removal efficiencies of CM and other adsorbents

Adsorbent	Metal ions	Removal (%)	Sources
Banana peel-derived activated carbon (BPAC)	Pb Cd	92.40 89.90	Mkilima *et al*., 2024
Phosphate modified sludge biochar	Cd	97.00	Zhou, 2024
Activated carbons derived from plant-based materials	Pb Cd	> 90 > 90	Raji *et al*., 2023
Sulfur-ferromagnetic nanoparticles (SFMNs)	Pb	98.00	Song *et al*., 2022
Adsorbents derived from agricultural residues, such as treated rice and wheat husks	Pb Cd	95.00 92.00	Kwikima *et al*., 2021
Activated carbon obtained from pyrolysis of rice husks	Pb	95.36	Olupot *et al.,* 2024
Melanin-impregnated activated carbon	Pb	91.10	Manirethan and Balakrishnan, 2020
Ion exchange resin	Cd	95.50	Marszałek *et al*., 2023
Bioadsorbent (Aged refuse)	Cd	97.30	Manimekalai, and Subramanian, 2024
Bamboo stem derived biochar	Cd	90.60	Sable *et al*., 2024
Carbon dots	Cd	99.00	Bhattacharjee *et al*., 2023
Graphene oxide–silica composite	Cd	94.00	Mahmoudi *et al*., 2020
Cross-linked alginate-rice husk ash-graphene Oxide-chitosan	Pb	95.20	Nassar *et al*. (2025)
MOF-808-EDTA	Pb	92.00	Saeed *et al*., 2024
MOF: UiO-66-(SH)2	Pb	97.00	Abdollahi *et al*., 2020
Resin synthesized from modified mineral coal	Cd Pb	99.11 92.00	The present study

High removal rates have also been reported for adsorbents based on agricultural residues, including treated rice and wheat husks (Kwikima *et al*., 2021; Olupot *et al*., 2024), as well as for activated carbon produced via pyrolysis of rice husks (Raji *et al*., 2023), which generally achieved efficiencies above 90% for both metals under comparable conditions. The modified resin's performance is on par with or superior to other materials such as banana peel-derived activated carbon (Mklima *et al*., 2024), MOF-808-EDTA (Saeed *et al*., 2024), melanin-impregnated activated carbon (Manirethan and Balakrishnan, 2020), and the composite of cross-linked alginate, rice husk ash, graphene oxide, and chitosan (Nassar *et al*., 2025). Ultimately, the findings emphasize the exceptional capability of the modified resin in removing Cd and its competitive effectiveness in Pb removal. The sustainability of this material is not only reflected in its effectiveness but also in its production, as a key environmental benefit of the developed CM adsorbent lies in its origin. CM is synthesized from coal waste, a material that often presents disposal challenges. Utilizing this waste stream directly supports the principles of a circular economy by valorizing a by-product that would otherwise have limited economic reuse and could contribute to environmental problems through leaching of pollutants if not properly managed. This strategy minimizes the ecological strain related to standard waste management practices and could lower the demand for adsorbents derived from raw materials.

CONCLUSION

According to the outcomes of this study, the proximate and ultimate analyses demonstrated that the coal employed for resin production is classified as metallurgical and thermal, noted for its high volatility and carbon content, coupled with low levels of ash, moisture, and sulfur levels. These physicochemical properties enhance the adsorption capacity of the adsorbent. The adsorption performance of the CM for Pb and Cd ions significantly improved compared to C, achieving high removal percentages (98% for Pb and 97% for Cd). This improvement is due to the effective integration of sulfur-containing functional groups, especially xanthates, which promote complexation with divalent metal ions. The equilibrium adsorption data best fit the Freundlich isotherm, confirming the heterogeneous nature of the adsorbent surface and suggesting multilayer adsorption and strong metal-sorbent interactions. Moreover, kinetic studies

showed that the pseudo-2nd-order model provided the best fit ($R^2 = 0.997$), indicating that the rate-limiting step is likely chemisorption, involving valence forces through sharing or exchange of electrons. The CM demonstrated swift kinetics, achieving equilibrium within 100 minutes, exceeding the performance of various adsorbents noted in previous studies. The CM demonstrated remarkable performance even in complex matrices such as wastewater containing NOM, achieving 99.11% and 92% removal of Cd and Pb, respectively. This points to its possible use in real-life contexts, where interference from competing ions frequently occurs. The interaction of NOM with heavy metals likely enhanced adsorption efficiency through additional complexation pathways. This study's findings demonstrate that xanthate-modified coal can be an effective, cost-effective, and sustainable option for adsorbing contaminants from water. Future studies could further explore its regeneration capacity and long-term operational stability, which are essential parameters for scaling up this material in practical water treatment applications.

AUTHOR CONTRIBUTIONS

F. Fuentes Gandara, as the corresponding author, was responsible for analyzing the data and drafting the manuscript. W. Cabrera Lafaurie contributed significantly to the creation of tables and figures and took part in writing the manuscript. I. Piñeres Ariza was in charge of supervising the experimental work and performing a preliminary data evaluation. E. Espinosa – Fuentes participated in shaping the research proposal and provided a critical revision of the manuscript. J. Marrugo Negrete monitored specific phases of the experimental process and contributed to the interpretation of the data obtained. J. Pinedo Hernández contributed to research supervision, analysis of the results, and the preparation of the final manuscript.

ACKNOWLEDGEMENT

The authors are grateful to Universidad de la Costa and Universidad de Córdoba for providing the necessary facilities that enabled the experimental activities of this study.

CONFLICT OF INTEREST

The authors declare no potential conflict of interest regarding the publication of this work. In addition, the ethical issues including plagiarism, informed consent, misconduct, data fabrication and, or falsification, double publication and, or submission, and redundancy have been completely witnessed by the authors.

OPEN ACCESS

©2025 The author(s). This article is licensed under a Creative Commons Attribution 4.0 International License, which permits use, sharing, adaptation, distribution and reproduction in any medium or format, as long as you give appropriate credit to the original author(s) and the source, provide a link to the Creative Commons license, and indicate if changes were made. The images or other third-party material in this article are included in the article's Creative Commons license, unless indicated otherwise in a credit line to the material. If material is not included in the article's Creative Commons license and your intended use is not permitted by statutory regulation or exceeds the permitted use, you will need to obtain permission directly from the copyright holder. To view a copy of this license, visit: http://creativecommons.org/licenses/by/4.0/

PUBLISHER'S NOTE

GJESM Publisher remains neutral regarding jurisdictional claims about published maps and institutional affiliations.

☑ Positive AI Statement

During the preparation of this work the author(s) have used Artificial Intelligence (exclusively for the translation into English of paragraphs originally written in Spanish). After using this tool/service, the authors reviewed and edited the content as needed and take full responsibility for the content of the publication.

(For this reason, the GPTZero detector will evaluate the manuscript utilizing Generative AI, ensuring a high detection rate. If the manuscript relies heavily on Generative AI and AI-assisted technologies, it will be archived without further options for appeal).

☐ Negative AI Statement

The author(s) declare that no AI tools or services were not used or not highly applied during the preparation of this work.

ABBREVIATIONS

2nd	Second
%	Percent
%T	Percentage transmittance
°C	Degrees Celsius
/cm	Per centimeter
/min	Per minute
µm	Micrometer
AIC	The Akaike Information Criterion
Al	Aluminum
ANOVA	Analysis of Variance
ASTM	American Society for Testing Materials
AIM	Adsorption isotherm models
ASTM	American Society of Testing and Materials
BET	Brunauer, Emmett, and Teller
C	Unmodified mineral coal
Cd	Cadmium
$Cd(OH)^+$	Cadmium hydroxide
$Cd(NO_3)_2{\cdot}4H_2O$	Tetrahydrated cadmium nitrate
C_0	Initial concentration
$CaCO_3$	Calcium carbonate
Ce	Equilibrium concentration
CH_2	Methylene
CH_3	Methyl
CM	Modified mineral coal
cm	Centimeter
Cr	Chromium
CS_2	Carbon disulfide
Cu	Copper
DNA	Deoxyribonucleic acid
EDTA	Ethylenediaminetetraacetic acid
Fe	Iron
Fig.	Figure
FAOSTAC	Food and Agriculture Organization of the United Nations Statistical Database
FTIR	Fourier transform infrared spectroscopy
Fig.	Figure
g	Gram
g/mg/min	Gram per milligram per minute
h	Hour
H	Hydrogen
H_3O^+	Hydronium ions
HCl	Hydrochloric acid
Hg	Mercury
HNO_3	Nitric acid
HSAB	Hard Soft Acid Base
ICP-OES	Inductively coupled plasma optical emission spectrometer
k	Constant associated with the adsorption capacity of the adsorbent
k_1	Rate constant for pseudo-first-order kineticS
k_2	Rate constant for the pseudo second-order kinetic model
KBr	Potassium bromide
K_f	Interaction coefficients of Freundlich
K_l	Interaction coefficients of Langmuir
K_{LF}	Interaction coefficients of Langmuir-Freundlich
KOH	Potassium hydroxide
L	Liter
L/mg	Liter per milligram
ln(qe−qt)	Logarithm of the adsorbate amount not yet reached equilibrium (*qt*) at a specific time (*t*)
Log qe	Logarithm of the amount of adsorbate adsorbed at equilibrium per unit mass of adsorbent
M	Molarity
min	Minute
mg/L	Milligram per liter
mg/mL	Milligram per milliliter

mg/g	Milligram per gram
m^2/g	Square meter per gram
mm^3/g	Cubic millimeters per gram
$mg/g\ (L/g)^{1/n}$	Milligram per gram, multiplied by liter per gram raised to the inverse power of *n*
mL	Milliliter
mm	Millimeter
n	Constant related to the affinity (adsorption intensity) between the adsorbent and the solute
NaOH	Sodium hydroxide
n_F	Constant that reflects the degree of heterogeneity of the adsorbent of Freundlich
Ni	Nickel
n_{LF}	Constant that reflects the degree of heterogeneity of the adsorbent of Langmuir-Freundlich
n_i	Number of data points
nm	Nanometer
NOM	Natural Organic Matter
O	Oxygen
Pb	Lead
$Pb(OH)^+$	Lead hydroxide
$Pb(NO_3)_2$	Lead nitrate
pH	Potential of hydrogen
pKa	Acid dissociation constant
Ppm	Parts per million
q	Quantity absorbed
qe	Equilibrium adsorption capacity
q_m	Highest adsorption capacity
qt	Amount adsorbed at time t
R^2	Correlation coefficients
rpm	Revolutions per minute
S	Sulfur
SSR	Sum of squared residuals
t	Time
UNDP	United Nations Development Programme
UV-Vis	Ultraviolet visible
V	Volume of solution
W	Adsorbent mass

REFERENCES

Abbas, A.; Al-Amer, A.M.; Laoui, T.; Al-Marri, M.J.; Nasser, M.S.; Khraisheh, M.; Atieh, M.A., (2016). Heavy metal removal from aqueous solution by advanced carbon nanotubes: critical review of adsorption applications. Sep. Purif. Technol., 157: 141–161 **(21 pages)**.

Abdollahi, N.; Razavi, S.A.A.; Morsali, A.; Hu, M.L., (2020). High capacity Hg (II) and Pb (II) removal using MOF-based nanocomposite: cooperative effects of pore functionalization and surface-charge modulation. J. Hazard. Mater., 387: 121667 (**8 pages**).

Abou El-Reash, Y.G., (2016). Magnetic chitosan modified with cysteine-glutaraldehyde as adsorbent for removal of heavy metals from water, J. Environ. Chem. Eng., 4: 3835–3847 **(13 pages)**.

Akinterinwa, A.; Reuben, U.; Atiku, J.U.; Adamu, M., (2022). Focus on the removal of lead and cadmium ions from aqueous solutions using starch derivatives: A review. Carbohydr. Polym., 290: 119463 **(19 pages)**.

Akpa, O.M.; Unuabonah, E.I., (2011). Small-sample corrected Akaike information criterion: an appropriate statistical tool for ranking of adsorption isotherm models. Desalination. 272: 20–26 **(7 pages)**.

Arul, A.; Kavitha, S.; Christus, A.A.B.; Surya, V.J.; Ravikumar, A.; Sivalingam, Y., (2023). Enhanced removal of Pb (II) and Cd (II) ions from aqueous systems using coated magnetic nanoparticles in activated carbon derived from corncob waste. Surf. Interfaces. 40: 103095 **(19 pages)**.

Ben-Ali, S.; Jaouali, I.; Souissi-Najar, S.; Ouederni, A., (2017). Characterization and adsorption capacity of raw pomegranate peel biosorbent for copper removal. J. Cleaner Prod., 142: 3809-3821 (**13 pages**).

Benkő, M.; Puskás, S.; Király, Z., (2013). Application of mass spectrometry for study of the adsorption of multicomponent surfactant mixtures at the solid/solution interface. Adsorption. 19: 71-76 (**6 pages**).

Borji, H.; Ayoub, G.M.; Bilbeisi, R.; Nassar, N.; Malaeb, L., (2020). How effective are nanomaterials for the removal of heavy metals from water and wastewater? Water Air Soil Pollut. 231: 1–34 (**35 pages**).

Cabrera-Lafaurie, W.A.; Román, F.R.; Hernández-Maldonado, A.J., (2012). Transition metal modified and partially calcined inorganic–organic pillared clays for the adsorption of salicylic acid, clofibric acid, carbamazepine, and caffeine from water. J. Colloid Interface Sci., 386(1): 381-391 (**11 pages**).

Chakraborty, S.; Tare, V., (2006). Role of various parameters in synthesis of insoluble agro-based xanthates for removal of copper from wastewater. Bioresour. Technol., 97: 2407–2413 (**7 pages**).

Chakraborty, R.; Asthana, A.; Singh, A.K.; Jain, B.; Susan, A.B.H., (2022). Adsorption of heavy metal ions by various low-cost adsorbents: a review. Int. J. Environ. Anal. Chem., 102(2):

342-379 (**38 pages**).
Cheng, S.; Zhao, S.; Guo, H.; Xing, B.; Liu, Y.; Zhang, C.; Ma, M., (2022). High-efficiency removal of lead/cadmium from wastewater by MgO modified biochar derived from crofton weed. Bioresour. Technol., 343: 126081 (**8 pages**).
Du, Y.; Lian, F.; Zhu, L., (2011). Biosorption of divalent Pb, Cd and Zn on aragonite and calcite mollusk shells. Environ. Pollut., 159: 1763–1768 (**6 pages**).
El Mouden, A.; El Messaoudi, N.; El Guerraf, A.; Bouich, A.; Mehmeti, V.; Lacherai, A.; Jada, A.; Américo-Pinheiro, J.H.P., (2023). Removal of cadmium and lead ions from aqueous solutions by novel dolomite-quartz@ Fe_3O_4 nanocomposite fabricated as nanoadsorbent. Environ. Res., 225: 115606 (**13 pages**).
Fakhar, N.; Khan, S.A.; Siddiqi, W.A.; Khan, T.A., (2021). Ziziphus jujube waste-derived biomass as cost-effective adsorbent for the sequestration of Cd^{2+} from aqueous solution: isotherm and kinetics studies. Environ. Nanotechnol. Monit. Manage., 16: 100570 (**8 pages**).
Franco da Rocha, S.A.; Rocha, B.C.d.S.; Moraes, L.E.Z.d.; Villaça, J.M.P.; Scapin, D.; Santo, D.E.; Gonzalez, R.d.S.; Junior, O.V.; Peron, A.P., (2024). Evaluation and simulation of the adsorption capacity of octocrylene sunscreen on commercial carbon and biochar from spent coffee beans. Processes., 12: 1249 (**15 pages**).
Fontenele, R.S.; Hidalgo, P.; Gutz, I.G.; Pedrotti, J.J., (2007). Flow injection analysis of ethyl xanthate by in-line dialysis and UV spectrophotometric detection, Talanta. 72(3): 1017-1022 (**8 pages**).
Fuentes-Gandara, F.; Pinedo-Hernández, J.; Gutiérrez, E.; Marrugo-Negrete, J.; Díez, S., (2021). Heavy metal pollution and toxicity assessment in Mallorquin swamp: a natural protected heritage in the Caribbean Sea, Colombia. Mar. Pollut. Bull., 167: 112271 (**8 pages**).
Fuentes-Gandara, F.; Piñeres, I.E.; Zambrano, A.M.; Castellar, G.; Herrera, C. H.; Castro, S.; Peluffo, G.; Pinedo-Hernández, J., (2024). Removal of direct navy-blue dye from aqueous solutions using banana peles. Global J. Environ. Sci. Manage., 10(3): 1067 – 1084 (**18 pages**).
Gebretsadik, H.; Gebrekidan, A.; Demlie, L., (2020). Removal of heavy metals from aqueous solutions using *Eucalyptus camaldulensis*: an alternate low-cost adsorbent. Cogent Chem., 6(1): 1720892 (**17 pages**).
Gode, F.; Pehlivan, E., (2003). A comparative study of two chelating ion-exchange resins for the removal of chromium (III) from aqueous solution. J. Hazard. Mater., 100(1-3): 231-243 (**13 pages**).
Guo, J.; Song, Y.; Ji, X.; Ji, L.; Cai, L.; Wang, Y.; Zhang, H.; Song, W., (2019). Preparation and characterization of nanoporous activated carbon derived from prawn shell and its application for removal of heavy metal ions. Materials. 12: 241 (**17 pages**).
Gurnule, W.B.; Katkamwar, S.S., (2012). Selective removal of toxic metal ions from waste water using phenol formaldehyde type chelating resins. Rasayan J. Chem., 5(3): 365 – 375 (**11 pages**).
He, X.; Liu, X.; Nie, B.; Song, D., (2017). FTIR and Raman spectroscopy characterization of functional groups in various rank coals. Fuel., 206: 555-563 (**9 pages**).
Jasim, A.Q.; Ajjam, S.K., (2024). Removal of heavy metal ions from wastewater using ion exchange resin in a batch process with kinetic isotherm. S. Afr. J. Chem. Eng., 49: 43-54 (**12 pages**).
Jawad, A.H.; Malek, N.N.A.; Abdulhameed, A.S.; Razuan, R., (2020). Synthesis of magnetic chitosan-fly ash/ Fe3O4 composite for adsorption of reactive orange 16 dye: optimization by Box–Behnken design. J. Polym. Environ., 28(3): 1068-1082 (**15 pages**).
Jia, L.; Wu, W.; Zhang, J.; Wu, H., (2021). Insight into heavy metals (Cr and Pb) complexation by dissolved organic matters from biochar: impact of zero-valent iron. Sci. Total Environ., 793: 148469 (**9 pages**).
Kamaraj, M.; Kiruthika, N.; Saranya, T.; Aravind, J., (2025). Bibliometric analysis and impact of heavy metals contamination in soils. Global J. Environ. Sci. Manage., 11(1): 321-342 (**22 pages**).
Karim, M.R.; Aijaz, M.O.; Alharth, N.H.; Alharbi, H.F.; Al-Mubaddel, F.S.; Awual, M.R., (2019). Composite nanofibers membranes of poly (vinyl alcohol)/chitosan for selective lead (II) and cadmium (II) ions removal from wastewater. Ecotoxicol. Environ. Saf., 169: 479-486 (**8 pages**).
Katariya, S.N.; Kumar, S.; Yadav, R.B., (2021). Kinetics and thermodynamics of removal of metal ions using EDTA-modified cation ion exchange resin. Desal. Water Treat., 233: 133-149 (**17 pages**).
Khalil, T.E.; El-Dissouky, A.; Rizk, S., (2016). Equilibrium and kinetic studies on Pb^{2+}, Cd^{2+}, Cu^{2+} and Ni^{2+} adsorption from aqueous solution by resin 2,2'–(ethylenedithio) diethanol immobilized Amberlite XAD-16 (EDTDE-AXAD-16) with chlorosulphonic acid. J. Mol. Liq., 219: 533–546 (**14 pages**).
Khan, S.A.; Siddiqui, M.F.; Khan, T.A., (2020). Ultrasonic-assisted synthesis of polyacrylamide/bentonite hydrogel nanocomposite for the sequestration of lead and cadmium from aqueous phase: Equilibrium, kinetics and thermodynamic studies. Ultrason. Sonochem., 60: 104761 (**11 pages**).
Kim, S.; Lee, S.E.; Baek, S.H.; Choi, U.; Bae, H.J., (2023). Preparation of activated carbon from Korean anthracite: simultaneous control of ash reduction and pore development. Processes. 11(10), 2877 (**14 pages**).
Kumar, A.; Bhattacharya, T.; Vithanage, M., (2023). Valorization of waste biomass for biochar production and arsenic removal: a comparative assessment. Groundwater Sustainable Dev., 22: 100972 (**10 pages**).
Kwikima, M.M.; Mateso, S.; Chebude, Y., (2021). Potentials of agricultural wastes as the ultimate alternative adsorbent for cadmium removal from wastewater. A review. Sci. Afr., 13: e00934 (**14 pages**).
Li, S.; Li, S.; Wen, N.; Wei, D.; Zhang, Y., (2021). Highly effective removal of lead and cadmium ions from wastewater by bifunctional magnetic mesoporous silica. Sep. Purif. Technol., 265: 118341 (**11 pages**).https://doi.org/10.1016/j.

seppur.2021.118341

Liang, S.; Guo, X.; Feng, N.; Tian, Q., (2009). Application of orange peel xanthate for the adsorption of Pb^{2+} from aqueous solutions. J. Hazard. Mater., 170: 425–429 (**5 pages**).

Liang, S., Guo, X.Y.; Feng, N.C.; Tian, Q.H., (2010). Effective removal of heavy metals from aqueous solutions by orange peel xanthate. Trans. Nonferrous Met. Soc. China. 20: S187–S191 (**5 pages**).

Mahmoudi, E.; Azizkhani, S.; Mohammad, A.W.; Ng, L.Y.; Benamor, A.; Ang, W.L.; Ba-Abbad, M., (2020). Simultaneous removal of Congo red and cadmium (II) from aqueous solutions using graphene oxide–silica composite as a multifunctional adsorbent. J. Environ. Sci., 98: 151-160 (**10 pages**).

Mandal, S.; Calderon, J.; Marpu, S.B.; Omary, M.A.; Shi, S.Q., (2021). Mesoporous activated carbon as a green adsorbent for the removal of heavy metals and congo red: characterization, adsorption kinetics, and isotherm studies. J. Contam. Hydrol., 243: 103869 (**11 pages**).

Manimekalai, B.; Subramanian, S., (2024). Synthesized bioadsorbent using aged refuse for heavy metal removal in aqueous solution. Desalin. Water Treat., 320: 100862 (**11 pages**).

Manirethan, V.; Balakrishnan, R.M., (2020). Batch and continuous studies on the removal of heavy metals using biosynthesised melanin impregnated activated carbon. Environ. Technol. Innov., 20: 101085 (**18 pages**).

Marszałek, M.; Knapik, E.; Piotrowski, M.; Chruszcz-Lipska, K., (2023). Removal of cadmium from phosphoric acid in the presence of chloride ions using commercially available anion exchange resins. J. Ind. Eng. Chem., 118: 488–498 (**11 pages**).

Memon, S.Q.; Memon, N.; Shah, S.W.; Khuhawar, M.Y.; Bhanger, M.I., (2007). Sawdust—a green and economical sorbent for the removal of cadmium (II) ions. J. Hazard. Mater., 139(1): 116-121 (**6 pages**).

Mitra, S.; Chakraborty, A.J.; Tareq, A.M.; Emran, T.B.; Nainu, F.; Khusro, A.; Idris, A.M.; Khandaker, M.U.; Osman, H.; Alhumaydhi, F.A.; Simal-Gandara, J., (2022). Impact of heavy metals on the environment and human health: novel therapeutic insights to counter the toxicity. J. King Saud. Univ. Sci., 34(3): 101865 (**23 pages**).

Mkilima, T.; Zharkenov, Y.; Abduova, A.; Sarypbekova, N.; Kudaibergenov, N.; Sakanov, K.; Zhukenova, G.; Omarov, Z.; Sultanbekova, P.; Kenzhaliyeva, G., (2024). Utilization of banana peel-derived activated carbon for the removal of heavy metals from industrial wastewater. Case Stud. Chem. Environ. Eng., 10: 100791 (**10 pages**).

Mohammed, A.A.; Mahmood, H.S., (2013). Removal of Cu^{2+}, Pb^{2+}, and Ni^{2+} ions from simulated wastewater by ion exchange method on zeolite and purolite C105 resin. J. Eng., 19(10): 1327-1340 (**14 pages**).

Mondal, A.K.; Hinkley, C.; Kondaveeti, S.; Vo, P.H.N.; Ralph, P.; Kuzhiumparambil, U., (2024). Influence of pyrolysis time on removal of heavy metals using biochar derived from macroalgal biomass (*Oedogonium sp*). Bioresour. Technol., 414: 131562 (**13 pages**).

Mouni, L.; Merabet, D.; Bouzaza, A.; Belkhiri, L., (2011). Adsorption of Pb (II) from aqueous solutions using activated carbon developed from Apricot stone. Desalination. 276: 148–153 (**6 pages**).

Nadarajah, K.; Bandala, E.R.; Zhang, Z.; Mundree, S.; Goonetilleke, A., (2021). Removal of heavy metals from water using engineered hydrochar: kinetics and mechanistic approach. J. Water Process Eng., 40: 101929 (**12 pages**).

Nassar, A.A.; Mubarak, M.F.; El-Sawaf, A.K.; Zayed, M.A.; Hemdan, M., (2025). Efficient lead ion removal from aqueous solutions for wastewater treatment using a novel cross-linked alginate-rice husk ash-graphene oxide-chitosan nanocomposite. Int. J. Biol. Macromol., 284: 137983 (**13 pages**).

Olupot, P.W.; Wakatuntu, J.; Turyasingura, M.; Jjagwe, J.; Menya, E.; Okure, M., (2024). Optimization of heavy metal removal by activated carbon obtained as a co-product from fast pyrolysis of rice husks. Results Mater., 21: 100545 (**18 pages**).

Ofudje, E.A.; Akiode, O.K.; Oladipo, G.O.; Adedapo, A.E.; Adebayo, L.O.; Awotula, A.O., (2015). Application of raw and alkaline-modified coconut shaft as a biosorbent for Pb^{2+} removal. BioResources. 10: 3462-3480 (**19 pages**).

Pagnanelli, F.; Esposito, A.; Toro, L.; Veglio, F., (2003). Metal speciation and pH effect on Pb, Cu, Zn and Cd biosorption onto *Sphaerotilus natans*: Langmuir-type empirical model. Water Res., 37: 627–633 (**7 pages**).

Panda, G.C.; Das, S.K.; Guha, A.K., (2008). Biosorption of cadmium and nickel by functionalized husk of *Lathyrus sativus*. Colloids Surf. B., 62: 173–179 (**7 pages**).

Patel, H., (2020). Environmental valorisation of bagasse fly ash: a review. RSC Adv., 10(52): 31611-31621 (**11 pages**).

Pentari, D.; Vamvouka, D., (2019). Cadmium removal from aqueous solutions using nano-iron doped lignite. IOP Conference Series: Earth Environ. Sci., 221: 012135 (**8 pages**).

Pereira, I.C.; Carvalho, K.Q.; Passig, F.H.; Ferreira, R.C.; Rizzo-Domingues, R.C.P.; Hoppen, M.I.; Perretto, F., (2018). Thermal and thermal-acid treated sewage sludge for the removal of dye reactive red 120: characteristics, kinetics, isotherms, thermodynamics and response surface methodology design. J. Environ. Chem. Eng., 6(6): 7233-7246 (**14 pages**).

Požgajová, M.; Navrátilová, A.; Kovár, M., (2022). Curative potential of substances with bioactive properties to alleviate Cd toxicity: a review. Int. J. Environ. Res. Public Health., 19(19): 12380 (**42 pages**).

Purkait, M.K.; Maiti, A.; Dasgupta, S.; De, S., (2007). Removal of congo red using activated carbon and its regeneration. J. Hazard. Mater., 145: 287–295 (**9 pages**).

Raji, Z.; Karim, A.; Karam, A.; Khalloufi, S., (2023). Adsorption of heavy metals: mechanisms, kinetics, and applications of various adsorbents in wastewater remediation—a review. Waste. 1: 775–805 (**31 pages**).

Ren, Q.; Ma, Y.; Wei, F.; Qin, L.; Chen, H.; Liang, Z.; Wang, S., (2023). Preparation of Zr-MOFs for the adsorption of doxycycline hydrochloride from wastewater. Green Process. Synth., 12(1): 20228127 (**10 pages**).

Sabilillah, A.M.; Palupi, F.R.; Adji, B.K.; Nugroho, A.P., (2023). Health risk assessment and microplastic pollution in streams

through accumulation and interaction by heavy metals. Global J. Environ. Sci. Manage., 9(4): 719-740 (**22 pages**).

Sable, H.; Kumar, V.; Mishra, R.; Singh, V.; Roy, A.; Rai, A.K.; Ranjan, N.; Rustagi, S.; Pandit, S., (2024). Bamboo stem derived biochar for biosorption of cadmium (II) ions from contaminated wastewater. Environ. Nanotechnol. Monit. Manage., 21: 100936 (**8 pages**).

Saeed, F.; Reddy, K.A.; Sridhar, S., (2024). Efficient removal of environmentally hazardous heavy metal ions from water by NH2-MIL-101-Fe and MOF-808-EDTA based polyether sulfone adsorbents. Chem. Eng. J., 497: 154688 (**18 pages**).

Shang, Z.; Zhang, L.; Zhao, X.; Liu, S.; Li, D., (2019). Removal of Pb (II), Cd (II) and Hg (II) from aqueous solution by mercapto-modified coal gangue. J. Environ. Manage. 231: 391-396 (**6 pages**).

Sheng, P.X.; Ting, Y.P.; Chen, J.P.; Hong, L., (2004). Sorption of lead, copper, cadmium, zinc, and nickel by marine algal biomass: characterization of biosorptive capacity and investigation of mechanisms. J. Colloid Interface Sci., 275: 131–141 (**11 pages**).

Sireesha, S.; Agarwal, A.; Sopanrao, K.S.; Sreedhar, I.; Anitha, K.L., (2022). Modified coal fly ash as a low-cost, efficient, green, and stable adsorbent for heavy metal removal from aqueous solution. Biomass Convers. Biorefin., 1-23 (**23 pages**).

Song, H.; Kumar, A.; Zhang, Y., (2022). A novel approach for the removal of Pb^{+2} and Cd^{2+} from wastewater by sulfur-ferromagnetic nanoparticles (SFMNs). Chemosphere. 287: 132156 (8 pages).

Sulistyowati, L.; Nurhasanah, N.; Riani, E.; Cordova. M.R., (2023). Heavy metals concentration in the sediment of the aquatic environment caused by the leachate discharge from a landfill. Global J. Environ. Sci. Manage., 9(2): 323-336 (**14 pages**).

Sun, Y.; Song, X.; Ma, J.; Yu, H.; Liu, G.; Chen, F., (2022). Preparation and characterization of a novel amidoxime-modified polyacrylonitrile/fly ash composite adsorbent and its application to metal wastewater treatment. Int. J. Environ. Res. Public Health. 19(2): 856 (**13 pages**).

Tambaru, D.; Djahi, B.S.; Ndii, M.Z., (2018). The effects of hard water consumption on kidney function: insights from mathematical modelling. In: AIP conference proceedings. 1. AIP Publishing LLC: 020020 (**8 pages**).

Tamizharasan, S.; Muralidharan, R.; Abirami, N.; Leelavathi, H.; Siva, A.; Kumarasamy, A.; Arulmozhi, R., (2023). Biomass derived carbon blended ion-exchange resins for the removal of toxic metal ions from wastewater. Optik., 283: 170930 (**11 pages**).

Tang, W.W.; Zeng, G.M.; Gong, J.L.; Liang, J.; Xu, P.; Zhang, C.; Huang, B.B., (2014). Impact of humic/fulvic acid on the removal of heavy metals from aqueous solutions using nanomaterials: a review. Sci. Total Environ., 468: 1014-1027 (**11 pages**).

UNDP, (2024). La dependencia del país y de los territorios de los hidrocarburos y el carbón en Colombia y la necesidad de la diversificación de las exportaciones y de la producción ante la transición energética.

Virolainen, S.; Wesselborg, T.; Kaukinen, A.; Sainio, T., (2021). Removal of iron, aluminium, manganese and copper from leach solutions of lithium-ion battery waste using ion exchange. Hydrometallurgy. 202: 105602 (**9 pages**).

Wang, F.; Lu, X.; Li, X.Y., (2016). Selective removals of heavy metals (Pb^{2+}, Cu^{2+}, and Cd^{2+}) from wastewater by gelation with alginate for effective metal recovery. J. Hazard. Mater., 308: 75–83 (**9 pages**).

Wang, W.; Chen, M.; Guo, L.; Wang, W.X., (2017). Size partitioning and mixing behavior of trace metals and dissolved organic matter in a south China estuary. Sci. Total Environ., 603: 434–444 (**11 pages**).

Wang, P.; Liu, W.; Xu, H.; Liu, G., (2021). Adsorption of Pb (II) cation from aqueous solutions by acid modified low-rank coal: an experimental study and simulation. Water Sci. Technol. 84(12): 3726-3737 (**12 pages**).

Wang, Y.; Li, J.; Wei, X.; Zhou, Z.; An, L.; Zheng, S., (2024a). Construction of two protein-SmtA-based bio-microspheres as efficient 'collector'of heavy metal ions. Int. Biodeterior. Biodegrad., 189: 105768 (**10 pages**).

Wang, L.; Zhao, H.; Li, S.; Guo, B.; Huang, X.; Gao, P.; Ji, P., (2024b). Simultaneous removal of methylene blue and cadmium from aqueous solution by a novel sulfonated material: Characterization, mechanism and application. Environ. Chem. Eng., 12(1): 111706 (**11 pages**).

Wattanakornsiri, A.; Rattanawan, P.; Sanmueng, T.; Satchawan, S.; Jamnongkan, T.; Phuengphai, P., (2022). Local fruit peel biosorbents for lead (II) and cadmium (II) ion removal from waste aqueous solution: a kinetic and equilibrium study. S. Afr. J. Chem. Eng., 42: 306-317 (**12 pages**).

Wong, C.W.; Barford, J.P.; Chen, G.; McKay, G., (2014). Kinetics and equilibrium studies for the removal of cadmium ions by ion exchange resin. J. Environ. Chem. Eng., 2(1): 698-707 (**10 pages**).

Yadav, S.K.; Singh, D.K.; Sinha, S., (2013). Adsorption study of lead (II) onto xanthated date palm trunk: kinetics, isotherm and mechanism. Desalin. Water Treat., 51(34-36): 6798-6807 (**10 pages**).

Yang, Y.; Wang, L.; Zhao, H.; Yan, F.; Li, S.; Guo, B.; Luo, C.; Huang, X.; Ji, P., (2023). Utilization of KOH-modified fly ash for elimination from aqueous solutions of potentially toxic metal ions. Environ. Res., 223: 115396 (**10 pages**).

Yuliani, G.; Qi, Y.; Hoadley, A.F.; Chaffee, A.L.; Garnier, G., (2012). Lignite clean up of magnesium bisulphite pulp mill effluent as a proxy for aqueous discharge from a ligno-cellulosic biorefinery. Biomass Bioenergy. 36: 411-418 (**8 pages**).

Zhou, Z.; Zhang, C.; Xi, M.; Ma, H.; Jia, H., (2023). Multi-scale modeling of natural organic matter–heavy metal cations interactions: aggregation and stabilization mechanisms. Water Res., 238, 120007 (**12 pages**).

Zhou, L., (2024). Improving the removal performance of cadmium from wastewater by phosphate modified sludge biochar: a mineral dissolution-precipitation perspective. Desalination Water Treat., 320: 100865 (**11 pages**).

Zhu, Y.; Fan, W.; Zhou, T.; Li, X., (2019). Removal of chelated heavy metals from aqueous solution: a review of current methods and mechanisms. Sci. Total Environ., 678: 253–266 (**14 pages**).

AUTHOR (S) BIOSKETCHES

Fuentes-Gandara, F., Ph.D., Professor, Department of Natural and Exact Sciences, Universidad de la Costa, Barranquilla, Colombia.
- Email: *fabioar20@hotmail.com*
- ORCID: 0000-0002-0681-0544
- Web of Science ResearcherID: GXV-7697-2022
- Scopus Author ID: 57192062455
- Homepage: https://www.researchgate.net/profile/Fabio-Fuentes

Cabrera-Lafaurie, W., Ph.D., Professor, Corporación Universitaria de Ciencias Empresariales, Educación y Salud – Corsalud, Barranquilla, Colombia.
- Email: *wilman.cabrera@unicorsalud.edu.co*
- ORCID: 0000-0002-9041-7576
- Web of Science ResearcherID: CIM-7743-2022
- Scopus Author ID: 37009535700
- Homepage: https://www.researchgate.net/profile/Wilman-Cabrera

Piñeres-Ariza, I., Ph.D., Professor, Department of Physics, Faculty of Basic Sciences, Universidad del Atlántico, Barranquilla, Colombia.
- Email: *ismaelpineres@mail.uniatlantico.edu.co*
- ORCID: 0000-0003-4871-6211
- Web of Science ResearcherID: GQB-0840-2022
- Scopus Author ID: 56017822200
- Homepage: https://www.researchgate.net/profile/Ismael-Pineres

Espinosa-Fuentes, E., Ph.D., Professor, Faculty of Engineering, Universidad Libre, Barranquilla, Colombia.
- Email: *eduardo.espinosaf@unilibre.edu.co*
- ORCID: 0000-0003-1653-5408
- Web of Science ResearcherID: DVL-0558-2022
- Scopus Author ID: 24340657400
- Homepage: https://www.researchgate.net/profile/Eduardo_Espinosa

Marrugo-Negrete, J., Ph.D. Professor, Faculty of Basic Sciences, Department of Chemistry, Universidad de Córdoba, Montería, Colombia.
- Email: *jmarrugo@correo.unicordoba.edu.co*
- ORCID: 0000-0002-3181-7529
- Web of Science ResearcherID: FJD-6078-2022
- Scopus Author ID: 23480310100
- Homepage: https://www.researchgate.net/profile/Jose-Marrugo-Negrete

Pinedo-Hernández, J., M.Sc., Assistant Professor, Faculty of Basic Sciences, Department of Chemistry, Universidad de Córdoba, Montería, Colombia.
- Email: *josejph@hotmail.com*
- ORCID: 0000-0002-4288-1788
- Web of Science ResearcherID: AAV-2548-2021
- Scopus Author ID: 55780076200
- Homepage: https://www.researchgate.net/profile/Jose-Pinedo-2

HOW TO CITE THIS ARTICLE

Fuentes-Gandara, F.; Cabrera-Lafaurie, W.; Piñeres-Ariza, I.; Espinosa-Fuentes, E.; Marrugo-Negrete, J.; Pinedo-Hernández, J., (2025). Removal of cadmium and lead using a sub-bituminous coal resin modified with xanthate groups. Global J. Environ. Sci. Manage., 11(3): 1035-1056.

DOI: 10.22034/gjesm.2025.03.10

URL: https://www.gjesm.net/article_724627.html

Global J. Environ. Sci. Manage. 11(3): 1057-1078, Summer 2025, Serial #43

Global Journal of Environmental Science and Management
(GJESM)

Homepage: https://www.gjesm.net/

Podcasts

ORIGINAL RESEARCH PAPER

Conserving biodiversity, carbon, and community values in a fragmented landscape

A. Susilowati[1,*], Y. Lisnawati[2] , H.H. Rachmat[2], H. Kurniawan[2], W.C. Adinugroho[2], R. Imanuddin[2], D. J. Sudrajat[3], I.W.S. Dharmawan[2], M. Iqbal[2], S. Fahmi[2], L.M. Nugraha[2], E. Novriyanti[3], E. Sutrisno[4], A.B. Siswanto[5]

[1] *Faculty of Forestry, Universitas Sumatera Utara. Kampus 2 USU Bekala, Deli Serdang 20353, North Sumatera, Indonesia*

[2] *Research Center for Ecology and Ethnobiology, Research Organization for Life Sciences and Environment, National Research and Innovation Agency, Cibinong, 16911, Indonesia*

[3] *Research Center for Applied Botany, Research Organization for Life Sciences and Environment, National Research and Innovation Agency, Cibinong, 16911, Indonesia*

[4] *Kampar Social Forestry Institute, Ministry of Forestry Republic of Indonesia, Jl., Kampar District, Riau Province, Indonesia*

[5] *Ministry of Forestry Republic of Indonesia, Jl., Kampar District, Riau Province, Indonesia*

ARTICLE INFO

Article History:
Received 08 February 2025
Revised 13 April 2025
Accepted 15 May 2025

Keywords:
Above-ground biomass
community perception
conservation
Ecosystem services
Forest fragmentation
Imbo Putui Customary Forest

ABSTRACT

BACKGROUND AND OBJECTIVES: Fragmenting forests into small and isolated areas due to deforestation increases the risk of species loss. To address global warming, it is crucial to manage fragmented forests, promote income diversification, recycle nutrients and water, and support habitats for numerous specie. One form of forest resulting from fragmentation is customary forests, which are managed by indigenous communities. The goals of this study included 1) assess the vegetation structure and biodiversity within customary fragmented forests, 2) evaluating the characteristics of the soil, 3) estimating the potential for carbon storage, and 4) analyzing community views and management practices associated these forests. The goal is to support the sustainable management of customary fragmented forests by providing scientific and social insights to maintain their ecological functions and community benefits.

METHODS: The study was conducted in the Imbo Putui Customary Forest in Petapahan Village, Kampar Regency, Riau Province, Indonesia. A total of 18 sample plots were subjected to observation. The analysis of vegetation aimed to assess the structure and composition of the stands, which served as the foundation for determining carbon stock potential. Biodiversity analysis was performed using open source software, which was used to calculate biodiversity indices (species richness, Shannon-Wiener diversity, and Simpson diversity). The analysis of variance was used for statistical tests comparing biodiversity metrics between tree and pole stage groups. Soil characteristics observed included physical, chemical, and biological aspects. The calculation of carbon stock focused on above-ground biomass from trees with diameters greater than 10 centimeters. The diversity of flora and fauna was sourced from general literature, and community perspectives were acquired through field surveys conducted via direct interviews.

FINDINGS: Five species with the highest importance index are Scorodocarpus borneensis, Syzygium glabratum, Richetia hopeifolia, Santiria oblongifolia, and Xylopia malayana. The Shannon-Wiener index value was 1.75, indicating relatively high species diversity. Simpson's index value was 0.8 at tree level, indicating relatively lower dominance of some species and higher overall diversity. This soil type is identified as Ultisol, known for its low fertility and acidic nature. Nevertheless, its cation exchange capacity and physical properties are conducive to plant growth and maintaining soil moisture. Carbon sequestration potential is significant, with potential above-ground biomass of 177.24 tons per hectare and carbon stock of 83.30 tons of carbon per hectare. Community perceptions are quite good towards conservation and environmental values, with a significance value greater than 0.05, indicating the same perceptions in all community structures and clusters.

CONCLUSION: Imbo Putui Customary Forest is a fragmented forest with relatively high species diversity. The physical characteristics of the soil at the site are conducive to supporting plant growth and providing access to groundwater. Generally, the forest continues to possess significant conservation value, notable carbon sequestration potential, positive perceptions from the community, and possibilities for the sustainable management of ecosystem services.

DOI: 10.22034/gjesm.2025.03.11

This is an open access article under the CC BY license (http://creativecommons.org/licenses/by/4.0/).

NUMBER OF REFERENCES
62

NUMBER OF FIGURES
9

NUMBER OF TABLES
6

*Corresponding Author:
Email: *arida.susilowati@usu.ac.id*
Phone: +62852 7080 1310
ORCID: 0000-0001-9608-4787

Note: Discussion period for this manuscript open until Sep 1, 2025 on GJESM website at the "Show Article".

INTRODUCTION

The escalating global deforestation rates have become a prominent concern in contemporary environmental discourse, resulting in the fragmentation of once-contiguous forests (Wingate *et al*., 2023). This fragmentation is characterized by fragmented and solitary patches of forest located within landscapes modified by human activity, including agricultural plantations, urban developments, and residential areas (Wingate *et al*., 2022). Habitat fragmentation is represents a major danger to the remaining forests; it is understood that this fragmentation impacts ecological dynamics, resulting in a higher extinction rate of species in smaller, isolated areas, whereas larger, less isolated fragments tend to lose species at a faster rate (Peh *et al*., 2014). Fragmentation will also cause direct loss of forest habitat and alter the structure and function of remaining forest patches. The increasing isolation of the remaining forest will result in changes in the composition of the forest plant community and nutrient cycling patterns (Yang *et al*., 2021). In spite of their disjointed nature, these forested regions play an important role in alleviating global warming (Janowiak *et al*., 2021), enabling income diversification (Garcia and Laurene, 2014), recycling nutrients and water resources, and providing habitats for many species (Kremen *et al*., 2018). The remaining forests become particularly important to preserve when land cover in the surrounding area substantially transforms into alternative land uses, such as agriculture, settlements, and plantations (Muche *et al*., 2023). Today's landscape is characterized by quick shifts in land cover and land use. The remaining indigenous forests are seen as important refuges for biodiversity and as areas that uphold cultural values often associated with religious significance (Lindenmayer *et al*., 2023). Indigenous peoples have inherited knowledge systems closely linked to biodiversity conservation (De Gregorio *et al*., 2023). Indigenous peoples and local communities are essential actors in environmental governance that maintain intergenerational relationships with nature through livelihood practices, cultural identity, worldviews, institutions, and ecological knowledge (Brondízio *et al*., 2021; Suyadi *et al*., 2025). Native forests serve as prime examples of natural vegetation, harbor a variety of rare plant species, and retain greater carbon levels compared to non-forested regions (Maru *et al*., 2023). The importance of indigenous forests in biodiversity conservation and climate change mitigation has received increasing attention in recent studies (Lynch *et al*., 2018; Ekaputri *et al*., 2024). In Indonesia, the concept of customary forests, including the Imbo Putui Customary Forest (IPCF), is one of the traditional forest concepts that has been legally acknowledged by the state. The IPCF was established through Kampar Regent Decree No. 660-491/X/2018 and Ministry of Environment and Forestry (MoEF) Decree No. 7503/Menlhk-PSKL/PKTHA/Kum.1/9/2019 with an area of 251 hectares (ha). Located in Petapahan Village, IPCF is one of the fragmented forest areas in Tapung District, Riau Province. Before its designation as an adat forest, the IPCF was a restricted area that required permission from traditional authorities ("ninik mamak") to access or extract resources for the collective welfare of Indigenous communities (Lestari and Kusuma, 2022). Customary values and practices are represented in local expertise that regulates the careful use of timber, prohibits the burning of forests, defends sialang trees (*Koompassia excelsa*), and maintains the conservation of forest fruit plants. In addition, institutional roles are enforced through customary and social sanctions, along with regulatory measures implemented by village officials and "ninik mamak", all of which contribute to preserving IPCF as a Prohibition Forest (Dasrol and Bachtiar, 2020). While, numerous studies have examined one certain aspect of IPCF, the present work provides the first comprehensive quantification of IPCF's multifunctional role as: a carbon sink, a biodiversity refuge, and a livelihood foundation for local communities. The created framework delivers transferable metrics for analyzing ecological and social compromises in human-modified landscapes. The study aims are to 1) assess the vegetation structure and biodiversity within customary fragmented forests, 2) evaluate soil characteristics, 3) estimate their carbon storage potential, and 4) analyze community perceptions and management practices. This study will focus on the significance of customary fragmented forests in safeguarding biodiversity and identifying variations in habitats. Understanding ecological conditions and local perceptions provides a basis for designing future policies and practical management strategies in the face of evolving environmental landscapes. This study was conducted in the IPCF, Riau Provinces-Sumatera-Indonesia, in 2024.

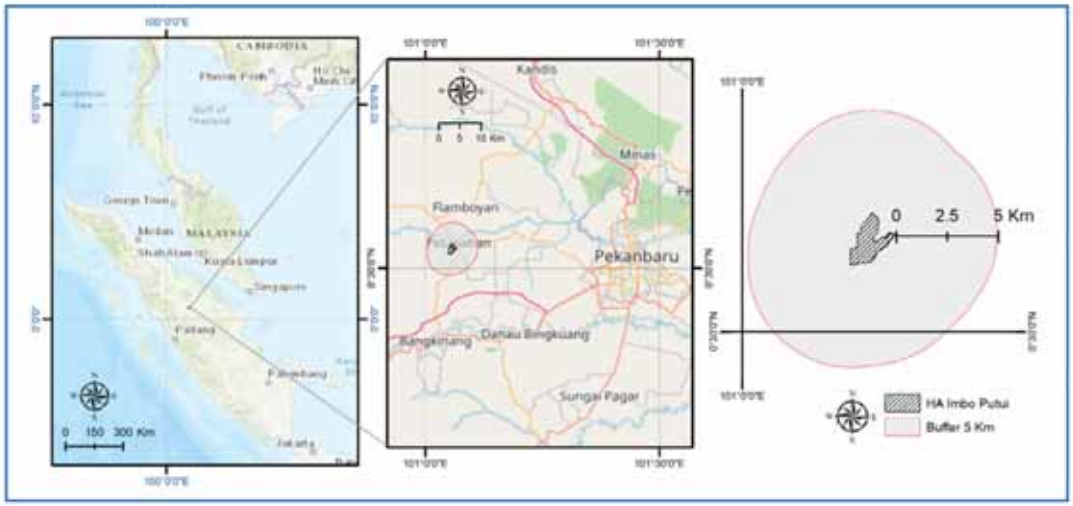

Fig. 1: Geographic location of the study área in the Imbo Putui Customary Forest of Riau Province, Indonesia

MATERIALS AND METHODS

Study area

IPCF is located in the administrative area of Petapahan Village, Tapung District, Kampar Regency, Riau Province, Indonesia. Petapahan Village is home to the indigenous people of Petapahan. The IPCF encompasses 251 hectares, with oil palm concessions surrounding it to the west, north, and south, and community fields and land plots in Petapahan Village lying to the east (Fig. 1).

Vegetation structure and biodiversity analysis

Vegetation analysis assessed stand structure and composition to estimate carbon stock potential. Data were collected from 18 systematically placed plots to ensure spatial representativeness across different forest condition as 20×20 meters (m) for trees, 10×10 m for poles, recording coordinates, species, diameter at breast height (DBH), and height. This number of plots corresponds with ecological studies conducted in tropical forests, where factors such as logistical challenges and landscape accessibility often impact the sampling process. Biodiversity analysis in R used packages (vegan, Biodiversity-R, Interpolation and Extrapolation (iNEXT) to compute indices (richness, Shannon/Simpson diversity). Analysis of variance (ANOVA) was applied for statistical comparisons of biodiversity indices. Significant species indicators were established through relative frequency, density, and dominance, which is assessed via basal area.

Soil characteristics

Soil data collected from field sampling and the Agricultural Land Resources Center (Ministry of Agriculture). Sampling covered nine points: three undisturbed IPCF areas, three human-disturbed areas, and three oil palm plantations. Soil cores as 0–20 centimeters (cm) depth) were collected using a brass tube (7.67 cm inner diameter, 7.97 cm outer diameter, 4 cm height) and analysed by the Agricultural Instruments Standardization Agency Laboratory. Chemical analysis included potential of hidrogen (pH) (electrometric), carbon (C) organic (Walkley and Black), macronutrients of nitrogen (N) total [Kjeldahl], phosphorus (P) total [hydrochloric acid (HCl) 25 percent: %], available P [Bray I], potassium (K) total [Morgan]), exchangeable cations (potassium (K), Calcium (Ca), Magnesium (Mg), Aluminium cation (Al^{3+}), hydrogen cation (H^{+}), cation exchange capacity (CEC) (amonium (NH_4)-acetate 1.0N pH 7), and base saturation (BS). Physical analysis measured bulk density, porosity, water content, and permeability. Soil fertility was evaluated using Prabowo and Subantoro (2017) criteria. T-tests were utilized for data comparisons and analyzed through statistical package for the social sciences (SPSS).

Carbon stock

Carbon stock in the IPCF was assessed by focusing on the above-ground biomass (AGB) of vegetation with a diameter greater than 10 cm. In mineral

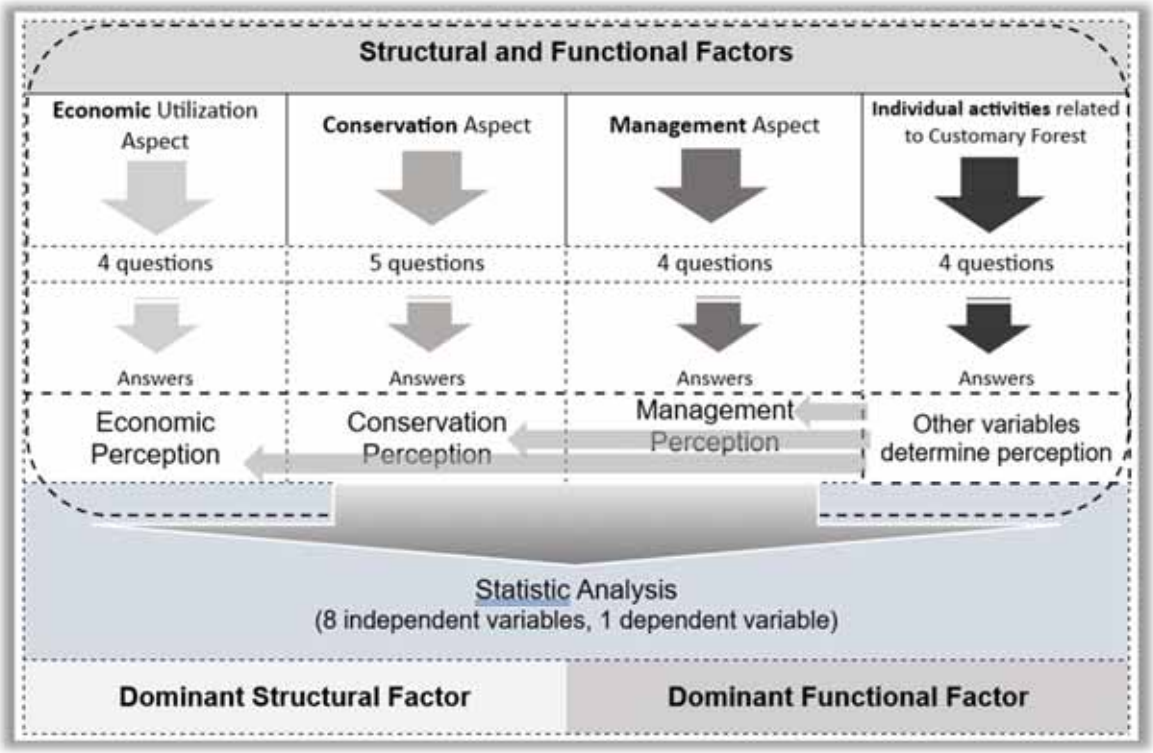

Fig. 2: Scheme of the research flow

soils, AGB is a key element of the carbon inventory (Krisnawati *et al*., 2014). AGB was estimated using Indonesia-specific allometric equations, particularly for the western region, using Eq. 1 (Manuri *et al*., 2017):

$$AGB = 0.167D^{2.56}G^{0.889} \quad (1)$$

Where; AGB = Above-ground biomass (kg), D = Tree diameter (cm), and G = Species Density (gram/cm^3). Because of its regional relevance and suitability for the vegetation types seen in the IPCF, this model was chosen. Although it provides a fair approximation for above-ground biomass (AGB), we note that destructive sampling within IPCF has not been used to confirm it. According to Yuen *et al*. (2016), utilizing site- or species-specific allometric equations is strongly recommended to reduce uncertainty and enhance the accuracy of biomass and carbon stock estimates in tropical ecosystem. A carbon fraction of 47% of biomass is employed to calculate the carbon stock in the ecosystem.

Community perception of customary forest

Public perception data came from direct interviews with 62 respondents divided into three groups: (1) 8 community/institutional leaders, (2) 24 direct IPCF users, and (3) 30 non-users. The questionnaire collected personal data (education, occupation) and 17 questions about IPCF perceptions, categorized into functional and structural factors. The analysis of responses was conducted as binary outcomes (positive/negative) concerning economic, conservation, and management dimensions. Fig. 2 presents the flowchart of the study

The perception questionnaire was formulated based on significant themes identified in the literature regarding ecosystem services and customary forest governance. It included 17 questions, grouped into economic, conservation, and management categories. A pre-test with five individuals helped refine language and structure for clarity. The responses were corroborated by cross-referencing field observations and secondary data. To ensure diverse

Table 1: The highest importance value index for both tree and pole stage

Species	Genus	Family	IV (%)
Tree			
Scorodocarpus borneensis (Baill.) Becc.	Scorodocarpus	Strombosiaceae	83.57
Syzygium glabratum (DC.) Veldkamp	Syzygium	Myrtaceae	35.42
Richetia hopeifolia (F.Heim) P.S.Ashton & J.Heck.	Richetia	Dipterocarpaceae	21.21
Santiria oblongifolia Blume	Santiria	Burseraceae	15.64
Xylopia malayana Hook. f. & Thomson	Xylopia	Annonaceae	10.68
Pole			
Scorodocarpus borneensis (Baill.) Becc.	Scorodocarpus	Strombosiaceae	46.02
Syzygium glabratum (DC.) Veldkamp	Syzygium	Myrtaceae	30.68
NN3_	nn	nn	29.39
NN7_	nn	nn	26.93
Rubroshorea macroptera (Dyer) P.S.Ashton & J.Heck.	Rubroshorea	Dipterocarpaceae	21.18

representation from important community groups, stratified sampling was applied, and interviews were conducted anonymously by trained enumerators to mitigate bias. Factor-perception relationships were analyzed using logistic regression (Sperandei, 2014), which models categorical dependent variables (Maalouf, 2011). Eight independent variables were tested: respondent cluster, age, education, gender, occupation, familiarity duration, information sources, and visit frequency. The study revealed the primary elements that had the greatest impact on community perceptions (both positive and negative) of the customary forest.

RESULTS AND DISCUSSION

Vegetation structure and composition

The five species with the highest importance value index (IVI) were Kulim (*Scorodocarpus borneensis*), Red Kelat (*Syzygium glabratum*), Meranti (*Richetia hopeifolia*), Lalan (*Santiria oblongifolia*), and Mempisang (*Xylopia malayana*) (Table 1 and Fig. 3). At the pole stage, which refers to young trees with a diameter of approximately 10–20 cm measured at breast height, the dominant species remained relatively consistent, with Kulim, Red Kelat, two unidentified species (NN3, NN7), and Meranti Merah (*Rubroshorea macroptera*) showing the highest IVI values.

The ANOVA findings indicated notable variations in diversity indices, including Chao species richness, Shannon's, and Simpson's, while highlighting *Scorodocarpus borneensis* as the predominant species ecologically at both tree and pole levels within the IPCF.

Chao species diversity was more pronounced in the tree stage (6) than the pole stage (2) (Fig. 4), probably as a result of human activities like selective logging, land clearing, and habitat fragmentation (Zamorano-Elgueta *et al*., 2014). The lower pole-stage richness may reflect disrupted regeneration caused by seed harvesting and microclimate changes (Gonçalves *et al*., 2017), particularly for kulim (*Scorodocarpus borneensis*), whose fruits are heavily collected for culinary use (Kustiawan *et al*., 2022). Diversity indices support this pattern: tree-stage Shannon (1.75) and Simpson (0.8) values indicate relatively even species distribution, while pole-stage values (Shannon 0.70; Simpson 0.5) suggest dominance by fewer species. This structural variation is likely a reflection of historical biological and environmental pressures (Mekonen *et al*., 2015), encompassing resource competition, the prevalence of pioneer species, and selective harvesting that have modified the forest's primary composition.

The three dominant families were Olacaceae (primarily *Scorodocarpus borneensis*), Myrtaceae (*Syzygium spp.*), and Dipterocarpaceae (*Shorea* spp.) (Fig. 5). Vegetation analysis across 18 plots showed higher pole density (205.5/ha) than tree density (169.4/ha), a pattern typical of natural

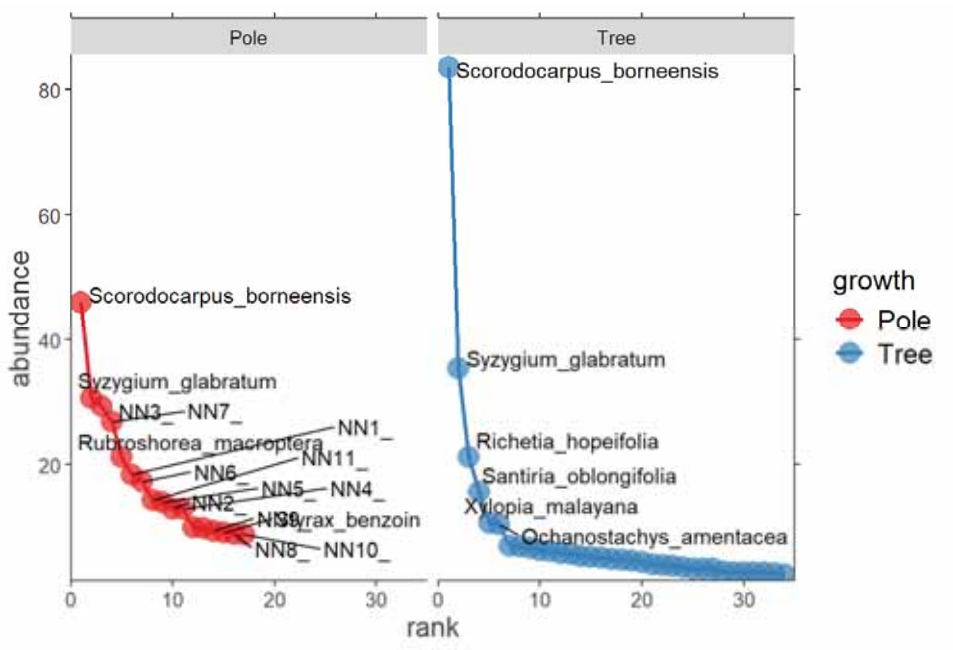

Fig. 3: Vegetation structure and composition

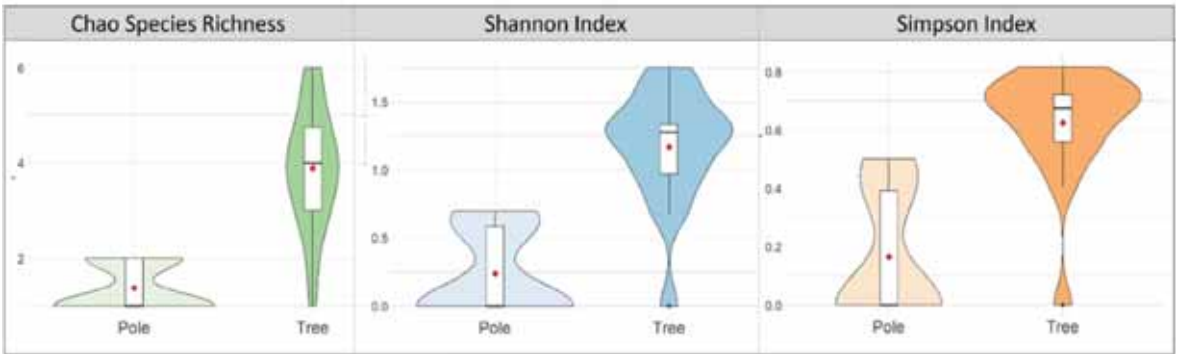

Fig. 4: The diversity indices for the tree and pole stage at Imbo Putui customary forest

forests though, less pronounced than in undisturbed stands. Undisturbed forests generally display an inverted J-shaped structure, signifying a consistent influx of late-successional species (Gonçalves *et al.*, 2017). The observed pole-tree distribution (Fig. 6) aligns with an interrupted inverse J-shape, one of four structural patterns identified by Mekonen *et al.* (2015) for woody plant populations. This shape suggests incomplete regeneration accompanied by inconsistencies in IPCF. Such a pattern suggests gaps in regeneration—possibly due to past disturbances in the IPCF—leading to an uneven transition from saplings to mature trees. If this trend remains, the forest might see shifts in its composition, promoting species that excel in disrupted conditions over those that are typically dominant in stable, late-successional dominance. Statistically, this is supported by the pole density (205.5/ha) exceeding tree density (169.4/ha), deviating from the smooth inverse J-curve typical of stable forests (Mekonen *et al.*, 2015). The fragmented structure relates to disturbed or secondary forests where regeneration is taking place, but balance has not yet been achieved. Thus, while some natural recovery is evident, long-term stability remains

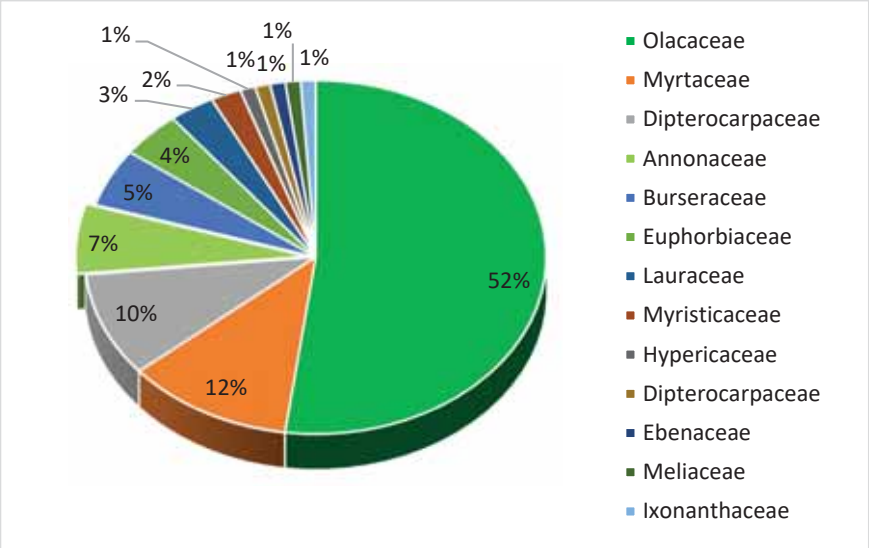

Fig. 5: Percentage of trees' family which composed IPCF

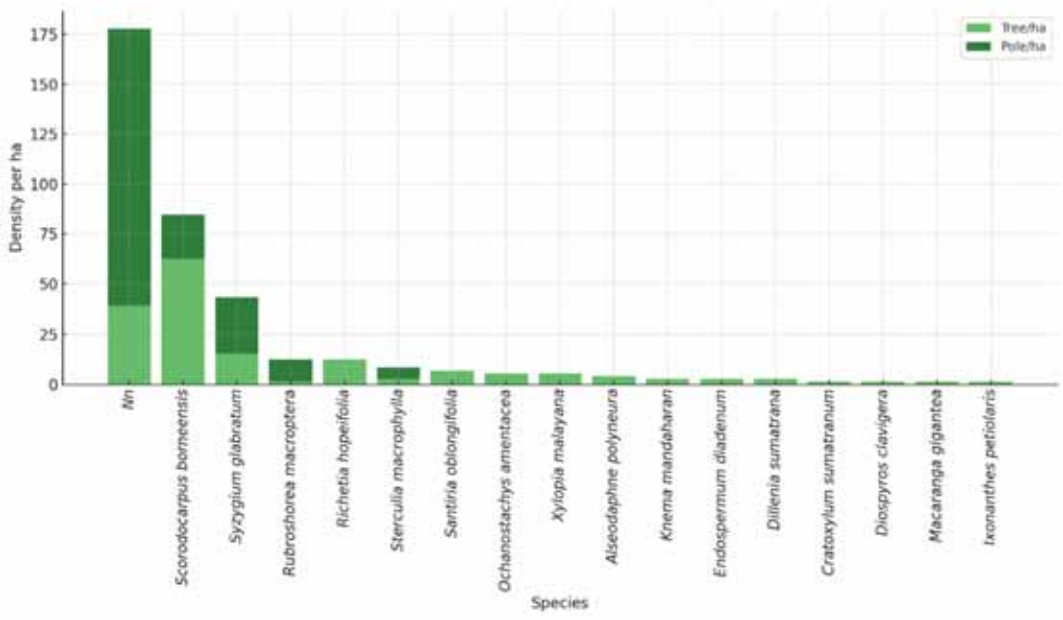

Fig. 6: Number of poles and trees per hectare in the Imbo Putui customary forest

uncertain without consistent recruitment into larger size classes. Though regeneration is uneven (pole density 205.5/ha > trees density 169.4/ha), the IPCF maintains greater biodiversity and carbon stocks than oil palm plantation (Lindh *et al.*, 2024). Its structural complexity including large trees such as *Scorodocarpus borneensis* and *Shorea* spp. Members of the Dipterocarpaceae family offer microhabitats for different species. Despite the carbon pool not being optimally sequestered because of disrupted recruitment, it remains greater than that of standard agroforestry and also oil palm plantation. Strategic conservation could amplify these benefits, as this fragmented IPCF retain higher ecological value than

Table 2: Physical properties of soil at the study site

Parameters	Imbo Putui customary forest (undisturbed)^{ns}	Imbo Putui customary forest (disturbed)^{ns}	Oil palm plantation^{ns}
Bulk Density (g/cc)	0.85	0.95	0.82
Total pore space (%)	59.4	57.0	61.2
Permeability (cm/h)	1.47	2.60	3.57
Water content (%)	34.13	34.67	32.43
Water availability (%)	15.93	15.10	10.27
Soil textura	Silt loam	Silt loam	Silt loam

the surrounding landscape that dominated by oil palm, serving as reservoirs for recovery and connectivity in human-modified landscapes. Disruption of ecological processes, including pollination and seed dispersal that rely on animal vectors, can occur due to forest fragmentation. While, this study did not explicitly evaluate faunal diversity, prior observations in the IPCF note the presence of potential pollinators (e.g., bees) and seed dispersers (e.g., rodents, mammals) (Arianto, 2021). The occurrence of Dipterocarpaceae (e.g., *Shorea* spp.) across both tree and pole stages confirms this keystone family's persistence in the IPCF, a critical family of tropical lowland forests. While their presence suggests ecological continuity, the species mismatch between size classes implies regeneration barriers (e.g., habitat alteration, logging). The Dipterocarp family is a favorable indicator of ecological resilience, supporting biodiversity, aiding in carbon sequestration, and maintaining forest structure (Saura *et al.,* 2019). To enhance conservation, restoration efforts should prioritize in protecting mature seed-bearing trees, enrichment planting in degraded IPCF areas, and community-based monitoring to reduce anthropogenic pressures. Understanding their natural regeneration is essential for developing adaptive management strategies that promote the enduring stability of this fragmented ecosystem.

Characteristics and soil fertility status in Imbo Putui Customary Forest and surrounding oil palm plantations

Soil characteristics

In the study area, the soils are identified as Ultisols (Soil Survey Staff, 2014), which generally possess advantageous physical traits yet exhibit low chemical fertility (Fitriatin *et al.,* 2014). This study compared soil's physical and chemical fertility in IPCF and surrounding oil palm plantations (Table 2). Analysis of the texture revealed consistency among the sites, as three locations (undisturbed IPCF, disturbed IPCF, and oil palm plantations) consisting of silt loam, which retains water moderately yet is prone to erosion. IPCF's superior water retention and carbon sequestration capacity can be a cornerstone for regional sustainable land-use planning by implementing it as a nature-based solution (NbS) alternative to conventional land uses like oil palm plantations. It is essential to require the integration of policy, ecological valuation, and participatory mechanisms to align conservation efforts with regional developmen. Water availability varied significantly ($p < 0.05$), being highest in undisturbed IPCF (15.93%), followed by disturbed IPCF (15.10%) and oil palm plantations (10.27%). The observed differences are likely a result of variations in permeability, pore space, and organic matter content that impact bulk density (BD). Undisturbed IPCF had the lowest BD (0.85 g/cm^3), while disturbed IPCF (0.95 g/cm^3) and oil palm plantations (0.82 g/cm^3) showed contrasting trends. The lower BD in plantations may result from compost application and root-induced soil aeration (Lucas *et al*., 2022). Despite higher permeability and pore space in plantations, their water availability was reduced due to oil palms' high water demand (~1000 l/ha/day; Safitri *et al*., 2018), which can decrease water discharge by 30–40% (Akram *et al*., 2021). The elevated water demand for oil palm plantations will decrease the potential for effective water retention. The potential for increasing water retention in oil palm plantations can be increased through agroforestry cropping patterns between oil palm and forest plant species.

Soil fertility status

Soil fertility analysis conducted at the three study sites indicated persistently low fertility levels, defined by extremely low base saturation (4-13%), inadequate total P and K levels, and elevated acidity (Table 3). The

Table 3: Soil fertility status evaluation results

Parameters	Imbo Putui customary forest (undisturbed)[ns]	Imbo Putui customary forest (disturbed)[ns]	Oil palm plantation[ns]
CEC (me/100g)	62.75 ± 11.39 (extremely high)	43.99 ± 28.48 (extremely high)	49.16 ± 4.22 (extremely high)
Base Saturation (%)	4 ± 0.76 (extremely low)	13 ± 15.16 (extremely low)	7 ± 1.70 (extremely low)
C-organic (%)	7 ± 3.01 (extremely high)	7 ± 0.56 (extremely high)	8 ± 1.48 (extremely high)
P-total (mg/100g)	4 ± 0.58 (extremely low)	2 ± 0.58 (extremely low)	4 ± 1.00 (extremely low)
K-total (mg/100g)	5 ± 1.00 (extremely low)	4 ± 1.00 (extremely low)	6 ± 1.00 (extremely low)
Fertility Status	Low	Low	Low
pH	3.44 (very acidic)	3.89 (very acidic)	4.61 (acidic)

observed conditions stem from various influences: base cations are prone to leaching, phosphorus is rendered unavailable, and high concentrations of aluminum and iron generate acidic conditions that negatively affect plant growth by limiting root expansion and nutrient acquisition (Chen *et al*., 2022). The pronounced soil acidity stems from organic matter adsorption/desorption processes and heterotrophic microbial respiration (Ding *et al*., 2021). Despite these fertility constraints, the soils exhibit remarkably high CEC due to substantial organic carbon content (7-8%), which provides abundant cation exchange sites (Ćirić *et al*., 2023; Zgorelec *et al*., 2019; Zhang *et al*., 2015). The elevated CEC present in IPCF facilitates the retention of limited base cations (Mg, K, Ca), providing a buffer against nutrient depletion in a fragmented environment where microclimatic variations and edge effects enhanceleaching. However, the low base saturation (4-13%) reflects, where decomposition and mycorrhizal networks are critical to mobilizing nutrients. The silt loam texture (62% silt) balances water retention (15.93% in undisturbed areas), reducing drought stress. These characteristics support the intricate structure of IPCF forests and their ability to sequester carbon, even when faced with fragmentation challenges.

The very low base saturation suggests a limited availability of base cations (Ca, Mg, K, Na). When a forest soil has high CEC but low base saturation it implies that the soil can retain a significant amount of nutrients (high CEC), yet the exchange sites are predominantly filled with acidic cations (H^+, Al^{3+}) rather than base cations (Ca^{2+}, Mg^{2+}, K^+, Na^+) that are essential for plant growth. This combination often occurs in weathered tropical soils or acidic forest soils, and limits nutrient availability. In order to preserve forest productivity under these conditions, a range of scientifically validated soil management strategies can be implemented, including liming, amending with organic matter, choosing nitrogen-fixing plants, and applying mycorrhizal inoculation. The deficient P and K levels likely originate from advanced mineral weathering and poor solubility (Zhang *et al*., 2021). High CEC (43.99-62.75 me/100g), driven by a 7-8% increase in organic carbon, enhances forest sustainability by improving nutrient retention, root growth and water retention (Sulieman *et al*., 2018). The integration of these soil attributes with proper fertilization can markedly boost forest productivity and resilience, facilitating sustainable land use practices. This finding underscores the importance of conserving IPCF so that soil organic matter can continue to accumulate in a closed nutrient cycle that will minimize nutrient losses. The shift from forests to monoculture plantations will disrupt the nutrient cycle, transitioning it to an open cycle, consequently leading to a decline in soil organic matter and nutrient content

Carbon stock potential

This study quantified carbon sequestration potential IPCF by analyzing vegetation across 18 plots, revealing substantial above-ground biomass with 177.24 ± 21.27 tons per hectare (t/ha) and carbon stocks with 83.30 ± 9.99 tons of carbon per hectare (t C/ha). While, this study presents a snapshot of the

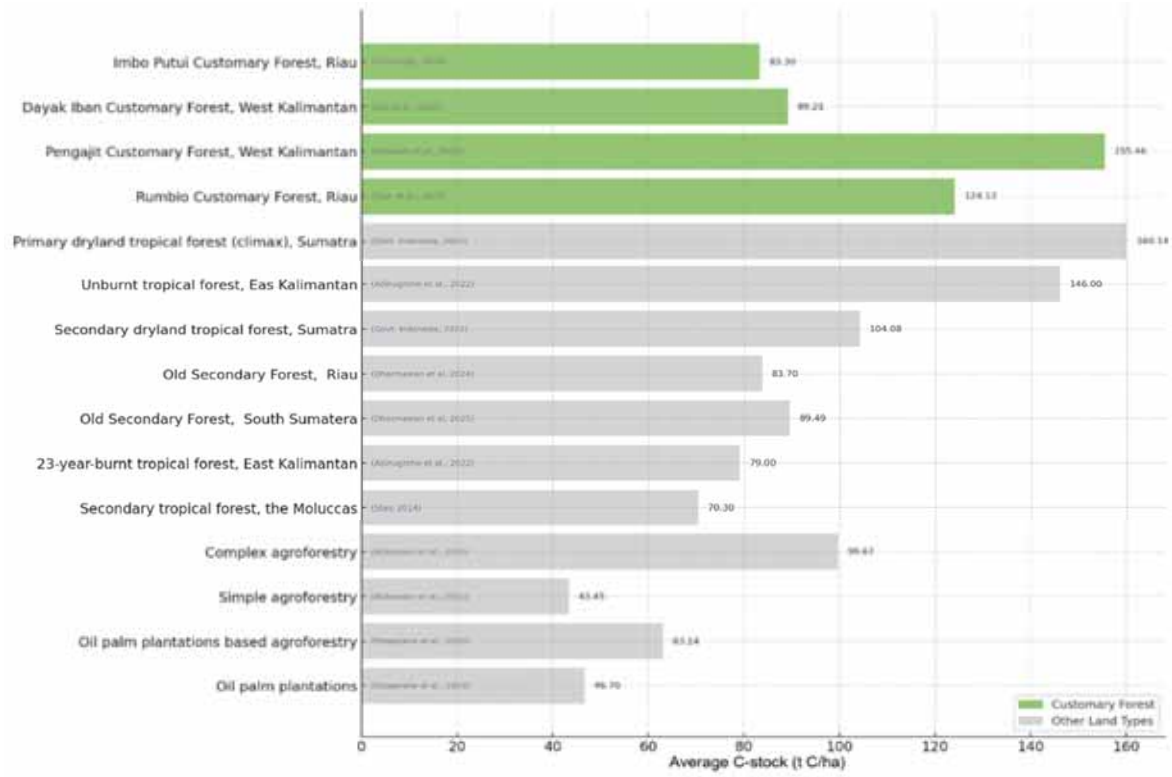

Fig. 7: A comparative of carbon stocks between the IPCF and various other customary forest sites and land uses

ecological condition in IPCF, long-term monitoring data are currently unavailable. However, comparative analysis with other forest systems (Fig. 7) indicates that IPCF's carbon storage is less than that of the traditional forests in Pengajit – West Kalimantan (155.46 t C/ha) and Rumbio-Riau (124.12 t C/ha) or Sumatra's primary dryland forests (160.14 t C/ha; (Government of Indonesia, 2022), significantly exceeds degraded landscapes such as oil palm plantations (46.70 t C/ha). The disparity with primary forests reflects differences in structural complexity—mature forests accumulate more carbon through large trees, deadwood, and understory development—whereas IPCF's intermediate values demonstrate its ecological resilience despite fragmentation. Remarkably, IPCF surpasses secondary forests (70.30 t C/ha) and straightforward agroforestry (59.37 t C/ha), which can be credited to its diverse stand composition and reduced anthropogenic interference (Murphy, 2024). This pattern supports broader findings in tropical forest ecology, where biodiversity and carbon stocks decline with increasing fragmentation and anthropogenic pressure. The findings emphasize IPCF's important role as a regional carbon sink and a sanctuary for biodiversity, underlining the urgent requirement for formal protection to sustain these functions as plantations continue to expand. By safeguarding such customary forests, Indonesia could synergize climate mitigation targets with indigenous livelihood security and ecosystem conservation.

The viability of customary forests, including Imbo Putui, is influenced by local governance practices, traditional laws, and outside pressures such as the growth of oil palm agriculture. IPCF's relatively lower carbon stock compared to other customary forests (Fig. 8) can be attributed to two key factors: 1) anthropogenic disturbances, including encroachment by oil palm plantations, and 2) its designation as an ecotourism area, which alters natural forest dynamics. Conversely, the Rumbio Customary Forest reveals superior conservation outcomes, largely owing to the application of stringent customary legal

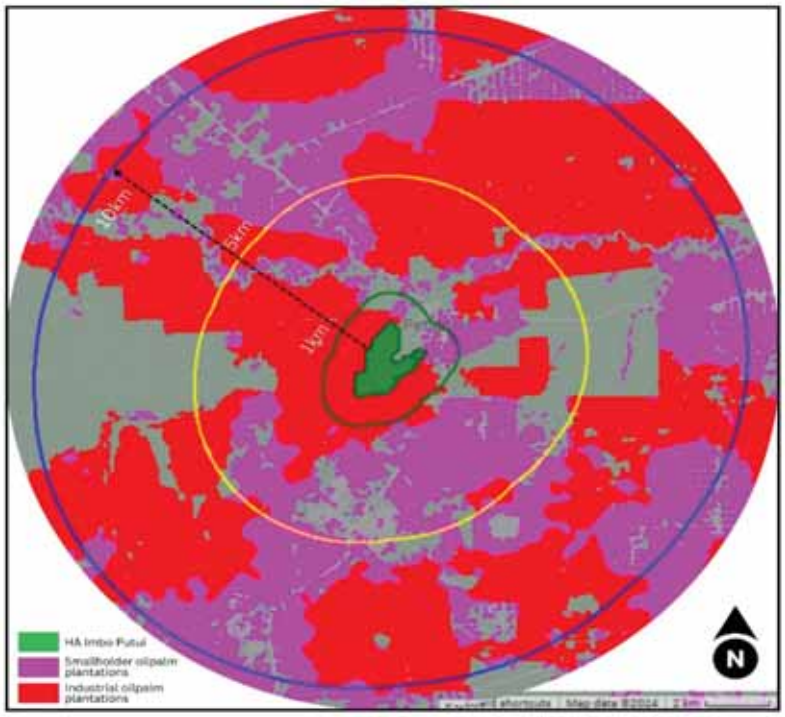

Fig. 8: The location of the IPCF surrounded by palm oil plantations

frameworks. The Rumbio community implements a 100-meter riparian buffer zone where logging is strictly prohibited, and the forest cannot be converted, inherited, or granted—regulations enforced through social sanctions. These measures not only reduce deforestation but also enhance hydrological functions, as evidenced by the presence of clean water springs in Rumbio, which correlate with higher carbon storage (Ritonga *et al.*, 2014). This combination of legal, cultural, and ecological influences emphasizes the vital contribution of effective customary governance to the resilience and maximizing carbon sequestration potential.

The IPCF exhibits significantly higher carbon stocks (86.03–396.20 t AGB/ha) compared to oil palm plantations, which typically store less than 50 t AGB/ha on drained peatlands (Lindh *et al.*, 2024). This disparity stems from the monoculture nature of oil palm systems, which limit species diversity and biomass accumulation (Ogbemudia *et al.*, 2023). In contrast, IPCF's diverse vegetation structure supports higher carbon retention despite selective harvesting pressures (Pelletier *et al.*, 2017). Converting from natural forests to plantations causes major substantial carbon depletion, while secondary forests and agroforestry practices usually retain more carbon compared to monoculture plantations. Although oil palm plantations offer economic benefits, their environmental impacts—particularly greenhouse gas (GHG) emissions and carbon loss—raise sustainability concerns. Agroforestry systems offer a more environmentally friendly land management alternative. Agroforestry's ability to store carbon is affected by the variety of plant species, the number of plants per area, and the practices used in land management (Karuru *et al.*, 2021). These factors influence overall carbon stock values, as ecosystems with higher biodiversity—especially those with structurally complex vegetation—tend to sequester more carbon than simplified monocultures. Consequently, increasing plant diversity and utilizing ecologically responsible land management techniques are vital for enhancing carbon sequestration in tropical landscapes. This contrast is critical for informing regional climate mitigation strategies, particularly as Indonesia advances its FOLU Net Sink

2030 commitment to achieve net-zero emissions in the forestry and land-use sector. It is recommend future research prioritize permanent plot monitoring to capture trends in ecological resilience and degradation under customary forest governance. IPCF's ecological resilience is under increasing threat due to a combination of human activities and ecological challenges. Encroachment and land conversion by expanding oil palm plantations, which directly reduce forest cover and fragment habitat.

Community perception of customary forest on the aspect of economic utilization, conservation, and management

The brief history of imbo putui customary forest

The existence of customary forests based on customary law is a source of law that applies in the community and applies across generations and is even adopted by state law. Customary forests serve as a means to protect ecological areas and biodiversity, while also prioritizing the religious beliefs and traditional wisdom of the local population (Nghi *et al*., 2025). Several versions of folklore stories through oral tradition have greatly colored and are even believed to be the origin stories of conditions, existence, and management of land, forests, nature, and existing community institutions. At present, the community can only utilize the IPCF under very strict conditions through permits from the village government and the customary leaders of the Petapahan Village community. The Village Regulation enacted in 2014 forbids hunting and deforestation in the IPCF. Those who violate this regulation will incur customary sanctions. For example, anyone who cuts down trees with a diameter of 20 cm or more will be fined with 50 bags of cement (Firmanda, 2017). Along with the development of time and changes in governance in Indonesia, the management of the IPCF is increasingly simplified in its utilization and management. Currently, the IPCF is managed by the Indigenous Community Institution led by the Supreme Datuk, assisted by customary and formal village government structures (Chahyana *et al.*, 2018). The IPCF gained governmental recognition in 2020 with the release of the MoEF Decree that designated customary forests, delivered personally by the President of the Republic of Indonesia to the Datuk forest manager. The extent of the IPCF has undergone changed over time, and it is experiencing shrinkage. Originally, the land covered more than 500 ha; however, parts of it have been appropriated by palm oil plantation firms and subsequently allocated for housing development. Currently, the officially designated customary forest through Decree No: SK.7503/Menlhk-PSKL/PKTHA/Kum.1/9/2019 dated September 17, 2019, regarding the Designation of the IPCF in Petapahan Territory to the Customary Law Community of Petapahan Territory covers an area of 251 ha. The utilization of the IPCF is increasingly restricted and diminished over time. The community no longer fully utilizes the customary forest to meet their needs, such as building houses and other things. Currently, the administration of the traditional forest has transitioned to leveraging environmental services, including ecotourism, education, and research, along with the potential for carbon sequestration services.

The community's perception of Imbo Putui customary forest

Although not always visible, the perception formed within the community, will significantly determine what steps should be taken to anticipate any potential changes that may occur in the future (Lin *et al*., 2021). Understanding the social value of urban green spaces can be achieved through perception, which is measurable against specific geographical conditions (Buchel and Frantzeskaki, 2015). The earlier perception is understood and mapped, the more accurate the management planning and policies for the IPCF, the Petapahan Village community, and the external community.

Multivariate logistic regression analysis was used instead of a risk factor model. The goal of this analysis is to uncover the main influencing factor, so that all variables expected to shape public perception are treated uniformly. The variables included in the logistic regression model were selected based on their relevance to understanding community perceptions of customary forests. Furthermore, interactions are not included in the analysis due to the absence of primary and confounding variables, unlike the risk factor model. However, further research into public perception utilizing the risk factor model is crucial after identifying the primary influencing factors. Given that the objective of this study on community perception is to assess the probability of dominant factors influencing perception, and that a quantitative approach was applied in the analysis, the use of the

Table 4: Significance values for logistic regression analysis

Variables \ Aspect	Economic utilization	Conservation and Environmental	Management
	Sig.value	Sig.value	Sig.value
Cluster	0.004	0.617	0.92
Age	0.972	0.997	0.103
Education	0.942	0.62	0.25
Gender	0.736	0.998	0.173
Occupation	0.525	0.687	0.012
Length of knowing	0.155	0.903	0.165
Source of information	0.017	0.657	0.584
Visitation	0.742	0.488	0.985

Table 5: Logistic regression analysis results for economic utilization aspect

Variable	B	S.E.	Wald	db	Sig.	Exp(B)
Cluster	-1.215	0.426	8.146	1	0.004	0.297
Constant	2.505	1.027	5.945	1	0.015	12.245

term 'no significant difference' is necessary. This implies that these factors may still influence the variations in perception that have been observed. According to the logistic regression analysis shown in Table 4, eight variables were found to influence community perceptions, classified into structural factors (cluster, education, occupation, familiarity duration, information source) and functional factors (age, gender, visitation frequency). For economic utilization perceptions, only two variables showed significant effects: cluster (p=0.004) and information source (p=0.017). Subsequent analysis indicated that these results were no longer significant (cluster p=0.058; information source p=0.500), resulting in their exclusion. Consequently, cluster emerged as the sole determinant of economic utilization perceptions (Table 5).

The significance values from simple logistic regression analysis are presented in (Table 4), and serve as the basis for selecting variables influencing the probability of community perceptions. A total of eight variables were selected and assessed to uncover the essential factors. These variables are grouped into two categories: structural factors (cluster, education, occupation, length of knowing, and information source about IPCF) and functional factors (age, gender, visitation). In terms of community perceptions related to economic utilization, Table 4 reveals that two variables significantly influence the probability of perception: These two variables are cluster (significance = 0.004) and information source (significance = 0.017). These were included in further logistic regression analysis. The results showed a significance value of 0.058 for cluster and 0.500 for information source. Thus, the sources of information were removed from the regression model. In the end, the cluster variable stands out as the sole candidate for inclusion, serving as the key determinant of perception probability concerning the economic benefits of customary forest. Final analysis results are shown in (Table 5). The IPCF ecosystem services that can provide direct benefits to the community are: 1) non timber forest products utilization for subsistence and tradition, like harvesting forest fruits (e.g., *kulim*) and edible mushroom for use in local cuisine, which also supports cultural practices; 2) controlled timber use: Despite being constrained by customary law, some regulated exploitation of forest resources aids in meeting housing demands and other customary uses under community oversight; 3) ecotourism and educational services: that will also generate potential income for local guides, service providers, and small businesses; 4) carbon sequestration services: the forest's carbon stock (83.3 tons C/ha) suggests potential for inclusion in carbon trading schemes or payment for ecosystem services (PES) in the

future. Viable and non-invasive economic initiatives that respect local culture and can benefit the IPCF surrounding communities consist of nature tourism and traditional ceremonies aimed at attracting visitors. During traditional events, the surrounding community can also sell food, drinks and other goods needed. The carbon market can also be utilized for the benefit of indigenous communities with assistance from non government organizations (NGOs) and the government. Harvesting of non-timber forest products (NTFPs), including kulim fruits and edible mushrooms, can bring direct financial benefits to the community. Kulim fruit not only serves as a cooking spice but also has significant market value. The study shows that most respondents prefer non-destructive forest uses such as recreation and education. This aligns with previous research (Lin *et al.*, 2021; Paudyal *et al.*, 2018), which show users value forests as habitat, recreational spaces, and service regulation sources. Gender, occupation, and income influence how ecosystem service utilization is perceived. In this study, perceptions differ significantly by cluster and information source regarding the IPCF.

For conservation and environmental value perceptions, Table 4 indicates no variable significantly influences perceptions. All eight variables exhibit significant values exceeding 0.05, indicating that perceptions of conservation and ecosystem services are largely uniform across community structures, reflecting a strong positive trend. This contrast with Porras-Salazar *et al.* (2023), who found age, gender and education as influential factors. Ecosystem services impact human life, and different stakeholders may disagree on the level of benefit (Thiemann *et al.*, 2022). Although there is a growing awareness of environmental issues, land degradation remains a challenge due to short-term economic practices, emphasizing the importance of enhancing the relationship between nature and urban environments (Yeo *et al.*, 2016). Although deforestation threats emerge from timber commodification and land demands, Hassen *et al.* (2023) found that indigenous governance systems and ecological knowledge can effectively support community-based conservation approaches. A majority (96.7%) of respondents recognize forests' role in climate change mitigation. According to Thompson (2015), mitigation and adaptation, biodiversity, and land use represent significant global concerns. Before 2012, customary forests were not recognized by the government as forests burdened with rights. However, after the Constitutional Court ruling (MK 35/2012), the government's recognition of customary forests clearly provides management and ownership rights to communities governed by customary law. Thus, recognition of conservation practices that arise from customary law also becomes legal. In regional context, IPCF is officially recognized by Kampar Regent Decree and the Ministry of Environment and Forestry (MoEF) Decree, which legally designates the forest as a customary forest. The leadership of IPCF Governance is provided by a traditional institution, headed by the Datuk, in conjunction with the formal village government, demonstrating co-management principles. In addition, village regulations that align with national conservation objectives prohibit hunting and tree felling without permits, strengthening conservation efforts through both customary sanctions and formal legal mechanisms. A clear legal structure will motivate the community to take part in the conservation of the IPCF. The community can support and be useful in utilizing the services offered with a willingness to pay and awareness not to damage the environment. Current revenue can be allocated for managerial salaries and enhancing community forest service. Given the strong conservation sentiment, the community can take an active role in monitoring forest health, tracking biodiversity, and enforcing local conservation laws. This can be incorporated into government-supported conservation programs to develop a hybrid governance system that integrates traditional insights with modern tools. Strengthening collaboration with local government bodies, NGOs, and academic institutions can help ensure that the current strategies are robust and adequately funded.

In management aspects, Table 4 shows only occupation has a significance value below 0.05 (0.012; Table 6), and is the sole variable included in further regression. A majority of participants highlight the significance of infrastructure, including fences and waste bins, for enhancing IPCF management. This aligns with the findings of Kabisch *et al.* (2015), which demonstrate that the quality of green spaces, accessibility, and infrastructure influence user perceptions. Similarly, understanding residents' attitudes aids policy and tourism planning (Obradovic and Stojanovic, 2021), and greenspace preferences

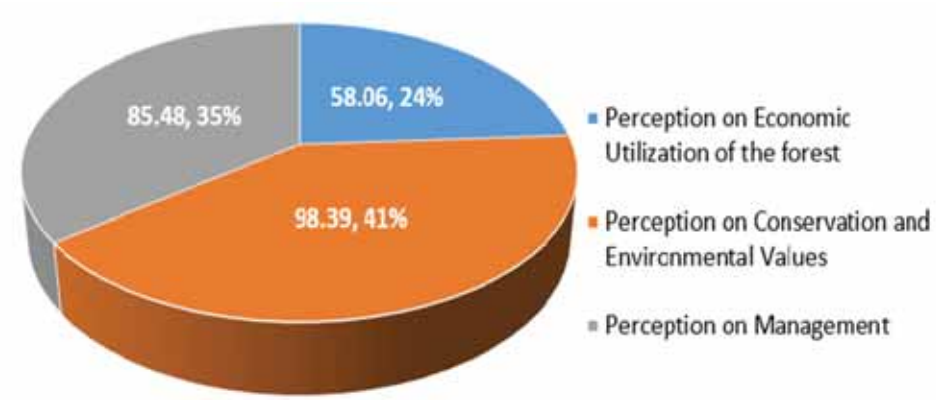

Fig. 9: Percentage graph of community perceptions according to three aspects

Table 6: The final result of the logistic regression on the management aspect

Variable	B	S.E.	Wald	df	Sig.	Exp(B)
Occupation	-1.138	0.451	6.358	1	0.012	0.320
Constant	0.479	0.807	0.352	1	0.553	1.614

support better design and development (Farahani and Maller, 2018). The management of customary forests significantly relies on the contributions of youth and women. Currently, a young man leads the management of these forests and has recently received a promotion. Even the management members are dominated by young people. Women play a very important role in customary ceremonies. Most of the decorative equipment can only be prepared by women. Women participate as members of forest farmer groups, engaging in all activities associated with customary forests. So far, we have not seen any marginalized groups being marginalized, even newcomers are given places to live around the forest and access to enter the forest. Furthermore, to mitigate biases concerning gender and age, the sample included women and individuals of different ages, as these factors were considered in the analysis. All stakeholders can focus at least on factors that influence community perception. Community clusters, especially local figures and ordinary people, greatly influence the resilience of external values. Promoting strong traditional values can help protect forests while still reaping the economic benefits of ecosystem services. In terms of management, increasing professionalism by using agreed work procedures and standards, the approval of village officials and traditional elders, will increase positive community perceptions, especially among more experienced professionals. This facilitates the differentiation of engagement strategies within co-management plans for traditional leaders, forest users, and local villagers, thereby increasing relevance and encouraging participation. Although the IPCF is not formally designated within Indonesia's protected area system, its ecological function within the fragmented landscape is critical. Surrounded by oil palm plantations, IPCF maintains a relatively intact forest patch that may act as a stepping-stone or ecological node facilitating species movement and maintaining genetic exchange. As emphasized by Saura *et al.* (2019), strengthening connectivity between protected and non-protected areas, including indigenous and community-managed forests, is essential for biodiversity resilience at a landscape scale. Frameworks could include customary forests like IPCF to connect ecological corridors, especially in the lowland forest areas of Sumatra. This is consistent with landscape-level strategies such as the RIMBA Corridor Initiative in Central Sumatra, which emphasizes integrated conservation planning that includes customary, state, and private

land (Sulistyawan *et al*., 2019). Although IPCF is not currently linked to any formal ecological corridor, it fits the profile of community-managed forests that can complement protected areas by enhancing ecological resilience across fragmented landscapes. Future regional spatial planning should take IPCF into account as an integral part of the biodiversity corridor network in Sumatra.

CONCLUSION

Customary forests, rooted in local law and intergenerational traditions, blend conservation with cultural and religious values. Overseen by native institutions following village guidelines, the IPCF restricts logging and hunting, with fines for breaches. Recognized by the Indonesian government in 2020, its area has shrunk from 500+ ha to 251 ha due to palm oil and settlements. In spite of its ongoing reduction and fragmentation, IPCF retains a comparatively high species diversity. The species with the highest importance value index in the area include Kulim (*Scorodocarpus borneensis* (Baill.) Becc.), Red Kelat (*Syzygium glabratum* (DC.) Veldkamp), Meranti (*Richetia hopeifolia* (F.Heim) P.S.Ashton & J.Heck), Lalan (*Santiria oblongifolia* Blume), and Mempisang (*Xylopia malayana* Hook.f. & Thomson). Several diversity indices—including Chao species richness, Shannon's index, and Simpson's index— demonstrate significant disparities in species composition. *Scorodocarpus borneensis* stands out as the most ecologically important species naturally occurring in the IPCF, present at both the tree and pole stages. Activities driven by humans, such as selective logging, agricultural land clearing, and the development of infrastructure, have led to a decline in habitat complexity and resilience, which in turn has created disparities in species richness between tree and pole stages. The presence of fewer dominant species in the pole stage suggests a less complex community structure or ecological conditions that support specific species. The soil in the IPCF is classified as Ultisol, characterized by low fertility, high acidity, and a high CEC. The average pH values for the undisturbed IPCF, disturbed IPCF, and nearby oil palm plantations are 3.44, 3.89, and 4.61, respectively. In contrast, CEC values are exceptionally high across all three sites, ranging from 43.99 to 62.75 me/100 g. Other soil chemical characteristics, like base saturation, are significantly low (4%–13%), reflecting limited amounts of crucial base cations (Ca, Mg, K, Na), which hinders their availability for plant nutrient uptake. In terms of texture, the soil falls under the silt loam category, dominated by the silt fraction (62%), followed by sand (19%) and clay (19%). When soil has a significant amount of silt, it becomes more susceptible to erosion, which means that improper land utilization can speed up both erosion and surface runoff. However, silt loam soils also have moderate pore sizes, allowing balanced water retention and drainage. The IPCF exhibits high water availability, with values of 15.93% (undisturbed), 15.10% (disturbed), and 10.27% (oil palm plantation). While the IPCF has a higher capacity for water storage than oil palm plantations, the difference does not reach statistical significance at the 5% level. The soil's physical attributes facilitate vigorous plant development and maintain sustainable water availability. The IPCF demonstrates significant carbon sequestration potential, with an above-ground biomass of 177.24 ± 21.27 tons/ha and a carbon stock of 83.30 ± 9.99 t C/ha. These data points underscore the forest's function as an essential carbon reservoir, particularly in contrast to human land uses such as oil palm plantations. Despite pressures from development and land conversion pressures, the IPCF retains substantial carbon storage capacity, aiding climate change mitigation while supporting biodiversity and indigenous livelihoods. The way communities perceive the IPCF significantly impacts the formulation of sustainable management strategies, guiding forest use and preservation. The study reveals that structural factors (such as cluster groups and information sources) and functional factors (including occupation and visitation frequency) significantly shape attitudes toward economic utilization. Across different demographics, conservation values continue to be viewed positively. Notably, most respondents favor non-destructive uses like recreation and education, reflecting a broader preference for ecosystem services over extractive activities. Occupation emerged as the key determinant in management perceptions, with infrastructure improvements (e.g., fences, waste facilities) highlighted as priorities. While a significant 96.7% of participants recognize the contribution of forests to climate mitigation, obstacles continue to arise from competing economic priorities and land-use pressures. The integration of Indigenous

governance and ecological insights presents valuable opportunities for conservation, highlighting the need for the effective inclusion of community perspectives into policy remains essential. The study emphasizes the importance of methods that integrate ecological protection with socio-economic demands, ensuring that management plans align with local values and long-term sustainability goals. By prioritizing inclusive decision-making and infrastructure development, allows stakeholders to enhance the IPCF's ecological resilience and its benefits to local communities.

AUTHOR CONTRIBUTIONS

A. Susilowati, the corresponding author, has contributed to funding acquisition, conceptualization, article writing, and editing. Y. Lisnawati has contributed to planned the experiment, article writing, data analysis, interpreted and discussed the results, validating and editing. H.H. Rachmat has contributed to planned the experiment, article writing, data analysis, interpreted and discussed the results, validating and editing. H. Kurniawan has contributed to planned the experiment, data collection, article writing, data analysis, interpreted and discussed the results, and editing. W.C. Adinugroho has contributed to article writing and data analysis, prepared the maps and figures, interpreted and discussed the results, and editing. R. Imanuddin has contributed to article writing and data analysis, prepared the maps and figures, interpreted and discussed the results, and editing. D.J. Sudrajat has contributed to article writing, interpreted and discussed the results, validation, and editing. I.W.S. Darmawan has contributed to article writing, interpreted and discussed the results, and editing. M. Iqbal has contributed to article writing, preparing figures, visualization and editing. S. Fahmi has contributed to article writing, preparing figures, and editing. L.M. Nugraha has contributed to article writing, preparing figures, and editing. E. Novriyanti has contributed to data collection and article writing. E. Sutrisno has contributed in data collection, data validation and article writing. A.B. Siswanto has contributed to data collection.

ACKNOWLEDGEMENT

The study was conducted in Petapahan Village, Tapung District, Kampar Regency, Riau Province, Indonesia. Data analysis and preparation of this manuscript are part of the Cooperation program between the Ecology and Ethnobiology Research Center, the National Research and Innovation Agency and the Faculty of Forestry, University of North Sumatra, with contract numbers [367/V/KS/09/2024] and [390/UN5.2.15.D/HK.09/2024] on Ecological, Social, and Molecular Genetics Research on Remnant Forest Areas as Biodiversity Preservation Areas in Sumatra's Anthropogenic Landscape to Support Ecosystem Resilience, as well as Decree Number [093/E5/PG.02.00.PL/2024] and Agreement/ Contract Letter Number [10/UN5.4.10.S/PPM/KP-DRTPM/2024] on National Competitive Research, Fundamental Research grant scheme, Ministry of Education, Culture, Research and Technology.

CONFLICT OF INTEREST

The authors declare that there is no conflict of interests regarding the publication of this manuscript. In addition, the ethical issues, including plagiarism, informed consent, misconduct, data fabrication and/ or falsification, double publication and/or submission, and redundancy have been completely observed by the authors.

OPEN ACCESS

©2025 The author(s). This article is licensed under a Creative Commons Attribution 4.0 International License, which permits use, sharing, adaptation, distribution and reproduction in any medium or format, as long as you give appropriate credit to the original author(s) and the source, provide a link to the Creative Commons license, and indicate if changes were made. The images or other third-party material in this article are included in the article's Creative Commons license, unless indicated otherwise in a credit line to the material. If material is not included in the article's Creative Commons license and your intended use is not permitted by statutory regulation or exceeds the permitted use, you will need to obtain permission directly from the copyright holder. To view a copy of this license, visit: http://creativecommons.org/licenses/by/4.0/

PUBLISHER'S NOTE

GJESM Publisher remains neutral with regard to jurisdictional claims in published maps and institutional afflictions.

Positive AI Statement

During the preparation of this work the author(s) have used Artificial Intelligence (AI) [NAME TOOL / SERVICE] in order to [REASON]. After using this tool/ service, the authors reviewed and edited the content as needed and take full responsibility for the content of the publication.

(For this reason, the GPTZero detector will evaluate the manuscript utilizing Generative AI, ensuring a high detection rate. If the manuscript relies heavily on Generative AI and AI-assisted technologies, it will be archived without further options for appeal).

Negative AI Statement

The author(s) declare that no AI tools or services were not used or not highly applied during the preparation of this work.

ABBREVIATIONS

%	Percent
AGB	Above-ground biomass
Al^{3+}	Aluminium cation
ANOVA	Analysis of variance
BD	Bulk density
BS	Base saturation
C	Carbon
Ca	Calsium
CEC	Cation Exchange Capacity
Cm	Centimeter
CO_2	Carbon dioxide
DBH	Diameter Breast Height
GHG	Greenhouse gas
H^+	Hidrogen cation
Ha	Hectare
HCl	hidrochloric acid
iNEXT	Interpolation and extrapolation
IPCF	Imbo Putui Customary Forest
K	Kalium
M	Meter
Meq	Milliequivalent
Mg	Magnesium
Mm	Millimeter
MoEF	Ministry of Envirenment and Forestry
N	Nitrogen
NbS	Nature-based Solution
NH4	Amonium acetate
NGOs	Nonorganization organizations
P	Phosphor
pH	Potential of Hidrogen
SPSS	Statistical package for the social sciences
t/ha	Ton per hectare
t C/ha	Ton of carbon per hectare

REFERENCES

Akram, H.; Levia, D.F.; Herrick, J.E.; Lydiasari, H.; Schütze, N., (2022). Water requirements for oil palm grown on marginal lands: a simulation approach. Agric. Water Manage., 260: 1-11 (**11 pages**).

Arianto., (2021). Keanekaragaman Jenis Mamalia Pada Kawasan Hutan Adat Imbo Putui Provinsi Riau. Pekanbaru : Universitas Riau –Fakultas Pertanian – Kehutanan **(107 pages).**

Brondízio, E.S.; Aumeeruddy-Thomas, Y.; Bates, P.; Carino, J.; Fernández-Llamazares, Á.; Ferrari, M.F.; Galvin, K.; Reyes-García, V.; McElwee, P.; Molnár, Z.; Samakov, A.; Shrestha, U.B., (2021). Locally based, regionally manifested, and globally relevant: indigenous and local knowledge, values, and practices for nature. Ann. Rev. Environ Resour., 46, 481–509 (**19 pages**).

Buchel, S.; Frantzeskaki, N., (2015). Citizens' voice: a case study about perceived ecosystem services by urban park users in Rotterdam, the Netherlands. Ecosyst. Serv., 12: 169–177 (**9 pages**).

Chahyana, I.; Hutomo, P.; Hernawan, E.; Titisari, P. W., (2024). The role of indigenous people to the viability of traditional forest management: A case study from Imbo Putui customary forest. In ICAGRI, 5th. Int. conf. on agriculture. Banda Aceh, Indonesia, 11–12 Oct. IOP Conference Series: Earth Environ. Sci., 1297(1): 1-14 **(14 pages)**.

Chen, W.W.; Tang, L.; Wang, J.Y.; Zhu, H.H.; Jin, J.F.; Yang, J.L.; Fan, W., (2022). Research advances in the mutual mechanisms regulating response of plant roots to phosphate deficiency and aluminum toxsicity. Int. J. Mol. Sci., 23(3): 1-20 (**20 pages**).

Ćirić, V.; Prekop, N.; Šeremešić, S.; Vojnov, B.; Pejić, B.; Radovanović, D.; Marinković, D., (2023). The implication of cation exchange capacity (cec) assessment for soil quality management and improvement. Agric. For., 69(4): 113–134 (**22 pages**).

Dasrol, D.; Bachtiar, M., (2020). Local wisdom at Kampar, Pekanbaru, Indonesia, to preserve traditional culture. Adv. Soc. Sci. Educ. Humanit. Res., 442: 111–114 (**4 pages**).

De Gregorio, E.; Caffaro, F.; Pirchio, S.; Tiberio, L.; Carrus, G. (2023). Editorial: current trends in environmental psychology, volume I. Front. Psychol., 14:1-2 (**2 pages**).

Ding, F.; Flury, M.; Schaeffer, S.M.; Xu, Y.; Wang, J., (2021). Does long-term use of biodegradable plastic mulch affect soil carbon stock?. Resour. Conserv. Recycl., 175(7): 1-2 (**2 pages**).

Ekaputri, R.Z.; Hidayat, T.; Surtikanti, H.K.; Surakusumah, W., (2024). Modeling vegetation density with remote sensing, normalized difference vegetation index and biodiversity plants in watershed area. Global J. Environ. Sci. Manage., 10(4): 1809-1826 **(18 pages).**

Farahani, L.M.; Maller, C., (2018). Perceptions and preferences of urban greenspaces: a literature review and framework for policy and practice. Landsc. Online. 61(1): 1–22 (**22 pages**).

Firmanda, H., (2017). Hukum adat masyarakat petapahan dalam pengelolaan lingkungan sebagai upaya pemenuhan hak masyarakat adat. Fikri : J. Kajian Agama Sos. Budaya. 2(1): 1-26 (**26 pages**).

Fitriatin, B.N.; Yuniarti, A.; Turmuktini, T.; Ruswandi, F.K., (2014). The effect of phosphate solubilizing microbe producing growth regulators on soil phosphate, growth and yield of maize and fertilizer efficiency on ultisol. Eurasian J. Soil Sci., 3(2): 101-107 (**7 pages**).

Garcia, C.A.; Laurene, F., (2014). Beyond the mirror: tropical forest fragmentation and its impact on rural livelihoods, in: Kettle, C.J.; Koh, L.P. (Eds.), Global forest fragmentation. Department of Environmental System Science, ETH Zurich, Switzerland (**17 pages**).

Gonçalves, F.M.P.; Revermann, R.; Gomes, A.L.; Aidar, M.P.M.; Finckh, M.; Juergens, N., (2017). Tree species diversity and composition of miombo woodlands in south-central Angola: a chronosequence of forest recovery after shifting cultivation. Int. J. For. Res., 2017(1): 1–13 (**13 pages**).

Government of Indonesia, (2022). National forest reference level for deforestation, forest degradation, and enhancement of forest carbon stock. Submission by Indonesia to the United Nations Framework Convention on Climate Change (UNFCCC) (**108 pages**).

Hassen, A.; Zander, K.K.; Manes, S.; Meragiaw, M., (2023). Local people's perception of forest ecosystem services, traditional conservation, and management approaches in North Wollo, Ethiopia. J. Environ. Manage., 330: 1–10 (**10 pages**).

Janowiak, M.K.; Brandt, L.A.; Wolf, K.K.; Brady, M.; Darling, L.; Derby-Lewis, A.; Fahey, R.T.; Giesting, K.; Hall, E.; Henry, M.; Hughes, M.; Miesbauer, J. W.; Marcinkowski, K.; Ontl, T.; Rutledge, A.; Scott, L.; Swanston, C. W., (2021). Climate adaptation actions for urban forests and human health. General Technical Report., NRS-203: 1-122 (**122 pages**).

Kabisch, N.; Qureshi, S.; Haase, D., (2015). Human-environment interactions in urban green spaces - A systematic review of contemporary issues and prospects for future research. Environ. Impact Assess. Rev., 50: 25–34 (**10 pages**).

Karuru, S. S.; Rasyid, B.; Millang, S., (2021). Carbon stock estimation on some land cover: Secondary forest, agroforestry, palm oil plantation and paddy fields. In ICSAE, 7th. Int. conf. on sustainable agriculture and environment. Surakarta, Indonesia, 25–27 Aug. IOP Conference Series: Earth Environ. Sci., 637(1): 1-8 **(8 pages)**.

Kremen, C.; Merenlender, A.M., (2018). Landscapes that work for biodiversity and people. Science, 362(6412): 1-11 (**11 pages**).

Krisnawati, H.; Adinugroho, W.C.; Imanuddin, R.; Hutabarat, S., (2014). Estimation of forest biomass for quantifying CO_2 emissions in Central Kalimantan. Research and Development Center for Conservation and Rehabilitation, Forestry Research and Development Agency, Ministry of Forestry, Bogor, Indonesia (**36 pages**).

Kustiawan, P.M.; Siregar, K.A.A.K.; Saleh, L.O.; Batistuta, M.A.; Setiawan, I.M., (2022). A review of botanical characteristics, chemical composition, pharmacological activity and use of *Scorodocarpus borneensis*. Biointerface Res. Appl. Chem., 12(6): 8324–8334 (**11 pages**).

Lestari, R.; Kusuma, Z. J., (2022). Customary law and challenges of Imbo Putui customary forest management. In RAMLAS, 2nd. Riau annual meeting on law and social sciences. Pekanbaru, Indonesia, 14-15 Sep. Atlantis Press: Paris (**3 pages**).

Lin, J.C.; Chiou, C.R.; Chan, W.H.; Wu, M.S., (2021). Public perception of forest ecosystem services in Taiwan. J. For. Res., 26(5) : 344–350 (**7 pages**).

Lindenmayer, D.; Scheele, B.C.; Lavery, T.; Likens, G.E., (2023). Biodiversity response to rapid successive land cover conversions in human-dominated landscapes. Global Ecol. Conserv., 45(5): 1-18 (**18 pages**).

Lindh, A.; Sundqvist, M.K.; Axelsson, E.P.; Hasselquist, N.J.; Aguilar, F.X.; Alloysius, D.; Ilstedt, U., (2024). Functional traits to predict financial value of enrichment planting in degraded tropical forests. New For., 55(5): 1283–1310 (**28 pages**).

Lucas, M.; Nguyen, L.T.T.; Guber, A.; Kravchenko, A.N., (2022). Cover crop influence on pore size distribution and biopore dynamics: Enumerating root and soil faunal effects. Front. Plant Sci., 13(8): 1–13 (**13 pages**).

Lynch, L.; Kokou, K.; Todd, S., (2018). Comparison of the ecological value of sacred and nonsacred community forests in Kaboli, Togo. Trop. Conserv. Sci., 11: 1–11 (**11 pages**).

Maalouf, M., (2011). Logistic regression in data analysis: an overview. Int. J. Data Anal. Tech. Strateg., 3(3): 281–299 (**19 pages**).

Manuri, S.; Andersen, H.E.; McGaughey, R.J.; Brack, C., (2017). Assessing the influence of return density on estimation of lidar-based aboveground biomass in tropical peat swamp forests of Kalimantan, Indonesia. Int. J. Appl. Earth Obs. Geoinf., 56: 24–35 (**12 pages**).

Maru, Y.; Gebrekirstos, A.; Haile, G., (2023). Indigenous sacred forests as a tool for climate change mitigation: lessons from gedeo community, Southern Ethiopia. J. Sustainable For., 42(3): 260–287 (**28 pages**).

Mekonen, T.; Ayele, B.; Ashagrie, Y., (2015). Woody plant species diversity, structure and regeneration status of Woynwuha Natural Forest, North West Ethiopia. J. Agric. Environ. Sci., 1: 67-83 (**17 pages**).

Muche, M.; Yemata, G.; Molla, E.; Adnew, W.; Muasya, A.M., (2023). Land use and land cover changes and their impact on ecosystem service values in the north-eastern highlands of Ethiopia. PLoS ONE, 18(9): 1–24 (**24 pages**).

Murphy, D.J. (2024). Carbon sequestration by tropical trees and

crops: a case study of oil palm. Agric., 14(7): 1133 (**31 pages**).
Nghi, T.H.; Tung, N.S.; Thu, N.Q., (2025). Community forestry practices of ta oi ethnic group in the Central Annamite of Indochina: a case study in a Luoi district, Thua Thien Hue province, Viet Nam. Open J. Plant Sci., 10(1): 009-016 (**8 pages**).
Obradović, S.; Stojanović, V., (2022). Measuring residents' attitude toward sustainable tourism development: a case study of the Gradac River gorge, Valjevo (Serbia). Tour. Recreat. Res., 47(5–6): 499–511 (**13 pages**).
Ogbemudia, F.O.; Ita, R. E.; Anwana, E.D., (2023). Tree-based carbon sequestration and storage abilities vary in natural and plantation forest ecosystems. World J. Appl. Sci. Technol., 15(1): 19–25 (**7 pages**).
Paudyal, R.; Stein, T.V.; Ober, H.K.; Swisher, M.E.; Jokela, E.J.; Adams, D.C., (2018). Recreationists' perceptions of scenic beauty and satisfaction at a public forest managed for endangered wildlife. Forests. 9(5): 1-13 (**13 pages**).
Peh, K.S.H.; YangChen, L.; Sarah, H.L.; William, A.F.; Edgar, C.T., (2014). Forest fragmentation and ecosystem function. In: Kettle, C. J.; Koh, L. P. (Eds.), Global forest fragmentation. Department of Environmental System Science, ETH Zurich, Switzerland: 96-114 **(19 pages)**.
Pelletier, J.; Siampale, A.; Legendre, P.; Jantz, P.; Laporte, N.T.; Goetz, S.J., (2017). Human and natural controls of the variation in aboveground tree biomass in African dry tropical forests. Ecol. Appl., 27(5): 1578–1593 (**16 pages**).
Porras-Salazar, J.A.; Flor, J.F.; Contreras-Espinoza, S.; Soto-Arce, M.; Castro-Salazar, R., (2023). The public perception of urban vegetation in metropolitan regions of Costa Rica. Environ. Adv., 13(9): 100422 (**14 pages**).
Prabowo, R.; Subantoro, R., (2017). Soil analysis as an indicator of the fertility level of agricultural cultivation land in the city of Semarang. Cendekia Eksakta., 2(2): 59-64 (**6 pages**).
Ritonga, A.; Mardhiansyah, M.; Kausar, K., (2014). Identifikasi kearifan lokal masyarakat hutan larangan adat Rumbio, Kabupaten Kampar terhadap perlindungan hutan. J. Online Mhs. Faperta UNRI., 1(1): 1–9 (**9 pages**).
Safitri, L.; Hermantoro, H.; Purboseno, S.; Kautsar, V.; Saptomo, S.K.; Kurniawan, A., (2018). Water footprint and crop water usage of oil palm (*Eleasis guineensis*) in Central Kalimantan: environmental sustainability indicators for different crop age and soil conditions. Water (Switz)., 11(1): 1–16 (**16 pages**).
Saura, S.; Bertzky, B.; Bastin, L.; Battistella, L.; Mandrici, A.; Dubois, G., (2019). Global trends in protected area connectivity from 2010 to 2018. Biol. Conserv., 238:108183 (**8 pages**).
Soil Survey Staff, (2014). Keys to soil taxonomy, 12th Ed. United States Department of Agriculture, Natural Resources Conservation Service. (**372 pages**).
Sperandei, S., (2014). Understanding logistic regression analysis. Biochem. Med., 24(1): 12–18 (**7 pages**).
Sulieman, M.; Saeed, I.; Hassaballa, A.; Rodrigo-Comino, J., (2018). Modeling cation exchange capacity in multi geochronological-derived alluvium soils: an approach based on soil depth intervals. Catena, 167: 327-339 **(13 pages).**
Sulistyawan, B.S.; Feger, C.; McKenzie, E.; Gallagher, L.A.; Verweij, P.A.; Verburg, R., (2019). Towards more effective landscape governance for sustainability: the case of RIMBA corridor, Central Sumatra, Indonesia. Sustainable Sci., 14: 1485–1502 **(18 pages).**
Suyadi; Basyuni, M.; Amukti, R.; Damayanti, C.; Stokes, D.; Mubaraq, A.; Rahmila, Y.I., (2025). Ecological features of mangroves as indicators of seawater intrusion. Global J. Environ. Sci. Manage., 11(2): 609-630 **(22 pages).**
Thiemann, M.; Riebl, R.; Haensel, M.; Schmitt, T. M.; Steinbauer, M. J.; Landwehr, T.; Fricke, U.; Redlich, S.; Koellner, T., (2022). Perceptions of ecosystem services: Comparing socio-cultural and environmental influences. PLoS ONE. 17(10): 1–20 (**20 pages)**.
Thompson, I.D., (2015). An overview of the science–policy interface among climate change, biodiversity, and terrestrial land use for production landscapes. J. For. Res., 20(5): 423–429 (**7 pages**).
Wingate, V.R.; Akinyemi, F.O.; Iheaturu, C.; Ifejika Speranza, C., (2022). A remote sensing-based inventory of West Africa tropical forest patches: a basis for enhancing their conservation and sustainable use. Remote Sens., 14(24): 1-16 (**16 pages**).
Wingate, V.R.; Akinyemi, F.O.; Speranza, C.I., (2023). Archetypes of remnant West African forest patches, their main characteristics and geographical distribution. Appl. Georgr., 158(J1): 1-12 (**12 pages**).
Yang, J.; Yang, J.; Xing, D.; Luo, X.; Lu, S.; Huang, C.; Hahs, A.K. (2021). Impacts of the remnant sizes, forest types, and landscape patterns of surrounding areas on woody plant diversity of urban remnant forest patches. Urban Ecosyst., 24(2): 345–354 (**10 pages**).
Yeo, L.B.; Said, I.; Saito, K.; Ling, G.H.T., (2016). Conceptual framework of ecosystem services in landscape planning, Malaysia. Int. J. Built Environ. Sustainable. 3(3): 142–149 (**8 pages**).
Yuen, J.Q.; Fung, T.; Ziegler, A.D., (2016). Review of allometric equations for major land covers in SE Asia: Uncertainty and implications for above-and below-ground carbon estimates. For. Ecol. Manag. 360: 323–340 (**18 pages**).
Zamorano-Elgueta, C.; Cayuela, L.; Rey-Benayas, J.M.; Donoso, P.J.; Geneletti, D.; Hobbs, R.J., (2014). The differential influences of human-induced disturbances on tree regeneration community: a landscape approach. Ecosphere., 5(7): 1–17 (**17 pages**).
Zgorelec, Z.; Grahovac, B.; Percin, A.; Jurkovic, V.; Gandjaeva, L.; Maurović, N., (2019). Comparison of two different CEC determination methods regarding the soil properties. Agric. Conspec. Sci., 84(2): 151–158 (**8 pages**).
Zhang, Y.G.; Yang, S.; Fu, M.M.; Cai, J.P.; Zhang, Y.Y.; Wang, R. Z.; Xu, Z. W.; Bai, Y. F.; Jiang, Y., (2015). Sheep manure application increases soil exchangeable base cations in a semi-arid steppe of inner Mongolia. J. Arid. Land., 7(3): 361–369 (**9 pages**).

AUTHOR (S) BIOSKETCHES

Susilowati, A., Professor, Faculty of Forestry, Universitas Sumatera Utara. Kampus 2 USU Bekala, Deli Serdang 20353, North Sumatera, Indonesia
- Email: *arida.susilowati@usu.ac.id*
- ORCID: 0000-0001-9608-4787
- Web of Science ResearcherID: AAF-6384-2021
- Scopus Author ID: 56102433700
- Homepage: https://fhut.usu.ac.id/id/dosen/arida-susilowati

Lisnawati, Y., Dr., Senior Researcher, Research Center for Ecology and Ethnobiology, Research Organization for Life Sciences and Environment, National Research and Innovation Agency (BRIN), Jalan Raya Jakarta, Bogor km 46, Cibinong, 169111, Indonesia.
- Email: *yuni028@brin.go.id*
- ORCID: 0000-0002-2601-4596
- Web of Science ResearcherID: NA
- Scopus Author ID: 57213351062
- Homepage: https://www.independent.academia.edu/LisnawatiYunita

Rachmat, H.H., Ph.D., Principal Researcher, Research Center for Ecology and Ethnobiology, Research Organization for Life Sciences and Environment, National Research and Innovation Agency (BRIN), Jalan Raya Jakarta, Bogor km 46, Cibinong, 169111, Indonesia.
- Email: *hent003@brin.go.id*
- ORCID: 0000-0003-4586-6820
- Web of Science ResearcherID: NA
- Scopus Author ID: 57193913977
- Homepage: https://www.researchgate.net/scientific-contributions/Henti-Hendalastuti-Rachmat-2124572622

Kurniawan, H., M.Sc., Senior Researcher, Research Center for Ecology and Ethnobiology, National Research and Innovation Agency (BRIN), Jalan Raya Jakarta-Bogor Km 46, Cibinong 16911, Indonesia.
- Email: *hery011@brin.go.id*
- ORCID: 0000-0002-7054-0921
- Web of Science ResearcherID: NA
- Scopus Author ID: 57193558098
- Homepage: https://brin.go.id/en/page/civitas

Adinugroho, W.C., Dr., Principal Researcher, Research Center for Ecology and Ethnobiology, Research Organization for Life Sciences and Environment, National Research and Innovation Agency (BRIN), Jalan Raya Jakarta – Bogor km 46, Cibinong, 169111, Indonesia.
- Email: *wahy060@brin.go.id*
- ORCID: 0000-0003-0687-5679
- Web of Science ResearcherID: AEL-2252-2022
- Scopus Author ID: 57193552889
- Homepage: https://wahyukdephut.wordpress.com/

Imanuddin, R., M.Sc., Senior Researcher, Research Center for Ecology and Ethnobiology, Research Organization for Life Sciences and Environment, National Research and Innovation Agency (BRIN), Jalan Raya Jakarta – Bogor km 46, Cibinong, 169111, Indonesia.
- Email:rina027@brin.go.id
- ORCID: 0000-0002-0252-7186
- Web of Science ResearcherID: NA
- Scopus Author ID: 57219599979
- Homepage: https://www.researchgate.net/profile/Rinaldi-Imanuddin

Sudrajat, D. J., Ph.D., Principal Researcher, Research Center for Applied Botany, National Research and Innovation Agency, Jl. Jakarta-Bogor. KM 46, Cibinong Bogor, West Java, Indonesia, 16911.
- Email: *djsudrajatbtp@yahoo.com*
- ORCID: 0000-0002-8256-8454
- Web of Science ResearcherID: NA
- Scopus Author ID: 56590048000
- Homepage: https://www.brin.go.id/

Dharmawan, I.W.S., Dr., Principal Researcher, Research Center for Ecology and Ethnobiology, National Research and Innovation Agency (BRIN), Jalan Raya Jakarta-Bogor Km 46, Cibinong 16911, Indonesia.
- Email: *iway028@brin.go.id*
- ORCID: 0000-0002-7007-393X
- Web of Science ResearcherID: NA
- Scopus Author ID: 58097512800
- Homepage: https://brin.go.id/en/page/civitas

Iqbal, M., M.Sc., Junior Researcher, Research Center for Ecology and Ethnobiology, Research Organization for Life Science and Environment, National Research and Innovation Agency, Jl. Raya Jakarta – Bogor km 46, Cibinong, 169111, Indonesia.
- Email: *moha071@brin.go.id*
- ORCID: 0009-0006-0291-713X
- of Science Researcher ID: NA
- Scopus Author ID: 57362407400
- Homepage: https://www.linkedin.com/in/mohamad-iqbal-b646bb248/

AUTHOR (S) BIOSKETCHES

Fahmi, S., M.Sc., Junior Researcher, Research Center for Ecology and Ethnobiology, Research Organization for Life Science and Environment, National Research and Innovation Agency, Jl. Raya Jakarta – Bogor km 46, Cibinong, 169111, Indonesia.
▪ Email: *saidfahmi88@gmail.com*
▪ ORCID: 0009-0003-0840-5598
▪ Web of Science Researcher ID: NA
▪ Scopus author ID: 58102659500
▪ Homepage: https://www.linkedin.com/in/said-fahmi-336a36133?utm_source=share&utm_campaign=share_via&utm_content=profile&utm_medium=android_app

Nugraha, L.M., M.Sc., Junior Researcher, Research Center for Ecology and Ethnobiology, Research Organization for Life Sciences and Environment, National Research and Innovation Agency (BRIN), Jalan Raya Jakarta-Bogor KM 46, Cibinong, Jawa Barat, Indonesia.
▪ Email: *luth007@brin.go.id*
▪ ORCID: 0000-0002-4054-3355
▪ Web of Science ResearcherID: NA
▪ Scopus Author ID: 57215651692
▪ Homepage: https://brin.go.id/orhl/pree/page/personil

Novriyanti, E., Ph.D., Senior Researcher, Research Center for Applied Botany, National Research and Innovation Agency, Jl. Jakarta-Bogor. KM 46, Cibinong Bogor, West Java, Indonesia, 16911.
▪ Email: *ekan006@brin.go.id*
▪ ORCID: 0000-0002-9160-3274
▪ Web of Science ResearcherID: ADZ-84845-2022
▪ Scopus Author ID: 55212232700
▪ Homepage: https://intra.brin.go.id/home/profile_sivitas/ekan006

Sutrisno, E., M.Sc., Field Instructor, Forest Ecosystem Controller at Kampar Social Forestry Institute, Ministry of Forestry Republic of Indonesia, Jl. Raya Bangkinang-Kuok km 9, Kampar District, Riau Province, Indonesia
▪ Email: *ekokuoksutrisno@gmail.com*
▪ ORCID: 0009-0003-5085-5584
▪ Web of Science Researcher ID: NA
▪ Scopus Author ID: 57216752503
▪ Homepage: https://scholar.google.co.th/citations?user=BoggtzwAAAAJ&hl=th

Siswanto, A.B., B.Sc., Forest Ecosystem Controller Supervisor, Ministry of Forestry, Jalan Bangkinang-Kuok Km. 9 Kabupaten Kampar, Provinsi Riau.
▪ Email: *arifin.bs31@gmail.com*
▪ ORCID: 0009-0005-1240-5974
▪ Web of Science researcher ID: NA
▪ Scopus Author ID: NA
▪ Homepage: www.kehutanan.go.id

HOW TO CITE THIS ARTICLE

Name, N., (2025). Title. Global J. Environ. Sci.Manage., 11(3): 1057-1078.

DOI: 10.22034/gjesm.2025.03.11

URL: https://www.gjesm.net/article_724187.html

Global J. Environ. Sci. Manage. 11(3): 1079-1096, Summer 2025, Serial #43

Global Journal of Environmental Science and Management
(GJESM)

Homepage: https://www.gjesm.net/

Podcasts

CASE STUDY

Passenger car emissions in urban areas based on local vehicle fleet and environmental conditions

A. Valdés-Montenegro, F.G. González-Olivardía*, C. Pinzón-Acosta

Air Engineering Studies Research Group, CINEMI, Universidad Tecnológica de Panamá

ARTICLE INFO

Article History:
Received 07 February 2025
Revised 25 April 2025
Accepted 25 May 2025

Keywords:
Air quality
Emission inventory
Greenhouse gases
On-road emission
Passenger car

DOI: 10.22034/gjesm.2025.03.12

ABSTRACT

BACKGROUND AND OBJECTIVES: For effective air quality management, suitable emission inventories must be classified for on-road mobile sources like cars, based on their usage, vehicle technology, and local environmental conditions. This study aims to estimate atmospheric pollutant emissions generated by passenger cars using the international vehicle emission model for the year 2023.

METHODS: To implement the international vehicle emission model and develop a baseline for an emissions inventory, vehicle technology in the study area was determined through surveys conducted at fuel filling stations in the two districts with the most significant traffic. The fleet was categorized based on criteria including emission control technology, fuel type, and engine displacement. Moreover, the research took into account geographic and environmental aspects, such as travel patterns on urban roads, fuel specifications, and elevation.

FINDINGS: In the province, 53 distinct vehicle categories were recognized and classified using the international vehicle emission model. Following the configuration of the fleet file detailing the distribution of vehicle categories and the location file outlining environmental conditions and representative characteristics, the model calculated atmospheric pollutant emissions for 2023 in metric tons. Passenger vehicles were the primary source of pollutant emissions, producing 1.78 million tons of carbon dioxide each year and 234.16 kilotons of carbon monoxide annually. Regarding emission factors, gasoline vehicles showed a proportional increase in carbon dioxide, nitrous oxide, nitrogen oxides, and sulfur oxides emissions per kilometer as vehicle size increased. A notable case was carbon monoxide emissions, where a medium-sized vehicle emitted approximately 41 grams per kilometer—twice the amount of a heavy car as 23 grams per kilometer, according to international vehicle emission model estimation. The majority of particulate matter emissions originated from heavy passenger vehicles, as opposed to light and medium cars, which contributed 90 percent and 83 percent of emissions, respectively.

CONCLUSION: This study developed an on-road mobile source emission inventory for 2023, focusing on passenger cars in Panama. A survey of 409 vehicles characterized a fleet of 534,322 cars, identifying 53 categories, with 94.8 percent running on gasoline and 5.12 percent on diesel. Over 45 percent of vehicles have traveled beyond 160,000 kilometers, leading to higher emissions. Medium-sized cars (1.5–3 liters) account for 61.1 percent of the fleet and are the largest emitters of carbon dioxide and nitrogen oxide. Although fewer in number, diesel vehicles produce nearly half of the particulate matter-10 emissions. Evaluations against national and international inventories affirm the impact of these vehicles on air pollution and the significance of each pollutant.

This is an open access article under the CC BY license (http://creativecommons.org/licenses/by/4.0/).

NUMBER OF REFERENCES
42

NUMBER OF FIGURES
9

NUMBER OF TABLES
6

*Corresponding Author:
Email: *franchesca.gonzalez@utp.ac.pa*
Phone: +507 6398 6687
ORCID: 0000-0002-9356-6016

Note: Discussion period for this manuscript open until Sep 1, 2025 on GJESM website at the "Show Article".

INTRODUCTION

Air emission inventories are essential tools for environmental management. Air emission inventories provide a detailed record of the types and quantities of atmospheric pollutants emitted by various sources over a defined period according to the United States Environmental Protection Agency (EPA, 2022). Among these pollutants are greenhouse gases, which contribute to the warming of the Earth's surface (Jones *et al.,* 2023; Shevlyakov *et al.,* 2024).

Decarbonizing gas emissions from petrochemical production using microalgae along with criteria air pollutants that have health repercussions for at-risk populations (Fogelbach *et al.,* 2020) including respiratory ailments (Duan *et al.,* 2020; Parvin *et al.,* 2023). and nervous system diseases (Costa *et al.,* 2020). Air emission inventories are divided into three categories: point sources, area sources, and mobile sources (Almetwally *et al.,* 2020). The latter contribute the largest share of emissions of volatile organic compounds (VOCs), nitrogen oxides (NOx) and carbon monoxide (CO), generated by incomplete combustion (Zhang *et al.,* 2021) (Ministerio del Medio Ambiente Chile, 2022). Mobile sources consist of road vehicles, aircraft, railway transportation, maritime transport, among others. Studies reveal that private vehicles and taxis are the main sources of these emissions (Liliana and Pérez, 2015). Stationary emissions, like manufacturing facilities and production plants, are known as point sources. Conversely, area sources consist of emissions from multiple small sources that, when considered individually, do not fulfill the requirements to be classified as point sources. Their effects are evaluated as a whole since these emissions are released in small volumes and are widely distributed (EPA, 2001). Panama's economy is mainly based on service-related activities (Ministerio de Economía y Finanzas, 2017), supported by transportation as shown before (Valdes-Montenegro *et al.,* 2024). Transportation is essential for people's lives, as there is a need to move and commute to work or do other activities efficiently and promptly daily. Therefore, as the country's economy grows, so does the need for mobility and the emissions generated by these activities unless mitigation plans are implemented. There are two main measurement methods for vehicle emissions: laboratory measurements (idling or dynamometer) and real-world measurements (Lyu *et al.,* 2021). In Panama, the environmental emission standards for motor vehicles define acceptable emission limits based on the fuel type, the year of engine manufacture, or the vehicle weight. Although this regulation was established in 2009, it is not being enforced at this time. This regulation indicates that the permissible minimum emission limit for gasoline-fueled or alternative-fueled cars for carbon dioxide (CO_2) is 10.5 percent (%) for vehicles manufactured before 1999 and 12.5% for those manufactured after 1999. For CO emissions, a maximum of 4.5% is allowed for models before 1999 and 0.5% for those after 1999. Engines built before 1999 have a maximum unburned hydrocarbon emission limit of 500 parts per million (ppm), whereas for engines made after that year, the limit is reduced to 125 ppm. The only parameter evaluated in diesel-fueled cars is opacity. For lighter cars (3.5 tons), it is 60 Hartridge Smoke Units (HSU), and for heavier cars (3.5 tons), it is 70 HSU. Recently, an electric mobility mitigation plan (Gaceta Oficial, 2022) has passed that aims to reduce the internal combustion engine vehicle fleet by implementing electric mobility. A crucial first step in managing air quality effectively is to assess the emissions from internal combustion engine vehicles, considering their specific characteristics, technology, fuel efficiency, and consumption. In Panama, the Ministry of Environment reported for 2019 that greenhouse gas emissions originating from fuel combustion processes were represented by 99.9% CO_2, 0.03% methane (CH_4), and 0.002% nitrous oxide (N_2O). According to estimates, the transportation sector is responsible for 7,301.52 kilotons (kt) of CO_2 emissions, accounting for 46.9% of the total. Road transport emerges as the primary contributor, as depicted in Fig. 1, which details the subcategories of the transportation sector and their respective contributions (Ministerio de Ambiente, 2021).

The methodology for estimating emissions in this sector follows the Intergovernmental Panel for Climate Change (IPCC) Guidelines of 2006, applying the Tier 1 method, which calculates CO_2 emissions by multiplying the fuel sold by a default CO_2 emission factor by Intergovernmental Panel on Climate Change (IPCC, 2006). However, a better estimation of the emissions from on-road vehicles will be required to feed the inventory with characteristics of the vehicles, including the number of vehicles, vehicle year, mileage, and average travel speed (USEPA, 1992).

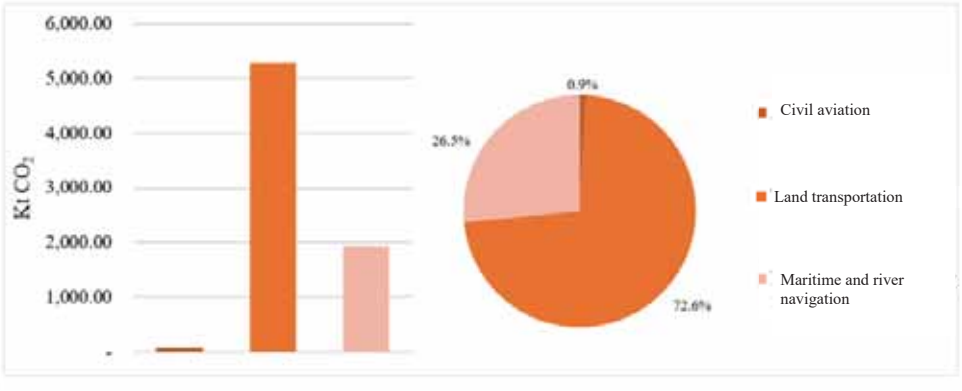

Fig. 1: Emissions from the transportation sector (2019) by activity (kt CO_2). From: Second Biennial Update Report: Learn About Climate Change Mitigation in Panama (Ministerio de Ambiente, 2021)

Tools for modeling that consider vehicle technology factors increase the accuracy of results (Tran *et al.*, 2024). The use of a vehicular emission estimation model, such as the international vehicle emissions (IVE) model, to to compile a mobile emissions inventory would greatly improve the decision-making process for formulating climate change mitigation strategies and preserving. These plans could include setting objectives for specific vehicle fleets and evaluating their progress. IVE model is able to estimate gases such as greenhouse gases (CO_2, N_2O, CH_4) and criteria air pollutants such as particulate matter (PM_{10}), CO, lead (Pb), sulfur dioxide (SO_2), and nitrogen dioxide (NO_2). Moreover, ammonia (NH_3) and VOCs are utilized to estimate the pollutants emitted by passenger cars in the IVE model. The Environmental Protection Agency (EPA) has defined air quality standards in the United States (Leland *et al.*, 2022) for the criteria for air pollutants. In 2023, in Panama, an executive order was passed to follow WHO guidelines regarding the short-term and long-term limits of fine particulate matter ($PM_{2.5}$), PM_{10}, CO, tropospheric ozone (O_3), sulfur dioxide (SO_2), and NO_2. Nonetheless, the absence of regulatory monitoring stations hinders the evaluation of how air pollutants behave. The IVE model is a multiscale model based on laboratory measurements, as it processes tens of thousands of datasets from tests conducted by the EPA, the California Air Resources Board (CARB), and the University of California, Riverside (UCR). This model further utilizes region-specific features, demonstrating a strong adaptability to developing countries (ISSRC, 2008) for estimating factors, greenhouse gases, and pollutant emissions of vehicles according to their technology (Outapa *et al.*, 2018). The emission factor is a measure of the mass of pollutant emissions relative to a unit of activity. The emissions are derived by multiplying this factor with the activity data (Fong *et al.*, 2022). Elements such as the travel distance of vehicles, the total number of vehicles, and emission factors significantly impact the amount of toxic emissions generated by vehicles (Outapa and Thepanondh, 2014). Although the IVE model has not seen significant updates in recent years, scientific publications using this model have been increasing compared to others with more recent updates (Cuba *et al.*, 2021). This is because the IVE model is a vehicular emissions estimation model developed for practical purposes, both for the United States and for developing countries (Marcela and Zapata, 2021). The IVE model would allow the establishment of a cost-effective method for evaluating vehicular air pollutants to develop a more representative emissions inventory for on-road mobile sources (Valdes-Montenegro *et al.*, 2024) and to evaluate the mitigation policies (Zhao *et al.*, 2021). Factors like traffic congestion are often seen in urban areas, producing harmful exhaust emissions that are discharged at breathing height and in crowded city environments, thus presenting a significant risk of human exposure (Trang *et al.*, 2015). Emissions can be calculated depending on the type of road (highway, avenue, or street), location (rural, urban) and population driving behaviors, all

these parameters differ by region. A study conducted in the city of Azogues, Ecuador, found that the highest emissions were recorded on highways, arterial roads, and commercial routes, respectively. Light gasoline vehicles equipped with a multi-point injection system largely represented the vehicle fleet (Peñafiel, 2019). In contrast, in the city of Guayaquil, a study using a high-resolution spatial breakdown of vehicle emissions indicated that the highest pollution rates were recorded in areas with high population density and an extensive network of secondary roads, rather than in areas with highways, which tend to have fewer connecting roads (Patiño-Aroca *et al.,* 2022This type of research, which assesses vehicle emissions using data like fuel type, daily or annual mileage, and vehicle weight, provides a crucial resource for government bodies in developing policies focused on enhancing air quality (Viteri *et al.,* 2023). Moreover, it enables the comparison with international contexts and allows for engagement in higher-level debates about air quality management. The objective of this study is to estimate the emissions of atmospheric pollutants generated by passenger cars, using the IVE model methodology to create an emissions inventory in the province of Panama in 2023.

MATERIALS AND METHODS

The information required to estimate the air emission inventory generated by passenger cars using the IVE model is shown in Table 1. The National Institute of Statistics and Census (INEC) of Panama defines a passenger car as one that is exclusively intended for the transportation of people, with a capacity of up to 13 people including SUVs, jeeps, coupes, and sedans. The methodology flowchart for estimating emissions from passenger cars is depicted in Fig. 2.

Passenger cars in circulation in the Republic of Panama are primarily found within the province of Panama, specifically in the Panama district, followed by the San Miguelito district. By 2022, 59.2% of the total vehicles in the country were in these districts. To determine the prevalent vehicle technologies in the country, various regions within these districts were studied. These areas are representative because they correspond to major high-traffic avenues in the Panama and San Miguelito districts, and they also cover areas of low, medium, and high incomes. Fig. 3 shows the chosen avenues; Centenario, Cincuentenario, Domingo Díaz, José Agustín Arango, and Simón Bolívar.

Data collection

In the process of data collection phase, drivers were interviewed at fuel stations found in the previously designated locations. The questionnaire was designed to obtain detailed information about vehicle characteristics and driving behavior. The questions included vehicle type, year of manufacture, type of car exhaust catalyst, engine size, type of fuel used, among others. In cases where the driver was unfamiliar with certain characteristics, the vehicle registration information was examined. Given that the

Table 1: Input parameters for the air emission inventory using the IVE Model

Report	Parameter	Description
Location	Environmental variables	Ambient temperature
		Ambient relative humidity
		Altitude
	Fuel specifications	Sulfur in gasoline and Diesel
		Lead in gasoline
		Benzene in gasoline
	Driving behavior	Driving patterns and Driving distance
		Slopes
		Use of air conditioning
		Cold start distribution
Fleet	Vehicle fleet fraction	Vehicle size
		Fuel type
		Vehicle use
		Fuel delivery system
		Evaporative emission control system
		Exhaust control system/Standard

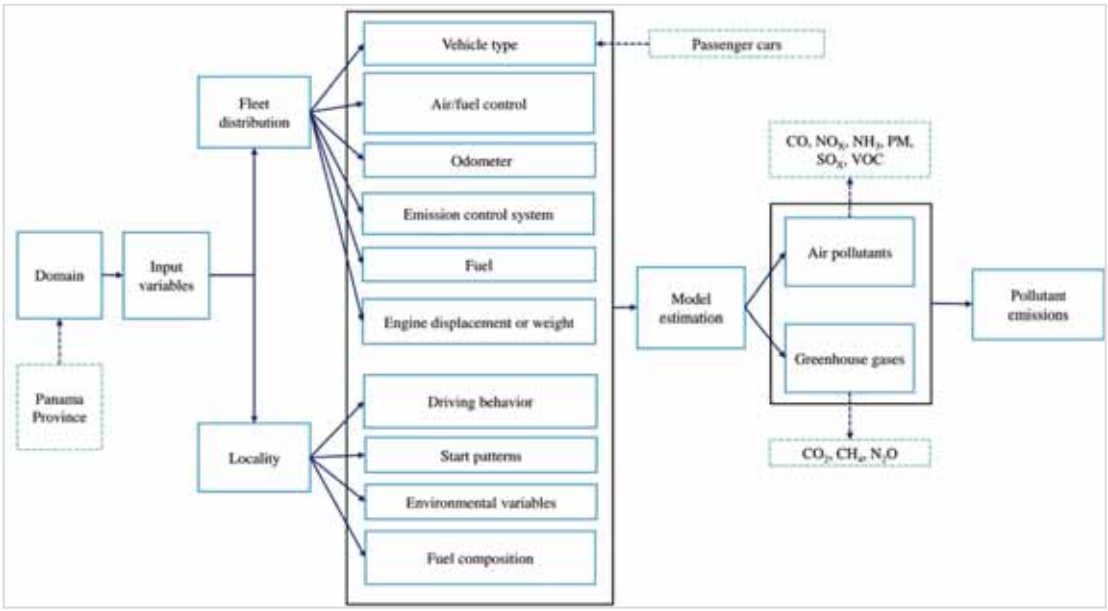

Fig. 2: Flowchart of the input variables in the IVE model

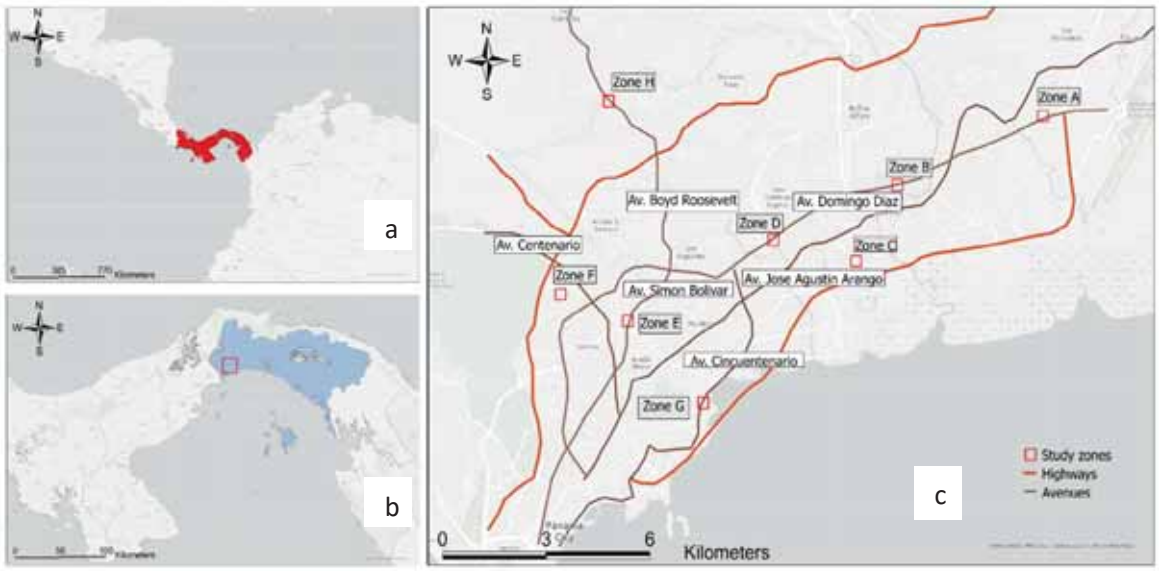

Fig. 3: Geographical location of the Republic of Panamá in Central America (a), location of the province of Panama in the Republic of Panamá (b), location of the study area in the main avenues within the districts of Panamá and San Miguelito (c)

survey concentrated on passenger vehicles, therefore, the inclusion of hatchbacks and pickup trucks was due to drivers reporting their personal usage rather than for business purposes. To represent a fleet of 534,322 passenger cars, a sample of 409 vehicles was surveyed. A convenience sampling (a non-probabilistic approach) method was applied to define the sample size. This technique was picked to evaluate the number of vehicle users to be surveyed, owing to its capability in pinpointing the qualitative features of the vehicle fleet in Panama province. It enables quick and easy access to participants, which is crucial for data collection

Table 2: Distribution of surveyed vehicle fleet by location

Avenue	Location of filling stations		No. of vehicles surveyed	Distribution (%)
	Zone	Coordinates		
Domingo Díaz	A	9° 4' 6.5" N 79° 24' 34.1" W	107	26.2 %
	B	9° 3' 6.0" N 79° 26' 50.1" W		
	D	9° 2' 17.9" N 79° 28' 46.2" W		
José Agustín Arango	C	9° 1' 59.5" N 79° 27' 28.9" W	25	6.1 %
Simón Bolívar	E	9° 1' 7.2" N 79° 31' 2.4" W	44	10.8 %
Centenario	F	9° 1' 30.4" N 79° 32' 5.3" W	102	24.9 %
Cincuentenario	G	8° 59' 55.5" N 79° 29' 51.8" W	82	20 %
Boyd Roosevelt	H	9° 4' 19.4" N 79° 31' 20.3" W	49	12 %
Total			409	100 %

in areas with high traffic density. The distribution by location is shown in Table 2.

Vehicle technology distribution

The pollutant emissions generated by vehicles are influenced by their mechanical characteristics and incorporated technology. The IVE Model includes a database with the most common characteristics of passenger cars, which was used for vehicle classification. Despite this, the IVE Model has not undergone recent updates, thereby limiting its effectiveness in characterizing vehicles that utilize more advanced technologies compliant with Euro 5 and Euro 6 standards. Consequently, spark-ignition vehicles that comply with these international standards have been categorized under the most stringent standard in the IVE model, which is European (Euro)- 4.

Geographic and environmental profile

Meteorological conditions have a significant impact on traffic behavior and vehicle performance. These parameters were established for the baseline year using data from weather monitoring stations at two locations within the province of Panama: Albrook "Marcos A. Gelabert" International Airport (8° 58' 00" N, 79° 34' 00" W) and Tocumen International Airport (9° 03' 56" N, 79° 23' 31" W), both near the study areas in the Panama district. The database was obtained using the OpenAir and worldmet (Carslaw, 2023) libraries in R (John Chambers, 2024). This dataset includes an hourly historical record of air temperature and relative humidity for the year 2023. To correlate these variables with peak traffic hours, values were limited to the period between 6:00 a.m. when traffic congestion is highest in the city (Banco Interamericano de Desarrollo and Alcaldía de Panamá, 2016) and 8:00 p.m., when vehicle flow begins to decrease on the city's main roads (Velasco Soldevila, 2014). In Table 3, the air temperature results derived from the software were evaluated against daily meteorological data from Institute of Meteorology and Hydrology of Panama (IMHPA), evaluating the percentage error between both values.

With respect to the monthly relative humidity for 2023, the data displayed in Table 4 was gathered exclusively from the R source.

Geographical elevation

The avenues above mentioned primarily extend within watershed 144 (Juan Díaz River and between Juan Díaz and Pacora) and watershed 142 (Rivers between El Caimito and Juan Díaz) of the country. The average elevation of watershed 144 is 90 meters above sea level (masl), in contrast to watershed 142, which has an average elevation of 67 masl.

Fuel composition

The fuel composition is subject to regional regulations according to the Central American

Table 3: Average monthly temperature for the year 2023

Months	Weather monitoring stations					
	Albrook "Marcos A. Gelabert" International Airport			Tocumen International Airport		
	Temp. R (°C) (6 a.m.-8 p.m.)	Temp. IMHPA (°C)	Error (%)	Temp. R (°C) (6 a.m.-8 p.m.)	Temp. IMHPA (°C)	Error (%)
January	27.8	27.3	1.9 %	27.9	27.8	0.3 %
February	28.8	28.1	2.4 %	28.6	27	6.1 %
March	28.8	27.9	3.2 %	28.7	27.1	5.9 %
April	29.7	29	2.4 %	29.6	27.9	5.9 %
May	29.5	29.3	0.5 %	29.6	28.8	2.8 %
June	28.7	28.2	1.7 %	28.5	27.9	2.0 %
July	28.5	28.5	0.0 %	28.4	28.1	1.1 %
August	28.5	28.4	0.5 %	28.3	27.9	1.3 %
September	28.7	28.5	0.6 %	28.3	27.8	1.9 %
October	28.2	28	0.8 %	27.5	27.3	0.8 %
November	28.1	27.9	0.6 %	27.9	27.5	1.5 %
December	29.2	28.9	1.2 %	28.9	27.9	3.5 %

Table 4: Monthly average relative humidity (RH) for the year 2023

Months	Weather monitoring stations	
	Albrook "Marcos A. Gelabert" International Airport	Tocumen International Airport
	RH (%)	RH (%)
January	73.38	68.55
February	64.74	64.11
March	66.54	65.45
April	63.29	63.23
May	74.47	72.49
June	80.59	81.93
July	81.50	82.74
August	81.60	83.14
September	80.84	83.04
October	82.67	87.73
November	83.28	84.99
December	75.00	76.70

Technical Regulation 75.01.20:19 for Petroleum products, where it is established the physical and chemical characteristics that automotive-grade premium gasoline must comply with, effective from February 2021 (Ministerio de Comercio e Industrias de la República de Panamá, 2022). For diesel, the specifications established in regulation RTCA 75.02.17:19 for automotive-grade diesel fuel have been in effect since October 2021 (Ministerio de Comercio e Industrias, 2021). The national regulations concerning fuel quality in vehicles are illustrated in Table 5. Fuel adulteration and unauthorized vehicle modifications were excluded from the input in the IVE model.

Driving patterns

In establishing the driving pattern for passenger cars in Panama province, the country lacks previous studies or available information on vehicle travel behavior. Upon examining vehicle travel behaviors and the implementation of the IVE model, it was determined to employ reference data obtained from Thailand (Outapa *et al.*, 2018). The similarities between the two countries allow these values to be used as a baseline, since both share urban congestion and similar weather conditions, notably a humid tropical climate. The driving patterns are mainly defined to establish a specific velocity profile. The input in the software requires non-discrete data. The data was derived sourced from driving behaviors in Thailand, yet in the current study, the profile was corroborated with the speed limits on the roads adjacent to the filling station where the survey occurred. The emission factors (EF) were calculated

using the results obtained.

Methodology for emission factors

The emission factors (EF) (g/km) were calculated by dividing the total emissions by the fleet size and the annual mileage, adjusting the emissions to a basis of grams per kilometer per vehicle. The emission factors are determined using Eq. 1 modified from (ISSRC, 2008):

$$EF_{i,j} = \frac{E_{i,j} \times 1,000,000}{NV_j \times (kma)} \quad (1)$$

Where;

Eij = Total fleet emissions for pollutant *i* and technology *j* (tons/year)

NVj = Number of vehicles corresponding to technology *j*

kma = Annual mileage (km/year)

RESULTS AND DISCUSSION

Driving distance

Concerning the kilometers driven by the vehicle fleet during a designated period, estimating the fleet's mileage annually is vital for compiling an emissions inventory for the year. This parameter was determined by using odometer reading collected from the vehicles during the survey, where the daily kilometers traveled (Daily km) of the vehicles were calculated in this study, using Eq. 2:

$$\text{Daily km} = \frac{\text{Odometer Lecture}}{(\text{Inventory year} - \text{manufacturing year}) * \left(365 - \frac{\text{holidays}}{2}\right)} \quad (2)$$

In Eq. 2, half of the holidays in the year were subtracted. This adjustment was made because vehicles are used less on holidays, and it improves accuracy by considering population behavior. The formula takes into account the inventory year, which aligns with the base year of the study, 2023, as well as the vehicle's manufacturing year. Fig. 4 presents a histogram showing the distribution of daily kilometers traveled by private passenger cars, representing 71% of the fleet identified in the sample. The figure indicates that 91% of private passenger cars travel less than 87 kilometers per day (km/d). The histogram illustrates a right-skewed distribution, revealing that the number of vehicles that travel longer daily distances diminishes considerably. This right-skewed pattern suggests that less than 87 km per day trips are the most common among private passenger cars. Consequently, vehicles with daily distances greater than 87 km were left out to prevent incorporating outliers. Fig. 5 presents a box-and-whisker plot representing the annual kilometers traveled by private passenger cars with daily distances of less than 157 km (1) and 87 km (2). Case 2 shows less dispersion; therefore, this data will represent the annual kilometers traveled, averaging 14,611 km/year, which accounts for 65.2% of the surveyed sample of 409 cars.

Throughout the Panama and San Miguelito districts, a total of 53 distinct vehicle categories were identified during the field campaign. The findings from the survey reveal that 94.80% of cars were powered by gasoline (known as petrol), and 5.12% ran on diesel. The cars have accumulative mileage greater than 160,000 km, representing 45.19%, followed by vehicles with odometer readings of less than 79,000 km (23.22%). Concerning the engine displacement, 61.1% of the fleet's passenger cars have an engine displacement between 1.5 and 3 liters (classified as medium size), followed by 34.7% with a displacement of less than 1.5 liters (light size) and 4.2% possess a displacement exceeding 3 liters (designated as heavy size). Fig. 6 shows that light and medium cars have a higher proportion of vehicles with mileage exceeding 160,000 km.

According to the survey results, the average age of the car fleet was 9. This compares with neighboring countries such as Costa Rica, where the average age is 16 (Arias-Arguedas *et al.*, 2023), and 13 in Colombia (Alejandra Rico, 2025). In this study, the vehicle's origin was not questioned (imported or second-hand owner), and there are no official statistics with this information. A law was proposed in Panama in 2017 to ban the importation of cars that are classified as total loss or scrap, or having reached the end of their useful life in the country of origin. However, this law did not pass the legislative chamber. Even without a specific incentive to lower emissions from older vehicles, a financial inclination is observed in the country. Loans for newer cars generally offer lower interest rates, approximately 5.5% per year, and longer repayment periods of up to 96 months.

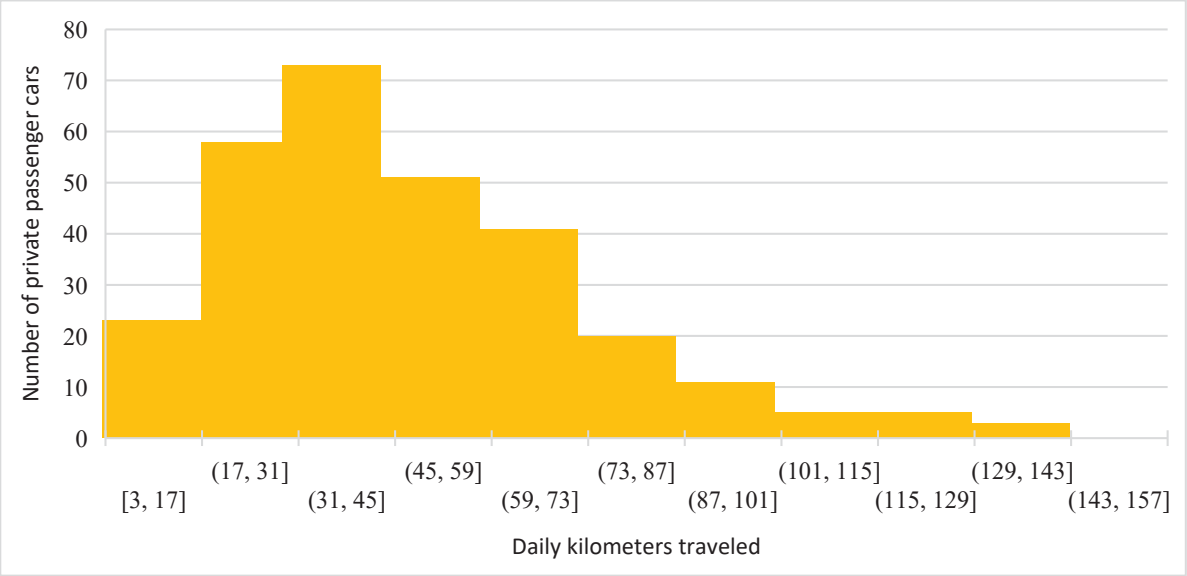

Fig. 4: Histogram of daily kilometers traveled by the passenger car fleet

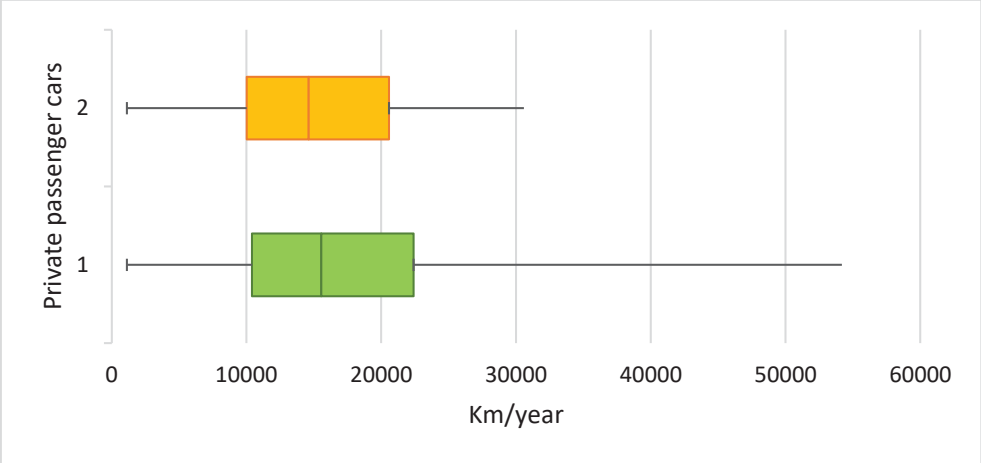

Fig. 5: Box-and-whisker plot of the annual kilometers traveled by passenger vehicles with daily ranges of up to 157 km (1) and up to 87 km (2)

In contrast, used vehicles typically have interest rates starting from approximately 7.75% annually.

Methodology for emission factors

The emissions of greenhouse gases and other atmospheric pollutants (in metric tons) generated by passenger cars in the province of Panamá in 2023, based on fuel type and vehicle, are displayed in Table 5. The results were obtained after setting the vehicle categories, the environmental conditions and the local profile in the IVE model.

The contribution of GHG pollutants from passenger vehicles is as follow: 1.78 Mt (Megatonnes) per year of CO_2, 1111.7 t per year of CH_4 and 58.3 t per year of N_2O. Regarding air pollutants, CO was the main pollutant emitted reaching 234.16 kt in the year of analysis, followed by VOCs (5.40 kt), NOx (4.95 kt), NH_3 (1.17 kt), PM_{10} (0.16 kt), and SOx (0.031 kt) (Fig 7.). With increasing vehicle mileage, there is a corresponding rise in engine wear, which affects the efficiency of combustion and leads to incomplete combustion. Also, the degradation of the emission control system occurs. Vehicles use lubricants to

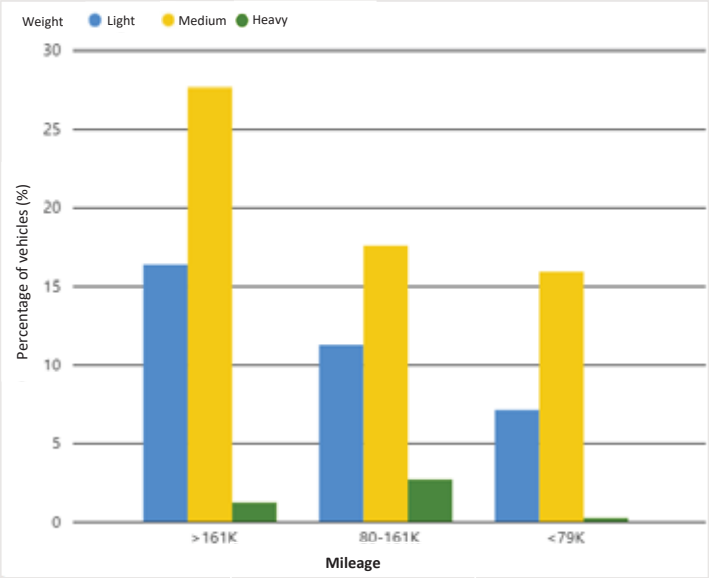

Fig. 6: Percentage of vehicles based on their weight (size) and accumulated mileage

Table 5: Physicochemical specs of fuels according to national regulations and the input in the IVE Model

Fuel	Physicochemical properties	Unit	Regulatory limit	Value employed in the IVE model
Gasoline	Sulfur	mg/kg (% mass)	150 (0.015) max.	50 (0.0050)
	Lead Content	g Pb/L	0.013 max.	0
	Benzene	% volume	1.5 max.	1.5
	Oxygenates	% volume	0.7 max.	0
Diesel	Sulfur	mg/kg (% mass)	15 (0.0015) max.	15 (0.0015)

reduce friction between engine components, which minimizes wear and improves engine efficiency. Furthermore, with the passage of time and continuous use, the oil breaks down and its efficiency diminishes, causing incomplete combustion in the vehicle and increasing emissions of VOCs and CO.

With respect to the fuel type used in vehicles, Fig. 8a. illustrates that diesel-powered vehicles, which constitute under 6% of the fleet, are accountable for almost 50% of the PM10 emissions, precisely 47% of the total emissions. In contrast, each gasoline vehicle emits approximately 169 grams of PM_{10} per year, while diesel vehicles emit significantly more, with 2779 grams of PM_{10} per year. In the analysis of emissions by vehicle size, Fig. 8b demonstrates that medium-sized cars are the largest sources of all gaseous emissions. Heavy vehicles, with engine displacements over 3000 cc (cubic centimeters), have the greatest impact on particulate matter emissions, contributing 15%. These data reflect the impact of diesel vehicles on air quality. Unlike CO_2, which primarily affects the atmosphere temperature, pollutants such as SOx, NOx, and particulate matter present a direct risk to human health. The contribution of vehicles to GHG emissions and air pollutants is depicted in Fig. 8c, which is based on the total mileage of the fleet. Vehicles with mileage over 160,000 km are the main contributors to emissions, with significant impacts on CO (79%), PM_{10} (80%), VOC (78%), and CH_4 (76%) emissions. In contrast, vehicles with mileage under 79,000 km, which have a lower travel distance, contribute relatively little to the emissions of CH_4 (4%), CO (3%), and VOC (4%). According to national statistics, hybrid vehicles represent less than 0.24% of the total cars in the study area. Consequently, hybrid and electric vehicles were excluded from the emission model. Current information about the passenger car fleet indicates that alternative fuels

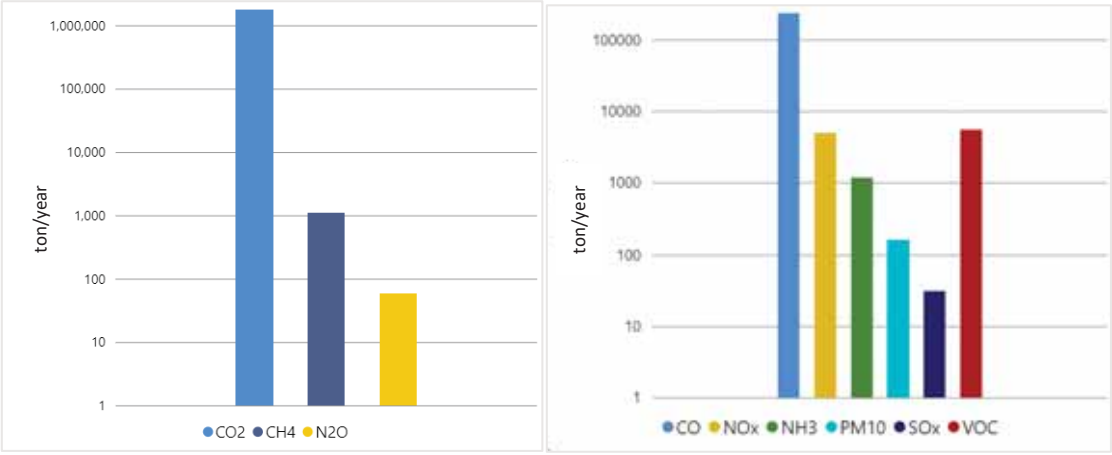

Fig. 7: Greenhouse Gas and Air Pollutant Emissions (ton/y)

were not employed in 2023. The assumptions made in the current model reflect the existing distribution of the vehicle fleet. However, it is understood that modifications will be essential as hybrid, electric, and various low-emission technologies become increasingly common in the region.

Performing a linear regression with a coefficient of determination of 95% on the emissions reported by the Ministry of Environment in the country to date, 5.78 Mt of CO_2 emissions generated by land transportation (cars, motorcycles, buses, trucks, machinery, etc.) are estimated for the year 2023. According to the IPCC methodology, these emissions have been calculated, revealing that 31% of the produced emissions associated with land transportation stem from passenger cars within the Province of Panama.

Emission factors

IVE model facilitates the determination of emission factors for future estimates, measured in grams of pollutants per kilometer. This calculation considers the emission control technology implemented in the fleet. Table 6 shows the emission factors calculated based on the 2023 emissions inventory, taking into account the fuel type and vehicle size (engine displacement). For gasoline-powered vehicles, emissions of CO_2, N_2O, NOx, and SOx per kilometer increase proportionally with vehicle size. However, this behavior varies for other air pollutants. Regarding CH4, light-duty vehicles release the least amount of this gas, in contrast to the higher and comparable emissions from medium and heavy vehicles. Diesel vehicles of medium size generate approximately 0.19 g/km of PM_{10}, whereas heavy vehicles emit 0.25 g/km. Although diesel vehicles without emission control systems belong only to the medium-size category, vehicle size remains a key parameter in determining emissions. When compared, heavy vehicles emit 31% more PM10 per kilometer than medium-sized vehicles, underscoring the influence of vehicle size on pollutant emissions.

Comparative analysis of the estimated emissions inventory versus other localities

The aim of this section is to present a comparative analysis of atmospheric pollutant emissions of CO, NOx, and VOCs generated by passenger cars in different cities or regions, alongside the results obtained in this study for the province of Panama. To achieve a proportional comparison, emissions were examined on a per capita basis, acknowledging the population disparities across different regions. These per capita emissions are shown in Fig. 9. CO is the primary pollutant emitted in all the analyzed locations, with the province of Panama reporting the highest emissions (446 g/d/per capita), three times higher than Guayaquil, Ecuador (138 g/d/capita). In Guayaquil, the IVE model was applied using 2018 dataA significant contrast between Panama and Guayaquil is evident in their vehicle counts: Panama had 371 cars for every 1,000 inhabitants, while

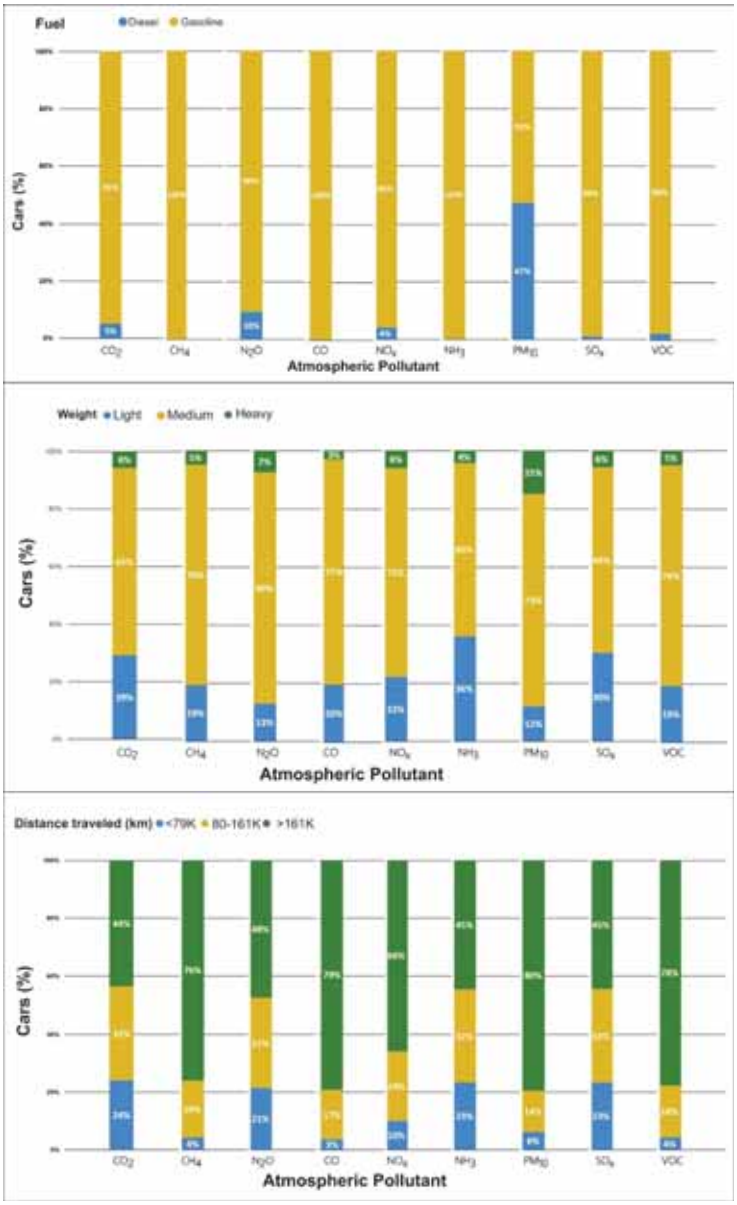

Fig. 8: Atmospheric pollutant emissions of CO_2, CH_4, N_2O, CO, NOx, NH_3, PM_{10}, SOx, and VOC (a) by fuel type (b) by vehicle size (c) by mileage (distance travel)

Guayaquil only had 114 in the same year of the study. The lowest CO emissions were found in Manizales, Colombia, based on a 2017 study using the COPERT model, which showed emissions 69% lower than those estimated by the IVE model for the same year—differences largely due to varying emission factors and calculation methods. Additionally, vehicle activity in Panama is higher (41 km/car/d) compared to Manizales (25 km/car/d). The second most significant pollutant is VOC, Guayaquil leading (15 g/day/per/ habitant), followed by Bogotá (13 g/d/capita) (Alcaldía Mayor de Bogotá D.C. and Secretaría de Ambiente, 2021) and Panama (10 g/d/capita). In Bogotá, there are 240 cars for every 1,000 people—twice as many as in Guayaquil, even though both cities demonstrate comparable levels of VOC

Table 6: Passenger vehicle emissions by vehicle category (ton/year)

Vehicle characteristics		%	CO_2	Methane (CH_4)	N_2O	CO	NO_x	Ammonia (NH_3)	PM_{10}	Sulfur oxides (SO_x)	VOC
Fuel	Weight			ton/y				ton/y			
Gasoline	Light	34.7	518430.7	214.8	7.5	45954.0	1094.6	424.4	19.4	9.3	1036.7
	Medium	56.2	1074562.6	842.9	40.9	180859.8	3375.6	699.2	46.1	19.4	3982.3
	Heavy	3.9	98011.3	54.0	4.3	7062.3	282.1	49.3	19.6	1.7	264.0
Diesel	Medium	4.9	84081.8	0.0	5.5	268.9	187.2	1.2	72.0	0.3	112.2
	Heavy	0.2	4947.8	0.0	0.0	13.4	14.3	0.1	4.7	0.0	5.4
Total		100	1780034.2	1111.7	58.3	234158.3	4953.9	1174.1	161.7	30.8	5400.6

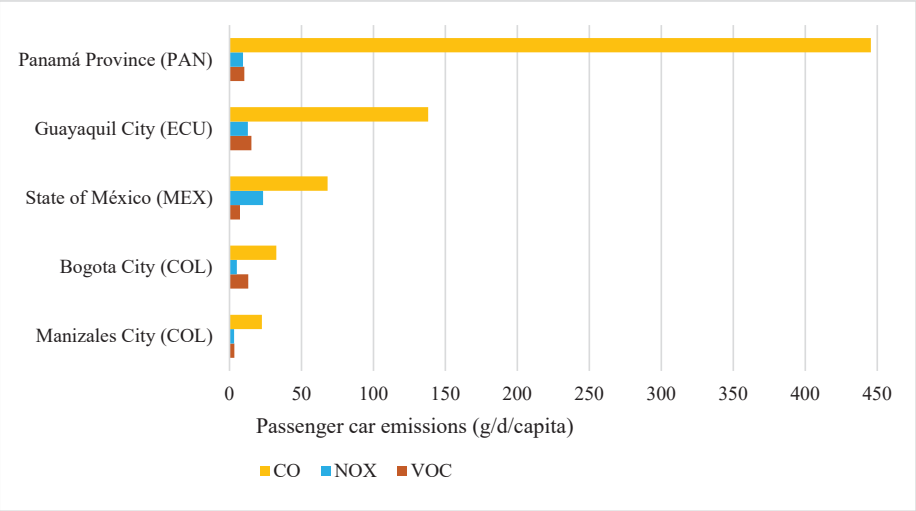

Fig. 9: Daily per capita emissions by location

emissions. NOx emissions were highest in the State of Mexico (23 g/d/capita in 2018) (Secretaría de Medio Ambiente y Recursos Naturales, 2024), 155% higher than in Panama, which ranks third. In 2018, the State of Mexico report 320 cars per 1,000 inhabitants (Dirección General de Estadística, 2024), while Panama had 16% more cars in 2023. PM_{10} emissions are below 1 g/d/capita and were not analyzed in detail. This study highlights the significance of local elements like the size of the vehicle fleet, vehicle activity, and the emission models employed to ensure accurate and representative emission estimates. Moreover, it indicates the situation in comparison to countries in the region and it will help as a reference to propose policies to improve air quality management at the district or provincial level in Panamá. In a study conducted in the city of Manizales, Caldas Department in Colombia (Cifuentes *et al.*, 2021), a comparison of COPERT/Top-down and IVE/Top-down shows that the IVE performed better than the COPERT because information about vehicle-specific power, which accounts not only for average speed, but for acceleration, vehicle weight, road slopes, among other variables. Nonetheless, future studies of this kind will offer enhanced information concerning the effectiveness of the IVE model in this context.

Uncertainty analysis

An uncertainty analysis was performed using error propagation method, as recommended by the IPCC. This method allows for quantifying the level of uncertainty associated with the product of the quantities involved in the emissions estimation. This approach for merging uncertainties was employed to determine the uncertainty percentage for the

Table 7: Emission factors for passenger vehicles per kilometer (g/km)

Vehicle characteristics		CO_2	CH_4	N_2O	CO	NO_x	NH_3	PM_{10}	SO_x	VOC
Fuel type	Weight	g/km					g/km			
Gasoline	Light	191.317	0.079	0.003	16.958	0.404	0.157	0.007	0.003	0.383
	Medium	244.957	0.192	0.009	41.229	0.770	0.159	0.011	0.004	0.908
	Heavy	321.906	0.177	0.014	23.195	0.927	0.162	0.064	0.006	0.867
Diesel	Medium	220.699	0.000	0.014	0.706	0.491	0.003	0.189	0.001	0.295
	Heavy	264.070	0.000	0.002	0.715	0.765	0.004	0.248	0.001	0.289

numerical input data in the IVE Model, taking into account the statistical variability of the associated variables. A method utilizing qualitative evaluation of the origin and characteristics of the data was employed for qualitative variables. The outcome revealed a roughly 14% uncertainty associated with the input data. On the other hand, the Second Biennial Update Report: Learn About Climate Change Mitigation in Panama in 2021 has an uncertainty of ±58.0 %, and the national inventory in 2024 indicates an uncertainty of ±194.5 % due to the use of Tier 1 methodology in both cases.

RECOMMENDATION

This study proposed the following recommendations: 1) *To disclose information about the emission standard and the emission control system in the vehicle registration*. Currently, there is no obligated for manufacturers to disclose information concerning the vehicle emission standard or the type of emission control system in the user manual. 2) *To update the emission test*. Environmental policies in other countries require tests on dynamometers that allow manufacturers to share information about the vehicle's emissions versus fuel consumption or kilometers travel. 3) *To continue implementing the recently approved electric mobility law*. As indicated, the government must replace the fleet with electric cars by 10% by 2025, 25% by 2027, and 40% by 2023. Establishments must reserve at least 15% of the parking lots for electric cars. Electric vehicles are exempt from paying for car plates for five years. 4) *To invest in public transportation*. The inaugural Metro line was launched in 2014 to reduce congestion between San Miguelito and Panama Districts. Later in 2019, Metro Line 2 was inaugurated with 18 stations, connecting the east side of Panama City. In 2023 (Quiñones, 2023), 255000 people commute daily on line 1 and 157000 on line 2. A Monorail is envisioned as Line 3 for 2025, aimed at connecting West Panama Province to Panama City. The original plan was to construct a bridge over the Panama Canal waterway by a bridge, but the proposal has recently shifted to a tunnel situated 60 meters beneath it. In Panama City, the metro line is supplied by the public transportation services provided by the buses known as "MiBus". However, users complain about frequency, schedules, security, and capacity. 5) *To allow greater transparency in government public data on vehicles registered nationwide, and to facilitate more effective collaboration among public institutions*. Making this data accessible and regularly updated would allow better air emission inventories estimations. 6) *To expand vehicle registration information.* Vehicle registration should encompass details regarding technological specifications, odometer mileage, maintenance schedule, type of fuel used, vehicle efficiency, and the categorization of vehicles (passenger, commercial, heavy-duty vehicle, L-category, etc.). 7) *To require car registration in the driver's residency municipality.* Currently, cars can be registered in any municipality in the country. However, this does not help with urban planning and local governments environmental policies. 8) *To initiate public awareness campaigns*. Clarify how fuel usage correlates with emissions and the subsequent health consequences for the community. 9) *To discourage the use of diesel-powered cars.* Currently, three types of fuel for vehicles are sold in Panama: Ultra-Low Sulfur Diesel (ULSD), 95-octane gasoline, and 91-octane gasoline. The prices vary depending on the province, but diesel per liter is lower than gasoline. In July 2022, following significant strikes throughout the country, a fuel price subsidy was approved for 91-octane gasoline and ULSD valid until January 2024. Policies aimed at reducing the use

of diesel-powered vehicles should start by raising public awareness about the impact of air pollution on community health to prevent social unres. 10) *To verify authorized car workshops*. The Land Transit and Transportation Authority (in Spanish: La Autoridad de Tránsito y Transporte Terrestre (ATTT)) is supposed to enforce the current vehicle emission regulation law. They must inspect authorized car workshops and verify that they have the certified equipment to conduct the annual emission inspection. 11) *To evaluate long-term strategies regarding phasing out or retrofit*. It is essential to consider these policies since they may not be suitable for the social context and might predominantly benefit vehicle dealers. Moreover, they could facilitate the second-hand black-market business. Retrofitting an internal combustion engine to an electric vehicle will require trained labor.

CONCLUSION

This study estimated the air emission inventory of on-road mobile sources in 2023 for passenger cars in the province of Panama. A field investigation was performed to recognize the technologies that characterize passenger vehicles within the designated study area. Fifty-three vehicle categories were identified, with gasoline-powered cars making up 94.8% of the fleet, while diesel vehicles represented only 5.12%. Results indicate that more than 45% of the vehicles exceed 160,000 km. The distribution by size shows that medium-sized vehicles (with an engine displacement between 1.5 and 3 liters) constitute the majority (61.1%) and are the highest emitters in all pollutant categories, particularly in CO_2 and N_2O. Although diesel vehicles are fewer, they account for nearly half of the PM_{10} emissions, especially those with engine displacements greater than 3 liters. CO_2 was identified as the main pollutant emitted by passenger cars. With the increase in vehicle mileage, a significant uptick in the emissions of pollutants including CO, NOx, and VOC is observed. Diesel vehicles are notable for their high NOx and PM_{10} emissions, which pose a considerable risk to human health. Additionally, reducing sulfur content in diesel has significantly contributed to decreasing NOx, PM_{10}, and SOx emissions, underscoring the importance of fuel quality regulations. Examining emission factors for passenger vehicles has uncovered trends that are influenced by the size of the vehicle and the type of fuel used. In gasoline-fueled vehicles, emissions of pollutants such as CO_2, N_2O, NOx, and SOx increase proportionally with vehicle size, while other gases such as CH_4 show more variable behavior. Ultimately, the comparative analysis with other regions emphasizes the variations in per capita emissions, which are affected by elements like vehicle density, distance traveled, and the software used. This analysis demonstrates that, although estimates may vary, the size and use of the vehicle fleet play a crucial role in determining atmospheric emissions. Moreover, the survey revealed that the public lacks awareness of the connection between air pollution and their car usage.

AUTHOR CONTRIBUTIONS

A. Valdés-Montenegro has analyzed the data, written the manuscript, prepared all the figures, and interpreted the results. F. González-Olivardía, the corresponding author, has contributed by supervising the work, interpreting the results, and writing the manuscript. C. Pinzón-Acosta participated in the interpretation of the results and manuscript revision. All the authors participated in the data collection process.

ACKNOWLEDGEMENT

The authors sincerely thank the Mahidol University Faculty of Public Health, particularly Professor Sarawut Thepanondh, for his guidance and data sharing of driving patterns to support this study. Moreover, the authors want to acknowledge the work of more than 20 volunteers who helped in the survey, especially the students from the AirES research group. The authors extend our gratitude to Joseph Asprilla for helping with the map drawings. Also, the Universidad Tecnológica de Panamá and the gas filling stations that allowed us to use their sites to conduct the surveys. SENACYT funds this article under contracts No. [141-2022 (IDDS22-43)] and No. [186-2022 (FIED22-12)].

CONFLICT OF INTEREST

The authors declare that there is no conflict of interest regarding the publication of this manuscript. In addition, ethical issues, including plagiarism, informed consent, misconduct, data fabrication and/or falsification, double publication and/or submission, and redundancy have been completely observed by the authors.

OPEN ACCESS

©2025 The author(s). This article is licensed under a Creative Commons Attribution 4.0 International License, which permits use, sharing, adaptation, distribution and reproduction in any medium or format, as long as you give appropriate credit to the original author(s) and the source, provide a link to the Creative Commons license, and indicate if changes were made. The images or other third-party material in this article are included in the article's Creative Commons license, unless indicated otherwise in a credit line to the material. If material is not included in the article's Creative Commons license and your intended use is not permitted by statutory regulation or exceeds the permitted use, you will need to obtain permission directly from the copyright holder. To view a copy of this license, visit: http://creativecommons.org/licenses/by/4.0/

PUBLISHER'S NOTE

GJESM Publisher remains neutral with regard to jurisdictional claims in published maps and institutional afflictions.

Positive AI Statement

During the preparation of this work the author(s) have used Artificial Intelligence (AI) [Grammar/English language writing assistant] in order to [Improving the English writing style]. After using this tool/service, the authors reviewed and edited the content as needed and take full responsibility for the content of the publication.

(For this reason, the GPTZero detector will evaluate the manuscript utilizing Generative AI, ensuring a high detection rate. If the manuscript relies heavily on Generative AI and AI-assisted technologies, it will be archived without further options for appeal).

Negative AI Statement

The author(s) declare that no AI tools or services were not used or not highly applied during the preparation of this work.

ABBREVIATIONS

%	Percent
°C	Degree Celsius
a.m.	ante meridiem or before noon.
CARB	California Air Resources Board
CH_4	Methane
CO	Carbon monoxide
CO_2	Carbon dioxide
EPA	United States Environmental Protection Agency
g/km	Grams per kilometer
HSU	Hartridge Smoke Units
IMHPA	Panama Institute of Meteorology and Hydrology
INEC	National Institute of Statistics and Census
IPCC	The Intergovernmental Panel for Climate Change
IVE	International vehicle emissions
km	Kilometer
kma	Annual mileage (km/vehicle)
Km/d	kilometers per day
km/kWh	electricity consumption
km/lt	fuel consumption
km/y	kilometers per year
kt	Kilotons
kt CO_2	Kilo-tonnes of carbon dioxide emissions
Mt	Megatons
masl	Meters above sea level
N	North
NH_3	Ammonia
N_2O	Nitrous oxide
No.	Number
NO_2	Nitrogen dioxide
NOx	Nitrogen oxides
O_3	Tropospheric ozone
p.m.	post meridiem or after noon
Pb	Lead
$PM_{2.5}$	Fine inhalable particles, with diameters that are generally 2.5 micrometers and smaller.
PM_{10}	Inhalable particles, with diameters that are generally 10 micrometers and smaller
ppm	parts per million

RH	Relative humidity
SO_2	Sulfur dioxide
SOx	Sulfur oxides
SUV	Sport Utility Vehicle
Temp.	Temperature
Ton/y	Tonnes per year
UCR	University of California, Riverside
ULSD	Ultra-low sulfur diesel
VOC	Volatile organic compounds
W	West

REFERENCES

Alcaldía Mayor de Bogotá, D.C.; Secretaría de Ambiente, (2021). Inventario de emisiones de Bogotá, contaminantes atmosféricos 2020 **(81 pages)**.

Alejandra Rico, A., (2025). El parque automotor se llenó de carros viejos y tiene una edad promedio de 13 años. LR MAS.

Almetwally, A. A.; Bin-Jumah, M.; Allam, A. A., (2020). Ambient air pollution and its influence on human health and welfare: an overview. Environ. Sci. Pollut. Res., 27(2): 24815–24830 **(16 pages).**

Arias-Arguedas, C.; Richmond-Navarro, G.; Gómez-Ramírez, G., (2023). Crecimiento de la flota vehicular en Costa Rica y sus emisiones de gases de efecto invernadero. Investiga. TEC, 16(46), **(5 pages)**.

Banco Interamericano de Desarrollo; Alcaldía de Panamá, (2016). Plan integral para la mejora de la movilidad y seguridad vial para el centro histórico de la ciudad de Panamá **(28 pages)**.

Carslaw, D., (2023). Worldmet (0.9.7.).

Cifuentes, F.; Gonzalez, C. M.; Trejos, E. M.; Lopez, L. D.; Sandoval, F. J.; Cuellar, O. A.; Mangones, S. C., Rojas, N. Y., Aristizabal, B. H., & Velasco, M. (2021). Comparison of emission models and top-down/bottom-up approaches on the estimation of vehicular emissions, and its use in air quality modeling in the city of Manizales. *2021* Congreso Colombiano y Conferencia Internacional de Calidad de Aire y Salud Pública (CASAP), **(4 pages)**.

Costa, L.G.; Cole, T.B.; Dao, K.; Chang, Y.C.; Coburn, J.; Garrick, J.M., (2020). Effects of air pollution on the nervous system and its possible role in neurodevelopmental and neurodegenerative disorders. Pharmacol Ther., 210: 107523 **(47 pages)**.

Cuba, C.; Cuba, R.; Arroyo, V.; Morales, J, (2021, 26th-28th August). Characterization of Air Pollution in Pre-COVID 19 Time Using the IVE Model Applied to Mobile Sources in Urban Areas The 7th International Conference on Advances in Environment Research (ICAER 2021), Sapporo, Japan **(9 pages)**.

Duan, R.R.; Hao, K.; Yang, T., (2020). Air pollution and chronic obstructive pulmonary disease. Chronic Diseases and Translational Medicine, 6(4) **(10 pages)**.

EPA, (2001). Introduction to stationary point source emission inventory development. EIIP Volume II: Chapter 1 **(316 pages)**.

Fogelbach, G.G.; Ramon, G.D.; Staffeld, P.L.; Sarabia, A.M.C.; López, C.A.S.R.; Duarte, P.A.; Calderón, O.M.; Romero, F.H C.; Diaz, S.G.; De-Ramos, R. S.; Piraino, P.; Repka-Ramirez, M.S.; Sisul, J.C.; Quezada, C.E.d.L.; Gonzalez, R.V.; Guzman-Avilán, R.I.; Silva, B.G.d.; Aguirre, J.C.F.d.C., (2020). Contaminacion atmosferica em America Latina: impacto em la salu Y regulacion actual: reporte de grupo de Comité de Aerobiologia Sociedad Latinoamericana de Asma, Alergia e Imunologia. Arquivos de Asmas Alergia e Imunologia. 4(4) **(12 pages)**.

Fong, W.K.; Sotos, M.; Doust, M.; Schultz, S.; Marques, A.; Deng-Beck, C., (2022). Protocolo global para inventarios de emisión de gases de efecto invernadero a escala comunitaria **(176 pages)**.

Gaceta Oficial, (2022). Ley N° 295 "Que incentiva la movilidad eléctrica en el transporte terrestre" **(8 pages)**.

IPCC, (2006). Directrices del IPCC de 2006 para los inventarios nacionales de gases de efecto invernadero. Intergovernmental Panel on Climate Change, Volume 2 **(78 pages)**.

ISSRC, (2008). Manual del usuario del Modelo IVE versión 2.0. International Sustainable Systems Research Center **(55 pages)**.

Jones, M.W.; Peters, G.P.; Gasser, T.; Andrew, R.M.; Schwingshackl, C.; Gütschow, J.; Houghton, R. A.; Friedlingstein, P.; Pongratz, J.; Le Quéré, C. (2023). National contributions to climate change due to historical emissions of carbon dioxide, methane, and nitrous oxide since 1850. Scientific Data, 10(1) **(23 pages)**.

Leland, E.M.; Vohra, V.; Seal, S.M.; Zhang, Z.; Ramanathan, M., (2022). Environmental air pollution and chronic rhinosinusitis: A systematic review. Laryngoscope Investigative Otolaryngol., 7(2): 349–360 **(12 pages).**

Liliana, A.; Pérez, R., (2015). Estimación de emisiones de contaminantes provenientes de fuentes móviles en la jurisdicción CAR **(120 pages)**.

Lyu, P.; Wang, P.; Liu, Y.; Wang, Y., (2021). Review of the studies on emission evaluation approaches for operating vehicles. J. Traffic Transport. Eng., 8(4): 493–509 **(17 pages).**

Marcela, E.; Zapata, T., (2021). Estimación de emisiones atmosféricas por fuentes móviles en ruta aplicando la metodología copert y determinación de las emisiones de material particulado resuspendido con información local **(171 pages)**.

Ministerio de Ambiente, (2021). Segundo informe bienal de actualización conoce sobre la mitigación del cambio climático en Panamá **(214 pages)**.

Ministerio de Comercio e Industrias, (2021). Gaceta oficial digital **(27 pages)**.

Ministerio de Comercio e Industrias de la República de Panamá, (2022). DGNTI-Reglamento técnico. Se aplica El RTCA 75.01.20:19 productos de petróleo. Gasolina superior. Especificaciones **(15 pages)**.

Ministerio de Economía y Finanzas, (2017). La actividad de transporte y su aporte a la plataforma logística de Panamá **(64 pages)**.

Ministerio del Medio Ambiente Chile, (2022). Norma primaria de calidad del aire para monóxido de carbono (CO). Qué es el monóxido de carbono?

Outapa, P.; Thepanondh, S., (2014). Development of air toxic emission factor and inventory of on-road mobile sources. Air Soil Water Res., 7 **(10 pages)**.

Outapa, P.; Thepanondh, S.; Kondo, A.; Pala-En, N., (2018). Development of air pollutant emission factors under real-world truck driving cycle. Int. J. Sustainable Transport., 12(6): 432–440 **(9 pages).**

Parvin, R.; Johora, F.T.; Alim, M.A., (2023). Environmental effect of the Coronavirus-19 determinants and lockdown on carbon

emissions. Global J. Environ. Sci. Manage., 9(1): 87-100 **(14 pages).**

Patiño-Aroca, M.; Parra, A.; Borge, R., (2022). On-road vehicle emission inventory and its spatial and temporal distribution in the city of Guayaquil, Ecuador. Sci. Total Environ., 848 **(11 pages)**.

Peñafiel, M., (2019). Estimación de un inventario de emisiones de fuentes móviles terrestres para la ciudad de Azogues aplicando el Modelo Internacional de Emisiones Vehiculares **(10 pages)**.

Quiñones, Erika, (2023). Nueve años y seguimos creciendo. Metro de Panamá.

Secretaría de Medio Ambiente y Recursos Naturales, (2024). Documentos del inventario nacional de emisiones. inventario nacional de emisiones 2018 Resumen, Sección 8.1: Emisiones de Fuentes Móviles Por Estado.

Shevlyakov, F.; Laptev, A.B.; Latypov, O.R.; Latypova, D.R., (2024). Decarbonizing gas emissions from petrochemical production using microalgae. Global J. Environ. Sci. Manage., 10(2): 733-742 **(10 pages).**

Tran, H.; Nghiem, T.D.; Hoang Vu, K.N.; Quoc Ho, B., (2024). Characteristics and distribution of greenhouse gas emissions from motorcycles in Hanoi, Vietnam. IOP Conference Series: Earth Environ. Sci., 1349(1) **(76 pages)**.

Trang, T.T.; Van, H.H.; Oanh, N.T.K., (2015). Traffic emission inventory for estimation of air quality and climate co-benefits of faster vehicle technology intrusion in Hanoi, Vietnam. Carbon Manage., 6(3–4): 117–128 **(12 pages).**

USEPA, (1992). Procedures for emission inventory preparation procedures for emission inventory preparation Volume IV: Mobile sources. United States Environmental Protection Agency **(240 pages)**.

USEPA, (2022). Managing air quality - Emissions inventories. United States Environmental Protection Agency.

Velasco Soldevila, M., (2014). Análisis de las vías interurbanas de acceso a la Ciudad de Panamá **(105 pages)**.

Viteri, R., Borge, R., Paredes, M., Pérez, M. A., (2023). A high resolution vehicular emissions inventory for Ecuador using the IVE modelling system. Chemosphere, 315 **(9 pages)**.

Zhang, M.; Shi, L.; Ma, X.; Zhao, Y.; Gao, L, (2021). Study on Comprehensive Assessment of Environmental Impact of Air Pollution. Sustainability. 13(2) **(18 pages)**.

Zhao, H.; Mu, L.; Li, Y.; Qiu, J.; Sun, C.; Liu, X., (2021). Unregulated Emissions from Natural Gas Taxi Based on IVE Model. Atmosphere, 12(4) **(9 pages)**.

AUTHOR (S) BIOSKETCHES

Valdés-Montenegro, A., B.Sc., Research Assistant, Air Engineering Studies Research Group, School of Industrial Engineering, Universidad Tecnológica de Panamá.
- Email: *ana.valdes@utp.ac.pa*
- ORCID: 0009-0002-3101-9452
- Web of Science ResearcherID: ND
- Scopus Author ID: ND
- Homepage: https://aires.utp.ac.pa/inicio-ingles/

González-Olivardía, F., Ph.D., Professor, Air Engineering Studies Research Group, CINEMI, Universidad Tecnológica de Panamá.
- Email: *franchesca.gonzalez@utp.ac.pa*
- ORCID: 0000-0002-9356-6016
- Web of Science ResearcherID: MXJ-6283-2025
- Scopus Author ID: 59163679100
- Homepage: https://aires.utp.ac.pa/inicio-ingles/

Pinzón-Acosta, C., Ph.D., Professor, Air Engineering Studies Research Group, School of Mechanical Engineering, Universidad Tecnológica de Panamá.
- Email: *cesar.pinzon1@utp.ac.pa*
- ORCID: 0000-0002-0417-5831
- Web of Science ResearcherID: MBH-7035-2025
- Scopus Author ID: 57190277215
- Homepage: https://aires.utp.ac.pa/inicio-ingles/

HOW TO CITE THIS ARTICLE

Valdés-Montenegro, A.; González-Olivardía, F.G.; Pinzón-Acosta, C., (2025). Passenger car emissions in urban areas based on local vehicle fleet and environmental conditions. Global J. Environ. Sci. Manage., 11(3): 1079-1096.

DOI: 10.22034/gjesm.2025.03.12

URL: https://www.gjesm.net/article_724743.html

Global J. Environ. Sci. Manage. 11(3): 1097-1124, Summer 2025, Serial #43

Global Journal of Environmental Science and Management
(GJESM)

Homepage: https://www.gjesm.net/

Podcasts

CASE STUDY

Infrared precipitation on climate hazards using rainfall dataset over inter-tropical convergence zone

A. Purwandani[1], Supari[2, *], W. Ambarwulan[3], U. Haryoko[4], I.P. Dewi[5], Y. Anantasena[6], Y.S. Djajadihardja[3], H. Sadmono[7], S.I. Sachoemar[8], D. Nugroho[9]

[1] *Research Center for Conservation of Marine and Inland Water Resources, National Research and Innovation Agency, Jl., Cibinong 16911 Jawa Barat, Indonesia*

[2] *Directorate of Climate Change, Agency for Meteorology, Climatology and Geophysics, Jl., Kemayoran, Central Jakarta, Indonesia*

[3] *Research Center for Limnology and Water Resources, National Research and Innovation Agency, Jl. Cibinong 16911 Jawa Barat, Indonesia*

[4] *Directorate of Applied Climate Services, Agency for Meteorology, Climatology and Geophysics, Jl., Kemayoran, Central Jakarta, Indonesia*

[5] *Marine Science Study Program, Faculty of Fisheries and Marine Sciences, Lambung Mangkurat University, Jl., Banjarbaru 70714 South Kalimantan, Indonesia*

[6] *Research Center for Mining Technology, National Research and Innovation Agency, Jl. Setu, Tangerang Selatan 15314 Banten, Indonesia*

[7] *Research Center for Geoinformatics, National Research and Innovation Agency, Jl., Cibinong 16911 Jawa Barat, Indonesia*

[8] *Research Center for Environmental and Clean Technology, National Research and Innovation Agency, Jl., Cibinong 16911 Jawa Barat, Indonesia*

[9] *Directorate of Research Vessel Management, National Research and Innovation Agency, Jl., Jakarta Pusat 10340 Indonesia*

ARTICLE INFO

Article History:
Received 28 February 2025
Revised 02 April 2025
Accepted 04 May 2025

Keywords:
Climate hazards
Precipitation
Annual
Cycle
Equatorial
Monsoonal
Seasonal

ABSTRACT

BACKGROUND AND OBJECTIVES: *Hydrometeorological disaster management and agriculture sectors require accurate spatial and temporal rainfall data. However, in situ rainfall gauges were very limited and distributed unevenly. Satellite-derived rainfall estimates served as a reference and supplement to on-site measurements in Kalimantan Island, Indonesia. The island exhibited intricate climatic phenomena, including the inter-tropical convergence zone. This study aimed to i) validate rainfall data estimates from climate hazards group infrared precipitation with stations, ii) identify movement in Inter-Tropical Convergence Zone variability, and iii) analyze the variability of rainfall in the inter-tropical convergence zone region.

METHODS: The study utilized a blend of descriptive and categorical statistics, relying on the European Centre for Medium-Range Weather Forecasts Reanalysis 5th generation data serving as the basis for identifying the inter-tropical convergence zone, while power spectrum density analysis was applied to analyze rainfall variability. A comparison is made of the standard characteristics of monthly rainfall across different seasonal types, utilizing observed rainfall data alongside climate hazards group infrared precipitation data, differentiated by stations with and without correction.

FINDINGS: The results showed that the best Climate Hazards Group InfraRed Precipitation with Stations performance was found in the southeast of Kalimantan, characterized by flat to undulating areas from the coast to the valley behind the hills, mainly forest and cultivated land cover types, and a high density of rainfall observations. The method of testing station performance for infrared precipitation by the climate hazards group, when comparing point to pixel and the Seasonal Zone region, shows similarities; nonetheless, point to pixel is distinctly the better option. The movement pattern of the intertropical convergence zone influences the accuracy of rainfall estimation using climate hazards group infrared precipitation with stations. The infrared precipitation dataset from the climate hazards group, validated against the shifts of the intertropical convergence zone in Kalimantan. Seasonal zones with equatorial, monsoonal, equatorial-1, equatorial-2, Monsoonal-1, and Monsoonal-2 types generally does not affect the performance differences of the climate hazards group infrared precipitation with stations. The discrepancies between infrared precipitation from climate hazard groups and the rainfall estimates recorded at stations do not exhibit a systematic difference.

CONCLUSION: Climate hazards group infrared precipitation with stations performance was strongly influenced by Inter-Tropical Convergence Zone movements, and the dataset was reliable in estimating rainfall for areas in Kalimantan with a reduced number of observation stations. Local, regional, and global climate variability, driven by land-sea-atmosphere interactions on the Indonesian maritime continent, affects the movement pattern of the inter-tropical convergence zone, causing significant fluctuations in its center and width. the major cycle of corrected and observed climate hazards group infrared precipitation with stations rainfall in the seasonal zone is annual and seasonal, with monsoonal and equatorial rainfall types.

DOI: 10.22034/gjesm.2025.03.13

This is an open access article under the CC BY license (http://creativecommons.org/licenses/by/4.0/).

NUMBER OF REFERENCES
79

NUMBER OF FIGURES
9

NUMBER OF TABLES
2

*Corresponding Author:
Email: *supari@bmkg.go.id*
Phone: +62819 9525 1300
ORCID: 0000-0002-0442-5183

Note: Discussion period for this manuscript open until Sep 1, 2025 on GJESM website at the "Show Article".

INTRODUCTION

Rainfall offers critical information on climate change, water availability, agricultural production, and natural disasters, which is critically required by government decision-makers in water resource management (Awange *et al*., 2019). For areas susceptible to hydrometeorological events such as floods and droughts, trustworthy and multi-temporal rainfall data are vital for formulating flood and drought models that align closely with actual situations (Baethgen and Goddard, 2012). According to (Fowler *et al*., 2021), global warming leads to increased rainfall, excessive atmospheric humidity, and catastrophic droughts. In 1970, rainfall-related disasters (floods, droughts, landslides, and forest fires) killed more than 1 million people (WMO, 2021). As a result, it is crucial to have exact, real-time, and fast rainfall statistics in every region of the world. Currently, rainfall data is collected using conventional ground-based rain gauges, meteorological radar, and satellites (Bai *et al*., 2018). Conventional rainfall measurements have become the primary source of rainfall data in many parts of the world (Katsanos *et al*., 2016). Nonetheless, the current in situ rainfall data collection is insufficient for generating accurate rainfall assessments. This can largely be attributed to poor spatial coverage, a high rate of missing data, and short record spans (Melo *et al*., 2015; Xavier *et al*., 2015). Meanwhile, the availability of high-resolution rainfall grid data is critical for disaster risk management (Shrestha *et al*., 2020). Satellite-based rainfall measurements present an effective approach to obtaining precipitation data in areas where traditional ground measurements are limited or absent (Funk, Verdin, *et al*., 2015). These measurements are favored for their wide coverage, high detail, and convenient accessibility (Tang *et al*., 2015). Rainfall measurement in Kalimantan is difficult due to the large and frequently inaccessible terrain and a lack of ground-based monitoring equipment. In situ measures, such as rain gauges and weather stations, give precise point data but are scarce, particularly in isolated and forested areas (Kidd *et al*., 2017). The climate hazards group infrared precipitation with station (CHIRPS) dataset solves this limitation by providing extensive spatial coverage, bridging key gaps where ground observations are lacking. Rainfall estimation databases based on satellite data cover the complete island, enabling more effective hydrological and climatic assessments (Skofronick-Jackson *et al*., 2017). While in situ measurements may suffer from data reporting delays, particularly at manual stations, CHIRPS rainfall estimate datasets provide near-real-time updates, which are critical for disaster planning. Severe rainfall in Kalimantan can trigger floods and peatland fires, notably during monsoon transitions and the phases of El Niño and La Niña events (Aldrian and Susanto, 2003). Satellite-based rainfall estimates improve in situ measurements in Kalimantan by providing spatial coverage, real-time data, and increased accuracy through calibration. Their integration enables flood forecasting, peatland conservation, and climate research, making them critical to the region's sustainable water resource management. Some worldwide rainfall data, such as CHIRPS (Funk, Peterson, *et al*., 2015), tropical rainfall measuring mission (TRMM) (Huffman *et al*., 2017)), and worldwide global satellite mapping of precipitation (GSMaP) (Kubota *et al*., 2007), are available and can help to address the issue of rainfall data availability. Despite this, international satellite data needs to be confirmed and adjusted due to anomalies. Several validation studies have been carried out in different countries to evaluate the reliability of the CHIRPS dataset. Arregocés *et al*. (2023) evaluated the CHIRPS data set for Colombia's coastal regions and complex topography. Thus, CHIRPS achieves the highest performance when assessed monthly and annually. The same effect was observed in Argentina from 1982 to 2019 (Medina *et al*., 2023). Meanwhile, (Rivera *et al*., 2018; Rivera *et al*., 2019) verified CHIRPS in Argentina and found that it was effective for assessing dry and wet conditions over a month. The analysis reveals that geographic influences, surface conditions, and seasonal changes in rainfall timing play a crucial role in determining the precision of CHIRPS estimates (Hobouchian *et al*., 2017; Rahmawati and Lubczynski, 2017). CHIRPS validation studies have only been conducted in a few places in Indonesia (Liu *et al*., 2020). conducted a comparative investigation of three satellite-based rainfall data sets on Bali Island, including CHIRPS, between 2015 and 2017 in locations with a high density of rain gauge stations. The results reveal that CHIRPS outperforms GSMaP and integrated multi-satellite retrievals for global precipitation measurement (GPM) on a monthly basis. (Wiwoho *et al*., 2021) evaluated three satellite products (CHIRPS,

GPM, and precipitation estimation from remotely sensed information using artificial neural networks for 30 years in the Brantas Watershed on Java Island. The results suggest that all satellite estimates are inadequate. Meanwhile, (Wahyuni *et al*., 2021) confirmed CHIRPS data (corrected and uncorrected) for the Wonorejo Reservoir on Java Island. The adjusted CHIRPS data produced significantly better outcomes than the uncorrected ones. Saragih *et al*. (2022) conducted a validation analysis of CHIRPS data from 2017 to 2019 in North Sumatra Province. Consequently, CHIRPS demonstrates a minimal correlation and a considerable average error in conjunction with observational data. The inter-tropical convergence zone (ITCZ) is a zone of convection and rainfall in the tropics where the northeastern and southeastern trade winds meet, with an average elevation of roughly 10°N over the ocean (Leech *et al*., 2013). The ITCZ plays a vital role in regulating flow and precipitation patterns, the development of tropical cyclones, and maintaining the hydrological cycle in tropical climates (Chan and Evans, 2002). There have been several techniques of identifying ITCZ. The detection of meridional migration patterns of the ITCZ in the western equatorial Pacific has heavily relied on satellite rainfall, sea surface temperature (SST), and surface winds (Chen *et al*., 2008). The ITCZ's diurnal cycle was imaged using infrared satellites that represented cold clouds (Bain *et al*., 2010). Meanwhile, Žagar *et al*. (2011) investigated the variability of ITCZ meridional movement over land and ocean using zonal and meridional wind data from the European Centre for Medium-range Weather Forecasts (ECMWF) Reanalysis (ERA-Interim) at eleven levels below 900 hPa. Meanwhile, Berry and Reeder (2014) created a method for automatically identifying the ITCZ using many layers of low-level wind data from ERA-Interim. This technique demonstrates ITCZ dynamics during El Niño and La Niña episodes in the Pacific Ocean and Indonesian Maritime Continent. Wodzicki and Rapp (2016) employed ERA-Interim, TRMM, and global precipitation climatology project (GPCP) rain rate data to determine the long-term characteristics of an ITCZ migration. During the period of northward ITCZ migration, generally from June to September, a reduction in convective activity leads to drier conditions that further aggravate peatland degradation and elevate the likelihood of wildfires, especially in the context of El Niño phenomena (Field *et al*., 2009). Conversely, enhanced ITCZ activity during southward displacement (December-March) produces intense rainfall that frequently exceeds drainage capacity, resulting in widespread flooding (Ward *et al*., 2016). Monitoring the dynamics of the ITCZ strategically allows for more precise seasonal predictions, crucial for optimizing reservoir operations, water allocation in agriculture, and early warning mechanisms. Based on the criteria outlined above, CHIRPS data validation should be intensified in Indonesia's equatorial tropical maritime country. Although accurate rainfall data is essential for climate change adaptation and disaster management, validation studies of satellite-based rainfall estimates such as CHIRPS in Indonesia are still limited. Despite some evaluations occurring in locations like Bali and Java, there is a critical lack of extensive validation in Kalimantan Island, an important region affected by the ITCZ. Existing studies have highlighted the variability of CHIRPS performance across different geographic regions, but the specific factors affecting its accuracy in the complex topography and climate of Kalimantan have not been adequately addressed. This study's uniqueness stems from its targeted evaluation of CHIRPS performance on Kalimantan Island, where the ITCZ traverses, by integrating local in situ observation data to corroborate rainfall estimates. The objectives of this study are i) validate CHIRPS rainfall estimates using in situ observation data, ii) analyze the variability of ITCZ movement, and iii) investigate rainfall variability in the ITCZ region. Additionally, this study aims to provide dependable rainfall information for Kalimantan, which will aid in improving disaster risk management and empower regional planners to make well-informed decisions. Furthermore, these findings will contribute to a broader understanding of the dynamics of the ITCZ in Indonesia, filling a significant gap in the current literature. In addition, this study helps the Meteorology, Climatology, and Geophysics Agency (BMKG) provide accurate, timely, and accountable climate data for Indonesia. This study has been condacted in Kalimantan Island, Indonesia in 2023-2024.

MATERIALS AND METHODS

Study area desciption

This study was performed on Kalimantan Island,

the third-largest island in the world and the second-largest in Indonesia (Fig. 1). Kalimantan Island is approximately 743,330 square kilometers (km²) and is shared between Indonesia as 73 percent (%), Malaysia (26%), and Brunei Darussalam (1%). Kalimantan Island is located at 4°24' north (N) – 4°10' N and 108°30' east (E) – 119° E. Kalimantan has a tropical climate with relatively stable temperatures throughout the year, ranging between 25 degrees Celsius (°C) and 35°C. The yearly average rainfall in

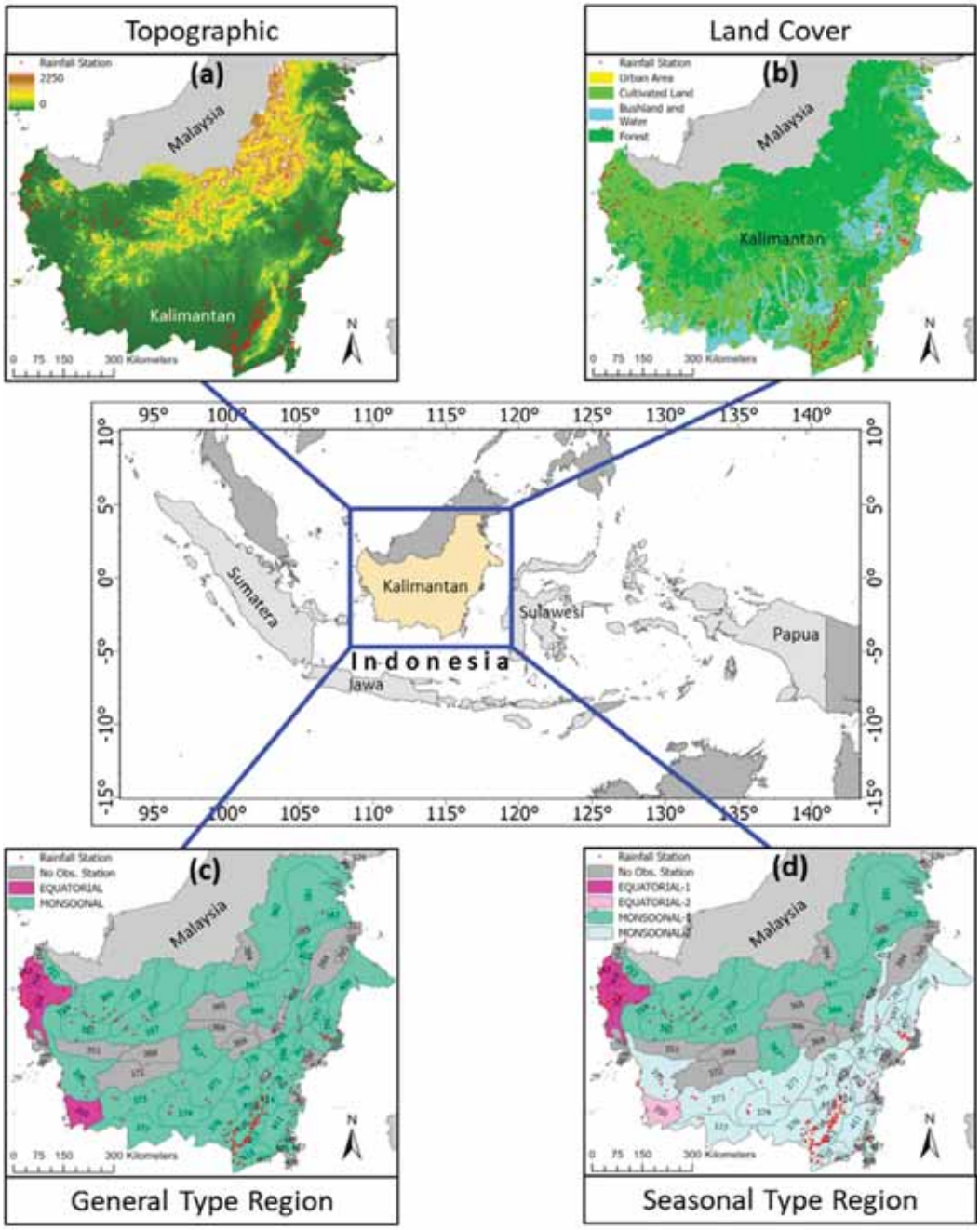

Fig. 1: Geographical location of the study area in Kalimantan Island, Indonesia (Topographic map (a), land cover (b), BMKG's ZOM as general rainfall types (c), and BMKG's ZOM as seasonal types, along with their ZOM area numbers (d). The red dots are BMKG rainfall observation stations)

Kalimantan is 2,992 millimeters (mm). Kalimantan has a very diverse geomorphology. There are several mountains, such as the Meratus, Schwaner, and Muller Mountains, as well as many significant rivers, including the Kapuas, Mahakam, and Barito. Most of Kalimantan features extensive lowlands with diverse attributes. In addition to hosting the planet's most diverse tropical forests, the lowlands encompass millions of hectares of peatland. The distribution of rainfall in Kalimantan is shaped by the island's challenging topography, geographic setting, land cover, and uneven terrain. Fig. 1 depicts the spatial distribution of Indonesia Agency for Meteorology, Climatology, and Geophysics (BMKG) rainfall observation stations overlaid with a topographic elevation profile (Fig. 1a), land cover types (Fig. 1b), seasonal zones (ZOM) (BMKG, 2022) areas classified by General Type (Fig. 1c), and ZOM areas classified by Seasonal Type (Fig. 1d). Meanwhile, ZOMs depicted in gray lack rainfall observation stations.

Rainfall ground-based data

BMKG established rainfall ground-based data (BMKG data), which consists of monthly observations of rainfall station data from 1991 to 2020. Kalimantan Island is home to 210 rain gauge stations, which are unevenly distributed across five provinces. The rain gauge network has a density of one gauge per 3,539.67 km², which is five times lower than the World Meteorological Organization's (WMO) recommendation for flat areas in temperate, Mediterranean, and tropical zones (one measuring instrument per 600 – 900 km²).

CHIRPS satellite-based data

CHIRPS is a satellite rainfall product for various countries that gives gridded daily rainfall estimates with a spatial resolution of 0.05° (degrees) (50° South (S) – 50°N), which is roughly comparable to 5 kilometers (km). It has been available since 1981 (Funk, Verdin, *et al*., 2015; Funk, Peterson, *et al*., 2015). The University of California, Santa Barbara provides free online access to CHIRPS, which delivers rainfall data spanning daily to annual time frames. This study employs the CHIRPS version 2 database in Network Common Data Form (NetCDF) format.

ERA5 reanalysis-based Data

The fifth generation of European Centre for Medium-range Weather Forecasts analysis is the fifth generation of ECMWF' atmospheric reanalysis of global climate, spanning from January 1940 to the present. The Copernicus Climate Change Service (C3S) at ECMWF produces ERA5 (Bell *et al*., 2021). The typical monthly displacement of the ITCZ across the studied area was assessed using convective precipitation data. Fig. 2 depicts the study's four phases. These steps include i) validating CHIRPS with BMKG data, ii) identifying ITCZ movement, and iii) analyzing rainfall variability in the ITCZ region.

CHIRPS performance and validation

The performance of CHIRPS was analyzed utilizing descriptive and categorical statistics (Table 1). Descriptive statistics for analyzing the performance of the monthly and standard monthly rainfall estimation by comparing the accuracy between BMKG data and the closest grid of CHIRPS data, including i) Pearson's correlation coefficient (r), ii) root mean square error (RMSE), iii) mean error (ME), (iv) mean absolute error (MAE), v) nash-sutcliffe efficiency (NSE), and (vi) percent bias (PB). Meanwhile, the categorical statistics used to assess satellite-derived rainfall detection capabilities (Fenta *et al*., 2018) include i) false alarm ratio (FAR), ii) frequency bias (FB), and iii) accuracy (ACR).

Indentification of ITCZ variability

This study employed convective precipitation data produced from monthly mean reanalysis data at the single level ECMWF ERA5 (Hersbach *et al*., 2020) by extending the coverage of the ECMWF ERA-Interim data period from 1979 to 1950 (Bell *et al*., 2021). With the ongoing research into ITCZ identification, rainfall and wind convergence have gained greater relevance. Converging winds concentrate water vapor, resulting in convergent rain clouds and the ITCZ band. Thus, this study applied convective rainfall as a concrete instance of convergent cloud formation to explore the movement, dynamics, and variability of the ITCZ over Kalimantan Island. The average monthly convective precipitation from 1991 to 2020 was evaluated. The ITCZ convergence zone is defined by convective rainfall values of 50 mm or more per month. The midpoint of the meridional contours of convective rainfall at the northern and southern boundaries was determined. These sites were joined in a zonal style to produce a line that represented the

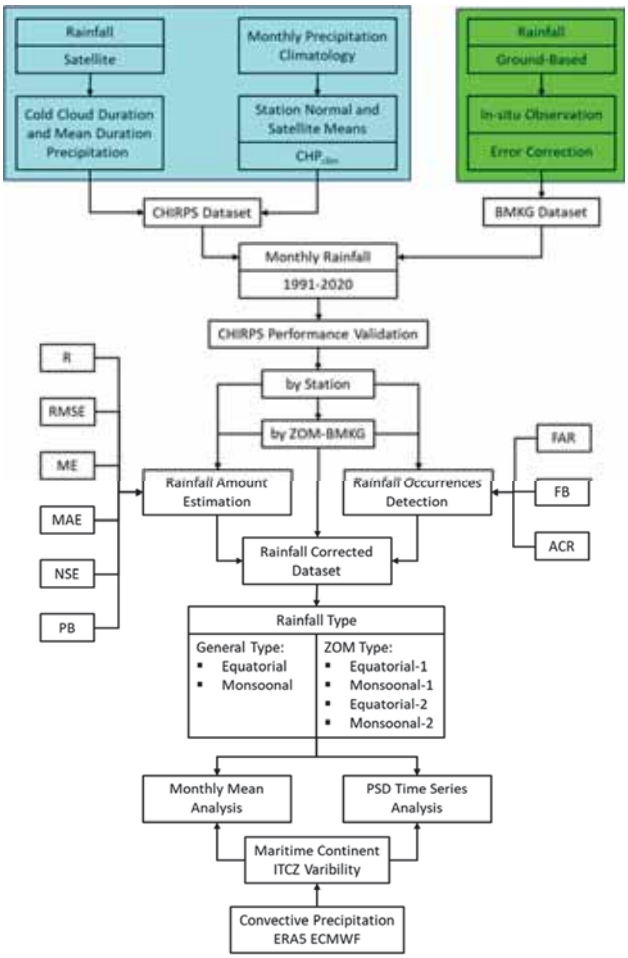

Fig. 2: Research flowchart, green box indicating process data

ITCZ's meridional center.

Investigating rainfall variability in the ITCZ region

The study of rainfall variability in the ITCZ zone of Kalimantan Island was performed by calculating power spectral density (PSD) from monthly rainfall time series data, supplemented by CHIRPS and BMKG information. PSD reveals the key recurring cycles associated with each rainfall category. These major rainfall recurrence cycles are analyzed in relation to Kalimantan Island's ITCZ position. The time series data of monthly rainfall in the diverse rainfall types undergo analysis by Fast Fourier Transform (FFT) utilizing Eq. 10 (Bendat and Piersol, 2010).

$$X(f_k) = h\sum_{t=0}^{N-1} exp\left[-1\frac{2\pi kt}{N}\right] \quad (10)$$

Eq. 11 (Bendat and Piersol, 2010) was used to compute the spectral density energy (Sx) obtained from the FFT analysis of rainfall time series data.

$$S_x = \frac{2h}{N}|X(f_k)|^2 \quad (11)$$

Where, $X(f_k)$ represents monthly rainfall time series data with a one-month interval (h), N is the total quantity of rainfall time series data, f_k is the k-th frequency, and i is an imaginary number. PSD findings for each type of rainfall location were utilized to explain the validation process. This was accomplished by displaying typical monthly rainfall patterns that included observed rainfall, corrected CHIRPS, and uncorrected CHIRPS. Furthermore, the map illustrates variations in rainfall across each ZOM

Table 1: Descriptive and categorical statistics

Statistical	Equation (Eq.)	Eq. No.	Range	Best value	Sources
Descriptive statistics					
r	$\frac{\sum_{i=1}^{n}(P_C-\overline{P_C})(P_o-\overline{P_o})}{\sqrt{\sum_{i=1}^{n}(P_C-\overline{P_C})^2}\sqrt{\sum_{i=1}^{n}(P_o-\overline{P_o})^2}}$	1	− 1 ≤ to ≤ 1	1	Valencia *et al*., 2023
Explanation	The correlation relationship between CHIRPS rainfall estimates and BMKG data				
RMSE	$\sqrt{\frac{1}{n}\sum_{i=1}^{n}(P_C-P_o)^2}$	2	0 ≤ to ≤ ∞	0	Valencia *et al*., 2023
Explanation	The average difference between CHIRPS and BMKG data provides a single number to assess the accuracy of CHIRPS.				
ME	$\frac{1}{n}\sum_{i=1}^{n}(P_C-P_o)$	3	-∞ ≤ to ≤ ∞	0	Medina *et al*. (2023)
Explanation	The average magnitude of error estimates for assessing the precision and fidelity of data-driven.				
MAE	$\frac{1}{n}\sum_{i=1}^{n}(\lvert P_C-P_o\rvert)$	4	0 ≤ to ≤ ∞	0	Arregocés *et al*. (2023)
Explanation	The average absolute magnitude of error estimates.				
NSE	$1-\frac{\sum_{i=1}^{n}(P_C-P_o)^2}{\sum_{i=1}^{n}(P_C-\overline{P_o})^2}$	5	-∞ ≤ to ≤ 1	1	Arregocés *et al*. (2023)
Explanation	The relative magnitude of the variance of residuals compared to the variance of the observed surface values provides valuable insights into the homoscedasticity of the data.				
PB	$\frac{\sum_{i=1}^{n}P_C-P_o}{\sum_{i=1}^{n}P_o}\,100$	6	-∞ ≤ to ≤ ∞	0	Arregocés *et al*. (2023)
Explanation	They consistently differ from actual values, showing whether they overestimate or underestimate.				
P_C = The precipitation estimates from CHIRPS.					
P_o = The observed rain gauge station.					
n = Number of data pairs.					
i = i^{th} data pair.					
Categorical statistic					
FAR	$\frac{B}{A+B}$	7	0 ≤ to ≤ 1	0	Arregocés *et al*. (2023)
Explanation	The fraction of events characterized by rainfall detection from CHIRPS but not captured by BMKG data				
FB	$\frac{A+B}{A+C}$	8	1 ≤ to ≤ ∞	1	Valencia *et al*., 2023
Explanation	Systematizing the frequency of observed rainfall events and CHIRPS estimates facilitates a comprehensive analysis of precipitation patterns over time.				
ACR	$\frac{A+D}{n}$	9	0 ≤ to ≤ 1	1	Medina *et al*. (2023)
Explanation	The accuracy of CHIRPS detection indicates the proportion of CHIRPS rainfall events that were correctly detected.				

A = Rainfall has been detected to occur (number of occurrences).
B = Detected rainfall that did not occur (number of false alarms).
C = Rainfall was detected not to occur but occurred (number of misses).
D = Rainfall was detected not to occur, and it indeed did not occur.

region, highlighting differences between the adjusted CHIRPS data and the actual measurements. This information was critical for assessing the validation performance in each ZOM. The CHIRPS correction was conducted using a simple linear regression equation between observed rainfall (R_{cor}) and CHIRPS rainfall (R_{CHIRPS}), where a and b are linear regression constants, using Eq. 12 (Bendat and Piersol, 2010):

$$R_{cor} = a.R_{CHIRPS} + b \quad (12)$$

RESULTS AND DISCUSSION

Fig. 1 demonstrates that the majority of the BMKG data is dispersed across Kalimantan's southeastern, northwestern, and somewhat northeastern regions. The inconsistent distribution has a notable influence on the average precipitation levels across each ZOM (Figs. 1c and d). More BMKG data results in more accurate average figures that reflect the specific rainfall in each ZOM. Such a level of complexity has repercussions on the reliability of the CHIRPS data performance assessment. In contrast, assessing each BMKG data and matching it with the nearest CHIRPS grid data enhanced analytical accuracy and performance validation compared to the ZOM method. Furthermore, the elevation profile affects

CHIRPS effectiveness (Fig. 1a), as established by numerous researches (Rivera *et al*., 2018; Macharia *et al*., 2020; Dogra *et al*., 2023). The kind of land cover exposure (Fig. 1b) significantly influenced the performance of CHIRPS (Bai *et al.,* 2018; Liu *et al.,* 2019; Nashwan *et al.,* 2019).

CHIRPS performance assessment for estimating rainfall amount

Fig. 3 and 4 show that the performance of CHIRPS appears to be similar for point-to-pixel and ZOM analyses. CHIRPS rainfall performance has the best r values between 0.67 and 0.75. It dominates the southeast region of Kalimantan (Fig. 3a). Areas exhibiting elevated r values correspond to a greater concentration of BMKG rainfall observation stations. The region is located in northwestern Kalimantan, with forest-covered hills in the form of lowlands (Fig. 1a) and is primarily agricultural (Fig. 1b). Meanwhile, Kalimantan's northern region shows the lowest r values, which can be linked to the few rainfall observation sites, inconsistent topography, and a landscape largely dominated by forests. Based on the RMSE value, the southeast has the best CHIRPS estimation performance, with a range of 88.63 – 104.41 mm/month, followed by the eastern region along Kalimantan's east coast (Fig. 3b). The region is characterized by a high density of rainfall stations, located in the low-lying areas near the Mahakam Delta, and is mainly covered with shrubbery and wetland woodlands. Conversely, the northern and northeastern sections of Kalimantan are known to have the highest RMSE values. CHIRPS rainfall performance was evaluated using the best ME values (-14 – 5.67 mm/month) found in central, northwest, northeast, and east Kalimantan (Fig. 3c). The distribution of rainfall observation stations is frequently sparse. Due to geographical and land cover features, it lacks differentiation. Additionally, the optimal MAE values (8.24 – 8.97 mm/month) closely resemble best RMSE values (Fig. 3d). Meanwhile, Kalimantan's southern, northeastern, and northern

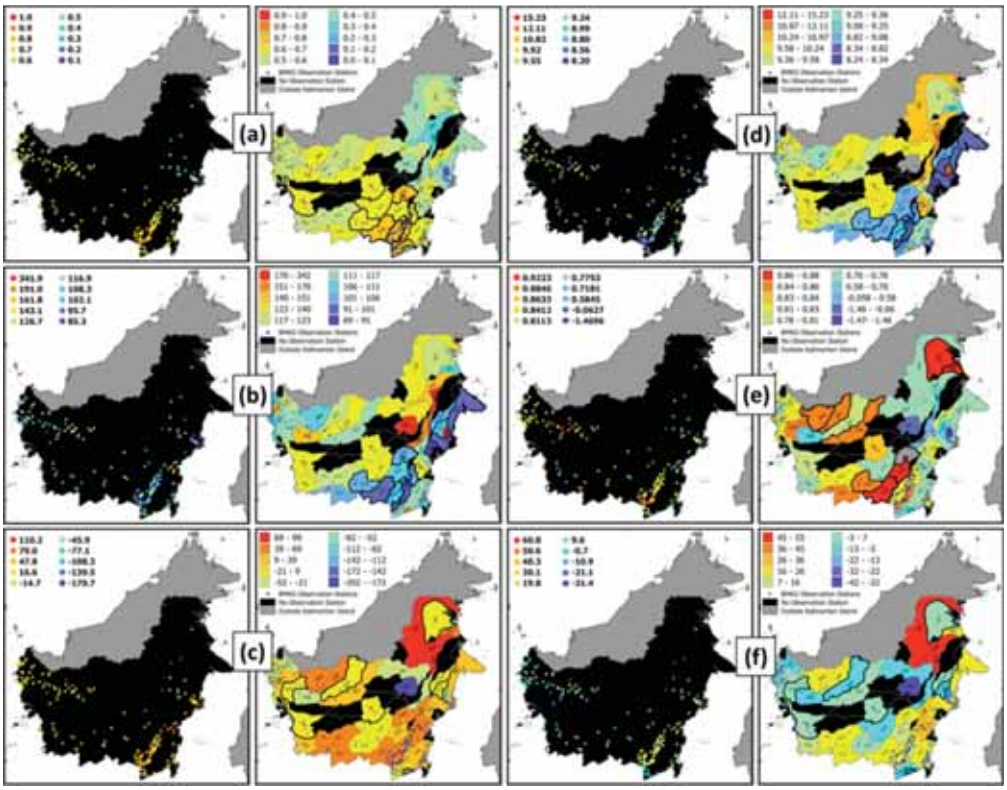

Fig. 3: Map of each BMKG station (dot) and BMKG ZOM (polygon), with descriptive statistics r (a), RMSE (b), ME (c), MAE (d), NSE (e), and PB (f). The thick black line border of ZOM BMKG represents the optimal value of the best percentile class

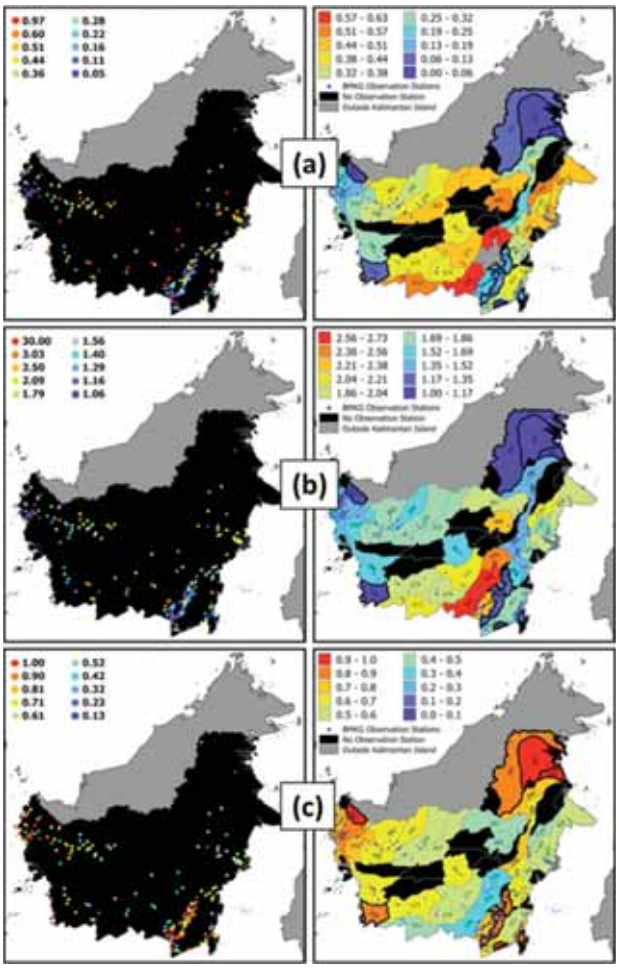

Fig. 4: Map of each station (dot) and BMKG ZOM (polygon), with categorical analyses of FAR (a), FB (b), and ACR (c). The thick black line border of ZOM BMKG represents the optimal value of the best percentile class

regions have the best NSE values (0.85 – 0.88). These regions are typically located close to hills that have a high concentration of BMKG rainfall stations and are predominantly utilized for agriculture. The best PB values (-4.65 – 2.78) fall in the same range as the best ME values. Based on categorical statistics, nine ZOMs performed well in predicting rainfall events: ZOMs 350, 352, 381, 382, 383, 405, 409, 413, and 416, which are distributed throughout Kalimantan's northeast, southeast, southwest, and northwest regions (Fig. 4a, b, and c). The ideal value ranges for FAR, FB, and ACR are 0 – 0.19, 1 – 1.29, and 0.81 – 1.

ITCZ Variability and CHIRPS Performance

BMKG has separated seasonal rainfall prediction areas according to ZOM (BMKG, 2022). This division illustrates that an individual ZOM possesses unique rainfall attributes. Kalimantan was separated into two types of ZOM: General and Seasonal, as indicated in Fig. 1c and d. The general type is separated into ZOM with Equatorial and Seasonal rain characteristics. Furthermore, 93% and 7% of the ZOM in Kalimantan are classed as Monsoonal and Equatorial respectively. BMKG classified seasonal types as Monsoonal-1 and Monsoonal-2 in the north and south, and Equatorial-1 and Equatorial-2 in the northwest and southwest (Fig. 1d). CHIRPS validation outcomes regarding ZOM rainfall, influenced by ITCZ movement, were successfully evaluated through continuous and categorical statistics. The apparent

path of the sun has a substantial effect on ITCZ dynamics. With the equator situated directly in the middle of the island, it significantly impacts the variability of precipitation. As a result, CHIRPS performance was confirmed on a monthly scale and correlated with changes in position movements. Fig. 5 depicts the anticipated usual monthly movement pattern, while Table 2 displays continuous statistics of CHIRPS performance on BMKG. Continuous statistical parameters explain the performance of the ITCZ and movement in Kalimantan. The results of categorical statistics demonstrate that event detection with FAR, FB, and ACR is effective in all areas; thus, the focus of the discussion is exclusively on continuous statistical data.

Fig. 5k-l depicts the meridional travel trajectory of the ITCZ band from north to south and vice versa. In November, it was above Kalimantan Island (around 4°N) and moved further south when the West (rainy) Season began in December (around 1.4°N). The ITCZ was at 2.5°S in January and moved further south in February, near the end of the West Season (around 3.5°S) (Fig. 5a-b), but it remained above Kalimantan Island. After February, the ITCZ drifted north until March, when it entered Transition Season I (about 2.1°S). In April, the ITCZ was around 1.5°S (Fig. 5c-d). When Transition Season I ended in May, the ITCZ band quickly moved away from Kalimantan Island to the north, approximately 10°N (Fig. 5e). During the East (dry) Season in June-August (Fig. 5f-h), the ITCZ

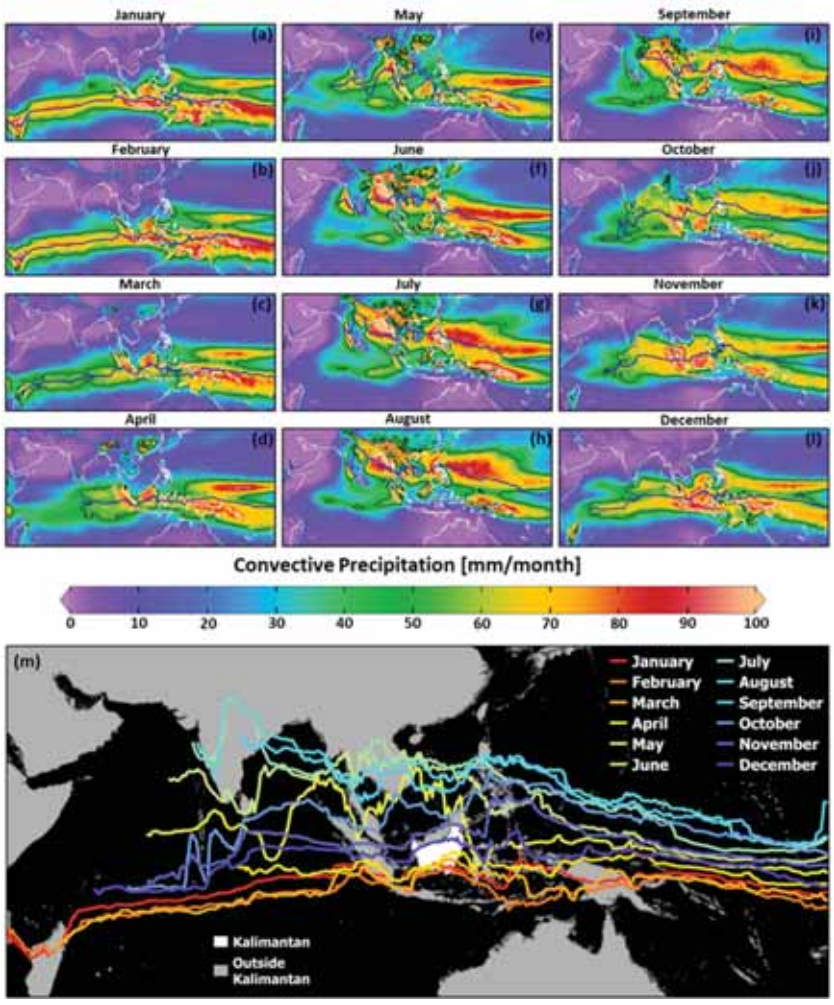

Fig. 5: Monthly mean convective precipitation (1991-2020) from January (a) to December (l), with a convergence boundary of 50 mm/month (black), and the estimated ITCZ position (blue) and monthly variations (m)

Table 2: Statistical indicators for each month were employed to assess the agreement between observations and CHIRPS estimations. Changes in color gradation reflect changes in value

Stat.	Class	Type	Month											
			1	2	3	4	5	6	7	8	9	10	11	12
r	General type	Equatorial	0.60	0.67	0.53	0.31	0.71	0.68	0.87	0.90	0.84	0.64	0.62	0.69
		Monsoonal	0.64	0.59	0.63	0.24	0.75	0.83	0.89	0.97	0.92	0.90	0.71	0.61
	Zom type	Equatorial-1	0.67	0.67	0.58	0.31	0.66	0.67	0.83	0.91	0.82	0.50	0.45	0.72
		Equatorial-2	0.24	0.44	0.24	0.15	0.46	0.64	0.80	0.88	0.77	0.82	0.48	0.36
		Monsoonal-1	0.59	0.63	0.54	0.43	0.63	0.60	0.76	0.90	0.88	0.82	0.52	0.50
		Monsoonal-2	0.64	0.57	0.66	0.22	0.69	0.88	0.92	0.93	0.95	0.93	0.72	0.60
RMSE	General type	Equatorial	76.9	50.8	64.7	62.0	61.9	52.0	49.2	40.8	57.4	70.9	53.1	62.7
		Monsoonal	42.7	43.7	54.0	59.7	69.7	49.2	55.9	67.8	61.7	60.7	43.1	36.2
	Zom type	Equatorial-1	89.1	57.2	58.9	65.5	59.5	58.1	55.4	45.6	59.9	82.4	61.9	69.1
		Equatorial-2	98.7	94.9	97.2	87.9	129.4	86.6	74.4	54.1	82.3	86.4	103.6	211.6
		Monsoonal-1	54.1	67.3	69.4	47.4	57.4	49.6	54.2	56.8	48.3	56.4	48.1	68.9
		Monsoonal-2	51.0	40.6	48.1	59.8	68.4	47.6	57.3	65.5	59.1	47.4	43.1	35.3
ME	General type	Equatorial	21.1	11.9	38.2	28.4	21.8	10.0	-21.2	2.6	-30.6	1.3	-26.3	-1.4
		Monsoonal	-15.9	14.3	29.4	38.2	61.1	37.6	46.7	64.2	55.3	51.4	22.5	12.1
	Zom type	Equatorial-1	49.1	19.2	29.4	24.7	7.8	8.9	-24.1	22.2	-28.4	19.3	-28.5	20.9
		Equatorial-2	1.0	-18.2	38.4	22.0	72.5	46.7	41.8	24.5	35.7	30.6	-7.5	-117.9
		Monsoonal-1	5.7	30.2	33.3	20.5	35.0	15.5	12.9	36.8	5.3	34.1	2.3	36.1
		Monsoonal-2	-31.3	3.7	21.4	33.5	56.1	37.8	48.9	58.4	53.1	36.9	15.7	-4.5
MAE	General type	Equatorial	7.88	6.42	7.25	7.34	7.04	6.58	6.35	5.71	6.83	7.54	6.52	7.42
		Monsoonal	5.92	5.98	6.65	6.91	7.89	6.40	7.01	8.01	7.45	7.29	5.92	5.31
	Zom type	Equatorial-1	8.50	6.43	6.78	7.32	7.05	6.73	6.79	5.99	6.66	8.19	7.07	7.53
		Equatorial-2	9.18	8.61	8.96	8.47	9.95	8.50	7.98	6.57	8.14	8.41	8.36	12.97
		Monsoonal-1	6.91	7.70	7.60	6.19	6.72	6.09	6.41	6.75	6.42	6.67	6.35	7.47
		Monsoonal-2	6.46	5.60	6.19	6.94	7.67	6.34	7.04	7.64	7.33	6.43	5.83	5.40
NSE	General type	Equatorial	0.96	0.97	0.95	0.95	0.93	0.96	0.85	0.98	0.88	0.92	0.98	0.96
		Monsoonal	0.98	0.96	0.97	0.96	0.93	0.96	0.82	0.95	0.87	0.95	0.98	0.98
	Zom type	Equatorial-1	0.96	0.95	0.96	0.95	0.90	0.93	0.84	0.97	0.85	0.91	0.98	0.95
		Equatorial-2	0.88	0.94	0.89	0.90	0.81	0.90	0.54	0.90	0.78	0.85	0.93	0.50
		Monsoonal-1	0.97	0.93	0.97	0.98	0.96	0.97	0.90	0.98	0.95	0.98	0.98	0.95
		Monsoonal-2	0.97	0.95	0.97	0.95	0.93	0.95	0.75	0.95	0.84	0.96	0.98	0.98
B	General type	Equatorial	7.4	6.1	19.0	12.3	9.1	5.1	-11.2	1.6	-14.3	0.4	-7.5	-0.4
		Monsoonal	-5.3	5.8	10.6	15.2	30.7	22.4	36.0	62.6	48.4	27.4	8.2	3.7
	Zom type	Equatorial-1	17.2	10.0	14.8	10.8	3.2	4.5	-12.4	12.8	-12.8	6.3	-8.1	5.9
		Equatorial-2	0.4	-8.4	17.7	9.0	35.2	30.2	34.3	21.2	26.8	12.8	-2.2	-25.9
		Monsoonal-1	1.8	11.3	10.8	6.7	12.8	7.1	6.6	19.3	2.4	11.4	0.7	10.2
		Monsoonal-2	-10.6	1.5	8.0	14.0	31.0	24.5	43.8	73.8	61.3	23.4	6.2	-1.4

band was to the north of Kalimantan, reaching its farthest point in July (Fig. 5g). The ITCZ band shifted southward in August (Fig. 5h). With the onset of Transition Season II in September-October, the ITCZ band progressed further south toward Kalimantan Island (Fig. 5i-j). In November, the ITCZ band was once again visible north of Kalimantan (Fig. 5k).

The correlation between CHIRPS rainfall and BMKG data was strongest between July and September, with r values ranging from 0.76 to 0.97. The highest association occurred in August (Table 2). During these months, the ITCZ was located in the northern hemisphere about 15.5° – 10.3°N (Fig. 5). The ITCZ was not directly above the island of Kalimantan. The closest point was in October (Fig. 5j), whereas the farthest was in July (Fig. 5g). The ITCZ was immediately above Kalimantan Island from October to April (Figs. 5j-l and a-d), with the lowest r value of 0.76. Throughout these months, Kalimantan faces the rainy season, distinguished by significant convective precipitation rates and a reduced width of the ITCZ zone relative to other times of the year. However, when the ITCZ track was not immediately above Kalimantan from May to September (Fig. 5e-i), it had a dry season with generally high r values and a larger ITCZ bandwidth. The ITCZ band failed to develop in many cases during this timeframe due to convective precipitation values being distributed at lower altitudes. On Kalimantan Island, the rainfall estimation error was assessed using the RMSE performance. The minimum and maximum RMSE values were 35.3 mm/month and 211.6 mm/month, respectively (Table 2). In contrast to the r assessment, RMSE failed to provide the best value for any specific month or season. The best RMSE values were often found in the ZOM for Monsoonal-2 and Monsoonal types. The RMSE range estimates for the Monsoonal-2 were 35.3 to 68.4 mm/month. The Monsoonal type produced 36.2 – 69.7 mm/month. However, when considering the Seasonal type, it was discovered that the lowest RMSE values occurred in ZOM with Monsoonal-1 and Monsoonal-2 types, with values of 47.4 – 69.4 mm/month and 35.3 – 68.4 mm/month. In contrast, ZOM with Equatorial-1 and Equatorial-2 kinds varied from 45.6 – 89.1 mm/month and 54.1 – 221.6 mm/month, respectively, and were not preferable to Monsoonal-1 and Monsoonal-2 types. Contrary to the r assessment, RMSE did not achieve the highest value for any designated scenario. However, a more in-depth analysis of the Seasonal type revealed that the Equatorial-1 and Equatorial-2 types demonstrated lower effectiveness. Based on the normal monthly pattern of RMSE, it is attainable to conclude that the types containing the Monsoonal (Monsoonal, Monsoonal-1, and Monsoonal-2) were more closely associated with the ITCZ's normal movement pattern (Fig. 5) than the types containing the Equatorial. The RMSE range for rainfall types containing the Monsoonal type, both General and Seasonal types, was 35.3 – 69.7 mm/month, which was better than the type containing Equatorial, which ranged from 40.8 – 211.6 mm/month (Table 2). When considered from ME, the average difference between CHIRPS rainfall and BMKG measurements proved to be more positive in both the General and Seasonal kinds. The negative ME values were larger, reaching up to -117.9 mm/month, while the positive value was only 72.5 mm/month (Table 2). The optimal value is typically observed from November to February. This indicates a correlation between the ME value and the movement pattern of the ITCZ, although no significant difference was noted. The Monsoonal rainfall type was more closely aligned to the ITCZ's regular monthly migration pattern than the Equatorial type (Fig. 5). Except for December, the Equatorial-2 had the best ME values, which ranged from -31.3 to 72.5 mm/month. When compared to ME, MAE easily exhibits its best value (Table 2). The CHIRPS rainfall estimation error exhibits an average deviation that is nearly zero. From June to August, the average rainfall was approximately 6.80 mm per month. This pattern corresponds to the intra-seasonal cycle rainfall pattern, which is compatible with the General and Seasonal kinds of Equatorial, Equatorial-1, and Equatorial-2. The rainfall pattern in the equatorial region includes two peaks of rain, with a dry interval in between. Conversely, the General and Seasonal classifications of Monsoonal, Monsoonal-1, and Monsoonal-2 display an annual precipitation pattern featuring one peak for rainy and dry periods. From November to February, the best value was around 6.24 mm/month, while the highest value was around 7.00 mm/month from May to August. Similarly to ME, the regular monthly pattern of MAE in the monsoonal ZOM follows the ITCZ movement pattern when compared to the Equatorial ZOM. The MAE range for the Monsoonal type, both General and Seasonal, is higher (5.31 – 8.01 mm/

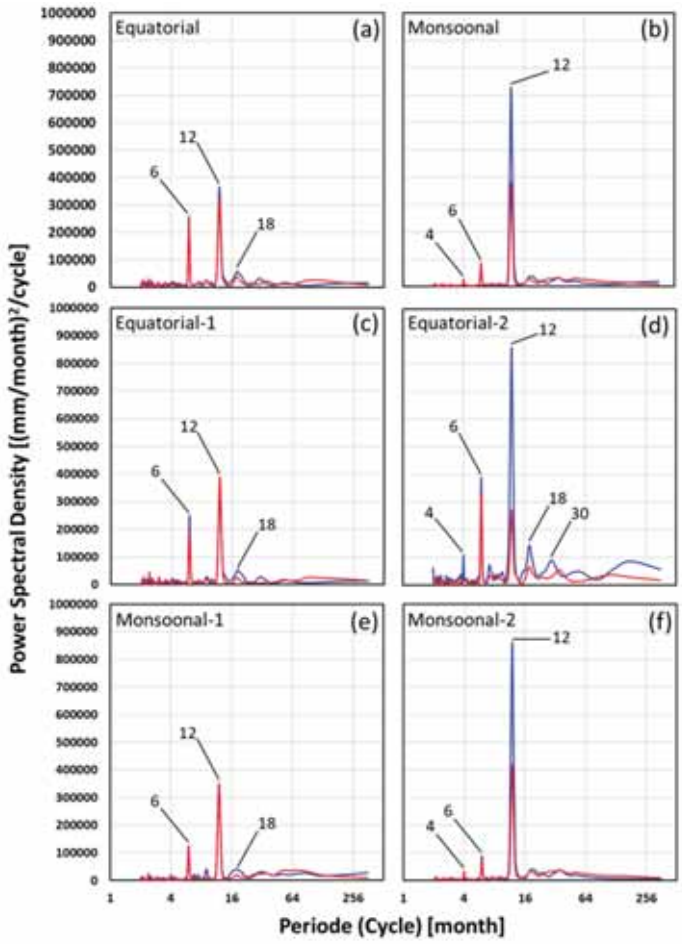

Fig. 6: PSD of General Types, Equatorial (a), Monsoonal (b), and BMKG Seasonal types, Equatorial-1 (c), Equatorial-2 (d), Monsoonal-1 (e) and Monsoonal-2 (f) from BMKG observation data (blue) and corrected CHIRPS (red)

month) than the Equatorial type, which has a range of 5.71 – 12.97 mm/month. Rainfall kinds have a big impact on the NSE value. The Monsoonal type has a greater residual variation of around 0.95 than the Equatorial type, which has a value of approximately 0.90. From November to April, the NSE value was at its strongest, ranging from 0.95 to 0.97. The NSE value was low from May to October, ranging from 0.78 to 0.95. The NSE value was higher in the ZOM with the Monsoon (0.75 – 0.98) than in the Equatorial ZOM (0.50 – 0.98). The study revealed a significant correlation between the patterns of ITCZ movement and the NSE value. Monsoonal-1 performed better than Monsoonal-2, with average scores of 0.97 and 0.95, respectively. These findings suggest that it is essential to take into account the types of rainfall and the movement patterns of the ITCZ when predicting NSE values. Every month in the ZOM, the PB parameter was overstated, with the exception of November and December, when it was underestimated. The highest overestimation occurred between May and September, with values ranging from 15.6% to 31.9%. On the other side, the best overstate value was often seen between October and April, with a range of -1.3% to 11.3%. The Equatorial-2 contributed the most to underestimate, with values as low as -25.9%. The ITCZ movement pattern appeared to be very similar to the PB value. In November and December, the negative PB value fluctuated between -0.5% and 1.3%. This pattern was comparable to the NSE value, which followed the movement pattern of the ITCZ.

CHIRPS performance, rainfall variability, and ITCZ

As per the PSD analysis, the modified CHIRPS and BMKG rainfall observation data show analogous cycles. The variation is in the energy, where greater energy corresponds to a more robust cycle (Fig. 6). The greatest variation in cycles occurred in ZOM with the Equatorial-2 type from BMKG observation, including 4 (intra-seasonal), 6 (seasonal), 12 (annual), 18 (semi-annual), and 30 monthly cycles (interannual), whereas CHIRPS only exhibits three dominating cycles. Meanwhile, other types of rainfall have three cycles. The Equatorial (Fig. 6a), Equatorial-1 (Fig. 6c), and Monsoonal-1 (Fig. 6e) rainfall types were found to follow seasonal, annually, and semi-annual cycles. Meanwhile, the monsoonal (Fig. 6b), equatorial-2 (Fig. 6d), and Monsoonal-2 (Fig. 6f) rainfall types have the shortest intra-seasonal cycle. The ZOM with monsoonal, equatorial-2, and monsoonal-2 categories contained the most energy over the annual cycle. The annual energy cycle was greater in BMKG rainfall compared to the adjusted CHIRPS data. The predominant cycle identified in the ZOM across all rainfall types is categorized into two primary cycles with notably higher energy levels: annual and seasonal. The variability of rainfall and its cycles was investigated by comparing the differences in the two biggest primary cycles of corrected CHIRPS performance for BMKG rainfall related with the ITCZ's southerly shift (Fig. 5).

The energy levels differed between the corrected CHIRPS and BMKG rainfall cycles. The disparity in energy value among various cycles and rainfall categories reflects the strengths and weaknesses inherent in each cycle. The values span from negative to positive infinity, with zero being the ideal number. Except for Equatorial-1, all forms of rainfall exhibit negative energy difference values in both annual and seasonal cycles. A negative finding reveals that the energy derived from the BMKG rainfall cycle was greater than that from CHIRPS, despite the two cycles being identical. The Monsoonal-1, Equatorial, and Equatorial-1 types had the greatest annual cycle energy disparities, with values of -798, -41784, and 48370 millimeters per month squared per cycle (mm/month)^2/cycle). Meanwhile, the best seasonal cycles were the Monsoonal, Monsoonal-1, and Monsoonal-2 rainfall types with values of -864, -5429, and -13045 (mm/month)^2/cycle (Fig. 6). The seasonal cycle has an absolute energy difference of 864 to 59446 (mm/month)^2/cycle, which is more than the annual cycle's range of 798 to 589022 (mm/month)^2/cycle.

In the equatorial type, the monthly rainfall pattern had a minimum average of 171 mm/month and a highest average of 354 mm/month (Fig. 7a). under contrast, under the Monsoonal type, the minimum was 106 mm/month and the highest was 326 mm/month (Fig. 7b). The equatorial type had a lower SD average of rainfall variations (127 mm/month) than the Monsoon type (131 mm/month). In the context of Equatorial rainfall, CHIRPS demonstrated greater accuracy in performance compared to Monsoon rainfall. However, the Monsoon type's normal monthly rainfall pattern appears more closely related to the ITCZ movement pattern than the Equatorial type. In the Equatorial type, there were two rainy seasons, peaking in May and December, and two dry seasons, February and August. Between January and May, both corrected and uncorrected CHIRPS rainfall estimates were overestimated. In contrast, from June to December, both types of estimates showed a slight improvement (Fig. 7a). The Monsoonal type has significantly different average minimum and maximum values than the Equatorial type, with a peak in the rainy season in December and a high in the dry season in August (Fig. 7b). During the period from February to October, CHIRPS rainfall data showed an overestimation, both in its corrected and uncorrected forms. It was discovered that corrected CHIRPS were more accurate in estimating BMKG rainfall amounts than uncorrected CHIRPS (Fig. 7c and d). This was particularly true for the Monsoonal rainfall type (Fig. 7d). The unadjusted CHIRPS data, in contrast, showed commendable performance for the Equatorial type (Fig. 7c). CHIRPS, corrected and uncorrected, fared better for the Equatorial type than the Monsoonal type. In terms of the ITCZ movement pattern (Fig. 5), CHIRPS performance differed depending on whether the Equatorial (Fig. 7c) or Monsoonal type (Fig. 7d) was used. When the ITCZ was not over Kalimantan Island, which was between May and October (Fig. 5e-j), CHIRPS performed better for the Equatorial type. Conversely, for the Monsoonal type, CHIRPS performed more effectively when the ITCZ was located Kalimantan Island from November to April (Fig. 5a-d and k-l). For the Monsoon type, when the ITCZ was not over Kalimantan Island (Fig. 5e-j), CHIRPS performance was either corrected or uncorrected, and the value was overestimated. Meanwhile, for

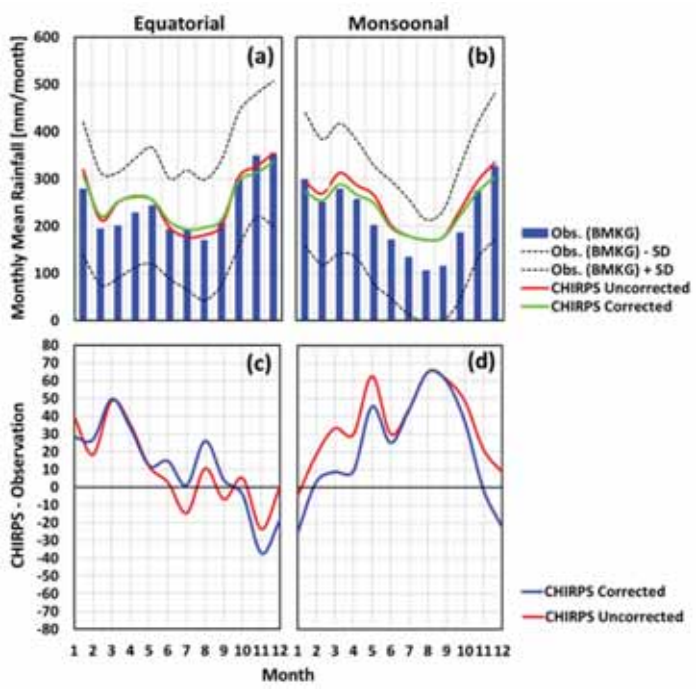

Fig. 7: The normal pattern of corrected (green) and uncorrected (red) CHIRPS and BMKG (bar) monthly rainfall data from 1991 to 2020 for the General Type area, Equatorial (a), and Monsoonal type (b). The dashed line represents the SD of observed rainfall. The difference between corrected CHIRPS rainfall (blue) and uncorrected (red) with observational data for the Equatorial (c) and Monsoonal (d) types

the Equatorial type, when the ITCZ passed over Kalimantan Island from January to April (Fig. 5a-d), CHIRPS rainfall was overestimated. This report shows the minimum and maximum rainfall values for various types of rainfall patterns, including Equatorial-1, Equatorial-2, Monsoonal-1, and Monsoonal-2. The lowest recorded rainfall amounts for these categories were 174, 120, 193, and 84 mm/month. In contrast, the highest rainfall measurements reached 350, 442, 367, and 316 mm/month. The Monsoonal-1, Equatorial-2, Equatorial-1, and Monsoonal-2 types have the highest SD values at 150, 133, 126, and 119 mm/month, respectively (Fig. 8a-d). In equatorial-1 and Equatorial-2, rainfall patterns had two different peaks: rainy and dry seasons. Equatorial-1 (Fig. 8a) experienced its primary rainy season from May and November, whereas Equatorial-2 (Fig. 8b) reached its peak in April and December. The Monsoonal-2 type was more powerful than the Monsoonal-1 type, with the rainy season peaking in December and the dry season in August in both types.

CHIRPS rainfall performed best in Equatorial-1, followed by Monsoonal-1, Monsoonal-2, and Equatorial-2, which had the greatest difference between CHIRPS and BMKG rainfall (Fig. 8e-f). In Equatorial-1, the difference between uncorrected and corrected CHIRPS rainfall was greater, whereas in Equatorial-2, the contrary was accurate. Excluding October, the monthly changes in adjusted CHIRPS rainfall in Equatorial-1 overstated the actual figures. Uncorrected CHIRPS, on the other hand, showed an overestimate from January to May, followed by a range of over- and underestimates. In contrast to Equatorial-1, whether CHIRPS was corrected or not, the Equatorial-2 overstated conditions between March and September. Subsequently, the December underestimation surpasses the peak overestimation recorded until January. Whether CHIRPS was corrected or not, the Monsoonal-1 had an overstated value from January to December, with the exception of November (Fig. 8g). Meanwhile, in the Monsoonal-2 type, corrected and uncorrected CHIRPS were overestimated in all months except December (Fig. 8h), where corrected CHIRPS

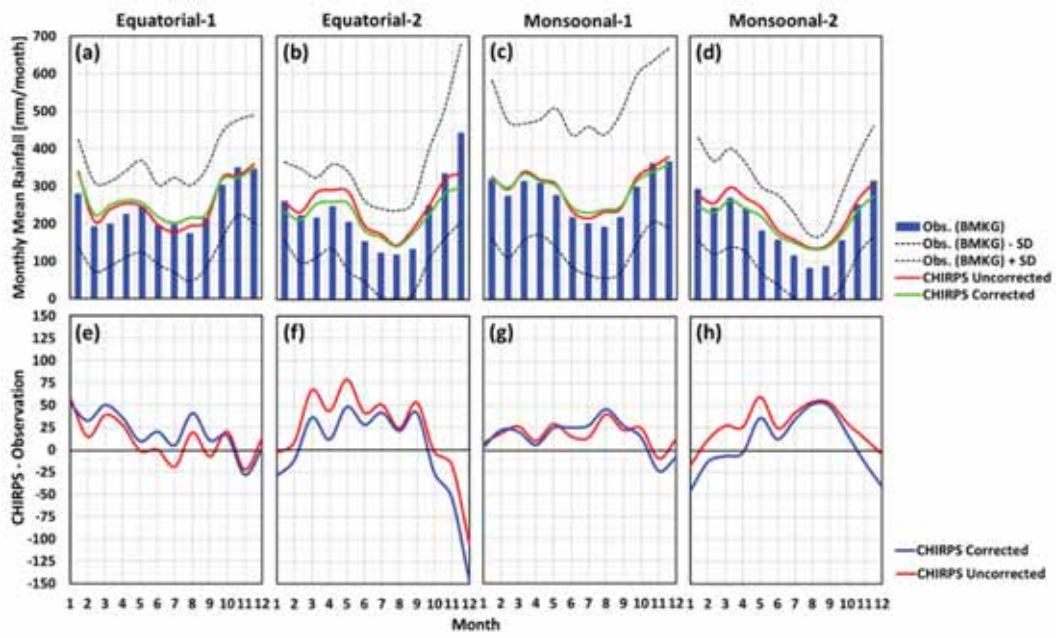

Fig. 8: The normal pattern of corrected (green) and uncorrected (red) CHIRPS and BMKG (bar) monthly rainfall from 1991 to 2020 in the BMKG Seasonal Zone type area, Equatorial-1 (a), Equatorial-2 (b), Monsoonal-1 (c), and Monsoonal-2 (d). The dashed line represents the SD of observed rainfall. The difference between corrected CHIRPS (blue) and uncorrected (red) rainfall using observational data for equal types of areas (e-h)

outperformed uncorrected CHIRPS. The effectiveness of CHIRPS in the Equatorial-1 and Equatorial regions improved when the ITCZ was positioned outside of Kalimantan from May to October, particularly in northern Kalimantan (Fig. 5e-j). Similarly, in the Equatorial-2 type (Fig. 8f), CHIRPS corrected and uncorrected performance improved when the ITCZ was not above the island of Kalimantan. However, CHIRPS' performance on Kalimantan Island was underestimated when compared to BMKG data from January to April. In the Monsoonal-1 rainfall type (Fig. 8g), CHIRPS performance was overestimated every month except in November, when the ITCZ was over Kalimantan Island (Fig. 8k). The Monsoonal-2 type (Fig. 8h) had essentially identical CHIRPS performance to the Monsoonal type (Fig. 7d). An overestimation took place when the ITCZ was not over Kalimantan between May and October (Fig. 5e-j). This category of CHIRPS exhibited its highest performance from November through April (Fig. 5a-d and k-l). The Monsoonal-2 type performed better than the Monsoonal type (Fig. 7d). This evaluation explores the distinctions between the corrected CHIRPS data and the BMKG records. The study found that CHIRPS overestimates rainfall between 0 and 36 mm/month while underestimating it between -36 and 0 mm/month. This study aims to investigate the spatial changes in CHIRPS performance under standard monthly conditions. In January (Fig. 9a), CHIRPS rainfall was overestimated northwest of Kalimantan but underestimated southeast of Kalimantan. In January, the ITCZ was located in the south (2.6°S), above Kalimantan Island. In February (Fig. 9b), An increase in the overestimated ZOM of more than 36 mm/month has been identified in the northern part of Kalimantan (ZOM 352, 356, and 387) as well as in the southeast of Kalimantan (ZOM 410, 411, 413, 414, 416, 396, and 393). The ITCZ shifted slightly south (3.2°S) across Kalimantan Island. In March (Fig. 9c), the elevated values in the southeast and north persisted in their expansion towards the southeast and from the southwest to the south. The ITCZ shifted northward to 1.7°S.

During April, the ZOM value gradually decreased in Kalimantan's northern region. In April, the ITCZ migrated further north around the middle of Kalimantan Island, precisely to 0.7°S. In May, the ITCZ moved further north, although there were no areas

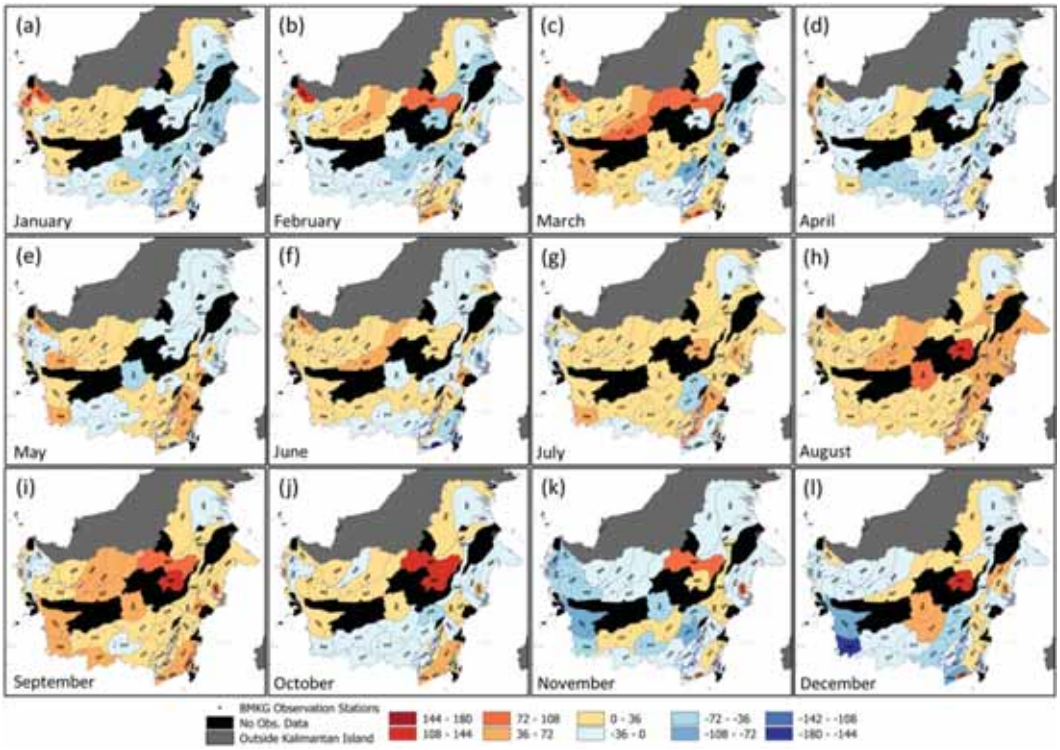

Fig. 9: The CHIRPS performance map was shown as the difference between the corrected monthly CHIRPS rainfall and observations (BMKG) from January (a) to December (l)

with concentrated rainfall contours more than 50 mm/month (Fig. 5e). Rainfall projections in various regions of Kalimantan experienced minor adjustments in June. In the northwest, ZOM 359, 361, and 364 had exaggerated readings. The same shift occurred in the northeast (ZOMs 387, 388, 397, and 383). In the northwest and southeast regions, the values that were previously underestimated and overestimated have been switched. The ITCZ has shifted further north than the previous month, from 9.7°N to 13.8°N. As July began, the ITCZ was the furthest north from Kalimantan Island, at 14.6°N. Except for some ZOMs in the southeast (ZOMs 353 and 361) and the southeast (ZOMs 370, 375, 410, 411, 405, and 409), the majority of Kalimantan's ZOMs now overestimate CHIRPS rainfall performance. During August, the ITCZ migrated southward to 12.8°N. Most ZOMs in Kalimantan overestimated CHIRPS rainfall. In September, ZOM increased, with CHIRPS performance underestimated, notably at southeast ZOMs (ZOMs 352, 361, and 364). In September, the ITCZ (10.9°N) shifted further south and remained below Kalimantan Island. In October, the ITCZ migrated further south, to 6.5°N. The ZOMs in the southeast were being considerably underestimated. Meanwhile, in the northwest, CHIRPS rainfall performance was improving. In November, with the ITCZ moving closer to the island of Kalimantan at roughly 3.5°N, it was revealed that the effectiveness of CHIRPS was underestimated. The only ZOMs with inflated values in the center of Kalimantan are 371, 373, 387, 388, 396, 398, 391, 402, 405, and 411. In December, the ITCZ shifted south to 1.4° N. CHIRPS performance improved when ZOMs overestimated values. An evaluation was conducted utilizing the ZOM grouping that exhibited optimal performance in CHIRPS rainfall ranging from -36 and 36 mm/month. It was discovered that the most accurate month for calculating CHIRPS rainfall in Kalimantan was October – December, with 38 ZOMs. However, there were 37 ZOMs from April to June, 35 ZOMs from July to September, and 30 ZOMs between January and March. The ZOM analysis with

rainfall types was between -36 and 36 mm/month for 12 months, revealing that the General type identified the Equatorial type at 6.25% and the Monsoonal type at 93.75%. Equatorial-1 accounted for 6.25% of the total 16 ZOMs, followed by monsoonal-1 at 56.25% and Monsoonal-2 at 37.5%. The best ZOM was between -36 and 36 mm/month for nine months with the General type, 15% Equatorial, and 85% monsoonal. Meanwhile, the ZOM types were Equatorial-1 (10%), Equatorial-2 (5%), Monsoonal-1 (15%), and monsoonal-2 (70%) of the 20 total ZOMs. Furthermore, the best ZOM ranged between -36 and 36 mm/month for six months, with the General Monsoonal type accounting for 100%. The distribution of ZOM types included Monsoonal-1 at 28.57% and Monsoonal-2 at 71.43% of the total 7 ZOMs. Rainfall estimation using CHIRPS was evaluated on Borneo Island, which traverses the ITCZ, has complex topography, and insufficient rainfall stations. The examination of CHIRPS rainfall performance demonstrates that the point-to-pixel observation method is preferable to the ZOM area. Compared to the ZOM method, the point-to-pixel technique provides a more accurate estimation of CHIRPS rainfall because it is dedicated to a single point, making its precision value easily identifiable. Meanwhile, in the ZOM approach, the rainfall value used is the area average between the observed rainfall and CHIRPS, resulting in bias from the averaging. Previous researchers have used a point-to-pixel technique (Mianabadi, 2023; Helmi and Abdelhamed, 2023). The CHIRPS dataset is utilized because it has been shown to be effective in estimating rainfall for a variety of meteorological occurrences at both high and low latitudes, including tropical regions crossed by the ITCZ (Mianabadi, 2023; Zhang *et al*., 2023; Bhattacharyya *et al*., 2022). Similarly, monthly timeframes have been adopted since CHIRPS operates best on a monthly scale and corresponds with the ITCZ cycle (Hisam *et al*., 2023; Valencia *et al*., 2023). BMKG developed a regional approach, ZOM, for Indonesia based on the stages of the K-Means (Ng, 2012) or Ward-SC (Batagelj, 1988) clustering methods, namely data standardization to equalize data variation, Principal Component Analysis (PCA) to generate the greatest diversity of principal components, and PCA clustering (BMKG, 2022). As a result, each ZOM exhibits identical rainfall characteristics. Furthermore, the ZOMs are generated by incorporating rainfall observation data alongside the dataset utilized in the current study, which is the CHIRPS rainfall dataset. Rainfall forecast utilizing regional areas can also be based on agroclimatic zones (Dayal *et al*., 2023), watershed zones (Chatterjee *et al*., 2023), agroecological zones (Macharia *et al*., 2020), and administrative areas (Nawaz *et al*., 2021). When employing a regional technique, the average rainfall data collected from multiple observation sites can result in misleading findings. Meanwhile, utilizing ZOM for seasonal forecasting and managing multi-source rainfall data for operational purposes is significantly more flexible and easier to implement than depending on point station measurements (BMKG, 2022). Based on the optimal percentile value of the best continuous statistical value, NSE, RMSE, and ME were used to assess the performance of the best CHIRPS rains at ZOM in Kalimantan. Previous studies have primarily concentrated on the strong correlation between CHIRPS rainfall and recorded observations (Rivera *et al*., 2018; Babaousmail *et al*., 2019; Aksu and Akgül, 2020). *NSE*'s weakness is its susceptibility to severe maximum and minimum values, such as in El Niño years with drought and La Niña with extreme rainfall in Kalimantan (Neelin *et al*., 1998; Wallace *et al*., 1998), or during natural disasters, MJO phases (Zhang, 2005) and tropical storms (Azgha and Mukminan, 2019). The majority of continuous and categorical statistical parameters exhibited optimal values predominantly at rainfall stations characterized by high density, forest cover, fertile soil, and flat to gently rolling terrain. These findings are consistent with prior research; satellite-based rainfall works well at low elevations and in agricultural areas (Macharia *et al*., 2020; Shrestha *et al*., 2017; Toté *et al*., 2015). ZOMs 413 and 416 had the best CHIRPS rainfall performance based on parameters such as optimum r, RMSE, MAE, FAR, FB, and ACR values (Figs. 3, and 4). They are located in the lowlands to the northwest of the hills, where green land is covered by farmed land. The region experiences a significant amount of rainfall measurements, which contributes to the superior performance of the ZOM's CHIRPS, as the methodology for creating the CHIRPS dataset incorporates the Climate Hazards Center's Precipitation Climatology (CHPclim) variable in its computations (Funk, Verdin, *et al*., 2015). The more rainfall monitoring stations, the higher the CHPclim

value. The ZOM region behind the hills improves CHIRPS performance because of high rainfall caused by the creation of orographic rain clouds during the Southern Hemisphere's rainy season. The accuracy of the CHPclim value improves with a greater number of rainfall observation stations. The more exact the value of CHPclim, the better the accuracy of CHIRPS rainfall. The ZOM is located behind the hill, and the precipitation that happens is caused by orographic rain clouds. The detection of cold clouds by satellite infrared sensors will improve in precision. As a result, the formation of orographic clouds behind the hills with a time lag prior to the occurrence of rain will improve the accuracy of CHIRPS rainfall estimates. Furthermore, the occurrence of orographic rain during the rainy season enhances the accuracy of CHIRPS estimates. This location is primarily surrounded by cultivated land and woodlands, which naturally fertilizes the area and increases the amount of cultivated land over time. CHIRPS (Medina *et al*., 2023; Cavalcante *et al*., 2020) generally validates the high rainfall phase. Previous research (Mu *et al*., 2021) focused on observation density and green vegetation landscapes, and (de Andrade *et al*., 2022) found that CHIRPS operates well in such environments. The strong relationship between CHIRPS data and field rainfall observations highlights its effectiveness. Parameter r has the highest value between July and September (Table 2); the middle band of the ITCZ is not exactly above Kalimantan, but rather the furthest away (Fig. 5). The existence of the ITCZ band is strongly linked to increased rainfall due to ERA5 convective precipitation. When there isn't much rain, CHIRPS does its best. CHIRPS operates most effectively in the absence of the ITCZ, typically during the dry season, as this leads to more straightforward atmospheric conditions and consistent infrared signals. The dataset's design favors regions like Southeast Kalimantan, where land cover and topography mitigate these seasonal biases. Prior studies have identified comparable trends during drought periods in northern Nigeria and mainland China (Usman *et al*., 2018; Zhong *et al*., 2019). Similarly, (Fenta *et al*., 2018) found that CHIRPS performs better in the secondary rainy season (March – May) than in the primary wet season (June – September). The rainfall in Kalimantan during this period is under 25 mm per month. Consequently, the Monsoonal-2 category in South Kalimantan exhibits the highest performance according to CHIRPS. Overall, the Monsoonal type surpasses the Equatorial type in effectiveness. The finest Seasonal type is Monsoonal-2, followed by Monsoonal-1, Equatorial-2, and Equatorial-1. Meanwhile, prior studies in Venezuela, which is near the equator, revealed that the best r occurred during the rainy season from April to September (Paredes Trejo *et al*., 2016). Similarly, in Pakistan's temperate regions, optimal rainfall occurs during the monsoon season, which spans from July to September and October to November (Nawaz *et al.,* 2021). Meanwhile, Kalimantan Island is situated near the intersection of the Hadley and Walker circulations on the Indonesian Maritime Continent (Schwendike *et al*., 2014). CHIRPS performance based on the RMSE value associated with ITCZ did not reveal meaningful results. In contrast to the Equatorial type, the Monsoonal type achieved the most favorable RMSE value. These findings are consistent with those reported by (Gao *et al*., 2018): the RMSE is low. The best ME for all types of rainfall showed CHIRPS performance between November and February (Table 2). In these months, the ITCZ is right above Kalimantan (Fig. 5k-b). The most significant rainfall was recorded in Kalimantan during November, whereas the peak rainfall was observed on the the island of Java from December to February. Saeidizand *et al*. (2018) investigated the performance of CHIRPS in Iran and discovered that it works effectively in places dominated by convective rain. The highest ME values are observed in the Monsoonal, Monsoonal-1, and Monsoonal-2 rainfall types, which adhere to an annual cycle. In contrast, the best values for the Equatorial, Equatorial-1, and Equatorial-2 rainfall types occur after the intra-seasonal cycle (Table 2). These two cycles are indirectly related to the ITCZ movement pattern (Fig. 5k-b). Unlike ME, the best MAE values occur during the intra-seasonal cycle for the Equatorial, Equatorial-1, and Equatorial-2 types, at the height of lowest rainfall (Fig. 5b and h). Meanwhile, during the period from November to February, Monsoonal-1 and Monsoonal-2 exhibit the highest values, coinciding with the peak heavy rainfall season (Fig. 5k-b). According to (López-Bermeo *et al*., 2022), the accuracy of CHIRPS in northern Colombia is determined by the geographical characteristics and climatic circumstances of the region where rainfall occurs. Similarly to MAE, the best NSE values occur from November to April, when they are over

Kalimantan (Fig. 5k-d). The best NSE occurs in rainfall types comprising the Monsoonal type, with the Monsoonal-1 type outperforming the Monsoonal-2 type (Table 2). In all months apart from November and December, PB values tend to be overestimated. The ITCZ movement pattern influences PB, with the highest value occurring when the ITCZ is directly above Kalimantan, specifically between November and April. The Equatorial rainfall type has a higher PB value than the Monsoonal type, similar to the MAE. Equatorial types often provide lower estimates, whereas Monsoonal types frequently give higher estimates. The PB underestimation value is less than the overestimation. CHIRPS validation parameters r, ME, MAE, NSE, and PB all have a link with the ITCZ movement pattern, with the exception of RMSE, which is unknown. Rainfall including Monsoonal types (Monsoonal, Monsoonal-1, and Monsoonal-2) is better to rainfall having Equatorial types (Equatorial-1, and Equatorial-2) and is well detected by r, RMSE, ME, and NSE, although MAE identifies both. Concurrently, PB illustrates that the Equatorial model is superior to the Monsoon mode. These six validation metrics can be linked to different patterns of ITCZ movement. It has also been explained that CHIRPS performs well when rainfall is influenced by ITCZ activity and rainfall convective systems in Venezuela (Paredes Trejo *et al*., 2016); similarly, Bai *et al*. (2018) stated that there are changes in CHIRPS performance patterns as the rainy season moves across the Chinese plains. Monsoonal, Equatorial-2, and Monsoonal-2 rainfall types showed intra-seasonal, seasonal, and annual cycles in CHIRPS or BMKG data (Fig. 6). Interannual cycles were found in Equatorial-2 as well. Meanwhile, the Equatorial, Equatorial-1, and Monsoonal-1 types only showed seasonal, annual, and semi-annual cycles. The energy magnitude of the cycles in the Equatorial, Equatorial-1, and Monsoonal-1 types is essentially same. In contrast, the annual cycle of the Monsoonal, Equatorial-2, and Monsoonal-2 categories indicate that the BMKG rainfall, which replenishes energy, is considerably greater than that of CHIRPS. Consequently, CHIRPS rainfall can identify the intricate patterns of rainfall variability throughout the annual cycle in the Monsoonal, Equatorial-2, and Monsoonal-2 categories, especially when contrasted with other rainfall types in Kalimantan. Jonah *et al*. (2021) discovered a bimodal rainfall pattern (Monsoonal type) in the annual cycle while conducting study in Rwanda using CHIRPS data. In March–May, it was discovered that it included a unimodal scheme (equatorial type). Equatorial rainfall is more compatible with CHIRPS compared to Monsoonal rainfall, whether corrected or uncorrected (Fig. 7). Meanwhile, the Monsoonal type can determine its link to the ITCZ movement pattern. In the Equatorial type, the best CHIRPS performance occurs when the ITCZ is not over Kalimantan, whereas in the Monsoonal type, the ITCZ rises above Kalimantan. The Equatorial-1 type has the best CHIRPS performance, followed by Monsoonal-1, Monsoonal-2, and Equatorial-2 (Fig. 8). Corrected CHIRPS rainfall is typically overestimated in the Equatorial-1, Monsoonal-1, and Monsoonal-2. Conversely, the Equatorial-2 type may be either overvalued or undervalued. Types Equatorial-1 and Equatorial-2 have strong CHIRPS performance when the ITCZ is not over Kalimantan, but Monsoonal-1 and Monsoonal-2 occur when the ITCZ is above Kalimantan. Prior studies have demonstrated that CHIRPS effectively captures rainfall characteristics across seasonal to inter-annual cycles within the monsoon regime in lowland areas (Rivera *et al*., 2018). The normal pattern of differences in CHIRPS rainfall corrected by BMKG was closely related to the ITCZ movement pattern (Fig. 9). This is seen in the variation in rainfall patterns between Equatorial and Monsoonal types, as well as between Equatorial-1 and 2 and Monsoonal-1 and 2. From July to September, nearly all ZOMs were overestimated. In October, the majority of the ZOM in the southeast of Kalimantan began to be underestimated, followed by September in the northwest. In December and January, the opposite situation occurred, initially overestimated in the northwest of Kalimantan and progressively spreading to the center of Kalimantan by March. The ideal circumstances for corrected CHIRPS performance in estimating BMKG rainfall occurred in April. Following that, until June, further overestimation was observed in Kalimantan's northwestern and southeastern ZOMs. The variations in over- and underestimating ZOM in Kalimantan are clearly associated with the movement pattern of the ITCZ. The ITCZ's movement has a significant impact on regional variations in CHIRPS performance across Kalimantan, with various accuracy patterns forming in different zones. In southern Kalimantan, the ITCZ

leads to substantial monsoon rains from December to March, but CHIRPS tends to overestimate coastal rainfall because of persistent warm cloud cover, while it underestimates precipitation in highland areas due to unresolved orographic influences. The mountainous geography of Central Kalimantan exacerbates underestimation (-20-30%), while CHIRPS struggles with localized convection. Northern locations have superior dry-season accuracy, but humid circumstances cause numerous false alarms when the ITCZ is distant. Distinct problems arise in the eastern coastal plains, where mangrove forests disrupt evapotranspiration signals, causing inflated estimates. Transitional zones in southeast Kalimantan (ZOM 413 and 416) have the strongest CHIRPS performance due to flatter terrain and denser gauge networks, which efficiently correct satellite biases. These regional differences highlight how microclimates influenced by the ITCZ interact with local terrain and land use, leading to inconsistent error patterns in rainfall estimates. The study's findings highlight the necessity of precise rainfall monitoring in enabling effective disaster risk management and planning in places impacted by complex climatic patterns such as the ITCZ. The findings of this study can be used to a variety of fields, including flood disasters (Puno *et al.,* 2021) and sustainable water management (Teweldebrihan and Dinka, 2024). Accurate rainfall data is critical for successful water and agricultural management, which improves food self-sufficiency and contributes to global food security (AlBtoosh *et al.*, 2024; Girsang *et al.,* 2025).

CONCLUSION

This study aims to validate CHIRPS over Kalimantan Island, which passes through the ITCZ. The study involved monthly validation conducted over a thirty-year timeframe, specifically from 1991 to 2020. A thorough analysis was carried out to evaluate the performance of CHIRPS and its interaction with ITCZ. According to the results, the optimal performance of the Climate Hazards Group InfraRed Precipitation with Stations was observed in the southeast of Kalimantan, an area characterized by its flat to undulating landscape stretching from the coast to the valleys behind the hills, mainly covered by forests and cultivated fields, and marked by a high frequency of rainfall data. Regionally, monsoon intensification and land-sea contrasts exacerbate rainfall variability, especially in southern areas where CHIRPS struggles with extreme events. Changes in local terrain and land cover contribute to further inaccuracies, as mountains experience a reduction in orographic rainfall and deforested regions generate misleading signals. These interactions clarify that CHIRPS is most effective during transitional seasons (March-May) and faces challenges in peak ITCZ months, highlighting the need for scale-aware adjustments to enhanceaccuracy for hydrometeorological applications. The ITCZ's seasonal migration affects Kalimantan's rainfall patterns, which shift from heavy monsoon rains (December-March) south of the equator to drier conditions (June-September) as it advances north. This variation leads to separate wet and dry seasons, greatly affecting water supply and influencing reservoir management, agricultural practices, and the risks associated with floods and droughts. During the ITCZ's overhead transit, southern regions see heavy rainfall, necessitating flood preparation, but its northward retreat makes northern areas more vulnerable to water scarcity. Understanding these ITCZ-driven trends improves seasonal water distribution, irrigation planning, and hydropower generation in Kalimantan's various climate zones. The seasonal shift of the ITCZ impacts climate variability by affecting local precipitation patterns (monsoons), regional weather systems (wind patterns), and global circulation (interaction with ENSO/IOD). Understanding these multi-scale interactions helps weather predictions by (1) anticipating seasonal rainfall variations for agriculture, (2) fine-tuning regional flood/drought forecasts, and (3) improving global climate models by better representing ITCZ dynamics. The fundamental cycle of modified and observed CHIRPS rainfall in ZOM is characterized by annual and seasonal patterns, including monsoonal and equatorial types of precipitation. The best CHIRPS performance, as measured by the difference in rainfall between adjusted CHIRPS and observations, occurred from March to May. The optimal CHIRPS performance was observed during the transitional months of March to May, where adjusted estimates aligned closely with actual observations, attributed to lower convective complexity and consistent rainfall patterns. Corrected CHIRPS is far more reliable for quantitative applications in Kalimantan. The adjustment process

mitigates infrared-based biases but cannot fully resolve challenges in extreme rainfall or complex terrain or climate phenomena. Identified biases may include infrared cold-cloud bias, land cover effects, severe convective rainfall, topographical factors, and seasonal bias trends. The CHIRPS performance testing approach from point to pixel and using the ZOM region is similar, although point to pixel is definitely preferable. CHIRPS in Kalimantan can be used to estimate rainfall in areas with a few monitoring stations. These findings are significant for operational rainfall monitoring and hydrometeorological disaster early warning systems in Kalimantan. The variable effectiveness of CHIRPS by season and location highlights the importance of calibration based on ZOM features, particularly in locations with complex topography and heterogeneous land cover. CHIRPS can accurately estimate rainfall in data-scarce areas by merging satellite infrared data with available ground stations, even when station networks are restricted. The system seamlessly integrates satellite observations with current station data, employing statistical correlations to remove biases—suggesting that strategically positioned gauges can significantly enhance accuracy over vast regions. CHIRPS excels in flat, low-elevation areas with uniform land cover, making it especially useful for drought monitoring and seasonal forecasting in remote tropical locations. While it may underestimate extreme rainfall in complex terrain, its freely available near-real-time data makes it a viable option for water resource management in underserved areas where traditional monitoring is difficult.

AUTHOR CONTRIBUTIONS

A. Purwandani contributed to the conceptualization, research design, data acquisition, analysis, interpretation, and manuscript drafting. W. Ambarwulan supervised the study, assisted in conceptualization and study design, and participated in data analysis, interpretation, and manuscript preparation. U. Haryoko provided supervision, supported data acquisition, and contributed to data analysis, interpretation, and statistical evaluation. S. Supari served as the corresponding author, supplied data, conducted analysis and interpretation, and assisted in drafting the manuscript. I. P. Dewi provided administrative, and technical support. Y. Anantasena revised the critically important intellectual content of the manuscript. Y.S. Djajadihardja reviewed, and revised the critically important intellectual content of the manuscript. H. Sadmono provided administrative, and visual design support. S.I. Sachoemar provided administrative support. D. Nugroho provided technical, and visual design support.

ACKNOWLEDGEMENT

The authors express their gratitude to the Meteorology, Climatology, and Geophysical Agency of Indonesia (BMKG) for providing the data for this study, as well as the National Research and Innovation Agency of Indonesia (BRIN) for their assistance. Authors also thank the reviewers for their contributions to the manuscript's quality.

CONFLICT OF INTEREST

The authors declare that there are no conflicts of interest regarding the publication of this manuscript. In addition, the ethical issues, including plagiarism, informed consent, misconduct, data fabrication and/or falsification, double publication and/or submission, and redundancy, were observed by the authors.

OPEN ACCESS

©2025 The author(s). This article is licensed under a Creative Commons Attribution 4.0 International License, which permits use, sharing, adaptation, distribution and reproduction in any medium or format, as long as you give appropriate credit to the original author(s) and the source, provide a link to the Creative Commons license, and indicate if changes were made. The images or other third-party material in this article are included in the article's Creative Commons license, unless indicated otherwise in a credit line to the material. If material is not included in the article's Creative Commons license and your intended use is not permitted by statutory regulation or exceeds the permitted use, you will need to obtain permission directly from the copyright holder. To view a copy of this license, visit: http://creativecommons.org/licenses/by/4.0/

PUBLISHER'S NOTE

GJESM Publisher remains neutral with regard to jurisdictional claims with regard to published maps and institutional affiliations.

Positive AI Statement

During the preparation of this work the author(s) have used Artificial Intelligence (AI) [NAME TOOL / SERVICE] in order to [REASON]. After using this tool/service, the authors reviewed and edited the content as needed and take full responsibility for the content of the publication.

(Furthermore, the GPTZero detector will evaluate the manuscript utilizing Generative AI, ensuring a high detection rate. If the manuscript relies heavily on Generative AI and AI-assisted technologies, it will be archived without further options for appeal).

Negative AI Statement

The author(s) declare that no AI tools or services were not used or not highly applied during the preparation of this work.

ABBREVIATIONS

%	Percent
°	Degrees
°C	Degrees Celsius
A	Rainfall has been detected to occur (number of occurrences)
ACR	Accuracy
B	Detected rainfall that did not occur (number of false alarms)
BMKG	Indonesia agency for meteorology, climatology, and geophysics
C	Rainfall was detected not to occur but occurred (number of misses)
CHIRPS	Climate hazards group infrared precipitation with station
CHPclim	Climate Hazards Center's Precipitation Climatology
CS3	Copernicus climate change service
D	Rainfall was detected not to occur, and it indeed did not occur
E	East
ECMWF	European centre for medium-range weather forecasts
Eq.	Equation
ERA5	the fifth generation of *ECMWF* reanalysis
ERA-Interim	*ECMWF* reanalysis
FAR	False alarm ratio
FB	Frequency bias
FFT	Fast fourier transform
GPCP	Global precipitation climatology project
GPM	Global precipitation measurement
GSMaP	Global satellite mapping of precipitation
h	Interval
i	i^{th} data pair
IMERG	Integrated multi-satellite retrievals for *GPM*
ITCZ	Inter-tropical convergence zone
km	Kilometers
km^2	Square kilometers
MAE	Mean absolute error
ME	Mean error
mm	Millimeters
mm/ month²/ cycle	Millimeters per square month per cycle
N	North
n	Number of data pairs
NetCDF	Network common data form
NSE	Nash-sutcliffe efficiency
Obs./ha	Observation per hectare
PB	Percent bias
P_c	Precipitation estimates from *CHIRPS*
P_o	Observed rain gauge station
PSD	Power spectral density
r	Pearson's correlation coefficient
R_{CHIRPS}	*CHIRPS* rainfall
R_{cor}	Observed rainfall
RMSE	Root mean square error
S	South
SD	Standard deviation
S_x	Spectral density energy
TRMM	Tropical rainfall measuring mission
$X(f_k)$	Monthly rainfall time series data with a one-month interval
ZOM	Seasonal zones

REFERENCES

Aksu, H.; Akgül, M.A., (2020). Performance evaluation of CHIRPS satellite precipitation estimates over Turkey. Theor. Appl. Climatol. , 142: 71–84 **(14 Pages)**.

AlBtoosh, J.; Abu-Awwad, A.; Obeidat, N., (2024). A statistical approach to the water scarcity implications on food security. Global J. Environ. Sci. Manage., 10(SI): 201-218 **(18 Pages)**.

Aldrian, E.; Susanto, R.D., (2003). Identification of three dominant rainfall regions within Indonesia and their relationship to sea surface temperature. Int. J. Climatol., 23(12): 1435-1452 **(17 Pages)**.

Arregocés, H.A.; Rojano, R.; Pérez, J., (2023). Validation of the CHIRPS dataset in a coastal region with extensive plains and complex topography. Case Stud. Chem. Environ. Eng., 8: 100452.

Awange, J.L.; Hu, K.X.; Khaki, M., (2019). The newly merged satellite remotely sensed, gauge and reanalysis-based multi-source weighted-ensemble precipitation: evaluation over Australia and Africa (1981–2016). Sci. Total Environ., 670: 448–465 **(18 Pages)**.

Azgha, R.; Mukminan, M., (2019). Analysis of the influence of tropical cyclones on rainfall in Indonesia. IOP Conference Series: Earth Environ. Sci, 271: 012035.

Babaousmail, H.; Hou, R.; Ayugi, B.; Gnitou, G.T., (2019). Evaluation of satellite-based precipitation estimates over Algeria during 1998–2016. J. Atmos. Sol. Terr. Phys., 195: 105139.

Baethgen, W.E.; Goddard, L., (2012). Latin American perspectives on adaptation of agricultural systems to climate variability and change. In Handbook of Climate Change and Agroecosystems. Imperial College Press, 2: 57–72 **(16 Pages)**.

Bai, L.; Shi, C.; Li, L.; Yang, Y.; Wu, J., (2018). Accuracy of CHIRPS satellite-rainfall products over mainland China. Remote Sens., 10(3).

Bain, C.L.; Magnusdottir, G.; Smyth, P.; Stern, H., (2010). Diurnal cycle of the intertropical convergence zone in the east Pacific J. Geophys. Res.: Atmos., 115(23).

Batagelj, V., (1988). Generalized Ward and related clustering problems. In Classification and Related Methods of Data Analysis, Ed. H.H. Bock, Amsterdam: North-Holland, 67-74 **(8 Pages)**.

Bell, B.; Hersbach, H.; Simmons, A.; Berrisford, P.; Dahlgren, P.; Horányi, A.; Muñoz-Sabater, J.; Nicolas, J.; Radu, R.; Schepers, D.; Soci, C.; Villaume, S.; Bidlot, J.R.; Haimberger, L.; Woollen, J.; Buontempo, C.; Thépaut, J.N., (2021). The ERA5 global reanalysis: preliminary extension to 1950. Q. J. R. Meteorolog. Soc., 147(741): 4186–4227 **(42 Pages)**.

Bendat, J.S.; Piersol, A.G., (2010). Data analysis. In Random Data: Analysis and Measurement Procedures: Fourth Edition. Wiley Blackwell. 359–416 **(58 Pages)**.

Berry, G.; Reeder, M.J., (2014). Objective identification of the intertropical convergence zone: climatology and trends from the ERA-Interim. J. Clim., 27(5): 1894–1909 **(16 Pages)**.

Bhattacharyya, S.; Sreekesh, S.; King, A., (2022). Characteristics of extreme rainfall in different gridded datasets over India during 1983–2015. Atmos. Res., 267:105930.

BMKG, (2022). Pemutahiran Zona Musim Indonesia Periode 1991-2020.

Cavalcante, R.B.L.; Ferreira, D.B.da S.; Pontes, P.R.M.; Tedeschi, R.G.; da Costa, C.P.W.; de Souza, E.B., (2020). Evaluation of extreme rainfall indices from CHIRPS precipitation estimates over the Brazilian Amazonia. Atmos. Res., 238: 104879.

Chan, S.C.; Evans, J.L., (2002). Comparison of the structure of the ITCZ in the West Pacific during the Boreal Summers of 1989-93 using AMIP simulations and ECMWF reanalysis. J. Clim., 15(24): 3549–3568 **(20 Pages)**.

Chatterjee, D.; Singh, D.; Singh, P.K.; Fohrer, N.; Singh, B.B., (2023). Performance evaluation of different gridded precipitation and CMIP6 model products with gauge observations for assessing rainfall variability under the historical and future climate change scenario over a semi-arid catchment, India. Phys. Chem. Earth., 131: 103433.

Chen, B.; Lin, X.; Bacmeister, J.T., (2008). Frequency distribution of daily ITCZ patterns over the western-central Pacific. J. Clim., 21(17): 4207–4222 **(16 Pages)**.

Dayal, D.; Pandey, A.; Gupta, P.K.; Himanshu, S.K., (2023). Multi-criteria evaluation of satellite-based precipitation estimates over agro-climatic zones of India. Atmos. Res., 292: 106879.

de Andrade, J.M.; Ribeiro N.A.; Bezerra, U.A.; Moraes, A.C.C.; Montenegro, S.M.G.L., (2022). A comprehensive assessment of precipitation products: Temporal and spatial analyses over terrestrial biomes in Northeastern Brazil. Remote Sens. Appl.: Soc. Environ., 28: 100842.

Dogra, A.; Thakur, J.; Tandon, A., (2023). Do satellite-based products suffice for rainfall observations over data-sparse complex terrains? Evidence from the North-Western Himalayas. Remote Sens. Environ., 299: 113855.

Fenta, A.A.; Yasuda, H.; Shimizu, K.; Ibaraki, Y.; Haregeweyn, N.; Kawai, T.; Belay, A.S.; Sultan, D.; Ebabu, K., (2018). Evaluation of satellite rainfall estimates over the Lake Tana basin at the source region of the Blue Nile River. Atmos. Res., 212; 43–53 **(11 Pages)**.

Field, R.D.; van der Werf, G.R.; Shen, S.S.P., (2009). Human amplification of drought-induced biomass burning in Indonesia since 1960. Nat. Geosci., 2: 185–188 **(4 Pages)**.

Fowler, H.J.; Lenderink, G.; Prein, A.F.; Westra, S.; Allan, R.P.; Ban, N.; Barbero, R.; Berg, P.; Blenkinsop, S.; Do, H.X.; Guerreiro, S.; Haeter, J.O.; Kendon, E.J.; Lewis, E.; Schaer, C.; Sharma, A.; Villarini, G.; Wasko, C.; Zhang, X.,

(2021). Anthropogenic intensification of short-duration rainfall extremes. Nat. Rev. Earth Environ., 2: 107–122 **(16 Pages)**.

Funk, C.; Peterson, P.; Landsfeld, M.; Pedreros, D.; Verdin, J.; Shukla, S.; Husak, G.; Rowland, J.; Harrison, L.; Hoell, A.; Michaelsen, J., (2015). The climate hazards infrared precipitation with stations - A new environmental record for monitoring extremes. Sci. Data, 2: 150066.

Funk, C.; Verdin, A.; Michaelsen, J.; Peterson, P.; Pedreros, D.; Husak, G., (2015). A global satellite-assisted precipitation climatology. Earth Syst. Sci. Data Discuss., 7: 275–287 **(13 Pages)**.

Gao, F.: Zhang, Y.; Chen, Q.; Wang, P.; Yang, H.; Yao, Y.; Cai, W., (2018). Comparison of two long-term and high-resolution satellite precipitation datasets in Xinjiang, China. Atmos. Res., 212: 150–157 **(8 pages)**.

Girsang, S.S.B.; Banurea, D.M.; Lestari P.; Nambela, J.B.; Verawaty, I.; Barus, J.; Jonharnas; Girsang, M.A.; Purba, T., (2025). Dynamics prediction of land use changes using cellular automata and artificial neural network modeling. Global J. Environ. Sci. Manage., 11(2): 427-442 **(16 Pages)**.

Helmi, A.M.; Abdelhamed, M.S., (2023). Evaluation of CMORPH, PERSIANN-CDR, CHIRPS V2.0, TMPA 3B42 V7, and GPM IMERG V6 satellite precipitation datasets in Arabian arid regions. Water (Switzerland), 15(1).

Hersbach, H.; Bell, B.; Berrisford, P.; Hirahara, S.; Horányi, A.; Muñoz-Sabater, J.; Nicolas, J.; Peubey, C.; Radu, R.; Schepers, D.; Simmons, A.; Soci, C.; Abdalla, S.; Abellan, X.; Balsamo, G.; Bechtold, P.; Biavati, G.; Bidlot, J.; Bonavita, M.; Thépaut, J.N., (2020). The ERA5 global reanalysis. Q. J. R. Meteorolog. Soc., 146(730): 1999–2049 **(51 Pages)**.

Hisam, E.; Mehr, A.; Alganci, U.; Seker, Z.D., (2023). Comprehensive evaluation of satellite-based and reanalysis precipitation products over the Mediterranean region in Turkey. Adv. Space Res, 71(7): 3005–3021 **(17 Pages)**.

Hobouchian, M.P.; Salio, P.; Skabar, G.Y.; Vila, D.; Garreaud, R., (2017). Assessment of satellite precipitation estimates over the slopes of the subtropical Andes. Atmos. Res., 190: 43–54 **(Pages)**.

Huffman, G.J.; Bolvin, D.T.; Nelkin, E.J., (2017). Integrated multi-satellite retrievals for GPM (IMERG) technical documentation.

Jonah, K.; Wen, W.; Shahid, S.; Ali, M.A.; Bilal, M.; Habtemicheal, B.A.; Iyakaremye, V.; Qiu, Z.; Almazroui, M.; Wang, Y.; Joseph, S.N.; Tiwari, P., (2021). Spatiotemporal variability of rainfall trends and influencing factors in Rwanda. J. Atmos. Sol. Terr. Phys., 219: 105631.

Katsanos, D.; Retalis, A.; Tymvios, F.; Michaelides, S., (2016). Analysis of precipitation extremes based on satellite (CHIRPS) and in situ dataset over Cyprus. Nat. Hazard., 83: 53–63 **(11 Pages)**.

Kidd, C.; Becker, A.; Huffman, G.J.; Muller, C.L.; Joe, P.; Jackson, G.S.; Kirschbaum, D.B, (2017). So, How Much of the Earth's Surface Is Covered by Rain Gauges? Bull. Am. Meteorol. Soc., 98(1): 69-78 **(9 Pages)**.

Kubota, T.; Shige, S.; Hashizume, H.; Aonashi, K.; Takahashi, N.; Seto, S.; Hirose, M.; Takayabu, Y.N.; Ushio, T.; Nakagawa, K.; Iwanami, K.; Kachi, M.; Okamoto, K., (2007). Global precipitation map using satellite-borne microwave radiometers by the GSMaP project: production and validation. IEEE Trans. Geosci. Remote Sens., 45(7): 2259–2275 **(17 Pages)**.

Leech, P. J.; Lynch-Stieglitz, J.; Zhang, R., (2013). Western Pacific thermocline structure and the Pacific marine intertropical convergence zone during the Last Glacial Maximum. Earth Planet. Sci. Lett., 363: 133–143 **(11 Pages)**.

Liu, C.Y.; Aryastana, P.; Liu, G.R.; Huang, W.R., (2020). Assessment of satellite precipitation product estimates over Bali Island. Atmos. Res., 244: 105032.

Liu, J.; Shangguan, D.; Liu, S.; Ding, Y.; Wang, S.; Wang, X., (2019). Evaluation and comparison of CHIRPS and MSWEP daily-precipitation products in the Qinghai-Tibet Plateau during the period of 1981–2015. Atmos. Res., 230: 104634.

López-Bermeo, C.; Montoya, R.D.; Caro-Lopera, F.J.; Díaz-García, J.A., (2022). Validation of the accuracy of the CHIRPS precipitation dataset at representing climate variability in a tropical mountainous region of South America. Phys. Chem. Earth., 127: 103184.

Macharia, J.M.; Ngetich, F.K.; Shisanya, C.A., (2020). Comparison of satellite remote sensing derived precipitation estimates and observed data in Kenya. Agric. For. Meteorol., 284: 107875.

Medina, F.D.; Zossi, B.S.; Bossolasco, A.; Elias, A.G., (2023). Performance of CHIRPS dataset for monthly and annual rainfall-indices in Northern Argentina. Atmos. Res., 283: 106545.

Melo, D.de C.D.; Xavier, A.C.; Bianchi, T.; Oliveira, P.T.S.; Scanlon, B.R.; Lucas, M.C.; Wendland, E., (2015). Performance evaluation of rainfall estimates by TRMM multi-satellite precipitation analysis 3B42V6 and V7 over Brazil. J. Geophys. Res., 120(18): 9426–9436 **(11 Pages)**.

Mianabadi, A., (2023). Evaluation of long-term satellite-based precipitation products for developing intensity-frequency (IF) curves of daily precipitation. Atmos. Res., 286: 106667.

Mu, Y.; Biggs, T.; Shen, S.S.P., (2021). Satellite-based precipitation estimates using a dense rain gauge network over the Southwestern Brazilian Amazon: Implication for identifying trends in dry season rainfall. Atmos. Res., 261: 105741.

Nashwan, M.S.; Shahid, S.; Wang, X., (2019). Assessment of satellite-based precipitation measurement products over

the hot desert climate of Egypt. Remote Sens., 11(5): 555.
Nawaz, M.; Iqbal, M. F.; Mahmood, I., (2021). Validation of CHIRPS satellite-based precipitation dataset over Pakistan. Atmos. Res., 248: 105289.
Neelin, J.D.; Battisti, D.S.; Hirst, A.C.; Jin, F.F.; Wakata, Y.; Yamagata, T.; Zebiak, S. E. (1998). ENSO theory. J. Geophys. Res.: Oceans, 103(C7): 14261–14290 **(30 Pages)**.
Ng, A.Y., (2012). Clustering with the k-means algorithm. Machine Learning, 1-2.
Paredes Trejo, F.J.; Barbosa, H.A.; Peñaloza-Murillo, M.A., Alejandra Moreno, M.; Farías, A., (2016). Intercomparison of improved satellite rainfall estimation with CHIRPS gridded product and rain gauge data over Venezuela. Atmosfera. 29(4): 323–342 **(20 Pages)**.
Puno, G.R.; Puno, R.C.; Maghuyop, I.V., (2021). Two-dimensional flood model for risk exposure analysis of land use/land cover in a watershed. Global J. Environ. Sci. Manage., 7(2): 225-238 **(14 Pages)**.
Rahmawati, N.; Lubczynski, M.W., (2017). Validation of satellite daily rainfall estimates in complex terrain of Bali Island, Indonesia. Theor. Appl. Climatol., 134(1–2): 513–532 **(20 Pages)**.
Rivera, J.A.; Hinrichs, S.; Marianetti, G., (2019). Using CHIRPS dataset to assess wet and dry conditions along the semiarid Central-Western Argentina. Adv. Meteorol., 2019(1): 8413964.
Rivera, J.A.; Marianetti, G.; Hinrichs, S., (2018). Validation of CHIRPS precipitation dataset along the Central Andes of Argentina. Atmos. Res., 213: 437–449 **(13 Pages)**.
Saeidizand, R.; Sabetghadam, S.; Tarnavsky, E.; Pierleoni, A., (2018). Evaluation of CHIRPS rainfall estimates over Iran. Q. J. R. Meteorolog. Soc., 144: 282–291 **(10 Pages)**.
Saragih, N.F.; Sitepu, S.; Simanungkalit, G.T.; Sinambela, M.; Rajagukguk, E.; Larosa, F.G.; Jaya, I.K., (2022). Validation of CHIRPS estimation rainfall data using numerical accuracy test with precitipation observation data. IOP Conference Series: Earth Environ. Sci, 1083: 012095.
Schwendike, J.; Govekar, P.; Reeder, M.J.; Wardle, R.; Berry, G.J.; Jakob, C., (2014). Local partitioning of the overturning circulation in the tropics and the connection to the Hadley and Walker circulations. J. Geophys. Res., 119(3): 1322–1339 **(18 Pages)**.
Shrestha, A.; Rahaman, M.M.; Kalra, A.; Thakur, B.; Lamb, K.W.; Maheshwari, P., (2020). Regional climatological drought: An assessment using high-resolution data. Hydrology, 7(2): 33.
Shrestha, N.K.; Qamer, F.M.; Pedreros, D.; Murthy, M.S.R.; Wahid, S.M.; Shrestha, M., (2017). Evaluating the accuracy of Climate Hazard Group (CHG) satellite rainfall estimates for precipitation based drought monitoring in Koshi basin, Nepal. J. Hydrol.: Reg. Stud., 13: 138–151 **(14 Pages)**.
Skofronick-Jackson, G.; Kirschbaum, D.; Petersen, W., Huffman, G.;Kidd, K.; Stocker, E.; Kakar, R., (2018). The Global Precipitation Measurement (GPM) mission's scientific achievements and societal contributions: reviewing four years of advanced rain and snow observations. Q. J. R. Meteorol. Soc., 144(51): 27-48 **(21 Pages)**.
Tang, L.; Tian, Y.; Yan, F.; Habib, E., (2015). An improved procedure for the validation of satellite-based precipitation estimates. Atmos. Res., 163: 61–73 **(13 Pages)**.
Teweldebrihan, M.D.; Dinka, M.O., (2024). The impact of climate change on the development of water resources. Global J. Environ. Sci. Manage., 10(3): 1359-1370 **(12 Pages)**.
Toté, C.; Patricio, D.; Boogaard, H.: van der Wijngaart, R.; Tarnavsky, E.; Funk, C., (2015). Evaluation of satellite rainfall estimates for drought and flood monitoring in Mozambique. Remote Sens., 7(2): 1758–1776 **(19 Pages)**.
Usman, M.; Nichol, J.E.; Ibrahim, A.T.; Buba, L.F., (2018). A spatio-temporal analysis of trends in rainfall from long term satellite rainfall products in the Sudano Sahelian zone of Nigeria. Agric. For. Meteorol., 260–261: 273–286 **(14 Pages)**.
Valencia, S.; Marín, D.E.; Gómez, D.; Hoyos, N.; Salazar, J.F.; Villegas, J.C., (2023). Spatio-temporal assessment of Gridded precipitation products across topographic and climatic gradients in Colombia. Atmos. Res., 285: 106643.
Wahyuni, S.; Sisinggih, D.; Dewi, I.A.G., (2021). Validation of climate hazard group infrared precipitation with station (CHIRPS) data in Wonorejo reservoir, Indonesia. IOP Conference Series: Earth Environ. Sci., 930(1): 012042.
Wallace, J.M.; Rasmusson, E.M.; Mitchell, T.P.; Kousky, V.E.; Sarachik, E.S.; Von Storch, H., (1998). On the structure and evolution of ENSO-related climate variability in the tropical Pacific: lessons from TOGA. J. Geophys. Res.: Oceans, 103(C7): 14241–14259 **(19 Pages)**.
Ward, P.J.; Kummu, M.; Lall, U., (2016). Flood frequencies and durations and their response to El Niño Southern Oscillation: Global analysis. J. Hydrol., 539: 358–378 (Pages).
Wiwoho, B.S.; Astuti, I.S.; Alfarizi, I.A.G.; Sucahyo, H.R., (2021). Validation of three daily satellite rainfall products in a humid tropic watershed, brantas, indonesia: Implications to land characteristics and hydrological modelling. Hydrology, 8(4): 154.
WMO, (2021). WMO Atlas of Mortality and Economic Losses from Weather, Climate and Water Extremes (1970-2019).
Wodzicki, K.R.; Rapp, A.D., (2016). Long-term characterization of the Pacific ITCZ using TRMM, GPCP, and ERA-Interim. J. Geophys. Res., 121(7): 3153–3170 **(18 Pages)**.
Xavier, P.K.; Petch, J.C.; Klingaman, N.P.; Woolnough, S.J.;

Jiang, X.; Waliser, D.E.; Caian, M.; Cole, J.; Hagos, S.M.; Hannay, C.; Kim, D.; Miyakawa, T.; Pritchard, M.S.; Roehrig, R.; Shindo, E.; Vitart, F.; Wang, H., (2015). Vertical structure and physical processes of the Madden-Julian oscillation: Biases and uncertainties at short range. J. Geophys. Res., 120(10): 4749–4763 **(15 Pages)**.

Žagar, N.; Skok, G.; Tribbia, J., (2011). Climatology of the ITCZ derived from ERA Interim reanalyses. J. Geophys. Res. D: Atmos., 116(D15).

Zhang, C., (2005). Madden-Julian Oscillation. Rev. Geophys., 43(2): 1–36 **(36 Pages)**.

Zhang, Y.; Wu, C.; Yeh, P.J.-F; Li, J.; Li, J.; Hu, B.X.; Feng, P., (2023). Evaluating drought monitoring utility of the top-down and bottom-up satellite precipitation products over mainland China from a three-dimensional perspective. J. Hydrol., 625(Part B): 130153.

Zhong, R.; Chen, X.; Lai, C.; Wang, Z.; Lian, Y.; Yu, H.; Wu, X., (2019). Drought monitoring utility of satellite-based precipitation products across mainland China. J. Hydrol., 568: 343–359 **(17 Pages)**.

AUTHOR (S) BIOSKETCHES

Purwandani, A., Ir., M.Si., in Climatology and Air-Sea Interaction, Associate Expert Engineer, Research Center for Conservation of Marine and Inland Water Resources, National Research and Innovation Agency (BRIN), Jl. Raya Bogor KM. 46, Cibinong (16911), Jawa Barat, Indonesia.
- Email: *andri.purwandani@brin.go.id*
- ORCID: 0000-0002-7675-5069
- Web of Science ResearcherID: MXL-9334-2025
- Scopus Author ID: 8335951000
- Homepage: https://brin.go.id/

Supari, Ph.D, work at Division for Climate Variability Analysis, Directorat of Climate Change, Agency for Meteorology, Climatology and Geophysics (BMKG), Jl. Angkasa I no 2, Kemayoran - Central Jakarta, Indonesia.
- Email: *supari@bmkg.go.id*
- ORCID: 0000-0002-0442-5183
- Web of Science ResearcherID: N-6071-2014
- Scopus Author ID: 57190939052
- Homepage: https://bmkg.go.id/

Ambarwulan, W., Ir., M.Sc., Dr., in Remote Sensing Application, Principal Researcher, Research Center for Limnology and Water Resources, National Research and Innovation Agency (BRIN), Jl. Raya Bogor KM. 46, Cibinong (16911), Jawa Barat, Indonesia.
- Email: *wiwi021@brin.go.id*
- ORCID: 0000-0002-5424-0152
- Web of Science ResearcherID: NA
- Scopus ID: 36508507500
- Homepage: https://brin.go.id/

Haryoko, U., Dr., work at Directorate of Applied Climate Services, Agency for Meteorology, Climatology and Geophysics (BMKG), Jl. Angkasa I No 2, Kemayoran - Central Jakarta, Indonesia.
- Email: *urip.haryoko@bmkg.go.id*
- ORCID: 0009-0008-5289-134X
- Web of Science ResearcherID: MYR-8509-2025
- Scopus Author ID: 55597703600
- Homepage: https://bmkg.go.id/

Dewi, I.P., S.Kel., M.Si. in the field of oceanography, Lecturer, Marine Science Study Program, Faculty of Fisheries and Marine Sciences, Lambung Mangkurat University (ULM), Jl. A. Yani KM. 36 Banjarbaru (70714), South Kalimantan, Indonesia.
- Email: *irapuspitadewi@ulm.ac.id*
- ORCID: 0009-0009-0559-7209
- Web of Science ResearcherID: DMYS-0193-2025
- Scopus Author ID: 57215986955
- Homepage: https://ulm.ac.id/id/

Anantasena, Y., Ir., M.Sc., Dr., in disaster management, Principal Expert Engineer, Research Center for Mining Technology, National Research and Innovation Agency (BRIN), Jl. Raya Puspiptek 60, Setu, Tangerang Selatan (15314), Banten, Indonesia.
- Email: *yudi.anantasena@brin.go.id*
- ORCID: 0009-0001-7518-6108
- Web of Science ResearcherID: MYR-8598-2025
- Scopus Author ID: 6506006371
- Homepage: https://brin.go.id/

AUTHOR (S) BIOSKETCHES

Name, N., Aff.

Djajadihardja, Y.S., Dr., in Hydrology and water resources, geology disaster, marine geology, tectonic, Research Center for Limnology and Water Resources, National Research and Innovation Agency (BRIN), Jl. Raya Bogor KM. 46, Cibinong (16911), Jawa Barat, Indonesia.
- Email: *yusu001@brin.go.id*
- ORCID: 0009-0008-3108-2172
- Web of Science ResearcherID: MYR-9461-2025
- Scopus Author ID: 7801687269
- Homepage: https://brin.go.id/

Sadmono, H., Ir., M.Sc., in Natural Resources Development, Associate Expert Engineer, Research Center for Geoinformatics, National Research and Innovation Agency (BRIN), Jl. Raya Bogor KM 46, Cibinong (16911), Jawa Barat, Indonesia
- Email: *heri008@brin.go.id*
- ORCID: 0009-0003-5668-4448
- Web of Science: MRY-8046-2025
- Scopus Author ID: 57202968301
- Homepage: Https://brin.go.id

Sachoemar, S.I., Ir., M.Si., Dr., Prof., in Fisheries Resources Management, Coastal Marine Environment, Climate Change, Air-Sea Interaction, Research Professor, Research Center for Environmental and Clean Technology, National Research and Innovation Agency (BRIN), Jl. Raya Bogor KM. 46, Cibinong (16911), Jawa Barat, Indonesia.
- Email: *suhe002@brin.go.id*
- ORCID: 0000-0002-9280-529X
- Web of Science Researcher ID : MYR-8840-2025
- Scopus Author ID: 6507712661
- Homepage: Https://brin.go.id

Nugroho, D., S.T., M.T., Dr., in groundwater protection and management, geohazard, Associate Expert Engineer, Directorate of Research Vessel Management, National Research and Innovation Agency (BRIN), Jl. M. H. Thamrin No. 8, Jakarta Pusat (10340), Indonesia.
- Email: *djok011@brin.go.id*
- ORCID: 0000-0002-6130-5671
- Web of Science ResearchedID: MYR-9158-2025
- Scopus Author ID: 57212285003
- Homepage: https://brin.go.id/

HOW TO CITE THIS ARTICLE

Purwandani, A.; Ambarwulan, W.; Supari; Haryoko, U.; Dewi, I.P.; Anantasena, Y.; Djajadihardja, Y.S.; Sadmono, H.; Sachoemar, S.I.; Nugroho, D. (2025). Infrared precipitation on climate hazards using rainfall dataset over inter-tropical convergence zoneer. Global J. Environ. Sci. Manage., 11(3): 1097-1124.

DOI: 10.22034/gjesm.2025.03.13

URL: https://www.gjesm.net/article_723457.html

Global J. Environ. Sci. Manage. 11(3): 1125-1142, Summer 2025, Serial #43

Global Journal of Environmental Science and Management
(GJESM)

Homepage: https://www.gjesm.net/

Podcasts

ORIGINAL RESEARCH PAPER

Ambient air nitrogen dioxide concentration and the growing incidence of asthma in school-aged children

P.N. Sari[1], D. Driejana[2,*], A.P. Yudison[2], D. Agustian[3], A.B. Kurnia[1], A. Riqqi[4]

[1] *Environmental Engineering Graduate Program, Faculty of Civil and Environmental Engineering, Institut Teknologi Bandung, Bandung 40132, West Java, Indonesia*

[2] *Air and Waste Management Research Group, Faculty of Civil and Environmental Engineering, Institut Teknologi Bandung, Bandung 40132, West Java, Indonesia*

[3] *Department of Public Health, Faculty of Medicine, Universitas Padjadjaran, Bandung 40161, West Java, Indonesia*

[4] *Remote Sensing and GIS Research Group, Faculty of Earth Science and Technology, Institut Teknologi Bandung Bandung 40132, West Java, Indonesia*

ARTICLE INFO

Article History:
Received 14 March 2025
Revised 18 May 2025
Accepted 25 June 2025

Keywords:
Air pollution
Passive sampler monitoring
Spatial analysis
Traffic-related air pollution (TRAP)
Urban air quality
Wheezing

DOI: 10.22034/gjesm.2025.03.14

ABSTRACT

BACKGROUND AND OBJECTIVES: Nitrogen dioxide, a significant air pollutant contributor to childhood asthma, is the focus of this study. In accordance with Sustainable Development Goals Target 3.9 and 11.6, this study plays a vital role in demonstrating the health effects of air pollution in developing nations, where such information is limited. The objectives of this study were to develop a more accurate early detection of nitrogen dioxide exposure related to asthma attacks to support more effective local asthma prevention and control strategies. This study explores the connection between nitrogen dioxide levels and asthma symptoms, including wheezing, in children residing in northeastern Bandung, Indonesia.

METHODS: Palmes's passive diffusion tubes measured weekly nitrogen dioxide measurements at 83 sampling sites to obtain the spatial and temporal concentration variations. The employment of a 30 x 30 meters' grid resolution model improved the accuracy of pollutant distribution, enabling consistent processing and interpretation of spatially resolved exposure data. The assessment of asthma symptoms was conducted using the International Study of Asthma and Allergies in Childhood questionnaire, administered to 842 individuals aged 6 to 12 years. The asthmatic children's residences were geocoded and linked to the modelled nitrogen dioxide concentration to assign individualized exposure values. Statistical analyses were performed to evaluate temporal trends, compare exposure groups, estimate wheezing risk, and assess spatial autocorrelation.

FINDINGS: The weekly nitrogen dioxide concentrations were persistently high, with a mean of 110.87 ± 42.38 micrograms per cubic meter. Significant nitrogen dioxide concentration spatial variation was found across the study area ($p < 0.001$). Locations close to significant roads recorded the highest nitrogen dioxide concentrations, surpassing 120 micrograms per cubic meter. Forty-seven (5.6 percent) of the 842 children surveyed had experienced asthma attacks. Thirty-seven of the 47 children lived in areas where nitrogen dioxide exposure levels exceeded 100 micrograms per cubic meter, indicating a strong association between elevated nitrogen dioxide concentrations and asthma symptoms ($p < 0.001$). In the region with the highest concentration, children aged nine and above suffered from more asthma attacks ($p = 0.026$). Analysis results demonstrated that asthmatic children living near major roads correlated spatially with high nitrogen dioxide concentrations. More asthma attacks occurred during periods when nitrogen dioxide levels exceeded 120 micrograms per cubic meter. The robust spatial alignment with established evidence validates a persuasive relationship that bolsters causal inference.

CONCLUSION: Children living near roadways are more prone to frequent asthma attacks. Apparent nitrogen dioxide concentration variations observed at fine spatial scales enable better detection of areas with elevated risk of asthma attacks, which provides detailed information for targeted health interventions. Future studies are being conducted based on these findings by incorporating longitudinal monitoring to gain a deeper understanding of causal pathways.

This is an open access article under the CC BY license (http://creativecommons.org/licenses/by/4.0/).

NUMBER OF REFERENCES
64

NUMBER OF FIGURES
4

NUMBER OF TABLES
2

*Corresponding Author:
Email: *driejana@itb.ac.id*
Phone: +62812 8072 0528
ORCID: 0000-0001-8432-1511

Note: Discussion period for this manuscript open until Sep 1, 2025 on GJESM website at the "Show Article".

INTRODUCTION

Sustainable Development Goals (SDG) Targets 3.9 and 11.6 aim to reduce death, illnesses and the environmental impact of cities with special attention to air quality by 2030. Human health is primarily at risk from air pollution, which is driven by a variety of pollutants produced by human activities (Crippa *et al.,* 2021). One of the air pollutants reported to cause health effects is nitrogen dioxide (NO_2), more commonly reported as nitrogen oxides (NO_x) for its combination with nitric oxide (NO) (Singh *et al.,* 2016). In many cities, road transport is the primary NO_2 source. Private cars contributed to 57 percent (%) of NO_2 emissions in road traffic in Hamburg (Ramacher and Karl, 2020). In Las Vegas, NO_2 levels rose within 20 meters (m) of roadways (Richmond-Bryant *et al.,* 2017). Nitrogen dioxide is a harmful gas that irritates the respiratory tract (Meulenbelt, 2016). Moreover, it has the potential to intensify bronchoconstriction and inflammation in the airways, possibly leading to a greater risk of infections affecting the respiratory organs (Petit *et al.,* 2017). The development of asthma is connected to NO_2 exposure, which causes airway inflammation, reduces airflow, and heightening the chances of new asthma cases (Anenberg *et al.,* 2022). These health risks are even more concerning in children due to a combination of several reasons. Factors include physiologies such as the immature immune system and still-developing vital organs, behaviors, and environmental influences. These elements, when combined, raise the propensity for infections and magnify the influence of pollutants on organs. Air pollutant exposure in children is higher than in adults because they spend more time outdoors (Gouveia *et al.,* 2018). Furthermore, because of their limited lung capacity, children tend to inhale a greater volume of air and pollutants, leading to respiratory complications, including asthma and wheezing (Olaniyan *et al.,* 2020). Recent meta-analyses reliably demonstrate a notable correlation between NO_2 exposure and asthma outcomes, especially among children. A study by Han *et al.* (2021) indicated that children exposed to NO_2 from traffic were more likely to develop asthma in children (meta-OR = 1.11, 95% CI: 1.06–1.17), with stronger effects observed in studies conducted in Asia. Similarly, another systematic review analysing 67 studies reported a pooled relative risk of 1.014 (95% CI: 1.008–1.020) per 10 micrograms per cubic meter ($\mu g/m^3$) increase in 24-hour (h) average NO_2 for asthma-related hospital admissions and emergency visits (Zheng *et al.,* 2021). An independent meta-analysis comprising 22 studies further validated a notable correlation between NO_2 and asthma exacerbations (RR = 1.024, 95% CI: 1.005–1.044) (Orellano *et al.,* 2017). These consistent findings across large-scale studies highlight the asthmatic relevance of NO_2, especially in urban environments with high traffic emissions. Although NO_2, Ozone (O_3), sulphur dioxide (SO_2), and fine particulate matter ($PM_{2.5}$) may have synergistic effects on health, NO_2 is still the most common pollutant linked to asthma pathophysiology (Mainka and Żak, 2022). A number of studies have examined the link between NO_2 levels in Indonesia and their health consequences at various spatial levels (Suryadhi *et al.,* 2020; Haryanto and Djafri, 2020; Prijanto and Hasan, 2024). These studies provided insight into the health risks associated with NO_2 in large urban areas. Suryadhi *et al.,* 2020 estimated NO_2 exposure using the Ministry of Environment passive samplers' data collected quarterly from 2009 to 2011 across 243 districts in 33 provinces. The NO_2 exposure data was combined with 2012 acute respiratory infection (ARI) data and averaged across provinces. At the provincial level, the concentrations of NO_2 were determined by averaging the minimum and maximum values. This study found an increase in the 18 % risk of ARI with the increase in NO_2 concentrations, which was valuable as a broad assessment of NO_2 exposure across Indonesia. A study by Haryanto and Djafri (2020) was performed in Jakarta to determine the high-risk zones for exposure to air pollution. The pollutants included NO_2, which used a concentration higher than 15 parts per billion (ppb) as the exposure limit. In Bandung, a study measured NO_2 at five health centers and found NO_2 associated with respiratory infections in children (Prijanto and Hasan, 2024). According to Suryadhi *et al.* (2020), the average NO_2 concentrations for the province were determined by taking the mean of the minimum and maximum values. Similarly, Haryanto and Djafri (2020) utilized data from five government monitoring sites to cover the Jakarta province of 662.33 square kilometers (km^2) with approximately 10 million populations. The exposure data collected from urban monitoring sites at the provincial level may not accurately depict individual exposure, since it overlooks the variations in pollution at intra-city

and micro-scale levels. Likewise, short-term and location-limited measurements may not represent actual exposure. Children's main exposure likely occurs at home or school, with variability due to differing distances. Utilizing sparse measurement data in prior studies might cause discrepancies in both spatial and temporal aspects. This can potentially obscure local and individual variations in air pollution exposure and fail to capture NO_2 concentrations in short-term variations, which is critical for exposure assessment. Hence, it might not entirely reflect spatial and temporal variations in individual exposure. The increase in NO_2 concentrations in Bandung is due to densely populated areas and growing vehicular emissions. Nonetheless, the existing assessments of air quality are irregular and not continuous. The lack of a long-term continuous air quality monitoring system (AQMS) in Bandung makes it challenging to analyze changes and trends in pollution (Pontoh *et al.,* 2023). Taking into account the uneven distribution of NO_2 concentrations, this study holds the promise of markedly improving the accuracy of assessments regarding NO_2 exposure evaluations and their associated health effects. The study aims to fill data gaps in resource-limited areas by integrating direct air pollutant measurements with high-resolution spatial modeling. The field measurement was designed to represent the population's inhaled pollutant levels and a spatial interpolation technique to extend data coverage to unmonitored areas. Due to the densely built environment of the study area, accurate representation of fine-scale NO_2 exposure variations is only achievable through high-spatial resolution modeling. The fine grid resolution makes possible a more accurate location for exposure evaluations and health effect forecasts. This approach captures localized variations in NO_2 levels across different areas. Additionally, it improves the precision of exposure impact estimates on health. The study presents the first evaluation of NO_2 concentrations and their relationship with childhood asthma in Bandung City and becomes a significant step forward in understanding these issues. It furnishes a more comprehensive assessment of the spatial distribution of NO_2 through precise measurements in an urban setting, enhancing understanding of local exposure trends. In evaluating these variables, the geographical pattern of NO_2 air pollution and the relationship between school children's asthma become a good starting point for targeted public health intervention. Moreover, the uneven distribution of NO_2 concentrations across urban spaces that are captured in this study increases critical concerns about environmental equity. Children residing in the vicinity subjected to detrimental air pollutants encounter social inequality as their living conditions increase their health risk. Some often reside where exposure to high-risk environmental hazards is vulnerable to health burdens (Barnes *et al.,* 2019). Based on this background, this study purposes to evaluate the spatial variability of NO_2 concentrations. Subsequently, by local-scale measurement and modelling, the study investigates uneven NO_2 concentrations association with asthma occurrences among school-aged children. Demographic information along with the features of their living environments, including indoor conditions, are utilized to enhance a deeper insight into the connection between NO_2 exposure and asthma outcomes in children. The strategy employed in this study will contribute to enhancing the accuracy of early detection of NO_2 exposure associated with asthma attacks, allowing for more focused prevention and control initiatives. This study has been conducted in Bandung, West Java, Indonesia, in 2023.

MATERIALS AND METHODS

Study design and location

This study took place in the northeastern area of Bandung, West Java, Indonesia, of *Cibeunying Kidul* and *Kiaracondong* sub-districts, Bandung City, from July 29 to October 21, 2023. The population densities of the two subdistricts are 21,883.1 and 22,691.7 people per km^2, respectively (BPS Kota Bandung, 2023a, 2023b). These sub-districts are located near four major roads (Jalan Ahmad Yani, Jalan PHH Mustofa, Jalan Ibrahim Adjie, and Jalan Terusan Jakarta), which significantly contribute to air pollution (Yudison and Driejana, 2015). Transportation emissions pose an urgent challenge as the number of motorized vehicles in Bandung has surged from 1.252.230 units in 2011 to 1.571.795 units in 2020 (BPS Kota Bandung, 2021). The population density has increased over the years (BPS Kota Bandung, 2024), hence space limitations have resulted in minimal land-use changes over time.

NO_2 *data collection*

Palmes's passive diffusion tube (PDT) samplers measured NO_2 concentrations weekly. The sampling

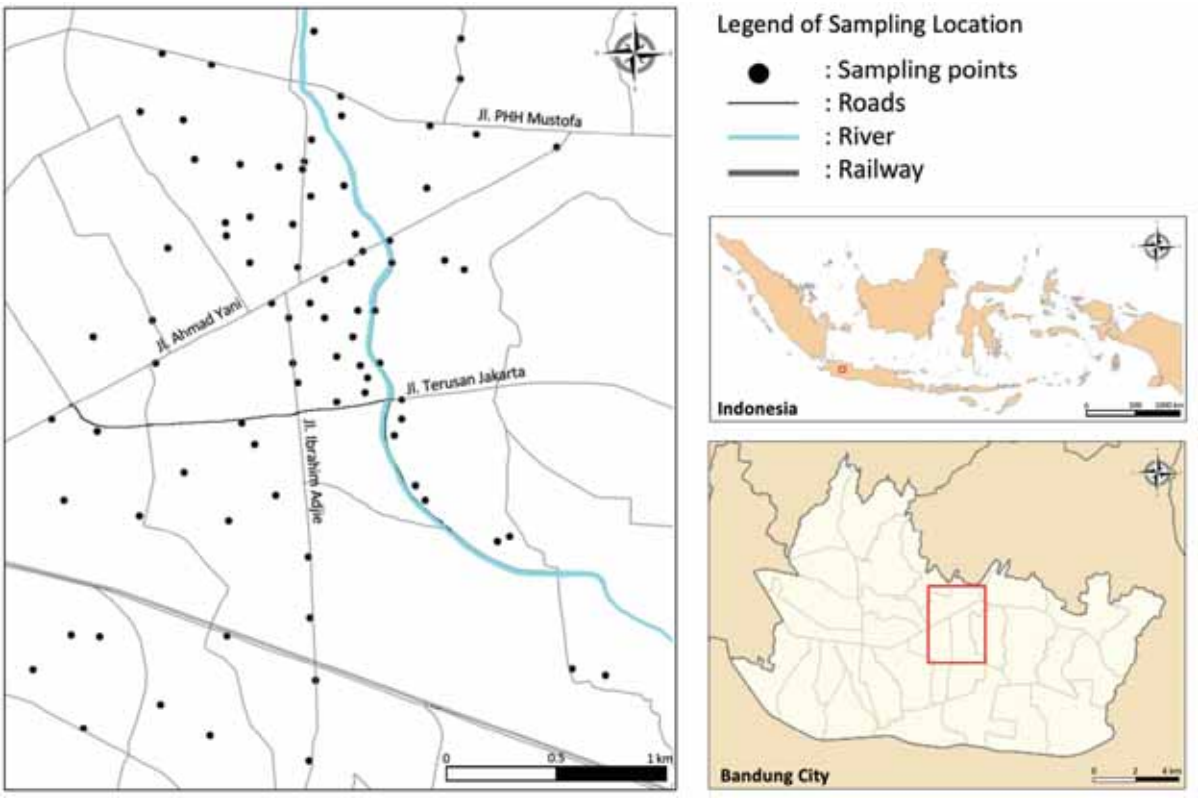

Fig. 1: Geographical location of the study area along with the sampling locations in Bandung, West Java, Indonesia (The map includes a scale bar (0-1 km) and a compass rose for spatial orientation)

of NO_2 was conducted simultaneously for 12 weeks (July 29 – October 21, 2023) at 83 measurement sites distributed across a 12 km^2 area (Fig. 1). The multiple points aimed to represent the small-scale spatial variation of NO_2 concentrations to reflect community exposure. The Palmes PDT is 71.0 millimeters (mm) in length and 11.0 mm in diameter (Zechmeister *et al.,* 2020). The caps made of polyethylene, which covered the top and bottom of the tube were unreactive to the reaction. Two stainless four-pore meshes per mm with a diameter of 12 mm held the absorbent solution at the closed end and were put inside the passive sampler cap. To provide the absorbent solution for NO_2 impregnation, 0.44 grams (g) sodium hydroxide (NaOH) and 3.95 g sodium iodide (NaI) were dissolved in methanol in 50 milliliters (mL) volumetric flask (Ngoasheng *et al.,* 2021). To enable free air circulation, the sampler was placed 1.5 to 3 meters (m) above the ground. Duplicate PDTs were deployed at each measurement location, with an additional 10% blank of the total deployed PDTs for quality control. The tubes were housed in a protective casing to lessen the effects of wind turbulence and to protect the tube from sunlight and rainwater. During the study period, consistent dry season conditions likely minimized variability due to weather-related factors (BMKG, 2023a). During the sampling phase, NO_2 molecules are drawn into the tube and are secured as nitrite ions in the absorbent solution via a diffusion process. Upon sampling, NO_2 was extracted from the exposed sample using 5 mL of Saltzman solution to quantify the concentration absorbed by the sampler. The sample was left in the dark for an hour until the solution created a pink azo dye complex. The amount of nitrite absorbed by the absorbent solution was quantified using a spectrophotometer at 550 nanometers (nm) wavelength (Gordon and Liptak, 2018). The validation of this approach is perceived as strong, highlighted by a prior study that identified a notable positive correlation coefficient of 0.84 in relation to the reference method (Estiri *et al.,* 2023).

Asthmatic data collection

Respondents for asthma data collection were selected from children residing within the areas covered by the NO_2 concentration mapping. Data regarding respondent characteristics and asthma symptoms was gathered through a survey questionnaire. The questionnaire was based on the International Study of Asthma and Allergies in Childhood (ISAAC) (Del-Rio-Navarro *et al.*, 2020) and was translated into *Bahasa Indonesia*. A certification of ethics for the research protocol guaranteed the quality of the study, the security of the data, and the rights of research subjects to their information. All asthma symptom data were obtained through parent/guardian-completed questionnaires. Only responses with signed informed consent were analyzed. To protect privacy, all geocoded residential data were anonymized and stored securely. The residential locations of children were not mapped using precise coordinates. Instead, symbolic markers were used to represent approximate residential areas. This makes certain that specific homes cannot be recognized, while permitting the examination of spatial clustering. The ethics approval was granted by the Research Ethics Committee of *Padjadjaran* University. To ensure quality assurance (QA), the questionnaire was pretested on 100 trial respondents who met the same criteria as the study population. Following the validation process, the approved questionnaires were distributed to the guardians of elementary school-aged children from two schools located within the study area. A method of sampling that is proportional to the size of the population was utilized to gather research samples from the complete population of 905 students. Random samples from each class were taken based on their respective proportions. The questionnaire included an informed consent section from the parents/guardians, and only responses with complete informed consent were further analyzed. Asthma status (ever/never) was assessed using the standardized ISAAC questionnaire. To capture recent asthma during a 12-week monitoring period, asthma symptoms in children were recognized by repeated episodes of cough, wheezing, and shortness of breath. This method refers to the Indonesian Paediatric Society in the National Asthma Guideline (Indonesian Paediatric Society, 2022), which is easily recognized by caregivers. To maintain uniformity in reporting, teachers from the school health unit, who are trained, confirmed the symptom episodes that parents reported using these criteria. This method uses community-based surveillance approaches (Benka-Coker *et al.*, 2018) and improves the use of questionnaire-based symptom identification, especially in large-scale population studies.

NO_2 *spatial distribution*

The interpolation method can generate the spatial distribution of pollutant concentrations to determine exposure level (Yudison and Driejana, 2015) and indicate the pollutant concentration in the subjects' residential area. This technique is more compatible with the measured concentration and yields superior representations of spatial patterns (Kamboj *et al.*, 2022). Nitrogen dioxide concentration data were interpolated at a 30 m × 30 m resolution based on the Indonesian Multiscale Grid System for Environmental Data using the inverse distance weighted (IDW) method, which effectively models concentrations around monitoring sites (Yudison and Driejana, 2015). Yadav and Ganguly (2025) revealed that IDW generated more accurate assessments of air quality than other techniques, such as Kriging, especially in cases where pollutants are distributed more uniformly across space. Therefore, the IDW method was chosen in this study to interpolate NO_2 exposure due to its suitability for relatively simple spatial patterns and moderate monitoring density. The 30 m × 30 m resolution model captures fine-scale spatial variability, including local factors such as land use, traffic density, and meteorological conditions. It is intended to be suitable for various urban settings that possess comparable features. The interpolation was performed using quantum geographic information system (QGIS) software (version 3.42). The locations of asthmatic children's houses were overlaid on the interpolated NO_2 concentration map to assess exposure distribution. The locations of the children-houses were checked to ensure they correspond with the actual building sites in the geographic information system (GIS), to reduce positional inaccuracies. Spatial linkage was confirmed by overlaying geocoded points onto the NO_2 exposure map to ensure each location accurately intersects with the corresponding modelled concentration grid.

Statistical test

Statistical analyses were performed to analyze

weekly fluctuations in NO_2 levels, investigate differences between concentration tiers, and estimate NO_2 concentrations at the residences of children suffering from asthma. All analyses were performed using Minitab® Statistical Software, licensed to *Institut Teknologi Bandung*.

Robustness check

To examine the spatial distribution of ambient NO_2 exposure among asthmatic children, a global Moran's I spatial autocorrelation analysis was performed using QGIS. Spatial relationships were defined via the k-nearest neighbours (KNN) method, which determines the closest features to a given location based on Euclidean distance. This technique facilitates adaptable definitions of neighborhoods and is successful in recognizing spatial clusters of adjacent features (Hu *et al.,* 2016). To evaluate the robustness and sensitivity of the spatial clustering patterns, the analysis was repeated using a range of K values (Abu Alfeilat *et al.,* 2019). For each number of nearest neighbouring locations (K), a spatial weights matrix was generated to calculate Moran's I, its expected value in a randomly spatially structured condition, and associated Z-scores and p-values. Calculation at an alpha (α) = 0.001 significance level and for multiple neighbourhood sizes was done to ensure that the identified spatial clustering was not an artefact of one definition of the neighbourhood. This technique provides greater assurance while ensuring the results remain consistent and interpretable.

RESULTS AND DISCUSSION

NO_2 temporal and spatial analysis

The duplicate PDTs resulted in the precision range of NO_2 measurements at 83 locations over 12 weeks from 92.59% to 95.27 %, with an average of 93.61%. The average precision means an average variation of approximately 6.39%, lower than the <7% duplicate relative standard deviation in the previously reported study (Masey *et al.,* 2017). In Fig. 2, the temporal variation over a period of 12 weeks is displayed, with each week's data collected from 83 sampling points. The minimum average concentration of 101.97 ± 39.22 µg/m^3 was observed in week 1. Meanwhile, the maximum average concentration of 117.06 ± 44.62 µg/m^3 was found in week 10. The median values for NO_2 concentrations remained relatively stable, with the highest median of 111.33 µg/m^3 in week 10 and the lowest median of 95.8 µg/m^3 in week 7. For the entire 12-week period, the average NO_2 concentration was 110.87 ± 42.38 µg/m^3. The average NO_2 concentration peaked at 270.21 µg/m^3 in week 7, while the lower-than-average values varied from 24.59 µg/m^3 in week 2 to 55.29 µg/m^3 in week 6. The Kruskal-Wallis's test was utilized to analyze variations in the weekly mean NO_2 levels over a period of 12 weeks. The statistical analysis yielded a p-value of 0.443 (> 0.05), suggesting no significant temporal variation in NO_2 concentrations, hence NO_2 levels were consistently high throughout the study period.

The 12-week mean concentrations of NO_2 at

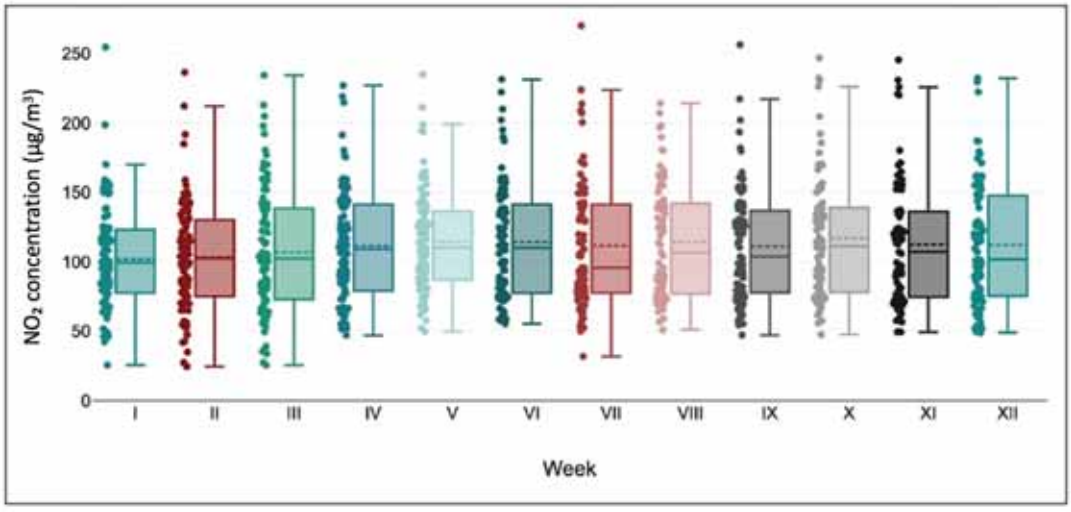

Fig. 2: Weekly Concentration of NO_2 (µg/m³) over 12 weeks
(Each bar represents weekly mean conce ntrations measured from 47 locations)

each sampling point across the study area were systematically classified into four categories to investigate the spatial variability based on scientifically justified thresholds. The critical reference level is set at 100 µg/m^3, highlighting its association with severe health consequences. Consequently, it functions as the foundational assessment standard for evaluating the necessity of implementing further monitoring actions to safeguard human health (Meulenbelt, 2016). Furthermore, the 120 µg/m^3 threshold marks the initial level associated with a higher NO_2 concentration found in downtown (Kijewska, 2016). The classification then adopts a 10 µg/m^3 incremental approach, according to Meng *et al.* (2021). The thresholds and the 10 µg/m^3 increment are applied in a systematic classification that resulted in Group 1 (>120 µg/m^3), Group 2 (111–120 µg/m^3), Group 3 (100–110 µg/m^3), and Group 4 (<100 µg/m^3). The IDW interpolation results indicated that the NO_2 level pattern always remained higher in areas near major roads. Locations close to rivers exhibited marginally diminished levels of NO_2, possibly due to the impact of rivers and water bodies on local airflow, which helps in the distribution of pollutants. This suggests that the proximity to water bodies may enhance air quality by facilitating air movement and minimizing pollutant buildup. The natural flow path has a cooling effect, reducing air pollution concentration locally (Guo *et al.,* 2023). Furthermore, bodies of water may chill the area, reducing the possibility of pollutants accumulating close to the ground (Shi *et al.,* 2020). Nonetheless, the significant effects of urban planning and traffic pollution render the river's moderating influence minimal and insignificant. This is because, even while natural characteristics are present, high-traffic locations have higher NO_2 concentrations.

As a short-lived pollutant, NO_2 remains concentrated near emission sources, serving as a key indicator of urban air pollution. In urban areas, NO_2 primarily originates from transportation fossil fuel combustion, which could contribute up to 80% of ambient NO_2 (Achakulwisut *et al.,* 2019). Several studies also reported high weekly NO_2 concentrations over 100 µg/m^3, such as 150 µg/m^3 in Holyoke, US (Beltran *et al.,* 2024), and 139 µg/m^3 in Accra, Ghana (Wang *et al.,* 2022), which were slightly higher but comparable to this finding. The increase in NO_2 levels in urban regions with fast-growing populations correlates with the escalation of transport-related emissions. On a global scale, since the 2000s, the average annual NO_2 concentration has increased by 71% in densely populated regions (Sicard *et al.,* 2023). Because of transportation-related activities, NO_2 concentrations in large European cities were above the annual NO_2 World Health Organization (WHO)'s air quality standard (40 µg/m^3) (Casquero-Vera *et al.,* 2019). Cities in south Asia also experienced significant increases in NO_2 concentrations. The growth in vehicle sales, intensified by the significant amount of traffic congestion, releases NO_x concurrently (Duncan *et al.,* 2016). NO_x emissions primarily originate from high-temperature reactions between nitrogen (N_2) and oxygen (O_2) during combustion (Wu *et al.,* 2020). Nitrogen dioxide in gaseous form can combine with other pollutants to produce secondary particulate matter, such as aerosols, that lower air quality and present health risks, particularly in urban settings (Lin *et al.,* 2019). These pollutants, particularly in city environments, create serious health threats, especially for those suffering from asthma. Sustained high temperature throughout the research period was another factor that might contribute to the elevated NO_2 concentrations. Peroxy-acyl nitrates and other long-lived reactive nitrogen compounds dissociate more quickly in hot temperatures (Romer *et al.,* 2018). During the measurement period, the highest weekly average temperature was 34 degrees Celsius (°C) in the 11th and 12th week measurements (BMKG, 2023b). West Java Province has been affected by a drought, going 50 days in a row without any rain. During this period, there was a notable reduction in rainfall, averaging only 8% (BMKG, 2023a). The dry season in Indonesia at the time of the measurement was drier than usual due to the combined impacts of El Niño and a positive Indian Ocean Dipole (IOD). It is well understood that a decrease in rainfall leads to a higher concentration of pollutants in the atmosphere (Liu *et al.,* 2024). The relatively stable weather throughout the study period suggests that spatial and temporal variations in NO_2 concentrations are predominantly driven by traffic emissions. This stable atmospheric context reinforces the notion that the NO_2 patterns observed are a result of local emissions rather than short-lived weather phenomena. The accuracy of PDT measurements for NO_2 is affected by humidity, especially in tropical environments. While low relative humidity (RH) can lead to potential underestimation

of NO_2 due to incomplete chemical reactions (Heal *et al.,* 2019), higher RH generally favors this chemical conversion and improves NO_2 uptake efficiency. However, excessive humid conditions, which are typical in tropical climates like Indonesia, may cause the NaOH/NaI solution to absorb excess moisture. It can reduce the concentration of the reagent and impact its stability during long exposure durations. In this study, all PDT samplers were protected within shielded cases designed to guard against direct rain, sunlight, and wind turbulence, with an exposure duration of no more than 7 days. This approach contributed to sustaining the chemical stability of the absorbent solution while reducing environmental interference. Although direct RH measurements were unavailable at every sampling location, the consistently high humidity during the monitoring period is expected to have supported effective NO_2 capture. Overall, the use of protective cases and the ambient conditions suggest that environmental effects on the measurement accuracy were mitigated to a considerable extent.

Asthma symptoms and spatial exposure to NO_2

842 children completed the survey, with a questionnaire response rate of 93%. This study found that 5.6% of children experienced wheezing, whereas 3.6% experienced wheezing in the previous 12 months. In total, 3.2% of children have been diagnosed with asthma or have a history of asthma verified by a physician. The residences of children suffering from asthma were geocoded and subsequently placed on the spatial distribution map of the modelled NO_2 concentration field. As depicted in Fig. 3 a significant number of children's residences were found in regions of elevated concentration. In total, 37 asthmatic children lived in areas with NO_2 concentrations greater than 100 µg/m^3 (Table 1) in

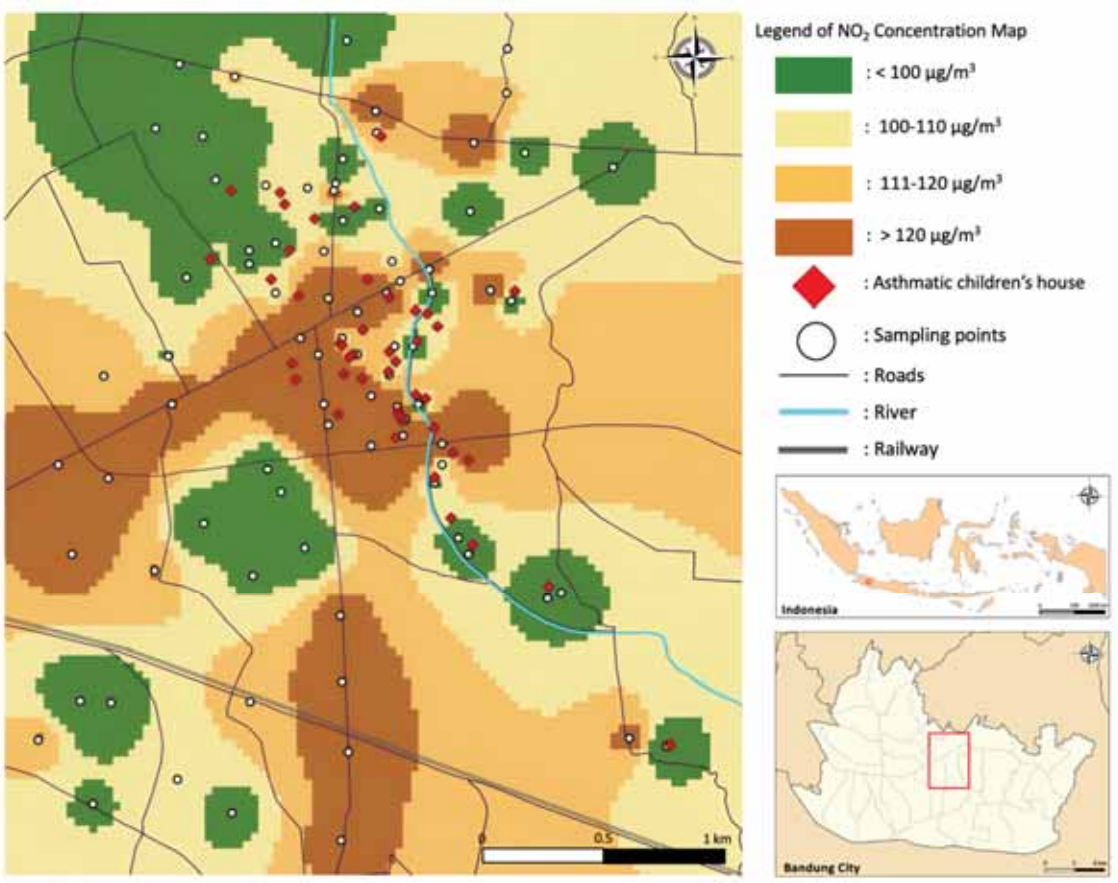

Fig. 3: Map of the 12-week average NO_2 concentration (µg/m^3) interpolation, sampling points, and asthmatic children's house location (The map includes a scale bar (0-1 km) and a compass rose for spatial orientation)

Table 1: Tukey-Kramer NO_2 mean differences based on IDW interpolation at measurement locations and asthmatic children's houses across exposure groups

Group (NO_2 exposure)	N	Mean ± standard deviation (SD)	95% confidence interval (CI)	Tukey grouping
Measurement Locations				
1 (>120 µg/m^3)	29	151.89 ± 25.20	145.45, 158.32	A
2 (111–120 µg/m^3)	6	113.91 ± 2.17	99.76, 128.05	B
3 (100–110 µg/m^3)	11	104.53 ± 4.05	94.09, 114.98	B
4 (<100 µg/m^3)	37	80.10 ± 12.86	74.41, 85.80	C
Asthmatic Children's Houses				
1 (>120 µg/m^3)	17	139.08 ± 15.66	134.18, 143.98	A
2 (111–120 µg/m^3)	5	118.34 ± 1.85	109.31, 127.37	B
3 (100–110 µg/m^3)	15	105.64 ± 3.36	100.42, 110.85	B
4 (<100 µg/m^3)	10	92.49 ± 4.94	86.10, 98.88	C

*Groups that do not share the same letter indicate a significant difference (Tukey-Kramer, $p < 0.001$)

the northern part of Kiaracondong sub-district. The sub-district is an area surrounded by three large roads (Jalan A. Yani, Jalan Ibrahim Adjie, and Jalan Terusan Jakarta) with dense traffic that contributes significantly to air pollution. The significant quantity of motor vehicles present in the vicinity is probably the main contributor to NO_2 emissions, leading to elevated levels of pollutants close to their residences. One-way ANOVA test investigated whether there was a difference between the concentration range groups. The study identified a considerable disparity ($p < 0.001$) in NO_2 levels among the four groups of concentration ranges, which is depicted in the IDW modeling map in Fig. 3. The *post-hoc* Tukey-Kramer test was used to further identify which groups were significantly different in all measurements area. The test result indicated that Group 1 (Mean = 151.89 µg/m^3) had significantly higher NO_2 levels than all other groups. In contrast, Group 4 (Mean = 80.10 µg/m^3) had the lowest concentrations and also differed significantly from other groups. However, the tests found no significant difference between Group 2 (113.91 µg/m^3) and Group 3 (104.53 µg/m^3) ($p > 0.05$) (Table 1). The findings indicated that the peak NO_2 levels observed in Group 1 corresponded to sampling locations near major roads, where the primary source of emissions is vehicle traffic (Fig. 3). The high concentrations also coincided with most of the children's house locations with asthma symptoms. Conversely, Group 4, demonstrating much lower concentrations, had a lesser number of children with asthma. The study also identified notable disparities in NO_2 levels and the number of residences of asthmatic children among the four groups ($p < 0.001$). Group 1 exhibited the highest mean NO_2 concentration (139.08 ± 15.66 µg/m^3). There were 17 asthmatic children's houses in the Group 1 area. Groups 2 and 3 showed intermediate values, with no significant difference between them (Tukey-Kramer test), each had 5 and 15 asthmatic children's houses. Conversely, Group 4, which was associated with residential zones situated at a greater distance from emission sources, exhibited the lowest concentration (92.49 ± 4.94 µg/m^3). It also had the least number of asthmatic children houses compared to other groups with concentrations larger than 100 µg/m^3 (Table 1). These findings confirm that the NO_2 distribution spatial pattern aligns with the proximity to traffic as the source of air pollution exposure.

Table 2 summarizes participant demographics and household characteristics stratified by NO_2 exposure group. Participant age distribution varied significantly across NO_2 exposure groups (Kruskal–Wallis, $p = 0.032$), with children aged nine and above predominantly residing in a high-exposure zones. Age was also significantly associated with total asthma attacks during the 12-week monitoring period (Negative Binomial Regression, $p = 0.026$). It appears that this relationship is predominantly caused by the spatial aggregation of older children in locations with increased NO_2 concentrations. Thus, the elevated asthma burden is more related to greater exposure to NO_2 pollution. Cheng *et al*. (2019) indicated a greater burden among older children, possibly due to cumulative exposure, increased time outdoors, or age-related susceptibility. Additional investigation is required to assess how age influences asthma exacerbations in this region characterized with elevated NO_2 levels. Other variables showed no statistically significant differences but exhibited

Table 2: Participant characteristics by NO_2 exposure group

Variables	Group 1 (>120 µg/m³)	Group 2 (111–120 µg/m³)	Group 3 (100–110/ µg/m³)	Group 4 (<100 µg/m³)	p-value for asthmatic symptom	p-value for total asthma attack
	n (%)	n (%)	n (%)	n (%)		
Age (years)					0.032*	0.026*
≥ 9	12 (70.6)	5 (100)	6 (40.0)	5 (50.0)		
< 9	5 (29.4)	0 (0)	9 (60.0)	5 (50.0)		
Sex					0.791	0.328
Female	5 (29.4)	2 (40.0)	7 (46.7)	4 (40.0)		
Male	12 (70.6)	3 (60.0)	8 (53.3)	6 (60.0)		
Cooking fuel type					NA	NA
LPG	17 (100)	5 (100)	15 (100)	10 (100)		
Kerosene/firewood	0 (0)	0 (0)	0 (0)	0 (0)		
Indoor smokers in family					0.422	0.544
No	6 (35.3)	2 (40.0)	2 (13.3)	2 (20.0)		
Yes	11 (64.7)	3 (60.0)	13 (86.7)	8 (80.0)		
Ventilation during cooking					0.689	NA
Open window	16 (94.1)	5 (100)	13 (86.7)	9 (90.0)		
Close window	1 (5.9)	0 (0)	2 (13.3)	1 (10.0)		
Ventilation during hot weather					0.197	1
Open window	17 (100)	4 (80.0)	15 (100)	10 (100)		
Close window	0 (0)	1 (20.0)	0 (0)	0 (0)		
Vehicle warm-up at home					0.19	0.478
No	17 (100)	5 (100)	13 (86.7)	10 (100)		
Yes	0 (0)	0 (0)	2 (13.3)	0 (0)		
Household size					0.929	NA
≤ 3 persons	2 (11.8)	1 (20.0)	2 (13.3)	2 (20.0)		
> 3 persons	15 (88.2)	4 (80.0)	13 (86.7)	8 (80.0)		
Residential density					0.472	0.395
Not dense	12 (70.6)	2 (40.0)	11 (73.3)	8 (80.0)		
Dense	5 (29.4)	3 (60.0)	4 (26.7)	2 (20.0)		
Presence of pets (dog/cat)					0.753	0.476
No	13 (76.5)	4 (80.0)	11 (73.3)	9 (90.0)		
Yes	4 (23.5)	1 (20.0)	4 (26.7)	1 (10.0)		
Transportation method to school					0.767	0.671
On foot	13 (76.5)	4 (80.0)	10 (66.7)	6 (60.0)		
Vehicle	4 (23.5)	1 (20.0)	5 (33.3)	4 (40.0)		
Commute time to school					0.4	0.351
≤ 5 minutes	8 (47.1)	1 (20.0)	4 (26.7)	2 (20.0)		
> 5 minutes	9 (52.9)	4 (80.0)	11 (73.3)	8 (80.0)		

*Statistically significant at $p < 0.05$

patterns of interest. All households reported using liquefied petroleum gas (LPG) for cooking, with no use of kerosene or firewood. Another observation is that most individuals practiced open-window ventilation during cooking; however, in Group 3, 13.3% did not participate in this practice, which raises potential concerns in areas with high exposure. Similarly, window opening during hot weather is common, which may facilitate outdoor NO_2 infiltration, particularly in polluted environments (Grigorieva and Lukyanets, 2021). Some variables were marked as not applicable (NA) in the statistical

tests due to limited variation or small subgroup sizes. For instance, all households utilized LPG, and none of the participants indicated the use of alternative fuels, which limits inferential analysis. Although these variables could not be statistically analysed, they remain important contextual factors in understanding indoor environmental quality. The prevalence of indoor smoking was noted in multiple groups, especially Groups 3 and 4, yet the differences did not reach statistical significance. Nonetheless, second-hand smoke is still a major contributor to respiratory health risk (Shargorodsky *et al.,* 2015). These findings demonstrate the dynamic relationship between environmental exposures and home behaviors. Living in a neighborhood with high exposure sets a baseline risk that may be lessened or intensified by typical ventilation and indoor smoking behaviors; other factors including household composition, pet ownership, residential density, mode of transportation, and commuting time showed no significant differences but should be retained for future exposure evaluations.

Robustness assessment of NO_2 concentration and asthma cases spatial distributions

A global Moran's I test was used to evaluate the spatial clustering of asthmatic children in relation to similar NO_2 exposure levels. The index ranges from -1 to +1, where values greater than zero indicate clustering of asthmatic children's house and NO_2 concentration, and values below zero indicate dispersion (O'Leary *et al*., 2016; Kumari *et al.,* 2019), or uncorrelated asthma cases with NO_2 concentration. A notably high Moran's I, along with a substantial z-score and a low p-value, implies that locations with elevated NO_2 levels are likely to spatially correlate with a greater residential presence of children suffering from asthma. Fig. 4 presents the results of the spatial autocorrelation analysis using Moran's I across a range of spatial neighborhood definitions (K = 1 to K = 46). The analysis shows a consistent and statistically significant positive spatial autocorrelation in NO_2 exposure among children with asthma for K = 1 to K = 36. In the KNN method, the parameter K refers to the number of closest neighbouring asthmatic locations considered for each sampling point. KNN spatial weights were applied with K values ranging from 1 to 46. This number accounts for all possible neighbours, excluding the focal point itself, given that the dataset contains 47 sampling locations. In the context of spatial analysis regarding NO_2 and asthma, the z-score denotes the potential for spatial

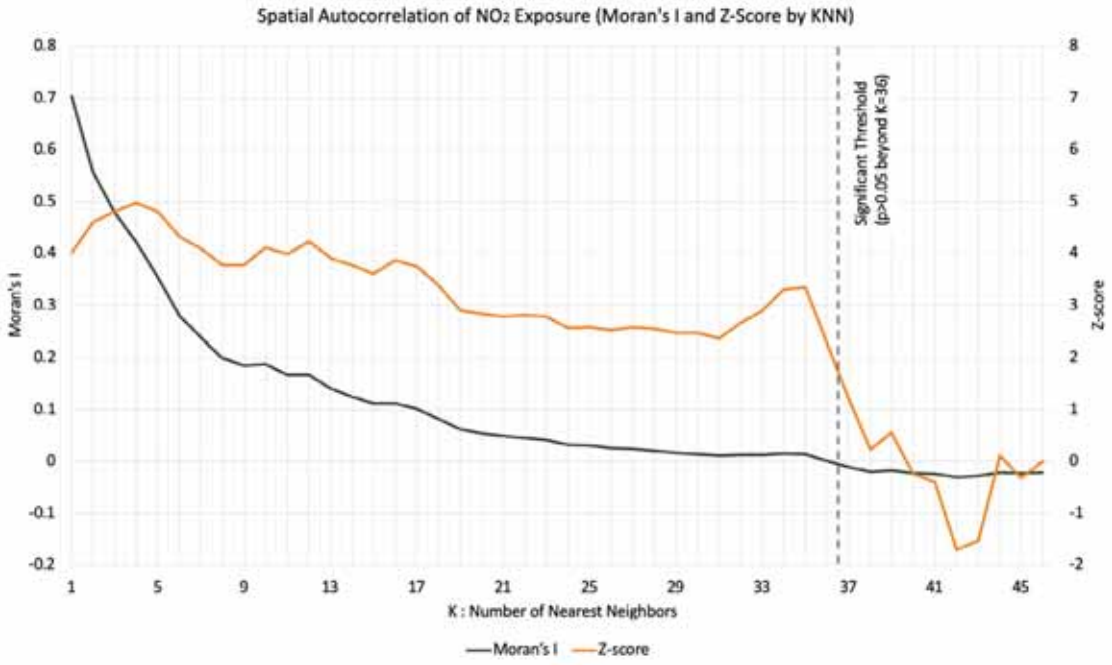

Fig. 4: Spatial autocorrelation of NO_2 exposure by k-nearest neighbor size (Statistical significance is based on corresponding Z-scores and p-values)

clustering, where a high positive z-score indicates that areas with increased NO_2 levels are likely prone to having a greater number of asthma cases. Corresponding Z-scores remain statistically significant ($p < 0.05$), indicating high confidence in the non-randomness of the clustering pattern. The highest Z-score (4.977) was found at K = 4, showing that a cluster of four closely located houses shows a strong spatial correlation with high NO_2 concentrations, indicating a localized clustering pattern. Nonetheless, when the distance between locations expands (with higher K values), the correlation diminishes, and the variability in NO_2 levels becomes less uniform, implying that a uniform spatial pattern is absent at a broader scale. These findings suggest that children with asthma tend to live in spatial clusters that correspond to areas with higher NO_2 concentrations, indicating a non-random spatial structure of exposure in urban settings. This imbalanced distribution reveals an environmental injustice, with some communities being more severely impacted by air pollution and its health consequences. Children residing in some neighborhoods, especially those near large highways, disproportionately carry the burden of increased NO_2 levels, which will heighten respiratory health risks such as asthma. This spatial condition corresponds with prior findings that underscores the influence of localized air pollution in influencing health disparities (Lindgren *et al.,* 2016).

The high NO_2 concentration and asthma, particularly in children living near the roads, suggest a strong association between asthma and exposure to traffic-related air pollution (TRAP), particularly NO_2. In densely populated urban areas, more individuals tend to live near roadways to enhance accessibility. This circumstance also increases the risk for children, where frequent outdoor activities will raise their exposure to air pollution. In an area of Bandung City characterized by high NO_2 levels (greater than 120 $\mu g/m^3$), fourteen asthmatic children lived in houses adjacent to a traditional market bustling with street vendors, a typical site of traffic congestion. Previous studies also found asthma exacerbation in hospital outpatients with increased NO_2 concentrations (Kowalska *et al.,* 2020). A retrospective cohort study also found an increased risk of asthma attacks after exposure to NO_2 at an early age (Kuiper *et al.,* 2021). The risk of new and persistent asthma was higher in people living <200 m from the main road (Bowatte *et al.,* 2018). Moreover, indoor NO_2 levels might be forecasted using outdoor concentration measurements in homes situated near major thoroughfares (Yudison and Driejana, 2011). This is particularly relevant for assessing asthma risk in children living in homes near major roadways. Urban inhabitants are likely to encounter a greater risk of asthma as a result of high mobility, the surge in transportation emissions, and the ongoing patterns of urbanization. Weekly interpolated raster data identified asthma attacks among 47 children that occurred specifically during weeks when the NO_2 concentration at their residential locations reached or exceeded 120 $\mu g/m^3$. These pollution-linked asthma cases were recorded in week 3 (2 children), week 4 (1 child), week 5 (2 children), week 6 (3 children), and weeks 7, 11, and 12 (1 child each). Despite the relatively low figures, the steady emergence of asthma episodes in the context of high pollution exposure was demonstrated. The need for timely response interventions is urgent in the management of asthma cases. Real-time NO_2 monitoring data in an area will provide air quality in a timelier manner to predict potential asthma risk. This monitoring activity is essential for developing successful public health interventions. Policymakers and urban planning authorities can implement targeted initiatives for specific areas, such as upgrading air quality monitoring systems and decreasing vehicle emissions in proximity to homes and educational institutions. In addition, the health sector can prioritize services in high-risk areas by acknowledging that certain communities are more impacted than others. This study had certain limitations. Firstly, the cases of asthmatic children were used to assess risk instead of prevalence, which is generally designated for comparing risk or likelihood. Second, the asthmatic condition was determined by self-report rather than the doctor's diagnosis or more objective measures such as spirometry or peak expiratory flow meter. Asthma management in Indonesia is commonly constrained by issues of underdiagnosis or inaccurate reporting, potentially causing the prevalence to be underestimated (Triasih *et al.,* 2023). To overcome these challenges, our study employed the ISAAC questionnaire, a widely accepted and validated tool for large-scale epidemiological studies. In addition, childhood asthma is commonly marked by repeated episodes of coughing, wheezing, and shortness

of breath (Indonesian Paediatric Society, 2022). These symptoms are typically detected by parents or caregivers, which aids in the early recognition of asthma symptoms, even when clinical testing is not conducted. Given the limited access to healthcare and diagnostic services in many parts of Indonesia, this symptom-based approach is both necessary and practical for community-level asthma identification. Second, IDW was selected due to its simplicity, computational efficiency, and suitability for capturing spatial patterns within the specific context of our study area, where monitoring data are relatively dense and spatial variation is moderate. Unlike Kriging, IDW does not explicitly model spatial autocorrelation, which may limit its performance in areas with complex spatial heterogeneity or sparse data coverage. Compared to land-use regression (LUR), IDW also does not incorporate covariates such as traffic intensity, land use type, or meteorological factors (Dirgawati *et al.,* 2015). The lack of these predictors indicates that IDW might not completely account for all sources of spatial variability. However, IDW provides a practical balance between accuracy and computational simplicity according to data availability and the scope of this study. It is essential to understand that alternative spatial interpolation techniques yield comparable results, but they are based on distinct assumptions and inputs; hence, their outcomes are not directly interchangeable. Third, while this study statistically evaluated several sociodemographic and indoor environmental factors, residual confounding may still exist. Aspects such as parental asthma history, exposure to indoor allergens (including dust mites or mold), and the condition of housing were not directly evaluated and may require inclusion in upcoming studies. These factors could be crucial for a thorough understanding of asthma. Future studies should consider measuring these variables for a more comprehensive analysis. A more comprehensive study is currently underway using cohort epidemiological design. In this study, NO_2 exposure and childhood asthma incidence are followed up at multiple intervals to more accurately predict asthma incidence and prevalence based on the representation of children's residential areas. Nevertheless, this study helps identifying high-risk regions, and supporting more focused health policies for asthma prevention and further investigation. Building on this, the follow-up study monitors weekly NO_2 concentrations alongside weekly asthma symptoms using a community-based surveillance method (Benka-Coker *et al.,* 2018). This design facilitates a clearer comprehension of the relationship between short-term fluctuations in air pollution relate to asthma attacks in children. Clinical examinations were conducted by health professionals at certain intervals to support more accurate diagnosis. The spatial patterns and exposure levels identified in the current study have informed the sampling strategy and exposure classification in the cohort, making it more targeted and policy relevant.

CONCLUSION

The weekly NO_2 concentrations in Bandung were relatively high, indicating a significant level of air pollution. The high-resolution spatial modeling improved the spatial coverage and temporal representation of passive sampler NO_2 measurements. The interpolation found high NO_2 concentration measurement sites on the roadsides. Transportation-related fuel burning is likely to contribute significantly to atmospheric NO_2 concentrations. Although the presence of a river may somewhat lessen local concentrations, its mitigating effect was negligible when compared to the significant influence of traffic emissions and urban design. The concentration pattern indicates that vehicle-related fuel combustion is a dominant contributor. The extended dry season observed during the study intensified these trends by decreasing rainfall and restricting atmospheric purification. As a result, pollutants were able to accumulate more easily. To improve geographical resolution and analytical accuracy and enable more methodical processing of environmental data, this study employed a 30 m x 30 m grid-based spatial methodology. This technique boosts the efficiency of spatial interpolation, facilitating a more precise assessment of population exposure and the distribution of pollutants. The enhanced spatial detail provided by the fine-resolution grid system also enabled clearer identification of exposure patterns in residential areas, particularly those with vulnerable populations such as children. Children are likely to develop asthma due to significant exposure to pollution from traffic. Some children experienced asthma attacks in the observed area, while others experienced wheezing in the last 12 months. Statistical analyses demonstrated significant differences in NO_2 concentration levels across different

exposure areas and in the spatial distribution of asthmatic children's homes. Regions characterized by elevated NO_2 concentrations close to major transport corridors reported the highest incidence of asthma among residents. This spatial gradient confirms the dominant influence of traffic emissions on air pollution exposure at the neighborhood level. The spatial analysis confirms older children living in high-exposure zones experienced asthma attacks during the monitoring period. However, this pattern is more likely the result of growing exposure to severely polluted locations rather than age being the primary cause. Spatial autocorrelation analysis (Moran's I) confirmed significant clustering of NO_2 exposure and asthma cases at the neighbourhood level. This emphasizes the disproportionate environmental burden on children in polluted areas. By Identifying these trends, city authorities and urban planners can direct their attention to the areas that are most affected. For instance, they can stop housing construction that is situated too near to heavily trafficked roads, enhance greenery to assist in filtering air pollutants, or refine traffic management to diminish emissions. Clustering also helps identify the potential locations for health surveillance. Improving air quality surveillance is crucial for safeguarding vulnerable groups. These findings suggest that neighbourhood environmental factors, such as traffic closeness and urban infrastructure, control air pollution exposure and its associated health burden. However, several limitations should be taken into account while considering these findings. Asthma symptoms were based on parental reports without clinical confirmation, and NO_2 exposure data were collected only at a single point in time. Although these were associated with a history of wheezing and the frequency of asthma episodes throughout the 12-week monitoring period, such limitations may affect the robustness and clarity of the observed relationships. Future research should aim to include clinical diagnoses and longer-term exposure tracking to strengthen the evidence base and better inform policy and targeted health interventions. An ongoing cohort-based epidemiological study aims to explore further the link between NO_2 exposure and children's health outcomes using updated data.

AUTHOR CONTRIBUTIONS

P.N. Sari prepared in data curation, formal analysis, investigation, visualization, and writing the original manuscript. Driejana, the corresponding author, contributed to conceptualization, methodology, resource management, supervision, validation, manuscript review, rewriting and editing. A.P. Yudison supervised air quality sampling, analysis methodology and manuscript review. Dwi Agustian provided advice for health data acquisition, health data analysis and manuscript review. A.B. Kurnia contributed to NO_2 investigation. A. Riqqi provided advice for geospatial analysis, review and rewriting. All authors contributed substantial edits to the final version of the article, read and approved the final manuscript.

ACKNOWLEDGEMENT

P.N. Sari was supported by the Center for Higher Education Funding and Assessment (PPAPT), Ministry of Higher Education, Science, and Technology of the Republic of Indonesia and the Indonesia Endowment Fund for Education (LPDP), Ministry of Finance of the Republic of Indonesia, through Beasiswa Pendidikan Indonesia (BPI) for her doctoral studies [Grant number: 202101121677]. ITB Riset Multidisiplin P2MI 2023 under the project title *'Dampak Emisi Transportasi Terhadap Penyakit Akibat Pencemaran Udara di Kota Bandung*' (PI: Dr. Driejana) supported air quality data for this study. Authors thank R.R. Hidayat for assisting with NO_2 data collection during weeks 1-3.

CONFLICT OF INTEREST

The authors declare that there is no conflict of interest regarding the publication of this manuscript. In addition, ethical issues, including plagiarism, informed consent, misconduct, data fabrication and/or falsification, double publication and/or submission, and redundancy have been completely observed by the authors.

OPEN ACCESS

©2025 The author(s). This article is licensed under a Creative Commons Attribution 4.0 International License, which permits use, sharing, adaptation, distribution and reproduction in any medium or format, as long as you give appropriate credit to the original author(s) and the source, provide a link to the Creative Commons license, and indicate if changes are made. The images or other third-party material in this article are included in the article's Creative Commons license, unless indicated otherwise in a

credit line to the material. If material is not included in the article's Creative Commons license and your intended use is not permitted by statutory regulation or exceeds the permitted use, you will need to obtain permission directly from the copyright holder. To view a copy of this license, visit: http://creativecommons.org/licenses/by/4.0/

PUBLISHER'S NOTE

GJESM Publisher remains neutral regarding jurisdictional claims in published maps and institutional afflictions.

☑ Positive AI Statement

During the preparation of this work the authors have used Artificial Intelligence (AI), Grammarly and Quillbot, in order to assist in checking grammar, diction errors and language refinement. After using this tool/service, the authors reviewed and edited the content as needed and took full responsibility for the content of the publication.

(For this reason, the GPTZero detector will evaluate the manuscript utilizing Generative AI, ensuring a high detection rate. If the manuscript relies heavily on Generative AI and AI-assisted technologies, it will be archived without further options for appeal).

☐ Negative AI Statement

The author(s) declared that no AI tools or services were not used or not highly applied during the preparation of this work.

ABBREVIATIONS

%	Percent
°C	Degree Celsius
α	Alpha
µg/m³	Microgram per cubic meter
AQMS	Air quality monitoring system
ARI	Acute respiratory infections
g	Grams
GIS	Geographic information system
IDW	Inverse distance weighted
IOD	Indian Ocean Dipole
ISAAC	International Study of Asthma and Allergies in Childhood
K	Number of nearest neighboring locations
km²	Square kilometer
KNN	K-nearest neighbours
LPG	Liquefied petroleum gas
LUR	land-use regression
m	Meter
mL	Milliliters
mm	Millimeters
N_2	Nitrogen
NaI	Sodium iodide
NaOH	Sodium hydroxide
nm	Nanometers
NA	Not applicable
NO	Nitric oxide
NO_2	Nitrogen dioxide
NO_x	Nitrogen oxides
O_2	Oxygen molecule
O_3	Ozone
PDT	Passive diffusion tube
$PM_{2.5}$	Fine particulate matter
ppb	Part per billion
QA	Quality assurance
QGIS	Quantum geographic information system
RH	Relative humidity
SDG	Sustainable development goal
SO_2	Sulphur dioxide
TRAP	Traffic-related air pollution
WHO	World Health Organization

REFERENCES

Abu-Alfeilat, H.A.; Hassanat, A.B.A.; Lasassmeh, O.; Tarawneh, A.S.; Alhasanat, M.B.; Eyal Salman, H.S.; Prasath, V.B.S., (2019). Effects of distance measure choice on k-nearest neighbor classifier performance: a review. Big Data. 7(4): 221–248 **(38 pages).**

Achakulwisut, P.; Brauer, M.; Hystad, P.; Anenberg, S.C., (2019) Global, national, and urban burdens of paediatric asthma incidence attributable to ambient NO_2 pollution: estimates from global datasets. Lancet Planet Health. 3: e166–78 **(13 pages).**

Anenberg, S.C.; Mohegh, A.; Goldberg, D.L.; Kerr, G.H.; Brauer, M.; Burkart, K.; Hystad, P.; Larkin, A.; Wozniak, S.; Lamsal, L., (2022). Long-term trends in urban NO_2 concentrations and associated

paediatric asthma incidence: estimates from global datasets. Lancet Planet. Health. 6(1): e49–e58 **(10 pages).**

Barnes, J.H.; Chatterton, T.J.; Longhurst, J.W.S., (2019). Emissions vs exposure: Increasing injustice from road traffic-related air pollution in the United Kingdom. Transp. Res. part D Transp. Environ., 73: 56–66 **(11 pages).**

Beltran, N.; Juda, L.; O'connor, S.; Wang, J.; Tejan Jalloh, K.; Lange, C.; Mottey, B.; Arku, R., (2024). Patterns of nitrogen dioxide (NO_2) pollution in Holyoke, MA. ISEE Conference Abstracts.

Benka-Coker, W.O.; Gale, S.L.; Brandt, S.J.; Balmes, J.R.; Magzamen, S., (2018). Optimizing community-level surveillance data for pediatric asthma management. Prev. Med. reports 10: 55–61 **(7 pages).**

BMKG, (2023a). Daily Climate Data of Bandung City. Meterological, Climatological and Geophysical Agency of Indonesia.

BMKG, (2023b). Seasonal Monitoring Bulletin July–September Q3 2023, Indonesia. Meterological, Climatological and Geophysical Agency of Indonesia **(22 pages).**

Bowatte, G.; Lodge, C.J.; Knibbs, L.D.; Erbas, B.; Perret, J.L.; Jalaludin, B.; Morgan, G.G.; Bui, D.S.; Giles, G.G.; Hamilton, G.S.; Wood-Baker, R.; Thomas, P.; Thompson, B.R.; Matheson, M.C.; Abramson, M.J.; Walters, E.H.; Dharmage, S.C., (2018). Traffic related air pollution and development and persistence of asthma and low lung function. Environ. Int., 113: 170–176 **(7 pages).**

BPS Kota Bandung, (2023a). Kiaracondong District in Figures 2023. Statistics of Bandung City **(179 pages)**.

BPS Kota Bandung, (2023b). Cibeunying Kidul District in Figures 2023. Statistics of Bandung City **(179 pages).**

BPS Kota Bandung, (2021). Potential of Motor Vehicles by Type in Bandung City. Statistics of Bandung City.

BPS Kota Bandung, (2024). Bandung City in Figures 2024. Statistics of Bandung City **(528 pages).**

Casquero-Vera, J.A.; Lyamani, H.; Titos, G.; Borrás, E.; Olmo, F.J.; Alados-Arboledas, L., (2019). Impact of primary NO_2 emissions at different urban sites exceeding the European NO_2 standard limit. Sci. Total Environ., 646: 1117–1125 **(9 pages).**

Cheng, C.-Y.; Cheng, S.-Y.; Chen, C.-C.; Pan, H.-Y.; Wu, K.-H.; Cheng, F.-J., (2019). Ambient air pollution is associated with pediatric pneumonia: A time-stratified case–crossover study in an urban area. Environ. Health. 18: 1–9 **(9 pages).**

Crippa, M.; Guizzardi, D.; Pisoni, E.; Solazzo, E.; Guion, A.; Muntean, M.; Florczyk, A.; Schiavina, M.; Melchiorri, M.; Hutfilter, A.F., (2021). Global anthropogenic emissions in urban areas: patterns, trends, and challenges. Environ. Res. Lett., 16(7): 74033 **(15 pages).**

Del-Rio-Navarro, B.E.; Navarrete-Rodríguez, E.M.; Berber, A.; Reyes-Noriega, N.; Álvarez, L.G.-M.; García-Almaraz, R.; Mérida-Palacio, J.V.; Saucedo-Ramirez, O.J.; Del-Rio-Chivardi, J.M.; Sienra-Monge, J.J.L., (2020). The burden of asthma in an inner-city area: A historical review 10 years after Isaac. World Allergy Organ., J. 13: 100092 **(12 pages).**

Dirgawati, M.; Barnes, R.; Wheeler, A.J.; Arnold, A.-L.; McCaul, K.A.; Stuart, A.L.; Blake, D.; Hinwood, A.; Yeap, B.B.; Heyworth, J.S., (2015). Development of land use regression models for predicting exposure to NO_2 and NO_x in metropolitan Perth, Western Australia. Environ. Model. Softw., 74: 258–267 **(10 pages).**

Duncan, B.N.; Lamsal, L.N.; Thompson, A.M.; Yoshida, Y.; Lu, Z.; Streets, D.G.; Hurwitz, M.M.; Pickering, K.E., (2016). A space-based, high-resolution view of notable changes in urban NO_x pollution around the world (2005–2014). J. Geophys. Res. Atmos., 121(2): 976–996 **(21 pages).**

Estiri, E.H.; Sani, A.R.; Dowlatabadi, A.; Estiri, R.H.; Miri, M., (2023). Development and validation of a nitrogen dioxide passive sampler. MethodsX. 11: 102334 (6 pages).

Grigorieva, E.; Lukyanets, A., (2021). Combined effect of hot weather and outdoor air pollution on respiratory health: Literature review. Atmosphere (Basel). 12: 790 **(30 pages).**

Guo, F.; Xu, S.; Zhao, J.; Zhang, H.; Liu, L.; Zhang, Z.; Yin, X., (2023). Study on the mechanism of urban morphology on river cooling effect in severe cold regions. Front. Public Health. 11: 1170627 **(11 pages).**

Gordon, R.J.; Lipták, B.G., (2018). Nitrogen Oxide Analyzers, in: Analytical Instrumentation. Routledge., London.

Gouveia, N.; Junger, W.L.; Romieu, I.; Cifuentes, L.A.; de Leon, A.P.; Vera, J.; Strappa, V.; Hurtado-Díaz, M.; Miranda-Soberanis, V.; Rojas-Bracho, L., (2018). Effects of air pollution on infant and children respiratory mortality in four large Latin-American cities. Environ. Pollut., 232: 385–391 **(7 pages).**

Han, K.; Ran, Z.; Wang, X.; Wu, Q.; Zhan, N.; Yi, Z.; Jin, T., (2021). Traffic-related organic and inorganic air pollution and risk of development of childhood asthma: A meta-analysis. Environ. Res., 194: 110493 **(14 pages).**

Haryanto, B.; Djafri, D., (2020). Air Pollution and School Children Respiratory Diseases in Indonesia: A Cohort Study. ASM Sci. J., 13(5): 24–29 **(6 pages).**

Heal, M.R.; Laxen, D.P.H.; Marner, B.B., (2019). Biases in the measurement of ambient nitrogen dioxide (NO_2) by Palmes passive diffusion tube: a review of current understanding. Atmosphere (Basel). 10: 357 **(28 pages).**

Hu, L.-Y.; Huang, M.-W.; Ke, S.-W.; Tsai, C.-F., (2016). The distance function effect on k-nearest neighbor classification for medical datasets. Springerplus. 5: 1–9 **(9 pages).**

Indonesian Pediatric Society, (2022). National Guidelines for Childhood Asthma, Third Edition. Jakarta, Indonesia (132 pages).

Kamboj, K.; Sisodiya, S.; Mathur, A.K.; Zare, A.; Verma, P., (2022). Assessment and spatial distribution mapping of criteria pollutants. Water, Air, Soil Pollut., 233(2): 82 **(15 pages).**

Kijewska, K., (2016). Analysis of the Christmas period impact on the freight transport demand in Szczecin. Transp. Res. Procedia. 16: 179–190 **(12 pages).**

Kowalska, M.; Skrzypek, M.; Kowalski, M.; Cyrys, J., (2020). Effect of NO_x and NO_2 concentration increase in ambient air to daily bronchitis and asthma exacerbation, Silesian voivodeship in Poland. Int. J. Environ. Res. Public Health. 17(3): 754 **(9 pages)**

Kuiper, I.N.; Svanes, C.; Markevych, I.; Accordini, S.; Bertelsen, R.J.; Bråbäck, L.; Christensen, J.H.; Forsberg, B.; Halvorsen, T.; Heinrich, J., (2021). Lifelong exposure to air pollution and greenness in relation to asthma, rhinitis and lung function in adulthood. Environ. Int., 146: 106219 **(10 pages).**

Kumari, M.; Sarma, K.; Sharma, R., (2019). Using Moran's I and GIS to study the spatial pattern of land surface temperature in relation to land use/cover around a thermal power plant in Singrauli district, Madhya Pradesh, India. Remote Sens. Appl. Soc. Environ., 15: 100239 **(10 pages).**

Lin, C.-A.; Chen, Y.-C.; Liu, C.-Y.; Chen, W.-T.; Seinfeld, J.H.; Chou, C.C.-K., (2019). Satellite-derived correlation of SO_2, NO_2, and

aerosol optical depth with meteorological conditions over East Asia from 2005 to 2015. Remote Sens., 11(5): 1738 **(21 pages).**

Lindgren, P.; Johnson, J.; Williams, A.; Yawn, B.; Pratt, G.C., (2016). Asthma exacerbations and traffic: examining relationships using link-based traffic metrics and a comprehensive patient database. Environ. Health. 15: 1–8 **(8 pages).**

Liu, S.; Yuan, C.; Behera, S.; Luo, J.; Yamagata, T., (2024). Indian Ocean Dipole changes during the Last Interglacial modulated by the mean oceanic climatology. Geophys. Res. Lett., 51(1): e(2023)GL106153 **(10 pages)**.

Mainka, A.; Żak, M., (2022). Synergistic or antagonistic health effects of long-and short-term exposure to ambient NO_2 and $PM_{2.5}$: a review. Int. J. Environ. Res. Public Health. 19: 14079 **(20 pages).**

Masey, N.; Gillespie, J.; Heal, M.R.; Hamilton, S.; Beverland, I.J., (2017). Influence of wind-speed on short-duration NO_2 measurements using Palmes and Ogawa passive diffusion samplers. Atmos. Environ., 160: 70–76 **(7 pages).**

Meng, X.; Liu, C.; Chen, R.; Sera, F.; Vicedo-Cabrera, A.M.; Milojevic, A.; Guo, Y.; Tong, S.; Coelho, M. de S.Z.S.; Saldiva, P.H.N., (2021). Short term associations of ambient nitrogen dioxide with daily total, cardiovascular, and respiratory mortality: multilocation analysis in 398 cities. BMJ., 372 **(9 pages).**

Meulenbelt, J., (2016). Irritant gases. Medicine (Baltimore). 44: 175–178 **(4 pages).**

Ngoasheng, M.; Beukes, J.P.; van Zyl, P.G.; Swartz, J.-S.; Loate, V.; Krisjan, P.; Mpambani, S.; Kulmala, M.; Vakkari, V.; Laakso, L., (2021). Assessing SO_2, NO_2 and O_3 in rural areas of the North West Province. Clean Air J., 31(1): 1–14 **(14 pages).**

Olaniyan, T.; Jeebhay, M.; Röösli, M.; Naidoo, R.N.; Künzli, N.; de Hoogh, K.; Saucy, A.; Badpa, M.; Baatjies, R.; Parker, B.; Leaner, J.; Dalvie, M.A., (2020). The association between ambient NO_2 and $PM_{2.5}$ with the respiratory health of school children residing in informal settlements: A prospective cohort study. Environ. Res., 186: 109606 **(8 pages).**

O'Leary, B.; Reiners Jr, J.J.; Xu, X.; Lemke, L.D., (2016). Identification and influence of spatio-temporal outliers in urban air quality measurements. Sci. Total Environ., 573: 55–65 (11 **pages).**

Orellano, P.; Quaranta, N.; Reynoso, J.; Balbi, B.; Vasquez, J., (2017). Effect of outdoor air pollution on asthma exacerbations in children and adults: systematic review and multilevel meta-analysis. PLoS One. 12: e0174050 **(15 pages).**

Petit, P.C.; Fine, D.H.; Vásquez, G.B.; Gamero, L.; Slaughter, M.S.; Dasse, K.A., (2017). The pathophysiology of nitrogen dioxide during inhaled nitric oxide therapy. ASAIO J., 63: 7–13 **(7 pages).**

Pontoh, R.S.; Saliaputri, L.; Nashwa, A.N.; Khairina, N.; Tantular, B.; Toharudin, T.; Gumelar, F., (2023). Air quality mapping in Bandung city. Atmosphere (Basel). 14(9): 1444 **(15 pages).**

Prijanto, T.B.; Hasan, N.Y., (2024). Spatial analysis of NO_2 and PM_{10} concentrations with the incidence of Acute Respiratory Tract Infection (ARI) in toddlers in Bandung City. African J. Biomed. Res., 27(3): 599–603 **(5 pages).**

Ramacher, M.O.P.; Karl, M., (2020). Integrating modes of transport in a dynamic modelling approach to evaluate population exposure to ambient NO_2 and $PM_{2.5}$ pollutions in urban areas. Int. J. Environ. Res. Public Health. 17(6): 2099 **(35 pages).**

Richmond-Bryant, J.; Chris Owen, R.; Graham, S.; Snyder, M.; McDow, S.; Oakes, M.; Kimbrough, S., (2017). Estimation of on-road NO_2 concentrations, NO_2/NO_x ratios, and related roadway gradients from near-road monitoring data. Air Qual. Atmos. Health. 10: 611–625 **(15 pages).**

Romer, P.S.; Duffey, K.C.; Wooldridge, P.J.; Edgerton, E.; Baumann, K.; Feiner, P.A.; Miller, D.O.; Brune, W.H.; Koss, A.R.; De Gouw, J.A., (2018). Effects of temperature-dependent NO_x emissions on continental ozone production. Atmos. Chem. Phys., 18(4): 2601–2614 **(14 pages).**

Shargorodsky, J.; Garcia-Esquinas, E.; Navas-Acien, A.; Lin, S.Y., (2015). Allergic sensitization, rhinitis, and tobacco smoke exposure in US children and adolescents, in: International forum of allergy & rhinology. Wiley Online Library. 471–476 **(11 pages).**

Shi, D.; Song, J.; Huang, J.; Zhuang, C.; Guo, R.; Gao, Y., (2020). Synergistic cooling effects (SCEs) of urban green-blue spaces on local thermal environment: A case study in Chongqing, China. Sustain. Cities Soc., 55: 102065 **(16 pages).**

Sicard, P.; Agathokleous, E.; Anenberg, S.C.; De Marco, A.; Paoletti, E.; Calatayud, V., (2023). Trends in urban air pollution over the last two decades: A global perspective. Sci. Total Environ., 858: 160064 **(13 pages).**

Singh, D.; Kumar, A.; Kumar, K.; Singh, B.; Mina, U.; Singh, B.B.; Jain, V.K., (2016). Statistical modeling of O_3, NO_x, CO, $PM_{2.5}$, VOCs and noise levels in commercial complex and associated health risk assessment in an academic institution. Sci. Total Environ., 572: 586–594 **(9 pages).**

Suryadhi, M.A.H.; Abudureyimu, K.; Kashima, S.; Yorifuji, T., (2020). Nitrogen dioxide and acute respiratory tract infections in children in Indonesia. Arch. Environ. Occup. Health. 75(5): 274–280 **(7 pages).**

Triasih, R.; Setyowireni, D.; Nurani, N.; Setyati, A., (2023). Prevalence, management, and risk factors of asthma among school-age children in Yogyakarta, Indonesia. J. Asthma Allergy., 23–32 **(11 pages).**

Wang, J.; Alli, A.S.; Clark, S.; Hughes, A.; Ezzati, M.; Beddows, A., (2022). Nitrogen oxides (NO and NO_2) pollution in the Accra metropolis: Spatiotemporal patterns and the role of meteorology. Sci Total Environ., 803: 149931 **(22 pages)**.

Wu, S.; Che, D.; Wang, Z.; Su, X., (2020). NO_x emissions and nitrogen fate at high temperatures in staged combustion. Energies. 13(14): 3557 **(17 pages).**

Yadav, V.; Ganguly, R., (2025). Evaluation and spatial mapping of criteria air pollutants in an industrial city in India. J. Hazardous, Toxic, Radioact. Waste., 29:4025011 **(10 pages).**

Yudison, A.P.; Driejana, (2015). Development of indoor air pollution concentration prediction by geospatial analysis. J. Eng. Technol. Sci., 47(3) **(14 pages).**

Yudison, A.P.; Driejana, D., (2011). Modeling of traffic-induced NO_2 concentration to predict the indoor air quality in houses near major road, in: Proceedings of the Eastern Asia Society for Transportation Studies Vol. 8. Eastern Asia Society for Transportation Studies. 174 **(11 pages).**

Zechmeister, H.G.; Rivera, M.; Köllensperger, G.; Marrugat, J.; Künzli, N., (2020). Indoor monitoring of heavy metals and NO_2 using active monitoring by moss and Palmes diffusion tubes. Environ. Sci. Eur., 32: 1–12 **(12 pages).**

Zheng, X.; Orellano, P.; Lin, H.; Jiang, M.; Guan, W., (2021). Short-term exposure to ozone, nitrogen dioxide, and sulphur dioxide and emergency department visits and hospital admissions due to asthma: A systematic review and meta-analysis. Environ. Int., 150: 106435 **(11 pages).**

AUTHOR (S) BIOSKETCHES

Sari, P.N., Ph.D. Candidate, Environmental Engineering Graduate Program, Faculty of Civil and Environmental Engineering, Institut Teknologi Bandung 40132, Bandung, West Java, Indonesia.
▪ Email: *nilam@ph.unand.ac.id*
▪ ORCID: 0000-0001-6122-1171
▪ Web of Science ResearcherID: AAR-1111-2021
▪ Scopus Author ID: 58150185300
▪ Homepage: https://www.researchgate.net/profile/Putri-Nilam-Sari

Driejana, D., Ph.D., Associate Professor, Air and Waste Management Research Group, Faculty of Civil and Environmental Engineering, Institut Teknologi Bandung, Bandung 40132, West Java, Indonesia.
▪ Email: *driejana@itb.ac.id*
▪ ORCID: 0000-0001-8432-1511
▪ Web of Science ResearcherID: NDT-0558-2025
▪ Scopus Author ID: 7409522726
▪ Homepage: https://itb.ac.id/staf/profil/raden-driejana

Yudison, A.P., Ph.D., Instructor, Air and Waste Management Research Group, Faculty of Civil and Environmental Engineering, Institut Teknologi Bandung, Bandung 40132, West Java, Indonesia.
▪ Email: *adyati@itb.ac.id*
▪ ORCID: 0000-0003-0234-8492
▪ Web of Science ResearcherID: NA
▪ Scopus Author ID: 56826043000
▪ Homepage: https://itb.ac.id/staf/profil/adyati-pradini-yudison

Agustian, D., Ph.D., Assistant Professor, Department of Public Health, Faculty of Medicine, Universitas Padjadjaran, Bandung 40161, West Java, Indonesia.
▪ Email: *dwi.agustian@unpad.ac.id*
▪ ORCID: 0000-0002-6122-0758
▪ Web of Science ResearcherID: MTA-3907-2025
▪ Scopus Author ID: 59345479100
▪ Homepage: https://fk.unpad.ac.id/dwi-agustian-dr-mph-phd/

Kurnia, A.B., Master Student, Environmental Engineering Graduate Program, Faculty of Civil and Environmental Engineering, Institut Teknologi Bandung 40132, Bandung, West Java, Indonesia.
▪ Email: *abalqisani@gmail.com*
▪ ORCID: 0009-0001-6589-1874
▪ Web of Science ResearcherID: NA
▪ Scopus Author ID: NA
▪ Homepage: https://id.linkedin.com/in/abalqisanikurnia

Riqqi, A., Ph.D., Associate Professor, Remote Sensing and GIS Research Group, Faculty of Earth Science and Technology, Institut Teknologi Bandung Bandung 40132, West Java, Indonesia
▪ Email: akhmad.riqqi@itb.ac.id
▪ ORCID: 0000-0002-0713-7208
▪ Web of Science ResearcherID: NA
▪ Scopus Author ID: 57195484781
▪ Homepage: https://itb.ac.id/staf/profil/akhmad-riqqi

HOW TO CITE THIS ARTICLE

Sari, P.N.; Driejana, D.; Yudison, A.P.; Agustian, D.; Kurnia, A.B.; Riqqi, A. (2025). Ambient air nitrogen dioxide concentration and the growing incidence of asthma in school-aged children. Global J. Environ. Sci. Manage., 11(3): 1125-1142.

DOI: 10.22034/gjesm.2025.03.14

URL: https://www.gjesm.net/article_725492.html

Global J. Environ. Sci. Manage. 11(3): 1143-1162, Summer 2025, Serial #43

Global Journal of Environmental Science and Management
(GJESM)

Homepage: https://www.gjesm.net/

Podcasts

CASE STUDY

Spatiotemporal analysis of rainfall variability using satellite precipitation in watersheds

M.D. Syaifullah[1], A. Purwandani[2], M. Kudsy[3,*], Tukiyat[3], S. Tikno[3], A.E. Sakya[4], F.H. Widodo[3], S. Bahri[3], Muktiyono[3]

[1] *Research Center for Climate and Atmosphere, National Research and Innovation Agency, Serpong 15314, Indonesia*

[2] *Research Center for Conservation of Marine and Inland Water Resources, National Research and Innovation Agency, Cibinong 16911, Indonesia*

[3] *Research Center for Limnology and Water Resources, National Research and Innovation Agency, Serpong 15314, Indonesia*

[4] *Research Center for Geological Disaster, National Research and Innovation Agency, Serpong 15314, Indonesia*

ARTICLE INFO

Article History:
Received 28 January 2025
Revised 02 April 2025
Accepted 05 May 2025

Keywords:
Asian Monsoon
Climate change
Rainfall variability
Spectral analysis
Watersheds

ABSTRACT

BACKGROUND AND OBJECTIVES: Comprehending spatial and temporal rainfall variability is essential for effective water resource management in Indonesia, where diverse landscapes and dynamic tropical climates lead to irregular precipitation patterns that can trigger localized floods or droughts. This study seeks to explore the impact of geomorphological and topographical differences across the Toba-Asahan, Brantas, and Larona-Malili watersheds in Indonesia influence rainfall distribution and trends, with the goal of enhancing adaptive and sustainable watershed management.

METHODS: This study analyzes rainfall variability in three distinct Indonesian watersheds, Toba-Asahan, Brantas, and Larona-Malili, using climate hazards group infrared precipitation with Station version 2 satellite precipitation data. The patterns of rainfall, both spatial and temporal, are analyzed in connection with the distinct geomorphological and topographical features of each watershed. Basic statistical analysis and mapping techniques are used to identify trends and visualize distribution patterns, with the goal of offering insights into the impact of natural landscape features on rainfall patterns and water availability within the watershed context.

FINDINGS: The results reveal a significant long-term increase in rainfall in the Larona-Malili watershed, while no statistically significant trends are observed in the Brantas and Toba-Asahan watersheds. The dominant rainfall patterns illustrate the distinct climatic features of each watershed region. Spectral analysis highlights the influence of El Niño Southern Oscillation and Indian Ocean Dipole, showing semi-annual rainfall patterns in Toba-Asahan and Larona-Malili, and an annual cycle in Brantas. The sensitivity to climate varies among the three watersheds, as indicated by the differing impacts of the Webster-Yang Monsoon Index, El Niño Southern Oscillation, and Indian Ocean Dipole.

CONCLUSION: This study comprehensively analyzes rainfall variability in three significant watersheds in Indonesia; the Brantas, the Toba-Asahan, and the Larona-Malili watersheds. The findings of this study further suggest that the Asian Monsoon plays a crucial role in shaping the seasonal rainfall patterns of the Brantas watershed. Conversely, the Toba-Asahan and Larona-Malili watersheds are influenced by both local and regional factors, where alterations in land use contribute to variations in rainfall and affect water resources. Annual patterns vary among the watershed, with Toba-Asahan experiencing year-round rainfall peaking from August to December, Brantas dominated by afternoon convection-driven rain from January to April and November to December, and Larona-Malili showing morning-to-noon rainfall from May to July due to local circulation and topographic effects. Another observation from this study indicates that the Asian Monsoon has a significant impact on the seasonal rainfall patterns within the Brantas watershed. Ultimately, the outcomes of this study could inform water resource management strategies in the three watersheds, particularly in response to anticipated climate change and extreme weather fluctuations

DOI: 10.22034/gjesm.2025.03.15

This is an open access article under the CC BY license (http://creativecommons.org/licenses/by/4.0/).

NUMBER OF REFERENCES	NUMBER OF FIGURES	NUMBER OF TABLES
41	8	3

*Corresponding Author:
Email: *maha001@brin.go.id*
Phone: +62811945991
ORCID: 0000-0001-8185-2958

Note: Discussion period for this manuscript open until Sep 1, 2025 on GJESM website at the "Show Article".

INTRODUCTION

Effective water resource management in tropical regions like Indonesia requires a comprehensive understanding of the spatial and temporal variability of rainfall at the watershed scale. Unpredictable rainfall patterns frequently result in hydrological extremes like floods and droughts, which can happen concurrently within the same region (Alemu and Bawoke, 2020). Climate change amplifies these challenges by increasing monsoonal variability and the frequency of extreme weather occurrences (Li *et al.,* 2023). Although satellite-based precipitation datasets such as Climate Hazards Group InfraRed Precipitation with Station (CHIRPS) and Global Satellite Mapping of Precipitation Near-Real-Time (GSMaP-GNRT) have enhanced rainfall monitoring, the relationship between rainfall variability, watershed geomorphology, and atmospheric circulation remains insufficiently explored (Saharia *et al.,* 2021). The diverse hydroclimatic conditions and complex geography of Indonesia create a perfect backdrop for studying the interplay between rainfall patterns, watershed attributes, and overarching climatic factors. The Brantas, Toba-Asahan, and Larona-Malili watersheds are strategically important for hydropower, irrigation, and tourism, yet are increasingly vulnerable to both climatic and anthropogenic pressures. Each basin represents distinct geomorphological and climatic conditions, ranging from the volcanic highlands of Lake Toba, the densely populated and intensively cultivated Brantas basin, to the mountainous terrain of the Larona-Malili region. The variability of rainfall throughout the archipelago is influenced by its physical geography, dominant wind patterns, and terrain, leading to distinct equatorial, monsoonal, and localized rainfall patterns (Kurniadi *et al.,* 2023). Previous studies have emphasized the importance of seasonal rainfall variability in water resource planning (Aksu, 2023; Narulita *et al.,* 2021) and the utility of satellite-derived products like CHIRPS for hydrological assessments (Wiwoho *et al.,* 2021). Furthermore, numerous research initiatives have investigated the hydrological and environmental dynamics in Indonesian watersheds, concentrating on flood susceptibility, alterations in land use, and the deterioration of water quality. For instance, Dede *et al.,* (2023) investigated the link between land use patterns and river ecosystem services using spatial correlation methods. The study conducted by Setiawan *et al.* (2024) employed the analytical hierarchy process (AHP) alongside a geographic information system (GIS) framework to identify suitable micro-hydropower dam sites in Banyumas, highlighting the importance of slope, land cover, and river proximity. Narendra *et al.,* (2024) used principal component analysis (PCA) and GIS to map flood vulnerability on Lombok Island, while Rosyidy and Frimawaty (2024) documented spatiotemporal patterns of oil palm expansion in Jambi Province. Furthermore, Marisi *et al.,* (2025) indicated that alterations in land use and land cover (LULC) within the Upper Bekasi watershed were associated with rising levels of pollutant concentrations. While these studies offer valuable insights, most emphasize spatial analyses and direct land use impacts, relying heavily on GIS-based methods and remote sensing, without fully integrating long-term temporal variability or the influence of large-scale climate oscillations. This study aims to fill this gap by performing an extensive spatiotemporal analysis of rainfall variability in the three primary Indonesian watersheds discussed earlier, covering the period from 2000 to 2023. By integrating high-resolution satellite precipitation datasets (CHIRPS and GSMaP-GNRT), applying Mann-Kendall trend tests, and employing fast fourier transform (FFT) analyses, this research captures both temporal trends and frequency-domain characteristics of rainfall. Moreover, it uniquely incorporates correlations with large-scale climate phenomena such as the El Niño-Southern Oscillation (ENSO), Indian Ocean Dipole (IOD), and Western Pacific Monsoon Index (WPMI), providing a more holistic understanding of how global climatic variability influences regional hydrological processes. The results indicate that only the Larona-Malili watershed exhibits a significant increasing trend in rainfall, implying varying climate sensitivities among the basins. This study provides insights that support the creation of more adaptable and region-specific strategies for water management. The insights generated aim to inform flood and drought mitigation planning, support climate adaptation policies, and enhance the long-term sustainability of water resources in Indonesia. This study's innovation is its comparative examination of rainfall variability through satellite data across various watersheds in Indonesia, highlighting specific results for each

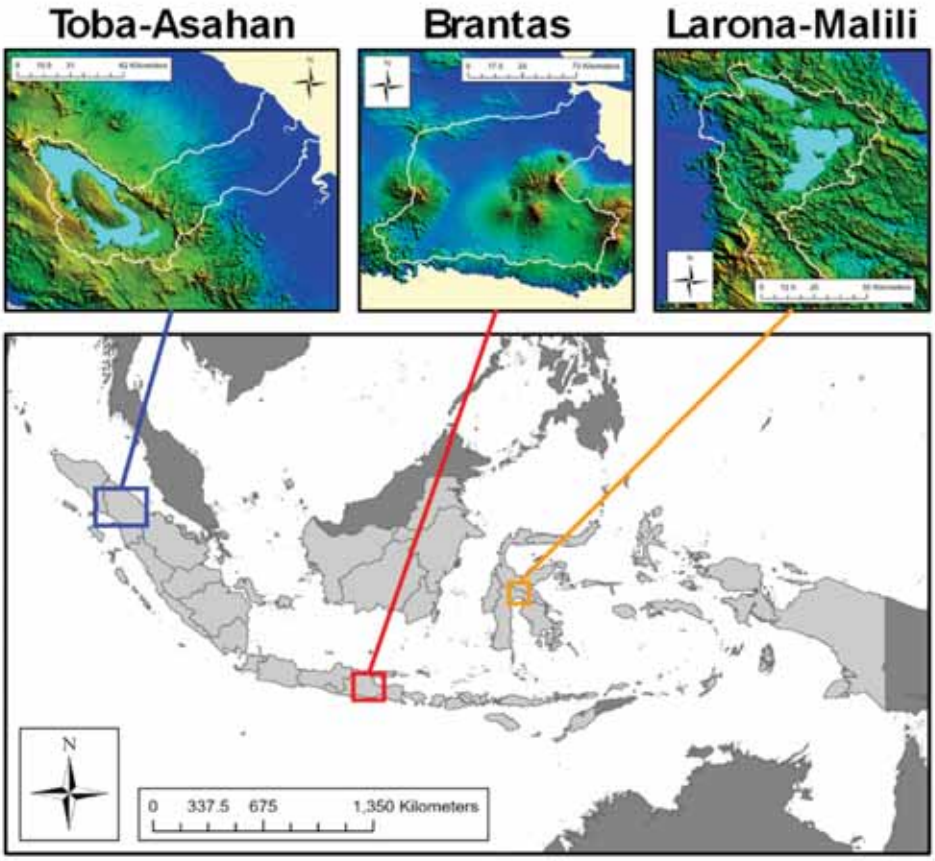

Fig. 1: Geographical location of the study area in the Toba-Asahan, Brantas, and Larona-Malili watershed regions, in Indonesia

basin. Notably, the Larona-Malili watershed shows a significant increasing rainfall trend that is not present in the other two watersheds; it also reveals distinct rainfall patterns that correspond to the unique climatic traits of each region, as well as varying climate sensitivities among the three watersheds. This study provides a foundation for more effective and sustainable water resource management strategies and supports the growing urgency for climate adaptation policies in Indonesia. This study has been condacted in Asahan Toba, Brantas, and Larona Malili watersheds, Indonesia in 2023-2024.

MATERIALS AND METHODS

The study area

The Larona-Malili watershed, in Sulawesi, is influenced by tropical rainforest ecosystems and hydroelectric power activities. These watersheds were selected due to their diverse hydrological and climatological conditions, illustrating a range of watershed traits across Indonesia. Fig. 1 shows the study area for the three watersheds.

Materials

GSMaP-GNRT data, part of the GPM dataset, was utilized to provide global rainfall information with high spatial and temporal resolution GPM uses radar instruments and microwave measurements on multiple satellites to collect rainfall data. The GSMaP-GNRT (version 6) Real-time Gauge-adjusted Precipitation product from Japan Aerospace Exploration Agency (JAXA) is processed 4 hours after observation and distributed with a spatial resolution of 0.1 degree (°) × 0.1° and a temporal resolution of 1 hour. This dataset has been available since April 2000. Generally, the accuracy of gauge-adjusted products is higher than that of uncorrected products (Kubota *et al.*, 2020; Li *et al.*, 2024). The dataset is

publicly accessible through the JAXA Global Rainfall Watch System (Kubota *et al.*, 2020). The GSMap_NRT data has been validated using rainfall data from three watersheds in Indonesia, which include the Brantas and Larona-Malili watersheds. Syaifullah (2014) found that the GSMap_NRT value has a pattern that follows the observed (actual) rainfall, although the value tends to be below the estimate. This variation could stem from the use of rain gauges that are not sufficiently representative of the watershed, causing the average rainfall in the region to be an unreliable indicator of the watershed's conditions. The CHIRPS exploited in this study is a satellite-based rainfall dataset designed to analyze rainfall in global land regions. This dataset is frequently utilized to investigate rainfall trends, climate variability, and the effects of extreme weather, particularly in tropical areas. Spatial resolution: 0.05° x 0.05° (~5 km), temporal resolution: daily, decadal (10 days), and monthly. The CHIRPS dataset (Funk *et al.*, 2015) covers the global region between 50° North (N) and 50° South (S), with a focus on tropical and subtropical areas. The dataset used includes monthly data from 1981 to 2024. The geomorphological analysis of the three catchments was carried out using the 2019 land use map published by the Ministry of Environment and Forestry (KLHK), the watershed boundary map, and the high-resolution topographic map (DEMNAS) obtained from the Geospatial Information Agency (BIG). The dipole mode index (DMI) is an essential indicator in climate studies. It is capable of assessing the fluctuations in sea surface temperature between two significant areas in the Indian Ocean. It is often used to monitor and analyze the phenomenon known as the Dipole Mode or Indian Ocean Dipole (IOD). Sea surface temperature (SST) in the Niño 3.4 region is a crucial indicator in climate studies used to monitor and analyze El Niño and La Niña phenomena. Data sources for DMI and Niño 3.4 SST anomalies are available from the Physical Sciences Laboratory (PSL) of the National Oceanic and Atmospheric Administration (NOAA) in the United States, and can be downloaded.

Methods

The study begins with the identification of the three watersheds, including their geomorphological and topographical characteristics, through a thematic watershed analysis that considers land use and cover. Land-use changes in Java's Brantas watershed from 1995 to 2015 were driven by economic, social, technological, and biophysical factors, leading to significant transitions from forests and agriculture to urban areas (Wiwoho *et al.*, 2023). The study of temporal analysis focuses on historical precipitation trends across daily and monthly intervals. Land-use changes, sedimentation, coastal erosion, and rainfall variability highlight the need for sustainable planning and adaptive strategies in Java (Nofirman *et al.*, 2023). The three selected watersheds—Toba-Asahan, Brantas, and Larona-Malili—exhibit varied hydrological and climatological conditions, representing different characteristics of Indonesian watersheds. The study initiates by identifying these watersheds, emphasizing their geomorphological and topographical characteristics through a thematic analysis that takes into account land use and cover. A temporal analysis investigates historical rainfall patterns on both monthly and daily scales. This study underlines the importance of managing water resources, which encompasses irrigation strategies and drought prevention measures. Rainfall distribution is analyzed by calculating the average CHIRPS rainfall during periods of significant climate phenomena, and descriptive statistics are used to assess regional average differences between phases with negative and positive standard deviations. An annual examination of daily variations in watersheds deepens insight into daily meteorological and hydrological behaviors, highlighting diurnal cycle trends and essential rainfall phases that can fluctuate across various watersheds. (Kamal *et al.*, 2019) Employed the non-parametric Mann-Kendall test to identify climate variable behavior using database records. Conducted a trend analysis of annual average temperature, rainfall, and river discharge in Afghanistan from 1980 to 2022 using the Mann-Kendall (MK) test and Sen's Slope estimator (SS) with ECMWF reanalysis v5 (ERA5) data (Akhundzadah, 2024). The Mann-Kendall and Sen's Slope tests identified a decreasing rainfall trend in Mempawah, an increasing trend in Kubu Raya, and significant drying in Sungai Kunyit as -33.20 milligrams per year (mm/y), highlighting the impact of climate change on water availability in West Kalimantan from 2000 to 2019 (Aditya *et al.*, 2021). Diurnal Hovmöller analysis for the three watersheds illustrates the temporal and spatial rainfall patterns specific to region. This strategy

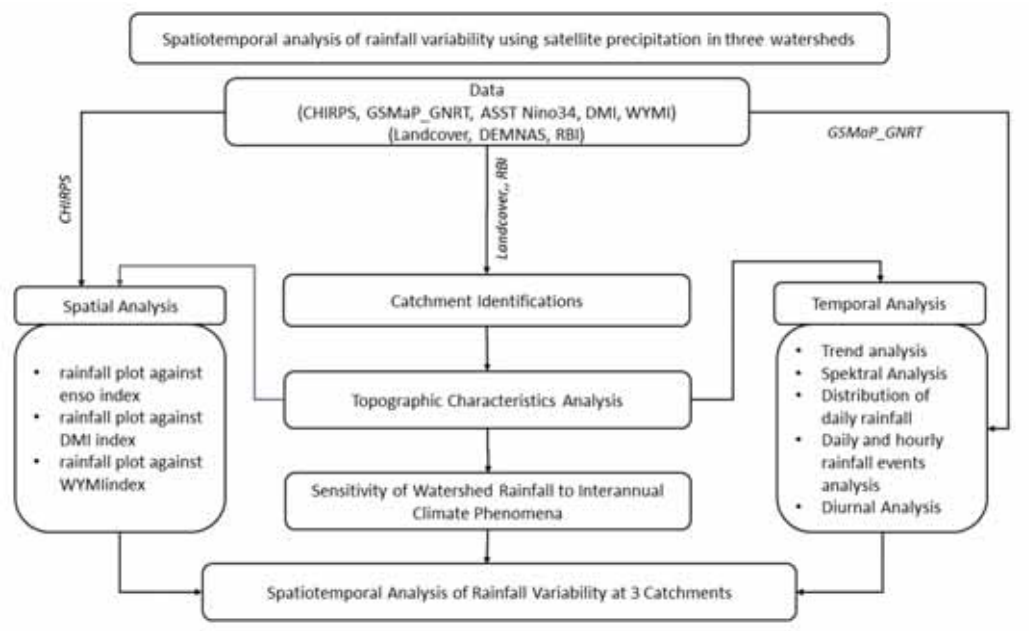

Fig. 2: Research flowchart

facilitates the visualization of daily fluctuations throughout the year, offering essential insights for watershed management, disaster prevention, and hydrological analysis. For instance, it can determine whether rainfall frequently occurs in the afternoon to evening due to topographical influences, valley-mountain wind cycles, or orographic effects. Rainfall patterns in the Ili region fluctuate according to the terrain, exhibiting afternoon peaks in mountainous areas and evening peaks in the valleys, largely driven by vertical velocity and the mixing ratio of water vapor (Li, *et al*., 2023). Organized convection drives most seasonal rainfall in South America, moving westward across the Amazon Basin, influenced by wind patterns, Convective Available Potential Energy (CAPE), and transient disturbances (Filho *et al*., 2015). The impact of climate phenomena on rainfall in the three watersheds is influenced by factors such as the monsoon, represented by the Webster and Yang Monsoon Index (Webster *et al*., 1992), IOD indicated by the Dipole Mode Index, and the El Niño Southern Oscillation (ENSO) measured using the Nino3.4 index (Trenberth *et al*., 1997). Conducting a sensitivity analysis of watershed rainfall to these interannual climate phenomena, including the El Niño-Southern Oscillation (ENSO), the Indian Ocean Dipole (IOD), and the Madden-Julian Oscillation (MJO), is essential for understanding their long-term effects. Utilizing spectral analysis allows for the identification of key frequencies or oscillation periods in time series data (Wilks, 2011), with a focus on detecting cyclical trends in rainfall data recorded on a daily or monthly basis. This method has been applied in various studies in Indonesia, such as analyzing zonal wind components in the Pontianak region to determine monsoon intensity and employing spectral analysis to investigate variations in sea level and wind fluctuations through cross-correlation spectrum analysis (Oktavia *et al*., 2011). Furthermore, spectral Fast Fourier Transform (FFT) analysis was applied to assess fluctuations in sea level and wind wind fluctuations using cross-correlation spectrum analysis, components such as cross-energy density spectrum, squared coherence, and phase difference. The Webster-Yang Monsoon Index (WYMI) is determined by the difference in zonal wind speed between the upper level as 200 hectoPascal (hPa) and the lower level (850 hPa) within the Asian monsoon core region (40° East (E)–110°E, 0°–20° North (N)), calculated as WYMI = U850 − U200. Here, U850 represents the zonal wind at 850 hPa and U200 at 200 hPa. Strong monsoon intensity is indicated by positive WYMI values, which are associated with a strong southwest monsoon flow, while negative values represent weak monsoon

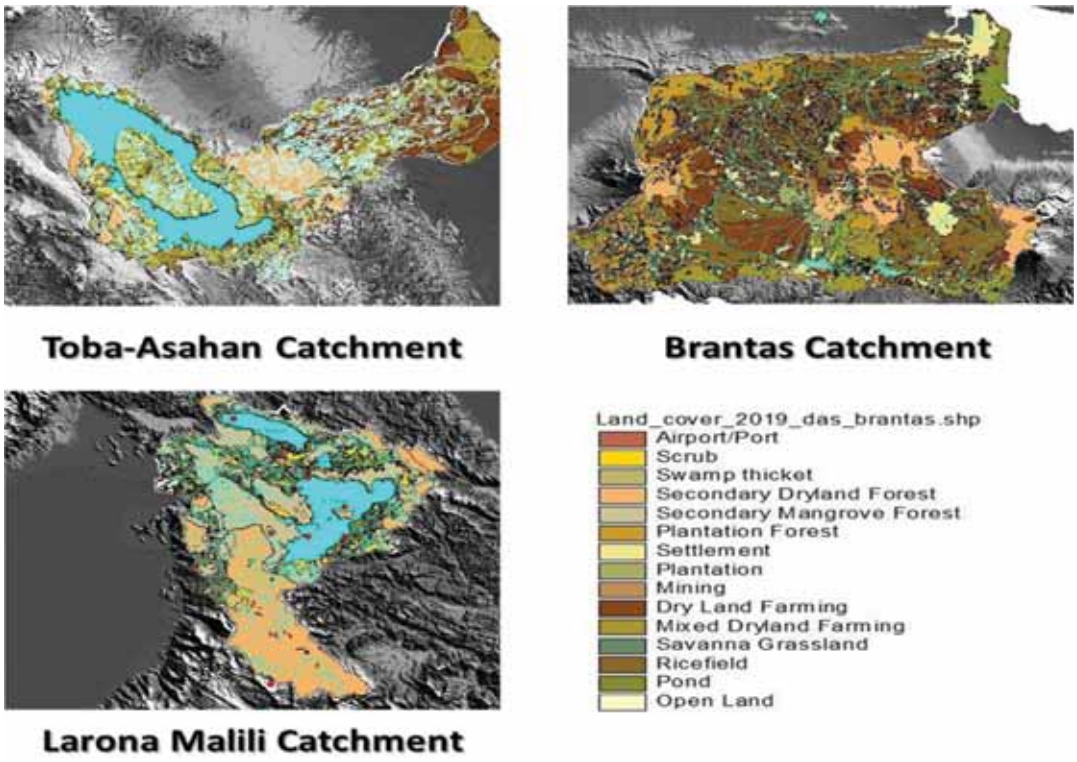

Fig. 3: Land cover map of the Toba-Asahan, Brantas and Larona-Malili watersheds.

conditions. Elevated WYMI values are generally linked to vigorous monsoon activity, potentially leading to severe rainfall occurrences in specific watersheds. Sensitivity analysis is performed utilizing correlation and regression models. The correlation model determines the relationship between rainfall and SST_Nino34, WYMI, and DMI. In contrast, the regression model measures the combined contribution or influence of SST_Nino34, WYMI, and DMI on rainfall in each watershed. Data processing is conducted using R studio. Fig. 2 shows the flowchart of the current study.

RESULTS AND DISCUSSION

Fig. 3 depicts the land cover maps of the Toba-Asahan, Brantas, and Larona-Malili watersheds issued by the Ministry of Environment and Forestry (KLHK) in 2019.

Topographic characteristics of the Toba-Asahan watershed

The Toba-Asahan watershed comprises Toba Lake and the Asahan River in North Sumatra, Indonesia. Covering an area of approximately 7,415 square kilometers (km^2), it is part of the Toba-Asahan River Region, designated as a national strategic river region by Presidential Decree No. 12 of 2012 of the Republic of Indonesia. Toba Lake, recognized as the largest volcanic lake globally, spans about 100 kilometers in length and 30 kilometers in width, with depths reaching as much as 508 meters. Water from Toba Lake flows through the Asahan River, a main river that stretches 153.82 km with an average width of 50 m, from the outlet of Toba Lake in Porsea District to the coast at the Malacca Strait (Tanjung Balai City). The geomorphology of the Toba-Asahan watershed in North Sumatra is notably complex, a result of ancient volcanic eruptions. This substantial eruption resulted in a large caldera that now contains Toba Lake, with the Asahan River being its primary drainage. The topography of the Toba-Asahan watershed ranges from the lake's surface level (approximately 905 meters above sea level) to the surrounding mountains, which reach heights of over 2,000 meters. The region surrounding the caldera is characterized by steep slopes and mountains.

Industrial activities such as the Asahan Hydroelectric Power Plant (PLTA Asahan) are significant elements in this watershed, utilizing the Asahan River's flow as an energy source. The geographical features of the Toba-Asahan watershed have a major impact on the area's precipitation trends. According to the 2019 land use map analysis by KLHK, the Toba-Asahan watershed is predominantly composed of dryland agriculture as 38.7 percent (%), plantations (25%), secondary dryland forest (14%), shrubs (6.2%), plantation forests (5.4%), and paddy fields (4%). Residential areas account for only about 1.3% of the total watershed area. Modifications to land cover in watershed zones greatly impact the nature of water flows and rainfall (Syarifuddin, 2022). This circumstance has a profound effect on the administration of water resources in the region. The land cover of the Toba-Asahan watershed (Fig. 3) significantly influence rainfall patterns. The mountains in the vicinity function as barriers to moist air masses, forcing them to rise, cool adiabatically, and undergo condensation. Due to the southwest monsoon, higher rainfall occurs on windward slopes, primarily in the west and southwest. In contrast, the rain shadow effect causes leeward slopes (those facing east and northeast) to be drier. Lake Toba increases local precipitation by releasing moisture through evaporation, especially during the afternoon when elevated temperatures initiate daily rain patterns in the vicinity of the lake. Dryland agriculture (38.7%) has lower infiltration rates than forests, resulting in increased runoff and a greater reliance on rainfall and irrigation. Plantations (25%) have high water demands, and poor conservation can accelerate runoff. Residential areas (1.3%) have relatively low water needs. The balance of agricultural activities, plantations, and forests is crucial for the watershed's water resources. Its dominance by dryland agriculture and plantations increases drought vulnerability. For sustainability, it is vital to implement effective land conservation, manage irrigation properly, and protect watersheds.

Topographic characteristics of the Brantas watershed

The Brantas watershed, one of Indonesia's largest, is in East Java Province. The Brantas River, the main river, is approximately 320 km long and is the second-longest river on Java Island after Bengawan Solo. The Brantas watershed spans an area of roughly 12,069 km², equivalent to around 25% of East Java Province's total area. Over thousands of years, volcanic activity and sediment deposition have sculpted the Brantas watershed. Topographically, the Brantas watershed encompasses a range of hilly to lowland areas. The upstream section is characterized by hilly and mountainous topography, particularly around Mount Arjuno and Welirang, with steep slopes. Downstream, the topography becomes gentler and tends to be flat. In the vicinity of the Sutami Reservoir, certain watersheds capture water from the Brantas River prior to its downstream flow. Elevation in the watershed ranges from over 3,000 meters in the upstream mountainous areas of Mount Arjuno to around 200 meters in the lowland areas near the reservoir. The Brantas watershed encompasses vast agricultural regions, mainly featuring irrigated rice fields in the low-lying areas and dryland farming in the hilly terrain. The main land use surrounding the reservoir is agriculture, which includes a variety of food crops, including rice, maize, and vegetables. These forests are crucial for maintaining soil stability and water flow to the reservoir. The Brantas watershed encompasses both residential and urban regions, particularly in the vicinity of Malang City. According to the 2019 land use map analysis by KLHK, the Brantas watershed is dominated by paddy fields (35.5%), residential areas (16.2%), plantation forests (15.5%), dryland agriculture (11.4%), mixed dryland agriculture (8.8%), secondary dryland forest (7.3%), fish ponds (2%), and plantations (1.3%). Urban and rural residential areas significantly dominate the total watershed area. The Brantas watershed features a varied landscape, shifting from steep mountainous terrains in the upstream regions surrounding Mount Arjuno and Welirang (exceeding 3,000 m) to more gradual lowlands close to the Sutami Reservoir (about 200 m). The upstream region features steep slopes and forested areas, whereas the middle and lower reaches become flatter, supporting extensive agricultural activities. The Sutami Reservoir and its adjacent watersheds are essential for managing water flow prior to its arrival in downstream regions. Agriculture dominates the watershed, particularly irrigated paddy fields (35.5%) and dryland farming, with crops such as rice, maize, and vegetables. Protected forests (15.5% plantation, 7.3% secondary) act as erosion buffers and help regulate river flow, although their limited coverage affects overall hydrological stability. Urban expansion of urban

environments, particularly in Malang City, leads to more infrastructure development and rising water demand, thereby affecting sedimentation and the quality of water. The watershed is facing significant pressure from urbanization and agricultural activities, resulting in increased erosion and potential sedimentation in rivers and reservoirs. The significant proportion of paddy fields, residential zones (16.2%), and dryland farming necessitates efficient land and water management approaches. If not correctly managed, sedimentation can reduce reservoir storage capacity, affecting water supplies for irrigation and domestic use. Achieving a balance between agricultural productivity, urban expansion, and hydrological sustainability remains a critical challenge for watershed management.

Topographic characteristics of the Larona-Malili watershed

The Larona-Malili watershed is in East Luwu Regency, South Sulawesi, Indonesia. This watershed comprises three large lakes that form a cascade: Lake Matano, Lake Mahalona, and Lake Towuti. Water from these lakes is channeled into the Larona River, which is utilized for the Larona Hydroelectric Power Plant (PLTA Larona). The Larona-Malili watershed covers a rainfall catchment area of approximately 4,943 km². The Larona-Malili watershed exhibits a varied topography, with elevation levels that transition from lowlands adjacent to valleys and lakes to the encircling mountain ranges. According to land use map analysis, the Larona-Malili watershed is predominantly covered by primary forests, consisting of primary dryland forests (36.3%) and secondary dryland forests (35.4%), followed by shrubs (10.4%), mixed dryland agriculture (8.8%), dryland agriculture (2.7%), open land (1.8%), and paddy fields and fish ponds, each comprising 1%. Approximately 0.4% of the entire watershed area is comprised of residential neighborhoods, predominantly found in the downstream region. Characterized by tropical forests, the Larona-Malili watershed functions as a conservation area and a hub for biodiversity. Besides forests, residential areas, small-scale agriculture, mining, and fishing activities surround the lakes. The extensive primary and secondary forests (71.7%) that dominate this area indicate that the watershed's condition is still relatively good. Maintaining the hydrological cycle heavily relies on primary and secondary dryland forests. The dense plant life within these forests promotes the infiltration of rainwater into the soil, curtails surface runoff, and sustains groundwater availability all year long, contributing to stable river discharge. It reduces drought risk during the dry season. Open land areas (1.8%) have a high risk of erosion due to the lack of vegetation protecting the soil from rain erosion. When found in upstream locations, this can result in heightened sedimentation within rivers and reservoirs, potentially reducing water storage capacity. The presence of reservoirs and the dominance of primary forests can help reduce sedimentation and maintain a stable water supply for existing hydroelectric power plants (PLTA). The limited residential zone (0.4%) located in the lower section of the watershed indicates that the demand for domestic water may remain relatively low in relation to the total water availability. However, if there is rapid residential growth, effective management of clean water and sanitation is necessary to prevent contamination of water sources. The central water bodies include the Larona River and Malili Reservoir, which play essential roles in irrigation and power generation. Certain regions show clear signs of environmental degradation, primarily due to deforestation linked to the expansion of plantations and mining operations. Overall, the Larona-Malili watershed has good water resource potential due to the dominance of primary forests, which contribute to water conservation and hydrological regulation. Nonetheless, challenges must be taken into account, including the possible degradation of open land regions and alterations in land use that may impact future water resources

Spatial distribution of rainfall in watersheds

The spatial rainfall assessment of the three watersheds utilizes precipitation data from CHIRPS, recognized for its relatively high resolution. Monthly rainfall maps were created using CHIRPS data from 2001 to 2024 for the three watersheds, linked to three climate phenomena: ENSO, represented by the Niño3.4 Index; Dipole Mode, represented by the DMI; and the monsoon, represented by the Webster-Yang Monsoon Index (WYMI). Each index was analyzed under two conditions: below the negative standard deviation of the index value (SD-) and above the positive standard deviation of the index value (SD+). The results are presented in Fig. 4. As illustrated in

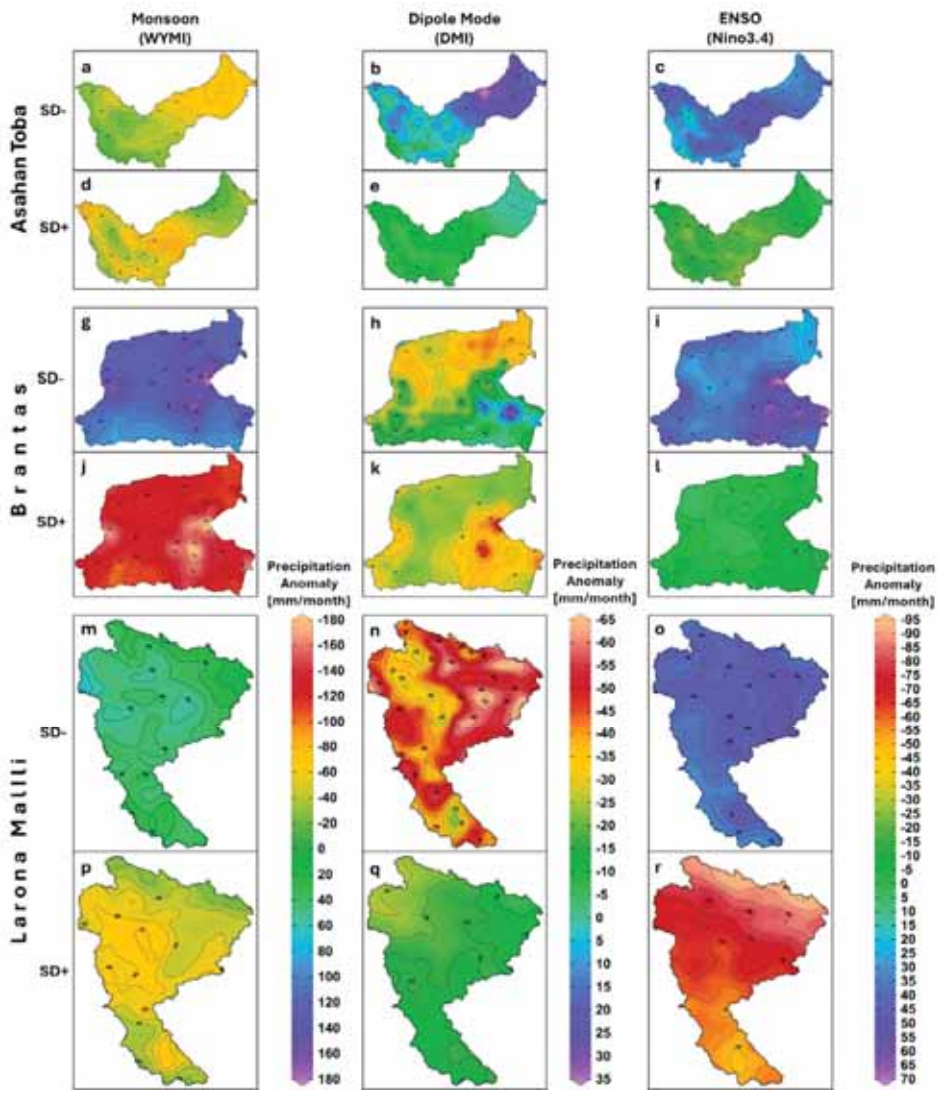

Fig. 4: Rainfall distribution patterns in the Asahan Toba, Branstas, and Larona Malili watersheds (from top to bottom) are influenced by WYMI, DMI, and Niño3.4 (from left to right) in the positive phase (SD+, above the positive standard deviation) and negative phase (SD-, below the negative standard deviation). The values in the rainfall legend for each climate phenomenon are different.

Fig. 4, the analysis of the distance from the watershed (DAS) to the source and the traits of each climate phenomenon indicates that the Brantas watershed is governed by a monsoon system, significantly influenced by the fluctuations in monsoon activity. Meanwhile, the Asahan Toba watershed, closest to the origin of the IOD, exhibits the most potent influence among the three climate phenomena. The Larona Malili watershed is notably impacted by the ENSO, given that its source is in close proximity to Larona Malili. When ranked by watershed, the Asahan Toba watershed demonstrates the most prominent climate phenomena in sequence: IOD, ENSO, and Monsoon. In contrast, the Brantas watershed is influenced by Monsoon, IOD, and ENSO, while the Larona Malili watershed is affected by ENSO, Monsoon, and IOD. Table 1 supports the findings illustrated in Fig. 4, highlighting the key climate phenomena that quantitatively impact each watershed. Conversely, it also reveals the ranking of watersheds based on the

Table 1: Minimum and maximum values and the difference between the average rainfall anomalies of each watershed area for each climate phenomenon between SD- and SD+

Climate phenomena	Phase	Asahan Toba			Brantas			Larona Malili		
		Min.	Max.	Mean	Min.	Max.	Mean	Min.	Max.	Mean
Monsoon (WYMI)	SD-	-75	-11	-45	84	184	123	15	64	38
	SD+	-89	-6	-47	-187	-104	-132	-79	-22	-50
Difference				2			255			88
Dipole Mode (DMI)	SD-	-12	38	11	-44	29	-21	-67	-18	-47
	SD+	-13	1	-7	-49	-20	-29	-26	-6	-16
Difference				18			7			-31
ENSO (Nino3.4)	SD-	14	57	38	18	73	40	29	56	44
	SD+	-27	5	-15	-14	5	-3	-95	-47	-71
Difference				52			43			115

(Green indicates the most significant difference, and red means the smallest)

strength of influence of each climate phenomenon. The more significant the difference between the SD- and SD+ mean rainfall areas, the stronger the impact of the respective climate phenomenon (highlighted in green). Furthermore, these values demonstrate the cumulative impacts of climatic factors across watersheds and different climate events. The maximum difference of 225 mm/month occurs in the Brantas watershed under the influence of the monsoon. The second highest difference is ENSO, with 115 mm/month, followed by another significant difference in the Brantas watershed, with a 43 mm/month value. This trend continues in subsequent different rankings. The rainy season has significantly affects rainfall variability in the Brantas watershed compared to Larona-Malili or Toba-Asahan. Of the three, Larona-Malili experiences the greatest impact from the rainy season, whereas Toba-Asahan is the least impacted. The rainy season has a considerable effect on Brantas due to its position in Region A, which is marked by a monsoonal climate featuring distinct wet and one dry season. The dipole mode event (DME) has a significant impact on Toba-Asahan, primarily because of its close geographical location to the DME activity center. This is supported by previous studies, including Khaldun *et al.* (2017) and Hendon (2003), which provide detailed analyses of the DME's influence on rainfall fluctuations in the Toba-Asahan region. Meanwhile, ENSO plays a dominant role in Larona-Malili, establishing it as a key ENSO-sensitive watershed. In terms of ENSO-related variability, Larona-Malili's rainfall ranks second, just behind Brantas, and is predominantly influenced by seasonal monsoon rains. Studies by Lestari *et al*. (2023) and Arsyad *et al.* (2023) have further explored the impact of ENSO on rainfall patterns in and around the Larona-Malili watershed.

Temporal trend of rainfall

The study employs the Mann-Kendall method to analyze temporal rainfall trends in the Toba-Asahan, Brantas, and Larona-Malili watersheds using monthly GSMaP_GNRT data from 2001 to 2024. The analysis provides the slope, Z-score, and P-value, where a positive slope represents a rising trend, a negative slope represents a falling trend, and a slope that is nearly zero implies no significant variation. The Z-score determines statistical significance, at $|Z|>1.96$ at $\alpha=0.05$ demonstrates a meaningful trend. Table 2 presents the results of the Mann-Kendall analysis. The findings of the Mann-Kendall test for the three watersheds, as presented in Table 2, can be interpreted in the following manner: For the Toba-Asahan watershed, the Z-score value of 1.178532946 is smaller than the critical value of 1.96 (for $\alpha=0.05$), indicating that there is no significant trend. The P-value of 0.2385842 is greater than 0.05; therefore, the null hypothesis is not rejected, meaning there is no significant trend. The Z-score of

Table 2: Mann-Kendall test results for the three watersheds with a data length of 288 months (2001 ~ 2024)

Parameters	Watershed		
	Toba-Asahan	Brantas	Larona-Malili
Trend	no-trend	no-trend	increasing
Z-Score	1.17853294649	1.19200323480	2.5052247900
P-Value	0.238584205709	0.23325997688	0.01223735914
Sen's slope estimated	0.092604347826	0.0437962962	0.257294323979

the Brantas watershed is 1.1920032, which is below the critical threshold of 1.96 (for α=0.05), suggesting that there is no observable trend. The P-value of 0.233260 is more significant than 0.05. Thus, the null hypothesis is accepted, meaning there is no trend. For the Larona-Malili watershed, the Z-score value of 2.50522479 is greater than the critical value of 1.96 (for α = 0.05), indicating that the trend is statistically significant and increasing. The P-value of 0.012237359 is smaller than 0.05; therefore, the null hypothesis is rejected, meaning there is a significant trend of an increased rainfall of 0.2573 mm/month. The findings indicate that the Larona-Malili watershed exhibits a notable upward trend, observed both statistically and in practical applications. Few publications discuss the rainfall trends and their relationship to the increase in water levels in the lakes within the Larona-Malili watershed, including Lake Matano, Lake Mahalona, and Lake Towuti. The growing levels of rainfall have a favorable effect on the Larona-Malili watershed, as it supports a hydroelectric power station that necessitates an adequate water for nickel manufacturing. Additionally, the adequate water resources in these three lakes benefit the surrounding communities. As for the Brantas watershed, there is no significant statistical trend. Thus, no definitive conclusion can be drawn about long-term changes in rainfall. The result of Toba-Asahan watershed suggests that observed variations in rainfall are more likely due to interannual fluctuations rather than a consistent long-term trend. Previous study by Irwandi et al. (2021) indicated that the water level of Lake Toba is affected by rainfall and runoff; however, the present analysis does not reveal any clear patterns of rainfall variation over time.

Spectral rainfall analysis in the watersheds

To perform spectral analysis of daily GSMaP data for the three watersheds, the fast fourier transform (FFT) technique is employed to transform the data from the time domain to the frequency domain, thereby identifying the spectral peaks. In Fig. 5, part a) presents the time series of daily rainfall data, while part b) displays the power spectrum for the Toba-Asahan, Brantas, and Larona-Malili watersheds. The outcomes of the spectral analysis regarding daily rainfall across the three watersheds can be articulated as follows. The FFT rainfall analysis in the Toba-Asahan watershed shows two spectral peaks at frequencies of 0.00272 (367 days or 12 months) and 0.00546 (182 days or 6 months). The FFT analysis of precipitation in the Brantas watershed reveals a single spectral peak at a frequency of 0.00271, corresponding to 369 days or one year. In the Larona-Malili watershed, the FFT analysis of precipitation identifies four prominent spectral peaks at frequencies of 0.00272 (367 days or one year), 0.00546 (183 days or 6 months), 0.0082 (122 days or 4 months), and 0.0109 (92 days or 3 months). Fig. 5 shows that for the Toba-Asahan watershed, the dominant period of 367 days/12 months shows an annual cycle reflecting the seasonal rainfall cycle, which is likely related to monsoon changes affecting the Toba-Asahan watershed following the tropical yearly cycle. The period of 182 days/6 months indicates a semi-annual cycle associated with the influence of two prominent rainy season peaks in a year. This occurrence is frequently seen in tropical regions that experience transitional seasons. The dominant period of the Brantas watershed is 369 days/12 months, which reflects a strong and regular monsoon cycle similar to that of the Toba-Asahan watershed. The absence of additional frequencies or periods suggests that a straightforward annual cycle predominates in the Brantas watershed, with minimal influence from semi-annual or shorter cycles. The Larona-Malili watershed's dominant period of 367 days, equivalent to 12 months, is also observed, indicating an annual pattern that reflects a significant monsoon influence in this watershed, similar to the Toba-Asahan and Brantas watersheds.

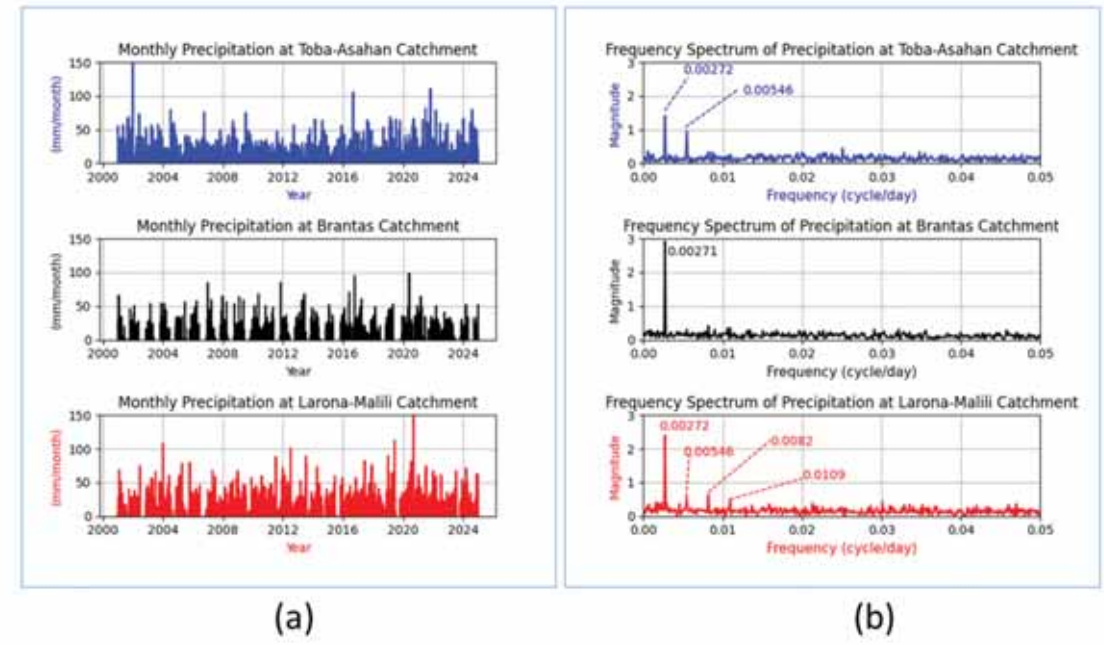

Fig. 5: Time series of monthly/daily rainfall (a) and its power spectrum (b)

There are also semi-annual, quarterly, and intra-seasonal patterns that correspond to durations of 6 months, 4 months, and ~2.5 months, respectively. The semi-annual pattern indicates the presence of two main rainy seasons within a year, similar to the Toba-Asahan watershed. The quarterly trend is probably connected to regional variations or the impact of sub-seasonal phenomena such as the MJO. Variability in local or regional weather systems, such as tropical cyclones, atmospheric waves, or micro-monsoon influences, can lead to a shorter intra-seasonal pattern. The dominant annual pattern observed in all three watersheds, lasting 12 months, highlights the significant impact of the annual monsoon cycle on rainfall. In contrast, the Toba-Asahan and the Larona-Malili watersheds have a semi-annual pattern (6 months), indicating two main rainy seasons within a year. The Brantas watershed exhibits a more straightforward spectral pattern, characterized by a single dominant frequency (~12 months), indicating that rainfall in this watershed tends to be relatively stable, with minimal sub-seasonal fluctuations. Factors that impact spectral variability in climatic occurrences imply that the both annual and semi-annual cycles are usually related to monsoon phenomena. Simultaneously, the quarterly and intra-seasonal trends may be associated with the MJO, Kelvin waves, or Rossby waves.

Distribution of daily rainfall in the watersheds

The examination of the daily rainfall distribution map facilitates the identification of both spatial and temporal rainfall trends and irregularities in the watershed regions under review. The daily rainfall distribution for the three watersheds is presented in Fig. 6, featuring the vertical axis indicating the dates from January 1 to December 31 and the horizontal axis representing the years 2001 to 2024. As depicted in Fig. 6, precipitation occurrences in the Toba-Asahan watershed are nearly constant throughout the month, with increased intensity observed from July to December. El Niño years (2002-2003, 2004-2005, 2006-2007, 2009-2010, 2014-2016, 2018-2019, and 2023-2024) do not significantly alter rainfall patterns in this watershed. This trend reveals that local conditions, particularly orographic effects and regional atmospheric circulation, are crucial in regulating rainfall pattern. In the Brantas watershed, rainfall is most frequent from January to May and November to December. During El Niño years, the

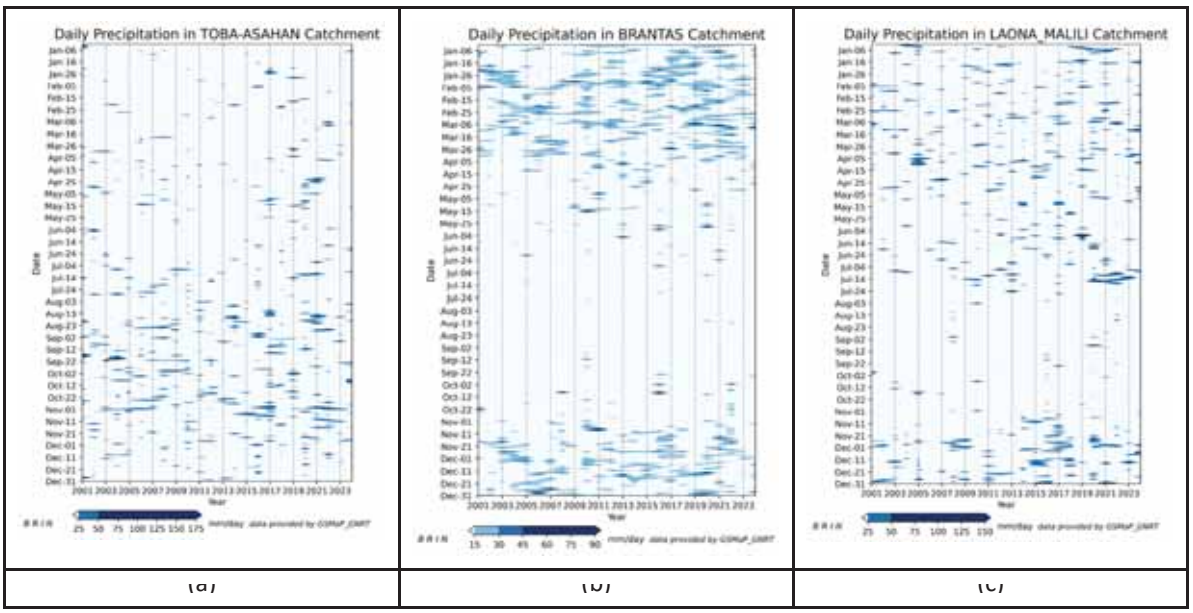

Fig. 6: Distribution of Daily Rainfall in the three watersheds Toba-Asahan (a), Brantas (b) and Larona-Malili (c) respectively from 2001 to 2023

dry season is prolonged due to a notable decrease in rainfall, as reflected in extended dry periods. Rainfall in the Larona-Malili watershed is particularly intense from January through July and from November to December. Unlike Brantas, El Niño years do not cause a substantial reduction in rainfall, as sporadic rainfall events persist even during typically dry months. These findings align with the classification of three distinct climatic regions in Indonesia, where ENSO has a strong influence on rainfall variability in Regions A and C. Conversely, Region B reveals a less pronounced ENSO signal, demonstrating notable correlations between SST and rainfall fluctuations, especially from June to November (Aldrian and Susanto, 2003).

Distribution of daily and hourly rainfall events

The data on rainfall can be segmented into predetermined intervals to evaluate the distribution of rainfall events within the three watersheds. For daily rainfall events, the intervals are: 15mm-20mm, 20mm-25mm, 25mm-30mm, 30mm-40mm, 40mm-50mm, 50mm-60mm, 60mm-80mm, 80mm-100mm, and >100mm. For hourly rainfall events, the intervals are 8mm-10mm, 10mm-12mm, 12mm-14mm, 14mm-16mm, 16mm-18mm, 18mm-20mm, and >20mm. The results are presented in Fig. 7.

The profile of daily rainfall distribution shows a gradual decrease, except for the 30-40 millimeters per day (mm/d) interval. According to the Meteorology, Climatology, and Geophysics Agency (BMKG), extreme rainfall is defined as rainfall with an intensity of more than 50 mm/day or 20 millimeters per hour (mm/h). In line with these criteria, the Toba-Asahan watershed encountered four significant hourly events, the Larona-Malili watershed experienced one, and the Brantas watershed did not experience any events that fulfilled these criteria. For daily rainfall events, the Toba-Asahan watershed experienced 180 extreme events, the Larona-Malili watershed experienced 232 events, and the Brantas watershed experienced 92 events. It is essential to recognize that rainfall measurements, whether conducted daily or hourly, rely on the average watershed area. Fig. 7 shows that the Toba-Asahan watershed (180 events) and the Larona-Malili watershed (232 events) experience a higher frequency of extreme daily rainfall compared to the Brantas watershed (92 events). The distinct characteristics are largely driven by the topographic and atmospheric conditions associated with each watershed. The Toba-Asahan watershed features

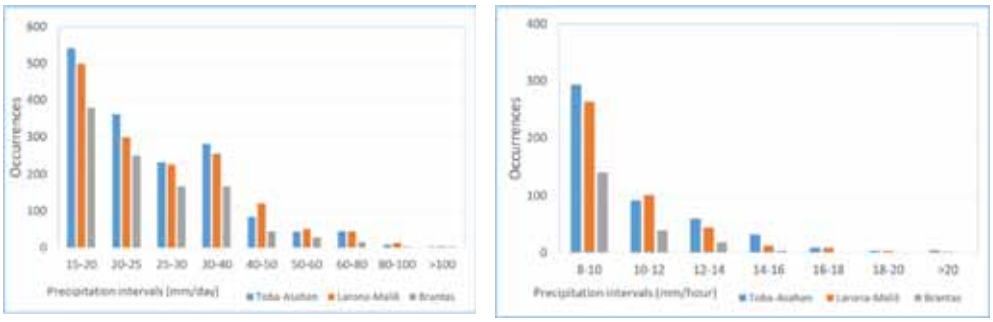

(a) (b)

Fig. 7: Distribution of the number of daily rainfall events (a) and hourly rainfall events (b) in the three watersheds from 2001 to 2024

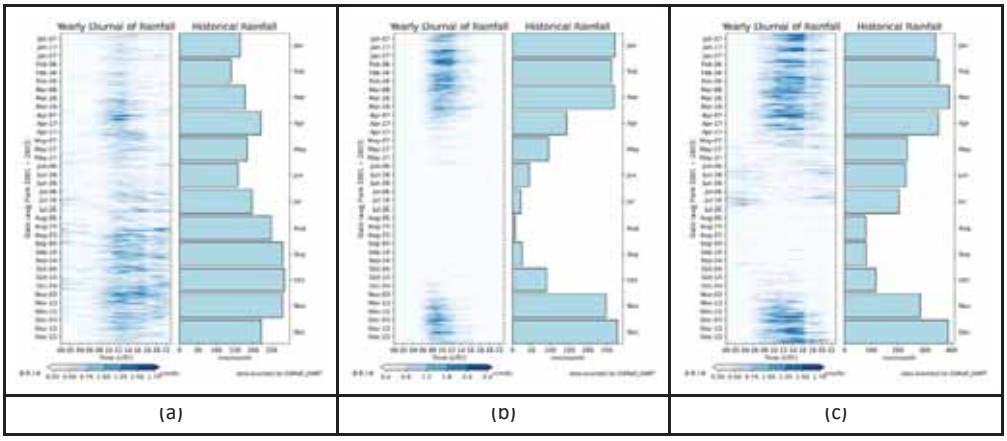

(a) (b) (c)

Fig. 8: Diurnal-daily analysis for each watershed Toba-Asahan (a), Brantas (b) and Larona-Malili (c), respectively from 2001 to 2024

significant mountainous terrain, particularly in the upstream region, which enhances orographic lifting and convective activity, leading to frequent heavy rainfall events. Likewise, the Larona-Malili watershed in South Sulawesi is shaped by monsoonal winds and its diverse mountainous topography, which results in significant rainfall intensity. In contrast, despite receiving high annual rainfall, the Brantas watershed exhibits a more uniform spatial distribution of rainfall with lower daily intensities. The middle and lower watershed regions experience reduced orographic effects, which likely contribute to a lower frequency of extreme rainfall events. The rate of extreme hourly rainfall occurrences is low in every watershed, implying that high-intensity rainfall over short timeframes is less prevalent than daily rainfall. The results, which show stark differences in extreme rainfall events among the three watersheds, are likely due to climatological, topographic, and atmospheric factors. Greater emphasis is necessary on flood management and disaster mitigation for the Toba-Asahan and Larona-Malili watersheds concerning severe rainfall occurrences. Further research can be conducted to understand the meteorological factors, atmospheric dynamics, and local rainfall patterns of each watershed, thereby supporting disaster risk mitigation and adaptation planning.

Diurnal-daily analysis in the watersheds

The diurnal-daily analysis observes the diurnal distribution of rainfall, determining whether rainfall predominantly occurs in the morning, afternoon, evening, or even at night. This technique is essential for analyzing the daily cycle patterns that are impacted by local conditions (such as topography and land use) and larger phenomena (including the monsoon and MJO). Besides identifying peak rainfall times (morning, afternoon, evening, and night), this

analysis provides valuable information for flood risk mitigation or water resource management. The following is the diurnal-daily analysis for the Toba-Asahan, Brantas, and Larona-Malili watersheds. The vertical axis (Y-axis) represents the average date from January 1 to December 31 for 2001 to 2024, while the horizontal axis (X-axis) represents the hours from 00 to 23 in Universal Time Coordinated (UTC). The annual distribution of rainfall on a daily basis is depicted in Fig. 8. The left profile shows the diurnal rainfall distribution, while the right profile shows the monthly average rainfall. According to Fig. 8, the Toba-Asahan watershed experiences rainfall nearly throughout the year, with peak intensity observed from August to December. Diurnally, it is not explicitly shown, but rainfall events occur from 08:00 UTC (15:00 Local Time (LT)) to nighttime, even into early morning, from August to December. The onset of morning rain occurs at 00:00 UTC (07:00 LT), implying that the lake plays a role in morning rainfall patterns or is related to nocturnal radiative cooling. The Brantas watershed exhibits different rainfall characteristics compared to the Toba-Asahan watershed; rainfall typically begins around 06:00 UTC (13:00 LT) and lasts until 14:00-16:00 UTC (21:00-23:00 LT), with no significant rainfall events occurring at dawn. Historically, rainfall is predominantly concentrated in the periods of January to April and November to December. The rainfall characteristics in the Brantas watershed indicate more frequent afternoon rainfall due to local convection from surface heating during the day and orographic factors. In mountainous regions, including the Brantas watershed, afternoon rainfall is common due to orographic lifting. The Larona-Malili watershed has rainfall characteristics that differ from those of the Brantas and Toba-Asahan watersheds. Rainfall events dominate from January to April and November to December, generally starting around 06:00 UTC (13:00 LT) and decreasing in intensity until early morning. Analysis of the rainfall characteristics in the Larona-Malili watershed shows that afternoon precipitation is often frequent, driven by local convection caused by daytime surface heating and the influence of orographic factors. Mountainous regions, such as the Larona-Malili watershed, tend to experience afternoon rainfall due to orographic lifting. Interestingly, rainfall events are observed from morning to noon and evening to early morning, with lower intensity from May to July. Rainfall occurring from morning to noon is frequently linked to the cooling of air at night, which leads to local convergence. This cooling enhances cloud formation through land breeze circulation or local convective processes triggered by morning solar heating. The topography in the Larona-Malili watershed, with hills or mountains, can amplify this pattern due to airlifting triggered by slope heating (orographic lifting). Wind patterns and rainfall in the Larona watershed are influenced by the El Niño-Southern Oscillation (ENSO), with El Niño reducing rainfall by up to 22% and La Niña increasing it by 50%, thereby affecting water availability for hydroelectric power generation. The most significant rainfall in the Larona watershed occurs in the regions surrounding Mahalona, southeastern Matano, and northwestern Towuti. The dry season occurs in August and September, while the watershed is considered a moderate water reservoir with a runoff coefficient of 0.6 (Syaifullah, 2013).

Sensitivity of rainfall conditions over the watershed to interannual climate phenomena

A correlation analysis examined the rainfall sensitivity in the three watersheds to ENSO, DMI, and Monsoon WYMI. This technique facilitates the assessment of the relationship strength between rainfall and the three parameters using the Pearson Correlation test, along with a 2-tailed significance test. The test criteria are that if the 2-tailed significance value is less than the significance level (alpha level), the test result is significant. Alternatively, a test result is regarded as insignificant when the two-tailed significance value exceeds the predetermined significance level. The analysis results are presented in Table 3. The statistical analysis components were essential in explaining the patterns and factors influencing rainfall variability in the studied watersheds. Specifically, correlation analysis was used to assess the relationships between rainfall and various spatiotemporal factors, revealing significant dependencies and highlighting the complexity of precipitation dynamics (Adler *et al.,* 2018).

The correlation coefficients have been obtained in this study, such as -0.122 and -0.141, indicate weak correlations. This suggests that the relationships among the analyzed variables are neither strong nor consistent. Rainfall data obtained from satellites are recognized to have significant uncertainty and bias, potentially impacting correlation outcomes.

Table 3: Correlation between the three watersheds with ESNO, DMI, and WYMI

Catchment area	Parameter	ASST-Nino34	WYMI	DMI
Toba-Asahan	Pearson correlation	-0.122*	0.205**	-0.033
	Sig. (2 tailed)	0.039	< 0.001	0.582
Brantas	Pearson correlation	-0.141*	0.732**	-0.138*
	Sig. (2 tailed)	0.016	< 0.001	0.019
Larona-Malili	Pearson correlation	-0.112	-0.591**	-0.043
	Sig. (2 tailed)	0.057	< 0.001	0.472

** Correlation is significant at the 0.001 level (2-tailed);
* Correlation is significant at the 0.05 level (2-tailed)

The variability of rainfall in Indonesia, influenced by climatic phenomena such as the El Niño Southern Oscillation (ENSO) and the Indian Ocean Dipole (IOD), may also contribute to these weak correlations, as noted by Aldrian and Susanto (2003). Additionally, alterations in land use and human activities can modify rainfall patterns, resulting in weak correlations. From a statistical perspective, Beck *et al.,* (2017) pointed out that correlations between global precipitation datasets can vary widely, indicating that weak correlations do not necessarily imply a lack of relationship, but rather reflect relationships that are not strong or consistent. Conducting a spatiotemporal analysis of rainfall variability is crucial for establishing climate-resilient watershed management strategies. It helps in recognizing changes in precipitation patterns, evaluating drought risks, and detecting extreme rainfall events, which in turn supports the formulation of adaptive measures such as optimized reservoir management, flood mitigation systems, and drought preparedness initiatives (Mishra and Singh, 2010; Ward *et al.,* 2020). This approach improves water allocation efficiency, supports early warning systems, and guides ecosystem-based adaptation strategies such as reforestation and wetland conservation, all of which improve natural water retention and reduce erosion (IPCC, 2022; Pahl-Wostl, 2019). Furthermore, such analysis feeds climate-smart agricultural practices and adaptive governance frameworks, ensuring long-term water resource management in the face of increased climate unpredictability. Utilizing spatiotemporal rainfall data enhances the resilience of watersheds, mitigates climate-related risks, and fosters enduring socio-ecological stability in at-risk areas (UNEP, 2023).

CONCLUSION

This study offers an in-depth spatiotemporal analysis of rainfall fluctuations in three major watersheds in Indonesia: Brantas, Toba-Asahan, and Larona-Malili. Key findings highlight a significant increasing rainfall trend in the Larona-Malili watershed, while no statistically significant trends were found in the Brantas and Toba-Asahan basins. Unique patterns of rainfall were noted across different seasons and times of day, influenced by regional climate systems, local air movements, and geographical features. Brantas is primarily influenced by the Asian Monsoon, while the Toba-Asahan and Larona-Malili watersheds are more sensitive to local and regional factors, including land-use changes. Spectral analysis further reveals that ENSO and IOD drive interannual rainfall variability, with semi-annual and annual rainfall cycles observed across the basins. The differing responses to climatic indices such as ENSO, IOD, and WPMI reflect the varied climate sensitivities among the watersheds. This comprehensive method connects local hydrological fluctuations with broader climate patterns, offering a fresh perspective on rainfall dynamics in Indonesian catchments. The findings contribute to improving adaptive water resource planning and climate risk mitigation strategies. However, this study is not without limitations. The analysis relies primarily on satellite-based rainfall datasets without extensive validation using ground-based observations, due to the limited availability of in-situ data across the study area. Furthermore, while the study spans a period of twenty years (2000–2023), extending the data records could enhance the identification of trends and the evaluation of variability. The study also does not incorporate hydrological modeling to assess runoff or water availability impacts. Future research should include ground-truthing with rain gauge data, integration of hydrological models to simulate water balance and streamflow response, and application of higher spatial-resolution datasets. Moreover, including more watersheds that exhibit a range of geomorphological conditions and land-use intensities

would strengthen the study's generalizability. Investigating the compound effects of anthropogenic changes and climate variability at finer temporal scales (e.g., sub-seasonal or diurnal) could further support the development of resilient and region-specific water management strategies under future climate change scenarios.

AUTHOR CONTRIBUTIONS

M.D. Syaifullah performed design, writing, review and editing, visualization, temporal and spectral analysis, research flowchart, writing original draft, methodology, and software. A. Purwandani has done the spatial distribution of rainfall in watersheds analysis, writing, visualization, editing, and software. Tukiyat performed the statistical analysis, sensitivity analysis, editing, reviewing of the manuscript. S. Tikno did the geomorphology and topography analysis. A.E. Sakya reviewed the geomorphology and topography, editing and reviewing the manuscript. M. Kudsy performed the corresponding author, reviewed meteorology and climatology, and edited the manuscript. F.H. Widodo performed the geomorphology and hydrology analysis, S. Bahri did the meteorology and climatology analysis. Muktiyono performed the writing, review, editing and visualization.

ACKNOWLEDGEMENT

The National Research and Innovation Agency of Indonesia (BRIN) is gratefully acknowledged by the authors for its support of this study. Additionally, the authors would like to thank the Japan Aerospace Exploration Agency (JAXA) for providing the GSMaP-GNRT data. The CHIRPS v2.0 data were provided by the Climate Hazards Center at the University of California, Santa Barbara. DMI and Niño 3.4 data were provided by the Physical Sciences Laboratory (PSL) of the National Oceanic and Atmospheric Administration (NOAA). Finally, we would like to extend our gratitude to the Ministry of Environment and Forestry (KLHK) and the Geospatial Information Agency (BIG) for their contributions to the watershed boundary and high-resolution topographic data (DEM Nasional/DEMNAS)

CONFLICT OF INTEREST

The authors declare that there is no conflict of interest regarding the publication of this manuscript. In addition, the authors have fully addressed the ethical issues, including plagiarism, informed consent, misconduct, data fabrication and/or falsification, double publication and/or submission, and redundancy.

OPEN ACCESS

©2025 The author(s). This article is licensed under a Creative Commons Attribution 4.0 International License, which permits use, sharing, adaptation, distribution and reproduction in any medium or format, as long as you give appropriate credit to the original author(s) and the source, provide a link to the Creative Commons license, and indicate if changes were made. The images or other third-party material in this article are included in the article's Creative Commons license, unless indicated otherwise in a credit line to the material. If material is not included in the article's Creative Commons license and your intended use is not permitted by statutory regulation or exceeds the permitted use, you will need to obtain permission directly from the copyright holder. To view a copy of this license, visit: http://creativecommons.org/licenses/by/4.0/

PUBLISHER'S NOTE

GJESM Publisher remains neutral with regard to jurisdictional claims in published maps and institutional afflictions.

Positive AI Statement

During the preparation of this work the author(s) have used Artificial Intelligence (AI) [NAME TOOL / SERVICE] in order to [REASON]. After using this tool/service, the authors reviewed and edited the content as needed and take full responsibility for the content of the publication.

(Furthermore, the GPTZero detector will evaluate the manuscript utilizing Generative AI, ensuring a high detection rate. If the manuscript relies heavily on Generative AI and AI-assisted technologies, it will be archived without further options for appeal).

☑ Negative AI Statement

The author(s) declare that no AI tools or services were used or applied during the preparation of this work.

ABBREVIATIONS

°	Degree
²	Square
%	Percent
AHP	Analytical hierarchy process
BIG	Badan informasi geospasial (Geospatial information agency)
CAPE	Convective available potential energy
CHIRPS	Climate hazards group infrared precipitation with station
DEM	Digital elevation model
DEMNAS	DEM nasional
DMI	Dipole mode index
E	East
ECMWF	European Center for medium-range weather forecasts
ENSO	El niño southern oscillation
ERA5	ECMWF reanalysis v5
FFT	Fast fourier transform
GIS	Geographic information system
GPM	Global precipitation measurement
GSMaP-GNRT	Global satellite mapping of precipitation near-real-time
hPa	Hectopascal
IOD	Indian ocean dipole
Km	Kilometers
Km²	Square kilometers
KLHK	Kementerian lingkungan hidup dan kehutanan (Ministry of environment and forestry)
LT	Local time
LULC	Land use and land cover
mm/d	Milimeter per day
mm/h	Milimeter per hour
MJO	Madden-julian oscillation
MK	Mann-Kendall
N	North
NetCDF	Network common data format
NOAA	National oceanic and atmospheric administration
PCA	Principal component analysis
PLTA	Pembangkit listrik tenaga air (hydroelectric power plant)
PSL	Physical sciences laboratory
S	South
SS	Sen's slope estimator
SST	Sea surface temperature
U850	Zonal wind component at 850 hPa
U200	Zonal wind component at 200 hPa
UTC	Universal time coordinated
WYMI	Webster-yang monsoon index

REFERENCES.

Aditya, F.; Gusmayanti, E.; Sudrajat, J., (2021). Rainfall trend analysis using Mann-Kendall and Sen's slope estimator test in West Kalimantan. IOP Conference Series: Earth Environ. Sci., 893(1): 1-9 **(9 Pages).**

Adler, R.F.; Sapiano, M.R.P.; Huffman, G.J.; Wang, J.J.; Gu, G.; Bolvin, D.; Chiu, L.; Schneider, U.; Becker, A.; Nelkin, E.; Xie, P.; Ferraro, R.; Shin, D. Bin., (2018). The Global Precipitation Climatology Project (GPCP) monthly analysis (New Version 2.3) and a review of 2017 global precipitation. Atmosphere. 9(4).

Akhundzadah, N.A., (2024). Analyzing temperature, precipitation, and river discharge trends in Afghanistan's main river basins using innovative trend analysis, Mann–Kendall, and Sen's slope methods. Climate. 12(12): 2-21 **(20 Pages)**.

Aksu, H.H., (2023). Estimation and analysis of seasonal rainfall distribution and potential of Türkiye and Its 25 main watersheds. Atmosphere. 14(5): 1-17 **(17 Pages)**.

Aldrian, E.; Susanto, R.D., (2003). Identify three dominant rainfall regions within Indonesia and their relationship to sea surface temperature. Int. J. Climatol., 23: 1435–1452 **(18 Pages)**.

Alemu, M.M.; Bawoke, G. T., (2020). Analysis of spatial variability and temporal trends of rainfall in Amhara Region, Ethiopia. J. Water Clim. Change. 11(4): 1505–1520 **(16 Pages)**.

Arsyad, M.; F. Fitriani, V. A. Tiwow, P. Palloan, S. Sulistiawaty, and A. Susanto, (2023). The Effects of El Nino Southern Oscillation on Rainfall in the Karst Area of Maros, National Park Bantimurung Bulusaraung South Sulawesi and its Impact on Flood Disasters, J. Ilmu Lingkungan. 21(4): 772-780 **(8 Pages).**

Beck, H.E.; Vergopolan, N., Pan, M.; Levizzani, V.; Van Dijk, A.I.J.M.; Weedon, G.P.; Brocca, L.; Pappenberger, F.; Huffman, G.J.; Wood, E.F., (2017). Global-scale evaluation of 22 precipitation datasets using gauge observations and hydrological modeling. Hydrol. Earth Syst. Sci., 21(12):6201–6217 **(17 Pages).**

Dede, M.; Sunardi, S.; Lam, K.; Withaningsih, S., (2023). Relationship between landscape and river ecosystem services. Global J. Environ. Sci. Manage., 9(3): 637–652 **(16 Pages)**.

Filho, A.J.P.; Carbone, R.E.; Tuttle, J.D.; and Karam, H.A., (2015). Convective Rainfall in Amazonia and Adjacent Tropics. Atmos. Clim. Sci., 05(02): 137–161.**(25 Pages).**

Funk, C.; Peterson, P.; Landsfeld, M.; Diego Pedreros, D.; Verdin, J.; Shukla, S.; Husak, G.; Rowland, J.; Harrison, L.; Hoell, A.; Michaelsen, J., (2015). The climate hazards infrared precipitation with stations—a new environmental record for monitoring extremes. Sci. Data. 2: 150066.

Hendon, H.H., (2023). Indonesian rainfall variability: Impacts of ENSO and local air–sea interaction. J, Clim. 16(11):1775–1790 **(15 pages)**

IPCC, (2022). Climate change 2022: Impacts, adaptation and vulnerability. Cambridge University Press.

Irwandi, H.; Rosid, M.S.; Mart, T., (2021). The effects of ENSO, climate change and human activities on the water level of Lake Toba, Indonesia: a critical literature review. Geosci. Lett. 8, 21.

Kamal, N.; and Pachauri, S., (2019). Mann-Kendall, and Sen's Slope Estimators for Precipitation Trend Analysis in North-Eastern States of India. Int. J. Comput. Appl. Technol., 177(11): 7–16 **(10 Pages)**.

Khaldun, M.H.I; Wirasatriya, A.; Suryo, A.A.D; Kunarso , (2017). The Influence of Indian Ocean Dipole (IOD) on the variability of sea surface temperature and precipitation in Sumatera Island. IOP Conference Series: Earth Environ. Sci., 165: 012008.

Kubota, T; Aonashi, K.; Ushio, T.; Shige, S.; Takayabu, Y.N.; Misako Kachi, M.; Arai, Y.; Tashima, T.; Masaki, T.; Kawamoto, N.; Mega, T.; Yamamoto, M.K.; Hamada, A.; Yamaji, M.; Liu, G.; Oki, R. (2020). Global satellite mapping of precipitation (GSMaP) products in the GPM Era. In satellite precipitation measurement. Springer, Cham. 355-373 **(19 Pages).**

Kurniadi, A.; Weller, E.; Salmond, J.; Aldrian, E., (2023). Future projections of extreme rainfall events in Indonesia. Int. J. Climatol., 44(1): 160–182 **(23 Pages)**.

Lestari, S.; Hamada,J.I; Syamsudin, F.; Sunaryo; Matsumoto, J.; Manabu D.Y., (2023). ENSO Influences on Rainfall Extremes around Sulawesi and Maluku Islands in the Eastern Indonesian Maritime Continent. Scientific Online Letters on the Atmosphere. 12 : 37-41 (**4 Pages)**.

Li, Z.; Abulikemu, A.; Zhu, K.; Mamtimin, A.; Zeng, Y.; Li, J.; Abulimiti, A.; Kadier, Z.; Abuduaini, A.; Li, C.; Sun, Q., (2023). Diurnal Variation Characteristics of Summer Precipitation and Related Statistical Analysis in the Ili Region, Xinjiang, Northwest China. Remote Sens., 15(16).

Li, Z; Liang, H.; Chen, S.; Li, X.; Li, Y.; Wei, C., (2024). Performance Assessment of Satellite-Based Precipitation Products in the 2023 Summer Extreme Precipitation Events over North China. Atmosphere.

Mishra, A.K.; Singh, V.P., (2010). A review of drought concepts. J. Hydrol., 391(1-2): 202-216 (15 Pages)

Marisi, D.; Hariyadi, S.; Kaswanto, R., (2025). The impacts of land use and cover change on water quality of watershed basin. Global J. Environ. Sci. Manage., 11(2): 573–592 **(20 Pages).**

Narendra, B.; Setiawan, O.; Hasan, R.; Siregar, C.; Pratiwi, N.; Sari, N.; Sukmana, A.; Dharmawan, I.; Nandini, R., (2024). Flood susceptibility mapping based on watershed geomorphometric characteristics and land use/land cover on a small island. Global J. Environ. Sci. Manage., 10(1): 301–320 **(20 Pages)**.

Narulita, I.; Fajary, F.R.; Syahputra, M.R.; Kusratmoko, E.; and Djuwansah, M.R., (2021). Spatio-temporal rainfall variability of equatorial small island: case study Bintan Island, Indonesia. Theor. Appl. Climatol., 144(1–2): 625–641 **(17 Pages)**.

Nofirman, N.; Harahap, M.A.K.; and Andiani, P., (2023). Studi Geomorfologi dan Perubahan Lanskap dalam Konteks Perubahan Lingkungan di Pulau Jawa. J. Geosains West Sci., 1(03): 126–133 **(8 Pages)**.

Oktavia, R.; Pariwono, J. I.; and Manurung, P., (2011). Sea Level Variation and Geostrophic Current of the Sunda Strait Based on Tidal and Wind Data in Year 2008. Jurnal Ilmu Dan Teknologi Kelautan Tropis. 3(2): 127–152 **(26 Pages)**.

Pahl-Wostl, C., (2019). Governance of the water-energy-food security nexus: A multi-level coordination challenge. Environ. Sci. Policy. 92: 356-367 **(12 Pages)**

Rosyidy, M.; Frimawaty, E., (2024). Spatiotemporal analysis of oil palm land clearing. Global J. Environ. Sci. Manage., 10(2): 821–836 **(16 Pages)**.

Setiawan, O.; Nugroho, H.; Wahyuningrum, N.; Auliyani, D.; Hardjo, K., (2024). A suitability modeling based on geographic information system for potential micro hydropower dam site. Global J. Environ. Sci.Manage., 10(2): 713–732 **(19 Pages)**.

Saharia, M.; Kirstetter, P.E.; Vergara, H.; Gourley, J.J.; Emmanuel, I.; and Andrieu, H., (2021). On the impact of rainfall spatial variability, geomorphology, and climatology on flash floods. Water Resour. Res., 57(9): 1–18 **(18 Pages)**.

Syaifullah, D., (2013). Karasteristik Curah Hujan Dan Aliran Das Larona Kabupaten Luwu Timur Sulawesi Selatan. J. Sains Teknologi Modifikasi Cuaca. 14(2): 83-93 **(11 Pages)**.

Syaifullah, M. D. (2014). Validasi Data TRMM Terhadap Data Curah Hujan Aktual di Tiga DAS di Indonesia. J. Meteorologi Dan Geofisika. 15(2): 109-118 (**10 Pages**).

Syarifuddin; Achmad; Sedyowati; Laksni; Suriptono, (2022). The Effect of land use changes on water availability as water resources conservation effort in Brantas Hulu Watershed. Int. J. Innovative Sci. Res. Technol., 7(2): 463-470 **(8 Pages)**.

Trenberth, K.E, (1997). The Definition of El Niño. Bull. Am. Meteorol. Soc., 78(12): 2771–2777 **(7 Pages)**.

UNEP, (2023). Adaptation Gap Report 2023: Underfinanced, Underprepared. United Nations Environment Programme.

Ward, P.J.; de Ruiter, M.C.; Mård, J.; Schröter, K,; Loon, A.V.; Veldkamp, T.; von Uexkull, N.; Wanders, N.; AghaKouchak, A.; Nielsen, K.A.; Capewell, L.; Llasat, M.C.; Day, R.; Dewals, B.; Di Baldassarre, G.; Huning, L.S.; Kreibich, H.; Mazzoleni, M.; Savelli, E.; Teutschbein, C.; van den Berg, H.; van der Heijden, A.; Vincken, J.M.R.; Waterloo, M.J.; Wens, M., (2020). The need to integrate flood and drought disaster risk reduction strategies. Water Security (11).

Webster, P.J.; Yang, S., (1992). Monsoon and ENSO: Selectively interactive systems. Q. Q. J. R. Meteorol. Soc., 118: 877–926 **(50 Pages).**

Wilks, D.S. (2011). Statistical methods in the atmospheric sciences (3rd ed.). Academic Press.

Wiwoho, B.S.; Astuti, I.S.; Alfarizi, I.A.G.; and Sucahyo, H.R., (2021). Validation of three daily satellite rainfall products in a humid tropic watershed, brantas, indonesia: Implications to land characteristics and hydrological modeling. Hydrology. 8(54): 1-22 **(22 Pages).**

Wiwoho, B.S.; Phinn, S.; and McIntyre, N., (2023). Two Decades of Land-Use Dynamics in an Urbanizing Tropical Watershed: Understanding the Patterns and Drivers. ISPRS Int. J. Geol.-Inf., 12(3): 1-26 **(26 Pages).**

AUTHOR (S) BIOSKETCHES

Syaifullah, M.D., M.Sc., Research Center for Climate and Atmosphere, National Research and Innovation Agency (BRIN), Serpong 15314, Indonesia.
- Email: *muha042@brin.go.id*
- ORCID: 0009-0005-8265-2620
- Web of Science ResearcherID: NA
- Scopus Author ID: 57211929385
- Homepage: http://brin.go.id/

Purwandani, A., M.Sc., Research Center for Conservation of Marine and Inland Water Resources, National Research and Innovation Agency (BRIN), Cibinong 16911, Indonesia.
- Email: *andri.purwandani@brin.go.id*
- ORCID: 0000-0002-7675-5069
- Web of Science ResearcherID: MXL-9334-2025
- Scopus Author ID: 8335951000
- Homepage: http://brin.go.id/

AUTHOR (S) BIOSKETCHES

Tukiyat, Ph.D., Principal Research Engineer, Research Center for Limnology and Water Resources, National Research and Innovation Agency (BRIN), Serpong 15314, Indonesia.
▪ Email: *tuki001@brin.go.id*
▪ ORCID: 0000-0001-7568-6237
▪ Web of Science ResearcherID: NA
▪ Scopus Author ID: NA
▪ Homepage: http://brin.go.id/

Tikno, S., M.Sc., Research Center for Limnology and Water Resources, National Research and Innovation Agency (BRIN), Serpong 15314, Indonesia.
▪ Email: *sunu001@brin.go.id*
▪ ORCID: 0009-0000-7675-8238
▪ Web of Science ResearcherID: NA
▪ Scopus Author ID: NA
▪ Homepage: http://brin.go.id/

Sakya, A.E., Ph.D., Principal Research Engineer, Research Center for Geological Disaster, National Research and Innovation Agency (BRIN), Serpong 15314, Indonesia.
▪ Email: *andi.eka.sakya@brin.go.id*
▪ ORCID: 0000-0002-5490-1846
▪ Web of Science ResearcherID: NA
▪ Scopus Author ID: 57201667644
▪ Homepage: http://brin.go.id/

Kudsy, M., Ph.D., Principal Research Engineer, Research Center for Limnology And Water Resources, National Research and Innovation Agency (BRIN), Serpong 15314, Indonesia.
▪ Email: *maha001@brin.go.id*
▪ ORCID: 0000-0001-8185-2958
▪ Web of Science ResearcherID: NA
▪ Scopus Author ID: 6602489366
▪ Homepage: http://brin.go.id/

Widodo, F.H., M.Sc., Research Center for Limnology and Water Resources, National Research and Innovation Agency (BRIN), Serpong 15314, Indonesia.
▪ Email: *flor003@brin.go.id*
▪ ORCID: 0009-0000-4984-6945
▪ Web of Science ResearcherID: NA
▪ Scopus Author ID: NA
▪ Homepage: http://brin.go.id/

Bahri, S., M.Sc., Research Center for Limnology and Water Resources, National Research and Innovation Agency (BRIN), Serpong 15314, Indonesia.
▪ Email: *sams001@brin.go.id*
▪ ORCID: 0009-0004-5954-6312
▪ Web of Science ResearcherID: NA
▪ Scopus Author ID: NA
▪ Homepage: http://brin.go.id/

Muktiyono, M.Sc., Research Center for Limnology and Water Resources, National Research and Innovation Agency (BRIN), Serpong 15314, Indonesia.
Email: *muktiyono@brin.go.id*
ORCID: 0009-0001-2639-9406
Web of Science ResearcherID: NA
Scopus Author ID: NA
▪ Homepage: http://brin.go.id/

HOW TO CITE THIS ARTICLE

Syaifullah, M.D.; Purwandani, A.; Kudsy, M.; Tukiyat, Tikno, S.; Sakya, A.E.; Widodo, F.H.; Bahri, S.; Muktiyono, (2025). Spatiotemporal analysis of rainfall variability using satellite precipitation in three watersheds.Global J. Environ. Sci. Manage., 11(3): 1143-1162.

DOI: 10.22034/gjesm.2025.03.15

URL: https://www.gjesm.net/article_723550.html

Global J. Environ. Sci. Manage. 11(3): 1163-1184, Summer 2025, Serial #43

Global Journal of Environmental Science and Management
(GJESM)

Homepage: https://www.gjesm.net/

Podcasts

CASE STUDY

Tracking Coronavirus 2019 pandemic-related waste generation in urban waterways

R.G. Banal [1,*], I.L.M. Abad [2]

[1] *Electrical and Electronics Engineering Department, College of Engineering, Mindanao State University – General Santos, Fatima, 9500 General Santos City, Philippines*

[2] *Mechanical Engineering Department, College of Engineering, Mindanao State University – General Santos, Fatima, 9500 General Santos City, Philippines*

ARTICLE INFO

Article History:
Received 27 April 2025
Revised 08 May 2025
Accepted 21 May 2025

Keywords:
Coronavirus 2019 (COVID-19)
Household waste
Non-household waste
Sustainable waste management
Waste characterization

ABSTRACT

BACKGROUND AND OBJECTIVES: The Coronavirus 2019 pandemic has revealed significant shortcomings in the Philippines' solid waste management system, particularly in addressing the surge of pandemic-related waste. Unreliable waste collection, insufficient public knowledge, and improper waste disposal practices have exacerbated risks to the environment and public health. Despite these concerns, the specific impacts of Coronavirus 2019 pandemic related waste on human health and the environment in the Philippines' context remain underexplored. This study aims to quantify Coronavirus 2019 related waste generated from both household sources and non-household establishments, assess disposal practices, characterize waste composition, determine generation rates, and classify waste types. Moreover, a comprehensive waste flow analysis will be carried out to monitor the movement of both appropriately and inappropriately managed Coronavirus 2019 waste, examining its implications on terrestrial and aquatic environments, as well as public health. Insights from the Philippines can significantly contribute to the formulation of resilient and adaptive waste management approaches in response to future public health emergencies worldwide.

METHODS: Coronavirus 2019 pandemic related waste generation from both household sources and non-household establishments was quantified through a 5-day at-source Waste Analysis and Characterization Study conducted in twenty-six urban and rural barangays of General Santos City. The determination of sample sizes was conducted using conventional statistical techniques, informed by the most up-to-date census data and business establishment profiles. Structured questionnaires and checklists were used to gather information from household respondents regarding Coronavirus 2019 related waste sources, generation rates, and disposal behaviors. To determine the degree of environmental contamination related to pandemic waste, further waste characterization was carried out in the Silway and Makar Rivers, two key urban waterways that pass through populated and commercial districts prior to their discharge into Sarangani Bay.

FINDINGS: According to the Waste Analysis and Characterization Study, waste linked to the Coronavirus 2019 pandemic totals about 52,877.7 kilograms per day, which is equivalent to 1.57 percent of the city's total daily waste. This equates to an estimated 4,654,720 discarded face masks from household sources and 633,050 from non-household establishments daily. Coronavirus 2019 pandemic related waste density in the Makar and Silway Rivers tributaries of the Sarangani Bay Protected Seascape was recorded at 0.238 gram per square meters and 0.706 gram per square meters, respectively. Mainly consisting of plastic face masks, this waste poses environmental threats as possible microplastic sources, jeopardizing both marine environments and human well-being. Waste flow analysis illustrated the management pathways of Coronavirus 2019 pandemic-related waste, underscoring its significant environmental and social repercussions.

CONCLUSION: The Coronavirus 2019 pandemic has highlighted critical gaps in waste management systems and the environmental and health hazards associated with emerging waste streams such as Coronavirus 2019. Mismanagement of this waste stream results in environmental damage and considerable threats to public health. The study emphasizes the pressing requirement for better waste governance, infrastructure enhancements, and public education to reduce the enduring effects of waste associated with the pandemic.

DOI: 10.22034/gjesm.2025.03.16

This is an open access article under the CC BY license (http://creativecommons.org/licenses/by/4.0/).

NUMBER OF REFERENCES
59

NUMBER OF FIGURES
7

NUMBER OF TABLES
8

*Corresponding Author:
Email: *ryan.banal@msugensan.edu.ph*
Phone: +63908 360 8971
ORCID: 0000-0001-6958-7354

Note: Discussion period for this manuscript open until Sep 1, 2025 on GJESM website at the "Show Article".

INTRODUCTION

The Coronavirus 2019 (COVID-19) pandemic placed unprecedented strain on municipal solid waste management (MSWM) infrastructure worldwide (Kulkarni and Anantharama, 2020; Roy *et al.,* 2021), particularly in developing countries (Yousefi *et al.,* 2021). When the World Health Organization (WHO) declared COVID-19 a pandemic (Cucinotta and Vanelli, 2020), the country's solid waste management sector was unprepared for the surge in pandemic-related waste. This increase in municipal waste posed significant challenges in collection, segregation, transport, treatment, and disposal (Limon *et al.,* 2022). In contrast, hospital-generated medical waste was managed more effectively through established treatment methods aimed at preventing viral transmission (Kulkarni and Anantharama, 2020; Sanito *et al.*, 2024). During the pandemic, one of the critical environmental challenges was the escalation of plastic waste, primarily caused by the growing demand for personal protective equipment (PPE) among healthcare staff, essential service personnel, and the general public (Klemeš *et al.,* 2020; Ragazzi *et al.,* 2020; Zhao *et al.,* 2021). The prevalent dependence on disposable plastics, including face masks and shields, originated from apprehensions regarding the spread of viruses (Nzediegwu and Chang, 2020; Roy *et al.,* 2021). The pandemic also altered waste generation patterns, particularly in household waste composition (Sharma *et al.,* 2020; Vanapalli *et al.,* 2021). Lockdowns and market restrictions fueled an increase in online deliveries, leading to greater volumes of organic and plastic waste from food packaging and consumer goods. The increase in plastic consumption after the COVID-19 pandemic emerged as a result of changes in human lifestyle during the pandemic, cheap prices, and enhanced accessibility. During the pandemic, the key determinant of plastic consumption patterns was the inadequate management of plastic waste by individuals, leading to a fourfold increase in plastic use among those with poor waste management practices versus those who were more responsible (Herdiansyah and Nuraeni, 2024). A previous study introduced solutions to the problems and challenges of the waste management sector by introducing recovery recycling stations (RSS) that optimize the solid waste collection system (Cuong *et al*., 2022). Although healthcare personnel generally demonstrate a high level of knowledge and awareness concerning the administrative procedures for managing COVID-19 medical waste (Alzghoul *et al*., 2022), it appears that similar efforts to enhance knowledge and awareness should be extended to the broader public. Ajbar El-Ghoriri *et al*. (2023) examined the characteristics of healthcare waste in regional hospitals and a private clinic related to waste generation during the COVID-19 pandemic. However, the limited scope of these investigations restricts their ability to capture the broader extent of waste generation associated with the pandemic. In another study, Ouhsine *et al*. (2020) analyzed the qualitative and quantitative impacts of the COVID-19 pandemic on household solid waste, reporting that 9 percent (%) of respondents disposed of used face masks in public spaces. While this highlights a potential risk for public exposure to infection, the study did not trace the waste flow resulting from such improper disposal practices. In spite of these difficulties, the overall consequences of pandemic-induced waste on public health and the environment in the Philippines have not been adequately examined (Limon *et al.,* 2022). Many national policies lack comprehensive data, peer-reviewed research, and expert recommendations, making it difficult to develop effective waste management strategies (Apostol *et al.,* 2022). Existing policies often rely on global statistics from organizations such as the WHO and the U.S. Centers for Disease Control and Prevention (CDC), but there is a critical gap in local quantitative and qualitative data. Without country-specific insights, long-term environmental and health risks may go unaddressed. Moreover, waste management practices adopted in developed countries (Sharma *et al.,* 2020; Vanapalli *et al.,* 2021) may not be directly applicable to developing nations like the Philippines due to disparities in infrastructure, resource availability, and public consciousness (Adusei-Gyamfi *et al.,* 2022). Following the declaration of COVID-19 as a pandemic, General Santos City implemented precautionary measures, including social distancing and various health protocols, such as the compulsory use of face masks in public areas and face shields in public transportation, shopping malls, government offices, and workplaces. Consequently, the government adopted multiple lockdown protocols, causing a significant decline in waste generated from residential and commercial sources. It is noteworthy that regulations stipulate that local government units (LGUs) are permitted

to collect only residual waste, which is the refuse remaining after proper sorting and management. This transition compelled the government to concentrate on the collection of COVID-19 pandemic-related waste (CRW) in isolation centers and treatment facilities, where the city produced an average of 1.5 tons of medical waste weekly. This waste included PPE, face masks, face shields, and test kits, all of which were disposed of separately (Philippine News Agency, 2021). Nevertheless, determining the apex of CRW formation is challenging due to the absence of comparative data. The implementation of these diverse lockdown strategies were accompanied by a surge in pandemic-related waste within the urban environment, notably affecting the water bodies. The study will be conducted through the Waste Analysis and Characterization Study (WACS) - a process of gathering information about the quantity and composition of solid waste generated by different sources (Japan International Cooperation Agency, 2020), and the conduct of survey. Furthermore, a waste flow assessment will be carried out to monitor the disposal routes of pandemic-related waste, both proper and improper, and its consequences for land and aquatic ecosystems. This study offers a novel perspective on COVID-19-related waste management by presenting empirical evidence from a developing country context, thereby addressing a gap in existing literature dominated by studies from more developed parts of the Asia-Pacific region. As a country with a high population density and significant challenges, the Philippines presents important insights that can inform global waste management approaches during future public health crises. This study aims to assess COVID-19 waste generation from both household sources and non-household establishments, providing insights into community disposal practices, waste composition, generation rate, and classification. This study has been carried out in General Santos City, the Philippines, in 2022-2023.

MATERIALS AND METHODS

Scope of the study

The systematic collection of COVID-19 pandemic-related waste was conducted in General Santos City, which consists of twenty-six barangays-the smallest administrative unit in the Philippines. The map of the city is depicted in Fig. 1. Of these barangays, twenty-

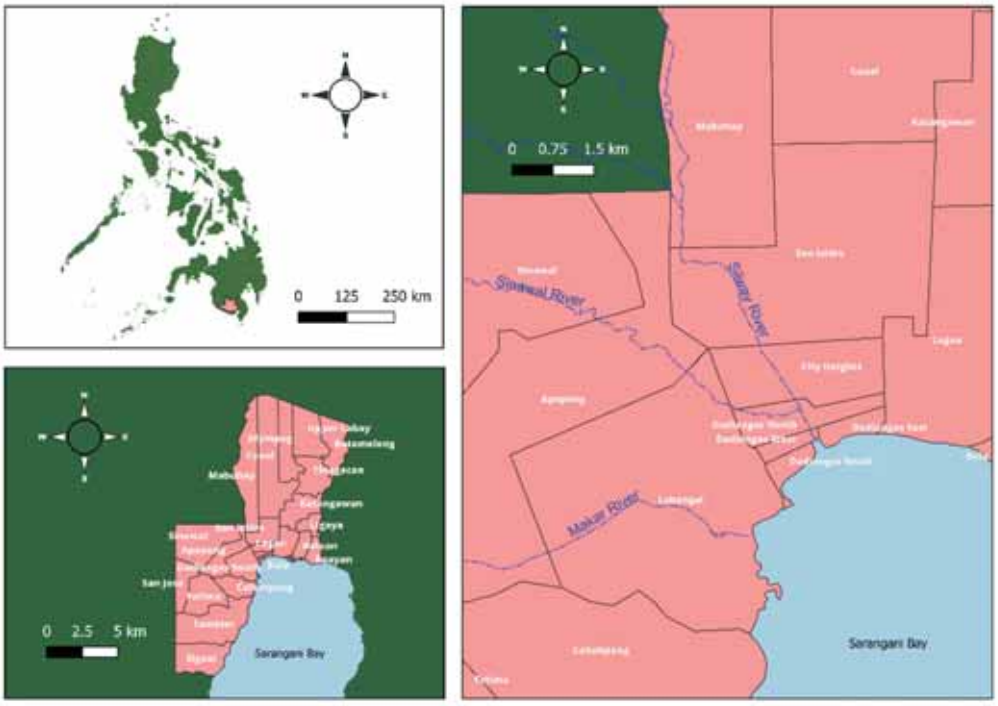

Fig. 1: Geographic location of the study area indicating the 26 barangays and major tributaries of General Santos City, Philippines

three are classified urban while the remaining three are classified as rural (LGU-GSC and ADB, 2022). According to the 2020 national census, General Santos City is the Philippines' 11th most populous city, with 697,315 residents and a population growth rate of 3.41% from 2015 to 2020 (Philippine Statistics Authority, 2021a). The city has a population density of 1,415 people per square kilometer (people/km^2) and an average household size of 4.0 (Philippine Statistics Authority, 2022a, 2021b).

General Santos City serves as the commercial and trade hub of Region XII, also known as the SOCCSKSARGEN (South Cotabato, Cotabato, Sultan Kudarat, Sarangani, and General Santos City). The dynamic economy of the city is supported by its range of industries, including fishing, farming, and commerce, which enhances its appeal to investors from both local and foreign markets. Due to its strategic location, well-developed infrastructure, and comprehensive support facilities, agriculture and fisheries largely drive the city's economy (LGU-GSC and ADB, 2022). Additionally, General Santos City is situated at the head of Sarangani Bay, a government-declared protected seascape (Office of the President, 1996).

Determination of COVID-19 generated waste and conduct of survey

CRW generated from household sources and non-household establishments was assessed through an at-source WACS (Japan International Cooperation Agency, 2020) between September 2022 and February 2023, which included a survey with identified respondents. This study was part of a comprehensive assessment of the city's solid waste management system for the development of a 10-year solid waste management plan (SWMP). The current study was conducted about two and a half years following the COVID-19 pandemic was officially declared. During this time, the city was under enhanced community quarantine (ECQ), where the requirement to wear face masks indoors and outdoors has been rescinded, except for healthcare facilities, medical transport vehicles, and all forms of public transportation. Quarantine facilities in the city were no longer in use. Both private and government offices embraced flexible work setups, and educational institutions shifted to virtual learning. The survey was carried out in this timeframe. To determine the appropriate sample size (n) for households and non-household establishments, the latest available population census and business establishment profiles were utilized. The sampling for household sources and non-household establishments is proportional to the total number of households in barangays or the total establishments of non-household generators within each subcategory. The sample for WACS seeks to obtain a representative subset that reflects the mix and characteristics of the total waste generated by various sources. Although enhanced sampling boosts the accuracy of outcomes, it demands extra resources including personnel, time, materials, and various expenditures. Consequently, due to constrained resources and the extensive sampling sizes, it has been determined to execute the 5-day WACS throughout 5 consecutive days, encompassing one market day, three regular days, and one weekend to analyze waste generation behavior. Moreover, sampling was purposefully bypassed during high garbage output periods, such as post-festival or significant events. The conventional statistical approach for determining sample size for representative household and non-household sources was employed, as outlined using Eq. 1 (Japan International Cooperation Agency, 2020; Krejcie *et al*., 1970; National Solid Waste Management Commission, 2020):

$$n = \frac{\frac{z^2 \times P(1-P)}{e^2}}{1 + \left(\frac{z^2 \times P(1-P)}{e^2 N} \right)} \quad (1)$$

Where,

n = representative number of households or non-household units

N = total number of households or total units of non-household generators per category

z = z score for 95% confidence level = 1.96

P = standard deviation = 0.20, and

e = 5% margin error for highly-urbanized cities.

Household respondents were identified through the head of the household or a representative. Data collection involved a survey questionnaire and checklist, which provided insights into the sources, percentage, and disposal practices of CRW. The survey focused exclusively on household respondents, with no participation from non-household entities. This consideration accounts for the fact that non-

household establishments are typically subject to more stringent regulations and policies on waste management than households. Financial incentives—such as tax breaks for recycling or penalties for improper disposal, can play a crucial role in shaping waste management behaviors. Furthermore, commercial establishments typically employ different recycling methods and systematic waste management strategies compared to residential households. The survey questionnaire was divided into three sections: 1) demographic profile of respondents, 2) waste generation and disposal practices, and 3) awareness of solid waste management. In accordance with the NSWMC guidelines (National Solid Waste Management Commission, 2020), the WACS was conducted in three stages. The stages are: 1) planning and preparation, 2) implementation of WACS, and 3) data processing and analysis (Japan International Cooperation Agency, 2020). The initial planning and preparation phase set the framework for the technical working group (TWG), waste collectors, and recorders was established. The TWG was tasked with identifying and categorizing waste generators, conducting orientations for respondents, distributing and collecting survey questionnaires, preparing WACS tools and materials, and providing appropriately labeled plastic bags for various waste categories. Identified participants were briefed and educated on their roles and duties in the study via guided discussions and pamphlets detailing the appropriate trash segregation protocols. Post-orientation, they received six assigned trash bags, each linked to a particular waste category: biodegradable waste, recyclable waste, residual waste with recycling potential, residual waste for disposal, and waste associated with COVID-19. It is crucial to acknowledge that waste linked to COVID-19 has been included in the conventional waste categorization. Then CRW was collected over five consecutive days during the WACS stage. An appropriate site was chosen that offered sufficient ventilation, accessibility, and ample room for waste sorting. Upon receiving the trash bags, sorters equipped themselves with PPE to ensure that the respondents had correctly sorted the waste. If discrepancies were found, they undertook further sorting and segregation prior to weighing the waste. Recorders recorded these measures using data entry forms. After the assessment of all waste, the space was adequately disinfected. The accumulated waste was subsequently transported to the sanitary landfill for appropriate disposal. The transport, treatment, and disposal of COVID-19-related waste were executed in compliance with Joint Memorandum Circular No. 2020-0001 issued by the Department of Health and the Department of the Interior and Local Government (Department of Health and Department of the Interior and Local Government, 2020). The data processing stage involved entering the data into Microsoft Office Excel and analyzing each component. The calculation of the CRW percentage from household (HH) sources utilized Eqs. 2, 3, 4, and 5, which were adapted to reflect total household waste generation rather than per capita generation, as detailed in the WACS handbook (Japan International Cooperation Agency, 2020).

$$\frac{CRW\ per\ HH}{day} = \frac{Total\ CRW\ generated\ by\ HH\ sampled}{No.of\ HH\ sampled \times No.\ of\ sampling\ days} \quad (2)$$

$$\frac{Brgy\ CRW\ HH}{day} = \frac{CRW\ per\ HH}{day} \times Total\ number\ of\ Brgy\ HH \quad (3)$$

$$\frac{City\ HH\ CRW\ generated}{day} = \sum\left(\frac{Brgy\ CRW}{day}\right)_1 + \left(\frac{Brgy\ CRW}{day}\right)_2 + \ldots + \left(\frac{Brgy\ CRW}{day}\right)_{N-1} + \left(\frac{Brgy\ CRW}{day}\right)_N \quad (4)$$

$$\%HH\ CRW = \frac{\frac{City\ HH\ CRW\ generated}{day}}{\frac{City\ Total\ HH\ waste\ generated}{day}} \times 100\%. \quad (5)$$

The percentage of CRW generated for each non-household establishment category has been calculated using Eqs. 6, 7, 8, 9 and 10, which were modified for total non-household waste generation, as outlined in the WACS handbook (Japan International Cooperation Agency, 2020):

$$\frac{Establishment\ CRW\ generation\left(ECG\right)}{day} = \frac{Total\ CRW\ generated\ by\ Establishments\ sampled}{No.of\ Establishments\ sampled \times No.\ of\ sampling\ days} \quad (6)$$

$$\frac{Total\ non-HH\ category\ CRW\ generation}{day} = \Sigma\left(\frac{ECG}{day}\right)_1 + \left(\frac{ECG}{day}\right)_2 + \ldots + \left(\frac{ECG}{day}\right)_{M-1} + \left(\frac{ECG}{day}\right)_M \quad (7)$$

$$\frac{non-HH\ category\ CRW\ generation}{day} = \frac{Total\ non-HH\ category\ CRW\ generation}{day} \times Total\ no.of\ establishments \quad (8)$$

$$\frac{Total\ non-HH\ CRW\ generation}{day} = \left(\frac{Commercial\ CRW\ generation}{day}\right) + \left(\frac{Industrial\ CRW\ generation}{day}\right) + \left(\frac{Institutional\ CRW\ generation}{day}\right) \quad (9)$$

$$\%non-HH\ CRW = \frac{\frac{Total\ non-HH\ CRW\ generation}{day}}{\frac{Total\ non-HH\ waste\ generated}{day}} \times 100\%. \quad (10)$$

Upon completion of data processing and analysis, an extensive report was generated. A total of 250 household sources and 651 non-household establishments participated in the study. Non-residential establishments were divided into commercial, industrial, and institutional sectors. Nevertheless, due to rigorous hospital protocols during the data collection phase, health-related institutions were confined to clinics, diagnostic centers, and laboratories. To assess the extent of waste pollution associated with COVID-19, waste characterization was conducted in the Silway and Makar Rivers. These waterways pass through several neighborhoods and non-domestic entities prior to flowing into Sarangani Bay (Fig. 1). The Silway River spans 7.35 kilometers (km) and consists of three main tributaries: Silway, Sinawal, and Klinan Rivers. In contrast, the Makar River is approximately 0.86 km long (Paringit and Puno, 2017). Waste characterization in these rivers involved collecting CRW using specialized garbage tongs. The study covered an area of 1,500 square meters (m²) for Makar River and 2,500 m² for Silway River, with sampling sites located 150–240 meters (m) from the river mouths. The collected refuse was categorized and sorted based on the household and non-household categories defined in the WACS. After weighing, the waste was sent to the city's sanitary landfill for disposal. Data analysis was conducted to determine the waste density per unit area. This approach facilitated a comprehensive understanding of CRW generation, disposal practices, and potential environmental impacts within General Santos City. This study is part of the waste flow assessment concerning improperly managed pandemic waste, while CRW collected by designated garbage trucks waste, even though it is intermixed with residual waste due to the unavailability of a dedicated facility.

RESULTS AND DISCUSSION

COVID-19-related wastes of household and non-household establishments

Fig. 2 illustrates examples of CRW collected from household sources and non-household establishments during WACS. The accumulated waste was predominantly made up of disinfectant containers and PPE, encompassing a variety of disposable and reusable face masks of various colors and materials, as well as face shields.

Table 1 presents the estimated daily CRW generation for each barangay from household sources, as well as for each subcategory of non-household establishments, based on a 5-day WACS conducted at the source. It is essential to note that the estimation of daily waste generation for each barangay is derived from multiplying the established representative samples by the total number of households in each barangay. Correspondingly, for non-household organizations, the daily waste generation is assessed by taking the representative samples and multiplying them by the overall number of establishments in each subcategory. The data presented in the table indicate that the urban barangay of San Isidro had the highest CRW generation rate, whereas the rural

barangay of Batomelong recorded the lowest CRW generation rate. This variation corresponds with previous findings that point out the significance of demographic, educational, and economic factors on CRW generation (Arumugam *et al.*, 2021; Saseanu *et al*., 2019). Specifically, the differences in waste generation rates can be attributed to the contrasting characteristics of Batomelong, which has a smaller household size in a rural area, compared to San Isidro, known for its larger household size and urban classification.

As depicted in Fig. 3, CRW generation correlated with the total number of households in every barangay due to increased use of PPE and disinfectant products. Among non-household organizations, the largest contributors to CRW were commercial establishments, succeeded by industrial facilities and institutional entities.

Table 1 also presents the daily waste generation from household sources and non-household establishments. On average, household sources generated a total of 46,547.2 kilograms per day (kg/day) of CRW, constituting 3.26% of the total municipal solid waste (MSW). Non-household establishments contributed a total of 6,330.5 kg/day, accounting for 0.33% of total MSW. Collectively, these sources produced a total of 52,877.7 kg/day of CRW, representing 1.57% of total MSW collected daily. This is expected that this will change according to the lockdown restrictions imposed on the community. Among the CRW collected, face masks were the predominant waste item, followed by disinfectant containers and face shields, which aligns with mask mandates in public spaces. The data reveals that CRW, notably in the form of face masks, creates a substantial challenge for landfill management. Furthermore, proper treatment is essential to mitigate virus transmission prior to final disposal. As the predominant CRW, and based on an estimated weight of 10 grams (g) per face mask, approximately 4,654,720 masks were used daily by the entire city's household sources, while non-household establishments accounted for a total of around 633,050 masks daily. Despite the constraints of the study's limited timeframe, it was hard to ascertain which lockdown measures produced the most significant in CRW generation. The CRW generation rate for household sources can be established using Eq. 11 (Japan International Cooperation Agency, 2020):

$$Household\ CRW\ Generation\ rate = \frac{Total\ CRW\ generated\ by\ household\ sources\left(g/day\right)}{Total\ number\ of\ households} \cdot \quad (11)$$

Based on the 2020 population census (Philippine Statistics Authority, 2021a), General Santos City had 175,345 households. Given a daily CRW generation of $4.65\acute{}10^7$ grams (g), the CRW generation rate was 273.7 grams per day (g/day) per household. With



Fig. 2: Examples of COVID-19 pandemic-related waste collected from (a) household sources and (b) non-household establishments during the 5-day WACS

Table 1: COVID-19 pandemic-related waste generated by barangay from household sources and by sub-categories from non-household establishments

Household sources

Name of Barangay	Classification of Barangay	Household Size (*N*)	Sample Size (*n*)	Daily waste generation of total households (kg/day)
Apopong	Urban	14,223	21	2,100.7
Baluan	Urban	2,893	4	1,384.7
Batomelong	Rural	724	1	74.6
Buayan	Urban	2,802	4	292.8
Bula	Urban	7,523	11	808.6
Calumpang	Urban	21,395	33	6,405.5
City Heights	Urban	5,937	9	690.7
Conel	Urban	3,886	6	520.7
Dadiangas East	Urban	826	1	103.3
Dadiangas North	Urban	1,659	2	140.2
Dadiangas South	Urban	1,174	2	111.5
Dadiangas West	Urban	3,193	5	725.4
Fatima	Urban	17,710	26	2,514.8
Katangawan	Urban	4,233	6	1,197.9
Labangal	Urban	18,793	27	6,760.6
Lagao	Urban	13,099	19	2,577.3
Ligaya	Urban	1,631	2	146.0
Mabuhay	Urban	9,178	13	1,671.8
Olympog	Rural	1,087	2	85.3
San Isidro	Urban	15,843	23	10,753.9
San Jose	Urban	3,294	5	4,352.7
Siguel	Urban	3,826	6	382.0
Sinawal	Urban	4,504	7	1,084.8
Tambler	Urban	7,692	11	1,039.0
Tinagacan	Urban	2,035	3	232.7
Upper Labay	Rural	917	1	389.7
Subtotal		170,077	250	46,547.2

Non-household establishments

Category/subcategory	Total Number of Units (*N*)	No. of collected establishments	Daily waste generation of total establishments (kg/day)
Institutions			
Offices	345	83	43.8
Schools	178	42	411.6
Parks	77	18	7.4
Churches	30	7	104.4
Healthcare-related	162	38	10.3
Commercial establishments			
General merchandise	1901	141	3,033.8
Food establishments	954	70	506.8
Hotels	220	16	44.6
Public market	16	1	45.1
Industrial establishments			
Manufacturing	649	30	104.4
Agribusiness	212	10	19.3
Service industries	4,249	195	2,101.8
Subtotal	8,993	651	6,330.5
Total			52,877.7

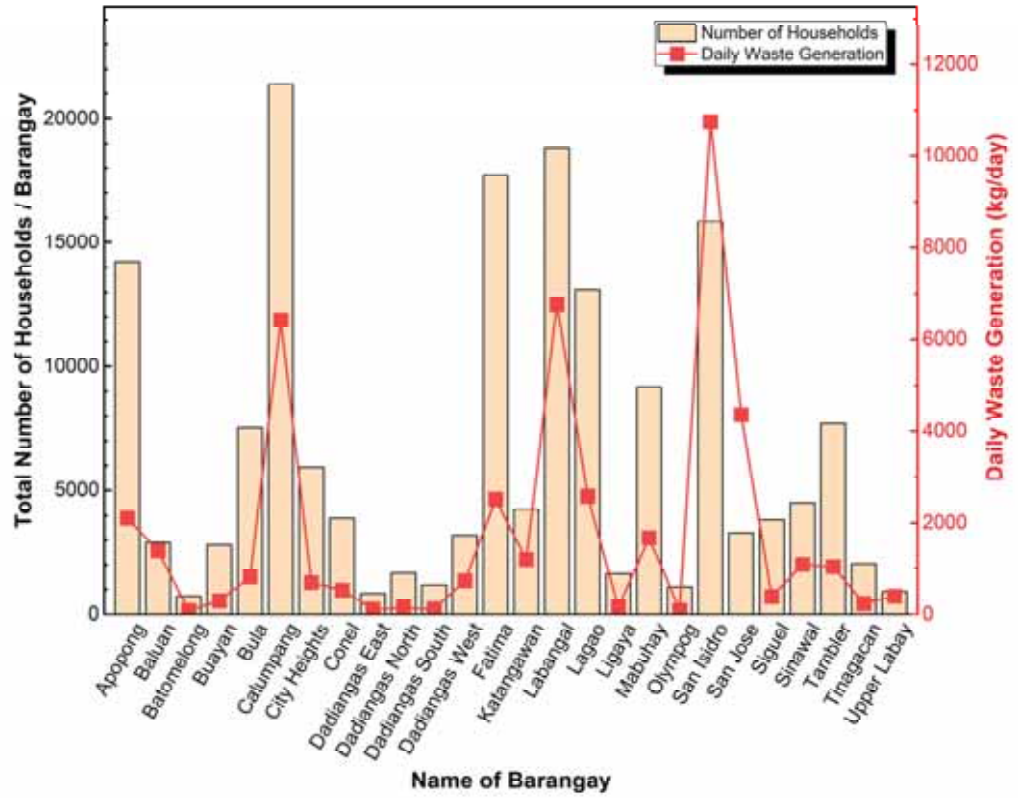

Fig. 3. Daily generation of COVID-19 pandemic-related waste from household sources across the 26 barangays of General Santos City

an average household size of four, each person contributed an approximately 68.4 g/day of CRW. The contribution of CRW non-household establishments is hard to quantify, as there is no data available on the workforce or waste generation associated with this particular subcategory. However, household sources generated a significantly larger number of face masks than non-household establishments, suggesting that face masks were primarily disposed of at home after daily activities. This underscores the importance of having a unique waste classification for CRW to facilitate proper disposal. Despite existing policies requiring immediate segregation of CRW (Apostol *et al.,* 2022), these policies generally classify CRW as hazardous waste without considering its point of generation. Given the highly contagious nature of Severe Acute Respiratory Syndrome Coronavirus 2 (SARS-CoV-2), a survey was conducted to assess household practices related to CRW disposal. The demographic profile of the 250 respondents surveyed is shown in Fig. 4. Among these participants, 210 were heads of their respective households, and 40 were other members of the household (Fig. 4a). The average household size was four, ranging from one to 21 members. Educational attainment varied, with 44.7% completing high school, 16.7% attaining a college degree, 1.2% earning postgraduate qualifications, 19.9% completing elementary education, and 15.0% having incomplete elementary education (Fig. 4b). The assessment also included household income levels, which play a role in shaping knowledge and practices concerning solid waste management (Kwakye *et al.,* 2024; Sarker *et al.,* 2024). Occupational classification followed the 2012 Philippine Standard Occupational Classification (PSOC) (Philippine Statistics Authority, 2022b), modeled after the 2008 International Standard Classification of Occupations (ISCO). A significant portion of the respondents held positions in service and sales (40.6%) or clerical support (20.3%), while 16.5% were engaged in agriculture, forestry, and fisheries. Studies indicate that labor market status influences virus transmission in urban

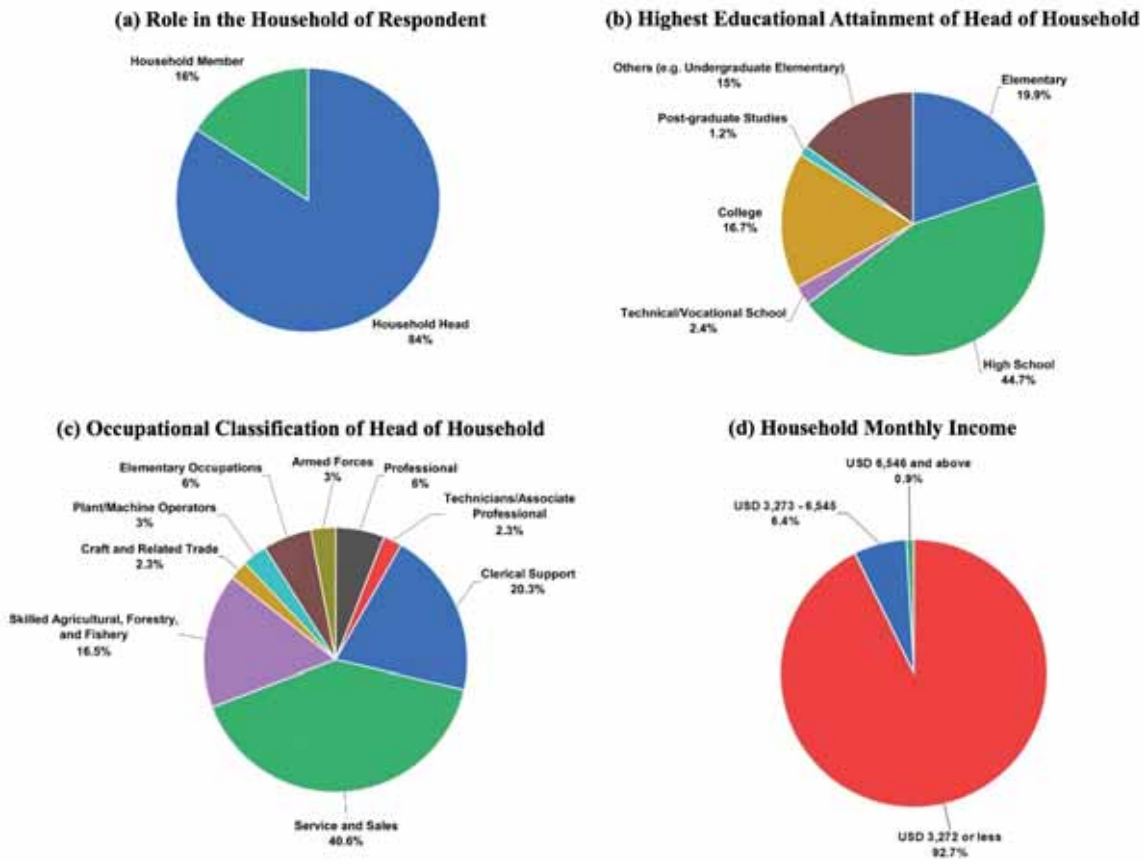

Fig. 4: Demographic profile of household respondents: (a) Role within the household; (b) Highest educational attainment; (c) Occupational classification; and (d) Monthly household income

settings (Hâncean *et al.,* 2022), with private-sector employees often initiating household transmission. Additionally, more than half of the respondents had a total annual income ranging from USD 3,272.00 or less (92.7%), USD 3,273.00 – 6,545.00 (6.4%), to USD 6,546.00 and above (0.9%) (Fig. 4d).

Fig. 5 outlines household disposal practices for CRW. Most respondents (84.0%) used disposable face masks, while 16.0% used reusable ones (Fig. 5a). The frequency of disposable face mask usage was less than what was previously indicated (Limon *et al.*, 2022), which may be attributed to economic factors and a shift in community attitudes toward COVID-19 risks. Among those using disposable face masks, 72.1% discarded them daily, while others disposed of them weekly (12.2%), monthly (0.9%), or irregularly (14.9%) (Fig. 5c). Disposal methods varied: 61.0% mixed face masks with common waste, 16.0% placed them in separate plastic bags, 4.0% discarded them in open areas, and 4.0% used city-designated garbage bags (Fig. 5e). Disinfection methods primarily included alcohol (65.2%) and disinfectant sprays (33.0%) (Fig. 5b). The frequency of disinfectant disposal is daily (4%), weekly (17%), monthly (12%), or as desired (67%) (Fig. 5d). Waste collection was managed by barangay garbage trucks and private waste collectors (73.0%), but some respondents resorted to burning (8.6%) or burying (5.2%) CRW due to irregular collection services. Despite government regulations that forbid open dumping and burning, these improper disposal techniques still persist (Congress of the Philippines, 2001; Hantoko *et al.,* 2021; Sangkham, 2020). During the pandemic, there was no citywide implementation of dedicated disposal bins for face masks, PPE, and other COVID-19-related waste. Although certain hospitals, clinics, and large organizations have set up separate receptacles for infectious waste as part of their

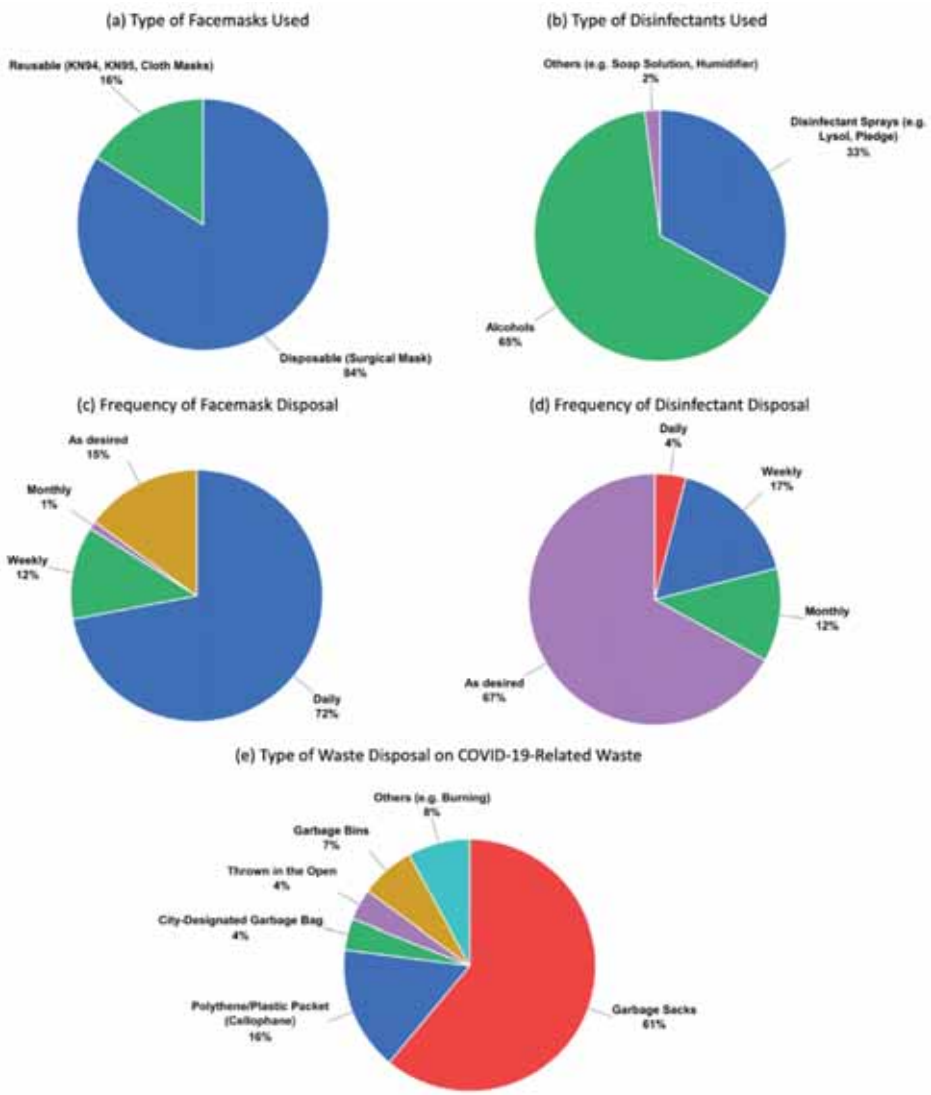

Fig. 5: COVID-19 pandemic-related waste disposal practices of respondents in General Santos City. (a) Type of face masks; (b) Type of disinfectants; (c) Face mask disposal frequency; (d) Disinfectant disposal frequency; and (e) Disposal type

operational guidelines, most public venues, schools, and smaller facilities neglected this practice, causing a mixture of these items with regular waste. Thus, most of CRW were observed to be mixed with general household waste and subsequently transported to the city's sanitary landfill. Due to the absence of a dedicated waste treatment facility, these wastes accumulated primarily at the landfill site, highlighting a gap in the city's waste segregation and treatment capacity during the pandemic. The lack of segregation increases the risk of toxic leachates contaminating groundwater and soil (El-Saadony *et al.,* 2023). Furthermore, inadequate landfill disposal obstructs the effective recycling and recovery of precious materials, causing resource loss and extended environmental degradation. Household CRW disposal lacks strict adherence to proper protocols. The co-disposal of CRW with general waste poses health risks to households and waste management workers. Without specific policies mandating CRW segregation, CRW is often mixed with regular solid waste (Hantoko *et al.,* 2021), which can disrupt subsequent waste management processes, including collection, transport, and disposal (Vanapalli *et al.,*



Fig. 6: Collection of COVID-19 pademic-related waste in General Santos City. (a) Silway River; (b) Makar Rivers; and (c) example of face masks collected during the activity

2021). Inadequate disposal of CRW raises the risk of exposure for informal waste pickers and contributes to environmental degradation (Shanmugasundaram, 2024). The improper disposal of used COVID-19-related waste poses a significant health risk (Al-Emam and Al-Yousfi, 2021), such as the spread of respiratory and skin diseases, which undermines national efforts to control the spread of infections in communities.

Impact of COVID-19-related wastes on Sarangani Bay

Sarangani Bay faces ongoing environmental challenges, including rapid population growth, coastal settlement expansion, urbanization, and pollution (Agduma and Cao, 2023; LGU-GSC and ADB, 2022). Improper disposal of waste significantly impacts marine ecosystems, primarily due to contributions from residential and industrial sectors (Acot *et al.,* 2022; Ng *et al.,* 2023). The conduct of CRW collection in Silway and Makar rivers is shown in Fig. 6.

Table 2 presents CRW densities in Silway and Makar Rivers, calculated by dividing collected waste mass by study area. The CRW density was 0.238 grams per square meters (g/m²) in Silway River and 0.707 g/m² in Makar River, with respective waste collections of 595 g and 1,060 g. Differences in CRW density may be attributed to river characteristics: Silway River has continuous flow, whereas Makar River has stagnant sections. The detection of CRW in these rivers reflects human activity, likely caused by insufficient disposal practices and the transfer of waste through stormwater runoff and wind. Other than disposable face masks, plastics such as single-use food wrappers, plastic bags, and bottles composed of plastic polymers such as polypropylene, polyethylene, and polyethylene terephthalate for various uses were found during collection.

Previous studies have reported that disposable face masks, composed of plastic polymers such as polypropylene, contribute to microplastic pollution upon degradation (Aragaw, 2020; Shukla *et al.,* 2022). The infiltration of microplastics into groundwater and marine environments could jeopardize aquatic life and posing health risks to humans (Fadare and Okoffo, 2020; Oliveira *et al.,* 2023; Tang *et al.,* 2021). The insufficiency of the public and government response during the pandemic has become apparent when improperly handled solid waste ultimately contaminates the aquatic environment (Bhat *et al.*, 2022). This situation is illustrated by the vast quantities of polluted PPE that have turned into waste found in oceans, along coastlines,

Table 2: Density of COVID-19 pandemic-related waste collected in major rivers in General Santos City

Name of River	Density (g/m^2)
Silway River	0.238
Makar River	0.706

Table 3: Model fit measures

Model	R	R^2
1	0.759	0.577

Note. Models estimated using sample size of N=26

Table 4: Model coefficients - daily CRW for Barangay households

Predictor	Estimate	SE	t	p
Intercept	-243.495	489.2280	-0.498	0.623
Number of Households	0.311	0.0544	5.717	<.001

and within rivers (Ammendolia *et al.*, 2021; Aragaw, 2020). Moreover, other investigations have detected COVID-19-related PPE debris in the marine waters off the shores of Palawan (Jarabe *et al.*, 2023) and Davao (Sajorne *et al.*, 2022). Improperly managed pandemic-related waste that entered waterways eventually accumulated along beaches and in nearby mangrove areas, where tidal action and vegetation trapped the debris. This created environmental and economic challenges by disturbing marine ecosystems, polluting fishing areas, and increasing microplastic contamination (Peng *et al.*, 2021). Unfortunately, there are currently no established local monitoring programs in General Santos City to assess microplastic contamination from degraded pandemic-related waste. Therefore, assessing its ecological impact on rivers and coastal zones poses a challenge. Consequently, developing organized monitoring strategies that feature standardized testing and their integration into existing waste and water management systems is crucial.

Correlation between the number of households and the daily waste generation across 26 barangays

A multiple linear regression was utilized to assess the relationship between household counts and daily CRW generation in 26 barangays. The analysis demonstrated a statistically significant connection between the two variables (Table 3). The model yielded a correlation coefficient (*R*) of 0.759 and a coefficient of determination (R^2) of 0.577, suggesting that 57.7% of the variation in daily waste generation can be accounted for by the number of households. This indicates that the number of households is an important element in comprehending trends in waste production. The regression coefficient for the number of households was 0.311, with a p-value of less than 0.001, indicating that the effect is statistically significant (Table 4). Practically, this means that for every additional household, there is an associated increase of approximately 0.311 kg of daily CRW generated, demonstrating that the amount of waste tends to scale with the number of household units. These outcomes imply that household data may be employed to anticipate waste generation, which can support LGUs in developing waste collection infrastructure and optimizing collection routes.

This study also investigated the differences in daily CRW generation across four sectors: commercial, household, industry, and institution. A Kruskal-Wallis H

Table 5: Kruskal-Wallis – Daily CRW Generation on Households and Non-household Establishments

Variable	χ^2	df	p	ε^2
Daily CRW Generation	10.6	3	0.014	0.287

Note: χ^2 (Chi-square); df (Degrees of Freedom); p (probability value) where $p < 0.05$ indicates statistically significant differences between at least two groups; ε^2 (Epsilon squared) where values closer to 1 indicate a stronger effect.

Table 6: Pairwise comparisons - Daily CRW Generation on Households and Non-household Establishments

1st Category type	2nd Category type	W	p
Commercial	Household	1.726	0.614
Commercial	Industry	-0.500	0.985
Commercial	Institution	-2.771	0.204
Household	Industry	-1.620	0.661
Household	Institution	-4.178	0.017
Industry	Institution	-1.897	0.537

Note: W (Test Statistic for DSCF): Larger absolute values of W indicate greater differences between specific group pairs.

test was conducted due to the non-parametric nature of the data and unequal group sizes. Table 5 revealed a statistically significant difference in daily CRW generation between groups ($\chi^2(3) = 10.6$, $p = 0.014$, $\varepsilon^2 = 0.287$). The effect size ($\varepsilon^2 = 0.287$) suggests a moderate to large effect, indicating meaningful variation in waste generation depending on the sector. To explore these differences further, Dwass-Steel-Critchlow-Fligner (DSCF) pairwise comparisons presented in Table 6 were performed. Among all comparisons made, the distinction between the household and institutional sectors was the only one that reached statistical significance ($W = -4.178$, $p = 0.017$). This implies that households contribute significantly more to COVID-related waste than institutions do. Other comparisons did not yield significant differences, though the commercial-institution comparison approached significance ($W = -2.771$, $p = 0.204$), indicating a potential trend that did not reach statistical reliability.

Waste flow analysis of COVID-19 pandemic-related waste generated from household sources and non-household establishments

Fig. 7 illustrates the flow of CRW, highlighting the pathways through which improper disposal contributes to environmental pollution and the potential transmission of pathogens. If CRW is not collected and disposed of properly, it may flow into neighboring river systems and eventually reach the bay. This situation emphasizes the pressing requirement for better waste collection systems and specific public awareness efforts to advocate for appropriate disposal practices. The analysis also reveals a bidirectional flow of CRW between household sources and non-household establishments, indicating complex inter-source waste circulation patterns. How CRW is administered, whether done appropriately or not, plays a crucial role in determining the extent of environmental pollution and the health hazards faced by the community. CRW that is collected by barangay garbage trucks or private waste contractors is typically directed to the sanitary landfill. However, waste disposed of through informal or inappropriate means-such as burying, open burning, mixing with general household waste, or discarding in open areas-can lead to the pollution of both inland and marine environments and may facilitate virus transmission. According to Ammendolia *et al*. (2021) and Limon *et al*. (2022), disposable masks (DM) found in oceans, along highways, in mountainous terrains, and other

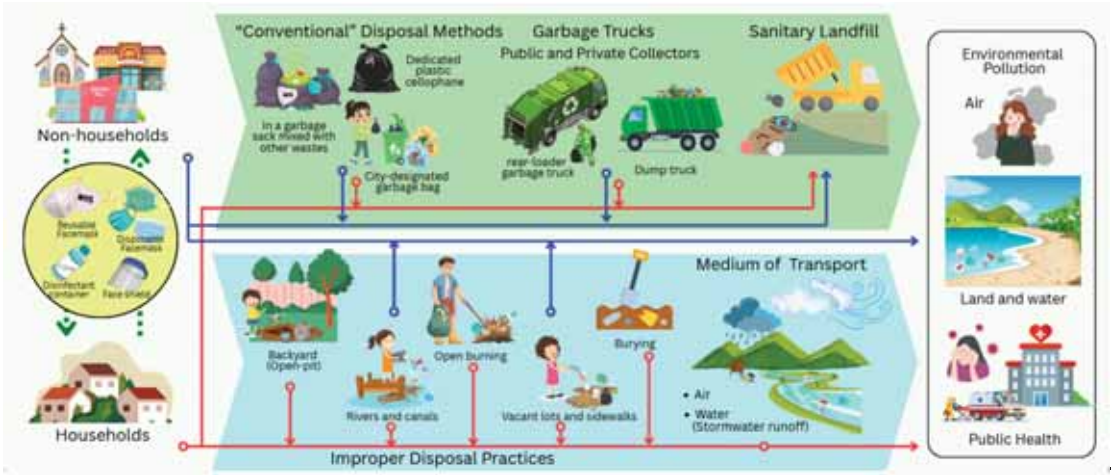

Fig. 7: Waste flow analysis of COVID-19 pandemic-related waste generated from household sources and non-household establishments

Table 7: Descriptives – Daily CRW generation on households and non-household establishments

Category	Sample Size	Median	Standard deviation (SD)
Households	26	767	2579
Commercial (Non-household)	4	276	1434
Institution (Non-household)	5	10.3	178
Industry (Non-household)	3	104	1179

open environments may primarily originate from household sources. CRW that is discarded in rivers or open spaces, or transported via stormwater runoff, wind, and flooding, can eventually reach coastal waters and marine ecosystems. To address these risks, consistent and organized CRW collection should be mandated, along with continuous community outreach initiatives that encourage appropriate waste disposal methods to safeguard both environmental and public health.

Descriptive statistics reinforce these findings as shown in Table 7. Households produced the highest average daily CRW (Median = 767), followed by commercial (Median = 276), industry (Median = 104), and institution (Median = 10.3). Significantly, households exhibited the greatest standard deviation (SD = 2579), indicating substantial variability in waste generation patterns across residential settings. In contrast, institutional settings consistently reported the lowest levels of CRW generation (SD = 178), supporting the statistical outcome of the pairwise comparison. These results may reflect differing operational scales and protocols across sectors. It is likely that household waste saw a significant rise due to the surge in home-centered activities during lockdowns, such as food deliveries, disposable plastics, and personal protective equipment. This observation aligns with studies reporting increased household waste generation during the pandemic due to factors such as heightened consumption of packaged food and PPE (Klemeš *et al.,* 2020; Patrício Silva *et al.,* 2021). Furthermore, the institutions' reports of low CRW may stem from behavioral tendencies in which individuals tend to throw away their CRW at home instead of their places of work. This behavior suggests a waste flow from non-household to household settings, as people may prefer to discard used masks, gloves, and other PPE at home for convenience or due to institutional disposal policies. Observations during the pandemic indicated that household waste became the central repository for waste linked to pandemic activities. These findings show the significant generation of CRW at the household level during the pandemic. Consequently, upcoming future policy initiatives should focus on bolstering the resilience of waste

Table 8: Summary of the key findings of the present study in comparison with previous research

Country/area	Methodology	Key findings	Novel contributions of the present study in the context of prior research	Sources
Morocco (Khenifra, Tighassaline)	Field survey (300 households); comparison of municipal waste tonnage (Feb–Mar 2019 vs. 2020)	Found an increase in the purchase of disinfectant products and a decrease in the consumption of meat and canned goods; masks mixed with general waste	Provides data not only on waste generation in households but also at the non-household level	Ouhsine *et al*. (2020)
Global / China (focus on Wuhan	Systems/lifecycle analysis; waste flow modeling; Life Cycle Assessment	Proposed Plastic Waste Footprint (PWF); life cycle assessments of plastic medical waste treatment (e.g., incineration with heat recovery)	Provides ground-level generation data during the peak of COVID-19, validating modeled forecasts from this study. Provides waste flow analysis of improperly disposed COVID-19-related wastes three years after the pandemic	Klemeš *et al*. (2020)
Australia, America, United Kingdom, Singapore, Sri Lanka, and India	Online survey of 1,033 individuals across multiple countries; literature review	Assessed types, usage, and disposal of face masks; proposed recycling/upcycling into construction materials	Provides daily COVID-19 waste generation data for both households and non-households, which considers not only face masks but also disinfectants and face shields	Selvaranjan *et al*. (2021)
Philippines	Online survey (Google Forms) with 13,116 respondents; statistical analysis using Pearson's r and regression	Evaluated public knowledge and practices for mask disposal; found high awareness but inconsistent practices; found improperly disposed of face masks in the ocean, on highways, and in the mountains	Provides not only qualitative data but also quantitative data on daily COVID-19 related waste generation. Conducts face-to-face interviews to assess the behavior and practices of households. Assesses and characterizes COVID-19 related waste in rivers	Limon *et al*. (2022)
General Santos City, Philippines	Waste characterization of daily COVID-related waste generation (kg/day) onsite for households, non-households, and waterways, with statistical analysis	Provided qualitative and quantitative COVID-19-related waste generation data from households, non-households (commercial, industrial, institutional), and waterways. Provided a comprehensive waste flow analysis of properly and improperly disposed COVID-19-related wastes	Provides unique data on COVID-19 waste generated from households, non-households, and waterways, along with a comprehensive waste flow analysis, potentially informing dynamic policy responses	Present Study

management systems in response to public health crises.

Table 8 summarizes the methodologies, key findings, and contributions of the present study in comparison to prior studies. These studies vary in geographic scope, methodology, and focus areas. For instance, Selvaranjan *et al*. (2021) and Limon *et al*. (2022) used online surveys to evaluate public behavior regarding face mask disposal, highlighting widespread improper disposal practices. Klemeš

et al. (2020) conducted systems-level modeling to propose waste treatment methods for medical plastics, while Ouhsine *et al*. (2020) surveyed Moroccan households and reported increased waste from disinfectants and food packaging. Conversely, the current study enhances its scope by merging qualitative and quantitative data related to CRW, encompassing disinfectants and face shields. It utilizes a combination of WACS and surveys directed at household sources, non-household entities, and local waterways in General Santos City, Philippines. Furthermore, while most studies reported general disposal methods, such as household bins or mixed waste, the present study includes a detailed waste flow analysis that distinguishes between properly and improperly managed waste streams, a feature largely absent in previous research. This strategy yields a more extensive dataset concerning COVID-19 waste generation, featuring insights into the composition and flow of waste, which in turn provides a unique lens on the wider waste management scenario.

In summary, the COVID-19 pandemic has highlighted the challenges of solid waste management and its adverse effects on communities, public health, and the environment. CRW has emerged as a significant waste stream, posing environmental and health risks when improperly handled. The absence of explicit regulations from government bodies has worsened improper disposal methods. The extensive mishandling of PPE has heightened environmental contamination and health risks (Benson *et al.,* 2021; Klemeš *et al.,* 2020; You *et al.,* 2020). Illegally discarded CRW often finds its way into water bodies, including the Sarangani Bay protected seascape, where polymer-based materials degrade into microplastics. Resolving this challenge necessitates the adoption of rapid and effective waste management practices, including suitable protocols for collection, disposal, and transportation to minimize pollution and hinder the spread of viruses. The waste management personnel faced significant challenges in handling the pandemic-related waste, especially infectious and medical waste generated from hospitals, quarantine facilities, and households, deficient PPE and safety apparatus, inadequate waste separation at the source, unavailability of treatment facilities, and operational disruption. Although some of these challenges were addressed by improved waste segregation and labeling, provision of PPE and disinfection supplies, worker training and public education, and financial and policy support, the pandemic exposed systemic gaps in the waste management infrastructure, prompting calls for better investment in treatment facilities, institutionalized PPE supply systems for sanitation workers, and integration of health and environmental protocols in emergency planning.

CONCLUSION

The COVID-19 pandemic has significantly disrupted waste management systems, highlighting critical vulnerabilities, particularly in low- and middle-income countries such as the Philippines. This analysis delivers a thorough examination of the amount, makeup, and management of pandemic-associated waste generated from domestic and non-domestic entities in General Santos City. The findings demonstrate that pandemic-related waste, although representing a small percentage of total municipal waste by weight, poses considerable dangers to terrestrial and aquatic ecosystems, as well as to public health, due to its lasting plastic nature and poor management. The daily generation of approximately 52,877.7 kilograms of COVID-19 pandemic-related waste, coupled with the alarming presence of discarded face masks in the Makar and Silway Rivers, underscores the environmental risks associated with inadequate pandemic waste governance. The analysis of waste flow highlighted the complicated channels through which inadequately handled waste is transported from urban centers to aquatic environments, potentially contributing to microplastic pollution in critical marine ecosystems such as Sarangani Bay. The evidence confirms that without focused measures, waste associated with the pandemic could result in enduring and cumulative consequences for ecosystem services, biodiversity, and public health. Given these challenges, it is evident that existing solid waste management frameworks are not sufficiently resilient to absorb the shocks of emerging waste streams associated with global public health emergencies. The subsequent recommendations should be considered to mitigate the effects of pandemic-related waste on the environment and public health. Enhancing waste management should therefore be recognized as a strategic objective. This involves the establishment of emergency waste management strategies, the optimization waste collection through source segregation and labeling,

deployment of mobile collection units, establishment of specialized disposal infrastructure in high pedestrian traffic areas such as shopping centers, medical facilities, educational institutions, and transportation terminals. These disposal units will be designed to be sealed, foot-operated, and routinely emptied by qualified personnel, and treatment infrastructure, and the formulation of circular economy strategies that embed biodegradability and recyclability into the design of PPE and other health-related materials. Equally significant is the urgent need for comprehensive public education initiatives to advocate responsible waste disposal behaviors, facilitate behavioral transformation, and cultivate a culture of environmental stewardship among citizens. Protocols for sanitation personnel must ensure the availability of adequate PPE and training on the safe collection and handling of potentially contaminated waste, in addition to implementing of disinfection procedures for vehicles and containers used in CRW collection. It is crucial to consider the final disposal method to ensure the elimination of pathogens. In cases where incineration is not feasible, landfilling must be conducted with stringent regulations and protective measures like liners and coverings. Furthermore, future policy directions should emphasize the integration of pandemic waste management strategies into broader disaster risk reduction and climate resilience frameworks. Multisectoral collaboration among public health authorities, environmental agencies, local government units, and community organizations is crucial to ensure coordinated and effective responses to similar crises. It is vital to invest in research and innovation, particularly focusing on biodegradable materials, advanced waste capture technologies, and environmental monitoring systems to track the behavior of emerging contaminants. The experience in the Philippines reflects the larger international challenges linked to waste produced during the pandemic. Establishing adaptive, inclusive, and sustainable waste management systems is crucial for both alleviating the short-term consequences of health emergencies and promoting long-term environmental sustainability and public health safety. As the world continues to grapple with the consequences of the COVID-19 pandemic, this study underscores the imperative for proactive, science-based, and policy-driven solutions to future-proof waste management systems against similar disruptions.

AUTHOR CONTRIBUTIONS

R.G. Banal conceptualized the entire project and managed the writing of the project proposal for funding acquisition. R.G. Banal co-supervised the activities, co-administered the project, and ensured adherence to the timeline and objectives. R.G. Banal was directly involved in the development of the methodology, acquisition, and curation of data, as well as in conducting formal analysis and visualization of the results. Additionally, R.G. Banal wrote the original draft of the manuscript and subsequent revisions through critical review and editing, and validated the final content for submission. I.L.M. Abad led the writing of the project proposal for funding acquisition. Throughout the project's execution, I.L.M. Abad supervised the activities, and ensured adherence to the timeline and objectives. I.L.M. Abad was directly involved in the development of the methodology, acquisition, and curation of data, as well as in conducting formal analysis and visualization of the results. Additionally, I.L.M. Abad contributed to the original draft of the manuscript, its subsequent revisions through critical review and editing, and validated the final content for submission.

ACKNOWLEDGEMENTS

The authors acknowledge the valuable support of the Waste Management Office (WMO) of the local government unit of General Santos City during the sampling period of the study. Furthermore, they are also grateful for the technical support the Department of Environment and Natural Resources Environmental Management Bureau – Region 12 provided. The authors acknowledge the contribution of Dr. Cristina P. Dadula, Dr. Danilo P. Dadula, Engr. Johanna Faith G. Israel, Engr. Vizzelle John J. Baliguat, Engr. Algem Cris B. Crusis, and Mr. John Duane L. Hitalia of WMO – General Santos City for the conduct of WACS. This w ork was supported by the Department of Science and Technology, Philippine Council for Industry, Energy, and Emerging Technology Research and Development (DOST-PCIEERD) GIA Program/Project [PCIEERD Project No. 10336 and PMIS No. 1212128].

CONFLICT OF INTEREST

The authors declare that there are no conflict of

interest regarding the publication of this manuscript. In addition, the ethical issues, including plagiarism, informed consent, misconduct, data fabrication and/or falsification, double publication and/or submission, and redundancy, were observed by the authors.

OPEN ACCESS

©2025 The author(s). This article is licensed under a Creative Commons Attribution 4.0 International License, which permits use, sharing, adaptation, distribution and reproduction in any medium or format, as long as you give appropriate credit to the original author(s) and the source, provide a link to the Creative Commons license, and indicate if changes were made. The images or other third-party material in this article are included in the article's Creative Commons license, unless indicated otherwise in a credit line to the material. If material is not included in the article's Creative Commons license and your intended use is not permitted by statutory regulation or exceeds the permitted use, you will need to obtain permission directly from the copyright holder. To view a copy of this license, visit:

http://creativecommons.org/licenses/by/4.0/

PUBLISHER'S NOTE

GJESM Publisher remains neutral with regard to jurisdictional claims with regard to published maps and institutional affiliations.

Positive AI Statement

During the preparation of this work the author(s) have used Artificial Intelligence (AI) [NAME TOOL / SERVICE] in order to [REASON]. After using this tool/ service, the authors reviewed and edited the content as needed and take full responsibility for the content of the publication.

(For this reason, the GPTZero detector will evaluate the manuscript utilizing Generative AI, ensuring a high detection rate. If the manuscript relies heavily on Generative AI and AI-assisted technologies, it will be archived without further options for appeal).

Negative AI Statement

The author(s) declare that no AI tools or services were not used or not highly applied during the preparation of this work.

ABBREVIATIONS

%	Percent
CDC	U.S. Centers for Disease Control and Prevention
COVID-19	Coronavirus 2019 disease
CRW	COVID-19 pandemic-related waste
df	Degrees of Freedom
DM	Disposable mask
e	Margin of error
ECQ	Enhanced community quarantine
Eq.	Equation
Fig.	Figure
g	Grams
g/day	Grams per day
g/m²	Grams per square meter
HH	Household
ISCO	International Standard Classification of Occupations
km	Kilometers
kg/day	Kilograms per day
LGUs	Local government units
m	Meter
m²	Square meters
MSW	Municipal solid waste
MSWM	Municipal solid waste management
N	Total number of households or total units of non-household generators
n	Sample size
NSWMC	National Solid Waste Management Commission
P	Standard deviation
p	p-value
PWF	Plastic waste footprint
people/km²	People per square kilometer
PPE	Personal protective equipment
PSOC	Philippine Standard Occupational Classification
R	Correlation coefficient
R²	Coefficient of determination

RSS	Recovery Recycling Stations
SARS-CoV-2	Severe acute respiratory syndrome coronavirus 2
SE	Standard Error
SOCSKSARGEN	South Cotabato, Sultan Kudarat, Sarangani Province, and General Santos City
SWMP	Solid waste management plan
t	t-statistic
US	United States
WACS	Waste analysis and characterization study
WMO	Waste Management Office
WHO	World Health Organization
χ^2	Chi-square

REFERENCES

Acot, F.T.; Sajorne, R.E.; Omar, N.-A.K.; Suson, P.D.; Rallos, L.E.E.; Bacosa, H.P., (2022). Unraveling Macroplastic Pollution in Rural and Urban Beaches in Sarangani Bay Protected Seascape, Mindanao, Philippines. J. Mar. Sci. Eng., 10: 1532 **(11 pages)**.

Adusei-Gyamfi, J.; Boateng, K.S.; Sulemana, A.; Hogarh, J.N., (2022). Post COVID-19 recovery: Challenges and opportunities for solid waste management in Africa. Environ. Chall., 6: 100442 **(9 pages)**.

Agduma, A.; Cao, K.-F., (2023). Species richness, extent and potential threats to mangroves of Sarangani Bay Protected Seascape, Philippines. Biodivers. Data J., 11: e100050 **(27 pages)**.

Ajbar El Gueriri, S.; El Mansouri, F.; Achemlal, F.; Lachaal, S.; Brigui, J.; Fakih Lanjri, A., (2023). Healthcare waste characteristics and management in the regional hospital and private clinic. Global J. Environ. Sci. Manage., 9(4): 805-818 **(14 pages)**.

Al-Emam, R.; Al-Yousfi, B., (2021). Waste management of used personal protective equipment during the COVID-19 pandemic in the Eastern Mediterranean Region. East Mediterr. Health J., 27: 1034-1035 **(2 pages)**.

Alzghoul, S.E.; Smadi, O.A.; Almomani, T.D.; Alzghoul, M.B.; Albataineh, O.M., (2022). Solid medical waste management practices and awareness in COVID-19 screening stations. Global J. Environ. Sci. Manage., 8(3): 327 **(12 pages)**.

Ammendolia, J.; Saturno, J.; Brooks, A.L.; Jacobs, S.; Jambeck, J.R., (2021). An emerging source of plastic pollution: Environmental presence of plastic personal protective equipment (PPE) debris related to COVID-19 in a metropolitan city. Environ. Pollut., 269: 116160 **(10 pages)**.

Apostol, G.L.C.; Acolola, A.G.A.; Edillon, M.A.; Valenzuela, S., (2022). How comprehensive and effective are waste management policies during the COVID-19 pandemic? Perspectives from the Philippines. Front. Public Health. 10: 958241 **(18 pages)**.

Aragaw, T.A., (2020). Surgical face masks as a potential source for microplastic pollution in the COVID-19 scenario. Mar. Pollut. Bull., 159: 111517 **(7 pages)**.

Arumugam, V.; Abdullah, I.; Yusoff, I.S.M.; Abdullah, N.L.; Tahir, R.M.; Nasir, A.M.; Omar, A.E.; Ismail, M.H., (2021). The Impact of COVID-19 on Solid Waste Generation in the Perspectives of Socioeconomic and People's Behavior: A Case Study in Serdang, Malaysia. Sustain., 13:13045 **(11 pages)**.

Bhat, R.A.; Singh, D.V.; Qadri, H.; Dar, G.H.; Dervash, M.A.; Bhat, S.A.; Unal, B.T.; Ozturk, M.; Hakeem, K.R.; Yousaf, B., (2022). Vulnerability of municipal solid waste: An emerging threat to aquatic ecosystems. Chemosphere, 287: 132223 **(13 pages)**.

Benson, N.U.; Bassey, D.E.; Palanisami, T., (2021). COVID pollution: impact of COVID-19 pandemic on global plastic waste footprint. Heliyon, 7: e06343 **(9 pages)**.

Congress of the Philippines, (2001). An Act Providing for an Ecological Solid Waste Management Program, Creating the Necessary Institutional Mechanisms and Incentives, Declaring Certain Acts Prohibited and Providing Penalties, Appropriating Funds Therefore, and for Other Purposes, Rep. Act No. 9003.

Cucinotta, D.; Vanelli, M., (2020). WHO Declares COVID-19 a Pandemic. Acta Biomedica, 91: 157-160 **(4 pages)**.

Cuong, L.D.; Fujiwara, T.; Asari, M.; Bao, N.D; Song Toan, P.P., (2022). Optimization of solid waste collection system in a tourism destination. Global J. Environ. Sci. Manage., 8(3): 419 (**18 pages**).

Department of Health, Department of the Interior and Local Government, (2020). Joint Administrative Order No. 2020-0001: Guidelines on Local Isolation and General Treatment Areas for COVID-19 cases (LIGTAS COVID) and the Community-based Management of Mild COVID-19 Cases.

El-Saadony, M.T.; Saad, A.M.; El-Wafai, N.A.; Abou-Aly, H.E.; Salem, H.M.; Soliman, S.M.; Abd El-Mageed, T.A.; Elrys, A.S.; Selim, S.; Abd El-Hack, M.E.; Kappachery, S.; El-Tarabily, K.A.; AbuQamar, S.F., (2023). Hazardous wastes and management strategies of landfill leachates: A comprehensive review. Environ. Technol. Innovation, 31: 103150 **(26 pages).**

Fadare, O.O.; Okoffo, E.D., (2020). Covid-19 face masks: A potential source of microplastic fibers in the environment. Sci. Total Environ., 737: 140279 **(4 pages)**.

Hâncean, M.-G.; Lerner, J.; Perc, M.; Oană, I.; Bunaciu, D.-A.; Stoica, A.A.; Ghiţă, M.-C., (2022). Occupations and their impact on the spreading of COVID-19 in urban communities. Sci. Rep., 12:14115 **(12 pages)**.

Hantoko, D.; Li, X.; Pariatamby, A.; Yoshikawa, K.; Horttanainen, M.; Yan, M., (2021). Challenges and practices on waste management and disposal during COVID-19 pandemic. J. Environ. Manage., 286: 112140 **(9 pages)**.

Herdiansyah, H.; Nuraeni, (2024). Environmental awareness and plastic use behavior during the Covid-19 pandemic. Global J. Environ. Sci. Manage., 10(2): 419 (**16 pages**).

Jarabe, J.G.P.; Torres, A.G.; Guihawan, J.Q.; Bacosa, H.P., (2023). Occurrence of COVID-19-Related Personal Protective Equipment (PPE) Litter in Mangroves and Beaches in Davao City, Philippines. Water Air Soil Pollut., 234: 395 **(11 pages)**.

Japan International Cooperation Agency, (2020). Waste Analysis and Characterization Study (WACS): A standardized and mandatory guide for Philippine Local Government Units and Solid Waste Management Practitioners **(62 pages)**.

Klemeš, J.J.; Fan, Y.V.; Tan, R.R.; Jiang, P., (2020). Minimising the present and future plastic waste, energy and environmental footprints related to COVID-19. Renewable Sustainable Energy

Rev., 127: 109883 **(7 pages)**.
Kulkarni, B.N.; Anantharama, V., (2020). Repercussions of COVID-19 pandemic on municipal solid waste management: Challenges and opportunities. Sci. Total Environ., 743: 140693 **(8 pages)**.
Krejcie, R. V.; Morgan, D. W., (1970). Determining sample size for research activities. *Educ. Psychol. Meas.*, 30: 607-610 (**4 pages**).
Kwakye, S.O.; Amuah, E.E.Y.; Ankoma, K.A.; Agyemang, E.B.; Owusu, B.-G., (2024). Understanding the performance and challenges of solid waste management in an emerging megacity: Insights from the developing world. Environ. Chall., 14: 100805 **(9 pages)**.
LGU-GSC; ADB, (2022). Green City Action Plan: General Santos City, Asian Development Bank **(204 pages)**.
Limon, M.R.; Vallente, J.P.C.; Cajigal, A.R.V.; Aquino, M.U.; Aragon, J.A.; Acosta, R.L., (2022). Unmasking emerging issues in solid waste management: Knowledge and self-reported practices on the discarded disposable masks during the COVID-19 pandemic in the Philippines. Environ. Chall., 6: 100435 **(14 pages)**.
National Solid Waste Management Commission, (2020). NSWMC Resolution No. 1380, Series of 2020: Adopting the Guidelines of the Waste Analysis and Characterization Study and its Related Manual **(48 pages)**.
Ng, C.H.; Mistoh, M.A.; Teo, S.H.; Galassi, A.; Ibrahim, A.; Sipaut, C.S.; Foo, J.; Seay, J.; Taufiq-Yap, Y.H.; Janaun, J., (2023). Plastic waste and microplastic issues in Southeast Asia. Front. Environ. Sci., 11: 1142071 **(15 pages)**.
Nzediegwu, C.; Chang, S.X., (2020). Improper solid waste management increases potential for COVID-19 spread in developing countries. Resour, Conserv. Recycl., 161: 104947 **(2 pages)**.
Ouhsine, O.; Ouigmane, A.; Layati, El.; Aba, B.; Isaifan, R.L.; Berkani, M., (2020). Impact of COVID-19 on the qualitative and quantitative aspect of household solid waste. Global J. Environ. Sci. Manage., 6(SI): 41-52 (**12 pages**).
Office of the President, (1996). Establishing Sarangani Bay and a Portion of the Municipal Waters of Maitum, Kiamba, and Maasim Sarangani Province as protected seascape for the purpose of protecting and maintaining its coastal and marine resources for the benefit and enjoyment of the people of the Philippines, Press. Proceeding. 756.
Oliveira, A.M.; Patrício Silva, A.L.; Soares, A.M.V.M.; Barceló, D.; Duarte, A.C.; Rocha-Santos, T., (2023). Current knowledge on the presence, biodegradation, and toxicity of discarded face masks in the environment. J. Environ. Chem. Eng., 11: 109308 **(17 pages)**.
Paringit, E.; Puno, G., (2017). LiDAR Surveys and Flood Mapping Report of Silway River. University of the Philippines Training Center for Applied Geodesy and Photogrammetry **(159 pages)**.
Patrício Silva, A.L.; Prata, J.C.; Walker, T.R.; Duarte, A.C.; Ouyang, W.; Barcelò, D.; Rocha-Santos, T., (2021). Increased plastic pollution due to COVID-19 pandemic: Challenges and recommendations. Chem. Eng. J., 405: 126683 (**9 pages**).
Peng, Y.; Wu, P.; Schartup, A.T.; Zhang, Y., (2021). Plastic waste release caused by COVID-19 and its fate in the global ocean. Proc. Natl. Acad. Sci. U.S.A., 118: e2111530118 (**6 pages**).
Philippine News Agency, (2021). GenSan to expand sanitary landfill.
Philippine Statistics Authority, (2022a). Household population, number of households, and average household size of the Philippines (2020 Census of Population and Housing).
Philippine Statistics Authority, (2022b). 2022 Updates to the 2012 Philippine Standard Occupational Classification (PSOC).
Philippine Statistics Authority, (2021a). 2020 Census of Population and Housing (2020 CPH) Population Counts Declared Official by the President.
Philippine Statistics Authority, (2021b). Highlights of the Population Density of the Philippines 2020 Census of Population and Housing (2020 CPH).
Ragazzi, M.; Rada, E.C.; Schiavon, M., (2020). Municipal solid waste management during the SARS-COV-2 outbreak and lockdown ease: Lessons from Italy. Sci. Total Environ., 745: 141159 **(6 pages)**.
Roy, P.; Mohanty, A.K.; Wagner, A.; Sharif, S.; Khalil, H.; Misra, M., (2021). Impacts of COVID-19 Outbreak on the Municipal Solid Waste Management: Now and beyond the Pandemic. ACS Environ. Au., 1: 32–45 **(14 pages)**.
Sajorne, R.E.; Cayabo, G.D.B.; Madarcos, J.R.V.; Madarcos, K.G.; Omar, D.M.; Ardines, L.B.; Sabtal, S.A.; Mabuhay-Omar, J.A.; Cheung, V.; Creencia, L.A.; Bacosa, H.P., (2022). Occurrence of COVID-19 personal protective equipment (PPE) litters along the eastern coast of Palawan Island, Philippines. Mar. Pollut. Bull., 182: 113934 **(8 pages)**.
Sangkham, S., (2020). Face mask and medical waste disposal during the novel COVID-19 pandemic in Asia. Case Stud. Chem. Environ. Eng., 2: 100052 **(9 pages)**.
Sanito, R.C.; Mujiyanti, D.R.; You, S.-J.; Wang, Y.-F., (2024). A review on medical waste treatment in COVID-19 pandemics: Technologies, managements and future strategies. J. Air Waste Manage. Assoc., 74: 72–99 **(29 pages)**.
Sarker, A.; Baul, T.K.; Nath, T.K.; Karmakar, S.; Paul, A., (2024). Household solid waste management in a recently established municipality of Bangladesh: Prevailing practices, residents' perceptions, attitude and awareness. World Development Sustainability, 4: 100120 **(12 pages)**.
Saseanu, A.S.; Gogonea, R.-M.; Ghita, S.I.; Zaharia, R.Ş., (2019). The Impact of Education and Residential Environment on Long-Term Waste Management Behavior in the Context of Sustainability. Sustain., 11: 3775 **(17 pages)**.
Selvaranjan, K., Navaratnam, S., Rajeev, P., Ravintherakumaran, N., 2021. Environmental challenges induced by extensive use of face masks during COVID-19: A review and potential solutions. Environ. Challenges, 3: 100039 **(11 pages)**.
Shanmugasundaram, L., (2024). Waste picking in the age of COVID-19: an environmental justice perspective. Discov. Environ., 2: 82 **(21 pages)**.
Sharma, H.B.; Vanapalli, K.R.; Cheela, V.S.; Ranjan, V.P.; Jaglan, A.K.; Dubey, B.; Goel, S.; Bhattacharya, J., (2020). Challenges, opportunities, and innovations for effective solid waste management during and post COVID-19 pandemic. Resour. Conserv. Recycl., 162: 105052 **(12 pages)**.
Shukla, S.; Khan, R.; Saxena, A.; Sekar, S., (2022). Microplastics from face masks: A potential hazard post Covid-19 pandemic. Chemosphere, 302: 134805 **(7 pages)**.
Tang, Y.; Liu, Y.; Chen, Y.; Zhang, W.; Zhao, J.; He, S.; Yang, C.; Zhang, T.; Tang, C.; Zhang, C.; Yang, Z., (2021). A review: Research progress on microplastic pollutants in aquatic environments. Sci. Total Environ., 766: 142572 **(80 pages)**.

Vanapalli, K.R.; Sharma, H.B.; Ranjan, V.P.; Samal, B.; Bhattacharya, J.; Dubey, B.K.; Goel, S., (2021). Challenges and strategies for effective plastic waste management during and post COVID-19 pandemic. Sci. Total Environ., 750: 141514 **(10 pages)**.

You, S.; Sonne, C.; Ok, Y.S., (2020). COVID-19's unsustainable waste management. Science: 368, 1438–1438 **(2 pages)**.

Yousefi, M.; Oskoei, V.; Jonidi Jafari, A.; Farzadkia, M.; Hasham Firooz, M.; Abdollahinejad, B.; Torkashvand, J., (2021). Municipal solid waste management during COVID-19 pandemic: effects and repercussions. Environ. Sci. Pollut. Res., 28: 32200–32209 **(10 pages)**.

Zhao, H.; Liu, H.; Wei, G.; Wang, H.; Zhu, Y.; Zhang, R.; Yang, Y., (2021). Comparative life cycle assessment of emergency disposal scenarios for medical waste during the COVID-19 pandemic in China. Waste Manage., 126: 388–399 **(12 pages)**.

AUTHOR (S) BIOSKETCHES

Banal, R.G., D.Eng., Professor, Electrical and Electronics Engineering Department, College of Engineering, Mindanao State University, General Santos, Fatima, General Santos City, 9500, Philippines.
- Email: ryan.banal@msugensan.edu.ph
- ORCID: 0009-0009-9338-4253
- Web of Science ResearcherID: NA
- Scopus Author ID: 24398302300
- Homepage: https://facultydirectory.msugensan.edu.ph/?facultyId=361-11

Abad, I.L.M., M.Sc., Associate Professor, Mechanical Engineering Department, Mindanao State University, Fatima, General Santos City, 9500, Philippines.
- Email: irenelara.abad@msugensan.edu.ph
- ORCID: 0009-0006-5392-1761
- Web of Science ResearcherID: NA
- Scopus Author ID: NA
- Homepage: https://facultydirectory.msugensan.edu.ph/?facultyId=360-07

HOW TO CITE THIS ARTICLE

Banal, R.G.; Abad, I.L.M., (2025). Tracking Coronavirus 2019 pandemic-related waste generation in urban waterways. Global J. Environ. Sci. Manage., 11(3): 1163-1184.

DOI: 10.22034/gjesm.2025.03.16

URL: https://www.gjesm.net/article_724551.html



Global J. Environ. Sci. Manage. 11(3): 1185-1198, Summer 2025, Serial #43

Global Journal of Environmental Science and Management
(GJESM)

Homepage: https://www.gjesm.net/

Podcasts

CASE STUDY

Sustainability of natural tourism attraction and satisfaction

Y. Yuliana[1,*], A.M. Ningsih[2], V. Kristiana[2], A.P. Maharani[2], C. Syahni[1]

[1] *Faculty of Economics and Business, Universitas Muslim Nusantara Al-Washliyah, Medan, North Sumatera, Indonesia*

[2] *Faculty of Letters, Universitas Muslim Nusantara Al-Washliyah, Medan, North Sumatera, Indonesia*

ARTICLE INFO

Article History:
Received 21 December 2024
Revised 26 February 2025
Accepted 09 April 2025

Keywords:
Natural tourism
Revisit intention
Tourist attraction
Tourism destination sustainability
Tourist satisfaction

DOI: 10.22034/gjesm.2025.03.17

ABSTRACT

BACKGROUND AND OBJECTIVES: Batu Katak is a small dream village located on the edge of Gunung Leuser National Park in North Sumatra, Indonesia. Nature tourism is full of natural charm. It serves as an ideal retreat from busy crowds, providing an opportunity to spend a vacation connecting with the natural world. One part of the village is home to a remarkable karst forest, teeming with diversity and characterized by its cave systems and intriguing landscapes, while the famous National Park is situated just across the river. The attraction of Batu Katak nature tourism is trekking, and the uniqueness of the flora and fauna offered, including the giant Rafflesia flower and Amorphophallus found in the area. This study aims to examine the effect of tourist attraction and tourist satisfaction on the revisit intention of tourists in the case of Batu Katak Natural Tourism in Indonesia.

METHODS: Tourists who had visited Batu Katak Nature Tourism comprised the study's population. In this investigation, the sample size was 350 people who had just visited the Batu Katak Park nature tourism. Structural equation modeling, a utilized in this study as a multivariate analysis technique, illustrates the concurrent linear relationships between unobserved elements (latent variables) and observation variables (indicators). A component-based model of structural equations method called partial least squares is implemented.

FINDINGS: This investigation discovered that tourist attraction affects the revisit intention positively and significantly. The influence of the tourist attraction was both positive and significant in enhancing satisfaction levels. Tourist satisfaction effect revisit Intention positively and significantly. This analysis also examines the indirect effects of a tourist attraction on revisit intention by tourist satisfaction as mediation. The study revealed that tourist satisfaction plays a mediating role in the relationship between tourist attractions and the likelihood of returning.

CONCLUSION: Tourist attractions have made strong effect on tourist satisfaction. Tourist satisfaction has a significant contribution to revisit intention, and tourist attractions have a strong effect on tourist revisit intention. The findings of this study reveal that the presence of tourist attractions is the key factor in establishing a tourist destination. Tourist attractions after visiting a natural tourist area will affect their desire and decision to revisit, and this requires the management's capacity to sustain and improve tourist sites according to tourist needs, desires, satisfaction, and perceptions. The findings also found that tourist attractions affect revisit intention through the satisfaction of tourists. Tourist satisfaction is a crucial factor in motivating individuals to revisit destinations. When tourists are content with their experiences, it amplifies the impact of attractions on their likelihood of returning.

This is an open access article under the CC BY license (http://creativecommons.org/licenses/by/4.0/).

NUMBER OF REFERENCES
67

NUMBER OF FIGURES
3

NUMBER OF TABLES
5

*Corresponding Author:
Email: *yayukyuliana@umnaw.ac.id*
Phone: +0821 6555 7651
ORCID: 0009-0000-4394-0359

Note: Discussion period for this manuscript open until Sep 1, 2025 on GJESM website at the "Show Article".

INTRODUCTION

Batu Katak is a small dream village located on the edge of Gunung Leuser National Park in North Sumatra. Nature tourism is full of natural charm. It serves as an ideal retreat from busy crowds, providing an opportunity to spend a vacation connecting with the natural world. On one side of the village, there is a very diverse and interesting karst forest, full of cave systems and interesting landscapes, and across the river is the famous National Park. The primary draw of Batu Katak nature tourism lies in its trekking experiences and the exceptional variety of flora and fauna, including the remarkable Rafflesia flower and Amorphophallus that inhabit the area. The wildlife found in Batu Katak Ecotourism are siamang (Hylobates syndactylus), Sumatra orangutan (pongo abelii), Sumatra tiger (Panthera tigris sumatrae), wild goat (Capricornis sumatraensis), kedih (Presbytis thomasi), sun bear (Helarctos malayanus), soft-shelled labi-labi (Dogania suplana), porcupine (Hystrix sumatrae), civet (Cynogale benettii) and otter (Lutra sumatrana). The wildlife live freely in Batu Katak Ecotourism (indarjo and Arifin, 2016). Batu Katak Ecotourism has tourist attractions consisting of natural panoramas, corpse flowers (Amorphophallus titanum), rafflesia, cave exploration, Batu Katak shrine, waterfalls, and wildlife. This feature represents a significant advantage of Batu Katak Ecotourism. Environmental issues are frequently a challenge within the Indonesian tourism sector. Tourist destinations that are not kept clean. In addition to positive effects, tourism also has negative effects on local communities and the local environment. Local communities play a crucial role in shaping tourism development, as they have both the moral authority and the right to be involved in this process. To increase local community trust in the tourism industry, local communities must be involved in decision-making and policy-making. Efforts made by the community at the Batu Katak natural tourism destination include renting mats, renting tires for tubing, and selling drinks and snacks. Moreover, the likelihood of tourists returning serves as a crucial measure for evaluating their experiences in a tourism area, especially if they take part in tourism-related activities (Kim and Park, 2017; Kridakorn Na Ayutthaya et al., 2024; Silalahi *et al.,* 2024). Previous research has identified numerous characteristics that influence revisit intention, particularly in the sectors of tourism. Prior studies have shown that there are elements beyond management and business education. The perceived environmental value can enhance the likelihood of returning. Several researchers have confirmed that tourist attraction and tourist satisfaction influence revisit intention (Diallo *et al*., 2015). However, this study has not discussed all variables as a whole. This research intends to fill the gap, by applying tourist satisfaction as mediation. One issue arising from the growing popularity of nature tourism is that the experiences provided do not consistently align with the desires of tourists. Tourists will be more satisfied with the features of a tourism product or service, and visitors are pleased when the experience of tourist exceeds tourist expectations (over-fulfillment); on the other side, visitors are often disappointed when their experience falls short of their expectations (Tan *et al*., 2019). Numerous studies indicate that various factors impact the intention to revisit (Marques *et al*., 2021). The study carried out by Song *et al*. (2019) indicates that tourist attractions have a significant and favorable effect on the satisfaction of tourists. A person's tendency to carry out a behavior is influenced by several factors such as attitude toward behavior, subjective norms, and perceived behavioral control known as the theory of planned behavior (Ajzen, 2011). Abbasi *et al.,* (2021) theory of planned behavior (TPB) is one of the predictors that can have a positive effect on revisit intention. Perceived behavior as a determinant of attitude rather than tourists positively affects the revisit intention. According to Bianchi *et al*. (2017), travel decision-making is influenced by multiple factors, particularly psychological aspects such as attitudes, visitor satisfaction, and the image of the destination. This study is important to perform because the research provides a significant contribution to the development of knowledge related to efforts to increase revisit intention in the tourism sector. Within the scientific context, this study identifies visitor satisfaction as a mediating element that reinforces the link between tourist attractions and the desire to return. This research also has a practical contribution for local governments as decision makers in formulating regulations to improve the performance and attractiveness of natural tourism. Consequently, it will affect the inclination to revisit. Interest refers to the emotional state that consumers experience before engaging in an action, which can

then be used as a standard for assessing the action itself (Jung *et al*., 2018). Purchase interest as a model and consumer attitudes towards objects that are very suitable for measuring attitudes towards a product, service, or brand class (Chou and Hsu, 2016). Revisit intention is the customer's willingness to visit a tourist destination, provide positive word of mouth, stay longer than expected, and spend more than expected. The concept of revisit intention is derived from behavioral intention. The concept of behavioral intention includes two key components: the intention to make repeat purchases and the intention to engage in word of mouth communication (Oliver, 1999). Behavioral intention refers to the visitor's plan to return within a year and to make repeated visits to the location (Baker *et al*., 2020). Positive word-of-mouth from visitors and the desire to refer to others are additional elements that are taken into consideration when evaluating behavioral intentions (Bigné *et a*l., 2001). A destination's ability to attract repeat visitors can be shaped by its overall performance, which encompasses advertising strategies and the circulation of news about newly available attractions (Ryan *et al*., 2012). Revisit intention can be defined as a strong willingness, whether or not one has a positive attitude about the service provider.

The intention to revise is influenced by environmental psychological aspects that are rooted in two behavioral foundations: approach and avoidance (Wirtz and Zeithaml, 2018). The interest in repeat visits is also influenced by tourist attractions or what is known as tourist attractions. The key influence on the willingness to revisit is the attractiveness of the tourist site. As one of the primary concerns in human life, ecotourism draws significant attention to the sustainability of natural resources and the environment on an economic, social, and political level (Wondirad *et al*., 2020). In alignment with the United Nations Sustainable Development Goals for 2030, sustainable tourism is emerging as a central theme in a growingly intricate area of research, discussion, and perspectives (Cotterell *et al*., 2020). Many destinations are finding it difficult to become sustainable due to globalization, the change in technology, the consumption of tourism trends, and growing international rivalry. Tourist attractions are resources and very important in attracting visitors (Navarro-Ruiz and McKercher, 2020; Zulvianti *et al.,* 2023). Tourist Attractions are an important determining factor for someone to decide to visit a tourist destination (Isa and Ramli, 2014). The main purpose of the formation of Tourist Attractions is to influence tourists' perceptions. The traits of natural tourism can serve as a foundation for creating tourist attractions (Camilleri, 2018). Tourist satisfaction refers to the emotions felt by tourists when receiving an opportunity or experience that exceeds their expectations. The level of customer satisfaction can be gauged by the interactions consumers have with product providers while utilizing the products (Semuel and Wibisono, 2019). Tourist satisfaction will influence trust and the willingness to revisit



Fig. 1: Jungle Trekking in Batu Katak, Indonesia

the destination (Pujiastuti *et al*., 2017). Seow *et al.,* (2024) argued that visitor satisfaction determines the visitor's attitude to make repeat visits in the future. The willingness to revisit describes tourists' inclination to return to the same place in the future (Arifin *et al*., 2021). Revisit intention is a visitor's assessment of the possibility of revisiting a tourist attraction (Herliza and Ferdian, 2024). Impressive positive experiences play an important role in influencing tourist satisfaction towards the intention to revisit (Mahdzar and Gani, 2018). The way tourists perceive and experience their visits plays a significant role in determining their intentions to return (Kim, 2014). Tourist satisfaction is required for the development of the tourism sector and tourist revisit destinations (Evren *et al*., 2020). Revisit intention is positively influenced by tourist satisfaction at rural tourist attractions (Chin *et al*., 2022). A key element that enhances the likelihood of tourists returning is their sense of well-being. Additionally, how recreation is perceived and the level of interest play significant roles in influencing well-being. The effects of spatial atmosphere, emotional connection to a place, perceived interest, and the perception of the environment on well-being are positively influenced by the richness of information available (Lin, 2024). Tourists will make repeat visits if their past experiences during their visits were not disappointing. Satisfaction in the past will make tourists make repeat visits. Thus, it can be assumed that tourist satisfaction plays a mediating role in the influence of tourist attraction dimensions on revisit intention in the context of nature tourism. Teeroovengadum, (2019) argues that a tourist behaves responsibly by referring to the factors of desire to travel. Responsible tourists have a profile of respecting the social, cultural, and natural capital of the visited area (Zgolli and Zaiem, 2018). The role of tourist attractions is crucial in influencing behaviors, particularly in terms of assessing satisfaction, intentions to return, and the propensity to recommend to others. Attractions are used as a means to determine the purpose of visiting a destination (Leask, 2016). Therefore, tourist attractions are the main reason why tourists choose the destination (Crouch and Ritchie, 1999). When a consumer compares a product's perceived performance or outcome to their expectations, consumer can feel either satisfied or disappointed (Kotler and Keller, 2009). Customer satisfaction arises when individuals perceive that their needs have been met exceptionally well during their assessment of a product or service (Oliver, 1999). Customer involvement is a function of expectations and perceptions related to a product or service. Dissatisfied consumers will usually switch to another brand and avoid the product that makes them dissatisfied (Kotler, 2012). In contrast, content customers tend to come back for more and recommend their favorable experiences to others. In addition to helping destination marketers enhance the quality of their offerings and create something new that can satisfy travelers' needs or desires, knowledge about visitor satisfaction at a specific location will also help the destination better meet the needs of tourists, and give an effect on revisit intention (Quintal and Polczynski, 2010). The key factor in visitor satisfaction is the awareness and knowledge gained during the visit (Woods and Moscardo, 2003). The remarkable natural features and welcoming atmosphere of a destination can draw tourists seeking a variety of experiences (Okello and Novelli, 2014). Attraction is a uniqueness and attribute in a tourist destination that can attract tourists. According to Cheng and Wu, (2015) environmental knowledge and awareness can influence tourists to behave responsibly towards the environment and natural sites. As highlighted by Schwartz (2019), attributes such as the beauty of nature, environmental conditions, and biodiversity play a crucial role in attracting tourists. Furthermore, environmental suitability has a positive effect on visitor satisfaction (Suanmali, 2014). According to Kotler and Keller (2009), a person's emotional response is influenced by how the perceived performance of a product aligns with their expectations, leading to either joy or disappointed. Simanihuruk *et al*. (2018) confirmed that tourist attraction effect the tourist satisfaction positively and significantly. The tourist Satisfaction variable is used to mediate Tourist Attraction towards revisit intention based on self-congruity (Sirgy and Su, 2000) namely self-concept is a cognitive mechanism that determines whether the values expressed by a tourist destination are in accordance with the tourist's self-concept. The notion of satisfaction explores the relationship between service satisfaction and customer satisfaction in particular circumstances. From an experiential perspective, satisfaction indicates how satisfied customers are with the service content associated with a transaction. Satisfaction is



Fig. 2: Flora, Fauna and the Cave in Batu Katak

defined as the "result of customer evaluations" of the content provided by a service provider and results from comparing customers' experiences with their prior expectations, leading to customer satisfaction or dissatisfaction (Kao *et al.,* 2019). The study aims to examines the effect of tourist attraction and tourist satisfaction on revisit intention of tousts in the case of Batu Katak Natural Tourism in Indonesia. This study has been carried out in Batu Katak Tourism Location, Indonesia, in 2024.

MATERIALS AND METHODS

Tourists who had visited Batu Katak Nature Tourism comprised the study's population. Conversely, a sample is a subset of components or individuals selected from a wider population, chosen through sampling methods to effectively represent the overall population. Since the identification of the respondents required to create the sampling framework cannot be provided in detail, the sample type employed in this study is the accidental sampling technique. Accidental sampling involves choosing respondents for a study based on those who are conveniently available to researchers during their data collection process (Uma and Roger, 2010). The population size in this study is not known with certainty, therefore the sample size developed by Krejcie and Morgan (Uma and Roger, 2010) is 350 people. The sample size of this study was 350 people who had just visited the Batu Katak Park nature tourism.

Based on Table 1 respondents based on gender in this study, out of 350 respondents, male respondents reached 205 respondents or 58.6 percent (%), and female respondents reached 145 respondents or

41.4%. Respondents based on age can be divided into 4 categories, namely: tourists aged < 25 years amounting to 181 respondents or 51.7%, tourists aged between 26-35 amounting to 68 respondents or 19.4%, tourists aged 36-45 years amounting to 59 respondents or 16.9%, tourists aged > 45 years amounting to 42 respondents or 12.0%. The predominant age group among respondents is tourists aged 17 to 25 years. High school education amounting to 154 people or 44.0%. Next, the second rank of tourists with a Bachelor's degree in education is 109 respondents or 31.1 %. Based on income level, it is divided into 4 categories. The initial category includes 49 respondents, or 14.0%, of tourists whose income surpasses 366.97 United States Dollars (USD). For the second category are tourists who have an income of 73,39 to 366,97 USD amounting to 124 respondents or 35.4%. For the category of 30,58 to 73,39 USD, the amount is 91 respondents or 26.0%. The income category of 21,41 to 30,58 USD, amounted to 86 respondents or 42.6%. According to the data presented, the majority of tourists belong to the income bracket of 73,39 to 366,97 USD.

The study consists of three variables, namely tourist attraction, tourist satisfaction, and tourist revisit intention. Tourist attraction uses 4 items adopted from Chi and Qu (2008) and Bhat and Darzi (2018). Tourist satisfaction uses 4 items adopted from Sulistyanto *et al*. (2022). Furthermore, revisit intention also uses 4 items adopted (Elsayeh, 2020; Kumar and Kaushik, 2017; Alrawadieh *et al*., 2019).

Structural equation modeling (SEM), a multivariate analysis tool used in this study, describes the concurrent linear relationship between factors that cannot be directly assessed (latent variables) and observation variables (indicators). The component-based structural equation modeling technique known as partial least squares (PLS) is utilized. The purpose is to analyze structural models and data. PLS has the advantage of working with nominal, ordinal, and interval scale variables and requiring less data for distribution. Moreover, this method is

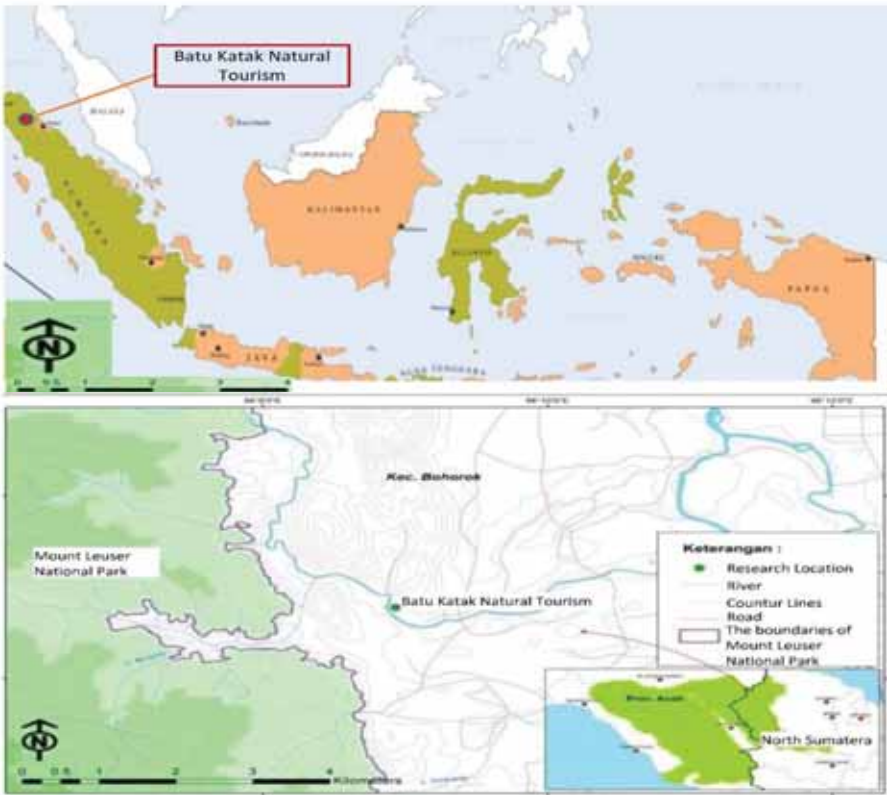

Fig. 3: Geographical location of the study area in Batu Katak Tourism Location, Indonesia

Table 1: Characteristics of respondents

No.	Characteristics	Choice	Number of respondents	
			F	%
1	Gender	Man	205	58.6
		Woman	145	41.4
2	Age	< 25 years	181	51.7
		26 -35 years	68	19.4
		36-45 years	59	16.9
		More than 45 years	42	12.0
3	Level of education	SENIOR HIGH SCHOOL	154	44.0
		Bachelor	109	31.1
		Diploma	62	17.7
		Postgraduate	25	7.1
4	Income	Over 366,97 USD	49	14.0
		73,39 – 366,97 USD	124	35.4
		30,58 – 73,39 USD	91	26.0
		21,41 - 30,58 USD	86	42.6

Table 2: Measurement of variables

Variables	Measurement	Sources
Tourist attraction	1. The uniqueness of tourist attraction compared to other tourist attractions 2. The beauty of tourist attractions compared to other tourist attractions 3. The authenticity of tourist attraction 4. The weather of tourist attraction	(Chi and Qu, 2008) (Bhat and Darzi, 2018)
Tourist satisfaction	1. Tourist enjoy all the existence of tourist destination 2. Tourist feel about all the existence in the tourist destination 3. Being at a Tourism destination was a vacation that went as I thought it would 4. Being at the tourist destination was the perfect vacation that I needed.	(Sulistyanto *et al.*, 2022)
Revisit intention	1. Intend to tourism place in the future. 2. Suggest/recommend others to visit. 3. Tell positive things to others. 4. Make it as first choice and destination for a vacation.	(Elsayeh, 2020) (Kumar and Kaushik, 2017) (Alrawadieh *et al.*, 2019)

superior for recognizing differences between groups in cases where the data lacks a normal distribution, and it is particularly well-suited for predicting a range of dependent variables from a substantial set of independent variables (Hair *et al*., 2019).

RESULTS AND DISCUSSION

Convergent validity is a component of the measurement model, which is known as confirmatory factor analysis (CFA) in Covariance-based SEM and the outer model in SEM-PLS (Hair *et al*., 2019). The measurement model fulfills the convergent validity standards for reflective constructs, which state that the loading must be greater than 0.7. Convergent validity assessment is carried out by looking at the average variance extracted (AVE) value for each construct (Hair *et al*., 2019) state that each construct is stated to be good, AVE value 0.5.

Three criteria were used to evaluate convergent validity: 1) composite reliability (CR) should be above

Table 3: Convergent validity

Indicator	Loading Factor	Composite Reliability	AVE	Cronbach Alpha
Tourist Attraction		0.984	0.940	0.968
The uniqueness of the Batu Katak natural tourist attraction compared to other tourist attractions I have visited	0.972			
The beauty of the Batu Katak natural tourist attraction compared to other tourist attractions I have visited	0.971			
I feel that the authenticity of Batu Katak nature tourism is in accordance with my personality or self-concept.	0.969			
The weather at Batu Katak nature tourism is pleasant	0.967			
Tourist Satisfaction		0.965	0.873	0.986
I enjoyed all the existence in the Batu Katak natural tourist destination	0.949			
I feel about all the existence in the Batu Katak natural tourist destination	0.944			
Being at the Batu Katak Nature Tourism destination was a vacation that went as I thought it would.	0.938			
Being at the Batu Katak natural tourist destination was the perfect vacation that I needed.	0.905			
Revisit Intention		0.981	0.867	0.974
I intend to revisit the Batu Katak nature tourism in the future.	0.968			
I would suggest/recommend others to visit Batu Katak nature tourism	0.969			
I will tell positive things about Batu Katak nature tourism to others.	0.901			
I will make Batu Katak nature tourism my first choice and destination for a vacation.	0.896			

0.70; 2) average variance extracted (AVE) should be greater than 0.50; and 3) all component loadings should be greater than 0.60. Good measurement reliability was also indicated by the fact that all Cronbach's alpha (CA) values were higher than 0.70. Adequate discriminant validity for all constructs was established because the square root of the AVE for each construct, indicated by the diagonal of each column, was greater than its correlations with other constructs (Usakli and Kucukergin, 2018). Discriminant validity testing can also be carried out by comparing the correlation of each construct with the square root of its AVE based on the Fornell-Lacker criteria (Hair *et al*., 2019). The square root value of AVE on the Fornell-Lacker criterion is obtained by performing the square root operation of the AVE value obtained on the SmartPLS algorithm. The result obtained from the square root of the AVE will act as a standard for measuring discriminant validity, which can be compared against the correlations between different constructs.

Table 4 informs the hypothesis testing result. This study found that tourist attraction has a significant influence on Revisit Intention (β =0.084, p < 0.020). The tourist attraction has a significant influence on tourist Satisfaction (β =0.153, p < 0.004). Tourist Satisfaction has a significant influence on Revisit Intention (β =0.217, p < 0.002). Beyond assessing the direct relationship between tourist attractions, tourist satisfaction, and the intention to return, this research delves into the indirect influences that tourist attractions have on tourist Satisfaction. Tourist Satisfaction mediates the impact of tourist attraction to revisit intention (β =0.033, p > 0.043).

The idea of sustainable tourism encompasses practices that can yield enduring benefits for the environment, society, culture, and economy, impacting both today and the future. Visitors are one of the factors that support the sustainability of Batu Katak Natural Tourism. With the presence of tourists, the economic life of the surrounding community can develop and become a source of income for the government. Rich in both flora and fauna, the Batu Katak natural tourism area, combined with the unique attributes of the surrounding community, serves as a fascinating natural laboratory for further research (Purwanto *et al*., 2014). Tourists can enjoy the natural panorama, besides that tourists can also do nature adventures, camping, bird watching, fishing, and rafting. The study explores the impact of tourist attractions and the level of satisfaction on the likelihood of tourists revisiting. The first hypothesis shows the result of a positive and significant influence on the relationship between tourist attraction and

Table 4: AVE root value Fornell-Lacker criterion

Variables	Revisit intention	Tourist attraction	Tourist satisfaction
Revisit Intention	0.934		
Tourist Attraction	0.493	0.970	
Tourist Satisfaction	0.634	0.519	0.934

Table 5: Direct effects, mediation, on variables

Hypothesis	β	p-values	Decisión
H1: Tourist attraction has an impact revisit Intention	0.084	0.020	Accepted
H2: Tourist attraction Has an impact on tourist satisfaction	0.153	0.004	Accepted
H3: Tourist satisfaction has an impact revisit intention	0.217	0.002	Accepted
H4: Tourist satisfaction mediates tourist attraction to revisit Intention	0.033	0.043	Accepted

tourist satisfaction. Tourist attractions play a crucial role in determining the satisfaction levels of visitors. A destination that features engaging attractions and ensures a pleasant experience will lead to higher levels of tourist satisfaction. Bagheri *et al*., (2024) state that the experience experienced by a visitor or tourist will have an impact on visitor satisfaction. The importance of nature-based and forest-based tourism, as well as the necessity for visitors to experience the introduction of nature, have all been covered in earlier studies. Consequently, it is essential for managers of tourist destinations to prioritize tourism development. The development of tourist sites takes into account not only the economic worth of travel but also its environment and services (Adam, 2021). Findings from the second hypothesis test reveal that tourist attractions play a crucial and beneficial role in influencing visitors' likelihood of returning. A research conducted by Bagheri *et al.* (2024) discovered that visitor experiences and attractions will eventually affect loyalty. Visitors are more inclined to return if visitors had a positive experience and are more satisfied. The tourism industry has extensively addressed orientation to tourist sites and its impact on visitor satisfaction, intention to return, and intention to return. The key factor influencing the intention to return is the perceived level of attractiveness. A tourist attraction is anything that has natural beauty and is found in tourist destinations, like waterfalls and caverns, as well as rich natural, cultural, and zoological resources that draw travelers. One of the primary reasons for wanting to return is the natural potential that has been developed and recognized as a tourist destination. The way that visitors evaluate tourist sites can vary from person to person (Park *et al*., 2018). Tourist satisfaction has an impact on revisit intention. The third hypothesis test proves that tourist satisfaction is a factor that determines whether a tourist will come back to visit or not. The uniqueness of Batu Katak is the biggest attraction factor for visitors as satisfaction determinat with a loading factor of 0.972. The second element is the charm of the Batu Katak natural tourist destination, boasting a loading factor of 0.971. The attachment visitors feel to the location is a distinctive appeal. This is also in accordance with the findings of research conducted by (Zou *et al*., 2022) relationship between place attachment and tourist loyalty was scientifically proven. The results of previous studies by Nguyen Huu *et al*. (2024) tourist attractions may acquire a competitive advantage by providing a higher perceived value, which increases tourist satisfaction and encourages return visits. The same findings were also found by Simanihuruk *et al*. (2018) found that tourist satisfaction will have an impact on revisit intention as a result of strengthening tourist attractions. This study has furthered theoretical insights and has practical implications for management. To begin with, it examines the direct impacts of tourist attraction on tourist satisfaction, in line with the proposed hypothesis. Tourist satisfaction will increase the number of tourist.

Satisfied tourists will have the potential to come back, and of course will recommend Batu Kata Natural tourism as a tourist destination. This study validates previous studies that demonstrated the influence of tourist visits on the environment and the local communities. Stylos, (2019) discovered a strong link between environmental tourism and sustainability. The findings are also congruent with the concept of sustainable tourism development, a concept that is widely accepted in tourist locations. Tourism destination performance must be considered in a broader perspective, encompassing not just growth of economic and output, but also the maturity of the tourism development and advantages. This comprehension originates from studies focused on sustainable development (Choi *et al*., 2020). This study also contributes to the mediation effect driven by tourist satisfaction from the influence of tourist attraction and tourist satisfaction toward revisit intention. Tourist satisfaction serves as an intermediary factor that affects how tourist attractions influence the likelihood of visitors returning. This shows that visitor satisfaction is very important to maintain, because satisfaction is very important for making decisions. Evidence shows that when tourists are satisfied, their inclination to revisit destinations rises significantly. This is in accordance with the findings of research conducted by Pavlic *et al.,* (2014) revealed that tourist satisfaction is one of the factors that can increase the growth of tourist destinations. In order to maximize the benefits of ecotourism—such as cultural exchange, the revitalization of traditional crafts and ceremonies, and the advancement of rural development—the government is making investments in tourism initiatives. Additionally, the government has a broad duty to protect people's social welfare, especially that of women and children, by lessening the detrimental sociocultural effects of tourism. Another factor is very crucial to limit tourism's environmental impact, such as pollution and other environmental risks. Nature tourism is also employed to maintain a healthy lifestyle balance. Nature tourism can revitalize the body and mind, allowing tourists to work more creatively since it provides both physical and spiritual pleasure. To boost tourist attraction and satisfaction, tourism managers must leverage their creativity, which in turn can lead to an increased intention for visitors to return. Creativity is essential for thriving in the business landscape (Siregar *et al*., 2022).

LIMITATIONS AND FUTURE RESEARCH DIRECTIONS

This study has made an essential contribution to the study of nature tourism, however, it does have certain drawbacks. To begin with, numerous important indicators were omitted from this study. As a result, future investigations could explore other factors, including waste management at tourist locations, to better understand and improve perceived environmental value. Furthermore, tourist attractiveness indicators like infrastructure and art must be enhanced. Furthermore, this study evaluates the degree of tourists' intention to revisit, while the tourism industry primarily aims to gauge the loyalty of its visitors. Consequently, it is expected that further studies will boost the intention to return. Additionally, given that all participants in this research were domestic travelers, future research is likely to involve international tourists.

CONCLUSION

The sustainability of Batu Katak natural tourism place is very important to maintain. Current research is very crucial because it can preserve natural tourism, in this case, Batu Katak natural tourism, and also improve the welfare of the surrounding community. Attractions for visitors include the exceptional qualities of Batu Katak, its authentic essence, and the stunning natural environment featuring diverse flora and fauna. The attractions in Batu Katak Ecotourism such as the Berkail River which is still clear and has many rocks, there are 8 karst caves, there is a corpse flower (Amorphophallus titanum) which is easy to find, there is a rafflesia flower (Rafflesia lawangensis), there are various types of wild animals such as Sumatran orangutans (pongo abelii), siamangs or gibbons (Hylobates syndactylus), sun bears (Helarctos malayanus) and Sumatran tigers (Panthera tigris sumatrensis). Maintaining and protecting these aspects is crucial for ensuring visitor satisfaction and encouraging them to plan future visits. Scientifically, this research also has an impact on increasing the scientific treasury, especially in the field revisit the intention to enhance natural tourism destination sustainability. The findings prove that all hypotheses are accepted. This result indicates that the desire to return is shaped by the attractiveness of tourist sites as well as the satisfaction experienced by visitors.

Tourist attractions have a significant impact on tourist satisfaction. Tourism managers and the government must pay more attention to tourism facilities and attractions so that visitors are not disappointed and feel satisfied. A commitment to innovation and quality enhancement is crucial. Additionally, destinations are encouraged to implement promotional strategies that cater to customer needs and satisfaction, crafting advertisements and promotions that evoke emotional connections. Tourist satisfaction is a determinant of whether tourists will come or not in the future. Tourist satisfaction is very important to manage so that tourists come back to visit. Tourist attractions have a significant effect on revisit intention. The findings also found that tourist attractions affect revisit intention through the satisfaction of tourists. To gain revisit intention, destinations can utilize various channels to strengthen their tourist satisfaction. The findings of this study reveal that the presence of tourist attractions is the key factor in establishing a tourist destination. Tourist attractions after visiting a natural tourist area will affect their desire and decision to revisit, and this depends on the management's ability to maintain and improve tourist sites according to tourist needs, desires, satisfaction, and perceptions. The findings of this study suggest that it is essential for all parties involved, such as government entities and tourism managers, to concentrate on enhancing tourist attractions. This focus will help create a comfortable environment for visitors and foster a favorable impression. As a policymaker or decision-maker, the government is in charge of preserving the environmental effects of tourist destinations, including the detrimental effects of pollution, other environmental hazards, and land use issues brought on by inadequate planning, regulation, and engineering of sites, tourist attractions, and facilities. Furthermore, tourist destinations can involve visitors in environmental conservation by creating communities focused on this purpose. Batu Katak must be maintained in its natural condition, with biodiversity and animals, and increasing visitor comfort, preparing other facilities such as rest areas and clean sanitation facilities. To preserve biodiversity and wildlife in Batu Katak, effective conservation strategies must be established. These strategies should prioritize the protection of forested regions, promote the sustainable use of biodiversity, and ensure that natural resources are not compromised. Furthermore, all activities should be designed to be environmentally friendly, minimizing any negative impact on the surroundings. Lastly, to satisfy the needs and preferences of visitors, tourism locations might collaborate with different parties. Local communities can be involved in tourism management such as being guides, providing restaurants, sanitation, and transportation. The process of formulating policy recommendations includes collaboration among local communities, government officials, Leuser Mountain area managers, and researchers to create landscapes that mitigate impacts and sustain current conditions. Encourage small and medium enterprises in tourist locations, and protect biodiversity and animals in the Batu Katak Natural Tourism area. The preservation of Batu Katak's natural attractions should also be a priority in environmental regulation. The uniqueness and biodiversity must be maintained, there is a prohibition on visitors from taking any biodiversity and animals at the Batu Katak natural tourism location.

AUTHOR CONTRIBUTIONS

Y. Yuliana performed conceptualization, formal analysis, investigation, methodology, and supervision, and analyzed and interpreted the data. A.M Ningsih performed project administration, validation and help conceptualization, data processing. V. Kristiana performed the methodology, the writing – original draft, help in conceptualization and investigation. A.P. Maharani performed methodology, help in writing – review and editing, investigation, and help interpreted data analysis, and supervision. C. Syahni performed writing – review and editing, visualization, help in the investigation, and project administration.

ACKNOWLEDGEMENT

DRTPM funded this study by of the Ministry of Education, Culture, Research, and Technology, Grant number [103/E5/PG.02.00.PL/2024], for the 2024 fiscal year.

CONFLICT OF INTEREST

The authors declare that there are no conflict of interest regarding the publication of this manuscript. In addition, the ethical issues, including plagiarism, informed consent, misconduct, data fabrication and/or falsification, double publication and/or submission, and redundancy, were observed by the authors.

OPEN ACCESS

©2025 The author(s). This article is licensed under a Creative Commons Attribution 4.0 International License, which permits use, sharing, adaptation, distribution and reproduction in any medium or format, as long as you give appropriate credit to the original author(s) and the source, provide a link to the Creative Commons license, and indicate if changes were made. The images or other third-party material in this article are included in the article's Creative Commons license, unless indicated otherwise in a credit line to the material. If material is not included in the article's Creative Commons license and your intended use is not permitted by statutory regulation or exceeds the permitted use, you will need to obtain permission directly from the copyright holder. To view a copy of this license, visit: http://creativecommons.org/licenses/by/4.0/

PUBLISHER'S NOTE

GJESM Publisher remains neutral with regard to jurisdictional claims with regard to published maps and institutional affiliations.

Positive AI Statement

During the preparation of this work the author(s) have used [NAME TOOL / SERVICE] in order to [REASON]. After using this tool/service, the authors reviewed and edited the content as needed and took full responsibility for the content of the publication. Furthermore, the GPTZero detector will evaluate the manuscript utilizing Generative AI, ensuring a high detection rate. If the manuscript relies heavily on Generative AI and AI-assisted technologies, it will be archived without further options for appeal.

Negative AI Statement

The author(s) declare that no AI tools or services were not used or not highly applied during the preparation of this work.

ABBREVIATIONS	DEFINITION
%	Percent
AVE	Average variance extracted
β	A beta coefficient
CA	Cronbach Alpha
CFA	confirmatory factor analysis
CR	composite reliability
H1	First hypothesis
H2	Second hypothesis
H3	Third hypothesis
H4	Fourth hypothesis
P	Probability
PLS	Partial least square
SEM	Structural equation modeling
USD	United States Dollar

REFERENCES

Abbasi, G. A.; Kumaravelu, J.; Goh, Y. N.; Dara Singh, K. S. (2021). Understanding the intention to revisit a destination by expanding the theory of planned behaviour (TPB). Spanish J. Market- ESIC. 25(2): 282–311 **(30 pages).**

Adam, I., (2021). Negative tourist-to-tourist interactions, value destruction, satisfaction, and post consumption behavioral intention. J. Dest. Market. Manage., 20: 100557 **(14 pages).**

Ajzen, I. (2011). The theory of planned behaviour: Reactions and reflections. Psychology and Health, 26(9): 1113–1127 **(15 pages)**.

Alrawadieh, Z.: Prayag, G.: Alrawadieh, Z.: Alsalameen, M., (2019). Self-identification with a heritage tourism site, visitors' engagement and destination loyalty: the mediating effects of overall satisfaction. The Ser. Ind. J., 39(7-8): 541-558 **(18 pages).**

Arifin, S.; Rachman Putra, A.; Seno Anjanarko, T.; Masithoh, N.; Ryadin, F.; Syaiful Anwar, M., (2021). Refrigerator purchase decisions are reviewed from the price level, product quality and promotion. J. Market. Bus. Res., 1(2): 2962–9012 **(51 pages).**

Bagheri, F.; Guerreiro, M.; Pinto, P.; Ghaderi, Z., (2024). From Tourist Experience to Satisfaction and Loyalty: Exploring the Role of a Sense of Well-Being. J. Travel Res., 63(8): 1989-2004 **(16 pages).**

Baker, T.L.; Chari, S.; Daryanto, A.; Dzenkovska, J.; Ifie, K.; Lukas, B.A.; Walsh, G., (2020). Discount venture brands: Self-congruity and perceived value-for-money? J. Bus. Res., 116: 412–419 **(8 pages).**

Bhat, S.A.; Darzi, M.A., (2018). Antecedents of tourist loyalty to tourist destinations: a mediated-moderation study. Int. J. Tourism Cities. 4(2): 261–278 **(17 pages).**

Bigné, J.E.; Sánchez, M.I.; Sánchez, J., (2001). Tourism image, evaluation variables and after purchase behavior: Inter-relationship. Tourism Manage., 22(6): 607–616 **(9 pages).**

Camilleri, M.A., (2018). Travel marketing, tourism economics and the airline product: An introduction to theory and practice. Springer.

Cheng, T.-M.; Wu, H.C., (2015). How do environmental knowledge, environmental sensitivity, and place attachment affect environmentally responsible behavior? An integrated approach for sustainable island tourism. J. Sustainable Tourism. 23(4): 557–576 **(19 pages).**

Chi, C.G.Q.; Qu, H., (2008). Examining the structural relationships of destination image, tourist satisfaction and destination loyalty: An integrated approach. Tourism Manage., 29(4) : 624–636 **(13 pages)**.

Chin, T; Shi, Y.; Singh, S.K.; Agbanyo, G.K.; Ferraris, A., (2022). Leveraging block chain technology for green innovation in ecosystem-based business models: a dynamic capability of values appropriation. Technol. Forecast. Soc. Change. 183: 121908 **(8 pages).**

Choi, H.C.; Huang, S.; Choi, H.; Chang, H.S., (2020). The effect attendants' physical attractiveness on satisfaction, positive emotion, perceived value, and behavioral intention of flight. J. Hosp. Tourism Manage., 44: 19–29 **(10 pages).**

Chou, S.-W.; Hsu, C.-S., (2016). Understanding online repurchase intention: social exchange theory and shopping habits. Inf. Syst. E-Bus. Manage. 14:19–45 **(27 pages)**.

Cotterell, D.; Ferreira, J.-A.; Hales, R.; Arcodia, C., (2020). Cultivating conscientious tourism caretakers: A phenomenographic continuum towards stronger sustainability. Curr. Issues. Tourism, 23(8): 1004–1020 **(17 pages)**.

Crouch, G.I.; Ritchie, J.R.B., (1999). Tourism, competitiveness, and societal prosperity. J. Bus. Res, 44(3): 137–152 **(16 pages).**

Diallo, M.F.; Diop-Sall, F.; Leroux, E.; Valette-Florence, P., (2015). Responsible tourist behavior: the role of social engagement. Rech. Appl. Mark., 30(3): 85–104 **(20 pages).**

Elsayeh, Y., (2020). The Impact of Destination Image on Tourists' Satisfaction and Loyalty: A Case of Egypt. Int.Tourism. Hosp. J., 3(3) : 1-13 **(13 pages).**

Evren, S.; Şimşek Evren, E.; Çakıcı, A.C., (2020). Moderating effect of optimum stimulation level on the relationship between satisfaction and revisit intention: the case of Turkish cultural tourists. Int. J. Culture Tourism. Hosp. Res., 14(4): 681–695 **(15 pages)**.

Hair, J.F.; Risher, J.J.; Sarstedt, M.; Ringle, C.M., (2019). When to use and how to report the results of PLS-SEM. Eur. Bus. Rev, 31(1): 2–24 **(23 pages).**

Herliza, S.; Ferdian, F., (2024). The influence of place attachment on revisit intention at gunung padang tourist attraction, west sumatra. Fil. Manage. Tourism. 2(2): 251–263 **(13 pages).**

Indarjo, S.; Arifin, S., (2016). Strategy and policy for the development of batu katak ecotourism as a buffer area for gunung leuser national park. Thesis.

Isa, SM.; Ramli, L., (2014). Factors influencing tourist visitation in marine tourism: Lessons learned from FRI Aquarium Penang, Malaysia. Int. J. Cult. Tourism Hosp. Res., 8(1) : 103–117 **(15 pages).**

Jung, TH.; Lee, H.; Chung, N.; Diek, MC., (2018). Cross-cultural differences in adopting mobile augmented reality at cultural heritage tourism sites. Int. J. Contemp. Hosp. Manage., 30(3): 1621-1645 **(19 pages).**

Kao, H.K.; Tsai, S.N.; Chang, J.H., (2019). Enhancing the Destination Loyalty in Taiwan's Hot Spring Industry. Proceedings of the 2019 5th International Conference on Industrial and Business Engineering. 76 – 81 **(6 pages).**

Kim, K.-H.; Park, D.-B., (2017). Relationships among perceived value, satisfaction, and loyalty: Community-based ecotourism in Korea. J. Travel. Tourism Mark., 34(2) : 171–191 **(21 pages)**.

Kim, J. H., (2014). The antecedents of memorable tourism experiences: The development of a scale to measure the destination attributes associated with memorable experiences. Tourism Manage., 44: 34–45 **(12 pages)**.

Kotler, P.; Keller, K.L., (2009). Marketing management (13th ed.). In Prentice Hall.

Kotler, P.; Keller, K.L., (2012), Marketing Management, 14 edition, Global Edition Pearson Prentice Hall.

Kridakorn Na Ayutthaya, T.; Jakrawatana, N.; Rinchumphu, D.; Owatsakul, V., (2024). Application of artificial neural networks for predictive model of municipal solid waste collection in tourist cities. Global J. Environ. Sci. Manage., 10(4): 1859-1876 **(18 pages).**

Kumar, V.; Kaushik, A.K., (2017). Achieving destination advocacy and destination loyalty through destination brand identification. J. Travel. Tourism Mark., 34(9): 1247–1260 **(14 pages)**.

Leask, A., (2016). Visitor attraction management: A critical review of research 2009–2014. Tourism Manage., 57: 334–361 **(28 pages).**

Lin, M., (2024). Understanding the influencing factors of tourists' revisit intention in traditional villages. Heliyon. 10(15): 1-15 **(15 pages).**

Mahdzar, M.; Gani, AA., (2018). Effects of destination attributes on tourists' behavioral intentions to Kuala Selangor. Int. J. Acad. Res. Bus. Soc. Sci., 8(16): 367–375 **(9 pages)**.

Marques, C.; da Silva, R.V.; Antova, S., (2021). Image, satisfaction, destination and product post-visit behaviours: How do they relate in emerging destinations? Tourism Manage., 85: 1-12 **(12 pages).**

Navarro-Ruiz, S.; McKercher, B., (2020). The usability of visitor attractions: State-of-the-art. Tourism Rev., 75(3): 497–509 **(13 pages).**

Nguyen Huu, T.; Nguyen Ngoc, H.; Nguyen Dai, L.; Nguyen Thi Thu, D.; Truc, L.N.; Nguyen Trong, L., (2024). Effect of tourist satisfaction on revisit intention in Can Tho City, Vietnam. Cogent. Bus. Manage., 11(1): 1-17 **(17 pages).**

Okello, M.M.; Novelli, M., (2014). Tourism in the East African community (EAC): Challenges, opportunities, and ways forward. Tourism Hosp. Res, 14(1–2): 53–66 **(14 pages).**

Oliver, R.L., (1999). When is consumer loyalty? J. Mark., 63(4.): 33–44 **(12 pages).**

Park, S.; Hahn, S.; Lee, T.; Jun, M., (2018). Two factor model of consumer satisfaction: International tourism research. Tourism Manage., 67 : 82–88 **(7 pages).**

Pavlic, I.; Perucic, D.; Portolan, A. (2014). Tourists' Satisfaction As an Important Tool for Increasing Tourism Destination Competitivness in the Globalization Conditions - the Case of Dubrovnik-Neretva County. Int. J. Manage. Cases. 13(3): 591–599 **(9 pages).**

Pujiastuti, E.E.; Nimran, U.; Suharyono, S.; Kusumawati, A., (2017). The antecedents of behavioral intention regarding rural tourism destination. Asia Pac. J. Tourism Res., 22(11): 1169–1181 **(13 pages).**

Purwanto, S.; Syaufina, L.; Gunawan, A., (2014). Study of Potential and Carrying Capacity of Bukit Kelam Natural Tourism Park for Ecotourism Development Strategy. J. Pengelolaan Sumberdaya Alam dan Lingkungan. 4(2): 119–125 **(7 pages).**

Quintal, V.A.; Polczynski, A., (2010). Factors influencing tourists' revisit intentions. Asia Pac. J. Mark. Logist., 22(4): 554–578 **(25 pages).**

Ryan, C.; Ninov, I.; Aziz, H., (2012). Ras Al Khor—Eco-tourism in constructed wetlands: Post modernity in the modernity of the Dubai landscape. Tourism Manage. Perspect., 4: 185–197 **(13 pages)**.

Semuel, H.; Wibisono, J., (2019). Brand image, customer satisfaction and customer loyalty of the Superindo supermarket chain in Surabaya. J. Manage. Pem., 13(1): 27–34 **(8 pages).**

Seow, A.N.; Foroughi, B.; Choong, Y.O., (2024). Tourists' satisfaction, experience, and revisit intention for wellness tourism: E Word-of-Mouth as the Mediator. SAGE Open. 14(3): 1–16 **(16 pages).**

Shkurti, F., (2019). National Marine Park Karaburun-Sazan and today's trends for tourism development. Int. J. Geoheritage Parks. 7(1): 1–14 **(14 pages).**

Silalahi, H.T.; Basyuni, M.; Aritonang, E.Y.; Slamet, B.; Hartini, K.S.; Wee, A., (2024). Management of mangrove landscape and ecosystem for ecotourism. Global J. Environ. Sci. Manage., 10(4): 1977-1992 **(16 pages).**

Simanihuruk, M.; Mumin, A. T.; Wulan, S., (2018). The Effect of Tourist Attraction Toward Visitor Satisfaction in Sindang Barang Cultural Village, Bogor Regency. TRJ Tourism Res. J., 2(2): 33-44 **(12 pages).**

Siregar, Z.M.E.; Supriadi, Y.N.; Pranowo, A.S.; Ende.; Harahap, N.J., (2022). A multidimensional approach in examining the role of self-efficacy on innovative work behavior: Evidence from the creative industry. Probl. Perspect. Manage., 20(2): 588–597 **(10 pages).**

Sirgy, M.J.; Su, C., (2000). Destination image, self-congruity, and travel behavior: Toward an integrative model. J. Travel. Res, 38(4): 340–352 **(13 pages).**

Song, H.; Wang, J.; Han, H., (2019). Effect of image, satisfaction, trust, love, and respect on loyalty formation for name-brand coffee shops. Int. J. Hosp. Manage., 79 (2019): 50–59 **(10 pages).**

Stylos, N., (2019). Beliefs, Destination Loyalty, and Tourists' need for Variety as Antecedents of their Intention to Revisit a Destination. In Travel and Tourism Research Association.

Suanmali, S., (2014). Factors affecting tourist satisfaction: An empirical study in the northern part of Thailand. SHS Web of Conferences, 4th International Conference on Tourism Research (4ICTR). 12, 1027.

Sulistyanto, A.; Mujab, S.; Harahap, H., (2022). Memorable cultural tourism experience: blogger narrative analysis. J. Pariw. Pesona, 7(1): 104-119 **(16 pages)**.

Tan, T.M.; Salo, J.; Juntunen, J.; Kumar, A., (2019). The role of temporal focus and self-congruence on consumer preference and willingness to pay: A new scrutiny in branding strategy. Eur. J. Mark, 53(1): 37–62 **(26 pages).**

Teeroovengadum, V., (2019). Environmental identity and ecotourism behavior: examination of the direct and indirect effects. Tourism Rev., 74(2): 257–269 **(13 pages).**

Uma, S.; Roger, B., (2010). Research methods for business. John Wiley & Son.

Usakli, A.; Kucukergin, K.G., (2018). Using partial least squares structural equation modeling in hospitality and tourism: Do researchers follow practical guidelines? Int. J. Contemp. Hosp. Manage., 30 (11): 3462-3512 **(51 pages).**

Wirtz, J.; Zeithaml, V., (2018). Cost-effective service excellence. J. Acad. Mark. Sci., 46: 59–80 **(22 pages)**.

Wondirad, A.; Tolkach, D.; King, B., (2020). Stakeholder collaboration as a major factor for sustainable ecotourism development in developing countries. Tourism Manage., 78: 1-21 **(21 pages**).

Woods, B.; Moscardo, G., (2003). Enhancing wildlife education through mindfulness. Australian J. Environ. Educ., 19: 97–108 **(12 pages).**

Zgolli, S.; Zaiem, I., (2018). The responsible behavior of tourists: The role of personnel factors and public power and effect on the choice of destination. Arab. Econ. Bus. J., 13(2): 168–178 **(11 pages)**.

Zulvianti, N.; Akmal, H.; Putra, M.R. (2023). The role of pro-environmental behavior in the development of sustainable tourism. Global J. Environ. Sci. Manage., 9(SI): 319-330 **(12 pages).**

Zou, W.; Wei, W.; Ding, S.; Xue, J., (2022). The relationship between place attachment and tourist loyalty: A meta-analysis. Tourism. Manage. Perspect, 43: 1-14 **(14 page).**

AUTHOR (S) BIOSKETCHES

Yuliana, Y., Dr., Faculty of Economics and Business. Universitas Muslim Nusantara Al-Washliyah. Kampus Arsyad Thalib Lubis, Jl. Garu II No. 93, Medan, Indonesia.
- Email: *yayukyuliana@umnaw.ac.id.*
- ORCID: 0009-0000-4394-0359
- Web of Science ResearcherID: NA
- Scopus Author ID: 58684623200
- Homepage: https://fe.umnaw.ac.id/teams/yayuk-yuliana-se-m-si-2/

Ningsih, A.M., M.Sc., Faculty of Letters, Universitas Muslim Nusantara Al-Washliyah. Kampus Arsyad Thalib Lubis, Jl. Garu II No. 93, Medan,Indonesia.
- Email: *ayumelati@umnaw.ac.id*
- ORCID: 0009-0004-4916-0002
- Web of Science ResearcherID: NA
- Scopus Author ID: NA
- Homepage: https://umnaw.ac.id/fakultas-sastra/

Kristiana, V., M.Pd., Faculty of Letters, Universitas Muslim Nusantara Al-Washliyah. Kampus Arsyad Thalib Lubis, Jl. Garu II No. 93, Medan,Indonesia.
- Email: *verakristiana@umnaw.ac.id*
- ORCID: 0009-0002-7177-0662
- Web of Science ResearcherID: NA
- Scopus Author ID: NA
- Homepage: https://umnaw.ac.id/fakultas-sastra/

Maharani, A.P., B.A. Student, Faculty of Letters, Universitas Muslim Nusantara Al-Washliyah. Kampus Arsyad Thalib Lubis, Jl. Garu II No. 93, Medan,Indonesia.
- Email: *adindaputrimaharani@umnaw.ac.id*
- ORCID: 0009-0009-9260-2239
- Web of Science ResearcherID: NA
- Scopus Author ID: NA
- Homepage: https://umnaw.ac.id/fakultas-sastra/

Syahni, C., B.A. Student, Faculty of Economics and Business. Universitas Muslim Nusantara Al-Washliyah. Kampus Arsyad Thalib Lubis, Jl. Garu II No. 93, Medan,Indonesia.
- Email: *cynthiasyahni@umnaw.ac.id*
- ORCID: 0009-0006-5083-3766
- Web of Science ResearcherID: NA
- Scopus Author ID: NA
- Homepage: https://fe.umnaw.ac.id/

HOW TO CITE THIS ARTICLE

Yuliana, Y.; Ningsih, A.M.; Kristiana, V.; Maharani, A.P.; Syahni, C., (2025). Sustainability of natural tourism attraction and satisfaction. Global J. Environ. Sci. Manage., 11(3): 1185-1198.

DOI: 10.22034/gjesm.2025.03.17

URL: https://www.gjesm.net/article_722586.html

Global J. Environ. Sci. Manage. 11(3): 1199-1220, Summer 2025, Serial #43

Global Journal of Environmental Science and Management
(GJESM)

Homepage: https://www.gjesm.net/

Podcasts

CASE STUDY

Allometric equations model for estimating an above and below ground biomass of dipterocarp forest in the tropics

I. Heriansyah[1], L. Abdulah[1], J.S. Rahajoe[1], R. Susanti[1], Y. Lisnawati[1], Subarudi[2], R. Dewi[1,3], Darwo[1], Mawazin[1], Abdurachman[1], Karmilasanti[1], N. Wakhid[1,*], D. Wicaksono[1], R. Effendi[1], A.S. Yunianto[1], M.A. Qirom[1], N. Mindawati[1]

[1] Research Center for Ecology and Ethnobiology, National Research and Innovation Agency, Jalan Raya Jakarta-Bogor, Cibinong, Bogor, Jawa Barat 16911, Indonesia

[2] Research Center for Population, National Research and Innovation Agency, Jalan Gatot Subroto, Mampang Prapatan Jakarta Selatan, DKI Jakarta 12710, Indonesia

[3] Department of Tropical Silviculture, Faculty of Forestry and Environment, IPB University, Jalan Raya Dramaga, Bogor 16680, Indonesia

ARTICLE INFO

Article History:
Received 28 december 2024
Revised 01 February 2025
Accepted 10 April 2025

Keywords:
Carbon dynamic
Natural forest
Tree diameter
Tree height

DOI: 10.22034/gjesm.2025.03.18

ABSTRACT

BACKGROUND AND OBJECTIVES: Accurate measurement of carbon stocks is essential for assessing the forest carbon dynamics. The measurement of carbon stocks can be achieved through an allometric equation, which offers a cost-efficient solution for estimating tree biomass and carbon stocks by measuring only specific tree features, including diameter and height. Many allometric equations have been developed for estimating the forest biomass in tropical región. However, only few studies were found focusing on dipterocarp species, and most of them applying allometric equations for aboveground biomass only. This study sought to refine the accuracy of allometric equations related to Dipterocarp Forest by creating new equations for above-ground, root, and total biomass.
METHODS: The study was conducted in tropical natural and planted forests in Indonesia (Sumatra, Java, and Kalimantan) and Peninsular Malaysia (Johor, Perak, and Pahang), with a total of eight plots at different provinces. Using destructive analysis, all tree samples were collected and divided into groups consisting of living branches and twigs, dead branches and twigs, leaves and roots. A series of general equations for an allometric model has been formulated to assess tree volume and biomass. Then, the allometric equations were validated using validation models.
FINDINGS: Generally, there are a positive relationship between tree diameter and height, tree volume and biomass. he study achieved the successful creation of various equations that represent above-ground, root, and total biomass, based on tree diameter alone and in conjunction with both tree diameter and height. Also, the validation of models against actual data showed that models for above-ground, root-, and total- biomass were not significantly different (probability value > 5 percent). Depending on the forest type, planted forests demonstrate more uniform relationships among tree diameter, height, and biomass components, which suggests the presence of controlled growing conditions. In contrast, natural forests display a higher degree of variability, particularly among larger trees, which mirrors the diversity found in natural ecosystems.
CONCLUSION: Allometric model for estimating biomass in dipterocarp forests was developed and validated using diameter and a combination of diameter and height as predictor variables. The models demonstrated a high coefficient of determination (> 90 percent), indicating strong predictive power for above-ground, root- and total biomass. Based on statistical significance and practical use, Model 1 for above-ground biomass, Model 7 for root biomass, and Model 8 for total biomass were recognized as the most suitable models.

This is an open access article under the CC BY license (http://creativecommons.org/licenses/by/4.0/).

NUMBER OF REFERENCES
41

NUMBER OF FIGURES
6

NUMBER OF TABLES
10

*Corresponding Author:
Email: *nur.wakhid@brin.go.id*
Phone: +62877 2305 8591
ORCID: 0000-0002-5065-8770

Note: Discussion period for this manuscript open until Sep 1, 2025 on GJESM website at the "Show Article".

INTRODUCTION

The dipterocarp forests, distributed across tropical and subtropical regions of Asia, are unique ecosystems that play a critical role in both conservation and production forests. Dominating the lowland landscapes of Indonesia and Malaysia, these forests play a critical role in providing habitats for a wide range of species. Additionally, they are important suppliers of timber and non-timber products, including medicinal plants and resins from dipterocarp species (Huy *et al*., 2019). The conservation and sustainable management of these forests are crucial for climate change mitigation and economic reasons. With the growing global focus on climate change mitigation, it is vital to thoroughly comprehend the dynamics of carbon (C) stocks in forest ecosystems (Debie and Abro, 2025; Siregar *et al.,* 2025). They have important role in regulating the C cycle and global climate mitigation, as forests are significant C sinks and store C dioxide from the atmosphere in biomass and soil (Pant *et al*., 2023). Reliable quantification and forecasting of biomass and carbon in forest ecosystems are necessary for assessing their C sequestration potential (Tian *et al*., 2023; Larekeng *et al.,* 2024). Destructive and non-destructive methods are often used to estimate biomass (Schettini *et al*., 2023). Although destructive techniques offer improved accuracy, they are often time-consuming and costly, involving the collection, oven-drying, and weighing plants (Suárez-Fernández *et al*., 2025). Non-destructive methods are based on allometric equations that related to forest inventory data, such as height (H) and diameter at breast height (D), to tree volume and biomass (Brede *et al*., 2022; Sumarga *et al.,* 2024). Nevertheless, these allometric equations necessitate extensive temporal data for each species and are complicated to scale. In addition, most recent research on forest biomass in the tropics has been conducted using remote sensing technology, which also requires appropriate allometric equations for validating through field measurements (Avitabile *et al*., 2016). To enhance forest management, particularly in relation to carbon sequestration and climate change mitigation, it is crucial to have reliable allometric equations that simplify the estimation of tree biomass of the forest. By having a more accurate and comprehensive biomass estimation model for dipterocarp forests, policy makers and conservation practitioners can optimize forest management strategies to increase C sequestration potential and reduce greenhouse gas emissions. Several field studies have been undertaken to formulate allometric equations that estimate forest biomass in tropical environments to date (Ketterings *et al*., 2001; Basuki *et al*., 2009; Chave *et al*., 2014; Manuri *et al*., 2014; Manuri *et al*., 2016). However, among those existing studies, only two have specifically focused on dipterocarp species, both of which dedicated to develop allometric equation for aboveground biomass (Basuki *et al*., 2009; Manuri *et al*., 2016). Furthermore, both studies conducted field sampling only in natural forest. Consequently, further field studies are required to improve the precision of allometric equations for Dipterocarp forests in tropical regions, utilizing diverse field sampling methods. Moreover, the process of developing an allometric equation for root biomass generally involves a higher level of effort and resource allocation. This study aimed to develope allometric equations of tropical forest biomass including above-ground biomass (AGB), root biomass (RB), and total biomass (TB), specifically focus on dipterocarp forests in tropical countries. To improve the accuracy of these equations, a comprehensive sampling strategy was adopted, both in natural and plantation forests with a wide range of tree age, D, and structure variation. In addition, a significant and diverse array of samples was obtained from multiple islands and countries. The study was conducted in tropical natural and production forests in Sumatra, Java, and Kalimantan as well as Johor, Perak, and Pahang of Indonesia during 2019 to 2022 (Fig. 1 and Table 1).

MATERIALS AND METHODS

Study site

The sites for this study are based in Malaysia and Indonesia, featuring both natural forest ecosystem and dipterocarp plantation forest. The topography ranges from flat to undulating as 5-25 percent (%) slope, with elevation varying between 200 - 600 meters (m) above sea level (asl). In total, eight measurement plots were established, consisting of four plots in natural forest and four in plantation forest (Fig. 1 and Table 1). This natural forest falls under the classification of lowland tropical forest, noted for its diverse mix of dipterocarp species along with other types of trees. These sites illustrate a typical

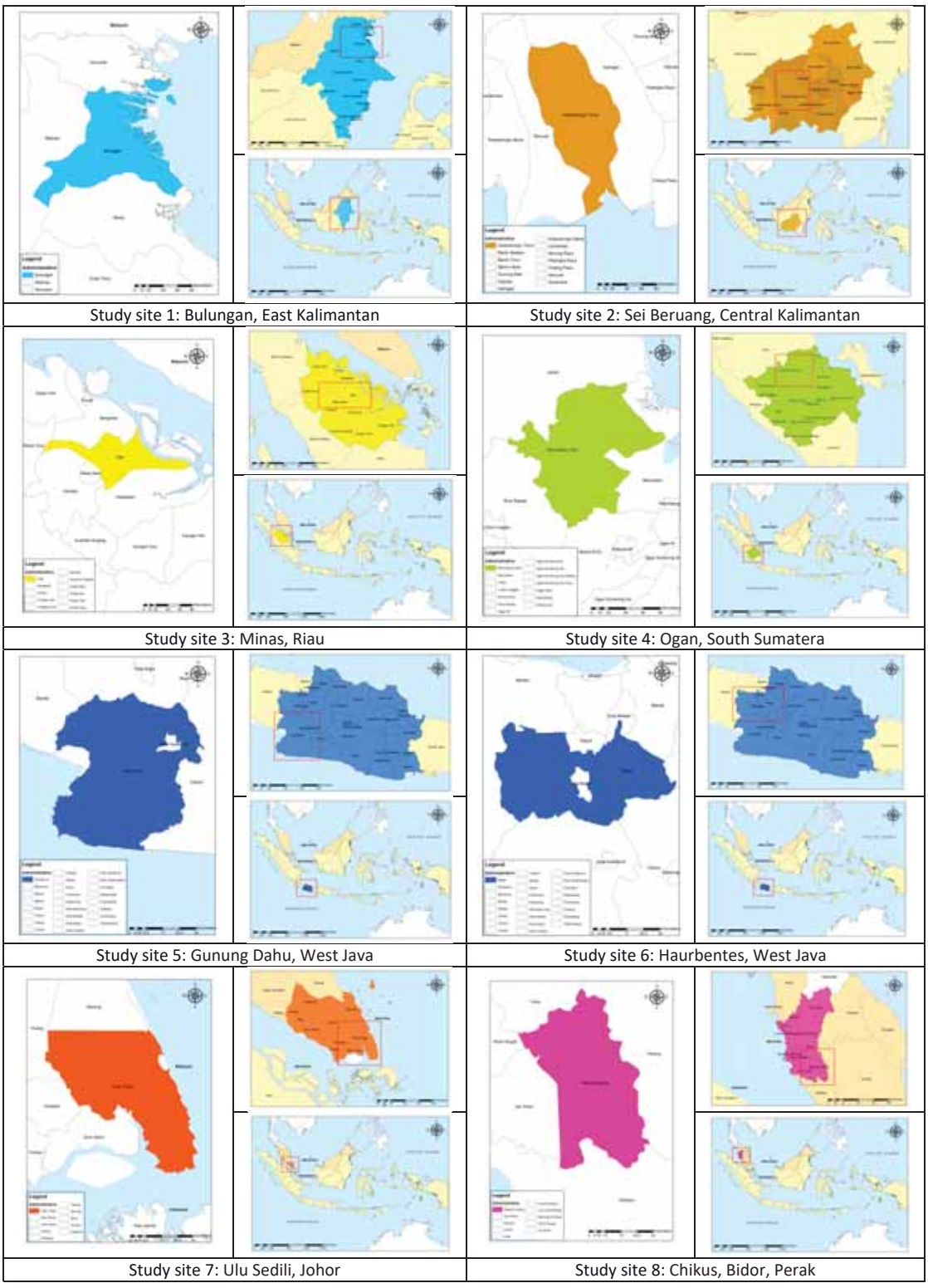

Fig. 1: Geographic location of the study area in in tropical natural production forests in Sumatra, Java, and Kalimantan and Johor, Perak, and Pahang of Indonesia

Table 1: Geographical position of the study plots

No.	Forest type	Site	Geographical coordinates	
Natural forest				
1	Primary forest	Bulungan, East Kalimantan	Latitude longitude altitude	02°56'093" - 02°58'057" North 116°32'557" - 116°35'101" East 200-600 m. asl
2	35 years - logged over area	Sei Beruang, Central Kalimantan	Latitude longitude altitude	00°52'30" - 01°22'30" South 111°30'00" - 112°07'30" East 111- 600 m. asl
3	15 years - logged over area	Minas, Riau	Latitude longitude altitude	00°49'438" – 00°50'138" North 101°28'340" – 101°28'499" East 8 – 100 m. asl
4	10 years - logged over area	Ogan, South Sumatera	Latitude Longitude Altitude	02°14'212" – 02°14'989" South 103°17'182" – 103°17'879" East 54 – 96 m.asl
Planted forest				
1	12 years - Spacing trial	Gunung Dahu, West Java	Latitude longitude altitude	06°36'535" – 06°37'766" South 106°33'844" – 106°35'712" East 694 – 917 m. asl
2	16 years – Ex-situ conservation	Haurbentes, West Java	Latitude longitude altitude	06°32 – 06°33 South 106°20 – 106°30 East 220 – 280 m. asl
3	6.5 years - Provenance trial	Ulu sedili, Johor	Latitude longitude altitude	01°44 – 01°95 North 103°53 – 103°88 East 30 – 60 m. asl
4	17 years - Restoration trial	Chikus, Bidor, Perak	Latitude Longitude Altitude	04°05'338" – 04°05'559" North 101°11'328" – 101°11'462" East 30 – 60 m. asl

sample of the natural forest landscapes that still exist in Southeast Asia. Vegetation analysis indicates that dipterocarp dominate the study area, with tree H up to 35 - 60 m. Additionally, dipterocarps are the predominant species in the stand composition, with individuals having a minimum D of 10 centimeters (cm). The vastness of the site, which covered the Island and several countries, necessitated greater effort and resources for data collection. Also, the times of the study were quite long up to about 4 years to compile the samples. Despite the fact that the sites are located in different countries, the data collection process does not present any major challenges.

Each sample plot measures 20 × 20 meters and has been strategically located to reflect the logging activities performed by the concession permit holder, which supports the collection of destructive sampling data. Data collected from each plot included tree species identification, D and H. Sample selection criteria focused on dipterocarp species with a minimum D of >10 cm. A total of 81 trees were sampled in natural forests, compared to 38 in plantation forests. In the natural forests, tree D's diameter varied from 10 to 75 cm, with the majority of specimens falling within the 20 to 25 cm category. Twenty dipterocarp species were identified, with *Shorea parvifolia* dyer being the most dominant, exhibiting a broad size distribution from <5 cm to 75 cm in D. In plantation forests, tree D ranged from 10 to 25 cm, with the majority in the 10–15 cm class. The dominant species in plantation forests was *Shorea leprosula Miq.* The collection of data for dipterocarp species was conducted without differentiating between the various species within this group. This study was designed to develop an allometric model specifically for dipterocarp species, considering the species diversity within the research plots and the relatively limited number of sampled individuals.

Destructive sampling

Tree samples obtained from natural forests were chosen based on the normality of tree structure during logging companies' operational felling activities. In contrast, samples from plantation forests were chosen based on D distribution. Destructive analysis samples were obtained from all eight plots (Table 2).

Table 2: Species and quantity of harvested samples that were collected from study plots. Superscript P and R mean samples from planted forest and species with roots unearthing, respectively

Group	Species	Quantity	Group	Species	Quantity
Red meranti	*Shorea (S) acuminate* dyer [R]	6	Red Meranti	*S. scaberiana* [R]	1
	S. assamica	1		*S. stenoptera* [R]	2
	S. falax [R]	1		*S. teysmanniana* Dyer	1
	S. glauca King	1		*S. virescens* [R]	1
	S. johorensis [R]	3		*S. xantophylla* [R]	1
	S. laevis [R]	2		*S. bracteolate* dyer [R]	7
	S. leprosula Miq. [R]	41 (38 [P])		*S. polyandra*	1
	S. ovalis Bl.	2	Kapur	*Dryobalanops fusca* V.Sl	3
	S. palembanica Miq [R]	3		*D. lanceolata* burck	1
	S. parvifolia dyer [R]	20	Keruing	*Dipterocarpus appendiculatus* Scheff [R]	5
	S. patoensis [R]	2	Majau	*Shorea compressa* burck	4
	S. pinanga [R]	1		*S. seminis* V.Sl	2
	S. platycarpa [R]	1	Yellow Meranti	*S. gibbosa* brandis	1
	S. platyclados V.Sl	1		*S. faguetiana* dyer	2
	S. polyandra [R]	1	White Meranti	*S. retinodes* V.Sl	2

Instead of cutting down tree D, the sample trees were gathered using a destructive approach that employed digging tools and heavy machinery. Trees with D less than 10 cm were directly pulled out including the root system using digging tools such as hoe, crowbar and hand tracker. The collection of trees exceeding 10 cm in diameter was facilitated by heavy machinery, such as an excavator. Initially, the process involved manually excavating to weaken the root systems, which was then complemented by spraying water using firefighting equipment. Then, followed by utilizing the above-ground weight as a driving force for unearthing the root system. All tree samples then cut and measured for H, D and weight in the field every 2 m. at subsequences of 0-0.3 m, 0.3-1.3 m, 1.3-3.3 m, and so on. Those samples then were categorized into living branches and twigs, dead branches and twigs, leaves and roots. Furthermore, root samples were collected whenever it was practical. All samples were then taken to the laboratory for the purpose of measuring their oven-dry weight. The sample trees with D more than 30 cm in the natural forest were measured with special procedures after felling. The procedures included measuring the stem D at the larger and smaller ends of the stump (the lower section of the stem left in the field after harvesting) and at the larger and smaller ends of substantial branches exceeding 20 cm in D. Moreover, measurements were obtained for the stems classified as commercial and non-commercial, the latter being segments deemed unsuitable for commercial use because of their defects). The tree volume was then calculated using Smalian's formula. Other components, such as small branches, twigs, and foliage, were weighed directly in the field using platform balance. A selection of sub-samples, each weighing 200 grams (fresh weight), was taken from every component and measured using a spring balance. Block-shaped sub-samples (2 cm x 2 cm x 5 cm) of wood from the stump, commercial stem, non-commercial stem, and substantial branches were obtained for biomass estimation, considering their specific wood density. All samples were systematically placed into coded paper bags and subsequently delivered to the laboratory for oven-drying. The biomass samples then were dried at 85 degrees Celsius (^{o}C) until reach consistent weight, using a drying oven (Memmert, Germany). The specific drying duration was: i) 48 hours (h) for leaves and wood biomass less than 10 cm in D, and ii) 96 h for wood biomass over 10 cm in D (Heriansyah *et al*., 2007; Miyakuni *et al*., 2004; Miyakuni *et al*., 2005). Once the dry weight was measured, the total dry weights were derived by taking the initial fresh weight of the samples and multiplying it by the dry-to-fresh weight ratio of each respective sample. The development of this model does not take into account variations in growing conditions such as rainfall, soil type, and

Table 3: Equation for general allometric models

ID	Equation	Model Type
1	$AGB = aD^b$	Exponential
2	$AGB = a(D^2H)^b$	This study
3	$AGB = \frac{aD}{(1+bD)}$	Michaelis-Menten
4	$AGB = \frac{a(D^2H)}{(1+b(D^2H))}$	This study
5	$AGB = exp\ (a + b * lnD - c * (lnD)^2)$	(Brown, 1997)
6	$AGB = exp\ (a + b * ln(D^2H) - c * (ln(D))^2)$	This study
7	$AGB = exp\ (a + b * lnD)$	(Basuki *et al.*, 2009)
8	$AGB = exp\ (a + b * ln\ (D^2H)\ )$	(Romero *et al.*, 2022)

temperature. The current study seeks to formulate a comprehensive allometric equation for dipterocarps, deliberately omitting specific environmental factors from consideration. This highlights a limitation of the model. Additionally, the model faces the challenge of differentiating components of the sample tree after it has been cut down. The high density of the stand causes the sample tree to be cut down and hit other trees around it. Then all parts of the tree are weighed. It is possible that some parts that are not from the sample tree are also weighed. A further complication is that while extracting and collecting roots from sample trees, it is often the case that not every root is gathered. This leads to uncertainty regarding whether the roots weighed are exclusively from the sample tree, a situation exacerbated by the dense stand. To address the potential sources of error in the destructive sampling method used to collect biomass data, the selection of sample trees considers the normality of the trees, including the ratio of D to H and the proportion of the crown.

Formulating and model fitting of allometric equation

To estimate tree volume and AGB, a set of general equations for allometric model was developed (Table 3). An exponential model was specifically utilized, incorporating D either independently or alongside H as independent variables to evaluate tree volume and biomass (Huang *et al.*, 2021). The study assessed the efficacy of linear and non-linear models in log-log space. The linear model is based solely on D as the independent variable, implying a linear D-biomass relationship in log-log space. Concurrently, non-linear models involved employing polynomials in D and incorporated various combinations of both D and H as independent variables.

The assessment of model fit for allometric equations adhered to specific criteria, including the significance of model coefficient at α of 5%, low standard error, high coefficient of determination (R^2), high adjusted coefficient of determination (R^2adj) and a low root mean square error (RMSE) (Chicco *et al.*, 2021).

Validation of the allometric equations

A validation analysis was conducted on the dataset comprising 119 sample trees to determine the general applicability of the derived equation. The analysis was conducted using a random dataset that did not involve replacement, and it was divided into two separate subsets. The larger dataset (67%) was utilized for model construction, involving the development of model equations, while the smaller subset (33%) served for model validation. For the construction process, the 67% subset was employed to ascertain the parameters of the equation linking biomass to D, with or without H considerations. Subsequently, the biomass values for the remaining 33% trees were validated based on this equation and compared against the measured biomass. The process involved recording the intercept, slope, R^2, and residual standard error that characterize the relationship between the developed model

Table 4: Distribution of D based on forest and tree type

Forest type	Species	Diameter (cm)																
		<5	5-10	10-15	15-20	20-25	25-30	30-35	35-40	40-45	45-50	50-55	55-60	60-65	65-70	70-75	>70	Grand total
Natural	Kapur					3		1										4
	Keruing	1					1			1	1			1				5
	Majau					2	1		1					1			1	6
	Red meranti	16	11	5	4	9		1	2	1	1	1	1	3	2		1	58
	White meranti							1					1					2
	Yellow meranti					1				1						1		3
Total		17	11	5	4	15	2	3	3	3	2	1	2	5	2	1	2	78
Plantation	Red meranti	3	17	11	3	1	4					1	1					41
Total		3	17	11	3	1	4	0	0	0	0	1	1	0	0	0	0	41
Grand total		20	28	16	7	16	6	3	3	3	2	2	3	5	2	1	2	119

and its validation. To ensure the accuracy of the model, the simulation model was compared with model validation using t-test with an α of 5% (95% confidence intervals). The model was deemed valid if it was determined to be statistically equivalent to the model validation.

RESULTS AND DISCUSSION

Available dataset

This study successfully collected 119 individuals representing 81 trees of Dipterocarp species in natural forest and 38 trees of *Shorea leprosula* in plantation forest (Table 4). The D and H of trees in natural forests ranged from 1.2 – 114.6 cm and 1.9 - 59.1 m, respectively. In the plantation forest, the D and H of the trees varied between 3.7 cm and 28.5 cm, and from 2.9 m to 23.1 m, respectively. Observations of the D distribution indicate that natural forests have a more extensive range of D compared to plantation forests, which is reflected in the elevated D values associated with natural forests. When compared to plantation forests, which are typically well-managed and often consist of a single species, natural forests display a more complex and uneven distribution of tree diameters, along with a greater diversity in tree sizes. Natural forests tend to have a more complex and diverse structure due to the natural processes of natural selection, interactions between species, and ecological succession that occur over a long period of time. The formation of natural forests occurs over time as a result of competition among and within species, which creates variations in wood density and a broad spectrum of tree sizes. Conversely, plantation forests typically exhibit a more consistent structure due to the intentional management practices employed, which often involve the cultivation of genetically uniform species. Compared to planted forests, natural forests tend to have higher specific gravity, leading to higher biomass content. Similarly, with tree D size, it is difficult to estimate the age of trees in natural forests. The longer rotation times of natural forests result in the cultivation of larger trees, which in turn increases the range of the model that is currently being developed.

Proportion of biomass

The proportion of stem biomass to AGB is higher than branches and foliage biomass (Fig. 2). The proportion of stem biomass ranges from 32 to 70%, with an average of 51.7%. The range becomes narrower when considering the first quartile (Q1) and third quartile (Q3), which varies between 46% to 58%. Branch biomass constitutes between 4% and 30% of the total AGB, averaging approximately 17.4%. The proportion of foliage varies from 2 to 26%, with an average of 12%. The proportion of root varies from 10.2 to 32.1%, with an average of 18.4%.

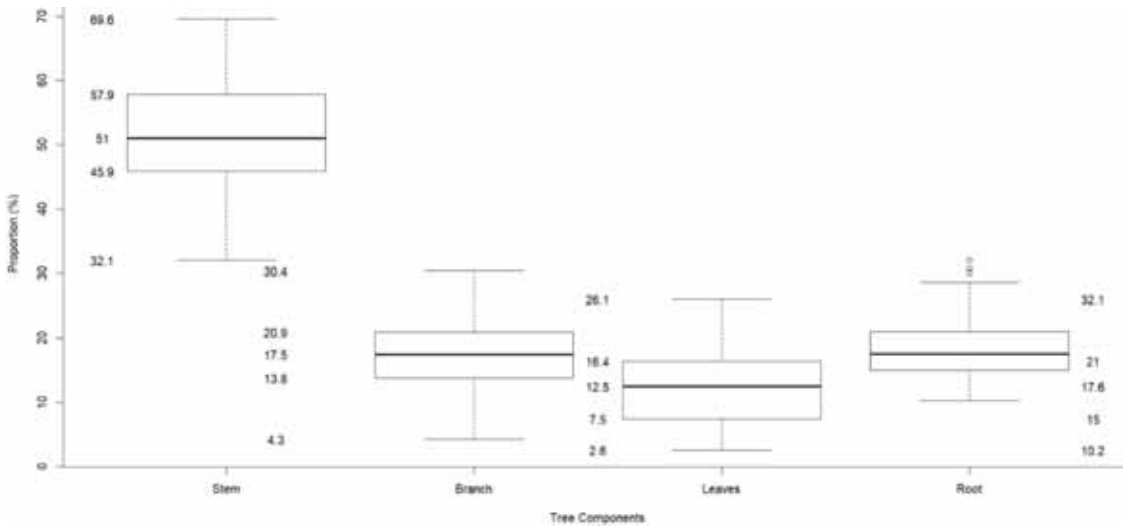

Fig. 2: Boxplot of the proportion of tree component biomass: stem, branches, leaves, and root to TB (%)

Biomass estimation variables

Results from the data distribution concerning biomass variables revealed a positive association between D and H, tree volume and biomass (Fig. 3). D to H and biomass relationship tend to be a relatively stable for planted and natural forests of D less than 20 cm as an effect of similar growing space. In natural forests with a D greater than 20 cm, the results demonstrated a relatively scattered pattern, influenced by the varying availability of growing space and competition among the trees.

Allometric model for biomass

Several equations using all data from natural and plantation forest were constructed following the scenarios for ABG, RB, and TB biomass using parameter D alone and a combination of D and H (Table 5).

Based on the criterion of R^2 and R^2adj, almost all models have high coefficient determination (>90%) except models 2 and 3. In terms of significance, where the coefficient is below 5%, models 1, 4, and 5 were recognized as the top-performing models, with model 1 being the most applicable. Unlike the AGB equation, almost all models for RB have moderate coefficient determination. However, when considering significance (coefficient less than 5%), model 7 emerged as the best-fitting model (Table 6).

For TB, based on the criteria of R^2 and R^2adj, almost all models have high coefficient determination (>94%), except models 3 and 4. Nevertheless, when evaluating significance at a coefficient of less than 5%, model 8 proved to be the optimal fitting model (Table 7).

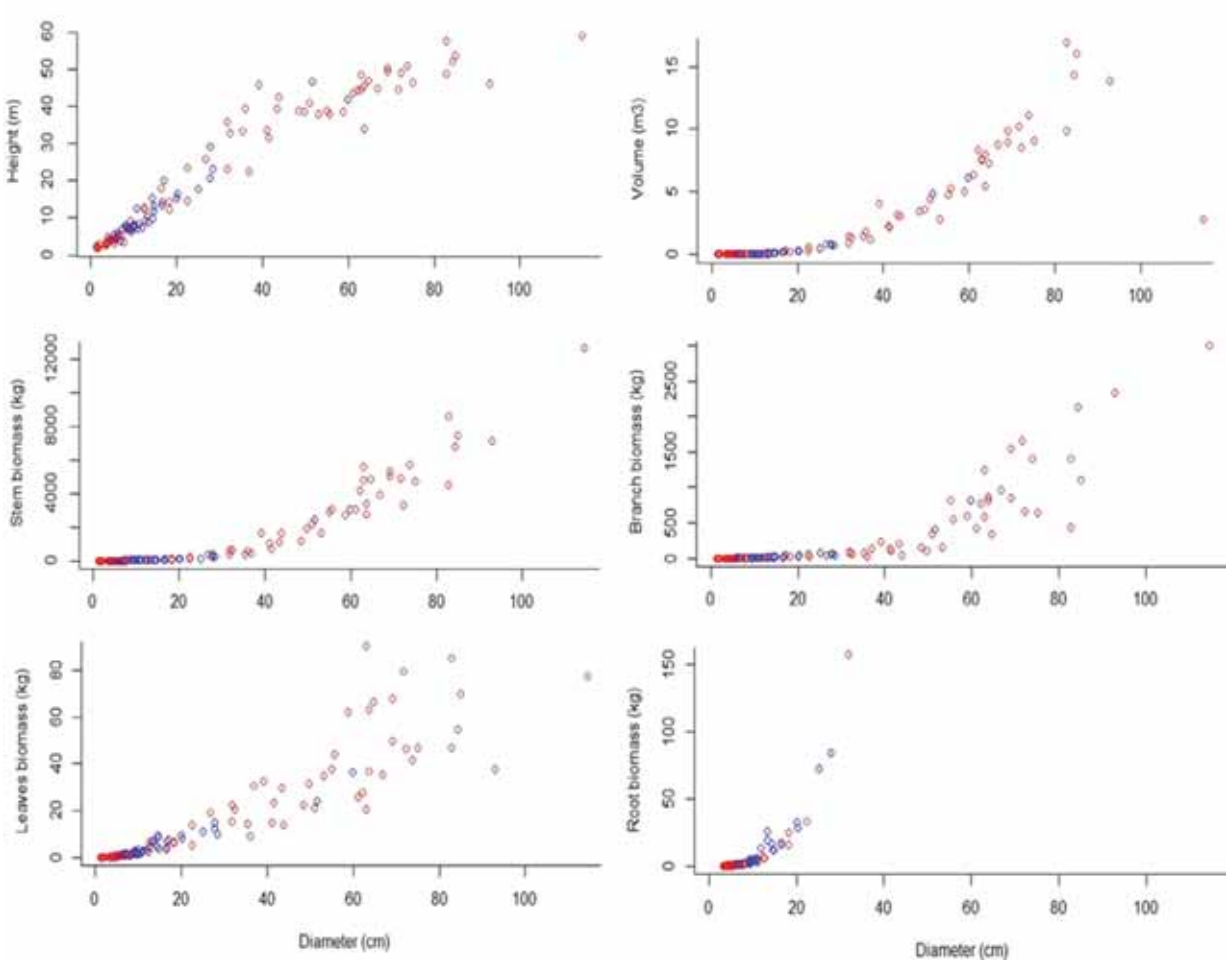

Fig. 3: Relationship between D and H, volume, stem, branch, leaves, and root-biomass. Red and blue colors represent natural and planted forests, respectively.

Table 5. Characteristics of allometric models for ABG

Model	R^2	R^2adj	RMSE	Coefficient		
				a	b	c
1	0.949	0.949	67.11	0.4244**	2.222***	
2	0.959	0.959	42.85	0.084*	0.8968***	
3	0.144	0.133	1063.09	5.4028*	0.8968***	
4	0.885	0.884	388.4	0.5614 ***	-7.9e-07 ***	
5	0.953	0.953	8.5	-9.867*	6.4095**	-0.4843
6	0.961	0.960	24.18	-4.956**	1.245***	-0.1
7	0.950	0.949	67.11	-0.857*	2.222***	
8	0.960	0.959	42.85	-2.474***	0.897***	

*Significant at 10% significant level, **Significant at 5% significant level, ***Significant at 1% significant level

Table 6: Characteristics of allometric models for RB

Model	R^2	R^2 adj	RMSE	Coefficient		
				a	b	c
1	0.867	0.867	0.314	0.028*	2.309***	
2	0.831	0.828	0.173	0.028	0.787***	
3	0.81	0.807	0.957	0.463***	-0.032***	
4	0.786	0.781	1.03	6.34e-01***	-8.23e-05***	
5	0.89	0.89	0.09	-14.647**	10.472**	-1.492*
6	0.86	0.85	19.73	-1.597	0.262	0.295**
7	0.87	0.87	0.314	-3.575***	2.309***	
8	0.83	0.83	0.831	-3.579***	0.787***	

*Significant at 10% significant level, **Significant at 5% significant level, ***Significant at 1% significant level

Table 7: Allometric model for TB

Model	R^2	R^2 adj	RMSE	Coefficient		
				a	b	c
1	0.927	0.925	1.4	0.094*	2.484***	
2	0.953	0.951	0.1	0.05**	0.925***	
3	0.86	0.857	5.326	2.391***	-0.033***	
4	0.19	0.17	25.11	6.34e-01***	-8.23e-05***	
5	0.96	0.96	1.02	-15.28***	11.85***	-1.69**
6	0.97	0.96	0.363	-2.46***	0.79***	0.07
7	0.94	0.94	1.4	-2.367***	2.484***	
8	0.96	0.96	0.1	-3.00***	0.925***	

*Significant at 10% significant level, **Significant at 5% significant level, ***Significant at 1% significant level

The allometric equation for tree volume and biomass was validated using the biometric data (Fig. 4, Table 8). The validation of models against actual data revealed no significant differences among the models for AGB, RB, and TB were not significantly different (probability value (p-value)) > 5%) (Table 8). The p-value of RB were quite low compared to AGB and TB. However, RB estimation in this study only need a data of D, same as AGB. While, for TB, the model need a combination data of D and H.

Comparative biomass predictions

Comparative analysis was conducted by evaluating the efficacy of the present equation against literature-based models. The plot-level biomass predicted by the optimum predictive equation derived in this study, employing the composite variable D while excluding the effect of forest type, were compared with those from various functions found in the literatures both in dipterocarp forest or non dipterocarp or mixed forest (Table 9). The results of the analysis, depicted in Fig. 5, showcase the comparisons made for equations based entirely on the log-log linear function of D for (Basuki *et al*., 2009; Brown, 1997; Chave *et al*., 2005), respectively.

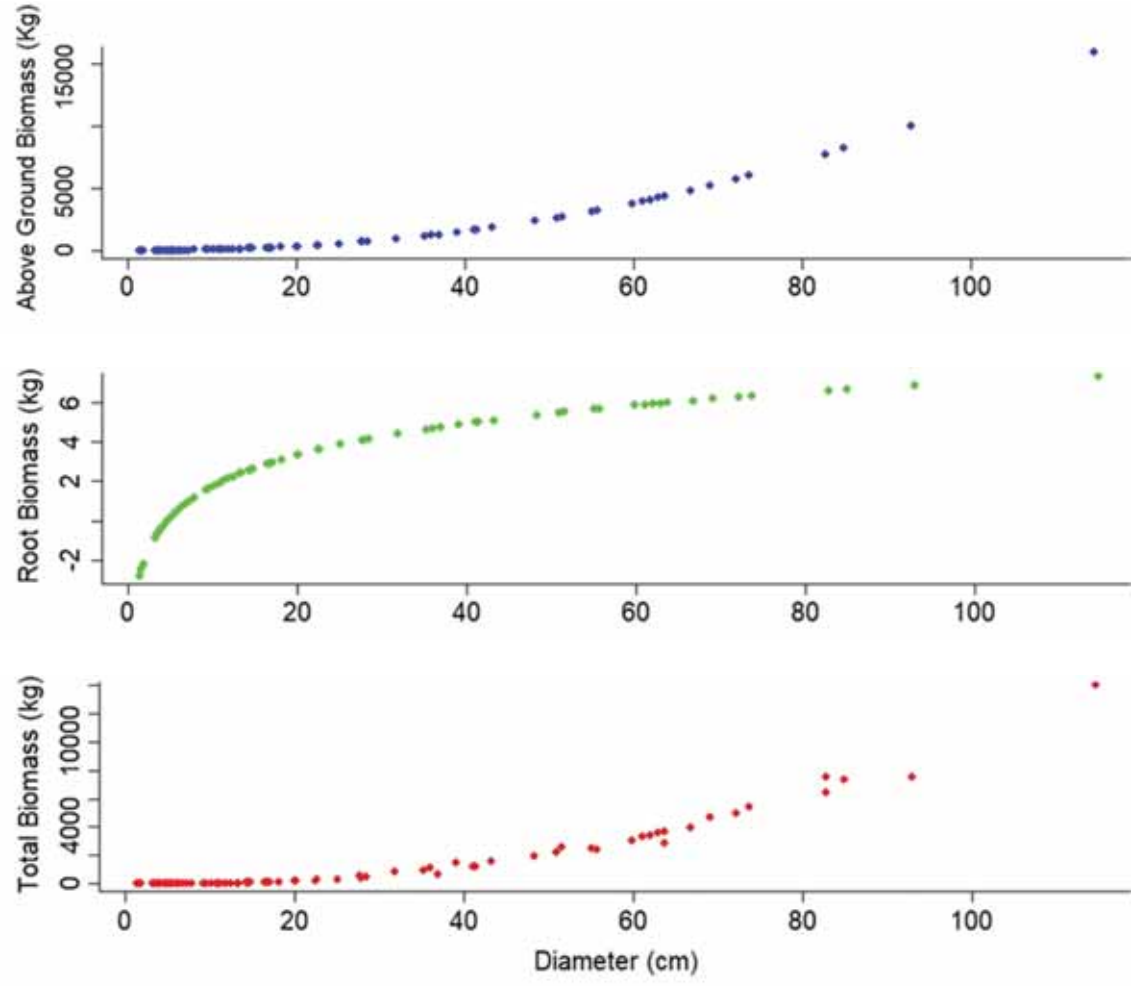

Fig. 4: Ratio observed value with model allometric

Table 8: Validation test for AGB, RB, and TB

Biomass	Equation	t-test	p-value
Above ground	$AGB = 0.4244(D)^{2.222}$	0.017	0.986
Root	$RB = -3.575 + 2.309(\ln D)$	0.60	0.55
Total	$TB = \exp(-3.00 + 0.925 * (\ln D^2 H)$	-0.016	0.987

In dipterocarp forest, the average deviation for individual trees models by Basuki *et al*. (2009) is lower than that of the study model (Fig. 5). In contrast to non-dipterocarp forests, the model examined in this study exhibits a greater average deviation (Ketterings *et al.,* 2001). The predicted values in the study were underestimated if the equation from Ketterings *et al.* (2001) were applied in the data of this study. However, the model developed by Manuri *et al*. (2014) and Brown (1997) in mixed forest has similar estimates for AGB at a deviation between 1 to 19% (average 10%) for D 35 to 115 cm, and a deviation between 1 to 20% (average 4%) for D 15 to 115 cm, respectively. In addition, the paired t-test presented in Table 8 shows that for one-tailed at $\alpha = 0.05$, the mean of our model is significantly similar at p-value 0.81 and 0.88 for the model of Manuri *et al*. (2014) and Brown (1997), respectively. Brown (1997) developed an equation

Table 9: The comparison of equations based on the log linear function of tree D

No.	Equation	t-test	p-value	Sources
1.	$AGB = 0.108 * (D)^{2.562}$	0.244	0.810	Manuri *et al*., 2014
2.	$AGB = 0.318 * (D)^{2.196}$	1.700	0.080	Basuki *et al*., 2009
3.	$AGB = 0.066 * (D)^{2.59}$	1.320	0.188	Ketterings *et al*., 2001
4.	$AGB = 42.69 - 12.8 * D + 1.242 * D^2$	0.150	0.880	Brown, 1997

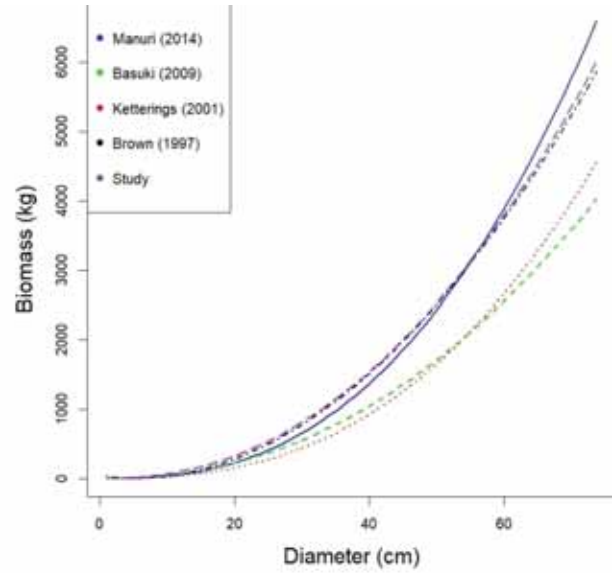

Fig. 5: Comparison of plot-level biomass using alternative equations from literature.

that almost precisely estimated the plot ABG relative to the equation developed here in all four cases. Comparative analysis with literature-based models (Basuki *et al*., 2009; Brown, 1997) showed that the study's models provided comparable or improved estimates for AGB, particularly for larger D classes. While the model from this study is comparable to findings from some non-dipterocarp forest studies, using a species grouping model significantly improves the precision of the estimation (Manuri *et al.,* 2014).

Biomass Conversion and Expansion Factor (BCEF)

This study's BCEF is associated with estimating TB from AGB. If AGB is estimated from D, the resulting estimation, when multiplied by the BCEF, provides the TB (Schepaschenko *et al*., 2018). The definition of BCEF depends on what is being estimated; at times, BCEF is utilized to calculate TB in hectares (ha), as demonstrated by Marziliano *et al*. (2017) which influences its applicability. Marziliano *et al*. (2017) emphasize that BCEF plays a crucial role in estimating the TB of stands using allometric equations. In cases where the equation is unknown, the BCEF used is based on stand age. BCEF is also expressed as the proportion of carbon dioxide (CO_2) in tree volume, denoted in ton carbon dioxide per cubic meter (tCO_2/m^3) (Petersson *et al*., 2012).

The value of BCEF is a crucial conversion factor for estimating TB from D parameters (Fig. 6). D is employed to estimate AGB, and the estimation of TB is derived by multiplying AGB and BCEF. Fig. 6 shows BCEF distribution at different D, with an average of 1.22 at a standard deviation of 8% (Table 10). As indicated in Table 10, the BCEF is 1.22 for the dipterocarp species, signifying that the TB is approximately 1.22 times the AGB. This BCEF value is practical within D range of 3.2 to 31.8 cm. The BCEF value of 1.22 indicates that TB is approximately 1.22 times the AGB, providing a practical conversion factor for dipterocarp species within a D range of 3.2 to 31.8 cm.

Predictive variables of allometric equations model

Results from the validation of the models against

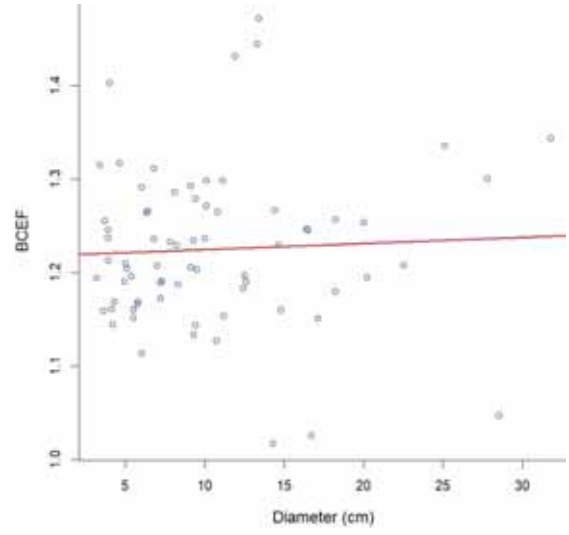

Fig. 6: BCEF value distribution at several D of trees

Table 10: BCEF for D ranges of dipterocarp species in tropics

D (cm)		BCEF			
Min	Max	Min	Max	Average	Deviation
3.2	31.8	1.02	1.47	1.22	0.08

actual data demonstrate a positive association with D (Fig. 4). Also, the models for AGB, RB, and TB were not significantly different from actual data, supporting their use for biomass estimation in dipterocarp species. This positive correlation implies that the models formulated in the research can effectively estimate the biomass of dipterocarp species within Indonesia's tropical dipterocarp forests (Basuki *et al*., 2009; Huy *et al*., 2016; Manuri *et al*., 2014; Manuri *et al*., 2016). In the context of dipterocarp species, the allometric equation utilizing D or a combination of D and H as predictor variables displayed consistent stability across the thirty dipterocarp species (Basuki *et al*., 2009; Chave *et al*., 2005; Hashimoto *et al*., 2004; Huy *et al*., 2016; Huy *et al*., 2019). The data reveals a stark contrast between the natural and plantation forests in terms of species diversity. The natural forest exhibits a rich composition of Dipterocarp species, including Kapur, Keruing, Majau, Red meranti, White meranti, and Yellow meranti. In contrast, the plantation forest consists exclusively of Red meranti (*S. leprosula*). This difference aligns with (Basuki *et al*., 2009; Huy *et al*., 2016; Manuri *et al*., 2014; Manuri *et al*., 2016) typical patterns observed in tropical forest ecosystems, where natural forests generally support higher biodiversity compared to monoculture plantations. In the natural forest, the D distribution displayed a reverse J-shaped curve, a hallmark of mixed-species forests characterized by uneven age distribution. About 66.7% of trees fall within smaller D classes (<25 cm). Large trees (>50 cm D) constitute only 16.7% of the total, indicating the presence of old-growth elements. Meanwhile, D distribution at planted forest showed more uniform D distribution, concentrated in 5-15 cm range (82.9% of trees). Maximum D reaches only 25-30 cm, suggesting a relatively young, even-aged stand. Contrast in D distribution reflects the fundamental differences between natural forest dynamics and managed plantation growth (Malik *et al.,* 2024). The robust proliferation of Dipterocarp species in their native forests might play a role in shaping allometric equations for biomass assessment. However, dipterocarp species are highly adaptable to the environment, especially light. The availability of light directly affects tree growth. Therefore, tree size is a key determinant of biomass, which subsequently shapes the dynamic allometric relationship. The allometric equations for planted forests were different with natural forests and

may the influence forest management practices. The consistent growth and lighter specific gravity found in planted forests yield less biomass than equivalent-sized trees in natural forests. In terms of forest management, tree size is a priority in planted forest management, while selective cutting is a primary consideration for natural forest management. Unlike natural forests, plantation forests create a managed setting that encourages a more uniform development of Dipterocarp species. This uniformity is achieved through a combination of ecological and management practices that directly influence the development and biomass accumulation of these trees. Natural forest root biomass is distributed across a wider range of D classes, up to 30-35 cm. A sophisticated subterranean framework that could play a role in improving ecosystem stability (Bardgett and van der Putten, 2014; Poorter *et al*., 2015). Root biomass in plantation forest is concentrated in the 5-15 cm D classes. Reflects a more homogeneous subsurface structure, which is typical of plantations that are even-aged. Estimating root biomass is often a challenge in forest biomass research. Root biomass is difficult to measure directly and requires careful sampling techniques. Moreover, variability in root distribution in the soil and the complexity of root structure can also complicate root biomass estimation. Consequently, additional study and the creation of more sophisticated techniques are essential to tackle the difficulties in precisely estimating root biomass. The study reveals distinct patterns in biomass allocation among different tree components. At stem biomass constitutes the largest proportion of AGB, ranging from 43.6% to 97%, with an average of 71.5%. With an interquartile range spanning from 60.2% to 81.2%, it can be inferred that the majority of trees consistently allocate a considerable amount of their biomass to stems. Branch biomass are representing a smaller but significant portion of AGB, ranging from 2.09% to 40.1%, with an average of 19.5%. The foliage biomass is forms the smallest component of AGB, ranging from 0.38% to 29.1%, with an average of 7.8%. The root biomass area accounts for 14.6% to 21.05% of total biomass, averaging 17.3%. Individual trees may show wider variation (1.7% to 32.1%) as reported by Heryati *et al*. (2011). This biomass allocation pattern aligns with the pipe model theory proposed by Lehnebach *et al.* (2018), which suggests that trees allocate resources to maintain a functional balance between water-conducting tissue (stem) and photosynthetic organs (leaves). The elevated stem biomass ratio demonstrates the trees' focus on structural support and water transport, which are critical for their survival and growth in forest ecosystems. This pattern is consistent with findings from other tropical forests, as reported by Poorter *et al.* (2015), who observed that stem biomass typically accounts for 72-79% of AGB in tropical trees. By integrating stem biomass variation into the model, this study has produced results that are predominantly aligned across different species and ecosystems. With these results, aboveground or total biomass, and sometimes root biomass, can be estimated from stem biomass. Once a tree has been transformed into a log, the volume of waste biomass that remains in the forest can still be assessed. The study demonstrates positive relationships between D, H, tree volume, and biomass components. The relationship between D and H is positively correlated, which is in line with the allometric growth patterns found in trees. The relationship is more consistent in planted forests and for trees with D < 20 cm in natural forests, likely due to similar growing conditions. Greater variability in D-H relationships for trees with D > 20 cm in natural forests, reflecting diverse growing spaces and competition levels. The performance of biomass varies according to forest type. In the case of planted forests, there is a more consistent correlation between D, H, and biomass components, which suggests that these forests are cultivated under controlled. Natural forests exhibit greater variability, especially for larger trees, reflecting the heterogeneity of natural ecosystems. These relationships are consistent with findings from Chave *et al*. (2014) who developed improved allometric models for tropical trees, emphasizing the importance of tree D, H, and wood density in estimating biomass. The fluctuations seen in natural forests, particularly among larger trees, are consistent with the research conducted by Feldpausch *et al*. (2011), which highlighted significant disparities in H-D relationships across diverse tropical forest types and areas. The significant proportion of root biomass (averaging 17.3%) highlights the importance of belowground C storage and soil stabilization. The findings on root biomass align with the global analysis by Cairns *et al.* (1997), who reported that root biomass in upland forests typically ranges from 18% to 30% of aboveground biomass, highlighting the significant contribution of roots to total forest biomass and C

storage. Qi *et al*. (2019), who observed that plants would allocate more biomass to roots to release the stress of water shortage and improve the effectiveness of nutrient and soil moisture. Variations in the biomass ratios of branches and leaves in natural forests may reflect the existence of diverse habitats suitable for canopy-dwelling species. These implications are supported by the work of Thompson *et al.* (2011), who emphasized the importance of forest biodiversity in delivering ecosystem services. This study delivers significant understanding of biomass allocation trends and growth interrelations in natural forests as well as in planted environments like community forest plantation. The findings emphasize the importance of considering forest type and tree size when estimating biomass and C stocks. Moreover, the findings of the study point to the requirement for management practices that are specifically designed to address the unique structural and functional characteristics of both natural and planted forest ecosystems. As suggested by Stephenson *et al*. (2014) the continuous increase in C accumulation with tree size underscores the importance of conserving large trees in natural forests for climate change mitigation strategies. Within the diverse range of ecosystems, the allometric equation formulated in this research acts as a crucial benchmark, reconciling overestimations and underestimations in the data, thereby mitigating possible errors. Therefore, the model will be effective for use in extensive forests with large datasets, but may be less accurate for plants with abnormal growth. Applying the model to planted forests with relatively uniform growth would be better if using a model from planted forests, and vice versa. Nevertheless, for extensive biomass estimation across diverse ecosystems, particularly when time and financial resources are limited, the model from this study will be effective and efficient. In addition, the application of the models to other dipterocarp species in is promising, but needs to consider the variability of environmental conditions that may differ in each region. Some considerations are needed to ensure broader application in different regions include:

1) Model calibration: The created models require modification to reflect the specific attributes of the leading dipterocarp species in various tropical region. Genetic and ecological variability among tree populations in different regions can affect the allometric relationships between the parameters used in the model. 2) Validation: To confirm the reliability of the models, it is essential to test them in different tropical regions, taking into account the distinct environmental conditions present. Validating the models with actual data from different locations can help assess the generalizability of the models. 3) Inclusion of additional parameters: To improve the model's accuracy, it is beneficial to integrate region-specific parameters that consider diverse environmental factors, including soil conditions, climate, and topography. 4) Collaboration and knowledge exchange: Collaboration among researchers from various tropical regions can help broaden the understanding of environmental condition variability and model adjustments. Knowledge exchange among experts can enrich the approaches used to expand the application of the models. By considering these factors, the application of the developed models to dipterocarp species in various tropical regions can be more successful and relevant to estimate tree biomass in different environments. It is anticipated that the allometric model from this research will provide a precise basis for ground truth data, aiding in the future large-scale estimation and monitoring of biomass using remote sensing techniques. Different forest cover typologies provide different image reflections. Thus, by knowing the biomass content of each different forest typology, the biomass contained in the forest could be estimated based on remote sensing. In addition, changes in forest cover based on the results of growth parameter measurements can be linked to the magnitude of C sequestration and climate change mitigation using the model from this study.

CONCLUSION

The study shows a direct field study in 8 different sites across 2 countries with a big forest holder in Southeast Asia, resulting in a wide range of data that is feasible for developing an accurate allometric model and indicating their potential applicability beyond the immediate study regions. Furthermore, samples were sourced from two different forest categories: natural and plantation. This approach ensures a robust sample that improves the model's precision. With a larger number of samples, more diverse species, and different forest types, this study produces an allometric model with broader application and more reliable results compared to other allometric models with more limited data. Findings from the study reveal that the variety of

trees in natural forests is more diverse compared to those in plantation forest. That data reveals that the growth of dipterocarp species in natural forest is more dynamic than that in plantation forest. The samples collected for this study are more than adequate, as they cover a full spectrum of D distribution, ranging from small to large trees, and include a diverse array of tree ages from young to mature, especially in the natural forest setting. Also, the study shows that the composition of dipterocarp species in natural forest is more heterogeneous than that in plantation forest. In simpler terms, the variety of life found in natural forests is considerably richer than that found in plantation forest. This study produces the best-fitting of 3 models of allometric equation with a combination predictor of D and H for estimating the biomass of dipterocarp species in the tropics (model 1, ABG = $0.4244(D)^{2.222}$; model 7, RB = $-3.575 + 2.309\ (\ln D)$; and model 8, TB = $\exp\ (-3.00 + 0.925 * (\ln D^2 H))$. The models were statistically valid as shown by a high coefficient of determination (R^2 > 90%) and not being significantly different from the validation test's actual data. Those accurate allometric models offer a significant advantage in practical applications to estimate the 3 variables of dipterocarp species biomass, AGB, RB, and TB by only employing the D or a combination of D and H as predictor variables. This study's allometric model for RB holds considerable practical significance, especially since estimating the root biomass of dipterocarp species often necessitates extensive direct measurement efforts in the field. Additionally, if the measurement of tree H is difficult in the field, especially for large trees, the TB could be estimated as the sum of ABG and RB, which requires D measurement only. Thus, increases the simplicity in the field process. In the next step, combining with the C content of trees, the biomass estimation from allometric equations in this study could also improve the accuracy of C stock or sequestration of dipterocarp forest estimation. In general, the study findings provide an important contribution to enhancing the accuracy of biomass and C dynamic estimation of dipterocarp forest, which is essential to support the sustainable forest management in tropical countries. This study's model may face limitations, particularly because it has not yet incorporated variables such as rainfall, soil type, and temperature that could impact its performance. However, with the assumption that the environmental conditions across the tropical countries are usually similar, the model developed in this study is potential to apply beyond the study areas. In addition, the model in this study were developed from samples across different province and country. A further limitation is that the stand's elevated density could result in the integration of elements from surrounding trees into the measurements, thereby potentially biasing the outcomes. The dense forest environment could also complicate the accuracy of root biomass measurements. Collecting roots from sample trees presents challenges in ensuring the complete transport of all origins and verifying that the weighed roots are exclusively from the sample tree. Expanding the range of dipterocarp species in future studies is essential for enhancing the models' generalizability across different forest types and conditions. Also, more studies on the effect of environmental growth conditions such as soil type, climate, and topography are needed to improve the model accuracy and applicability. Furthermore, conducting longitudinal studies to track growth patterns over time would provide insights into biomass dynamics and C sequestration potential. The allometric model tailored for specific sites serves as an essential foundation for developing biomass estimation models based on land cover. In the future, the accurate allometric models that combine with remote sensing data could facilitate large-scale biomass estimation and monitoring faster and more precisely.

AUTHOR CONTRIBUTIONS

I. Heriansyah has contributed in conceptualization, planned the experiment, data collection, data analysis, interpreted and discussed the results, article writing and funding acquisition. L. Abdulah performed in article writing, data analysis and curation, results interpretation, and visualization. J.S. Rahajoe has contributed in article writing, data analysis, editing, results discussion and validation. R. Susanti has contributed in article writing, data analysis, editing, and results discussion. Y. Lisnawati has contributed in article writing, data analysis, editing, and results discussion. Subarudi has contributed in article writing, data analysis, editing, and results discussion. R. Dewi has contributed in article writing, data analysis, editing and validation. Darwo has contributed in article writing, data analysis, editing and validation. Mawazin has contributed in article writing, editing

and validation. Abdurachman has contributed in article writing, editing and validation. Karmilasanti has contributed in article writing and editing. N. Wakhid, the corresponding author has contributed in article writing, editing, validation, results interpretation and discussion. D. Wicaksono, has contributed in article writing, editing and data visualization. R. Effendi has contributed in article writing, editing and validation. A.S Yunianto has contributed in article writing, editing and data visualization. M.A. Qirom has contributed in article writing, editing and data interpretation. N. Mindawati has contributed in article writing, editing and data interpretation.

ACKNOWLEDGEMENT

The authors would like to thank Professor Hazandy Abdul Hamid, Universiti Putra Malaysia (UPM) and Professor Maurizio Mencuccini, University of Edinburgh (UK) for providing valuable insights and feedback on the manuscript. Authors are grateful to Indonesian Forestry and Environment Research, Development, and Innovation Agency (FOERDIA) and UPM for providing laboratory facilities.

CONFLICT OF INTEREST

The authors declare that there is no conflict of interests regarding the publication of this manuscript. In addition, the ethical issues, including plagiarism, informed consent, misconduct, data fabrication and/or falsification, double publication and/or submission, and redundancy have been completely observed by the authors.

OPEN ACCESS

©2025 The author(s). This article is licensed under a Creative Commons Attribution 4.0 International License, which permits use, sharing, adaptation, distribution and reproduction in any medium or format, as long as you give appropriate credit to the original author(s) and the source, provide a link to the Creative Commons license, and indicate if changes were made. The images or other third-party material in this article are included in the article's Creative Commons license, unless indicated otherwise in a credit line to the material. If material is not included in the article's Creative Commons license and your intended use is not permitted by statutory regulation or exceeds the permitted use, you will need to obtain permission directly from the copyright holder. To view a copy of this license, visit: http://creativecommons.org/licenses/by/4.0/

PUBLISHER'S NOTE

GJESM Publisher remains neutral with regard to jurisdictional claims in published maps and institutional afflictions.

☐ Positive AI Statement

During the preparation of this work the author(s) have used [NAME TOOL / SERVICE] in order to [REASON]. After using this tool/service, the authors reviewed and edited the content as needed and took full responsibility for the content of the publication. Furthermore, the GPTZero detector will evaluate the manuscript utilizing Generative AI, ensuring a high detection rate. If the manuscript relies heavily on Generative AI and AI-assisted technologies, it will be archived without further options for appeal.

☑ Negative AI Statement

The author(s) declare that no AI tools or services were not used or not highly applied during the preparation of this work.

ABBREVIATIONS

%	Percent
^oC	Degree Celsius
AGB	Above-ground biomass
asl	Above sea level
BCEF	Biomass conversion and expansion factor
BGB	Below-ground biomass
C	Carbon
cm	Centimeter
CO_2	Carbon dioxide
D	Diameter at breast height
FOERDIA	Forestry and Environment Research, Development, and Innovation Agency
H	Height
h	Hours
ha	Hectare
Kg	Kilogram

m	Meter
p	Planted forest
p-value	Probability value
Q1	First quartile
Q3	Third quartile
R	Roots unearthing
R^2	Coefficient of determination
R^2adj	Adjusted coefficient of determination
RB	Root biomass
RMSE	Root mean square error
S	Shorea
TB	Total biomass
tCO_2/m^3	Ton carbon dioxide per cubic meter
UPM	Universiti Putra Malaysia
UK	University of Edinburgh

REFERENCES

Avitabile, V.; Herold, M.; Heuvelink, G.; Lewis, S.L.; Phillips, O.L.; Asner, G.P.; Armston J.; Ashton, P.S.; Banin, L.; Bayol, N., (2016). An integrated pan-tropical biomass map using multiple reference datasets. Global Change Biol., 22(4) **(14 pages).**

Bardgett, R.D.; van der Putten, W.H., (2014). Belowground biodiversity and ecosystem functioning. Nature. 515: 505–511 **(7 pages).**

Basuki, T.M.; van Laake, P.E.; Skidmore, A.K.; Hussin, Y.A., (2009). Allometric equations for estimating the above-ground biomass in tropical lowland dipterocarp forests. For. Ecol. Manage. 257 (8): 1684-1694 **(11 pages)**.

Brede, B.; Terryn, L.; Barbier, N.; Bartholomeus, H.M.; Bartolo, R.; Calders, K.; Derroire, G.; Moorthy, S.M.K.; Lau, A.; Levick, S.R.; Raumonen, P.; Verbeeck, H.; Wang, D.; Whiteside, T.; van der Zee, J.; Herold, M., (2022). Non-destructive estimation of individual tree biomass: Allometric models, terrestrial and UAV laser scanning. Remote Sens. Environ., 280: 1-20 **(20 pages).**

Brown, S., (1997). Estimating biomass and biomass change of tropical forests: A Primer. FAO Forestry Paper 134. Food and Agriculture rganization of the United Nations. Rome. **(55 pages)**.

Brown, S., (2002). Measuring carbon in forests: current status and future challenges. Environ. Pollut. 116(3): 363–72 **(10 pages)**.

Cairns, M.A.; Brown, S.; Helmer, E. H.; Baumgardner, G.A. (1997). Root biomass allocation in the world's upland forests. Oecologia. 111(1): 1-11 **(11 pages)**.

Chave, J.; Andalo, C.; Brown, S.; Cairns, M.A.; Chambers, J.; Eamus, D.; Folster, H.; Fromard, F.; Higuchi, N.; Kira, T.; Lescure, J.P.; Nelson, B.W.; Ogawa, H.; Puig, H.; Riere, B.; Yamakura, T., (2005). Tree allometry and improved estimation of carbon stocks and balance in tropical forests. Oecologia. 145(1): 87–99 **(12 pages)**.

Chave, J.; Réjou-Méchain, M.; Búrquez, A.; Chidumayo, E.; Colgan, M.S.; Delitti, W.B.; Duque, A.; Eid, T.; Fearnside, P.M.; Goodman, R.C.; Henry, M.; Martínez-Yrízar, A.; Mugasha, W.A.; Muller-Landau, H.C.; Mencuccini, M.; Nelson, B.W.; Ngomanda, A.; Nogueira, E.M.; Ortiz-Malavassi, E.; Pélissier, R.; Ploton, P.; Ryan; C.M.; Saldarriaga, J.G.; Vieilledent, G., (2014). Improved allometric models to estimate the aboveground biomass of tropical trees. Global Chang. Biol., 20(10): 3177–3190 **(14 pages)**.

Chicco, D.; Warrens, M.J.; Jurman, G., (2021). The coefficient of determination r-squared is more informative than SMAPE, MAE, MAPE, MSE and RMSE in regression analysis evaluation. PeerJ Comput. Sci., 5(7): e623 **(24 pages)**.

Debie, E.; Abro, T.W., (2025). Carbon stock dynamics in biosphere reserves and mountainous forest ecosystems. Trees, Forest People. 19: 1-11 **(11 pages)**.

Divya Pant, D.; Shah, K.K.; Sharma, S.; Bhatta, M.; Tripathi, S.; Pandey, H.P.; Tiwari, H.; Shrestha, J.; Bhat, A.K., (2023). Soil and ocean carbon sequestration, carbon capture, utilization, and storage as negative emission strategies for global climate change. J. Soil Sci. Plant Nutr., 23: 1421–1437 **(17 pages)**.

Feldpausch, T.R.; Banin, L.; Phillips, O.L.; Baker, T. R.; Lewis, S.L.; Quesada, C.A.; Affum-Baffoe, K.; Arets, E.J.M.M.; Berry, N.J.; Bird, M.; Brondizio, E.S.; de Camargo, P.; Chave, J.; Djagbletey, G.; Domingues, T.F.; Drescher, M.; Fearnside, P.M.; França, M. B.; Fyllas, N. M.; Lopez-Gonzalez, G., Hladik, A.; Higuchi, N.; Hunter, M.O.; Iida, Y.; Salim, K. A.; Kassim, A.R.; Keller, M., Kemp, J.; King, D.A.; Lovett, J.C.; Marimon, B.S.; Marimon-Junior, B.H.; Lenza, E., Marshall, A.R., Metcalfe, D.J., Mitchard, E.T.A., Moran, E.F., Nelson, B.W.; Nilus, R.; Nogueira, E.M.; Palace, M.; Patiño, S.; Peh, K.S.-H.; Raventos, M.T.; Reitsma, J.M.; Saiz, G.; Schrodt, F.; Sonké, B.; Taedoumg, H.E.; Tan, S.; White, L.; Wöll, H., Lloyd, J., (2011). Height-diameter allometry of tropical forest trees. Biogeosciences. 8(5): 1081-1106 **(26 pages).**

Hashimoto, T.; Tange, T.; Masumori, M.; Yagi, H.; Sasaki, S.; Kojimas, K., (2004). Allometric equations for pioneer tree species and estimation of the aboveground biomass of a tropical secondary forest in East Kalimantan. Tropics. 14(1): 123–30 **(8 pages).**

Heriansyah, I.; Miyakuni, K.; Kato, T.; Kiyono, Y.;

Kanazawa, Y., (2007). Growth characteristics and biomass accumulations of acacia mangium under different management practices in Indonesia. J. Trop. For. Sci., 19(4): 226–35 **(10 pages).**

Heryati, Y., Abdu, A., Mahat, M. N., Abdul-Hamid, H., Jusop, S., Majid, N. M., Heriansyah, I., Ahmad, K. (2011). Assessing forest plantation productivity of exotic and indigenous species on degraded secondary forests. Am. J. Agric. Biol. Sci., 6(2): 201-208 **(9 pages).**

Huang, Y.; Ciais, P.; Santoro, M.; Makowski, D.; Chave, J.; Schepaschenko, D.; Abramoff, R. Z.; Goll, D. S.; Yang, H.; Chen, Y.; Wei, W.; Piao, S., (2021). A global map of root biomass across the world's forests. Earth Syst. Sci. Data. 13: 4263–4274 **(12 pages).**

Huy, B.; Poudel, K.P.; Kralicek, K.; Hung, N.D.; Khoa, P.V.; Temesgen, H., (2016). Allometric equations for estimating tree aboveground biomass in tropical dipterocarp Forests of Vietnam. Forest. 7(8): 180 **(19 pages).**

Huy, B.; Tinh, N.T.; Krishna, P.; Poudel, K.P.; Frank, B.M.; Temesgen, H., (2019). Taxon-specific modeling systems for improving reliability of tree aboveground biomass and its components estimates in tropical dry dipterocarp forests. For. Ecol. Manage. 437: 156–74 **(19 pages).**

Ketterings, Q.M.; Coe, R.; Noordwijk, M.N.; Ambagau', Y.; Palm, C.A., (2001). Reducing uncertainty in the use of allometric biomass equations for predicting above-ground tree biomass in mixed secondary forests. For. Ecol. Manage. 146(1–3): 199–209 **(11 pages).**

Larekeng, S.H.; Nursaputra, M.; Mappiasse, M.F.; Ishak, S.; Basyuni, M.; Sumarga, E.; Arifanti, V.B.; Aznawi, A.A.; Rahmila, Y.I.; Yulianti, M.; Rahmania, R.; Mubaraq, A.; Salmo III, S.G.; Ali, H.; Yenny, I., (2024). Estimation of mangrove carbon stocks using unmanned aerial vehicle over coastal vegetation. Global J. Environ. Sci. Manage., 10(3): 1133-1150 **(18 pages).**

Lehnebach, R.; Beyer, R.; Letort, V.; Heuret, P., (2018). The pipe model theory half a century on : a review. Ann. Bot., 121: 773-795 **(22 pages).**

Malik, A.D.; Arief, M.C.W.; Withaningsih, S.; Parikesit, P., (2024). Modeling regional aboveground carbon stock dynamics affected by land use and land cover changes. Global J. Environ. Sci. Manage., 10(1): 245-266 **(12 pages).**

Manuri, S., Brack, C.; Nugroho, N.P.; Hergoualc'h, K.; Novita, N.; Dotzauer, H.; Verchot, L.; Putra, C.A.S.; Widyasari, E., (2014). Tree biomass equations for tropical peat swamp forest ecosystems in Indonesia. For. Ecol. Manage. 334: 241-253 **(13 pages).**

Manuri, S.; Brack, C.; Noor'an, F.; Rusolono, R.; Anggraini, S.M.; Dotzauer, H.; Kumara, I., (2016). Improved allometric equations for tree aboveground biomass estimation in tropical dipterocarp forests of Kalimantan, Indonesia. For. Ecosyst., 3: 28 **(10 pages).**

Marziliano, P.A.; Menguzatto, G.; Scuderi, A.; Scalise, C.; Coletta., (2017). Biomass conversion and expansion factors in Douglas-fir stands of different planting density: variation according to individual growth and prediction equations. For. Syst., 26(1): e003 **(12 pages).**

Miyakuni, K.; Heriansyah, I.; Heriyanto, N.M.; Kiyono, Y., (2004). Allometric biomass equations, biomass expansion factors and root-to-shoot ratios of planted acacia mangium willd. forests in West Java, Indonesia. J. For. Plan., 10(2): 69–76 **(8 pages).**

Miyakuni, K.; Heriansyah, I.; Heriyanto, N.M.; Kiyono, Y., (2005). Allometric equations and parameters for estimating the biomass of planted pinus merkusii jungh. et de vr. forests. Japan. J. For. Environ., 47(2): 95–104 **(10 pages).**

Petersson, H.; Holm, S.; Ståhl, G.; Alger, D.; Fridman, J.; Lehtonen, A.; Lundström, A.; Mäkipää, R., (2012). Individual tree biomass equations or biomass expansion factors for assessment of carbon stock changes in living biomass - a comparative study. For. Ecol. Manage. 270: 78–84 **(7 pages).**

Poorter, H.; Jagodzinski, A.M.; Ruiz-Peinado, R.; Kuyah, S.; Luo, Y.; Oleksyn, J.; Usoltsev, V.A.; Buckley, T.N.; Reich, P.B.; Sack, L., (2015). How does biomass distribution change with size and differ among species? An analysis for 1200 plant species from five continents. New Phytologist. 208(3): 736-749 **(16 pages).**

Poorter, L.; van der Sande, M. T.; Thompson, J.; Arets, E. J. M. M.; Alarcón, A.; Álvarez-Sánchez, J.; Ascarrunz, N.; Balvanera, P.; Barajas-Guzmán, G.; Boit, A.; Bongers, F.; Carvalho, F.A.; Casanoves, F.; Cornejo-Tenorio, G.; Costa, F.R.C.; de Castilho, C.V.; Duivenvoorden, J.F.; Dutrieux, L.P.; Enquist, B.J.; Fernández-Méndez, F.; Finegan, B.; Gormley, L.H.L.; Healey, J.R.; Hoosbeek, M.R.; Ibarra-Manríquez, G.; Junqueira, A.B.; Levis, C.; Licona, J.C.; Lisboa, L.S.; Magnusson, W.E.; Martínez-Ramos, M.; Martínez-Yrizar, A.; Martorano, L.G.; Maskell, L.C.; Mazzei, L.; Meave, J.A.; Mora, F.; Muñoz, R.; Nytch, C.; Pansonato, M.p.; Parr, T.W.; Paz, H.; Pérez-García, E.A.; Rentería, L.Y.; Rodríguez-Velazquez, J.; Rozendaal, D.M.A.; Ruschel, A.R.; Sakschewski, B.; Salgado-Negret, B.; Schietti, J.; Simões, M.; Sinclair, F.L.; Souza, P.F.; Souza, F.C.; Stropp, J.; ter Steege, H.; Swenson, N.G.; Thonicke, K.; Toledo, M.; Uriarte, M.; van der Hout, P.; Walker, P.; Zamora, N.; Peña-Claros, M., (2015). Diversity enhances carbon storage in tropical forests. Global Ecol. Biogeogr., 24(11): 1314-1328 **(15 pages).**

Qi, Y.; Wei, W.; Chen, C.; Chen, L., (2019). Plant root-shoot biomass allocation over diverse biomes: A global synthesis. Global Ecol. Conserv., 18: 1-14 **(14 pages)**

Romero, F.M.B.; Jacovine, L.A.G; Torres, C.M.M.E.; Ribeiro, S.C.; da Rocha, S.J.S.S.; Novais, T.D.O.; Gaspar, R.D.G.; da Silva, L.F.;Vidal, E.; Leite, H.G.; Staudhammer, C.L.; Fernside, P.M., (2022). Aboveground biomass

allometric models for large tres in southwestern Amazonia. Trees For. People. 9: 100317 **(13 pages).**

Schepaschenko, D.; Moltchanova, E.; Shvidenko, A.; Blyshchyk, V.; Dmitriev, E.; Martynenko, O.; See, L.; Kraxner, F., (2018). Improved estimates of biomass expansion factors for russian forests. Forests. 9: 312.

Schettini, B.L.S.; Jacovine, L.A.G.; Torres, C.M.M.E.; Carneiro, A.D.O.; Renato Vinícius Oliveira Castro, R.V.O.; Villanova, P.H.; da Rocha, S.J.S.S.; Rufino, M.P.M.X.; Silvio Nolasco de Oliveira Neto, S.N.D.N.; Junior, V.T.M.D., (2022). Use of destructive and non-destructive methodologies to estimate stem biomass accumulation and carbon stock in an eucalypys forest. Revista Árvore, 46: 1-9 **(9 pages).**

Siregar, C.A.; Narendra, B.H.; Abywijaya, I.K.; Pratiwi, P.; Alhamd, L.; Dharmawan, I.W.S.; Hadi, E.E.W.; Kurniawan, H., (2025). A model designed for estimating biomass and carbon pool stock in over-mature plantations of teak; Tectona grandis. Global J. Environ. Sci. Manage., 11(2): 677-694 **(18 pages).**

Stephenson, N.L.; Das, A.J.; Condit, R.; Russo, S.E.; Baker, P.J.; Beckman, N. G.; Coomes, D.A.; Lines, E.R.; Morris, W.K.; Rüger, N.; Álvarez, E.; Blundo, C.; Bunyavejchewin, S.; Chuyong, G.; Davies, S.J.; Duque, Á.; Ewango, C.N.; Flores, O.; Franklin, J.F.; Grau, H.R.; Hao, Z.; Harmon, M.E.; Hubbell, S.P.; Kenfack, D.; Lin, Y.; Makana, J.R.; Malizia, A.; Malizia, L.R.; Pabst, R.J.; Pongpattananurak, N.; Su, S.H.; Sun, I.F.; Tan, S.; Thomas, D.; van Mantgem, P.J.; Wang, X.; Wiser, S.K; Zavala, M.A., (2014). Rate of tree carbon accumulation increases continuously with tree size. Nature. 507: 90-93 **(4 pages).**

Suarez-Fernandez, G.E.; Martínez-Sanchez, J.; Arias, P., (2025). Enhancing carbon stock estimation in forests: Integrating multi-data predictors with random forest method. Ecol. Inf., 86: 1-20 **(20 pages).**

Sumarga, E.; Rosleine, D.; Hutajulu, G.B.; Plaurint, R.P.; Basyuni, M.; Larekeng, S.H.; Taqiyudin, M.F.; Shohihah, N.N.; Ali, H.M., (2024). Quantification of ecosystem services from mangrove silvofishery. Global J. Environ. Sci. Manage., 10(3): 1333-1344 **(12 pages)**.

Thompson, I.D.; Okabe, K.; Tylianakis, J.M.; Kumar, P.; Brockerhoff, E.G.; Schellhorn, N.A.; Parrotta, J.A.; Nasi, R., (2011). Forest biodiversity and the delivery of ecosystem goods and services: translating science into policy. BioScience. 61(12): 972-981 **(10 pages).**

Tian, L.; Wu, X.; Tao, Y.; Li, M., Qian, C.; Liao, L.; Fu, W., (2023). Review of Remote Sensing-Based Methods for Forest Aboveground Biomass Estimation: Progress, Challenges, and Prospects. Forests. 14: 1-31 **(31 pages).**

AUTHOR (S) BIOSKETCHES

Heriansyah, I., Ph.D., Principal Researcher, Research Center for Ecology and Ethnobiology, Research Organization for Life Sciences and Environment, National Research and Innovation Agency (BRIN), Jalan Raya Jakarta – Bogor km 46, Cibinong, 169111, Indonesia.
- Email: *ika.heriansyah@brin.go.id*
- ORCID: 0000-0002-2396-1475
- Web of Science ResearcherID: EXS-5346-2022
- Scopus Author ID: 10440172700
- Homepage: https://www.researchgate.net/profile/ika-heriansyah-2

Abdulah, L., Dr., Senior Researcher, Research Center for Ecology and Ethnobiology, Research Organization for Life Sciences and Environment, National Research and Innovation Agency (BRIN), Jalan Raya Jakarta – Bogor km 46, Cibinong, 169111, Indonesia.
- Email: *lutf008@brin.go.id*
- ORCID: 0000-0002-0916-5974
- Web of Science ResearcherID: NA
- Scopus Author ID: 55135251300
- Homepage: https://scholar.google.com/citations?hl=id&user=aTPXiXUAAAAJ

Rahajoe, J.S., Ph.D., Principal Researcher, Research Center for Ecology and Ethnobiology, Research Organization for Life Sciences and Environment, National Research and Innovation Agency (BRIN), Jalan Raya Jakarta – Bogor km 46, Cibinong, 169111, Indonesia.
- Email: *joen001@brin.go.id*
- ORCID: 0000-0002-5581-4058
- Web of Science ResearcherID: GNP-8203-2022
- Scopus Author ID: 15761031600
- Homepage: https://scholar.google.co.id/citations?user=DEaJcK4AAAAJ&hl=en

Susanti, R., Ph.D., Principal Researcher, Research Center for Ecology and Ethnobiology, Research Organization for Life Sciences and Environment, National Research and Innovation Agency (BRIN), Jalan Raya Jakarta – Bogor km 46, Cibinong, 169111, Indonesia.
- Email: *ruliyanas@gmail.com*
- ORCID: 0000-0003-0342-2906
- Web of Science ResearcherID: NA
- Scopus Author ID: 57210910758
- Homepage: https://scholar.google.co.id/citations?hl=en&user=DsZe-q4AAAAJ

AUTHOR (S) BIOSKETCHES

Lisnawati, Y., Dr., Principal Researcher, Research Center for Ecology and Ethnobiology, Research Organization for Life Sciences and Environment, National Research and Innovation Agency (BRIN), Jalan Raya Jakarta – Bogor km 46, Cibinong, 169111, Indonesia.
- Email: *yuni028@brin.go.id*
- ORCID: 0000-0002-2601-4596
- Web of Science ResearcherID: NA
- Scopus Author ID: 57213351062
- Homepage: https://www.independent.academia.edu/LisnawatiYunita

Subarudi, Dr., Principal Researcher, Research Center for Population, National Research and Innovation Agency (BRIN), Jalan Raya Jakarta – Bogor km 46, Cibinong, 169111, Indonesia.
- Email: *subarudi@brin.go.id*
- ORCID: 0000-0001-8278-0378
- Web of Science ResearcherID: NA
- Scopus Author ID: 7409630160
- Homepage: https://www.scopus.com/authid/detail.uri?authorId=7409630160

Dewi, R., Ph.D. Candidate, Department of Tropical Silviculture, Faculty of Forestry and Environments, IPB University, Jalan Raya Dramaga, Bogor 16680, Indonesia. Senior Researcher, Research Center for Ecology and Ethnobiology, Research Organization for Life Sciences and Environment, National Research and Innovation Agency (BRIN), Jalan Raya Jakarta – Bogor km 46, Cibinong, 169111, Indonesia.
- Email: *rosi015@brin.go.id*
- ORCID: 0000-0003-4629-7084
- Web of Science ResearcherID: NA
- Scopus Author ID: 57519367700
- Homepage: https://independent.academia.edu/rositadewi231

Darwo, Dr., Principal Researcher, Research Center for Ecology and Ethnobiology, Research Organization for Life Sciences and Environment, National Research and Innovation Agency (BRIN), Jalan Raya Jakarta – Bogor km 46, Cibinong, 169111, Indonesia.
- Email: *darw004@brin.go.id*
- ORCID: 0000-0002-4196-9984
- Web of Science ResearcherID: NA
- Scopus Author ID: 57213353672
- Homepage: https://independent.academia.edu/Darwo

Mawazin, S.Si., Senior Researcher, Research Center for Ecology and Ethnobiology, Research Organization for Life Sciences and Environment, National Research and Innovation Agency (BRIN), Jalan Raya Jakarta – Bogor km 46, Cibinong, 169111, Indonesia.
- Email: *mawa001@brin.go.id*
- ORCID: 0000-0002-6062-4400
- Web of Science ResearcherID: NA
- Scopus Author ID: 57201287955
- Homepage: https://independent.academia.edu/MawazinMawazin

Abdurachman, M.P**.,** Senior Researcher, Research Center for Ecology and Ethnobiology, Research Organization for Life Sciences and Environment, National Research and Innovation Agency (BRIN), Jalan Raya Jakarta – Bogor km 46, Cibinong, 169111, Indonesia.
- Email: *abdu082@brin.go.id*
- ORCID: 0000-0001-8856-510X
- Web of Science ResearcherID: LJK-1045-2024
- Scopus Author ID: 59291756000
- Homepage: https://www.researchgate.net/profile/Abdurachman-Abdurachman-3

Karmilasanti, S.Hut., Junior Researcher, Research Center for Ecology and Ethnobiology, Research Organization for Life Sciences and Environment, National Research and Innovation Agency (BRIN), Jalan Raya Jakarta – Bogor km 46, Cibinong, 169111, Indonesia.
- Email: *karmilasanti@brin.go.id*
- ORCID: 0000-0003-4768-2793
- Web of Science ResearcherID: NA
- Scopus Author ID: 57685888300
- Homepage: https://scholar.google.co.id/citations?user=6-_tAAQAAAAJ&hl=id

Wakhid, N., Ph.D., Senior Researcher, Research Center for Ecology and Ethnobiology, Research Organization for Life Sciences and Environment, National Research and Innovation Agency (BRIN), Jalan Raya Jakarta – Bogor km 46, Cibinong, 169111, Indonesia.
- Email: *nur.wakhid@brin.go.id*
- ORCID: 0000-0002-5065-8770
- Web of Science ResearcherID: KLZ-5679-2024
- Scopus Author ID: 57192961613
- Homepage: https://scholar.google.com/citations?user=WcjCchUAAAAJ&hl=en

Wicaksono, D., M.Sc., Junior Researcher, Research Center for Ecology and Ethnobiology, Research Organization for Life Sciences and Environment, National Research and Innovation Agency (BRIN), Jalan Raya Jakarta – Bogor km 46, Cibinong, 169111, Indonesia.
- Email: *donny.wicaksono@brin.go.id*
- ORCID: 0009-0008-3672-6256
- Web of Science ResearcherID: NA
- Scopus Author ID: 58042016700
- Homepage: https://scholar.google.com/citations?user=KpWmMrMAAAAJ&hl=en

AUTHOR (S) BIOSKETCHES

Effendi, R., M.Sc., Principal Researcher, Research Center for Ecology and Ethnobiology, Research Organization for Life Sciences and Environment, National Research and Innovation Agency (BRIN), Jalan Raya Jakarta – Bogor km 46, Cibinong, 169111, Indonesia.
▪ Email: *rach026@brin.go.id*
▪ ORCID: 0009-0009-2335-3187
▪ Web of Science ResearcherID: NA
▪ Scopus Author ID: 57223125592
▪ Homepage: https://scholar.google.com/scholar?hl=id&as_sdt=0%2C5&q=rachman+effendi&btnG=

Yunianto, A.S., S.Hut., Researcher, Research Center for Ecology and Ethnobiology, Research Organization for Life Sciences and Environment, National Research and Innovation Agency (BRIN), Jalan Raya Jakarta – Bogor km 46, Cibinong, 169111, Indonesia.
▪ Email: *andh008@brin.go.id*
▪ ORCID: 0009-0006-3672-5515
▪ Web of Science ResearcherID: NA
▪ Scopus Author ID: 0009-0006-3672-5515
▪ Homepage: https://scholar.google.com/citations?hl=en&user=Y3nYbcgAAAAJ

Qirom, M.A., M.Si., Senior Researcher, Research Center for Ecology and Ethnobiology, Research Organization for Life Sciences and Environment, National Research and Innovation Agency (BRIN), Jalan Raya Jakarta – Bogor km 46, Cibinong, 169111, Indonesia.
▪ Email: *muhammad.abdul.qirom@brin.go.id*
▪ ORCID: 0000-0002-8708-212X
▪ Web of Science ResearcherID: NA
▪ Scopus Author ID: 56012934200
▪ Homepage: https://scholar.google.co.id/citations?hl=en&user=0Ytm-cAAAAAJ

Mindawati, N., Dr., Principle Researcher, Research Center for Ecology and Ethnobiology, Research Organization for Life Sciences and Environment, National Research and Innovation Agency (BRIN), Jalan Raya Jakarta – Bogor km 46, Cibinong, 169111, Indonesia.
▪ Email: *nina017@brin.go.id*
▪ ORCID: 0000-0001-7368-1351
▪ Web of Science ResearcherID: NA
▪ Scopus Author ID: 104404844000
▪ Homepage: http://www.researchgate.net/profile/nina-mindawati

HOW TO CITE THIS ARTICLE

Heriansyah, I.; Abdulah, L.; Rahajoe, J.S.; Susanti, R.; Lisnawati, Y.; Subarudi; Dewi, R.; Darwo; Mawazin; Abdurachman; Karmilasanti; Wakhid, N.; Wicaksono, D.; Effendi, R.; Yunianto, A.S.; Qirom, M.A.; Mindawati, N., (2025). Allometric equations model for estimating an above and below ground biomass of dipterocarp forest in the tropics. Global J. Environ. Sci. Manage., 11(3): 1199-1220.

DOI: 10.22034/gjesm.2025.03.18

URL: https://www.gjesm.net/article_722661.html

Global J. Environ. Sci. Manage. 11(3): 1221-1240, Summer 2025, Serial #43

Global Journal of Environmental Science and Management
(GJESM)

Homepage: https://www.gjesm.net/

Podcasts

CASE STUDY

Carcinogenic and non-carcinogenic hazards associated with trace elements and organochlorines from fish consumption in tropical river watershed

D. Dwiyitno[1,*], F. Ariyani[2], G.R. Barokah[3,4], D. Yogaswara[5], R. Grandiosa[6], E. Frimawaty[7], H.E. Irianto[2,8], Y. Sani[1]

[1] *Research Center for Veterinary Science, National Research and Innovation Agency, Cibinong 16911 Indonesia*

[2] *Research Center for Marine and Land Bioindustry, National Research and Innovation Agency, Tangerang Selatan, 15310 Indonesia*

[3] *Research Center for Food Technology and Processing, National Research and Innovation Agency, Gunungkidul 55681 Indonesia*

[4] *Department of Biotechnology, Graduate School of Engineering, University of Osaka, 2-1 Yamada-Oka, 565-0871 Japan*

[5] *Research Center for Oceanography, National Research and Innovation Agency, Jakarta 14430 Indonesia*

[6] *Faculty of Fisheries and Marine Science, Padjadjaran University, Sumedang 45363 Indonesia*

[7] *School of Environmental Science, Universitas Indonesia, Jakarta 10430 Indonesia*

[8] *Faculty of Food Technology and Health, Sahid University, Jl., Jakarta 12870, Indonesia*

ARTICLE INFO

Article History:
Received 20 February 2025
Revised 24 April 2025
Accepted 24 May 2025

Keywords:
Carcinogenic
Health risk
Non-carcinogenic
Organochlorines
River watershed
Trace elements

ABSTRACT

BACKGROUND AND OBJECTIVES: Trace elements and pesticide residues are among the crucial problems in the river Watershed ecosystem. The current study sought to evaluate the health risks associated with trace elements and organochlorines from fish consumption for the local population in the Citarum Watershed, Indonesia. This study is important as the rapid development of population and industrial activities along Citarum Watershed has contributed to domestic waste production, agricultural run-off, and industrial emissions that could leak into the river watershed.

METHODS: This risk assessment was conducted based on the framework according to the Codex Alimentarius Commission. The concentrations of selected trace elements and organochlorines in fish species from Citarum Watershed were obtained from fish farms in 3 reservoirs (Saguling, Cirata, and Jatiluhur). Data pertaining to food consumption, which was employed to evaluate contaminant exposure, was gathered from individual food consumption surveys conducted by the Ministry of Health as part of the National Total Diet Study. A deterministic approach was used to estimate the dietary exposure to trace elements and organochlorine pesticides from fish consumption related to the Citarum Watershed in different age groups of the local population. The health risk assessment is categorized into chronic/non-carcinogenic health risks (hazard quotient) as well as carcinogenic risk.

FINDINGS: The study found that trace elements and organochlorine pesticides were detected in freshwater fish from Citarum Watershed with concentration orders of copper > chrome > lead > mercury > cadmium. The concentrations are fall below the maximum permitted limit in accordance with Indonesian and global standards. Additionally, organochlorine levels in fish samples were also relatively low compared to the official threshold, with concentration order of heptachlor > lindane > dichloro-diphenyl-trichloroethane > endosulfan > aldrin > endrin > dieldrin, respectively. Chrome and lead showed the highest contributors for non-carcinogenic and carcinogenic risks from trace element exposure, respectively. Moreover, aldrin and heptachlor are the key contributors for non-carcinogenic and carcinogenic risks stemming from organochlorine exposure, respectively.

CONCLUSION: The present study revealed that trace elements and organochlorines are unlikely to pose non-carcinogenic and carcinogenic risks to the local populations in Citarum Watershed. However, the worst estimation of cumulative exposure revealed that children are particularly vulnerable to the highest level of risk. The result of the present study is considered as the lowest risk scenario. Additionally, if there is no improved mitigation program to reduce contamination to Citarum Watershed, there is a possible increased health risks to the local population. There may be an increased risk from various contaminants and dietary sources, along with the potential for synergistic toxicity among the compounds. To provide a more reliable health risk, further research is required to identify the contamination in wild fish and other dietary sources, as well as to include emerging contaminants. Furthermore, it is essential for the associated governmental organizations to create a routine monitoring system and to keep track of the biota samples. Identification of contaminant sources is important to develop a mitigation strategy and law enforcement for minimizing the use and leakage of the contaminants in the ecosystem and reducing the hazards to public health.

DOI: 10.22034/gjesm.2025.03.19

This is an open access article under the CC BY license (http://creativecommons.org/licenses/by/4.0/).

NUMBER OF REFERENCES
74

NUMBER OF FIGURES
3

NUMBER OF TABLES
9

*Corresponding Author:
Email: ***
Phone: ***
ORCID: ***

Note: Discussion period for this manuscript open until Sep 1, 2025 on GJESM website at the "Show Article".

INTRODUCTION

Anthropogenic pollutants such as trace elements and pesticide residues are among the crucial problems in river watersheds of many countries, including Indonesia (Chen *et al.*, 2020a; Fahimah *et al*., 2023; Oginawati *et al*., 2021; Olayinka-Olagunju *et al*., 2021; Salami *et al*., 2025; Wulandari *et al*., 2022). A range of industrial operations has been identified as sources of trace elements that are released into the atmosphere, aquatic systems, and soil environments (Briffa *et al*., 2020). Additionally, large amounts of organochlorine pesticides (OCPs) have been used for a long time until replaced by more environmentally friendly pesticides (Jürgens *et al*., 2016). The continuous existence of trace elements and organochlorines, as well as their potential harmful impacts on ecosystems and human health, has raised global awareness (IPCS-WHO, 2025; IRIS, 2025). Edible fish is the primary protein source in Indonesia, with an annual consumption of 54.49 kilograms (kg). Furthermore, freshwater fish play a crucial role in both the production and consumption of aquaculture in Indonesia. Out of 7.4 million tons of aquaculture production in 2021, freshwater aquaculture shared 3.7 million tons, as 50 percent (%), and mainly produced from floating cages (BPS-Statistics Indonesia, 2023). A total diet study (TDS) revealed that freshwater fish accounted for 23.4% of total fish consumption (Ministry of Health, 2015). Furthermore, the levels of pollutants found in fish can serve as indicators of the overall state of environmental contamination (Ahmed *et al*., 2019; Cui *et al*., 2015). Citarum Watershed is among the largest watersheds in Java Island, the most populated island in Indonesia. Known as the longest river in West Java Province with 297 km, the Citarum Watershed covers an area of approximately 6,617 square kilometers (km^2) (DIKPLHD West Java, 2021). Three hydropower dams, namely Saguling, Cirata, and Jatiluhur, are situated along Cirarum Watershed. The dams are also known as fish farming centers of 141,219 net cages with an annual production of 224,962 tons, or 27.5% of the locally farmed fish production (BPS-Statistics Indonesia, 2023 Moreover, the deterioration of water quality resulting from anthropogenic pollution poses a critical challenge in the Citarum Watershed (Idris *et al*., 2019). This river plays a vital role for more than 35 million people around it, including for drinking water, agricultural irrigation, hydroelectric power plants, and for net cage fish farming (ADB, 2013; Idris *et al*., 2019). The quick expansion of both population and industrial operations within the Citarum Watershed has resulted in the decline of the river watershed (DIKPLHD West Java, 2021; Idris *et al*., 2019). The population around the Citarum Watershed potentially produces 15,838 tons of organic and inorganic waste daily. Industrial growth in this area is also rapid, from 4,845 units in 2014 to 7,046 units in 2021 (ADB, 2013; Idris *et al*., 2019). Trace element residues have been reported in fish species from the Citarum Watershed (Astuti *et al*., 2021; Murtini and Rachmawati, 2007; Nuraeni *et al*., 2021; Priyanto *et al*., 2008; Salami *et al*., 2008; Sutrisno *et al*., 2007; Wulandari *et al*., 2022). Rahmawati *et al*. (2013) and Oginawati *et al*. (2021) reported organochlorine pesticides in fish and mollusks from the Citarum Watershed. Household wastewater, industrial processes, and agricultural activities are the main sources of trace elements and organochlorine pesticide pollution in the Citarum Watershed. Industries of textile (60%), food/beverage (13%), slaughterhouses (13%), tanneries (9%), and electroplating are the major contributors for trace element pollution. Additionally, agriculture is the main contributor of organochlorine residue (ADB, 2013; Roosmini *et al.,* 2020). Consumption of fish with elevated trace element contamination could result in detrimental health impacts, such as neurological disorders, cancer, and injury to crucial body organs (ATSDR, 2020, 2022b, 2022d). Furthermore, some organochlorine compounds and their derivatives are classified as persistent organic pollutants (POPs), which can cause cancers to the liver, testes, pancreas, and breast (ATSDR, 2021, 2022a, 2022c, 2023). To date, there is no comprehensive assessment of chemical contaminants hazard in fish species from the Citarum Watershed to the local population. It is essential to assess the contaminant risks linked to fish consumption from this watershed to safeguard the health assurance of the local population. Risk assessment on the different age groups of local populations is essential to provide a more reliable health risk assessment (Zhao *et al*., 2023). Moreover, assessing the risks of various chemicals is regarded as a more realistic approach to understanding simultaneous exposure to multiple agents (OECD, 2025). This analysis of multiple substances emphasized the health risks associated with carcinogenic and non-carcinogenic factors (More *et al*., 2019). The findings from this study will be valuable

for providing food safety status, dietary guidance, and environmental management for protecting the public health in the related region. Therefore, the objective of this study were to: a) assess dietary exposure to trace elements and organochlorines through farmed fish consumption from the Citarum Watershed; and b) calculate the hazard index (HI) and carcinogenic risk (CR) to estimate the non-carcinogenic and carcinogenic health risks to different age groups of local population. This study was conducted in the Citarum Watershed, Indonesia performed in 2024.

MATERIALS AND METHODS

Trace elements and organochlorine pesticides in fish samples

This risk assessment was conducted based on the framework according to the Codex Alimentarius Commission (CAC) (FAO/WHO, 2011). Data on trace element concentrations and organochlorine pesticide levels in fish species from the Citarum Watershed were collected from prior studies spanning 2007 to 2022 (Murtini and Rachmawati, 2007; Oginawati *et al*., 2021; Priyanto *et al*., 2008; Rahmawati *et al*., 2013; Salami and Rizaldi, 2016; Sutrisno *et al*., 2007; Wardhani *et al*., 2017, 2018; Wulandari *et al*., 2022). Studies on trace-element monitoring in fish samples were typically conducted more often than on organochlorine pesticides. These studies were conducted in three reservoirs along the Citarum Watershed (Saguling, Cirata, and Jatiluhur). Fig. 1 illustrates an overview of the Citarum Watershed and the distribution of samples.

Trace element concentrations were evaluated based on 204 fish samples, whereas organochlorine levels were collected from 44 fish samples. A summary of the trace element and organochlorine levels in fish species from Citarum Watershed is presented in Figs. 2 and 3. In those studies, trace elements were assessed via atomic absorption spectroscopy (AAS), while organochlorines were quantified using



Fig. 1: Geographic location of the study area in Citarum Watershed along with the fish sampling collection in Indonesia

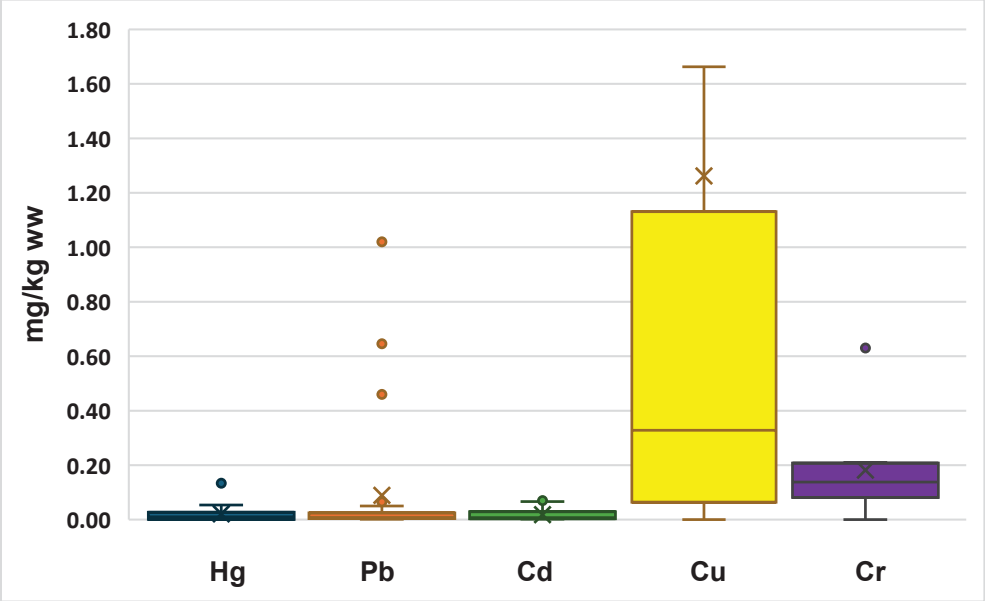

Fig. 2: Concentration of selected trace elements in fish samples from Citarum Watershed

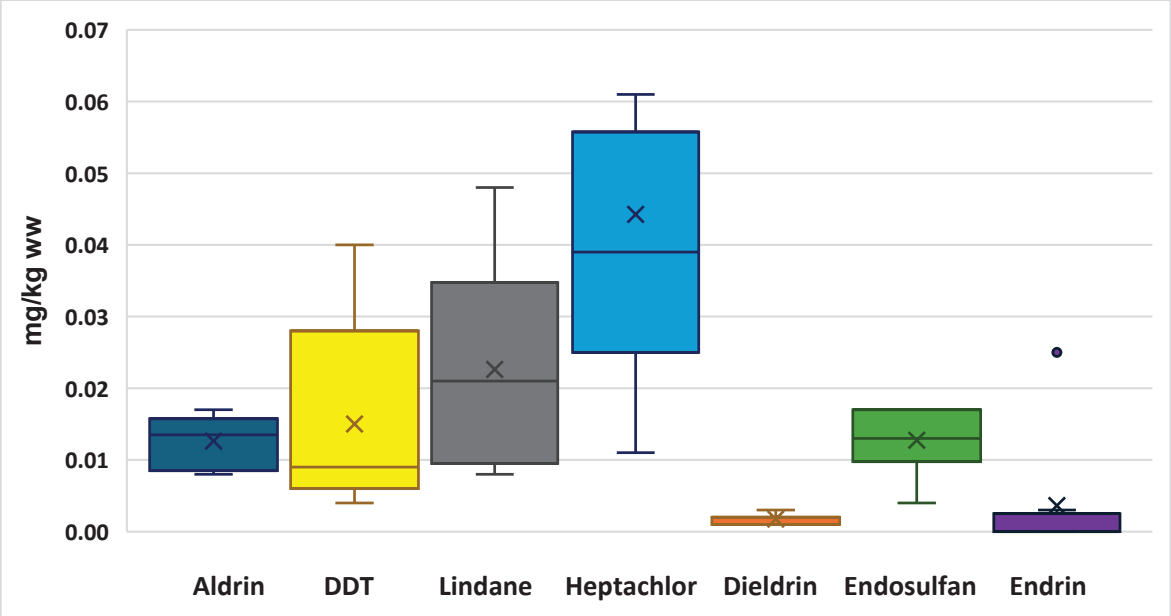

Fig. 3: Concentration of organochlorine pesticides in fish samples from Citarum Watershed

gas chromatography (GC). Contaminant levels are presented as mean, standard deviation (SD), median, minimum, percentile 95 (P_{95}), and maximum values. The P_{95} of consumption is utilized to gauge the potential health hazards related to the maximum levels of fish consumption or the exposure to contaminants from consuming fish (US EPA, 2019).

Fish consumption data

Data on food consumption to estimate the exposure to the concerned trace elements and organochlorines were obtained from the National

Table 1: Distribution of body weight and fish consumption of different age group population

Category	Age group (years old)					Sources
	0-5	5-12	13-18	19-55	>55	
Mean body weight (kg)	11.67	27.5	46.33	57.87	50.78	Ministry of Health, 2015
Freshwater fish consumption (g/day)	16.38	28.38	25.63	31.50	26.25	BPS-Statistics Indonesia, 2023

Total Diet Study (TDS) (Ministry of Health, 2015). The personal food consumption surveys were carried out in 2014-2015, employing a 1x24-hour food recall technique. The surveys involved 162,044 respondents, who were divided into five age groups: toddlers, children, adolescents, adults, and seniors aged over 55 years old. The mean body weights of these age groups were between 11.67 and 57.87 kg (Table 1). Since the current study emphasized the Citarum Watershed, data pertaining to fish consumption was chosen specifically for freshwater fish consumption in West Java Province, where the Citarum Watershed is located. Based on the data of fish consumption (BPS-Statistics Indonesia, 2023), national fish consumption was 54,49 kg/year, and the West Java population consumed 35.81 kg/year [98.22 gram (g)/day]. Therefore, the freshwater fish consumption rates in different age groups were between 16.38 and 31.50 g/day (Table 1). The data was further applied to calculate the exposure to the concerned contaminants in the population of the Citarum Watershed.

Dietary exposure

A deterministic strategy was utilized to evaluate the dietary exposure to trace elements and organochlorine pesticides linked to fish consumption among different age demographics of the local community (FAO/WHO, 2011). Only contaminant levels in fish muscle samples were included in this study, while contaminant levels in fish organs (liver, gill, and skin) were excluded from the calculation. Molluscan samples were also excluded from the exposure calculation because their availability and consumption rates were relatively minor. It was presumed that entire identified concentration in tainted food was taken in through dietary consumption. Contaminant exposure was calculated by multiplying the consumption rate of freshwater fish (Table 1) by the concentration of trace elements (Fig. 2) and organochlorines in fish samples (Fig. 3). The average exposure of trace elements and organochlorine pesticides was estimated as daily intake (EDI) and presented as the mean, minimum, maximum, and P_{95} values, using Eq. 1 (FAO/WHO, 2011):

$$EDI\left(\frac{\frac{\mu g}{kg}bw}{day}\right) = \frac{\Sigma\left[\text{consumption rate}\left(\frac{g}{day}\right)x\ \text{contaminant level}\left(\frac{\mu g}{g}\right)\right]}{\text{Body weight (kg bw)}} \quad (1)$$

Health risk characterization

In the current study, chronic health risks are divided into non-carcinogenic and carcinogenic hazards. The non-carcinogenic risk is calculated as a percentage of EDI relative to the provisional tolerable daily intake (TDI) values. Tables 2 and 3 provide the toxicological profiles of oral reference doses and toxicity endpoints for the risks associated with trace elements and organochlorines, covering both non-carcinogenic and carcinogenic aspects. Accordingly, if the risk percentage value is greater than 100%, there is a potential risk (FAO/WHO, 2011). Non-carcinogenic risk was estimated using the target hazard quotient (THQ) equation developed by the United States Environmental Protection Agency (US EPA) (2019). The higher the THQ value, the higher the hazard probability to the exposed population, using Eq. 2 (FAO/WHO, 2011):

$$THQ = \frac{EDI}{TDI} \quad (2)$$

Where; EDI is daily exposure or estimated daily intake [microgram (µg)/kg body weight (bw)/day], and TDI is the oral reference dose representing no expected adverse health effects (µg/kg bw/day). The potential cumulative non-carcinogenic effects from exposure to multi-contaminants were calculated by

Table 2: Toxicological profiles of the concerned trace elements

Criteria	Trace element					Sources
	Hg	Cd	Pb	Cr	Cu	
Maximum Permissible Limit (MPL)	0.5	0.3	0.3	0.5	30.0	EFSA, 2010; FAO/WHO, 2023; NADFC, 2022; IPCS-WHO, 2025
TDI (µg/kg bw/day)	0.7	1.0	3.6	3.3	500.0	IPCS-WHO, 2025
SF (µg/kg bw/day)	-	6.1	8.5	41.0	-	Loomis *et al*., 2018; ; Zhao *et al*., 2023
Carcinogenicity category	-	1[a], A2[b], B1[c]	2B[d]	1[a]	-	IARC, 2019; IRIS, 2025; Loomis *et al*., 2018

[a] 1: Carcinogenic to humans (ATSDR, 2025); [b]A2: Suspected human carcinogen (IRIS, 2025);
[c]B1: Probable human carcinogen (IRIS, 2025); [d] 2B: Possibly carcinogenic to humans (ATSDR, 2020)

Table 3: Toxicological profiles of the concerned organochlorine pesticides

Criteria	Organochlorine pesticides							Sources
	Aldrin	Dieldrin	Lindane	Heptachlor	DDT	Endosulfan	Endrin	
MPL	0.2-0.3	0.2-0.3	0.2	0.2-0.3	0.7	0.2	0.1	ATSDR, 2022a, 2022c; BSN, 2025; FAO/WHO, 2023
TDI (µg/kg bw/day)	0.1	0.1	5.0	0.5	10.0	5.0	0.2	FAO/WHO, 2023
SF (µg/kg bw/day)	17.0	16.0	1.8-6.3	4.5	340.0	-	-	IARC, 2018, 2019; Loomis *et al*., 2018
Carcinogenicity criteria	2A[a] B2[b]	2A[a] B2[b]	1[c], 2B[d], B2[b]	2B[d] B2[b]	-	-	-	ATSDR, 2022a; IARC, 2018; Loomis *et al*., 2018

[a]2A: Probably carcinogenic to humans (ATSDR, 2022a); [b]B2: Probable human carcinogen (ATSDR, 2022a);
[c]1: Carcinogenic to humans (IARC, 2018); [d]2B: Possibly carcinogenic to humans (ATSDR, 2022a)

the sum of individual hazard (THQ) and represented as HI. A HI values below 1 implies minimal or no risk of adverse effects, in contrast with values exceeding 1. Furthermore, chronic risk levels < 0.1 is categorized as negligible, and for ≥ 0.1 <, ≥ 1 < 4, and ≥ 4) are low, medium, and high risk, respectively (US EPA, 2019). The HI of trace elements (*HIe*) and organochlorines (*HIo*) were calculated separately, using Eqs. 3 and 4 (FAO/WHO, 2011):

$$HIe = \mathrm{THQ(Hg)} + \mathrm{THQ(Cd)} + \mathrm{THQ(Pb)} + \mathrm{THQ(Cu)} + \mathrm{THQ(Cr)} \quad (3)$$

$$HIo = \mathrm{THQ(Aldrin)} + \mathrm{THQ(Dieldrin)} + \mathrm{THQ(Lindane)} + \mathrm{THQ(Heptachlor)} + \mathrm{THQ(DDT)} + \mathrm{THQ(Endosulfan)} + \mathrm{THQ(Endrin)} \quad (4)$$

For carcinogenic contaminants, the health risks were estimated as the probability of exposure to a potential carcinogen (Sultana *et al*., 2017; US EPA, 2019; Zhao *et al*., 2023). Cd, Pb, and Cr are categorized as carcinogenic elements, whereas aldrin, dieldrin, lindane, and heptachlor are classified as carcinogenic organochlorines (IARC, 2019; Loomis *et al*., 2018). The CR values were estimated using Eq. 5 (FAO/WHO, 2011):

$$CR = EDI \times SF \quad (5)$$

Where; SF is the cancer slope factor (µg/kg bw/day) adopted from the earlier databases (IARC, 2018, 2019; Loomis *et al*., 2018; Zhao *et al*., 2023).

RESULTS AND DISCUSSION

Trace elements concentration

From 2007 to 2022, multiple studies found trace elements of Hg, Pb, Cd, Cr, and Cu in fish samples from Citarum Watershed at various concentrations (Fig. 2). The mean concentrations of trace elements (0.01-0.60 mg/kg ww) are generally below the MPL according to Indonesian and global regulations (FAO/WHO, 2023; IRIS, 2025; NADFC, 2022;). Only the maximum concentration of Pb (0.46 mg/kg) was over the MPL of 0.3 mg/kg. In general, the concentration

of Cu in fish was relatively high compared to the other trace elements, with a concentration order of Cu > Cr > Pb > Hg > Cd (Fig. 2). This concentration order could indicate the pollution level in the Citarum Watershed. Cu, Cr, and Pb were also reported as the main trace elements in Citarum water and sediment (Murtini and Rachmawati, 2007; Priyanto *et al*., 2008; Roosmini *et al*., 2022; Salami and Rizaldi, 2016; Sutrisno *et al*., 2007; Wardhani *et al*., 2017, 2018).

Trace elements may find their way into the Citarum Watershed either through natural means or from human-induced sources related to domestic, agricultural, or industrial operations in the region. Contaminants concentration in the fish from the upper dams (Saguling and Cirata) are relatively comparable but higher than those from the downstream dams (Jatiluhur). This could be attributed to the fact that the majority of contaminant sources are found in the upper watershed. Contamination of Cu, Cr, Pb, Cd, and Hg is commonly present in the industrial waste of textiles, smelting, tannery, painting, dyes, and battery. Furthermore, the combustion of fossil fuels will generate emissions of Hg and Pb, whereas agricultural pesticides and fertilizers have the potential to introduce Cu and Cd into the ecosystem (Briffa *et al*., 2020). The relatively high concentration of Pb in fish indicated by the high emission of this element, which is also represented in the sediment accumulation. Various sources contribute to Pb contamination in the Citarum Watershed, such as the lead-acid battery industry, paints, electronic goods household emission, agriculture pesticides and fuel additives. There is no seasonal pattern of the contaminant concentration, as some higher during wet season due to higher emission loads, but some others higher during dry season due to concentration (Priyanto *et al.,* 2008). Therefore, the contaminant concentration in Citarum River is typically affected by the effluent loads from the different point of sources which vary seasonally. No consistent pattern exists regarding the fluctuation of contamination levels over time. Nevertheless, there has been a minor rise in contaminant levels in the upper dams, while a slight decline has been observed downstream. This could be affected by the development of industrial and urban activities in the upper region (Bandung City), compared to the lower region (Purwakarta District). Accumulating trace elements in river sediment can also be naturally derived from geogenic sources, such as volcanic precursor rocks (Sindern *et al*., 2016). Environmental contaminants could enter the food chain through various pathways, such as bioconcentration, bioaccumulation, and biomagnification in different trophic levels (Ahmed *et al*., 2019; Olayinka-Olagunju *et al*., 2021). This current study reveals that the mean levels of trace elements in fish samples collected from the Citarum Watershed are generally low, apart from the peak concentration of Pb (P_{95}: 0.46 mg/kg). This concentration is over the MPL according to official regulations for fish products in Indonesia, CAC, and Thailand, i.e., 0.3 mg/kg (BSN, 2025; FAO/WHO, 2023; MPH Thailand, 2020). However, the concentration is below the threshold in Australia, New Zealand, Hong Kong, and the EU, i.e., 0.5 mg/kg (CFS, 2019; EFSA, 2010; FSANZ, 2016). Biological and environmental aspects may impact how heavy metals accumulate in fish, with considerations such as age, body size, feeding patterns, habitat, and the nature and levels of pollutants. In comparison to other studies of trace elements in fish from Indonesian waters, the trace elements in fish from the Citarum Watershed are higher than those of fish from the Musi River (Putri *et al*., 2016). Relatively comparable levels of trace elements in fish from Citarum Watershed were reported from Cikaniki River, Bogor (Azizah and Maslahat, 2021). Additionally, a relatively high concentration of trace elements Pb, Cu, As, Cr, and Cd was reported in commercial fish from Karnaphuli River-Bangladesh (Ahmed *et al*., 2019). The estimated bioconcentration factor (BCF) for different trace elements in fish from Citarum Watershed were between 5-47, while for organochlorines were 40-65. BCF value >1 means the contaminant is bioaccumulative, but the value < 100 is categorized a low accumulation (Wassenaar et al., 2020). Moreover, as the fish are raised near the surface water, the bioaccumulation factors influenced by sediment effects cannot be determined with precision. A BCF value of 1.25-6 was reported from heavy metal contamination in tilapia from Central Java (Hidayah et al., 2014). Furthermore, Nędzarek et al. (2021) reported BCF of heavy metals between <10 and 50 on *Rutilus rutilus* and *Perca fluviatilis* from 2 lakes in Poland. Sanou et al (2021) reported BCF of heavy metals between 1-85 in tilapia from Bandama River in the Côte d'Ivoire. There are 3 species of farmed fishes in Citarum Watershed, i.e. tilapia (*Oreochromis niloticus*), common carp (*Cyprinus*

carpio), and catfish (*Pangasius pangasius*). The fish are farmed in a net-cage of 2-4 m under surface with a harvesting size of 300-400 g/fish from 4–5-month aquaculture. Crucially, reports indicate that both fish species and the cereal crop of rice in the Citarum Watershed have trace elements present, with levels varying from low to relatively high. A study conducted by Handayani *et al*. (2022) revealed contamination of Pb, Cd, Cu, Cr, Zn, Ni, and Co in rice from the upper Citarum Watershed.

Organochlorine pesticide concentration

Organochlorine compounds were detected in fish samples from Citarum Watershed, i.e., aldrin, DDT, lindane, dieldrin, heptachlor, endosulfan, and endrin (Fig. 3). In a manner akin to trace element contaminants, the levels of organochlorines found in fish samples from the Citarum Watershed were notably lower than the established threshold (ATSDR, 2022c, 2022a; BSN, 2025; FAO/WHO, 2011). Dieldrin represented the lowest concentration (0.002 mg/kg), while heptachlor showed the highest concentration (0.044 mg/kg).

To date, there is no MPL in Indonesian regulation for organochlorine residues in fish products. However, the present assessment showed that organochlorines in fish from the Citarum Watershed were lower than the MPL for meat products (BSN, 2025) or from global regulations (FAO/WHO, 2023). In general, heptachlor showed the highest accumulation level with concentration order in fish samples as heptachlor > lindane > DDT > endosulfan > aldrin > endrin > dieldrin (Table 3). A study performed in the Citarum Watershed indicated that heptachlor, lindane, and aldrin were the leading organochlorines detected in sediment samples, whereas aldrin was the most frequently found in water samples (Oginawati *et al*., 2021). Other studies in Indonesian regions reported organochlorines in fish samples from freshwater and marine water. Sudaryanto *et al*. (2007) reported that DDTs were the predominant contaminants in fish samples collected from different locations (Ciliwung River and bays of Jakarta, Lampung, Cirebon, and Lada-Banten). Accordingly, hexachlorocyclohexane (HCH), chlordane (CHL), and hexachlorobenzene (HCB) were identified up to 24, 81, and 28 ng/g lipid, respectively. In the southern English river, roach fish (*Rutilus rutilus*) exhibited a notably high level of DDT, surpassing the Canadian residue limit of 14 µg/kg (Jürgens *et al*., 2016). Similar to trace element contaminants, vegetable crops around Citarum Watershed have also been reported to contain organochlorines. A study conducted by Rahmawati *et al*. (2017) reported aldrin, DDT, lindane, heptachlor, dieldrin, endosulfan, and endrin in carrots and potatoes from the upper Citarum Watershed. This also reveals the potential origin of pesticide emissions from agricultural activities in the Citarum Watershed. Nevertheless, due to the high persistence of organochlorine compounds in the environment, the concentration noted in this study may have resulted from prolonged exposure to agricultural or household practices. For example, the half-life of DDT and its metabolites in soil varies from 2 to 15 years (ATSDR, 2022c). However, there are limited data or samples of wild-caught fish in the study area. Typically, wild-caught fish are not officially recorded due to limited amount compared to the aquaculture ones. According to the limited samples of *Clarias* sp., it appears that the concentration of organochlorines is lower in comparison to farmed fish, yet there is no information concerning the size or age of the fish. Additionally, trace elements in wild-pangasius are comparable to the farmed-pangasius.

Dietary exposure to trace elements and organochlorine pesticides

The current study indicates that the predominant pathway for exposure to trace elements and organochlorines was via dietary fish sourced from the Citarum Watershed, with other routes of exposure, including dermal and inhalation, were not considered. The EDI values of trace elements from Citarum Watershed's fish ranged from 0.005 µg/kg bw/day (Cd) and 0,60 µg/kg bw/day (Cu). Additionally, Cd contributed as the lowest trace element exposure (showed in the senior group), while Cu was the highest contributor (in the toddler group), as presented in Table 4. In general, Cu contributed predominantly (69.93%) to the trace element exposure, followed by Cr, Pb, Hg, and Cd, with contributions of 21.85%, 3.99%, 2.57%, and 1.67%, respectively.

Among organochlorines, dieldrin showed the lowest exposure (0.001µg/kg bw/day) to the population, especially for the senior group (>55 years old). Simultaneously, heptachlor was found to have the highest exposure rate (0.062 µg/kg bw/d), especially within the group of toddlers. Based on the high intake

Table 4: Exposure of concerned trace elements (µg/kg bw/day) to fish consumption from Citarum Watershed

Trace elements		Age group (years)					TDI	SF
		Toddler (0-5)	Children (5-12)	Adolescent (13-18)	Adult (19-55)	Senior (>55)		
Pb	Mean	0.0340	0.0250	0.0134	0.0132	0.0125	3.6	8.5
	P_{95}	0.0754	0.0555	0.0297	0.0293	0.0278		
Cd	Mean	0.0142	0.0104	0.0056	0.0055	0.0052	1.0	6.1
	P_{95}	0.0552	0.0406	0.0218	0.0214	0.0203		
Cr	Mean	0.1862	0.1369	0.0734	0.0722	0.0686	3.3	41
	P_{95}	0.2719	0.1999	0.1072	0.1055	0.1002		
Hg	Mean	0.0219	0.0161	0.0086	0.0085	0.0081	0.7	-
	P_{95}	0.0676	0.0497	0.0266	0.0262	0.0249		
Cu	Mean	0.5958	0.4382	0.2349	0.2311	0.2195	500.0	-
	P_{95}	1.9109	1.4052	0.7532	0.7413	0.7040		

Table 5: Exposure of organochlorine pesticides (µg/kg bw/day) to fish consumption from Citarum Watershed

Organochlorine pesticides		Age group (years)					TDI	SF
		Toddler (0-5)	Children (5-12)	Adolescent (13-18)	Adult (19-55)	Senior (>55)		
Aldrin	Mean	0.0177	0.0130	0.0070	0.0069	0.0065	0.1	17.0
	P_{95}	0.0234	0.0172	0.0092	0.0091	0.0086		
DDT	Mean	0.0210	0.0155	0.0083	0.0082	0.0078	10.0	34.0
	P_{95}	0.0527	0.0387	0.0208	0.0204	0.0194		
Lindane	Mean	0.0317	0.0233	0.0125	0.0123	0.0117	8.0	6.3
	P_{95}	0.0629	0.0463	0.0248	0.0244	0.0232		
Heptachlor	Mean	0.0621	0.0457	0.0245	0.0241	0.0229	0.5	4.5
	P_{95}	0.1248	0.0918	0.0492	0.0484	0.0460		
Dieldrin	Mean	0.0025	0.0018	0.0010	0.0010	0.0009	0.1	16.0
	P_{95}	0.0037	0.0027	0.0015	0.0014	0.0014		
Endosulfan	Mean	0.0179	0.0132	0.0071	0.0069	0.0066	5.0	-
	P_{95}	0.0239	0.0175	0.0094	0.0093	0.0088		
Endrin	Mean	0.0051	0.0037	0.0020	0.0020	0.0019	0.2	-
	P_{95}	0.0243	0.0179	0.0096	0.0094	0.0089		

scenario (P_{95}), heptachlor contributed to the highest exposure of organochlorine (0.12 µg/kg bw/day) in the toddler group (Table 5). The contribution of heptachlor, lindane, DDT, aldrin, endosulfan, endrin, and dieldrin to the total organochlorine exposure was 39.29%, 20.08%, 13.32%, 11.32%, 11.20%, 3.22%, and 1.55 %, respectively.

Risk characterization and health risk evaluation

The total non-carcinogenic risk from trace elemental exposure for all aged groups through fish consumption from the Citarum Watershed was well below the chronic threshold (mean HI: 4.11-11.25 %). According to Table 6, Cu had a minimal impact on trace element exposure, while Cr exhibited the highest

Table 6: Non-carcinogenic health risk (%) of concerned element exposure to fish consumption from Citarum Watershed

Trace elements		Age group (years)				
		Toddler (0-5)	Children (5-12)	Adolescent (13-18)	Adult (19-55)	Senior (>55)
Pb	Mean	0.94	0.69	0.37	0.37	0.35
	P_{95}	2.10	1.54	0.83	0.81	0.77
Cd	Mean	1.42	1.04	0.56	0.55	0.52
	P_{95}	5.52	4.06	2.18	2.14	2.03
Cr	Mean	5.64	4.15	2.22	2.19	2.08
	P_{95}	8.24	6.06	3.25	3.20	3.04
Hg	Mean	3.13	2.30	1.23	1.21	1.15
	P_{95}	7.10	3.80	3.74	3.56	9.65
Cu	Mean	0.09	0.05	0.05	0.04	0.12
	P_{95}	0.38	0.28	0.15	0.15	0.14
Hazard index	Mean	11.25	8.27	4.43	4.36	4.14
	P_{95}	25.89	19.04	10.20	10.04	9.54

Table 7: Carcinogenic risk (%) of concerned trace elements to fish consumption from Citarum Watershed

Trace elements		Age group (years)				
		Toddler (0-5)	Children (5-12)	Adolescent (13-18)	Adult (19-55)	Senior (>55)
Pb	Mean	0.40	0.29	0.16	0.16	0.15
	P_{95}	0.89	0.65	0.35	0.34	0.33
Cd	Mean	0.23	0.17	0.09	0.09	0.09
	P_{95}	0.91	0.67	0.36	0.35	0.33
Cr	Mean	0.45	0.33	0.18	0.18	0.17
	P_{95}	0.66	0.49	0.26	0.26	0.24
Cancer risk	Mean	1.09	0.80	0.43	0.42	0.40
	P_{95}	2.46	1.81	0.97	0.95	0.90

levels of contribution. Furthermore, the anticipated worst-case scenario regarding high exposure (P_{95}) was still under the defined limit. The population over 55 years old has the lowest non-carcinogenic risk (P_{95} HI: 9.54%), while the toddlers' group has the highest chance (P_{95} HI: 25.89%).

Table 7 presents the total CR from trace elemental exposure for all age groups through fish consumption from the Citarum Watershed, which was lower than the threshold (mean CR: 0.40-1.09%). Cd contributed minimally to the CR, accounting for 0.09%, while Pb represented the highest level at 0.40%. Furthermore, the estimated worst-case scenario for high exposure (P_{95}) was still under the advised threshold for carcinogenic risk. The population over 55 years old has the lowest carcinogenic risk (P_{95} CR: 0.90%), while the toddlers' group has the highest chance (P_{95} CR: 2.46%).

Some trace elements show nutritional or pharmaceutical benefits. Cr, for example, is required to metabolize glucose, protein, and fat. Furthermore, Cu is utilized for iron metabolism, as a coenzyme in glucose synthesis, and to control hemoglobin, connective tissue, and phospholipids (Chen *et al.*, 2020b). Nevertheless, consuming these elements at specific levels may lead to toxicity and result

in either acute or chronic poisoning (IPCS-WHO, 2025). The chronic effect of Cu is associated with hepatic and kidney diseases and brain damage. Additionally, carcinogenic Pb, Cd, and Cr potentially adversely affect the central nervous system, blood constituents, lungs, liver, kidneys, and other vital organs. Extended exposure to heavy metals may damage nucleic acids, resulting in mutations, disturb the endocrine and reproductive systems, and eventually lead to cancer (IRIS, 2025). Due to the possible harmful effects on the environment and human health, DDT was globally banned and categorized as POPs according to the Stockholm Convention in 2001. Exposure to DDT and other organochlorines has been associated with adverse effects on hepatic, reproductive, developmental, and endocrine functions, and type-2 diabetes (IRIS, 2025). Unlike the maximum concentration and EDI value of Cu, the HQ value of Cu was the lowest when compared to the other elements. This is due to Cu's having a relatively high TDI value (500 µg/kg BW/d), indicating less harmful compared to the other elements with higher TDI values of 0.7-3.3 µg/kg BW/day (IRIS, 2025). In the present study, Cr showed the highest HQ value, with an HQ order of Cr > Cd > Hg > Pb > Cu. The mean HI value from trace element exposure in the present study (11.07%) is much lower than that of fish consumption in Karnaphuli River-Bangladesh (Ahmed *et al*., 2019). Accordingly, the HI value from arsenic (As), Pb, Cd, Cr, and Cu exposure in the adult population was 22.23%. Furthermore, HI values from trace element exposure (Zn, Pb, Mn, Hg, Cu, Co, Cd, As) via *C. carpio* and *Sparus aurata* fishes from the Caspian Sea were 14.3% and 12.9%, respectively (Solgi *et al*., 2019). Since Pb, Cd, Cr, DDT, lindane, heptachlor, and dieldrin are categorized as potentially carcinogenic, the carcinogenic risk was calculated based on carcinogenic SF (IARC, 2018, 2019). This assessment has demonstrated that the exposure to trace elements and organochlorines through fish consumption in the Citarum Watershed is relatively minimal. The total mean and the worst risk (P_{95}) from trace elements and organochlorines were 9.39% and 24.10%, respectively. Moreover, children between the ages of 0 and 12 were identified as the most at risk for this carcinogenic threat, in contrast to individuals over 55 years old. Cd and Chromium (VI) are designated as group 1 carcinogens, while inorganic Pb is categorized as a group 2B carcinogen (IARC, 2019). The carcinogenicity of these compounds is relatively similar, such as Cd, Cr, and Pb are associated with lung/respiratory, stomach/gastrointestinal, and kidney cancers. Additionally, Cd and Pb may control kidney cancer, while Cd exposure is reported to cause cancer in the prostate, liver, and hematopoietic system (Briffa *et al*., 2020; IRIS, 2025). For organochlorines, lindane is among the most priority carcinogens (group 2B), the same group as DDT and heptachlor, while aldrin and dieldrin are known as group 2A carcinogens (IARC, 2018, 2019). Toxicological studies reveal that contact with organochlorines is associated with cancer development in several organs, especially the liver, testis, breast, prostate, and pancreas (ATSDR, 2022c; IARC, 2018; Loomis *et al*., 2018). The cumulative non-carcinogenic risk from organochlorine exposure for individuals of all ages through fish consumption sourced from the Citarum Watershed remained well beneath the chronic threshold (mean HI: 12.23-33.19%). As indicated in Table 8, the contribution of DDT to organochlorine exposure was minimal, while aldrin represented the highest level. Additionally, the estimated worst scenario of the high exposure (P_{95}) was still below the established threshold of the non-carcinogenic risk. The population over 55 years old has the lowest non-carcinogenic risk (P_{95} HI: 19.66%), while the toddlers' group has the highest chance (P_{95} HI: 53.36%).

This study revealed that non-carcinogenic risk (HI) from 7 organochlorine pesticides is relatively comparable to that of the five trace elements, with an order value of aldrin > heptachlor > endrin > dieldrin > lindane > endosulfan > DDT. The toddler group exhibits a relatively elevated HI value (P_{95}: 53%), suggesting a moderate risk of exposure to organochlorines, especially among children. A study on organochlorine exposure from fish consumption in Mansoura, Egypt, reported the HI values from consumption of *Clupea harengus, Sardinella aurata*, and *Mugil cephalus* were 31.3, 19.33, and 7.3%, respectively (Hussein *et al*., 2022). The mean total CR from organochlorine exposure through fish consumption from the Citarum Watershed was well below the threshold for all aged groups (mean CR: 0.76-2.07%). Table 9 reveals that dieldrin's contribution to the CR was minimal, while heptachlor had the highest level. Additionally, the estimated worst-case scenario for high exposure (P_{95}) was still

Table 8: Non-carcinogenic health risk (%) of organochlorine pesticide exposure to fish consumption from Citarum Watershed

Organochlorine pesticides		Age group (years)				
		Toddler (0-5)	Children (5-12)	Adolescent (13-18)	Adult (19-55)	Senior (>55)
Aldrin	Mean	17.72	13.03	6.98	6.87	6.53
	P_{95}	23.36	17.18	9.21	9.06	8.61
DDT	Mean	0.21	0.15	0.08	0.08	0.08
	P_{95}	0.53	0.39	0.21	0.20	0.19
Lindane	Mean	0.40	0.29	0.16	0.15	0.15
	P_{95}	0.79	0.58	0.31	0.31	0.29
Heptachlor	Mean	12.42	9.13	4.89	4.82	4.57
	P_{95}	24.96	18.36	9.84	9.68	9.20
Dieldrin	Mean	2.46	1.81	0.97	0.95	0.90
	P_{95}	3.72	2.73	1.47	1.44	1.37
Endosulfan	Mean	0.36	0.26	0.14	0.14	0.13
	P_{95}	0.48	0.35	0.19	0.19	0.18
Endrin	Mean	2.54	1.87	1.00	0.99	0.94
	P_{95}	12.14	8.93	4.78	4.71	4.47
Hazard index	Mean	33.19	24.41	13.08	12.87	12.23
	P_{95}	53.36	39.24	21.03	20.70	19.66

Table 9: Carcinogenic risk (%) of organochlorine pesticides to fish consumption from Citarum Watershed

Organochlorine pesticides		Age group (years)				
		Toddler (0-5)	Children (5-12)	Adolescent (13-18)	Adult (19-55)	Senior (>55)
Aldrin	Mean	0.10	0.08	0.04	0.04	0.04
	P_{95}	0.14	0.10	0.05	0.05	0.05
DDT	Mean	0.06	0.05	0.02	0.02	0.02
	P_{95}	0.15	0.11	0.06	0.06	0.06
Lindane	Mean	0.50	0.37	0.20	0.20	0.19
	P_{95}	1.00	0.73	0.39	0.39	0.37
Heptachlor	Mean	1.38	1.01	0.54	0.54	0.51
	P_{95}	2.77	2.04	1.09	1.08	1.02
Dieldrin	Mean	0.02	0.01	0.01	0.01	0.01
	P_{95}	0.02	0.02	0.01	0.01	0.01
Cancer risk	Mean	2.07	1.52	0.81	0.80	0.76
	P_{95}	4.09	3.01	1.61	1.59	1.51

below the carcinogenic threshold. The population over 55 years old has the lowest carcinogenic risk (P_{95} CR: 1.51%), while the toddlers' group has the highest chance (P_{95} CR: 4.09%). A CR value less than the carcinogenic limit of 10^{-6} was reported from the carcinogenic elements (As, Pb, Cd) exposure via various river fish consumption in Bangladesh (Ahmed *et al*., 2019). A similar result was revealed

on the organochlorine exposure (heptachlor epoxide, heptachlor, *para-para (p,p')*-DDE, and *p,p'*-DDD) in farmed and wild fish from Bangladesh (Habibullah-Al-Mamun *et al*., 2023). A CR value greater than one was reported on trace elements exposure from 2 fish species (*Aristichthys nobilis* and *Hypophthalmichthys molitrix*) from Wuhan, China (Cui *et al*., 2015). Accordingly, Cr and As were the predominant contributors to the carcinogenic risk, while the CR of organochlorines was less than 1.

The interplay between various trace elements and organochlorine pesticides may produce either diminished (antagonistic) or heightened (synergistic) toxicity. Heavy metals and organic pollutants can interact in aquatic organisms, potentially exhibiting synergistic effects. Due to a lack of information on its antagonistic or synergistic effects, this element is not included in the risk evaluation. Some contaminants can also alter the bioavailability of other contaminants, making them increase or reduce the uptake by aquatic organisms. The interaction between pesticides and metals contaminants is mainly synergistic (Dinh *et al.,* 2022). Consequently, there may be an increased risk from various contaminants and dietary sources, along with the potential for synergistic toxicity between the compounds. Additionally, climate change may affect the contamination properties as increased rainfall or flooding can generate more pollutants load, while droughts can concentrate the pollutants. Warmer temperatures can increase or reduce the toxicity of some contaminants. Metal uptake increases at high potential of hydrogen (pH), while the toxicity increases at low pH (Kicinska *et al.,* 2022). The land use in the Citarum watershed will significantly influence pollution emissions, particularly due to population growth, industrial activities, and the transformation of forests into residential areas. The recent study showed that during 2013-2023, population, urban area, and industries in this region increased 11%, 8%, and 45% respectively, while forest areas reduced 2% (Hakim *et al.,* 2025). Currently, official bodies have not released any advisories concerning fish consumption from the Citarum Watershed aimed at vulnerable populations. Therefore, to reduce the health risk from trace elements and organochlorines, vulnerable groups are advised to consume fish not exceeding the TDI of concerned contaminants. The groups are advised to limit their consumption of fish during the period of heightened concentration or from fish farms that are more contaminated. Importantly, these groups must keep the attention to possible contaminants from other dietary sources. Consuming more variety of dietary sources with less contaminant concentration is important to reduce health risk. In the future, evaluating additional priorities and emerging contaminants will improve the hazard assessment related to the health of the affected population. Earlier studies in Citarum Watershed or other Indonesian regions revealed contamination of PAHs, organometals and pharmaceutical and personal care products (PPCPs) in aquatic ecosystem (Koagouw *et al.,* 2021; Zait *et al.,* 2022). Mitigation has been carried out by the local government by establishing *Citarum Harum* campaign since 2018 (Idris *et al*., 2019). Nonetheless, it requires effective and efficient enhancements through improved strategies and regulations to expedite the program.

Limitations and uncertainties of the study

The health risk estimation in the present study may be underestimated due to limited to available data from previous studies (Hg, Pb, Cd, Cr, Cu, heptachlor, lindane, DDT, endosulfan, aldrin, endrin, and dieldrin). Due to its toxicity, As for example, has been gaining concern for human health exposure through fishery products (Bentley and Soebandrio, 2017; Silva *et al*., 2020; Tanamal *et al*., 2021). Other organochlorines were reported from fish and other foodstuffs from Citarum Watershed or other regions in Indonesia, namely HCB, DDE, DDD, chlordane, heptachlor epoxide, and HCHs (Shoiful *et al*., 2013). The various organochlorine groups might influence the exposure levels of organochlorines within the study region. Moreover, there is a likelihood of bias in the health risk assessment, as the cumulative risk was computed by summing the individual risks of the contaminants in question, irrespective of their interactions. Other bias could be resulted from the exclusion of wild fish samples as contaminant sources. However, contribution of wild fish to total fish production from Citarum Watershed is minor and the limited samples showed comparable contaminant concentration to farmed fish (Astuti *et al.,* 2021; Rahmawati *et al.,* 2013). This study reveals that there is no available data or information on the demographic or medical variability of the population, nor on gender or socioeconomic disparities. However, in the present study the assessment is focused on the

different age groups of population as the commonly main classification of exposure impact (Zhao *et al*., 2023). Given the stated limitations and uncertainties, this risk assessment in the current study is regarded as the data representing the lowest risk scenario.

CONCLUSION

Earlier studies detected trace elements of Hg, Pb, Cd, Cr, and Cu in fish samples from Citarum Watershed, with concentration orders as Cu > Cr > Pb > Hg > Cd. The concentrations are generally below the MPL according to Indonesian and global regulations. Additionally, organochlorine compounds detected in fish samples from the Citarum Watershed included aldrin, DDT, lindane, dieldrin, heptachlor, endosulfan, and endrin. Organochlorine levels in fish samples were relatively low compared to the official threshold, with concentration order of heptachlor > lindane > DDT > endosulfan > aldrin > endrin > dieldrin. The anticipated exposures of trace elements and organochlorine residues remained well beneath the TDI thresholds defined by regulatory bodies. In general, Cu contributed predominantly to the trace element exposure, followed by Cr, Pb, Hg, and Cd. Organochlorine exposure is predominantly contributed by heptachlor, followed by lindane, DDT, aldrin, endosulfan, and dieldrin. Cr and Pb showed the highest contributors for non-carcinogenic and carcinogenic risks from trace element exposure. Among the organochlorine compounds, aldrin and heptachlor are the primary contributors to non-carcinogenic and carcinogenic risks. The present study revealed that trace elements and organochlorines are unlikely to pose non-carcinogenic and carcinogenic risks to the local populations in Citarum Watershed. Nevertheless, the most unfavorable estimation (P_{95}) of total exposure indicated that the child demographic (ages 0-12) faces the greatest risk. The result of the present study is considered as the lowest risk scenario. Moreover, in the absence of a better mitigation strategy to diminish contamination in the Citarum Watershed, local consumers could face an increased health risk. There is possible additional risk from other contaminants and other dietary sources, as well as the possible synergistic toxicity among the compounds. To guarantee a more trustworthy evaluation of health risks, further studies are needed to detect contamination in wild fish and various dietary sources, as well as to account for emerging contaminants. Additionally, it is essential for the local or central government to set up a regular monitoring initiative based on the current results, as well as to enhance the current program to incorporate biota samples. Furthermore, identification of contaminant sources is important to develop a mitigation strategy and law enforcement for minimizing the use and leakage of the contaminants in the ecosystem and reducing the hazards to public health.

AUTHOR CONTRIBUTIONS

D. Dwiyitno is the corresponding author and has contributed to designing the study, collected and analyzed the data, interpreted the results, and prepared the manuscript. F. Ariyani contributed to the result interpretation, finalizing the manuscript, reviewing, and revising. G.R. Barokah contributed to data analysis, result interpretation, and manuscript preparation. D. Yogaswara contributed to data analysis, result interpretation, and manuscript preparation. R. Grandiosa contributed to data analysis and manuscript preparation. E. Frimawaty contributed to the result interpretation and manuscript preparation. H.E. Irianto contributed to the supervision and manuscript preparation. Y. Sani contributed to the result interpretation, reviewing, and editing.

CONFLICT OF INTEREST

The authors declare that there is no conflict of interest regarding the publication of this manuscript. In addition, ethical issues, including plagiarism, informed consent, misconduct, data fabrication and/or falsification, double publication and/or submission, and redundancy, were observed by the authors.

ACKNOWLEDGEMENT

This study was supported by a grant from the National Research and Innovation Agency of Indonesia: Research Program of Model Development for Priority River Basin and Lake (FR-3); [No.5/III.4/HK/2023].

OPEN ACCESS

©2025 The author(s). This article is licensed under a Creative Commons Attribution 4.0 International License, which permits use, sharing, adaptation, distribution and reproduction in any medium or format, as long as you give appropriate credit to the

original author(s) and the source, provide a link to the Creative Commons license, and indicate if changes are made. The images or other third-party material in this article are included in the article's Creative Commons license, unless indicated otherwise in a credit line to the material. If material is not included in the article's Creative Commons license and your intended use is not permitted by statutory regulation or exceeds the permitted use, you will need to obtain permission directly from the copyright holder. To view a copy of this license, visit: http://creativecommons.org/licenses/by/4.0/

PUBLISHER'S NOTE

GJESM Publisher remains neutral with regard to jurisdictional claims in published maps and institutional afflictions.

Positive AI Statement

During the preparation of this work the author(s) have used Artificial Intelligence (AI) [NAME TOOL / SERVICE] in order to [REASON]. After using this tool/service, the authors reviewed and edited the content as needed and take full responsibility for the content of the publication.

(For this reason, the GPTZero detector will evaluate the manuscript utilizing Generative AI, ensuring a high detection rate. If the manuscript relies heavily on Generative AI and AI-assisted technologies, it will be archived without further options for appeal).

Negative AI Statement

The author(s) declare that no AI tools or services were not used or not highly applied during the preparation of this work.

ABBREVIATIONS

%	Percent
µg	Microgram
AAS	Atomic absorption spectroscopy
ADB	Asian Development Bank
As	Arsenic
ATSDR	Agency for Toxic Substances and Disease Registry
BCF	Bioconcentration factor
BPS	Badan Pusat Statistik (Statistics Indonesia)
BSN	Badan Standardisasi Nasional (National Standardization Agency of Indonesia)
bw	Body weight
CAC	Codex Alimentarius Commission
FSANZ	Food Standards Australia New Zealand
Cd	Cadmium
CHL	Chlordane
Co	Cobalt
Cr	Chrom
CR	Carcinogenic risks
Cu	Copper
DDD	Dichloro-diphenyl-dichloroethane
DDE	Dichloro-diphenyl-dichloroethylene
DDT	Dichloro-diphenyl-trichloroethane
DIKPLHD	*Dokumen Informasi Kinerja Pengelolaan Lingkungan Hidup* (Document of Environmental Management Performance Information)
EDI	Estimated daily intake
EFSA	European Food Safety Authority
EU	European Union
FAO	Food and Agriculture Organization
Fe	Iron
g	Gram
GC	Gas chromatography
ha	Hectares
HCB	Hexachlorobenzene
HCH	Hexachlorocyclohexane
Hg	Mercury

HI	Hazard index
IARC	International Agency for Research on Cancer
IPCS	International Programme on Chemical Safety
IRIS	Integrated Risk Information System
JECFA	Joint FAO/WHO Expert Committee on Food Additives
kg	Kilograms
km	Kilometers
km²	Square kilometers
mg	Milligram
Mn	Manganese
MPL	Maximum Permissible Limit
MPH	Ministry of Public Health
NADFC	National Agency for Drug and Food Control
Ni	Nickel
OCPs	Organochlorine pesticides
OECD	Organization for Economic Co-operation and Development
P_{95}	95th percentile
Pb	Lead
pH	Potential of hydrogen
POPs	Persistent Organic Pollutants
p,p'	Para-para
SD	Standard deviation
SF	Cancer slope factor
TDI	Tolerable daily intake
TDS	Total diet study
THQ	Target hazard quotient
US EPA	United States Environmental Protection Agency
WHO	World Health Organization
ww	Wet weight (basis)
Zn	Zinc

REFERENCES

ADB, (2013). Downstream impacts of water pollution in the upper Citarum River, West Java, Indonesia: economic assessment of interventions to improve water quality. Water and Sanitation Program. Asian Development Bank. 1–44 **(44 pages)**.

Ahmed, A.S.S.; Sultana, S.; Habib, A.; Ullah, H.; Musa, N.; Hossain, M.B.; Rahman, Md.M.; Sarker, Md. S.I., (2019). Bioaccumulation of heavy metals in some commercially important fishes from a tropical river estuary suggests higher potential health risk in children than adults. PLOS ONE, 14(10): e0219336 (**21 pages**).

Astuti, L.P.; Warsa, A.; Nurfiarini, A. Tjahjo, D.W.H., (2021). Bioaccumulation of non-essential heavy metals in fish in Ir H Djuanda Reservoir, West Java. IOP Conference Series: Earth Environ. Sci., 744(1) (**8 pages**).

ATSDR, (2020). Toxicological profile for lead. Agency for Toxic Substances and Disease Registry (ATSDR). Atlanta, GA: U.S. Department of Health and Human Services, Public Health Services (**583 pages**).

ATSDR, (2021). Toxicological profile for endrin. Agency for Toxic Substances and Disease Registry (ATSDR). Atlanta, GA: U.S. Department of Health and Human Services, Public Health Services (**196 pages**).

ATSDR, (2022a). Toxicological profile for aldrin and dieldrin. Agency for Toxic Substances and Disease Registry (ATSDR). Atlanta, GA: U.S. Department of Health and Human Services, Public Health Services (**318 pages**).

ATSDR, (2022b). Toxicological profile for copper draft for public comment. Agency for Toxic Substances and Disease Registry (ATSDR). Atlanta, GA: U.S. Department of Health and Human Services, Public Health Services (**369 pages**).

ATSDR, (2022c). Toxicological profile for DDT, DDE, and DDD. Agency for Toxic Substances and Disease Registry (ATSDR). Atlanta, GA: U.S. Department of Health and Human Services, Public Health Services (**510 pages**).

ATSDR, (2022d). Toxicological profile for mercury. Agency for Toxic Substances and Disease Registry (ATSDR). Atlanta, GA: U.S. Department of Health and Human Services, Public Health Services (**959 pages**).

ATSDR, (2023). Toxicological profile for hexachlorocyclohexane (HCH). Agency for Toxic Substances and Disease Registry (ATSDR). Atlanta, GA: U.S. Department of Health and Human Services, Public Health Services (**479 pages**).

Azizah, M.; Maslahat, M., (2021). Concentration of lead (Pb), cadmium (Cd), and mercury (Hg) in barbodes fish (*Barbodes binotatus*) and water of Cikaniki River, Bogor. Limnotek Trop. Freshwater Indones., 28(2): 83–93 (**11 pages**).

Bentley, K.; Soebandrio, A., (2017). Arsenic and mercury concentrations in marine fish sourced from local fishermen and fish markets in mine-impacted communities in Ratatotok Sub-

district, North Sulawesi, Indonesia. Mar. Pollut. Bull., 120(1–2): 75–81 (**6 pages**).

BPS-Statistics Indonesia, (2023). Statistical Yearbook of Indonesia 2023. Directorate of Statistical Dissemination - BPS Statistics Indonesia, 1 (**830 pages**).

Briffa, J.; Sinagra, E.; Blundell, R., (2020). Heavy metal pollution in the environment and their toxicological effects on humans. Heliyon, 6(9): e04691 (**26 pages**).

BSN, (2025). Maximum permissible limit of microbe contaminants and maximum residue limit in food product from animal origin. National Standard Agency (BSN), SNI-01-6366-2000: 1–16 (**16 pages**).

CFS, (2019). Food adulteration: metallic contamination (amendment) regulation 2018. Centre for Food Safety - The Government of the Hong Kong Special Administrative Region. 1–27 (**27 pages**).

Chen, C.; Zou, W.; Chen, S.; Zhang, K. Ma, L., (2020a). Ecological and health risk assessment of organochlorine pesticides in an urbanized river network of Shanghai, China. Environ. Sci. Eur., 32(1): 42 (**14 pages**).

Chen, J.; Jiang, Y.; Shi, H.; Peng, Y.; Fan, X.; Li, C., (2020b). The molecular mechanisms of copper metabolism and its roles in human diseases. Pflügers Archiv Eur. J. Physiol., 472(10): 1415–1429 (**15 pages**).

Cui, L.; Ge, J.; Zhu, Y.; Yang, Y.; Wang, J., (2015). Concentrations, bioaccumulation, and human health risk assessment of organochlorine pesticides and heavy metals in edible fish from Wuhan, China. Environ. Sci. Pollut. Res., 22(20): 15866–15879 (**14 pages**).

DIKPLHD West Java. (2021). Performance report: environmental management of West Java Province in 2021. Environmental Office of West Java Province (**2065 pages**).

Dinh, K.V.; Konestabo, H.S.; Borgå, K.; Hylland, K.; Macaulay, S.J.; Jackson, M.C.; Verheyen, J.; Stoks, R., (2022). Interactive Effects of Warming and Pollutants on Marine and Freshwater Invertebrates. Curr. Pollut. Rep., 8: 341–359 **(19 pages).**

EFSA, (2010). Scientific opinion on lead in food. EFSA J., 8(4) (**151 pages**).

Fahimah, N.; Salami, I.R.S.; Oginawati, K.; Yapfrine, S.J.; Supriatin, A.; Thaher, Y.N., (2023). Mapping and determining chemical of potential concerns from heavy metals in water usage in the uppers watershed. Global J. Environ. Sci. Manage., 9(4): 765-788 **(24 pages).**

FAO/WHO, (2011). Joint FAO/WHO Expert meeting on dietary exposure assessment methodologies for residues of veterinary drugs. Food and Agriculture Organization and World Health Organization of the United Nations. (**83 pages**).

FAO/WHO, (2023). General standard for contaminants and toxins in food and feed: CXS 193-1995. Codex Alimentarius FAO-WHO, 8(5): 55 (**77 pages**).

FSANZ, (2016). Australia New Zealand food standards code - standard 1.4.1 - Contaminants and natural toxicants. Australia New Zealand Food Legislation, 1.4.1: 1–11 (**11 pages**).

Habibullah-Al-Mamun, Md.; Tanima, S.A.; Paul, B.; Al Zahid, Md.; Kabir, Md.H.; Ahmed, S.; Mandal, S.C.; Hossain, A., (2023). Occurrence of organochlorine pesticides (OCPs) residues in farmed and wild fish in Bangladesh and implications for human health. Exposure Health. 15(2): 425–437 (**13 pages**).

Hakim, A.M.Y.; Santosa, B.H.; Martono, D.N.; Sencaki, D.B.; Prayogi, H.; Arifandri, R.; Apip, A.; Ningrum, W.; Schröter, K.; Steinhausen, M.J., (2025). Exploring land cover change impacts on ecosystem services using machine learning technique and scenario simulation: case study of the Upper Citarum River Basin, Indonesia. Model. Earth Syst. Environ. 11, 211 (**11 pages**).

Handayani, C.O.; Sukarjo, S.; Dewi, T.; Zu'amah, H., (2022). Heavy metal and health risk assessment via rice consumption from upper Citarum Basin. Indones. Environ. Health J., 21(2): 225–234 (**10 pages**).

Hidayah, A.M.P; Soeprobowati, T.R., (2014). Bioconcentration of heavy metal factors Pb, Cd. Cr and Cu in tilapia (*Oreochromis niloticus* Linn.) at Rawa Pening Lake. Bioma., 16 (1): 1-9 (**9 pages**).

Hussein, M.A.; Hammad, O.S.; Tharwat, A.E.; Darwish, W.S.; Sayed-Ahmed, A.; Zigo, F.; Farka ová, Z.; Rehan, I.F., (2022). Health risk assessment of organochlorine pesticide residues in edible tissue of seafood. Front. Vet. Sci., 9 (**11 pages**).

IARC, (2018). DDT, lindane, and 2,4-D: Monograph on the evaluation of carcinogenic risks to human. International Agency for Research on Cancer (IARC). 113 (**513 pages**).

IARC. (2019). Agents classified by the IARC monographs. International Agency for Research on Cancer (IARC). Vol. 138 (**134 pages**).

Idris, A.M.S.; Permadi, A.S.C.; Kamil, A.I.; Wananda, B.R.; Taufani, A.R., (2019). Citarum harum project: A restoration model of river basin. Indones. J. Dev. Plann., 3(3): 310–324 (**25 pages**).

IPCS-WHO, (2025). WHO human health risk assessment toolkit: chemical hazards. International Programme on Chemical Safety (IPCS) harmonization project document, xv. (**87 pages**).

IRIS, (2025). IRIS assessments. Integrated Risk Information System. (**11 pages**).

Jürgens, M.D.; Crosse, J.; Hamilton, P.B.; Johnson, A.C.; Jones, K.C., (2016). The long shadow of our chemical past high DDT concentrations in fish near a former agrochemicals factory in England. Chemosphere. 162: 333–344 (**12 pages**).

Kicińska, A., Pomykała, R., & Izquierdo-Diaz, M. (2022). Changes in soil pH and mobility of heavy metals in contaminated soils. Eur. J. Soil Sci., 73(1), e13203 (**14 pages**).

Koagouw, W.; Arifin, Z.; Olivier, J.W.J.; Ciocan, C., 2021. High concentrations of paracetamol in effluent dominated waters of Jakarta Bay, Indonesia, Mar. Pollut. Bull., 169: 112558 (**6 pages**)

Loomis, D.; Guha, N.; Hall, A.L.; Straif, K., (2018). Identifying occupational carcinogens: An update from the IARC Monographs. Occup. Environ. Med., 75(8): 593–603 (**11 pages**).

Ministry of Health, (2015). Total diet study (consumption survey of individual diet and food contaminant analysis). Ministry of Health, Republic of Indonesia (**232 pages**).

More, S.J.; Hardy, A.; Bampidis, V.; Benford, D.; Hougaard Bennekou, S.; Bragard, C.; Boesten, J.; Halldorsson, T.I.; Hernández-Jerez, A.F.; Jeger, M.J.; Knutsen, H.K.; Koutsoumanis, K.P.; Naegeli, H.; Noteborn, H.; Ockleford, C.; Ricci, A.; Rychen, G.; Schlatter, J.R.; Silano, V.; Nielsen,S.S.; Schrenk, D.; Turck, D.; Younes, M.; Benfenati, E.; Castle, L.; Cedergreen, N.; Hardy, A.; Laskowski, R.;

Leblanc, J.C.; Kortenkamp, A'; Ragas, A.; Posthuma, L.; Svendsen, C.; Solecki, R.; Testai, E.; Dujardin, B.; Kass, G.E.N.; Manini, P.; Jeddi, M.Z.; Dorne, J.C.M.; Hogstrand, C., (2019). Guidance on harmonised methodologies for human health, animal health and ecological risk assessment of combined exposure to multiple chemicals. EFSA J., 17(3) (**77 pages**).

MPH Thailand, (2020). Food act B.E. 2522: Standards for contaminants in food. Ministry of Public Health: Nonthaburi, Thailand, 1(1): 105–112 (**8 pages**).

Murtini, J.; Rachmawati, N., (2007). Heavy metals content of fish, water, and sediment in Saguling Dam, West Java. Mar. Fish. Postharvest Biotechnol. J., 2(2): 153–159 (**7 pages**).

Nędzarek, A.; A. Rybczyk, M.; Bonisławska, A.; Tański; Tórz, A., (2021) Bioaccumulation of metals in tissues of Rutilus rutilus and Perca fluviatilis from lakes with poor ecological status – human health risk assessment. Eur. Zool. J., 88: 1084-1095 (**12 pages**).

NADFC, (2022). Heavy metals requirements in processed foods. National Agency for Drug and Food Control (NADFC), Republic of Indonesia, Art. No. 9/2022 (**18 pages**).

Nuraeni, A.; Samosir, A.; Sulistiono., (2021). Heavy metal (Pb) on hearth of catched fish (*Pangasius djambal*) in Saguling reservior, West Java. Mar. Fish. Technol. J., 12(2): 113–123 (**11 pages**).

OECD, (2025). Considerations for assessing the risks of combined exposure to multiple chemicals: series on testing and assessment No. 296 (**119 pages**).

Oginawati, K.; Susetyo, S.H.; Rahmawati, S.I.; Kurniawan, S.B.; Abdullah, S.R.S., (2021). Distribution of organochlorine pesticide pollution in water, sediment, mollusk, and fish at Saguling Dam, West Java, Indonesia. Toxicol. Res., 38(2): 149–157 (**9 pages**).

Olayinka-Olagunju, J.O.; Dosumu, A.A.; Olatunji-Ojo, A.M., (2021). Bioaccumulation of heavy metals in pelagic and benthic fishes of Ogbese River, Ondo State, South-Western Nigeria. Water, Air, Soil Pollut., 232(2): 44 (**19 pages**).

Priyanto, N.; Dwiyitno, D.; Ariyani, F., (2008). Heavy metals (Hg, Pb, Cd, and Cu) in fish, water, and sediment in Cirata Dam, West Java. Mar. Fish. Postharvest Biotechnol. J., 3(1): 69-78 (**10 pages**).

Putri, W.A.E.; Bengen, D.G.; Prartono, T.; Riani, E., (2016). Accumulation of heavy metals (Cu and Pb) in two consumed fishes from Musi River Estuary, South Sumatera. Indones. J. Mar. Sci., 21(1): 45-42 (**8 pages**).

Rahmawati, S.; Margana, G.; Yoneda, M.; Oginawati, K., (2013). Organochlorine pesticide residue in catfish (*Clarias* sp.) *Collected from Local Fish Cultivation* at Citarum watershed, West Java Province, Indonesia. Procedia Environ. Sci., 17: 3–10 (**8 pages**).

Rahmawati, S.; Kirana, L.C.; Yoneda, M.; Oginawati, K., (2017). Risk analysis on organochlorine pesticides residue in potato and carrot from conventional and organic farms in Citarum watershed Area, West Java Province, Indonesia. Sci. Environ. Technol. J., 9(1): 1–15 (**15 pages**).

Roosmini, D.; Wardhani, E.; Notodarmojo, S., (2022). Risk assessment and fractionation of cadmium contamination in sediment of Saguling Lake in West Java Indonesia. J. Eng. Technol. Sci., 54(2) (**15 pages**).

Salami, I.R.S.; Rahmawati, S.; Sutarto, R.I.H.; Jaya, P.M., (2008). Accumulation of heavy metals in freshwater fish in cage aquaculture at Cirata reservoir, West Java, Indonesia. Ann. New York Acad. Sci., 1140: 290–296 (**7 pages**).

Salami, I.R.S.; Rizaldi, D.K., (2016). Organics and heavy metals content in river receiving the effluent of municipal landfill leachate treatment. Trends Asian Water Environ. Sci. Technol., 127-136. (**10 pages**).

Salami, I.R.S.; Thufailah, N.A.; Fahimah, N.; Roosmini, D., (2025). Health risk assessment of physicochemical and heavy metals exposures of the usage of shallow groundwater located at the proximity to Citarum River, Indonesia. Case Stud. Chem. Environ. Eng., 11: 101153 (**11 pages**).

Sanou A.; Coulibaly S.; Coulibaly M.; N'dri, S.N.; Atse, B.C, (2021). Assessment of heavy metal contamination of fish from a fish farm by bioconcentration and bioaccumulation factors. Egypt. J. Aquat. Biol. Fish., 49, 25(1), 821-841 (**21 pages**)

Shoiful, A.; Fujita, H.; Watanabe, I.; Honda, K., (2013). Concentrations of organochlorine pesticides (OCPs) residues in foodstuffs collected from traditional markets in Indonesia. Chemosphere. 90(5): 1742-1750 (**9 pages**).

Silva, C.A.; Santos, S.O.; Garcia, C.A.B.; de Pontes, G.C.; Wasserman, J.C., (2020). Metals and arsenic in marine fish commercialized in the NE Brazil: risk to human health. Hum. Ecol. Risk Assess., 26(3): 695–712 (**8 pages**).

Sindern, S.; Tremöhlen, M.; Dsikowitzky, L.; Gronen, L.; Schwarzbauer, J.; Siregar, T.H.; Ariyani, F.; Irianto, H.E., (2016). Heavy metals in river and coast sediments of the Jakarta Bay region (Indonesia) - Geogenic versus anthropogenic sources. Mar. Pollut. Bull., 110(2): 624–633 (**10 pages**).

Solgi, E.; Alipour, H.; Majnooni, F., (2019). Investigation of the concentration of metals in two economically important fish species from the Caspian Sea and assessment of potential risk to human health. Ocean Sci. J., 54(3): 503–514 (**12 pages**).

Sudaryanto, A.; Monirith, I.; Kajiwara, N.; Takahashi, S.; Hartono, P.; Muawanah; Omori, K.; Takeoka, H.; Tanabe, S., (2007). Levels and distribution of organochlorines in fish from Indonesia. Environ. Int., 33(6): 750–758 (**9 pages**).

Sultana, M.S.; Rana, S.; Yamazaki, S.; Aono, T.; Yoshida, S., (2017). Health risk assessment for carcinogenic and non-carcinogenic heavy metal exposures from vegetables and fruits of Bangladesh. Cogent Environ. Sci., 3(1): 1–17 (**17 pages**).

Sutrisno, S.; Koesoemadinata, S.; Taufik, I., (2007). Levels of heavy metal pollution in the reservoir ecosystems of West Java (Saguling, Cirata, and Jatiluhur). Aquacult. Res. J., 2(2): 103–115 (**13 pages**).

Tanamal, C.; Blais, J.M.; Yumvihoze, E.; Chan, H.M., (2021). Health risk assessment of inorganic arsenic exposure through fish consumption in Yellowknife, Northwest Territories, Canada. Hum. Ecol. Risk Assess., 27(4): 1072–1093 (**22 pages**).

US EPA, (2019). Guidelines for human exposure assessment. U.S. Environmental Protection Agency. (**223 pages**).

Wardhani, E.; Notodarmojo, S.; Roosmini, D., (2017). Heavy metal speciation in sediments in Saguling lake West Java Indonesia. Int. J. GEOMATE, 12(34): 146–151 (**6 pages**).

Wardhani, E.; Notodarmojo, S.; Roosmini, D., (2018). Assessment of heavy metal contamination in Saguling reservoir water West Java Province Indonesia. E3SvWeb of Conferences 73: 06009 ICENIS (**5 pages**).

Wassenaar, P.N.H.; Verbruggen, E.M.J.; Cieraad, E.; Peijnenburg, W.J.G.M,; Vijver, M.G., (2020). Variability in fish bioconcentration factors: Influences of study design and consequences for regulation, Chemosphere. 239, 124731 (**9 pages**).

Wulandari, N.; Trilaksani, W.; Suwandi, R., (2022). Risk assessment of heavy metals Cd, Hg and Pb in carp (*Cyprinus carpio*) from Jatiluhur Reservoir, West Java in rainy season. IOP Conference Series: Earth Environ. Sci., 967(1) (**12 pages**).

Zait, R.; Sluser, B.; Fighir, D.; Plavan, O.; Teodosiu, C., (2022). Priority pollutants monitoring and water quality assessment in the Siret River Basin, Romania. Water. 14(1) (**23 pages**).

Zhao, S.; Gong, Y.; Yang, S.; Chen, S.; Huang, D.; Yang, K.; Cheng, H., (2023). Health risk assessment of heavy metals and disinfection by-products in drinking water in megacities in China: A study based on age groups and Monte Carlo simulations. Ecotoxicol. Environ. Saf., 262: 115330 (**8 pages**).

AUTHOR (S) BIOSKETCHES

Dwiyitno, D., Ph.D., Associate Professor, Research Center for Veterinary Science, National Research and Innovation Agency, Jl. Raya Jakarta-Bogor Km.46, Bogor 16911 Indonesia
- Email: *dwiyitno@brin.go.id*
- ORCID: 0000-0001-5451-1947
- Web of Science ResearcherID: AAA-1657-2022
- Scopus Author ID: 57191071175
- Homepage: https://intra.brin.go.id/home/profile_sivitas/dwiy007

Ariyani, F., M.Sc., Senior researcher, Research Center for Marine and Land Bioindustry, National Research and Innovation Agency, Jl. Raya Puspiptek 60, Tangerang Selatan, 15310 Indonesia.
- Email: *fari019@brin.go.id*
- ORCID: 0009-0002-9458-0167
- Web of Science ResearcherID: JFE-3509-2023
- Scopus Author ID: 57846471800
- Homepage: https://intra.brin.go.id/home/profile_sivitas/fari019

Barokah, G.R., Ph.D. Candindate, Department of Biotechnology, Graduate School of Engineering, University of Osaka, 2-1 Yamada-oka, Suita-shi, Osaka-fu 565-0871 Japan;
Research Center for Food Technology and Processing, National Research and Innovation Agency,
Jl. Jogja-Wonosari KM 31.5, Gunungkidul 55681 Indonesia
- Email: *giri004@brin.go.id*
- ORCID: 0000-0002-7009-0756
- Web of Science ResearcherID: NA
- Scopus Author ID: 57215085499
- Homepage: https://intra.brin.go.id/home/profile_sivitas/giri004

Yogaswara, D., M.Sc., Researcher, Research Center for Oceanography, National Research and Innovation Agency, Jl. Pasir Putih 1 Ancol Timur, Jakarta 14430 Indonesia
- Email: *deny.yogaswara@brin.go.id*
- ORCID: 0000-0002-3931-5486
- Web of Science ResearcherID: HSE-5793-2023
- Scopus Author ID: 57201066185
- Homepage: https://intra.brin.go.id/home/profile_sivitas/deny003

Grandiosa, R., Ph.D., Faculty of Fisheries and Marine Science, Padjajaran University, Jl. Raya Bandung -Sumedang KM.21, Sumedang 45363 Indonesia
- Email: *roffi.grandiosa@unpad.ac.id*
- ORCID: 0000-0003-0498-7220
- Web of Science ResearcherID: AGN-2057-2022
- Scopus Author ID: 56998831000
- Homepage: https://fpik.unpad.ac.id/sdm/

Frimawaty, E., Ph.D., School of Environmental Science, Universitas Indonesia, Jl. Salemba Raya No.4, Jakarta 10430 Indonesia
- Email: *evi.frimawaty11@ui.ac.id*
- ORCID: 0000-0002-9016-4062
- Web of Science ResearcherID: AAC-8694-2021
- Scopus Author ID: 8128517300
- Homepage: https://ppsml.sil.ui.ac.id/team-members/dr-evi-frimawaty-s-pt-m-si-2/

Irianto, H.E., Ph.D., Professor, [2]Research Center for Marine and Land Bioindustry, National Research and Innovation Agency, Jl. Raya Puspiptek 60, Tangerang Selatan, 15310 Indonesia. 8Faculty of Food Technology and Health, Sahid University, Jl. Prof DR Soepomo No. 84, Jakarta 12870, Indonesia.
- Email: *hari057@brin.go.id*
- ORCID: 0000-0001-9984-0592
- Web of Science ResearcherID: ADU-7100-2022
- Scopus Author ID: 57194878429
- Homepage: https://intra.brin.go.id/home/profile_sivitas/hari057

AUTHOR (S) BIOSKETCHES

Sani, Y., Ph.D., Associate Professor, Research Center for Veterinary Science, National Research and Innovation Agency, Jl. Raya Jakarta-Bogor Km.46, Cibinong 16911 Indonesia
- Email: yulv001@*brin.go.id*
- ORCID: 0000-0003-0861-4624
- Web of Science ResearcherID: NGS-3331-2025
- Scopus Author ID: 57214755677
- Homepage: https://intra.brin.go.id/home/profile_sivitas/yulv001

HOW TO CITE THIS ARTICLE

Dwiyitno, D.; Ariyani, F.; Barokah, G.R.; Yogaswara, D.; Grandiosa, R.; Frimawaty, E.; Irianto, H.E.; Sani, Y., (2025). Carcinogenic and non-carcinogenic hazards associated with trace elements and organochlorines from fish consumption in tropical river watershed. Global J. Environ. Sci. Manage., 11(3): 1221-1240.

DOI: 10.22034/gjesm.2025.03.19

URL: https://www.gjesm.net/article_724868.html

Global J. Environ. Sci. Manage. 11(3): 1241-1258, Summer 2025, Serial #43

Global Journal of Environmental Science and Management
(GJESM)

Homepage: https://www.gjesm.net/

Podcasts

CASE STUDY

The impact of renewable energy technology innovation on the low-carbon economic transition

X.Y. Liu, X. Shao, X.F. Li, C. Dong*

School of Economics, Hebei university, Baoding 071000, China

ARTICLE INFO

Article History:
Received 04 February 2025
Revised 08 April 2025
Accepted 12 May 2025

Keywords:
Climate risk
Low-carbon economic transition
Policy regulation
Renewable energy technology innovation

ABSTRACT

BACKGROUND AND OBJECTIVES: Within the framework of sustainable development, advancements in renewable energy technologies are essential for boosting energy efficiency and play a significant role in facilitating a low-carbon economic shift. Throughout this process, the importance of climate risks and policy regulations has become increasingly apparent. This study aims to empirically examine the impact of renewable energy technology innovation on the transition to a low-carbon economic with a particular focus on the roles of climate risks and policy regulations.

METHODS: This study establishes a benchmark regression model to empirically examine the impact of renewable energy technology innovation on low-carbon economic transition, analyzing panel data from 30 Chinese provinces from 2000 to 2021. Subsequently, the essential influence of climate risk is explored, focusing on its moderating and threshold effect. Furthermore, a difference-in-differences model is constructed to evaluate the efficacy of policy interventions in this transformative process. Finally, mediation analysis is carried out to examine the mediating influences of air pollution intensity.

FINDINGS: The benchmark regression analysis revealed a statistically significant negative association between renewable energy technology innovation and low-carbon economic transition. Moderation effect tests indicated a positive coefficient for the interaction term, indicating that climate risk imposes a restrictive effect on advancement. Threshold regression findings further indicated that rising climate risk levels increasingly enhance its restrictive influence. Analysis through difference-in-differences estimation demonstrated the notable impact of policy interventions on accelerating transition dynamics. The intermediary effect shows that air pollution intensity plays an intermediary role in the progression.

CONCLUSION: 1) renewable energy technology innovation contributes to low-carbon economic transition, and this effect remains consistent after a series of robustness tests; 2) The impact of climate risk is negatively moderating, revealing a threshold effect in the transition to a low-carbon economic system; 3) policy regulation can significantly promote low-carbon economic transition. Additionally, it is found that renewable energy technology innovation promotes low-carbon economic transition by reducing air pollution intensity. In regions with higher economic development, the innovation of renewable energy technologies significantly influences the transition to a low-carbon economy.

DOI: 10.22034/gjesm.2025.03.20

This is an open access article under the CC BY license (http://creativecommons.org/licenses/by/4.0/).

NUMBER OF REFERENCES
64

NUMBER OF FIGURES
4

NUMBER OF TABLES
10

*Corresponding Author:
Email: *dongchi30@163.com*
Phone: +312 507 9484
ORCID: 0009 0006 4143 3912

Note: Discussion period for this manuscript open until Sep 1, 2025 on GJESM website at the "Show Article".

INTRODUCTION

In the pursuit of sustainable development, the transition of low-carbon economic transition (LCET) has become the development focus of all countries, and it is also a key strategy to address the challenges of global emission reduction. The considerable growth in carbon emissions associated with economic development has emphasized the pressing importance of the LCET (Ahmad *et al.*, 2023), perceived as a connection to achieve sustainability (Wei *et al.*, 2022). The notion of "low-carbon economic" was first defined in the United Kingdom (UK)'s Energy White Paper in 2003, which pointed out that it is a new economic system characterized by "low energy consumption, low emissions, and low pollution". This approach can realize the least carbon emissions and financial costs, enabling the harmonious advancement of ecological preservation alongside economic prosperity. Researchers have extensively explored the factors influencing the LCET. Zhang *et al.* (2024) emphasized that the transformation towards a low-carbon economic is inseparable from policy guidance. Policies related to environmental regulation can deliver subsidies and tax advantages to businesses focused on low carbon emissions, while simultaneously bolstering support for these companies (Liu *et al.*, 2024). Some scholars also contend that enhancing the energy structure can significantly contribute to the LCET. Enhancing clean energy adoption and fostering a greener transition in the energy structure, a new energy system can be established, which is reducing emissions and advancing the LCET. Additionally, advancements in technology deliver a reliable promise for the LCET. Integrating low-carbon technologies can support the transformation and advancement of industries, while also promoting key emerging sectors such as energy efficiency and ecological sustainability (Cheng *et al.*, 2023). Additionally, low-carbon technologies contribute to reducing pollution control costs, achieving energy savings and consumption reductions, and leveraging the innovation compensation effect. This enhances enterprises' confidence in pursuing green development, thereby advancing the LCET. Among various influencing factors, technological innovation serves as a central pillar across all forms of innovation and contributes significantly in driving the shift toward LCET. Specifically, within the energy industry, it sets up a beneficial cycle where innovation in technology enhances renewable energy. Consequently, from a theoretical perspective, through innovations in renewable energy technology innovation (RETI), reducing dependence on fossil fuels to foster the adoption of LCET. As an emerging technological paradigm, RETI represents a key area of focus within the field of energy and environmental economics research. This development has led to considerable low-carbon achievements across different sectors. Zhao *et al.* (2022) emphasized that RETI plays an emission reduction role in the transportation sector. Experts have drawn attention to the crucial part that RETI in promoting industrial energy conservation (Mu *et al.*, 2018), realizing ultra-low energy consumption of buildings (Zang *et al.*, 2024; Rashif *et al.*, 2025), and developing ecological agriculture (Lai *et al.*, 2024). Furthermore, innovations in renewable energy technologies can produce spillover effects and energy-related consequence. On one side, RETI has promoted the dissemination and influence of technology among various regions, thereby advancing the level of technological innovation in diverse locations (Imran *et al.*, 2024). And RETI fosters the progress of renewable energy and then achieve sustainable economic expansion (Huang *et al.*, 2025). Simultaneously, confronting climate risks has turned into an immediate worldwide concern. Research has also indicated that physical risk triggered by climate change, such as storms, floods, heatwaves, and droughts, create significant uncertainty in financial markets and continue to affect economic and social development (Murphy, 2024). First, climate risk brings investment risk. Increasing concerns among investors about climate risk could result in alterations to their investment approaches, which might heighten volatility in the financial markets. Moreover, investment in renewable energy, will have a greater negative impact, leading to increased investment losses (Sun *et al.*, 2022). Second, climate risks pose risks to supply chains. Extreme weather events may lead to the interruption of enterprise supply chain (Gao *et al.*, 2025), reduce the resilience of enterprise development, and have a significant impact on enterprise operation and supply chain. Third, climate risks create transition risks. Evidence suggests that climate risks will cause a reduction in the assets necessary for the production and operation of businesses, which will impair their capacity to repay

debts and severely impact their routine operations (Ma *et al.,* 2025). Moreover, governments around the world are taking measures to mitigate climate issues, further strengthening the uncertainty of business environment and bringing low-carbon transition risks to enterprises (Ma *et al.,* 2024). However, others have also shown that climate risks increase the possibility of energy system disruption, forcing governments to strengthen the research of RETI (Olmos *et al.,* 2012). In regions that frequently experience extreme weather events, governments tend to implement regulations to foster the advancement of RETI in the industry (Jacobson *et al.,* 2010). Conversely, policy regulations are vital for promoting the structural transition towards a low-carbon economic framework. The Paris Agreement stands as a landmark in the global fight against carbon emissions, and its important role in fostering sustainable and low-carbon growth has been recognized by the international community. It reflects the collaborative efforts of all countries in reducing carbon emissions and realizing LCET (Salman *et al.,* 2022). However, there are two different perspectives when considering the consequences of the policy regulation of the Paris Agreement. Findings from various studies reveal that excessive regulatory measures may suppress innovation within companies, elevate costs of operation, and negatively impact economic growth (Parise, 2016). Overly restrictive policies may impose additional burdens on enterprises and expand into new markets (Jiang *et al.,* 2025). Moreover, the rise of environmental regulation enforcement may force highly polluting enterprises to engage in hidden activities that damage the environment and exacerbate regional environmental deterioration. The "Porter hypothesis" from the 1970s suggests that strict regulations may enhance corporate competitiveness through fostering innovation. In order to alleviate the challenges posed by negative externalities on environmental quality, it is crucial to integrate government intervention with market strategies to facilitate. According to Holmes *et al.* (2013), regulatory measures can foster both innovation and the use of emerging technologies, which in turn supports low-carbon development (Fan and Xu, 2025). the RETI. Strict policies may encourage enterprises to boost investment in technological innovation, attain technological breakthroughs, improve development efficiency, and empower enterprises to obtain competitive advantages in the global market (Han, 2020). China, recognized as the top carbon emitter worldwide, aimed for carbon peak and carbon neutrality by 2020 (Cao *et al.,* 2024). With the remarkable progress in RETI and the continuous optimization of the energy mix, China has emerged as a key driving force within the global renewable energy market. Enhancing RETI and fast-tracking LCET are now urgent priorities in China, calling for swift intervention and systematic approaches. Moreover, this situation provides a valuable context to examine related research. Based on these analyses, this study identifies the following gaps. First, existing research seldom centers on the influence of RETI on the LCET, indicating room for further study. Second, existing literature lacks a consensus on the moderating effects of climate risk, necessitating in-depth research to clarify their specific effects. Third, few studies explore the role of the Paris Agreement's policy regulation in promoting the LCET, and the significance of policy implementation needs further examination. The objective of this study is to assess how RETI influences the LCET and to investigate the mechanistic functions of climate risks and policy regulations within this framework. This study was conducted at Hebei University in Baoding City, Hebei Province, China, and completed in 2025.

MATERIALS AND METHODS

Theoretical analysis and research hypotheses

As a newly emerging area around innovation, RETI centers on the advancing and implementing of new technologies (Lin and Xie, 2024) for enhancing the utilization efficiency. LCET is showcased through the transformation of the established energy structure (Yan *et al*., 2020). In contrast, it is also represented in the LCET (Zhang *et al*., 2025), where RETI can mitigate pollution and foster a new avenue for cooperative advancement (Khan *et al.,* 2021). The transition of economic development can not only significantly reduce pollution, but also effectively promote endogenous economic (Dong *et al*., 2023). Ge *et al*., (2022) argued that RETI can optimize regional industrial structure. The principle of biased technological evolution suggests that the unequal allocation of limited resources by research and development between different manufacturing industries serves as the catalyst for structural shifts in the economy. In addition, RETI can stimulate and foster

the development of green industries and enterprises' productivity (Yan *et al*., 2020), then promote the industrial development of clean production (Tambo, 2016; Chatjuthamard, 2024; Jiang *et al*., 2024). The subsequent hypothesis is put forward.

H1: RETI promotes the LCET

Climate risk has a profound effect on RETI. Firstly, severe weather events lead to climate-related risks that can harm energy infrastructure, posing great challenges to the integrity and sustainability of the renewable energy system (Feng *et al*., 2023). Secondly, these climate risks may heighten negative sentiments among investors, thereby diminishing their willingness to invest in RETI (Anupam *et al*., 2022). Due to insufficient disclosure of climate risks and the existence of information asymmetry, investors will be more cautious about financing needs such as RETI, which will further inhibit the innovation ability of enterprises (Rabeh *et al*., 2022). Thirdly, intense weather phenomena have the potential to damage regional infrastructure, cause interruptions in production, exacerbate the operational climate, and elevate the daily costs of running a business, thereby hindering investments in technological advancements (Rao *et al*., 2023). Therefore, climate risk can impact the effectiveness of RETI and is not conducive to the development of RETI. However, climate risk up to a certain threshold may also reduce the role of hindering RETI. Climate risks may force the government to introduce investment policies to support RETI to alleviate the negative effect of climate risks (Dietz *et al*., 2016). as the threat of climate change grows, there may be a greater tendency for individuals to pursue alternative energy solutions. To increase the efficiency of renewable energy sources, businesses could also be forced to develop innovative technologies.

H2: Climate risk exerts moderating and threshold impacts on the RETI and the LCET

The study of the impact of policy instruments has long been the focus of academic research. Policies can guide relevant industries to minimize fossil fuel usage, promote the LCET. The objective of policies and regulations is to regulate the harmful effects of activities within the ecosystem's tolerance thresholds and support the development of a low-carbon economy (Tang *et al*., 2024). Policy regulation can increase the support and guarantee for low-carbon industries and provide necessary policy support to enhance enterprises' confidence in low-carbon development (Li and Qi, 2025). Nonetheless, burdensome regulations and policy requirements may prolong the timeline and inflate the costs of renewable energy projects, limit their development potential, and impede the LCET (Wu *et al*., 2023). If environmental regulations are inflexible, they may weaken incentives for low-carbon development and hinder the LCET (Tang *et al*., 2020). Among policies, the signing of the Paris Agreement was a turning point. In this context, countries achieve their emission reduction commitments through their nationally determined contributions, representing a new era in global climate governance (Li *et al*., 2024), and emphasizing the critical role of policy regulation. However, the specific impact of policy regulation still needs to be further verified.

H3: Policy regulation moderates the process by which RETI promotes the LCET

RETI can promote the transition of employment industries and jobs to "go green," reduce air pollution caused by fossil fuel combustion (Obiora *et al*., 2024), reduce industrial pollutant emissions, and reduce $PM_{2.5}$ concentrations, thus significantly improving air quality (Yu *et al*., 2023). The presence of air pollution may result in health complications, diminish workers' cognitive skills and creativity, lower labor efficiency, and impede economic advancement. Therefore, reducing air pollution concentration can not only improve productivity, but also provide the economic foundation for the LCET (Jaffe *et al*., 2004). The economic losses caused from air pollution can also encourage to invest more in LCET and further promote the LCET (Fisher *et al*., 2004).

H4: RETI promotes the LCET by reducing air pollution intensity

China has a wide territory and obvious differences in the level of economic development between different regions, which leads to the differentiation of the impact of RETI on LCET (Conway *et al*., 2023). Regions with strong economies have adequate funding,

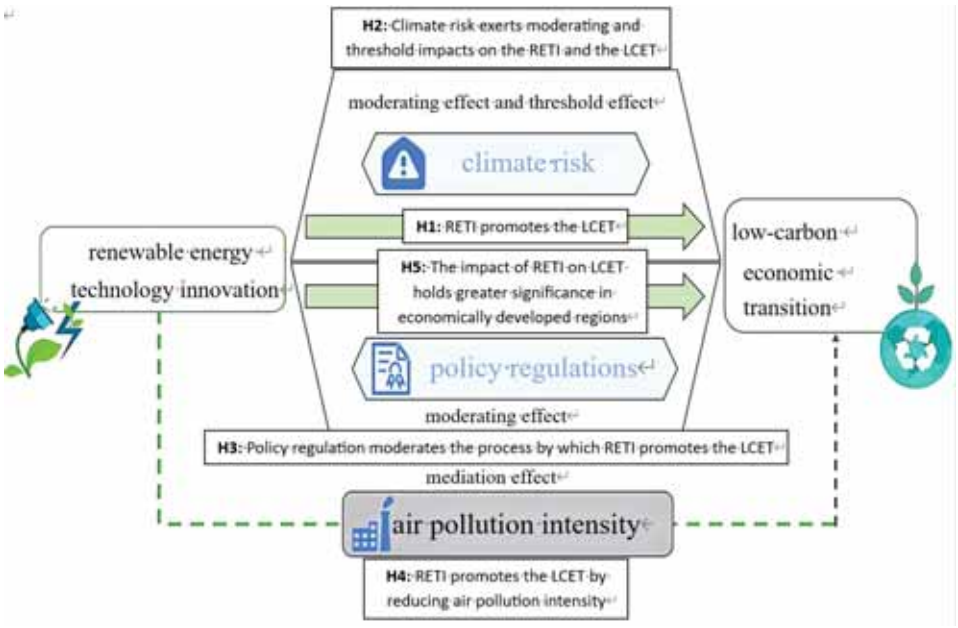

Fig. 1: methods and assumptions

modern infrastructure, and advanced technological assets that contribute to the evolution of technologies (Bai and Lin, 2024). Conversely, regions with lagging economic development struggle with challenges such as inadequate infrastructure and an overdependence on fossil fuels, hindering their ability to reach CET in a timely manner. Moreover, economically developed regions have sufficient talent reserves, which can attract a large number of talents to participate in green product research and development (R&D), while regions with slow economic progress confront serious brain drain and weak economic growth, which not only aggravates the pressure of industrial transition, but also hinders the process of local LCET. Consequently, regions with economic development have several benefits that increase the significance of RETI on LCET in these areas.

H5: The impact of RETI on the LCET holds greater significance in economically developed regions.

Fig. 1 illustrates a flowchart that represents the research methodology implemented in this work and the relevant research hypotheses.

Data and variables

This analysis is based on panel data collected from 30 provinces in China, with Tibet excluded, covering the timeframe from 2000 to 2021. Data on renewable energy technology innovation, specifically green patents, originated from the Chinese Research Data Services Platform (CNRDS), with supplementary information sourced from the "China Statistical Yearbook," EPS Database, CEIC, and Chinese Provincial Statistical Yearbooks.

Dependent variable

LCET: The research measures low-carbon economic transition using carbon emission intensity, following Qiao *et al*. (2024), Zhang *et al*. (2024), and Bai *et al*. (2023). LCET is computed as the proportion of carbon dioxide (CO_2) emissions to gross domestic product (GDP). An elevated LCET reflects a lag in the shift towards a low-carbon economic transition.

Key independent variable

RETI: Given data availability, this study measures RETI assessed through the number of green patent applications (Yang *et al*., 2024). Because of the slow process in awarding green patents, there might be hindrances in assessing local technological innovation (Yao *et al*., 2021). While patent data is not without its shortcomings, it continues to serve as a credible and valuable instrument for research. It showcases

Table 1: Descriptive statistics

Variables	Definition	Observations	Mean	SD	Min.	Max.	Jarque-bera statistic	p-value
LCET (Ton / 100 million yuan)	the proportion of CO_2 emissions to GDP	660	0.0256	0.0177	0.00157	0.126	0.0708	0.9652
RETI (Unit)	the number of green patent applications	660	4091	8078	3	67258	1.4475	0.4849
URB	the ratio of urban population to total population	660	0.517	0.158	0.139	0.896	0.0014	0.9993
OPEN	the proportion of export and import value to GDP	660	0.298	0.364	0.00757	1.721	0.0819	0.9599
lnPGDP (100 millions yuan/person)	the logarithm scale of per capita GDP	660	9.185	0.522	7.887	10.78	0.0072	0.9964
IS	the ratio of the tertiary industry to the secondary industry	660	1.064	0.588	0.494	5.297	0.7409	0.6904
lnAPI ($\mu g/m^3$) /100 million yuan	the logarithm of the annual average PM2.5 emissions of each province divided by the GDP	660	-5.516	1.134	-8.632	-1.937	0.0001	0.9999
CRI	climate physical risk index	660	43.64	8.74	19.08	84.34	0.0044	0.9978

spending on research and development and the success of technological advancements (Yu *et al.*, 2024).

Control variables

1) Foreign trade dependence (OPEN): Calculated as the proportion of export and import value to GDP.

2) Urbanization level (URB): Calculated as the ratio of urban population to total population.

3) Industrial structure (IS): Represented by the ratio of the tertiary industry to the secondary industry.

4) Economic development level (lnPGDP): Calculated as the logarithm scale of per capita GDP to reflect the economic development level of a region.

Moderating variable

Climate risk (CRI): Climate risk data are derived from daily observations by the National Oceanic and Atmospheric Administration (NOAA) and calculated based on the number of extreme cold, heat, precipitation, and drought days. These are normalized and weighted to develop a complete climate physical risk index (Guo *et al.*, 2024).

Mediating variable

Air pollution intensity (lnAPI): As referenced by Jiang *et al*. (2024), the current study introduces a new variable, air pollution intensity, which is calculated as the logarithm of the annual average PM2.5 emissions for each province, normalized by the GDP of the corresponding year.

Model specification

In order to evaluate the impact of RETI on LCET, Eq. 1 was used for LCET based on previous studies (Li *et al.*, 2024):

$$\mathrm{LCET}_{it} = \alpha_0 + \alpha_1 \mathrm{RETI}_{it} + \alpha_2 \mathrm{Control}_{it} + \delta_i + \varphi_t + \varepsilon_{it} \quad (1)$$

Where;

LCET_{it} represents the low−carbon economic transition, RETI_{it} denotes renewable energy technology innovation, δ_i and φ_t respectively denote province and time fixed effects.

Furthermore, assuming that CRI moderates the impact of RETI on CEI, the following moderation effect model is established, referencing previous

work, using Eq. 2 (Khan *et al.,* 2021):

$$LCET_{it} = \alpha_3 + \alpha_4 RETI_{it} + \alpha_5 CRI_{it} + \alpha_6 RETI_{it} \times CRI_{it} + \alpha_7 Control_{it} + \delta_i + \varphi_t + \varepsilon_{it} \quad (2)$$

Where;

CRI_{it} is the moderating variable, representing the climate risk index. The interaction terms are mean-centered.

RESULTS AND DISCUSSION

Empirical analysis

This study included an empirical analysis carried out utilizing Stata. As shown in Table 1, there is a significant variation between the minimum and maximum LCET values, which underscores the inconsistencies among provinces in LCET. The high standard deviation of RETI indicates considerable differences in the number of RETI among provinces, ranging from a maximum of 67,258 to a minimum of merely 3, which further illustrates the vast variation in the advancement of technological innovation. The p - values are uniformly well in excess of 0.05, substantiating the normal distribution of the study's data.

As shown in Table 2, the regression coefficient of RETI on LCET is -5.44e-07, and it is statistically significant at the 1% level. The results indicate that RETI has a significant negative impact on LCET. Hence, H1 is validated.

Robustness checks

To enhance the reliability of the model's estimation results, the following tests were performed as shown in Table 3. 1) Endogeneity Test: Using the lagged four periods of RETI as an instrumental variable for analysis. 2) Replacing the Dependent Variable: As noted by Yi *et al*. (2022), the ratio of carbon emissions to the added value generated by the secondary industry served as an alternative metric for low-carbon economic transition (CESI). 3) Excluding Special Years: Considering the impact of the 2008 global financial crisis on China's economy and RETI, data from the year 2008 was excluded. 4) Handling Outliers: both ends of all continuous variables were constrained to the 1% level. All results of robustness

Table 2: Baseline regression results

Variables	1	2	3	4	5
	LCET	LCET	LCET	LCET	LCET
RETI	-5.44e-07***	-5.20e-07***	-5.11e-07***	-4.48e-07***	-4.47e-07***
	(1.56e-07)	(1.52e-07)	(1.50e-07)	(1.39e-07)	(1.38e-07)
URB		0.00708***	0.00648***	-0.00580	-7.95e-05
		(0.00198)	(0.00213)	(0.00820)	(0.00822)
OPEN			-0.00399	-0.00387	-0.00885*
			(0.00349)	(0.00414)	(0.00487)
lnPGDP				0.0122**	0.0124***
				(0.00468)	(0.00415)
IS					-0.00462**
					(0.00226)
Constant	0.0278***	0.0241***	0.0255***	-0.0809**	-0.0785**
	(0.000638)	(0.00132)	(0.00169)	(0.0390)	(0.0350)
ID FE	YES	YES	YES	YES	YES
Year FE	YES	YES	YES	YES	YES
Observations	660	660	660	660	660
R^2	0.106	0.111	0.113	0.138	0.152

Notes: Robust standard errors in parentheses; ***, **, and * denote significance at the 1, 5, and 10 percent (%) levels, respectively. (The explanations in the following table are the same).

Table 3: Robustness tests

Variables	(1)		(2)	(3)	(4)
	2SLS (First stage)	2SLS (Second stage)	Replacing the explained variable	Excluding specific year	Dealing with outliers
	RETI	LCET	CESI	LCET	LCET
L4. RETI	0.739***				
	(0.0406)				
RETI		-7.90e-07***	-9.49e-07***	-5.10e-07***	-5.96e-07***
		(1.03e-07)	(3.33e-07)	(1.52e-07)	(1.35e-07)
URB	-1,724	0.0249***	-0.00638	-2.53e-05	-0.00111
	(2,477)	(0.00627)	(0.0240)	(0.00888)	(0.00839)
IS	531.3	-0.00537***	-0.0117**	-0.00461**	-0.00384
	(1,183)	(0.00122)	(0.00502)	(0.00223)	(0.00277)
lnPGDP	-8,002***	0.00579**	0.0245**	0.0112**	0.0113**
	(2,490)	(0.00260)	(0.0111)	(0.00426)	(0.00432)
OPEN	2,372	-0.0145***	-0.0126	-0.00757	-0.00696
	(2,681)	(0.00292)	(0.0117)	(0.00471)	(0.00452)
Constant	76,033***	-0.0288	-0.141	-0.0676*	-0.0692*
	(22,612)	(0.0214)	(0.0928)	(0.0356)	(0.0360)
ID FE	YES	YES	YES	YES	YES
Year FE	YES	YES	YES	YES	YES
Observations	540	540	660	630	660
R^2	0.423	0.273	0.110	0.144	0.184
F-statistic	259.41				

checks reveal that RETI exerts a statistically significant negative influence on LCET, with the corresponding regression coefficients being significant at the 1% level.

The impact of climate risks

To better understand the mechanism through which RETI influences the LCET, this study evaluates the mediating and threshold impacts of climatic risk.

The moderating effect of climate risks

To enhance the validation of the moderating role of climate risks, the outcomes are displayed in Table 4. The findings indicate that climate risks obstruct the transition from RETI to LCET.

The threshold effect of climate risks

This model accounts for the nonlinearity present in the relationship with RETI and allows for threshold variables to be endogenous, thereby improving the precision of the estimation results (Lee et al., 2024). It is constructed based on Eq. 3 (Lee *et al.*, 2024):

$$LCET_{it} = \beta_0 + \beta_1 CEI_{i,t-1} + \beta_2 RETI_{it} + (1, RETI_{it})\delta 1\{CRI_{it} > \gamma\} + \omega Controls_{it} + (1, Controls_{it})\delta 1\{CRI_{it} > \gamma\} + \varepsilon_{it} \quad (3)$$

Given the extensive geography of China and the considerable regional differences in climate risks, the effect of RETI on the LCET could vary according to these climate risk differences. Therefore, this study selects CRI as the threshold variable for the fast bootstrap test. After repeatedly resampling the samples, the optimal threshold for climate risk is chosen for subgroup regression, as shown in Table 5. As a result, H2 is substantiated. In Table 5, the first column reveals that a CRI below the threshold, the RETI coefficient is negative at the 1% significance level. As shown in Column (2), exceeding the CRI threshold results in a negative outcome at the 1% level, with an increase in its magnitude. A reduction in climate risks results in a more stable external environment for businesses, fostering increased investment in RETI. In locations with significant climate threats, more resources might need to be directed towards managing natural disasters, enacting policy reforms, and addressing environmental concerns, potentially constraining the resources available for fostering technological innovation and pursuing low-carbon transition. This increases operational costs and investment risks, hindering the LCET.

As shown in Fig. 2, after passing the threshold point,

Table 4: The moderating effect

Variables	Coefficient
	LCET
RETI	-0.744
	(-1.547)
LCET	0.000978***
	(3.331)
RETI×CRI	0.0413**
	(2.281)
URB	0.00884
	(1.030)
IS	0.0109***
	(3.349)
lnPGDP	-0.0215**
	(-2.467)
OPEN	0.0224**
	(2.138)
Constant	0.218***
	(3.764)
ID FE	YES
Year FE	YES
Observations	660
R^2	0.263

Table 5: The threshold effect

Variables	(1)	(2)
	LCET	LCET
	RETI (below γ)	RETI (above γ)
	-9.474440e-07 ***	-7.005026e-07 ***
	(2.598079e-07)	(9.044027e-08)
Control	Yes	Yes
Bootstrap test (p-value)	0.000	0.000
Optimal threshold	34.574	34.574
95% C.I.	[-1.880104e-06, -4.642863e-07]	[-9.439224e-07, -5.202866e-07]

the threshold effect exerted by CRI gradually decreases.

Analysis of policy regulation effects

Among the numerous policy regulations, the Paris Agreement stands out as a pivotal milestone. In 2015, China confirmed its participation in the Paris Agreement. This study applies the difference-in-differences methodology, treating 2015 as the policy implementation year, to investigate the distinct influence and effectiveness of the Paris Agreement in fostering China's LCET.

Stability test

Parallel trend test

Fig. 3 shows that prior to policy intervention (before 2015), the trends of different groups were roughly the same. Once the policy was enacted, its impact saw a significant decline, indicating adverse effects on the treatment group. This alteration in trend indicates that the policy intervention fulfilled its purpose, thereby validating the research design. It shows that the difference in trends is primarily due to the policy implementation, rather than other factors.

Incorporating the importance of the energy sector within the economic framework of each province, along with the share of fossil fuels in industrial output, 17 provinces that heavily rely on fossil energy, including Shanxi and Shaanxi, are designated as the treatment group. The constructed difference-in-differences (DID) model, using Eq. 4 (Wang and Zhang, 2020):

$$LCET_{it} = \beta_3 + \beta_4 treat_i \times post_t + \beta_5 Contral_{it} + \delta_i + \varphi_t + \varepsilon_{it} \quad (4)$$

Where;

$post_t$ is a time dummy variable, and taking the value 0 for the years 2015 and earlier, and 1 for the years after 2015 $treat_i$ is a regional dummy variable, taking the value 1 for provinces that rely on fossil energy and 0 for provinces that do not. As shown in Table 6, the findings indicate that the policy effectively curtailed carbon emissions from fossil energy sources and advanced the implementation of LCET. This confirms that the policy achieved the desired improvements in environmental quality.

Placebo test

The purpose of the placebo test is to ascertain

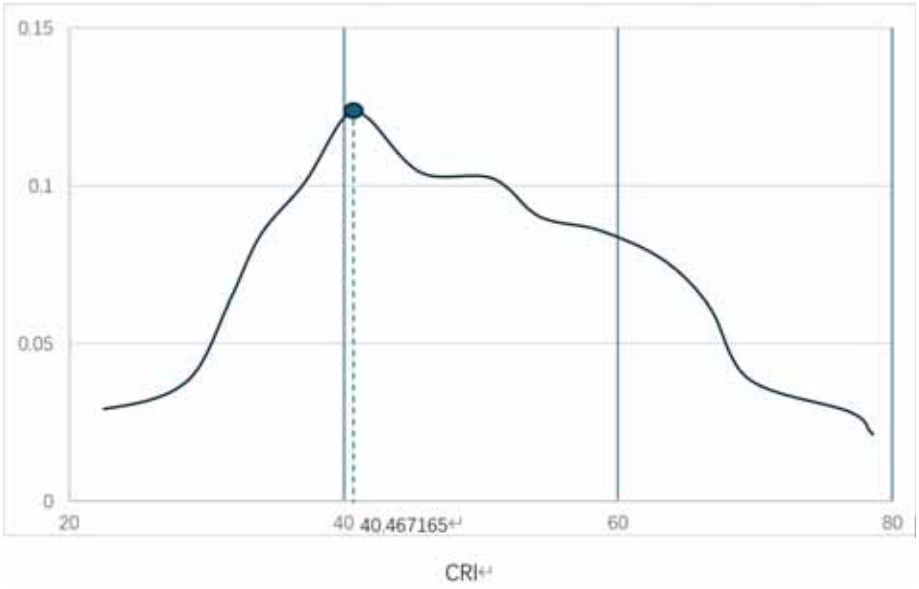

Fig. 2: The threshold effect

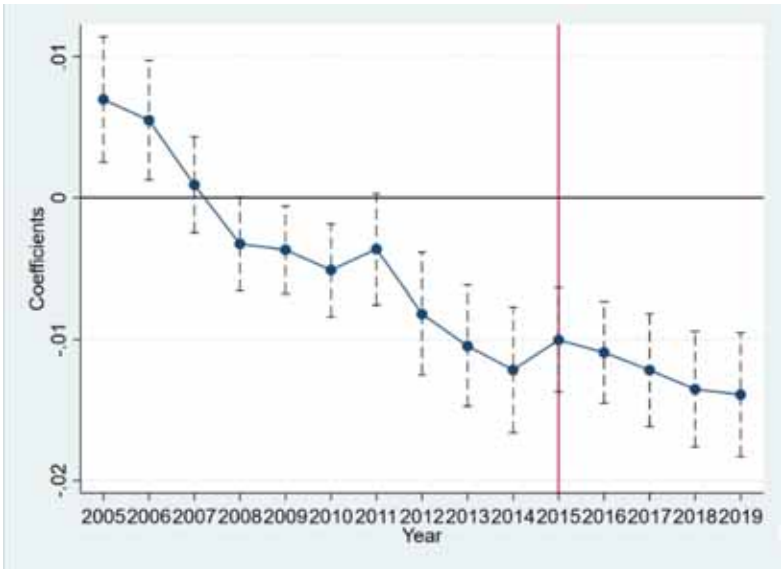

Fig. 3: Parallel trend test

Table 6: Baseline regression results

Variables	(1)	(2)
	LCET	LCET
Treat × post	-1.53***	-0.415*
	(0.184)	(0.214)
URB		-0.870
		(1.04)
IS		-0.626**
		(0.242)
lnPGDP		0.778*
		(0.446)
OPEN		0.291
		(0.364)
Constant	2.81***	-3.15
	(0.030)	(3.68)
ID FE	YES	YES
Year FE	YES	YES
Observations	660	660
R^2	0.227	0.351

Table 7: Placebo test

Variables	Coefficient
	LCET
placebo	2.53e-05
	(0.000952)
URB	-5.13e-05
	(0.00878)
OPEN	-0.0117**
	(0.00531)
lnPGDP	0.0168***
	(0.00403)
IS	-0.00469*
	(0.00234)
Constant	-0.120***
	(0.0336)
ID FE	YES
Year FE	YES
Observations	660
R^2	0.088

whether significant effects existed before the policy was implemented, as indicated in Table 7. In this study, a fictitious policy implementation time was set to 2009. According to Table 7, the placebo treatment variable had no significant effect on LCET, which implies that the treatment effect found in the original DID analysis is strong and not a result of random fluctuations.

This study employs a placebo test by randomly changing the schedule for policy implementation. Specifically, each sample firm has a year randomly selected from the study period to act as a pseudo-adoption year of the Paris Agreement, with this simulation conducted 500 times. Fig. 4 presents the distribution of estimated coefficients for these artificially generated treatment variables. As shown, the coefficients are tightly clustered around zero, following an approximately normal distribution. This indicates that the pseudo-treatment variables exert no statistically significant effect on LCET when policy timing is randomly assigned. The results suggest that the primary findings concerning the treatment effect are unlikely to be attributed to random chance, thereby reinforcing the empirical conclusions.

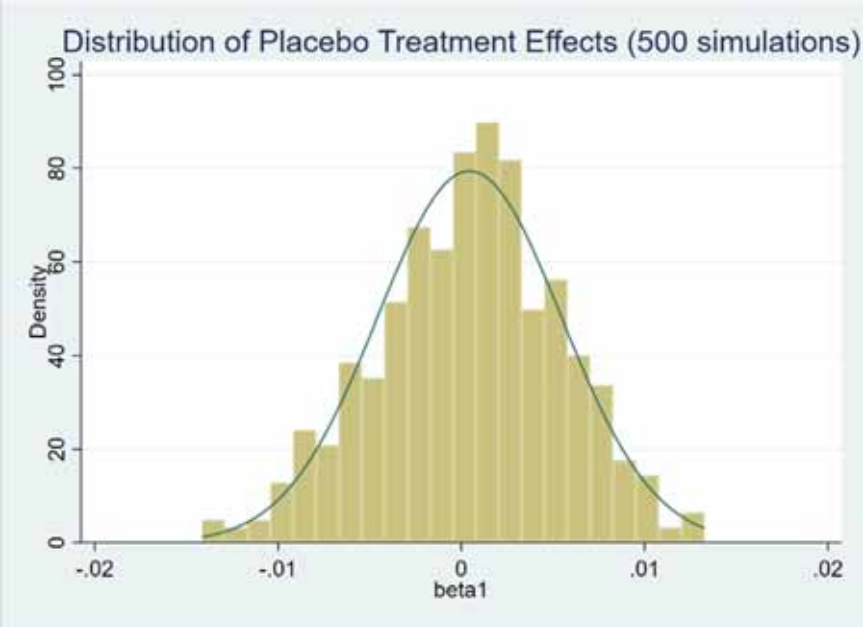

Fig. 4: Placebo test

Table 8 : PSM-DID

Variables	(1)	(2)	(3)	(4)
	K-proximity matching	Logit matching	Radius matching	Kernel matching
treat×post	-0.0160***	-0.0158***	-0.0149***	-0.0150***
	(0.00217)	(0.00215)	(0.00195)	(0.00210)
URB	-0.00350	-0.00451	-0.00787	-0.00781
	(0.0114)	(0.0114)	(0.0100)	(0.0133)
OPEN	0.00102	-0.000552	-0.00209	-0.00165
	(0.00528)	(0.00594)	(0.00547)	(0.00595)
lnPGDP	0.00892*	0.00924*	0.0122***	0.0123**
	(0.00493)	(0.00479)	(0.00413)	(0.00571)
IS	-0.00761*	-0.00724*	-0.00461**	-0.00497*
	(0.00408)	(0.00380)	(0.00209)	(0.00278)
Constant	-0.0410	-0.0443	-0.0743**	-0.0745
	(0.0422)	(0.0405)	(0.0339)	(0.0472)
ID FE	YES	YES	YES	YES
Year FE	YES	YES	YES	YES
Observations	510	540	660	648
R^2	0.297	0.286	0.267	0.268

PSM-DID

The analysis results using the PSM-DID method are shown below. Columns (1), (2), (3), and (4) of Table 8 represent k-proximity (k = 1), logit, radius, and kernel matching, respectively. Table 8 illustrates that the coefficient of the interaction term and its statistical significance remain relatively stable.

This study also included control variables that were lagged by one period. The tests show that the findings are consistent and reliable. Hence, H3 is validated. To understand the mechanism through which RETI affects the LCET, this study will conduct mediation effect analysis and heterogeneity tests.

Mediation effect

Following Jiang's (2022) insights on mediation effect

Table 9: The role of air pollution intensity

Variables	(1) lnAPI	(2) lnAPI
RETI	-7.12e-05***	-6.33e-05***
	(1.55e-05)	(1.42e-05)
URB		-0.0274
		(0.499)
IS		-0.481***
		(0.117)
lnPGDP		0.972***
		(0.206)
OPEN		-1.095***
		(0.290)
Constant	-5.225***	-13.34***
	(0.0636)	(1.707)
ID FE	YES	YES
Year FE	YES	YES
Observations	660	660
R^2	0.299	0.358

Table 10: Heterogeneity test

Variables	(1)	(2)	(3)
	LCET	LCET	LCET
RETI	0.0710	-1.6467***	-0.8959***
	(0.3418)	(-7.5309)	(-8.0254)
URB	0.0638*	-0.0054	-0.0055
	(1.6568)	(-0.4657)	(-1.1295)
IS	-0.0038	-0.0030	0.0003
	(-0.3671)	(-0.5443)	(0.2551)
lnPGDP	-0.0211	0.0118*	0.0039
	(-1.1442)	(1.7608)	(1.2137)
FDI	-0.0148	-0.0049	-0.0111***
	(-0.4066)	(-0.5228)	(-3.2873)
Constant	0.2202	0.0152	0.0526*
	(1.3688)	(0.2604)	(1.9414)
ID FE	YES	YES	YES
Year FE	YES	YES	YES
Observations	220	220	220
R^2	0.0161	0.2468	0.2843

analysis, this study aims to resolve the estimation bias found in the standard stepwise regression technique by analyzing the effect of the RETI on the API. Therefore, the following mediation effect model is established, using Eq. 5 (Li *et al.,* 2024):

$$\ln\mathrm{API}_{it} = \beta_6 + \beta_7\mathrm{RETI}_{it} + \beta_8\mathrm{Control}_{it} + \delta_i + \varphi_t + \varepsilon_{it} \quad (5)$$

Where;

$\ln\mathrm{API}_{it}$ represents the mediating variable, which is air pollution intensity.

The role of air pollution in the impact of RETI on the LCET cannot be ignored. Evidence from existing research shows that RETI substantially cuts down on air pollutant emissions, virtually eliminating harmful agents including sulfur dioxide and PM2.5 (Saidur *et al.,* 2011). It also significantly improves energy utilization efficiency, reduces the demand for traditional energy, and further lowers pollution intensity (Green *et al.,* 2019). Consequently, RETI effectively cuts down on air pollution intensity. This decline in intensity benefits the LCET in two

important aspects. First, as public awareness of reducing air pollution increases, governments adopt more proactive environmental protection measures and low-carbon development strategies, reducing reliance on high-carbon industries and shifting towards sustainable development (Thomas *et al.,* 2009). Second, mitigating air pollution intensity can promote the health of workers, increase productivity in the labor force, and elevate economic performance, laying a solid economic groundwork for the transition to a low-carbon economy (Song *et al.,* 2020). Table 9**.** indicates that lnAPI plays a significant mediating role between RETI and LCET. The renewable energy technology innovation can lower air pollution intensity. Additionally, lnAPI has impact on LCET, indicating that a reduction in air pollution intensity is conducive to the LCET. Hence, H4 is validated.

Heterogeneity analysis

This study continues to investigate the heterogeneous impact of RETI on LCET by analyzing the differences in economic development levels. The provinces are categorized into three groups: the bottom one-third of the provinces as low economic development regions, the middle one-third as medium economic development regions, and the top one-third as high economic development regions. The outcomes are presented in columns (1), (2), and (3) of Table 10. Column (1) shows that in areas with low economic development levels, the impact of RETI on the LCET is not clear. Column (3) illustrates that in provinces with higher economic development levels, RETI significantly promotes the LCET. Hence, H5 is validated.

CONCLUSION

The study quantitatively explores how RETI affects the LCET, considering the moderating effects of climate risk and regulatory policies. The principal findings and conclusion are as follows:

1) Baseline Regression Results: RETI significantly promotes the LCET by reducing carbon emission intensity. This finding is supported by several robustness tests. 2) Moderating Effects: Climate-related risks impede the development of renewable energy technology innovations that enhance the LCET. 3) Difference-in-Differences Results: The Paris Agreement policy significantly improves the LCET in fossil fuel-dependent provinces, achieving the expected environmental effects. This demonstrates the important role of the Paris Agreement in guiding RETI and promoting the LCET. 4) Mediation Effects: RETI significantly promotes the LCET by reducing air pollution intensity. 5) Heterogeneity Results: In more economically developed provinces, RETI significantly promotes the LCET. In contrast, the effect is negligible in areas of lesser economic advancement. The Paris Agreement has become an important opportunity for China to participate in the global low-carbon transformation. This policy not only fulfills the aspirations of the global community and showcases China's dedication to lowering emissions, but also aligns with China's historical focus on low-carbon development. It demonstrates China's determination to deal with climate change and plays a leading role in setting an example for other countries to achieve low-carbon economic transformation. This study delivers empirical validation for RETI's role in enhancing the LCET and proposes offers the following policy recommendations: 1) Strengthen R&D Investment and Collaboration: The government can increase investment in RETI and promote research and development in renewable energy by companies and research institutions. Investments should focus on technologies that reduce carbon emissions. Moreover, it is essential for the government to foster collaboration between companies and research institutions, enhance the efficiency of the patent application and approval process, and minimize the authorization duration for green patents to enable rapid transformation of innovative results into productive applications. 2) Establish a specific Climate Risk Management system: The government should establish a comprehensive climate risk assessment system, conduct regular assessments of climate risks in different regions, identify potential risks, and enhance emergency response capabilities to extreme weather events. This will reduce damage to renewable energy projects and ensure the steady progress of RETI. 3) Upgrade the industrial structure: Efforts must be made to refine and elevate industrial infrastructures, facilitating the shift of industries towards sustainable practices and minimizing reliance on fossil fuels. Cultivate new technologies and business models through investment in scientific research, boost the economic level, and create an environment for the renewable energy. 4) Strengthen Environmental Policy Execution: It is essential for the

government to establish supportive policy guidelines and incentive programs aimed at boosting innovation through fiscal subsidies and tax regulations. At the same time, we will strengthen the implementation and supervision of environmental protection policies, establish a scientific evaluation system, and create favorable conditions for RETI. China, being the foremost emerging market, offers valuable insights and experiences in promoting the LCET that can benefit other emerging nations and are relevant to different regions worldwide.

AUTHOR CONTRIBUTIONS

X.Y. Liu conceived the writing, original draft, methodology, and software design. X. Shao assisted on visualization, methodology, and formal analysis. X.F. Li interpreted the data curation, visualization, and investigation; C. Dong as the corresponding author supervised the project, performed the writing, review and editing the manuscript.

ACKNOWLEDGEMENT

This study was supported by Hebei Province Social Science Fund project: [Approval No: HB22YJ046], Philosophy and the social science training project of Hebei University: [Approval No: 2022HPY028] and S and T Program of Baoding [Approval No: 2363P022].

CONFLICT OF INTEREST

The authors declare that there is no conflict of interests regarding the publication of this manuscript. In addition, the ethical issues, including plagiarism, informed consent, misconduct, data fabrication and/or falsification, double publication and/or submission, and redundancy have been completely observed by the authors.

OPEN ACCESS

©2025 The author(s). This article is licensed under a Creative Commons Attribution 4.0 International License, which permits use, sharing, adaptation, distribution and reproduction in any medium or format, as long as you give appropriate credit to the original author(s) and the source, provide a link to the Creative Commons license, and indicate if changes were made. The images or other third-party material in this article are included in the article's Creative Commons license, unless indicated otherwise in a credit line to the material. If material is not included in the article's Creative Commons license and your intended use is not permitted by statutory regulation or exceeds the permitted use, you will need to obtain permission directly from the copyright holder. To view a copy of this license, visit: http://creativecommons.org /licenses/by/4.0/

PUBLISHER'S NOTE

GJESM Publisher remains neutral with regard to jurisdictional claims with regard to published maps and institutional affiliations.

☐ **Positive AI Statement**

During the preparation of this work the author(s) have used Artificial Intelligence (AI) [NAME TOOL / SERVICE] in order to [REASON]. After using this tool/service, the authors reviewed and edited the content as needed and take full responsibility for the content of the publication.

(For this reason, the GPTZero detector will evaluate the manuscript utilizing Generative AI, ensuring a high detection rate. If the manuscript relies heavily on Generative AI and AI-assisted technologies, it will be archived without further options for appeal).

☑ **Negative AI Statement**

The author(s) declare that no AI tools or services were not used or not highly applied during the preparation of this work.

ABBREVIATIONS

%	Percent
CESI	the ratio of carbon emissions to the secondary industry's added value
CO_2	carbon dioxide
CNRDS	Chinese Research Data Services Platform
DID	Difference-in-differences
IS	Industrial structure
lnAPI	Air pollution intensity
LCET	Low-carbon economic transition
lnPGDP	Economic development level
GDP	gross domestic product
NOAA	National Oceanic and Atmospheric Administration
OPEN	Foreign trade dependence
R&D	*research and development*

RETI	Renewable energy technology innovation
UK	United Kingdom
URB	Urbanization level

REFERENCES

Ahmad, N.; Youjin, L.; Žiković, S.; Belyaeva, Z., (2023). The effects of technological innovation on sustainable development and environmental degradation: Evidence from China. Technol. Soc., 72: 102184 **(13 pages)**.

Anupam, D.; Elie, B.; Timo, R.; Gazi, S., (2023). Climate risk and green investments: New evidence. Energy. 265 **(13 pages)**.

Bai, L.; Guo, T.; Xu, W.; Liu, Y.; Kuang, M.; Jiang, L., (2023). Effects of digital economy on carbon emission intensity in Chinese cities: A life-cycle theory and the application of nonlinear spatial panel smooth transition threshold model. Energy Policy. 183: 113792 **(13 pages)**.

Cao, H.; Zhao, Y.; Yuan, L.; Li, K., (2024). Does legislation promote technological innovation in renewable energy enterprises? Evidence from China. Energy Policy. 188: 114111 **(17 pages)**.

Chatjuthamard, P.; Singh S.; Jiraporn, P.; Lee, S. M., (2024). Climate change exposure, shareholder wealth, and the adoption of the Paris agreement: A text-based approach. Int. Rev. Finance. Anal., 94: 103327 **(13 pages)**.

Cheng, Z.; Kai, Z.; Zhu, S., (2023). Does green finance regulation improve renewable energy utilization? Evidence from energy consumption efficiency. Renew. Energy. 208: 63–75 **(13 pages).**

Chi-Chuan, L.; Hepeng, S.; Jiafu., A., (2024) The impact of green finance on energy transition: Does climate risk matter? Energy Econ., 129: 107258 **(12 pages).**

Feng, C.-Y.; Yang, X.; Afshan, S.; Irfan, M., (2023). Can renewable energy technology innovation promote mineral resources' green utilization efficiency? Novel insights from regional development inequality. Resour. Policy. 82 **(11 pages).**

Congyu, Z.; Kun, W.; Xiucheng, D., (2022). Is smart transportation associated with reduced carbon emissions? The case of China. Energy Econ., 105 **(14 pages).**

Conway, D.; Nicholls, J R.; Brown, S., (2019). The need for bottom-up assessments of climate risks and adaptation in climate-sensitive regions. Nat. Clim. Change., 9(7): 503-511 **(9 pages).** https://doi.org/10.1038/s41558-019-0502-0

Dietz, S.; Bowen, A.; Dixon, C.; Gradwell, P., (2016). 'Climate value at risk' of global financial assets. Nat. Clim. Change., 6(7): 676-679 **(4 pages).**

Dong, K.; Yang, S.; Wang, J.; Dong, X., (2023). Revisiting energy justice: Is renewable energy technology innovation a tool for realizing a just energy system? Energy Policy. 183: 113820 **(15 pages).** https://doi.org/10.1016/j.enpol.2023.113820

Fan, L.; Xu, W., (2025). The Impact of Green Finance Policies on Corporate Debt Default Risk-Evidence from China. Sustainability. 17(4): 1648 **(13 pages).** https://doi.org/10.3390 /su17041648

Fisher-Vanden, K.; Jefferson G. H.; Liu, H.; Tao, Q., (2004). What is driving China' s decline in energy intensity? Resour. Energy Econ., 26(1): 77–97 **(21 pages).**

Gao, X.; He, X.; Sun, C.; Wu, D.; Zhang, J., (2025). Innovation in shouldering green responsibility: ESG performance and green technology innovation. Energy Econ., 142: 108197 **(14 pages).**

Green, A M., (2019). How Did Solar Cells Get So Cheap? J. Joule., 3(3):631-633 **(3 pages).**

Guo, K.; Ji, Q.; Zhang, D., (2024). A dataset to measure global climate physical risk. Data Brief. 54: 110502 **(6 pages).**

Han, Y., (2020). Impact of environmental regulation policy on environmental regulation level: A quasi-natural experiment based on carbon emission trading pilot. Environ. Sci. Pollut. Res., 27(19): 23602–23615 **(14 pages).**

Holmes, M R.; Miller, T.; Hitt, A M., (2013). The Interrelationships Among Informal Institutions, Formal Institutions, and Inward Foreign Direct Investment. J. Manage., 39(2): 531-566 **(36 pages).**

Huang, S.; Wang, X.; Xue, Y., (2024). CEOS' climate risk perception bias and corporate debt structure. J. Int. Money Finance. 151: 103254 **(17 pages).**

Imran, A H.; Ikram, J.; Sudhara, S T.; Mehmood, R., (2023). How do corporate governance and corporate social responsibility affect credit risk? Res. Int. Bus. Finance. 67(PA) **(21 pages).**

Jaffe, AB.; Newell, RG.; Stavins, RN., (2005). A tale of two market failures: Technology and environmental policy. Ecol. Econ., 54(2–3): 164–174 **(11 pages).**

Jiang, C.; Li, Y.; Zhang, X., (2024). Climate risk and corporate debt decision. J. Int. Money Finance. 151: 103261 **(20 pages).** https://doi.org/10.1016/ j.jimonfin.2024.103261

Jiang, L.; Yang, Y.; Wu, Q., (2023). Hotter days, dirtier air: The impact of extreme heat on energy and pollution intensity in China. Energy Econ., 130: 107291 **(12 pages).** https://doi.org/10.1016/j.eneco.2023.107291

Jiang, Y.; Guo, Y.; Bashir, M F.; Shahbaz, M., (2024). Do renewable energy, environmental regulations and green innovation matter for China' s zero carbon transition: Evidence from green total factor productivity. J. Environ. Manage., 352: 120030 **(11 pages).**

Jacobson, Z M.; Delucchi, A M., (2010). Providing all global energy with wind, water, and solar power, Part I: Technologies, energy resources, quantities and areas of infrastructure, and materials. Energy Policy. 39(3): 1154-1169 **(16 pages).**

Lai, A.; Du, Q.; Wang, Q., (2024). One region's gain is another's loss: The impact of market segmentation on renewable energy development in China. Energy Policy. 192: 114215 **(14 pages).**

Li, T.; Qi, F., (2025). Fiscal reform and green innovation: Evidence from China's local debt management reform. Finance Res. Lett., 6: 106937 **(7 pages).**

Li, J.; Qu, S.; Peng, Z., (2024). The impact of green finance on carbon productivity: The mediating effects of the quantity and quality of green innovation. Energy Policy. 370: 122952 **(11 pages).**

Lin, B.; Xie, Y., (2024). Driving renewable energy innovation investments: Is venture capital a novel strategic choice? Evidence from China. Renew. Energy. 237: 121856 **(10 pages).** https://doi.org/10.1016/j.renene.2024.121856

Liu, J.; Jiang, T.; Ye, Z., (2020). Information efficiency research of China's carbon markets Renew. Energy. 38: 101444 **(8 pages).**

Liu, L.; Fu, P.; He, K., (2024). Impact assessment and mechanism analysis of the construction of pilot free trade zones on the efficiency of urban green technology innovation. Ecol. Indic., 163: 112137 **(13 pages).**

Liu, X.; Li, J.; Bai, C., (2024). Optimum low-carbon transformation pathways of China's iron and steel industry towards carbon neutrality based on a dynamic CGE model. Energy. 313: 134023 **(14 pages).**

Ma, Y.; Zhou, M.; Li, S., (2024). Weathering market swings: Does climate risk matter for agricultural commodity price predictability? J. Commod. Mark. 36: 100423 **(15 pages).**

Ma, Z.; Xie, Y.; Wang, K., (2025). Corporate climate risk perception and debt concentration. Finance Res. Mark., 77: 107022 **(15 pages).**

Murphy, R., (2023). What is undermining climate change mitigation? How fossil-fuelled practices challenge low-carbon transitions. Energy Res. Soc. Sci., 108: 103390 **(11 pages).**

Mu, Y.; Cai, W.; Evans, S., (2018). Employment impacts of renewable energy policies in China: A decomposition analysis based on a CGE modeling framework. Appl. Energy. 210: 256-267 **(12 pages).**

Obiora, C S.; Bamisile, O.; Hu, Y., (2024). Assessing the decarbonization of electricity generation in major emitting countries by 2030 and 2050: Transition to a high share renewable energy mix. Heliyon. 10 (8): e28770 **(20 pages).**

Olmos, L.; Ruester, S.; Liong, S., (2012). On the selection of financing instruments to push the development of new technologies: Application to clean energy technologies. Energy Policy. 43: 252-266 **(15 pages).**

Parise, S., (2016). Big data: A revolution that will transform how we live, work, and think, by Viktor Mayer-Schonberger and Kenneth Cukier. Int. Inf. Technol. Case Appl. Res., 18(3): 186–190 **(5 pages).**

Qiao, J.; Li, Y.; Yu, J., (2024). Admin Strative-led urbanization and urban carbon emission intensity: Evidence from city-county merger in China. Energy Econ., 136: 107615 **(11 pages).**

Rabeh, K.; Salma, M.; Jean-Laurent, V., (2022). How do climate risk and clean energy spillovers, and uncertainty affect U.S. stock markets? Technol. Forcast. Soc. Sci., 185: 122083 **(20 pages).**

Rashif, M.N.; Hartini, S.; Sari, D.P.; Ramadan, B.S.; Matsumoto, T.; Balasbaneh, A.T., (2025). Life cycle assessment of biomass waste briquettes as renewable energy. Global J. Environ. Sci. Manage., 11(1): 207-224 **(18 pages).**

Rao, A.; Lucey, B.; Kumar, S., (2023). Climate risk and carbon emissions: Examining their impact on key energy markets through asymmetric spillovers. Energy Econ., 126: 106970 **(16 pages).**

Saidur, R.; Islam, M.; Rahim, N., (2010). A review on global wind energy policy. Renew. Sustainable Energy Rev., 14(7): 1744-1762 **(19 pages).**

Sun, Y.; Razzaq, A.; Sun, H., (2022). The asymmetric influence of renewable energy and green innovation on carbon neutrality in China: Analysis from non-linear ARDL model. Renew. Energy. 193: 334–343 **(10 pages).**

Tambo, E.; Duo-quan, W.; Zhou, X., (2016). Tackling air pollution and extreme climate changes in China: Implementing the Paris climate change agreement. Environ. Int., 95: 152-156 **(5 pages).**

Tang, H.; Liu, J.; Wu, J., (2020). The impact of command-and-control environmental regulation on enterprise total factor productivity: A quasi-natural experiment based on China's "Two Control Zone" policy. J. Cleaner Product., 254: 120011 **(14 pages).**

Tang, T.; Jiang, X.; Zhu, K., (2023). Effects of the promotion pressure of officials on green low-carbon transition: Evidence from 277 cities in China. Energy Econ., 129: 107159 **(11 pages).** https://doi.org/10.1016/j.eneco.2023.107159

Thomas, D.; T G.; Jonathan, G., (2009). Household actions can provide a behavioral wedge to rapidly reduce US carbon emissions. PNAS. 106(44): 18452-18456 **(5 pages).**

Wang, C.; Zhang, Y., (2019). Does environmental regulation policy help improve green production performance? Evidence from China's industry. Corporate Soc. Responsibility Environ. Manage., 27(2): 937–951 **(15 pages).**

Wei, D.; Ahmad, F.; Chandio, A., (2024). Digital financial inclusion role to promote renewable energy technology innovation in Chinese prefectural cities: Moderating role of environmental governance. Renew. Energy. 237: 121704 **(14 pages).**

Wu, J.; Segerson, K.; Wang, C., (2023). Is environmental regulation the answer to pollution problems in urbanizing economies? J. Environ. Econ. Manage., 117: 102754 **(26 pages).**

Yan, S.; Aina, Z.; Ming, Z., (2020). Exploring the effect of subjective air pollution on happiness in China. Environ. Sci. Pollut. Res., 27(34): 43299-43311 **(13 pages).**

Yan, Z.; Zou, B.; Du, K., (2020). Do renewable energy technology innovations promote China's green productivity growth? Fresh evidence from partially linear functional-coefficient models. Energy econ., 90: 104842 **(11 pages).**

Yang, X.; Ran, R.; Chen, Y., (2024). Does digital government transformation drive regional green innovation? Evidence from cities in China. Energy Policy. 187: 114017 **(16 pages).**

Yao, S.; Yu, X.; Yan, S., (2021). Heterogeneous emission trading schemes and green innovation. Energy Policy. 155: 112367 **(13 pages).**

Yu, C.; Long, H.; Zhang, X., (2023). The interaction effect between public environmental concern and air pollution: Evidence from China. J. Cleaner Product., 391: 136231 **(11 pages).**

Yu, Z.; Chen, G.; Pei, X., (2024). The impact of corporate social responsibility on green technology innovation: An empirical study of listed companies in China. Finance Res. Lett., 66: 105699 **(8 pages).**

Zeeshan, K.; Shahid, A.; Kangyin, D., (2020). How does fiscal decentralization affect CO_2 emissions? The roles of institutions and human capital. Energy econ., 94: 105060 **(10 pages).**

Zhang, R.; Li, W.; Li, Y., (2024). Job losses or gains? The impact of supply-side energy transition on employment in China. Energy. 308: 132804 **(15 pages).**

Zhang, S.; Miao, X.; Zheng, H., (2024). Spatial functional division in urban agglomerations and carbon emission intensity: New evidence from 19 urban agglomerations in China. Energy. 300: 131541 **(9 pages).**

Zhang, X.; Zhang, R.; Feng, C., (2024). Decomposition analysis of renewable energy demand and coupling effect between renewable energy and energy demand: Evidence from China. Renew. Energy. 237: 121839 **(16 pages).**

Zhang, Y.; Liu, B.; Xue, J., (2024). Would geopolitical risks be the new driver of the energy transition? An empirical study on renewable energy technology innovation. Energy Econ., 141: 108100 **(13 pages).**

AUTHOR (S) BIOSKETCHES

X.Y. Liu, Ph.D. Candidate, School of Economics, Hebei university, Baoding 071000, China.
- Email: *13463498718@163.com*
- ORCID: 0009-0004-0401-2049
- Web of Science ResearcherID: NCV-4405-2025
- Scopus Author: NA
- Homepage: https://www.researchgate.net/scientific-contributions/Liu-Xiaoya-2178939245

X. Shao, M.Sc. Student, School of Economics, Hebei university. Baoding 071000, China.
- Email: *sxt720611@163.com*
- ORCID: 0009-0005-7490-9836
- Web of Science ResearcherID: NCV4433-2025
- Scopus Author: NA
- Homepage: https://www.researchgate.net/scientific-contributions/Shao-Xintong-2186855035

X.F. Li, M.Sc., Student, School of Economics, Hebei university. Baoding 071000, China.
- Email: *17889846146@163.com*
- ORCID: 0009-0001-8980-4771
- Web of Science ResearcherID: NCV4470-2025
- Scopus Author: NA
- Homepage: https://www.researchgate.net/scientific-contributions/Li-Xiaofang-2176329835

C. Dong, Ph.D., Professor, School of Economics, Hebei university. Baoding 071000, China.
- Email: *dongchi30@163.com*
- ORCID: 0009-0006-4143-3912
- Web of Science ResearcherID: LJL-4068-2024
- Scopus Author: 57193058700
- Homepage: https://www.researchgate.net/profile/Chi-Dong-2?ev=hdr_xprf

HOW TO CITE THIS ARTICLE

Liu, X.Y.; Shao, X.; Li, X.F.; Dong, C., (2025). The impact of renewable energy technology innovation on the low-carbon economic transaction. Global J. Environ. Sci. Manage., 11(3): 1241-1258.

DOI: 10.22034/gjesm.2025.03.20

URL: https://www.gjesm.net/article_724006.html

Global J. Environ. Sci. Manage. 11(3): 1259-1280, Summer 2025, Serial #43

Global Journal of Environmental Science and Management
(GJESM)

Homepage: https://www.gjesm.net/

Podcasts

CASE STUDY

Integrating building information modeling and bayesian network for enhanced go/ no-go decisions in building demolition projects

T.J.W., Adi[1,*], Y.P. Devia[2], N. Andriyani[3]

[1] *Department of Civil Engineering, Sepuluh Nopember Institute of Technology, Surabaya, 60111, Indonesia*

[2] *Department of Civil Engineering, Brawijaya University, Malang, 65145, Indonesia*

[3] *Research Centre for Industrial Systems and Sustainable Manufacturing, National Research and Innovation Agency, Tangerang Selatan, 15314, Indonesia*

ARTICLE INFO

Article History:
Received 23 February 2025
Revised 27 April 2025
Accepted 02 June 2025

Keywords:
Bayesian network
Building information modeling
Building demolition
Decision making
Go/No-Go demolition

ABSTRACT

BACKGROUND AND OBJECTIVES: Decision-making in building demolition is complex, involving structural, environmental, economic, and regulatory considerations. Traditional approaches often rely on subjective judgment and lack data-driven analysis. This study seeks to create a comprehensive decision-support framework that integrates Building Information Modeling and Bayesian Networks to optimize go or no-go decision processes. The objectives of the study were to provide a more accurate, reliable, and systematic tool that improves planning, reduces uncertainty, and promotes safety, efficiency, and sustainability in building demolition practices.

METHODS: This study integrates Building Information Modeling data with Bayesian Network probabilistic analysis to assess structural, environmental, and managerial factors influencing demolition decisions. A case study was conducted on a three-story market building located in South Jakarta. Expert insights were utilized to create conditional probability tables, improving the model's precision and its applicability to actual demolition situations. The model was validated through simulation and sensitivity analysis, identifying key variables affecting go or no-go outcomes.

FINDINGS: The integrated Building Information Modeling–Bayesian Network model effectively supports go or no-go demolition decisions by addressing uncertainty and risk factors probabilistically. According to the case study findings, there is a 55.10 percent chance of demolition, influenced by inadequate structural integrity (70 percent) and significant retrofit costs (59 percent). Mechanical demolition was preferred (56 percent) for its efficiency and lower risk. Sensitivity analysis identified structural integrity, retrofit cost, building age, environmental impact, and permit status as key influencing variables. Validation by experts has established the model's practical importance, illustrating its potential to boost planning accuracy and encourage sustainable, data-centric decision-making in complex urban demolition endeavors.

CONCLUSION: Integrating Building Information Modeling and Bayesian Network improves demolition decision-making by addressing uncertainty and supporting risk-informed analysis. The model boosts the precision of planning and aids in pinpointing significant influencing factors, like structural integrity and the costs associated with retrofitting. Furthermore, it fosters sustainable, data-driven approaches, rendering it an effective tool for complicated urban demolition initiatives.

DOI: 10.22034/gjesm.2025.03.21

This is an open access article under the CC BY license (http://creativecommons.org/licenses/by/4.0/).

NUMBER OF REFERENCES	NUMBER OF FIGURES	NUMBER OF TABLES
61	10	6

*Corresponding Author:
Email: *trijoko.riset@gmail.com*
Phone: +62-8113322774
ORCID: 0000-0001-9303-1479

Note: Discussion period for this manuscript open until Sep 1, 2025 on GJESM website at the "Show Article".

INTRODUCTION

Demolition is the process of dismantling or removing an existing building or any other types of structures due to a variety of reasons. A significant factor is the extensive structural damage that renders rehabilitation unfeasible, exemplified by buildings in specific areas of Türkiye (Caglar *et al.*, 2023). Demolition is also essential for replacing outdated transportation infrastructure and highway bridges that have exceeded the original design life (Davis *et al.*, 2019). Abandoned structures, such as neglected houses, also require demolition (Nowogońska *et al.*, 2021). Innovative technologies have profoundly impacted the demolition industry, which seek to decrease the need for human labor and mitigate risk. Although demolition provides solutions in certain situations, it is essential to consider its environmental, financial, and social impacts and to manage demolition waste properly (Menegaki *et al.*, 2018). Building demolition initiatives require attention to numerous complicated elements that must be thoroughly assessed to guarantee both success and safety, taking into account the threats posed by structural collapse and the potential dangers to employees and the surrounding area (Patel *et al.*, 2023). Environmental impacts are also a significant concern, as the demolition process can generate dust, debris, and pollution that affect air quality and local ecosystems (Ding *et al.*, 2016). Additionally, demolition costs must be meticulously calculated, including direct costs, such as equipment and labor, as well as indirect costs like waste management (Andriyani *et al.*, 2023) and site restoration (Nesticò *et al.*, 2024). Ensuring compliance with regulations and industry standards is essential for conducting all demolition activities legally and following the appropriate guidelines (Zhao *et al.*, 2021). A go or no-go (Go/No-Go) decision represents a pivotal phase of a project's life cycle, signifying a transition from planning and evaluation to execution. This decision necessitates a comprehensive analysis of all contributing factors to effectively identify and mitigate risks, ensuring that the project proceeds as intended and meets its objectives (Patel *et al.*, 2023). Demolition projects frequently encounter uncertainties concerning the structural state of buildings, environmental implications, and external influences such as weather. If not managed well, these uncertainties can make decision-making difficult and risky. According to Fang *et al.* (2021), the lack of clarity about the structural condition of buildings may result in complications when planning safe demolition techniques and sequences. Ding *et al.*, (2016) also highlighted that environmental impacts such as dust and noise pollution require careful assessment and mitigation to minimize adverse effects on the surrounding environment. The weather serves as an unpredictable external element impacting project schedules and costs (Ballesteros-Pérez *et al.*, 2018). Therefore, effective risk management Faiier2019is essential in demolition projects to mitigate these uncertainties and ensure the safety and sustainability of the project (Andriyani *et al.*, 2024). Several studies have been undertaken to identify efficient decision-making techniques for demolition projects. Wafiq and Adi (2016) applied the analytic hierarchy process (AHP) to choose demolition methods based on building characteristics. Even though AHP delivers a structured approach, it heavily relies on expert judgment, which can result in subjectivity and bias, particularly during the weighting of criteria. Other methods used in demolition planning include fuzzy analytic hierarchy process (Fuzzy AHP) (Khoshand *et al.*, 2020), analytic network process (ANP) (Chen *et al.*, 2014), and a combination of ANP and fuzzy multi attributive border approximation area comparison (Fuzzy MABAC) (Zhang *et al.*, 2021). For scheduling and prioritization, techniques such as preference ranking organization method for enrichment evaluation (PROMETHEE II) (Morkunaite *et al.*, 2019), Resource constrained project scheduling problem (RCPSP) (Pellerin *et al.*, 2020), and fuzzy multimode resource constrained project scheduling problem (Fuzzy MRCPSP) (Yuan *et al.*, 2021) have also been applied. Although these methods have theoretical advantages, they encounter numerous obstacles when applied in real-world scenarios. For example, ANP and PROMETHEE II require large amounts of input data and are computationally complex, making these methods challenging to apply without adequate information (Xu *et al.*, 2022). Likewise, AHP, fuzzy AHP, and ANP are commonly scrutinized for their subjective aspects, potentially causing inconsistencies in the decision-making process (Zhang *et al.*, 2021). In addition, RCPSP and Fuzzy MRCPSP struggle to manage uncertainties and variations in resource availability (Patoghi *et al.*, 2021). Furthermore, while each

technique has its strengths, these strategies also exhibit limitations like intricate execution, reliance on personal input, and struggles with uncertainty. Meanwhile, research on *Go/No-Go* decisions in demolition remains complex, as it involves multiple factors influencing the decision, such as structural conditions, cost, environmental impact, and safety. Zha *et al*. (2023) noted that these decisions often rely on expert opinion and past experience, which may lead to bias and uncertainty in the final outcome. The advent of building information Modeling (BIM) technology has significantly altered demolition planning by supplying more detailed structural data and superior visualization of building conditions (Alavi *et al*., 2022) along with potential hazards (Zou *et al.*, 2017). However, existing study reveals multiple shortcomings; first, the integration of BIM with risk management tools has not been fully realized in industry practice, resulting in less comprehensive and data-driven risk analysis (Waqar *et al.*, 2023). Second, a majority of studies have not successfully dealt with the intrinsic uncertainties associated with demolition projects, including changes in field conditions and other external factors (Roberts *et al.*,2022). Although BIM offers many advantages in decision-making (Han *et al.*, 2024), a more holistic and integrative approach is needed to manage uncertainties and risks more effectively. Several case studies show that the use of advanced technologies, such as BIM (Sopaheluwakan *et al.*, 2020) or Bayesian Network (BN) (Hoang *et al.*, 2017) has yielded positive results in construction and demolition projects. Hu *et al.* (2022) found that BIM improves planning accuracy and reduces on site errors, while Liu *et al.*, (2022) showed that BN effectively manages project risks and uncertainties. Moreover, only a small selection of studies examining the integration of BIM and BN exists in earlier literature, especially with an emphasis on the decision-making process related to building demolitions. Alavi *et al.*, (2022) suggested that integrating BIM with BN could provide a more comprehensive, data-driven approach to risk analysis. TohidiFar *et al.*, (2021) illustrated the efficacy of integrating BIM and BN to aid managers in healthcare facilities in evaluating disaster impacts on utilities and comprehending the ramifications of those choices. The recommended model successfully boosted and hastened the reactions of healthcare teams to emergency scenarios. The proposed model successfully improved and accelerated hospital teams' responses to critical situations. Research on combining BIM and BN in building demolition projects is still limited and rarely applied in practice. Although structured techniques like AHP and ANP have been widely applied in demolition planning, these methods remain limited due to reliance on subjective expert judgment, static outputs, and assumptions of variable independence. These limitations reduce flexibility in adapting to evolving project data. In contrast, the BN model utilized in this research provides a probabilistic framework that can manage uncertainty and represent interdependencies among variables. To address these shortcomings, this study proposes an integrated decision-support model that combines BIM's structured data environment with BN's adaptive reasoning capabilities. The combination of BIM and BN supports real-time sensitivity analysis and encourages more adaptive, evidence-based choices in complicated demolition contexts. A case study involving a three-story market building in Jakarta illustrates the model's practical application. Conducted at the Sepuluh Nopember Institute of Technology (ITS) in Surabaya and the National Research and Innovation Agency (BRIN) in Tangerang Selatan, Indonesia, in 2024, this study aims to enhance Go/No-Go decision-making in demolition projects. The central hypothesis is that integrating BIM and BN improves the objectivity, accuracy, and reliability of demolition decisions, providing a more transparent and robust alternative to conventional expert-based approaches.

MATERIALS AND METHODS

BIM, BN, and factors influencing Go/No-Go demolition choices are used as essential materials in this study. This discussion will concentrate on the methodological framework that merges BIM and BN to evaluate whether a building ought to be demolished, whether the demolition should be delayed, or whether the building should be preserved. This integration framework will be implemented in a case study of building demolition.

BIM for building demolition

BIM is vital in construction and demolition project management by offering detailed digital building representations (Nikmehr *et al.*, 2021). It enhances visualization, structural analysis, and planning

efficiency (Adi *et al.*, 2023). Utilizing BIM in demolition enhances the precision of planning and minimizes errors typically encountered during construction stages (Han *et al.*, 2021). BIM also identifies potential issues early, saving time and costs (Almujibah, 2023). In 3-dimensional (3D) BIM, building material specifications complement 3D visualizations as input data (Andriyani *et al.*, 2024). During quantity take-off (QTO), the model automatically processes volumes based on material types and specifications (Andriyani *et al.*, 2024). Nonetheless, BIM alone is insufficient to tackle every uncertainty and risk in demolition projects; unpredictable environmental conditions and weather still present challenges (Eastman *et al*., 2018). Integration of BIM with risk management, particularly probabilistic models like BN, is necessary to simulate uncertainties and support decisions. While BIM provides structured component data, attributes such as material degradation or undocumented changes introduce uncertainty. BN incorporates probabilistic values in conditional probability tables (CPTs) to capture these uncertainties, facilitating effective risk analysis despite the presence of imperfect or incomplete BIM data.

Fundamentals of BN for demolition decision modeling

A BN depicts the interrelationships of variables through a probability graphic model (Liu *et al.*, 2022). This model consists of nodes representing variables and probabilistic relationships among the variables, structured as a directed acyclic graph (DAG). Every node is linked to a conditional probability table (CPT), that specifies the likelihood of each variable based on the current state of its parent nodes. Using Bayes' theorem, a BN can perform probabilistic inference and estimate the probability of target variables based on existing evidence. This model is advantageous in a variety of contexts that involve uncertainty, including predicting weather patterns, analyzing risks, and making decisions, due to its ability to represent complex interrelations between variables and merge expert knowledge with empirical data for enhanced accuracy in estimates (Elmousalami, 2020). A BN comprises two parts: the structure and parameters. The structure graph shows the relationship between variables (Gao *et al.*, 2019). An arc going through variable Xi towards Xj indicates that Xj is contingent upon Xi. The arrangement comprises nodes that denote variables and directed edges that associate these nodes. The parameters comprise CPTs that define the intensity of the relationships among variables (Rodrigues *et al.*, 2024). The table elements were determined using Bayes' formula, using Eq. 1 (Liu *et al.*, 2022):

$$P(Xj) = \frac{P(Xi)\,xP(Xi)}{P(Xj)} \quad (1)$$

Where;

$P(X_i)$ is the probability of observing X_i;

$P(X_j)$ is the probability of observing X_j;

$P(X_i|X_j)$ is the conditional probability of X_i given X_j;

$P(X_j|X_i)$ is the conditional probability of X_j given X_i; and

$P(X_j|X_i) / P(X_j)$ is the Bayes factor.

The configuration and variables of a BN can be determined using the following approaches: (i) utilizing data, (ii) leveraging expert information, or (iii) integrating data with knowledge from experts (Kaikkonen *et al.*, 2021). Upon construction, a BN enables various types of inference, such as "forecasting inference," which elucidates the outcomes of an event based on its causes, and "diagnostic inference," which deduces the causes of a condition based on its effects (McLachlan *et al.*, 2019).

Factors influencing Go/No-Go demolition decisions

The decision to Go/No-Go for building demolition depends upon various interrelated factors, including building characteristics, retrofitting costs, demolition methods, environmental impact, owner constraints, and local government regulations. First, building attributes such as age, structural integrity, and material type are crucial. Structures that are aged and exhibit poor structural stability or include dangerous substances like asbestos are more prone to demolished. Retrofitting costs are also a significant consideration; buildings with high retrofitting costs are often more economical to demolish and rebuild (Higney and Gibb, 2024). The chosen demolition method, whether manual, mechanical, or chemical/explosive, affects environmental impacts like dust pollution, vibration, and noise (Chen *et al.*, 2021). Manual methods tend to produce less pollution but require more time and higher costs. In contrast, mechanical and explosive methods can cause significant pollution and vibration but are

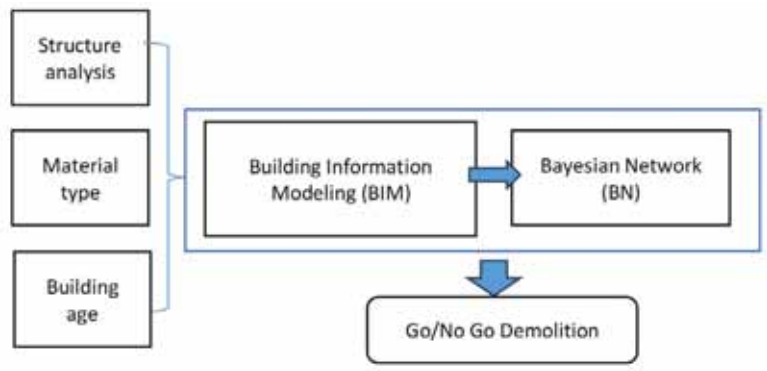

Fig. 1: Integration of BN and BIM framework

faster and more efficient (Eastman *et al.*, 2018). Owner constraints, including time and budget constraints, significantly influence this decision. Finally, compliance with local government permits and regulations is a nonnegotiable factor because every demolition project must meet safety and environmental standards (Zhao *et al.*, 2021). Taking all these factors into account, decisions regarding demolition should be made with caution to guarantee that the selected option is the safest, most cost-effective, and environmentally friendly.

Integration of BN and BIM framework

Multiple internal and external elements play a role in the decision to undertake demolition. Internal elements include the characteristics of the building, including its structural soundness, the type of materials, its age, and the financial implications of retrofitting (Kamissoko *et al.*, 2022). Information about these factors is obtained through BIM (Andriyani *et al.*, 2024). External factors include the demolition method used (manual, mechanical, chemical/explosive), environmental impact of demolition (dust, vibration, and noise) (Andriyani *et al.*, 2023), and government permits and regulations (Andriyani *et al.*, 2024). All these factors are then integrated through a BN to determine whether the building should be demolished, postponed, or not demolished at all. Merging building information from BIM with multiple facets from BN boosts decision-making, guaranteeing that demolition projects are efficient, safe, and environmental friendly (Fig. 1).

Combining a BN with BIM can provide a more holistic framework for decision-making in demolition projects. BIM provides data and visualizations of building structures, whereas a BN assesses related risks and uncertainties. As noted by Alavi *et al*. (2022), this integration facilitates a deeper examination of possible issues and provides more prompt and efficient solutions. Integrating the visualization benefits of BIM with the analytical power of BN empowers decision-makers to understand the full scope of the project, which includes potential risks and outcomes, leading to better-informed choices. Liu *et al.*, (2022) also mentioned that this integration provides a more comprehensive approach to managing uncertainty and risk, ultimately enhancing the effectiveness and efficiency of demolition project execution.

Proposed BN diagram

The BN in Fig. 2 depicts the decision-making process for building demolition by integrating various interrelated factors. Blue nodes indicate BIM and structural analysis outputs, while yellow nodes represent variables influencing decisions. The factors consist of structural integrity, types of materials, the age of the structure, and the expenses associated with retrofitting (Okoye *et al.*, 2023). The decision accounts for manual, mechanical, or chemical/explosive demolition methods and environmental impacts such as dust, vibration, and noise (Chen *et al.*, 2021). Manual methods produce less pollution but require more time and higher costs; mechanical and explosive methods generate more pollution and vibration but offer faster and more efficient execution (Eastman *et al.*, 2018). Owner limitations such as time and budget are also significant factors. Adhering to local permits and regulations guarantees compliance with safety and environmental standards (Zhao *et*

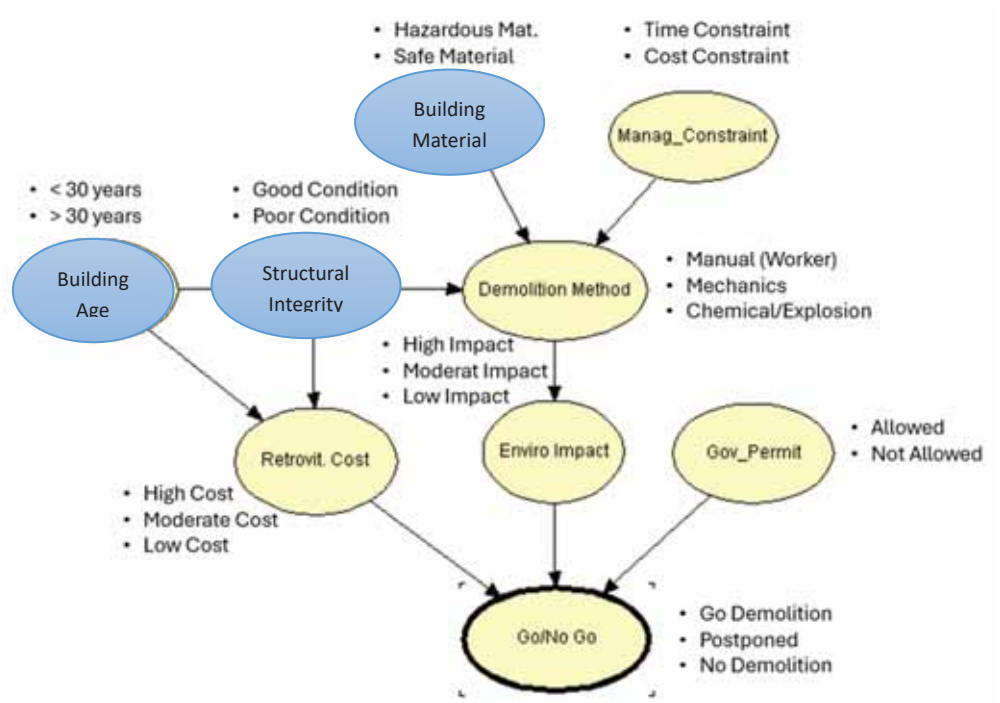

Fig. 2: BN diagram

al., 2021). This BN enables practical risk assessment and outcome prediction by mapping complex relationships visually and analytically.

Additionally, the age of a structure significantly influences its structural soundness and the cost-effectiveness of retrofitting. Structures that are older often exhibit more material wear, diminished energy efficiency, and greater maintenance requirements. Elevated long-term operational costs necessitate life cycle cost (LCC) analysis to determine retrofit viability. Demolition becomes cost-effective when retrofit expenses surpass reconstruction costs, especially for severely deteriorated buildings. The model's Retrofit Cost variable quantifies these cumulative financial burdens, incorporating structural decline and maintenance inefficiencies to support Go/No-Go decisions. Age influences structural conditions, which dictate the selection of demolition methods (Xiong *et al.*, 2019). Mechanised demolition suits sound structures, while compromised buildings require manual dismantling. Retrofit cost assessments, tied to age and condition, critically guide repair-or-demolish decisions (He *et al.*, 2021). Material composition plays a significant role in shaping strategy, with particular materials leaning towards manual or mechanical techniques based on considerations of safety and recyclability (Andriyani *et al.*, 2024). Budget and time limitations directly shape demolition method selection in public and private projects. The model encodes these as Management Constraints with two conditions: Time Constraints and Cost Constraints. Manual demolition suits are preferred in scenarios where costs are a primary concern, despite their extended execution durations. Conversely, mechanical demolition fits tight schedules due to faster operation and moderate environmental impact, especially in dense urban areas. Chemical or explosive methods execute fastest but incur the highest costs, ecological risks, and regulatory hurdles. These findings corroborate Ivanica *et al.*, (2022), who identified financial and scheduling pressures as primary determinants of demolition method choice. When choosing a demolition method, environmental considerations such as dust, vibration, and noise are also factored in to lessen negative impacts on the surrounding environment (Wu *et al.*, 2019). Economic assessments in demolition extend beyond retrofit cost to include waste handling, operational efficiency,

Table 1: Relationship between parent nodes and demolition method decisions (Kuzhin *et al.*, 2023)

Management constraint	Structural integrity condition	Building material	Recommended method
Time	Good	Safe	Mechanical
Time	Good	Hazardous	Manual
Time	Poor	Safe	Mechanical/Chemical
Time	Poor	Hazardous	Manual
Cost	Good	Safe	Manual
Cost	Good	Hazardous	Manual
Cost	Poor	Safe	Mechanical
Cost	Poor	Hazardous	Manual

Table 2: Relationship between demolition methods, and environmental impact (Zhu *et al.*, 2019)

Demolition method	Dust	Vibration	Noise	Environmenat impact
Manual	Low	Low	Low	Low
Mechanical	Moderate	Moderate	High	Moderate
Chem/explosion	High	High	Very high	High

and potential disruptions to adjacent activities. Although these factors are not separate variables, the 'Environmental Impact' category captures indirect financial and social effects, such as noise complaints, traffic delays, and community safety concerns. Official permits remain mandatory, defining demolition eligibility and identifying heritage-protected structures. Municipal authorities factor in social aspects—including resident displacement, safety concerns, and environmental disruptions (dust, noise, vibration)—when setting approval guidelines, particularly in densely populated regions. Public consultation also influences permit outcomes, as feedback or opposition can halt projects when safety or environmental risks emerge. Integration of these factors determines whether demolition proceeds are postponed or are deemed unnecessary. Decision-makers use BN to holistically evaluate diverse factors, enabling more comprehensive, efficient, safe, and environmentally sustainable demolition planning (Contreras Llanes *et al.*, 2021). IoT-based structural sensors feed real-time measurements of cracks, load variations, and other anomalies into the BIM environment. Environmental monitors report dust, noise, and vibration levels continuously. The 3D model integrates these live data streams for real-time visualization and contextual analysis. Administrative systems update permit status instantly in response to regulatory changes or public feedback. Project management tools adjust time and cost constraints on the fly. The BIM–BN model takes in all inputs to uphold adaptability, legal compliance, and alignment with safety and sustainability objectives during demolition planning phase.

Transitional and conditional probabilities in BN

Transitional probability in a BN describes the flow of probabilistic information between nodes, where each node is a random variable, and edges represent dependencies. This explains the transfer of probabilities between nodes through these connections. generally, the calculation employs the use of Bayes' theorem along with probability distributions (Kaplan *et al.*, 2023). This study's transitional probabilities were derived from subjective assessments by five experts in high-rise building demolition from academia and state-owned Indonesian construction firms. Probability values were calculated as the geometric mean of expert responses. The influence of parent nodes on the selection of demolition methods is depicted in Fig. 3.

The transitional probability matrix for demolition methods establishes logical relationships between building characteristics, management constraints, demolition techniques, and environmental impact. Table 1 links time-cost trade-offs, structural integrity, and material type to demolition method selection. Poor structural integrity (POOR_COND) and hazardous materials (HAZARDOUS_MAT) necessitate manual demolition for safety. Table 2 compares

Table 3: Pollution parameter limits (Hong *et al.*, 2020)

Type of pollution	Parameter	Limit	Measured method	Environmental impact
Dust	PM10 consentration	≤ 150 µg/m^3	High volume air sampler	Respiratory issues, decreased air quality
	PM2.5 Consentration	≤ 35 µg/m^3	Beta attenuation monitor	Healthy problems, reduced visibility
Vibration	Peak particle velocity (PPV)	≤ 5 mm/s (sensitive buildings) ≤ 10 mm/s (general)	Seismometer	Structural demage to building, discomfort
Noise Level	Noise level	≤ 85 dB	Sound level meter	Hearing loss, stress, sleep disturbance

Table 4: Transitional probability matrix result for demolition methods

STRUCTURAL_INTEGRITY	GOOD_COND				POOR_COND			
BUILDING_MATERIAL	HAZARDOUS_MAT		SAFE_MAT		HAZARDOUS_MAT		SAFE_MAT	
MANAG_CONSTRAINT	TIME_CONST	COST_CONST	TIME_CONST	COST_CONST	TIME_CONST	COST_CONST	TIME_CONST	COST_CONST
MANUAL	0.83	0.81	0.15	0.85	0.81	0.81	0.15	0.11
MECHANICS	0.12	0.14	0.82	0.1	0.14	0.14	0.62	0.82
CHEM/EXPLOSION	0.05	0.05	0.03	0.05	0.05	0.05	0.23	0.07

demolition techniques and environmental effects. By minimizing dust and noise, manual demolition promotes safer conditions for adjacent communities, but it necessitates additional time and labor, leading to higher costs. Explosive and mechanical methods accelerate demolition and reduce expenses, yet generate higher dust and vibration, posing risks to nearby structures and residents. The conclusions underscore the necessity of achieving a balance between environmental effects, public safety, and operational efficiency, with consideration for technical performance and the surrounding context. Table 3 defines regulatory thresholds for airborne particles, vibration, and noise exposure. Particulate matter less than 10 µm (micrometers) (PM10) ≤ 150 µg/m³ and particulate matter less than 2.5 µm (PM2.5) ≤ 35 micrograms per cubic meter (µg/m³) maintain air quality. Peak Particle Velocity (PPV) limits restrict vibration to 5 millimeters per second (mm/s) for sensitive structures and 10 mm/s for general buildings. Sound levels must remain below 85 decibels (dB) to comply with environmental guidelines. These specifications assist in the organization of demolition projects, ensuring a regulated impact on the environment

Table 4 consolidates data from the previous tables to show how demolition method selection probabilities vary by project conditions. Specialists with considerable experience in demolition formulated CPTs by evaluating the likelihood of techniques for predetermined situations. Estimates were aggregated using the geometric mean to reduce extreme-value bias and build consensus. Follow-up discussions addressed significant discrepancies, while validation compared CPTs against real case data, including structural degradation and retrofit costs. This validation process ensured that CPTs accurately reflected expert knowledge and real field conditions. Manual demolition had a high selection probability (0.81) under hazardous materials and financial constraints, prioritizing safety and environmental control. Conventional methods are still preferred in sound structures to lessen ecological effects and manage expenses. Mechanical demolition has taken precedence in environments without risks and tight deadlines, owing to its superior operational efficiency.

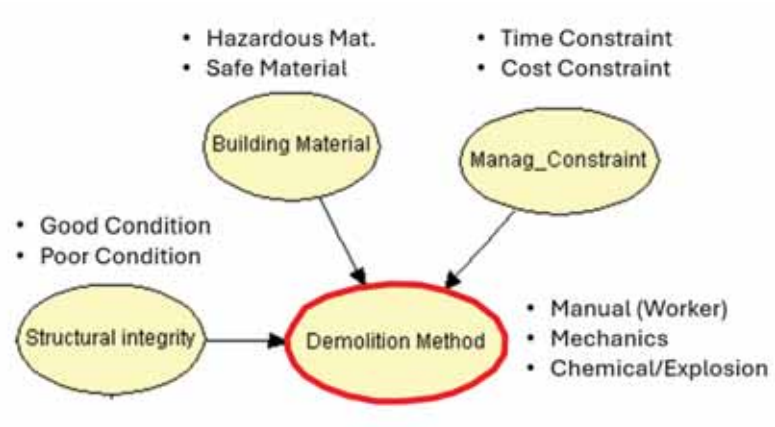

Fig. 3: Parent node used for selecting demolition method

Bayes factor
X1=P(Building Material)
X2=P(Management Constraint)
X3=P(Demolition Method | Building Material, Management Constraint, Structural Integrity)
X4=P(Building Age)
X5=P(Structural Integrity | Building Age)
X6=P(Retrofit Cost | Structural Integrity, Building Age)
X7=P(Environment Impact | Demolition Method)
X8=P(Government permission)
X9=P(Go/No-Go | Retrofit Cost, Environment Impact, Government Permission)

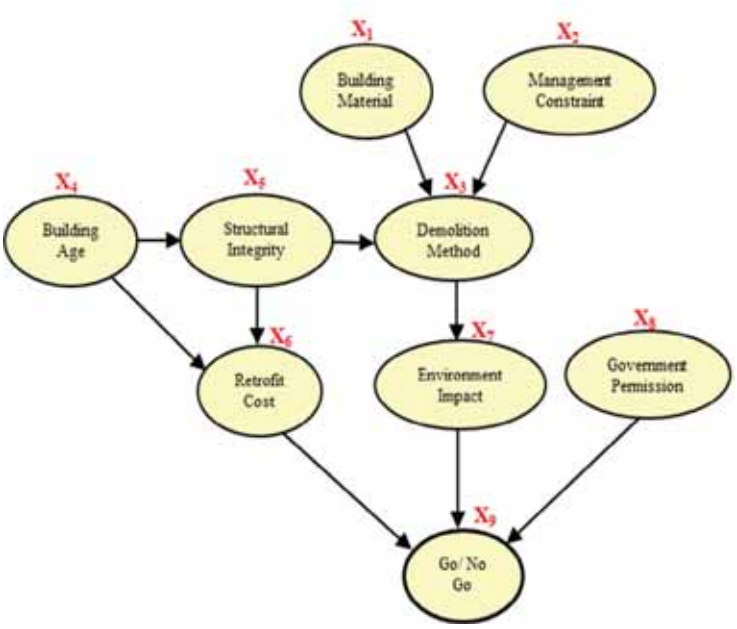

Fig. 4: Joint probability variables

Model inference in BN

Inference in a BN estimates unobserved variables using observed data (Marcot *et al.*, 2019). BN addresses inference problems by modelling probabilistic relationships between variables as graphs (Kitson *et al.*, 2023). The current study employs Bayes' theorem and a variable elimination algorithm for the purpose of inference. Incorporating observational data into a BN boosts decision-making accuracy and reliability, while inference supports precise, evidence-based predictions. Fig. 4 shows the BN joint probability structure, representing the likelihood of variable combinations co-occurring. Calculation multiplies each node's individual and conditional probabilities, accounting for network dependencies. This method enables a comprehensive assessment of factors influencing decisions. The analysis of joint probability facilitates precise assessment of possible outcomes and risks in various scenarios.

Eq. 2 demonstrates that calculating the joint probability of the entire network is the product of the individual and conditional probabilities of each node (Liu *et al.*, 2022).

$$P(X_1 = x_1, \ldots, X_n = x_n) = \prod_{i=1}^{n} P\left(x_{parent\,(i)}\right) \quad (2)$$

Where;

$P(X_1 = x_1, \ldots, X_n = x_n)$ is the joint probability distribution over all variables X_1 to X_n;

$\prod_{i=1}^{n} P\left(x_{parent\,(i)}\right)$ is a product of the probabilities of all parent variables for each node X_i

Therefore, the joint probability of the entire network (Eq. 2) in this study can be calculated as follows (Eq. 3):

$$P(X_1, X_2, X_3, X_4, X_5, X_6, X_7, X_8, X_9) =$$
$$P(X_1).P(X_2).P(X_3|X_1, X_2, X_5).P(X_4).P(X_5|X_4).$$
$$P(X_4, X_5).P(X_6).P(X_8).P(X_6, X_7, X_8) \quad (3)$$

This study employed BN simulations with Hun Lite (version 7), which is recognized for its user-friendly interface and robust probabilistic modelling capabilities. This software streamlines the input of CPT and the visualization of inferences, addressing the needs of academic modeling. Limitations include scalability constraints and lack of integration with external data sources like BIM. Subsequent studies ought to focus on examining open-source or customizable BN tools to boost interoperability and flexibility for extensive applications.

Case study as model implementation

The demolition target was a three-story market covering 918 square meter (m^2) in Pasar Manggis, South Jakarta, Indonesia. The structure, which is more than thirty years old, displayed notable structural damage resulting from the deterioration of materials and extensive environmental exposure. Located in a densely populated metropolitan area, safety and environmental impacts became primary concerns in demolition planning (Fig. 5).

The scenario was chosen to replicate authentic urban demolition circumstances, evaluating the BIM-BN model's capacity to manage structural damage, hazardous substances, regulatory requirements, and environmental hazards. As a high-risk demolition example in fast-urbanizing areas with limited documentation, it provided a valuable context for testing practical implementation. While confirmed through one case study, the BN structure continues to be versatile for different types of buildings and locations. Adjusting variables like structural conditions, materials, costs, environmental limits, and regulations allows the model to reflect local characteristics and account for variations in construction practices, policies, and risks. This flexibility supports broader application across urban environments and infrastructure types.

RESULTS AND DISCUSSION

In the Results and Discussion section, the validation of the proposed integration model, which combines BN and BIM for demolition decision-making, is presented through a real-world case study. The



Fig. 5: Demolition of a three-story market building

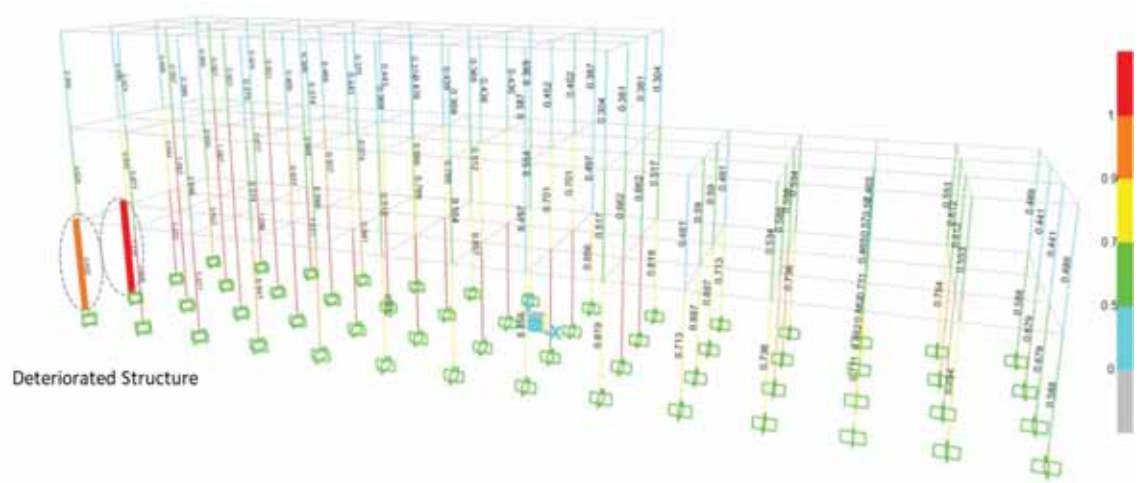

Fig. 6: Structural Integrity analysis result

evaluation involves structural condition analysis and material quantity assessment through BIM, followed by the inclusion of time and cost constraints to determine the most appropriate demolition method while addressing retrofit costs and environmental impact. To enhance validation beyond a singular instance, focus group discussions (FGDs) with contractors, consultants, building owners, and government representatives generated professional feedback on the model's applicability, interpretability, and consistency with field practices. The feedback indicate that the model adeptly merges technical, managerial, environmental, and regulatory factors, enabling broader applicability in various demolition contexts

Structural analysis result

Structural analysis using Structure Analysis Program (SAP)2000 software evaluated the integrity of the three-story market building (Fig. 6). The evaluation indicated considerable material degradation in structural components, highlighted by diminished strength and weakened joint connections. Colour-coded zones highlighted critical areas—yellow and red segments indicated elements unable to sustain design loads, with integrity values approaching 1.0, suggesting high failure risk. Structural assessment based on Indonesian national standards (SNI) 2847:2019 and SNI 1726:2019 identified several columns and beams that fell below safety thresholds, prompting the need for reinforcement or demolition. The analysis of economic, safety, and environmental aspects suggested that demolition is a more practical alternative than the high costs associated with retrofitting. By merging BIM-generated quantity take-off with BN analysis, it became possible to engage in predictive planning for material recovery, waste categorization, and impact alleviation. These findings align with Selim *et al.*, (2023), who reported long-term wear in reinforced concrete structures, and Wang and Lu (2024), who demonstrated BIM-based structural deformation tracking. The decision-support framework improves upon previous methods by integrating BIM visualization with probabilistic inference boost the accuracy of demolition planning.

BIM result

Integrating BIM and BN enhances sustainability in demolition planning by linking demolition waste quantification with risk-informed decision-making. BIM identifies and categorizes materials—such as concrete, reinforcing steel, bricks, and ceramic tiles—into reusable, recyclable, or residual types. BN then assesses the associated environmental impacts and recommends mitigation strategies based on waste type, volume, and project constraints. For example, high volumes of concrete combined with tight demolition schedules can increase environmental pressure and elevate overall impact levels. The integrated BIM–BN framework further optimizes waste transport schedules by aligning demolition sequences with quantified material outputs, thereby reducing landfill dependence and reinforcing circular economy goals. As depicted in Fig. 7, QTO details the

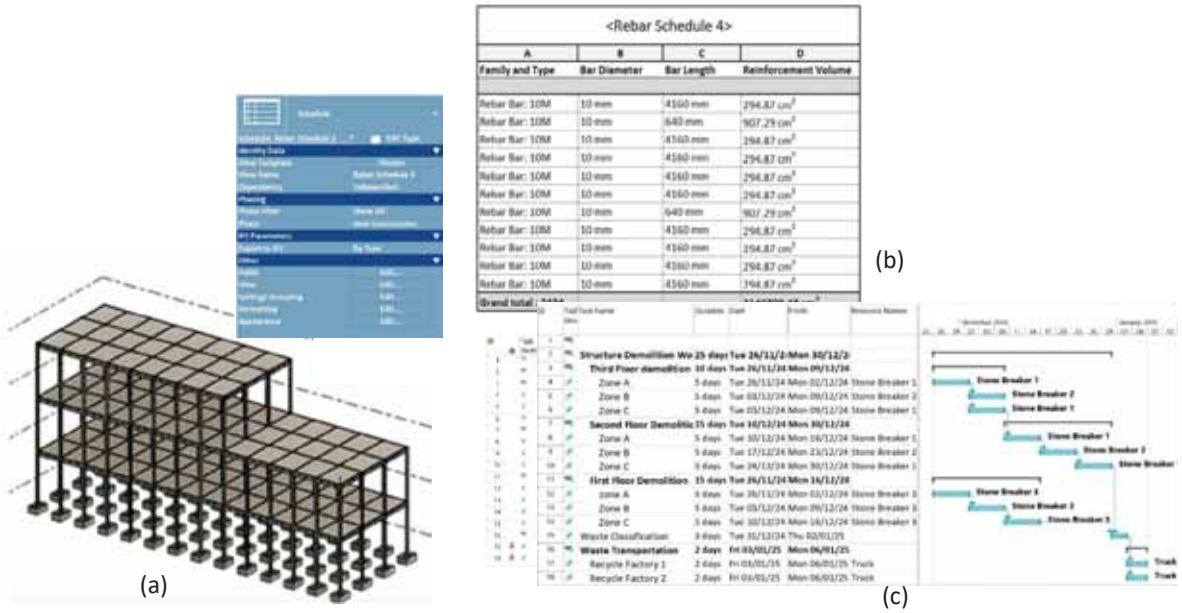

Fig. 7: BIM model for classifying (a), quantifying (b), and scheduling demolition waste (c)

various material types and their volumes, allowing for well-informed decisions about reuse, recycling, scheduling, and waste management.

Demolition activities contribute significantly to global solid waste, representing one of the most significant fractions of construction-related debris. According to Wijewickrama *et al.*, (2021), demolition accounts for nearly 50% of total construction and demolition (C&D) waste, highlighting the urgent need for effective material recovery strategies. Proper classification, handling, and diversion of these materials are essential to reduce environmental degradation, ease landfill burden, and lower carbon emissions. Based on BIM-derived quantity take-off (QTO) data, this study identified substantial volumes of recoverable materials, including 290 cubic meters (m^3) of recyclable concrete (comprising 136 m^3 from slabs, 95 m^3 from columns, and 59 m^3 from beams), 1,000 kilograms (kg) of reusable reinforcing steel, 32,055 kg of recyclable steel, 331 m^3 of bricks, and 918 m^2 of ceramic tiles. The integrated BIM-BN framework systematically categorizes these materials to support environmental impact assessments by evaluating recovery potential, material degradation, and final disposal outcomes. Unlike the study by Andriyani *et al.*, (2024), which concentrated only on waste composition in the context of the circular economy, this framework also includes structural conditions, material degradation, and environmental aspects in the demolition decision-making process. The model also captures post-demolition effects—such as landfill burden and transport-related emissions—through the "Environmental Impact" variable. Simulation results demonstrate improved accuracy in volume estimation and scheduling of waste disposal, which are typically lacking in conventional landfill-based methods. While a comprehensive life-cycle assessment is beyond the scope of this study, the framework lays the groundwork for future incorporation of carbon tracking and site rehabilitation strategies, thereby encouraging circular and sustainable demolition methods.

BN results for demolition decision

The BN simulation in Fig. 8 provides a comprehensive analysis of the interconnected probabilistic factors that influence the Go/No-Go decision for building demolition. The model integrates key parameters, including building age, structural integrity, retrofit costs, demolition methods, environmental impacts, and regulatory approvals. Every parameter is represented as a node, while directional arrows depicting the causal connections between variables. The BN model simulates these dependencies to

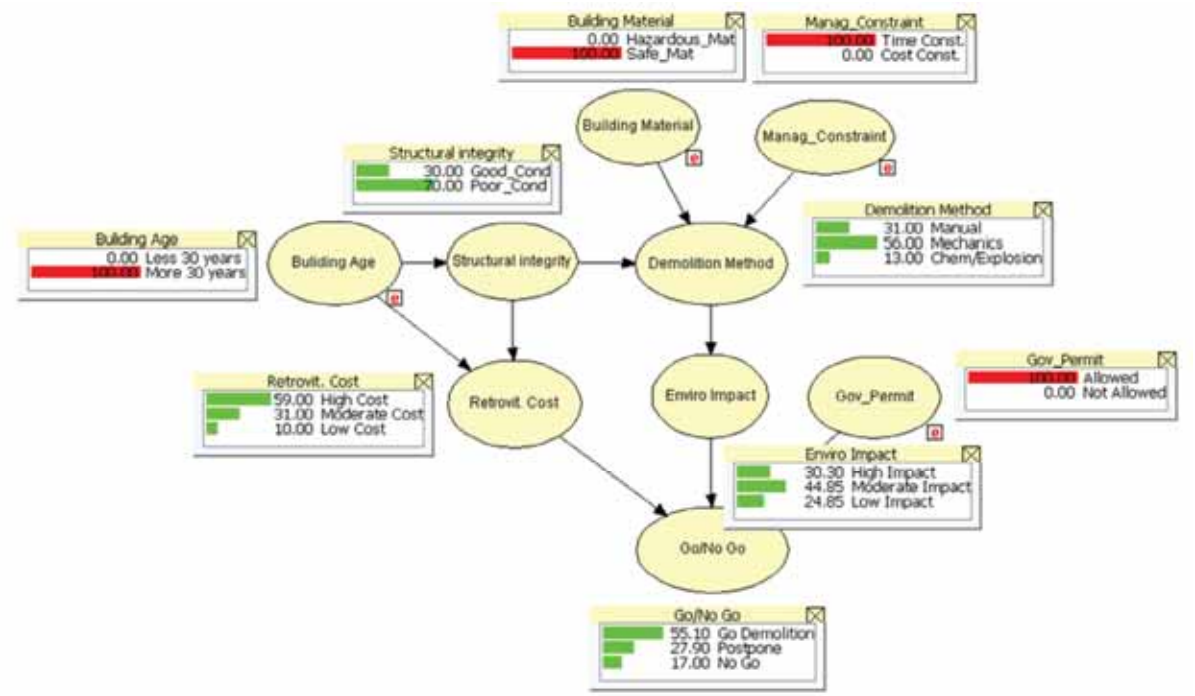

Fig. 8: BN simulation results for the Go/No-Go demolition decision

support a data-driven, risk-informed decision-making process that determines whether a building should be demolished, postponed, or retained.

Utilizing a data-centric method, this approach depicts the relationships among risks and facilitates better decision-making based on information. The following analysis elaborates on critical factors derived from the BN simulation and the influence of each factor on the final Go/No-Go decision:

1) *Building condition and structural integrity*

The analysis indicates that the building has been in use for more than 30 years, with a probability of 100 percent (%), which directly correlates with its structural integrity. A total of 70% of the building is classified as being in Poor Condition, while only 30% remains in Good Condition. This structural decline elevates the risk of collapse in buildings and markedly lessens their ability to resist loads and environmental force. As a result, safety considerations become the primary factor in the demolition decision.

2) *Retrofit costs and demolition alternatives*

High retrofit costs are another crucial factor to consider. The analysis reveals that 59% of retrofit scenarios require high costs, whereas only 10% fall under the low-cost category. This implies that restoring the building may not represent a cost-effective solution, especially in light of the substantial degree of structural deterioration

3) *Demolition methods and their impacts*

Mechanical demolition yields a 56% preference, manual methods 31%, and chemical/explosive methods 13 %. Additionally, mechanical demolition offers a safer alternative, ensuring that the potential hazards associated with manual or explosive techniques are minimized. Environmental impact distributes as moderate in 44.85% of scenarios, high in 30.30%, and low in 24.85%, necessitating implementation of mitigation strategies. Comparative assessment of dust, vibration, and noise levels across methods informs environmental planning. Manual methods lessen the impact but involve considerable labor. On the other hand, mechanical demolition hastens the removal, resulting in more dust and noise, thereby requiring water spraying and the installation of acoustic barriers.. Explosive demolition

Table 5. Demolition Methods, Environmental Impacts, and Recommended Mitigation (Zhao *et al.*, 2021; Zhu *et al.*, 2019)

Demolition method	Dust	Vibration	Noise	Recommended mitigation
Manual demolition (Handy tools)	Low	Very low	Low	Schedule during daytime, use of personal protective equipment (PPE) (e.g., masks), gradual waste handling and disposal
Mechanical demolition (excavator, hydraulic stone breaker)	High	High	High	Water spraying to reduce dust, acoustic barriers, restricted work hours, vibration and noise monitoring systems
Chemical/ Explosive Demolition	Very High	Very high	Very high	Site clearance, pre-blast simulation, dust containment covers, community alerts, installation of vibration and sound sensors

produces the highest risk profile, mandating site clearance and community notification. Alignment of each method with specific environmental outcomes and mitigation measures supports evidence-based demolition planning (Table 5).

4) *Regulatory and permit considerations*

One important factor in demolition decisions is government approval. The analysis shows a 100% probability that the required permit has been granted, meaning there are no regulatory barriers to the project. Additionally, these permits are essential in assessing the status of a building as a heritage site or its eligibility for removal from the public asset registry, directly impacting the approval of demolition activities. In this case, the results indicate that all legal requirements have been met, allowing the demolition to move forward in accordance with regulations.

5) *Final decision: Go/No-Go demolition*

The probability of Go Demolition reaching 55.10%, Postpone 27.90%, No Go 17%. The demolition decision was supported by poor structural conditions (70% Poor Condition) and high retrofit costs (59% High), making repairs uneconomical. Mechanical Demolition provides enhanced safety, efficiency, and a managed environmental footprint via waste management. The permit is approved by the regulator. The probability of delay (27.90%) arose from environmental management optimization efforts and retrofit benefit review. CPT in BN encodes expert probabilities for variable interactions, handling trade-offs. Probabilistic inference assesses the likelihood of a combined scenario, objectively resolving competing factors. The likelihood of Go Demolition remains elevated due to low environmental risks, inadequate structure, and substantial retrofit expenses. The structure of the model maintains a balance of data-driven decisions according to field conditions.

6) *Sensitivity analysis*

The sensitivity analysis in Fig. 9 and Fig. 10, highlights the most influential factors affecting the Go Demolition decision within the BN model. Key variables include retrofit cost, structural integrity, building age, environmental impact, and permit status. The sensitivity chart (Fig. 10) employs red bars to signify conditions that heighten the likelihood of demolition, while green bars represent those that diminish it. The highest demolition probability is observed when buildings are over 30 years old, structurally poor, and associated with high retrofit costs. Conversely, good condition and low retrofit costs tend to favor non-demolition. These results emphasize the model's ability to dynamically modify decision outcomes in response to changing inputs. By incorporating technical, regulatory, and environmental variables, the BN framework enhances decision accuracy and supports adaptive, evidence-based demolition planning under uncertainty.

BN model reveals key demolition decision factors: hazardous materials, time and budget constraints, and structural condition. This case study focuses on a three-story market building that is more than 30 years old and exhibits significant structural damage; it appears that mechanical demolition with heavy equipment is the most suitable approach, as it offers moderate dust, mild vibrations, and superior

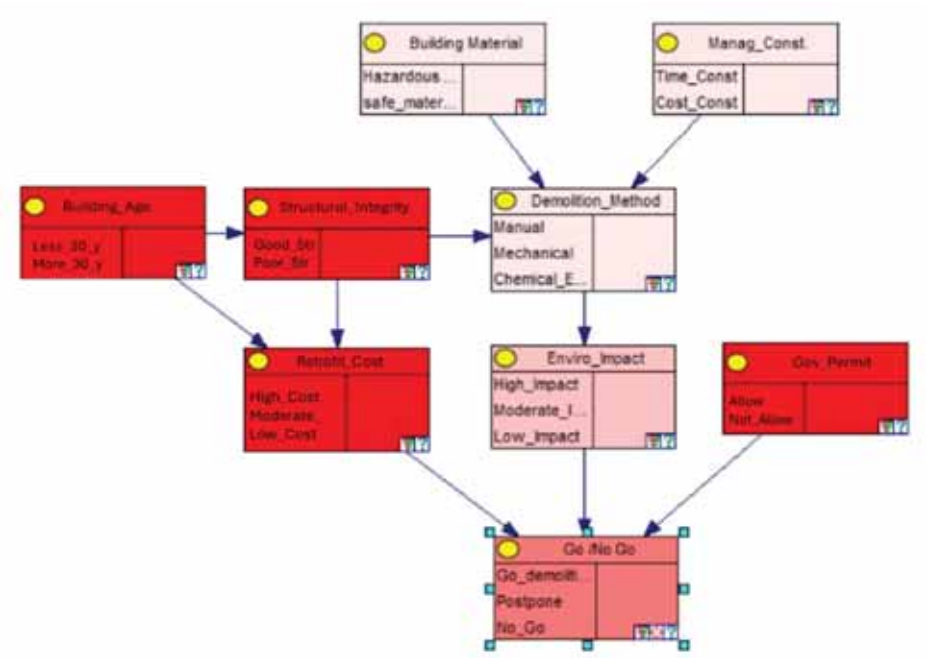

Fig. 9: Key variables influencing Go/No-Go demolition decision

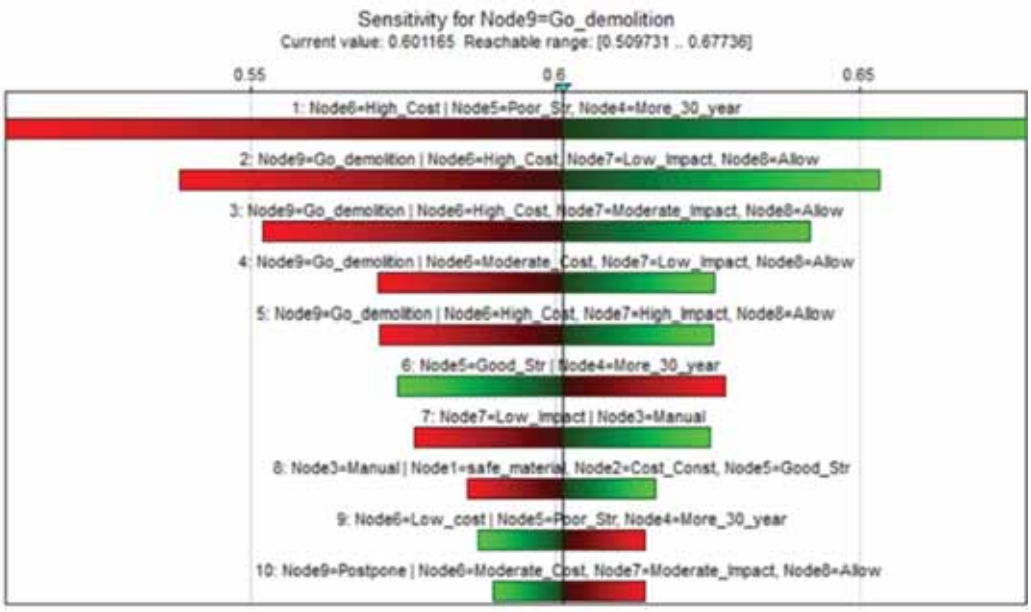

Fig. 10: Sensitivity analysis of demolition decision

noise control compared to the higher-risk options of blasting or chemical methods. The simulation indicates the highest selection probability for mechanical demolition under time constraints and moderate environmental risk. Operational efficiency, reduced labour intensity, and schedule adherence provide crucial advantages in dense urban zones. Manual demolition yields lower dust and noise

but demands more time and labour, rendering it unsuitable when speed and cost prevail. Manual methods remain viable under hazardous-material presence or stringent environmental restrictions. Trade-offs demonstrate the model's capacity to balance safety, ecological impact, and project performance. According to the BN simulation, there is a 55.10% chance for "Go Demolition," which aligns with the industry's preference for excavators and rock breakers. BIM integration delivers structured data on building conditions, demolition-material types and volumes, and execution sequence, enabling efficient material sorting, reuse, and recycling. Supplementary actions—dust control, noise management, vibration tracking—improve environmental effectiveness. Permit acquisition completes the framework, showcasing a public-private collaboration model for large-scale demolition projects. Sensitivity analysis adjusted each input parameter by 10% to gauge each variable's influence. The findings highlight retrofit expenses, the condition of the structure, the age of the building, environmental considerations, and the status of permits as major determinants in decision-making. Cultural or historical value variables remain excluded, with heritage considerations only via the permit variable reflecting government protection. Poor structural integrity coupled with high retrofit cost sharply increases demolition probability. Influence weights rank structural condition and retrofit costs highest. The economic rationale often renders retrofit on severely degraded structures unfeasible compared to demolition and rebuilding. Multiple risk factors further justify demolition. The BIM–BN framework delivers a probabilistic, dynamic sensitivity analysis that reduces reliance on expert judgment (Zhang *et al.*, 2021). It strengthens the depiction of uncertainty by associating 3D data modeling to risk-oriented decision analysis.

FGDs results

To assess the model's real-world applicability and practical value, a structured FGDs was conducted involving eight participants from four key stakeholder groups: contractors, consultants, building owners, and government officials. Each group evaluated the model based on three criteria: applicability, interpretability, and multidimensional coverage (technical, environmental, managerial, and regulatory aspects). In Table 6, the agreement rates and representative feedback from participants across four stakeholder groups are summarized, with averages of 86.25% applicability, 87.5% interpretability, and 89.75%-dimension coverage. Contractors validated the mechanical sequencing by comparing it with on-site workflows and actual waste volumes. Consultants lauded the clear presentation of cost-risk relationships and the metrics concerning structural integrity. Building owners cited precise budget insights and strong Go-Demolition justification. Government officials noted accurate environmental thresholds and permit-compliance outputs. Such consistently positive reviews affirm the model's technical robustness, contextual importance, and practical usefulness for urban demolition planning.

Table 6: Stakeholder feedback on the BN model for demolition decision-making

Stakeholder Group	Number of participants	Applicable (%)	Interpretability (%)	Dimension coverages (%)	Representative comment
Contractors	2	90	88	92	• Mechanical sequencing aligns with site operations. • Waste outputs match actual volumes.
Consultants	2	85	87	90	• Risk–cost probabilities are clear. • Structural metrics reflect engineering standards.
Building Owners	2	88	90	89	• Budget and schedule insights are precise. • Go-demolition justification is well supported.
Government Officials	2	82	88	92	• Regulatory limits are accurately represented. • Compliance flags expedite permit review.

Stakeholder feedback recognized model clarity in visualizing causal relationships and simulating real-world decision pathways. Mechanical demolition emerged as the most probable method (56%), followed by manual (31%) and chemical (13%), consistent with 70% structural integrity classified as "Poor" and 59% retrofit cost categorized as "High Cost." Assessments of material quantities and recognition of reusable elements facilitated environmental adherence and sustainable developmen. Hydraulic excavators and breakers offered optimal speed, safety, and efficiency for dismantling large reinforced structures. FGDs confirmed alignment with site operations (92%-dimension coverage by contractors), efficiency in processing concrete volumes (90%-dimension coverage by consultants), and compliance with noise and vibration thresholds (92%-dimension coverage by government officials). Simulation and sensitivity analysis substantiated the hypothesis that BIM–BN integration enhances objectivity, accuracy, and reliability of Go/No-Go decisions through probabilistic reasoning, BIM-based QTO data integration, and real-time updates. Ethical considerations in highly populated urban regions were incorporated into the "Environmental Impact" variable, highlighting public health concerns associated with noise, dust, vibration, and structural integrity. The "Permit" node addressed local government assessments of social risks. The BIM–BN framework thus advances socially responsible demolition planning within complex regulatory environments.

CONCLUSION

Integrating BIM and BN in this study offers a more objective, adaptive, and data-driven approach to demolition decision-making. In contrast to conventional methods like AHP or ANP that are significantly based on subjective evaluations from experts, the BN framework employs probabilistic reasoning to model uncertainty, thereby reducing cognitive bias and enabling dynamic scenario analysis. The model continuously adjusts decision outputs by leveraging BIM data based on evolving technical conditions, environmental risks, and regulatory factors. The case study of a three-story market building in Jakarta illustrates the model's practical applicability. Simulation and sensitivity analysis (±10% parameter variation) revealed that structural condition, building age, and retrofit cost are the dominant variables influencing Go/No-Go decisions. Furthermore, while the structural integrity was deemed acceptable, factors such as the presence of hazardous substances and budget limitations were found to change the preferred demolition technique from mechanical to manual. The result shows the model's efficacy in elucidating complex interactions among multiple variables. The integration of BIM improves material quantification, supporting recycling and waste reduction, while BN enhances decision quality by evaluating risks, costs, and environmental impacts under uncertainty. Together, these technologies enable informed, transparent, and sustainable demolition planning. The model's ability to adjust to changes in project scope or site conditions makes it particularly useful in ever-changing urban landscapes. A FGDs involving eight stakeholders—contractors, consultants, building owners, and government officials, was conducted to validate real-world applicability. Results showed high consensus, with mean agreement scores of 86.25% for applicability, 87.5% for interpretability, and 89.75% for multidimensional coverage. Participants affirmed that the model's results were in harmony with site practices and regulatory requirements, with feedback indicating that mechanical sequencing corresponded with operational workflows and that compliance-related outputs supported permit processes. While this study confirms the model's effectiveness in one case, broader validation is required. Future research should test its scalability across diverse building types, including heritage sites and industrial facilities, as well as in different regulatory environments. Extending the framework to integrate sustainability metrics—such as estimates of carbon footprints or indices for green demolition—and real-time data from IoT sensors may further improve its significance. In conclusion, this integrated BIM–BN framework establishes a robust foundation for modern, sustainable demolition planning by addressing uncertainty, improving accuracy, and supporting holistic decision-making.

AUTHOR CONTRIBUTIONS

T.J.W. Adi, the corresponding author, conceptualized the main idea of the research, designed the study, executed the scientific review, carried out experiments plus exploratory research, and composed the research paper. Y.P. Devia contributed to manuscript

drafting, provided critical revisions, and assisted in the discussion and critical analysis of the findings. N. Andriyani contributed to the exploratory work, data analysis, result interpretation, and preparation of the manuscript.

ACKNOWLEDGEMENT

This study was carried out in the Civil Engineering Department, Institut Teknologi Sepuluh Nopember (ITS), Surabaya, Indonesia; the Department of Civil Engineering, Brawijaya University, Indonesia; and the Research Center of Sustainable Production Systems Research and Life Cycle Assessment, National Research and Innovation Agency (BRIN), Serpong, Indonesia. This study did not receive specific funds from government, business, or non-profit funding agencies.

CONFLICT OF INTEREST

The authors confirm that there are no conflicts of interest related to the publication of this article. The authors have addressed ethical concerns such as plagiarism, informed consent, misconduct, data fabrication and falsification, multiple submissions and publications, and redundancy thoroughly

OPEN ACCESS

©2025 The author(s). This article is licensed under a Creative Commons Attribution 4.0 International License, which permits use, sharing, adaptation, distribution and reproduction in any medium or format, as long as you give appropriate credit to the original author(s) and the source, provide a link to the Creative Commons license, and indicate if changes were made. The images or other third party material in this article are included in the article's Creative Commons license, unless indicated otherwise in a credit line to the material. If material is not included in the article's Creative Commons license and your intended use is not permitted by statutory regulation or exceeds the permitted use, you will need to obtain permission directly from the copyright holder. To view a copy of this license, visit: http://creativecommons.org/licenses/by/4.0/

☐ Positive AI Statement

During the preparation of this work the author(s) have used Artificial Intelligence (AI) [NAME TOOL / SERVICE] in order to [REASON]. After using this tool/service, the authors reviewed and edited the content as needed and take full responsibility for the content of the publication.

(For this reason, the GPTZero detector will evaluate the manuscript utilizing Generative AI, ensuring a high detection rate. If the manuscript relies heavily on Generative AI and AI-assisted technologies, it will be archived without further options for appeal).

☑ Negative AI Statement

The author(s) declare that no AI tools or services were not used or not highly applied during the preparation of this work.

ABBREVIATIONS

%	Percent
3D	3-dimensional
AHP	Analytic hierarchy process
ANP	Analytic network process
BIM	Building information modeling
BN	Bayesian network
C&D waste	Construction and demolition waste
Cost_Const	Cost constraint
CPT	Conditional probability table
CPTs	Conditional probability tables
DAG	Directed acyclic graph
dB	Decibels
Fuzzy AHP	Fuzzy analytic hierarchy process
Fuzzy MABAC	Fuzzy multi attributive border approximation area comparison
Fuzzy MRCPSP	Fuzzy multimode resource constrained project scheduling problem
FGDs	Focus group discussions

Go/No-GO	Go or no-go
Good_Cond	Good structural condition
Hazardous_Mat	Hazardous materials
kg	Kilogram
LCC	Life cycle cost
MABAC	Multi attributive border approximation area comparison
Manag_Constraint	Management constraint
m^2	Square meter
m^3	Cubic meter
mm/s	Millimeters per second
µm	Micrometers
$\mu g/m^3$	Microgram per cubic meter
PM2.5	Particulate matter (less than 2.5 µm)
PM10	Particulate matter (less than 10 µm)
Poor_Cond	Poor structural integrity
PPE	Personal protective equipment
PPV	Peak particle velocity
PROMETHEE II	Preference ranking organization method for enrichment evaluation
$P(X_i)$	Probability of observing X_i
$P(X_j)$	Probability of observing X_j
$P(X_i \mid X_j)$	Conditional probability of Xi given Xj
$P(X_j \mid X_i)$	Conditional probability of Xj given Xi
$P(X_j \mid X_i) / P(X_j)$	Bayes factor
$P(X_1 = x_1, \ldots, X_n = x_n)$	Joint probability distribution over all variables X_1 to X_n
$\prod_{i=1}^{n} P(x_{parent(i)})$	Product of the probabilities of all parent variables for each node X_i
QTO	Quantity take-off
RCPSP	Resource constrained project scheduling problem
Safe_Mat	Safe material
SAP	Structure analysis program
SNI	Indonesian national standards
Time_Const	Time constraint

REFERENCES

Adi, T.J.W.; Andriyani, N., (2023). Model dekonstruksi bangunan berkelanjutan berbasis "reverse 4D BIM". PADURAKSA: J. Teknik Sipil Universitas Warmadewa, 12(2): 228-234 **(7 pages)**.

Alavi, H.; Bortolini, R.; Forcada, N., (2022). BIM-based decision support for building condition assessment. Autom. Constr., 135(2022): 104117 **(15 pages)**.

Andriyani, N.; Adi, T.J.W.; Suprobo, P.; Aspar, W.A.; Rachmawati, F.; Pradono, M.H., (2023). The framework of green deconstruction planning system in Indonesia: Maximizing the conservation of construction resources. AIP Conference Proceeding. 2847(1): 040007-1 – 040007-7 **(8 pages)**.

Andriyani, N.; Suprobo, P.; Adi, T.J.W.; Aspar, W.A.N.; Jatmiko, A.D.; Santoso, A.D., (2024). Integrating urban building information modeling and circular economy framework for green sustainability. Global J. Environ. Sci. Manage., 10(3): 1313-1332 **(20 pages)**.

Andriyani, N.; Adi, T.J.W.; Suprobo, P.; Aspar, W.A.; Widiyanto, A.; Firdana, F.; Yunus, A.F., (2024). The role of Building Information Modelling (BIM) in waste management deconstruction plan via 3D reconstruction model. AIP Conference Proceeding. 3069(2024): 020115-1 - 020115-9 **(10 pages)**.

Almujibah, H., (2023). Assessment of building information modeling (BIM) as a time and cost-saving construction management tool: Evidence from two-story villas in Jeddah. Sustainability, 15(9): 7354 **(26 Pages)**.

Ballesteros-Pérez, P.; Smith, S.T.; Lloyd-Papworth, J.G.; Cooke, P., (2018). Incorporating the effect of weather in construction scheduling and management with sine wave curves: application in the United Kingdom. Construct. Manage. Econ., 36(12): 666-682 **(18 pages)**.

Caglar, N.; Vural, I.; Kirtel, O.; Saribiyik, A.; Sumer, Y., (2023).

Structural damages observed in buildings after the January 24, 2020, Elazığ-Sivrice earthquake in Türkiye. Case Stud. Constr. Mater., 18: e01886 **(21 pages)**.

Chen, Z.; Abdullah, A.B.; Anumba, C.J.; Li, H., (2014). ANP experiment for demolition plan evaluation. J. Constr. Eng. Manage., 140(2): 06013005 **(4 pages)**.

Chen, K.; Wang, J.; Yu, B.; Wu, H.; Zhang, J., (2021), Critical evaluation of construction and demolition waste and associated environmental impacts: a scientometric analysis. J. Cleaner Prod., 287(2021): 125071 **(16 pages)**.

Contreras Llanes, M.; Romero Pérez, M.; Gázquez González, M.J.; Bolívar Raya, J.P., (2021). Construction and demolition waste as recycled aggregate for environmentally friendly concrete paving. Environ. Sci. Pollut. Res., 29: 9826–9840 (**15 pages**).

Davis, N.T.; Hoomaan, E.; Agrawal, A. K.; Sanayei, M.; Jalinoos, F.F., (2019). Foundation reuse in accelerated bridge construction. J. Bridge Eng., 24(10): 05019010 (**13 Pages**).

Ding, Z.; Wang, Y.; Zou, P.X., (2016). An agent based environmental impact assessment of building demolition waste management: conventional versus green management. J. Cleaner Prod., 133(2016): 1136-1153 **(18 pages)**.

Eastman, C.M. (2018). Building product models: computer environments, supporting design and construction. CRC press **(424 Pages)**.

Elmousalami, H.H., (2020). Artificial intelligence and parametric construction cost estimate modeling: state-of-the-art review. J. Constr. Eng. Manage., 146(1): 03119008 **(30 pages)**.

Fang, C.; Linzell, D.G., (2021). Examining progressive collapse robustness of a high-rise reinforced concrete building. Eng. Struct., 248: 113274 **(16 pages)**.

Gao, X.G.; Guo, Z.G.; Ren, H.; Yang, Y.; Chen, D.Q.; He, C.C., (2019). Learning Bayesian network parameters via minimax algorithm. Int. J. Approximate Reasoning, 108(2019): 62-75 **(14 Pages)**.

Han, D.; Kalantari, M.; Rajabifard, A., (2021). Building information modeling (BIM) for construction and demolition waste management in Australia: a research agenda. Sustainability. 13(23): 12983 **(22 Pages)**.

Han, D.; Kalantari, M.; Rajabifard, A., (2024). The development of an integrated BIM-based visual demolition waste management planning system for sustainability-oriented decision-making. J. Environ. Manage., 351: 119856 **(26 Pages)**.

He, Q.; Hossain, M. U.; Ng, S. T.; Augenbroe, G., (2021). Identifying practical sustainable retrofit measures for existing high-rise residential buildings in various climate zones through an integrated energy-cost model. Renewable Sustainable Energy Rev., 151(2021): 111578 **(21 Pages)**.

Higney, A.; Gibb, K., (2024). Net zero retrofit of older tenement housing–The contribution of cost-benefit analysis to wider evaluation of a demonstration project. Energy Policy. 191: 114181 **(11 pages)**.

Hoang, M.; Fujiwara, T.; Pham Phu, S.; Nguyen Thi, K., (2017). Predicting waste generation using bayesian model averaging. Global J. Environ. Sci. Manage., 3(4): 385-402 **(18 pages)**.

Hong, J., Kang, H., Jung, S., Sung, S., Hong, T., Park, H. S., & Lee, D. E. (2020). An empirical analysis of environmental pollutants on building construction sites for determining the real-time monitoring indices. Build. Environ., 170(2020): 106636 **(17 pages)**.

Hu, X.; Zhou, Y.; Vanhullebusch, S.; Mestdagh, R.; Cui, Z.; Li, J., (2022). Smart building demolition and waste management frame with image-to-BIM. J. Build. Eng., 49(2022): 104058 **(16 pages)**.

Ivanica, R.; Risse, M.; Weber-Blaschke, G.; Richter, K., (2022). Development of a life cycle inventory database and life cycle impact assessment of the building demolition stage: A case study in Germany. J. Cleaner Prod., 338(2022): 130631 **(12 Pages)**.

Kaikkonen, L.; Sutinen, K.; Tuominen, S.; Maijanen, P.; Luoma, J., (2021). Bayesian networks for environmental risk assessment: A review. Integr. Environ. Assess. Manage., 17(3): 456-469 **(17 Pages)**.

Kamissoko, D.; Gourc, D.; Marmier, F.; Clement, A., (2022). A go/no-go decision-making model based on risk and multi-criteria techniques for project selection. Int. J. Decis. Support Syst. Technol., 15(2): 1-21 **(21 Pages)**.

Kaplan, D., (2023). Bayesian Statistics for the Social Sciences, 2nd. Ed. Guilford Publications.

Khoshand, A.; Khanlari, K.; Abbasianjahromi, H., Zoghi, M., (2020). Construction and demolition waste management: fuzzy analytic hierarchy process approach. Waste Manage. Res., 38(7): 773-782 **(11 pages)**.

Kitson, N.K.; Constantinou, A.C.; Guo, Z., Liu, Y.; Chobtham, K., (2023). A survey of Bayesian Network structure learning. Artif. Intell. Rev., 56(8): 8721-8814 **(94 Pages)**.

Kuzhin, M., (2023). Ensuring safety during the demolition and dismantling of buildings. In E3S Web of Conferences. EDP Science, 457: 02009 **(12 pages)**.

Liu, N.; Hu, M.; Wang, J.; Ren, Y.; Tian, W., (2022). Fault detection and diagnosis using Bayesian network model combining mechanism correlation analysis and process data: Application to unmonitored root cause variables type faults. Process Saf. Environ. Prot., 164: 15-29 **(15 Pages).**

Marcot, B.G.; Penman, T.D., (2019). Advances in Bayesian network modelling: Integration of modelling technologies. Environ. Modell. Software, 111: 386-393 **(8 Pages)**.

McLachlan, G.J.; Lee, S.X.; Rathnayake, S.I., (2019). Finite

mixture models. Annu. Rev. Stat. Appl., 6(1): 355-378 **(24 pages)**.

Menegaki, M.; Damigos, D., (2018). A review on current situation and challenges of construction and demolition waste management. Curr. Opin. Green Sustainable Chem., 13: 8-15 **(8 Pages)**.

Morkunaite, Z.; Podvezko, V.; Zavadskas, E. K.; Bausys, R., (2019). Contractor selection for renovation of cultural heritage buildings by PROMETHEE method. Arch. Civ. Mech. Eng., 19: 1056-1071 **(16 pages)**.

Nesticò, A.; D'Ambrosio, G.; Ghisellini, P.; Maselli, G.; Ulgiati, S., (2024). Environmental reclamation of limestone mining sites in Italy: financial evaluation, challenges and proposals for sustainable development. Resour. Policy, 89: 104534 **(14 pages).**

Nikmehr, B.; Hosseini, M.R.; Wang, J.; Chileshe, N.; Rameezdeen, R., (2021). BIM-based tools for managing construction and demolition waste (CDW): a scoping review. Sustainability. 13(15): 8427 **(19 Pages)**.

Nowogońska, B.; Mielczarek, M., (2021). Renovation management method in neglected buildings. Sustainability., 13(2): 929 **(20 pages)**.

Okoye, J.U.; Apeh, S.T.; Olaye, E.; Osuji, S.O., (2023). Towards automation of building integrity tracking: review of critical causes and its Impact on building structures in Nigeria. J. Sci. Technol. Res., 5(2): 166-183 **(18 pages)**.

Patel, D.J.; Patel, D.A., (2023). Identification of potential demolition hazard attributes: an exploratory factor analysis approach. J. Leg. Aff. Dispute Resolut. Eng. Constr., 15(2): 04522061 **(12 pages)**.

Patel, D.J.; Ponnana, S.A.; Patel, D.A.; Patel, M.B., (2023). Development of a framework for risk assessment in building demolition works. J. Leg. Aff. Dispute Resolut. Eng. Constr., 15(3): 04523016 **(16 pages)**.

Patoghi, A.; Mousavi, S.M., (2021). A new approach for material ordering and multi-mode resource constraint project scheduling problem in a multi-site context under interval-valued fuzzy uncertainty. Technol. Forecasting Soc. Change. 173:121137 **(16 Pages)**.

Pellerin, R.; Perrier, N.; Berthaut, F., (2020). A survey of hybrid metaheuristics for the resource-constrained project scheduling problem. Eur. J. Oper. Res., 280(2): 395-416 **(22 pages).**

Roberts, R.E.; Okanya, O., (2022). Measuring the socio–economic impact of forced evictions and illegal demolition; a comparative study between displaced and existing informal settlements. Soc. Sci. J., 59(1): 119-138 **(14 pages)**.

Rodrigues, M.R.R.; Natal, J.; Polpo de Campos, C.; Dias Maciel, C., (2024). Conditional probability table limit-based quantization for Bayesian networks: model quality, data fidelity and structure score. Appl. Intell., 54(6): 4668-4688 **(21 pages)**.

Selim, M.; Ibrahim, Y.E.; Emara, M., (2023). Seismic retrofitting of a deteriorated RC building. Case Stud. Constr. Mater., 18(2023): e01758 **(12 pages)**.

Sopaheluwakan, M.P.; Adi, T.J.W., (2020). Adoption and implementation of building information modeling (BIM) by the government in the Indonesian construction industry. In IOP Conference Series: Mater. Sci. Eng., 930(1): 012020 **(12 pages)**.

TohidiFar, A.; Mousavi, M.; Alvanchi, A., (2021). A hybrid BIM and BN-based model to improve the resiliency of hospitals' utility systems in disasters. Int. J. Disaster Risk Reduct., 57(2021): 102176 **(13 pages).**

Wafiq, L.; Adi, T.J.W., (2016). Model alat bantu pengambilan keputusan metode demolisi pada proyek konstruksi. Master Thesis, Institut Technology Sepuluh Nopember, **(155 pages)**.

Wang, D.; Lu, H., (2024). Development of a BIM Platform for the Design of Single-Story Steel Structure Factories. Buildings, 14(3): 747 **(19 pages)**.

Waqar, A.; Othman, I.; Shafiq, N.; Deifalla, A.; Ragab, A.E.; Khan, M., (2023). Impediments in BIM implementation for the risk management of tall buildings. Results Eng., 20: 101401 **(18 pages)**.

Wijewickrama, M.K.C.S.; Chileshe, N.; Rameezdeen, R.; Ochoa, J.J., (2021). Minimizing macro-level uncertainties for quality assurance in reverse logistics supply chains of demolition waste. Sustainability. 13(23): 13069 **(35 pages)**.

Wu, H.; Zuo, J.; Yuan, H.; Zillante, G.; Wang, J., (2019). A review of performance assessment methods for construction and demolition waste management. Resour. Conserv. Recycl., 150: 104407 **(15 Pages)**.

Xiong, J.J.; Shenoi, R.A.; (2019). General aspects on structural integrity. Chin. J. Aeronaut., 32(1): 114-132 **(19 Pages)**.

Xu, J.; Li, L.; Ren, M., (2022). A hybrid ANP method for evaluation of government data sustainability. Sustainability, 14(2): 884 **(32 Pages).**

Yuan, Y.; Ye, S.; Lin, L.; Gen, M., (2021). Multi-objective multi-mode resource-constrained project scheduling with fuzzy activity durations in prefabricated building construction. Comput. Ind. Eng., 158: 107316 **(16 pages)**.

Zha, Q.; Zhou, W.; Gu, J., (2023). Time uncertainty and random opinion based group decision making for demolition negotiations. J. Oper. Res. Soc., 74(11): 2455-2471 **(17 pages)**.

Zhang, F.; Ju, Y.; Gonzalez, E.D.S.; Wang, A.; Dong, P.; Giannakis, M., (2021). Evaluation of construction and demolition waste utilization schemes under uncertain environment: A fuzzy heterogeneous multi-criteria decision-making approach. J. Cleaner Prod., 313: 127907. **(14 Pages)**.

Zhao, X., (2021). Stakeholder-associated factors influencing

construction and demolition waste management: a systematic review. Buildings. 11(4): 149 **(22 Pages)**.

Zhu, J.; Zheng, W.; Sneed, L.H.; Xu, C.; Sun, Y., (2019). Green demolition of reinforced concrete structures: Review of research findings. Global J. Res. Eng., 19(4): 1-18 **(19 pages)**.

Zou, Y.; Kiviniemi, A.; Jones, S.W., (2017). A review of risk management through BIM and BIM-related technologies. Saf. Sci., 97(2017): 88-98 **(11 pages)**.

AUTHOR (S) BIOSKETCHES

Adi, T.J.W., Ph.D., Associate Professor, Department of Civil Engineering, Sepuluh Nopember Institute of Technology, Surabaya, 60111, Indonesia.
- Email: *tri_joko@ce.its.ac.id*
- ORCID: 0000-0001-9303-1479
- Web of Science ResearcherID: NA
- Scopus Author ID: 5546802290Hom
- epage: https://scholar.its.ac.id/en/persons/tri-joko-wahyu-adi

Devia, Y.P., Dr. Eng., Lecturer at Department of Civil Engineering, Brawijaya University, Indonesia.
- Email: *yatnanta@ub.ac.id*
- ORCID: 0000-0001-8354-3008
- Web of Science ResearcherID: NA
- Scopus Author ID: 57200255989
- Homepage: https://sipil.ub.ac.id/sumber-daya-manusia/dosen/

Andriyani, N., Dr., Senior Researcher at Research Centre for Industrial Systems and Sustainable Manufacturing, National Research and Innovation Agency, Tangerang Selatan, 15314, Indonesia.
- Email: *nofa001@brin.go.id*
- ORCID: 0000-0002-6241-3869
- Web of Science ResearcherID: NA
- Scopus Author ID: 55906618400
- Homepage: https://brin.go.id/

HOW TO CITE THIS ARTICLE

Adi, T.J.W.; Devia, Y.P.; Andriyani, N., (2025). Integrating building information modeling and bayesian network for enhanced go/no go decisions in building demolition projects. Global J. Environ. Sci. Manage., 11(3): 1259-1280.

DOI: 10.22034/gjesm.2025.03.21

URL: https://www.gjesm.net/article_725008.html

Global J. Environ. Sci. Manage. 11(3): 1281-1298, Summer 2025, Serial #43

Global Journal of Environmental Science and Management
(GJESM)

Homepage: https://www.gjesm.net/

Podcasts

CASE STUDY

Sustainable approach for biocontrol of biostimulants derived from endophytic bacteria and seaweed extracts

Y. Suryadi[1,*], D.N. Susilowati[1], Wartono[1], Hanudin[1], E. Korlina[1], N. Gunaeni[1], E. Diningsih[1], M. Assad[1], S. Widawati[2], Suliasih[2]

[1] *Research Centre of Horticulture, National Research and Innovation Agency, Jl., Cibinong, Bogor, West Java 16911, Indonesia*

[2] *Research Center for Applied Microbiology, National Research and Innovation Agency, KST Soekarno, Jl. Raya Jakarta-Bogor, Cibinong, West Java 16915, Indonesia*

ARTICLE INFO

Article History:
Received 09 January 2025
Revised 14 March 2025
Accepted 19 May 2025

Keywords:
Endophyte
Fusarium oxysporum f.sp. cepae (Foc)
Shallot
Ulva sp.
Wilt

ABSTRACT

BACKGROUND AND OBJECTIVES: Shallot yields are significantly threatened by Fusarium wilt disease, caused by the fungus *Fusarium oxysporum* f.sp. cepae. Management strategies predominantly utilize synthetic fungicides along with established cultural techniques. To find a more sustainable and cost-effective alternative, this research explored the potential of microbial biocontrol. This study aims to evaluate the efficacy of a biostimulant mixture that includes a seaweed extract from *Ulva sp*. and two endophytic bacteria isolates (*Bacillus subtilis DK5 and Kosakonia* sp. DBS2) in controlling shallot wilt disease.

METHODS: The efficacy of this formulation was assessed by examining bacterial antagonism, fungal mortality rates, and the biostimulant's production capabilities.

FINDINGS: The results of this study highlight the promising capabilities of endophytic bacterial isolates, particularly *Bacillus subtilis* DK5 and K osakonia sp. DBS2 inhibits the growth of *Fusarium oxysporum* f.sp. cepae in vitro and suppresses wilt disease in shallot plants. Results demonstrated that the created biostimulants significantly inhibited pathogen growth across various concentrations. In vitro testing showed that a 2.5 percent biostimulant treatment led to a greater *Fusarium oxysporum* f.sp. cepae growth reduction than the control. Moreover, within greenhouse conditions, the treated group demonstrated a significantly lower severity of wilt disease (Probability ≤ 0.05) relative to the control group, implying that the biostimulant formulation was effective in controlling the disease.

CONCLUSION: These bacteria exhibited notable antagonistic properties and compatibility, making them suitable for incorporation into a biostimulant formulation. When combined with *Ulva sp*. extract, the biostimulant mixture not only reduced disease severity by up to 58.76 percent but also enhanced key agronomic parameters such as plant height, leaf number, clump weight, and tuber dry weight, most notably at the 3.5 percent concentration. The effectiveness of the biostimulant can be attributed to its antimicrobial properties as well as its ability to promote growth, which includes enhanced nutrient absorption and increased phytohormone synthesis.

This study provides promising evidence for the integrated use of microbial and seaweed-based biostimulants as a sustainable alternative for managing Fusarium wilt and improving the productivity of shallot cultivation within a greenhouse environment.

DOI: 10.22034/gjesm.2025.03.22

This is an open access article under the CC BY license (http://creativecommons.org/licenses/by/4.0/).

NUMBER OF REFERENCES
49

NUMBER OF FIGURES
4

NUMBER OF TABLES
4

*Corresponding Author:
Email: *yadi007@brin.go.id*
Phone: +62812 1947 7022
ORCID: 0000-0003-2790-7529

Note: Discussion period for this manuscript open until Sep 1, 2025 on GJESM website at the "Show Article".

INTRODUCTION

Indonesia ranks fourth as a shallot (*Allium cepa*) producer after New Zealand, France, and the Netherlands.

For smallholder farmers, shallot farming is the second most crucial agricultural activity after rice production, especially in the northern coastal regions of Subang, Indramayu (West Java), and Brebes (Central Java), significantly improving their quality of life. According to Indonesian agricultural statistical data, harvested areas were reported to increase by 1.54 percent (%) during 2019 compared to the previous year, with the total amount of shallot production in 2019 reaching 1.58 million tons and increasing to 1.81 million tons in 2020 (Central Bureau Statistic, 2021). *Fusarium oxysporum f.sp. cepae* (Foc) is one of the most prevalent fungal pathogens affecting roots and tubers, leading to root rot or wilt disease in shallots across Indonesia. These infections, caused by Foc, lead to a range of symptoms, including seedling blight and root hypocotyl rot, which have been observed under suitable environmental conditions and in susceptible cultivars. Other signs may involve color changes, necrosis, the presence of false stems, excessive leaf elongation, and yellowing. It has been reported that shallots are susceptible to fungal pathogens at different plant growth stages, and the seedling stage is very susceptible to pathogen infection. The prevalence of wilt and tuber rot during the initial growth period may cause yield losses ranging from 60% to 90%, underscoring the importance of implementing suitable control measures (Hanci, 2018). Many control efforts, such as the use of seed treatment, cultural practices, the planting of resistant cultivars, and pesticides, in agricultural goods have been applied to overcome pests. The over-application of chemical treatments, particularly synthetic fungicides, can jeopardize human health and environmental safety, leading to detrimental effects on living beings (Sintayehu *et al*., 2011; Manggala *et al*., 2023). Soil-borne diseases have also been controlled by the use of biocontrol techniques that employ biological control agents with different modes of action. It is crucial to establish efficient approaches to combat Fusarium wilt, especially for smallholder farmers. Endophytic bacteria are the most common microorganisms found in plant tissues; they do not harm plants and have potential antibacterial and antifungal properties (Katoch *et al*., 2014). Some endophytic bacteria, such as *Pseudomonas fluorescens*, *Bacillus* spp., and *Serratia marcescens*, have been reported to reduce disease caused by multiple cucumber pathogens (Raupach and Kloepper, 1998; Shafi *et al*., 2017). A previous study showed that some endophytic bacteria isolated from the shallot rhizosphere could suppress the growth of Foc. Alongside endophytes, biostimulants may be utilized to improve the efficiency of nutrient uptake in horticultural and food crops (Ali *et al*., 2021; Sandepogu, 2018). As a result, plant extracts with bioactive compounds, particularly alkaloids, flavonoids, and glycosides have demonstrated encouraging outcomes in preventing the spread of soil-borne diseases (Rafiee *et al*., 2016). Several studies have explored the antibacterial and antifungal properties of seaweed extracts. The diverse algal extract also demonstrates antifungal action (Pourakbar *et al*., 2021; Noorjahan *et al*., 2022). *Ulva* sp., in particular, is a common genus of green algae grown in coastal regions. Belonging to the Chlorophyta division, it possesses antioxidant, antibacterial, antifungal, and antitumor characteristics, which may be linked to the presence of compounds including phenolic, sterol (ergosterol), and polysaccharides (Domínguez and Loret, 2019). It has been reported that sea lettuce ethanol extracts can inhibit fungal growth (Rouphael and Colla, 2020; Dominguez and Loret, 2019; Bhattacharyya *et al*., 2015). Although many optimistic findings exist concerning the biocontrol of soil-borne pathogens in shallots, there is a significant lack of documentation on the role of seaweed algae in managing wilt disease (WD) induced by Foc. Hence, this study hypothesizes that *Ulva* sp. combined with endophytic bacteria can effectively suppress Foc and reduce shallot wilt disease severity, offering a more environmentally friendly approach for Indonesian farmers. Therefore, the objective of this study is to investigate the effectiveness of a biostimulant mixture of *Ulva* sp. and endophytic bacteria in controlling shallot WD. Utilizing this blend for soil drenching and foliar application aims to establish a sustainable crop management approach that mitigates shallot wilt disease while improving overall yield. This study has been conducted in the greenhouse (GH) of Biotechnology Standardization and Instrumentation, Bogor, West Java, in the planting season in 2022.

MATERIALS AND METHODS

Preparation of material sources and site location study

The shallot tubers of cultivar (cv.) 'Bima' were obtained from the Brebes region, while *Ulva* sp. was obtained from the coastal region of Bayah, Banten, Indonesia (6°56'10.8924", 106°14'35.3364"). The experiments were conducted in the microbiology laboratory and GH of Bogor, West Java, Indonesia (6°34'31.044", 106°47'10.464", 221 meters (m) above sea level). During the dry season, the average temperature in GH ranges from 24 to 32 degrees Celsius (°C).

Laboratory assay (in vitro)

Bacterial and fungal preparation

The bacteria used in this study were isolated from shallot roots. Following sterilization with sterile water and 96% alcohol, the samples were pulverized using a mortar and pestle. The finely ground chives were cultivated on nutrient agar (NA) media, diluted with 10 milliliters (mL) of distilled water, and incubated for twenty-four hours. A single colony of bacteria was used to purify the bacteria on agar plates. Cultures of slimy isolates were subsequently grown and maintained at room temperature for a duration of three days. In this study, the selected bacterial endophyte isolates were identified as *Kosakonia* sp. DBS2 and *Bacillus subtilis* DK5. The bacteria were freeze-dried in ampoules at -80 °C and kept with 25% glycerol cryoprotectant. To utilize the culture, bacterial cultivation is performed using nutrient agar medium preserved with glycerol. A fungal isolate known as Foc UBS 3 was derived from a shallot displaying symptoms of WD. The pathogen was subsequently grown on potato dextrose agar (PDA) for 7 days at 25 °C, after which it was purified by growing fungal mycelium colonies on PDA media until fungal hyphae formed; afterward, the fungal hyphae were incubated for 5-7 days at room temperature (Caligiore-Gei *et al*., 2014).

Selection for antagonistic assay and bacterial isolate compatibility test (synergistic assay)

An antagonistic test against Foc was carried out utilizing a dual culture assay in a Petri dish with a diameter of 9 centimeters (cm) using PDA media to identify possible antagonistic-endophytic bacteria. Discs of fungus, each 5 millimeters (mm) in diameter, derived from seven-day-old cultures, were arranged on the opposite side of the Petri plates at a right angle to the bacterial streaks, with the bacterial colonies being streaked on one side of the dish. Petri dishes inoculated with fungi alone served as controls. The observation was performed by measuring the radius of the fungal pathogen colonies (Kalimutu *et al*., 2020), whereas the degree percentage of inhibition (I) of endophytic bacteria against Foc was determined using Eq. 1 (Li *et al*., 2003):

$$I = \frac{R1 - R2}{R1} \times 100\% \quad [1]$$

Where, I = percentage of inhibition; R1 = Foc radius as opposed to endophytic bacterial colonies; and R2 = Foc radius facing endophytic bacterial colonies.

Compatibility tests were carried out to make a mixture of endophytic bacteria, and if the endophytic bacteria were compatible or synergistic, they could be used together in mixed cultures. The procedure consisted of applying 2-3 various endophytic bacterial isolates onto NA media in a two-compartment Petri dish. The clearing zone was seen when the plates were incubated for 24 to 72 hours (h). In the presence of antagonist activity, the bacteria are clearly separated and do not interact with each other. The endophytic bacteria can be further combined if there is no distinct zone since they are compatible or synergistic (Dinata *et al*., 2021).

Preparation of the seaweed (Ulva sp.) extract

A field-collected sample of Ulva sp. was processed in the laboratory. The 1 kilogram (kg) of healthy materials was chopped into fine powder, dried in an oven, and cleaned with hot water. Seaweed was extracted using a drying process. In brief, 250 mL of distilled water (dH_2O) (1:5) weight per volume (w/v), was mixed with 50 gram (g) of seaweed powder, and the mixture was then centrifuged (Sorval-Legend Micro 21; Thermo Scientific). After mashing the mixture, Whatman #1 filter paper was used to filter it. Following filtration with a Millipore 0.22 micrometer (µm) filter paper, the filtrate was permitted to stand at room temperature (27 °C). The dried seaweed extract was suspended in dH_2O, and the remaining supernatant was stored (4 °C) until further use.

Preparation of biostimulant mixtures

The selected synergistic endophyte isolates (*B.*

subtilis DK5 and *Kosakonia* sp. DBS2) were cultured in 10 mL of nutrient broth (NB) media, homogenized using a shaker (IKA K-260), and incubated for 1-2 days at room temperature. Furthermore, 100 mL of NB media was utilized to culture 5 mL of each isolate, followed by a two-day incubation period. The formula for the microbe-based biostimulant was made by combining the following ingredients: 5% of a 48-h-old bacterial culture, 40 mL of seaweed extract solution as potential of hydrogen (pH) = 6.8, 80 mL of fructose, 5 mL of humic acid, 10 mL of 10% glycerol, and sterilized micronutrient stock. For 15 minutes, a magnetic stirrer was utilized to combine the materials in a 5-liter Erlenmeyer flask, producing a consistent liquid. The biostimulant was then diluted by dissolving it in dH_2O at concentrations of 1.5%, 2.5%, and 3.5% using dH_2O that had been sterilized following the procedures.

Effect of biostimulant mixtures on the mycelial growth of Foc (in vitro) and Biostimulant combination application on Foc mycelial growth (in vitro)

In 200 mL bottles with PDA, the selected biostimulants of *Ulva* sp. 1:1, volume per volume (v/v), and endophytes were well combined before being transferred into a 9 cm Petri plate. Cultures that were 7 days old and actively developing were utilized to create a 5 mm diameter disk of Foc, which was subsequently placed at the center of PDA Petri plates containing biostimulant-modified material. The plates were then cultured for seven days at 25 °C. The fungal infections were grown alone to create control treatments (non-amended PDA). After seven days, the fungal growth diameter was measured and used to determine the fungal growth inhibition (GI), using Eq. 2 (Sarven *et al*., 2020):

$$GI = \left[\frac{T}{C} - 1\right] \times 100\% \quad [2]$$

Where, T is the average fungal colony diameter in the treatment, C is the average fungal colony diameter in the control, and GI is growth inhibition (Hlokwe *et al*., 2020).

The lethal concentration-50 (LC_{50}) was calculated using probit analysis (Chandra *et al*., 2014). To assess their defense activity against Foc, bioassays of biostimulant mixtures (*Ulva* sp. plus endophytic bacteria) were performed using various gradient concentrations (5%, 3.5%, 2.5%, 1.5%, 0.75%, and 0.375%).

GH experiment

Plant preparation and fungal inoculation on shallots

The GH experiment employed 30 polybags measuring 25 cm in diameter, organized into five treatments with six replications each. Before planting, all polybags filled with soil medium were positioned in a greenhouse, ensuring a 5-by-5 cm gap between them, followed by the addition of 2.5 kg of sterile soil into each. After 20 discs of a 7-day-old Foc isolate were inoculated into autoclaved PDA medium and cultured for 14 days at 25 °C, *Fusarium* sp. was artificially inoculated into the soil medium. The pathogen was given one week to establish itself within the soil. The early-stage maturity of the shallot tuber cv. 'Bima' was buried with soil 3/4 of the way, with the bud facing upward. Three tubers, spaced about 5 cm apart, were placed in each polybag. The suggested amounts of inorganic fertilizers include urea at 0.3325 g, SP-36 at 0.1042 g, and potassium chloride (KCl) at 0.165 g for each soil medium. The first urea treatment at 7 days after planting (DAP) was applied along with KCl or SP-36 at all rates. Three centimeters from the plant's edge, the fertilizer was misted on.

Biostimulant treatment, disease assessment, and agronomic parameter observations

The biostimulant extracts were tested for pathogen growth suppression in vitro at concentrations of 1.5%, 2.5%, and 3.5% in 1000 mL of dH_2O. The positive control was established with a commercial fungicide (mancozeb) at a concentration of 2.5%, while the negative control was maintained without any treatment. When the plants were 14, 28, or 42 days old, the biostimulant formula was applied using soil drenching treatment every two weeks, while the soil was soaked with the biostimulant solution before planting. A volume of 100 mL of tap water was utilized for irrigation of the polybags assigned to both the biostimulant treatment and the control treatment every three days. The Rengwalska and Simon (1986) method was used to assess disease severity using a five-point rating system: 1 representing no symptoms (0%), 2 representing rotted roots (<10%), 3 representing 10-30% rotted roots, 4 representing completely rotted roots (10-30%), and 5 representing completely rotted roots (>30%). The efficacy of the

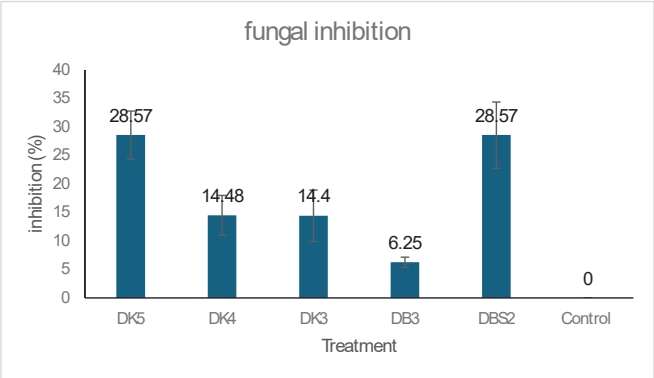

Fig. 1: Effect of selected endophytic bacterial isolates on Foc growth inhibition on PDA (in vitro). Vertical bars correspond to standard deviation (SD)

biostimulant treatment was evaluated for disease suppression (DS), using Eq. 3 (Ponsankar *et al*., 2023):

$$DS = \left[\frac{T}{C} - 1\right] \times 100\%, \quad [3]$$

Where, DS = disease suppression, T = treatment, and C = untreated control.

The height of the shallot plants was recorded weekly using a ruler, starting from two weeks to six weeks after planting (WAP). To determine the cumulative area under the plant height progress curve (AUHPC), using Eq. 4 (Simko and Piepho, 2012):

$$AUHPC = \sum_{i=1}^{n-1} (ti + 1 - ti)\left(\frac{yi + yi + 1}{2}\right) \quad [4]$$

Where, t is the observation period (days), y is the parameter plant height at the ith observation, n is the total number of observations, and AUHPC is the area under the plant height progress curve. The leaves on the shoot plants were counted on a weekly basis. Shallot plants were harvested by removing them from the soil and washing them. Shallot postharvest processing involved determining tuber counts, followed by a drying step. Upon completion of a three-day drying at 80 °C in an oven, the dried material was weighed, and the number of tubers and clump weight were evaluated.

Analysis of data

A completely randomized design (CRD) was utilized for the experiment, and analysis of variance (ANOVA) was performed on the data using Statistical Package for the Social Sciences (SPSS) software version 16. The application of Duncan's multiple range test (DMRT) aimed to assess the differences between the various treatments. A 5% probability threshold (P< 0.05) was applied while calculating the mean separation.

RESULTS AND DISCUSSION

Effect of bacterial isolates against the fungus Foc in vitro

The results of the bacterial screening of the isolates were tested in vitro on PDA media. Five endophytic isolates, namely, DK5, DK4, DK3, DB3, and DBS2, were obtained from the phyllosphere of the shallot cv. Bima', which inhibited the growth of Foc. Isolates DK5 and DBS2 exhibited a greater percentage of inhibition (28.57%), whereas the DB3 isolate had the lowest rate of inhibition (6.25%) (Fig. 1).

Consequently, the DK5 and DBS2 isolates were chosen for further use in the formulation of the biostimulant mixture. The identified isolates include *B. subtilis*, a gram-positive bacterium, and *Kosakonia sp*., a gram-negative bacterium. All the isolates produced enzymes i.e., glucanase (glucanolytic index ranged 0.61 – 0.80) and chitinase (chitinolytic index ranged 0.63 – 0.64). The presence of a clearing zone in the antagonism experiment indicates that interactions between microorganisms in shared habitats, particularly competition for nutrients, inhibit the growth of the pathogenic fungus (Müller *et al*., 2018; Rengwalska and Simon, 1986). The level of inhibition is influenced by the nature and

Table 1: Effect of the biostimulant concentration on the lethal concentration (LC_{50}) of Foc

Treatment	LC_{50} (mL/L)[a]	95% confidence Interval	Slope ± SE	Intercept	χ^2 (chi sq)
Biostimulant	2.415	0.822 – 7.095	0.688 ± 0.239	4.737	0.966

[a]LC_{50} values were significantly different (P≤0.05) based on Probit analysis.

stability of the metabolites produced by bacteria to control fungal expansion. Endophytic bacteria have the ability to inhibit fungal growth by producing antibiotic substances, such as volatile compounds that permeate the surrounding environment (Joshi *et al*., 2013). Beneficial bacteria, such as *Bacillus subtilis* DK5 and *Kosakonia* sp. DBS2, controls plant diseases via a complex network of molecular interactions and mechanisms that limit pathogen growth while increasing plant health. Both of these microorganisms provide biocontrol effects through a variety of mechanisms, including direct pathogen inhibition (by antimicrobial chemical production), promotion of plant defenses, and microbial competition to reduce Fusarium wilt and other diseases. The collaboration of these microorganisms enhances their ability to suppress pathogens and promote plant health, thereby making them essential elements of an integrated pest management (IPM) approach. Compatibility between microbial strains is critical not only for disease suppression but also for the stability and functionality of microbial consortia in field circumstances.

Effect of biostimulant mixture and bacterial synergistic assay on the in vitro mycelial growth of Foc

The compatibility and synergism of the antagonistic endophytic bacterial isolates were examined to determine whether they interacted with each other. The findings indicated that only the *B. subtilis* DK5 and *Kosakonia* sp DBS2 isolates exhibited compatibility, as they did not produce a clearing zone following 24-48 hours of incubation at 30 °C on NA media. The Probit analysis, as shown in Table 1, revealed that the biostimulant mixtures (*Ulva* sp. plus endophytic bacteria) at various concentrations (5%, 3.5%, 2.5%, 1.5%, 0.75%, and 0.375%) had LC_{50} values of 2.415 mL/L. The result also exhibited significantly different slopes (0.688) (chi square ($\chi 2$) = 0.966, degree of freedom (DF) = 4, P ≤ 0.05).

Biostimulant formulations at various concentrations inhibited the growth of Foc on PDA media after eight days of incubation. All biostimulant concentrations resulted in reduced mycelial growth of Foc compared to the control group. Mycelial growth was more inhibited at higher biostimulant doses. Ensuring bacterial compatibility or synergism is essential for effective co-application and beneficial effects on plant growth without adverse interactions. Bacterial synergy is influenced by factors like the ability of one genus member to provide essential nutrients, degrade otherwise indigestible organic matter, or protect other sensitive genus members from harmful organic materials (Dinata *et al*., 2021; Deng and Wang, 2016). Typically, there is a concentration of biostimulant that optimally balances controlling diseases and fostering plant growth. This optimal concentration is usually found through dose-response studies, in which several application rates of the biostimulant are tested under controlled or field circumstances to assess their impact on plant health and disease severity. In such studies, various concentrations are applied to shallot plants that are infected or at risk of Fusarium wilt. For example, in a typical trial, a 2.5% concentration of a microbial-based biostimulant could lower disease severity by 60-70% while increasing bulb production by 30-40% compared to untreated controls. However, levels above 4% might not provide further benefits in disease reduction and may negatively influence growth as a result of nutritional or microbial imbalances. The optimal concentration is thus defined as the rate at which maximal or near-maximum disease suppression and growth benefit are obtained while producing no negative effects. Analytical tools including ANOVA and regression analysis are utilized to assess the importance of treatment effects and ascertain which concentration delivers the best overall results.

Effect of biostimulant formulation on the disease suppression of shallot caused by WD

Concentrations of 3.5%, 2.5%, and 1.5% were selected for further application in the GH experiment because of their similar degrees of inhibition. Shallot

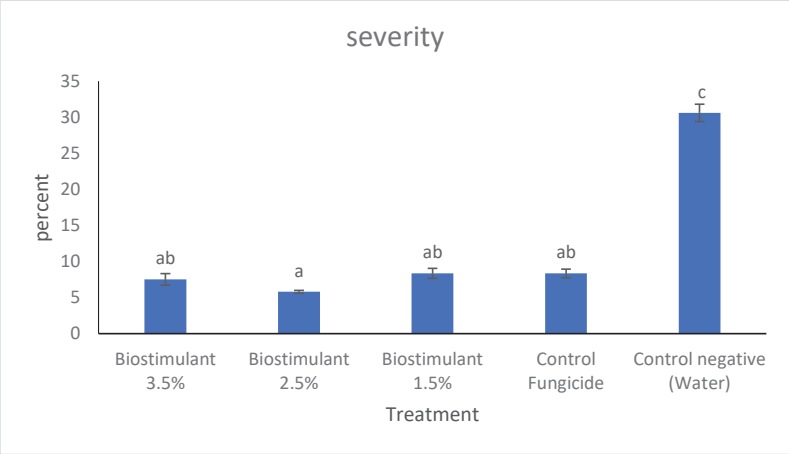

Fig. 2: Effect of biostimulant concentration on WD severity. Different letters on bars indicate significant differences according to DMRT ($P \leq 0.05$). Vertical bars correspond to SD.

plants may exhibit symptoms like wilting at the leaf tips, yellowing, and eventual death. The disease severity of wilt caused by Foc in the treatments ranged from 5.8% to 8.35% (Fig. 2). Different concentrations of the biostimulant (endophytes and *Ulva* sp.) exhibited varying effects, ranging from low to high suppression of WD severity. The effectiveness of disease suppression was assessed in comparison to an untreated control to verify the differences among treatments (Fig. 3).

Significant differences were found among biostimulant concentrations in their ability to reduce wilt severity. The DS values ranged from 40.9% to 58.76%. Despite these variations, the treatments had greater suppressive effects than the control. For instance, the biostimulant at a concentration of 1.5% significantly reduced wilt by 40.98%, while the largest reduction of 58.76% was recorded at a concentration of 2.5% (Fig. 3). Despite the lack of a clear change at a 1.5% concentration relative to the control group, the three biostimulants studied exhibited a marked effectiveness in mitigating Fusarium wilt during the greenhouse trial. The study's primary focus was on controlling Foc-induced WD in shallots. In addition to Fusarium wilt, shallots are vulnerable to a variety of other soil-borne pathogens and foliar diseases, which could have been influenced by the biostimulant's impact study. However, common diseases such as downy mildew (*Peronospora destructor*) and the bacterial pathogen *Pseudomonas* spp. were not detected during the investigation. Determining whether the biostimulant can indirectly safeguard against fungal diseases by boosting the plant's overall resistance is crucial. Various biostimulants, including extracts from seaweed, can boost plant health and trigger systemic resistance, thereby helping to lower the risk of other infections by reinforcing the plant's protective system. 2.5% biostimulant formulation significantly inhibited Foc growth through a synergistic mechanism involving both the bioactive compounds in the *Ulva* sp. seaweed extract and the antagonistic activities of beneficial microbes, specifically *Bacillus subtilis* DK5 and *Kosakonia* sp. DBS2. When concentrated at 2.5%, these chemicals are projected to attain levels that greatly hinder the growth and development of Foc mycelial structures. *Bacillus subtilis* DK5 and *Kosakonia* sp. DBS2 may contribute to pathogen suppression through molecular processes. The 2.5% biostimulant's substantial inhibition of Foc is due to a dual mechanism: 1) direct antifungal actions of *Ulva* sp. bioactives, and 2) microbial antagonism via lipopeptide synthesis, enzymatic degradation, and competition. This molecular synergy explains the increased efficacy seen at this concentration. Studies have demonstrated that seaweed is effective in preventing root infections caused by plant pathogenic fungi in okra seedlings (Sultana *et al*., 2005). Furthermore, spraying with seaweed extract has been demonstrated to increase strawberry yields, reduce fruit rot, and inhibit the spread of gray mold (Washington *et al*., 1999). Aligned with these findings, the present study showed increased Foc inhibition with increasing concentrations of a biostimulant formulation containing green seaweed. The biostimulant combination is

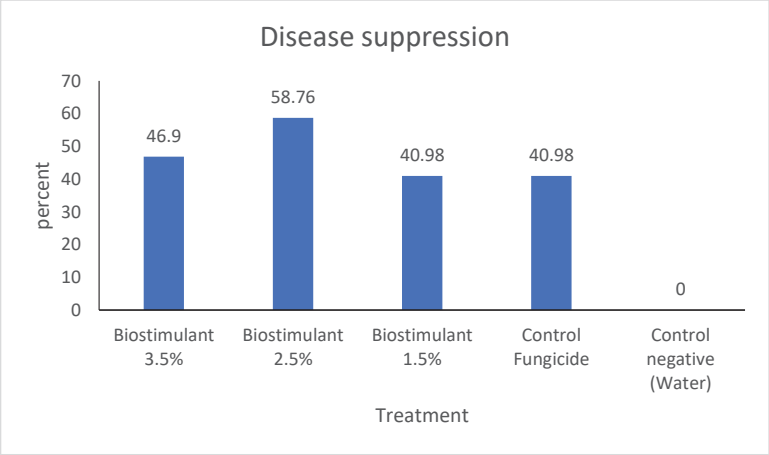

Fig. 3: Effect of the biostimulant concentration on disease suppression (DS)

believed to be utilizing nutrients from PDA media and converting them into antibiotics that restrain the spread of Foc. Visible indicators of Foc infection include twisting leaflets and yellowing commencing from the shoots, ultimately culminating in leaf drying and wilting. Endophytic bacteria are thought to possess enzymes involved in plant defense mechanisms. The elevated peroxidase activity observed in shallot plants treated with endophytic bacteria might indicate plant resistance and reduced disease severity. The presence of bacterial endophytes aids in the suppression of Fusarium wilt through the secretion of antibiotics and other inhibitory agents (Katoch *et al*., 2014). Several environmental factors, including spore dispersal, the relationship between host and pathogen, and overall environmental conditions, had a significant impact on the infection rate of wilt disease (Rengwalska and Simon, 1986; Promsai *et al*., 2023). Control of Foc and reduction in WD severity were achieved when biostimulant formulations were applied at concentrations of 2.5% and 3.5%, suggesting the effectiveness of using high concentrations. Extracts from seaweed, particularly *Ulva* sp., are highly regarded for their ability to act as biostimulants, significantly aiding in plant growth, enhancing stress tolerance, and suppressing diseases. The observed effects of *Ulva* sp. extracts are largely attributed to their unique composition, which includes nutrients, hormonal compounds, and bioactive molecules. These elements not only enhance plant growth but also interact synergistically when used in combination with other biocontrol agents like *Bacillus subtilis* or *Kosakonia* sp., optimizing their overall effectiveness. A synergistic approach to stress management is achieved through the competition among beneficial microbes and the hormonal properties of *Ulva* sp. extracts. When plants are treated with a combination of biostimulants and biocontrol agents, they typically show improved tolerance to environmental stresses such as drought, high salinity, and pathogen attacks, which contributes to more sustainable crop production. The presence of growth-promoting compounds in *Ulva* sp. extracts, such as auxins and cytokinins, directly influences plant morphology and physiology. The improvements in root system development, leaf area, and flowering help plants establish robust growth in the early stages. Moreover, the nutrient profile of *Ulva* sp. extracts facilitates ongoing growth, improves photosynthesis, and increases the plant's potential for biomass production. The observed 58.76% suppression of Fusarium wilt disease at the 3.5% biostimulant concentration demonstrates a clear concentration-response relationship, indicating that increasing concentrations of the biostimulant enhance disease control efficacy, up to a certain threshold. The 58.76% suppression at 3.5% suggests that this concentration offers a robust protective effect against Foc under controlled conditions. This level of suppression, though not complete, represents a significant reduction in disease severity, especially when compared to lower concentrations or untreated controls. These findings validate the biostimulant's overall effectiveness as a biological control agent, particularly when utilized at or

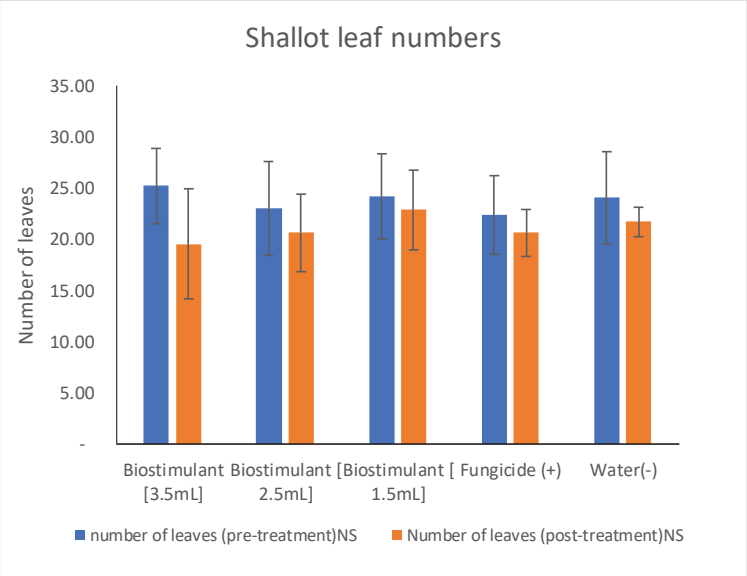

Fig. 4: Effect of the biostimulant on the number of shallot leaves. NS= not significant (DMRT, P≤0.05). Vertical bars correspond to SD

near ideal concentrations. It also highlights that disease suppression is dose-dependent, aligning with the principle that greater concentrations typically provide increased levels of active compounds and microbial populations capable of pathogen antagonism.A concentration-response trend was observed in the trials, with increasing concentrations (e.g., 1.5%, 2.5%, 3.5%) yielding progressively higher levels of wilt suppression. However, the relationship may plateau beyond 3.5%, meaning that it may represent a practical upper threshold for effective field use and balancing efficacy.

Effects of biostimulant formulations on shallot agronomic components:

The quantity of leaves

Fig. 4 shows the average number of leaves on the shallot plants before and after the biostimulant treatment. 3.5% was the ideal concentration of biostimulant to provide the nutrients that plants need throughout the vegetative growth stage, such as when leaves are forming. Shallot plants treated with biostimulants on a weekly basis produced a higher quantity of leaves. The quantity of leaves on a plant is one item that could indicate its growth. Although the DMRT test revealed no discernible changes across treatments, the biostimulant pre-treatment group had more leaves than the post-treatment group (Fig. 4).

Height of plants

The ANOVA test at the 95% confidence level revealed that the combination of biostimulant formulations had a significant effect on shallot plant height from 7 to 56 DAP (Table 2). The application of the biostimulant compound to the shallot plants significantly affected plant height at 6 and 8 weeks after planting (WAP), but not at 2 or 4 WAP, according to subsequent DMRT tests (Table 2).

The negative control treatment had the lowest plant height (39.10 cm), whereas the data obtained at 6 WAP indicated the highest plant height at a concentration of 3.5% (45.62 cm). It is hypothesized that the seaweed extract mixture (*Ulva* sp.) within the biostimulant may play a role in determining plant height. Nevertheless, a decline in height was recorded after 8 weeks post-planting. This decrease was evident from the increased occurrence of yellowing, wilting, and rapid drying of the leaves, which could be attributed to Fusarium WD. In the GH environment (mean temperature = 23.9 °C/month; relative humidity = 51-52.8%/month), the plants treated with the biostimulant grew taller (6 WAP), but at 8 WAP, this gain was slightly increased, corresponding with plant growth stages. Furthermore, it inhibits excessive plant height and directs nutrients to meet the requirements for the formation and maturation of shallot tubers. The cumulative height (AUHPC) of the shallot plants under each treatment

Table 2: Effect of biostimulant on shoot height

Treatment	Plant height at week after planting (WAP)			
	2WAP^{NS}	4 WAP^{NS}	6 WAP	8 WAP
Biostimulant 3.5%	21.11	38.63	45.62 ^{a*}	40.55 ^{a*}
Biostimulant 2.5%	20.65	37.68	42.62 ^{ab}	42.25 ^{b}
Biostimulant 1.5%	21.38	35.68	39.44 ^{ab}	45.91 ^{bc}
Control+ (fungicide)	22.23	39.09	42.18 ^{b}	39.04 ^{c}
Control- (Water)	20.81	35.63	39.10 ^{b}	36.75 ^{b}

*The DMRT did not show a significant difference between means that were followed by the same letter (P≤0.05). WAP = week after planting; NS = not significant.

Table 3: Effect of biostimulant on the shoot cumulative plant height

Treatment	Cumulative plant height (AUHPC)**	Difference with control (%)
Biostimulant 3.5%	1165.45	5.19
Biostimulant 2.5%	1107.05	0.19
Biostimulant 1.5%	1094.06	-0.99
Control+ (fungicide)	1173.36	5.83
Control- (Water)	1104.94	0

**AUHPC=area under the plant height progress curve (cumulative plant height).

(Table 3) ranged from the highest to the lowest, corresponding to the following treatments: 1173.36 for the fungicide control treatment, 1165.45 for the biostimulant treatment (3.5%), and 1104.94 for the control treatment (water alone). The cumulative plant height difference ranged from 0.19 to 5.19%.

Yield parameters (clump weight, number of tubers, and tuber weight)

In all treatments, there was no substantial difference in the quantity of shallot tuber. The treatment with 3.5% biostimulant had the greatest number of tubers (16.17). However, the lowest number of tubers (13.5) was obtained for the 2.5% biostimulant. The assessment of yield parameters, particularly the clump weight of shallots, indicated that distinct concentrations of the biostimulant formulation resulted in notably varied outcomes (Table 4). Because there are more tubers per clump as a result of the increased leaf count, shallot yield rises. The highest clump weight was observed for the treatment with a biostimulant concentration of 3.5% (47.76 g). Furthermore, the application of the biostimulant formula at a concentration of 3.5% to shallot plants at 8 WAP resulted in the highest clump weight compared to that of the control (Table 4). ANOVA results demonstrated that the concentration of the biostimulant had a significant impact on the dry weight of shallot tubers. A subsequent DMRT test revealed significantly different tuber dry weights between treatments. The 3.5% biostimulant treatment had the highest tuber dry weight (30.16 g), but this value did not differ significantly from that of the 2.5% biostimulant treatment (28.62 g). At a concentration of 3.5%, the biostimulant formula exhibited a more substantial effect on tuber count and weight than the control treatment. On the other hand, the dry weight of tubers at 1.5% concentration was reduced.

Seaweed extracts are recognized for their ability to enhance photosynthesis, increase chlorophyll content, and support root development, resulting in improved yields. Notably, while there were no significant variations in the number of tubers, the increased weight and health of tubers indicate superior nutrition allocation and physiological performance. The rise in plant height along with the greater number of leaves underscores the treatment's effectiveness in promoting growth, validating the biostimulant's function as a biocontrol and biofertilizer in greenhouse environments. The improved plant performance following biostimulant application can be attributed to

Table 4: Effect of biostimulant on the shoot clump weight, number of tubers, and tuber weight.

Treatment	Clump weight (g)	Number of tubers^{NS}	Tuber dry weight (g)
Biostimulant 3.5%	47.76 ^{a}	16.17	30.16 ^{a}
Biostimulant 2.5%	35.97 ^{ab}	13.5	28.62 ^{ab}
Biostimulant 1.5%	32.67 ^{b}	14.83	15.16 ^{c}
Control + (fungicide)	33.44 ^{b}	13.33	20.98 ^{ab}
Control - (Water)	33.93 ^{b}	14.17	23.32 ^{bc}

According to the DMRT, means in the same column that are followed by the same letter do not differ significantly (P≤0.05). NS stands for not significant.

several key growth parameters, with nutrient uptake efficiency and hormonal regulation playing dominant roles in enhancing physiological and morphological development. The primary growth parameters responsible for the noted enhancement included better nutrient uptake and hormonal stimulation, especially from auxins and cytokinins. These effects were mediated by both the microbial and seaweed components of the biostimulant, resulting in better root development, photosynthesis, and biomass accumulation. The application of biostimulants containing extracts from *Ascophyllum nodosum* at particular concentrations is recognized to affect leaf quantity in *Arabidopsis* (Rayorath *et al*., 2008). Moreover, extracts from the green sea algae *U. fasciata* and *U. lactuca* have served as biocides to inhibit the cotton pest *Dysdercus cingulatus* (Asha *et al*., 2012). Enhancing mineral uptake, as well as promoting plant growth and yield, represent key benefits of using biostimulants on plants (Vernieri *et al*., 2005; Mancuso *et al*., 2006). The application of nutrient components derived from biostimulants is believed to enhance chlorophyll synthesis, promote greener foliage, and directly impact the rates of photosynthesis, root-to-shoot ratios, and overall plant growth. Through the influence of the studied biostimulants involving microorganisms, including *Kosakonia* sp. DSB2 and *Bacillus subtilis* DK5 have been known to potentially promote nutritional absorption. It is known that these bacteria could produce indole acetic acid (IAA), nitrogen fixers, and phosphate solubilizers, which encourage plant development (Singh and Reddy, 2014). The elevation in shoot height suggests that plants have the ability to take in nutrients. In this research, variations in cumulative plant heights were observed to set apart the biostimulant formulation group from the control group (Table 3). Based on the ability and effectiveness of the root system, the improved growth rate, which is then connected to the used biostimulant formulation, is known to absorb nutrients and motivate plant growth and is known to influence the rate of overall plant height. Many minerals, amino acids, cytokines, and auxins included in seaweed extracts in biostimulant formulations stimulate plant metabolism, thereby boosting vegetative plant growth and yield (Rouphael and Colla, 2020; Yusuf *et al*., 2020). In relation to the generative and vegetative stages of plant growth, the GH environment biostimulant treatments resulted in increased plant heights. Four weeks after planting (WAP), it was noted that plant height continued to improve from the earlier two. Slight plant height rate improvements were only seen after six WAP. It was demonstrated that the plant has a high rate of leaf production that did not yield symptoms of yellowing or wilting. It is thought that the synergy between indole acetic acid (IAA), a plant physiological hormone, and endophytic bacteria works alongside other processes to support the delivery of crucial nutrients during plant development. This has resulted in significant improvements in photosynthetic activity rates and cell differentiation, lengthening, and division rates (Singh and Reddy, 2014; Ngoroyemoto *et al*., 2020). The quality of seed tubers has a well-known and long-studied impact on the productivity rate in shallots. Known infections and diseases are often connected to disease-carrying bacteria such as Foc (Sintayehu *et al*., 2011). Observations indicate that the application of biostimulants has a positive impact on shallot productivity rates. Additionally, it is known that biostimulant formulation provides an improved rate of soil fertility, which then will encourage the production and growth of high-value tuber production. Different types of seaweeds have been found to positively affect the dry-weight of tuber clumps (Nasmia *et al*., 2021; Nabti *et al*., 2017; Latique *et al*., 2021). An important indicator used to understand the state of the quality that determines shallot production often involves the assessment of total tuber clump weight. Plant height, leaf number, clump weight, and tuber dry weight are

all substantially correlated with final shallot yield because they are important markers of both vegetative vigor and reproductive efficiency. These aspects indicate the plant's physiological capability to facilitate vigorous development and substantial biomass distribution into vital storage organs, including shallot bulbs. These features are strongly associated with final shallot production, making them credible predictors of productivity and validating the positive effect of the biostimulant on agricultural output**.** *Ulva* sp. contains various phytochemical compounds commonly found in many plant extracts. Furthermore, research has demonstrated that diverse extract formulations can exhibit notable antimicrobial properties, which play a crucial role in enhancing overall disease suppression rates (Hernández-Herrera *et al*., 2016). There is well-studied potential that the application of biostimulants can contribute to improvements in the state and health of plant growth, quality, and overall soil state. In addition, it has been suggested that by enhancing different rates of soil nutrient processes, the plant may be in prime and effective health to improve different rates of plant stress, soil production, and overall soil health (Meena *et al*., 2025). The findings of this study confirm that endophytes (*B. subtilis* DK5 and *Kosakonia sp*. DBS2 isolates) and extracts from *Ulva sp*. have been successfully tested for their application. Even then, additional improvements and research are required to determine different rates of synergetic improvement that can be achieved with new or existing formulations. In general, the use of biostimulants is seen as a potential and effective mechanism in providing integrated control against WD, with other qualities that include safety, affordability, and availability that can benefit small farmers for their needs and applications. The present state of knowledge demands comprehensive research into how biostimulant formulations affect the soil and rhizosphere microbiome, with a focus on beneficial microbes in GH environments. The efficacy of the biostimulant in field conditions compared to GH settings may vary significantly due to a range of environmental and biological factors. While GH provide a controlled environment with stable temperature, humidity, and light levels, field settings introduce unpredictability, which can impair the biostimulant's effectiveness. Within a GH settings, optimal factors for plant growth—such as managed irrigation, temperature regulation, and protection from outside pathogens—facilitate the consistent performance of the biostimulant, promoting disease suppression and encouraging growth. This controlled environment avoids factors that might normally interfere with the biostimulant's activity, such as soil nutrient imbalances, extreme water stress, or pest pressure (Wadduwage *et al.,* 2023). However, in the field, the biostimulant's performance may be influenced by a broader range of environmental factors, such as shifting soil moisture, temperature extremes, variations in soil pH and nutrient levels, and the presence of competing bacteria and pathogens. Such factors may modify the microbial function of the biostimulant, leading to a decrease in its ability to suppress Fusarium wilt while simultaneously fostering plant growth. Furthermore, field conditions may result in increased variation in biostimulant uptake and immune response development, depending on factors such as plant health and soil composition. These disparities must be considered in real agricultural applications. In the field, application processes may need to be modified to account for differences in environmental circumstances. For instance, the timing of treatment, which may involve offering further formulation enhancements such as improving microbial strain stability in field conditions or developing slow-release formulations, might also enhance effectiveness (Chaudhary *et al*., 2020). Although this study focused primarily on controlled conditions and a single shallot cultivar (cv. 'Bima'), preliminary observations and related literature indicate that the effectiveness of the biostimulant may vary across different environmental conditions and shallot genotypes due to interactions between biotic and abiotic factors. While not explicitly examined in this study, it is expected that environmental conditions and the traits of shallot cultivars will affect the effectiveness of biostimulants. To encourage widespread use, future research should incorporate multi-location field experiments and cultivar screening to assure consistency, scalability, and targeted recommendations in a variety of growing conditions. The long-term impact of a biostimulant on soil microbiota composition and overall soil health is crucial for both environmental sustainability and agricultural production. The use of biostimulants, especially those that include beneficial bacteria or organic materials, greatly influences soil microbiota, which is vital for nutrient cycling, disease management, and maintaining soil fertility (Khoulati *et al*., 2025). Biostimulants applied regularly may

introduce new microbial strains or stimulate the growth of native beneficial microbes in the soil, resulting in increased microbial diversity that can improve the soil's ability to suppress pathogens like *Fusarium* spp. and support plant growth through nutrient cycling and disease resistance without the use of excessive synthetic fertilizers/pesticides. It is vital to examine the influence of biostimulants on the resilience of soil over time, especially its capacity to withstand environmental challenges like droughts and disease occurrences (Haque *et al*., 2023). The long-term impact of biostimulants will be determined by various factors, including the biostimulant's content (for example, microbial strains, chemical compounds), as well as the frequency and method of application. Extended use of the biostimulant may promote soil health, lower the frequency of Fusarium wilt, and reinforce the agroecosystem. Its dual effect improves soil microbiome function and plant defense capacity, makes it a promising tool for sustainable crop production over multiple planting cycles (Carillo, 2025). This study demonstrates the potential of *Ulva*-based biostimulants and beneficial bacteria in minimizing Fusarium wilt in shallots. However, significant limits remain, namely: 1) Scalability remains an issue; results obtained in controlled or small-scale field settings may not translate effectively to large-scale agricultural systems due to unpredictable environmental factors and the logistical hurdles of consistent implementation. 2) Natural variability in seaweed composition, caused by factors such as harvest location, season, and processing techniques, can affect in variations in biostimulant activity, posing challenges for standardization and commercial formulation. 3) The durability and viability of microbial strains in adverse field conditions are not well understood. Variations in soil type, temperature shifts, and competition from native bacteria can all compromise their effectiveness. The scalability and replicability of biostimulant production are crucial in determining its commercial potential and practicality for large-scale agricultural applications. Several elements enhance the current formulation's appropriateness for broader application, which includes *Ulva* sp. seaweed extract and microbial strains such as *Bacillus subtilis* DK5 and *Kosakonia* sp. DBS2. As a result, the biostimulant formulation using Ulva sp. extract and beneficial microorganisms is highly scalable, repeatable, and commercially feasible. The high potential of this biostimulant for large-scale implementation is attributed to its ample raw material availability, established manufacturing processes, and growing interest in sustainable farming inputs. To facilitate wider acceptance, future efforts should prioritize field-scale validation, product registration, and farmer training. The cost-benefit analysis suggests that biostimulants may be economically competitive with synthetic fungicides, especially when long-term benefits like improved soil health, reduced chemical reliance, and increased plant development are considered. The shift to integrated pest management (IPM), in which biostimulants can play an important role in lowering chemical inputs, is likely to benefit both the economy and the environment (Szparaga *et al*., 2019). The extensive adoption of biostimulants can support the rising need for sustainable farming methods, simultaneously protecting agricultural operations from surging chemical prices, regulatory challenges, and ecological concerns. Future research should include long-term, multi-site field tests to assess formulation options that improve microbial inoculant shelf life and field performance. The use of biostimulants to control Fusarium wilt in shallot farming has important implications for the future of IPM. Biostimulants serve as a long-lasting and eco-friendly substitute for traditional chemical management, as they enhance plant vitality, strengthen systemic resistance, and improve the balance of soil microorganisms. The long-term sustainability of utilizing biostimulants to manage Fusarium wilt is largely depends on their mode of action, crop-pathogen dynamics, and how they are integrated into a larger IPM strategy. Biostimulants, which include microbial inoculants, plant extracts, and organic substances, typically work by boosting the plant's natural defenses, improving root health, or indirectly suppressing pathogens in the rhizosphere. In contrast to synthetic fungicides that directly target infections, biostimulants are less likely to cause resistance development due to their complex and often indirect methods of action. Biostimulants can maintain their effectiveness across several growing seasons when integrated into a holistic disease management approach. When combined with crop rotation, resistant cultivars, and good agronomic practices, biostimulants improve soil health and microbial diversity, all of which are important factors in the long-term suppression of soil-borne diseases such as

Fusarium spp. However, sustainability also depends on environmental conditions, continuous product quality, and the potential adaptation of microbial communities.

CONCLUSION

The study showed the potential of endophytic bacterial isolates *Bacillus subtilis* DK5 and *Kosakonia* sp. DBS2 to act as biocontrol agents against *Fusarium oxysporum f.sp. cepae*, the pathogen responsible for wilt disease in shallots. The antagonistic activity observed in vitro, particularly the significant inhibition of *Fusarium oxysporum f.sp. cepae* mycelial growth by DK5 and DBS2, highlights the role of microbial secondary metabolites and enzymatic degradation (chitinase and glucanase) in pathogen suppression, which enables these bacteria to compromise fungal integrity, thereby inhibiting its proliferation. The synergistic relationship between DK5 and DBS2, as shown by their harmonious growth on nutrient agar, plays a vital role in developing a potent biostimulant mixture. When combined with *Ulva* sp. extract, the biostimulant formulation exhibited concentration-dependent inhibition of *Fusarium oxysporum f.sp. cepae* growth in vitro, with a notably low LC_{50} value of 2.415 mL/L. This outcome demonstrates that even small concentrations of the formulation can significantly decrease pathogen counts, probably owing to the combined or enhanced effects of bioactive substances found in seaweed extract, including phenolics, polysaccharides, and plant growth hormones, alongside microbial enzymes (chitinase and glucanase). In GH experiments, disease suppression rates up to 58.76% and reduced severity of wilt symptoms confirm the practical application of the biostimulant under GH conditions. At a concentration of 3.5%, the biostimulant significantly boosted critical growth factors, including plant height, clump weight, and tuber dry weight. The use of *Ulva*-based biostimulants (containing endophytic bacteria and marine algae extracts) in controlling fusarium wilt in shallots has been considered, as the broader implications for sustainable agricultural practice. Field validation plays a vital role in verifying the efficacy of biostimulants in diverse environmental contexts, since information gathered from controlled settings may not completely represent the nuances of field-related factors, including soil composition, microclimates, and pathogen diversity. Furthermore, optimizing biostimulant formulations is critical to ensuring their scalability, stability, and cost-effectiveness for large-scale use. Microbial strain selection, formulation stability, and application methods all need to be addressed to improve both short- and long-term effectiveness.

AUTHOR CONTRIBUTIONS

Y. Suryadi, has contributed in conceptualization, methodology, interpreted the results, preparing the manuscript., and final manuscript; D.N. Susilowati, contributed in methodology, formal analysis, preparing the manuscript., and final manuscript; Wartono contributed in software, validation, investigation, writing-original draft; Hanudin, prepring the manuscript, writing-review and editing, E. Korlina, contributed in writing original draft, and visualization, N. Gunaeni, contributed in software, and writing original draft, E. Diningsih, contributed in validation, data curation, and writing original draft, M. Assad, contributed in preparing the manuscript and final manuscript; S. Widawati contributed in writing original draft, review the muscript, and validation; Suliasih contributed in formal analysis, preparing the manuscript, writing the final manuscript. All co-authors reviewed the final version and approved the manuscript before submission.

ACKNOWLEDGEMENT

The authors would like to thank the Microbiology Laboratory Technicians for preparing the biostimulant formulations and performing the GH trials. The authors gratefully acknowledge the Indonesian Institute of Standard Testing for Biotechnology and Genetic Resources for the research support. The research was partially funded by [APBN No.FY 2021].

CONFLICT OF INTEREST

The authors declare that there are no conflict of interest regarding the publication of this manuscript. In addition, the ethical issues, including plagiarism, informed consent, misconduct, data fabrication and/or falsification, double publication and/or submission, and redundancy, were observed by the authors.

OPEN ACCESS

©2025 The author(s). This article is licensed under a Creative Commons Attribution 4.0 International License, which permits use, sharing, adaptation, distribution and reproduction in any medium or

format, as long as you give appropriate credit to the original author(s) and the source, provide a link to the Creative Commons license, and indicate if changes were made. The images or other third-party material in this article are included in the article's Creative Commons license, unless indicated otherwise in a credit line to the material. If material is not included in the article's Creative Commons license and your intended use is not permitted by statutory regulation or exceeds the permitted use, you will need to obtain permission directly from the copyright holder. To view a copy of this license, visit: http://creativecommons.org/licenses/by/4.0/

PUBLISHER'S NOTE

GJESM Publisher remains neutral with regard to jurisdictional claims with regard to published maps and institutional affiliations.

Positive AI Statement

During the preparation of this work the author(s) have used Artificial Intelligence (AI) [NAME TOOL / SERVICE] in order to [REASON]. After using this tool/ service, the authors reviewed and edited the content as needed and take full responsibility for the content of the publication.

(For this reason, the GPTZero detector will evaluate the manuscript utilizing Generative AI, ensuring a high detection rate. If the manuscript relies heavily on Generative AI and AI-assisted technologies, it will be archived without further options for appeal).

Negative AI Statement

The author(s) declare that no AI tools or services were not used or not highly applied during the preparation of this work.

ABBREVIATIONS

%	Percent
°C	Degree Celcius
ANOVA	Analysis of variance
AUHPC	Area under height of the plant curve
cm	Centimeter
CRD	Complete randomized design
Cv	Cultivar
DAP	Days after planting
DF	Degree of freedom
dH_2O	Distilled water
DMRT	Duncan's multiple range test
DS	Disease suppression
Foc	Fusarium oxysporum fsp. cepae
fsp	Forma species
g	Gram
GH	Green house
GI	Growth inhibition
h	Hours
I	Percentage of inhibition
IAA	Indole acetic acid
IPM	Integrated pest management
ISR	Induced systemic resistance
KCl	Potassium chloride
kg	Kilogram
L	Liter
LC_{50}	Lethal concentration
m	Meter
min	Minutes
mL	Mililiter
mL/L	Mililiter per liter
mm	Milimeter
NA	Nutrient agar
NB	Nutrient broth
NS	Not significant
P	Probability threshold
PDA	Potato dextrose agar
pH	Potential of hydrogen
SD	Standard deviation
SE	Standard error
SP-36	Super phosphate-36
SPSS	Statistical Package for the Social Sciences
µm	Micrometer
v/v	Volume per volume
WAP	Week after planting
WD	Wilt disease
w/v	Weight per volume
χ2(chi sq)	Chi square

REFERENCES

Ali, O.; Ramsubhag, A.; Jayaraman, J., (2021). Biostimulant properties of seaweed extracts in plants: implications toward sustainable crop production. Plants. 10(3): 1-27 **(27 pages)**.

Asha, A.; Rathi, J. M.; Raja, P.D.; Sahayaraj, K., (2012). Biocidal activity of two marine algal extracts against third instar nymph of Dysdercus cingulatus (Fab.) (Hemiptera, Pyrrhocoridae). J. Biopesticide. 5:129–134 **(6 pages)**.

Battacharyya, D.; Babgohari, M.Z.; Rathor, P.; Prithiviraj, B., (2015). Seaweed extracts as biostimulants in horticulture. Sci. Horticulturae. 196: 39-48 **(10 pages)**.

Central Bureau Statistic., (2020). Production of vegetables 2020. statistical yearbook of Indonesia in infographics 2021. Jakarta, Indonesia **(748 pages)**.

Caligiore-Gei, P.F.; Valdez, J.G.; Piccolo, R.J.; Galmarini, C.R., (2014). Influence of Fusarium spp. isolate and inoculum density on resistance screening tests in onion. Trop. Plant Pathol., 39(1): 19-27 **(9 pages)**.

Carillo, P., (2025). Can biostimulants enhance plant resilience to heat and water stress in the Mediterranean hotspot? Plant Stress, 16, 100802 (**21 pages**).

Chandra, M.; Raj, J.; Dogra, T.D.; Rajvanshi, A.C.; Raina, A., (2014). Determination of median lethal dose of triazophos with DMSO in Wistar rats. Asian J. Pharmaceut. Clinic. Res., 7(4): 64-67 **(4 pages).**

Chaudhary, T., Dixit, M., Gera, R., Shukla, A.K., Prakash, A., Gupta, G., Shukla, P., (2020). Techniques for improving formulations of bioinoculants. 3 Biotech, 10(5): 199 **(9 pages).**

Deng, Y.J.; Wang, S.Y., (2016). Synergistic growth in bacteria depends on substrate complexity. J. Microbiol., 54(1): 23-30 **(8 pages)**.

Dinata, G.F.; Aini, L.Q.; Abadi, A.L., (2021). The synergy between several bacteria isolated from the biodiversity of UB forest coffee litter in vitro. Nusantara Science Technology Proceeding. 25-30 **(6 pages)**.

Dominguez, H.; Loret, E.P., (2019). Ulva lactuca, a source of troubles and potential riches. Mar. Drugs. 17(6): 1-20 **(20 pages)**.

Hanci, F., (2018). A comprehensive overview of onion production: worldwide and Turkey. J. Agric. Vet. Sci., 11(9): 17-27 **(11 pages)**.

Haque, Z.; Pandey, K.; Zamir, S., (2023). Bio-management of Fusarium wilt of tomato (Fusarium oxysporum f.sp. lycopersici) with multifacial Trichoderma species. Discov Agric 1, 7 (**10 pages**).

Hernández-Herrera, R.M.; Santacruz-Ruvalcaba, F.; Zañudo-Hernández, J.; Hernández-Carmona, G., (2016). Activity of seaweed extracts and polysaccharide-enriched extracts from Ulva lactuca and Padina gymnospora as growth promoters of tomato and mung bean plants. J. Appl. Phycol., 28(4): 2549-2560 **(12 pages)**.

Hlokwe, M.T.P.; Kena, M.A.; Mamphiswana, D.N., (2020). Application of plant extracts and Trichoderma harzianum for the management of tomato seedling damping-off caused by Rhizoctonia solani. South Afr. J. Sci., 116(11/12): Art. #7860, **(5 pages)**.

Joshi, M.; Srivastava, R.; Sharma, A.K.; Prakash, A., (2013). Isolation and characterization of Fusarium oxysporum, a wilt causing fungus, for its pathogenic and non-pathogenic nature in tomato (Solanum lycopersicum). J. Appl. Nat. Sci., 5 (1): 108-117 **(10 pages)**.

Kalimutu, P.K.; Komang Mahardika, I.B.; Anak Agung Sagung, P.R.A., (2020). Antagonism test of Trichoderma atroviride and Gliocladium sp. Bali local isolates as a disease control of 'blendok' disease (Botryodiplodia theobromae) in grapefruit (Citrus grandis L. Osbeck). Sustainable Environ. Agric. Sci., 4(2): 102-110 **(9 pages)**.

Katoch, M.; Salgotra, A.; Singh, G., (2014). Endophytic fungi found in association with Bacopa monnieri as potential producers of industrial enzymes and antimicrobial bioactive compounds. Brazilian Arch. Biol. Technol., 57(5): 714-722 **(9 pages)**.

Khoulati, A.; Ouahhoud, S.; Taibi, M.; Ezrari, S.; Mamri, S.; Merah, O.; Hakkou, A.; Addi, M.; Maleb, A.; Saalaoui, E., (2025). Harnessing biostimulants for sustainable agriculture: innovations, challenges, and future prospects. Discov Agric 3, 56 (**28 pages**).

Latique, S.; Mrid, R.B.; Kabach, I.; Kchikich, A.; Sammama, H.; Yasri, A.; Nhiri, M.; El Kaoua, M.; Douira, A.; Selmaoui, K., (2021). Foliar application of Ulva rigida water extracts improves salinity tolerance in wheat (Triticum durum L.). Agron., 11: 265 **(17 pages)**.

Li, J.; Lu, Y.; Ye, Q.; Cinke, M.; Han, J.; Meyyappan, M., (2003). Carbon nanotube sensors for gas detection. Nano Lett., 3(7): 929–933 (**5 pages**).

Mancuso, S.; Azzarello, E.; Mugnai, S.; Briand, X., (2006). Marine bioactive substances (IPA extract) improve ion fluxes and water stress tolerance in potted Vitis vinifera plants. Advances in Hort. Sci., 20: 156-161 **(6 pages)**.

Manggala, B.; Chaichana, C.; Syahputra, W.N.H.; Wongwilai, W., (2023). Pesticide residues detection in agricultural products: a review. Nat.Life Sci. Comm., 22(3):e2023049 **(36 pages)**.

Meena, D.C.; Birthal, P.S.; Kumara, T.M.K., (2025). Biostimulants for sustainable development of agriculture: a bibliometric content analysis. Discov Agric **3**, 2 (**14 pages**).

Müller, T.; Ruppel, S.; Behrendt, U.; Lentzsch, P.; Müller, M.E.H., (2018). Antagonistic potential of fluorescent Pseudomonads colonizing wheat heads against mycotoxin-producing Alternaria and Fusaria. Front. Microbiol., 9: 1-14 **(14 pages)**.

Nabti, E.; Jha, B.; Hartmann, A., (2017). Impact of seaweeds on agricultural crop production as biofertilizer. Int. J. Environ. Sci. Technol., 14 (5): 1119-1134 **(16 pages)**.

Nasmia.; Rosyida, E.; Masyahoro, A.; Putera, F.H.A.; Natsir, S., (2021). The utilization of seaweed-based liquid organic fertilizer to stimulate Gracilaria verrucosa growth and quality. Int. J. Environ. Sci. Technol., 18(6): 1637-1644 **(8 pages)**.

Ngoroyemoto, N.; Kulkarni, M.G.; Stirk, W.A.; Gupta, S.; Finnie, J.F.; van Staden, J., (2020). Interactions between microorganisms and a seaweed-derived biostimulant on the growth and biochemical composition of Amaranthus hybridus L. Nat. Product Comm., 15(7):1-11 **(11 pages)**.

Noorjahan, A.; Mahesh, S.; Anantharaman, P.; Aiyamperumal, B., (2022). Antimicrobial potential of seaweeds: critical review. In: Ranga Rao, A., Ravishankar, G.A. (eds) Sustainable global resources of seaweeds Volume 1. Springer, Cham., (**21 pages**).

Ponsankar, A.; Senthil-Nathan, S.; Vasantha-Srinivasan, P.; Pandiyan, R.; Karthi, S.; Kalaivani, K.; Chellappandian, M.; Narayanaswamy, R.; Thanigaivel, A.; Patcharin, K.; Mahboob, S.; Al-Ghanim, K.A., (2023). Systematic induced resistance in solanum lycopersicum (l.) against vascular wilt pathogen (fusarium oxysporum f. sp. lycopersici) by citrullus colocynthis and trichoderma viride. Plos

One. 18(5): 1-20 **(20 pages)**.
Pourakbar, L.; Moghaddam, S.S.; Enshasy, H.A.E.; Sayyed, R.Z., (2021). Antifungal activity of the extract of a macroalgae, Gracilariopsis persica, against four plant pathogenic fungi. Plants (Basel). 10(9):1781 (**13 pages**).
Promsai, S.; Tragoolpua, Y.; Thongwai, N., (2023). Biological control of bacterial wilt in Pathumma; Curcuma alismatifolia. Global J. Environ. Sci. Manage., 9(SI): 127-144 **(18 pages)**.
Rafiee, H.; Badi, H.N.; Mehrafarin, A., (2016). Application of plant biostimulants as new approach to improve the biological responses of medicinal plants-a critical review. J. Med. Plants, 15(59): 6-39 **(34 pages)**.
Raupach, G.S.; Kloepper, J.W., (1998). Mixtures of plant growth-promoting rhizobacteria enhance biological control of multiple cucumber pathogens. Phytopathol., 88(11): 1158-1164 **(7 pages)**.
Rayorath, P.; Narayanan, J.M.; Farid, A.; Khan, W.; Palanisamy, R.; Hankins, S.; Critchley, A.T.; Prithiviraj, B., (2008). Rapid bioassays to evaluate the plant growth-promoting activity of Ascophyllum nodosum (L.) Le Jol. using a model plant, Arabidopsis thaliana (L.) Heynh. J. Appl. Phycol., 20: 423-429 **(7 pages)**.
Rengwalska, M.M.; Simon, P.W., (1986). Laboratory evaluation of pink root and fusarium basal rot resistance in garlic. Plant Dis., 70(7): 670-672 **(3 pages)**.
Rouphael, Y.; Colla, G., (2020). Biostimulants in agriculture. Front. Plant Sci., 11(40): 1-7 **(7 pages)**.
Sandepogu, M., (2018). Seaweed extract and humic acids biostimulant to improve growth and post-harvest quality of spinach and lettuce. University of Halifax. **(108 pages)**.
Sarven, M.S.; Hao, Q.; Deng, J.; Yang, F.; Wang, G.; Xiao, Y.; Xiao, X., (2020). Biological control of tomato gray mold caused by Botrytis cinerea with the entomopathogenic fungus Metarhizium anisopliae. Pathogens, 9(213):1-17 **(17 pages)**.
Szparaga, A.; Kuboń, M.; Kocira, S.; Czerwińska, E.; Pawłowska, A.; Hara, P.; Kobus, Z.; Kwaśniewski, D., (2019). Towards sustainable agriculture—agronomic and economic effects of biostimulant use in common bean cultivation. Sustainability. 11(17):4575 (**21 pages**).
Simko, I.; Piepho, H., (2012). The area under the disease progress stairs: calculation, advantage, and application. Phytopathology. 102 (4): 381-389 **(9 pages)**.
Shafi, J.; Tian, H.; Ji, M., (2017). Bacillus Species as versatile weapons for plant pathogens: a review. Biotechnol. Biotechnol. Equip., 31(3): 446-459 **(14 pages)**.
Singh, R.P.; Reddy, C.R.K., (2014). Seaweed-microbial interactions: key functions of seaweed-associated bacteria. FEMS Microbiol. Ecol., 88(2): 213-230 **(18 pages)**.
Sintayehu, A.; Sakhuja, P.K.; Fininsa, C.; Ahmed, S., (2011). Management of Fusarium basal rot (Fusarium oxysporum f.sp. cepae) on shallot through fungicidal bulb treatment. Crop Prot., 30(5): 560-565 **(6 pages)**.
Sultana, V.; Ehteshamul-Haque, S.; Ara, J.; Athar, M., (2005). Comparative efficacy of brown, green, and red seaweeds in the control of root infecting fungi and okra. Int. J. Environ. Sci. Technol., 2:129–132 **(4 pages).**
Vernieri, P.; Borghesi, E.; Ferrante, A.; Magnani, G., (2005). Application of biostimulants in floating system for improving rocket quality. J. Food, Agric. Environ., (3&4): 86-88 **(3 pages)**.
Wadduwage, J., Liu, H., Egidi, E., Singh, B. K., & Macdonald, C. A. (2023). Effects of biostimulant application on soil biological and physicochemical properties: A field study. J. Sustainable Agric. Environ., 2(3): 285-300 (**16 pages**).
Washington, W.S.; Engleitner, S.; Boontjes, G.; Shanmuganathan, N., (1999). Effect of fungicides, sea-weed extracts, tea tree oil, and fungal agents on fruit rot and yield in strawberry. Australian J. Experiment Agric., 39: 487- 494 **(8 pages)**.
Yusuf, R.; Syakur, A.; Kalaba, Y.; Fatmawati, F., (2020). Application of some types of local seaweed extract for the growth and yield of shallot (*Allium wakegi*). AACL Bioflux. 13(4): 2203-2210 **(8 pages)**.

AUTHOR (S) BIOSKETCHES

Suryadi, Y., M.Sc., Senior Researcher, Research Center for Horticulture, National Research and Innovation Agency, KST Soekarno, Jl. Raya Jakarta-Bogor, Cibinong, West Java 16915, Indonesia.
- Email: *yadi007@brin.go.id*
- ORCID: 0000-0003-2790-7529
- Web of Science ResearcherID: E-5997-2015
- Scopus Author 55625328400
- Homepage: https://brin.go.id/

Susilowati, D.N., Ph.D., Senior Researcher, Research Center for Horticulture, National Research and Innovation Agency, KST Soekarno, Jl. Raya Jakarta-Bogor, Cibinong, West Java 16915, Indonesia.
- Email: *d_nengsusi@yahoo.com*
- ORCID: 0000-0002-3061-9758
- Web of Science ResearcherID: NA
- Scopus Author ID: 55468022900
- Homepage: https://brin.go.id/

Wartono, Ph.D., Junior Researcher, Research Center for Horticulture, National Research and Innovation Agency, KST Soekarno, Jl. Raya Jakarta-Bogor, Cibinong, West Java 16915, Indonesia.
- Email: *wart005@brin.go.id*
- ORCID: 0000-0002-1645-1493
- Web of Science ResearcherID: NA
- Scopus Author ID: 57212248046
- Homepage: https://brin.go.id/

AUTHOR (S) BIOSKETCHES

Hanudin, B.Sc., Senior Researcher, Research Center for Horticulture, National Research and Innovation Agency, KST Soekarno, Jl. Raya Jakarta-Bogor, Cibinong, West Java 16915, Indonesia.
▪ Email: *hanu004@brin.go.id*
▪ ORCID: 0000-0001-8615-1552
▪ Web of Science ResearcherID: NA
▪ Scopus Author ID: 57210145156
▪ Homepage: https://brin.go.id/

Korlina, E., M.Si., Senior Researcher, Research Center for Horticulture, National Research and Innovation Agency, KST Soekarno, Jl. Raya Jakarta Bogor, Cibinong, West Java 16915, Indonesia.
▪ Email: *korlina64@gmail.com*
▪ ORCID: 0000-0003-3419-3835
▪ Web of Science ResearcherID: NA
▪ Scopus Author ID: 57196081528
▪ Homepage: https://brin.go.id/

Gunaeni, N., B.Sc., Senior Researcher, Research Center for Horticulture, National Research and Innovation Agency, KST Soekarno, Jl. Raya Jakarta-Bogor, Cibinong, West Java 16915, Indonesia.
▪ Email: *gunaenineni323@gmail.com*
▪ ORCID: 0000-0003-2937-4105
▪ Web of Science ResearcherID: NA
▪ Scopus Author ID: 57222179209
▪ Homepage: https://brin.go.id/

Diningsih, E., PhD., Junior Researcher, Research Center for Horticulture, National Research and Innovation Agency, KST Soekarno, Jl. Raya Jakarta-Bogor, Cibinong, West Java 16915, Indonesia.
▪ Email: *diningsiherniawati@gmail.com*
▪ ORCID: 0000-0002-9678-8415
▪ Web of Science ResearcherID: NA
▪ Scopus Author ID: 56719651100
▪ Homepage: https://brin.go.id/

Asaad, M., M.Sc., Senior Researcher, Research Center for Horticulture, National Research and Innovation Agency, KST Soekarno, Jl. Raya Jakarta-Bogor, Cibinong, West Java 16915, Indonesia.
▪ Email: *asaadmuh0@gmail.com*
▪ ORCID: 0000-0001-6058-2987
▪ Web of Science ResearcherID: NA
▪ Scopus Author ID: 57217523084
▪ Homepage: https://brin.go.id/

Widawati, S., B.Sc., Senior Researcher, Research Center for Applied Microbiology, National Research and Innovation Agency, KST Soekarno, Jl. Raya Jakarta-Bogor, Cibinong, West java 16915, Indonesia.
▪ Email: *sriw001.go.id*
▪ ORCID: 0000-0003-2717-9146
▪ Web of Science ResearcherID: NA
▪ Scopus Author ID: 57192115090
▪ Homepage: https://brin.go.id/

Suliasih., B.Sc., Senior Researcher, Research Center for Applied Microbiology, National Research and Innovation Agency, KST Soekarno, Jl. Raya Jakarta-Bogor, Cibinong, West java 16915, Indonesia.
▪ Email: *lishadari@yahoo.co.id*
▪ ORCID: 0000-0002-5296-7171
▪ Web of Science ResearcherID: NA
▪ Scopus Author ID: 57196169410
▪ Homepage: https://brin.go.id/

HOW TO CITE THIS ARTICLE

Suryadi, Y.; Susilowati, D.N.; Wartono; Hanudin; Korlina, E.; Gunaeni, N.; Diningsih, E.; Assad, M.; Widawati, S.; Suliasih, (2025). Sustainable approach for biocontrol of biostimulants derived from endophytic bacteria and seaweed extracts. Global J. Environ. Sci. Manage., 11(3): 1281-1298.

DOI: 10.22034/gjesm.2025.03.22

URL: https://www.gjesm.net/article_724380.html

Global J. Environ. Sci. Manage. 11(3): 1299-1318, Summer 2025, Serial #43

Global Journal of Environmental Science and Management
(GJESM)

Homepage: https://www.gjesm.net/

Podcasts

REVIEW PAPER

Bibliometrics analysis and the role of nanocatalysts in wastewater remediation

J. Aravind[1,*], M. Kamaraj[2], P. Suresh Babu[1]

[1] *Department of Biotechnology, Saveetha School of Engineering, Saveetha Institute of Medical and Technical Sciences, Chennai-602105, Tamil Nadu, India*

[2] *Department of Biotechnology, Faculty of Science and Humanities, SRM Institute of Science and Technology, Ramapuram, Chennai 600089, Tamil Nadu, India*

ARTICLE INFO

Article History:
Received 27 February 2025
Revised 02 May 2025
Accepted 01 June 2025

Keywords:
Hybrid catalytic materials
Nanocatalysts
Resource Recovery
Sustainable water management
Wastewater recycling

ABSTRACT

To address global concerns such as population expansion, urbanization, and industrialization, which are contributing to increased water pollution and shortages, sustainable water management relies on wastewater reuse. The purpose of this review is to investigate the significant role that hybrid catalytic materials and nanocatalysts play in the process of improving wastewater treatment technologies. By employing these materials and other advanced oxidation techniques, nanocatalysts are evaluated to assess their effectiveness in eliminating heavy metals and degrading persistent organic contaminants. The bibliometric assessment of research trends from 2015 to 2024 reveals a growing emphasis on the applications of nanotechnology in wastewater treatment. Within the scope of this review, the internal and extrinsic parameters that influence catalytic performance are investigated. These factors include particle size, light intensity, catalyst loading, and ambient pH conditions. Nanocatalysts hold great promise; however, several lingering concerns need to be addressed. These issues include high synthesis costs, scalability challenges, and environmental toxicity. These issues underscore the need to develop sustainable synthesis procedures, improved recovery mechanisms, and policy frameworks. Recent achievements in this sector include synthesizing nanomaterials that are safe for the environment, developing hybrid catalytic systems, and integrating these systems into existing treatment infrastructures to enhance efficiency and cost-effectiveness. The resolution of these issues will contribute to the establishment of nanocatalysts as transformative tools and green materials for wastewater treatment, for promoting the sustainability of water on a global scale and protecting the environment. The application of these hybrid materials for wastewater treatment is a topic of significant interest in environmental research.

DOI: 10.22034/gjesm.2025.03.23

This is an open access article under the CC BY license (http://creativecommons.org/licenses/by/4.0/).

NUMBER OF REFERENCES	NUMBER OF FIGURES	NUMBER OF TABLES
119	6	2

*Corresponding Author:
Email: *dr.j.aravind@gmail.com*
Phone: +9194 4351 8878
ORCID: 0000-0001-9699-2312

Note: Discussion period for this manuscript open until Sep 1, 2025 on GJESM website at the "Show Article".

INTRODUCTION

Driven by industrial development and increasing population growth, the global problems of water shortages and contamination are becoming more severe. Traditional wastewater treatment techniques highlight the need for creative and sustainable solutions, as they often struggle to remove persistent pollutants. Emerging as a key method in wastewater treatment, nanocatalysis (NC) improves pollution degradation and supports resource recovery. Emphasizing the functions of NC and hybrid catalytic materials (HCM) (Yaqoob *et al.,* 2020; Patra *et al.,* 2023; Tripathy *et al.,* 2024), this work investigates developments in chemical catalysis for wastewater treatment. NC enhances procedures utilizing catalysts that remain unaltered after the reaction. Catalysts help to break down difficult pollutants in wastewater treatment into simpler, less dangerous molecules. Conventional catalysts, such as metal oxides, have been employed; however, their efficacy is sometimes limited by factors including a restricted surface area and susceptibility to deactivation (Mahadevan *et al.,* 2023; Zheng *et al.,* 2024; Razzaq *et al.,* 2024). Defined by their nanoscale size, nanocatalysts offer a significantly larger surface area and unique electrical properties, thereby enhancing their catalytic efficacy. Under photocatalytic mechanisms, materials such as titanium dioxide (TiO_2), zinc oxide (ZnO), and cerium oxide (CeO_2) nanoparticles have demonstrated efficacy in the destruction of organic contaminants. For instance, TiO_2 nanoparticles have been extensively studied for their ability to degrade several organic pollutants in wastewater, including dyes (Nawaz *et al.,* 2023; Gunasekaran *et al.,* 2023; Abass *et al.,* 2024). Combining several catalytic components has yielded hybrid materials that exhibit multiple functional characteristics. Combining these materials maximizes the qualities of every element, improving stability, reusability, and catalytic efficiency. For example, hybrid nanocomposites combining carbon-based materials with metal nanoparticles have shown promise in enhancing the rates of pollution degradation (Das *et al.,* 2023; Rashid *et al.,* 2024; Godja and Munteanu, 2024). Several difficulties still arise in using hybrid materials and NCs for wastewater treatment, as well as environmental and health issues. The potential discharge of nanoparticles into the environment raises significant toxicity concerns that necessitate careful risk assessments. Translating lab successes into broad applications involves substantial challenges, particularly in terms of cost and process integration. Ensuring economic viability depends on the effective recovery and reuse of catalysts to maintain their activity (Ahmed *et al.,* 2022; Sanni *et al.,* 2024). Eco-friendly synthesis techniques, which utilize sustainable processes for catalyst creation to minimize environmental impacts, design catalysts that operate under visible light to capture solar energy efficiently, and integrate catalytic processes into existing treatment systems for seamless functionality, are progressively emerging as key trends and future paths in research. Particularly by utilizing NCs and hybrid materials, photocatalysis shows significant promise for enhancing wastewater recycling. Achieving their best efficacy for environmental cleanup will depend on addressing challenges through creative research and pragmatic solutions (Aragaw et al., 2021; Silerio-Vázquez *et al.,* 2024). This study aimed to investigate the significant role that hybrid catalytic materials and nanocatalysts play in enhancing wastewater treatment technologies. This study was conducted in India, specifically in Tamil Nadu, in 2025.

METHODOLOGY

Bibliometric analysis

With the support of software, bibliometric analysis is gaining popularity in systematic reviews of published documents. The visual presentations generated from this software analysis make it more attractive, comprehensive, and informative, providing a general overview of a specific topic. The bibliometric analysis involves inputs such as key terms, including authors, source type, subject area, publishing country, affiliation, author network, and funding, among others, to identify the trending theme and research network on a specific topic (Danya *et al.,* 2024). The documents published in the Scopus database are retrieved using the keywords “nanocatalysts AND wastewater AND treatment” searched within the “Abstract title, Abstracts, Keywords” section. The query search was limited to the period between 2015 and 2024 to retrieve document information from the last 10 years. The search displayed 850 documents; 708, 66, 52, 14, and 07 documents belong to an article, review, book chapter, conference paper, and book, respectively. The annual publication data have found an increasing trend from 2015 to 2022; in the recent

2 years, it has been observed as stagnant (Fig. 1). The country-wise data shows that China, India, and Iran are the top 3 positions by publishing documents such as 299, 207 and 103 in the last 10 years. The major sponsoring agencies for the documents are from China, and the National Natural Science Foundation of China has been identified as the highest funding agency for 174 documents listed in the search.

The output retrieved as of December 24th, 2024, signifies the research progress and selectively organized information on the documents published in the SCOPUS database on nanocatalysts in wastewater treatment. These documents are extracted in a BibTeX format and evaluated using the RStudio software-based Bibliometrix package (Aria and Cuccurullo, 2017). The overall summary of key information, including comprehensive documents, sources, average citations per document, keywords, and more, is illustrated in Fig. 2.

The three-field plot (Fig. 3), created using Biblioshiny, shows a relationship between countries with the highest scientific production and the major journal sources related to catalytic nanocomposites, as well as the affiliations for the Top 10 categories in each. The plot illustrates the connections of keywords such as wastewater treatment, photocatalysis, nanocatalyst, degradation, and nanocomposites, which have high-intensity connections with the top publishing countries and sources. The journals such as Chemosphere, Journal of Environmental Chemical Engineering, Ceramic International, Journal of Hazardous Materials, and Chemical Engineering Journal are identified as the top 5 sources with high-intensity connections between the top countries and Keywords.

Resource sharing, research ideas, and national variety will aid research expansion. The periodical plays a significant role in bolstering the nation's scientific infrastructure. Therefore, a major determinant of the progress of the chosen field of

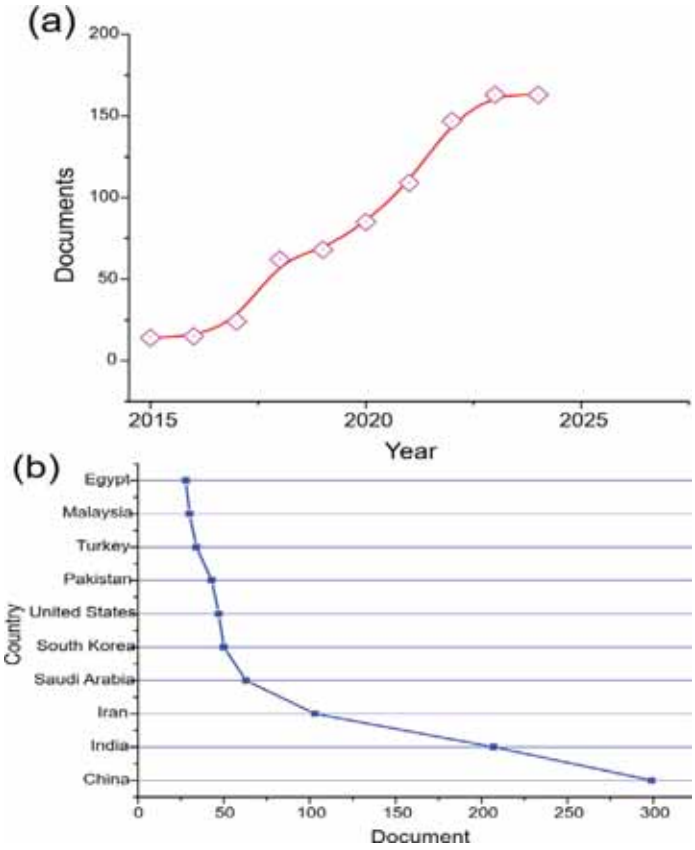

Fig. 1: Bibliometric output of research articles in Scopus database. Annual production (a) and Top 10 country-wise documents (b) for the given keywords



Fig. 2: Overview of key information associated with the database search

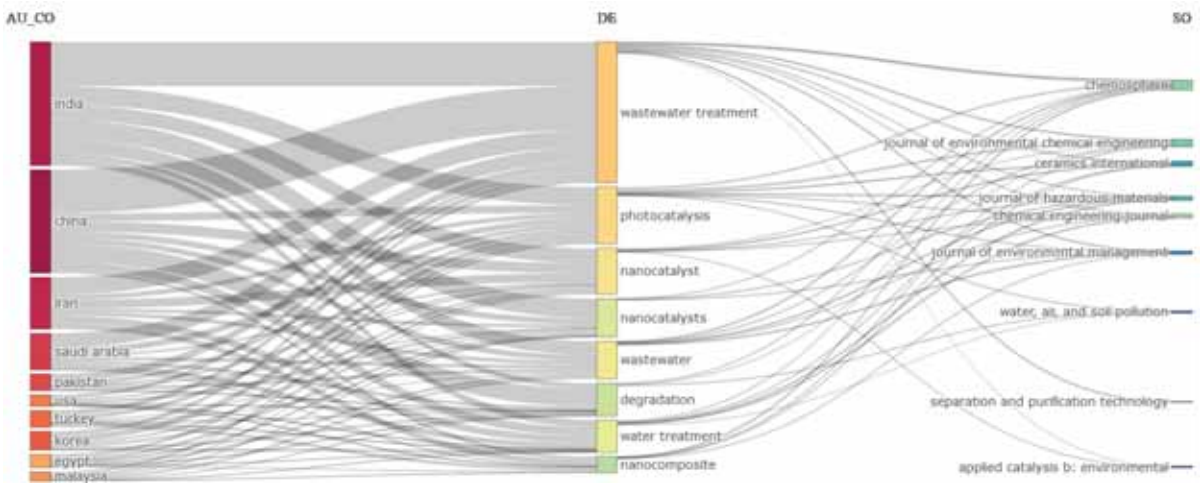

Fig. 3: Three-field plot for the selective keywords

research is international research partnership. The collaboration network (Fig. 4) illustrates the country collaboration map related to the keyword search. To compensate for their familiarity, several public documents portrayed a thorough cooperation with other nations. The collaboration between India and Saudi Arabia, as well as India and South Korea, is more significant, with 21 and 19 frequencies, respectively. Apart from that, a global network pattern is observed in the collaboration of published documents related to the given keyword search, which indicates that nanocatalyst-empowered wastewater research has a high degree of connection intensity, especially over the last 10 years.

Factors affecting the nanocatalytic activity

NCs can be synthesized through various mechanisms, including physical, chemical, and biological methods. The synthesis involves a range of external and internal factors that influence the characteristics of NCs (Fig. 5) and their photocatalytic performance. External factors are outside the reaction medium but impact the surrounding environment of the reaction. The external factors encompass initial dye concentration, catalyst loading, light intensity, irradiation duration, the potential of hydrogen (pH), and the type of effluent oxidant. Intrinsic factors also play a significant role in internal reactions, encompassing aspects such as crystal structure, particle size, morphology, surface area, pore density, pore volume, and the functional group of the catalyst (Gupta and Xie, 2018; Gupta *et al.*, 2021; Sinha and Ghosal, 2023).

The level of contaminants has a significant influence on the efficiency of degradation and removal processes. The primary element influencing

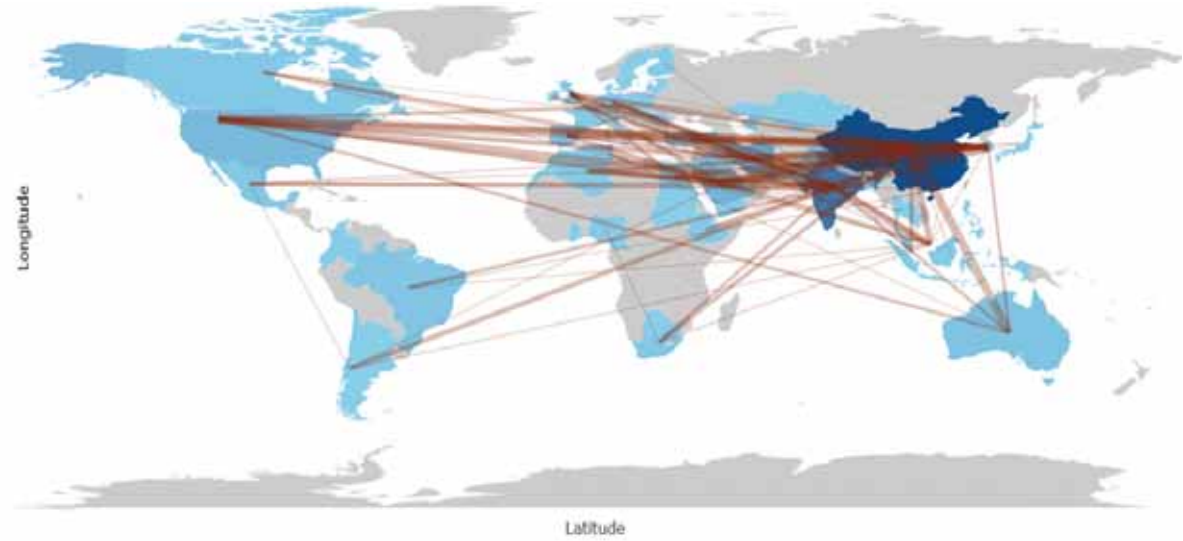

Fig. 4: A world collaboration map created for the keywords

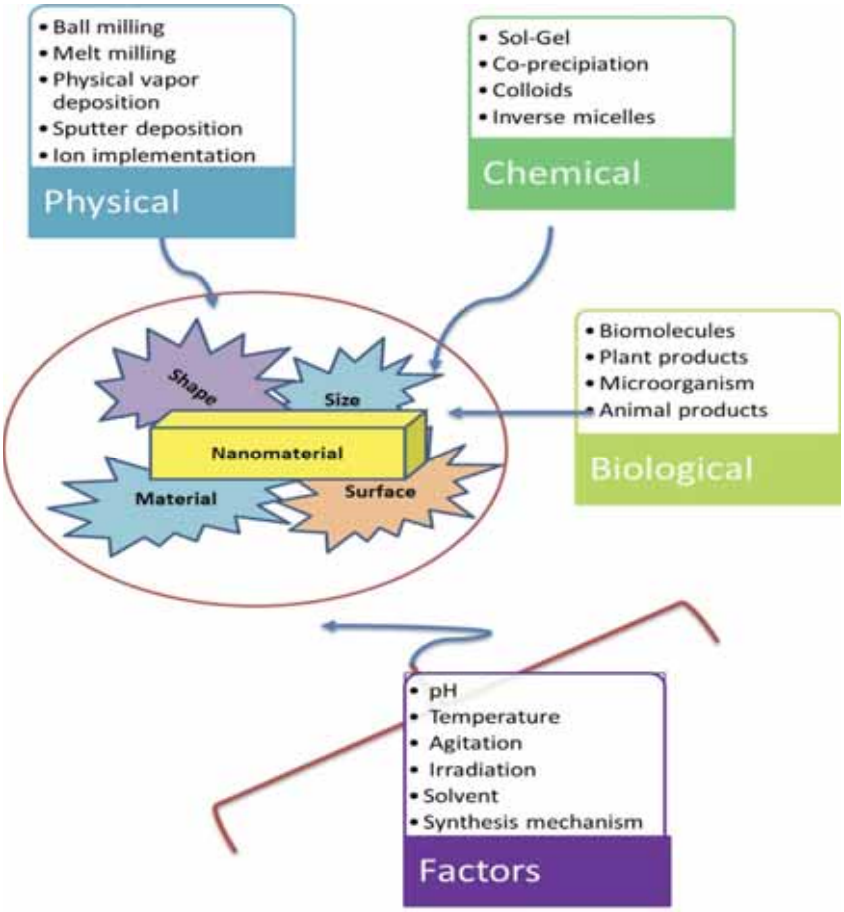

Fig. 5: Synthesis mechanisms and factors affecting the Nanocatalyst properties

Photocatalysis is the generation of hydroxyl radicals (•OH) on the catalyst's surface and their interaction with the dye. Increasing the initial dye concentration resulted in a decrease in photodegradation efficiency (Rafiq *et al.,* 2021). At elevated dye concentrations, numerous dye molecules adhere to the surface of the photocatalyst, occupying active sites and significantly hindering photon production, which reduces the generation of •OH radicals (Azad and Gajanan, 2017). Introducing the concentrated dye solution reduced the photon path length and hindered light transmission to the catalyst, decreasing photocatalytic activity (Zhu *et al.,* 2012). The study investigated the impact of varying initial dye concentrations on the degradation process of reactive yellow dye. The dye degradation efficiency diminished from 89.62 percent (%) to 35.79% as the initial dye concentration rose from 25 to 100 milligram per liter (mg/L). The explanation could be attributed to the higher dye concentration, which allowed more dye molecules to be available for excitation and energy transfer (Ilinoiu *et al.,* 2013). A group observed that the efficiency of photodegradation for Methyl Orange (MO) dye (45 mg/L) utilizing NCs decreased (23.0%) as the initial dye concentration increased (to 50 mg/L) under sunlight exposure. This finding was obtained by obstructing the infiltration of simulated solar light into the dye solution (Al-Mamun *et al.,* 2021). The quantity of NCs affects the degradation process. It is essential to ascertain the optimal loading to eliminate surplus photocatalysts. The notable photocatalytic percentage corresponds to the liquid volume ratio to the appropriate NCs. An elevated catalyst dose correlates with an enhanced ability of the catalyst to generate a significant amount of •OH radicals (Ahmad *et al.,* 2016). The degradation efficiency of reactive yellow 14 dye improved from 52.6% to 91.3% with the incorporation of NCs [1–6 gram per liter (g/L)] over 40 minutes (min). A higher concentration of NCs often leads to agglomeration, which reduces the surface area, diminishes the number of absorbed photons, and increases light dispersion, thereby hindering the penetration of Ultra-violet (UV) or solar light into the solution (Rafiq *et al.,* 2021). A study examined the dosage of NCs ranging from 0.5 to 1.5 g/L for the degradation of azo dye and determined that the optimal catalyst dosage was 1.0 g/L after three hours of UV irradiation (Çalışkan and Yatmaz, 2017). The effectiveness of photodegradation is directly related to the duration of irradiation. The photocatalytic process progresses rapidly for a specific duration of irradiation; however, as the temperature rises, evaporation commences, leading to an inverse relationship with irradiation time. As a result, the efficiency of photodegradation for organic pollutants diminished with prolonged irradiation time, attributed to the increased generation of intermediate compounds (Groeneveld *et al.,* 2023). These minor chain aliphatic compounds interact with •OH, reducing the reaction rate until the optimal contact time is reached (Singh *et al.,* 2023a). The application of NCs in the remediation of cationic Yellow dye was investigated. The photodegradation efficiencies were recorded at 95.53%, 95.84%, and 99.14% after 1, 2, and 3 days of UV irradiation, respectively. The degradation of organic pollutants by the light source is crucial, as it influences the effectiveness of the catalyst (Suhan *et al.,* 2023). The strength of UV light is contingent upon the distance separating the UV lamp from the photocatalyst, thereby affecting the effectiveness of pollutant degradation by the photocatalyst particles. As the light intensity increased, many electron pairs were produced in the metal NCs. The adsorbed contaminants on the surface of the photocatalyst are degraded by free radicals (Mariselvam *et al.,* 2016). The artificial UV light source demonstrates greater consistency and is preferred over solar light exposure due to its enhanced effectiveness in photodegrading textile colors. Consequently, solar light irradiation is anticipated to serve as a cost-effective alternative to traditional light sources. The findings indicate that the degradation efficiency notably improved to 56% with increased UV light intensity from 0 to 3.0 milliwatts per square centimeter (mW/cm^2). A comparable pattern was observed in the degradation of MO dye by applying NC at power levels of 17.25 and 65.85 watts per square meter (W/m^2), achieving efficiencies between 58.1% and 97.6% following 180 minutes of UV irradiation (Bouarioua and Zerdaoui, 2017). The increase in light intensity did not enhance degradation due to the restricted number of active sites present on the surface of the NC. Thus, suitable light intensity is crucial for improving the effectiveness of photocatalytic processes (Chen *et al.,* 2020). The pH of the solution plays a vital role in influencing the degradation of organic compounds and the stability of the catalyst in photocatalysis. The outcome often

depends on the photocatalyst's charge and the properties of the pollutant within the reaction medium. The pH has consistently demonstrated its importance in pollution remediation through various catalysts. The oxidation kinetics exhibited a marked increase as pH values rose. Studies indicate that dye adsorption is enhanced in acidic pH environments (Kumari *et al.,* 2023; Baral *et al.,* 2024). The metallic surface exhibits a positive charge in an acidic solution (pH <6.8) due to strong dye adsorption onto the metal-nanocatalyst due to electrostatic attraction. Consequently, a negative charge was obtained in an alkaline environment (pH > 6.8) due to the elevated presence of metal groups within the NCs. The heightened oxidizing activity of NCs was observed at low pH; however, at very low pH levels, producing a larger quantity of H^+ ions leads to a reduction in the reaction rate. The interaction between the catalyst surface and solvent molecules in photocatalytic processes is significantly influenced. The results have a substantial influence on the adsorption of solutes, thereby affecting the photodegradation rate. Studies show that the photodegradation of specific organic contaminants using NCs is significantly more efficient in acidic environments than in basic or neutral conditions (de la Flor *et al.,* 2022). The efficiency of photodegradation of MO dye utilizing NCs was enhanced at an acidic pH of 3.0 after 5 hours of exposure to direct sunlight (Al-Mamun *et al.,* 2021). The photocatalytic degradation of reactive orange dye exhibited decolorization rates ranging from 24.14% to 89.10% as the pH increased from 1 to 10 during an 80 min reaction period. As a result, the increase in pH from 10 to 12 led to a decrease in decolorization efficacy, which fell from 89.31% to 81.20%. Various oxidants were utilized with NCs, significantly influencing bio-persistent toxic dyes. The introduction of an oxidant serves as a potent electron scavenger, enhancing the photodegradation efficiency of intermediate molecules via three distinct mechanisms. The dual functional properties of intermediate oxidants, which include strong oxidants and electron acceptors, are evident in photocatalytic reactions (Akerdi and Bahrami, 2019). Peroxide acts as a source of oxygen, exhibiting notable oxidizing capabilities that enhance the reaction rate. Integrating hydrogen peroxide (H_2O_2) into photocatalysis for degrading organic color compounds in textile effluent proved to be significant. Introducing H_2O_2 has increased photo-oxidation rates by enhancing the generation of extra •OH through the reduction of surface-trapped electrons (Merdoud *et al.,* 2024). As a result, the effectiveness of photodegradation can be reliably improved through oxidative conversion by adding H_2O_2. As a result, •OH is generated by interacting conduction band electrons with hydroxide ions originating from water molecules. On the other hand, introducing the metal-oxidant substantially impacts the mineralization rate, decreasing the pH of the dye solution (Al-Mamun *et al.,* 2021). The inclusion of metal is an effective electron acceptor, enhancing the kinetics of NCs and the photodegradation efficiency of dye-laden textile effluent. This phenomenon arose from the interplay between the electron band and the oxidant, influenced by the scavenging effect of the latter. However, the overuse of metal reduced the photocatalytic effectiveness of NCs when exposed to UV or solar light. Adding Potassium Bromate ($KBrO_3$) at concentrations between 1 and 3 g/L significantly improves the degradation efficiency of reactive orange dye in textile wastewater from 64.4% to 97.97% over a 20 min irradiation period (Almulhem *et al.,* 2022; Bopape *et al.,* 2024). The surface characteristics of a semiconductor are considered essential for enhancing photocatalytic activity, which can be achieved through the optimization of bandgap energy and the reduction of photogenerated electron-hole recombination (Akerdi and Bahrami, 2019). The degradation rate is notably influenced by the surface characteristics of the materials produced, including zeta potential, acidity, and isoelectric point (Rashid *et al.,* 2021). The surfaces of both nano and bulk-sized NC have been meticulously evaluated, uncovering significant variations in their photodegradation effectiveness and photochemical processes (Hu *et al.,* 2017). Many studies have shown that smaller forms result in a greater surface-to-volume ratio, increase the internal recombination of electron/hole pairs, and enhance the active sites of surface area, thereby improving the availability of •OH for the degradation of organic pollutants (Rashid *et al.,* 2021). The enhanced surface area notably elevated the separation rate of photogenerated charge carriers and promoted charge transport efficiency (Gupta *et al.,* 2021). The ideal particle size of the NCS for the degradation of methylene blue dye under UV irradiation was determined to be 35

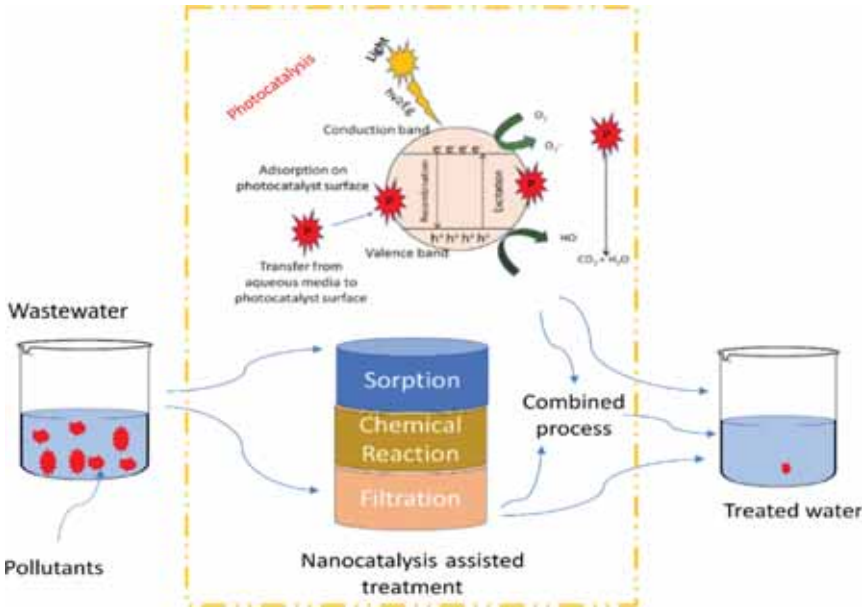

Fig. 6: Application of nanocatalyst in wastewater treatment

nanometers (nm) (Chen *et al.,* 2020). Bisphenol A (11.2 mg/L) demonstrated a degradation rate of 96% for nanostructured NCs and 84% for micro-structured NCs following 2 hours of UV irradiation. The photocatalytic activity of NCs is greatly affected by surface morphological factors, including phase composition, crystallinity, crystal structure, porosity, pore volume, and surface hydroxyl groups (Rani and Shanker, 2020).

Nanocatalysts in wastewater processing and remediation

NC, defined by their nanoscale dimensions, have become crucial players in wastewater recycling through various mechanisms. The most commonly recognized mechanisms include photocatalytic degradation, filtration, sorption, and chemical reaction (Fig. 6). The catalysts demonstrate unique physicochemical properties, such as high surface area-to-volume ratios, tunable surface chemistry, and enhanced catalytic performance. These traits make them highly effective at removing contaminants from wastewater, including organic pollutants, heavy metals, and other persistent environmental toxins. NC plays a vital role in sustainable water management by enabling efficient degradation of pollutants and recovery of resources. Increased catalytic activity reduces reaction times and energy consumption, allowing the precise targeting of specific contaminants based on their chemical characteristics. Various NCs can be reactivated and utilized again with negligible reduction in effectiveness. Recent developments in nanotechnology make the large-scale production of NC financially feasible (Yaqoob *et al.,* 2020; Baig *et al.,* 2021; Raza *et al.,* 2022; Thakur *et al.,* 2024).

NCs originated from TiO_2 and ZnO harness solar or ultraviolet light to generate reactive oxygen species (ROS), breaking organic pollutants into harmless byproducts such as CO_2 and H_2O. TiO_2, ZnO, iron oxide (Fe_3O_4), silver (Ag), and gold (Au) nanoparticles are widely employed for the photocatalytic degradation of organic pollutants, microbial disinfection and the sequestration of heavy metals. Carbon-based nanomaterials can absorb heavy metals and transform them into less harmful or recoverable forms, such as carbon nanotubes, graphene oxide, and activated carbon nanocomposites. Carbon nanoparticles are utilized for adsorption, electrochemical oxidation, and hybrid catalysis due to their exceptional conductivity and surface functionality (Jiang *et al.,* 2021; Wang *et al.,* 2022a, b, c; Chauke and Raphulu, 2024; Pinzari, 2024). Photodegradation plays a crucial role in environmental studies, as it facilitates the decomposition of harmful substances present in

air, water, and soil (Etafo *et al.,* 2024). NCs sourced from TiO_2 and ZnO demonstrate photocatalytic activity that varies based on the materials used and the surrounding environmental conditions; superoxide radicals play a crucial role in oxidizing and breaking down persistent organic pollutants (POPs) into smaller, less harmful molecules. Photocatalytic degradation exhibits significant efficacy in addressing persistent organic pollutants (POPs) characterized by conjugated double bonds and aromatic rings within their chemical structure (Zhang *et al.,* 2023; Meng *et al.,* 2023). NCs that incorporate transition metal ions, such as iron (Fe), copper (Cu), or manganese (Mn), are capable of facilitating oxidative reactions, which contribute to the degradation of POPs via oxidation mechanisms (Sun *et al.,* 2023). The presence of metal ions on the surface of NCs facilitates the activation of molecular oxygen (O^{2+}) or H_2O_2, leading to the generation of ROS that effectively converts POPs into non-toxic byproducts (Chen *et al.,* 2023a). Oxidative catalysis enhances the efficiency and selectivity of degrading various persistent organic contaminants in wastewater. NCs featuring acidic or basic surface sites have the potential to improve hydrolytic reactions, facilitating the degradation of POPs through nucleophilic attack by hydroxide ions (OH-) or via mechanisms of protonation and deprotonation (Xiao *et al.,* 2023). Hydrolysis demonstrates significant efficacy for POPs that possess ester, amide, or ether functional groups, facilitating the cleavage of chemical bonds when water molecules are present. Nanocatalysts designed with specific surface chemistry can enhance hydrolytic degradation rates and increase selectivity for specific persistent organic pollutants (POPs). Specific NC, including palladium (Pd) and platinum (Pt) nanoparticles, exhibit reductive catalytic activity by transferring electrons to POP molecules, effectively reducing them to less harmful or inert substances (Sun *et al.,* 2023). Reductive catalysis demonstrates efficacy for endocrine-disrupting compounds (EDCs) with functional groups amenable to reduction reactions. NCs enhance electron transfer activities, facilitating the degradation of persistent organic pollutants under mild reaction conditions (Lu *et al.,* 2023). Ultrasonic irradiation, when combined with NC, significantly enhances the breakdown of persistent organic pollutants through a mechanism known as sonocatalysis (Zhao *et al.,* 2023). Ultrasonic waves produce cavitation bubbles in wastewater, resulting in localized hotspots and high-pressure zones near the surface of the NC. The specified conditions promote the activation of NCs, enabling the degradation of persistent organic pollutants through sonochemical reactions, which involve the generation of hydroxyl radicals and the cleavage of chemical bonds (Varela *et al.,* 2021). Nano-zeolites and metal-organic frameworks (MOFs) utilize ion exchange and molecular sieving techniques to extract heavy metals and other dissolved materials. Au-Pd, Pt-Cu, and Fe-Co nanocomposites, functioning as bimetallic nanocatalysts, exhibit synergistic effects that improve their ability to break down complex contaminants and boost catalytic efficiency (Chen and Xu, 2019; Kaur *et al.,* 2023; Liu *et al.,* 2024). Specific nanomaterials serve as electrocatalysts, enabling advanced oxidation processes (AOPs) to remove persistent organic pollutants (POPs) effectively. A comprehensive assessment of specific NC's potential toxicity and environmental stability is essential. Increased production costs persist in hindering broader acceptance. Incorporating NC into current wastewater treatment systems presents significant challenges (Cardoso *et al.,* 2021; Masood *et al.,* 2022). Future studies should focus on creating biocompatible, sustainable NC and exploring hybrid systems that integrate NC with biological processes for effective wastewater recycling solutions. NC holds considerable promise for improving wastewater recycling systems (Cardoso et al., 2024; Kumar *et al.,* 2024). The combination of advanced materials science and environmental engineering enables these catalysts to significantly enhance the efficiency, sustainability, and cost-effectiveness of wastewater treatment systems, thereby supporting global water conservation efforts. Table 1 presents a compilation of various nanocelluloses (NCs) and their applications in wastewater remediation.

Hybrid catalytic materials and their application in wastewater recycling

HCM represents a significant advancement in environmental remediation, combining the unique catalytic properties of various components to address the complex challenges of wastewater recycling. The design of these materials involves integrating multiple catalytic systems, including metallic, semiconductor, or polymeric catalysts, aimed at improving efficiency in pollutant degradation, heavy metal removal, and

Table 1: Nanocatalysts and their applications in wastewater recycling

Nanocatalyst	Application	Mechanism	Sources
TiO_2 Nanoparticles	Degradation of organic pollutants (e.g., industrial dyes)	Photocatalytic oxidation under UV light generates reactive oxygen species that decompose pollutants	Anucha *et al.,* 2022
ZnO Nanoparticles	Removal of pharmaceutical contaminants	Photocatalytic degradation under UV light, breaking down complex pharmaceutical compounds	Singh *et al.,* 2022
Ag Nanoparticles	Antibacterial activity	Release of Ag^+ ions disrupts microbial cell membranes, leading to cell death	Yaqoob *et al.,* 2020
Iron Oxide Fe_3O_4 Nanoparticles	Removal of heavy metals (e.g., arsenic, lead)	Adsorption of metal ions onto nanoparticle surfaces, followed by magnetic separation	Masood *et al.,* 2022
Graphene Oxide Nanosheets	Adsorption of organic pollutants	High surface area facilitating adsorption of pollutants; potential for photocatalytic degradation	Ugwuanyi *et al.,* 2024
Carbon Nanotubes	Filtration and adsorption of contaminants	High surface area and porosity enable the adsorption of various pollutants	Sajid *et al.,* 2022
Au Nanoparticles	Catalytic degradation of pollutants	Facilitation of electron transfer reactions, enhancing the breakdown of contaminants	Desseigne *et al.,* 2023
CeO_2 Nanoparticles	Oxidation of organic pollutants	Redox cycling between Ce^{3+} and Ce^{4+} states, promoting oxidative degradation	Pansambal *et al.,* 2023
Magnetic Nanoparticles	Separation of pollutants	Magnetic properties allow for easy separation after pollutant adsorption	Dhadda *et al.,* 2024
Nanosponges	Removal of organic contaminants	Porous structure traps pollutants; can be functionalized for specific contaminants	Kumari *et al.,* 2023

wastewater recycling (Li *et al.,* 2022; Lu *et al.,* 2023; Mahmoud *et al.,* 2024). Hybrid catalysts typically integrate nanostructured materials, such as metal oxides, carbon-based materials, and polymeric frameworks, to leverage their synergistic properties. For example, TiO_2 is frequently combined with carbon-based materials to enhance light absorption, charge separation, and surface area. Furthermore, incorporating metals or non-metals improves electron transport and catalytic activity when exposed to visible light (Godja and Munteanu, 2024; Navrotskaya *et al.,* 2020; Mushahary *et al.,* 2024). The operational principles of hybrid catalysts often rely on adsorption; an enhanced surface activity ensures that contaminants, such as dyes, pharmaceuticals, and pesticides, adhere to the material's surface. The active sites in catalysis are crucial for initiating oxidation or reduction reactions, which are essential for degrading organic pollutants and reducing heavy metals. Some hybrids facilitate self-cleaning or straightforward regeneration, rendering them economical for multiple cycles (Rigoletto *et al.,* 2022; Farwa *et al.,* 2024; Satyam and Patra, 2024).

Photocatalytic Degradation of Organic Pollutants: Hybrid materials such as TiO_2-carbon or ZnO-g-C_3N_4 composites are extensively utilized for the breakdown of complex organic pollutants into innocuous byproducts when exposed to sunlight or artificial UV light. The combination of metal-organic frameworks (MOFs) with metal nanoparticles enables the selective and efficient adsorption and reduction of toxic heavy metals, including lead (Pb), cadmium (Cd), and arsenic (As) (Sewnet *et al.,* 2022; Qamar *et al.,* 2023; El Gaini *et al.,* 2024). Hybrid materials are integrated into filtration membranes to enhance fouling resistance and catalytic activity. These membranes physically filter contaminants while degrading them in situ via catalytic reactions. Their multifunctional capabilities enable the concurrent elimination of various pollutant categories, including a combination of dyes and heavy metals, rendering them particularly suitable for intricate wastewater streams. The enhancement of photocatalytic and adsorption properties decreases treatment duration and energy usage (Qi *et al.,* 2020; Chen *et al.,* 2023b). Hybrid materials often employ eco-friendly synthesis techniques and operate under gentle conditions; their resilience and recyclability reduce operational costs. The adaptability of hybrid catalysts enables their incorporation into current wastewater

treatment systems (Ghazal *et al.,* 2022; Elgarahy *et al.,* 2023). While there are notable benefits, obstacles persist, such as elevated synthesis expenses, the risk of material leaching, and constraints on large-scale implementation. Future investigations aim to create environmentally sustainable and economically viable synthesis techniques, catalysts exhibiting improved stability and reusability, and functional materials suitable for various environmental conditions (Alraae *et al.,* 2024). NC demonstrates improved degradation of organic dyes under simulated sunlight, as electrons and holes interact with adsorbed O_2 and H_2O molecules to produce reactive species that decompose organic dyes. The NC developed by a team in 2019 demonstrated significant degradation activity towards methylene blue. At pH 10, BWO achieved a remarkable reduction of 99.87% of methylene blue (MB) within 160 min (Shivani *et al.,* 2019). In 2020, researchers utilized Sn(II) meso-tetra(4-carboxyphenyl) porphyrin-modified NPC to break down organic dye. The breakdown mechanism of the dye was examined through ultra-performance liquid chromatography, revealing that the dye molecules transform carbon intermediates through N-demethylation and a two-step demethylation process. The C intermediates undergo dehydroxylation, ethylation, and deamidation, forming H and I products. The J intermediate is generated by removing the amino group and the cleavage of the aromatic rings from H intermediates. The cleavage of the aromatic rings in J products leads to the formation of K products, which subsequently undergo decomposition into carbon dioxide (CO_2) and water (H_2O) (He *et al.,* 2020). Song et al. (2022) developed the photocatalyst NC aimed at MB degradation. The dyes adsorbed on the catalyst surface may undergo sensitization, leading to an increase in the photodegradation rates of the dyes. Upon exposure to light, dyes produce photoelectrons. The electrons within the lowest unoccupied molecular orbital (LUMO) of the dyes can be transferred to the conduction band of NPC, thereby increasing the generation of superoxide anions. (Zn-Bi-NPC) composites were developed by Bahadoran *et al.* (2021), demonstrating an 86% degradation of MG. The degradation mechanisms of MG-sensitized composites were also examined. The MG-sensitized catalyst demonstrated a clearance rate for 2,4-dichlorophenol that exceeded that of the unmodified catalyst, attributed to the process of dye sensitization. Research indicates that NPC effectively removes antibiotics from wastewater. Li *et al.* (2023) created a MIL(Fe)/NPC heterojunction. This heterojunction exhibited notable deterioration efficiency, achieving approximately 82.8% disintegration within 60 minutes (min.). The MIL-100(Fe)/NPC nanocomposites demonstrated advantages such as an extended light absorption spectrum, efficient carrier separation, and enhanced redox potential due to the formation of S-scheme heterojunctions. Wang *et al.* (2022a) developed Cu/NC photocatalysts, resulting in a degradation of 91% TC-HCl within 60 min. Two mechanisms of antibiotic degradation have been documented. The Bi-Br-NPC photocatalysts created by Zhang *et al.* (2022) achieved a 91.79% degradation of POPs within 120 min. They recorded intermediate products and various degradation mechanisms. The dominant degradation mechanisms observed were the cleavage of piperazinyl rings, defluorination, and decarboxylation. The oxidation of the piperazine moiety resulted in the degradation of antibiotics, yielding small-molecule compounds. The findings demonstrate the effectiveness of NPC in degrading antibiotics. Recent studies have concentrated on developing effective methods to decompose antibiotics and produce Hydrogen (H_2) from wastewater. A technique involves using antibiotics as sacrificial agents in processes for photocatalytic hydrogen generation (Wei *et al.,* 2020). A study utilized a Bi/Zn-NPC with platinum (Pt) as a co-catalyst to successfully decompose antibiotics, producing approximately 27 micromoles per gram (µmol/g) of hydrogen in 120 minutes (Wang *et al.,* 2022b). A study showed that a CTF/ZnO-NPC catalyst demonstrated enhanced effectiveness in hydrogen generation and antibiotic degradation (Tahir *et al.,* 2021). Table 2 outlines a range of beneficial characteristics of NC.

Cai et al. (2023) developed a novel S-scheme heterojunction Cd/Zn/Bi photocatalyst using the solvothermal method. This photocatalyst demonstrated an impressive degradation rate of 77.5% for norfloxacin within just 20 min of exposure to visible light. Mustafa and Oladipo (2021) investigated the effectiveness of Ag-doped Ni-Zn-Fe-NPC in removing metronidazole-based pharmaceuticals. The synthesized photocatalyst demonstrated an impressive removal rate of 99.9%, accompanied

Table 2: Catalytic Materials and their merits in wastewater remediation

Catalytic material	Composition/structure	Catalytic mechanism	Application	Advantages	Sources
TiO_2/ZnO Nanocomposites	TiO_2 and ZnO nanostructures	Photocatalytic degradation	Removal of organic dyes (e.g., methylene blue)	High photostability and efficiency	Ayu *et al.*, 2023
g-C_3N_4/$BiVO_4$	Graphitic carbon nitride and bismuth vanadate	Photocatalysis	Degradation of pharmaceutical residues	Visible light activity, low toxicity	Varmaziar *et al.*, 2024
Fe_3O_4/SiO_2/TiO_2	Magnetic core-shell structure with TiO_2 coating	Fenton-like reaction and Photocatalysis	Removal of heavy metals and dyes	Magnetic recovery, multifunctional activity	González-Fernández *et al.*, 2024
ZnO/Ag	ZnO doped with silver nanoparticles	Surface Plasmon Resonance-Enhanced Photocatalysis	Antimicrobial activity in wastewater	Enhanced visible light absorption	Kareem et al., 2022
CeO_2/MOF-199	CeO_2 integrated with metal-organic framework MOF-199	Adsorption and catalysis	Removal of phenolic pollutants	High surface area, tunable pore size	Zango *et al.*, 2020
CuO/C_3N_4	Copper oxide integrated with graphitic carbon nitride	Photocatalysis	Degradation of dyes	High charge separation, visible light activity	Vijayakumar *et al.*, 2022
ZrO_2/Graphene Oxide	Zirconia nanoparticles on graphene oxide sheets	Adsorption and photocatalysis	Heavy metal removal	High stability and reusability	Al-Mhyawi *et al.*, 2023
$MnFe_2O_4$/Activated Carbon	Magnetic spinel ferrite supported on activated carbon	Advanced oxidation processes	Remediation of industrial effluents	Strong magnetic properties, reusability	Esteves *et al.*, 2024
Ni/TiO_2	Nickel-doped titanium dioxide	Photocatalysis and hydrogenation	Degradation of xenobiotic compounds	Improved redox potential	Sharma *et al.*, 2023
Ag_2O/TiO_2	Silver oxide incorporated with titanium dioxide	Photocatalysis	Disinfection and organic pollutant degradation	Better antimicrobial properties	Endo-Kimura *et al.*, 2019

by a rate constant of 0.0103 per minute (/min). Yi *et al.* (2023) developed hollow Bi/NPC hierarchical microspheres by annealing Bismuth microsphere precursors generated using the solvothermal method. The unique hollow structure of the microspheres provided a mesoporous configuration with numerous active sites, improving the adsorption and breakdown of antibiotics. The performance of this photocatalyst in degrading antibiotics reached 83% in 100 minutes. HCM significantly advances wastewater recycling, effectively tackling environmental sustainability and resource management issues. Their capacity to combine catalytic efficiency, environmental compatibility, and cost-effectiveness establishes them as fundamental for realizing sustainable water management objectives. Ongoing advancements in this area are expected to enhance the implementation and scalability of these technologies, thereby propelling the evolution of worldwide wastewater treatment methodologies (Singh *et al.,* 2023b).

FUTURE PROSPECTS

Driven by developments in nanotechnology, material science, and environmental engineering, the future of wastewater treatment using HCM and NC provides exciting prospects. Still, reaching their full potential requires addressing current issues and seizing new opportunities by employing group research and innovative approaches (Bamisaye *et al.,* 2024). Developing environmentally friendly synthesis techniques is a top priority at present. Current methods often rely on hazardous compounds and energy-intensive processes, which contradict the goals of wastewater treatment in the environment. Minimizing environmental impact, green synthesis techniques using plant extracts, microorganisms, or biopolymers as reducing and stabilizing agents show promise for generating NCs. Future studies should concentrate on standardizing these techniques and enhancing their scalability while maintaining the physicochemical qualities of the produced materials. The broad application of NCs depends on their seamless integration into conventional wastewater treatment systems. There are excellent prospects in reactor design developments and hybrid systems combining nanocatalysis with biological processes, such as microbial fuel cells or enzymatic degradation. These hybrid systems enhance treatment efficiency, economic viability, and resource recovery while simultaneously addressing multiple contaminants and promoting resource recovery (Ma *et al.,* 2024). Using traditional techniques, future NC should demonstrate enhanced sensitivity for breaking down challenging molecules, including endocrine-disruption chemicals, medicines, and microplastics. Changing surfaces and adding metals or non-metals helps NC to target particular pollutants. Recent advancements in computational modeling and machine learning can significantly enhance the design of NCs, ensuring they possess the ideal characteristics for specific applications. The significant costs associated with producing and using NC pose major challenges to its widespread adoption in industrial-scale applications. Affordable, high-efficiency production techniques—including co-precipitation, sol-gel procedures, or thermal decomposition—which can be scaled up for mass production—should take center stage in these efforts. Investigating substitute raw materials for catalyst manufacture, such as agricultural or industrial byproducts, can help improve sustainability and potentially reduce prices. Reducing operating costs and minimizing environmental risks depends on efficiently recovering and reusing NC (Nizam *et al.,* 2021). Promising prospects are presented by magnetically responsive NC, which are easily separable and regenerable under magnetic fields. Long-term performance and financial viability can be significantly improved by developing self-cleaning or regenerable materials that sustain catalytic activity across multiple cycles. Still, a significant obstacle is the potential leaching of nanoparticles into treated water and their subsequent environmental impact. Developing biocompatible NC with minimal toxicity and operational condition stability should be the main priority of the subsequent studies. Developing safety rules about using and disposing of NC depends on thorough lifetime assessments and risk evaluations. Given only a small fraction of the solar spectrum, UV radiation significantly limits the effectiveness of current photocatalysts. Advancing visible-light-active NCs through bandgap engineering, doping, or heterojunction creation should be the primary focus of future efforts. The present advances could significantly increase the feasibility and efficiency of photocatalysis in practical applications. Including solar or wind power in NC will substantially increase attempts at sustainability. Moreover, combining wastewater treatment techniques with circular

economy concepts—such as the recovery of valuable byproducts like metals, fertilizers, or hydrogen gas—may help transform wastewater from a burden into a useful resource. Artificial intelligence and machine learning will transform the design and optimization of nanocrystals (NCs) (Salahshoori *et al.,* 2024). Predictive modeling can significantly accelerate the discovery of new materials with enhanced properties. Conversely, real-time monitoring and control systems can adjust operational settings to achieve optimal performance. The safe application of NC depends on strict policy and regulatory structures; therefore, their practical implementation requires them. Given their possible environmental and health effects, providing explicit instructions for the production, use, and disposal of NC is imperative. Fostering an atmosphere that encourages invention and adoption depends on joint projects among academics, government representatives, and business leaders. NCs and HCM can transform wastewater recycling by addressing these challenges and seizing new opportunities, providing an effective, sustainable, and reasonably priced solution. Their inclusion in forthcoming water management systems could significantly enhance global efforts to address pollution and water shortages, thereby fostering a more sustainable ecology (Linghu *et al.,* 2023).

CONCLUSION

Nanocatalysts (NCs) and hybrid catalytic materials (HCMs) have emerged as transformative tools in wastewater remediation, offering exceptional catalytic efficiency, selectivity, and multifunctionality. This review has explored the synergistic potential of these advanced materials in degrading persistent organic pollutants (POPs), facilitating resource recovery, and promoting sustainable water purification. Their unique physicochemical properties, including high surface-to-volume ratios and tunable reactivity, make them ideal candidates for next-generation wastewater treatment technologies. Despite their promising performance, several critical challenges must be addressed to enable the widespread adoption of nanocatalysts (NCs) and hybrid carbon materials (HCMs). High synthesis costs, issues with long-term stability, environmental toxicity concerns, and difficulties in scaling laboratory successes to industrial applications remain major bottlenecks. The risk of nanoparticle leaching and their uncertain ecological impact further necessitate robust environmental assessments and regulatory frameworks. Integrating these materials into existing treatment infrastructure requires innovations in reactor design and system compatibility. Future advancements will likely hinge on interdisciplinary collaboration among material scientists, environmental engineers, policymakers, and industry stakeholders. Emphasis should be placed on developing cost-effective, eco-friendly synthesis methods, such as green chemistry approaches using biological agents and engineering NCs that function effectively under visible light to maximize solar energy utilization. Moreover, coupling NC-based systems with biological or electrochemical processes promises to create hybrid treatment platforms that can address complex pollutant matrices with improved energy and cost efficiency. Policy support and regulatory clarity are essential to ensure the safe deployment, monitoring, and disposal of these nanomaterials. Artificial intelligence and machine learning can play a vital role in the predictive design of catalysts, real-time monitoring of processes, and optimization of treatment conditions, thereby accelerating innovation and deployment. Hence, NCs and HCM represent a paradigm shift in environmental remediation technologies. Their integration into wastewater treatment systems has the potential to significantly enhance purification efficiency, reduce operational costs, and contribute to achieving global water sustainability goals. By addressing the current limitations through strategic research, responsible innovation, and policy integration, NCs and HCMs can lead the transition toward a cleaner, safer, and more resilient water future.

AUTHOR CONTRIBUTIONS

J. Aravind's contribution in writing, editing, original draft, and conceptualization; M Kamaraj's contribution was writing bibliometric analysis, tables, and figures; P Sureshbabu's contribution to writing, editing, and review.

ACKNOWLEDGEMENT

The authors are grateful for the support provided by the institution.

CONFLICT OF INTEREST

The authors declare no potential conflict of interest regarding the publication of this work. In addition,

the ethical issues including plagiarism, informed consent, misconduct, data fabrication and, or falsification, double publication and, or submission, and redundancy have been completely witnessed by the authors.

OPEN ACCESS

©2025 The author(s). This article is licensed under a Creative Commons Attribution 4.0 International License, which permits use, sharing, adaptation, distribution and reproduction in any medium or format, as long as you give appropriate credit to the original author(s) and the source, provide a link to the Creative Commons license, and indicate if changes were made. The images or other third-party material in this article are included in the article's Creative Commons license, unless indicated otherwise in a credit line to the material. If material is not included in the article's Creative Commons license and your intended use is not permitted by statutory regulation or exceeds the permitted use, you will need to obtain permission directly from the copyright holder. To view a copy of this license, visit:

http://creativecommons.org/licenses/by/4.0/

PUBLISHER'S NOTE

GJESM Publisher remains neutral with regard to jurisdictional claims with regard to published maps and institutional affiliations.

Positive AI Statement

During the preparation of this work, [the author(s) have used Artificial Intelligence (AI) [Quillbot in order to minimize similarity in few sentences]. After using this tool/service, the authors reviewed and edited the content as needed and take full responsibility for the content of the publication.

(For this reason, the GPTZero detector will evaluate the manuscript utilizing Generative AI, ensuring a high detection rate. If the manuscript relies heavily on Generative AI and AI-assisted technologies, it will be archived without further options for appeal).

Negative AI Statement

The author(s) declare that no AI tools or services were not used or not highly applied during the preparation of this work.

ABBREVIATIONS

%	Per cent
µmol/g	Micromole per gram
/min	Per minutes
•OH	Hydroxyl radical
AOPs	Ddvanced oxidation processes
Ag	Silver
As	Arsenic
Au	Gold
Cd	Cadmium
CeO_2	Cerium oxide
CO_2	Carbon dioxide
Cu	Copper
EDCs	Endocrine-disrupting compounds
Fe	Iron
Fe_3O_4	Iron oxide
g/L	Gram per liter
H_2	Hydrogen
H_2O	Water
H_2O_2	Hydrogen peroxide
HCM	Hybrid catalytic materials
$KBrO_3$	Potassium Bromate
LUMO	lowest unoccupied molecular orbital
mg/L	Milligram per liter
min.	Minutes
Mn	Manganese
MB	Methyl Blue
MO	Methyl Orange
MOFs	Metal-organic frameworks
mW/cm^2	Milliwatt per centimeter square
NCs or NC	Nanocatalysts
nm	Nanometer
OH^-	Hydroxide ions
Pb	Lead
Pd	Palladium
pH	Potential of hydrogen
POPS	Persistent organic pollutants

Pt	Platinum
ROS	Reactive oxygen species
TiO_2	Titanium dioxide
UV	Ultra-violet
W/m²	Watt per mete square

REFERENCES

Abass, A.M.; Abdoon, F.M., (2024). Synthesis, characterization, and applications of metal oxides of ZnO, CuO, and CeO_2 nanoparticles: A review. J. Appl. Organomet. Chem., 24 (4): 349–366 **(18 pages)**.

Ahmad, R.; Ahmad, Z.; Khan, A.U.; Mastoi, N.R.; Aslam, M.; Kim, J., (2016). Photocatalytic systems as an advanced environmental remediation: Recent developments, limitations and new avenues for Applications. J. Environ. Chem. Eng., 4(4): 4143–4164 **(22 pages)**.

Ahmed, S.F.; Mofijur, M.; Ahmed, B.; Mehnaz, T.; Mehejabin, F.; Maliat, D.; Hoang, A.T.; Shafiullah, G.M., (2022). Nanomaterials as a sustainable choice for treating wastewater. Environ. Res., 214(1): 113807 **(19 pages)**.

Akerdi, A.G.; Bahrami, S.H., (2019). Application of heterogeneous nano-semiconductors for photocatalytic advanced oxidation of organic compounds: A review. J. Environ. Chem. Eng., 7(5): 103283 **(19 pages)**.

Al-Mamun, M.R.; Kader, S.; Islam, M.S., (2021). Solar-TiO_2 immobilized photocatalytic reactors performance assessment in the degradation of Methyl Orange dye in aqueous solution. Environ. Nanotechnol. Monit. Manage., 16: 100514 **(12 pages)**.

Al-Mhyawi, S.R.; Bader, D.M.D.; Bajaber, M.A.; El Dayem, S.M.A.; Ragab, A.H.; Abd El-Rahem, K.A.; Gado, M.A.; Atia, B.M.; Cheira, M.F., (2023). Zirconium Oxide with Graphene Oxide anchoring for improved heavy metal ions adsorption: Isotherm and kinetic study. J. Mater. Res. Technol., 22: 3058–3074 **(17 pages)**.

Almulhem, N.K.; Awada, C.; Alnaim, N.M.; Al Taisan, N.; Alshoaibi, A.A.; Shaalan, N.M., (2022). Synergistic effect of the $KBrO_3$ electron acceptor on the photocatalytic performance of the Nb-TiO_2 nanocomposite for polluted Phenol Red wastewater treatment. Crystals. 12(12): 1758 **(11 pages)**.

Alraae, A.; Moussadik, A.; Benzaouak, A.; Kacimi, M.; Dahhou, M.; Sifou, A.; El Hamidi, A., (2024). Eco-friendly synthesis and catalytic activity of Cu nanoparticles deposited on expanded Muscovite to reduce organic pollutants. Results Surf. Interfaces., 17: 100343 **(14 pages)**.

Anucha, C.B.; Altin, I.; Bacaksiz, E.; Stathopoulos, V.N., (2022). Titanium Dioxide (TiO_2)-based photocatalyst materials activity enhancement for contaminants of emerging concern (CECs) degradation: In the light of modification strategies. Chem. Eng. J. Adv., 10: 100262 **(16 pages)**.

Aragaw, T.A.; Bogale, F.M.; Aragaw, B.A., (2021). Iron-based nanoparticles in wastewater treatment: A Review on synthesis methods, applications, and removal mechanisms. J. Saudi. Chem. Soc., 25(8): 101280 **(28 pages)**.

Aria, M.; Cuccurullo, C., (2017). Bibliometrix: An R-Tool for comprehensive science mapping analysis. J. Inf., 11(4): 959–975 **(17 pages)**.

Ayu, D.G.; Gea, S.; Andriayani.; Telaumbanua, D.J.; Piliang, A.F.R.; Harahap, M.; Tok, A.I.Y., (2023). Photocatalytic degradation of Methylene Blue using N-doped ZnO/carbon dot (N-ZnO/CD) nanocomposites derived from organic soybean. ACS Omega., 8(17): 14965–14984 **(20 pages)**.

Azad, K.; Gajanan, P.J., (2017). Photodegradation of Methyl Orange in aqueous solution by the visible light active Co:La:TiO_2 nanocomposite. Chem. Sci. J., 8(3): 1000164 **(9 pages)**.

Bahadoran, A.; Farhadian, M.; Hoseinzadeh, G.; Liu, Q., (2021). Novel flake-like Z-scheme Bi_2WO_6-$ZnBi_2O_4$ heterostructure prepared by sonochemical assisted hydrothermal procedures with enhanced visible-light photocatalytic activity. J. Alloys Compd., 883: 160895 **(14 pages)**.

Baig, N.; Kammakakam, I.; Falath, W., (2021). Nanomaterials: A review of synthesis methods, properties, recent progress, and challenges. Mater. Adv., 2(6): 1821–1871 **(52 pages)**.

Bamisaye, A.; Abati, S.M.; Ige, A.R.; Etafo, N.O.; Alli, Y.A.; Bamidele, M.O.; Okon-Akan, O.A.; Adegoke, K.A.; Abiola-Kuforiji, O.T.; Idowu, M.A.; Bello, O.S., (2024). Metal-oxide nanocatalysts for spontaneous sequestration of endocrine-disrupting compounds from wastewater. Chemosphere. 367: 143569 **(23 pages)**.

Baral, S.C.; Maneesha, P.; Mishra, P.K.; Dhanapal, P.; Sen, S., (2024). Rapid photocatalytic degradation of organic pollutants by Al^{3+} doped CuO powders under low power visible light and natural sunlight. Opt. Mater., 147: 114653 **(17 pages)**.

Bopape, D.A.; Ntsendwana, B.; Mabasa, F.D., (2024). Photocatalysis as a pre-discharge treatment to improve the effect of textile dyes on human health: A critical review. Heliyon. 10(20): e39316 **(31 pages)**.

Bouarioua, A.; Zerdaoui, M., (2017). Photocatalytic activities of TiO_2 layers immobilized on glass substrates by dip-coating technique toward the decolorization of Methyl Orange as a model organic pollutant. J. Environ. Chem. Eng., 5(2): 1565–1574 **(10 pages)**.

Cai, M.; Liu, Y.; Dong, K.; Wang, C.; Li, S., (2023). A novel S-scheme heterojunction of CD0.5Zn0.5S/BiOCl with Oxygen defects for antibiotic Norfloxacin photodegradation: Performance, mechanism, and intermediates toxicity evaluation. J. Colloid Interface Sci., 629(A): 276–286 **(11 pages)**.

Çalışkan, Y.; Yatmaz, H.C., (2017). Bektaş N. Photocatalytic oxidation of high concentrated dye solutions enhanced by hydrodynamic cavitation in a pilot reactor. Process Saf. Environ. Prot. 111: 428–438 **(11 pages)**.

Cardoso, I.M.F.; Cardoso, R.M.F.; da Silva, J.C.G.E., (2021). Advanced oxidation processes coupled with nanomaterials for water treatment. Nanomaterials (Basel)., 11(8): 2045 **(13 pages)**.

Cardoso, R.M.F.; da Silva, J.C.G.E.; da Silva L.P., (2024). Application of engineered nanomaterials as nanocatalysts in catalytic ozonation: A review. Materials (Basel)., 17(13):3185 **(15 pages)**.

Chauke, N.M.; Raphulu, M., (2024). A review: Simultaneous one-Pot Pollution mitigation and hydrogen production from industrial wastewater using photoelectrocatalysis process. Mater. Today Catalysis., 5: 100052 **(26 pages)**.

Chen, C.; Lu; L.; Fei, L.; Xu, J.; Wang, B.; Li, B.; Shen, L.; Lin, H., (2023a). Membrane-catalysis integrated system for contaminants degradation and membrane fouling mitigation: A review. Sci. Total Environ., 904: 166220 **(28 pages)**.

Chen, D.; Cheng, Y.; Zhou, N.; Chen, P.; Wang, Y.; Li, K.; Huo, S.; Cheng, P.; Peng, P.; Zhang, R.; Wang, L.; Liu, H.; Liu, Y.; Ruan, R., (2020). Photocatalytic degradation of organic pollutants using TiO_2-based photocatalysts: A review. J. Cleaner Prod., 268:

121725 **(14pages)**.
Chen H, Han Z, Cao S, Li Y, Kang X, Cheng C, Chen X, Xu Y, Zhang H., (2023b). Ultra-facile fabrication of Oxygen vacancy-laden catalyst for peroxymonosulfate activation to degrade organic pollutant in water: Performance and mechanism. Chem. Eng. J., 453: 139660 **(12 pages)**.
Chen, L.; Xu, Q., (2019). Metal–organic framework composites for catalysis. Matter., 1(1): 57–89 **(33 pages)**.
Danya, U.; Kamaraj, M.; Suresh Babu, P.; Aravind, J., (2024). Bibliometric analysis and review of food waste management via sustainable approaches. Glob. J. Environ. Sci. Manage., 10(4): 2127–2144 **(18 pages)**.
Das, T.K.; Jesionek, M.; Çelik, Y.; Poater, A., (2023). Catalytic polymer nanocomposites for environmental remediation of wastewater. Sci. Total Environ., 901: 165772 **(22 pages)**.
de la Flor, M.P.; Camarillo, R.; Martínez, F.; Jiménez, C.; Quiles, R.; Rincón, J., (2022). Synthesis and Characterization of bimetallic TiO_2/CNT/Pd-Cu for efficient remediation of endocrine disruptors under solar light. J. Environ. Chem. Eng., 10(2): 107245 **(15 pages)**.
Desseigne, M.; Madigou, V.; Coulet, M-V.; Heintz, O.; Chevallier, V.; Arab, M., (2023). Au/WO_3 nanocomposite based photocatalyst for enhanced solar photocatalytic activity. J. Photochem. Photobiol. A., 437: 114427 **(12 pages)**.
Dhadda, S.; Jangir, N.; Sihag, P.; Bagaria, S.K.; Jangid, D.K., (2024). The designing of magnetic nanomaterials synthesis and applications in dye degradation: A Review. Environ. Sci. Pollut. Res., 2024: 1–23 **(24 pages)**.
El Gaini, L., (2024). Enhancing Solar-driven photocatalysis: Synergistic integration of biochar, semiconductors, and magnetic materials for degrading organic pollutants. Desalin. Water Treat., 320: 100798 **(25 pages)**.
Elgarahy, A.M.; Maged, A.; Eloffy, M.G.; Zahran, M.; Kharbish, S.; Elwakeel, K.Z.; Bhatnagar, A. (2023). Geopolymers as sustainable eco-friendly materials: Classification, synthesis routes, and applications in wastewater treatment. Sep. Purif. Technol., 324: 124631 **(26 pages)**.
Endo-Kimura, M.; Janczarek, M.; Bielan, Z.; Zhang, D.; Wang, K.; Markowska-Szczupak, A.; Kowalska, E., (2019). Photocatalytic and antimicrobial properties of Ag_2O/TiO_2 heterojunction. ChemEngineering., 3(1): 3 **(18 pages)**.
Esteves, B.M.; Morales-Torres, S.; Maldonado-Hódar, F.J.; Madeira, L.M., (2024). Catalytic peroxidation of winery wastewater contaminants using activated carbon-supported magnetite nanoparticles. J. Water Process Eng., 58: 104772 **(13 pages)**.
Etafo, N.O.; Bamidele, M.O.; Bamisaye, A.; Alli, Y.A., (2024). Revolutionizing photocatalysis: Unveiling efficient alternatives to Titanium (IV) Oxide and Zinc Oxide for comprehensive environmental remediation. J. Water Process Eng., 62: 105369 **(25 pages)**.
Farwa, U.; Sandhu, Z.A.; Kiran, A.; Raza, M.A.; Ashraf, S.; Gulzarab, H.; Fiaz, M.; Malik, A.; Al-Sehemi, A.G., (2024). Revolutionizing environmental cleanup: The evolution of MOFs as catalysts for pollution remediation. RSC Adv., 14(50): 37164–37195 **(32 pages)**.
Ghazal, H.; Koumaki, E.; Hoslett, J.; Malamis, S.; Katsou, E.; Barcelo, D.; Jouhara, H., (2022). Insights into current physical, chemical and hybrid technologies used for the treatment of wastewater contaminated with pharmaceuticals. J. Cleaner Prod., 361: 132079 **(22 pages)**.
Godja, N-C.; Munteanu, F-D., (2024). Hybrid nanomaterials: A brief overview of versatile solutions for sensor technology in healthcare and environmental applications. Biosensors., 14(2): 67 **(23 pages)**.
González-Fernández, C.; Bringas, E.; Rivero, M.J.; Ortiz, I., (2024). Revealing the role of magnetic materials in light-driven advanced oxidation processes: Enhanced degradation of contaminants and facilitated magnetic recovery. Front. Chem. Eng., 6: 1430773 **(22 pages)**.
Groeneveld, I.; Kanelli, M.; Ariese, F.; van Bommel, M.R., (2023). Parameters that affect the photodegradation of dyes and pigments in solution and on substrate–an overview. Dyes Pigments., 210: 110999 **(14 pages)**.
Gunasekaran, A.; Rajamani, A.K.; Masilamani, C.; Chinnappan, I.; Ramamoorthy, U.; Kaviyarasu, K., (2023). Synthesis and characterization of ZnO Doped TiO_2 nanocomposites for their potential photocatalytic and antimicrobial applications. Catalysts. 13(2): 215 **(23 pages)**.
Gupta, R.; Xie, H., (2018). Nanoparticles in daily life: Applications, toxicity and regulations. J. Environ. Pathol. Toxicol. Oncol., 37(3): 209–230 **(22 pages)**.
Gupta, T.; Samriti, J.; Cho, J.; Prakash, J., (2021). Hydrothermal synthesis of TiO_2 nanorods: Formation chemistry, growth mechanism, and tailoring of surface properties for photocatalytic activities. Mater. Today Chem., 20: 100428 **(40 pages)**.
He, Y.; Lv, H.; Daili, Y.; Yang, Q.; Junior, L.B.; Liu, D.; Liu, H.; Ma, Z., (2020). Construction of a new cascade photogenerated charge transfer system for the efficient removal of bio-toxic Levofloxacin and Rhodamine B from aqueous solution: Mechanism, Degradation Pathways and Intermediates Study. Environ. Res. 187: 109647 **(14 pages)**.
Hu, X.; Hu, X.; Tang, C.; Wen, S.; Wu, X.; Long, J.; Yang, X.; Wang, H.; Zhou, L., (2017). Mechanisms underlying degradation pathways of Microcystin-LR with doped TiO_2 photocatalysis. Chem. Eng. J., 330: 355–371 **(17 pages)**.
Ilinoiu, E.C.; Pode, R.; Manea, F.; Colar, L.A.; Jakab, A.; Orha, C.; Ratiu, C.; Lazau, C.; Sfarloaga, P., (2013). Photocatalytic activity of a Nitrogen-doped TiO_2 modified Zeolite in the degradation of Reactive Yellow 125 Azo dye. J. Taiwan Inst. Chem. Eng., 44(2): 270–278 **(9 pages)**.
Jiang, D.; Otitoju, T.A.; Ouyang, Y.; Shoparwe, N.F.; Wang, S.; Zhang, A.; Li, S., (2021). A review on metal ions modified TiO_2 for photocatalytic degradation of organic pollutants. Catalysts. 11(9): 1039 **(82 pages)**.
Kareem, M.A.; Bello, I.T.; Shittu, H.A.; Sivaprakash, P.; Adedokun, O.; Arumugam, S., (2022). Synthesis, characterization, and photocatalytic application of silver doped zinc oxide nanoparticles. Cleaner Mater., 3: 100041 **(7 pages)**.
Kaur, H.; Devi, N.; Siwal, S.S.; Alsanie, W.F.; Thakur, M.K.; Thakur, V.K., (2023). Metal–organic framework-based materials for wastewater treatment: Superior adsorbent materials for the removal of hazardous pollutants. ACS Omega. 8(10): 9004–9030 **(27 pages)**.
Kumar, A.; Mohite, P.; Munde, S.; Puri, A.; Edet, H.O.; Ochoule, D.O.; Chidrawar, V.R.; Nagime, P.V.; Uddin, M.J.; Singh, S., (2024). Revolutionizing the biomedical and environmental cleanup through polymeric nano-sponges: A review. Nano. Struct. Nano. Objects., 39: 101193 **(19 pages)**.

Kumari, H.; Sonia, S.; Suman, R.; Ranga, R.; Chahal, S.; Devi, S.; Sharma, S.; Kumar, S.; Kumar, P.; Kumar, S.; Kumar, A.; Parmar, R., (2023). A review on photocatalysis used for wastewater treatment: Dye degradation. Water Air Soil Pollut., 234(6): 349 **(46 pages)**.

Li, S.; Wang, C.; Liu, Y.; Liu, Y.; Cai, M.; Zhao, W.; Duan, X., (2023). S-Scheme MIL-101 (Fe) Octahedrons modified Bi_2WO_6 microspheres for photocatalytic decontamination of Cr(VI) and Tetracycline Hydrochloride: Synergistic insights, reaction pathways, and toxicity analysis. Chem. Eng. J., 455: 140943 **(12 pages)**.

Li, X.; Chen, Y.; Tao, Y.; Shen, L.; Xu, Z.; Bian, Z.; Li, H., (2022). Challenges of photocatalysis and their coping strategies. Chem. Cat., 2(6): 1315–1345 **(31 pages)**.

Linghu, X.; Shu, Y.; Liu, L.; Zhao, Y.; Zhang, J.; Chen, Z.; Shan, D.; Wang, B., (2023) Hydro/solvothermally synthesized Bismuth Tungstate nanocatalysts for enhanced photocatalytic degradation of ayes, antibiotics, and bacteria in wastewater: A review. J. Water Process Eng. 54: 103994 **(26 pages)**.

Liu, Z.; Bakhtari, M.F.; Han, X., (2024). Preparation of bimetallic Pb/Zn metal-organic framework @Graphene Oxide composite and its adsorption performance for Pb(II) and Zn(II). Environ. Eng. Res., 29(6): 240198 **(12 pages)**.

Lu, Z.; Cai, B.; Xie, Q.; Hu, C.; Liu, Q.; Cai, X., (2023). Preparations of Cyclodextrin polymer and MgO jointly entrapped Iron(III)-TAML catalysts for the removal of aromatic pollutants in water. Sep. Purif. Technol., 304: 122311 **(10 pages)**.

Ma, X.; Tian, Y.; Yang, R.; Wang, H.; Allahou, L.W.; Chang, J.; Williams, G.; Knowles, J.C.; Poma, A., (2024). Nanotechnology in healthcare, and its safety and environmental risks. J. Nanobiotechnol., 22(1): 715 **(81 pages)**.

Mahadevan, R.; Palanisamy, S.; Sakthivel, P., (2023). Role of nanoparticles as oxidation catalyst in the treatment of textile wastewater: Fundamentals and Recent Advances. Sustain. Chem. Environ., 4: 100044 **(17 pages)**.

Mahmoud, M.A.; Alsehli, B.R.; Alotaibi, M.T.; Hosni, M.; Shahat, A., (2024). A comprehensive review on the application of semiconducting materials in the degradation of effluents and water splitting. Environ. Sci. Pollut. Res. Int., 31(3): 3466–3494 **(29 pages)**.

Mariselvam, R.; Ranjitsingh, A.J.A.; Mosae Selvakumar, P.; Alarfaj, A.A.; Munusamy, M.A., (2016). Spectral studies of UV and solar photocatalytic degradation of Azo dye and textile dye effluents using green synthesized Silver nanoparticles. Bioinorg. Chem. Appl., 2016(1): 8629178 **(8 pages)**.

Masood, Z.; Ikhlaq, A.; Akram, A.; Qazi, U.Y.; Rizvi, O.S.; Javaid, R.; Alazmi, A.; Madkour, M.; Qi, F., (2022). Application of nanocatalysts in advanced oxidation processes for wastewater purification: Challenges and future prospects. Catalysts. 12(7): 741 **(23 pages)**.

Meng, Y.; Wang, Y.; Ye, Z.; Wang, N.; He, C.; Zhu, Y.; Fujita, T.; Wu, H.; Wang, X., (2023). Three-dimension Titanium phosphate aerogel for selective removal of radioactive Strontium (II). J. Environ. Manage., 325(B): 116424 **(11 pages)**.

Merdoud, R.; Aoudjit, F.; Mouni, L.; Ranade, V.V., (2024). Degradation of Methyl Orange using hydrodynamic cavitation, H_2O_2, and photocatalysis with TiO_2-coated Glass fibers: Key operating parameters and synergistic effects. Ultrason. Sonochem., 103: 106772 **(9 pages)**.

Mushahary, N.; Sarkar, A.; Basumatary, F.; Brahma, S.; Das, B.; Basumatary, S., (2024). Recent developments on Graphene Oxide and its composite materials: from fundamentals to applications in biodiesel synthesis, adsorption, photocatalysis, supercapacitors, sensors, and antimicrobial activity. Results Surf. Interfaces., 15: 100225 **(37 pages)**.

Mustafa, F.S.; Oladipo, A.A., (2021). Photocatalytic degradation of Metronidazole and bacteria disinfection activity of Ag–Doped $Ni0.5Zn0.5Fe_2O_4$. J. Water Process Eng., 42: 102132 **(11 pages)**.

Navrotskaya, A.G.; Aleksandrova, D.D.; Krivoshapkina, E.F.; Sillanpää, M.; Krivoshapkin, P.V., (2020). Hybrid materials based on Carbon nanotubes and nanofibers for environmental applications. Front. Chem., 8: 546 **(9 pages)**.

Nawaz, R.; Ullah, H.; Ghanim, A.A.J.; Irfan, M.; Anjum, M.; Rahman, S.; Ullah, S.; Abdel Baki, Z.; Kumar Oad, V., (2023). Green synthesis of ZnO and black TiO_2 materials and their application in photodegradation of organic pollutants. *ACS* Omega., 8(39): 36076–36087 **(12 pages)**.

Nizam, N.U.M.; Hanafiah, M.M.; Woon, K.S., (2021). A content review of life cycle assessment of nanomaterials: Current practices, challenges, and future prospects. Nanomaterials (Basel)., 11(12): 3324 **(27 pages)**.

Pansambal, S.; Oza, R.; Borgave, S.; Chauhan, A.; Bardapurkar, P.; Vyas, S.; Ghoteka, S., (2023). Bioengineered cerium oxide (CeO_2) nanoparticles and their diverse applications: a review. Appl. Nanosci., 13: 6067–6092 **(26 pages)**.

Patra, R.; Dash, P.; Panda, P.K.; Yang, P-C., (2023). A breakthrough in photocatalytic wastewater treatment: the incredible potential of g-C_3N_4/titanate Perovskite-based nanocomposites. Nanomaterials (Basel)., 13(15): 2173 **(32 pages)**.

Pinzari, F., (2024). Synthesis, photocatalytic and bio activity of ZnO-TiO_2 nanocomposites: A review study. Reactions. 5(4): 680–739 **(60 pages)**.

Qamar, M.A.; Javed, M.; Shahid, S.; Shariq, M.; Fadhali, M.M.; Ali, S.K.; Khan, M.S., (2023). Synthesis and applications of graphitic carbon nitride (g-C_3N_4) based membranes for wastewater treatment: A critical review. Heliyon., 9(1): e12685 **(31 pages)**.

Qi, K.; Liu, S.Y.; Zada, A., (2020). Graphitic carbon nitride, a polymer photocatalyst. J. Taiwan Inst. Chem. Eng., 109: 111–123 **(13 pages)**.

Rafiq, A.; Ikram, M.; Ali, S.; Niaz, F.; Khan, M.; Khan, Q.; Maqbool, M., (2021). Photocatalytic degradation of dyes using semiconductor photocatalysts to clean industrial water pollution. J. Ind. Eng. Chem., 97: 111–128 **(18 pages)**.

Rani, M.; Shanker, U., (2020). Efficient photocatalytic degradation of Bisphenol A by metal ferrites nanoparticles under sunlight. Environ Technol Innov., 19, 100792 **(17 pages)**.

Rashid, A.B.; Haque, M.; Islam, S.M.M.; Uddin Labib, K.M.R., (2024). Nanotechnology-enhanced fiber-reinforced polymer composites: Recent advancements on processing techniques and applications. Heliyon., 10(2): e24692 **(29 pages)**.

Rashid, M.M.; Simončič, B.; Tomšič, B., (2021). Recent advances in TiO_2-functionalized textile surfaces. Surf. Interfaces., 22: 100890 **(33 pages)**.

Raza, A.; Altaf, S.; Ali, S.; Ikram, M.; Li, G., (2022). Recent advances in carbonaceous sustainable nanomaterials for Wastewater Treatments. Sustain. Mater. Technol., 32: e00406 **(50 pages)**.

Razzaq, U.; Nguyen, T-B.; Saleem, M.U.; Le, V-R.; Chen, C-W.; Bui, X-T.; Dong, C-D., (2024). Recent progress in electro-fenton

technology for the remediation of pharmaceutical compounds in aqueous environments. Sci. Total Environ., 946: 174253 **(16 pages)**.

Rigoletto, M.; Calza, P.; Gaggero, E.; Laurenti, E., (2022) Hybrid materials for the removal of emerging pollutants in water: Classification, Synthesis, and Properties. Chem. Eng. J. Adv., 10: 100252 **(16 pages).**

Sajid, M.; Asif, M.; Baig, N.; Kabeer, M.; Ihsanullah, I.; Mohammad, A.W., (2022) Carbon nanotubes-based adsorbents: Properties, functionalization, interaction mechanisms, and applications in water purification. J. Water Process Eng., 47: 102815 **(19 pages)**.

Salahshoori, I.; Yazdanbakhsh, A.; Namayandeh Jorabchi, M.N.; Kazemabadi, F.Z.; Khonakdar, H.A.; Mohammadi, A.H., (2024). Recent advances and applications of stimuli-responsive nanomaterials for water treatment: A comprehensive review. Adv. Colloid Interface Sci., 333: 103304 **(30 pages)**.

Sanni, S.E.; Oni, B.A.; Okoro, E.E.; Pandya, S., (2024). Recent advances in the use of biogenic nanomaterials and photocatalysts for wastewater treatment: Challenges and future prospects. Front. Nanotechnol. 6: 1469309 **(45 pages)**.

Satyam, S.; Patra, S., (2024). Innovations and challenges in adsorption-based wastewater remediation: A comprehensive review. Heliyon. 10(9): e29573 **(24 pages)**.

Sewnet, A.; Abebe, M.; Asaithambi, P.; Alemayehu, E., (2022). Visible-light-driven g-C_3N_4/TiO_2 based heterojunction nanocomposites for photocatalytic degradation of organic dyes in wastewater: A review. Air Soil Water Res. 2022: 15 **(23 pages)**.

Sharma, S.; Devi, A.; Bhattacharyya, K.G., (2023). Nickel-Titanium dioxide-fuller's earth nanocomposites: synthesis, characterization and application as a photocatalyst in aqueous methylene blue degradation under visible light irradiation. Inorg. Chem. Commun., 151: 110550 **(10 pages)**.

Shivani, V.; Harish, S.; Archana, J.; Navaneethan, M.; Ponnusamy, S.; Hayakawa, Y., (2019). Highly efficient 3-D hierarchical Bi_2WO_6 catalyst for environmental remediation. Appl. Surf. Sci., 488: 696–706 **(11 pages)**.

Shoaib, H.; Butt, T.E.; Hina, A.; Hina, F., (2024). Life cycle of medicinal compounds from lifesaving to life threating component in environment-innovative use of nanotechnology for treatment. Cleaner Water., 2: 100046 **(17 pages)**.

Silerio-Vázquez, F.J.; González-Burciaga, L.A.; Antileo, C.; Núñez-Núñez, C.M., Proal-Nájera, J.B., (2024). Photocatalytic degradation of antibiotics in water via TiO_2-x: Research needs for technological advancements. J. Hazard. Mater. Adv., 16: 100506 **(20 pages)**.

Singh, B.J.; Chakraborty, A.; Sehgal, R., (2023a). A systematic review of industrial wastewater management: evaluating challenges and enablers. J. Environ. Manage., 348: 119230 **(34 pages)**.

Singh, G.; Ubhi, M.K.; Jeet, K.; Singla, C.; Kaur, M., (2023b). A review on impacting parameters for photocatalytic degradation of organic effluents by ferrites and their nanocomposites. Processes., 11(6): 1727 **(23 pages)**.

Singh, P.; Mohan, B.; Madaan, V.; Ranga, R.; Kumari, P.; Kumar, S.; Bhankar, V.; Kumar, P.; Kumar, K., (2022). Nanomaterials photocatalytic activities for waste water treatment: A review. Environ. Sci. Pollut. Res. Int., 29(46): 69294–69326 **(33 pages)**.

Sinha, R.; Ghosal, P.S., (2023). A comprehensive appraisal on status and management of remediation of DBPs by TiO_2 based-photocatalysts: Insights of technology, performance and energy efficiency. J. Environ. Manage., 328: 117011 **(19 pages)**.

Song, R.; Yao, J.; Yang, M.; Ye, Z.; Xie, Z.; Zeng, X., (2022). Active site regulated Z-scheme MIL-101(Fe)/Bi2WO6/Fe(III) with the synergy of hydrogen peroxide and vsible-light-driven photo-fenton degradation of organic contaminants. Nanoscale., 14(18): 7055–7074 **(20 pages)**.

Suhan, M.B.K.; Al-Mamun, M.R.; Farzana, N.; Aishee, S.M.; Islam, M.S.; Marwani, H.M.; Hasan, M.M.; Asiri, A.M.; Rahman, M.M.; Islam, A.; Awual, M.R., (2023). Sustainable pollutant rRemoval and wastewater remediation using TiO_2-based nanocomposites: A critical review. Nano Struct. Nano Objects., 36: 101050 **(26 pages)**.

Sun, W.; Hong, Y.; Li, T.; Chu, H.; Liu, J.; Feng, L.; Baghayeri, M., (2023). Biogenic synthesis of reduced Graphene Oxide decorated with Silver nanoparticles (rGO/Ag NPs) using table Olive (*Olea europaea*) for efficient and rapid catalytic reduction of organic pollutants. Chemosphere., 310: 136759 **(8 pages)**.

Tahir, M.B.; Nabi, G.; Sagir, M.; Rafique, M.; Alrobei, H.; Nawaz, T.; Inayat, A.; Hussain, S.; Naz, G.; Iqbal, K.; Tahir, M.S., (2021). Role of CTF in Bi_2WO_6/ZnO photocatalysts for effective degradation and hydrogen energy evolution. Int. J. Hydrog. Energy., 46(59): 30606–30614 **(9 pages)**.

Thakur, S.; Ojha, A.; Kansal, S.K.; Gupta, N.K.; Swart, H.C.; Cho, J.; Kuznetsov, A.; Sun, S.; Prakash, J., (2024). Advances in powder nano-photocatalysts as pollutant removal and as emerging contaminants in water: Analysis of pros and cons on health and environment. Adv. Powder Mater., 3(6): 100233 **(37 pages)**.

Tripathy, J.; Mishra, A.; Pandey, M.; Thakur, R.R.; Chand, S.; Rout, P.R.; Shahid, M.K., (2024). Advances in nanoparticles and nanocomposites for water and wastewater treatment: A review. Water., 16(11): 1481 **(26 pages)**.

Ugwuanyi, E.D.; Nwokediegwu, Z.Q.S.; Dada, M.A.; Majemite, M.T.; Obaigbena, A., (2024). The impact of nanomaterials in enhancing wastewater treatment processes: A review. Magna Sci. Adv. Res. Rev., 10(1): 273–285 **(13 pages)**.

Varela, C.F.; Pazos, M.C.; Alba, M.D., (2021). Organophilization of acid and thermal treated sepiolite for its application in BTEX adsorption from aqueous solutions. J. Water Process Eng., 40: 101949 **(9 pages)**.

Varmaziar, M.; Amooey, A.A.; Ghasemi, S., (2024). $BiVO_4$/Sulfur-doped g-C_3N_4 nanocomposite as photocatalyst for degradation of Ciprofloxacin under visible light irradiation. Diam. Relat. Mater., 149: 111539 **(13 pages)**.

Vijayakumar, T.P.; Benoy, M.D.; Duraimurugan, J.; Suresh Kumar, G.; Shkir, M.; Maadeswaran, P.; Senthil Kumar, A.; Ramesh Kumar, K.A., (2022). Hydrothermal synthesis of CuO/g-C_3N_4 nanosheets for visible-light driven photodegradation of Methylene Blue. Diam. Relat. Mater., 121: 108735 **(9 pages)**.

Wang, K.; Shao, X.; Zhang, K.; Wang, J.; Wu, X.; Wang, H., (2022b). 0D/3D Bi_3TaO_7/$ZnIn_2S_4$ heterojunction photocatalyst towards degradation of antibiotics coupled with simultaneous H_2 evolution: In situ irradiated XPS investigation and S-scheme mechanism insight. Appl. Surf. Sci., 596: 153444 **(10 pages)**.

Wang, L.; Liu, Y.; Lin, Y.; Zhang, X.; Yu, Y.; Zhang, R., (2022a). Z-Scheme $Cu_2(OH)_3F$ nanosheets-decorated 3D Bi_2WO_6 heterojunction with an intimate hetero-surface contact through a hydrogen bond for enhanced photoinduced charge separation and transfer. Chem. Eng. J., 427: 131704 **(12 pages)**.

Wang, S.; Alenius, H.; El-Nezami, H.; Karisola, P., (2022c). A new

look at the effects of engineered ZnO and TiO_2 nanoparticles: evidence from transcriptomics studies. Nanomaterials (Basel)., 12(8): 1247 **(34 pages)**.

Wei, Z.; Liu, J.; Shangguan, W., (2020). A review on photocatalysis in antibiotic wastewater: Pollutant degradation and hydrogen production. Chin. J. Cat., 41(10): 1440–1450 **(11 pages)**.

Xiao, Z.; Wu, R.; Shu, T.; Wang, Y.; Li, L., (2023). Synthesis of Co-doped Fe metal–organic framework MIL-101(Fe,Co) and efficient degradation of organic dyes in water. Sep. Purif. Technol., 304: 122300 **(11 pages)**.

Yaqoob, A.A.; Parveen, T.; Umar, K.; Mohamad Ibrahim, M.N., (2020). Role of nanomaterials in the treatment of wastewater: A review. Water., 12(2): 495 **(30 pages)**.

Yi, J.; Xie, R.; Liu, R.; Li, M.; Zeng, H.; Chen, Q.; Cai, L.; Li, N.; Yu, C.; Liu, Z.; Li, D., (2023). Hollow BiOI/Bi_5O_7I hierarchical microsphere with S-Scheme heterostructure for efficiently removal of Tetracycline Hydrochloride. J. Water Process Eng., 53: 103798 **(11 pages)**.

Zango, Z.U.; Jumbri, K.; Sambudi, N.S.; Ramli, A.; Abu Bakar, N.H.H.; Saad, B.; Rozaini, M.N.H.; Isiyaka, H.A.; Jagaba, A.H.; Aldaghri, O.; Sulieman, A.A., (2020). A critical review on metal–organic frameworks and their composites as advanced materials for adsorption and photocatalytic degradation of emerging organic pollutants from wastewater. Polymers., 12(11): 2648 **(42 pages)**.

Zhang, Q.; Zhang, Z.; Zhao, D.; Wang, L.; Li, H.; Zhang, F.; Huo, Y.; Li, H., (2023). Synergistic photocatalytic-photothermal contribution enhanced by rRecovered Ag+ ions on MXene membrane for organic pollutant removal. Appl. Cat. B., 320: 122009 **(11 pages)**.

Zhang, Y.; Li, Y.; Yuan, Y., (2022). Carbon quantum dot-decorated BiOBr/Bi2WO6 photocatalytic micromotor for environmental remediation and DFT calculation. ACS Cat., 12(22): 13897–13909 **(13 pages)**.

Zhao, J.; Wang, P.; Liu, C.; Zhao, Q.; Wang, J.; Shi, L.; Xu, G.; Abudula, A.; Guan, G., (2023). Nanosheet-state Cobalt-Manganese Oxide with multifarious active regions derived from oxidation-etching of metal organic framework precursor for catalytic combustion of Toluene. J. Coll. Interface Sci., 629(A): 706–722 **(17 pages)**.

Zheng, Z.; He, J.; Zhang, Z.; Kumar, A.; Khan, M.; Lung, C.W.; Lo, I.M.C., (2024). Magnetically recyclable nanophotocatalysts in photocatalysis-involving processes for organic pollutant removal from wastewater: current status and perspectives. Environ. Sci. Nano., 2024;11(5):1784–1816 **(33 pages)**.

Zhu, H.; Jiang, R.; Fu, Y.; Guan, Y.; Yao, J.; Xiao, L.; Zeng, G., (2012). Effective photocatalytic decolorization of Methyl Orange utilizing TiO_2/ZnO/Chitosan nanocomposite films under simulated solar irradiation. Desalination. 286: 41–48 **(8 pages)**.

AUTHOR (S) BIOSKETCHES

Aravind, J., Ph.D. Professor, Department of Biotechnology, Saveetha School of Engineering, Saveetha Institute of Medical and Technical Sciences, Chennai- 602105, Tamil Nadu, India
- Email: *dr.j.aravind@gmail.com*
- ORCID: 0000-0001-9699-2312
- Web of Science ResearcherID: O-9296-2015
- Scopus Author ID: 23569355700
- Homepage: https://www.grd.org/grdcs/bio-technology/

Kamaraj, M., Ph.D., Associate Professor, Department of Biotechnology, Faculty of Science and Humanities, SRM Institute of Science and Technology -Ramapuram Campus, Chennai- 600089, Tamil Nadu, India.
- Email: *drkamarajm@gmail.com*
- ORCID: 0000-0002-0111-8524
- Web of Science ResearcherID: AAP-1422-2020
- Scopus Author ID: 55645159500
- Homepage: https://fsh.srmrmp.edu.in/department-of-biotechnology/faculty/dr-kamaraj-m/

Suresh Babu, P., Ph.D., Assocaite Professor, Department of Biotechnology, Saveetha School of Engineering, Saveetha Institute of Medical and Technical Sciences, Chennai- 602105, Tamil Nadu, India.
- Email: *suresh78785@rediffmail.com*
- ORCID: 0000-0001-9859-2208
- Web of Science ResearcherID:
- Scopus Author ID: 57226597886
- Homepage: https://saveetha.irins.org/profile/286107

HOW TO CITE THIS ARTICLE

Aravind, J..; Kamaraj, M.; Sureshbabu, P. (2025). Bibliometrics analysis and the role of nanocatalysts in wastewater remediation. Global J. Environ. Sci. Manage., 11(3): 1299-1318.

DOI: 10.22034/gjesm.2025.03.23

URL: https://www.gjesm.net/article_724943.html

Global J. Environ. Sci. Manage. 11(3): 1319-1342, Summer 2025, Serial #43

Global Journal of Environmental Science and Management
(GJESM)

Homepage: https://www.gjesm.net/

Podcasts

REVIEW PAPER

A bibliometric study on Sordariales fungi covering genetic diversity, ecological interactions and biotechnological applications

N.F. Wulandari[1*], A.R. Syam[2], L. Alhamd[3], B. Gunadi[4], Yosmaniar[5], E. Widjaja[6], B.N. Utomo[7], S. Wahyuwardani[7], R. Widiastuti[7], T. Kadarini[4], S. Dody[8]

[1] *Research Center for Biosystematics and Evolution, National Research and Innovation Agency, Cibinong 16911, Indonesia*

[2] *Research Center for Conservation of Marine and Inland Water Resources, National Research and Innovation Agency, Cibinong 16911, Indonesia*

[3] *Research Center for Ecology and Ethnobiology, National Research and Innovation Agency, Cibinong 16911, Indonesia*

[4] *Research Center for Fishery, National Research and Innovation Agency, Cibinong 16911, Indonesia*

[5] *Research Center for Marine and Land Bioindustry, National Research and Innovation Agency, Serpong 15314, Indonesia*

[6] *Research Center for Sustainable Production System and Life Cycle Assessment, National Research and Innovation Agency, Serpong 15314, Indonesia*

[7] *Research Center for Veterinary Science, National Research and Innovation Agency, Cibinong 16911, Indonesia*

[8] *Research Center for Oceanography, National Research and Innovation Agency, Serpong 15314, Indonesia*

ARTICLE INFO

Article History:
Received 02 January 2025
Revised 08 March 2025
Accepted 16 April 2025

Keywords:
Bibliometric analysis
Biotechnology
Ecological interactions
Genetic diversity
Sordariales

ABSTRACT

The kingdom fungi, with its vast diversity and applications, is crucial in maintaining ecosystem balance and supporting industries like food production and environmental protection. Despite their ecological value, research on Sordariales is limited compared to other fungal orders. The aims include outlining the Sordariales research landscape, recognizing important themes and areas lacking attention, and showcasing potential uses in biotechnology. The data retrieval from Scopus from 1978 to 2024 for various aspects of Sordariales, including agricultural, nutritional, and industrial dimensions. Carefully selected search terms were implemented throughout all sections, such as titles, abstracts, and keywords. These terms were subsequently filtered to incorporate the latest relevant literature and subjected to a comprehensive bibliometric analysis, employing visualization of similarities (version 1.6.20) and the bibliometric R package. Publication trends with minimal research output were recorded until the 1990s, and an increase starting in 1995, which was widely published in high-impact journals with the top journals. Sordariales studies emphasize its ecological, genetic, and industrial importance across multiple scientific fields. The worldwide distribution of Sordariales research indicates that China is in the lead, with the United States ranking second. Research pattern shows the first cluster was fungal ecology and microbial diversity, the second cluster delves into the genetic and molecular biology of Sordariales, and the third cluster centers on the biochemical and enzymatic properties of Sordariales, despite emerging research assisting researchers in recognizing key trends and future directions. The role of Sordariales in carbon and nitrogen processes, as demonstrated by biotechnological applications, is crucial for converting livestock waste into compost, bio-based products, or biofuels. This conversion can help mitigate the environmental impact of animal agriculture and improve soil health and nutrient availability, which are vital for supporting plant growth and the functioning of microbial communities. Soil-related function highlights Sordariales fungi's significant role in soil ecosystems, underscoring their interactions with other microorganisms and their impact on nutrient cycling. Sordariales contribute to soil health by decomposing organic matter, recycling nutrients, and supporting biogeochemical cycles, thus aiding ecosystem stability. he metabolic diversity and biotechnological possibilities of fermentation and enzymes are prominently displayed. Plant-root related function reveals significant linkages between Sordariales and plant-root functions. Concurrently, enzymes decompose cellulose into simpler sugars, promoting nutrient cycling and boosting soil fertility. Co-occurrence analysis of Sordariales identified major clusters-fungal ecology, molecular genetics, biochemistry, and phylogenetics-reflecting interconnected research themes and highlighted genetic studies, soil functions, and enzyme applications. Sordariales' roles in carbon and nitrogen cycling, enzyme production, and plant interactions. Upcoming studies should enhance data collection methods and delve into the molecular mechanisms, since Sordariales fungi are essential for ecological functions and offer promising opportunities for biotechnological advancements.

DOI: 10.22034/gjesm.2025.03.24

This is an open access article under the CC BY license (http://creativecommons.org/licenses/by/4.0/).

NUMBER OF REFERENCES
108

NUMBER OF FIGURES
7

NUMBER OF TABLES
2

*Corresponding Author:
Email: *nila003@brin.go.id*
Phone: : +62896 2862 5156
ORCID: 0000-0003-4467-075

Note: Discussion period for this manuscript open until Sep 1, 2025 on GJESM website at the "Show Article".

INTRODUCTION

With its vast diversity and applications, the kingdom of Fungi is crucial in maintaining ecosystem balance and supporting industries like food production and environmental protection (Corbu *et al*., 2023; Hussin *et al*., 2023). Fungi linked to marine plastic waste, such as those from the Sordariales order, demonstrate intricate relationships with different ecosystems, highlighting the significance of researching fungi to gain deeper insights into ecological dynamics (Vaksmaa *et al.,* 2024; Nakbi *et al.,* 2024). The Sordariales, an order within the Sordariomycetes class in the phylum Ascomycota, occupy diverse ecological niches, playing essential roles in nutrient cycles, decomposition, and symbiotic relationships in both terrestrial and aquatic ecosystems (Bao *et al.,* 2023; Debeljak and Baltar, 2023). Although Sordariales hold significant ecological importance, studies focusing on this fungal order are relatively scarce in comparison to others (Wang *et al.,* 2023b). Sordariales serve as reservoirs of secondary metabolites, offering valuable applications and warranting further study, especially given the potential of omics tools for discovering new secondary metabolites in this group (Charria-Girón *et al.,* 2022; Shao *et al.,* 2022). The complexity of Sordariales is further demonstrated through interactions with animals, as they serve dual roles as both pathogens and symbionts. For example, species like *Sordaria fimicola* typically release spores from mammalian dung, playing a role in nutrient cycles. Their spores found in ancient sediments can even indicate past herbivore activity (Wang, 2020). In addition to their role in decomposition, Sordariales species establish advantageous partnerships with plants, promoting their growth and resilience, which is essential for sustainable agricultural practices (Voigt *et al.,* 2021). This study uses a bibliometric approach to explore Sordariales genetic diversity, ecological interactions, and biotechnological applications, reviewing research trends and identifying areas for further analysis (Bao *et al.,* 2023). The progress in genomics and molecular biology, particularly through high-throughput sequencing and bioinformatics, has paved the way for new research into the genetic diversity of Sordariales. These technologies help uncover new genes and metabolic pathways, potentially leading to discoveries in enzymes, antibiotics, and bioactive compounds. Given the extensive data available, a systematic literature review is necessary to synthesize insights effectively and drive biotechnological advancements (Hensen *et al.,* 2023). Conducting a bibliometric analysis is vital for recognizing major research areas, impactful studies, and leading scholars in the Sordariales discipline (Maltseva and Batagelj, 2024). Citation patterns and publication trends reveal the evolution and expansion of Sordariale's research, benefiting researchers navigating vast literature and funding agencies allocating resources efficiently (Hensen *et al.,* 2023). Combining bibliometric and content analyses yields an in-depth understanding of themes and trends, highlighting dominant research methods, focal topics, and emerging patterns (Wang *et al.,* 2023a). This approach, widely used across various fields from 2000 to 2024, gives a holistic view of current knowledge, helping identify areas needing further exploration (Corbu *et al.*, 2023; Marin-Felix *et al.,* 2020). Combining bibliometric and content analysis offers a comprehensive insight into Sordariale's research. While bibliometric analysis offers quantitative insights into publication and citation patterns (Charria-Girón *et al.,* 2022; Hensen *et al.,* 2023; Marin-Felix and Miller, 2022; Bao *et al.,* 2023), content analysis delivers qualitative assessments. These techniques facilitate an in-depth evaluation, steer research initiatives, and encourage cooperation among scholars. Currently, a dedicated bibliometric study on Sordariales is lacking, highlighting the need for systematic analysis to map this study landscape (Wang *et al.,* 2023b). This study improves the understanding of the ecological roles and genetic diversity of Sordariales by analyzing publication and citation trends, pinpointing key themes, identifying knowledge gaps, and exploring potential biotechnological applications (Voigt *et al.,* 2021; Wang *et al.,* 2023b). This analysis will spotlight prevalent topics in current literature, reflecting the group's ecological significance and opening doors for future research and innovation. Interdisciplinary collaboration, integrating biosystematics, and biotechnology promises to accelerate discoveries in Sordariales research, enhancing both ecological insights and industrial applications. The aims include outlining the Sordariales research landscape, recognizing important themes and areas lacking attention, and showcasing potential uses in biotechnology. By mapping the research landscape, we aim to highlight opportunities for future innovation. Specifically, the study addresses several questions: 1) What are the key publication and citation trends in Sordariales

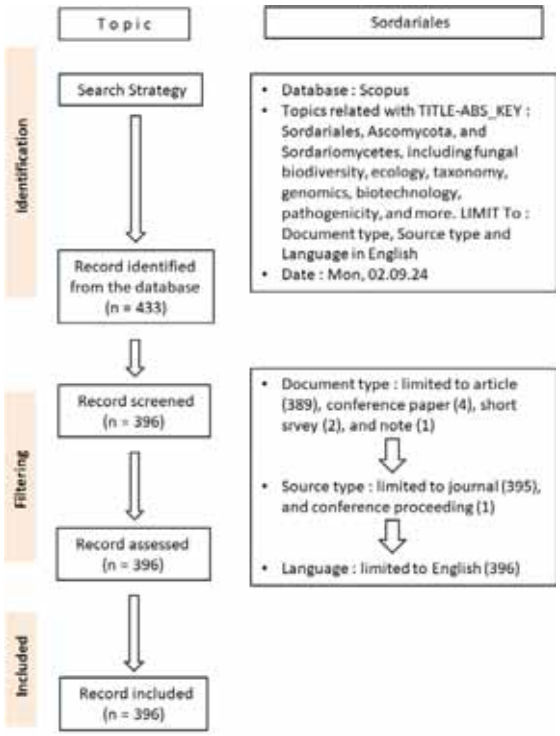

Fig. 1: A review procedure adapted from the preferred reporting items for systematic reviews and meta-analyses (PRISMA) flow diagram

research? 2) What predominant themes and topics emerge What significant patterns can be observed in the publication and citation of the current literature? 3) How do these themes reflect the ecological roles and genetic diversity of Sordariales? 4) What potential biotechnological applications have been explored? 5) What new opportunities exist for future research and innovation? Achieving these goals contributes to the expanding knowledge base on Sordariales, stimulating further research in mycology. This study underscores the importance of Sordariales in both ecological and biotechnological contexts, urging a comprehensive analysis of their diverse contributions, such as nutrient cycling, plant symbiosis, and industrial applications. This study has been carried out in National Research and Innovation Agency of Indonesia, in 2024.

METHODOLOGY

The data extraction from Scopus database was executed with a systematic and rigorous methodology. Scopus, an Elsevier-managed database, provides access to over 70 million records, offering researchers a vast repository of high-quality publications and analytical tools for efficient research. In order to address the comprehensive aspects of Sordariales, which include agricultural, nutritional, and industrial factors, strategically selected search terms were employed throughout all sections, including titles, abstracts, and keywords. This comprehensive strategy yielded 433 data points (Fig. 1), essential for a multidimensional analysis of Sordariales research.

A temporal filter limited results to the last five years (2020–2024), including the latest relevant literature. This period was selected to capture the latest research trends and developments in the field. Notably, between 2020 and 2024, there has been a significant increase in publications related to Sordariales, reflecting growing global interest in the topic. Concentrating on this specific time period allows for a more pertinent and current analysis, which can aid in shaping future research endeavors. After the initial search, records underwent thorough screening with stringent criteria, primarily focusing on English-language articles and proceedings. Through a meticulous selection process, the dataset was condensed to 396 entries, providing a strong foundation for an extensive bibliometric analysis of current research on Sordariales.

Table 1. Terminology mapping for network visualization: VOSviewer Term Replacement Data

Label	Replace by	Label	Replace by
Animals		Deoxyribonucleic acid (DNA), fungal	Fungal DNA
Article		DNA, ribosomal	Ribosomal DNA
Comparative Study		Fungal proteins	Fungal protein
Controlled Study		Fungus	Fungi
Human		Gene expression regulation, fungal	Gene expression regulation
Humans		Gene, fungal	Gene
Nonhuman		Genes, fungal	Gene
Priority Journal		Ribosome DNA	Ribosomal DNA
Unclassified Drug		Soils	Soil
Bacteria (Microorganisms)	Bacteria	Sp.	Species
Bacterium	Bacteria	Spores, fungal	Spore

Bibliometric and content analysis

The bibliometric analysis of Scopus metadata utilized visualization of similarities (VOSviewer) (version 1.6.20) and the Bibliometrix R package (version 4.1.1 on R software 4.4.1) to explore the key trends and future directions in Sordariales research (van Eck and Waltman, 2023; Aria and Cuccurullo, 2017; Team, 2018). Through a meticulous selection process, the dataset was condensed to 396 entries, providing a strong foundation for an extensive bibliometric analysis of current research on Sordariales. Bibliometric tools are useful for tracking research trends in Sordariales, but they have limitations. High impact factor (IF) journals are often used as quality indicators, yet studies show that significant fungal discoveries frequently occur in journals with low or no impact factors (Ifs). Furthermore, the presence of incomplete author information in databases, along with biases associated with gender or institutions, can distort the findings. These issues highlight the need for cautious interpretation of bibliometric data, especially in niche fields like fungal taxonomy. The research used both descriptive and co-occurrence analyses, combining Bibliometrix descriptive capabilities with VOSviewer structured keyword mapping. By analyzing co-occurrence patterns, VOSviewer grouped frequently occurring keywords into clusters, highlighting the thematic connections present the literature (Baker *et al.,* 2020). Sordiariales order is gaining more attention for their roles in nature and their uses in science. Nevertheless, the fungal order *Sordariales* remains largely unexplored in terms of bibliometric analysis. There is no comprehensive overview of how research on this group has grown or changed over time. The current study aims to bridge that gap by implementing a minimum occurrence threshold of five, thereby ensuring the inclusion of pertinent results and excluding less important keywords. The 100 keywords with the highest total link strength were selected to capture core themes and emerging trends within Sordariale's research. The next step in the refinement process included the standardization of keywords by consolidating both singular and plural forms (for instance, "bacterium" with "bacteria") and uniting synonyms (such as "fungus" with "fungi"), while eliminating irrelevant terms like "animals," "article," and "controlled study." This ensured the analysis focused solely on Sordariales-relevant literature (Table 1).

The visualization of keyword clusters was achieved through network maps, illustrating that keywords with a high degree of co-occurrence are situated near each other and connected by network pathways. An overlay visualization was generated with nodes meeting a minimum strength of 30 and displaying the 500 strongest links among them. It established a network of nodes in yellow or bright green, signifying the most recent research topics (Fig. 2).

Finally, these clusters were further explored within Bibliometrics to retrieve full-text papers. Prominent and well-cited articles from each cluster were identified, serving as a foundation for grasping upcoming research paths in the field of Sordariales studies. No bibliometric studies specifically addressing the order Sordariales were identified in the search. Nonetheless, there is relevant research, particularly in the form of phylogenetic studies concerning Sordariales. This work has culminated in the formation of several new families that more effectively illustrate the natural relationships among various taxa. While not

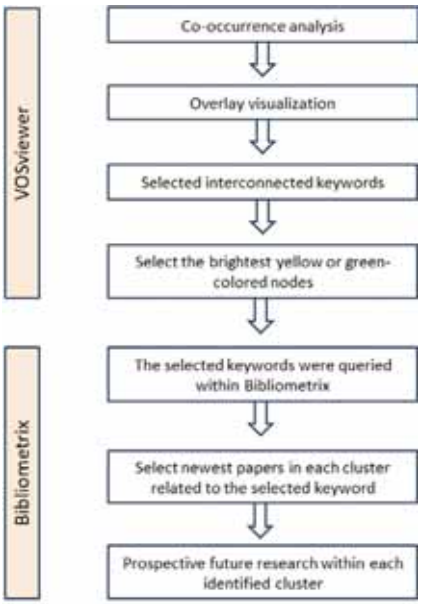

Fig. 2: Procedure of content analysis created by the authors

bibliometric in nature, such studies can still contribute valuable context and understanding of research trends related to Sordariales. This rigorous approach enables a comprehensive insight into evolving topics and identifies critical research areas for continued exploration in the field.

Descriptive analysis

Through descriptive analysis, one can investigate publication trends, research platforms, and the contributions of different countries, yielding a detailed understanding of patterns within a discipline. This encompasses the frequency of topics, leading journals, and the regions that are most prolific in research output (Nielsen, 2022).

Publication trend

The examination of Sordariales research articles over time, including their average yearly citation rates from 1978 to 2024, reveals a rising interest and significance in this field (Fig. 3). Research trends concerning Sordariales, a fungal order within the class Sordariomycetes, have markedly progressed from 1978 to 2024, highlighting improvements in molecular phylogenetics, genomics, and insights into ecological roles and secondary metabolites. The study originally focused on morphological classification, but recent research has shifted towards molecular systematics and genomic analysis, leading to a deeper comprehension of the evolutionary relationships and functional diversity within Sordariales. This shift in study emphasis underscores both the advancements achieved and the persisting deficiencies in the literature relative to other fungal taxa. Minimal research output was recorded until the 1990s, with a noticeable increase starting in 1995 and a surge in 1998, when publications reached 11 with a mean citation rate of 2.84 per year. Key years include 2006, 2009, 2014, 2016, 2019, and 2021, with 2020 peaking at 32 articles and the highest mean citations per year (7.01), signaling rapid growth.

This upward trend underscores the increasing interest in Sordariales, particularly in genetic diversity, ecology, and biotechnology. The findings suggest a bright outlook for future research, propelled by advancements in technology and efforts that span multiple disciplines. Similar trends in other fields reflect this heightened interest in biology and biotechnology globally (Castillo *et al.*, 2023; Gupta and Ahmed, 2019; Pautasso, 2012). In addition, a bibliometric analysis of *Nattrassia mangiferae* research revealed a sharp increase in studies, particularly from 2018 to 2021, reflecting increased attention to its pathogenicity and broader climate change implications on plant and human health (Samad, 2022). The effects of climate change are notably altering the distribution and ecological functions of Sordariales, which are fungi

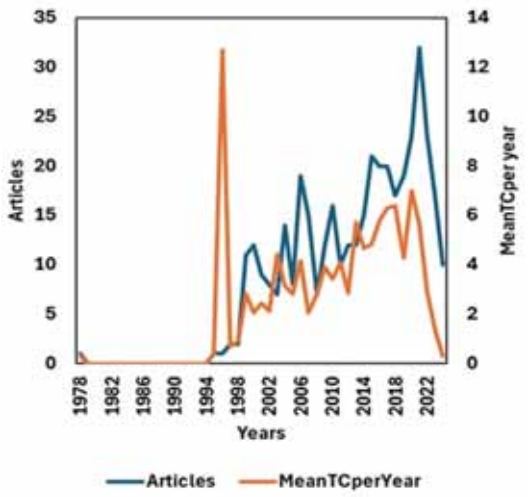

Fig. 3: Temporal trends in article count and mean citations per year (1978-2024)

that inhabit soil, wood, and aquatic environments. Factors such as temperature, humidity, and rainfall patterns greatly influence the life cycle and distribution of these groups. Studies conducted recently reveal that Sordariales species with particular substrate preferences, like Sordaria fimicola found in mammalian feces, are likely to shift towards higher latitudes and altitudes as global temperatures continue to increase. Changing environmental conditions can also affect the process of sporulation, mycelium growth, and secondary metabolite production, thereby interfering with their ecological function as a decomposer and an indicator of paleoecology. However, the case of Zootaxa, a mega-journal in zoological taxonomy, highlights the complexity and potential pitfalls of relying heavily on bibliometric indices such as the Journal Impact Factor, which can sometimes misrepresent the true impact and importance of research in a particular field (Pinto *et al.,* 2021). Numerous significant studies have greatly influenced research on Sordariales by offering essential insights into their classification and evolutionary connections. One key study created a detailed framework for Sordariomycetes using a four-gene phylogeny, which has greatly improved our understanding of their evolution. In a different study, researchers merged molecular and morphological data to refine the classification within the Sordariaceae family. Additionally, a third paper redefined the taxonomy of both Sordariales through molecular systematics. These studies are frequently cited because of their rigorous methods and clear taxonomic contributions, making them foundational to the understanding of fungi and evolutionary biology. Their widespread citation reflects their crucial role within the discipline.

Publication outlet

Research on Sordariales is widely published in high-impact journals, each offering essential advancements. According to Table 2, this distribution plays a vital role for researchers looking to emphasize the importance of their work to stakeholders, including funding bodies and government officials (Nielsen, 2022). The top journals publishing Sordariales studies emphasize its ecological, genetic, and industrial importance across multiple scientific fields.

Leading the list, Mycologia holds significant influence with 36 articles and a strong h-index of 20, reflecting its focus on fungal biology and ecology (Mondal *et al.,* 2023; Rousseau and Zhang, 2019). PLoS One and Fungal Diversity contribute substantially, underscoring Sordariales' broad relevance. Emerging journals like Frontiers in Microbiology highlight its interdisciplinary appeal and potential (Mylonakis, 2023). The movement towards open-access (OA) publishing has greatly enhanced the accessibility of research, particularly in areas such as mycology and Sordariales. From 2015 to 2020, the percentage of openly accessible full-text articles rose from 56.5% to 61.8%, with Gold OA publications increasing from 24.1% to 37.4%. This trend emphasizes a global effort to advance the openness and sharing of scientific information. While specific

Table 2. Top 10 journals publishing articles on Sordariales from 1978-2024

Journals	Publication on year start	Number of articles	Total citation	Production and citation impact (h-index)	Cumulative citation (g-index)	Productivity speed (m-index)
Mycologia	1996	36	1921	20	36	0.690
PLOS One	2008	16	816	12	16	0.706
Applied Microbiology and Biotechnology	1999	11	470	10	11	0.385
Fungal Diversity	2006	10	1458	10	10	0.526
Molecular Microbiology	2001	10	398	10	10	0.417
Applied and Environmental Microbiology	2004	11	492	9	11	0.429
Mycological Research	2002	10	434	9	10	0.391
Bioresource Technology	2012	8	317	8	8	0.615
Frontiers in Microbiology	2016	9	400	7	9	0.778
Fungal Genetics and Biology	2002	7	209	7	7	0.304

data on OA in Sordariales is scarce, it is likely to benefit from this broader momentum in fungal taxonomy and ecology. Open access fosters collaboration, particularly in resource-limited regions, while enhancing the visibility and citation opportunities for authors.

Country scientific production

The global distribution of research on Sordariales, depicted in Fig. 4, highlights notable regional disparities, with China leading by a significant margin, contributing 686 publications (Fig. 5). This preeminence showcases China's considerable investment in mycological studies, concentrating on fungal biodiversity and biotechnology, underpinned by a solid research framework and ample funding (Dong *et al.,* 2017; Wang *et al.,* 2023b; Zhang and Xie, 2023; Abdukerim *et al.,* 2025).

Following China, the United States ranks second with 283 publications, driven by its renowned research institutions and interdisciplinary collaborations that have expanded knowledge on Sordariales' genetic diversity and ecological roles, which are key to biotechnological advancements (Newcombe *et al.,* 2016; U'Ren *et al.,* 2016). The quick increase in omics data has significantly contributed to the progress of Sordariomycetes research, with various institutions concentrating on evolutionary genomics and transcriptomics. These studies have been instrumental in understanding the genetic and biological characteristics of Sordariales, with significant contributions from researchers (Wang *et al*., 2023). Institutions focused on the diversity of secondary metabolites within Sordariales have pointed out the potential medicinal and industrial applications of these substances (Charria-Girón *et al*., 2022). With 271 publications, Germany excels in genetic and molecular studies, employing advanced technologies to investigate fungal genomes (Blumenstein *et al*., 2021). A total of 112 publications from Spain examine the ecological relationships and biotechnological applications associated with Sordariales (Agustí-Brisach *et al.,* 2021; Charria-Girón *et al.,* 2022). But multidisciplinary approaches combine ideas from several fields to respond coherently to challenging problems (Li *et al.,* 2024). Thailand and Brazil, with 87 and 81 publications, respectively, utilize their rich biodiversity to explore Sordariales' ecological and economic potential, indicating an increasing interest in fungal research in these biodiversity-rich regions (U'Ren *et al.,* 2016). Concurrently, the Netherlands, boasting 74 publications, and France, with 73 publications, highlight the significant presence of mycological research in Western Europe, particularly in the areas of advanced diagnostics and collaborative efforts (Hannula *et al.,* 2020; Salmanton-García *et al.,* 2023). With long traditions of excellence in biological sciences, these countries focus on both fundamental and applied aspects of Sordariales, advancing the understanding of fungal biology and its applications (Bretagne *et al.,* 2022; Buil *et al.,* 2020). India, boasting 66 publications, and Canada, with 40, are emerging research hubs that highlight the environmental and biotechnological significance of Sordariales (Gnanesh *et al.,* 2021; Haldeman, 2021). Collaboration between

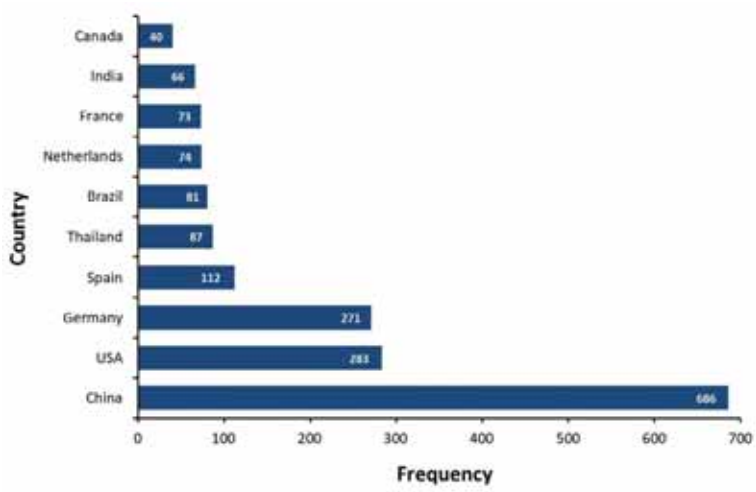

Fig. 4: The top 10 country ranks of the scientific paper production

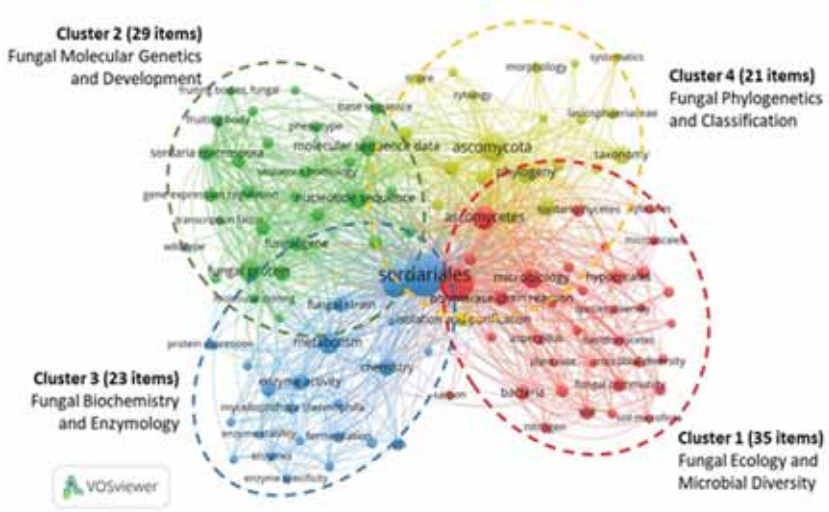

Fig. 5: Network visualization from co-occurrence analysis

developing countries in Sordariales research is still relatively limited, but is starting to show improvement, especially through regional cooperation in the exploration of local biodiversity. Nations like Indonesia, Thailand, Brazil, and India, which possess tropical ecosystems, significantly contribute to the discovery of new Sordariales species owing to their diverse biological resources. International partnerships have contributed significantly to the progress of Sordariales research, in several ways viz: 1) Access to advanced molecular technologies and methods, such as DNA sequencing and phylogenetic analysis, which are often not readily available in developing countries. 2) Capacity building of human resources through joint training, researcher exchange and publication collaboration. 3) Strengthening global scientific networks that accelerate data dissemination, new taxonomic discoveries, and potential applications of Sordariales in industry and ecology. 4) International collaborative funding that enables exploration of biodiversity and development of cross-border studies. The collaboration of developing countries in Sordariales research plays a crucial role in advancing the field, facilitated by mechanisms like the sharing of knowledge and resources. Together, these nations contribute substantially to the field, advancing fundamental and applied research on Sordariales and

reinforcing the importance of fungal studies globally. Research funding on Sordariales fungi remains limited, especially in developing countries, where attention tends to focus on more commercially valuable fungi. Nevertheless, there is a glimmer of optimism as global initiatives are starting to create new opportunities for researching Sordariales, particularly in tropical regions. The lack of funding has hindered the ability to investigate local species, employ advanced molecular methods, and produce significant publications or engage in international collaboration. The advancement is particularly apparent in the discovery of new species and the examination of their potential applications in biotechnology and environmental sustainability.

Research pattern

The co-occurrence analysis of research on Sordariales reveals distinct thematic clusters, each underscoring unique areas of study within the field. These clusters reveal significant insights into the diversity of research subjects and the connections among various scientific areas linked to Sordariales (Fig. 5). The first cluster was fungal ecology and microbial diversity, especially around the taxonomy and classification of fungi such as Ascomycetes and their interactions with soil microorganisms, with Sordariales standing out for their ecological significance. The importance of fungi, particularly those in microbial communities, is critical for sustaining environmental equilibrium. Their substantial representation, indicated by a count of 238 in community analyses, underscores their essential function in these ecosystems (Niego *et al.*, 2023). Ascomycetes are crucial in nutrient cycling, decomposition, and forming symbiotic relationships with plants, especially through mycorrhizal associations that enhance nutrient absorption and support plant growth (TlÁskal *et al.*, 2021). Other notable fungal orders, such as Hypocreales and Eurotiales, illustrate fungal communities' diversity and ecosystem contributions (Khaliq *et al.*, 2022; Devi *et al.*, 2020). The first cluster investigates the influence of fungi on plant ecosystems, underscoring their critical role in improving water and nutrient absorption, which is essential for sustainable agriculture. It also points out that recognizing this diversity is key to effective ecosystem management and conservation.

Fungi significantly influence plant ecosystems by affecting plant health, growth, and productivity. Mycorrhizal fungi, which belong to the Ascomycetes and Basidiomycetes groups, establish mutualistic associations with plant roots, enhancing water absorption and essential nutrients such as phosphates and nitrates (Ayana, 2020). Saprophytic fungi from the Ascomycetes and Basidiomycetes classes are integral to forest ecosystems, as they decompose organic material and facilitate the recycling of vital nutrients like nitrogen and phosphorus into the soil (Khaliq *et al.*, 2022; Leifheit *et al.*, 2024). Key genera, including Aspergillus and Penicillium, play pivotal roles in these processes. Innovations in molecular methods, including polymerase chain reaction and high-throughput sequencing, have substantially advanced the knowledge of microbial diversity and species identification, which in turn supports ecosystem management and conservation efforts (Gnanesh *et al.*, 2021; Voigt *et al.*, 2021). A second cluster delves into the genetic and molecular biology of Sordariales, where studies focus on terms like "fungal protein," "nucleotide sequence," and "gene expression." Model organisms such as *Sordaria macrospora* and *Neurospora crassa* are central to this research, contributing significantly to the understanding of fungal development, gene regulation, and protein synthesis. The findings from these studies might facilitate the discovery of new genes and pathways that could be utilized in biotechnological applications, including the production of enzymes and the creation of pharmaceuticals. Further, research has identified key genes involved in fruiting body development through transcriptional studies, thus expanding the prospects for biotechnological innovation (Kim *et al.*, 2022; Wang *et al.*, 2023b). Studies have demonstrated the significance of model organisms like *Neurospora crassa* and *Sordaria macrospora,* which play a crucial role in elucidating gene regulation and developmental processes. As an example, research has demonstrated the critical roles chromatin-associated proteins such as ASF1 (Anti-Silencing Function 1, a histone chaperone) and RTT109, a histone acetyltransferase (HAT) play in the development of sexual behavior and the DNA damage response in *Sordaria macrospora* (Breuer *et al.*, 2024). This second cluster enhances the understanding of fungi and opens up new possibilities for biotechnological applications, such as the production of enzymes and pharmaceuticals. The third cluster emphasizes fungi's promise in environmental biotechnology and bioenergy. It shows that fungi

can do much more than play ecological roles. The cluster centers on the biochemical and enzymatic properties of Sordariales, highlighting terms such as "enzyme activity" and "metabolism." Research on fungi like *Myceliophthora thermophila* has shown great promise in industrial applications, especially in biofuel production, waste degradation, and synthesis of valuable chemical compounds. Known for its production of potent enzymes in harsh conditions, this fungal species is well-suited for applications in environmental biotechnology and bioenergy (Dahiya *et al.*, 2021; Zhang *et al.*, 2023). Finally, the phylogenetic and taxonomic cluster underscores the importance of understanding evolutionary relationships through terms like "phylogeny," "taxonomy," and "classification." Genetic data, such as fungal DNA sequences, are instrumental in refining taxonomic classifications and providing a more comprehensive picture of Sordariales' evolutionary history (Voigt *et al.*, 2021). *Sordariales* taxonomy uses several genetic markers for better accuracy. The high variability of ITS is instrumental in identifying different species. Furthermore, the large subunit (LSU) and small subunit (SSU) ribosomal ribonucleic acid (rRNA) genes facilitate a more comprehensive classification. β-tubulin and ribosomal-ribonucleic-acid polymerase II subunit B (RPB2) improve resolution at species and genus levels. Combining markers gives clearer, more reliable evolutionary insights. This avoids the limits of single-gene analysis. The importance of this phylogenetic framework cannot be overstated in the fields of ecology, agriculture, and medicine, where accurate classifications are essential for elucidating ecological roles and interactions (Marin-Felix *et al.*, 2020). The final cluster is crucial for many areas, such as ecology, agriculture, and medicine. Accurate classifications help us understand ecological roles and interactions. New biosystematic approach using phylogenetic data can refine Sordariales classification, aiding ecological and functional studies. This facilitates a more efficient evaluation of fungal diversity and the creation of robust ecosystem management strategies. Within plant ecosystems, Sordariales fungi are essential for symbiotic associations, particularly mycorrhizal relationships that improve nutrient absorption, supporting plant growth and soil health (Frac *et al.*, 2018; Khaliq *et al.*, 2022). Achieving taxonomic clarity enhances biodiversity conservation efforts, allowing for improved assessments of fungal diversity and more effective strategies for managing ecosystems (Zeng *et al.*, 2019). Understanding these relationships helps ecologists maintain ecosystems where Sordariales fungi contribute significantly.

Emerging topics

A thematic map offers a structured overview of central themes and emerging research areas within Sordariales studies, assisting researchers in recognizing key trends and future directions (Pillay *et al.*, 2019). This visualization plays a crucial role in pinpointing major topics and comprehending the progression of research in this area throughout the years. The effectiveness of thematic mapping in observing spatiotemporal changes has been demonstrated across multiple domains, particularly in the context of shifts in forest cover (Dias *et al.*, 2020). When linked open data (LOD) is integrated with spatial data infrastructures, it enhances the interoperability of geospatial data, which is vital for creating effective thematic maps (Wiafe, 2018). Moreover, universities highlight the principles of thematic mapping, stressing its importance in education and training for effective communication through maps (Köbben, 2018). Thus, thematic maps are powerful tools for illustrating complex data, aiding decision-making processes in fields like Sordariales research (Köbben, 2018; Lange and Raposo, 2022; Pillay *et al.*, 2019). In Sordariale's research, "motor themes" are essential topics characterized by high centrality and density, marking them as well-developed, vital areas pushing the field forward. These subjects typically highlight important breakthroughs in genetic and developmental studies, with essential keywords including "gene," "sordaria," "macrospora," and "development" (Fig. 6). These terms highlight *Sordaria macrospora* as a crucial model organism, contributing profoundly to understanding fungal biology and molecular mechanisms. Research on this organism's developmental genes and regulatory proteins of this organism have revealed critical mechanisms such as autophagy and transcriptional regulation, which are vital for the growth of fungi (Teichert *et al.*, 2020; Werner *et al.*, 2021). Such themes reflect innovation in genetic research, advancing insights into fungal growth and development with broad applications in biotechnology and other scientific domains.

"Niche themes" within Sordariales research represent well-developed topics but are less central to the field, characterized by high density yet low centrality.

Examples include “fungal DNA,” “soil,” “diversity,” and “microbial.” These topics focus primarily on ecological factors and genetic variation of Sordariales fungi within soil habitats. By focusing on the contributions of microbial and fungal communities to soil health and ecosystem processes, these specific topics provide significant understanding of the ecological dynamics associated with Sordariales fungi (Corbu *et al.*, 2023). Even though these themes possess significant depth, they often occupy a marginal position within the wider research agenda, typically failing to take on a central role in guiding the field’s trajectory. They delve into specialized areas, such as Sordariales’ role in nutrient cycling, yet have limited influence on the larger scientific discourse. Themes in Sordariales research that are either emerging or in decline, characterized by low centrality and density, represent research areas gaining attention or losing relevance. The terms “species,” “molecular,” and “phylogeny” highlight the active research focused on species classification and the evolutionary relationships present within Sordariales. These areas are still developing and may grow in importance with new methodologies and discoveries. While peripheral to the core research focus, they provide essential insights that support the foundation without serving as the main drivers of the research. The dynamic nature of these themes shows how some areas may gain prominence, while others may fade as scientific priorities shift. “Primary themes,” marked by high centrality but low density, spotlight fundamental yet developing concepts central to Sordariale’s research. Keywords like “fungi,” “production,” “myceliophthora,” “characterization,” and “thermophile” indicate essential study areas related to Sordariales fungi biology and industrial applications. These themes are indeed crucial, yet their development is still underway, emphasizing the importance of ongoing research to fully grasp their effects in both industrial and scientific applications. This thematic map is a valuable bibliometric tool, allowing researchers to categorize and analyze Sordariale’s research themes based on density and centrality, thus helping shape the research landscape.

Potential biotechnological applications

Carbon (C)-related function of Sordariales

The network map’s visualization highlights the intricate interactions and relationships among key terms associated with Sordariales research, revealing their vital role in carbon-related functions. A key theme that has emerged from the network is the important ecological and biotechnological relevance of Sordariales fungi in carbon cycling (Fig. 7A). These fungi are pivotal in breaking down and transforming organic matter, thus playing a crucial role in the global carbon cycle (Leifheit *et al.*, 2024). Their metabolic processes enable the decomposition of complex organic compounds, contributing to the development of soil organic matter and the emission of carbon dioxide, essential for nutrient cycling and the overall fertility of the soil (Ye *et al.*, 2020). Sordariales fungi produce a variety of extracellular enzymes, such as cellulases, hemicellulases, and ligninases, which are instrumental in breaking down plant cell walls. This enzymatic

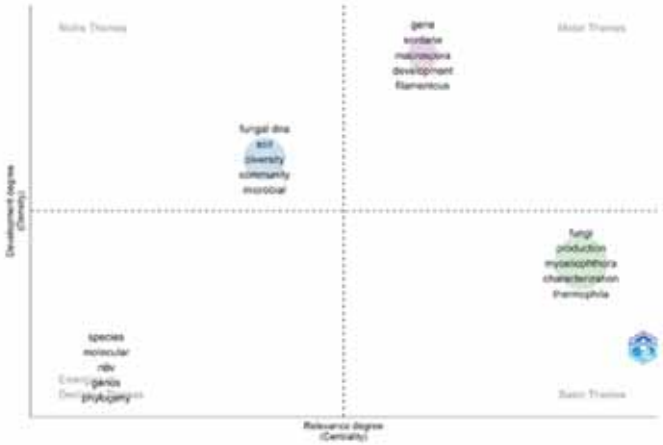

Fig. 6: Thematic map of Sordariales research using bibliometric analysis to identify and describe research themes, divided into four quadrants based on density and centrality

activity, influenced by the transcriptional control of genes involved in carbon metabolism, plays a crucial role in ecological nutrient cycling and is also applicable in industries such as biofuel production (Manuela del Rosario and Rita, 2022). The network map also shows a strong connection between Sordariales and "soil," underscoring their role in soil carbon sequestration. By decomposing organic matter and enhancing soil structure, these fungi contribute to carbon storage within the soil ecosystem (Rodrigues *et al.*, 2023). The study focus on Sordariales' carbon-related functions has intensified recently, with particular emphasis on their metabolic applications for industrial processes. Studies since 2010 have explored these fungi's potential in developing efficient biofuel production techniques and sustainable agricultural practices. The scalability of Sordariales-based bioprocessing is evidenced by their high enzyme yields and adaptability to industrial conditions, making them viable for large-scale applications such as biofuel production and bioremediation. Studies at the pilot scale has illustrated the capability of converting lignocellulosic biomass into bioethanol, resulting in a reduced reliance on chemical pretreatment processes (Manikandan *et al.*, 2022). Sordariales fungi play an essential role in animal husbandry systems by decomposing carbon-rich compounds like cellulose and lignin found in livestock waste. By releasing carbon back into the soil, this decomposition process enhances soil fertility and stimulates plant growth, contributing to the nutrient cycling in pasture ecosystems (Jørgensen *et al.*, 2007; Fu *et al.*, 2021). Moreover, the carbon degradation pathways of Sordariales offer biotechnological potential for converting livestock waste into compost, bio-based products, or biofuels, potentially reducing the environmental impact of animal farming (Xie *et al.*, 2014). Seeking sustainable biofuel production, researchers are exploring Sordariales microbes as a groundbreaking substitute for traditional chemical pretreatments, which typically rely on hazardous substances. Instead, these microbes produce enzymes like cellulases and xylanases that efficiently break down lignocellulose into simple sugars, which can be fermented into ethanol. By facilitating quicker biomass conversion, this enzymatic process boosts production efficiency and sustainability, playing a vital role in fostering a greener future (Mignogna *et al.*, 2024; Manikandan *et al.*, 2022). Research by Nargotra *et al.*, (2022) demonstrated the isolation of lignocellulolytic enzymes from Sordariales species with high efficiency in biomass pretreatment for biofuel production.

Nitrogen (N)-related function of Sordariales

The network image presents a detailed perspective on research concerning Sordariales fungi, underlining their contributions to the nitrogen cycle in multiple ecosystems (Fig. 7B). It shows the significant impact of Sordariales in nitrogen cycling, highlighting their contributions to soil health and nutrient availability, which are essential for plant growth and microbial community dynamics (Zeng *et al.*, 2019; Li *et al.*, 2023). Sordariales fungi transform nitrogenous substances in the soil, releasing nitrogen in forms that plants and other organisms can absorb. This process of nitrogen transformation boosts soil fertility, which in turn supports plant development. Sordariales interact with soil, nitrogen, and the broader fungal community, releasing enzymes and secondary chemicals that affect nitrogen availability and influence bacterial communities vital to the nitrogen cycle. The nitrogen cycle, shaped by fungi and bacteria, involves mineralization, nitrification, and nitrogen immobilization processes. In this context, Sordariales play a crucial role by metabolizing a range of nitrogen sources, including ammonium, nitrates, and organic nitrogen (Li *et al.*, 2023). The adaptability of Sordariales to different nitrogen types renders them particularly beneficial in high-nitrogen intensive agricultural environments. Nitrogen leaching and imbalances between nitrogen sources and crop demand are common issues in these settings. Sordariales fungi contribute to reducing these challenges by metabolizing excess nitrogen, making them essential players in nutrient cycling in diverse environments (Tei *et al.*, 2020). The interest in the nitrogen-related contributions of Sordariales has markedly intensified since 2010, indicating a heightened understanding of the significance of nitrogen cycling for sustainable agricultural practices and overall ecosystem well-being. Understanding Sordariales' nitrogen usage is crucial for advancing organic and sustainable farming practices. Their denitrification capabilities are also critical, as they help reduce nitrates to nitrogen gases, mitigating excess nitrogen's adverse effects, especially where nitrate-rich soils can foster bacterial pathogens (Huang *et al.*, 2020). Furthermore, some species within the Sordariomycetes class generate nitrous oxide (N_2O), which affects the cycling of nitrogen in soil and

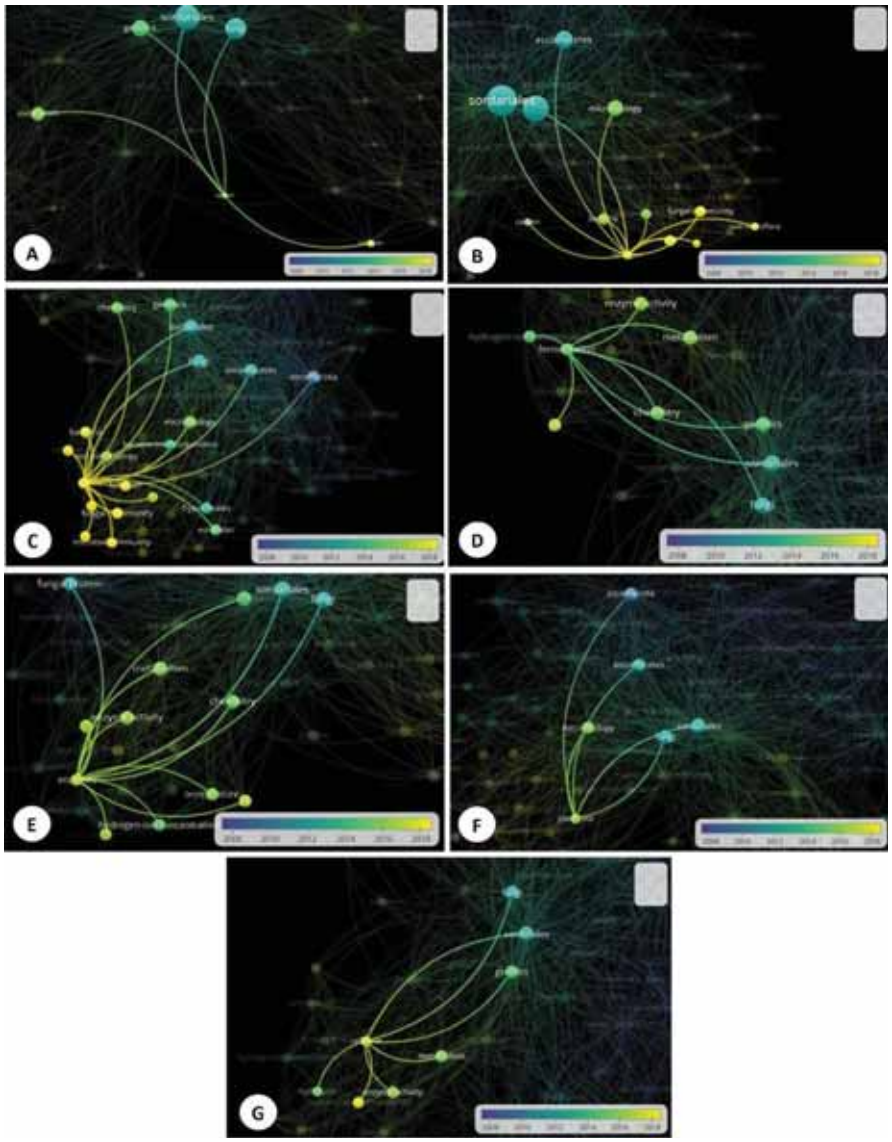

Fig. 7: Potential biotechnological relevance of Sordariales fungi A) Carbon-related function, B) Nitrogen-related function, C) Soil-related function, D) Fermentation-related function, E) Enzyme-related function, F) Plant root-related function, and G) Cellulose-related function of Sordariales

its emissions. The role of Sordariales in the nitrogen cycle extends to soil biocrusts, where nitrogen-related activities such as mineralization and nitrification occur more actively than in deeper soil layers. A range of functional groups, including bacteria and fungi, contributes to nutrient cycling, emphasizing the vital ecological role of microbial diversity in optimizing nitrogen efficiency (Mueller *et al.*, 2015). Sordariales fungi, especially within the Sordariomycetes group, are essential denitrifiers in various ecosystems, notably in arable soils where denitrification processes are crucial. Although fungal denitrifiers remain underexplored, Sordariales contain genes like nitrite reductase (nirK), which are linked to denitrification. The relationship between Sordariales and bacteria is shaped by certain genes and soil factors, including hydrogen (pH) and nitrate levels, which play a crucial role in determining nitrogen availability and enhancing soil fertility (Xu *et al.*, 2019). This process, regulated by nitrogen-responsive genes, mitigates excess nitrogen in agricultural soils,

supporting plant growth and microbial dynamics (Li *et al.*, 2023). Their metabolic flexibility permits them to utilize a range of nitrogen sources, including ammonium and organic nitrogen, making them essential for sustainable farming practices. Molecular studies reveal how these fungi influence bacterial communities through secondary metabolites, further shaping nitrogen cycles (Zeng *et al.*, 2019). The findings of Ibrahim *et al.* (2021) revealed that bioactive compounds derived from Sordariales demonstrate antibacterial and anticancer effects, pointing to their possible applications in the pharmaceutical industry. In addition to their ecological roles, Sordariales are significant in biotechnology, agriculture, and medicine. For instance, members of the Lamiaceae family generate enzymes and bioactive substances that could be valuable in industrial and pharmaceutical applications. Their antifungal properties offer promising avenues for new antibiotics and plant protection agents. Additionally, marine fungi within Sordariales demonstrate diverse functions such as saprotrophy, parasitism, and symbiosis, with potential applications in marine biotechnology (Ibrahim *et al.*, 2021; Cunliffe, 2023). Sordariales play a significant role in nutrient cycling in livestock farming, especially nitrogen. *Sordaria fimicola* and similar species serve as saprotrophs, decomposing organic substances, including animal dungs. This decomposition process liberates nitrogen into the soil, fostering plant growth that is crucial for the health of pasture ecosystems (Zhang *et al.*, 2021). This activity also helps maintain soil structure and microbial diversity, which are crucial for the health of grazing lands (Jørgensen *et al.*, 2007). Sordariales flourish in nitrogen-rich habitats thanks to their adaptability, allowing them to break down substances such as urea and undigested proteins found in dung. This transformation of nitrogen into usable forms supports soil fertility in agricultural contexts. Their spores, preserved in ancient sediments, offer insights into past herbivore activity and nitrogen dynamics, providing a historical perspective on ecosystems (Lee *et al.*, 2022). Recent studies suggest that some Sordariales may live endophytically within plant tissues, potentially influencing plant nitrogen metabolism, which expands their ecological role beyond decomposition (Sieber, 2007). Studies on Sordariales highlight their essential contributions to nitrogen dynamics and their significant ecological roles. In aquatic environments, these fungi contribute to the breakdown of organic matter, affecting nitrogen and carbon cycles (Goh *et al.*, 2020; Gutiérrez *et al.*, 2020). Sordariales' involvement in marine nitrogen cycling demonstrates the importance of fungi in nutrient regulation, supporting the view that fungi are central to nitrogen balance in diverse ecosystems. While the challenges associated with nitrogen cycling are often more localized than those related to carbon dioxide, the roles of Sordariales underscore their significance in maintaining ecosystem health and nutrient cycling (Zhang *et al.*, 2020). Sordariales' flexible metabolism makes them particularly effective in nutrient-poor environments. Although nitrogen deficiency might reduce their growth rate, it does not obstruct their contribution to nutrient cycling. For instance, *Sordaria macrospora*, a Sordariales species, serves as a model organism for studying fungal development and nitrogen's influence on growth (Charria-Girón *et al.*, 2022; Teichert *et al.*, 2020).

Soil-related function of Sordariales

The network visualization highlights Sordariales fungi's significant role in soil ecosystems, underscoring their interactions with other microorganisms and their impact on nutrient cycling (Fig. 7C). Co-occurrence analysis indicates potential connections; however, further studies are needed to substantiate these interactions (Wang *et al.*, 2023). Sordariales contribute to soil health by decomposing organic matter, recycling nutrients, and supporting biogeochemical cycles, thus aiding ecosystem stability (Charria-Girón *et al.*, 2022; Zhang *et al.*, 2024). These fungi decompose intricate organic compounds, thereby releasing vital nutrients that promote plant growth and sustain soil fertility (Du *et al.*, 2024; Leifheit *et al.*, 2024). Sordariales association with "decomposition" and "nutrient cycling" reflects their role in carbon and nitrogen cycling, which enhances soil structure and water retention. Their interactions with bacteria shape microbial communities, reinforcing soil health and agricultural productivity. Interest in soil functions has surged since 2012, propelled by developments in molecular biology and the critical need for sustainable agricultural practices (Mamatha *et al.*, 2024).

Fermentation-related functions of Sordariales

The network visualization underscores the fermentation capabilities of Sordariales fungi, demonstrating their diverse metabolic processes

and promising biotechnological prospects (Fig. 7D). Known for their robust enzyme production, these fungi break down complex organic compounds through fermentation, crucial for nutrient cycling and energy flow within ecosystems. Important concepts such as "fermentation," "enzyme activity," and "metabolism" underscore the significance of Sordariales in transforming plant biomass into valuable products, including biofuels (Li *et al.*, 2020). Fungi in the Chaetomiaceae family, such as *Myceliophthora thermophila*, produce enzymes like cellulases and xylanases, essential for industrial fermentation processes. Fungal phytases are widely used in food and animal feed additives. They facilitate better phosphorus uptake in animals and aid in decreasing phosphorus-related environmental pollution, highlighting their importance in agricultural and ecological settings. Fungi from the order Sordariales, particularly *Neurospora species*, show strong potential in biotechnology, especially fermentation. *Neurospora sitophila* showed the highest level of phytase production at 195.66 unit per gram (U/g) followed by Jatuwong *et al.* (2020). Conditions like pH and temperature are vital for optimizing these enzymes, as demonstrated by *M. thermophila*'s endoxylanase activity at pH 5.0 and 60 degrees Celsius (°C) (Dahiya *et al.*, 2021). Developments in genetic engineering have increased the fermentative efficiency of Sordariales, facilitating their application in bioenergy and organic acid production, which underscores their importance in sustainable technology (Naureen *et al.*, 2024; Aguilar-Paredes *et al.*, 2023).

Enzyme-related function of Sordariales

The network visualization highlights key terms connected to the enzyme-related functions of Sordariales, illustrating their ecological and biotechnological importance (Fig. 7E). These fungi are recognized for their powerful enzymatic functions, making them vital to nutrient cycling in ecosystems and leading to a wide range of industrial applications. Marine and freshwater environments host rich microbial communities, including fungi that decompose organic matter and regenerate nutrients. Tailored to thrive in marine settings, Sordariales synthesize hydrolytic and oxidative enzymes that are utilized in a variety of industrial applications (Bonugli-Santos *et al.*, 2015). Sordariales are prolific producers of enzymes like cellulases, hemicellulases, ligninases, and proteases, which break down complex organic materials, playing a crucial role in nutrient cycling and energy flow (Hemati *et al.*, 2022; Leifheit *et al.*, 2024). Their enzymatic processes they exhibit enable extensive industrial applications, particularly in biofuel generation and waste management. Large-scale bioprocessing becomes more viable due to the production of stable enzymes that can function under different conditions, which helps to decrease costs relative to synthetic alternatives (Alabdalall *et al.*, 2023). Fungi from the order Sordariales produce diverse enzymes like phytase, cellulases, laccases, and proteases, which are valuable in industries such as animal feed, textiles, biofuels, and bioremediation. Species like *Sporotrichum thermophile* and *Neurospora nobile* are notable for phytase production. These enzymes aid in biomass degradation and dye removal. While their industrial capabilities are promising, obstacles like the cost of production and the stability of enzymes still exist. Progress in fermentation, genetic engineering, and enzyme immobilization are vital for facilitating more extensive application. The activity of enzymes, vital for applications including biofuel production, waste management, and the paper industry, is heavily influenced by factors such as temperature, pH, and hydrogen-ion concentration (Sedek *et al.*, 2024; Abdel-Azeem *et al.*, 2021). Specifically, cellulases and ligninases from Sordariales facilitate plant biomass conversion into fermentable sugars, supporting bioethanol production and reducing fossil fuel dependency (Alabdalall *et al.*, 2023; Ilić *et al.*, 2023). The network map further links "enzyme activity", "metabolism", and "chemistry", emphasizing the study of Sordariales' enzymatic reactions and metabolic pathways (Kalntremtziou *et al.*, 2023). The degradation of cellulose by glycoside hydrolase genes is fundamentally linked to their expression, which is augmented by metabolic pathways that feature β-glucosidases and oxidative enzymes such as laccases. Genetic research advances the understanding of the genes responsible for enzyme production, aiming to enhance enzyme stability and specificity for industrial applications. Biotechnological techniques, such as Clustered regularly interspaced short palindromic repeats-based gene (CRISPR)-based gene editing can enhance enzyme production for industrial use by precisely modifying Sordariales' genomes to overexpress genes encoding enzymes like cellulases and ligninases, increasing yields and improving

stability for applications such as biofuel production. This approach, when combined with synthetic biology and directed evolution, maximizes enzyme efficiency and adaptability, thereby decreasing costs and improving scalability in industrial bioprocessing. These advancements further optimize enzyme yields, making Sordariales a promising candidate for industrial-scale biorefineries (Hensen *et al.*, 2023; Alabdalall *et al.*, 2023). In natural ecosystems, Sordariales enzymes like lignin peroxidase and laccase decompose lignin, while cellulases and hemicellulases release nutrients such as nitrogen, phosphorus, and carbon, improving soil fertility and plant growth (Kalntremtziou *et al.*, 2023; Kumar and Chandra, 2020). Moreover, Sordariales enzymes are effective in decomposing organic substances in animal excrement, facilitating nutrient cycling and providing possibilities for biofuel creation and eco-friendly agricultural practices, including the use of bio-based fertilizers and soil enhancements (Aguilar-Paredes *et al.*, 2023; Mignogna *et al.*, 2024).

Plant-root-related function of Sordariales

The network visualization reveals significant linkages between Sordariales and plant root functions, emphasizing their ecological and agricultural roles (Fig. 7F). Sordariales facilitate the uptake of essential nutrients, particularly phosphorus, in plants, in return for carbohydrates that are vital for plant development and soil vitality (Zhang *et al.*, 2020; Khaliq *et al.*, 2022; Tejakusuma *et al.*, 2025). Root metabolites play a crucial role in regulating root-fungi interactions. Agaricales and Sordariales are beneficial fungal orders with increased tread, possibly because of root compounds that aid nutrient absorption and soil carbon protection (Jingjing *et al*., 2022). The network demonstrates considerable connections among "Sordariales," "plant root," "fungi," and "microbiology," underscoring the critical nature of these connections (Pellerigno *et al.*, 2022). Additionally, Sordariales produce phytohormones that promote root growth and health, decompose organic matter, and recycle nutrients, benefiting soil fertility and plant vitality (Charria-Girón *et al.*, 2022). By controlling pathogens and strengthening soil structure, they facilitate better root access to nutrients, a vital aspect of sustainable agricultural methods (Aguilar-Paredes *et al.*, 2023). The presence of "Sordariales" in the soil is linked to soil structure and health improvements. Their hyphal networks help to stabilize soil aggregates, improving soil aeration and water retention. Modifications to the soil conditions can promote deeper root penetration and increase nutrient availability. The association with "fungi" and "microbiology" underscores the integral role of Sordariales in the soil ecosystem, contributing to the overall health and productivity of the soil (Alahmad *et al.*, 2023).

Cellulose-related function of Sordariales

The network visualization reveals key connections between Sordariales and cellulose-related functions, emphasizing their ecological and biotechnological importance (Fig. 7G). Sordariales, a group within the Sordariomycetes, decompose cellulose-a major plant biomass component-using cellulolytic enzymes like endoglucanases, exoglucanases, and β-glucosidases (Li *et al.*, 2012). These enzymes decompose cellulose into basic sugars, promoting nutrient cycling and improving soil fertility. This process can be scaled for biofuel production, transforming lignocellulosic biomass into fermentable sugars (Wu *et al.*, 2024). The network map shows strong associations between "Sordariales", "cellulose", "enzyme activity", and "hydrolysis" highlighting their roles in both natural and industrial contexts. Research focuses on optimizing enzyme production for cost-effective biomass conversion. Research focuses on refining enzyme production to facilitate affordable, large-scale biomass conversion, with successful trials indicating its feasibility for industrial applications (Bello *et al.*, 2022). Genetic advancements aim to boost enzyme yields, enhancing Sordariales' potential in large-scale industrial applications (Komorowicz *et al.*, 2023). The network connections between "Sordariales", "genetics", and "fungi" reflect this focus, indicating a substantial interest in understanding and leveraging the genetic basis of these fungi's cellulolytic functions. The progress in genetics is essential for maximizing the potential of Sordariales in various industrial and environmental applications (Sruthy *et al.*, 2023). From an ecological perspective, Sordariales contribute to soil health through the decomposition of plant litter, which helps in the creation of humus. This not only supports carbon sequestration but also releases nutrients, both of which are critical for maintaining forest sustainability (Wang *et al.*, 2024; Naureen *et al.*, 2024).

Sordariales in bioremediation

Evidence and potential applications: Despite the

limited research specifically addressing Sordariales in the context of bioremediation, recent evidence points to the promising capabilities of certain species in this order for environmental cleanup, particularly in the degradation of complex organic pollutants and the enhancement of soil health. Genera such as Chaetomium, Neurospora, and Sordaria well-known members of Sordariales produce robust extracellular enzymes like cellulases, laccases, peroxidases, and esterases. These enzymes are crucial for breaking down lignocellulosic compounds, dyes, pesticides, and polycyclic aromatic hydrocarbons (PAHs). For instance, *Chaetomium globosum* has been studied for its ability to degrade textile dyes and reduce heavy metal toxicity in soil, showcasing its role in mycoremediation. Sordariales have been noted to recolonize and restore ecological functions in agricultural soils that have been contaminated following pollution incidents. Their adaptability to stressful environments, such as areas affected by salinity, drought, or chemical exposure, is partly due to their strong antioxidant and detoxification systems, which may be harnessed for remediation purposes. Furthermore, the fact that certain species, like Sordaria fimicola, thrive in dung indicates their potential application in the biotransformation of animal waste and organic contaminants. These species thrive in nitrogen-rich, microbially active conditions, which are commonly found in contaminated compost or sludge environments. The evolution of omics technologies, particularly in the fields of transcriptomics and proteomics, has the potential to identify stress-response pathways and gene clusters that degrade pollutants in Sordariales, thus creating new opportunities for focused bioremediation strategies. Future research integrating metabolic profiling, microcosm experiments, and genetic manipulation is crucial to fully validate and optimize their application in polluted terrestrial and aquatic ecosystems. While still underexplored compared to other fungal taxa like Trametes or Aspergillus, Sordariales exhibit substantial untapped potential for bioremediation and deserve greater attention in mycoremediation research and sustainable environmental management.

Past and future recommendations

Research to date highlights the ongoing necessity for enhanced taxonomic clarity in the Sordariales order, especially concerning families such as Lasiosphaeriaceae, where the boundaries between genera and species are often ambiguous. Advances in molecular systematics, especially through the use of LSU rDNA sequences, offer promising tools to revisit and refine these classifications. Improving taxonomic resolution enables scientists to better understand the evolutionary relationships that exist within this wide-ranging group of fungi. Model organism utilization, *Sordaria macrospora* continues to serve as a valuable model for unraveling the complexities of fruiting body development in fungi. Its use has already contributed significantly to the understanding of fungal genetics and developmental biology. In order to delve deeper into the complex molecular mechanisms that control fungal growth and reproduction, it is vital to enhance genetic resources, such as well-organized mutant libraries and cutting-edge molecular tools (Teichert *et al*., 2020). For future research, exploration of marine fungi, marine fungi, especially those belonging to the Sordariales represent a largely untapped area of research with immense potential. These organisms could serve as a significant source of innovative enzymes with important applications in industry. Nevertheless, they have not been thoroughly investigated. Future research should prioritize bioprospecting marine-derived fungal enzymes, not only to expand the understanding of their unique adaptations but also to help tackle existing challenges in enzyme technology and bioprocess development (Muthusamy and Murugaiyan, 2023). In the climate change and fungal interactions, Sordariales fungi play a vital, yet often overlooked, role in the global climate system. In particular, understanding how Sordariales species interact with their surrounding ecosystems could shed light on their contributions to carbon cycling and ecosystem resilience. This information might be crucial in the development of nature-oriented solutions for mitigating climate impacts and restoring ecological balance. As climate change continues to reshape ecosystems, exploring the ecological functions of fungi becomes more urgent than ever (Case *et al.*, 2022).

CONCLUSION

This study delves deeply into Sordariales fungi, focusing on their ecological roles and significant potential for biotechnological advancements. Through bibliometric and content analysis, identified key research trends and themes that shape the scientific understanding of this fungal group. The results

highlight four major interconnected research areas: fungal ecology, molecular genetics, biochemistry, and phylogenetics. Additionally, thematic mapping demonstrated their vital contributions to nutrient cycling, enzyme generation, and their relationships with plants and animals, further reinforcing their ecological and industrial significance. Large-scale bioprocessing of Sordariales is feasible due to their metabolic flexibility and enzyme efficiency, as demonstrated in biofuel production and waste management. Sordariales fungi are essential decomposers in natural ecosystems, playing a fundamental role in breaking down organic matter and maintaining soil health. These fungi play an essential role in the carbon and nitrogen cycles, which is critical for the stability of ecosystems. Furthermore, they demonstrate considerable potential for applications in biotechnology. Their ability to produce diverse and powerful enzymes enables their use in industries such as biofuel production, bioremediation, and pharmaceuticals. Although these applications show great potential, a substantial lack of understanding persists regarding the molecular and biochemical processes that underpin their ecological roles and industrial functions. One major limitation of this study is its dependence on bibliometric analysis, which primarily reflects published research and may not capture ongoing or unpublished findings. As a result, while this study effectively maps broad scientific trends, it does not necessarily represent the latest experimental breakthroughs. Moreover, bibliometric approaches, despite their usefulness in mapping research trends, lack the capacity to deliver direct experimental validation concerning the ecological roles or industrial applications of Sordariales fungi. Future research should prioritize experimental studies alongside bibliometric analysis to gain a more comprehensive understanding of Sordariales fungi. Analyzing their genetic regulation, the processes involved in enzyme production, and their responses to diverse environmental factors will yield greater insights into their biological functions. The deployment of advanced omics technologies, which encompass genomics for the identification of functional genes linked to decomposition, transcriptomics for exploring environmental responses including stress adaptation, proteomics for optimizing enzyme production to improve industrial yields, and metabolomics for assessing metabolites such as biofuels and signaling compounds, can substantially enrich the understanding of the biochemical processes that underscore the importance of these fungi. Interdisciplinary collaboration will be essential in unlocking the full potential of Sordariales fungi. By bringing together experts in biosystematics and evolutions, mycology, biotechnology, marine and freshwater environment, animal husbandry, veterinary, ecosystem function, agriculture, researchers can develop innovative applications ranging from sustainable agriculture to industrial bioprocesses. By leveraging phylogenetic data, biosystematics enhances taxonomic structures, whereas biotechnology increases enzyme output through gene editing methods such as CRISPR. Furthermore, AI-driven strategies, particularly machine learning, enable predictions of metabolic functions and ecological roles, facilitating rapid research advancements. These efforts can address knowledge gaps, fostering sustainable solutions in agriculture and industry through enhanced collaboration across mycology, biotechnology, and computational sciences. In addition to their scientific and industrial relevance, studying Sordariales fungi can also contribute to broader sustainability goals. Their proficiency in breaking down sophisticated organic compounds and contributing to natural recycling processes positions them as vital players in confronting environmental challenges such as waste management and soil recovery. Harnessing their capabilities can support the development of greener technologies, contributing to a more sustainable future. As research on fungal biotechnology continues to expand, Sordariales fungi remain an exciting and dynamic field of study. Their vital ecological contributions, paired with a wide range of applications, emphasize the importance of sustained exploration and creative advancements. By deepening the understanding of these fungi, scientists can unlock new possibilities for sustainable solutions, environmental conservation, and biotechnological advancements that can benefit both nature and industry.

AUTHOR CONTRIBUTIONS

N.F. Wulandari performed the study conception and methodologies, conducted data analysis, collected data, drafted the manuscript, performed validation of results, and drafted and edited manuscript. A.R. Syam performed study methodologies, conducted data analysis, analyzed data using bibliometrix and VOSviewer, drafted the manuscript, and performed

validation of results. L. Alhamd conducted study methodologies, collected data, performed validation of results, drafted the manuscript, and performed validation of results. B. Gunadi collected and visualized the findings, analyzed data, drafted the manuscript, and performed validation of results. Yosmaniar drafted the manuscript, and validated the results. E. Widjaja drafted the manuscript, and validated the results. B.N. Utomo drafted the manuscript, and validated the results. S. Wahyuwardani drafted the manuscript, and validated the results. R. Widiastuti drafted the manuscript, and validated the results. T. Kadarini drafted the manuscript, and validated the results. S. Dody performed study conception, drafted the manuscript, and validated the results.

ACKNOWLEDGMENTS

The authors thank the National Research and Innovation Agency, Indonesia for granting access to the Scopus database and enabling training on producing scientific papers on secondary research. This study was produced without any financial grant from any source.

CONFLICT OF INTEREST

The authors declare that there is no conflict of interest regarding the publication of this manuscript. In addition, ethical issues, including plagiarism, informed consent, misconduct, data fabrication and/or falsification, double publication and/or submission, and redundancy have been completely observed by the authors.

☐ Positive AI Statement

During the preparation of this work the author(s) have used Artificial Intelligence (AI) [NAME TOOL / SERVICE] in order to [REASON]. After using this tool/service, the authors reviewed and edited the content as needed and take full responsibility for the content of the publication. Furthermore, the GPTZero detector will evaluate the manuscript utilizing Generative AI, ensuring a high detection rate. If the manuscript relies heavily on Generative AI and AI-assisted technologies, it will be archived without further options for appeal.

☑ Negative AI Statement

The author(s) declare that no AI tools or services were not used or not highly applied during the preparation of this work.

ABBREVIATIONS

°C	Degree Celsius
ASF1	Anti-silencing function 1, a histone chaperone, a protein support histone, fold and interact correctly
BRIN	Badan Riset dan Inovasi Nasional (National Research and Innovation Agency)
C	Carbon
CO_2	Carbon dioxide
CRISPR-based gene	Clustered regularly interspaced short palindromic repeats-based gene
DNA	Deoxyribonucleic acid
IF	Impact factor
ITS	Internal Transcribed Spacer
LOD	Linked open data
LSU	Large subunit
LSU nrDNA	Large subunit nuclear ribosomal DNA
N	Nitrogen
N_2O	Nitrogen oxide
nirK	Nitrite reductase
OA	Open access
PAHs	polycyclic aromatic hydrocarbons
pH	Potential of hydrogen
PRISMA	Preferred reporting items for systematic reviews and meta-analyses
R	Programming language
rRNA	Ribosomal ribonucleic acid
RPB2	Ribosomal-ribonucleic-acid polymerase II subunit B
RTT109	A histone acetyltransferase, an enzyme that catalyzes the addition of an acetyl group to lysine residues on histones.
SSU	Small subunit
TC	Total citation

U/g	Unit per gram
USA	United States of America
VOS	Visualization of similarities

REFERENCES

Abdel-Azeem, A.M.; Abu-Elsaoud, A.M.; Abo Nahas, H H.; Abdel-Azeem, M.A.; Balbool, B.A.; Mousa, M.K.; Ali, N.H.; Darwish, A.M.G., (2021). Biodiversity and industrial applications of genus Chaetomium. In Abdel-Azeem, A.M.; Yadav, A.N.; Yadav, N.; Usmani, Z., (Eds.), Industrially important fungi for sustainable development. Biodivers. Ecol. Perspectives. 1: 147–206 **(60 pages).**

Abdukerim, R.; Khidirov, K.; Amangeldikyzy, Z.; Mussina, M.; Yeszhanov, T.; Gritsenko, D.; Mendybayeva, A.; Tursynkulov, A., (2025). Biodiversity of entomopathogenic fungi genus Beauveria in the soils of arid zone. Global J. Environ. Sci. Manage., 11(1): 193-206 **(14 pages).**

Aguilar-Paredes, A.; Valdés, G.; Araneda, N.; Valdebenito, E.; Hansen, F.; Nuti, M., (2023). Microbial community in the composting process and its positive impact on the soil biota in sustainable agriculture. Agronomy. 13(2): 1-24 **(24 pages).**

Agustí-Brisach, C.; Jiménez-Urbano, J.P.; del Carmen Raya, M.; López-Moral, A.; Trapero, A., (2021). Vascular fungi associated with branch dieback of olive in super-high-density systems in Southern Spain. Plant Dis., 105(4): 797–818 **(22 pages).**

Alabdalall, A.H.; Almutari, A.A.; Aldakeel, S.A.; Albarrag, A.M.; Aldakheel, L.A.; Alsoufi, M.H.; Alfuraih, L.Y.; Elkomy, H.M., (2023). Bioethanol production from Lignocellulosic biomass using Aspergillus niger and Aspergillus flavus hydrolysis enzymes through immobilized S. cerevisiae. Energies. 16(2): 1-16 **(16 pages).**

Alahmad, A.; Edelman, L.; Castel, L.; Bernardon-Mery, A.; Laval, K.; Trinsoutrot-Gattin, I.; Thioye, B., (2023). Prebiotics: A solution for improving plant growth, soil health, and carbon sequestration? J. Soil Sci. Plant Nutr., 23(4): 6647–6669 **(23 pages).**

Aria, M.; Cuccurullo, C., (2017). Bibliometrix: An R-tool for comprehensive science mapping analysis. J. Informetr., 11(4): 959–975 **(17 pages).**

Ayana, B., (2020). Symbiotic association of beneficial fungal Species with plants to enhance agricultural production and productivity. Int. J. Res. Agric. Sci., 7(2): 2348–3997 **(50 pages).**

Bao, D.F.; Hyde, K.D.; Maharachchikumbura, S.S.N.; Perera, R.H.; Thiyagaraja, V.; Hongsanan, S.; Wanasinghe, D.N.; Shen, H.W.; Tian, X.G.; Yang, L.Q.; Nalumpang, S.; Luo, Z.L., (2023). Taxonomy, phylogeny and evolution of freshwater Hypocreomycetidae (Sordariomycetes). Fungal Diversity. 121(1): 1-94 **(94 pages).**

Bello, A.; Ogundeji, A.; Yu, S.; Jiang, X.; Deng, L.; Zhao, L.; Jong, C.; Xu, X., (2022). Dynamics of fungal species related to nitrogen transformation and their network patterns during cattle manure–corn straw with biochar composting. Arch. Microbiol., 204(4): 1-16 **(16 pages).**

Betancur-Corredor, B.; Lang, B.; Russell, D.J., (2023). Organic nitrogen fertilization benefits selected soil fauna in global agroecosystems. Biol. Fertil. Soils. 59(1): 1–16 **(16 pages).**

Blumenstein, K.; Bußkamp, J.; Langer, G. J.; Langer, E.J.; Terhonen, E., (2021). The diplodia tip blight pathogen Sphaeropsis sapinea is the most common fungus in Scots pines' mycobiome, irrespective of health status: A case study from Germany. J. Fungi, 7(8): 607 **(23 pages)**.

Bretagne, S.; Sitbon, K.; Desnos-Ollivier, M.; Garcia-Hermoso, D.; Letscher-Bru, V.; Cassaing, S.; Millon, L., Morio, F.; Gangneux, J.-P.; Hasseine, L., (2022). Active surveillance program to increase awareness on invasive fungal diseases: the French RESSIF Network (2012 to 2018). MBio, 13(3): e00920-22 **(16 pages).**

Breuer, J.; Ferreira, D.E.A.; Kramer, M.; Bollermann, J.; Nowrousian, M., (2024). Functional analysis of chromatin-associated proteins in Sordaria macrospora reveals similar roles for RTT109 and ASF1 in development and DNA damage response. G3: Genes, Genomes, Genet., 14(3): 1–13 **(13 pages).**

Buil, J.B.; Meijer, E.F.J.; Denning, D.W.; Verweij, P.E.; Meis, J.F., (2020). Burden of serious fungal infections in the Netherlands. Mycoses, 63(6): 625–631 **(7 pages).**

Case, N.T.; Berman, J.; Blehert, D.S.; Cramer, R.A.; Cuomo, C.A.; Currie, C.R.; Ene, I.V.; Fisher, M.; Fritz-Laylin, L.K.; Gerstein, A.C.; Glass, N.L.; Gow, N.A.R.; Gurr, S.J.; Hittinger, C.T.; Hohl, T.M.; Iliev, I.D.; James, T.Y.; Jin, H.; Klein, B.S.; … Cowen, L.E., (2022). The future of fungi: threats and opportunities. G3: Genes, Genomes, Genetics, 12(11) **(11 pages).**

Castillo, D.; Vega-Muñoz, A.; Salazar-Sepúlveda, G.; Contreras-Barraza, N.; Torres-Alcayaga, M., (2023). Bibliometric mapping of school garden studies: A thematic trends analysis. Horticulturae, 9(3): 359 **(21 pages).**

Charria-Girón, E.; Surup, F.; Marin-Felix, Y., (2022). Diversity of biologically active secondary metabolites in the ascomycete order Sordariales. Mycol. Prog., 21(4): 43 **(33 pages).**

Corbu, V.M.; Gheorghe-Barbu, I.; Dumbravă, A.Ş.; Vrâncianu, C.O.; Şesan, T.E., (2023). Current insights in fungal importance—A comprehensive review. Microorganisms, 11(6): 1–52 **(52 pages).**

Cunliffe, M., (2023). Who are the marine fungi? Environ. Microbiol., 25(1): 131–134 **(4 pages).**

Dahiya, S.; Kumar, A.; Malik, V.; Kumar, V.; Singh, B., (2021). Biochemical characterization and enhanced production of endoxylanase from thermophilic mould Myceliophthora thermophila. Bioprocess. Biosyst. Eng., 44(7): 1539–1555 **(17 pages).**

da Silva, S.G.M.; de Melo, B.A.; dos Santos, M.T.; Rios, R.R.S.; de Santa'Anna Santos, C.M.; Júnior, R.K.A. L.; de Albuquerque Maranhão, F.C.; Carvalho dos Santos, T.M.; Fraga, A.B., (2022). Endophytic fungi: Benefits for plants and biotechnological potential. Res. Soc. Dev., 11(4): 1–20 **(20 pages).**

Debeljak, P.; Baltar, F., (2023). Fungal diversity and community composition across ecosystems. J. Fungi, 9(5) **(10 pages).**

Devi, R.; Kaur, T.; Kour, D.; Rana, K.L.; Yadav, A.; Yadav, A.N., (2020). Beneficial fungal communities from different habitats and their roles in plant growth promotion and soil health. Microb. Biosyst., 5(1): 21-47 **(27 pages).**

Dias, A.D.O.; Ladwig, N.I.; Conto, D.De., (2020). Thematic mapping in landscape analysis: hydrographic basin of the Urussanga river, Santa Catarina, Brazil. Geosul. Florianopolis, 35(75): 418–440 **(23 pages).**

Dong, L.; Xu, J.; Zhang, L.; Yang, J.; Liao, B.; Li, X.; Chen, S., (2017). High-throughput sequencing technology reveals that continuous cropping of American ginseng results in changes in the microbial community in arable soil. Chin. Med., 12(1): 1-12 **(12 pages).**

Du, J.; Yu, Y.; Tang, C.; Zong, K.; Zhang, S.; Zhang, Q.; Fang, L.; Li, Y., (2024). Organic fertilizers increase the proportion of saprotrophs favoring soil nitrification under medicinal plants Fritillaria thunbergii. Ind. Crops Prod., 219: 119129 **(10 pages).**

Frac, M.; Hannula, S.E.; Belka, M.; Jędryczka, M., (2018). Fungal biodiversity and their role in soil health. Front. Microbiol., 9(4): 1–9 **(9 pages).**

Fu, Z.; Chen, Q.; Lei, P.; Xiang, W.; Ouyang, S.; Chen, L., (2021). Soil fungal communities and enzyme activities along local tree species diversity gradient in subtropical evergreen forest. Forests. 12(10): 1321 **(16 pages).**

Gnanesh, B.N.; Tejaswi, A.; Arunakumar, G.S.; Supriya, M.; Manojkumar,

H.B.; Tewary, P., (2021). Molecular phylogeny, identification and pathogenicity of Rhizopus oryzae associated with root rot of mulberry in India. J. Appl. Microbiol., 131(1): 360–374 **(15 pages).**

Goh, J.; Mun, H.Y.; Jeon, Y.J.; Chung, N.; Park, Y.H.; Park, S.; Hwang, H.; Cheon, W., (2020). First report of six Sordariomycetes fungi isolated from plant litter in freshwater ecosystems of Korea. Kor. J. Mycol., 48(2): 103–116 **(14 pages).**

Gupta, B.M.; Ahmed, K.K.M., (2019). Research on Withania somnifera (Ashwaganda): A scientometric assessment of global publications output during 1995-2018. Int. J. Pharm. Investig., 9(2): 59–66 **(8 pages).**

Gutiérrez, M.H.; Vera, J.; Srain, B.; Quiñones, R.A.; Wörmer, L.; Hinrichs, K.U.; Pantoja-Gutiérrez, S., (2020). Biochemical fingerprints of marine fungi: implications for trophic and biogeochemical studies. Aquat. Microb. Ecol., 84(1): 75–90 **(16 pages).**

Haldeman, M., (2021). New and interesting records of lichens, Lichenicolous fungi and other Ascomycota from Northwestern USA III. Evansia. 37(3): 71–80 **(10 pages).**

Hannula, E.; Ma, H.; Perez Jaramillo, J.E.; Pineda, A.M.; Bezemer, T.M., (2020). Structure and ecological function of the soil microbiome affecting plant–soil feedbacks in the presence of a soil-borne pathogen. Environ. Microbiol., 22(2): 660–676 **(17 pages).**

Hemati, A.; Nazari, M.; Asgari Lajayer, B.; Smith, D. L.; Astatkie, T., (2022). Lignocellulosics in plant cell wall and their potential biological degradation. Folia Microbiol., 67(5): 671–681 **(11 pages).**

Hensen, N.; Bonometti, L.; Westerberg, I.; Brännström, I.O.; Guillou, S.; Cros-Aarteil, S.; Calhoun, S.; Haridas, S.; Kuo, A.; Mondo, S.; Pangilinan, J.; Riley, R.; LaButti, K.; Andreopoulos, B.; Lipzen, A.; Chen, C.; Yan, M.; Daum, C.; Ng, V.; Johannesson, H., (2023). Genome-scale phylogeny and comparative genomics of the fungal order Sordariales., Mol. Phylogenet. Evol., 189(11): 1-11 **(11 pages).**

Huang, G.; Liao, J.; Han, Z.; Li, J.; Zhu, L.; Lyu, G.; Lu, L.; Xie, Y.; Ma, J., (2020). Interaction between fungal communities, soil properties, and the survival of invading e. Coli o157:H7 in soils. Int. J. Environ. Res. and Public Health. 17(10) **(17 pages).**

Hussin, M.S.; Nuaman, R.S.; Al-Shammari, R.H.H., (2023). Fungal importance in our environment. South Asian Res. J. Bio. Appl. Biosci., 5(06): 123–128 **(6 pages).**

Ibrahim, S.R.M.; Mohamed, S.G.A.; Sindi, I.A.; Mohamed, G.A., (2021). Biologically active secondary metabolites and biotechnological applications of species of the family Chaetomiaceae (Sordariales): an updated review from 2016 to 2021. Mycol. Prog., 20(5): 595-639 **(6 pages).**

Ilić, N.; Milić, M.; Beluhan, S.; Dimitrijević-Branković, S., (2023). Cellulases: from lignocellulosic biomass to improved production. Energies, 16(8): 1–21 **(21 pages).**

Jamali, S., (2022). A review of research trends on Natassia mangiferae from 1966-2022: A bibliometric approach. Scie. Res. Essays. 17(4): 73–86 **(14 pages).**

Jatuwong, K.; Suwannarach, N.; Kumla, J.; Penkhrue, W.; Kakumyan, P.; Lumyong, S., (2020). Bioprocess for Production, Characteristics, and Biotechnological Applications of Fungal Phytases. Front Microbiol. 14(11): 188 **(18 pages).**

Jingjing, Y.; Huiqin, G.; Fry, E.L.; de Long, J.R.; Shiming, T.; Ting, Y.; Weibo, R., (2022). Plant roots send metabolic signals to microbes in response to long-term overgrazing. Sci. Total Environ., 842(24): 1–10 **(10 pages).**

Kalntremtziou, M.; Papaioannou, I. A.; Vangalis, V.; Polemis, E.; Pappas, K.M.; Zervakis, G.I.; Typas, M.A., (2023). Evaluation of the lignocellulose degradation potential of Mediterranean forests soil microbial communities through diversity and targeted functional metagenomics. Front. Microbiol., 14: 1–16 **(16 pages).**

Khaliq, A.; Perveen, S.; Alamer, K.H.; Ul Haq, M.Z.; Rafique, Z.; Alsudays, I.M.; Althobaiti, A.T.; Saleh, M.A.; Hussain, S.; Attia, H., (2022). Arbuscular mycorrhizal fungi symbiosis to enhance plant–soil interaction. Sustainability (Switzerland). 14(13) **(16 pages).**

Kim, W.; Wang, Z.; Kim, H.; Pham, K.; Tu, Y.; Townsend, J.P.; Trail, F., (2022). Transcriptional divergence underpinning sexual development in the fungal Class Sordariomycetes. mBio. 13(3): 1–18 **(18 pages).**

Köbben, B., (2018). Open educational resources for cartography: the thematic mapping tutor. PeerJ. 6: 2–5 **(4 pages).**

Komorowicz, M.; Janiszewska-Latterini, D.; Przybylska-Balcerek, A.; Stuper-Szablewska, K., (2023). Fungal biotransformation of hazardous organic compounds in wood waste. Molecules. 28(12): 4823 **(21 pages).**

Kumar, A.; Chandra, R., (2020). Ligninolytic enzymes and its mechanisms for degradation of lignocellulosic waste in environment. Heliyon. 6(2): e03170 **(18 pages).**

Lange, V.; Raposo, P., (2022). MapColPal – a color palette generation and testing tool for thematic maps. ICA. 5(9): 1–3 **(3 pages).**

Lee, C.M.; van Geel, B.; Gosling, W.D., (2022). On the use of spores of coprophilous fungi preserved in sediments to indicate past herbivore presence. Quaternary. 5(3): 1-23 **(23 pages).**

Leifheit, E.F.; Camenzind, T.; Lehmann, A.; Andrade-Linares, D.R.; Fussan, M.; Westhusen, S.; Wineberger, T.M.; Rillig, M.C., (2024). Fungal traits help to understand the decomposition of simple and complex plant litter. FEMS Microbiol. Ecol., 100(5): 1-12 **(12 pages).**

Li, D.; Meng, M.; Ren, B.; Ma, X.; Bai, L.; Li, J.; Bai, G.; Yao, F.; Tan, C., (2023). Different responses of soil fungal and bacterial communities to nitrogen addition in a forest grassland ecotone. Front. Microbiol., 14(9): 1–15 **(15 pages).**

Li, J.; Lin, L.; Sun, T.; Xu, J.; Ji, J.; Liu, Q.; Tian, C., (2020). Direct production of commodity chemicals from lignocellulose using Myceliophthora thermophila. Metab. Eng., 61(5): 416–426 **(11 pages).**

Li, X.; Cai, F.; Bao, J.; Jian, Y.; Sun, Z.; Xie, X., (2024). Navigating interdisciplinary research: Historical progression and contemporary challenges. J. Data Inf. Sci., 9(3): 14–28 **(15 pages).**

Maltseva, D.; Batagelj, V., (2024). Citation and bibliographic coupling between authors in the field of social network analysis. J. Data Inf. Sci., 9(4): 1–45 **(45 pages).**

Mamatha, B.; Mudigiri, C.; Ramesh, G.; Saidulu, P.; Meenakshi, N.; Prasanna, C.L., (2024). Enhancing soil health and fertility management for sustainable agriculture: A review. Asian J. Soil Sci. Plant Nutr., 10(3): 182–190 **(9 Pages).**

Manikandan, S.; Subbaiya, R.; Biruntha, M.; Krishnan, R.Y.; Muthusamy, G.; Karmegam, N., (2022). Recent development patterns, utilization and prospective of biofuel production: Emerging nanotechnological intervention for environmental sustainability A review. Fuel. 314: 1-12 **(12 pages).**

Manuela del Rosario, G.G.; Rita, M.L., (2022). Cellulases, hemicellulases and ligninolytic enzymes: mechanism of action, optimal processing conditions and obtaining value-added compounds in plant matrices. MOJ Food Process Technol., 10(1): 30–37 **(8 pages).**

Marin-Felix, Y.; Miller, A.N., (2022). Corrections to recent changes in the taxonomy of the Sordariales. Mycol. Prog., 21: 1-15 **(15 pages).**

Marin-Felix, Y.; Miller, A.N.; Cano-Lira, J.F.; Guarro, J.; García, D.; Stadler, M.; Huhndorf, S.M.; Stchigel, A.M., (2020). Re-evaluation of the order sordariales: Delimitation of lasiosphaeriaceae s. str., and introduction of the new families diplogelasinosporaceae, naviculisporaceae, and schizotheciaceae. Microorganisms. 8(9): 1–41 **(41 pages).**

Mignogna, D.; Szabó, M.; Ceci, P.; Avino, P., (2024). Biomass energy and biofuels: perspective, potentials, and challenges in the energy transition. Sustainability. 16(16): 1–33 **(33 pages).**

Mondal, H.; Deepak, K.K.; Gupta, M.; Kumar, R., (2023). The h-index: Understanding its predictors, significance, and criticism. J. Family Med. Prim. Care. 12(11): 2531–2537 **(7 pages).**

Muthusamy, C.; Murugaiyan, K., (2023). Bioprospecting Marine Fungal Enzymes-Scope and Challenges. Kavaka, 59(1), 33–47 (14 Pages).

Mylonakis, E., (2023). Frontiers in bacteriology: Challenges and opportunities. Front. Bacteriol., 1 **(4 pages).**

Nakbi, A.; Banaoues, R.C.; Dhiab, R.Ben; Ghozzi, K.; Belgacem, S.; Challouf, R.; Haouas, N.; Babba, H., (2024). Marine fungal community composition and diversity across a polluted site in the South Mediterranean coast: The Monastir Bay, Tunisia. Water Sci. Technol., 89(2): 319–332 **(24 pages).**

Nargotra, P.; Sharma, V.; Lee, Y.C.; Tsai, Y.H.; Liu, Y.C.; Shieh, C.J.; Tsai ML.; Dong, D.H.; Kuo, C.H., (2022). Microbial lignocellulolytic enzymes for the effective valorization of lignocellulosic biomass: a review. Catalysts, 13(1), 83 **(28 pages).**

Naureen, U.; Kayani, A.; Akram, F.; Rasheed, A.; Saleem, M., (2024). Protease production and molecular characterization of a protease dipeptidyl-aminopeptidase gene from different strains of Sordaria fimicola. Braz. J. Biol., 84: 1-13 **(13 pages).**

Newcombe, G.; Campbell, J.; Griffith, D.; Baynes, M.; Launchbaugh, K.; Pendleton, R., (2016). Revisiting the life cycle of dung fungi, including Sordaria fimicola. PLoS ONE. 11(2) **(12 pages).**

Niego, A.G.T.; Rapior, S.; Thongklang, N.; Raspé, O.; Hyde, K.D.; Mortimer, P., (2023). Reviewing the contributions of macrofungi to forest ecosystem processes and services. Fungal Biol. Rev., 44: 1-18 **(18 pages).**

Nielsen, C., (2022). Providing evidence of the impact of university research. J. Behaviour. Econ. Soc. Sys., 4(2): 1-10 **(10 pages).**

Pellegrino, E.; Piazza, G.; Helgason, T.; Ercoli, L., (2022). Microbiome structure and interconnection in soil aggregates across conservation and conventional agricultural practices allow to identify main prokaryotic and fungal taxa related to soil functioning. Soil Biol. Biochem., 175(7): 108833 **(19 pages).**

Pillay, L.; Schaab, G.; Coetzee, S.; Rautenbach, V., (2019). A comprehensive workflow for automating thematic map geovisualization from univariate big geospatial point data. Proceedings of the ICA, 2(July): 1–8 **(8 pages)**.

Pinto, Â.P.; Mejdalani, G.; Mounce, R.; Silveira, L.F.; Marinoni, L.; Rafael, J.A., (2021). Are publications on zoological taxonomy under attack? R. Soc. Open Sci., 8: 201617 **(22 pages).**

Prieto, A.; de Eugenio, L.; Méndez-Líter, J.A.; Nieto-Domínguez, M.; Murgiondo, C., Barriuso, J., Bejarano-Muñoz, L.; Martínez, M.J., (2021). Fungal glycosyl hydrolases for sustainable plant biomass valorization: Talaromyces amestolkiae as a model fungus. Int. Microbiol., 24(4): 545–558 **(14 pages).**

Radujković, D.; van Diggelen, R.; Bobbink, R.; Weijters, M.; Harris, J.; Pawlett, M.; Vicca, S.; Verbruggen, E., (2020). Initial soil community drives heathland fungal community trajectory over multiple years through altered plant–soil interactions. New Phytol., 225(5): 2140–2151 **(12 pages).**

Rodrigues, C.I.D.; Brito, L.M.; Nunes, L.J.R., (2023). Soil carbon sequestration in the context of climate change mitigation: A review. Soil Syst., 7(3): 64 **(21 pages).**

Rousseau, R.; Zhang, X., (2019). Reflections on tools and methods for differentiated assessments of individual scientists, groups of scientists and scientific journals. J. Data Inf. Sci., 4(3): 1–5 **(5 pages).**

Salmanton-García, J.; Hoenigl, M.; Gangneux, J.P.; Segal, E.; Alastruey-Izquierdo, A.; Arikan Akdagli, S.; Lagrou, K.; Özenci, V., Vena, A.; Cornely, O.A., (2023). The current state of laboratory mycology and access to antifungal treatment in Europe: A european confederation of medical mycology survey. The Lancet Microbe. 4(1): 1–10 **(10 pages).**

Sedek, M.Y.; Megahed, M.M.; El-Shamy, A.M., (2024). Integrating science, culture, and conservation in safeguarding brass antiquities from microbial corrosion. J. Bio- Tribo-Corros. 10(3): 1-23 **(23 pages).**

Shao, Y.; Molestak, E.; Su, W.; Stankevič, M.; Tchórzewski, M., (2022). Sordarin-An anti-fungal antibiotic with a unique modus operando. Br. J. Pharmacol., 179(6): 1125–1145 **(21 pages).**

Sruthy, K.S.; Shukla, L.; Kundu, A.; Singh, S.K.; Alodaini, A.H., Hatamleh, A.A.; Santoyo, G.; Kumar, A., (2023). Effect of microbial consortium constructed with lignolytic ascomycetes fungi on degradation of rice stubble. J. Fungi. 9(5) **(15 pages).**

Team, R.C., (2018). R : A Language and Environment for Statistical Computing. R foundation for statistical computing, 1: 1-3915 **(3915 pages).**

Teichert, I.; Pöggeler, S.; Nowrousian, M., (2020). Sordaria macrospora: 25 years as a model organism for studying the molecular mechanisms of fruiting body development. Appl. Microbiol. Biotechnol., 104(9): 3691–3704 **(15 pages).**

Tejakusuma, I.G.; Sittadewi, E.H.; Handayani, T.; Hernaningsih, T.; Wisyanto, W.; Rifai, A., (2024). Root growth and arbuscular mycorrhizal fungi on woody plants for vegetative stabilization of tropical slopes. Global J. Environ. Sci. Manage., 10(1): 267-286 **(10 pages).**

Tiaskal, V.; BrabcovÁ, V.; Větrovský, T.; Jomura, M.; López-Mondéjar, R.; Oliveira Monteiro, L.M.; Saraiva, J. P.; Human, Z. R.; Cajthaml, T.; Nunes da Rocha, U.; Baldrian, P., (2021). Complementary roles of wood-inhabiting fungi and bacteria facilitate deadwood decomposition. MSystems. 6(1) **(12 pages).**

U'Ren, J.M.; Miadlikowska, J.; Zimmerman, N.B.; Lutzoni, F.; Stajich, J.E.; Arnold, A.E., (2016). Contributions of North American endophytes to the phylogeny, ecology, and taxonomy of Xylariaceae (Sordariomycetes, Ascomycota). Mol. Phylogenet. Evol., 98: 210–232 **(23 pages).**

Vaksmaa, A.; Vielfaure, H.; Polerecky, L.; Kienhuis, M.V.M.; van der Meer, M.T. J.; Pflüger, T.; Egger, M.; Niemann, H., (2024). Biodegradation of polyethylene by the marine fungus Parengyodontium album. Sci. Total Environ., 934 (4): 172819 **(11 pages).**

van Eck, N.J.; Waltman, L., (2023). VOSviewer manual. Manual for VOSviewer version 1.6.20 software documentation. Univeristeit Leiden, October, 31, 2023 **(54 pages).**

Voigt, K.; James, T.Y.; Kirk, P.M.; Santiago, A.L.C.M.d.A.; Waldman, B.; Griffith, G.W.; Fu, M.; Radek, R.; Strassert, J.F.H.; Wurzbacher, C.; Jerônimo, G.H.; Simmons, D.R.; Seto, K.; Gentekaki, E.; Hurdeal, V. G.; Hyde, K.D.; Nguyen, T.T.T.; Lee, H.B., (2021). Early-diverging fungal phyla: taxonomy, species concept, ecology, distribution, anthropogenic impact, and novel phylogenetic proposals. Fungal Diversity. 109(1): 59-98 **(40 pages).**

Wang, C., (2020). Grand challenges in the research of fungal interactions with animals. Front. Fungal Biol., 1: 602032 **(5 pages).**

Wang, X.; Zhang, Q.; Zhang, Z.; Li, W.; Liu, W.; Xiao, N.; Liu, H.; Wang, L.; Li, Z.; Ma, J.; Liu, Q.; Ren, C.; Yang, G.; Zhong, Z.; Han, X., (2023a). Decreased soil multifunctionality is associated with altered microbial network properties under precipitation reduction in a semiarid grassland. IMeta. 2(2): 1–14 **(14 pages).**

Wang, Y.; Zhai, D.; Cheng, X., (2024). Soil nitrogen and phosphorus dynamics respond divergently to afforestation. For. Ecol. Manage., 555: 121705 **(10 pages).**

Wang, Z.; Kim, W.; Wang, Y.-W., Yakubovich, E.; Dong, C.; Trail, F.; Townsend, J.P.; Yarden, O., (2023b). The Sordariomycetes: an expanding resource with Big Data for mining in evolutionary genomics and transcriptomics. Front. Fungal Biol., 4(6): 1214537 **(19 pages).**

Werner, A.; Otte, K.; Stahlhut, G.; Hanke, L.M.; Pöggeler, S., (2021). The glyoxysomal protease LON2 is involved in fruiting-body development, ascosporogenesis and stress resistance in Sordaria macrospora. J. Fungi. 7(2): 1–18 **(18 pages).**

Wiafe, O.-B., (2018). Making attributes from the linked open data (LOD) cloud a part of spatial data infrastructures (SDIS) for thematic mapping. Int. J. Sci.Technol., 7(1): 20–33 **(14 pages).**

Wu, H.; Cui, H.; Fu, C.; Li, R.; Qi, F.; Liu, Z.; Yang, G.; Xiao, K.; Qiao, M., (2024). Unveiling the crucial role of soil microorganisms in carbon cycling: A review. Sci. Total Environ., 909(11): 168627 **(16 pages).**

Xie, N.; Chapeland-Leclerc, F.; Silar, P.; Ruprich-Robert, G., (2014). Systematic gene deletions evidences that laccases are involved in several stages of wood degradation in the filamentous fungus Podospora anserina. Environ. Microbiol., 16(1): 141–161 **(21 pages).**

Xu, H.; Sheng, R.; Xing, X.; Zhang, W.; Hou, H.; Liu, Y.; Qin, H.; Chen, C.; Wei, W., (2019). Characterization of fungal nirK-containing communities and N2O emission from fungal denitrification in arable soils. Front. Microbiol., 10(2): 117 **(12 pages).**

Ye, G.; Lin, Y.; Luo, J.; Di, H. J.; Lindsey, S.; Liu, D.; Fan, J.; Ding, W., (2020). Responses of soil fungal diversity and community composition to long-term fertilization: Field experiment in an acidic Ultisol and literature synthesis. Appl. Soil Ecol., 145(12): 1–9 **(9 pages).**

You, C.; Liu, Y.J.; Cui, Q.; Feng, Y., (2023). Glycoside Hydrolase Family 48 Cellulase: A Key Player in Cellulolytic Bacteria for Lignocellulose Biorefinery. Fermentation. 9(3): 1–15 **(14 pages).**

Zeng, Q.; Jia, P.; Wang, Y.; Wang, H.; Li, C.; An, S., (2019). The local environment regulates biogeographic patterns of soil fungal communities on the Loess Plateau. Catena. 183(8): 104220 **(10 pages).**

Zhang, G.; Bai, J.; Zhai, Y.; Jia, J.; Zhao, Q.; Wang, W.; Hu, X., (2024). Microbial diversity and functions in saline soils: A review from a biogeochemical perspective. J. Adv. Res., 59(6): 129–140 **(12 pages).**

Zhang, J.; Li, H.; Zhang, H.H.; Zhang, H.H.; Tang, Z., (2021). Responses of litter decomposition and nutrient dynamics to nitrogen addition in temperate shrublands of North China. Front. Plant Sci., 11(1): 1–10 **(10 pages).**

Zhang, L.; Xie, Z., (2023). Research agendas and organizational commitment among academics in mainland China. Higher Educ., 86(2): 429–448 **(20 pages).**

Zhang, X.; Ward, B.B.; Sigman, D.M., (2020). Global nitrogen cycle: critical enzymes, organisms, and processes for nitrogen budgets and dynamics. Chem. Rev., 120(12): 5308–5351 **(44 pages).**

Zhang, Y.; Sun, T.; Wu, T.; Li, J.; Hu, D.; Liu, D.; Li, J.; Tian, C., (2023). Consolidated bioprocessing for bioethanol production by metabolically engineered cellulolytic fungus Myceliophthora thermophila. Metab. Eng., 78(3): 192–199 **(8 pages).**

AUTHOR (S) BIOSKETCHES

Wulandari, N.F., Ph.D., Senior Researcher, Research Center for Biosystematics and Evolution, National Research and Innovation Agency (BRIN), Jalan Raya Jakarta-Bogor Km 46, Cibinong 16911, Indonesia.
- Email: *nila003@brin.go.id*
- ORCID: 0000-0003-4467-0754
- Web of Science Researcher ID: ABG-9009-2021
- Scopus Author ID: 15830722600
- Homepage: https://brin.go.id/en/page/civitas

Syam, A.R., M.Si., Senior Researcher, Research Center for Conservation of Marine and Inland Water Resources, National Research and Innovation Agency (BRIN), Jalan Raya Jakarta-Bogor Km 46, Cibinong 16911, Indonesia.
- Email: *amra002@brin.go.id*
- ORCID: 0000-0002-9986-0339
- Web of Science Researcher ID: JLM-9097-2023
- Scopus Author ID: 57208086343
- Homepage: https://brin.go.id/en/page/civitas

Alhamd, L., Ph.D., Senior Researcher, Research Center for Ecology and Ethnobiology, National Research and Innovation Agency (BRIN), Jalan Raya Jakarta-Bogor Km 46, Cibinong 16911, Indonesia.
- Email: *laod003@brin.go.id*
- ORCID: 0000-0002-2574-5952
- Web of Science Researcher ID: JQW-2182-2023
- Scopus Author ID: 55488921400
- Homepage: https://brin.go.id/en/page/civitas

Gunadi, B., Ph.D., Senior Researcher, Research Center for Fishery, National Research and Innovation Agency (BRIN), Jalan Raya Jakarta-Bogor Km 46, Cibinong 16911, Indonesia.
- Email: *bambang.gunadi@brin.go.id*
- ORCID: 0000-0002-2912-6761
- Web of Science Researcher ID: HNI-9891-2023
- Scopus Author ID: 57217585215
- Homepage: https://brin.go.id/en/page/civitas

Yosmaniar, Y., M.Si., Senior Researcher, Research Center for Marine and Land Bioindustry, National Research and Innovation Agency (BRIN), Gedung TMC 120 KST B.J. Habibie, Serpong, Tangerang Selatan 15314, Indonesia.
- Email: *yosm003@brin.go.id*
- ORCID: 0000-0001-9931-2669
- Web of Science Researcher ID: LDL-6343-2024
- Scopus Author ID: 57218545896
- Homepage: https://brin.go.id/en/page/civitas

AUTHOR (S) BIOSKETCHES

Widjaja, E., Ph.D., Senior Researcher, Research Center for Sustainable Production System and Life Cycle Assessment, National Research and Innovation Agency (BRIN), Gedung Pusat Inovasi dan Bisnis Teknologi, No. 720, KST BJ. Habibie, Serpong, Tangerang Selatan 15314, Indonesia.
- Email: *ermi005@brin.go.id*
- ORCID: 0009-0007-2993-0577
- Web of Science Researcher ID: EED-5296-2022
- Scopus Author ID: 57217826643
- Homepage: https://brin.go.id/en/page/civitas

Utomo, B.N., Ph.D., Senior Researcher, Research Center for Veterinary Science, National Research and Innovation Agency (BRIN), Jalan Raya Jakarta-Bogor Km 46, Cibinong 16911, Indonesia.
- Email: *bamb063@brin.go.id*
- ORCID: 0000-0003-3472-515X
- Web of Science Researcher ID: JFJ-3890-2023
- Scopus Author ID: 57211914562
- Homepage: https://brin.go.id/en/page/civitas

Wahyuwardani, S., Ph.D., Senior Researcher, Research Center for Veterinary Science, National Research and Innovation Agency (BRIN), Jalan Raya Jakarta-Bogor Km 46, Cibinong 16911, Indonesia.
- Email: *suti010@brin.go.id*
- ORCID: 0000-0003-4566-3775
- Web of Science Researcher ID: KXR-1714-2024
- Scopus Author ID: 57204476536
- Homepage: https://brin.go.id/en/page/civitas

Widiastuti, R., Ph.D., Principal Researcher, Research Center for Veterinary Science, National Research and Innovation Agency (BRIN), Jalan Raya Jakarta-Bogor Km 46, Cibinong 16911, Indonesia.
- Email: *raph001@brin.go.id*
- ORCID: 0000-0002-3291-200X
- Web of Science Researcher ID: A-8471-2017
- Scopus Author ID: 57202236919
- Homepage: https://brin.go.id/en/page/civitas

Kadarini, T., M.Si., Principal Researcher, Research Center for Fishery, National Research and Innovation Agency (BRIN), Jalan Raya Jakarta-Bogor Km 46, Cibinong 16911, Indonesia.
- Email: *tuti006@brin.go.id*
- ORCID: 0000-0009-9321-2464
- Web of Science Researcher ID: NA
- Scopus Author ID: 57195980531
- Homepage: https://brin.go.id/en/page/civitas

Dody, S., Ph.D., Senior Researcher, Research Center for Oceanography, National Research and Innovation Agency (BRIN), Jl. Raya Puspitek 60, Serpong 15314, Tangerang Selatan, Indonesia.
- Email: *safa001@brin.go.id*
- ORCID: 0000-0002-0073-2151
- Web of Science Researcher ID: NA
- Scopus Author ID: 5705481638
- Homepage: https://brin.go.id/en/page/civitas

HOW TO CITE THIS ARTICLE

Wulandari, N.F.; Syam, A.R.; Alhamd, L.; Gunadi, B.; Yosmaniar, Y.; Widjaja, E.; Utomo, B.N.; Wahyuwardani, S.; Widiastuti, R.; Kadarini, T.; Dody, S., (2025). A bibliometric study on Sordariales fungi covering genetic diversity, ecological interactions and biotechnological applications. Global J. Environ. Sci. Manage., 11(3): 1319-1342.

DOI: 10.22034/gjesm.2025.03.24

URL: https://www.gjesm.net/article_722780.html

Global J. Environ. Sci. Manage. 11(3): 1343-1360, Summer 2025, Serial #43

Global Journal of Environmental Science and Management
(GJESM)

Homepage: https://www.gjesm.net/

Podcasts

REVIEW PAPER

Application of marine bacterial alginate lyases in wastewater treatment, biofilm removal and green technology

M.U.K. Anjung[1,2], H. Nursyam[3], A.A. Prihanto[3,*], E. Chasanah[4]

[1] *Doctoral Program in Fisheries Science and Marine, Faculty of Fisheries and Marine Sciences, Universitas Brawijaya East Java, Indonesia*

[2] *Secondary Fisheries Business School, Jl Pantai Harapan, Tanggamus, Lampung, Indonesia*

[3] *Department of Fishery Product Technology, Faculty of Fisheries and Marine Science, rawijaya University, JL. Veteran, Malang 65415, East Java, Indonesia*

[4] *Research Center for Marine and Inland Bioindustry, Research Organization of Earth and Maritime, National Research, and Innovation Agency, Serpong, Indonesia*

ARTICLE INFO

Article History:
Received 24 February 2025
Revised 30 April 2025
Accepted 04 June 2025

Keywords:
Alginate lyase
alginate oligosaccharides
Green Technology
Marine bacteria
Seaweed

ABSTRACT

Alginate lyases are a class of enzymes capable of cleaving alginate, a major structural polysaccharide presents in the cell walls of brown algae. In recent years, marine bacteria have emerged as a valuable and diverse source of these enzymes, owing to their unique adaptations to extreme marine conditions such as high salinity, variable potential of hydrogen, and fluctuating temperatures. Marine-derived alginate lyases exhibit outstanding enzymatic traits, including their ability to withstand salt, maintain thermal stability, exhibit substrate specificity, and employ various catalytic mechanisms, making them highly desirable for a variety of various industrial applications. The primary function of these enzymes lies in depolymerizing alginate into alginate oligosaccharides, which possess notable biological activities. The potential of alginate oligosaccharides is significant across diverse industries, such as pharmaceuticals (for instance, antitumor and immunomodulatory uses), agriculture (like plant biostimulants), food (serving as prebiotics), wastewater treatment, and the production of bioenergy. These applications are further enhanced by the enzymes' compatibility with green processing technologies and sustainable resource utilization. This study provides a comprehensive overview of marine alginate lyases, focusing on their enzymatic properties, catalytic mechanisms, and industrial relevance. It also highlights future directions for their development and application. Advancements in molecular biology, protein engineering, and synthetic biology have accelerated the identification and development of novel alginate lyases, expanding the repertoire of polysaccharide lyase families. Furthermore, in-depth understanding of their β-elimination catalytic mechanisms—whether via histidine/tyrosine-based or metal ion-assisted pathways—has enabled enzyme engineering for improved performance under industrial conditions. Although significant advancements have been made, obstacles still exist in attaining efficient large-scale production, improving enzyme stability, and optimizing catalytic characteristics. This review discusses the enzymatic features, catalytic mechanisms, and emerging applications of alginate lyases from marine bacteria, while exploring future perspectives including biofilm degradation, wastewater treatment, and biodegradable materials. The strategic development of alginate lyases may play a vital role in advancing sustainable biotechnologies and circular bioeconomy. The study aimed to deliver a thorough introduction to the recent progress in discovering and characterizing alginate lyases sourced from marine bacteria.

DOI: 10.22034/gjesm.2025.03.25

This is an open access article under the CC BY license (http://creativecommons.org/licenses/by/4.0/).

NUMBER OF REFERENCES
132

NUMBER OF FIGURES
3

NUMBER OF TABLES
4

*Corresponding Author:
Email: *asep_awa@ub.ac.id*
Phone: +62 341 553512
ORCID: 0000-0003-4180-1325

Note: Discussion period for this manuscript open until Sep 1, 2025 on GJESM website at the "Show Article".

INTRODUCTION

With the ongoing increase in the world population, the assurance of sustainable food production is becoming progressively vital. According to projections from the Food and Agriculture Organization of the United Nations (FAO), global food production must expand by 70 percent (%) by 2050 to accommodate demand (Crona *et al.,* 2023; Munialo and Mellor, 2024). Efforts made to overcome these challenges, the sustainable blue economy has developed into a strategic approach in optimizing the use of marine resources to produce innovative food products and supplements, especially in the European Union (EU) (Rotter *et al.,* 2023; Gaceu *et al.,* 2023). The fisheries sector plays a significant role in supplying essential food items like fish, seaweed, and shellfish, while also serving as a source of raw materials for multiple industries, including food production, cosmetics, and pharmaceuticals (Naseem *et al.,* 2024). Marine enzymes, including proteases, lipases, and alginate lyase (Aly), exhibit considerable potential for enhancing the value of fisheries products via biotechnology (Sarkar *et al.,* 2023; Shankar *et al.,* 2024; Irianto *et al.,* 2024). The ability of Aly to degrade alginate is a major attraction for various parties. Alginate as one of the largest polysaccharides in brown algae, can be converted into oligosaccharides with valuable bioactivities (Severo *et al.,* 2024; Liu *et al.,* 2024). Enzymes serving as facilitators of sustainable manufacturing practices in environmentally conscious chemical processing methods (Senadheera *et al.,* 2023; Sanjeewa *et al.,* 2023). Research on Alys mainly focuses on their biochemical traits and food industry uses, while new studies suggest broader applications like wastewater treatment and green chemicals (Xu *et al.,* 2021). Marine bacteria, including *Pseudoalteromonas* and *Flammeovirga* sp., synthesize Alys characterized by distinctive enzymes. Furthermore, enzyme-driven processing provides eco-friendly options by minimizing waste and facilitating energy-efficient manufacturing of valuable products in contrast to traditional techniques. Marine-derived enzymes are used in pharmaceuticals and nutraceuticals (Gholami-Shabani *et al.,* 2023; Ramya *et al.,* 2025) and in agriculture as fertilizers and feed supplements (Cheng *et al.,* 2024; Bi *et al.,* 2024). With increasing awareness of natural products and environmental sustainability, the role of enzymes in fishery product biotechnology is expected to expand across various industrial sectors (Augusto *et al.,* 2024; Khiari, 2024). The objective of this study is to present a comprehensive overview to the recent progress made in discovering and analysis of Alys derived from marine bacteria. It focuses on their unique enzymatic properties, catalytic mechanisms, and potential industrial applications. Furthermore, it examines how molecular biology and enzyme engineering have contributed to the evolution of these enzymes, while considering the current challenges and future opportunities in their research and application. This study is a part of a doctoral dissertation titled as "Characterization of alginate oligosaccharides resulting from enzymatic degradation by Aly from bacteria from Lampung waters". The research was conducted at Brawijaya University, Malang, Indonesia, from 2021 to 2025.

METHODOLOGY

The study covers literature published between 2020 and 2025. A systematic search was conducted using Google Scholar and ResearchGate and technical literature with keywords including "alginate lyase," "marine bacteria," "enzymatic degradation,"and" biotechnological applications". Additional pertinent studies were identified through citation tracking. Enzyme classification followed the Enzyme Commission (EC) number system established by the International Union of Biochemistry and Molecular Biology (IUBMB), and the latest updates on polysaccharide lyase (PL) families were obtained via the carbohydrate-active enzymes (CAZymes) Database. The initial search resulted in 1,399 records. Following the removal of duplicates, 1,185 records were reviewed by title and abstract, which led to the evaluation of 290 full-text articles assessed for eligibility. Based on predefined inclusion criteria, 132 articles were selected for this review. Exclusion criteria comprised studies that were not centered on marine bacteria, those that lacked thorough enzymatic or methodological data, as well as grey or low-quality literature. Only peer-reviewed publications with clear experimental insights were included to ensure scientific rigor and relevance.

Marine-derived bacteria as a source of Aly

Marine bacteria are known as promising sources of Aly enzymes due to their adaptation to extreme marine environments such as high salinity, osmotic pressure, and

Table 1: Marine-derived bacteria as sources of alginate lyase and their characteristics

Bacterial species	Source of isolation	Aly type	Enzyme characteristics	Applications	Sources
Vibrio sp.	Seawater, marine sediment	Endo-type lyase	Salt-tolerant, active at neutral pH	Biotechnology and Food Industry, Waste Treatment, Pharmaceuticals	Peng *et al.* (2024)
Pseudoalteromonas spp.	Brown algae	Endo-type lyase	Cold-adapted, high substrate specificity	Food, pharmaceutical, and cosmetic industries	Sun *et al.* (2024)
Flavobacterium spp.	Brown seaweed	Polysaccharide lyase	High activity at moderate temperatures	Food additives, enhancing texture and stability in food products.	Morley *et al.* (2025)
Shewanella oneidensis	Marine sediment	Exo-type lyase	Halotolerant, metal-ion influenced	Eectrochemical activity can be harnessed for electro-fermentation processes	Nah *et al.* (2023)
Zobellia galactanivorans	Decomposing seaweed	Endo-type lyase	Degrades both poly-mannuronate (M-blocks) and poly-guluronate (G-blocks)	AOs, food additives, agricultural biotechnology	Barbeyron *et al.* (2023)

temperature fluctuations (Pedraza-Segura *et al.,* 2023; Ye *et al.,* 2025). These changes facilitate the generation of stable and active enzymes under conditions of high salt concentrations and diverse pH levels, which is perfect for industrial applications. Certain marine habitats, like deep-sea hydrothermal vents, polar areas, coastal algal beds, and marine sediments, host many new Aly -producing bacteria. For instance, coastal areas rich in brown algae provide ample sources of alginate, fostering microbial development for effective enzymatic degradation (Flores-Contreras *et al.,* 2023). Extreme environments have bacteria with unique enzymes. Different habitats have distinct bacterial communities. Recently discovered Alys from the ocean, along with their characteristics and applications (Rahmati *et al.,* 2024).

Table 1. presenting various marine bacterial species that serve as sources of Alys enzymes. *Vibrio* sp., isolated from seawater and marine sediments, produces a salt-tolerant endo-type enzyme active at neutral pH (Peng *et al.*, 2024). *Pseudoalteromonas* spp., extracted from brown algae, these enzymes are cold-adapted endo-types that possess high substrate specificity, which is ideal for use in food, pharmaceutical, and cosmetic industries (Sun *et al.*, 2024). *Flavobacterium* spp., secrete moderate-temperature-active polysaccharide lyases used to improve food texture and stability (Morley *et al.*, 2025). *Shewanella oneidensis*, produces salt-tolerant exo-type enzymes influenced by metal ions, suitable for electroactive fermentation in waste treatment and bioenergy (Nah *et al.*, 2023). *Zobellia galactanivorans*, derived from decaying seaweed, generates an endo-type Alys that degrades both M-blocks and G-blocks, applied in AOs production, food additives, and agriculture (Barbeyron *et al.*, 2023). The bacterial source affects AOs yield and bioactivity, due to specific enzyme functions and degradation patterns. *Wenyingzhuangia fucanilytica* produces four synergistic lyases yielding AOs from disaccharides to heptasaccharides (Li *et al.*, 2023b). Aly5 from *Flammeovirga* sp. targets guluronate blocks, creating oligosaccharides with unique terminal structuresthat enhance AOs bioactivities such as antioxidant, antimicrobial, and immunomodulatory effects (Xing *et al.*, 2020; Barzkar *et al.*, 2022). The breakdown of alginate by marine bacteria is also a factor in carbon cycling, underscoring their ecological importance (Barzkar *et al.*, 2022; Balmonte *et al.*, 2024). However, not all enzymes are fully functional or efficient, highlighting the need to study less-explored marine bacteria for new enzymes with industrial and ecological relevance.

Mechanism of action of Alys

Alys degrade alginate through beta-elimination

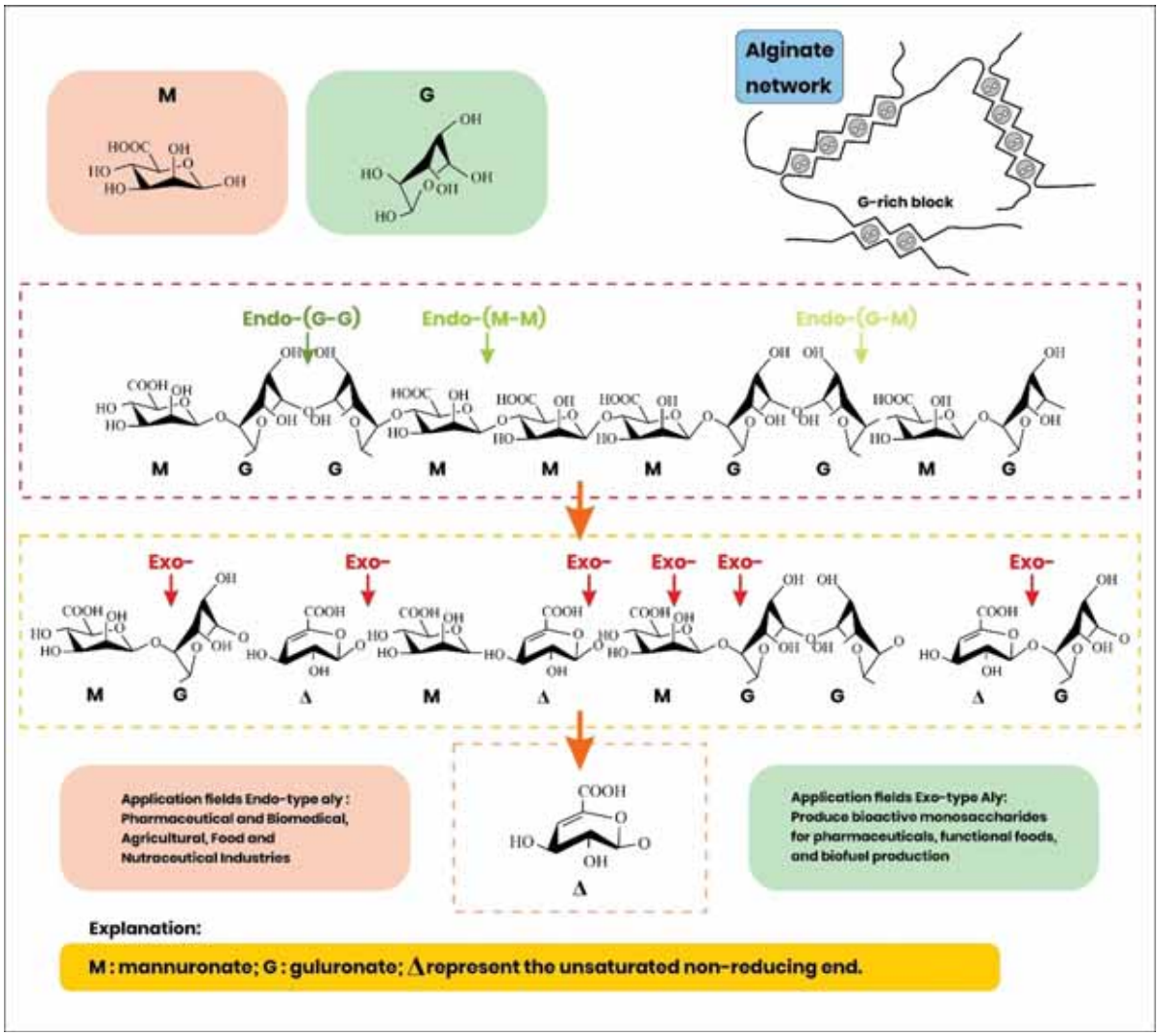

Fig. 1: Mechanism of action of Aly

(β-elimination), breaking 4-O-glycosidic bonds and forming a C4–C5 double bond, which is important for biological, biorefinery, and agricultural applications (Xiao *et al*., 2024). This enzymatic reaction results in oligosaccharides featuring 4-deoxy-L-erythro-hex-4-enopyranosyluronic acid (DEH) at the non-reducing terminus. The reaction involves three steps: carboxyl group charge neutralization, proton abstraction at fifth carbon (C5), and electron rearrangement to cleave the bond and form the double bond (Chen *et al*., 2024a). During proton abstraction at C5, the proton's position can vary, producing either syn or anti configurations. Syn configuration occurs with mannuronate (M) residues, while anti configuration arises from guluronate (G) residues. The general catalytic mechanism is shown in Fig. 1. Alys utilize two main catalytic strategies: The Histidin (His)/ Tyrosin (Tyr) elimination and the metal ion-assisted mechanism, differing in how they neutralize the carboxyl group and manage proton transfers (Cao *et al*., 2022). In Fig. 1, the action mechanism of Aly on alginate, made up of M and G monomers, is depicted. Alginate's structure is marked by a complex network with a predominance of G-blocks, as depicted in the upper right section. Alys are divided into two types: endo-type and exo-type. Endo-type lyases randomly

Table 2: Enzymatic properties of alginate lyases from marine bacteria

Marine bacterium	Optimum pH and temperature in degree Celsius (°C)	Substrate specificity	Catalytic mechanism	Sources
Pseudoalteromonas carrageenovora ASY5	6, 35	M-block and G-block	Lys/tyr acid–base catalysis	Tang *et al.* (2022)
Vibrio splendidus	7.5-8.5, 20-25	G-block > M-block	His/Tyr elimination	Bao *et al.* (2024)
Zobellia galactanivorans	7, 35	M-block	His/Tyr elimination	Xia *et al.* (2023)
Flavobacterium sp.	7.6, 30	M-block and G-block	Metal ion-assisted	Morley *et al.* (2025)
Paenibacillus sp.	7, 45	M-block and G-block	Novel Lys/Lys elimination mechanism	Wei *et al.* (2025)

cleave internal bonds in alginate represented by green arrows to produce oligosaccharides used in various sectors. Exo-type lyases, indicated by red arrows, eliminate segments from the ends of the chain, contributing to biofuels and pharmaceuticals.

His/Tyr-based and metal ion-assisted Alys exhibit distinct 3D structures and catalytic mechanisms, as shown by crystallographic and cryo-EM studies. Lyases that are based on His/Tyr (for instance, PL5, PL7, PL17) utilize conserved residues for syn or anti β-elimination and typically have flexible loops or mobile domains to allow for substrate access and product release. In contrast, metal-assisted lyases such as AlyGC (PL6) utilize Ca^{2+} ions at the active site to neutralize carboxyl groups and support catalysis. These enzymes are characterized by a right-handed β-helix fold and the rotation of structural subunits, which limits substrate binding to one monomer at a time. His/Tyr-based lyases have groove-like active sites, while metal-dependent enzymes show narrow, metal-coordinated catalytic pockets. Alys, particularly in enzymes sourced from marine environments, could demonstrate allosteric regulation, impacting enzyme activity through alterations in conformation. In AlyC8, deletion of catalytic domains revealed synergistic effects between domains, indicating potential allosteric interactions (Sun *et al*., 2022). Kinetic studies on *Stenotrophomonas maltophilia* lyases showed that specific residue mutations disrupt exolytic activity, highlighting the role of structural changes in allosteric control (Chu *et al*., 2020).

Enzymatic properties of Alys from marine bacteria

Marine bacterial Alys are predominantly endolytic, cleaving internal glycosidic bonds to yield unsaturated AOs with low degrees of polymerization (DP) (Wang *et al*., 2023a; Zhu *et al*., 2024). Certain enzymes exhibit exolytic activity, decomposing alginate from the ends into monosaccharides. Their specificity depends on the active site and the bonds in alginate. Some target M–M or G–G linkages, while others can degrade both, based on their structure. For instance, *Vibrio splendidus* makes lyases with different domains for M-block and G-block breakdown (Zhang *et al*., 2023a; Wang *et al*., 2023). Table 2, outlines the enzymatic properties of Alys obtained from various marine bacteria.

Marine Alys demonstrate different catalytic mechanisms, substrate preferences, and optimal conditions, which are affected by their bacterial origin and structural attributes. *Pseudoalteromonas carrageenovora* ASY5 hydrolyzes both M-block and G-block via Lysin (Lys)/Tyr acid-base catalysis, with peak activity at pH 6 and 35°C (Tang *et al*., 2022). *Vibrio splendidus* favors G-block over M-block, works best at pH 7.5-8.5 and 20-25°C, and employs a His/Tyr elimination mechanism (Bao *et al*., 2024). *Zobellia galactanivorans* prefers M-block, with optimal activity at pH 7 and 35°C using the His/Tyr pathway (Xia et al., 2023). *Flavobacterium* sp. acts on both substrates at pH 7.6 and 30°C through a metal ion-assisted mechanism (Morley *et al*., 2025). *Paenibacillus* sp. hydrolyzes M-block and G-block optimally at pH 7 and 45°C using a novel Lys-based elimination process (Wei *et al*., 2025). Alginate lyase has specific substrate preferences, some enzymes show a wider substrate range, so they can be used in various fields in biotechnology processes. This

Table 3: Comparative performance metrics of selected alginate lyases

Enzyme	Optimum Temp. (°C)	Optimum pH	Specific activity (Units per milligram (U/mg)	Stability profile	Features/ activation	Source
AlyRm4 (*Rhodothermus marinus*)	81	6.5	Not specified	Thermostable	Exolytic	Dobruchowska *et al*., 2022
AlyRm3 (*R Rhodothermus marinus*)	70–75	5.5–8.0	37,315.08	Stable at 65°C, 30% activity at 90°C	Highly thermophilic, endolytic	Dobruchowska *et al*., 2022; Li *et al*., 2023d
AlgL6 (*Microbulbifer* sp.)	35	8.0	Not specified	Stable ≤30°C, pH 5–9, Sodium Chloride (NaCl)/Detergent stable	Exolytic, Ca2+-dependent	Long *et al*., 2022
TAPL7B (*Tenacibaculum algicola*)	20	11.0	Not specified	Stable pH 4–12, cold-adapted, metal stable	Ca2+-activated, polyM-preferred	Chen *et al*., 2023b
Payn ALyase (*Paenibacillus* sp.)	55 (WT), 70 (mutant)	8.0	90.3 (WT)	Mutant: 83.3% activity after 30min at 65°C	Thermostability improved by mutation	Zhang *et al*., 2023b
Immobilized Alginate Lyase (unspecified)	45	9.0	Not specified	Thermostable at 45°C for 3h, reusable	Immobilized, industrial focus	Kaur *et al*., 2024

adaptability can increase the benefits of alginate lyase in various industrial applications, such as food processing and bioremediation (Barzkar *et al*., 2022). Post-translational modifications (PTMs), such as glycosylation, enhance enzyme activity, stability, and specificity. Aly7Ce shows catalytic stability influenced by glycosylation (Li *et al*., 2023c), while N-glycosylation in Pichia pastoris reduced substrate inhibition in d-lactonohydrolase, boosting biocatalysis efficiency (Sun *et al*., 2025). According to Couto *et al*. (2024), higher PTM occupancy might result in diminished enzyme stability. Alys have demonstrated to be beneficial for the breaking down of brown algae into AOs, with synergistic enzymes managing to achieve total polymer degradation (Li *et al*., 2023e). Structural and molecular advancements have expanded their industrial application in AOs production (Chen *et al*., 2024a). Enzyme combinations like Alys and cellulases enhance seaweed fertilizer production enriched with phytohormones (Zhang *et al*., 2023a). Table 3, illustrates the different optimal conditions and stability characteristics of the selected Alys and also emphasizes the ideal performance metrics and potential applications of different Alys. These enzymes exhibit a broad temperature range, from cold-adapted TAPL7B at 20°C to thermostable AlyRm4 at 81°C, making them suitable for diverse industrial settings.

Most Alys function effectively in neutral to alkaline conditions (pH 7.0–11.0), with some showing broad pH tolerance. AlyRm3 stands out with exceptionally high specific activities (8,306.7 and 37,315.08 U/mg), reflecting strong catalytic efficiency. A number of enzymes preserve stability across diverse pH and temperature conditions, with metal ions enhancing their catalytic performance. Some Alys are activated by NaCl or Ca^{2+} and exhibit substrate preferences for M-block or G-block, while others are bifunctional.

Applications of Alys

Alys sourced from marine bacteria is capable of efficiently and adaptively degrading alginate into bioactive oligosaccharides, showcasing remarkable catalytic efficiency in saline and fluctuating temperature conditions, rendering them perfect for industrial applications. Fig. 2 illustrates the application of Alys from marine bacteria.

Fig. 2 illustrates five key applications of Alys: biofilm inhibition, intermediates in drug synthesis, AOs production for food, health, and agriculture,



Fig. 2: Application of Alys from marine bacteria

eco-friendly biopolymer generation, and antibiotic support, showcasing their biotechnological and circular economy relevance. Optimizing Alys performance is vital for boosting biofuel precursor production from alginate-rich biomass through metabolic integration and enzyme optimization (Cao *et al*., 2022). These enzymes decompose alginate into oligosaccharides, which can subsequently be transformed into biofuels; therefore, the focus is on enhancing catalytic efficiency and thermal stability through strategic design and directed evolution. Recombinant expression in *E. coli* boosts Aly yields and facilitates purification for industrial-scale use (Dharani *et al*., 2020), while thermophilic enzymes like AlyRm3 increase saccharification efficiency (Li *et al*., 2023d). Process strategies involve combining endo- and exo-lyases for complete degradation and using low-cost feedstocks like *Sargassum* to enhance economic viability (Mohapatra, 2022). Fine-tuning enzyme ratios and conditions boosts biofuel yields, notwithstanding the challenges posed by production costs. The successful combination of endolytic and exolytic lyases efficiently transforms alginate into oligosaccharides or monosaccharides. Pathway modeling shows that complementary enzymes and optimal conditions enhance biorefinery efficiency. Fusion enzymes that combine both functions enhance thermostability and catalysis, which supports their application in bioconversion systems for commercial purposes (Zhu *et al*., 2024).

Biofilm degradation

Aly has shown great potential for biofilm degradation, especially those formed by *Pseudomonas aeruginosa*, by targeting alginate in the matrix and enhancing antibiotic penetration (Bi *et al*., 2023; Zanditenas and Ankri, 2024). Table 4 presents a comparative overview of various antibiofilm enzymes and their respective effectiveness. According to the summary in Table 4, the enzyme functions through β-elimination to undermine the structural integrity of the biofilm, thereby diminishing its resistance antibiotics. Alys from *P Pseudomonas aeruginosa* and *Azotobacter vinelandii* have improved antibiotic efficacy in cystic fibrosis (CF) patients by breaking down biofilms (Kanwar *et al*., 2024). According to Wang *et al*. (2024c), these enzymes have the ability to degrade biofilms of *Staphylococcus aureus* and *Pseudomonas aeruginosa*, particularly when they are combined with Deoxyribonuclease (DNase I) and antibiotics. Al-Madboly *et al*. (2024) further emphasized the enzyme's specificity for alginate, making it highly effective in synergistic applications for chronic infections and medical devices.

Table 4: Comparison of antibiofilm enzyme effectiveness

Enzyme	Biofilm forming bacteria	Mechanism of action	Effectiveness	Sources
Alginate Lyase	*Pseudomonas aeruginosa*	Degrades poly-mannuronic acid and poly-glucuronic acid	A concentration of 50 U/mL can reduce *P. aeruginosa* biofilm biomass by up to 70% within 24	Al-Madboly *et al.* (2024)
Dispersin B	*Staphylococcus*	Breaks glycosidic bonds in polysaccharides	Effective in inhibiting the formation and release of biofilms in more than 25 species of bacteria	Breslawec *et al.* (2023)
DNase I	Various biofilm-forming bacteria	Hydrolyzing extracellular DNA	Concentrations of 0.5–5 µg/mL can reduce biofilm biomass by up to 70% within 24 hour.	Lin *et al.* (2024)
Amylase	*Staphylococcus. aureus*	Hydrolyzes polysaccharides	A concentration of 100 U/mL α-amylase can reduce *Staphylococcus aureus* biofilm biomass by up to 79% in 5 minutes.	Aksoy *et al.* (2023)

Marine Alys disrupt antibiotic-resistant bacteria biofilms, influenced by enzyme and biofilm composition. Studies suggest enzymes may disperse biofilms without their catalytic roles. Alys show varying activity based on substrate, with Alg2A effective due to M-block and G-block degradation (Blanco-Cabra *et al.,* 2020). Alys help antibiotics penetrate biofilms; dosage affects effectiveness (Blanco-Cabra *et al.,* 2020; Wang *et al.,* 2024c).

Wastewater treatment

The introduction of Alys may boost alginate breakdown and carbon cycling, yet it demands meticulous evaluation to ensure that native microbial communities and nutrient balances are not disrupted (Zhu *et al*., 2024; Wang *et al*., 2024b). Recent studies underscore the critical role of monitoring alterations in microbial diversity following enzyme application to protect environmental safety (Zhang *et al*., 2023c; Liu *et al*., 2024). Aly has exhibited capability in the field of wastewater treatment by overseeing biofilms and breaking down organic pollutants sourced from algal biomass (Saini *et al*., 2023). In industrial systems, where biofilms often contain alginate produced by *Pseudomonas* species, Aly disrupts the matrix structure, thereby improving system cleanliness (Tao *et al*., 2024; Rehman *et al*., 2024). The enzyme also reduces alginate levels in seaweed-based processes, lowering biochemical and chemical oxygen demand (Abdelfattah *et al*., 2023; Yang *et al*., 2024), enhancing organic matter breakdown and microbial activity (Ye *et al*., 2025; Tang *et al*., 2025). Aly boosts the quality of treated wastewater and aids in the implementation of advanced technologies including membrane filtration and activated sludge systems (Vera-Villalobos *et al*., 2023; Singh *et al*., 2023). Its eco-friendly nature contributes to wastewater treatment sustainability by reducing maintenance costs and enhancing system stability (Luo *et al*., 2024; Khan, 2025). Aly is instrumental in sludge management, aiding in the recovery and application of extracellular polysaccharides, including alginate, which enhances coagulation, sedimentation, and dewatering, and facilitates the conversion of excess sludge into valuable biomaterials (Zeng *et al*., 2023; Hu et al., 2023). As a biocompatible and biodegradable agent, Aly reduces the environmental footprint of chemical treatments and supports greener technologies (Ramesh *et al*., 2023; Radoor *et al*., 2024). Fig. 3 illustrates the industrial production pipeline of marine Alys, starting from environmental screening and microbial strain selection, followed by gene cloning, expression, optimization, immobilization, purification, and enzymatic conversion of alginate into oligosaccharides (AOs), which are then applied in areas such as wastewater bioremediation, biofuel production, heavy metal adsorption, biofilm control, and alginate waste valorization.

Employing Alys for wastewater treatment can increase degradation efficiency while decreasing costs. The immobilization of these enzymes within bioreactors promotes greater oligosaccharide production. Techniques like chitosan beads improve enzyme stability, aiding pollutant removal and

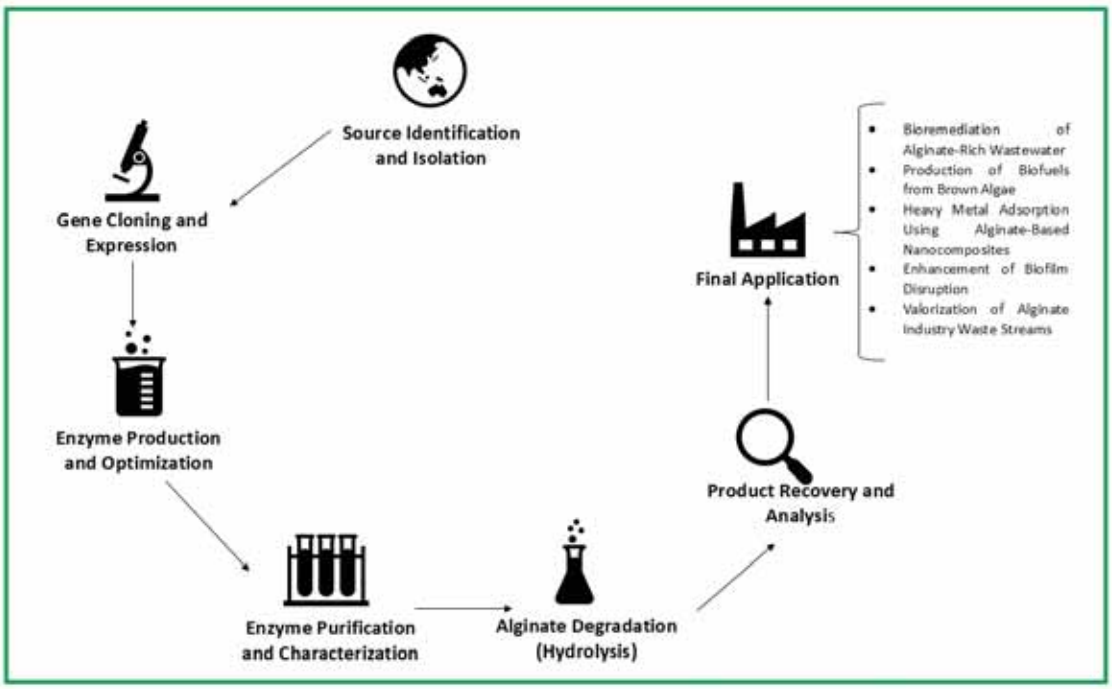

Fig. 3: Production of marine Alys for industrial waste treatment

sustainability. Coupled models can lower energy usage and costs while meeting effluent standards Dai *et al*. (2024). Furthermore, employing of chemical engineering simulation tools supports the modeling and optimization of system configurations, thereby enhancing efficiency (Obiuto *et al.,* 2024). Strains modified through genetic engineering that generate Alys pose biosafety concerns and require risk evaluations under international agreements like the Cartagena Protocol on Biosafety (Liu *et al.,* 2024). Using safe hosts like *Pichia pastoris* can reduce safety issues, but regulatory approval still demands (Wang *et al.,* 2024a). Continuous oversight and adherence to biosafety regulations are crucial for the responsible implementation of genetically modified Aly producers (Zhu *et al.,* 2024).

Oligosaccharide production

Aly can be used for producing AOs. In enzymatic hydrolysis, pure alginate is incubated with Alys under controlled circumstances. Enzymes sever glycosidic linkages between guluronic acid and mannuronic acid residues by β-elimination, resulting in oligosaccharides with varying DP (Wang *et al.,* 2024a; Gu *et al.,* 2024). The AOs produced are generally purified by means of ultrafiltration, ethanol precipitation, or chromatographic procedures (Li *et al.,* 2023e; Yan *et al.,* 2024). Other approaches, including acid hydrolysis and oxidative degradation, are not as selective and might produce undesirable byproducts or decrease bioactivity. AOs are widely studied for their biocompatibility and bioactivity in agriculture, medicine, and the food industry, especially for their antioxidant, antibacterial, and plant growth-promoting properties (Zhang *et al.,* 2023a; Sreya *et al.,* 2024; Akhtar *et al.,* 2024). AOs demonstrate high stability and effectiveness under various storage and formulation conditions AOs are stable and effective in different storage and formulation conditions, indicating strong cryoprotective and preservative effects that helping reduce losses in frozen foods and stabilize proteins (Zhang *et al.,* 2023a; Liu *et al.,* 2024). AOs utilized in agriculture boost fruit quality, inhibit decay, and extend shelf life through their impact on hormone signaling and the degradation of cell walls. They are valuable for storage and processing quality. Isolating AOs with specific effects, like immunomodulatory or antitumor, is challenging due to their complex structure (Li *et al.,* 2021; Wang *et al.,* 2023a; Zhang *et al.,* 2023a). Analytical techniques

including fast protein liquid chromatography (FPLC), thin-layer chromatography (TLC), and electrospray ionization mass spectrometry (ESI-MS) are essential for the separation and identification of AOs with specific DP and monomeric composition, which are critical determinants of their bioactivity (Li *et al.,* 2023e; Wang *et al.,* 2023b). Conducting studies on structure–function relationships necessitates organized investigations and particular assessments; however, the similarity of oligosaccharides introduces complications (Zhang *et al.,* 2023a; Wang *et al.,* 2023b). Alys breaks down alginate from brown algae efficiently and yields bioactive AOs for several industries. It is preferred over chemical methods because it requires milder conditions and results in AOs with specific DP important for their biological activities (Li *et al.,* 2024; Akoulina *et al.,* 2025). Furthermore, AOs may be synthesized using chemical oxidation and physical processes like radiation, alongside enzymatic methods. These methods involve dissolving alginic acid or its salts in water, followed by oxidation under controlled conditions to prevent over-oxidation and ensure a specific degree of polymerization (Bi *et al.,* 2023). Further studies delve into the processes of fermentation and biosynthesis aimed at generating AOs, capable of producing AOs that possess unique structural traits and bioactive properties (Long *et al.,* 2024).

Biodegradable material

Alys play a critical role in producing biodegradable materials by enzymatically breaking down alginate from brown algae into simpler molecules suitable for eco-friendly biopolymer synthesis (Severo *et al*., 2024; Munyiri *et al*., 2025). Through enzymatic breakdown, it is possible to control important material properties such as flexibility, solubility, and degradation rate, thus making alginate-based materials highly appropriate for packaging and biomedical purposes (Aarsen *et al*., 2024). Marine-derived Alys demonstrate high stability under extreme conditions, improving the efficiency and scalability of large-scale biopolymer production (Flemming *et al*., 2023; Weng *et al*., 2023; Metha *et al*., 2024). Increasing worldwide anxiety about plastic pollution necessitates sustainable alternatives; Aly presents biodegradable products. Adjusting temperature and pH enhances enzyme activity and hydrolysis efficiency, while optimizing AOs yield is vital for economic sustainability, influenced by molecular weight and structure (Kaur *et al*., 2024; Noach *et al*., 2024). Challenges include ensuring a steady supply of brown seaweed, managing enzyme logistics, and meeting regulations. Marine Alys contributes to the circular bioeconomy by transforming alginate into bioactive oligosaccharides, which are utilized in hydrogels, bioplastics, and films (Santana *et al*., 2024). These processes lower energy use, eliminate toxic chemicals, and reduce carbon emissions by 60-70%, promoting waste valorization and biodegradability, thus supporting circular economy principles.

Pharmaceutical intermediates

Alys from marine bacteria are valued in pharmaceuticals for degrading alginate into bioactive oligosaccharides (Morparia and Suvarna, 2024; Xie *et al*., 2024). Alys develops unsaturated oligosaccharides that boost solubility and activity, making them appropriate for use as pharmaceutical intermediates (Gao *et al*., 2022; Wawszczak *et al.,* 2024). Low molecular weight, hydrophilic oligosaccharides enhance drug dispersion, uptake, and delivery for antiviral and anticancer agents. They can stabilize antibiotics like neomycin, polymyxin, and framycetin with alginate derivatives (Žigrayová *et al*., 2023; Mohite *et al*., 2023; Osmokrovic *et al*., 2025). The pharmaceutical effectiveness of AOs depends on their structure, like degree of polymerization and M/G ratio. Reducing the degree of polymerization improves solubility and bioavailability, while G-block-rich Oligo G exhibits more effective bacterial interaction and inhibition than M-block-rich Oligo M, which enhances its antimicrobial and anti-biofilm capabilities (Lu *et al*., 2022; Pritchard *et al*., 2023). Targeted production of mannuronic, guluronic, or hybrid AOs forms can yield oligosaccharides with tailored bioactivities. Bioassay-guided fractionation further supports that the bioactivity of AOs, including antioxidant and immunomodulatory functions, depends on their DP and block sequences, with G-block structures exhibiting strong radical scavenging and electrostatic interactions (Li *et al*., 2023; Zhang *et al*., 2023a).

FUTURE PROSPECTS AND DIRECTION

Advances in synthetic biology and metabolic engineering

Integrating synthetic biology with metabolic engineering provides a promising method to boost Alys production, increase yield rates, and minimize

costs for industrial applications (Patel *et al*., 2023; Mirsalami and Mirsalami, 2025). Genetically engineered microbes employing Clustered Regularly Interspaced Short Palindromic Repeats (CRISPR) toolkits, modular design, and rational protein engineering have successfully boosted Alys expression and efficiency (Cao *et al*., 2022; Gao *et al*., 2022; Buller *et al*., 2023; Li *et al*., 2023d). Alys, which have been engineered, additionally generate bioactive oligosaccharides (AOs) that possess capabilities for promoting plant growth and biorefinery applications (Barzkar *et al*., 2022; Wang *et al*., 2024b). Marine-derived Alys operate well in saline conditions, making them suitable for seaweed-based bioprocesses at reduced cost (Zhu *et al*., 2024; Liu *et al*., 2024). In bioenergy, Alys facilitates the conversion of alginate into fermentable sugars for renewable fuel production (Zhuang *et al*., 2024). Approaches in systems biology, such as modular pathway engineering and genome-scale modeling, further refine the expression of microbial Alys (Han *et al*., 2023; Zhou *et al*., 2024b). Enzyme immobilization improves stability and reusability, enhancing economic feasibility (Li *et al*., 2020). Techno-economic modeling and pilot-scale employing using seaweed validate the industrial potential of Alys via solid-state and fed-batch fermentation (Perumal *et al*., 2023; Wang *et al*., 2023b; Zhang *et al*., 2023b).

Emerging applications

The application of Alys is expanding beyond pharmaceuticals and food, with growing relevance in biofuels, agriculture, and bioplastics (Samoraj *et al*., 2024). Alys catalyzes the conversion of alginate-rich seaweed to fermentable sugars for bioethanol, in addition to supporting the production of biodegradable materials. Enzymatic hydrolysis yields AOs with bioactivities—prebiotic, immunomodulatory, anticoagulant, antioxidant, and anticancer—showing potential in functional foods and pharmaceuticals (Akoulina *et al*., 2025; Chavan *et al*., 2023). Alys also aids in the synthesis of trisaccharides for nutritional supplements (Guo *et al*., 2023) and antioxidant-rich food additives (Perumal *et al*., 2023). Immobilization through nanoparticles or biopolymers boosts the ability of enzymes to withstand salt and temperature changes (Jiang *et al*., 2021; Mohapatra, 2022; Kaur *et al*., 2024). The expanding Intellectual Property landscape, including patents on therapeutic (US9220761B2), industrial (US11993795B2), and thermostable Alys (US5139945A), underscores innovation in the field.

Enzyme engineering

Protein engineering, through directed evolution and rational design, enables the development of robust Alys variants for industrial use (Song *et al*., 2023; Li *et al*., 2023a; Zhou *et al*., 2024a; Che *et al*., 2024). The activity and stability of AlyG2 have been improved through rational design (Huang *et al*., 2024), while computational approaches and domain-truncation techniques further boost performance and thermostability (Cui *et al*., 2024; Ye *et al*., 2025). Nonetheless, the ability to scale is restricted due to the intricate nature of enzymes, high costs of development, and expression hurdles including low yield, misfolding, and host toxicity (Meng *et al*., 2021; Guo *et al*., 2024; Sharma and Bhende, 2024). Addressing these challenges is key to realizing efficient and scalable Alys production systems. Various difficulties in AOS study are mapped out, and future directions—particularly on recombinant systems for AOS synthesis—are specified to more expand the range of these amazing oligosaccharides (Vasudevan *et al*., 2021).

CONCLUSION

Presenting remarkable opportunities for enhancing sustainability and efficiency across various industrial sectors, the utilization of marine bacterial Alys constitutes a highly promising advancement in biotechnology. Enzymes obtained from marine bacteria are recognized for their exceptional traits, including substrate specificity, salt tolerance, and thermal stability, permitting them to perform effectively in harsh environmental settings. Alys has elicited significant interest in their contributions to applications ranging from wastewater treatment, biofilm disruption, and sustainable chemical processes to pharmaceuticals and agriculture. Recent developments in the understanding of Alys' enzymatic traits and catalytic functions have notably increased their potential applications. Possessing the ability to hydrolyze interior glycosidic linkages in alginate, marine-derived Alys generate bioactive oligosaccharides (AOs), thereby facilitating novel avenues for their application in functional foods, nutraceuticals, and drug delivery systems. These

AOs have exhibited remarkable bioactivities, encompassing antioxidant, antibacterial, and immunomodulatory effects. A key application of their role, particularly in antibiotic-resistant bacterial biofilms, has been underscored; in particular, Alys has shown effectiveness in boosting antibiotic penetration, consequently improving treatment efficacy for stubborn infections. Moreover, their ability to degrade alginate in wastewater treatment systems has demonstrated potential for enhancing water quality through the reduction of organic pollutants and the augmentation of microbial activity. In addition to their environmentally beneficial enzymatic activity, this reinforces their function in green biotechnologies, wherein Alys contribute to reduced energy consumption and chemical utilization. Furthermore, while Alys research has made considerable strides, there are still challenges to overcome, especially regarding the increasing enzyme production and the improvement of their catalytic efficiency for industrial applications. Challenges that hinder their extensive commercial implementation encompass enzyme stability, yield, and cost-efficiency, among other concerns. However, with the growing emphasis on synthetic biology, protein engineering, and metabolic optimization, significant efforts are underway to overcome these challenges. Currently, genetic modification—encompassing the use of CRISPR technology and enzyme immobilization techniques—has led to improvements in enzyme activity, stability, and production efficiency, thereby making large-scale applications more feasible. Moreover, employing cutting-edge techniques like directed evolution and systems biology elevates Alys' capabilities, resulting in greater operational efficiency in numerous industrial contexts. The increasing demand for eco-friendly and sustainable solutions has driven the evolution of Alys as a crucial component of the circular bioeconomy. Marine-derived Alys play a crucial role in transforming alginate, a significant byproduct of the seaweed industry, into bioactive oligosaccharides that have applications in pharmaceuticals, biodegradable substances, and biofuels. A significant development in decreasing plastic waste and fostering sustainability in packaging and biomedical uses is their capability to generate biopolymers, which, including biodegradable films and hydrogels. Moreover, underscoring the significance of these enzymes in advancing green energy technology is exemplified by the ascendant utilization of alginate-rich biomass biofuels generated through Alys. Anticipating future trends, the relentless evolution of Alys—especially through genetic and enzymatic engineering—reveals considerable promise for broadening their applications within the biotechnology sector. Further exploration of the diverse microbial sources of Alys is essential to identify novel enzymatic pathways that could lead to the development of more efficient and versatile enzymes. The attainment of their full potential is also contingent upon the enhancement of Alys's industrial manufacturing capabilities. Future research ought to focus on the integration of Alys into more intricate bioprocesses, such as those utilizing marine biomass waste, to facilitate the creation of more cost-effective and sustainable production systems. The merging of Alys with extra biotechnological approaches, including membrane filtration systems, can boost wastewater treatment processes, producing more effective and sustainable water management solutions. In conclusion, Alys derived from marine bacteria represents a significant and versatile category of enzymes poised to tackle some of the most critical challenges in biotechnology, such as environmental conservation, waste remediation, and sustainability. By providing sustainable alternatives to standard practices, their roles in wastewater treatment, biofilm eradication, and sustainable chemistry are consistently increasing. While challenges persist regarding large-scale production and optimization, current research and development of Alys are poised to reveal new opportunities, thereby promoting both industrial applications and environmental sustainability in the future.

AUTHOR CONTRIBUTIONS

M.U.K. Anjung was responsible for conceptualizing the draft, searching the bibliography, selecting the relevant references, coding the references, writing the initial manuscript draft, synthesizing the manuscript, and revising the final manuscript version. H. Nursyam was responsible for reviewing the whole manuscript and validating it. A.A. Prihanto was responsible for conceptualizing the draft, writing the initial manuscript draft, revising the final manuscript version, the project administration and resources. E. Chasanah was responsible for reviewing the whole

manuscript, supervising the research, and responsible for the funding acquisition.

ACKNOWLEDGEMENT

The authors thank to the Center for Marine Fisheries Education, the Marine and Fisheries Extension and Human Resources Development Agency, the Indonesian Ministry of Marine Affairs and Fisheries for providing financial support [No. 218/SJ/KP.532/XI/2021].

CONFLICT OF INTEREST

The authors declare no potential conflict of interest regarding the publication of this work. In addition, the ethical issues including plagiarism, informed consent, misconduct, data fabrication and, or falsification, double publication and, or submission, and redundancy have been completely witnessed by the authors.

OPEN ACCESS

©2025 The author(s). This article is licensed under a Creative Commons Attribution 4.0 International License, which permits use, sharing, adaptation, distribution and reproduction in any medium or format, as long as you give appropriate credit to the original author(s) and the source, provide a link to the Creative Commons license, and indicate if changes were made. The images or other third-party material in this article are included in the article's Creative Commons license, unless indicated otherwise in a credit line to the material. If material is not included in the article's Creative Commons license and your intended use is not permitted by statutory regulation or exceeds the permitted use, you will need to obtain permission directly from the copyright holder. To view a copy of this license, visit:

http://creativecommons.org/licenses/by/4.0/

PUBLISHER'S NOTE

GJESM Publisher remains neutral with regard to jurisdictional claims with regard to published maps and institutional affiliations.

☒ **Positive AI Statement**

During the preparation of this work the author(s) have used Artificial Intelligence (AI) ChatGPT in order to solely to check the grammar and clarity of the manuscript. After using this tool/service, the authors reviewed and edited the content as needed and take full responsibility for the content of the publication.

(For this reason, the GPTZero detector will evaluate the manuscript utilizing Generative AI, ensuring a high detection rate. If the manuscript relies heavily on Generative AI and AI-assisted technologies, it will be archived without further options for appeal).

☐ **Negative AI Statement**

The author(s) declare that no AI tools or services were not used or not highly applied during the preparation of this work.

ABBREVIATIONS

%	Percent
^{O}C	Degree Celsius
β-elimination	beta-elimination
Alg	Name Alginate lyase from Polysaccharide Lyase family
AO	Alginate oligosaccharides
Alg	Name Alginate lyase from PL
Aly	Alginate lyase
BOD	Biochemical oxygen demand
C	Carboxyl group
Ca^{2+}	Calcium Ion
CAZy	Carbohydrate-Active Enzymes (CAZymes)
CF	Cystic fibrosis
CRISPR	Clustered Regularly Interspaced Short Palindromic Repeats
COD	chemical oxygen demand
DEH	4-deoxy-L-erythro-hex-4-enopyranosyluronic acid
DNase	Deoxyribonuclease
DP	Degrees of polymerization
EC	Enzyme Commission
ESI-MS	Electrospray Ionization Mass Spectrometry
EU	European Union's
FAO	The Food Agriculture Organization
FPLC	Fast Protein Liquid Chromatography
G	α-L-guluronic acid

G-block	Poly Guluronate
H_2O	Dihydrogen monoxide
IUBMB	International Union of Biochemistry and Molecular Biology
M	β-D-mannuronic acid
M-block	poly Mannuronate
NaCl	Sodium Chloride
pH	Potential of hydrogen
PTMs	Post-translasional modifications
TLC	Thin-Layer Chromatography
U/mg	Units per milligram

REFERENCES

Aarsen, C.V.; Liguori, A.; Mattsson, R.; Sipponen, M.H.; Hakkarainen, M., (2024). Designed to degrade: tailoring polyesters for circularity. Chem. Rev., 124(13): 8473-8515 **(43 pages).**

Abdelfattah, A.; Ramadan, H.; Elsamahy, T.; Eltawab, R.; Mostafa, S.; Zhou, X.; Cheng, L., (2023). Multifaced features and sustainability of using pure oxygen in biological wastewater treatment: a review. J. Water Process Eng., 75(2023): 103883 **(14 pages).**

Akhtar, H.; Usman, M.; Binyamin, R.; Hameed, A.; Arshad, S.F.; Aslam, H.M.U.; Shahid, M.S., (2024). Traditional strategies and cutting-edge technologies used for plant disease management: a comprehensive overview. Agronomy, 14(9): 2175 **(37 pages).**

Akoulina, E.A.; Bonartseva, G.A.; Dudun, A.A.; Kochevalina, M.Y.; Bonartsev, A.P.; Voinova, V.V., (2025). Current state of research on the mechanisms of biological activity of alginates. Biochemistry, 90: S263–S286 **(24 pages).**

Aksoy, N.; Vatansever, C.; Adalı, C.; Adaklı Aksoy, B.; Fışgın, T., (2023). The inhibitory effects of amylase and streptokinase on minimum inhibitory concentration of antibiotics used to treat gram negative bacteria biofilm infection on indwelling devices. Indian J. Microbiol., 63(4): 533–540 **(8 pages).**

Al-Madboly, L.A.; Aboulmagd, A.; El-Salam, M.A.; Kushkevych, I.; El-Morsi, R.M., (2024). Microbial enzymes as powerful natural anti-biofilm candidates. Microb. Cell Fact., 23(1): 343 **(16 pages).**

Augusto, A.; Lemos, M.F.L.; Silva, S.F.J., (2024). Exploring marine-based food production: the challenges for a sustainable and fast biotechnology-based development. Appl. Sci., 14(18): 8255 **(12 pages).**

Balmonte, J.P.; Giebel, H.; Arnosti, C.; Simon, M.; Wietz, M., (2024). Distinct bacterial succession and functional response to alginate in the South, Equatorial, and North Pacific Ocean. Environ. Microbiol., 26(3) **(14 pages).**

Bao, K.; Yang, M.; Sun, Q.; Zhang, K.; Huang, H., (2024). Genome analysis of a potential novel vibrio species secreting pH and thermo-stable alginate lyase and its application in producing alginate oligosaccharides. Mar. Drugs., 22(9): 414 **(22 pages).**

Barbeyron, T.; Le Duff, N.; Duchaud, E.; Thomas, F., (2023). *Zobellia alginoliquefaciens* sp. nov.: a new flavobacteria isolated from the epibiota of the brown alga *Ericaria zosteroides* (C. agardh) Molinari and Guiry 2020. Int. J. Sist. Evol. Microbiol., 73(6) **(4 pages).**

Barzkar, N.; Sheng, R.; Sohail, M.; Jahromi, S.T.; Babich, O.; Sukhikh, S.; Nahavandi, R., (2022). Alginate lyases from marine bacteria: An enzyme ocean for sustainable future. Molecules., 27(11): 3375 **(27 pages)**.

Bi, D.; Yang, X.; Lu, J.; Xu, X., (2023). Preparation and potential applications of alginate oligosaccharides. Crit. Rev. Food Sci. Nutr., 63(29): 10130–10147 **(18 pages).**

Bi, A.Z.; Umesh, K.B.; Md Abdul, B.; Sivakumar, D.; Srikanth, P., (2024). Economic and environmental sustainability of agriculture production at the crop level. Global J. Environ. Sci. Manage., 10(3): 1433-1456 **(14 pages).**

Blanco-Cabra, N.; Paetzold, B.; Ferrar, T.; Mazzolini, R.; Torrents, E.; Serrano, L.; LLuch-Senar, M., (2020). Characterization of different alginate lyases for dissolving Pseudomonas aeruginosa biofilms. Sci. Rep., 10(1): 9390 (10 pages).

Breslawec, A.P.; Wang, S.; Monahan, K.N.; Barry, L.L.; Poulin, M.B., (2023). The endoglycosidase activity of dispersin B is mediated through electrostatic interactions with cationic poly-β-(1→6)-N-acetylglucosamine. The FEBS J., 290(4): 1049–1059 **(11 pages).**

Buller, R.; Lutz, S.; Kazlauskas, R.J.; Snajdrova, R.; Moore, J.C.; Bornscheuer, U.T., (2023). From nature to industry: harnessing enzymes for biocatalysis. Sci., 382:(6673) **(11 pages).**

Cao, S.; Li, Q.; Xu, Y.; Tang, T.; Ning, L.; Zhu, B., (2022). Evolving strategies for marine enzyme engineering: recent advances on the molecular modification of alginate lyase. Mar. Life Sci. Technol., 1-11 **(11 pages).**

Chavan, A.R.; Singh, A.K.; Gupta, R.K.; Nakhate, S.P.; Poddar, B.J.; Gujar, V.V.; Khardenavis, A.A., (2023). Recent trends in the biotechnology of functional non-digestible oligosaccharides with prebiotic potential. Biotechnol. Genet. Eng. Rev., 39(2): 465–510 **(45 pages).**

Che, Y.; Feng, Z.; He, D.; Cao, F.; Chen, X.; Huang, A.; Xie, Z., (2024). Microhabitat-differentiated distribution of culturable and antagonistic bacteria in marine ecosystem: seawater as the original microbial provider. Ocean Coastal Manage, 256: 107304 (**18 pages**).

Chen, C.; Cao, S.; Zhu, B.; Jiang, L.; Yao, Z., (2023). Biochemical characterization and elucidation the degradation pattern of a new cold-adapted and Ca^{2+}-activated alginate lyase for efficient preparation of alginate oligosaccharides. Enzyme Microb. Technol., 162: 110146 (**10 pages**).

Chen, C.; Li, X.; Lu, C.; Zhou, X.; Chen, L.; Qiu, C.; Jin, Z.; Long, J., (2024a). Advances in alginate lyases and the potential application of enzymatic prepared alginate oligosaccharides: a mini review. Int. J. Biol. Macromol., 260: 129506 (**18 pages**).

Chen, C.; Li, X.; Lu, C.; Zhou, X.; Chen, L.; Qiu, C.; Long, J., (2024b). Significantly improving the thermal stability of alginate lyase AlyC3 from *Psychromonas* sp. C-3 by computational redesign. Food Biosci., 59: 103973 (**12 pages**).

Cheng, C.; Chen, L.; Zhang, D.; Yu, J.; Zhu, M.; Li, C.; Li, S., (2024). Value-added utilization of hemoglobin and its hydrolysis products from livestock and poultry blood processing by-products: a review. Trends Food Sci Technol., 104645 (**13 pages**).

Chu, Y.J.; Kim, H.S.; Kim, M.S.; Lee, E.Y.; Kim, H.S., (2020). Functional characterization of a novel oligoalginate lyase of Stenotrophomonas maltophilia KJ-2 using site-specific mutation reveals bifunctional mode of action, possessing both endolytic and exolytic degradation activity toward alginate in seaweed biomass. Front. Mar. Sci., 7: 420 (**11 pages**).

Couto, P.M.; Guardia, C.M.; Couto, F.L.; Labriola, C.A.; Labanda, M.S.; Caramelo, J.J., (2024). Acceptors stability modulates the efficiency of post-translational protein N-glycosylation. FASEB J., 38(13): e23782 (**21 pages**).

Crona, B.I.; Wassénius, E.; Jonell, M.; Koehn, J.Z.; Short, R.; Tigchelaar, M.; Wabnitz, C.C., (2023). Four ways blue foods can help achieve food system ambitions across nations. Nature., 616(7955): 104–112

(**25 pages**).

Cui, Y.; Yang, M.; Liu, N.; Wang, S.; Sun, Y.; Sun, G.; Zhou, D., (2024). Computer-aided rational design strategy to improve the thermal stability of alginate lyase AlyMc. J. Agric. Food Chem., 72(6): 3055-3065 (**10 pages**).

Dai, W.; Pang, J.W.; Zhao, Y.J.; Ding, J.; Sun, H.J.; Cui, H.; Mi, H.R.; Zhao, Y.; Zhang, L.Y.; Ren, N.; Yang, S., (2024). Machine learning assisted combined systems of wastewater treatment plants with constructed wetlands optimal decision-making. Bioresour. Technol., 130643 **(12 pages)**.

Dharani, S.R.; Srinivasan, R.; Sarath, R.; Ramya, M., (2020). Recent progress on engineering microbial alginate lyases towards their versatile role in biotechnological applications. Folia Microbiol., 65(6): 937–954 **(18 pages).**

Dobruchowska, J.M.; Bjornsdottir, B.; Fridjonsson, O.H.; Altenbuchner, J.; Watzlawick, H.; Gerwig, G.J.; Hreggvidsson, G.O., (2022). Enzymatic depolymerization of alginate by two novel thermostable alginate lyases from *Rhodothermus marinus*. Front. Plant Sci., 13: 981602 **(18 pages).**

Flemming, H.C.; van Hullebusch, E.D.; Neu, T.R.; Nielsen, P.H.; Seviour, T.; Stoodley, P.; Wuertz, S., (2023). The biofilm matrix: multitasking in a shared space. Nat. Rev. Microbiol., 21(2): 70-86 **(16 pages).**

Flores-Contreras, E.A.; Araújo, R.G.; Rodríguez-Aguayo, A.A.; Guzmán-Román, M.; García-Venegas, J.C.; Nájera-Martínez, E.F.; Parra-Saldivar, R., (2023). Polysaccharides from the Sargassum and brown algae genus: extraction, purification, and their potential therapeutic applications. Plants., 12(13): 2445 **(26 pages).**

Gaceu, L.; Gruia, R.; Oprea, O.B., (2023). Use of marine biomass resources as raw material in bakery. J. Eco. Agri. Tourism., 19(1) **(6 pages).**

Gao, J.; Xu, J.; Zuo, Y.; Ye, C.; Jiang, L.; Feng, L.; Lian, J., (2022). Synthetic biology toolkit for marker-less integration of multigene pathways into Pichia pastoris via CRISPR/Cas9. ACS Synth. Biol., 11(2): 623–633 **(12 pages).**

Gholami-Shabani, M.; Shams-Ghahfarokhi, M.; Razzaghi-Abyaneh, M., (2023). food microbiology: application of microorganisms in food industry. In Arshad, M.S.; Khalid W., (Eds), Health Risks of Food Additives – Recent Developments and Trends in Food Sector. (pp. 1-27). IntechOpen. London **(27 pages)**.

Gu, X.; Fu, L.; Wang, Z.; Cao, Z.; Zhao, L.; Seswita-Zilda, D.; Li, J., (2024). A novel bifunctional alginate lyase and antioxidant activity of the enzymatic hydrolysates. J. Agric. Food Chem., 72(8): 4116-4126 **(8 pages)**.

Guo, Q.; Dan, M.; Zheng, Y.; Shen, J.; Zhao, G.; Wang, D., (2023). Improving the thermostability of a novel PL-6 family alginate lyase by rational design engineering for industrial preparation of alginate oligosaccharides. Int. J. Biol. Macromol., 249: 125998 **(15 pages).**

Guo, Q.; Dan, M.; Zheng, Y.; Zhao, G.; Wang, D., (2024). Construction and characterization of a novel fusion alginate lyase with endolytic and exolytic cleavage activity for industrial preparation of alginate oligosaccharides. Food Chem., 453: 139695 **(12 pages)**.

Han, T.; Nazarbekov, A.; Zou, X.; Lee, S.Y., (2023). Recent advances in systems metabolic engineering. Curr. Opin. Biotechnol., 84: 103004 **(8 pages).**

Hu, Z.Y.; Lin, Y.P.; Wang, Q.T.; Zhang, Y.X.; Tang, J.; Hong, S.D.; Zhang, F., (2023). Identification and degradation of structural extracellular polymeric substances in waste activated sludge via a polygalacturonate-degrading consortium. Water Res., 233: 119800 **(10 pages).**

Huang, J.P.; Zhao, J.X.; Zhang, M.J.; Han, J.; Han, Y.T.; Wang, X.T.; Zhou, Y.X., (2025). Rational design of alginate lyase ALYI1 for improving the antioxidant activity of the alginate oligosaccharides. Food Chem., 143075 **(10 pages).**

Irianto, I.; Naryaningsih, A.; Trisnawati, N.W.; Astuti, A.; Komariyah, K.; Qomariyah, L., (2024). From sea to solution: a review of green extraction approaches for unlocking the potential of brown algae. South Afr. J. Chem. Eng., 48(1): 1-21 **(21 pages).**

Jiang, Z.; Zhang, X.; Wu, L.; Li, H.; Chen, Y.; Li, L.; Zhu, Y., (2021). Exolytic products of alginate by the immobilized alginate lyase confer antioxidant and antiapoptotic bioactivities in human umbilical vein endothelial cells. Carbohydr. Polym., 251: 116976 (**8 pages)**.

Kanwar, K.; Sharma, D.; Singh, H.; Pal, M.; Bandhu, R.; Azmi, W., (2024). In vitro effects of alginate lyase SG4+ produced by *Paenibacillus lautus* alone and combined with antibiotics on biofilm formation by mucoid *Pseudomonas aeruginosa*. Braz. J. Microbiol., 55(2), 1189–1203 **(15 pages).**

Kaur, S.; Abraham, R.E.; Franco, C.M.M.; Puri, M., (2024). Production of alginate oligosaccharides (AOSs) using enhanced physicochemical properties of immobilized alginate lyase for industrial application. Mar. Drugs **(14 pages).**

Khan, M.F., (2025). Recent advances in microbial enzyme applications for sustainable textile processing and waste management. Sci., 7(2): 46 **(12 pages)**.

Khiari, Z., (2024). Enzymes from fishery and aquaculture waste: research trends in the era of artificial intelligence and circular bio-economy. Mar. Drugs., 22(9): 411 **(10 pages).**

Li, C.; Tang, T.; Du, Y.; Jiang, L.; Yao, Z.; Ning, L.; Zhu, B., (2023a). Ulvan and ulva oligosaccharides: a systematic review of structure, preparation, biological activities and applications. Bioresour. Bioprocess., 10(1): 66 **(17 pages)**.

Li, J.; Pei, X.; Xue, C.; Chang, Y.; Shen, J.; Zhang, Y., (2023b). A repertoire of alginate lyases in the alginate polysaccharide utilization loci of marine bacterium Wenyingzhuangia fucanilytica: biochemical properties and action pattern. J. Sci. Food Agric., 104(1): 134–140 **(29 pages).**

Li, J.; Xue, C.; Shen, J.; Liu, G.; Mei, X.; Sun, M.; Chang, Y., (2023c). Action pattern of a novel G-specific alginate lyase: determination of subsite specificity by HPAEC–PAD/MS. J. Agric. Food Chem., 72(2): 1170-1177 **(8 pages).**

Li, J.; Yan, F.; Huang, B.; Zhang, M.; Wu, X.; Liu, Y.; Zheng, H., (2024a). Preparation, structural characterization, and enzymatic properties of alginate lyase immobilized on magnetic chitosan microspheres. Appl. Biochem. Biotechnol., 196(8): 5403-5418 **(16 pages).**

Li, L.; Cao, S.; Zhu, B.; Yao, Z.; Zhu, B.; Qin, Y.; Jiang, J., (2023d). Efficient degradation of alginate and preparation of alginate oligosaccharides by a novel biofunctional alginate lyase with high activity and excellent thermophilic features. Mar. Drugs, 21(3): 180 **(14 pages).**

Li, L.; Zhu, B.; Yao, Z.; Jiang, J., (2023e). Directed preparation, structure–activity relationship and applications of alginate oligosaccharides with specific structures: A systematic review. Food Res. Int., 170: 112990 **(12 pages).**

Li, Q.; Hu, F.; Wang, M.; Zhu, B.; Ni, F.; Yao, Z., (2020). Elucidation of degradation pattern and immobilization of a novel alginate lyase for preparation of alginate oligosaccharides. Int. J. Biol. Macromol., 146: 579-587 (**9 pages**).

Li, Q.; Zheng, L.; Guo, Z.; Tang, T.; Zhu, B., (2021). Alginate degrading enzymes: an updated comprehensive review of the structure, catalytic mechanism, modification method and applications of alginate lyases. Crit. Rev. Biotechnol., 41(6): 953–968 **(10 pages).**

Lin, Q.; Sheng, M.; Tian, Y.; Li, B.; Kang, Z.; Yang, Y.; Tan, Y., (2024). Antibiofilm activity and synergistic effects of DNase I and lysostaphin against *Staphylococcus aureus* biofilms. Food Qual. Saf., 8: 024 **(12 pages).**

Liu, C.; Gao, J.; Jiang, H.; Sun, J.; Gao, X.; Mao, X., (2024). Value-added

utilization technologies for seaweed processing waste in a circular economy: developing a sustainable modern seaweed industry. Compr. Rev. Food Sci. Food Saf., 23(6): e70027 **(17 pages).**

Long, J.; Ye, Z.; Li, X.; Tian, Y.; Bai, Y.; Chen, L.; Svensson, B., (2024). Enzymatic preparation and potential applications of agar oligosaccharides: a review. Crit. Rev. Food Sci. Nutr., 64(17): 5818-5834 **(17 pages).**

Long, L.; Hu, Q.; Wang, X.; Li, H.; Li, Z.; Jiang, Z.; Zhu, Y., (2022). A bifunctional exolytic alginate lyase from Microbulbifer sp. ALW1 with salt activation and calcium-dependent catalysis. Enzyme Microb. Technol., 161: 110109 **(10 pages)**.

Lu, S.; Na, K.; Wei, J.; Zhang, L.; Guo, X., (2022). Alginate oligosaccharides: The structure-function relationships and the directional preparation for application. Carbohydr. Polym., 284: 119225 **(18 pages).**

Luo, X.; Wu, Y.; Wang, S.; Xiong, Z.; Du, X.; Zheng, M.; Chen, Z., (2024). Frontier review of key reduction technologies and resource utilization of waste during the seaweed gel production process. Blue Biotechnol., 1(1): 12 **(14 pages).**

Meng, Q.; Tian, X.; Jiang, B.; Zhou, L.; Chen, J.; Zhang, T., (2021). Characterization and enhanced extracellular overexpression of a new salt-activated alginate lyase. J. Sci. Food Agric., 101(12): 5154-5162 **(9 pages).**

Metha, C.; Pawar, S.; Suvarna, V., (2024). Recent advancements in alginate-based films for active food packaging applications. Sustain. Food Technol., 2(5): 1246-1265 **(20 pages).**

Mirsalami, S.M.; Mirsalami, M., (2025). Advances in genetically engineered microorganisms: transforming food production through precision fermentation and synthetic biology. Future Foods., 11: 100601 **(12 pages).**

Mohapatra, B. R., (2022). Fermentation medium optimization, molecular modelling and docking analysis of the alginate lyase of a novel *Pseudomonas* sp. LB56 isolated from seaweed waste. Biotechnol. Biotechnol. Equip., 36(1): 281–291 **(12 pages).**

Mohite, P.; Shah, S.R.; Singh, S.; Rajput, T.; Munde, S.; Ade, N.; Dudhrejiya, A.V., (2023). Chitosan and chito-oligosaccharide: a versatile biopolymer with endless grafting possibilities for multifarious applications. Front. Bioeng. Biotechnol., 11: 1190879 **(24 pages)**.

Morley, C.; Yau, H.C.; Houppy, W.; Singh, W.; Lant, N.J.; Black, G.W.; Munoz-Munoz, J., (2025). Structure/activity relationships of two alginate lyases from *Flavobacterium* spp. and their potential application in detergents. Int. J. Biol. Macromol., 143524 **(11 pages)**.

Morparia, S.; Suvarna, V., (2024). Recent advancements in applications of alginates in drug delivery, tissue engineering, and biomedical fields. Nat. Prod. J., 14(9): 83-100 **(17 pages).**

Munialo, C.D.; Mellor, D.D., (2024). A review of the impact of social disruptions on food security and food choice. Food Sci. Nutr., 12(1): 13-23 (**11 pages)**.

Munyiri, C.N.; Madivoli, E.S.; Kisato, J.; Gichuki, J.; Kareru, P.G., (2025). Biopolymer-based hydrogels: crosslinking strategies and their applications. Int. J. Polymeric Mater. Polymeric Biomater., 74(7): 625-640 **(15 pages).**

Nah, H.S.; Kim, D.H.; Lee, H.Y.; Yoo, H.J.; Park, M.S.; Woo, K.E.; Ahn, D.H., (2023). Palatability-enhancing effect of the alcohol precipitate of *Sargassum confusum* C. Agardh extracts using an alginate-degrading crude enzyme. Korean J. Fish. Aquat. Sci., 56(2): 204-211 **(8 pages)**.

Naseem, S.; Imam, A.; Rayadurga, A.S.; Ray, A.; Suman, S.K., (2024). Trends in fisheries waste utilization: a valuable resource of nutrients and valorized products for the food industry. Crit. Rev. Food Sci. Nutr., 64(25): 9240-9260 **(21 pages).**

Noach, M.N.; Mampana, R.L.; van Rensburg, E.; Goosen, N.J.; Pott, R.W.M., (2024). Chemical and enzymatic hydrolysis of alginate: a review. Bot. Mar **(10 pages)**.

Obiuto, N.C.; Olu-lawal, K.A.; Ani, E.C., Ugwuanyi, E. D.; Ninduwezuor-Ehiobu, N., (2024). Chemical engineering and the circular water economy: Simulations for sustainable water management in environmental systems. World J. Adv. Res. Rev., 21(3): 001-009 **(9 pages)**.

Osmokrovic, A.; Stojkovska, J.; Krunic, T.; Petrovic, P.; Lazic, V.; Zvicer, J., (2025). Current state and advances in antimicrobial strategies for burn wound dressings: From metal-based antimicrobials and natural bioactive agents to future perspectives. Int. J. Mol. Sci., 26(9): 4381 **(25 pages).**

Patel, A.K.; Dong, C.D.; Chen, C.W.; Pandey, A.; Singhania, R.R., (2023). Production, purification, and application of microbial enzymes. In Biotechnology of Microbial Enzymes. Academic Press **(32 pages).**

Pedraza-Segura, L.; Esparza, K.M.R.; Pedroza-Islas, R., (2023). Microbial bioresource for the production of marine enzymes. In Microbial Bioreactors for Industrial Molecules (pp. 17-37). Springer **(17 pages).**

Peng, C.; Wang, Q.; Xu, W.; Wang, X.; Zheng, Q.; Liang, X.; Peng, L., (2024). A bifunctional endolytic alginate lyase with two different lyase catalytic domains from *Vibrio* sp. H204. Front. Microbiol., 15: 1509599 **(14 pages).**

Perumal, P.K.; Dong, C.D.; Chauhan, A.S.; Anisha, G.S.; Kadri, M.S.; Chen, C.W.; Patel, A.K., (2023). Advances in oligosaccharides production from algal sources and potential applications. Biotechnol. Adv., 67: 108195 **(23 pages).**

Pritchard, M.F., Powell, L.C., Adams, J.Y., Menzies, G., Khan, S., Tøndervik, A., Buurma, N. J.; Sletta, H.; Aarstad, O.; Skjåk-Bræk, G.; McKenna, S.; Farnell, D.J.J.; Rye, P.D.; Hill, K.E.; Thomas, D.W. (2023). Structure‐activity relationships of low molecular weight alginate oligosaccharide therapy against *Pseudomonas aeruginosa*. Biomolecules, 13(9): 1366 **(17 pages)**.

Radoor, S.; Karayil, J.; Jayakumar, A.; Kandel, D.R.; Kim, J.T.; Siengchin, S.; Lee, J., (2024). Recent advances in cellulose- and alginate-based hydrogels for water and wastewater treatment: a review. Carbohydr. Polym., 323: 121339 **(24 pages).**

Rahmati, F.; Sethi, D.; Shu, W.; Lajayer, B.A.; Mosaferi, M.; Thomson, A.; Price, G.W., (2024). Advances in microbial exoenzymes bioengineering for improvement of bioplastics degradation. Chemosphere., 355: 141749 **(19 pages)**.

Ramesh, M.; Balaji, D.; Rajeshkumar, L.; Sivalingam, S., (2023). Aerogels of sodium alginate and their behavior toward wastewater treatment. In Sodium Alginate-Based Nanomaterials for Wastewater Treatment. Elsevier **(14 pages).**

Ramya, P.; Ezhilarasi, P.; Aanandhalakshmi, R.; Ferdhous, P.B.; Vanavil, B., (2025). Oligosaccharides as nutraceuticals. In The Nature of Nutraceuticals (pp. 335-364). Apple Academic Press. **(30 pages)**.

Rehman, Z.U.; Ghaani, M.; Mohamed, A.Y.; Gallagher, J.; Saikaly, P.E.; Ali, M., (2024). Alginate-like exopolysaccharides extracted from different waste sludges exhibit varying physicochemical and material properties. Front. Microbiol., 15: 1493782 **(12 pages)**.

Rotter, A.; Giannakourou, A.; Argente García, J.E.; Quero, G.M.; Auregan, C.; Triantaphyllidis, G.; Chiavetta, C., (2023). Identification of marine biotechnology value chains with high potential in the northern Mediterranean region. Mar. Drugs, 21(7): 416 **(26 pages).**

Saini, S.; Tewari, S.; Dwivedi, J.; Sharma, V., (2023). BiofilpolyMediated wastewater treatment: a comprehensive review. Mater. Adv., 4(6): 1415-1443 **(29 pages).**

Samoraj, M.; Çalış, D.; Trzaska, K.; Mironiuk, M.; Chojnacka, K., (2024). Advancements in algal biorefineries for sustainable agriculture: biofuels, high-value products, and environmental solutions. Biocatal. Agric. Biotechnol., 58: 103224 **(24 pages).**

Sanjeewa, K.A.; Herath, K.H.I.N.M.; Kim, Y.S.; Jeon, Y.J.; Kim, S.K., (2023).

Enzyme-assisted extraction of bioactive compounds from seaweeds and microalgae. TrAC Trends Anal. Chem., 167: 117266 **(8 pages).**

Santana, I.; Felix, M.; Bengoechea, C., (2024). Seaweed as basis of eco-sustainable plastic materials: focus on alginate. Polymers, 16(12): 1662 **(18 pages).**

Sarkar, M.S.I.; Hasan, M.M.; Hossain, M.S.; Khan, M.; Al Islam, A.; Paul, S.K.; Kamal, M., (2023). Exploring fish in a new way: a review on non-food industrial applications of fish. Heliyon, 9: e22673 **(17 pages).**

Senadheera, T.R.L.; Hossain, A.; Shahidi, F., (2023). Marine bioactives and their application in the food industry: a review. Appl. Sci., 13: 12088 **(29 pages).**

Severo, I.A.; Mariano, A.B.; Vargas, J.V.C.; Surguchov, A., (2024). Alginate: Applications and Future Perspectives. BoD–Books on Demand **(146 pages).**

Shankar, A.; Ali, A.; Abdullah, H.M.; Balaji, J.; Kaur, J.; Saeed, F.; Islam, F., (2024). Nutritional composition, phytochemical profile, therapeutic potentials, and food applications of rosemary: a comprehensive review. J. Food Compos. Anal., 106688 **(12 pages).**

Sharma, S.; Bhende, M., (2024). An overview: non-toxic and eco-friendly polysaccharides-its classification, properties, and diverse applications. Polym. Bull., 81(14): 12383-12429 **(47 pages).**

Singh, D.; Satpute, S.K.; Ranga, P.; Saharan, B.S.; Tripathi, N.M.; Aseri, G.K.; Joshi, S., (2023). Biofouling in membrane bioreactors: mechanism, interactions and possible mitigation using biosurfactants. Appl. Biochem. Biotechnol., 195(3): 2114-2133 **(20 pages).**

Sun, R.; Yan, Q.; Deng, W.; Chen, P.; Wu, D.; Zheng, P., (2025). N-glycosylation-modifications-driven conformational dynamics attenuate substrate inhibition of d-lactonohydrolase. Bioorg. Chem., 155: 108122 **(11 pages).**

Sun, X.H.; Zhang, X.D.; Zhang, X.R.; Wang, X.F.; Zhang, X.Y.; Zhang, Y.Z.; Xu, F., (2024). Direct preparation of alginate oligosaccharides from brown algae by an algae-decomposing alginate lyase AlyP18 from the marine bacterium *Pseudoalteromonas agarivorans* A3. Mar. Drugs., 22(11): 483 **(14 pages).**

Sun, X.M.; Xue, Z.; Sun, M.L.; Zhang, Y.; Zhang, Y.Z.; Fu, H.H.; Wang, P., (2022). Characterization of a novel alginate lyase with two alginate lyase domains from the marine bacterium Vibrio sp. C42. Mar. Drugs., 20(12): 746 (13 pages).

Song, Z.; Zhang, Q.; Wu, W.J.; Pu, Z.J.; Yu, H., (2023). Rational design of enzyme activity and enantioselectivity. Front. Bioeng. Biotechnol., 11: 1129149 **(9 pages)**.

Sreya, E.S.; Kumar, D.P.; Balakrishnan, P.; Gopi, S., (2024). Science and technology of alginates: A review. Handbook of Biomass., 1229-1255 **(26 pages)**.

Tang, X., Jiao, C., Wei, Y., Zhuang, X. Y., Xiao, Q., Chen, J., Chen, F.; Yang, Q.; Weng, H.; Fang, B.; Zhang, Y.; Xiao, A. F. (2022). Biochemical characterization and cold-adaption mechanism of a PL-17 family alginate lyase Aly23 from marine bacterium *Pseudoalteromonas* sp. ASY5 and its application for oligosaccharides production. Mar. Drugs., 20(2): 126 **(17 pages)**.

Tang, Y.; Song, Z.; Xu, X.; Li, Y.; Wang, L., (2025). Insights into the mechanism of substrate specificity in a novel PL15_3 subfamily oligo-alginate lyase VBAly15A. Appl. Environ. Microbiol., 91(3): e02351-24 **(17 pages)**.

Tao, X.; Zou, K.; Yuan, M.; Wen, Y.; Liu, B.; Qing, T.; Zhang, P., (2024). Beyond denitrification: Alginate production by mucoid *Pseudomonas aeruginosa* using wastewater nitrate as electron acceptor. J. Environ. Chem. Eng., 12(5): 113679 **(9 pages).**

Vasudevan, U.M.; Lee, O.K.; Lee, E.Y., (2021). Alginate derived functional oligosaccharides: Recent developments, barriers, and future outlooks. Carbohydr. Polym, 267: 118158 **(18 pages)**.

Vera-Villalobos, H.; Riquelme, C.; Silva-Aciares, F., (2023). Use of Alteromonas sp. Ni1-LEM supernatant as a cleaning agent for reverse-osmosis membranes (ROMs) from a desalination plant in northern Chile affected by biofouling. Membranes, 13(5): 454 **(12 pages).**

Wang, H.; Wen, J.; Ablimit, N.; Deng, K.; Wang, W.; Jiang, W., (2024). Degradation of natural Undaria pinnatifida into unsaturated guluronic acid oligosaccharides by a single alginate lyase. Mar. Drugs., 22(10): 453 **(20 pages).**

Wang, H.Y.; Chen, Z.F.; Zheng, Z.H.; Lei, H.W.; Cong, H.H.; Zhou, H.X., (2023). A novel cold-adapted and high-alkaline alginate lyase with potential for alginate oligosaccharides preparation. Molecules, 28(17): 6190 **(19 pages)**.

Wang, X.; Xu, W.; Dai, Q.; Liu, X.; Guang, C.; Zhang, W.; Mu, W., (2023). Characterization of a thermostable PL-31 family alginate lyase from *Paenibacillus ehimensis* and its application for alginate oligosaccharides bioproduction. Enzyme Microb. Technol., 166: 110221 **(8 pages)**.

Wang, X.-H.; Zhang, Y.-Q.; Zhang, X.-R.; Zhang, X.-D.; Sun, X.-M.; Wang, X.-F.; Sun, X.-H.; Song, X.-Y.; Zhang, Y.-Z.; Wang, N.; Chen, X.-L.; Xu, F., (2024). High-level extracellular production of a trisaccharide-producing alginate lyase AlyC7 in *Escherichia coli* and its agricultural application. Mar. Drugs., 22 **(16 pages).**

Wang, Z.; Vanbever, R.; Lorent, J.H.; Solis, J.; Knoop, C.; Van Bambeke, F., (2024). Repurposing DNase I and alginate lyase to degrade the biofilm matrix of dual-species biofilms of *Staphylococcus aureus* and *Pseudomonas aeruginosa* grown in artificial sputum medium: in-vitro assessment of their activity in combination with broad-spectrum antibiotics. J. Cystic Fibrosis., 23(6): 1146-1152 (**7 pages**).

Wawszczak, A.; Kocki, J.; Kołodyńska, D., (2024). Alginate as a sustainable and biodegradable material for medical and environmental applications-the case studies. J. Biomed. Mater. Res. Part B: Appl. Biomater., 112(9): e35475 (**12 pages**).

Wei, Q.; Li, Z.; Liang, M.; Shen, N.; Pan, L.; Jiang, M.; Yang, D., (2025). Discovery and characterization of a novel alginate lyase PeAly15 and its truncated protein DUF4962 domain from *Paenibacillus elgii* HSFD1: Elucidation the molecular mechanism of endolytic mode. Int. J. Biol. Macromol., 306: 141822 (**9 pages**).

Weng, Y.; Yang, G.; Li, Y.; Xu, L.; Chen, X.; Song, H.; Zhao, C.X., (2023). Alginate-based materials for enzyme encapsulation. Adv. Colloid Interface Sci., 318: 102957 (**15 pages**).

Xing, M.; Cao, Q.; Wang, Y.; Xiao, H.; Zhao, J.; Zhang, Q.; Ji, A.; Song, S., (2020). Advances in research on the bioactivity of alginate oligosaccharides. Mar. Drugs., 18(3): 144 (**26 pages**).

Xia, H.F.; Jia, X.Y.; Zhou, Y.X.; Du, Z.J.; Mu, D.S.; Chen, G.J., (2023). Comparative genomics reveal distinct potential of *Tamlana* sp. S12 for algal polysaccharide degradation. Front. Mar. Sci., 10: 985514 **(14 pages).**

Xiao, Z.; Li, K.; Li, T., (2024). Characterization and mechanism study of a novel PL7 family exolytic alginate lyase from marine bacteria *Vibrio* sp. W13. Appl. Biochem. Biotechnol., 196: 68–84 (**17 pages**).

Xie, F.; Gao, C.; Avérous, L., (2024). Alginate-based materials: enhancing properties through multiphase formulation design and processing innovation. Mater. Sci. Eng. R Rep., 159: 100799 **(30 pages).**

Xu, F.; Cha, Q.Q.; Zhang, Y.Z.; Chen, X.L., (2021). Degradation and utilization of alginate by marine Pseudoalteromonas: a review. Appl. Environ. Microbiol., 87(17): e00368-21 **(17 pages).**

Yan, C.; Pan, M.; Geng, L.; Zhang, Q.; Hu, Y.; Wang, J.; Ye, S., (2024). A novel enzyme-assisted one-pot method for the extraction of fucoidan and alginate oligosaccharides from *Lessonia trabeculata* and their bioactivities. J. Oceanol. Limnol., 1-15 **(15 pages)**.

Yang, L.; Liu, Y.; Li, C.; Li, P.; Zhang, A.; Liu, Z.; Li, Z., (2024). Optimizing carbon sources regulation in the biochemical treatment systems for

coal chemical wastewater: aromatic compounds biodegradation and microbial response strategies. Water Res., 256: 121627 **(13 pages).**

Ye, Y.; Zhang, Y.; Zhou, Y.; Gao, Y., (2025). Molecular engineering of alginate lyases and the potential agricultural applications of their enzymatic products. J. Agric. Food Chem., 73(10): 5666-5684 **(10 pages).**

Zanditenas, E.; Ankri, S., (2024). Unraveling the interplay between unicellular parasites and bacterial biofilms: implications for disease persistence and antibiotic resistance. Virulence, 15(1): 2289775 **(19 pages).**

Zeng, R.G.; Shi, C.; Hao, L.T.; Huang, A.; Yuan, T.; Zhang, N., (2023). A review of alginate-like extracellular polymers from excess sludge: extraction, characterization, and potential application. J. Water Process Eng., 56: 104346 **(8 pages)**.

Zhang, C.; Li, M.; Rauf, A.; Khalil, A.A.; Shan, Z.; Chen, C.; Wan, C., (2023a). Process and applications of alginate oligosaccharides with emphasis on health beneficial perspectives. Crit. Rev. Food Sci. Nutr., 63(3): 303-329 **(27 pages).**

Zhang, W.; Ren, H.; Wang, X.; Dai, Q.; Liu, X.; Ni, D.; Zhu, Y.; Xu, W.; Mu, W. (2023b). Rational design for thermostability improvement of a novel PL-31 family alginate lyase from Paenibacillus sp. YN15. Int. J. Biol. Macromol., 253: 126919 **(8 pages)**.

Zhang, Y.; Wang, W.; Meng, Q.; Li, X.; Su, H.; Li, R.; Zhang, W., (2023c). A review on comprehensive analysis and potential applications of alginate based on the extracellular polymers in sludge. J. Water Process Eng., 56: 104540 **(12 pages).**

Zhou, L.; Zhang, R.; Jiang, B.; Meng, Q.; Chen, J.; Liu, X., (2024a). Efficient production of an alginate lyase in Bacillus subtilis with combined strategy: vector and host selection, promoter and signal peptide screening, and modification of a translation initiation region. J. Agric. Food Chem., 72(35): 19403-19412 **(10 pages)**.

Zhou, J.; Li, J.; Chen, G.; Zheng, L.; Mei, X.; Xue, C.; Chang, Y., (2024b). Discovery and characterization of a novel poly-mannuronate preferred alginate lyase: the first member of a new polysaccharide lyase family. Carbohydr. Polym., 343: 122474 **(7 pages).**

Zhu, B.; Li, L.; Yuan, X., (2024). Efficient preparation of alginate oligosaccharides by using alginate lyases and evaluation of the development promoting effects on *Brassica napus* L. in saline-alkali environment. Int. J. Biol. Macromol., 270: 131917 **(9 pages).**

Zhuang, H.; Zheng, F.; Zhang, H.; Wang, J.; Chen, J., (2024). Efficacious bioconversion of alginate/cellulose to value-added oligosaccharides by alginate-degrading GH5 endoglucanase from *Trichoderma asperellum*. Int. J. Biol. Macromol., 270: 131968 **(12 pages).**

Žigrayová, D.; Mikušová, V.; Mikuš, P., (2023). Advances in antiviral delivery systems and chitosan-based polymeric and nanoparticulate antivirals and antiviral carriers. Viruses, 15(3): 647 **(56 pages).**

AUTHOR (S) BIOSKETCHES

Anjung, M.U.K., Ph.D. Candidate, Doctoral Program in Fisheries Science and Marine, Faculty of Fisheries and Marine Sciences, Universitas Brawijaya East Java, Indonesia.
- Email: *mumpuni@student.ub.ac.id*
- ORCID: 0009-0007-7936-2731
- Web of Science ResearcherID: NA
- Scopus Author ID: NA
- Homepage: https://kkp.go.id/unit-kerja/bppsdmkp/upt/supm-kota-agung.html

Nursyam, H.; Ph.D., Professor; Department of Fishery Product Technology, Faculty of Fisheries and Marine Science, Brawijaya University, JL. Veteran, Malang 65415, East Java, Indonesia
- Email: *happy_nsy@ub.ac.id*
- ORCID: 0000-0002-6508-5493
- Web of Science ResearcherID: NA
- Scopus Author ID: 5569368600
- Homepage: https://fpik.ub.ac.id/dosen/prof-dr-ir-happy-nursyapolyM-s/

Prihanto, A.A, Ph.D., Professor, Department of Fishery Product Technology, Faculty of Fisheries and Marine Sciences, Brawijaya University, Jl Veteran, Malang, East Java, 65145, Indonesia.
- Email: *asep_awa@ub.ac.id*
- ORCID: 0000-0003-4180-1325
- Web of Science ResearcherID: AAB-9087-2021
- Scopus Author ID: 58165089800
- Homepage: https://fpik.ub.ac.id/dosen/prof-dr-sc-asep-awaludin-prihanto-s-pi-m-p/

Chasanah, E., Ph.D., Professor, Research Center for Marine and Inland Bioindustry, Research Organization of Earth and Maritime, National Research and Innovation Agency (BRIN), KST BJ Habibie, Serpong, Indonesia.
- Email: *Ekowati.chasanah@brin.go.id*
- ORCID: 0000-0002-5974-0690
- Web of Science ResearcherID: NA
- Scopus Author ID: 25931488000
- Homepage: https://brin.go.id/orkm/pusat-riset-bioindustri-laut-dan-darat/page/kr-mikrobiologi-dan-bioteknologi-akuatik

HOW TO CITE THIS ARTICLE

Anjung, M.U.K.; Nursyam, H.; Prihanto, A.A.; Chasanah, E., (2025). Application of marine bacterial alginate lyases in wastewater treatment, biofilm removal and green technology. Global J. Environ. Sci. Manage., 11(3): 1343-1360.

DOI: 10.22034/gjesm.2025.03.25

URL: https://www.gjesm.net/article_725046.html

PUBLICATION ETHICS

The ethical policy of GJESM is based on the Committee on Publication Ethics (COPE) guidelines and complies with International Committee of GJESM Editorial Board codes of conduct. Readers, authors, reviewers and editors should follow these ethical policies once working with GJESM. The ethical policy of GJESM is liable to determine which of the typical research papers or articles submitted to the journal should be published in the concerned issue. For information on this matter in publishing and ethical guidelines please visit http://publicationethics.org

Duties and Responsibilities of Publishers

1. GJESM is committing to ensure that editorial decisions on manuscript submissions are the final.
2. GJESM is promising to ensure that the decision on manuscript submissions is only made based on professional judgment and will not be affected by any commercial interests.
3. GJESM is committing to maintain the integrity of academic and research records.
4. GJESM is monitoring the ethics by Editor-in-Chief, Associate Editors, Editorial Board Members, Reviewers, Authors, and Readers.
5. GJESM is always checking the plagiarism and fraudulent data issues involving in the submitted manuscript.
6. GJESM is always willing to publish corrections, clarifications and retractions involving its publications as and when needed.

Duties and Responsibilities of Editors

1. The Editors of the journal should have the full authority to reject/accept a manuscript.
2. The Editors of the journal should maintain the confidentiality of submitted manuscripts under review or until they are published.
3. The Editor-in-Chief should take a decision on submitted manuscripts, whether to be published or not with other editors and reviewers
4. The Editors of the journal should preserve the anonymity of reviewers.
5. The Editors of the journal should disclose and try to avoid any conflict of interest.
6. The Editors of the journal should maintain academic integrity and strive to meet the needs of readers and authors.
7. The Editors of the journal should be willing to investigate plagiarism and fraudulent data issues and willing to publish corrections, clarifications, retractions, and apologies when needed.
8. The Editors of the journal should have the limit themselves only to the intellectual content.
9. The Editors of the journal must not disclose any information about submitted manuscripts to anyone other than the corresponding author, reviewers, potential reviewers, other editorial advisers, and the publisher, as appropriate.
10. Unpublished materials disclosed in a submitted paper will not be used by the editor or the members of the editorial board for their own research purposes without the author's explicit written consent.

Duties and Responsibilities of Reviewers

1. The Reviewers of the journal should assist the Editors in taking the decision for publishing the submitted manuscripts.
2. The Reviewers should maintain the confidentiality of manuscripts, which they are invited to review.
3. The Reviewers should provide comments in time that will help editors to make decision on the submitted manuscript to be published or not.
4. The Reviewers are bound to treat the manuscript received for peer reviewing as confidential, and must not use the information obtained through peer review for personal advantage.
5. The Reviewers comments against each invited manuscript should be technical, professional and objective.
6. The Reviewers should not review the manuscripts in which they have found conflicts of interest with any of the authors, companies, or institutions.
7. The Reviewers should disclose and try to avoid any conflict of interest.

Duties and Responsibilities of Authors

1. Manuscripts must be submitted only in English and should be written according to sound grammar and proper terminology.
2. Manuscripts must be submitted with the understanding that they have not been published elsewhere (except in the form of an abstract or as part of a published lecture, review, or thesis) and are not currently under consideration by another journal published by or any other publisher.
3. The submitting (corresponding) author is responsible for ensuring that the manuscript article's publication has been approved by all the other coauthors.
4. In order to sustain the peer review system, authors have an obligation to participate in peer review process to evaluate manuscripts from others.
5. It is also the authors' responsibility to ensure that the manuscripts emanating from a particular institution are submitted with the approval of the necessary institution.
6. It is a condition for submission of a manuscript that the authors permit editing of the paper for readability.
7. Authors are requested to clearly identify who provided financial support for the conduct of research and/or preparation of the manuscript and briefly describe the role of the funder/sponsor in any part of the work.
8. A copy right release and conflict of interest disclosure form must be signed by the corresponding author in case of multiple authorships, prior to the acceptation of the

manuscript, by all authors, for publication to be legally responsible towards the Journal ethics and privacy policy.

9. Under open access license, authors retain ownership of the copyright for their content, but allow anyone to download, reuse, reprint, modify, distribute, and/ or copy the content as long as the original authors and source are cited properly.
10. All authors have agreed to allow the corresponding author to serve as the primary correspondent with the editorial office, to review the edited manuscript and proof.
11. When author(s) discovers a significant error or inaccuracy in his/her own published work, it is the author's obligation to promptly notify the journal editor or publisher to retract or correct the manuscript.
12. All authors must know that that the submitted manuscripts under review or published with GJESM are subject to screening using Plagiarism Prevention Software. Plagiarism is a serious violation of publication ethics.

Violation of Publication Ethics

1. **Plagiarism:** Plagiarism is intentionally using someone else's ideas or other original material as if they are one's own. Copying even one sentence from someone else's manuscript, or even one of your own that has previously been published, without proper citation is considered by GJESM Journals as plagiarism. All manuscripts under review or published with GJESM are subject to screening using plagiarism prevention software. Thus, plagiarism is a serious violation of publication ethics. The development of CrossCheck is a service that helps editors to verify the originality of papers. CrossCheck is powered by the Ithenticate software from iParadigms, known in the academic community as providers of Turnitin. For a searchable list of all journals in the CrossCheck database, please visit: www.ithenticate.com/search
2. **Data Fabrication and Falsification:** Data fabrication and falsification means the researcher did not really carry out the study, but made up data or results and had recorded or reported the fabricated information. Data falsification means the researcher did the experiment, but manipulated, changed, or omitted data or results from the research findings.
3. **Simultaneous Submission:** Simultaneous submission occurs when a manuscript (or substantial sections from a manuscript) is submitted to a journal when it is already under consideration by another journal.
4. **Duplicate Publication:** Duplicate publication occurs when two or more papers, without full cross referencing, share essentially the same hypotheses, data, discussion points, and conclusions.
5. **Redundant Publications:** Redundant publications involve the inappropriate division of study outcomes into several articles, most often consequent to the desire to plump academic vitae.
6. **Improper Author Contribution or Attribution:** All listed authors must have made a significant scientific contribution to the research in the manuscript and approved all its claims. Don't forget to list everyone who made a significant scientific contribution, including students and laboratory technicians.
7. **Citation Manipulation:** Citation Manipulation is including excessive citations, in the submitted manuscript, that do not contribute to the scholarly content of the article and have been included solely for the purpose of increasing citations to a given author's work, or to articles published in a particular journal. This leads to misrepresenting the importance of the specific work and journal in which it appears and is thus a form of scientific misconduct.

Handling Cases of Misconduct

Once GJESM confirms a violation against GJESM's publication ethics, GJESM addresses ethical concerns diligently following an issue-specific standard practice as summarized below.

1. The first action of the journal Editor is to inform the Editorial Office of GJESM by supplying copies of the relevant material and a draft letter to the corresponding author asking for an explanation in a nonjudgmental manner.
2. If the author's explanation is unacceptable and it seems that serious unethical conduct has taken place, the matter is referred to the Publication Committee via Editorial Office. After deliberation, the Committee will decide whether the case is sufficiently serious to warrant a ban on future submissions.
3. If the infraction is less severe, the Editor, upon the advice of the Publication Committee, sends the author a letter of reprimand and reminds the author of GJESM publication policies; if the manuscript has been published, the Editor may request the author to publish an apology in the journal to correct the record.
4. Notification will be sent to corresponding author and any work by the author responsible for the violation or any work these persons coauthored that is under review by GJESM journal will be rejected immediately.
5. The authors are prohibited from serving on GJESM editorial board and serving as a reviewer for GJESM Journal. GJESM reserves the right to take more actions.
6. In extreme cases, notifications will be sent to the affiliations of the authors and the authors are prohibited from submitting their work to GJESM for 5 years.
7. In serious cases of fraud that result in retraction of the article, a retraction notice will be published in the journal and will be linked to the article in the online version. The online version will also be marked "retracted" with the retraction date.

GUIDE FOR AUTHORS

"Global Journal of Environmental Science and Management" (GJESM) is a double blind peer reviewed electronic and print quarterly publication concerned with all aspects of environmental science and management. GJESM publishes original research papers, review papers, case reports and short communications, letters to editor and authors' response about letters to editor across the broad field of environment. These include but are not limited to environmental science, environmental management, environmental engineering, environmental planning and design, urban and regional landscape design and industrial ecology. Environmentalist disciplines are invited to contribute their knowledge and experience. The publication appears at regular intervals time quarterly. The Journal database is fully open access and full text of published articles are available for everyone who can get access to the Journal website free of cost. The authors never pay any charges for submission, article processing and publication.

Guide for Authors: More details on guide for authors refer: http://gjesm.net/journal/authors.note

GENERAL

1. Authors should submit their contributions electronically through the GJESM website submission system to the Editorial Office.

2. Manuscripts must be submitted only in English and should be written according to sound grammar and proper terminology. Manuscripts should be typed in Times New Roman of 11 pt. font and in MS-Word format in one column with 2.5 cm margin at each side. Manuscript submission must be applied once in order to obtain only one submission ID number. More than one submission for a single manuscript can lose the chance of the manuscript consideration. Manuscript must be accompanied by a covering letter including title and author(s) name.

3. There are no strict formatting requirements but all manuscripts must contain the essential elements needed to convey your manuscript, for example Abstract, Keywords, Introduction, Materials and Methods, Results, Conclusions, Artwork and Tables with Captions. Please ensure the figures and the tables included in the single file are placed next to the relevant text in the manuscript, rather than at the bottom or the top of the file. There are no strict requirements on reference formatting at submission. References can be in any style or format as long as the style is consistent.

BEFORE YOU BEGIN

1. Peer-Review Process: In order to sustain the peer review system, authors have an obligation to participate in peer review process to evaluate manuscripts from others. When appropriate, authors are obliged to provide retractions and/or corrections of errors to the editors and the Publisher. All papers submitted to GJESM journal will be peer reviewed for at least one round. GJESM journal adopts a double-blinded review policy: authors are blind to reviewers, but reviewers are not blind to authors. After receiving reviewers' comments, the editorial team member makes a decision. Because reviewers sometimes do not agree with each other, the final decision sent to the author may not exactly reflect recommendations by any of the reviewers. The decision after each round of peer review may include (a) Accept without any further changes, (b) Accept with minor revision, (c) Major changes are necessary for resubmission and (d) Decline without encouraging resubmission.

2. Post-Publication Evaluation: In addition to rapid Peer Review Process, the GJESM Journal has Post-Publication Evaluation by the scientific community. Post-Publication Evaluation is concentrated to ensure that the quality of published research, review and case report meets certain standards and the conclusions that are presented are justified. The post-publication evaluation includes online comments and citations on published papers. Authors may respond to the comments of the scientific community and may revise their manuscript. The Post-Publication Evaluation is described in such a way; it is allowing authors to publish quickly about Environmental science, management, engineering and technology concepts.

3. Publication Ethics: The ethical policy of GJESM is based on the Committee on Publication Ethics (COPE) guidelines and complies with International Committee of GJESM Editorial Board codes of conduct. Readers, authors, reviewers and editors should follow these ethical policies once working with GJESM. The ethical policy of GJESM is liable to determine which of the typical research papers or articles submitted to the journal should be published in the concerned issue. The ethical policy insisted the Editor-in-Chief, may confer with other editors or reviewers in making the decision. Visit at: http://publicationethics.org

4. Conflict of Interest: Authors are requested to evident whether impending conflicts do or do not exist. A copyright transfer agreement is signed by the corresponding author, upon the acceptance of the manuscript, on behalf of all authors, for publication to be legally responsible towards the journal ethics and privacy policy. Authors will be notified as soon as possible of decisions concerning the suitability of their manuscripts for publication in the journal. The submitted materials may be considered for inclusion but cannot be returned and Editors of the journal reserve the right to accept or reject any article in any stage, if necessary. Conflict of Interest Disclosure form can be found at: www.gjesm.org/conflict_of_interest_discloure_form.docx

5. Submission Declaration and Verification: While submitting a manuscript to GJESM, all contributing author(s) must verify that the manuscript represents authentic and valid work and that neither this manuscript nor one with significantly similar content under their authorship has been published or is being considered for publication elsewhere including electronically in the same form, in English or in other language, without the written consent the copy right holder.

6. Authorship: All contributing authors should qualify for authorship and corresponding author should sign the authorship form while submitting the manuscript. It can be found at: (http://www.gjesm.net/data/gjesm/news/authorship_form.docx).

7. Changes to Authorship: After the manuscript is submitted or accepted for publication, the corresponding author is required to send a request to add or remove an author or to rearrange the author names of the submitted/accepted manuscript by sending the change of authorship form to editorial office. No authorship change is allowed after publication of manuscript. More details may be found at: (http://www.gjesm.net/data/gjesm/news/change_of_authorship_form.docx)

8. Retained Author Rights: As an author, author or authors' employer or institution retains certain rights. For more information on author rights, found at: www.gjesm.org/retained_authors_right.docx.

9. Copy Right: Journals should make clear the type of copyright under which authors' work will be published. For open access articles the publisher uses an exclusive licensing agreement in which authors retain copyright in their manuscript. More details may be found at: (www.gjesm.org/copyright_form.docx)

10. User license Agreement: GJESM provides access to archived material through GJESM archives. Manuscripts are the parts of an open archive are made freely available from GJESM website after certain period, which begins from the final publication date of the manuscript. All articles published open access will be immediately and permanently free for everyone to read and download. Permitted reuse is defined by Creative Commons user license called ***Creative Commons Attribution***. Visit at: **(**Creative Commons Attribution 4.0 International (CC BY 4.0)**)**

11. Plagiarism Prevention and Violation of Publication Ethics: All manuscripts under review or published with GJESM are subject to screening using Plagiarism Prevention Software. Plagiarism is a serious violation of publication ethics. Other violations include duplicate publication, data fabrication and falsification, and improper credit of author contribution. Thus, the Plagiarism or Fraudulent or knowingly inaccurate statements constitute unethical behavior are unacceptable and submitting the same manuscript to more than one journal concurrently constitutes unethical publishing behavior and is unacceptable. The development of CrossCheck is a service that helps editors to verify the originality of papers. CrossCheck is powered by the Ithenticate software from iParadigms, known in the academic community as providers of Turnitin. For more details visit at: www.ithenticate.com/search

12. Handling Cases of Misconduct: Once GJESM confirms a violation against GJESM's publication ethics, the following actions will be taken.

a. The work is rejected / retracted immediately. Notification will be sent to corresponding authors. In extreme cases, notifications will be sent to the affiliations of the authors.
b. The authors are prohibited from submitting their work to GJESM for 5 years.
c. Any work by the authors responsible for the violation or any work these persons coauthored that is under review by any GJESM journal will be rejected immediately.
d. The authors are prohibited from serving on GJESM editorial board. GJESM reserves the right to take more actions.

MANUSCRIPT PREPARATION

1. Title Page: The title page should include: the name(s) of the author(s), a concise and informative title, the affiliation(s) and address (es) of the author(s), and e-mail address, telephone and fax numbers of the corresponding author.

2. Manuscript Title: Title of up to 17 words should not contain the name of locations, countries or cities of the research as well as abbreviations. The title should be oriented to Environmental issues while not being obscure or meaningless.

3. Abstract: An abstract of 150 to 250 words that sketches the purpose of the study; basic procedures; main findings its novelty; discussions and the principal conclusions, should not contain any undefined abbreviations or references.

4. Keywords: Provide 5 to 7 keywords which can be used for indexing purposes. Keywords should not repeat the words of the manuscript title or contain abbreviations and shall be written in alphabetical order as separated by semicolon.

5. Introduction: The Introduction should state the purpose of the investigation and identify clearly the gap of knowledge that will be filled in the Literature review study. Date and location of the research carried out throughout the study must be mentioned at the end of this section.

6. Materials and methods: The Materials and Methods section should provide enough information to permit repetition of the experimental work. It should include clear descriptions and explanations of sampling procedures, experimental design, and essential sample characteristics and descriptive statistics, hypothesis tested, exact references to literature describing the tests used in the manuscript, number of data involved in statistical tests, etc.

7. Results and Discussion: The Results section should describe the outcome of the study. Data should be presented as concisely as possible - if appropriate in the form of tables or figures, although very large tables should be avoided. The Discussion should be an interpretation of the results and their significance with reference to work by other authors. Please note that the policy of the Journal with respect to units and symbols is that of SI symbols.

8. Tables: Do not submit tables and graphs as photograph. Place explanatory matters in footnotes, not in the heading. Do not use internal horizontal and vertical rules. Tables should be called out in the text and should have a clear and rational structure and consecutive numerical order. All tables should be numbered 1, 2, 3, etc. Give enough information in subtitles so that each table is understandable without reference to the text. Footnotes to tables should be indicated by superscript lower-case letters (or asterisks for significance values and other statistical data) and included beneath the table body.

9. Figures: Figures/ illustrations should be in high quality art work, within 200-300 dpi and separately provided in Excel format. Ensure that figures are clear, labeled, and of a size that can be reproduced legibly in the journal. Each figure should have a concise caption describing accurately what the figure depicts. Figure captions begin with the term Fig. Figures should be with the captions placed below in limited numbers. No punctuation is to be placed at the end of the caption.

10. Conclusion: This section should highlight the major, firm discoveries, and state what the added value of the main finding is, without literature references.

11. Acknowledgements: Acknowledgments of people, grants, funds, etc. should be placed in a separate section before the reference list. The names of funding organizations should be written in full. Financial support affiliation of the study, if exists, must be mentioned in this section. Thereby, the Grant number of financial support must be included.

12. References: All the references should be cited throughout the manuscript text as well as in the Reference section organized in accordance with Harvard system. Groups of references should be listed first alphabetically, then chronologically. The number of references extracted from each journal should not exceed 3 to 5 citations, which is the average acceptable amount. The number of references should not be less than 30 for original paper, less than 100 for review paper. It is substantially recommended to the authors to refer to more recent references rather than old and out of date ones. Volume, issue and pages of the whole references must be specified according to the GJESM format.

Citing and listing of Web references: As a minimum, the full URL should be given. Any further information, if known (Author names, dates, reference to a source publication, etc.), should also be given.

Text: All citations in the text should refer to: 1. Single author: the author's name (without initials, unless there is ambiguity) and the year of publication; 2. Two authors: both authors' names and the year of publication; and 3. Three or more authors: first author's name followed by "et al." and the year of publication. Citations may be made directly (or parenthetically). Groups of references should be listed first alphabetically, then chronologically. Examples: "as demonstrated (Allan, 1996a, 1996b, 1999; Allan and Jones, 1995). Kramer *et al.,* (2000) have recently shown …".

List: References should be arranged first alphabetically and then further sorted chronologically if necessary. More than one reference from the same Author(s) in the same year must be identified by the letters "a", "b", "c", etc., placed after the year of publication.

Journal article: Nouri J.; Lorestani B.; Yousefi N.; Khorasani N.; Hassani A. H.; Seif, F.; Cheraghi M., (2011). Phytoremediation potential of native plants grown in the vicinity of Ahangaran lead-zinc mine. Environ. Earth Sci., 62(3): 639-644.

Book: Davis, M. L., (2005). Introduction to Environmental Engineering, 3rd. Ed. McGraw Hill Inc.

Book chapter: Mettam, G. R.; Adams, L. B., (1999). How to prepare an electronic version of your article, in: Jones, B. S., Smith, R. Z. (Eds.), Introduction to the electronic age. E-Publishing Inc., New York.

Conference paper: Brown, J., (2005). Evaluating surveys of transparent governance. In UNDESA, 6th. Global forum on reinventing government: towards participatory and transparent governance. Seoul, Republic of Korea 24-27 May. United Nations: New York.

Dissertation: Trent, J. W., (1975). Experimental acute renal failure. Ph.D. Dissertation, University of California. USA.

Online document: Cartwright, J., (2007). Big stars have weather too. IOP Publishing Physics Web.
http://physicsworld.com/cws/article/news/2007/jun/26/big-stars-have-weather-too

AFTER ACCEPTANCE

1. Online Proof Correction: Corresponding authors will receive an e-mail with a link to our online proofing system, allowing annotation and correction of proofs online. Use this proof only for checking the typesetting, editing, completeness and correctness of the text, tables and figures. Significant changes to the article as accepted for publication will only be considered at this stage with permission from the Editor-in-Chief. It is important to ensure that all corrections are sent back to us in one communication. Please check carefully before replying, as inclusion of any subsequent corrections cannot be guaranteed. Proofreading is solely the corresponding author responsibility.

2. Offprints: The offprints can be downloading from the GJESM website once the final corrected manuscripts are disseminated.

AUTHORS INQUIRIES

Authors can track their submitted article through GJESM website on author's login section at: http://gjesm.net/contacts?_action=login

Copyright Transfer Agreement

1. Parties of the agreement

Author (s):

Manuscript Title:

Manuscript ID:

(Herewith referred to as the "materials"),

Journal Title: Global Journal of Environmental Science and Management (GJESM)

2. Subject of the agreement

A) Copyright
1- The Author and each co-authors shall transfer and sell to the Publisher for the length of the copyright starting from the moment the present agreement comes into force the exclusive rights to the materials, including the rights to translate, reproduce, transfer, distribute or otherwise use the materials or parts (fragments) contained therein, for publication in scientific, academic, technical or professional journals or other periodicals and in derivative works thereof, worldwide, in English, in print or in electronic editions of such journals, periodicals and derivative works in all media or formats now existing or that may exist in future, as well as the right to license (or give permission to) third parties to use the materials for publication in such journals, periodicals and derivative works worldwide. The transfer under this agreement includes the right to adapt the presentation of the materials for use in conjunction with computer systems and programs, reproduction or publication in machine-readable format and incorporation into retrieval systems.
2- Reproduction, placement, transfer or any other distribution or use of the materials, or any parts of the materials contained therein, in any way permitted under this Agreement, shall be accompanied by reference to the Journal and mentioning of the Publisher, namely: the title of the article, the name of the Author (Co-authors), the name of the Journal, volume/number, copyright of the publisher.

B) Reserved Rights
The Author (Co-authors) or the employer of the Author (Co-authors) of the materials shall retain all proprietary rights (with the exception of the rights transferred to the Publisher under the present Agreement).

C) Author Guarantee
The Author (Co-authors) guarantees that the materials are an original work, submitted only to GJESM, and have not been published previously.
In case the materials were written jointly with co-authors, the Author guarantees that he/she has informed them of the terms of this Agreement and obtained their signatures or written permission to singe on their behalf.
The Author guarantees as well that:
The materials do not contain libelous statements.
The materials do not infringe on other persons' rights (including without limitation copyrights, patent rights and the trademark right).
The materials do not contain facts or instructions that can cause damage or injury to third parties and their publication does not cause the disclosure of any secret or confidential information

---

Author (Corresponding Author):

Correspondence Address:

Phone:

Fax:

Email:

Corresponding Author Name: Signature Date

On Behalf of the Publisher:

Iran Solid Waste Association,
Faculty of Environment, University of Tehran,
Postal Code: 1417854511, Tehran,
Iran

Telefax: (+9821) 2610 5110

Email: *editor@gjesm.net*

Gjesm.publication@gmail.com

Website: www.gjesm.net

Accepted for publication ☑ Signature Date

PLEASE NOTE: The accepted manuscript cannot be processed for publication until the publisher has received this signed form. The form MUST be signed by the Corresponding Author and then scanned and sent through the system or email. If the manuscript is not published in the Journal, this release will not take effect.

The sole responsibility for the whole content (s) of the article remains only with the corresponding author. However, Editor would reserve the right to adjust the style to certain standards of uniformity before publication.

CONFLICT OF INTEREST DISCLOSURE FORM

Conflict of Interest is defined as a set of conditions in which professional judgment concerning a primary interest, such as the validity of research, may be influenced by a secondary interest, such as financial gain. A Conflict of Interest Disclosure is an agreement or notification from the authors that they have not been paid for the work, or if they have, stating the source of their payment. The purpose of Conflict of Interest Disclosure form is to provide readers of authors' manuscript with information about authors' interests that could influence how the authors receive the work. The corresponding author (on behalf of all co-authors) should submit a conflict of interest disclosure form and is responsible for the accuracy and completeness of the submitted manuscript. Conflict of Interest Disclosure form can be signed by the corresponding author on behalf of all co-authors and stating that the submitted manuscript is the authors' original work, has not received prior publication and is not under consideration for publication elsewhere, permission has been received to use any material in the manuscript much as tables, figures etc. or no permissions have necessary to publish the authors' work.

1. Name of the corresponding author

2. Affiliation including e-mail and phone number

3. Manuscript Title

4. Do the authors or authors' institution at any time receive payment or services from a third party (government, commercial, private foundation, etc.) for any aspect of the submitted manuscript (including but not limited to grants, data monitoring board, study design, manuscript preparation, statistical analysis, etc.)?

   Are there any relevant conflicts of interest? Yes / No

5. Do the authors have any patents, whether planned, pending or issued, broadly relevant to the work?

   Are there any relevant conflicts of interest? Yes / No

6. Are there other relationships or activities that readers could perceive to have influenced, or that give the appearance of potentially influencing, what the authors' information in the submitted manuscript?

   Are there any relevant conflicts of interest? Yes / No

7. Are there any aspect of the work covered in this manuscript that has involved either experimental animals or human patients has been conducted with the ethical approval of all relevant bodies or not.

   Are there any relevant conflicts of interest? Yes / No

Corresponding Author Signature | Print Name | Date

AUTHORSHIP FORM

By completing and signing the following statements, the corresponding author acknowledges and accepts the responsibility on behalf of all contributing authors, if any, concerning Authorship Responsibility.

Manuscript title:

Corresponding author:

Affiliation:

Email:

Phone No:

By signing and filling this form, the corresponding author certifies that each author has met all criteria below (A, B, C, and D) and indicates each author general and specific contributions by listing his or her name next to the relevant section.

A. I certify that

- The manuscript is authentic and valid and that neither this manuscript nor one with considerably similar content under my authorship has been published or is being considered for publication elsewhere, except as described in an attachment, nor copies of closely related manuscripts are provided.
- I will provide the data or will contribute fully in providing and obtaining the data on which the manuscript is based for examination by the editors or their assignees, if requested.
- Every author has agreed to allow the corresponding author to serve as the primary correspondent with the editorial office, to review the edited manuscript and proof.

B. Each author has given final approval of the submitted manuscript.

C. Each author has participated sufficiently in the work to take public responsibility for the whole content.

D. Each author qualifies for authorship by listing his or her name on the appropriate line of the categories of contributions listed below. List appropriate author next to each section – each author must be listed in at least 1 field. More than 1 author can be listed in each field.

- conception and design
- acquisition of data
- analysis and interpretation of data
- drafting of the manuscript
- critical revision of the manuscript for important intellectual content
- statistical analysis
- obtaining funding
- administrative, technical, or material support
- supervision
- no additional contributions
- other (specify)

Corresponding Author Signature **Print Name** **Date**

CHANGE OF AUTHORSHIP FORM

Manuscript Title:

Corresponding Author:

Please check all that apply.

☐ New author(s) have been added.

☐ There is a change in the order of authorship.

☐ An author wishes to remove his/her name. An author's name may only be removed at his/her own request in writing.

ORIGINAL AUTHORSHIP

List ALL AUTHORS in the same order as the original (first) submission.

Print Name	Print Name
Name (1)	Name (6)
Name (2)	Name (7)
Name (3)	Name (8)
Name (4)	Name (9)
Name (5)	Name (10)

NEW AUTHORSHIP

List the ALL AUTHORS in same order as the new version.

Print Name	Print Name
Name (1)	Name (6)
Name (2)	Name (7)
Name (3)	Name (8)
Name (4)	Name (9)
Name (5)	Name (10)

I attest that:

1. The manuscript is not currently under consideration, in press, or published elsewhere, and the research reported will not be submitted for publication elsewhere until a final decision has been made as to its acceptability by the journal (posting of submitted material on a web site may be considered prior publication-note this in your cover letter).
2. The manuscript is truthfully original work without fabrication, fraud, or plagiarism.
3. I have made an important scientific contribution to the study and am thoroughly familiar with the primary data.
4. I have read the complete manuscript and take responsibility for the content and completeness of the manuscript and understand that I share responsibility if the paper, or part of the paper, is found to be faulty or fraudulent.

Corresponding Author Signature Name Date

SUBSCRIPTION FORM

Subscription form

Global Journal of Environmental Science and Management

Please enter my annual subscription to the Global Journal of Environmental Science and Management (GJESM), including 4 quarterly issues for the Year ..... Vol. ..... Nos.....

	Domestic (Rials)	International (USD)
▪ Institutional	3,000,000	150
▪ Individual	2,000,000	100
▪ Student	1,000,000	80
▪ Single Copy	500,000	50

Name: **Tel.:** **Email:**

Mailing Address:

Payment method: Check or money order must be made in order of:
Account #. 0101834143005, Account name: J. Nouri
Bank Melli Iran, IAU Branch, Code 1017, Tehran, Iran

□ Bank receipt enclosed

** Please allow 3 to 5 weeks for delivery*

Please send this filled in order form along with the Bank receipt payment to:

Global Journal of Environmental Science
and Management
No. 2, Kouhestan Deadend, Janpour Street,
Darabad, Tehran 1956934461 Iran

CONTENTS

Volume 11, Issue 3, Summer 2025

1.	Neuro-fuzzy inference system and white shark optimization of coagulation-flocculation of aquaculture wastewater treatment	857
2.	A spatial slip plane-based vegetation model for slope reinforcement and shallow landslide mitigation	875
3.	The potential of carbon emission reduction through the transition to battery electric vehicles	897
4.	Microplastic contamination in river and its impact on fish health	915
5.	Carbon footprint associated with a small-scale emissions reduction initiative for sustainable event management	941
6.	The role of marine protected areas in enhancing coral cover and reef fish communities	963
7.	Eco-friendly pest management in integrated rice-fish farming systems using plant-derived biopesticides to promote sustainable agriculture	983
8.	The significance of clean energy, education, and environmental managament in fostering a sustainable future	1001
9.	Monsoonal influence on particulate organic carbon variability through satellite data analysis	1019
10	Removal of cadmium and lead using a sub-bituminous coal resin modified with xanthate groups	1035
11.	Conserving biodiversity, carbon, and community values in a fragmented landscape	1057
12.	Passenger car emissions in urban areas based on local vehicle fleet and environmental conditions	1079
13.	Infrared precipitation on climate hazards using rainfall dataset over inter-tropical convergence zone	1097
14.	Ambient air nitrogen dioxide concentration and the growing incidence of asthma in school-aged children	1125
15.	Spatiotemporal analysis of rainfall variability using satellite precipitation in watersheds	1143
16.	Tracking Coronavirus 2019 pandemic-related waste generation in urban waterways	1163
17.	Sustainability of natural tourism attraction and satisfaction	1185
18.	Allometric equations model for estimating an above and below ground biomass of dipterocarp forest in the tropics	1199
19.	Carcinogenic and non-carcinogenic hazards associated with trace elements and organochlorines from fish consumption in tropical river watershed	1221
20.	The impact of renewable energy technology innovation on the low-carbon economic transition	1241
21.	Integrating building information modeling and bayesian network for enhanced go/no-go decisions in building demolition projec	1259
22.	Sustainable approach for biocontrol of biostimulants derived from endophytic bacteria and seaweed extracts	1281
23.	Bibliometrics analysis and the role of nanocatalysts in wastewater remediation	1299
24.	A bibliometric study on Sordariales fungi covering genetic diversity, ecological interactions and biotechnological applications	1319
25.	Application of marine bacterial alginate lyases in wastewater treatment, biofilm removal and green technology	1343